GEOLOGICAL SURVEY OF CANADA
COMMISSION GÉOLOGIQUE DU CANADA

PAPER
ÉTUDE 81-1A

CURRENT RESEARCH
PART A

RECHERCHES EN COURS
PARTIE A

Energy, Mines and Resources Canada
Énergie, Mines et Ressources Canada

1981

Notice to Librarians and Indexers

The Geological Survey's thrice-yearly *Current Research* series contains many reports comparable in scope and subject matter to those appearing in scientific journals and other serials. All contributions to the Scientific and Technical Report section of *Current Research* include an abstract and bibliographic citation. It is hoped that these will assist you in cataloguing and indexing these reports and that this will result in a still wider dissemination of the results of the Geological Survey's research activities.

Avis aux bibliothécaires et préparateurs d'index

La série Recherches en cours *de la Commission géologique paraît trois fois par année; elle contient plusieurs rapports dont la portée et la nature sont comparable à ceux qui paraissent dans les revues scientifiques et autres périodiques. Tous les articles publiés dans la section des rapports scientifiques et techniques de la publication* Recherches en cours *sont accompagnés d'un résumé et d'une bibliographie, ce qui vous permettra, nous l'espérons, de cataloguer et d'indexer ces rapports, d'où une meilleure diffusion des résultats de recherche de la Commission géologique.*

Technical editing and compilation
Rédaction et compilation techniques
R.G. Blackadar
P.J. Griffin
H. Dumych
E.R.W. Neale

Production editing and layout
Préparation et mise en page
Leona R. Mahoney
Lorna A. Firth
Michael J. Kiel

Typed and checked by
Dactylographie et vérification
Debby Busby
Judy Côté
Susan Gagnon
Janet Gilliland
Janet Legere
Sharon Parnham

GEOLOGICAL SURVEY
PAPER 81-1A

COMMISSION GÉOLOGIQUE
ÉTUDE 81-1A

CURRENT RESEARCH
PART A

RECHERCHES EN COURS
PARTIE A

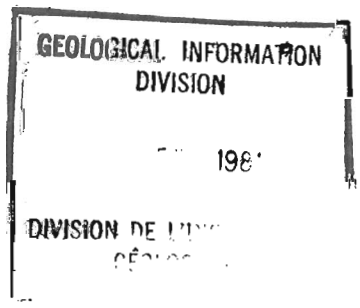

1981

Available in Canada through

authorized bookstore agents
and other bookstores

or by mail from

Canadian Government Publishing Centre
Supply and Services Canada
Hull, Québec, Canada K1A 0S9

and from

Geological Survey of Canada
601 Booth Street
Ottawa, Canada K1A 0E8

A deposit copy of this publication is also available
for reference in public libraries across Canada

Cat. No. M44-81-1AE
ISBN 0-660-10725-2

Canada: $8.00
Other countries: $9.60

Price subject to change without notice

ERRATUM

Current Research, Part C

Geological Survey of Canada, Paper 80-1C

Summary of conodont biostratigraphy of the Blue Fiord and Bird Fiord Formations (Lower-Middle Devonian) at the type and adjacent areas, southwestern Ellesmere Island, Canadian Arctic Archipelago; T.T. Uyeno and G. Klapper; Paper 80-1C, p. 81-93.

p. 82, right column, caption to Fig. 8.1, 3rd line from top:
. . . the type section of the Bird Fiord Formation.

p. 83, left column, note under Table 8.1, 9th line from top:
The **partitus** Zone . . .

p. 83, right column, last line:
Fåhraeus

p. 85, right column, 2nd paragraph, 4th line from bottom:
tentaculite

p. 85, right column, 2nd line from bottom:
Princess

p. 87, left column, explanation to Plate 8.1, under Figures 28-31,
Pandorinellina expansa Uyeno and Mason:
29-31. GSC 64495, lateral, upper and lower views, . . .

p. 89, left column, explanation to Plate 8.2, under Figures 5, 7, 8, 14, 27-30, 35, and 36:
S_{2a}, S_{2b}, S_{2c}

p. 89, left column, explanation to Plate 8.2, under Figures 12, 13:
Steptotaxis glenisteri

p. 89, right column, 6th to 11th line, not to read like titles, but as follows:
(starting at left margin)
Polygnathus inversus Klapper and D.B. Johnson, 1975, p. 73, Pl. 3, figs. 15-39 [synonymy through 1974].

Polygnathus inversus Klapper and Johnson, in Klapper and J.G. Johnson, 1980, p. 45? [synonymy through 1979].

p. 91, left column, explanation to Plate 8.3, under Figures 2, 7-9, 14-16:
S_{2a}, S_{2c}

p. 91, right column, 2nd paragraph, 15th line from top:
S_{2c}

p. 91, right column, under Al-Rawi, D., 1977:
Senckenbergiana lethaea

p. 91, right column, under Brice, D., in press:
Brachiopodes du Devonien . . .

p. 92, left column, under Fåhraeus, L., 1971:
Michelle and Prongs Creek Formations, . . .

p. 92, right column, under Mayr, U. et al., 1980:
Paper 80-1A

p. 92, right column, under McGregor, D.C. and Uyeno, T.T.:
Paper 71-13

SCIENTIFIC AND TECHNICAL REPORTS
RAPPORTS SCIENTIFIQUES ET TECHNIQUES

ECONOMIC GEOLOGY/GÉOLOGIE ÉCONOMIQUE

Page

R.T. BELL: Preliminary evaluation of uranium in Sustut and Bowser successor basins, British Columbia 241

K.H. POULSEN and J.M. FRANKLIN: Copper and gold mineralization in an Archean trondhjemitic intrusion, Sturgeon Lake, Ontario 9

V. RUZICKA and A.L. LITTLEJOHN: Studies on uranium in Canada, 1980 133

D.F. SANGSTER: Three potential sites for the occurrence of stratiform, shale-hosted lead-zinc deposits in the Canadian Arctic 1

H.P. TRETTIN: A tennantite deposit in the M'Clintock Inlet area, northern Ellesmere Island, District of Franklin 103

P.J. WHITTAKER and D.H. WATKINSON: Chromite in some ultramafic rocks of the Cache Creek Group, British Columbia 349

GEOCHRONOLOGY/GÉOCHRONOLOGIE

F.W. CHANDLER and R.D. STEVENS: Potassium-argon age of the late Proterozoic Fury and Hecla Formation, northwest Baffin Island, District of Franklin 37

A.V. OKULITCH, W.D. LOVERIDGE, and R.W. SULLIVAN: Preliminary radiometric analyses of zircons from the Mount Copeland syenite gneiss, Shuswap Metamorphic Complex, British Columbia 33

GEOPHYSICS/GÉOPHYSIQUE

C.F. HUANG and J.A. HUNTER: The correlation of "tube wave" events with open fractures in fluid filled boreholes 361

MARINE GEOSCIENCE/ÉTUDES GÉOSCIENTIFIQUES DU MILIEU MARIN

G.B. FADER and L.H. KING: A reconnaissance study of the surficial geology of the Grand Banks of Newfoundland 45

MINERALOGY/MINÉRALOGIE

J. RIMSAITE: Petrochemical and mineralogical evolution of radioactive rocks in the Baie-Johan-Beetz area, Quebec: a preliminary report 115

PALEONTOLOGY/PALÉONTOLOGIE

M.J. COPELAND: **Bungonibeyrichia** n. gen. (Ostracoda, Beyrichiidae) from New South Wales, Australia , with observations on the genus **Velibeyrichia** Henningsmoen, 1954 41

H.J. HOFMANN and M.P. CECILE: Occurrence of **Oldhamia** and other trace fossils in Lower Cambrian(?) argillites, Niddery Lake map area, Selwyn Mountains, Yukon Territory 281

M.J. ORCHARD: Triassic conodonts from the Cache Creek Group, Marble Canyon, southern British Columbia 357

QUATERNARY GEOLOGY/GÉOLOGIE DU QUATERNAIRE

Inventory Mapping and Stratigraphic Studies/Inventaire cartographique et stratigraphique

R.A. KLASSEN: Aspects of the glacial history of Bylot Island, District of Franklin 317

D.A. ST-ONGE, M.A. GEURTS, F. GUAY, V. DEWEZ, F. LANDRIAULT, and P. LÉVEILLÉ: Aspects of the deglaciation of the Coppermine River region, District of Mackenzie 327

Paleoecology and Geochronology/Paléoécologie et géochronologie

W. BLAKE, JR.: Lake sediment coring along Smith Sound, Ellesmere Island and Greenland 191

SIGRID LICHTI-FEDEROVICH: Contribution to the diatom flora of Arctic Canada: Report 2. Arctic representatives of the genus **Navicula** 57

Page

Sedimentology and Geomorphology/Sédimentologie et géomorphologie

L.A. DREDGE: Trace elements in till and esker sediments in northwestern Manitoba 377

LARRY D. DYKE: Bedrock heave in the central Canadian Arctic 157

P.A. EGGINTON: The impact of disturbance on mudboil activity, north Henik Lake, District of Keewatin 299

J. ROSS MACKAY: An experiment in lake drainage, Richards Island, Northwest Territories: a progress report 63

REGIONAL GEOLOGY/GÉOLOGIE RÉGIONALE

Appalachian Region/Région des Appalaches

K.L. CURRIE, R.D. NANCE, G.E. PAJARI, JR., and R.K. PICKERILL: Some aspects of the pre-Carboniferous geology of Saint John, New Brunswick 23

Arctic Islands/Archipel Arctique

P.R. MOORE: Mesozoic stratigraphy in the Blue Mountains and Krieger Mountains, northern Ellesmere Island, Arctic Canada: a preliminary account 95

Cordilleran Region/Région de la Cordillère

B.E.B. CAMERON and H.W. TIPPER: Jurassic biostratigraphy, stratigraphy and related hydrocarbon occurrences of Queen Charlotte Islands, British Columbia 209

W.H. FRITZ: Two Cambrian stratigraphic sections, eastern Nahanni map area, Mackenzie Mountains, District of Mackenzie 145

H. GABRIELSE: Stratigraphy and structure of Road River and associated strata in Ware (west half) map area, northern Rocky Mountains, British Columbia 201

J.W.H. MONGER: Geology of parts of western Ashcroft map area, southwestern British Columbia 185

CHRISTOPHER OKE and P.S. SIMONY: Basement gneisses of the western Rocky Mountains, Hugh Allan Creek area, British Columbia 181

N.C. OLLERENSHAW: Cadomin Formation, Flathead Ridge vicinity, southeastern British Columbia 341

JENNIFER PELL and P. SIMONY: Stratigraphy, structure, and metamorphism in the southern Cariboo Mountains, British Columbia 227

P.B. READ and D.W. KLEPACKI: Stratigraphy and structure: northern half of Thor-Odin nappe, Vernon east-half map area, southern British Columbia 169

C.J. REES: Western margin of the Omineca Belt at Quesnel Lake, British Columbia 223

K.R. SHANNON: The Cache Creek Group and contiguous rocks near Cache Creek, British Columbia 217

L.C. STRUIK: Snowshoe Formation, central British Columbia 213

Precambrian Shield/Bouclier précambrien

I.R. ANNESLEY: Field characteristics, petrology and geochemistry of the Amer Lake ultramafic metavolcanics, District of Keewatin 275

K.E. ASHTON: Preliminary report on geological studies of the "Woodburn Lake Group" northwest of Tehek Lake, District of Keewatin 269

F.H.A. CAMPBELL: Stratigraphy and tectono-depositional relationships of the Proterozoic rocks of the Hadley Bay area, northern Victoria Island, District of Franklin 15

K.D. CARD, J.A. PERCIVAL, J. LAFLEUR, and D.D. HOGARTH: Progress report on regional geological synthesis, central Superior Province 77

A. DAVIDSON and W.C. MORGAN: Preliminary notes on the geology east of Georgian Bay, Grenville Structural Province, Ontario 291

R.M. EASTON: Stratigraphy of a Proterozoic volcanic complex at Tuertok Lake, Wopmay Orogen, District of Mackenzie 305

Page

INGO ERMANOVICS and J.A. KORSTGÅRD: Geology of Hopedale block and adjacent areas, Labrador: report 3 69

THOMAS FRISCH: Further reconnaissance mapping of the Precambrian Shield on Devon Island, District of Franklin 31

R.A. FRITH: Preliminary account of the geology of the Beechey Lake-Duggan Lake map areas, District of Mackenzie 333

E. FROESE and Q. GALL: Geology of the eastern vicinity of Kisseynew Lake, Manitoba 311

T.M. GORDON: Metamorphism in the Crowduck Bay area, Manitoba 315

J.B. HENDERSON and P.H. THOMPSON: The Healey Lake map area and the enigmatic Thelon Front, District of Mackenzie 175

W.W. HEYWOOD and MIKKEL SCHAU: Geology of Baker Lake region, District of Keewatin 259

P.F. HOFFMAN: Revision of stratigraphic nomenclature, foreland thrust-fold belt of Wopmay Orogen, District of Mackenzie 247

P.F. HOFFMAN and M.R. ST-ONGE: Contemporaneous thrusting and conjugate transcurrent faulting during the second collision in Wopmay Orogen: implications for the subsurface structure of post-orogenic outliers 251

LÉOPOLD NADEAU: The geology of Whitehills Lake map area, District of Keewatin 265

SUBHAS TELLA, K.E. EADE, A.R. MILLER, and C.G. LAMONTAGNE: Geology of the west-half of the Kamilukuak Lake map area, District of Keewatin: a part of the Churchill Structural Province 231

Interior Plains/Plaines intérieures

D.W. MORROW and N.C. MEIJER-DREES: The Early to Middle Devonian Bear Rock Formation in the type section and in other surface sections, District of Mackenzie 107

SCIENTIFIC AND TECHNICAL NOTES
NOTES SCIENTIFQUES ET TECHNIQUES

MIKKEL SCHAU: Direction of movement of glacially transported boulders not necessarily shown by preserved ice-movement direction indicators, Baker Lake, District of Keewatin 383

J.R. HENDERSON: Strain ratios measured across a Hudsonian deformation front at Kaminak Lake, District of Keewatin 384

P.A. EGGINTON: Stability problems associated with sand and gravel pads, central District of Keewatin 385

S.H. WATTS: Near-coastal and incipient weathering features in the Cape Herschel-Alexandra Fiord area, Ellesmere Island, District of Franklin 389

S.P. GORDEY, D. WOOD, and R.G. ANDERSON: Stratigraphic framework of southeastern Selwyn Basin, Nahanni map area, Yukon Territory and District of Mackenzie 395

BRIAN MacLEAN and S.P. SRIVASTAVA: Petroliferous core from a diapir east of Cumberland Sound, Baffin Island 399

E.M. LEVY and B. MacLEAN: Natural hydrocarbon seepage at Scott Inlet and Buchan Gulf, Baffin Island Shelf: 1980 update 401

Author Index 404

Separates

A limited number of separates of the papers that appear in this volume are available by direct request to the individual authors. The addresses of the Geological Survey of Canada offices follow:

601Booth Street,
OTTAWA, Ontario
K1A 0E8

Institute of Sedimentary and Petroleum Geology,
3303-33rd Street N.W.,
CALGARY, Alberta
T2L 2A7

Cordilleran Geology Division
100 West Pender Street,
VANCOUVER, B.C.
V6B 1R8

Atlantic Geoscience Centre,
Bedford Institute of Oceanography,
P.O. Box 1006,
DARTMOUTH, N.S.
B2Y 4A2

When no location accompanies an author's name in the title of a paper, the Ottawa address should be used.

Tirés à part

On peut obtenir un nombre limité de "tirés à part" des articles qui paraissent dans cette publication en s'adressant directement à chaque auteur. Les adresses des différents bureaux de la Commission géologique du Canada sont les suivantes:

601, rue Booth
OTTAWA, Ontario
K1A 0E8

Institut de géologie sédimentaire et pétrolière
3303-33rd, St. N.W.,
CALGARY, Alberta
T2L 2A7

Division de la géologie de la Cordillère
100 West Pender Street
VANCOUVER, Colombie-Britannique
V6B 1R8

Centre géoscientifique de l'Atlantique
Institut océanographique de Bedford
B.P. 1006
DARTMOUTH, Nouvelle-Ecosse
B2Y 4A2

Lorsque l'adresse de l'auteur ne figure pas sous le titre d'un document, on doit alors utiliser l'adresse d'Ottawa.

1. # THREE POTENTIAL SITES FOR THE OCCURRENCE OF STRATIFORM, SHALE-HOSTED LEAD-ZINC DEPOSITS IN THE CANADIAN ARCTIC

Project 650056

D.F. Sangster
Economic Geology Division

Sangster, D.F., Three potential sites for the occurrence of stratiform, shale-hosted lead-zinc deposits in the Canadian Arctic; in Current Research, Part A, Geological Survey of Canada, Paper 81-1A, p. 1-8, 1981.

Abstract

Published literature describing the geology of the Canadian Arctic was examined relative to known attributes of shale-hosted lead-zinc deposits. Particular emphasis was placed on the search for evidence of depocentres, synsedimentary growth faults, and local geothermal anomalies. In this manner, Franklinian Basin, Baffin Basin, and Foxe Fold Belt were recognized to contain particular sedimentary formations favourable for the occurrence of shale-hosted lead-zinc deposits.

In a previous note (Sangster, 1970) the author listed ten areas in Canada regarded by him as favourable for the occurrence of undiscovered carbonate-hosted lead-zinc deposits. To date, all but two or three of these areas have been prospected to some degree and appear to be devoid of mineralization of any kind.

Having thus established his credibility as a prognosticator of potential lead-zinc bearing areas, the author now suggests three areas in Canada which he considers to be favourable for shale-hosted lead-zinc deposits. These areas were recognized as a result of the author's participation in a resource evaluation study of the Canadian Arctic Islands (Geological Survey of Canada, 1980).

Briefly, shale-hosted lead-zinc deposits are stratiform bodies consisting of layers of massive galena, sphalerite, pyrite and/or pyrrhotite occurring in shaly sedimentary rocks. Because "shales" are recognized more by their mechanical properties (i.e. they break along bedding and may possess a slaty cleavage) than by their mineralogical/chemical composition, deposits of this type are found in "shales" which may be argillaceous (Meggen, Rammelsberg in West Germany), extremely siliceous (i.e. cherty) (Howard's Pass, Yukon), silty or fine grained quartzite (Sullivan, B.C.), or dolomitic (Mt. Isa, HYC in Australia). In view of this wide range in host rock lithologies, the sedimentary environments in which these deposits are found also exhibit a wide range. Indeed, they range from starved basins with little or no detrital sedimentation (e.g. Howard's Pass), to those continuously, or periodically, receiving detrital material in abundance (e.g. Sullivan, Broken Hill) and from deep-water environments (e.g. Howard's Pass) to those in which shallow water features are abundant (e.g. HYC).

The deposits themselves are regarded as being of exhalative origin, albeit in essentially nonvolcanic terranes. The metalliferous solutions are considered to have debouched from unknown sources, through fractures, onto the ocean floor. Most deposits can be shown to occur in topographic lows on the seafloor and, in some cases, the metalliferous solutions (or a fluidic slurry of fine grained sulphide particles constituting essentially a "sulphide turbidite") appear to have migrated away from the exhalative centre before coming to rest in the ore-forming "depocentre".

Table 1.1

Basin classification and characteristics
(modified slightly from Krebs (1979))

First Order Basins
Lateral dimensions in hundreds of kilometres
Epicontinental re-entrant
On continental crust basement
Thick sedimentary sequence
Second Order Basins
Lateral dimensions in tens of kilometres
Local basins, troughs, and highs
Abrupt changes in sedimentary thickness
Local igneous activity
Third Order Basins
Lateral dimensions up to 5-6 km
"Black Shale" environment
Local synsedimentary faults

The depocentres in any one region are commonly arranged in a linear pattern which, in some instances, can be shown to lie within a graben or half-graben. Thus both the depocentres and the exhalative vents may be genetically related by virtue of the mutual relationship to synsedimentary growth faults.

The concept of relating "basins-within-basins" (i.e. depocentres in sedimentary basins), growth faults, and shale-hosted lead-zinc deposits has been portrayed by Krebs (1979) with reference to the Meggen and Rammelsberg deposits, West Germany, in Middle Devonian shales. The geological characteristics of Krebs' first, second and third order basins, summarized in Table 1.1, were considered to be of sufficiently large scale to be potentially recognizable from existing geological literature of the Canadian Arctic region. In this manner three basins were recognized to contain several of the geological features listed in Table 1.1 and hence regarded as favourable for the occurrence of stratiform lead-zinc deposits.

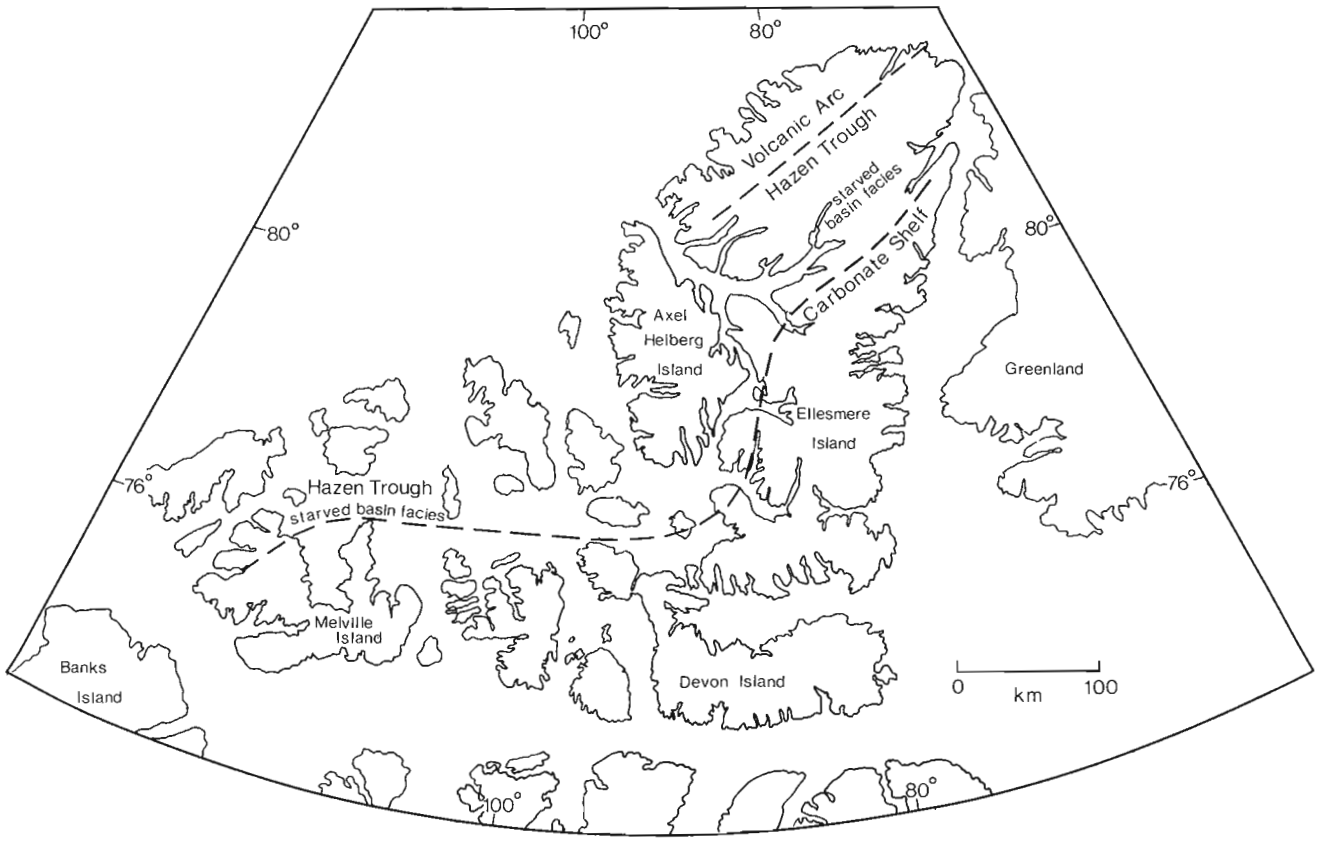

Figure 1.1. *Facies relationships and paleogeography, Franklinian Basin, during late middle Devonian (from Trettin and Balkwill, 1979).*

At this point it must be stressed that the evaluation process involved a literature search only; no field checks were possible under the assigned time constraints of the study which took place in January and February, 1980. The three basins, and specific formations within them regarded to be the most likely to contain shale-hosted lead-zinc deposits, are described in turn below.

Franklinian Basin (Fig. 1.1)

Occupying a major portion of the Queen Elizabeth Islands, the lower Paleozoic Franklinian Basin (Trettin and Balkwill, 1979, p. 752) stretches more than 1200 km southwesterly from northeastern Ellesmere Island to Banks Island. It evidently lies on continental crust as Trettin and Balkwill (1979, p. 750) stated "Precambrian crystalline terrains are exposed both north and southeast of the lower Paleozoic basin and probably underlie it in its entirety". On Ellesmere Island, the only region where a cross-section of the entire basin is exposed, the lower Paleozoic sedimentary sequence is more than 2500 m thick (Trettin, 1971). The Franklinian Basin, therefore, appears to fulfill the major requirements of Krebs' first-order basins.

Situated roughly along the axial line of the Franklinian Basin, the Hazen Trough, where exposed, is roughly 175 km wide (Fig. 1.1), bounded on the northwest by contemporaneous volcanic rocks and on the southeast by a carbonate platform. Table 1.2 shows the sedimentary sequence in northern Ellesmere Island.

The Grant Land Formation, consisting of nonmarine and marine sandstones and shales, was largely deposited under alluvial conditions (Trettin, 1971, p. 36). The assemblage represents a normal continental to shallow marine transgression onto the Precambrian craton.

The lithologies and depositional conditions of the Grant Land Formation contrast markedly with those of the overlying Hazen Formation which represents a "starved basin" facies, consisting as it does of a condensed succession of radiolarian cherts, shales, and resedimented carbonates. The overlying "flysch facies" of the Imina Formation effectively brought to a close deep-water sedimentation in the Hazen Trough.

Of these three formations, the Hazen on Ellesmere Island (including equivalent Canrobert and Ibbet Bay formations on Melville Island) is considered to have the most potential for stratiform lead-zinc deposits. The slow sedimentation rate, synchronous volcanism, and the possibility of coeval growth faulting make it the most attractive unit in Hazen Trough.

Filling of the Hazen Trough was a process of progradation along strike from northeast to southwest. Consequently, starved basin conditions prevailed much longer in the southwest. For example, the Canrobert-Ibbet Bay Formations starved basin facies on Melville Island range from late Cambrian to late Early Devonian (Trettin, personal communication, 1980).

Features considered to be particularly relevant to the occurrence of stratiform lead-zinc deposits are as follows:

1. The sudden and abrupt transition from continental and shallow marine conditions (Grant Land Formation) to a deep-water, starved basin environment (Hazen Formation). Such a dramatic deepening could most readily be achieved by synsedimentary faulting along the margins of the Hazen Trough. Growth faults such as these are extremely important because they serve not only as trans-strata channelways along which potential

Table 1.2

Table of formations, northern Ellesmere Island*

	Age	Formation	Thickness (m)	Lithologies
Hazen Trough	E Sil. to E Dev.	Imina	more than 2800	Calcareous greywacke, mudstone
	E Camb. to E Sil.	Hazen	390	Chert, graptolitic shale, limestone, minor breccia
	E Cambrian	Grant Land	more than 1100	Quartzitic sandstone, phyllite, conglomerate

*From Trettin, 1971; Trettin and Balkwill, 1979; Trettin et al., 1979

metal-bearing solutions may rise but they also produce local depocentres in which the exhalative metalliferous brines collect. Synsedimentary faulting during Hazen time may also be recorded in the abrupt appearance of local sedimentary breccias in the Hazen Formation (Trettin, 1971).

2. The presence of contemporaneous volcanic activity to the northwest is important for establishing higher-than-normal thermal gradients in the Hazen Trough sedimentary basin. Anomalous thermal gradients would be capable of heating connate water in the Trough sediments; the heated water could then leach metals from the surrounding sediments, and then be driven up along synsedimentary faults to debouch onto the floor of the deep-water Hazen Trough.
3. The extremely slow sedimentation rate of the Hazen Formation is ideal for the accumulation of sulphides; the lack of detrital material would allow even slow rates of exhalation of metalliferous brines to produce strata of significant metal content.
4. The overall stratigraphic succession in northern Ellesmere Island is comparable in age, lithology, and depositional environments to those in Selwyn Basin where numerous stratiform lead-zinc deposits have been discovered (e.g. Wheeler and Gabrielse, 1972; Blusson, 1976; Gabrielse, 1976; Morganti, 1979). The analogy is further strengthened by the fact that the carbonate platforms of both basins contain important lead-zinc deposits (Brock, 1976; Kerr, 1977b).

In addition to the Hazen Formation of northern Ellesmere Island (and the correlative Canrobert and Ibbett Bay formations on Melville Island), the Cape Phillips Formation elsewhere in the Franklinian Basin possesses certain features which render it somewhat attractive for stratiform lead-zinc deposits. The largely Silurian shales of the latter formation have been interpreted by Trettin and Balkwill (1979, p. 756) as having been deposited in a backreef basin on the southeast rim of Hazen Trough (see Trettin and Balkwill, 1979, Fig. 5). Within this basin, possibly formed by faulting, sedimentation was slow (Trettin and Balkwill, 1979, p. 756). Kerr (1977a, p. 1383) described the Cape Phillips Formation as comprising "dark grey graptolitic shaly limestone, shale, and some chert" and as having been deposited in an euxinic basin. Again, the coincidence in time and space of slow sedimentation rates, euxinic conditions, and synsedimentary faulting make the Cape Phillips Formation a potential host to stratiform lead-zinc deposits in Franklinian Basin.

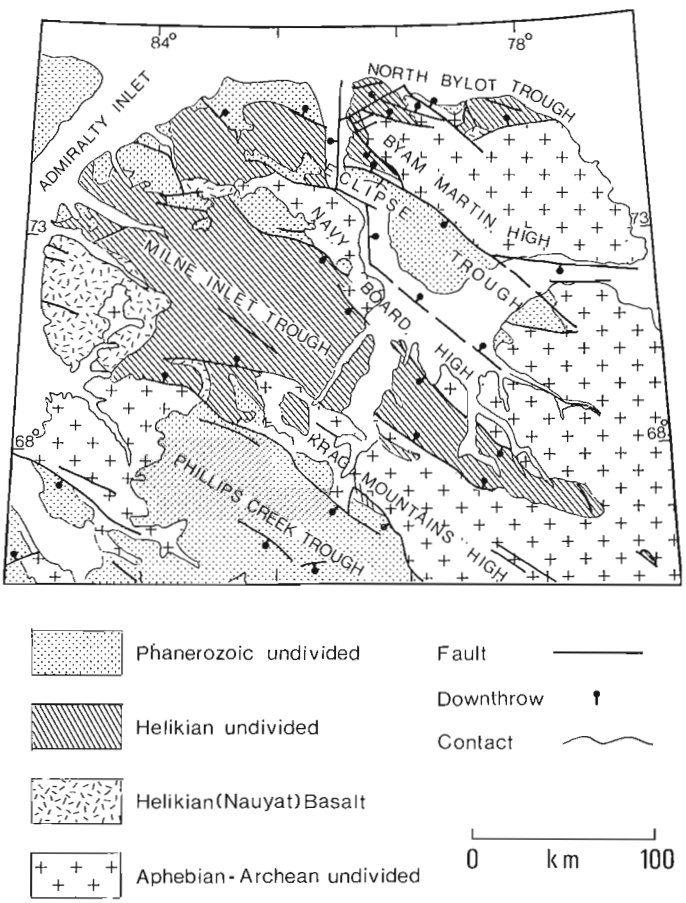

Figure 1.2. *Borden Basin within the North Baffin Rift Zone. Borden Basin is shown as Milne Inlet Trough on this diagram (Jackson et al., 1975).*

Borden Basin (Fig. 1.2)

One of a series of parallel northwest-trending horsts and grabens in the North Baffin Rift Zone (Jackson et al., 1975), Borden Basin extends southeasterly 325 km from Admiralty Inlet in northern Baffin Island (Fig. 1.2). Within the basin, up to 6000 m of Upper Proterozoic strata lie either in fault contact with, or unconformably on, older crystalline rocks.

Table 1.3

Table of formations, Eclipse Sound area, Borden Basin*

Age	Group	Formation	Thickness (m)	Lithology
Hadrynian		Franklinian Intrusions		Diabase
Neohelikian	Uluksan	Elwin	700+	Siltstone, quartzarenite
		Strathcona Sound/ Athole Point	870+/585	Arkose, conglomerate, shale/limestone, sandstone, shale
		Victor Bay	724	Limestone, dolostone, shale, siltstone
		Society Cliffs	825+	Dolostone, shale, sandstone, gypsum
		Fabricius Fiord/ Arctic Bay	1500+/600	Conglomerate, sandstone/calcareous shale, siltstone
	Eqalulik	Adams Sound	340	Quartzarenite
		Nauyat	90	Basalt, quartzarenite
Archean-Aphebian				Granitic gneiss complex

*From Jackson et al., 1980

Near the centre of the Borden Basin, the generalized upper Proterozoic stratigraphy is as shown in Table 1.3. A characteristic feature of the Rift Zone, however, is the effect syndepositional faulting has had on sedimentation, resulting in numerous facies changes and wide ranges in thicknesses of all formations. Jackson et al. (1978, p. 14) summarized the structural/sedimentological association as follows: "Abrupt vertical and lateral changes in lithologies and depositional environments, the cyclic nature of many of the formations, changes in transportation directions, and the presence of interformational unconformities, all indicate that syndepositional faulting played an important role in the sedimentation patterns within the basin...However, most of the faulting...seems to have occurred after deposition of the Eqalulik and Uluksan groups...". Significant to the possible occurrence of stratiform lead-zinc mineralization, however, is that some faulting did occur during deposition of the Uluksan Group, specifically during Fabricius Fiord/Arctic Bay time. Iannelli (1979) has described in some detail the relationship between these two formations. The former is largely conglomerate and coarse sandstone deposited in large delta fan complexes emanating from the southern margin of Borden Basin as a result of block faulting. The Fabricius Fiord Formation changes facies laterally, northward toward the centre of the basin, into the Arctic Bay Formation consisting predominantly of shale (locally pyritic) with minor dolostone and siltstone (Iannelli, 1979, Fig. 11.6, 11.7). The Arctic Bay Formation ranges in thickness from about 100 m in the type area near the western end of the Rift Zone (Lemon and Blackadar, 1963) to more than 1200 m near the eastern end (Jackson et al., 1975).

Features within Borden Basin, and in particular the Arctic Bay Formation, considered to be relevant to the possible occurrence of shale-hosted stratiform lead-zinc deposits, are the following:

1. The abundant evidence of synsedimentary faulting during deposition of the Arctic Bay Formation sediments.

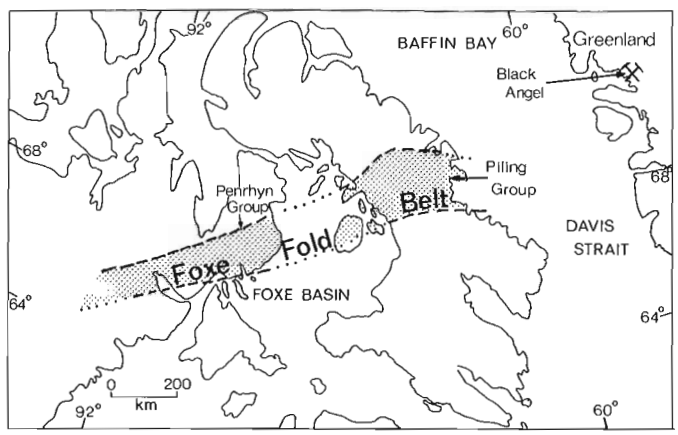

Figure 1.3. Position of Foxe Fold Belt, northeastern Canadian Shield (from Jackson and Taylor, 1972).

2. The series of horsts and grabens identified as "highs" and "troughs" in Figure 1.2 (equivalent to the submarine "Schwellen" and "Becken" of Krebs (1979)), produce second-order basins. These, in turn, suggest the possibility of third-order basins, of the size of individual lead-zinc deposits, occurring in the area. The wide range in thickness of the Arctic Bay Formation, for example, might be an indication of these smaller basins.
3. An early geothermal anomaly in the area is suggested by the presence of alkalic basalts at the west end of the basin which were extruded in the early stages of rifting.
4. The presence of the Nanisivik lead-zinc deposit in Society Cliffs dolomite (Olson, 1977) suggests that the region lies within at least a local lead-zinc metallogenic province. Olson (1977), in fact, concluded that the source of the metals in the Nanisivik deposit was the underlying Arctic Bay Formation.

Table 1.4

Comparison of lithologies and stratigraphic successions in three areas of the Foxe Fold Belt (see Fig. 3).*

Penrhyn Group	Piling Group	Marmorilik Formation
Psammites, pelitic metaturbidites (more than 1000 m)	Metagreywacke, psammite, slate minor amphibolite (more than 3000 m)	Semi-pelite (more than 200 m)
(possible unconformity)		
Marble, calc-silicate gneiss Paragneiss (in part rusty, graphitic) } 1000 m Marble, calc-silicate gneiss	Graphitic sulphide schist (up to 200 m)	
	Marble, quartzite, calc-silicate (up to 200 m)	Marbles (1600 m)
Quartzite, minor amphibolite (up to 100 m)	Quartzite, minor amphibolite (up to 200 m)	Quartzite, conglomerate (60 m)
unconformity	unconformity	unconformity
Basement Complex	Basement Complex	Basement Complex

* Penrhyn Group stratigraphy from Okulitch et al. (1977) and J.R. Henderson (personal communication, 1980); Piling Group as in Table 1.5, and Marmorilik area from Garde (1978).

Table 1.5

Comparison of Aphebian Piling Group, Baffin Island and Lower Paleozoic formations, northern Ellesmere Island.*

Piling Group, Baffin Island		Northern Ellesmere Island	
Unit/Lithology	Thickness (m)	Unit/Lithology	Thickness (m)
Metagreywacke, psammite, slate, minor amphibolite	>3000	Imina Fm.: subgreywacke, greywacke, argillaceous greywacke	more than 2800
Graphitic sulphide schist, metachert	up to 200	Hazen Fm.: chert, shale	400
Marble, quartzite, calc-silicates	up to 200	limestone, chert, shale	
Quartzite, minor amphibolite	up to 200	Grant Land Fm.: quartzite, sandstone, shale	more than 1100
unconformity		unconformity	
Basement Complex		Basement Complex	

* Piling Group information from Morgan et al. (1975, 1976); Tippett (1978, 1979); Henderson et al. (1979); Henderson and Tippett (1980); Jackson and Taylor (1972); W.C. Morgan and J.R. Henderson (personal communication, 1980). Ellesmere Island information from Trettin (1971), Trettin and Balkwill (1979), and Trettin et al. (1979).

Foxe Fold Belt (Fig. 1.3)

"The Foxe Fold Belt is a continuous zone composed mainly of folded Aphebian rocks that extends on the mainland from west of Repulse Bay to the east coast of Melville Peninsula, and extends east across Baffin Island... The Aphebian strata comprising the fold belt were named the Penrhyn Group on the mainland by Heywood (1967), and the Piling Group on Baffin Island by Jackson (1971)" (Jackson and Taylor, 1972, p. 1657).

Most of the discussion that follows refers to the Piling Group on Baffin Island but many comments may apply also to the Penrhyn Group if for no other reason than the lithologies and stratigraphic successions of the two groups are so similar (Table 1.4).

Because of the regional upper greenschist to granulite facies metamorphism and attendant complex structure, favourable features for lead-zinc mineralization such as those discussed in the previous two basins (growth faults, variations in stratigraphic thickness, sedimentary breccias, etc.) cannot be evaluated in the Foxe Fold Belt.

Table 1.6

Geological attributes of three Canadian Arctic sedimentary basins compared to Krebs' (1979) basin classification

Basin Classification and Characteristics (Krebs, 1979)	Canadian Arctic Sedimentary Basins		
	Franklinian Basin	Borden Basin	Foxe Fold Belt
First Order Basins			
Lateral dimensions in hundreds of kilometres	1200 x 200 km	North Baffin Rift Zone; full extent unknown	1300 x 160 km
Epicontinental re-entrant	yes	yes	yes
On continental crust basement	yes	yes	yes
Thick sedimentary sequence	more than 2300 m	up to 6100 m	more than 3600 m
Second Order Basins			
Lateral dimensions in tens of kilometres	Hazen Trough; ca 175 km wide, min. length 600 km	Borden Basin; 330 x 80 km	"Piling Basin" 250 x 160 km
Local basins, troughs, and highs	not identified	yes	not identified
Abrupt changes in sediment thickness	not documented	Arctic Bay Fm., 75 to 1200 m	obscured by metamorphism
Local igneous activity	contemporaneous volcanics	alkalic basalts	contemporaneous mafic volcanics
Third Order Basins			
Lateral dimensions up to 5-6 km	not identified	not identified	not identified
"Black shale" environment	Hazen Fm., pyritic, cherty, carbonaceous	Arctic Bay Fm., black, pyritic calcareous shale	Graphitic sulphide schist
Local synsedimentary faults	inferred	well documented	inferred

In spite of this, however, the Piling Group, in particular the graphitic sulphide schist, is regarded as a potential host for stratiform, shale-hosted lead-zinc mineraliation for the following reasons:

1. The Piling Group sequence quartzite-marble-graphitic pyritic schist-metagreywacke is remarkably similar to that in Hazen Trough (Table 1.2). There, the abrupt transition from the continental to shallow marine conditions of Grant Land Formation sedimentation to the euxinic, starved basin facies of the Hazen Formation was attributed to possible rifting along synsedimentary faults. Much the same argument could apply to the Piling Group and, to a lesser extent, the Penrhyn Group. In both groups, the quartzite and marble would represent the shallow marine environment, the graphitic sulphide schist (Jackson and Taylor (1972) reported "metachert" in the unit as well) a possible starved basin facies of pyritic, carbonaceous, siliceous shale. In Penrhyn Group (Okulitch et al., 1977), the basal quartzite and marble units are present but the position of the graphitic sulphide schist of Piling Group is taken by paragneiss, in part rusty and graphitic.
2. From the evidence of minor volcanic lithologies in both groups, an elevated geothermal gradient may be inferred throughout Foxe Fold Belt. Tippett (1978, 1979) referred to metavolcanic rocks possibly overlying the quartzite in the central part of Piling basin. Elsewhere Morgan et al. (1975) reported basic volcanics with amygdules and pillows occur ring in the upper metagreywacke unit. In Penrhyn Group, Okulitch et al. (1977) recorded minor amphibolites, of probable volcanic origin, associated with the basal quartzite unit there.
3. As with the previous two basins (Franklinian and Borden), the Foxe Fold Belt is, or lies within, a probable lead-zinc metallogenic province. This is suggested by the presence of a major lead-zinc deposit (Black Angel) in carbonates of the Marmorilik Formation on the coast of Greenland (Fig. 1.3). The Marmorilik area is not only along strike with the Foxe Fold Belt, but its lithologies and stratigraphic succession (Table 1.5) are so similar to Piling Group that direct correlation seems unavoidable. If this correlation is correct and allowing for the relatively recent opening of Davis Strait, the Black Angel deposit must be regarded, geologically, as part of the Foxe Fold Belt.

The graphitic sulphide schist unit in both Piling and Penrhyn groups contains scattered occurrences of more massive sulphide lenses, some of which contain minor amounts of sphalerite. This suggests that the Piling and Penrhyn basins, in particular the sulphidic schist unit, could be part of a zinc metallogenic province. This was also suggested earlier by Cameron (1979) on the basis of a strong correlation between zinc anomalies in lake sediments and waters and sulphidic paragneiss in Penrhyn Basin.

Discussion

Various attributes of the three sedimentary basins (probably better described as "troughs") referred to in the previous pages are summarized and compared with Krebs' basin classification in Table 1.6. The 'degree of fit' depends almost entirely on the level of published geological detail and the metamorphic history of the basin. These two factors have largely determined whether critical geological features such as synsedimentary faults and protoliths were directly observable, as in some basins, or merely inferred, as in others.

It must be stressed here that none of the features discussed in the previous pages nor summarized in Table 1.1 are necessarily unique to basins containing lead-zinc deposits. Anomalous features leading to, or a result of, lead-zinc mineralization occur only on the scale of third-order basins or less and are not likely to be recorded in reconnaissance-scale mapping, the scale of the data base used in this report. A review of the world literature, together with personal experience, has revealed to this author that, although stratiform lead-zinc deposits rather consistently occur in sedimentary basins with the attributes summarized in Table 1.1, direct evidence of their presence seldom extends much beyond the ore basin (third-order basin) itself.

An illustration of this point would be pyrite content of the host rock shale. Unlike volcanogenic massive sulphide deposits, individual shale-hosted lead-zinc deposits may be pyrite-poor (e.g. Howard's Pass and Broken Hill) and, in these deposits, the surrounding host rock sediments are not noticeably pyrite-rich. The same is true for the base-metal content of the host rock. Only 22 km from the HYC deposit (190 million tonnes, 9.5% Zn, 4.1% Pb, 40 g/t Ag), but still within a second-order basin, the host dolomitic shale averages about 28 ppm Zn (Corbett et al., 1975). This should be compared with averages of 90 ppm for shale in general, 200 ppm for carbonaceous shales, and 20 ppm for carbonates (Wedepohl, 1972).

These examples serve to illustrate, once again, the well-known fact that regional geological mapping programs, and the resource evaluation studies based on them, serve mainly to identify only large-scale permissive evidence for mineralization. Direct evidence of the mineralizing process must be sought in follow-up studies on a much smaller scale. In the context of shale-hosted stratiform lead-zinc deposits, the scale of the target sought (metal-bearing third-order basins) would be of the order of a few hundred metres to a few kilometres.

Acknowledgments

Information and ideas from the author's colleagues at the Geological Survey of Canada have made significant contributions to this study. In particular the author wishes to acknowledge discussions with H.P. Trettin, G.D. Jackson, W.C. Morgan, J.R. Henderson, and A. Okulitch. Diagrams were competently drafted by S.B. Green.

References

Blusson, S.L.
1976: Selwyn Basin, Yukon and District of Mackenzie; in Report of Activities, Part A, Geological Survey of Canada, Paper 76-1A, p. 131-132.

Brock, J.S.
1976: Selwyn-Mackenzie lead-zinc province, Yukon and Northwest Territories; Western Miner, v. 49, no. 3, p. 9-16.

Cameron, E.M.
1979: Investigation of base metal mineralization in Proterozoic metasediments, Melville Peninsula, District of Franklin; in Current Research, Part A, Geological Survey of Canada, Paper 79-1A, p. 187-196.

Corbett, J.A., Lambert, I.B., and Scott, K.M.
1975: Results of analyses of rocks from the McArthur area, Northern Territory; Commonwealth Scientific and Industrial Research Organization (C.S.I.R.O.), Minerals Research Laboratories, Technical Communication 57.

Gabrielse, H.
1976: Environments of Canadian Cordillera depositional basins; in Circum-Pacific Energy and Mineral Resources; American Association of Petroleum Geologists, Memoir 25, p. 492-502.

Garde, A.A.
1978: The Lower Proterozoic Marmorilik Formation, East of Marmorilik, West Greenland; Meddelelser Om Grønland, Bd. 200, Nr. 3.

Geological Survey of Canada
1980: Non-hydrocarbon mineral resources of parts of northern Canada; Geological Survey of Canada Open File 716.

Henderson, J.R. and Tippett, C.R.
1980: Foxe Fold Belt in eastern Baffin Island, District of Franklin; in Current Research, Part A, Geological Survey of Canada, Paper 80-1A, p. 147-152.

Henderson, J.R., Shaw, D., Mazuraki, M., Henderson, M., Green, R., and Brisbin, D.
1979: Geology of part of the Foxe Fold Belt, central Baffin Island, District of Franklin; in Current Research, Part A, Geological Survey of Canada, Paper 79-1A, p. 95-99.

Heywood, W.W.
1967: Geological notes, northeastern District of Keewatin and southern Melville Peninsula, District of Franklin, Northwest Territories; Geological Survey of Canada, Paper 66-40.

Iannelli, T.R.
1979: Stratigraphy and depositional history of some Upper Proterozoic sedimentary rocks on northwestern Baffin Island, District of Franklin; in Current Research, Part A, Geological Survey of Canada, Paper 79-1A, p. 45-56.

Jackson, G.D.
1971: Operation Penny Highlands, south-central Baffin Island; Geological Survey of Canada, Paper 71-1, Part A.

Jackson, G.D. and Taylor, F.C.
1972: Correlation of major Aphebian rock units in the northern Canadian Shield; Canadian Journal of Earth Sciences, v. 9, p. 1650-1669.

Jackson, G.D., Davidson, A., and Morgan, W.C.
1975: Geology of the Pond Inlet map-area, Baffin Island, District of Franklin; Geological Survey of Canada, Paper 74-25.

Jackson, G.D., Iannelli, T.R., Narbonne, G.M., and Wallace, P.J.
1978: Upper Proterozoic sedimentary and volcanic rocks of northwestern Baffin Island; Geological Survey of Canada, Paper 78-14.

Jackson, G.D., Iannelli, T.R., and Tilley, B.J.
1980: Rift-related Late Proterozoic sedimentation and volcanism on northern Baffin Island and Bylot Islands, District of Franklin; in Current Research, Part A, Geological Survey of Canada, Paper 80-1A, p. 319-328.

Kerr, J.Wm.
1977a: Cornwallis Fold Belt and the mechanism of basement uplift; Canadian Journal of Earth Sciences, v. 14, p. 1374-1401.

1977b: Cornwallis lead-zinc district; Mississippi Valley-type deposits controlled by stratigraphy and tectonics; Canadian Journal of Earth Sciences, v. 14, p. 1402-1426.

Krebs, W.
1979: Devonian basinal facies; in The Devonian System; The Paleontological Association, Special Papers in Paleontology 23, p. 125-139.

Lemon, R.R.H. and Blackadar, R.G.
1963: Admiralty Inlet area, Baffin Island, District of Franklin; Geological Survey of Canada, Memoir 328.

Morgan, W.C., Bourne, J., Herd, R.K., Pickett, J.W., and Tippett, C.R.
1975: Geology of the Foxe Fold Belt, Baffin Island, District of Franklin; in Report of Activities, Part A, Geological Survey of Canada, Paper 75-1A, p. 343-347.

Morgan, W.C., Okulitch, A.V., and Thompson, P.H.
1976: Stratigraphy, structure, and metamorphism of the west half of the Foxe Fold Belt, Baffin Island; Report of Activities, Part A, Geological Survey of Canada, Paper 76-1A, p. 387-391.

Morganti, J.M.
1979: The geology and ore deposits of the Howard's Pass area, Yukon and Northwest Territories: The origin of basinal sedimentary stratiform sulphide deposits; unpublished Ph.D. thesis, University of British Columbia, Vancouver.

Okulitch, A.V., Gordon, T., Henderson, J.R., Reesor, J.E., and Hutcheon, I.E.
1977: Geology of Barrow River map-area, Melville Peninsula, District of Franklin; in Report of Activities, Part A, Geological Survey of Canada, Paper 77-1A, p. 213-215.

Olson, R.A.
1977: Geology and genesis of zinc-lead deposits within a Late Proterozoic dolomite, northern Baffin Island, N.W.T.; unpublished Ph.D. thesis, University of British Columbia, Vancouver, 371 p.

Sangster, D.F.
1970: Geological exploration guides for Canadian lead-zinc deposits in carbonate rocks; Canadian Mining Journal, v. 91, no. 4, p. 49-51.

Tippett, C.R.
1978: A detailed cross-section through the southern margin of the Foxe Fold Belt in the vicinity of Dewar Lakes, Baffin Island, District of Franklin; in Current Research, Part A, Geological Survey of Canada, Paper 78-1A, p. 169-173.

Tippett, C.R. (cont.)
1979: Basement-supracrustal rock relationships on the southern margin of the Foxe Fold Belt, central Baffin Island, District of Franklin; in Current Research, Part A, Geological Survey of Canada, Paper 79-1A, p. 101-105.

Trettin, H.P.
1971: Geology of Lower Paleozoic formations, Hazen Plateau and southern Grant Land Mountains, Ellesmere Island, Arctic Archipelago; Geological Survey of Canada, Bulletin 203.

Trettin, H.P. and Balkwill, H.R.
1979: Contributions to the tectonic history of the Innuitian Province, Arctic Canada; Canadian Journal of Earth Sciences, v. 16, p. 748-769.

Trettin, H.P., Barnes, C.R., Kerr, J.W., Norford, B.S., Pedder, A.E.H., Riva, J., Tipnis, R.S., and Uyeno, T.T.
1979: Progress in lower Paleozoic stratigraphy, northern Ellesmere Island, District of Franklin; in Current Research, Part B, Geological Survey of Canada, Paper 79-1B, p. 269-279.

Wedepohl, K.H.
1972: Zinc-abundance in common sediments and sedimentary rocks; in Handbook of Chemistry, K.H. Wedepohl, editor, Volume II/3, Section 30-K, Springer-Verlag, Berlin.

Wheeler, J.O. and Gabrielse, H.
1972: The Cordilleran Structural Province; in Variations in Tectonics Styles in Canada, Geological Association of Canada, Special Paper 11.

2. COPPER AND GOLD MINERALIZATION IN AN ARCHEAN TRONDHJEMITIC INTRUSION STURGEON LAKE, ONTARIO

Project 750098

K.H. Poulsen[1] and J.M. Franklin,
Economic Geology Division

Poulsen, K.H. and J.M. Franklin, Copper and gold mineralization in an Archean trondhjemitic intrusion, Sturgeon Lake, Ontario; in Current Research, Part A, Paper 81-1A, p. 9-14, 1981.

Abstract

The Beidelman Bay intrusion is an Archean synvolcanic trondhjemitic sill near the base of the South Sturgeon Lake homoclinal sequence of epiclastic, felsic and mafic volcanic rocks which contain five massive sulphide deposits.

A broad zone of low grade disseminated copper mineralization, with up to 0.2% Cu amd 400 ppb Au, occurs in the western part of the intrusion; it has locally developed hydrothermal biotite and associated but more widespread sericite alteration. Breccia development, metal distribution and alteration in this zone are all similar to typical porphyry copper deposits.

Gold at the Darkwater Mine occurs in principal veins, central to shear zones that are dominant in the central and eastern parts of the intrusion. Shear zone development occurred prior to prograde metamorphism, and caused a total change in both textural and chemical characteristics including loss of Na_2O, CaO, CO_2, S and Cu, and addition of MgO, K_2O, FeO, Fe_2O_3, and H_2O, all apparently at constant volume. Au was possibly remobilized during the destruction of the porphyry copper zone and precipitated in the principal veins; alternatively, gold was introduced from an external source during the shear zone formation.

Introduction

The South Sturgeon Lake volcanic sequence is part of the Archean Wabigoon belt in northwestern Ontario (Trowell, 1974). It hosts at least five volcanogenic massive sulphide deposits: Mattabi, Sturgeon Lake, F zone, Lyon Lake and Creek Zone (Franklin et al., 1978). The Beidelman Bay trondhjemitic body is within the volcanic sequence approximately 3 km to the south of these deposits and is probably a synvolcanic intrusion. The intrusion hosts both copper and gold mineralization, each in different settings. The present study was initiated to document the setting of both types of mineralization, and to test whether the intrusion and its mineralization types represent an Archean porphyry system.

Geology of the Intrusion

The Beidelman Bay intrusion outcrops over a strike length of 20 km and has an average exposed width of 2 km (Trowell, 1974). At the regional scale the body is concordant with metavolcanic strata (Fig. 2.1). Contacts with the country rocks are generally sharp with only local development of xenolithic breccias. Most of the rocks of the intrusion are undeformed while at some localities deformed plutonic equivalents occur in ductile shear zones.

The intrusion is composed mainly of trondhjemite with subordinate quantities of quartz diorite and feldspar porphyry. The chemical and mineralogical characteristics of these phases are presented in Table 2.1. Dykes of feldspar porphyry, 0.5 to 1 m wide, cut the main mass of the intrusion. In this rock type, phenocrysts, usually of zoned plagioclase and subordinate quartz, are set in a fine grained quartz-sericite matrix. The quartz diorite forms an irregular border phase of the intrusion and has gradational contacts with the trondhjemite. It is generally coarse grained and equigranular and commonly contains plagioclase with oscillatory zoning. The undeformed trondhjemite (Figure 2.2a) is also equigranular and typically contains sub-equal quantities of albite and quartz which generally occur as myrmekitic intergrowths. The deformed equivalent of this rock (Fig. 2.2b) is markedly schistose with prophyroclasts of quartz set in a matrix of biotite or chlorite-sericite.

The chemical composition of the above phases clearly reflects their mineralogical composition. The dominance of albitic plagioclase in the modes of the undeformed rocks (Table 2.1) is confirmed by the high sodium:potassium and sodium:calcium ratios (analyses 1 through 3). The quartz diorite shows some variation in chemical composition that may be attributed either to disequilibrium crystallization of a trondhjemitic melt or to contamination of the melt by reaction with country rocks. The major and trace element compositions of the trondhjemite are similar to those of rhyolites within the volcanic sequence suggesting that the intrusion represents a subvolcanic equivalent to overlying felsic pyroclastic products (Franklin et al., 1978).

Copper Mineralization

Conventional prospecting and trenching by J. Gareau led to the discovery of copper near the northwest margin of the Beidelman Bay intrusion. Subsequent exploration by Steep Rock Iron Mines Ltd. and Noranda Mines Ltd. resulted in the partial definition of three zones of subeconomic mineralization (Fig. 2.1). Chalcopyrite and pyrrhotite occur in sub-equal quantities as disseminations and fracture fillings in massive trondhjemite. Pyrite, sphalerite and molybdenite are also present in variable but minor quantities. Grades of 0.2% Cu, and 0.03% MoS_2, with minor zinc, silver and gold, are indicated in trenches over lengths of at least 50 m.

The sulphide-bearing zones are spatially related to abundant xenoliths of metavolcanic country rock and at some localities the mineralization occupies the matrix of a distinctive breccia (Fig. 2.2c) composed of angular to slightly rounded fragments, mainly of feldspar porphyry with subordinate trondhjemite and metavolcanic rock. The breccia zones are highly irregular in shape. Sulphides are confined to the matrix of the breccia; no sulphide-bearing breccia clasts are present. Although alteration mineralogy is similar to regional metamorphic mineralogy, certain types of alteration are spatially related to the sulphide zones. Whereas some distance away from the mineralized zone undeformed trondhjemite is relatively fresh, feldspar in the mineralized trondhjemite is strongly sericitized.

[1]Department of Geology, Queen's University, Kingston, Ontario.

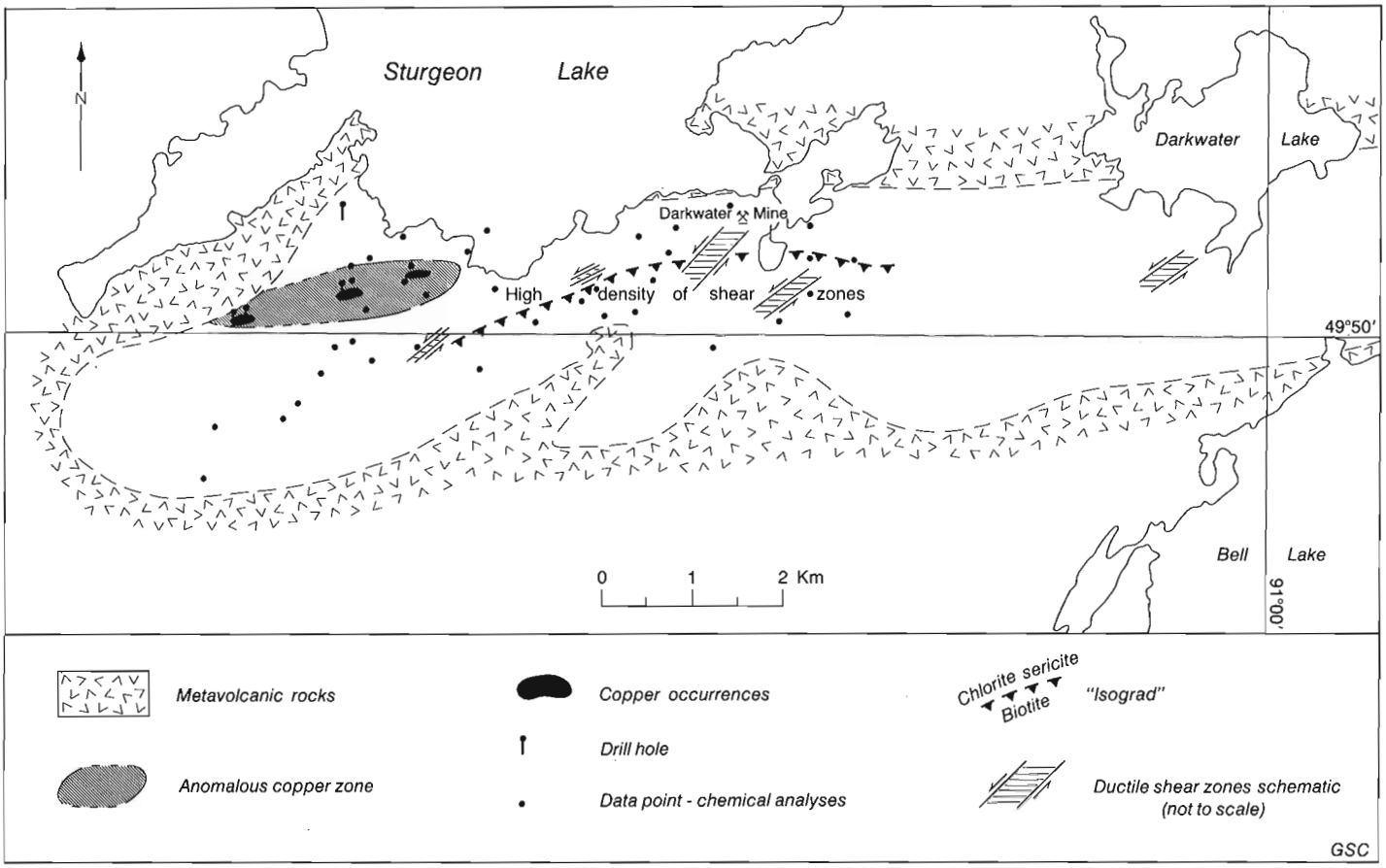

Figure 2.1. *Western end of the Beidelman Bay intrusion (not patterned), showing sample locations, distribution of anomalous copper and a metamorphic "isograd". The area of shear-zone development is illustrated schematically; individual shear zones increase in number and width near the Darkwater Mine. Geology after Trowell, 1974.*

Silicification, in the form of quartz stringers, is more common near the mineralization. There are two optically distinctive varieties of biotite. The first is dark brown, is weakly pleochroic, has a dark brown anomalous colour, and appears to be unrelated to the mineralization. The second type is tan-coloured, strongly pleochroic, has an orange interference colour, and is fine grained compared with the first variety. The latter variety is found only in copper-enriched (samples with 0.1 %Cu) rocks. Chemical analyses of mechanically separated biotites confirm this distinction as the first type of biotite (FeO:MgO equals 3:1) is low in copper while the second (FeO:MgO equals 2.3:1) contains 600 ppm Cu.

In an effort to delineate the large scale distribution of copper within the Beidelman Bay intrusion, 60 hand specimens and drillcore samples from representative localities were analyzed by atomic absorption spectrophotometry (Table 2.2). Statistical treatment of the data indicates a bimodal copper distribution; the median concentration of copper in sulphide poor undeformed trondhjemite is 18 ppm Cu while most samples from a broad but undeformed anomalous zone about the copper occurrences (Fig. 2.1) contain in excess of 250 ppm Cu.

Quartz diorite is absent from the sulphide-enriched area, and where present has a low copper content. Feldspar porphyry away from the sulphide zone has a similar low copper content, but two samples taken from the trenches have high (190 and 700 ppm) Cu contents.

Zinc analyses for the same groupings of samples have similar distributions (Table 2.2). A zone of zinc enrichment is centred on the copper occurrences, but it is broader and less clearly defined than the anomalous copper zone.

The deformed trondhjemite contains significantly less copper than its undeformed equivalent; six out of the eight samples of deformed rock contain less than 10 ppm Cu, whereas only 3 out of 14 samples of undeformed, but sulphide-poor, rock have less than 10 ppm Cu. The zinc contents of deformed and undeformed zones are not substantially different, however.

Gold Mineralization

Underground exploration for gold was conducted at the Darkwater Mine between 1934 and 1937, from quartz-ankerite-tourmaline veins (Horwood, 1937). Veins of this type are notably poor in sulphide and are found in ductile shear zones throughout the intrusion but are widest and most abundant in the mine area. The shear zones are similar in their geometry to those described by other authors (Ramsay and Graham, 1970) with the important distinction that the quartz-ankerite-tourmaline veins, here termed principal veins, occupy a position central to the shear zones (Fig. 2.2d). En echelon second order tensional veins are also present but commonly are composed only of quartz. Magnetite and hematite occur in some veins. The principal

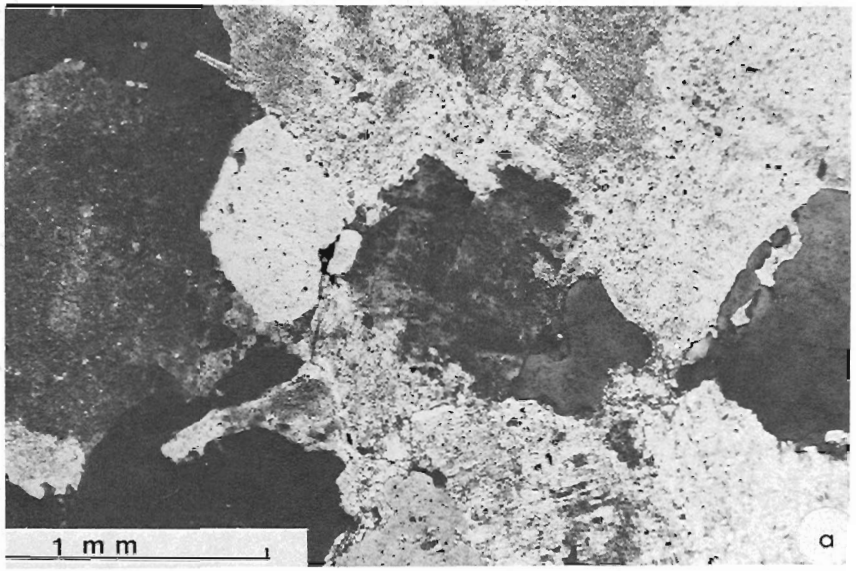

Figure 2.2a. *Undeformed trondhjemite composed of quartz, albite and chlorite.*

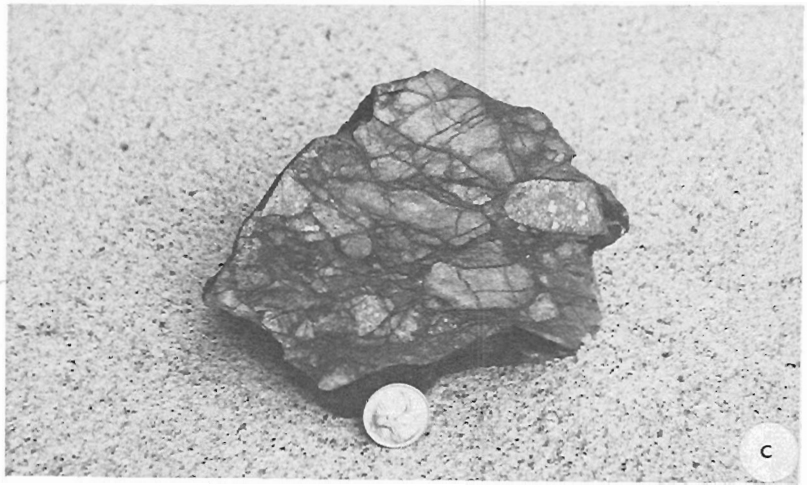

Figure 2.2c. *Breccia from central copper occurrence (Fig. 2.1) with clasts of trondhjemite and feldspar porphyry. Chalcopyrite is confined to the matrix.*

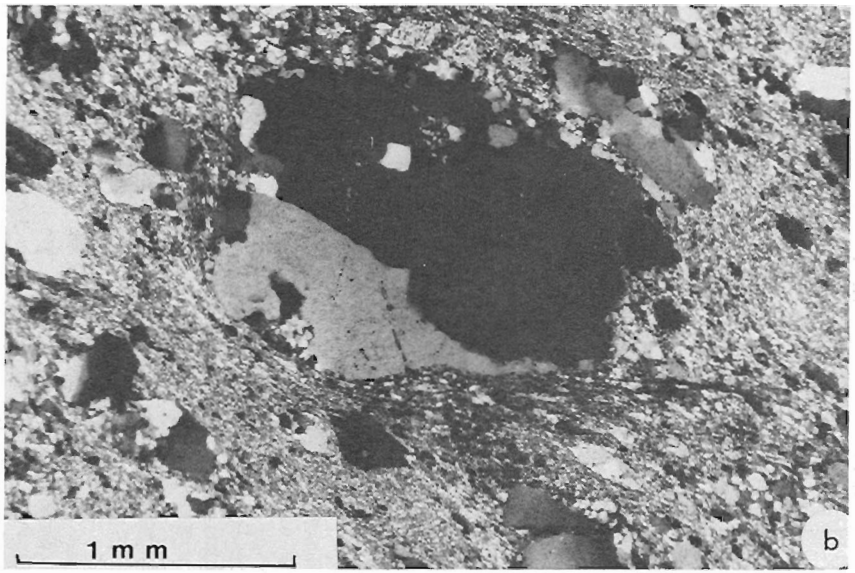

Figure 2.2b. *Deformed trondhjemite with a porphyroclast of quartz set in a sericite matrix.*

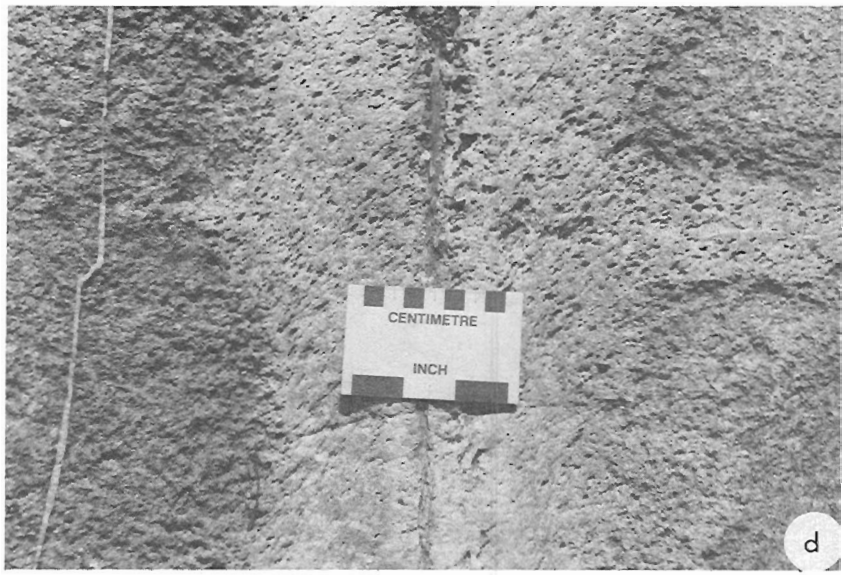

Figure 2.2d. *Typical shear zone with a principal vein in its centre.*

Table 2.1

Chemical and Mineralogical Data: Beidelman Bay Intrusion whole rock analyses

	Feldspar Porphyry	Quartz Diorite	Undeformed Trondhjemite	Deformed Trondhjemite	Relative gains/losses
SiO_2	66.76	58.01	76.30	76.47	+2%
Al_2O_3	15.60	16.44	12.05	11.83	0
Fe_2O_3	.72	2.25	.80	1.35	+73%
FeO	1.94	5.21	1.85	2.37	+30%
MgO	.87	2.49	.39	1.46	+280%
CaO	3.06	5.13	1.04	.58	-53%
Na_2O	4.76	4.62	4.75	.84	-82%
K_2O	1.77	1.03	1.16	2.76	+142%
MnO	.04	.12	.05	.06	+20%
TiO_2	.35	1.10	.27	.27	0
P_2O_5.	05	.20	.03	.06	+50%
CO_2	1.35	1.20	.77	.39	-48%
H_2O_T	.99	1.51	.61	1.60	+167%
TOTAL	98.26	99.31	100.07	100.04	+1.7%
No. of samples	(3)	(5)	(12)	(12)	

Modal Analyses

	Feldspar Porphyry	Quartz Diorite	Undeformed Trondhjemite	Deformed Trondhjemite
Quartz	present as phenocrysts	16	43	common as porphyroclasts
Plagioclase	common as phenocrysts	50	53	rare as porphyroclasts
Microcline		nil	trace	
Biotite		5	3	
Hornblende		24	trace	
Opaques		5	1	

veins are coplanar with the shear zones and strong schistosity oblique to the zones establishes the sense of shear (Fig. 2.3). The shear zones, veins and schistosity all dip steeply.

The textural development of the shear zones is characterized by the cataclastic deformation of plagioclase in preference to quartz with the result that quartz porphyroclasts are enclosed by a fine grained matrix (Fig. 2.2b). Progressive deformation results in a transition from somewhat angular quartz porphyroclasts showing undulose extinction to ellipsoidal augen showing subgrains to polycrystalline quartz ribbons with strong undulose extinction. Touching porphyroclasts commonly share sutured stylolitic boundaries. Tourmaline is a common constituent of the matrix which, in the northern half of the intrusion, is composed of chlorite-sericite and, in the southern half, abundant biotite (Fig. 2.1). Development of this "isograd" suggests that the shear zones developed prior to or during regional metamorphism.

The absence of plagioclase in the shear zones is also clearly indicated chemically (Table 2.1). A mass balance calculation (Krauskopf, 1979, p. 83), which assumes conservation of Al_2O_3, demonstrates that appreciable Na_2O, CaO, and CO_2 have been removed from the system while MgO, K_2O, FeO, Fe_2O_3 and H_2O have clearly been added in

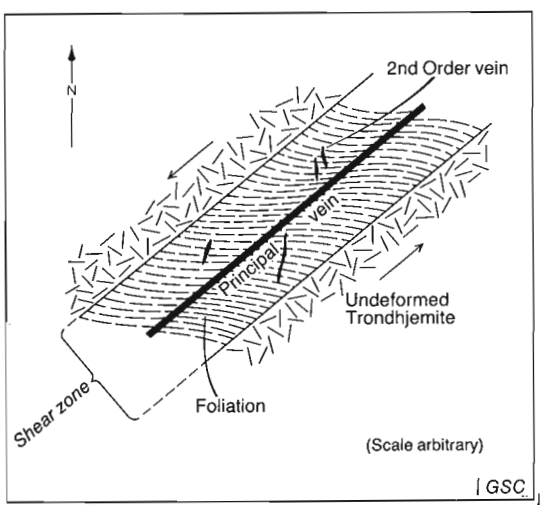

Figure 2.3. *Morphology of a typical shear zone.*

Table 2.2

Chemical Data on Sulphide and Gold Mineralization

	median	range	No. samples
Copper ppm			
Feldspar Porphyry	50	7 – 700	7
Quartz Diorite	24	9 – 50	5
Undeformed Trondhjemite	18	4 – 200	20
Undeformed Mineralized Trondhjemite	620	250 – 13,000	29
Deformed Trondhjemite	4	2 – 34	8
Zinc ppm			
Feldspar Porphyry	60	33 – 110	7
Quartz Diorite	110	60 – 170	5
Undeformed Trondhjemite	36	8 – 160	20
Undeformed Mineralized Trondhjemite	72	18 – 600	29
Deformed Trondhjemite	45	30 – 55	8
Gold ppb			
Feldspar Porphyry	5.5	2 – 22	4
Quartz Diorite	11	–	1
Undeformed Trondhjemite	11.5	0.5 – 40	14
Undeformed Mineralized Trondhjemite	10.5	4 – 410	26
Deformed Trondhjemite	3	0.5 – 20	7
Darkwater Mine	6800	after Horwood (1937)	

the transformation from undeformed to schistose trondhjemite. The net increase in total mass is reflected by an equivalent increase in specific gravity (2.683 for undeformed trondhjemite versus 2.725 for deformed trondhjemite) suggesting an equal volume transformation.

The distribution of gold in the various phases of the intrusion was determined by trace analysis by the neutron activation method (X-ray Assay Labs Ltd.). The data (Table 2.2) show that there is little difference in gold concentration among the undeformed plutonic phases. The schistose trondhjemite is somewhat depleted in gold and samples containing low copper concentrations (less than 0.1% Cu) show no appreciable gold content. However, six samples, each exceeding 0.1% Cu (average 0.4% Cu) contain an average of 104 ppb Au. Inferred reserves for the Darkwater Mine are approximately 50 000 tonnes of material grading 0.2 ounces of Au per ton (6800 ppb). Horwood (1937) reported that most of the gold is confined to the principal veins, and that gold distribution is erratic.

Summary

The zones of anomalous, subeconomic gold and copper are separate; each has a distinct setting and different mode of occurrence. Chalcopyrite, with very minor molybdenite, is clearly disseminated and in randomly oriented fracture fillings in undeformed trondhjemite. The textural and alteration characteristics are similar to younger porphyry copper deposits, as well to other Precambrian examples (Kirkham, 1972; Goldie et al., 1979). In contrast, the gold deposits are tectonically localized in veins in shear zones. Furthermore, copper is distinctly lacking in the gold-enriched zones at the Darkwater Mine.

Since the geometry of the shear zones implies a maximum compressional stress from the north (Fig. 2.3), the shear zones probably developed contemporaneously with the regional compression that produced the easterly-striking cleavage and a set of easterly-trending minor folds in the volcanic and volcaniclastic sedimentary rocks surrounding the Beidelman Bay complex. Similarly, the metamorphic assemblages in the shear zone rocks are consistent with the greenschist facies of metamorphism observed in the volcanic rocks.

The principal veins are presumably derived from an effective extensional stress, normal to the shear zone, but their precise relationship to the mechanism of shear zone formation is not known. The second order veins are en-echelon tension fractures (Ramsay and Graham, 1970) that initially develop at 90° to the schistosity, and remain planar unless there is additional movement on the shear zone. In the latter case, the second order veins become sigmoidal.

The shear system incorporated large amounts of Mg, K and H_2O, with an accompanying almost total loss of Na and Ca from the trondhjemite. This large chemical transfer exceeds that expected solely from a pressure-solution mechanism (Kerrich et al., 1977). The source of the large volumes of K and Mg are unclear; however, a large water:rock ratio in the shear system would enable such introductions to occur from fluids of moderate K and Mg contents, whether these fluids be of metamorphic or seawater origin.

Since the vein material contains no Na_2O-bearing minerals, and there is no obvious source for the introduced elements, we assume that substantial fluid transport accompanied shear zone development; vein materials were at least in part derived from this fluid.

The chemical characteristics of the alteration within the shear zone are remarkably similar to those observed below volcanic-related massive sulphide deposits (e.g. Riverin and Hodgson, 1980; Roberts and Riordon, 1978; Franklin et al., 1975). Recent studies of gold deposits at Red Lake (Hodgson and MacGeehan, 1980), and Timmins (Fryer et al., 1979) also note alteration patterns similar to those observed below massive sulphide deposits, except that the alteration associated with gold deposits tends to be symmetrical to the gold zones.

The fluid conditions enabled dissolution of albite and transport of Na and Ca, and promoted the formation of muscovite (or sericite) rather than K-feldspar. Examination of relevant ionic equilibria systems indicates that over the temperature range of 150-300°C, these conditions are met by a solution of acid pH. The stabilization of hematite and magnetite, and lack of sulphide in these veins indicates a relatively high fO_2 in the vein forming environment, relative to fS_2.

A preliminary evaluation of the petrochemical characteristics of the unaltered and nonfoliated parts of the intrusion (Franklin et al., 1978; Friske et al., 1979) indicates that it is a subvolcanic intrusion. The remarkable similarity in texture of the pre- or syn-sulphide breccia developed in the trench area at the Beidelman Bay copper occurrences (Fig. 2.1 and 2.2c) with that typical of many porphyry occurrences (see McMillan and Panteleyev, 1980, p. 56, fig. 4) strongly indicates that a porphyry-type system formed the sulphides. In addition, the distinctive biotite associated with the most intense copper mineralization, and the possible association of sericite (formed at the expense of the small amount of K-feldspar molecule in the albitic feldspar), are similar to alteration products observed at typical porphyry deposits. This alteration, however, is weakly developed.

The high fO_2 conditions prevalent in the shear zones probably destroyed any pre-existing sulphide minerals. Conversion of sulphide to either HSO_4^- (at low pH) or $SO_4^=$ (at higher pH) would be accompanied by a dramatic increase in the solubility of copper, while iron would be stabilized as

hematite or magnetite. Thus, if the porphyry copper zone (Fig. 2.1) did extend further to the east of its present position, it may have been destroyed by the formation of the shear zones. Gold, already concentrated in the more copper-rich portions of the porphyry copper zone, may have been ultimately redistributed into the shear-controlled quartz veins. Thus destruction of a pre-existing anomalous, but subeconomic, gold concentration by development of a shear zone, and ultimate redeposition and concentration of gold into the related veins may be a viable mechanism for formation of some gold deposits. Such deposits however, would likely be small, as in order to accommodate a concentration factor of ten, the volume of 'source' porphyry (or other type of sulphide accumulation) would probably be ten-times as large as the existing gold deposit. Furthermore, a pervasive shear zone throughout the source rock would be required in order to allow for a sufficient volume of gold to be mobilized. Large, low grade, Archean porphyry deposits, and possibly large, low grade copper-nickel deposits in gabbro sills, might be suitable candidates for ultimate gold concentration by this mechanism.

Alternatively, gold may have been introduced into the shear zones from an external source. Either metamorphic fluids (Fryer et al., 1979) or seawater might be suitable sources; isotopic data might elucidate this problem.

Acknowledgments

Peter Friske contributed considerable data regarding the prophyry copper occurrence. Discussions with Rod Kirkham and Dave Sinclair gave us an insight into porphyry copper geology. Wally Gibb and Adele Tamman of the Mattagami Lake Division of Noranda Mines Limited have continually supported our metallogenic studies at Sturgeon Lake. Mel Bartley, consulting geologist, and the staff of Noranda Mines Limited (Thunder Bay office) contributed useful exploration data.

References

Franklin, J.M., Kasarda, J., and Poulsen, K.H.
1975: Petrology and chemistry of the alteration zone of the Mattabi massive sulphide deposit; Economic Geology, v. 70, no. 1, p. 63-79.

Franklin, J.M., Gibb, W., Poulsen, K.H., and Severin, P.
1978: Archean metallogeny and stratigraphy of the South Sturgeon Lake Area; Guidebook, Institute on Lake Superior Geology, Lakehead University, Thunder Bay, Ontario, 73 p.

Friske, P., Poulsen, K.H., and Franklin, J.M.
1979: The Beidelman Bay porphyry copper-gold occurrences, northwestern Ontario; Geological Association of Canada., Program with Abstracts, v. 4.

Fryer, B.J., Kerrich, R., Hutchinson, R.W., Peirce, M.G. and Rogers, D.S.
1979: Archean precious metal hydrothermal systems, Dome Mine, Abitibi greenstone belt, I. Patterns of alteration and metal distribution; Canadian Journal of Earth Sciences, v. 16, no. 3 (pt. 1), p. 421-439.

Goldie, R., Kotila, B., and Seward, D.
1979: The Don Rouyn Mine: an Archean porphyry copper deposit near Noranda, Quebec; Economic Geology, v. 74, no. 8, p. 1680-1684.

Hodgson, C.J. and MacGeehan, P.J.
1980: The relationship of gold mineralization to volcanic and alteration features in the area of Campbell Red Lake and Dickenson Mines, Red Lake District, Western Ontario; Ontario Geological Survey, Open File Report 5293, p. 212-242.

Horwood, H.C.
1937: Geology of the Darkwater Mine; Ontario Div. Mines, v. 46, pt. 6, p. 26-35.

Kerrich, R., Fyfe, W.S., Gorman, B.E., and Allison, I.
1977: Local modification of rock chemistry by deformation; Contributions to Mineralogy and Petrology, v. 65, p. 183-190.

Kirkham, R.V.
1972: Geology of copper and molybdenum deposits; in Report of Activities, Part A, Geological Survey of Canada Paper 72-1A, p. 82-87.

Krauskopf, K.
1979: Introduction to Geochemistry; 2nd edition, McGraw-Hill, New York, 600 p.

McMillan, W.J.,and Panteleyev, A.
1980: Ore deposits models I. Porphyry Copper Deposits; Geoscience Canada, v. 7, p. 52-63.

Ramsay, J.G. and Graham, R.H.
1970: Strain variation in shear belts; Canadian Journal of Earth Sciences, v. 7, p. 786-813.

Riverin, G. and Hodgson, C.J.
1980: Wall-rock alteration at the Millenbach Cu-Zn Mine, Noranda, Quebec; Economic Geology, v. 75, no. 3, p. 424-444.

Roberts. R. Gwilym and Riordon, E.J.
1978: Alteration and ore-forming processes at Mattagami Lake Mine, Quebec; Canadian Journal of Earth Sciences, v. 15, no. 1, p. 1-21.

Trowell, N.F.
1974: Geology of the Bell Lake-Sturgeon Lake Area, Districts of Kenora and Thunder Bay; Ontario Division of Mines, Geological Report GR114, 67 p.

3. STRATIGRAPHY AND TECTONO-DEPOSITIONAL RELATIONSHIPS OF THE PROTEROZOIC ROCKS OF THE HADLEY BAY AREA, NORTHERN VICTORIA ISLAND, DISTRICT OF FRANKLIN

Project 740092

F.H.A. Campbell
Precambrian Geology Division

Campbell, F.H.A., Stratigraphy and tectono-depositional relationships of the Proterozoic rocks of the Hadley Bay area, northern Victoria Island, District of Franklin; in Current Research, Part A, Geological Survey of Canada, Paper 81-1A, p. 15-22, 1981.

Abstract

Proterozoic sedimentation in the northernmost part of the Kilohigok Basin commenced with deposition of shallow marine to nonmarine quartzose clastics of the Hadley Formation in depressions on dissected Archean(?) basement. Fine grained sandstones then accumulated on a periodically-exposed shelf. As terrigenous sedimentation diminished, clastic and stromatolitic carbonates spread across the slowly subsiding basin. Intertidal to shallow subtidal bioherms developed in the northeastern part of the area, while calcareous siltstones were deposited in the southwest. Renewed uplift in the source areas supplied fine grained sands and silts to the again periodically emergent shelf, and their deposition continued until the end of Hadley Formation sedimentation.

Syndepositional faults and regional tilting supplied large volumes of coarse debris to northerly- and northwesterly-flowing fluvial systems. Unsorted conglomerates were deposited close to active faults, while better-sorted congomerates and trough crossbedded sands were deposited in the more distal regions.

Subsequent subsidence of the entire area, coupled with reactivated uplift in the southerly and easterly source areas, caused marine sands to spread over the shallow shelf. These were dispersed by large sand waves which produced the very large scale trough crossbeds characteristic of this unit.

Gentle tilting and regional peneplanation followed, and led to the deposition of fine reddish sands, muds, and coarse white quartzites of the Glenelg(?) Formation.

Paleocurrent and facies analyses of the Hadley Formation, together with data from the Eastern Platform of the Kilohigok Basin to the south, indicate that an east-west trending aulacogen off the Wopmay Orogen was present in the Coronation Gulf area during deposition of the sediments of the Kilohigok Basin.

Introduction

Precambrian rocks of the Hadley Bay area (Fig. 3.1) were initially mapped by Thorsteinsson and Tozer (1962). They identified an older sequence of rocks which they interpreted to be intruded by a granodiorite (dated at 2405 Ma, K-Ar) because of supposedly metamorphic muscovite in the sediments. Dixon (1979) interpreted the muscovite as detrital, and suggested that these sediments were early Proterozoic. During mapping of the Hadley Bay area in 1980, Dixon's interpretation was confirmed. Detrital muscovite is abundant throughout the lower part of the succession, and there is no indication of either regional or contact metamorphism.

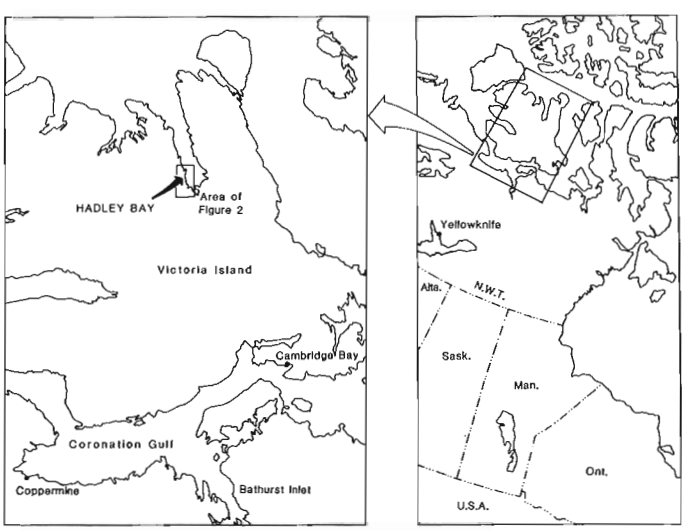

Figure 3.1. *Location map of the area, showing the location of Victoria Island in the northwestern Canadian Shield and the position of Hadley Bay on Victoria Island.*

The stratigraphy of the Proterozoic sediments in the Hadley Bay area has been considerably revised (Fig. 3.2; Table 3.1). Four unconformities are now recognized, separating three distinct successions from one another, and from underlying basement and overlying Paleozoic units. Due to a paucity of topographic names, none of the individual mappable units is formally named, although all merit at least member if not formation status. The lowermost group of three units is here named the Hadley Formation, as all contained units merit at least member rank.

The various rock units of the area are described in ascending stratigraphic order below.

Unit 1

This unit outcrops at the southwestern end of Hadley Bay, and on a small island offshore (Thorsteinsson and Tozer, 1962). It consists of massive, coarse grained, pink granodiorite locally with xenoliths of fine grained micaceous metasediments(?). The contact with the overlying Proterozoic sediments was not observed during the course of mapping. The closest sediments (Fig. 3.2) show no evidence of deformation or metamorphism, nor do they contain clasts which can be identified as having been derived from the granodiorite.

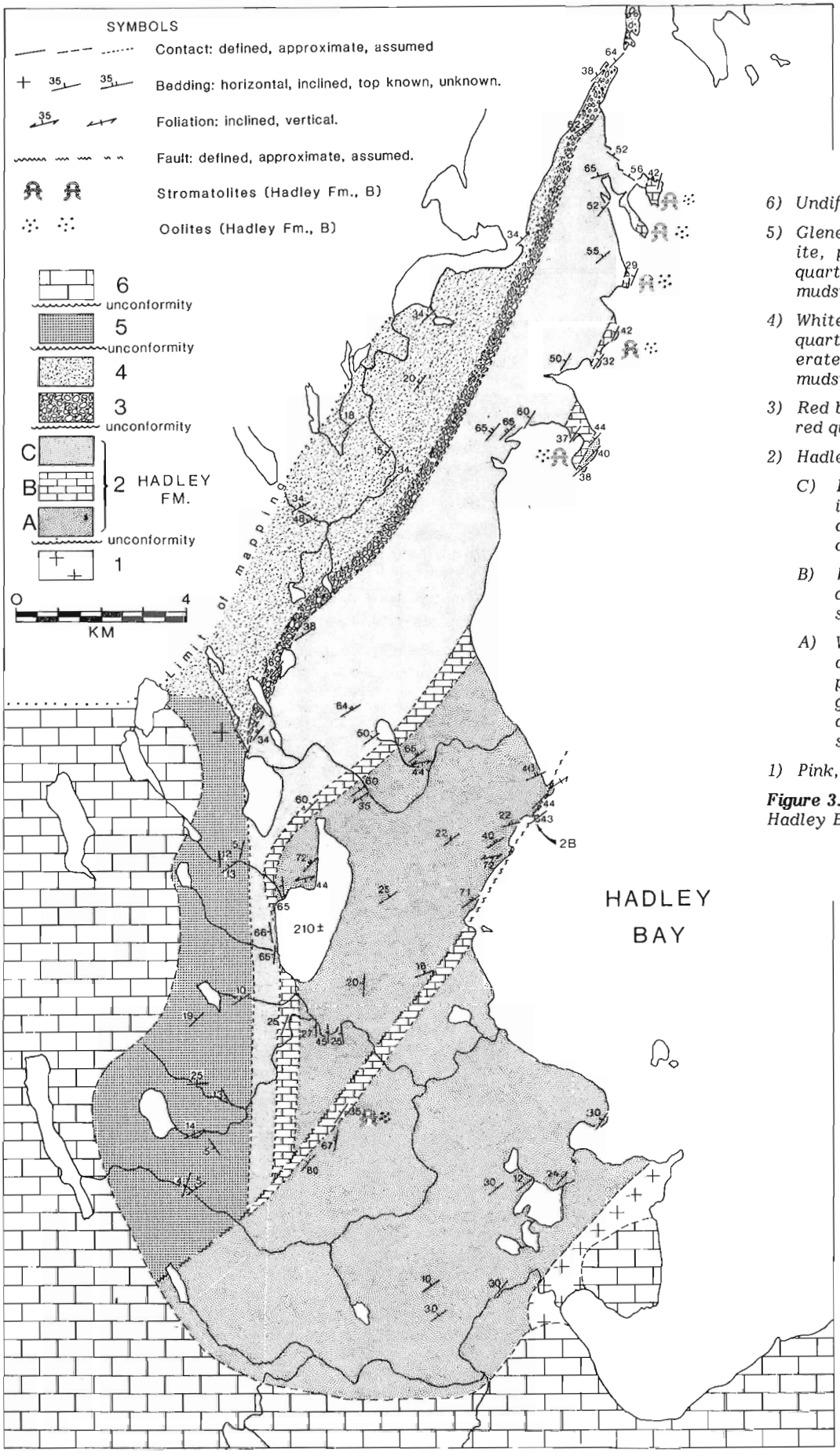

6) *Undifferentiated Paleozoic rocks.*

5) *Glenelg(?) Formation: white quartzite, pink to red fine grained quartzite; minor siltstone and mudstone.*

4) *White, massive, coarse grained quartzite; minor pebble conglomerate and red quartzite or mudstone near the base.*

3) *Red boulder conglomerate; minor red quartzite.*

2) *Hadley Formation:*

- *C) Red and grey quartzite and immature sandstone; siltstone and minor mudstone; rare conglomerate.*
- *B) Doloarenite, stromatolitic dolomite, oolite; grey-green siltstone.*
- *A) White quartzite; red quartzite and siltstone; rare quartz-pebble conglomerate; minor grey immature sandstone and mudstone; micaceous sandstone.*

1) *Pink, coarse grained granodiorite.*

Figure 3.2. *Geological map of the Hadley Bay area.*

Table 3.1

	Hadley Bay Area	Possibly Correlative Unit
	Undifferentiated Paleozoic	Undifferentiated Paleozoic
	unconformity	
PROTEROZOIC	Unit 5	Glenelg Formation (Shaler Group)
	unconformity	
	Units 3 and 4	Ellice Formation
	unconformity	
	Hadley Formation	Western River Formation (Goulburn Group)
	unconformity	
	Granodiorite (Archean ? basement)	Archean basement

Hadley Formation (Unit 2)

The Hadley Formation consists of at least three units of member rank, here informally termed the lower (A), middle (B), and upper (C) (see Table 3.1 and Fig. 3.2). All form extensive mappable units throughout the southern part of the area, and extend for unknown distances on small islands to the northeast.

Lower Member (A)

The lowermost member in the Hadley Formation consists of trough crossbedded white, pink, and light grey quartzite near the base, with increasing amounts of red to reddish grey fine grained sandstone toward the top. White quartzite in the lower part of this member contains rare thin beds of quartz-pebble conglomerate, with individual clasts up to 4 cm. Planar crossbedded quartzose doloarenite with small quartz pebbles is also rarely intercalated with this part of the member. The lowermost exposed section of the member is in a creekbed approximately 1 km from the closest exposure of the "basement" granodiorite. There, the sediments consists of medium to coarse grained, locally pebbly, trough crossbedded quartzite. Quartz pebbles are the predominant large clasts. The troughs are typically 1.5-2.0 m wide, up to 0.75 m deep, and are not part of fining-upward cycles. Paleocurrent data from these troughs and others in the Hadley Formation show the dominant transport direction was to the southwest (Fig. 3.3A).

Upward in this member, particularly near the contact with the Middle member (B), the sediments are much finer grained, less quartzose, and show little if any crossbedding. Immediately below the middle member, fine grained, dark grey-red sandstones and siltstones show abundant desiccation cracks. These generally overlie massive, red, fine grained sandstones and mudstones.

Where exposed, the contact with the overlying Middle member is sharp and conformable, with no apparent interbedding of lithologies.

Middle Member (B)

This unit, which outcrops sporadically throughout the area (Fig. 3.2), forms the only marker unit in the Hadley Formation. It consists of clastic, stromatolitic, and oolitic carbonate intimately interstratified with grey-green calcareous siltstones and mudstones. The stromatolitic and oolitic carbonates are abundant in the northern part of the area, while the siltstones and mudstones are dominant in the laterally equivalent part of the member in the south.

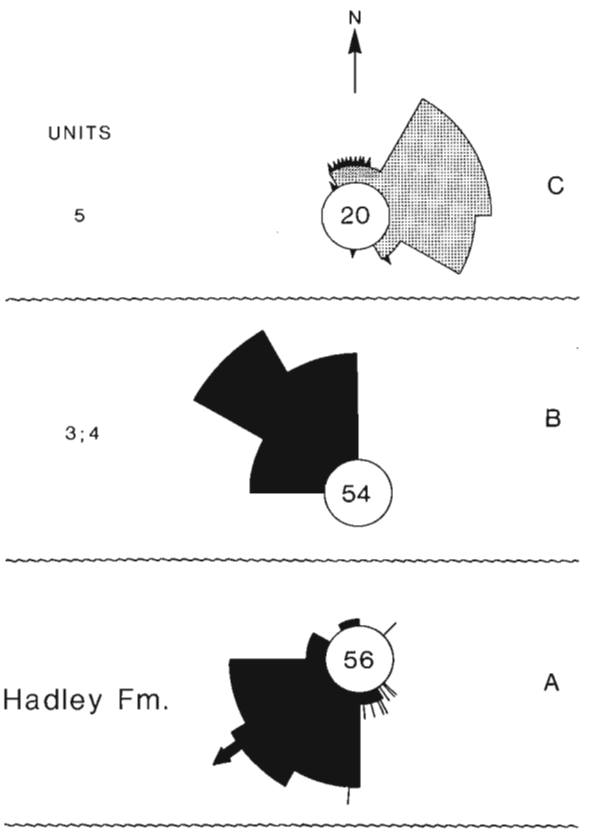

A) Trough crossbeds from the Hadley Formation. The solid arrow to the southwest shows the orientation of the elongate asymmetric stromatolites of the B member. The short lines show individual current ripple directions.

B) Trough crossbeds from units 3 and 4.

C) Current ripples from unit 5. The arrowheads are individual trough crossbeds from this same unit.

Figure 3.3. *Paleocurrent roses from various units in the area. The number of readings is as shown, and the diameter of the centre circle is 20 per cent.*

The stromatolites characteristic of this member are nearly continuous throughout the northern part of the area, where they are particularly well displayed in shoreline exposures. The stromatolites, however, occur only rarely in the southern part of the area, south of the major fault (Fig. 3.2). Small to large (0.5-3.0 m) bioherms of pseudocolumnar stromatolites show little evidence of well developed lateral linkage. Both the individual columns and the bioherms themselves are strongly elongated northeast-southwest, and the bioherms are locally inclined to the southwest (Fig. 3.4). The bioherms are separated by channels filled with calcareous siltstone and bioclastic debris presumably derived from the flanks of the bioherms.

Oolite beds up to 1.5 m thick are locally common in the member, particularly where the stromatolites are well developed. They typically over-and underlie the stromatolites. At one locality, a thin (5 cm) stromatolite bed is contained entirely within an oolite bed. The oolites apparently pinch out to the southwest in the semi-continuous section north of the major fault (Fig. 3.2), but are present in the member south of this fault (Fig. 3.2).

Both the oolites and stromatolites appear to increase in number, and the stromatolites in size, to the northeast, suggesting that the paleoslope was to the southwest.

Upper Member (C)

Red, fine grained sandstone and minor siltstone predominate throughout this unit, which conformably overlies the stromatolitic and oolitic carbonate and siltstone at all localities. Sedimentary structures, other than well developed shaly rip-ups, mud-chip conglomerates, and poorly to well developed shaly rip-ups, mud-chip conglomerates, and poorly to well preserved planar crossbedding are rare. Desiccation cracks, however, are common in the lower part of the member.

Typically, the beds in this member are less than 40 cm thick, show no internal grading, and are rarely capped by thin films of shale or mudstone. Some sequences, particularly in the centre of the member, show well developed planar crossbedding which is commonly only identifiable on subvertical joint surfaces. The top of this member, and the whole Hadley Formation, is defined as the base of the characteristic boulder and cobble conglomerate which unconformably overlies the member at all exposed localities.

Unit 3

Cobble and boulder conglomerate, locally interstratified with red coarse grained grit and pebbly sandstone, comprise this unit. The base of the unit rests unconformably on the top of the upper member of the Hadley Formation, and the contact is exposed only in the northern part of the area (Fig. 3.2) at the northeastern tip of the peninsula. Although bedding is obscure in the conglomerate, there is an apparent angular discordance of up to 30° between it and the underlying rocks of the Hadley Formation. This apparent variation in attitude is also maintained on a regional scale (Fig. 3.2), although dips are very similar at some localities.

The conglomerate consists predominantly of boulders of red and grey quartzite, and lithologies typical of underlying

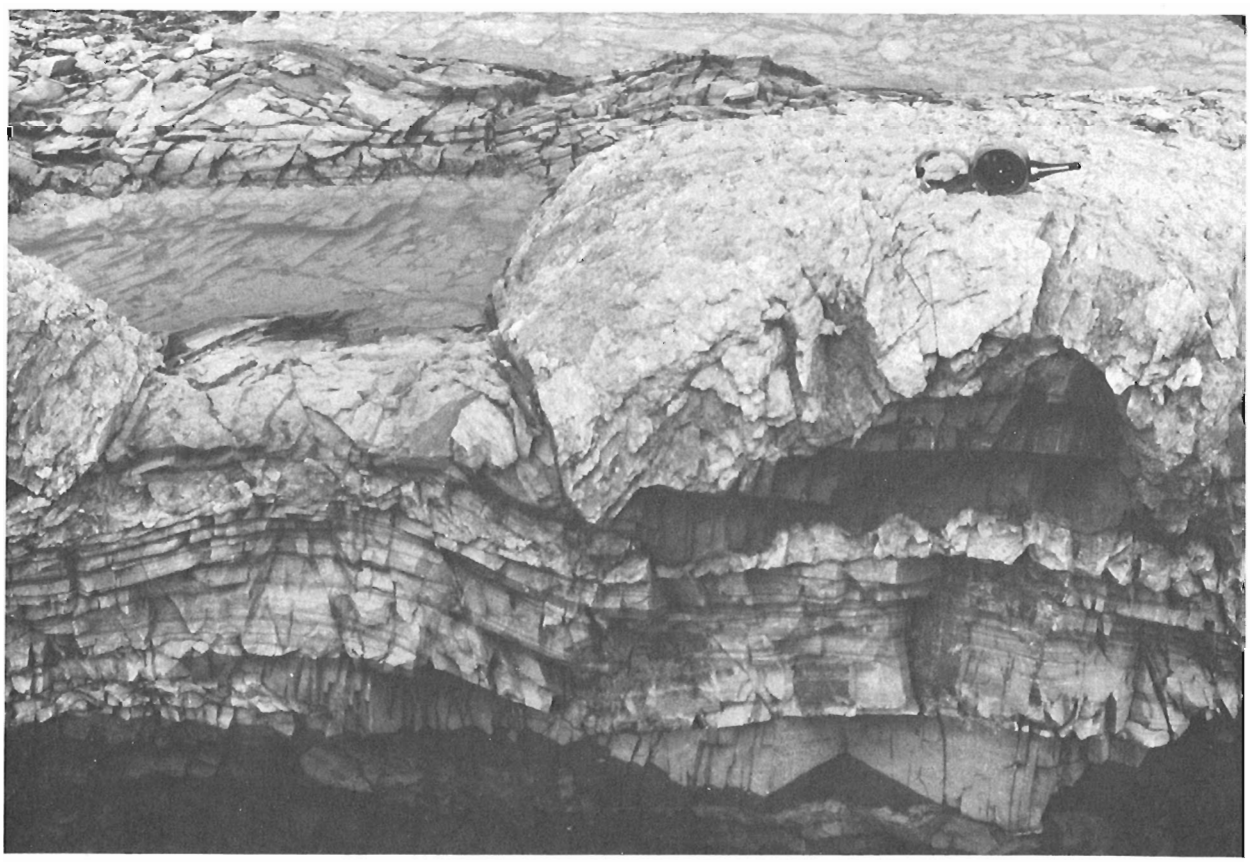

Figure 3.4. *Small stromatolite bioherms from the B member of the Hadley Formation. The bioherms are separated by calcareous grey-green siltstone, and rest on fine grained doloarenite and siltstone. (GSC 203062-K)*

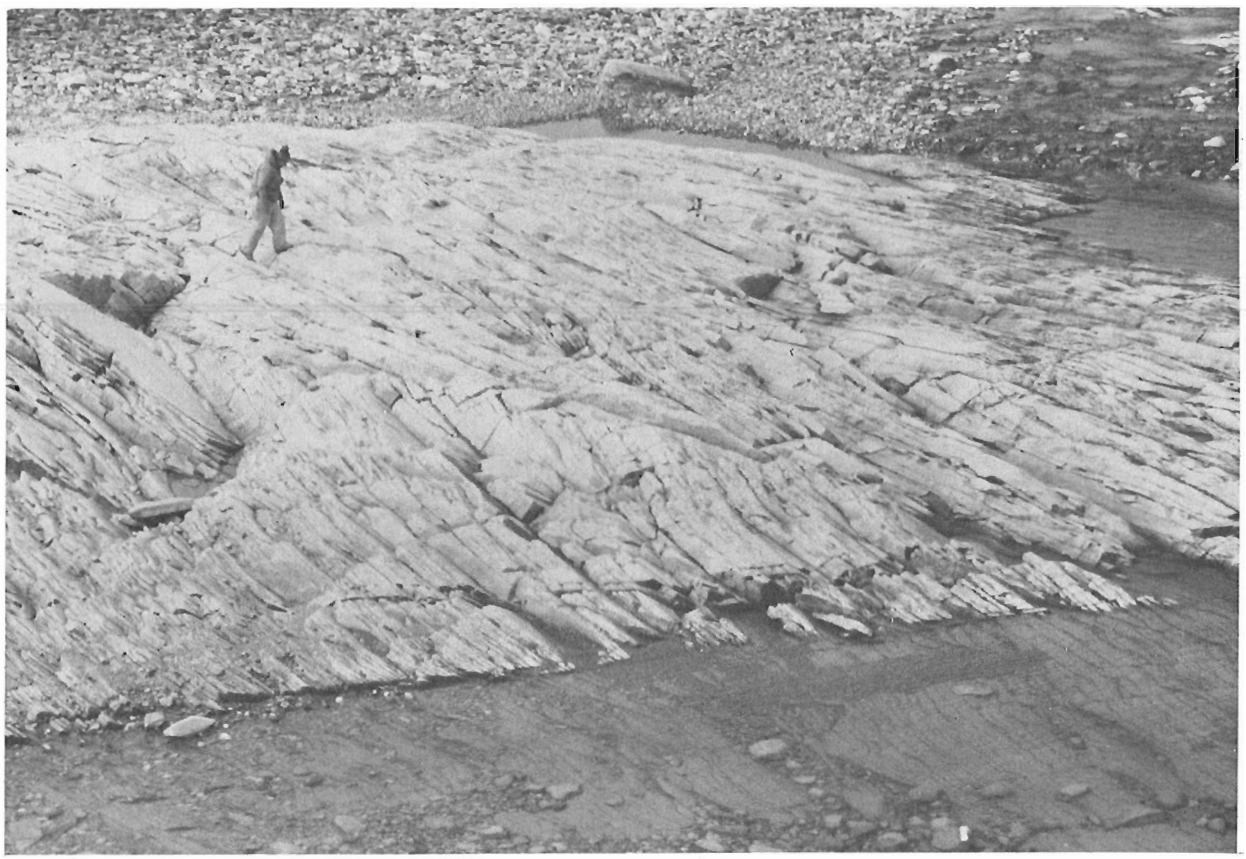

Figure 3.5. *Very large-scale trough crossbeds from unit 4, in the northwestern part of the area. Figure 3.6 is from this same exposure, at the left margin of this figure. (GSC 203062-P)*

units. No carbonate clasts were noted. Clasts near the base of the unit are relatively angular, but become well rounded within 2 m of the basal contact. The majority of the clasts is less than 30 cm in longest exposed dimension, but clasts up to 50 cm occur locally. There is no apparent change in the clast dimensions from the northeastern to the southwestern part of the unit.

Many of the quartzite clasts contain thin veinlets of quartz which are terminated at the clast margins, indicating that the veining occurred prior to their incorporation in the conglomerate. Clasts of pure quartz, however, are rare, suggesting that the veining was minor and possibly local.

In the northern part of the conglomerate, trough cross-bedded pebbly grit and coarse sandstone in thin (0.75 m) fining-upward cycles directly overlie and are locally interstratified with, the uppermost part of the basal conglomerate. Large boulders which typically occupy the lower parts of these cycles are locally abundant, angular, and up to 45 cm in exposed dimension. Limited paleocurrent data from this part of the unit suggest transport to the west and northwest (Fig. 3.3B).

The top of unit 3 is defined as the first appearance of massive, trough crossbedded quartzite, conformably overlying the conglomerate, red grit and coarse sandstone.

Unit 4

Massive, very large-scale trough crossbedded white quartzite with minor pebble conglomerate and rare red quartzite or mudstone near the base characterize this unit at all localities. It conformably overlies the basal conglomerate (Unit 3) everywhere.

Trough crossbeds of this unit are extremely large – up to 25 m wide and over 4 m deep (Fig. 3.5). Although the succession dips at approximately 30°, measured downcutting of individual troughs is commonly 3 m, and may exceed 5 m in some cases. At most localities the troughs are so large that they cannot be identified on a single exposure, and are inferred from the variable dips within the area. The troughs typically have curviplanar bases, and the filling consists of regularly arranged (10-25 cm) beds of uniform thickness which mimic the contour of the lowermost bounding surface of the trough (Fig. 3.6). There is no apparent change in grain size within the troughs from the base to the top, and no pebble concentrations were noted.

There is no variation in the character of this unit from the base to the top, but the contact with the overlying sequence is not exposed in the area examined, and an unconformity is inferred from variations in lithology and bedding attitudes.

Paleocurrent data from the troughs indicate that transport was strongly unimodal to the northwest (Fig. 3.3C).

Unit 5 (Glenelg(?) Formation)

White, pink to red, fine grained thin bedded quartzite, minor reddish siltstone and mudstone apparently unconformably overlie the white quartzites of Unit 4 in the southwestern part of the area (Fig. 3.2). In turn, these rocks are unconformably overlain by red shaly mudstones, shales, and limestones which form the basal Paleozoic strata in the area (Thorsteinsson and Tozer, 1962).

Figure 3.6. *Detail of intersecting bedding planes from the outcrop in Figure 3.5. The Brunton compass for scale is in the centre right of the photograph. (GSC 203062-O)*

Descriptions of the Glenelg Formation (Thorsteinsson and Tozer, 1962; Young and Jefferson, 1975), together with the stratigraphic succession and various unconformities within the rocks of the area, strongly suggest that these rocks are the basal equivalents of the Glenelg to the northwest.

The quartzites of this unit are thin- to medium-bedded (10-30 cm) throughout the area. However, generally more massive, coarse grained white quartzites commonly occur in beds to 65 cm thick in the upper part of the sequence. Sedimentary structures present in the unit include trough and planar crossbeds, oscillation and current ripples, and rare desiccation cracks. Paleocurrent data from the unit suggest transport to the northeast (Fig. 3.3C).

Interpretation

Hadley Formation

Lithologies and contained sedimentary structures in the formation suggest that the Hadley Formation was deposited in a fluvial to shallow marine environment, on a periodically-exposed, relatively stable shelf.

Paleocurrent data (Fig. 3.3A), together with stromatolite elongations and asymmetry indicate that the southwest-dipping shelf was continuously supplied with terrigenous detritus from rising source areas to the north and northeast. Following the initial transgression, and infilling of the paleotopographic depressions with coarse clastics of the lower member (A), shallow subtidal to intertidal muds, silts, and fine sands of the upper part of this same member were deposited. With decreasing terrigenous sediment supply and periodic emergence, carbonate sedimentation commenced with the gradual accumulation of shallow, possibly intertidal stromatolite banks and subtidal oolite shoals. The northeast-to-southwest pinching out of the stromatolites, together with the increasing amount of possibly resedimented carbonate detritus, suggests that the carbonate platform deepened to the southwest.

With renewed uplift in the source areas, and a consequent increase in terrigenous clastics, the carbonate shelf was rapidly buried beneath a sandy intertidal delta complex.

Units 3 and 4

Following uplift and erosion, a coarse basal conglomerate was deposited during renewed transgression of the underlying succession. As the paleotopography was rapidly buried, rising source areas in the southeast(?) supplied large volumes of quartz sand to the stable shelf. The sands were dispersed across the shallow(?) shelf bay, large marine sand waves, which constructed the trough crossbeds typical of Unit 4.

Unit 5

Following a second period of uplift and erosion, the shallow marine sands of the Glenelg(?) Formation were deposited on the relatively flat surface of the underlying successions.

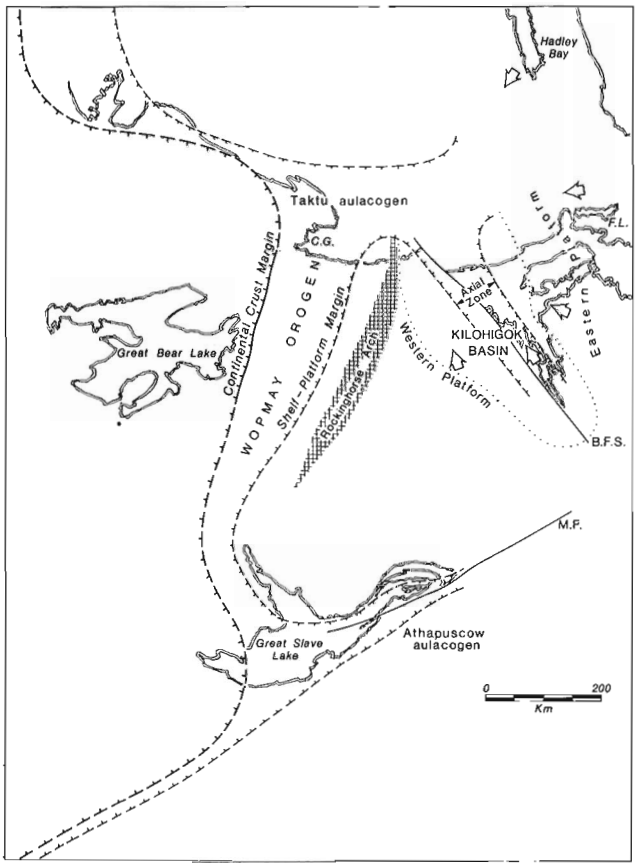

Figure 3.7. *Interpreted tectonic relationships between the Wopmay Orogen, Taktu aulacogen, Athapuscow aulacogen, and the various elements of the Kilohigok Basin. The Bathurst Fault System is shown as restored to its original position. The open arrows show the regional paleocurrent pattern derived from rose diagrams of the Burnside River and Hadley Formations. Lithostratigraphic correlation of the successions in the region are given elsewhere in this volume (Hoffman, 1981). Letter abbreviations are as follows:*

B.F.S. - Bathurst Fault System

M.F. - MacDonald Fault

C.G. - Coronation Gulf

F.L. - Ferguson Lake

Regional Correlation and Tectonics

The pre-Glenelg(?) Formation Proterozoic sediments of the Hadley Bay region were not previously correlated with other successions in the area, although Dixon (1979) suggested that they might be the equivalents of the Goulburn Group to the south.

Campbell and Cecile, 1979 had earlier mapped a continuous sequence of Burnside River and possible Western River Formation in the Wellington High area to the south on Victoria Island (Fig. 3.7). However, there are no sediments in the Hadley Bay area which resemble the rather distinctive red to purple trough crossbedded pebbly quartzites of the Burnside River Formation. The Hadley Formation may be the equivalent of the quartzite and carbonate succession which underlies the Burnside River in the Ferguson Lake area of the Wellington High (Fig. 3.7), which was previously correlated with the Western River Formation of the Goulburn Group of the Kilohigok Basin to the south (Campbell and Cecile, 1979).

Thus, the Hadley Formation is tentatively correlated with the Western River Formation of the Goulburn Group, based on its position in the succession, relationship with the underlying granodiorite, and the fact that it is unconformably overlain by two other Proterozoic successions.

Units 3 and 4, which are bounded above and below by regional unconformities, are similar to a single outlier noted by Campbell and Cecile (1979) in the Ferguson Lake area to the south (Fig 7). There, conglomerate overlain by large-scale trough crossbedded white quartzite, rests unconformably on Burnside River Formation quartzites. Campbell and Cecile (1979) suggested that this succession might be correlative with the Glenelg Formation to the north, based on its relationship to the underlying Burnside River Formation, and its geographic position relative to other possibly correlative units. The presence of Glenelg(?) Formation in southwestern Hadley Bay, unconformably overlying very similar rocks, suggests that the previous interpretation was incorrect.

The Ellice Formation fluvial to shallow marine sediments of the Elu Basin occupy an identical position relative to the Goulburn Group, and closely resemble both Units 3, 4 and the outlier at Ferguson Lake (Campbell, 1979; Campbell and Cecile, 1979). If this interpretation is correct, then the northern margin of the Elu Basin, or an equivalent of the Hiukitak Platform, would have extended at least as far as Hadley Bay. The northwesterly directed paleocurrents in Units 3 and 4 suggest that the continental shelf edge in this area lay to the west and/or northwest. This broad, tentative interpretation is in part supported by paleocurrent data from the equivalent rocks in the Ferguson Lake area, and also from the Ellice Formation outlier on northeastern Kent Peninsula (see Campbell and Cecile, 1979).

Regional Tectonic Implications

Correlation of the Hadley Formation with the Western River Formation of the Kilohigok Basin significantly extends the northern limit of the Eastern Platform (Fig. 3.7). However, lithofacies, paleocurrents, and stromatolite elongations and asymmetry indicate that the Hadley Formation was deposited on a southwest-dipping shallow to emergent shelf. This is in marked contrast to the orientation of the depositional slope in the remainder of the Kilohigok Basin to the south.

Paleoslope trends indicated by palocurrent data from the Western River and Burnside River formations of the Axial Zone and central part of the Eastern Platform of the Kilohigok Basin, together with those from the Hadley Formation, describe a subradial pattern about a proposed east-west trending depositional trough in the Coronation Gulf area. The existence of such a depression was first postulated by Hoffman (in press), which he interpreted as a failed arm developed off the Coronation Geosyncline. The continental re-entrant structure proposed by Hoffman and supported by evidence above, is here termed the Taktu* aulacogen.

The Axial Zone of the Kilohigok Basin, and possibly a similar structure extending toward Hadley Bay, developed as splays off the eastern terminus of the Taktu aulacogen. The scale, orientation, and in part the sedimentary fill, are similar to the Lancaster Aulacogen (Kerr, 1980). The significance of the Taktu failed arm, its control over sedimentation and dispersal patterns in the Kilohigok, Takijuq and Tree basins is the subject of another paper (Campbell and Cecile, in press).

If the admittedly tenuous correlation between Units 3, 4 and the Ellice Formation is correct, then the Elu Basin of the Bathurst Inlet-Melville Sound area (Campbell, 1979) may have developed in an embayment separated from correlative craton-margin basins or embayments by an elevated area approximately in the central part of Victoria Island.

Economic Geology

No significant mineral showings or anomalous zones of radioactivity were located during the course of the mapping.

Acknowledgments

Field work was generously supported through the facilities and staff of the Polar Continental Shelf Project in Resolute. Dr. W.A. Gibbins of DIAND, Yellowknife, arranged for all logistical support and assisted in the field.

Discussions with P.F. Hoffman and J.C. McGlynn were of considerable help. The manuscript was critically read and improved by G.D. Jackson and J.C. McGlynn.

References

Campbell, F.H.A.
1979: Stratigraphy and sedimentation in the Helikian Elu Basin and Hiukitak Platform, Bathurst Inlet-Melville Sound, Northwest Territories; Geological Survey of Canada, Paper 79-8, 18 p.

Campbell, F.H.A. and Cecile, M.P.
1979: The northeastern margin of the Aphebian Kilohigok Basin, Melville Sound, Victoria Island, District of Franklin; in Current Research, Part A, Geological Survey of Canada, Paper 79-1A, p. 91-94.

The evolution of the early Proterozoic Kilohigok Basin; in Proterozoic Basins of Canada; Geological Survey of Canada, Paper 81-10. (in press).

Dixon, J.
1979: Comments on the Proterozoic stratigraphy of Victoria Island and the Coppermine area, Northwest Territories; in Current Research, Part B, Geological Survey of Canada, Paper 79-1B, p. 263-267.

Hoffman, P.F.
1981: Revision of stratigraphic nomenclature, foreland thrust-fold belt of Wopmay Orogen, District of MacKenzie; in Current Research, Part A, Geological Survey of Canada, Paper 81-1A, Report 34.

Wopmay Orogen: a Wilson Cycle of early Proterozoic age in the northwest of the Canadian Shield; in The Crust of the Earth and its Mineral Resources, D.W. Strangway, editor, Geological Association of Canada Special, Paper 20. (in press)

Kerr, J. Wm.
1980: Structural framework of Lancaster Aulacogen, Arctic Canada; Geological Survey of Canada, Bulletin 319, 24 p.

Thorsteinsson, R. and Tozer, E.T.
1962: Banks, Victoria, and Stefansson Islands, Arctic Archipelago; Geological Survey of Canada, Memoir 330, 83 p.

Young, G.M. and Jefferson, C.W.
1975: Late Precambrian shallow water deposits, Banks and Victoria Islands, Arctic Archipelago; Canadian Journal of Earth Sciences, v. 12, p. 1734-1748.

*Taktu is the Inuit word for fog, thus an appropriate name for the structure.

4. SOME ASPECTS OF THE PRE-CARBONIFEROUS GEOLOGY OF SAINT JOHN, NEW BRUNSWICK

Project 730044

K.L. Currie, R.D. Nance[1], G.E. Pajari Jr.[2] and R.K. Pickerill[2]
Precambrian Geology Division

Currie, K.L., Nance, R.D., Pajari, G.E., Jr., and Pickerill, R.K., Some aspects of the pre-Carboniferous geology of Saint John, New Brunswick; in Current Research, Part A, Geological Survey of Canada, Paper 81-1A, p. 23-30, 1981.

Abstract

Much of the ground examined is underlain by a major antiform with a diapiric core of Brookville Gneiss of probable Aphebian age. About 850 Ma ago this core penetrated the unconformably overlying Green Head Group, a platformal carbonate assemblage. The Brookville Gneiss had already undergone one episode of partial melting prior to this event, and diapirism probably was triggered by another episode of intensive partial melting, generating major plutons emplaced essentially contemporaneously with diapirism. Both the Brookville Gneiss and the Greenhead Group were relatively cold and brittle during emplacement of the Coldbrook Group of acid volcanics about 750 Ma ago, but the gneiss underwent another period of partial melting in Ordovician time which created or strengthened the D_1 flow fabric in the Green Head Group. The Green Head, Coldbrook and (Paleozoic) Saint John groups underwent flexural slip deformation (D_2, D_3) and low grade regional metamorphism subsequent to this event, but evidence of these events is sparse in the core, possibly due to reworking during the Devonian Acadian orogeny.

Introduction

A succession of geologists have studied the geology of the city and district of Saint John for more than 130 years. Despite a vast amount of work, many of the relations between the major units and the relations of plutonic rocks to supracrustal units remain obscure. We here report the initial results of a multidisciplinary study intended to elucidate the origin and development of the rocks of the St. John area, and to interpret them in terms of current tectonic models.

Regional Geology

Since the work of Hayes and Howell (1937) and Alcock (1938), a five-fold division of the rocks of the Saint John region has become traditional, namely (i) a suite of plutonic rocks, termed Golden Grove suite by Hayes and Howell (1937), (ii) the Green Head Group, an assemblage of metamorphosed platformal sedimentary rocks, (iii) the Coldbrook Group, predominantly acid volcanic rocks with lesser amounts of sedimentary rocks, (iv) the Saint John Group of sedimentary rocks of Cambrian to early Ordovician age, and (v) a heterogeneous suite of Carboniferous and younger sedimentary and volcanic rocks. Much of the Carboniferous succession has been involved in a series of northerly transported thrust slices (Rast and Grant, 1973), and displays a structural style quite different from that of the older rocks. We here confine our remarks to the pre-Carboniferous succession and the Mississippian Kennebecasis Formation as exposed in the ground between St. John and Hammond rivers, and between Kennebecasis Bay and the 'Variscan Front' of Rast and Grant (1973), a rhombohedral area of about 300 km^2 (Fig. 4.1).

The major units within this area exhibit a crudely concentric pattern, with the plutonic rocks forming a central core, surrounded successively by the Green Head Group, the Coldbrook Group and the Saint John Group. In a general way this succession corresponds to decreasing age, and the pattern therefore appears antiformal. In the following descriptions of lithologic units we discuss the units in order of deduced decreasing age of protolith. However within the central plutonic core the concept of relative age bristles with difficulties, as will become clear from subsequent discussion. We have therefore elected to discuss all of the units of this core together.

Description of Units

The central plutonic core Hayes and Howell (1937) introduced the name Golden Grove suite for a variety of plutonic and metamorphic rocks crossing the mapped area in a narrow belt from northeast to southwest. This belt rarely exceeds one kilometre in width, although it branches in complex fashion. Despite a variety of compositions, textures and contact relations, the rocks of this belt differ in both composition and structural style from other units in the region. In order to emphasize this kinship while avoiding any implication of temporal relations between the various units, we term this belt the central plutonic core.

The oldest protolith appears to be a rather homogeneous biotite-quartz-feldspar and biotite-hornblende-quartz-feldspar gneiss, termed the Brookville Gneiss by Wardle (1977). the Brookville Gneiss (unit A_b) can be traced along the southeastern side of the central core for almost 20 km from Golden Grove to Green Head, distinguished by (a) strong planar structure, commonly gneissosity but locally schistosity, (b) abundance of aligned biotite, and (c) paucity of potash feldspar. Commonly the gneiss appears homogeneous on outcrop scale, although a variety of boudins, dykes and inclusions occur locally. Basic and salic bands, varying from a few millimetres to a few centimetres in width differ only in relative contents of minerals. The proportions of minerals change gradually from northeast to southwest, becoming richer in amphibole. The Brookville Gneiss is truncated by the basic complex (H_b) along a line extending from Golden Grove to south of Duck Lake, and has not been seen to the northeast. The southwestern termination of the belt has not been observed by us.

The gneiss does not exhibit a great deal of small scale folding, although complex minor folding occurs within narrow linear zones a few metres across. Numerous generations of small folds are implied by complex interference patterns among small folds which are roughly coplanar but show very diverse hinge lines. Gentle sinuosities in gneissosity are ubiquitous, but difficult to relate to any major structure. Large outcrops exhibit "necking" of gneissosity similar to boudinage but not obviously related to competency contrast. The necking appears regularly distributed, about one per 100 m^2. Inclusions or boudins in the gneiss commonly exhibit margins of disturbed gneissosity reminiscent of turbulent flow.

[1] Department of Geology, Ohio University, Athens, Ohio 45701

[2] Department of Geology, University of New Brunswick, Fredericton, N.B., E3B 5A3

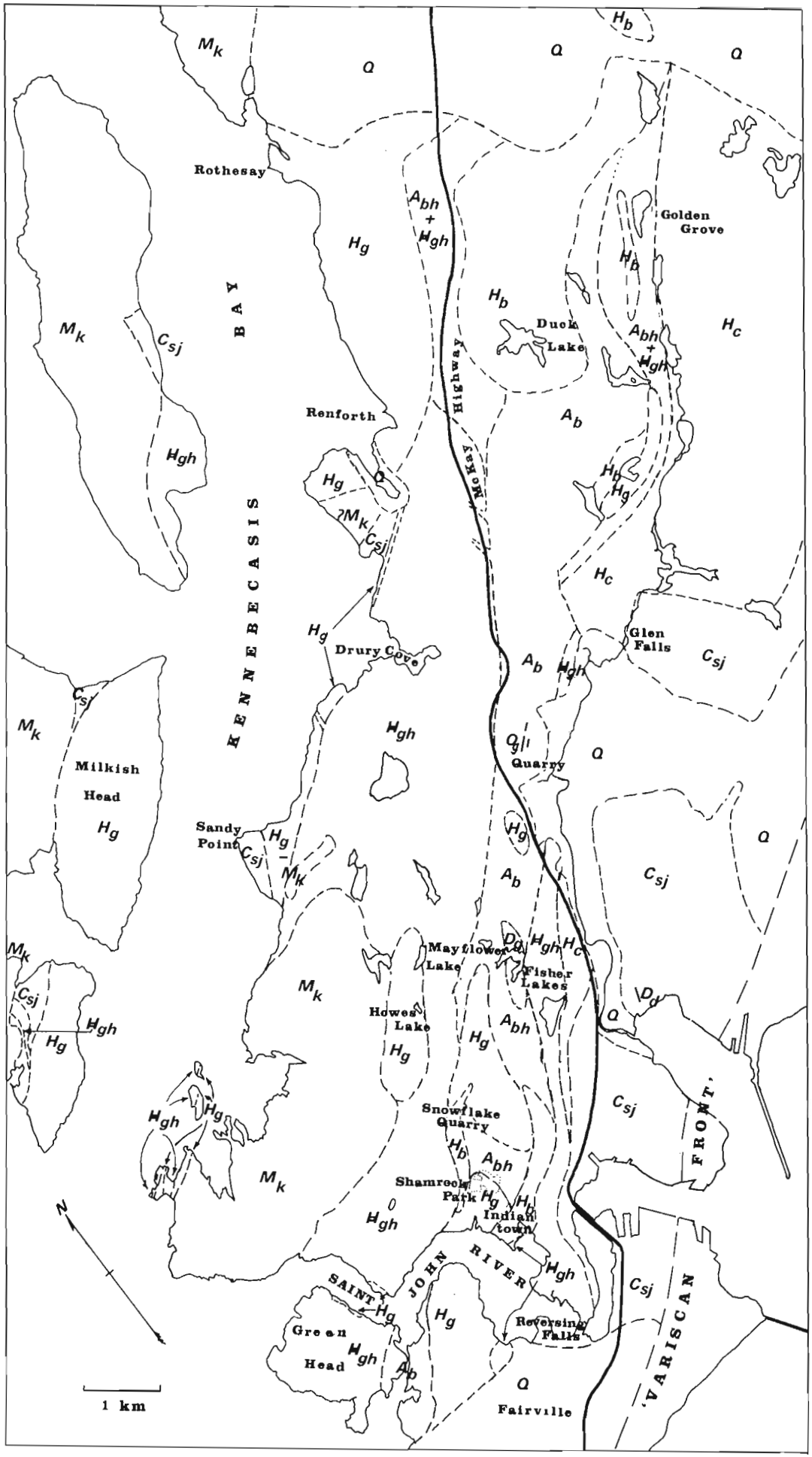
Rothesay
Golden Grove
Duck Lake
Highway
Renforth
Glen Falls
Drury Cove
Milkish Head
Sandy Point
Quarry
Mayflower Lake
Fisher Lakes
Howes Lake
Snowflake Quarry
Shamrock Park
Indian town
Reversing Falls
Green Head
Fairville
KENNEBECASIS BAY
SAINT JOHN RIVER
VARISCAN FRONT
N
1 km

LEGEND

QUATERNARY

Q — Glacial drift: ss – stratified sand and gravel; b – boulder till

– unconformity –

MISSISSIPPIAN

M_K — Kenebecasis Formation: cg – conglomerate;
ss – red sandstone and siltstone

– unconformity –

DEVONIAN ?

D_g — Biotite-hornblende granite and quartz monzonite: fl – Fisher Lakes pluton

– intrusive to gradational contact –

D_d — Doleritic and diabasic plugs (may be younger than D_g)

– intrusive contact –

ORDOVICIAN

O_g — Tourmaline-muscovite leucogranite

– intrusive to gradational contact –

CAMBRIAN TO EARLY ORDOVICIAN

C_{SJ} — Saint John Group: mc – Middle Cambrian to early Ordovician black to grey siltstone and shale;
gf – Glen Falls Formation; quartzite, pebble conglomerate;
rb – Ratcliffe Brook Formation; red sandstone and conglomerate

– unconformity –

HADRYNIAN

H_d — Chloritized basic dykes

– intrusive contact –

H_C — Coldbrook Group: t – red to green tuff, siltstone, shale;
f – red to green agglomerate, crystal tuff, lahar deposits;
a – grey green to violet fine-grained acid igneous rocks

– unconformity or intrusive contact –

H_g — Granitoid plutonic rocks: ea – epidote alaskite;
hb – biotite-hornblende quartz diorite and granodiorite;
mi – migmatite of H_g with H_b

– intrusive to gradational contact –

H_b — Basic complex: i – gabbro, diorite, hornblendite with relict igneous textures;
a – amphibolite, chloritized mafic rocks, with mafic dyke complex;
mc – mafic rocks with megacrysts of alkali feldspar;
d – dykes related to H_b

– intrusive contact –

HELIKIAN ?

H_{GH} — Green Head Group: c – grey blue calcite marble;
d – brownish dolomitic marble;
q – fine grained white quartzite;
s – rusty black siltstone and semi-pelite;
sm – thin-banded siltstone-marble sequence

(NOTE: Subdivisions not in stratigraphic order)

– unconformity –

APHEBIAN ?

A_g — Gneissic, fine grained biotite leucogranite

– gradational contact –

A_{bh} — Chloritized, epidotized Brookville Gneiss with potash feldspar porphyroblasts (younger than H_{GH} in part)

– gradational contact –

A_b — Brookville Gneiss: mesocratic, fine-banded biotite-quartz-feldspar gneiss with amphibolitic intercalations and boudins

Figure 4.1 *Geological sketch of the Saint John region, New Brunswick. Geology in part after Wardle (1977) and Hayes and Howell (1937).*

Many contacts between the Green Head Group and Brookville Gneiss are exposed in roadcuts on McKay Highway. In general the gneissosity in the gneiss and Green Head Group is close to parallel. In detail, marbles and siltstones of the Green Head Group commonly intrude the gneiss either in the form of dykes or as bulbous protrusions. Many marble dykes, some with screens or inclusions of siltstone, were mapped within the gneiss complex. Projections of gneiss into the Green Head Group are fairly common, and major boudins of Green Head Group within the gneiss occur at two localities. These complex relations led earlier workers to suggest that the Brookville Gneiss represented highly metamorphosed Green Head Group (Alcock, 1938; Wardle, 1977). We consider this unlikely because (a) the generally tonalitic composition of the gneiss is incompatible with derivation from a platformal sedimentary assemblage (no quartzite, marble or pelitic units), (b) the gneiss exhibits at least two periods of mafic dyke emplacement not seen in the Green Head, and (c) the structural style shows that the gneiss has been mobilized on several occasions compared to only one for the Green Head Group. On field mapping grounds we believe the Brookville Gneiss to be substantially older than the Green Head Group. Olszewski et al. (1980) dated zircons from the Brookville Gneiss, and obtained a discordant age with an upper intercept of 1640 Ma and a lower intercept of 380 Ma. Stevens (personal communication, 1980) reports a similar lower intercept for another zircon sample, with an ill-defined upper intercept in excess of 1100 Ma. We believe the older ages (Paleohelikian or Aphebian) represent the age of the protolith, with the younger ages showing the date of latest metamorphism during the Acadian orogeny.

The Brookville Gneiss exhibits little retrogressive metamorphism in typical outcrops, but large areas of gneiss have been chloritized and epidotized to the extent that the rock takes on a greenish hue. Such rocks contain large numbers of small pink feldspar porphyroblasts aligned in the gneissosity plane (unit A_{bg}). Such gneisses characteristically occur along the margins of younger plutons. The rocks abound in inclusions and boudins of amphibolite, and locally grade to agmatite. Along the margins of plutons of unit H_g altered gneisses may show megacrysts of orange potash feldspar up to 10 cm across. Altered megacrystic gneisses locally grade imperceptibly to unit $H_{g_{hb}}$.

The Brookfield Gneiss terrane contains significant amounts of a leucocratic, fine grained biotite granite gneiss (unit A_g) which commonly forms a minor but intimate component of the gneiss, but is locally found in mappable amounts. This material exhibits the complex small structure of the gneiss previously referred to. The contacts with more typical gneiss are nebulous and gradational, commonly of lit-par-lit type, rather than cross cutting.

The oldest discrete plutons of the central core appear to be mafic bodies (unit H_b). These bodies differ considerably among themselves. North of Duck Lake and at Indiantown, small areas display relict igneous textures, including cumulate ultramafic pods. However most bodies consist of amphibolites of varying grain size and degree of alteration, commonly riddled with several generations of dykes, most of which are probably related to their host. Although the mafic plutons are commonly intensely brecciated and altered, locally almost beyond recognition, they rarely show distinct foliation. The marginal parts of the basic bodies grade to, interdigitate with, and are hybridized by a white hornblende quartz diorite (unit $H_{g_{hb}}$). Although units H_g and H_b display many similarities, including similar degrees of sericitization and epidotization, and similar histories of dyke intrusion, as well as the transitions just noted, the granitoid rocks consistently intrude the mafic rocks. In addition to the type of relation just noted, the mafic complex may exhibit agmatite of mafic blocks in granitoid matrix (Duck Lake region) or marginal zones overprinted by megacrysts of orange potash feldspar (along contacts with $H_{g_{hb}}$ in the northern part of Shamrock Park). We estimate that one quarter to one third of the central core is underlain by mafic rocks, and in the northeastern part of the core no other rock types were observed.

Hornblende-bearing granitoid rocks (unit H_g) probably genetically related to the mafic complexes, form the largest and most easily recognized plutons within the central core. We distinguish five major bodies, the Renforth, Milkish Head, Fairville, Mayflower Lake and Rockwood Park plutons, as well as several minor bodies. Most of the major plutons intrude the Green Head Group as well as the central core. The Renforth Pluton lies on the shore of Kennebecasis Bay for 10 km from Rothesay to Sandy Point. The rock grades inward from fine grained hornblende quartz diorite to biotite hornblende granodiorite or quartz monzonite. Rocks of this pluton can be easily distinguished by their finely poikilitic (with plagioclase) hornblende. The Milkish Head Pluton consists of roughly equal amounts of potash feldspar, plagioclase and quartz with biotite as the predominant mafic mineral. Wardle (1977) correlated this mass with the Renforth pluton, which would make a mass of batholithic dimensions. In our opinion this correlation is incorrect, since the body at Milkish Head is much richer in potash feldspar and biotite. The Fairville pluton stretches from south of Green Head across the St. John River into the southern part of Shamrock Park. The pluton contains euhedral to ovoid megacrysts of pink potash feldspar scattered throughout, and is surrounded by an aureole of megacrysts. The Mayflower Lake pluton, emplaced in the Green Head Group, is a homogeneous mass of quartz diorite, while the nearby Rockwood Park pluton almost totally lacks dark minerals, consisting of potash feldspar, quartz and epidotized plagioclase. Where plutons of unit H_g intrude the gneissic core, they tend to be potassic and megacrystic, with nebulous boundaries, whereas plutons intruding the Green Head Group tend to be low in potassium feldspar, equigranular, and display sharp contacts, commonly with contact aureoles.

The hornblendic granitoid rocks are commonly massive, but layering is locally seen for example on Somerset Street at the power line. Some outcrops display striking evidence of remobilization and crystallization. At the east end of the running track in Shamrock Park, separated and partially assimilated blocks of two ages of mafic dykes can be seen, as well as a large inclusion of Brookville Gneiss. This outcrop, as well as many other exposures of unit H_g, displays two generations of hornblende phenocrysts (or porphyroblasts).

Major mafic dyke swarms occur in and around the Renforth and Mayflower Lake plutons. Dykes of these swarms can be distinguished by (1) abundant epidote-filled fractures, (2) weak fabric but no gneissosity. Such dykes can easily be distinguished from older gneissic, amphibolitic dykes and two or more generations of younger dykes lacking epidote.

The hornblendic plutonic rocks (units H_b and H_g) exhibit abundant cataclastic zones consisting of assemblages of fragments 5-10 cm on a side in a sheared chlorite-epidote paste. Such breccias commonly rim plutons, presumably due to late relative movement between pluton and host.

In some regions the Brookville Gneiss is infested by small, diffuse bodies of muscovite-tourmaline granite (unit O_g), for example in the quarry south of Rothesay interchange on McKay Highway. Granites tend to occur in zones some tens of metres across, commonly along the axial planes of small folds. Individual bodies rarely exceed 60 by 15 cm in plan, although larger dyke-like bodies occur. Tourmaline occurs in poikilitic clots up to one centimetre across, while distinctly greenish muscovite forms books up to

2 cm across. The granite is massive, but slightly altered, and the contacts are not sharp, but diffuse across several centimetres. Quarrying with a sledge-hammer showed that the individual bodies are not connected. The number, diffuseness and lack of feeders suggests that these bodies formed in situ, presumably by partial melting, possibly modified by metasomatism. Olszewski et al. (1980) obtained a discordant zircon age from these rocks with an upper intercept of 465 Ma (Ordovician).

The youngest plutonic rock within the central plutonic core appears to be a massive biotite-hornblende granite outcropping around Fisher Lakes (unit D_g), with unusual, almost round quartz grains up to 2 cm across. No dykes have been observed in this pluton, which is essentially unaltered. The pluton is weakly megacrystic near its boundaries, which are gradational. Although the pluton resembles other hornblendic acid plutons (of unit H_g) it appears to be younger since it clearly intrudes the Rockwood Park pluton, and shows no evidence of dyking, alteration, or later remobilization. The lack of alteration suggests that it may be younger than the Ordovician (?) muscovite-tourmaline granite, hence we tentatively conclude that it may be of Acadian (Devonian) age.

With the exception of unit O_g, dated only by radiometric methods, the plutonic rocks of the central core can all be relatively dated by intrusive relationships to give the relative ages shown in the legend. The Brookville Gneiss, Greenhead Group and units H_g and H_b are all cut by dykes of Coldbrook Group. No dykes of any kind have been found within the Fisher Lakes pluton. In addition to these classical intrusive relationships, the Brookville Gneiss, Green Head Group and hornblendic plutons have been remobilized subsequent to original emplacement. The intrusive relations of these remobilized bodies fix the age and style of tectonic disturbances within the crystalline core subsequent to formation.

Green Head Group

The Green Head Group consists of marble, calcareous quartz siltstones, quartz-rich semipelitic rocks and lesser amounts of quartzite. The Green Head Group lies roughly symmetrically about the central plutonic core, although the southeastern belt is narrower than the northwestern one. Well preserved primary sedimentary structures can locally be detected, such as stromatolites in the marbles and depositional structures in the siltstones, and attempts have been made to erect a detailed stratigraphy within the Green Head Group (Wardle, 1977; Leavitt and Hamilton, 1962). We found these subdivisions to be unmappable because of the undetermined, but apparently large, amount of flowage within the group. Evidence of flow can be found on all scales from hand specimen folds with enormously attenuated limbs to marble dykes within Brookville Gneiss up to 10 m across. Attempts to trace units within areas of favourable outcrop suggest that few units can be traced more than 200 m without being truncated by boudinage, or lost in zones of massive, featureless marble. Even relatively large scale units, such as siltstone horizons tens of metres thick, do not persist over one kilometre. Detailed observations show that colour banding in marble is an unreliable guide to bedding, and usually represents a gneissosity. We believe that primary features within the Green Head Group were preserved because of small competency contrasts, and carried passively along in a surrounding plastic medium. In essence they represent tectonic inclusions. Stromatolite occurrences, though widely scattered, are small, and surrounded by banded marbles which are presumed to have flowed.

The most reliable guide to the early history of the Green Head Group seems to be its regional distribution. The group is essentially continuous around the central crystalline core, absent only in a small area near Glen Falls where it has been cut out by faults. However in the northern part of the mapped area the contact relations between the Green Head Group and the older gneisses are anomalous. Along McKay Highway and the parallel hydro line to the east, north to northwest trending septa of gneiss and Green Head Group from 20 to 200 m in width are exposed in a generally northeast trending zone over 2 km in width and more than 6 km in length. In general the gneissosities in the two units are parallel, but in detail the contacts are intrusive. Gneiss intrudes the Green Head Group and vice versa, often within a few metres. Faults of unknown, but probably small, displacement are common within the gneiss close to, but not on, the contacts. We interpret this zone to represent complex flowage of both Green Head Group and Brookville Gneiss, possibly related to the emplacement of the major Renforth and Duck Lake plutons which bound the zone.

Coldbrook Group

The Coldbrook Group, in general terms, surrounds the central core, separated from it by rocks of the Green Head Group. The Coldbrook Group is absent in the Reversing Falls region, due to tectonic or erosional removal, and near Glen Falls it contacts the Brookville Gneiss along a complex of faults. We have nowhere observed an untectonized contact between the main part of the Coldbrook Group and older rocks. However many dykes identical to grey green Coldbrook Group rhyolite and rhyodacite cut the central plutonic core and the Green Head Group. Along Golden Grove Road an embayment of Coldbrook Group rhyolite into the rocks of unit H_g could be a feeder to the nearby acid volcanics. In any event, the presence of the dykes and their similarity to the lower part of the Coldbrook Group shows that the displacement between the Coldbrook Group and the older rocks cannot be large. The intricately indentate character of the contact near Glen Falls suggests that the movements must be mainly vertical rather than strike slip. In light of the aphanitic character of the dykes in the central core, we regard the estimate of 5 km of vertical movement by Gupta (1975) to be grossly excessive. We see no obvious reason why the sequence Brookville Gneiss-Green Head Group-Coldbrook Group should not be an essentially complete, autochthonous sequence, presumably with unconformities separating the various units.

Within the Coldbrook Group there is a general tendency for the parts of the Group closest to older rocks to consist of distinctive pale grey green, dense, fine grained to aphanitic igneous rocks, whereas away from the older rocks the Group includes more fragmental and sedimentary material, and the colour becomes more reddish. As yet we have established no stratigraphy within the Coldbrook Group but in general the lower parts consist of more or less massive acid volcanic rocks, while the upper parts consist of reddish lahar material, crystal tuffs, tuffs, minor massive acid volcanics, and erratically distributed volcanogenic sandstone. Primary structures appear to be fairly widely distributed, but difficult to recognize due to the nature of the outcrop.

Kennebecasis Formation

The Kennebecasis Formation occurs as relatively large masses with linear boundaries (possibly fault bounded troughs), and as a great number of small outliers on older rocks. This formation appears to have covered much of the map area at one time. The lower part of the formation consists of very coarse conglomerate with chocolate brown matrix. The cobbles, up to 30 cm diameter consist of local lithologies densely packed together and locally imbricated.

The conglomerate contains lenses of brick-coloured, cross-bedded sandstone, and such sandstones become predominant in the upper part of the formation, although conglomerate lenses reappear erratically throughout the section, suggesting reactivated uplift of the source areas. All of the older lithologies, including all of the plutonic types, have been identified as cobbles within the Kennebecasis Formation. The age of the formation, although slightly uncertain, is commonly accepted on the basis of spore evidence as Early Mississippian (van de Poll, 1970).

Structure of the Green Head Group

We consider three aspects of the structure of the St. John area, namely late deformation by flexural slip and related mechanisms, early deformation dominated by flowage, and, finally, the megascopic structure of the region. Information on all three of these aspects can be gained from the Green Head Group, which was studied in detail in three sections of nearly continuous outcrop at Drury Cove, Howes Lake and the Snowflake Quarry. This belt of Green Head Group consists of two contrasting lithologies, namely marbles and rusty siliceous siltstones with minor quartzite. In addition to colour banding, blue-grey calcite marbles display a strongly orientated fabric of coarse calcite grains which commonly parallels the banding. The concordant lenses of brown dolomite marbles exhibit a less well defined fabric. The marbles contain thin intercalations of black chloritic phyllite. Centimetre-laminated grey and green siltstones occur as 5-50 m intercalations in the marble, and as large lensoid bodies up to 0.5 km across, where they are associated with 1-10 m beds of massive white quartzite and rare pelitic units. A weak fabric ranging locally to phyllitic cleavage and micaceous schistosity is invariably present and parallels the commonly preserved bedding. Primary structures include slumping, grading and crossbedding. Although bedding and carbonate banding are regionally parallel, they are locally discordant. Dyke-like apophyses of marble in siltstones, and complexly contorted boudins of siltstone in marble are common features of marble/clastic contacts.

Three phases of deformation can be determined on the basis of style, orientation and overprinting. Some of these may represent a single polyphase event, but we argue below that D_1 is a highly composite deformation, involving earlier, undifferentiated, events.

A pervasive bedding (S_0) or layering-parallel fabric (S_1) forms the earliest recognizable structure in outcrop. In the marbles this fabric is axial planar to centimetre-scale F_1 folds which are typically upright, similar-style structures with attenuated steep limbs and thickened hinge zones. Axes plunge broadly northeast or southwest at gentle to steep angles. The folds are defined by marble colour bands such that these are discordant to the fabric in hinge zones. (The colour bands are presumed due to pre-F_1 deformation by flowage, as discussed below.) F_1 folds are notably absent from the clastic lithologies except where these are layered with marble on a centimetre-scale. We suggest that the bulk of the D_1 strain was accommodated by flow in the marbles which shielded the clastic rocks from stress. Weak fabric in the dolomitic rocks, and preservation of stromatolites suggests that deformation was strongly inhomogeneous, presumably controlled by slight competency contrasts.

The most abundant mesoscopic structures are close to tight asymmetric folds (F_2) that deform S_1 in carbonates and clastics. These folds are broadly coaxial and coplanar with F_1, plunging to northeast or southwest at shallow to moderate angles. However rare mesoscopic interference in areas where F_1 and F_2 are not coplanar produces Type III refolded isoclines (Ramsay, 1962, p. 531).

F_2 folds in carbonates range from parallel to similar style structures with a local axial plane calcite fabric (S_2) which overprints S_1. In the clastics, F_2 folds are typically flexural structures with parallel or Class 3 profiles (Ramsay, 1962) and curvilinear axes. S_2 fracture cleavage fans are weakly developed in some siltstone laminae at Howes Lake, and intense fracturing parallel to the axial plane is common at fold closures and along the steeper limbs. Typically these folds lack an axial fabric however. At Drury Cove a locally intense S_2 crenulation cleavage produces an S_1/S_2 crenulation lineation (L_2) plunging south southwest at 40°.

At Drury Cove and Snowflake Quarry the asymmetry of F_2 folds varies systematically about similarly oriented megascopic structures which control the regional orientation of S_0/S_1 and have wavelengths up to 0.5 km. Fold closures are associated with faulting along axial surfaces, and axial traces show little continuity along strike. In the Snowflake Quarry several F_2 folds with wavelengths of the order of 100 m are arranged in en echelon fashion, and show rapid variations in amplitude along their axial traces, which do not exceed 0.5 km in length.

Close to tight flexural folds (F_3) locally deform both S_1 and F_2. These upright to reclined structures plunge broadly east or west. At Drury Cove, upright mesoscopic F_3 folds of parallel profile locally deform the L_2 crenulation lineation such that it preserves its angular relationship with respect to the F_3 axis, consistent with a flexural fold mechanism. Elsewhere at Drury Cove similarly oriented folds, whose asymmetry is inconsistent with their position within the megascopic F_2 structure, show an axial plane fracture cleavage considered to be S_3.

At Howes Lake the asymmetry of steeply southwest plunging minor folds varies systematically about a megascopic F_3 reclined structure, while mesoscopic F_2 folds of constant asymmetry are refolded such that they plunge west on the northern limb and south on the southern limb. No axial fabric is associated with this structure.

Kink bands occur occasionally in well cleaved pelitic lithologies. Sets dipping north and northeast occur at Drury Cove, and sets dipping southwest and southeast occur in the Snowflake Quarry. Intersecting kink bands have not been observed, and the relationships between these sets is unknown. They are probably late structures reflecting local fault movement. Numerous fractures, commonly displaying calcitic and chloritic slickensides, cut all lithologies of the Green Head Group. Three sets occur in the Snowflake Quarry, one parallel to S_1, others dipping east southeast and northwest, as well as rare vertical east-west fractures. No systematic study of these fractures has been attempted, and their significance is presently unknown.

Structure of the Saint John and Coldbrook Groups

D_2 and D_3 deformation of the Green Head Group appears to be related to deformation of the Saint John Group. The earliest deformation of the Saint John Group involved formation of a muscovite-chlorite fabric axial planar to the megascopic Saint John syncline, and broadly conformable with S_1 in the Green Head Group. As with the Green Head clastics, it is not associated with minor structures, but is refolded about mesoscopic northeast and southwest trending axes that parallel the Green Head F_2 folds (Wardle, 1977). In the Kennebecasis Bay area these second folds are refolded by gently west-plunging structures (Wardle, 1977) that are compatible with the F_3 folds in the Green Head.

Little is known about the internal structure of the Coldbrook Group, since its internal stratigraphy has not yet been established. However we observed mesoscopic folds

north of Glenview United Church which are apparently related in style and orientation to F_2 in the Green Head Group.

The ages of D_1, D_2 and D_3 are not definitely known, but if the above correlations are accepted, they postdate the youngest (Arenig) members of the St. John Group. Radiometric dating suggests partial melting in the plutonic core in Caradoc (465 Ma) time. We are inclined to put the early plastic (hot) deformation (D_1) at this time (Taconic), and the later flexural (cold) deformation at a later time, whether in the late stages of Taconic orogeny, the Devonian Acadian orogeny, or even in post-Devonian time. If the latter is the case, further study should reveal D_2 and/or D_3 in the Kennebecasis Formation.

Structure of the Plutonic Core

We have already noted that minor folds are scarce in the central plutonic core, and those that are present cannot be profitably applied to orthodox structural analysis. A number of qualitative but persuasive arguments suggest repeated deformation by flow and diapirism.

The Brookville Gneiss exhibits an early period of migmitization, now witnessed by the biotite granite gneiss (unit A_g). No trace of this episode is found in the Green Head Group. Hence this migmitization must either have occurred in pre-Green Head time, or at a time when the Brookville Gneiss was at a much deeper level than the Green Head Group.

The hornblende-bearing plutons (units H_g and H_b) produced major hybridization and metasomatism of the Brookville Gneiss, but very limited contact aureoles about chilled margins in the Green Head Group. These observations require that the present configuration of the Green Head Group and Brookville Gneiss results from relatively large upward movement of the latter (infrastructure) with respect to the former (superstructure). Wardle (1977) reached the same conclusion from quite different arguments, and emphasized the diapiric character of the gneiss. However the presence of fine-grained to aphanitic Coldbrook dykes cutting central core and Green Head Group alike shows that in Coldbrook time the plutonic core and the Green Head Group were at roughly similar tectonic levels and relatively cold.

The presence of apparently anatectic Ordovician granite in the plutonic core (unit O_g) suggests that further flowage of the core rocks may have occurred at this time, a suggestion enhanced by the notable lack of flexural slip structure in the core rocks. The relatively young (Acadian) ages obtained from some zircons suggests that the core rocks may also have been reactivated during Acadian orogeny.

Metamorphism

Metamorphic assemblages in the core rocks (quartz-plagioclase-biotite, quartz-plagioclase-biotite-hornblende) are compatible with upper amphibolite facies metamorphism, and partial melting of compositionally suitable bands, although they do not demonstrate such conditions. Many of the assemblages are now overprinted by retrograde assemblages dominated by chlorite and epidote. The hornblende-bearing granites were associated with extensive potash metasomatism which characteristically is found associated with amphibolite grade metamorphism.

Within the Green Head Group, sillimanite-bearing assemblages occur only within 200 m of the central plutonic core. The relations are best explained by contact metamorphism by the hot, rising core. Contact aureoles with local development of brucite, wollastonite and vesuvianite occur in marbles around basic dykes of H_g and younger age. However the bulk of the Green Head Group lies at low metamorphic grade characterized by coexistence of dolomite+quartz in marbles, and chlorite+muscovite in clastic rocks. Andalusite occurs locally in the latter, but we have not determined whether it is a regional or a contact metamorphic mineral. The Coldbrook and Saint John groups exhibit regional muscovite+chlorite assemblages. Allowing for the demonstrated temperature gradients outward from the central plutonic core, these assemblages are compatible with the regional metamorphic grade within the Green Head Group.

Discussion

We interpret the central plutonic core to form the core of a major antiform whose formation was dominated by upward flowage of the core. Within this structure virtually all major contacts have been modified by faulting, but we see no evidence of displacements on a km scale. A major diapiric episode occurred in post-Green Head pre-Coldbrook time (before 750 Ma according to Cormier, 1969), when the central core intruded the Green Head Group. This episode appears to have been closely linked to major plutonism in the core and Green Head Group (emplacement of units H_g and H_b) dated by Olszewski et al. (1980) at about 850 Ma.

Perhaps buoyancy associated with the generation of these units may have triggered diapirism. Within the central plutonic core a still earlier episode of partial melting had formed biotite granite gneiss (A_g). Subsequent to diapirism the rocks were cold and brittle during emplacement of the Coldbrook Group. By Ordovician time however the central core was again hot enough to generate partial melt (O_g). We assume the sillimanite-bearing assemblages in the Green Head Group, and initiation, or modification of the D_1 (flow) fabric in the Green Head Group, as well as regional metamorphism of the Green Head, Coldbrook and Saint John groups are related to this episode, which probably also included diapiric movement of the core. Yet further metamorphism and diapirism may have taken place during the Acadian orogeny, but evidence for this is at present scarce and equivocal. The surroundings of the central core deformed by flexural slip in post-Ordovician time.

We have at present no explanation for the confinement of diapirism to a narrow elongate zone. We assume it to be related to the megatectonic position of the Saint John area at the relevant times, but our present information is insufficient to permit informed speculation on plate tectonic considerations. It already seems clear that the Brookville Gneiss must be a fragment of an ancient continental basement, upon which formed a carbonate platform (Green Head Group). Since the Brookville Gneiss represents the oldest fragment yet discovered in the eastern Appalachians, the Saint John area promises the possibility of working out events leading up to and including the formation and destruction of the Iapetus Ocean.

References

Alcock, F.J.
1938: Geology of Saint John region, New Brunswick; Geological Survey of Canada, Bulletin 216, 65 p.

Cormier, R.F.
1969: Radiometric dating of the Coldbrook Group of southern New Brunswick, Canada; Canadian Journal of Earth Sciences, v. 6, p. 393-398.

Gupta, V.K.
1975: An interpretation of aeromagnetic and gravity data of Caledonian area, in southern New Brunswick; unpublished Ph.D. thesis, University of New Brunswick, Fredericton, New Brunswick.

Hayes, A.O. and Howell, B.F.
1937: Geology of Saint John, New Brunswick; Geological Society of America, Special Paper 5, 146 p.

Leavitt, E.M. and Hamilton, J.B.
1962: Geology of the Saint John area; New Brunswick Department of Natural Resources, Map 62-4 (sheets A and B).

Olszewski, W.J., Gaudette, H.E., and Poole, W.H.
1980: Rb-Sr whole rock and U-Pb zircon ages from the Greenhead Group, New Brunswick; Geological Society of America, Abstracts with Program, v. 12, no. 2, p. 76.

Ramsay, J.G.
1962: Folding and fracturing of rocks; McGraw-Hill, 568 p.

Rast, N. and Grant, R.J.
1973: The Variscan Front in southern New Brunswick; American Journal of Science, v. 273, p. 572-579.

van de Poll, H.W.
1970: Stratigraphical and sedimentological aspects of Pennsylvanian strata in southern New Brunswick; unpublished Ph.D. thesis, University of Wales, Cardiff, Great Britain.

Wardle, R.J.
1977: The stratigraphy and tectonics of the Greenhead Group: its relations to Hadrynian and Paleozoic rocks, southern New Brunswick; unpublished Ph.D. thesis, Unviersity of New Brunswick, Fredericton, New Brunswick.

5. FURTHER RECONNAISSANCE MAPPING OF THE PRECAMBRIAN SHIELD ON DEVON ISLAND, DISTRICT OF FRANKLIN

Project 760023

Thomas Frisch
Precambrian Geology Division

Frisch, Thomas, Further reconnaissance mapping of the Precambrian Shield on Devon Island, District of Franklin; in Current Research, Part A, Geological Survey of Canada, Paper 81-1A, p. 31-32, 1981.

Abstract

The Precambrian basement of eastern Devon Island appears to consist of alternating, broad, easterly-trending belts of biotite- and hypersthene-bearing granulites and chiefly pelitic metasediments, all in the granulite facies of metamorphism. The easterly structural grain in eastern Devon Island contrasts with the predominantly northerly trends in the adjacent basement terrane of southeastern Ellesmere Island and Coburg Island. Paleozoic carbonate rocks, previously unknown east of the Devon Ice Cap, were found over an extensive area on western Philpots Island.

Introduction

Project 760023 involves the reconnaissance mapping, at 1:250 000 scale, of the Canadian Shield on Ellesmere, Devon and Coburg islands, which constitutes the northernmost part of the Churchill Structural Province. Mapping on Ellesmere and Coburg islands was completed in 1977 (Frisch et al., 1978). Geological reconnaissance of eastern Devon Island (Fig. 5.1) was begun in 1978 and focused on the crystalline areas of the south coast and west of Sverdrup Glacier on the north coast (Frisch, 1979). Completion of the mapping was planned during a two-week period in 1980, using a helicopter under charter to the Polar Continental Shelf Project. Reconnaissance of the eastern coast and of Philpots Island was completed but persistent low cloud prevented access to much of the nunatak terrain in the interior of Devon Island.

Crystalline Basement

The crystalline basement terrane along the eastern coast consists essentially of alternating tracts of biotite-hypersthene granulite and metasediments. Gneissic trends, which parallel the margins of the tracts, generally strike east to northeast. The easterly preferred orientation contrasts markedly with the northerly trends in the adjacent granulite facies basement on Coburg Island and southeastern Ellesmere Island.

Granulite and granulite gneiss underlie the north coastal area from Belcher Point to Sverdrup Inlet and occur, on the east coast, between Johnson Point and Cape Parker and on southern Philpots Island. These are relatively homogeneous, medium grained, quartzofeldspathic rocks, greenish on fresh, and brown or red on weathered surfaces. Garnet is locally an important constituent and, where abundant, may signify a metasedimentary origin. Pink granite is almost invariably associated with the granulitic rocks. It forms veins, sheets, and larger intrusions, and predates the main deformation. Major granitic bodies, suspected to be hypersthene-bearing, occur along the coast westward from Cape Hardy.

Two major metasedimentary tracts form the coast between Belcher Point and Johnson Point and from south of Cape Parker to central Philpots Island. The presence of metasedimentary terranes around the head of Sverdrup Glacier and east of Sverdrup Inlet, on strike with the northern of these two tracts, suggests that the tract is at least 150 km long. Clearly, much of eastern Devon Island consists of supracrustal rocks.

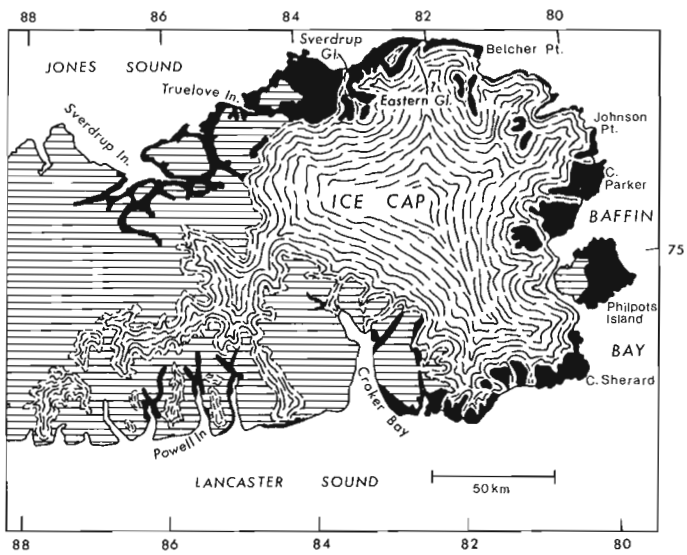

Figure 5.1. *Geological sketch-map of eastern Devon Island, showing the areas of Precambrian crystalline basement (black) and Paleozoic rocks (lined) and localities mentioned in the text.*

The metasedimentary belts are dominated by pelitic garnet-biotite schists and gneisses, commonly with sillimanite. Subordinate rocks include schistose psammitic rocks (metaquartzite and metagreywacke) and fine grained, garnetiferous, banded rocks possibly of metavolcanic origin. Amphibolite is relatively uncommon and only one thin marble bed was seen. The scarcity of marble provides another sharp contrast with the basement of Ellesmere and Coburg islands.

Pretectonic granite and pegmatite vein the supracrustals. A white weathering, garnetiferous, pegmatitic granite mass, several hundreds of metres thick, is associated with metasedimentary rocks east of the snout of Eastern Glacier.

All the metamorphic rocks appear to be in the granulite facies.

Diabase Dykes

Easterly- and southeasterly-trending diabase dykes form impressive swarms between Sverdrup Glacier and Truelove Inlet and on northern Philpots Island. They are present in smaller numbers throughout the rest of the Precambrian terrane.

Basement-Paleozoic Contact in Powell Inlet

Strongly weathered Precambrian basement rocks below basal Paleozoic sediments in steep cliffs on the eastern shore of Powell Inlet were first recognized by U. Mayr and R. Thorsteinsson of the Geological Survey of Canada, Calgary (personal communication, 1978). This occurrence is, in the author's experience, unique in the Ellesmere-Devon basement terrane.

The locality was briefly visited in 1980. About 35 m below essentially flat-lying Paleozoic strata, little-weathered Precambrian metasedimentary rocks grade rapidly into deeply-weathered material, some of which resembles fault gouge. Cutting the weathered zone are numerous shear planes, between some of which slivers of less altered rocks remain. The strong weathering was probably promoted by intense shearing, apparently of only local extent. Less than 20 km to the south, at the mouth of Powell Inlet, Proterozoic sedimentary rocks rest on fresh, hard granulite gneiss.

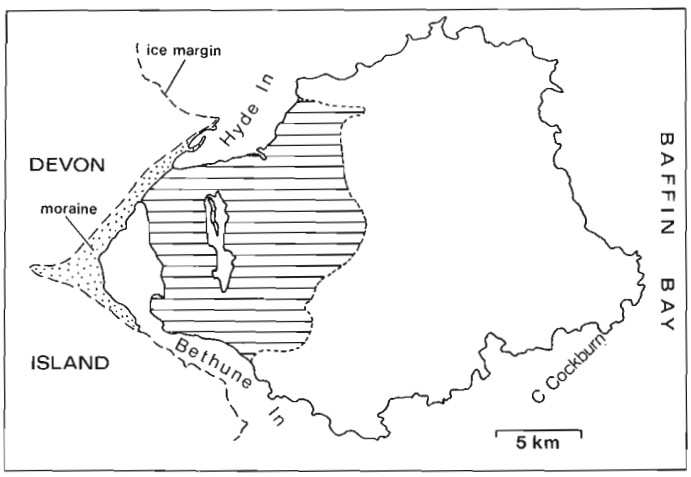

Figure 5.2. *Geological sketch-map of Philpots Island, showing the area underlain by Paleozoic rocks (lined). The eastern boundary of the Paleozoic area is interpretive, being based on limited outcrop and topography. The remainder of Philpots Island consists of Precambrian crystalline rocks.*

Paleozoic Rocks on Philpots Island

Prior to the present work, Philpots Island was generally considered to be underlain entirely by Precambrian crystalline rocks. However, on the basis of airphoto interpretation, L. Lazic (Petro-Canada, Calgary) recently suggested (personal communication to R.L. Christie, 1979) the presence of younger sedimentary, probably Paleozoic, rocks in the western part of the island, a low, swampy area of poor exposure. A brief visit by the author fully bore out Mrs. Lazic's prediction: scattered outcrops (now chiefly rubble), up to 5 m high, of flat-lying buff and orange dolomite and thin patches of felsenmeer of similar lithology occur in the area delineated in Figure 5.2. From samples and descriptions given him by the author, R. Thorsteinsson (Geological Survey of Canada, Calgary) considers it likely that the rocks belong to the Cass Fjord Formation of Middle Cambrian to Early Ordovician age. The nearest Paleozoic outcrops on Devon Island lie some 60 km to the west. There, the Cass Fjord Formation outcrops extensively near the base of the Paleozoic Arctic Platform sequence, in which it is generally separated from the Precambrian basement by thin Cambrian sandstones. On Philpots Island, no contact with the basement was seen.

The possibility remains that the sedimentary rocks on Philpots Island are Proterozoic in age, correlative with strata at the mouth of Powell Inlet, 155 km to the west, and on Bylot Island, 150 km to the south. However, lithologic differences render such correlation unlikely. Furthermore, easterly-trending diabase dykes, which postdate the Proterozoic, and predate the Paleozoic, strata of the region, are numerous in eastern Philpots Island; none was seen in the sedimentary terrane to the west.

Acknowledgments

I am indebted to the Polar Continental Shelf Project for generous helicopter and Twin Otter flying time and other support and assistance at Resolute Bay. I also thank Tom Stauffer (Okanagan Helicopters) for his outstanding flying. The Arctic Institute of North America kindly allowed use of their camp at Truelove Inlet.

References

Frisch, T.
1979: Reconnaissance studies of the Precambrian crystalline basement on Devon Island, District of Franklin; in Current Research, Part A, Geological Survey of Canada, Paper 79-1A, p. 113-114.

Frisch, T., Morgan, W.C., and Dunning, G.R.
1978: Reconnaissance geology of the Precambrian Shield on Ellesmere and Coburg islands, Canadian Arctic Archipelago; in Current Research, Part A, Geological Survey of Canada, Paper 78-1A, p. 135-138.

6.

PRELIMINARY RADIOMETRIC ANALYSES OF ZIRCONS FROM THE MOUNT COPELAND SYENITE GNEISS, SHUSWAP METAMORPHIC COMPLEX, BRITISH COLUMBIA

Project 730046

A.V. Okulitch[1], W.D. Loveridge[2], and R.W. Sullivan[2]

Okulitch, A.V., Loveridge, W.D., and Sullivan, R.W., Preliminary radiometric analyses of zircons from the Mount Copeland syenite gneiss, Shuswap Metamorphic Complex, British Columbia; in Current Research, Part A, Geological Survey of Canada, Paper 81-1A, p. 33-36, 1981.

Abstract

The isotopic ratios resulting from Pb and U analyses on three zircon fractions from syenite gneiss intrusive into metasediments of the Shuswap Metamorphic Complex are collinear on a concordia plot and yield upper and lower intercepts of about 773 Ma and 70 Ma. The upper intercept is tentatively interpreted as the minimum age of emplacement. The lower intercept is suggested to be the time of uplift and cooling associated with tectonic denudation of the Shuswap Complex. The implied age of the country rocks is pre-late Proterozoic and they may be correlatives of the Purcell Supergroup.

Introduction

The setting, petrology, origin and structure of the Mount Copeland syenite gneiss (Fig. 6.1) have been fully described by Fyles (1970) and Currie (1976a) who suggested an igneous origin prior to polyphase deformation and high grade metamorphism of the syenite and its host sedimentary rocks. Although neither its age nor that of the sediments was known, studies elsewhere in the Shuswap Complex (Wheeler, 1965; Reesor and Moore, 1971; Höy, 1979) gave rise to hypotheses correlating the sedimentary rocks with late Proterozoic to early Paleozoic strata in the Kootenay Arc east of the Complex. The emplacement of the syenite was implied to follow early Paleozoic sedimentation and to precede the Jura-Cretaceous Columbian Orogeny. A K-Ar date of 48 Ma from the intrusion (Currie, 1976b) is similar to many obtained from Shuswap Complex and probably represents a time of rapid uplift and cooling (cf. Okulitch, 1978).

Determination of the age of the syenite and definition of closer limits on the age of strata in the Shuswap Complex was deemed necessary for clearer understanding of the evolution of the Complex and its role in Cordilleran tectonics.

Analytical Procedures and Results

Zircon concentrates were prepared and analyzed using standard procedures established by the Geological Survey's geochronology laboratory, Ottawa (Sullivan and Loveridge, 1980). Results are presented in Table 6.1 and Figure 6.2.

Zircons from the +149 µm non-magnetic fraction are short, subeuhedral, with dark, "bubbly" textured, inclusion rich, brown inner zones which we interpret as cores, and clear to pale yellow outer zones which we interpret as overgrowths. The cores are generally rounded and constitute about 50 per cent of the total volume. The magnetic +149 µm fraction is similar (Fig. 6.3A) except that core material is more plentiful. The -64 µm + 44 µm fraction (Fig. 6.3B) contains numerous euhedral crystals with small, rounded and irregular cores. Clear material predominates.

Interpretations

Zircon morphology suggests that clear euhedral material grew over the dark cores. The core zircons are interpreted to have formed about 773 Ma ago during crystallization of the alkaline magma. The possibility that the core zircons are detrital and that the magma was emplaced much later is not considered likely. Alkaline magmas are postulated to be derived from sub-crustal sources (Currie, 1976b); they are not the products of crustal anatexis. Available chemical and petrographic data do not suggest significant crustal contamination of the magma (Currie, 1976a).

After emplacement, the core zircons suffered polyphase deformation, metamorphism and local anatexis (Currie, 1976a) during which they were rounded and overgrown by clear zircon material. Growth of the latter presumably ended prior to 70 Ma ago and final uplift and cooling occurred about 50 Ma ago. Zircon morphology is consistent with analytical results; the fraction with the greatest proportion of core material lies highest on the concordia plot chord; the fraction containing mostly clear overgrowths lies near the lower intercept (Fig. 6.2).

Emplacement of the syenite coincided approximately with a thermal event (circa 772 Ma; R.K. Wanless, personal communication, 1974) in the Malton Gneiss 125 km to the north, granitic intrusion in the Thor-Odin nappe (750 Ma, 755 Ma; Read, 1980a) 75 km to the south and with the East Kootenay Orogeny (Douglas et al., 1970, p. 373).

The age of the sediments intruded by the syenite must be greater than 773 Ma and less than about 2000 Ma, a date obtained from granitoid gneiss (Duncan, 1978; R.L. Armstrong, personal communication, 1979) lying unconformably (Fyles, 1970) below the sediments. Tentative correlation of the sedimentary rocks with late Proterozoic to early Paleozoic strata of the Kootenay Arc is not supported by data presented here, nor by detailed studies near Mount Copeland (Fyles, 1970, p. 37-39) and to the south (Read, 1980b). These sedimentary rocks may be correlative with strata of the Purcell Supergroup in southeastern British Columbia (Read, 1980b) or may predate them.

The results reported here have high analytical uncertainty (Fig. 6.2) but will be refined by additional analyses using improved techniques currently under development by the geochronology laboratory. If confirmed, these results will necessitate significant revision of models of the tectonic evolution of the Shuswap Complex. For example, the Complex must now be viewed as predominantly Precambrian crystalline basement mantled by Helikian to Early Hadrynian metasedimentary rocks without significant amounts of Paleozoic rock. The relationship of this basement mass to the North American craton must be re-assessed; the former may be allochthonous. The development of the Complex has clearly involved numerous episodes of deformation, metamorphism and plutonism from Archean to Tertiary times. It is not necessarily, therefore, primarily a product of Mesozoic orogenesis. Its final exposure must have

[1] Institute of Sedimentary and Petroleum Geology

[2] Precambrian Geology Division

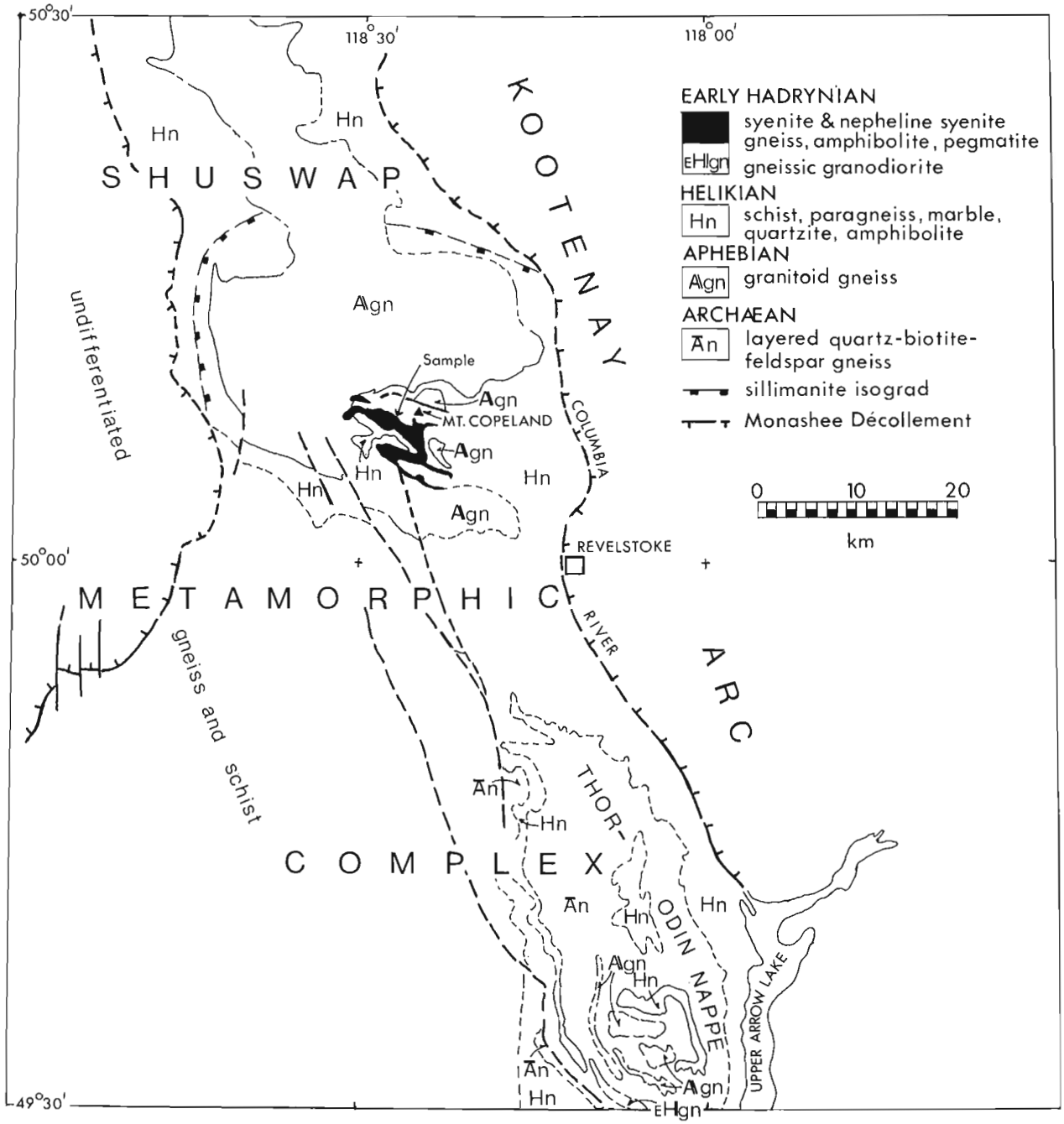

Figure 6.1. *Setting of the Mount Copeland syenite gneiss and geology of part of the Shuswap Metamorphic Complex. Data primarily from Read (1980a), Brown (1980), Currie (1976a) and Fyles (1970).*

Table 6.1

Mount Copeland Syenite Gneiss

Sample Number:		WN-4-74		
Location:		51°07'30"N, 118°26'30"W		
Lithology:		porphyritic syenite gneiss		
Size fraction (μm)		+149 magnetic	+149 non-magnetic	-64 + 44
Observed	$^{206}Pb/^{204}Pb$	50.5	71.9	62.2
Abundances* ^{206}Pb=100	^{204}Pb	1.783	1.168	1.439
	^{207}Pb	31.965	22.886	26.136
	^{208}Pb	138.67	122.78	84.522
Weight (mg)		6.29	5.98	4.93
Total Pb (ng)		26.4	24.7	30.1
Pb blank (%)		7.6	8.1	7.5
Radiogenic Pb	(ppm)	7.722	6.417	6.863
	(%)	53.31	66.25	51.54
U (ppm)		115.9	108.1	434.3
Atomic ratios	$^{206}Pb/^{238}U$	0.036543	0.033437	0.012532
	$^{207}Pb/^{235}U$	0.31003	0.27390	0.086687
	$^{207}Pb/^{206}Pb$	0.061527	0.059407	0.050165
Age (Ma)	$^{206}Pb/^{238}U$	231.4	212.0	80.3
	$^{207}Pb/^{235}U$	274.2	245.8	84.4
	$^{207}Pb/^{206}Pb$	657.7	582.1	202.7

*After subtraction of lead blank.

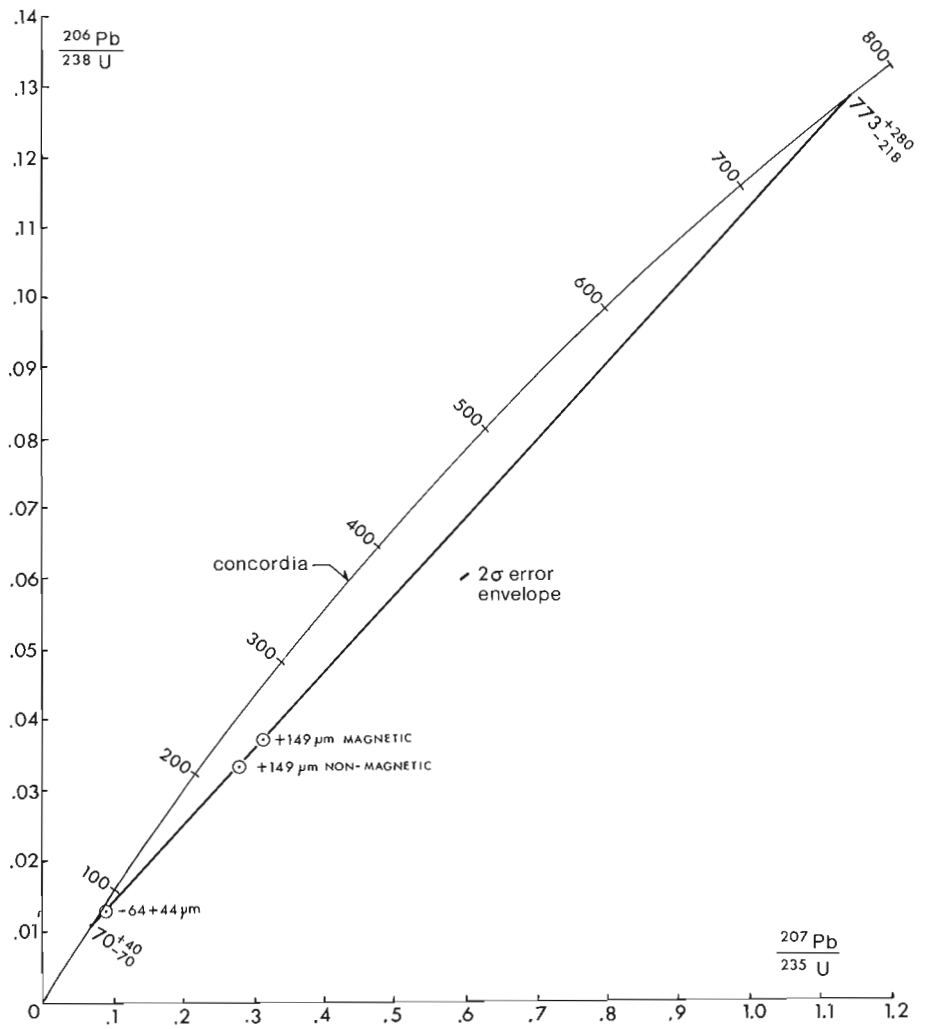

Figure 6.2

Concordia diagram for zircons in the Mount Copeland syenite gneiss.

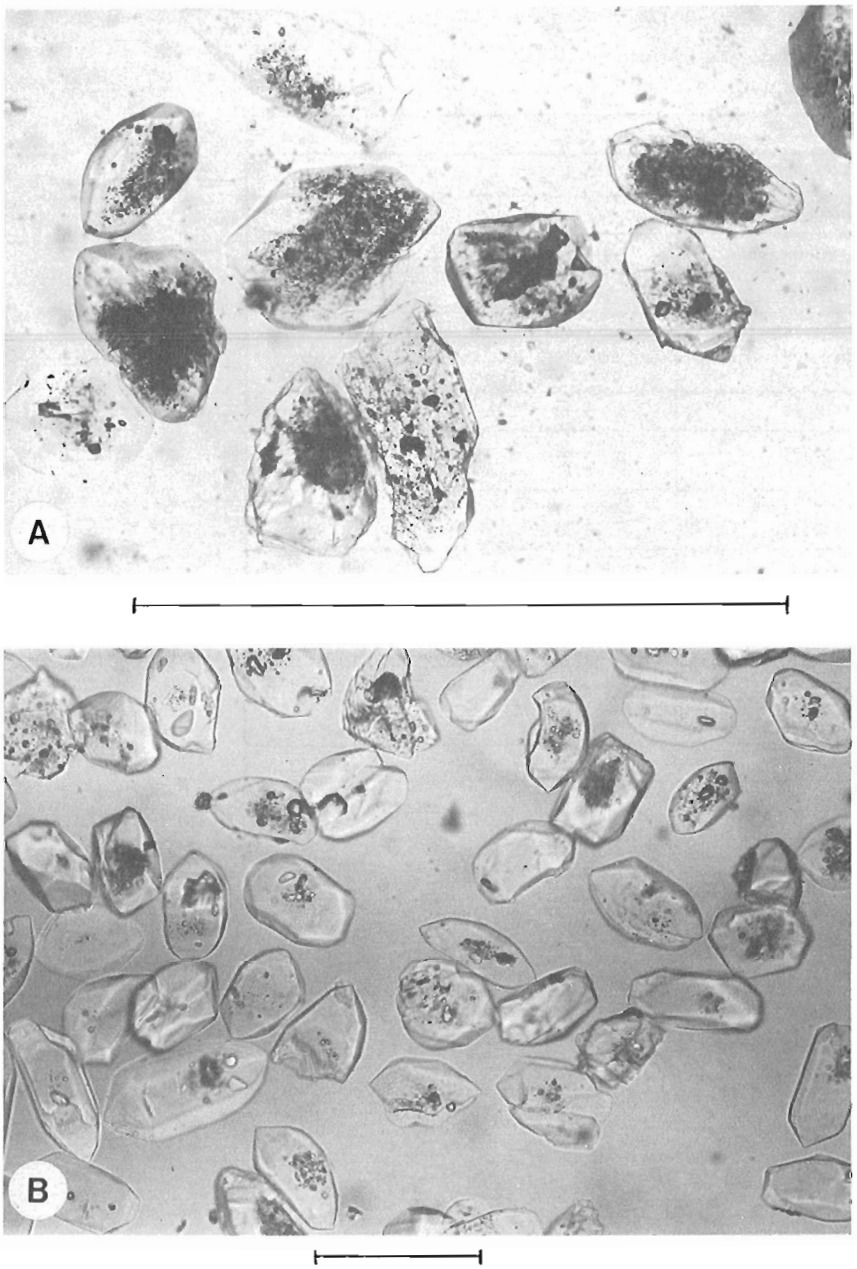

Figure 6.3. *Photomicrographs of zircons from the Mount Copeland syenite gneiss, sample WN-4-74, +149 μm magnetic fraction (6.3A) and -64 + 44 μm fraction (6.3B). Scale bar represents 1.0 mm for 6.3A and 0.1 mm for 6.3B.*

resulted from large scale rapid uplift from 70 to 50 Ma ago within an evolving orogen that extended from the eastern limits of the Rocky Mountain Fold and Thrust Belt to the Pacific Ocean, rather than from eastward and upward flow associated with thrusting. Mechanisms for this uplift and its relationship to adjacent tectonism remain vital problems for students of Cordilleran evolution.

References

Brown, R.L.
1980: Frenchman Cap Dome, Shuswap Complex, British Columbia: A progress report; in Current Research, Part A, Geological Survey of Canada, Paper 80-1A, p. 47-51.

Currie, K.L.
1976a: Notes on the petrology of nepheline gneisses near Mount Copeland, British Columbia; Geological Survey of Canada, Bulletin 265.

Currie, K.L. (cont.)
1976b: The alkaline rocks of Canada; Geological Survey of Canada, Bulletin 239.

Douglas, R.J.W., Gabrielse, H., and Wheeler, J.O.
1970: Geology of Western Canada (R.J.W. Douglas, ed.); Geological Survey of Canada, Economic Geology Report No. 1, p. 366-428.

Duncan, I.J.
1978: Rb/Sr whole rock evidence for three Precambrian events in the Shuswap Complex, southeast British Columbia; Geological Association of Canada, Mineralogical Association of Canada and Geological Society of America, Abstracts with programs, v. 10, p. 392-393.

Fyles, J.T.
1970: The Jordan River area; British Columbia Department of Mines and Petroleum Resources, Bulletin 57.

Höy, T.
1979: Stratigraphic and structural setting of strata-bound lead-zinc deposits in the Shuswap Complex; Geological Association of Canada, Cordilleran Section, Annual Meeting, Program with Abstracts, p. 18.

Okulitch, A.V.
1978: Discussion of results of K-Ar radiometric analyses; in Wanless et al., Age Determinations and Geological Studies, K-Ar Isotopic Ages, Report 13, Geological Survey of Canada, Paper 77-2, p. 24-26.

Read, P.B.
1980a: Geology and mineral deposits, eastern part of the Vernon east-half map-area; Geological Survey of Canada, Open File 658.

1980b: Stratigraphy and structure: Thor-Odin to Frenchman Cap "domes", southern British Columbia; in Current Research, Part A, Geological Survey of Canada, Paper 80-1A, p. 19-25.

Reesor, J.E. and Moore, J.M., Jr.
1971: Thor-Odin gneiss dome, Shuswap Metamorphic Complex, British Columbia; Geological Survey of Canada, Bulletin 195.

Sullivan, R.W. and Loveridge, W.D.
1980: Uranium-lead age determinations on zircon at the Geological Survey of Canada: current procedures in concentrate preparation and analysis; in Loveridge, W.D., Rubidium-strontium and uranium-lead isotopic age studies, Report 3; in Current Research, Part C, Geological Survey of Canada, Paper 80-1C, p. 161-246.

Wheeler, J.O.
1965: Big Bend map-area, British Columbia; Geological Survey of Canada, Paper 64-32.

7. POTASSIUM-ARGON AGE OF THE LATE PROTEROZOIC FURY AND HECLA FORMATION, NORTHWEST BAFFIN ISLAND, DISTRICT OF FRANKLIN

Project 790016

F.W. Chandler and R.D. Stevens
Precambrian Geology Division

Chandler, F.W. and Stevens, R.D., Potassium-argon age of the Late Proterozoic Fury and Hecla Formation, northwest Baffin Island, District of Franklin; in Current Research, Part A, Geological Survey of Canada, Paper 81-1A, p. 37-40, 1981.

Abstract

About 6000 m of Proterozoic clastic sediments overlie basement of the Churchill Province in northern Baffin Island. Mafic volcanic rocks near the base of the lower, quartzite-rich Fury and Hecla Formation yield ages of 1089, 1117 and 1121 Ma. A sill cutting the overlying black, shale-rich Autridge Formation gives ages of 716 and 746 Ma. Two mafic dykes cutting both formations, one probably cutting the sill, have ages of 631 and 643 Ma.

Validity of these ages is enhanced by their being reasonably close to the Mackenzie and Franklin igneous events. The dates indicate that sedimentation of the two formations commenced in the Neohelikian sub-era and may have extended into the middle of the Hadrynian era. Similarity between this succession and the Proterozoic sedimentary succession on Borden Peninsula to the north suggests that the latter succession might be of similar age.

Introduction, Previous Work and its Interpretation

Two sequences, several thousand metres thick, of late Precambrian sedimentary strata overlie gneiss of the Churchill Province in northwest Baffin Island. One sequence (Fig. 7.1) comprises the Fury and Hecla Formation and the overlying Autridge Formation (Blackadar, 1970; Chandler et al., 1980). The other is composed of the Eqalulik and overlying Uluksan groups (Blackadar, 1970; Jackson and Davidson, 1975; Jackson et al. 1975, 1978). The latter sequence is overlain by early Paleozoic strata (Trettin, 1969). There are lithological similarities between the basal parts of the two sequences including newly discovered mafic volcanics at the base of the Fury and Hecla Formation that may be equivalent to the Nauyat volcanics at the base of the Eqalulik Group. These volcanics lie within the lower redbed formation of Chandler et al. (1980) who originally thought them to be sills.

Both sequences are transected by northwest-striking mafic dykes and a mafic sill is present in the Autridge Formation (Fig. 7.2). The sequences are part of a group of broadly lithologically similar late Precambrian sedimentary sequences of the Canadian Arctic.

Earlier K/Ar ages from the mafic volcanic and intrusive rocks from these two sequences (Blackadar, 1970) did not agree with field relations among the enclosing sedimentary rocks. The purpose of this paper is to report new K/Ar whole rock dates from these igneous rocks from within the Fury and Hecla and Autridge formations that fit better (Table 7.1, Fig. 7.2).

Blackadar (1970) derived a K/Ar whole rock age from the Nauyat volcanics of 903 ± 140 Ma. Jackson et al. (1980) have reported Rb/Sr and K/Ar ages by the Geological Survey of Canada with the range 917-1032 Ma. Early dates from a mafic sill within the Autridge Formation (Blackadar, 1970, p. 76) by the K/Ar method were 475 ± 81 and 639 ± 25 Ma. The former date, from the coarse interior of the sill was regarded as unrealistic because of "geological considerations". The latter number was determined from a chilled margin. From the abundant northwest-trending mafic dykes that cut the Eqalulik and Uluksan groups Blackadar obtained K/Ar dates of 915 and 1140 Ma.

Accordingly interpretation of the geochronology of the late Proterozoic rocks of northwest Baffin Island was not straightforward. Blackadar (1970) observed that the sill he had dated was cut by dykes, but that the dykes had yielded greater ages. Noting that there were two sets of dykes with different trends, he wondered if there were several groups of different age. Equally confusing was the slightly younger age of the Nauyat volcanics than that of the dykes cutting the overlying sediments. This latter disparity was explained by experimental error. Blackadar concluded that an age in the range 900-1000 Ma should be assigned to the crystallization of the igneous rocks and that the Eqalulik and Uluksan groups were Neohelikian. This implied to him a similar age for the Fury and Hecla Formation.

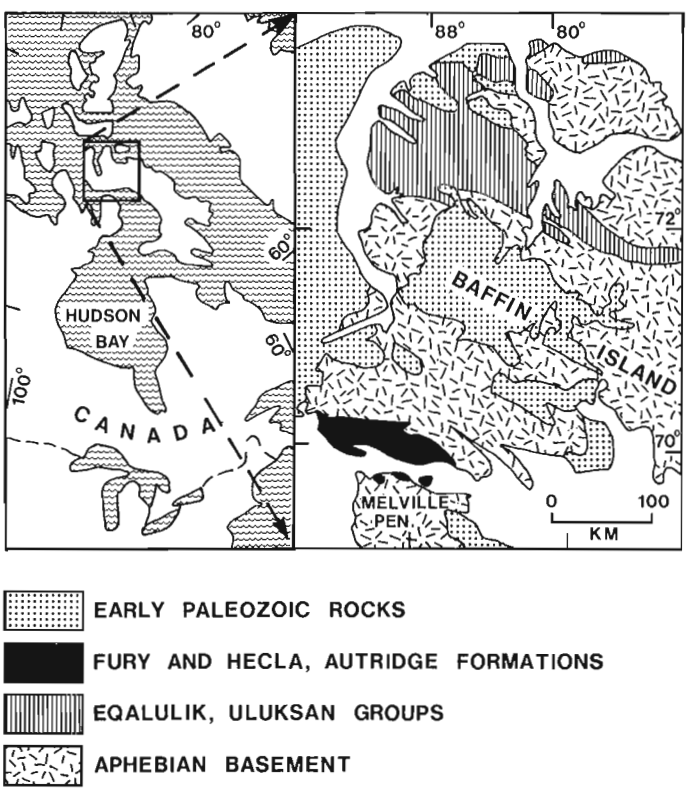

Figure 7.1. *The Fury and Hecla and Autridge formations and the Eqalulik and Uluksan groups, Late Precambrian sedimentary sequences of northern Baffin Island.*

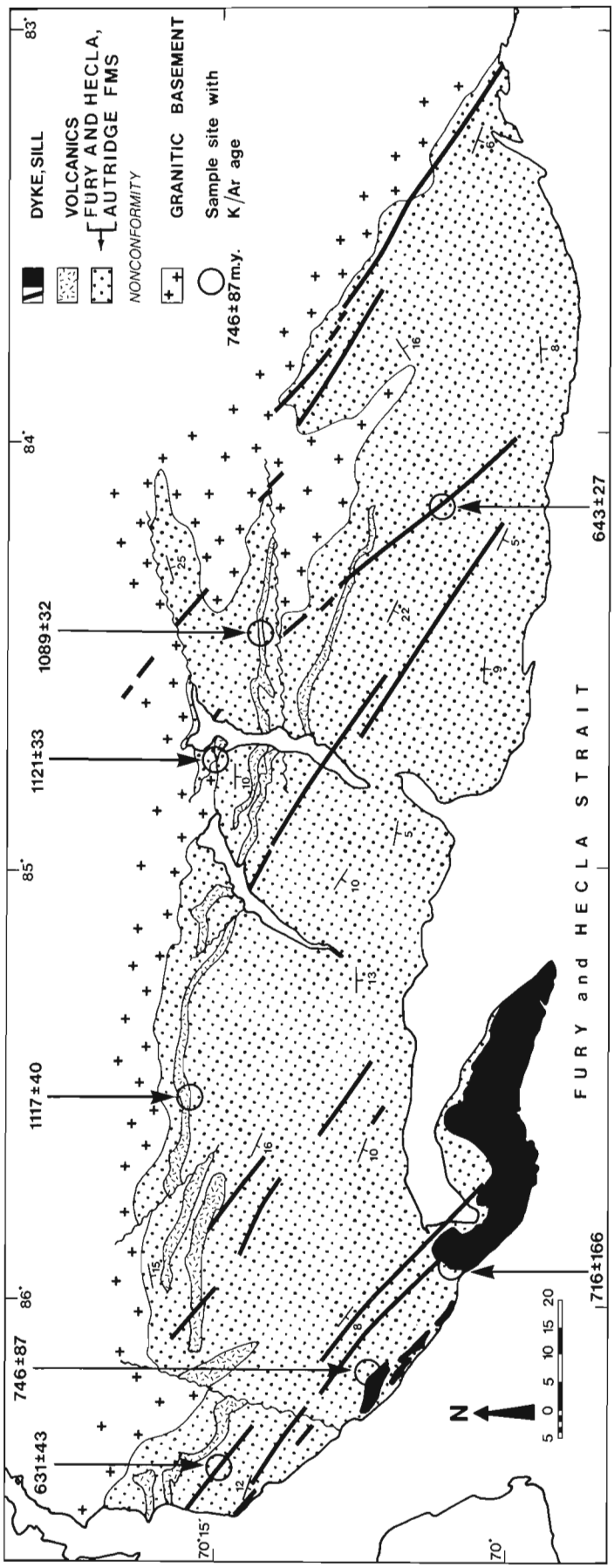

Figure 7.2. Potassium/Argon whole rock ages of mafic igneous rocks in the Fury and Hecla and Autridge formations.

Others have interpreted Blackadar's (1970) geochronology differently. Geldsetzer (1973) invoked loss of argon, choosing the 1140 Ma age for one of the dykes to indicate a Helikian age for sedimentation of the Eqalulik and Uluksan groups. Douglas (1970) thought that the dates represented two phases of igneous activity, one at 1100-1200 Ma and the other in the later part of the Hadrynian. In consequence he regarded the Eqalulik Group as probably Paleohelikian and the Uluksan Group as Neohelikian to Hadrynian.

Fahrig et al. (1971) found some dykes of northwestern Baffin Island and northern Melville Peninsula to have paleomagnetic characteristics similar to those of the Franklin Episode and therefore likely to have an age of about 675 Ma. He used the near equatorial paleolatitude of dyke intrusion, coupled with the presence of warm climate indicators (sulphates and stromatolites) in the Uluksan Group to imply a comparable age for the sediments. Jackson (Jackson and Davidson, 1975, Jackson et al. 1975, 1978) accepted a Franklin age for the dykes but regarded the age of the sediments as not well established. Great thickness of the Eqalulik and Uluksan groups, evidence of disconformities within the groups and of deformation before the intrusion of the dykes persuaded him that the sediments were significantly older than the dykes, that is Neohelikian, with an age greater than 950 Ma.

New Data and Discussion

Three K/Ar ages (1089 ± 32, 1117 ± 40 and 1121 ± 33 Ma) have been determined from a newly discovered volcanic unit near the base of the Fury and Hecla Formation. This unit is a likely correlative of the Nauyat Formation that occurs at the base of the Eqalulik Formation 300 km to the north. Two samples from the sill previously dated by Blackadar (1970) yielded dates of 716 ± 166 and 746 ± 87 Ma. Two dykes cutting the Fury and Hecla Formation gave dates of 631 ± 43 and 643 ± 27 Ma. One dyke probably transects the above sill (Fig. 7.2, Table 7.1).

Thin sections are not available for the dated volcanic samples. In four other less fresh samples from the volcanic unit pyroxene was generally fresh and plagioclase had varied sericite-like alteration. Olivine was pseudomorphed by serpentine and iron oxide. Both dated sill samples had fresh pyroxene and plagioclase. In one, olivine was fresh and in the other possibly represented by patches of iddingsite. The two dyke samples were fresh apart from minor patches of sericite-like alteration of both pyroxene and plagioclase.

The K/Ar age determinations reported here were carried out on whole rock samples of basalt and diabase crushed to -28, +48 mesh. A first split of each was processed "as is" for argon extraction, and a second split was ground very finely for postassium determination.

Argon extraction was accomplished by fusion in a high vacuum furnace and gas purification system heated by a high frequency induction generator. A calibrated, enriched argon-38 internal standard ("spike") was added to each extraction and the liberated gas was purified by passing it through liquid nitrogen cold traps, a copper oxide furnace and a titanium-sponge getter. The spiked argon was isotopically analyzed in a modified A.E.I. MS-10 mass spectrometer operated in the static mode. Potassium contents of the samples were determined by X-ray fluorescence spectroscopy (Lachance, in Wanless et al., 1965, p. 4-7). Age computations were

Table 7.1

Analytical data from mafic igneous rocks in the Fury and Hecla and Autridge formations

Rock unit	Age, Ma	K., %	Radiogenic ^{40}Ar., %	$^{40}Ar/^{40}K$	Location	Geol. Survey Sample No.
Dyke	631 ± 43	0.50	96.6	0.04388	70°15.8'N, 86°28'W	CGA79C323
Dyke	643 ± 27	0.86	94.5	0.04491	70°05'N, 84°08'W	CGA79C131
Sill	716 ± 166	0.14	82.5	0.05102	70°04'N, 85°55'W	CGA79Z257
Sill	746 ± 87	0.28	88.7	0.05365	70°08'N, 86°12.5'W	CGA79Z218A
Volcanic	1089 ± 32	2.41	99.4	0.08691	70°13'N, 84°26'W	CGA79C74A
Volcanic	1117 ± 40	1.55	98.9	0.08988	70°17.5'N, 85°32'W	CGA79C408
Volcanic	1121 ± 33	2.42	98.0	0.09035	70°16'N, 84°44'W	CGA79C37

based on the decay constants of Steiger and Jäger (1977) and the various factors involved in assigning experimental errors to individual age determinations are as detailed by Wanless et al. (1965). All errors are reported at the 95% (2 sigma) confidence level.

Analytical data, calculated ages, sample identifications and sample locations are listed in Table 7.1.

Among widespread diabase dyke-forming events in the North American Precambrian Shield two well-documented examples include the Mackenzie episode, first mentioned as such by Silver (1961), that occurred about 1200 Ma ago, and the Franklin Episode that occurred about 700 Ma ago. The Mackenzie Diabases, a northwest-striking set of dykes have approximate K/Ar age of 1200 Ma and diagnostic paleomagnetic properties (Fahrig and Jones 1969). Dykes with similar characteristics are present on the northern part of Melville Peninsula (Fahrig and Jones (1969)). Burke and Dewey (1973) considered that the Mackenzie event reflects widespread rifting of a large continental mass.

The north- to northwest-striking Franklin Dykes also have a paleomagnetic signature and have a probable K/Ar mean age of 675 Ma. Members of this swarm cutting the Eqalulik and Uluksan groups have been identified paleomagnetically by Fahrig et al. (1971).

The writers' ages for the volcanics in the Fury and Hecla Formation agree with the K/Ar age of the Mackenzie event. Further, Mackenzie dykes have been recognized on the nearby Melville Peninsula. The internal agreement of the three ages from the Fury and Hecla Formation volcanics over a strike length of 80 km argues against local argon loss. The presence of prehnite and pumpellyite (visual identification by R.K. Herd) in one thin section from one of the dated samples suggests however that conditions suitable for loss of argon might have been reached. With the above caveat it is suggested that a Mackenzie age for the volcanics might be more realistic than Blackadar's (1970) 903 Ma date for the Nauyat volcanics – a possible correlative.

Similarly, the writers' ages for a sill and dykes in the Fury and Hecla Strait area are close to those of the Franklin dykes. The dykes show a close correspondence if ages from the Franklin dykes of Baffin Island, taken from Table 3 of Fahrig et al. (1971) are recalculated using the potassium decay constants of Steiger and Jäger (1977). Of the 12 Franklin dykes only the 6 with a radiogenic argon content of over 80% were employed in the belief that they represent the best sample material and analyses. Those used have an age range of 555-720 Ma and an arithmetic mean age of 641 Ma, surprisingly close to the average of the two dyke dates introduced in this report, i.e. 631 ± 43 and 643 ± 27 Ma.

On the basis of field relations, at least some dykes cut the sill in the Autridge Formation, an observation that Blackadar (1970) found to be at variance with his geochronology. The writers' dates are, on the other hand, consistent with the field relations and suggest separate phases of sill and dyke intrusion, though the low potassium content of the sill samples gave a high experimental error.

Further supporting evidence for these two phases of close-to-Franklin age comes from Somerset Island 300 km northwest where Kerr and de Vries (1976) observed a set of mafic dykes and sills cutting the Aston Formation (a sandstone possibly correlative of the Fury and Hecla Formation), and truncated against the base of the overlying Hunting Formation. A second set of dykes cuts both formations. Of course the earlier phase could be equivalent to the volcanics in the Fury and Hecla Formation, a question that might be resolved by radiometric studies on Somerset Island. Further the volcanics, sill and dykes (Table 7.1) appear to have different potassium contents. This also could be evidence of three distinct times of crystallization.

The writers' K/Ar dates explain geological relations in the Late Proterozoic rocks of northwest Baffin Island better than do those of Blackadar (1970). They also are similar to the ages of major dyke swarms that have representatives nearby. Therefore, bearing in mind the limitations of the K/Ar method (Faure, 1977, p. 150), the new dates are felt to be reasonable approximations to the ages of the igneous events listed in Figure 7.1. It is likely then that sedimentation of the Fury and Hecla Formation, and possibly that of the Eqalulik Group, commenced close to the time of the Mackenzie event.

Similarly sedimentation terminated before the Franklin event. Fahrig et al. (1971) speculated that sedimentation of the Uluksan Group might have been little earlier than the Franklin event. According to Irving (1979) northwest Baffin Island was several times between 1250 and 950 Ma at moderate to low latitudes, for example at 1250 Ma, 10°; at 1100 Ma, 10°; at 1050 Ma, 25°; and at 950 Ma, 30°. Therefore, if late Proterozoic evaporites were a low latitude phenomenon they could have formed somewhat earlier than suggested by Fahrig.

Based on the K/Ar dating of micas Stockwell (1968) placed the boundary between the Helikian and the Hadrynian intervals at 945 Ma. Later Stockwell (1973) placed the same boundary at 1000 Ma, based on the U/Pb method and by the Rb/Sr method at 1010 Ma (Decay constant, 1.47) and 1070 Ma (Decay constant 1.42). In a revised time scale, using the Rb decay constant of 1.42 (Wanless et al., 1979) the boundary defined by Rb/Sr was moved to 1045 Ma. Recalculation of the 945 Ma K/Ar boundary using the decay constants of

Steiger and Jäger yields a change only to 956 Ma. Thus ages reported here for the volcanics in the Fury and Hecla Formation clearly fall on the Helikian side of the K/Ar boundary and do so even when compared with the Rb/Sr scale. Bearing in mind that as a general rule K/Ar ages tend to be younger than Rb/Sr ages the preference is for assignment of a Helikian age to the volcanics.

The Neohelikian/Paleohelikian boundary is close to 1400 Ma (Stockwell, 1968, 1972; Wanless et al. 1979). So the volcanics, and the commencement of sedimentation of the Fury and Hecla Formation that preceded it by a short time, are likely to be Neohelikian rather than Paleohelikian in age.

The oldest ages for intrusives postdating the Fury and Hecla Formation are those of the sill, 716 and 746 Ma. These numbers, even allowing for some difference with the other times scales, lie close to the middle of the Hadrynian Era. Sedimentation could have, but did not necessarily, continue into the early half of the Hadrynian.

References

Blackadar, R.G.
1970: Precambrian geology of northwestern Baffin Island, District of Franklin; Geological Survey of Canada, Bulletin 191, 89 p.

Burke, Kevin and Dewey, J.F.
1973: Plume generated triple junctions: Key indicators in applying plate tectonics to the old rocks; Journal of Geology, v. 81, p. 406-433.

Chandler, F.W.
1980: Proterozoic redbed sequences of Canada; Geological Survey of Canada, Bulletin 311, 53 p.

Chandler, F.W., Charbonneau, B.W., Ciesielski, A., Maurice, Y.T. and White, S.
1980: Geological studies of the Late Precambrian supracrustal rocks and underlying granitic basement, Fury and Hecla Strait area, Baffin Island, District of Franklin; in Current Research, Part A, . Geological Survey of Canada, Paper 80-1A, p. 125-132.

Douglas, R.J.W., (Ed.)
1970: Geology and Economic Minerals of Canada; Geological Survey of Canada, Economic Geology Report No. 1, 838 p.

Fahrig, W.F. and Jones, D.L.
1969: Paleomagnetic evidence for the extent of Mackenzie igneous events; Canadian Journal of Earth Sciences, v. 6, p. 679-688.

Fahrig, W.F., Irving, E., and Jackson, G.D.
1971: Paleomagnetism of the Franklin Diabases; Canadian Journal of Earth Sciences, v. 8, p. 455-467.

Faure, G.
1977: Principles of Isotope Geology; John Wiley & Sons, New York, 464 p.

Geldsetzer, Helmut
1973: The tectono-sedimentary development of an algal-dominated Helikian succession on northern Baffin Island, N.W.T.; in Symposium on the geology of the Canadian Arctic, Proceedings; Canadian Society of Petroleum Geologists, Saskatoon. May, 1973, p. 99-126.

Irving, E.
1979: Paleopoles and paleolatitudes of North America and speculations about displaced terrains; Canadian Journal of Earth Sciences, v. 16, p. 669-694.

Jackson, G.D. and Davidson, A.
1975: Bylot Island map-area, District of Franklin; Geological Survey of Canada, Paper 74-29, 12 p.

Jackson, G.D., Davidson, A., and Morgan, W.C.
1975: Geology of the Pond Inlet map-area, Baffin Island, District of Franklin; Geological Survey of Canada, Paper 74-25, 33 p.

Jackson, G.D., Iannelli, T.R., Narbonne, G.M., and Wallace, P.J.
1978: Upper Proterozoic sedimentary and volcanic rocks of northwestern Baffin Island; Geological Survey of Canada, Paper 78-14, 15 p.

Jackson, G.D., Iannelli, T.R., and Tilley, B.J.
1980: Rift-related late Proterozoic sedimentation and volcanism on northern Baffin and Bylot Islands, District of Franklin; in Current Research, Part A, Geological Survey of Canada, Paper 80-1A, p. 319-328.

Kerr, J.Wm., and de Vries, C.D.S.
1976: Structural geology of Somerset Island, District of Franklin; in Report of Activities, Part A, Geological Survey of Canada, Paper 76-1A, p. 493-495.

Silver, L.T.
1961: Major gabbroic magmatic events and geochronology; Journal of Geophysical Research, v. 66, No. 7, p. 2560.

Steiger, R.H. and Jäger, E.
1977: Subcommission on Geochronology: Convention on the use of decay constants in geo- and cosmochronology; Earth and Planetary Science Letters, v. 36, p. 359-362.

Stockwell, C.H.
1968: Geochronology of stratified rocks of the Canadian Shield; Canadian Journal of Earth Sciences, v. 5, p. 693-698.

1973: Revised Precambrian time scale for the Canadian Shield; Geological Survey of Canada, Paper 72-53, 4 p.

Trettin, H.P.
1969: Lower Palaeozoic sediments of northwestern Baffin Island, District of Franklin; Geological Survey of Canada, Bulletin 157, 70 p.

Wanless, R.K., Stevens, R.D., Lachance, G.R., and Delabio, R.N.
1979: Age determinations and geologic studies; K-Ar isotopic ages Report 14; Geological Survey of Canada, Paper 79-2, 67 p.

Wanless, R.K., Stevens, R.D., Lachance, G.R., and Rimsaite, J.Y.H.
1965: Age determinations and geological studies, Part 1 – Isotopic ages, Report 5; Geological Survey of Canada, Paper 64-17, p. 1-126.

8. BUNGONIBEYRICHIA N. GEN. (OSTRACODA, BEYRICHIIDAE) FROM NEW SOUTH WALES, AUSTRALIA, WITH OBSERVATIONS ON THE GENUS VELIBEYRICHIA HENNINGSMOEN, 1954

Project 720072

M.J. Copeland
Institute of Sedimentary and Petroleum Geology, Ottawa

*Copeland, M.J., **Bungonibeyrichia** n. gen. (Ostracoda, Beyrichiidae) from New South Wales, Australia, with observations on the genus **Velibeyrichia** Henningsmoen, 1954; in Current Research, Part A, Geological Survey of Canada, Paper 81-1A, p. 41-44, 1981.*

Abstract

*A new genus, **Bungonibeyrichia**, is proposed for a species of amphitoxotidine ostracode from southern New South Wales. The morphology of this genus is compared with that of **Velibeyrichia**, a poorly understood genus from the central Appalachians of North America.*

Introduction

The genus **Velibeyrichia** was erected by Henningsmoen (1954) to include lobally reticulate Beyrichiidae with three ventrally united lobes and a well developed velar frill. Martinsson (1962) redefined this description of **Velibeyrichia**, based on the type species **Beyrichia moodeyi** Ulrich and Bassler, 1908 (mainly from the more definitive illustration of one of the type specimens in Ulrich and Bassler, 1923, plate LXIII, figure 27), as having a tubulous, unrestricted, but deflected velum and broad lobes (Plate 8.1, fig. 11-14). At the same time, Martinsson (1962, p. 236) erected the somewhat similar genera **Hoburgiella** for Beyrichiidae with a narrow syllobium and a wide, undeflected velum that is inconsiderably restricted posteroventrally, and **Hemsiella** for Beyrichiidae with a restricted, undeflected velum, the tecnomorphs of which have a denticulate border crest and a broad syllobium (see Martinsson, 1964). Other amphitoxotidines are less similar to **Velibeyrichia**, such as **Migmatella** which has essentially no velum. **Cryptolopholobus** and **Lophoctenella** have tecnomorphic lobes that are cristate and restricted vela, and **Juviella**, **Amphitoxotis** and **Huntonella** also have restricted, undeflected vela. The taxonomic importance of the deflected velum (ventrally flexed) above the torus on the crumina of **Velibeyrichia**, unlike the undeflected vela of these other genera, is presently unknown but may reflect a relict, more primitive morphologic characteristic of **Velibeyrichia** within this assemblage of amphitoxotidines. These morphologic mixtures of velar and lobal characteristics leave one unresolved combination (if the deflection of the heteromorphic velum of **Velibeyrichia** is considered a generic characteristic), i.e. Beyrichiidae species with unrestricted velum and narrow lobes. The new genus **Bungonibeyrichia** is proposed for such a taxonomic combination.

Through the kindness of A.J. Wright, The University of Wollongong, Wollongong, New South Wales, the writer was able to study more than two dozen beyrichiacean specimens (casts and moulds) from near Bungonia Creek, New South Wales. Some aspects of the geology and paleontology of the Bungonia-Marulan South area, about 150 km southwest of Sydney, New South Wales, are discussed by Jones et al. (in preparation). Fossil Locality 3 of their Figure 1 will more precisely locate the site from which the specimens were obtained. Stratigraphically, the specimens occur in the upper shale unit of the Bungonia Limestone, a formation that rests unconformably on the Tallong Beds of Late Ordovician age, and is overlain by the Tangerang volcanics of early Devonian age. Talent et al. (1975, p. 41) considered the entire Bungonia Limestone as Late Silurian, but Jones et al. conclude that the fauna of the upper portion of the formation (including the upper shale unit) is Lochkov. The ostracode specimens contribute only marginally in determining the stratigraphic position of these beds, but specimens apparently similar to those discussed here were reported by Chapman (1903) from Kilmore in Central Victoria and by Talent (1963) from eastern Victoria in the lower half of the Kilgower Member, Tabberabbera Formation. Talent (1963) considered that fauna to be Siegen.

The present specimens appear more similar to those illustrated by Chapman (1903, Plate XVI, figures 6-8) in that the lobes of the type material as drawn are long and relatively slender. The apparent dorsal splitting of the syllobium of the type specimen is considered by Talent (1963, p. 109) as "completely abnormal". The specimens figured by Talent (1963) appear to have broader lobation than those figured here but many of the Tabberabbera Formation specimens are internal casts and a broader lobation is to be expected as shown by similar casts from the Bungonia Creek locality on Plate 8.1.

Systematic Paleontology

Family Beyrichiidae Matthew, 1886

Subfamily Amphitoxotidinae Martinsson, 1962

Genus **Bungonibeyrichia** n. gen.

Type species: **Beyrichia wooriyallockensis** Chapman, 1903

Diagnosis. Reticulate Amphitoxotidinae with narrow lobes, a wide, tubulous, unrestricted velum and an indistinct torus. The velar edge crosses the crumina without deflection.

Bungonibeyrichia wooriyallockensis (Chapman)

Plate 8.1, figures 1-10

Beyrichia kloedeni M'Coy. Chapman, 1903, p. 109, 110.

Beyrichia kloedeni var. **granulata** Jones. Chapman, 1903, p. 110, Plate XVI, fig. 8.

Beyrichia wooriyallockensis Chapman, 1903, p. 110, Plate XVI, fig. 6.

Beyrichia maccoyiana var. **australiae** Chapman, 1903, p. 111, Plate XVI, fig. 7.

Velibryrichia worriyallockensis (Chapman). Talent, 1963, p. 27, 108, Plate 74, fig. 13-26; Plate 78, fig. 1-3, 5. Talent, 1965, p. 51. De Deckker and Jones, 1978, p. 13, 24.

Description. Valves semi-elliptical, slightly preplete, with long, straight hinge; cardinal angles abrupt, obtuse. Trilobate, lobes club shaped, broadening dorsally and rising at right angles from the domicilial wall to their flattened or slightly curved distal surfaces and with continuous cristae at the point of juncture of the distal and lateral surfaces. Distal surfaces of the lobes enclosed by the cristae are finely reticulate except on dorsal cusps of the anterior and syllobial lobes. Lateral surfaces of the lobes smooth as are the sulci and proximal portion of the velar ridge. Lobes forming a complete (but much reduced in width) juncture above the distinct anteroventral domicilial invagination (anteroventral depression of Martinsson, 1962). Anterior lobe (L1) banana shaped, concave posteriorly, with an acutely pointed dorsal cusp extending to the dorsal margin. Preadductorial lobe (L2) oval, not extending to the dorsum. Syllobium (L3, the largest lobe) curved concave anteriorly, club shaped, extending to, and, on some specimens, above the dorsum with an unornamented dorsal cusp more pronounced than that of the anterior lobe. All three lobes are joined dorsal of the anteroventral domicial invagination by lobal rami (lobal connections of Martinsson, 1964, not to be confused with a zygal ridge or crista).

Bisulcate, preadductorial sulcus (S1) near vertical, narrow and deep throughout its length and slightly posteriorly curved ventral of the preadductorial lobe, ending at the juncture of the rami of the anterior and preadductorial lobes. Adductorial sulcus (S2) broader, especially dorsally and equally as deep as the preadductorial sulcus, curved anteriorly ventral of the preaductorial lobe, ending at the juncture of the rami of the preadductorial and syllobial lobes. Both sulci are in contact dorsal of the preadductorial lobe.

Plate 8.1
(GSC 203201-I)

(All specimens X30)

Figures 1-10. **Bungonibeyrichia wooriyallockensis** (Chapman), 1903

1,10. Natural mould and artificial cast of the exterior of a tecnomorphic right value, hypotype, AMF 61381.
2. Natural cast of the interior of a tecnomorphic left valve, hypotype, AMF 61382.
3. Artificial cast from the mould of the exterior of a postplete tecnomorphic right valve, hypotype, AMF 61383.
4. Natural cast of the interior of a tecnomorphic right valve, hypotype, AMF 61384.
5. Artificial cast of the exterior of a tecnomorphic left valve, hypotype, AMF 61385.
6. Artificial cast of the exterior of a tecnomorphic right valve, hypotype, AMF 61386.
7,8. Artificial cast from the mould of the exterior of a crushed heteromorphic left valve in ventral and oblique lateral views, hypotype, AMF 61387.
9. Natural mould of the exterior of a tecnomorphic right valve, hypotype, AMF 61388.

Figures 11-14. **Velibeyrichia moodeyi** (Ulrich and Bassler), 1908

11. Lateral view of a tecnomorphic right valve, hypotype, USNM 306766.
12,13. Lateral and ventral views of a heteromorphic right valve, hypotype, USNM 306767.
14. Lateral view of a heteromorphic right valve, hypotype, USNM 306768.

(McKenzie Formation, 2.4 km east-northeast of Great Cacapon, West Virginia along the Baltimore and Ohio Railway tracks, 65-66 m north of the most prominent outcrop of Keefer Sandstone, Pawpaw 15 minute quadrangle, Pennsylvania-Maryland-West Virginia, collected by Berdan, Martinsson and Pokorný, September 9, 1967).

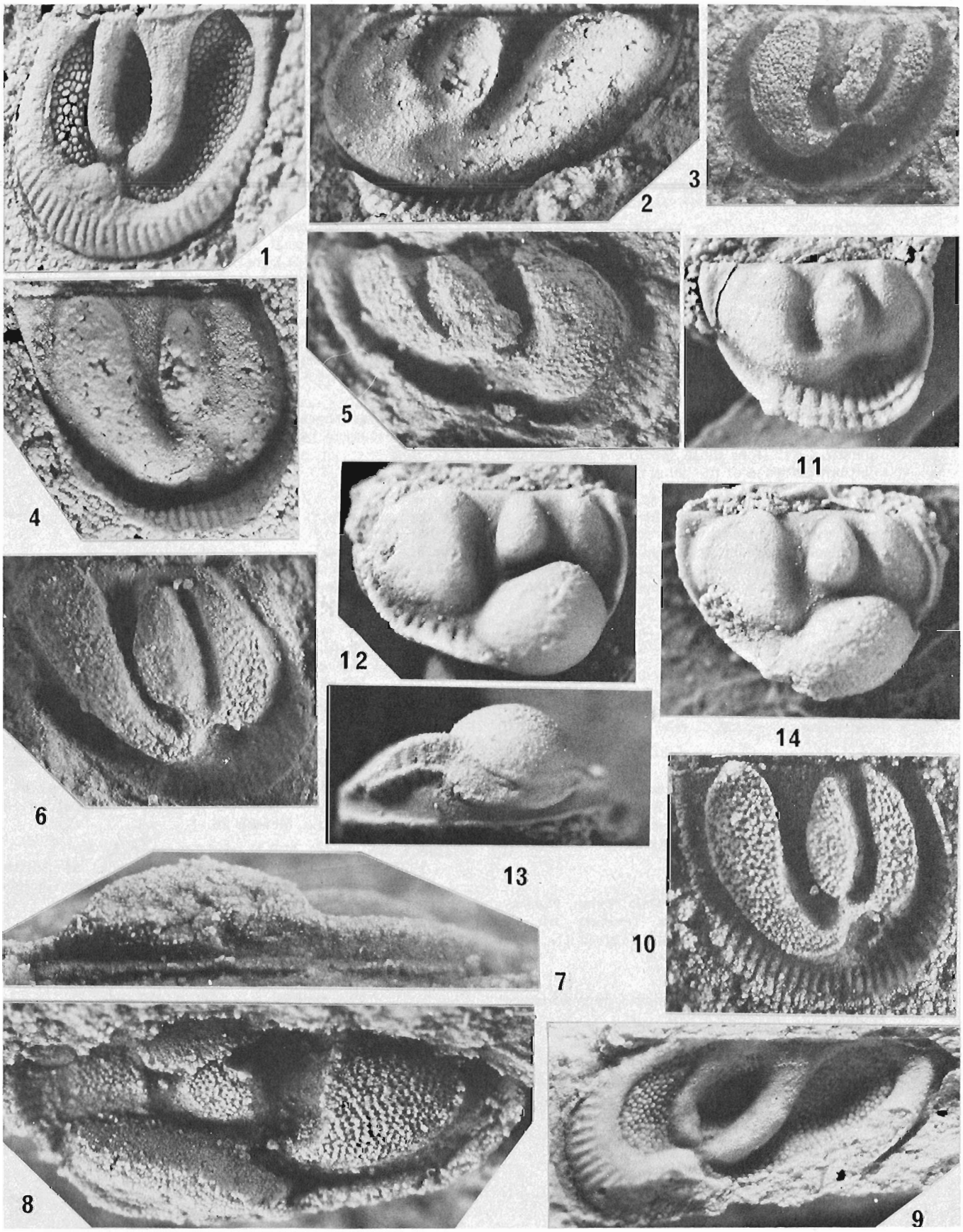
1
2
3
4
5
11
12
14
6
13
10
7
8
9

Tecnomorphic velum complete, tubulous, curved outwardly at an angle to the line of closure, broadest anteroventrally and narrowing gradually toward the cardinal angles. Heteromorphic velum apparently generally similar to that of the tecnomorphic velum but crosses the crumina as a narrow ridge without deflection. Crumina large, ovate, occupying the entire anteroventral area of the heteromorphic valve, cruminal ornamentation not discernible on the present specimens but is reported by Talent (1963) as "elongate pits oriented parallel to the long axis of the pouch". A trace of the torus may be present ventral of the velum.

Length of hypotype, AMF 61381, 1.8 mm, height, 1.5 mm

Number of specimens studied, 32.

Types. Figured hypotypes, AMF 61381-61388, unfigured hypotypes, AMF 61389-61400 deposited in the Australian Museum, Sydney, New South Wales. Unfigured hypotypes, GSC 65864-65867, deposited in the National Type Fossil Collection, Geological Survey of Canada.

Occurrence. Near the top of the upper shale unit, Bungonia Limestone, ca 9.7 km northeast of Bungonia, New South Wales and 0.35 km north of Bungonia Creek (Fossil Locality 3, Figure 1 of Jones et al., in preparation). Age: Early Devonian, Lochkov by Jones et al.; Late Silurian, Pridoli(?) by Talent et al. (1975). Either age is possible as species of amphitoxotidine genera range from late Wenlock to Siegen.

Remarks. The specimens of **B. wooriyallockensis** from the Bungonia Limestone appear unusual in that both preplete and postplete tecnomorphic specimens (i.e. compare Plate 8.1, figures 3 and 10) occur in the same fauna. These undoubtedly conspecific specimens must be distorted tectonically, as such has not been reported by Talent (1963) for the Victoria specimens.

All of the specimens from the Bungonia Limestone have lobes connected by short, thin rami. Some specimens reported by Talent (1963, p. 109) from the Tabberabbera Formation are described as lacking rami between the anterior and preadductorial lobes and some lack rami entirely. It may be questioned if all of those specimens are conspecific or if some casts of internal moulds may show less distinct evidence of this lobal connection.

Photographs of three specimens of **Velibeyrichia moodeyi** were kindly provided by J.M. Berdan (United States Geological Survey, Washington, D.C.) for comparison with **B. wooriyallockensis.** These show the broad lobation and complete, deflected velum that characterizes the genus. It is not known if other species presently assigned to **Velibeyrichia** because of their velar structure have this deflection. No deflected velum has yet been reported but this may be due to preservation or lack of observation. Possibly, **Velibeyrichia** is represented only by its type species, **V. moodeyi** (Ulrich and Bassler).

References

Chapman, F.
1903: New or little-known Victorian fossils in the National Museum, Melbourne. Part I. – Some Palaeozoic species; Royal Society of Victoria, Proceedings, v. XV, new series, Part II, p. 104-122.

De Deckker, P. and Jones, P.J.
1978: Check list of Ostracoda recorded from Australia and Papua New Guinea 1945-1973; Australia, Department of National Development, Bureau of Mineral Resources, Geology and Geophysics, Report 195.

Henningsmoen, G.
1954: Silurian ostracods from the Oslo region, Norway. 1. Beyrichiacea. With a revision of the Beyrichiidae; Norsk Geologisk Tidsskrift, v. 34, no. 1, p. 15-71.

Jones, J.G., Carr, P.F. and Wright, A.J.
Silurian and Early Devonian geochronology; Alcheringa. (in preparation)

Martinsson, A.
1962: Ostracodes of the Family Beyrichiidae from the Silurian of Gotland; Uppsala, University, Palaeontological Institution, Publication No. 41.

Martinsson, A. (cont.)
1964: **Hemsiella andincola,** a new beyrichiacean ostracode from the Silurian of Venezuela; Uppsala, University, Palaeontological Institution, Publication No. 55, p. 238-247.

Talent, J.A.
1963: The Devonian of the Mitchell and Wentworth Rivers; Geological Survey of Victoria, Memoir 24.

1965: The Silurian and Early Devonian faunas of the Heathcote District, Victoria; Geological Survey of Victoria, Memoir 26.

Talent, J.A., Berry, W.B.N., and Boucot, A.J.
1975: Correlation of the Silurian rocks of Australia, New Zealand, and New Guinea; The Geological Society of America, Special Paper 150.

Ulrich, E.O. and Bassler, R.S.
1908: New American Paleozoic Ostracoda. Preliminary revision of the Beyrichiidae with descriptions of new genera; United States National Museum, Proceedings, v. XXXV, p. 277-340.

1923: Systematic paleontology of the Silurian deposits; Ostracoda; Maryland Geological Survey, Silurian, p. 500-704.

9.

A RECONNAISSANCE STUDY OF THE SURFICIAL GEOLOGY OF THE GRAND BANKS OF NEWFOUNDLAND

Project 730072

Gordon B. Fader and Lewis H. King
Atlantic Geoscience Centre, Dartmouth

Fader, Gordon B. and King, Lewis H., A reconnaissance study of the surficial geology of the Grand Banks of Newfoundland; in Current Research, Part A, Geological Survey of Canada, Paper 81-1A, p. 45-56, 1981.

Abstract

The results of a reconnaissance study of the surficial and near-surface bedrock marine geology of the Grand Banks of Newfoundland are presented. On the basis of high-resolution seismic reflection profiles, sidescan sonograms, and bottom samples, the position of a Late Wisconsin low sea level stand is tentatively identified at 110-120 m. Above these depths, glacial sediments were eroded and redistributed during the Holocene transgression. Stable areas of lag gravel and large patches of sand have been desposited. Iceberg furrows occur at the seabed and are up to 5 m deep. On the basis of the distribution and stratigraphic relationships of the surficial sediments, it is suggested that above a 110 m depth the iceberg furrows were formed during the last 10 000-12 000 years and that these furrows may represent the total number developed during this time interval.

Introduction

Our purpose was to survey the surficial and bedrock geology of the Grand Banks of Newfoundland. Recent hydrocarbon discoveries at the Hibernia P-15 well site on the northeastern part of the Grand Banks has greatly increased the need for geological studies both on regional and site specific scales. To the south of Newfoundland, on the western Grand Banks, and on the adjacent Scotian Shelf the surficial and bedrock geology has been studied and mapped in a systematic format. Previous studies east of Newfoundland to the Virgin Rocks area have concentrated on a section of Ordovician-Silurian bedrock nearly exposed at the seabed (King and Fader, 1976). Prior to the present survey little was known of the stratigraphy, lithology, and morphology of the surficial sediments on the eastern Grand Banks of Newfoundland.

The survey was conducted aboard **CSS Hudson** (Cruise 80-010) in four weeks, and Figure 9.1 shows the ship's tracks along which data were collected. The cruise was primiarly an on-line geophysical survey and only a limited number of samples were obtained to provide ground truth for the acoustic data. A more detailed survey was conducted on the northern part of Grand Bank in the Hibernia discovery area, and the ship's tracks were chosen to best define anticipated structural and stratigraphic relationships. Only selected aspects of the geology are presented and discussed here.

Objectives

The specific objectives of the cruise were: (1) to obtain reconnaissance data on the distribution of surficial sediments and near-surface bedrock geology; (2) to study the Wisconsin glacial limits on the Grand Banks; (3) to study the nature, distribution, and age of bedforms and iceberg furrows at the seabed; (4) and to study the late glacial and postglacial eustatic and isostatic history of the shelf area. During the cruise, data were collected to help develop a framework for the surficial geological history; these were limited in scope by the large size of the survey area and the low density of coverage.

Methods

A multiparameter integrated geophysical and geological approach was used to collect data. High resolution seismic reflection data on the surficial sediments and near-surface bedrock were obtained with the Huntec Deep Towed High Resolution Seismic Reflection System (DTS) (Hutchins et al., 1976). The DTS was equipped with an Acoustic Reflectivity Module (ARM) that produced on-line acoustic reflectivity values to provide lithologic information on seabed materials (Parrott et al., 1980). The reflected energy of the DTS was measured in two time windows, r_1 and r_2, that represented the top metre of the seabed. Reflectivity r_1 is a measure of the energy which is coherently reflected from the seabed and r_2 is a measure of the scattered energy from the top metre of sediment. The energy values were used to calculated acoustic reflectivity as a percentage of the energy content of the outgoing acoustic pulse and were displayed on the seismic section. The spread of the distribution of the values between the 20th and 80th percentile points is shown as a grey band on the reflectivity profile, and the median as a black line within the grey band. For deeper seismic penetration, a 40 in^3 air-gun reflection system was employed. Bathymetric data were collected with Edo Western and Kelvin-Hughes echo sounder systems. A Bedford Institute of Oceanography designed sidescan sonar with a range of 750 m to each side of the ship provided sonograms of the seabed. Magnetic data were collected with a Barringer proton precession magnetometer. Surficial sediment samples were obtained with a van Veen sediment grab, and seabed photographs were taken with E.G. and G. underwater cameras. During the cruise, navigational control was provided by Loran-C and satellite navigation systems.

Central and Southern Grand Banks – Surficial Geology

Interpretation of the Huntec DTS and sidescan sonar profiles from the central and southeastern Grand Banks area indicates that complex distributions of sand patches, sand waves, megaripples, gravel deposits, and shell beds are present. Although acoustic control is limited across the Grand Banks, large sand bodies with amplitudes of up to 12 m and wavelengths of 2.7 km appear to be confined to the southern half of Grand Bank (Fig. 9.1). Figure 9.2 shows a Huntec DTS profile and a sidescan sonogram across an area of sand bodies. Because of their long wavelengths, the shape of the sand bodies is not resolved on the sonogram. However, the dark patches are believed to be shell deposits on the seabed. Other studies on the Scotian Shelf (Parrott et al., 1980) have revealed similar areas of shells associated with a basal transgressive sand and gravel formation. The acoustic reflectivity values (Fig. 9.2) which

occur over these zones indicate that there is a decrease in the amount of coherent energy reflected from the seafloor (r_1) and an increase in the amount of scattered energy (r_2). Over the sand facies the trend of the r_1 median profile has a value of about 25% and falls to 15% over the shells. The reflectivity values for the sand facies are lower than for similar deposits on the Scotian Shelf and this may be the result of loose packing of the sand particles or due to the presence of shell debris or small ripples at the seabed. The trend through the r_2 median profile increases from 2% in the sand facies to 20% over the shells, and there is an increase in the variability about the trend of r_2. Across the shell areas as well, the grey level of the seismic profiles increases at the seabed which results from high surface scatter. Shells are widespread on the Grand Banks, covering as much as 20% of the seabed and they often occur in conjunction with sand waves and sand ridges. The shell deposits range from circular to oval in shape, up to 100 m in diameter on Green Bank, to complex linear bodies on Grand Bank (Fig. 9.2). In most cases the shells are associated with 1-2 m depressions. Not enough high resolution seismic and sidescan sonar data exist to map the distribution of the deposits, and bottom samples and photographs would be essential for a complete interpretation.

To underscore the importance of obtaining sidescan sonar and seismic reflection data concurrently to understand complex sediment distributions, profiles from Green Bank are presented (Fig. 9.3). The Huntec DTS profile shows a thin surficial sediment layer overlying a buried erosional surface. The seabed across the profile is very flat. The trend of the r_1 median profile has an average value of 35% with values in the range of 30-45% for the median. The r_1 median profile is highly variable, which indicates rapidly changing sediment type at the seabed. The reflectivity values are similar to those obtained on the Scotian Shelf over sand and gravel facies (Parrott et al., 1980). The sonogram along the same track is a herringbone pattern of light and dark zones, which may represent thin patches of sand overlying a gravel substrate, or windrows of shell across sand. Sample data are required to confirm this interpretation. This sediment distribution occurred for 8 km along the ship's track over Green Bank.

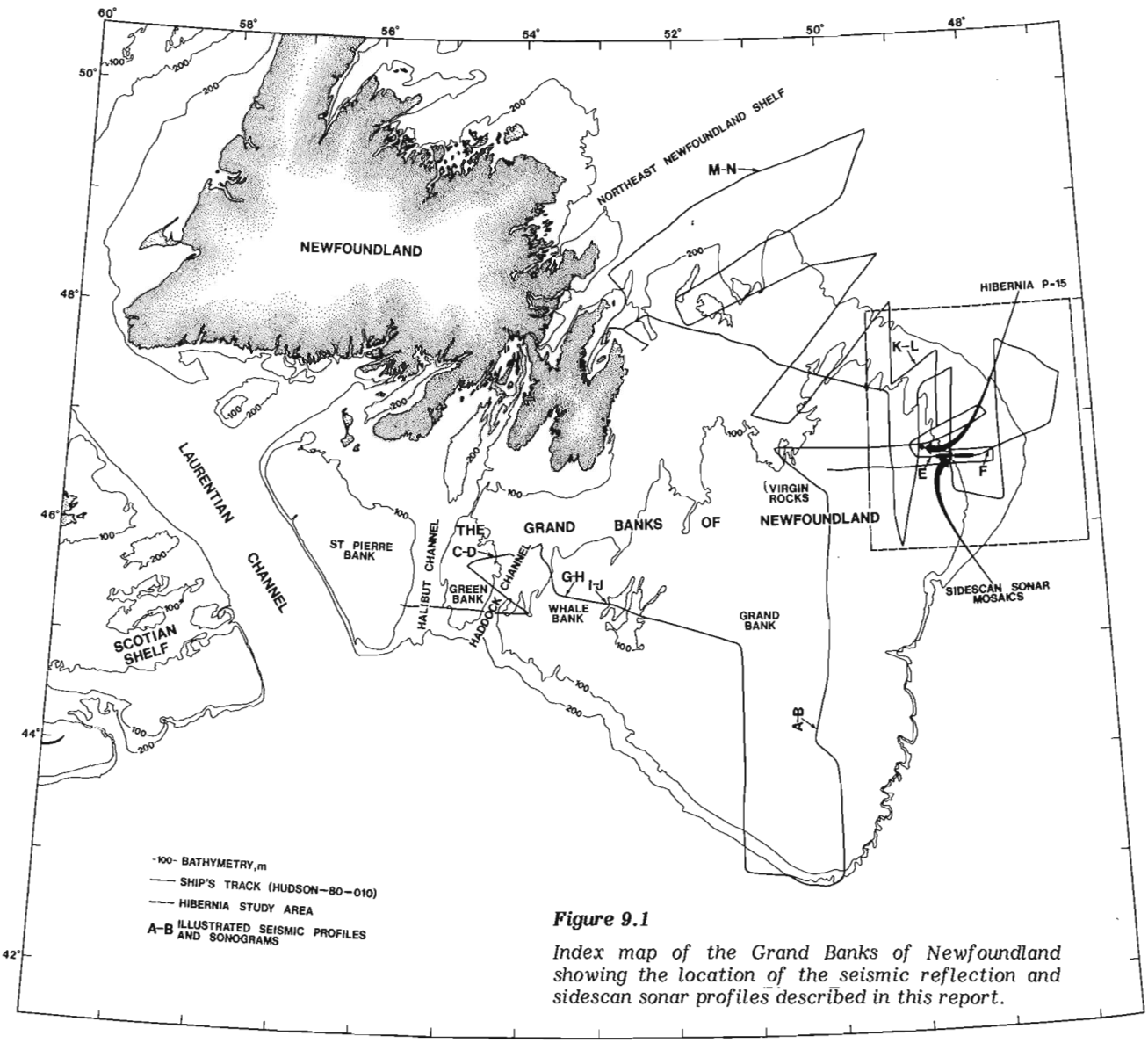

Figure 9.1

Index map of the Grand Banks of Newfoundland showing the location of the seismic reflection and sidescan sonar profiles described in this report.

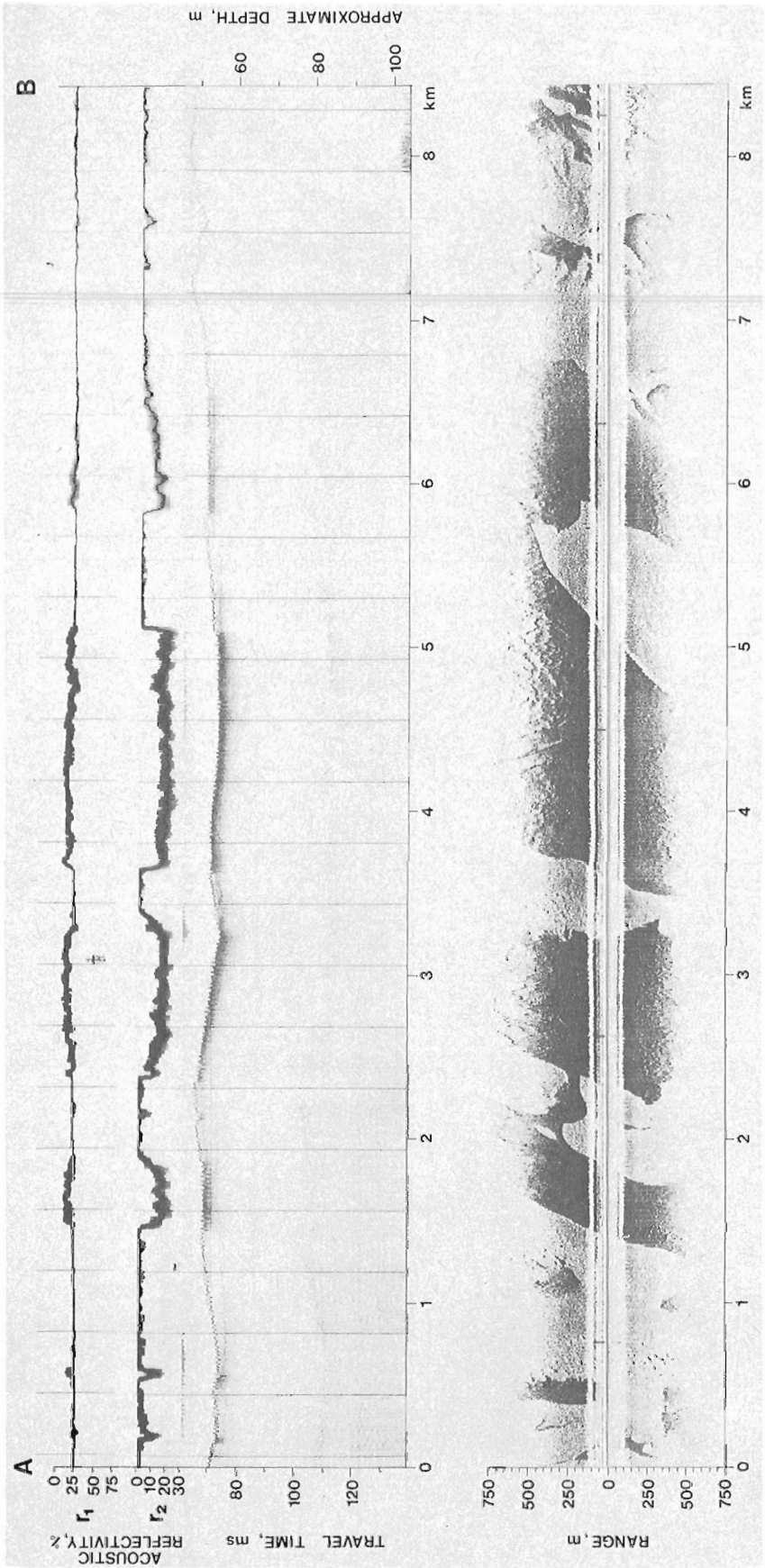

Figure 9.2. *Huntec (DTS) and sidescan sonar profiles across an area of sand bodies on Grand Bank. The dark patches on the sonogram which appear as areas of high acoustic scatter on the DTS profile are interpreted as representing shell beds on the seafloor. The highly irregular seabed on the DTS profile is due to extreme weather conditions.*

Hibernia Study Area – Northeast Grand Banks

A detailed survey was conducted in the Hibernia study area (Fig. 9.1); and two sidescan sonar mosaics were constructed. During collection of the data over the second mosaic area, the sidescan range was reduced due to temperature variations in the water column. Twenty-five surficial grab samples and 13 bottom photographic stations were completed.

Interpretation of Seismic Reflection Data

An airgun seismic reflection profile (E-F) (Fig. 9.1) from the Hibernia study area is presented in Figure 9.4, together with Huntec DTS sections along the same track. Interpretation of the airgun profile, which is typical of the study area, shows a seismic unit which consists of a series of parallel reflectors with gentle dips of 1-2° to the east. The truncation of the reflectors occurs within the 10 m "bubble pulse" and cannot be delineated on the airgun profiles. The absence of buried channels at this surface is characteristic of the Hibernia study area, and contrasts other areas of the Grand Banks to the south and west where channeling is highly developed. Figure 9.5 (G-H) is a Huntec DTS profile across a buried channel on Whale Bank. The channel is completely infilled with sediment and the surface expression of the feature at the seabed cannot be detected. Published well history reports from nearby exploratory wells on the Grand Banks indicate that the seismic unit consists of semi-consolidated "bedrock", of Tertiary age. The Huntec DTS profiles provide the increased resolution to define accurately the "bedrock" surface and the thickness of the overlying surficial sediment. An interpretation of Huntec DTS data along the airgun profile (Fig. 9.4) shows two zones of surficial cover. From the eastern section of the airgun profile the DTS record indicates a diffuse undulating subsurface horizon that is overlain by a more recent sediment with a smooth surface from 2-8 m thick. The subsurface horizon, which probably represents the "bedrock" surface, is defined by a large amount of backscatter resulting possibly from a highly irregular morphology and/or the presence of a lag gravel at this interface. The "bedrock" as represented on the DTS profiles, does not show well-developed stratification but where it is present the horizons can be traced to within 3-5 m of the seabed, which indicates a relatively thin surficial cover. Along the eastern DTS section the trend of the r_1 median profile has a uniform value of 35% and

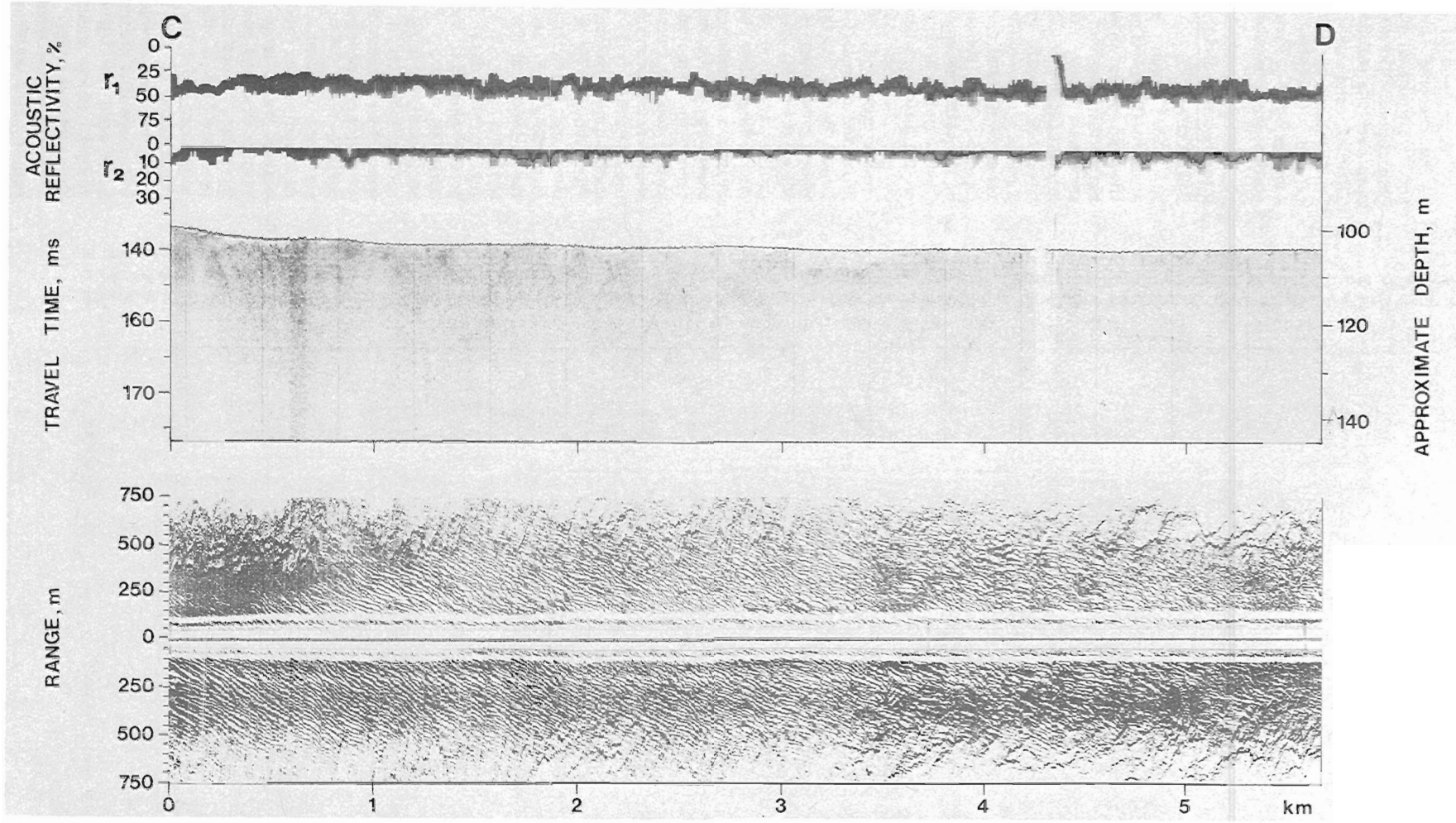

Figure 9.3. *Huntec (DTS) and sidescan sonar profiles from Green Bank. The sidescan profile and the reflectivity values show a highly variable sediment distribution across a very flat seabed.*

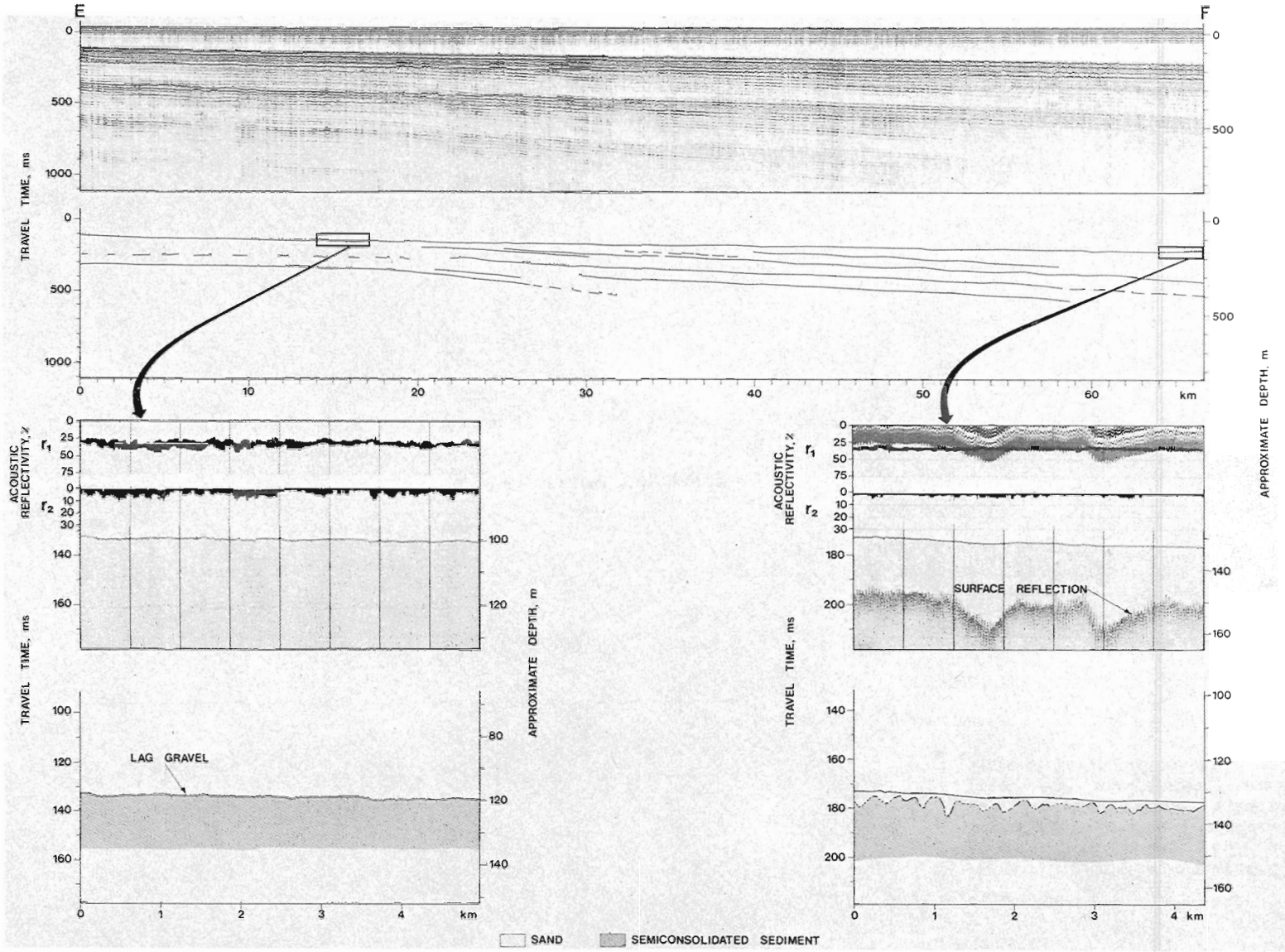

Figure 9.4. *Airgun seismic reflection profile E-F, and selected Huntec DTS profiles along the airgun profile; from Hibernia study area.*

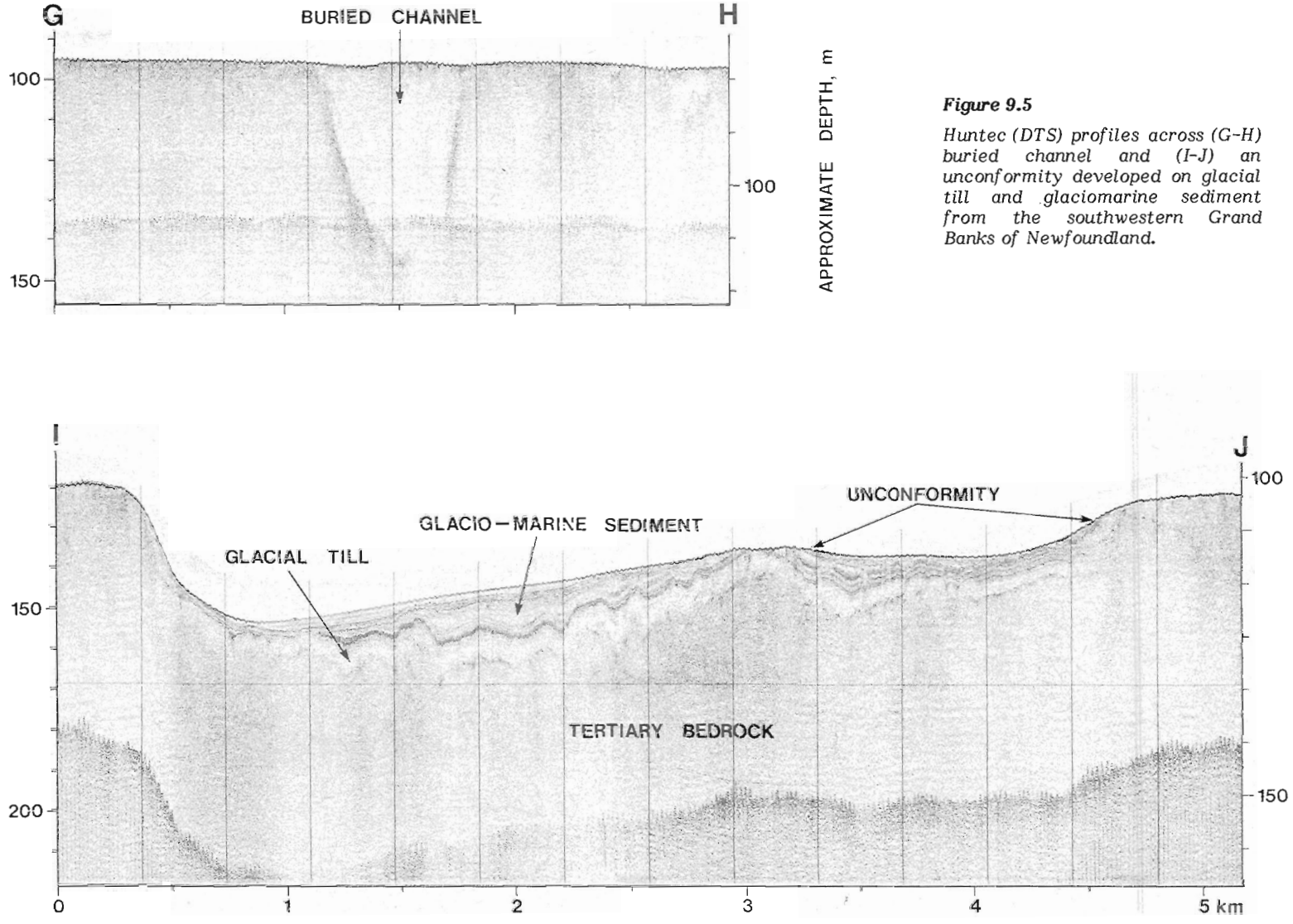

Figure 9.5

Huntec (DTS) profiles across (G-H) buried channel and (I-J) an unconformity developed on glacial till and glaciomarine sediment from the southwestern Grand Banks of Newfoundland.

compares well with values obtained over sand formations on the adjacent Scotian Shelf. The low values of r_2 indicate little backscatter from the surface or within the sediment. The Huntec profile to the west indicates that there is no surficial cover and the "bedrock" surface is interpreted as occurring at the seabed overlain by a lag gravel veneer and thin sand. The r_1 median profile is highly variable over the gravel facies with the trend line at 38%. Over the sand facies the r_1 profile is more uniform with values in the range of 35-40%. Interpretation of the reflectivity profiles together with the sidescan sonograms indicates a surficial sediment distribution of gravel (0-3 km) and thin sand (3-5 km) along this section.

In addition to lithostratigraphic information, the Huntec DTS provides a very accurate bathymetric profile of the seabed. The DTS system is heave compensated to remove unwanted, wave-induced, vertical motions from the profiles. The DTS profile (Fig. 9.4 to the east) shows up to 5 m wave heights as measured from the surface reflection, and an additional long period motion of up to 6 minutes duration. The heave compensated system effectively removes the excursions from the seismic profiles and the seafloor is presented in its true perspective. Accurate bathymetric data are essential in the recognition and measurement of very shallow iceberg furrows, which would not be resolved on conventional echo sounders under normal operating conditions.

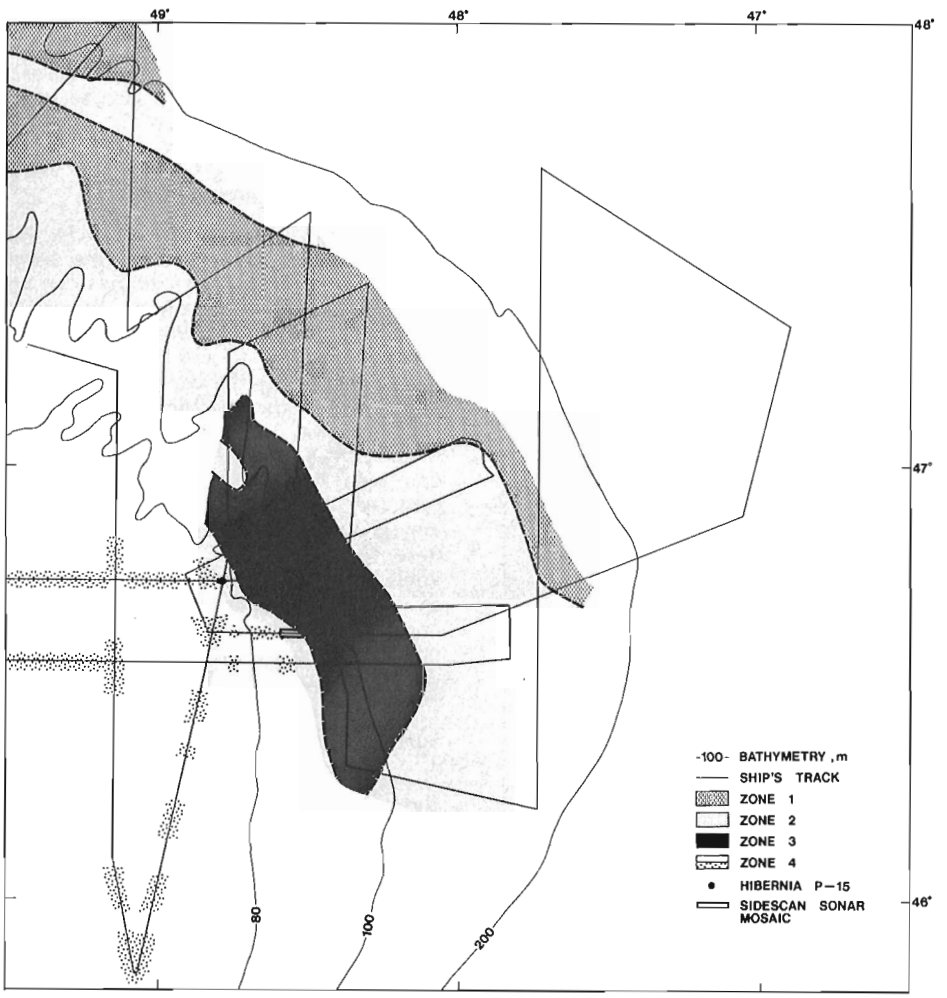

Figure 9.6. *Interpretation of sidescan sonograms from the Hibernia study area. Zone 1 is interpreted as a partially buried iceberg furrowed surface; Zone 2 is a flat sand bottom; Zone 3 consists of a gravel lag overlain by thin sand ribbons and sand waves; and Zone 4 is an area of broad patches of sand and gravel.*

Sidescan Sonogram Interpretation and Sample Data

Interpretation of the sidescan sonograms from the Hibernia study area is presented in Figures 9.6 and 9.7. Four zones of sonogram character can be recognized. Zone 1 occurs in the northeast part of the study area in depths greater than 110 m. The sonogram character consists of a network of randomly oriented discontinuous lineations, expressed as a dark tone against a light background (Fig. 9.8). The sonogram character is interpreted as representing a partially buried iceberg furrowed surface beneath thin sand. The dark lineations represent the ridges of the iceberg furrows. A few relatively recent furrows cut across this older surface and can be differentiated from the partially buried furrows by their continuous aspect, their raised rims, and their lack of sediment infilling. This partially buried furrowed surface continues along the northeast flank of Grand Bank and grades, in the deeper water of the southern part of the Northeast Newfoundland Shelf, into a zone of well-defined furrows (Fig. 9.9). The DTS profiles across this zone indicate that the buried furrowed surface is developed within the surficial sediment and that the seabed is moderately undulating. The trend of the r_1 median profile has a consistent value of 37%, which indicates that the partially buried furrowed surface is defined on the sonograms on the basis of its topographic expression and not on textural variations at the seabed.

To the west a second zone is represented on the sonograms by a continuous light tone and is interpreted as consisting of sand. Relatively few iceberg furrows occur across the seabed in contrast to the heavily furrowed areas of the Northeast Newfoundland Shelf. Sets of parallel marks, 75 m apart (Fig. 9.7) are numerous and are interpreted as originating from otter boards of fishing trawls. They provide a measure of the resolution ability of the sidescan sonar system as these marks are approximately 2 m wide, and cannot be detected on the bathymetric profiles. Surficial samples from the seabed consist of sand-sized sediment with minor gravel and contain less than 1% silt- and clay-sized particles. The gravel fraction appears to increase with depth. Bedforms are generally absent over this zone and the seabed is very flat. Figure 9.10 shows a large number of brittle starfish, sand dollars, worm tubes, and broken shell debris. The sediment varies from yellow-brown to light brown in colour. A more detailed description of the lithostratigraphy as interpreted from the DTS profiles is provided in the previous section on seismic reflection data in the discussion of Figure 9.4.

Zone 3 occurs to the west of zone 2 in depths of less than 110 m, and shows a distribution of light toned areas (sand ribbons) against a dark

background (lag gravel) (Fig. 9.11, 9.12). The sand ribbons tend to infill reflief of 1-2 m that occurs on the gravel surface and smooth the seabed profile. Arcuate shaped sand waves occur normal to the sand ribbons and both indicate a current direction from north to south. Megaripples and sand waves on the flanks of the sand ribbons, have been recognized by C.L. Amos (personal communication, 1980) using a higher resolution sidescan sonar system. Bottom photographs across the seabed show a sediment distribution of sand and gravel (Fig. 9.10c). The gravel-sized fraction ranges from subrounded to rounded in shape. On several photographs, local patches of sand with ripple marks developed across their surface can be seen lapping on the gravel lag. The ripple marks are being eroded by browsing organisms at the seabed and would quickly be removed. This indicates some recent mobility of the sand.

The description of the western Huntec DTS profile (Fig. 9.4) across Zone 3 given in the previous section, is typical of other profiles from the zone. From the DTS record the r_1 median profile is uniform over the sand facies with values in the range of 35-40%. Over the gravel facies the r_1 median is highly variable with the trend line at 38%. The seismic section also shows that the gravel facies has a moderately rough surface. Iceberg furrows also occur over the zone and are up to 75 m wide. They are more difficult to recognize, however, because their depths are limited to less than 1 m. In some areas, perhaps because of the harder surficial materials or the close proximity of the underlying "bedrock" surface, the furrows are discontinuous and appear on the sonogram as isolated depressions (iceberg pits). These furrows contrast to the smooth, continuous ones over Zone 2. Figure 9.12 is an enlargement of a section of the sidescan mosaic shown in Figure 9.11. Iceberg furrows cut across both the gravel and sand. In some cases the furrows appear to be discontinuous and may indicate recent mobility of the sand.

Zone 4 occurs to the west of Zone 3 in shallower water and consists of broad areas of light and dark tone on the sonograms. Samples from the dark areas contain well-rounded lag gravels with minor shell debris (Fig. 9.10a) and those from the light areas consist of well-sorted, buff-white sand (Fig. 9.10b). This pattern continues across the entire northern part of Grand Bank to the west. The reflectivity values from the Huntec DTS profiles show well-defined contacts between the sand and gravel facies and correlates well with the sonograms. The r_1 median profile is uniform over the sand facies with values about a trend through the median of 30%. Over the gravel facies, r_1 is variable about a median of 40%. The values of r_2 across the sand facies are uniform with values in the range of 4-8% about a trend through the median of 6%. Over the gravel facies the r_2 median profile is highly variable about a trend through the median of 12%. An area of sand waves, with wavelengths of between 20 and 125 m, occurs along the eastern boundary of the zone, 0-7 km along the mosaic. Bottom photographs (Fig. 9.10b) across the sand show well developed ripple marks. Iceberg furrows in this zone are sparse, and across the entire northern Grand Bank along the ship's tracks indicated in Figure 9.1, only 6 furrows were encountered on each pass.

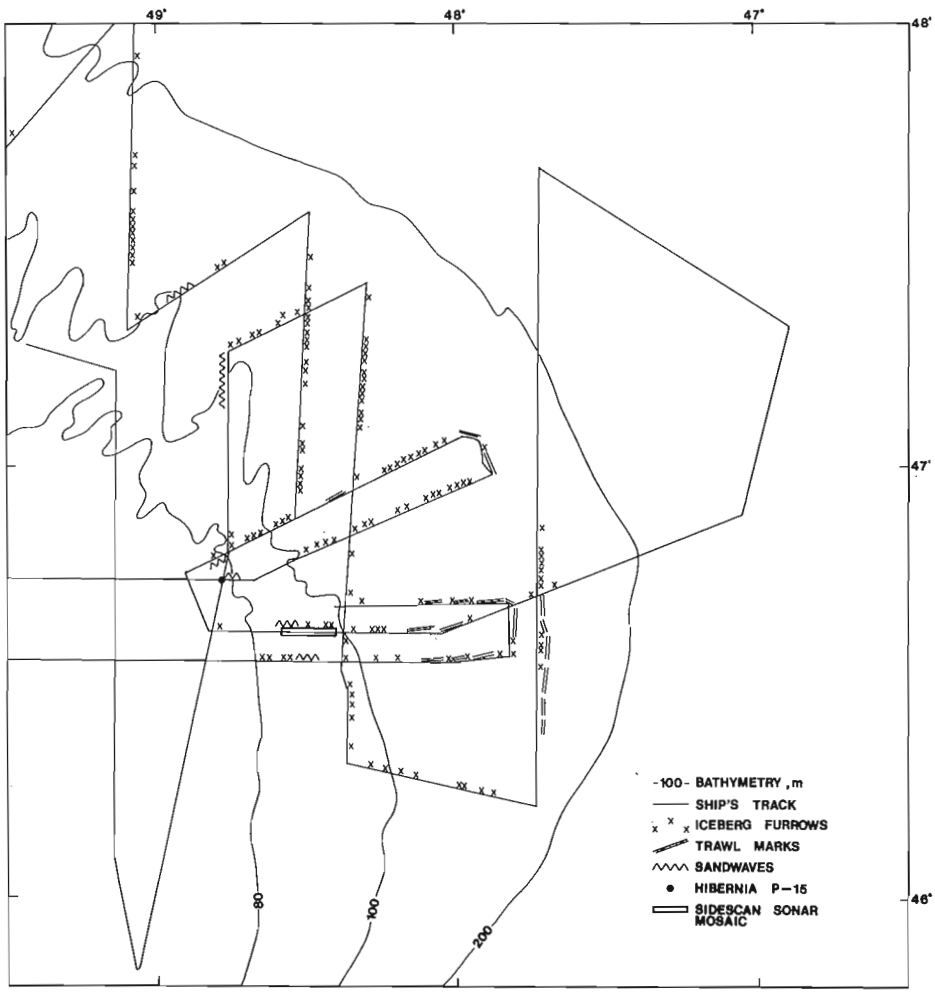

Figure 9.7. *Distribution of iceberg furrows, sand waves and trawl marks from an interpretation of sidescan sonograms in the Hibernia study area.*

In the Hibernia area (Fig. 9.7), the furrows range in size and shape from extensive linear depressions that can be detected for up to 8 km along the ship's track, to circular isolated depressions (iceberg pits) up to 100 m in diameter. The furrows near the edge of the banks appear to follow curvilinear paths that parallel the bathymetric contours. Most furrows seen on the sonograms can also be recognized on the DTS profiles. Occasionally a furrow may appear on a sonogram that cannot be detected on a DTS profile, and vice versa. This illustrates the importance of heave compensated bathymetry, concurrent with sidescan sonar data collection, in providing an accurate description of iceberg furrows.

Surficial Geological Framework

Studies on the Scotian Shelf and the western Grand Banks of Newfoundland (King 1970; Fader et al., in press), have identified a pre-Holocene low sea level stand at 110-120 m. This low sea level stand is critical to the distribution of the surficial formations identified in these areas. Above the low sea level stand, previously deposited glacial materials were reworked and redistributed by the subsequent Holocene transgression and a basal transgressive sand and gravel formation was developed. The low sea

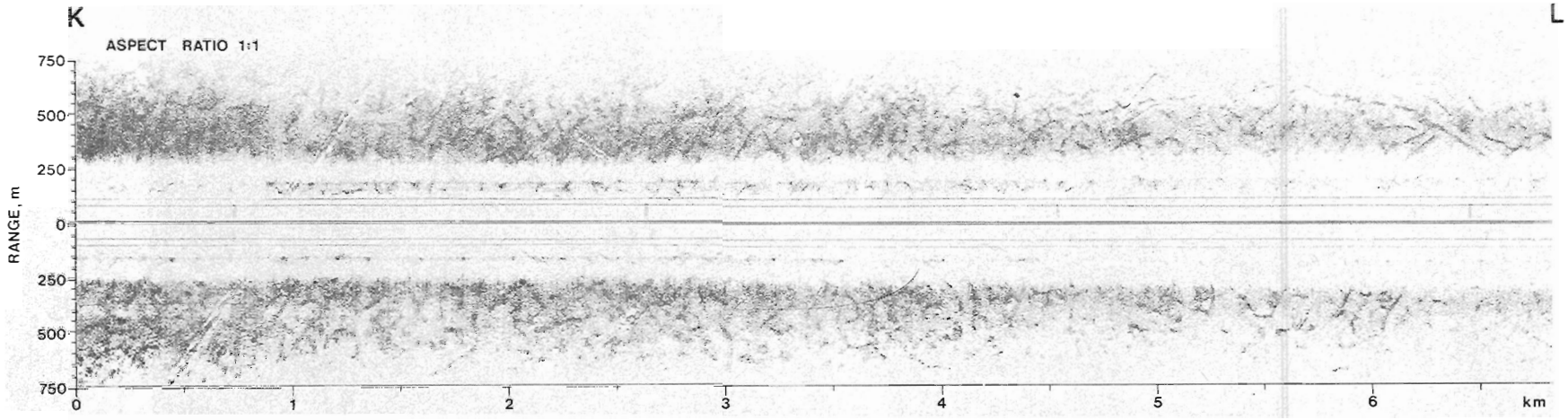

Figure 9.8. *Sidescan sonogram K-L across a partially buried iceberg furrowed surface in the Hibernia study area. A few recent furrows occur at the 0-2.5 km marks along the profile.*

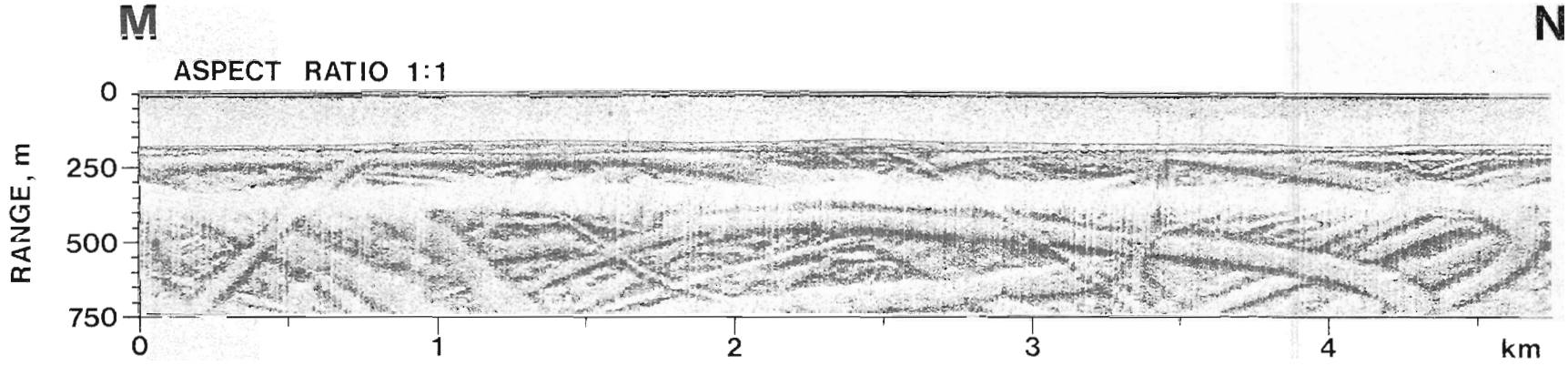

Figure 9.9. *Sidescan sonogram M-N across an intensely furrowed seabed, Northeast Newfoundland Shelf.*

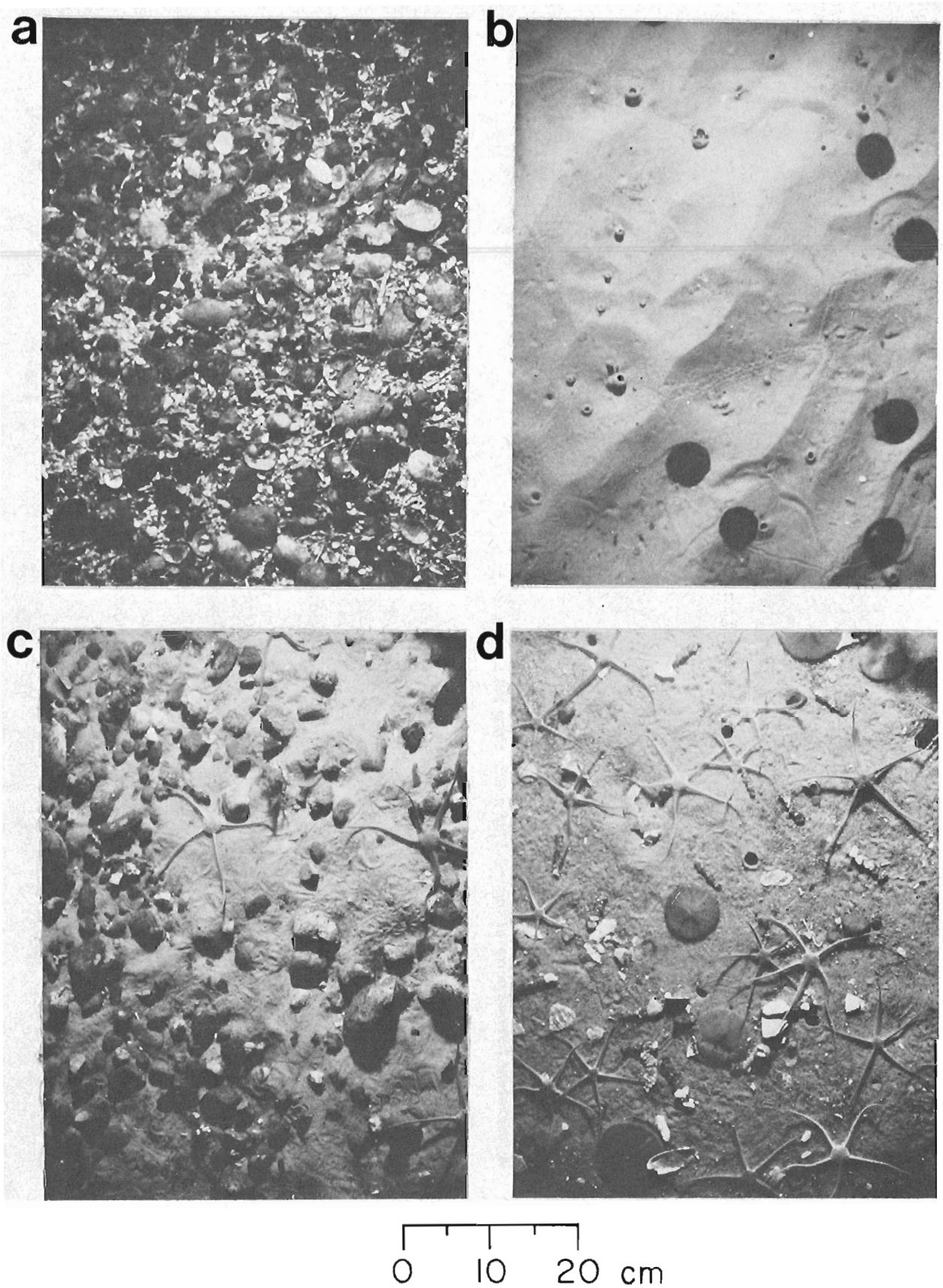

Figure 9.10. *Bottom photographs from the Hibernia study area showing variations in sediment texture.*

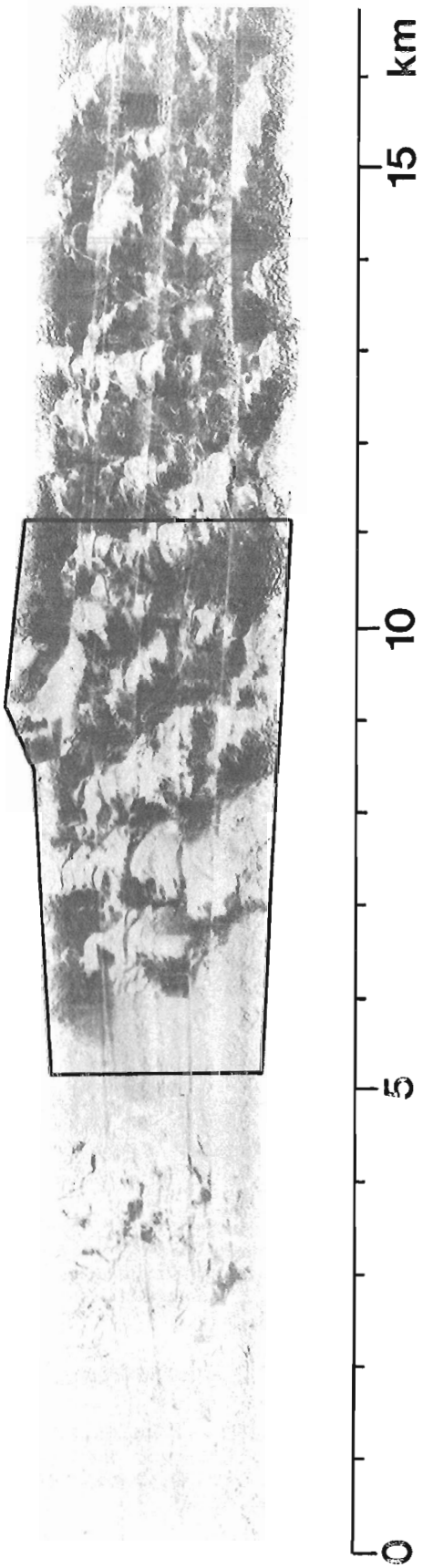

Figure 9.11. Sidescan sonar mosaic across Zones 3 and 4 from the Hibernia study area.

level stand appears to coindice with the minimum sea level curves of Milliman and Emery (1968) at 15 000 years B.P.

In the study area, the distribution of the surficial sediments, their sedimentological characteristics and stratigraphic relationships, and the distribution and significance of the partially buried iceberg furrowed surfaces indicate that the low sea level stand may have occurred at approximately the same depths (110-120 m). The distribution of the lag gravels in Zones 3 and 4, which could only have been formed in a high energy beach zone, indicates a former position for the pre-Holocene sea level, at or below the present 110 m contour. From the southern area of the Grand Banks, in Halibut and Haddock channels, and in some of the isolated depressions on the northern Grand Banks, the unconformities that were developed on glacial till and on glaciomarine sediments (Fig. 9.5, I-J) at depths of 110-120 m provide evidence for a low sea level stand at or below these depths. We assume that similar sediments existed in the Hibernia area and were completely removed during the transgression. Above depths of 110 m, the surficial sediments are well sorted and a definite change from light brown to buff-white occurs.

The above evidence suggests that the Late Wisconsin low sea level stand occurs at 110-120 m and that much of the Grand Banks was subaerially exposed prior to the Holocene transgression. In the sublittoral zone of the Holocene sea, the seabed was intensely furrowed by grounded icebergs associated with the retreating Late Wisconsin ice sheet. The present distribution of these furrows, now partially buried at depths below 110 m (Zone 1) provides a lower limit for the sea level stand, and above these depths any previously formed furrows would have been removed. This also indicates that furrows above the pre-Holocene low sea level stand (Zones 3 and 4) of the Hibernia study area are mainly Holocene and recent in age, about 10 000 to 12 000 years old.

To further refine the relative ages of these furrows is a difficult problem. Oceanographic data are lacking to investigate the dynamic setting of the area and to determine the temporal variations with respect to furrow formation and preservation. The distribution and relationship of trawl marks to iceberg furrows may provide some information on the age of the furrowing. If iceberg furrows can be found that transect trawl marks, then these furrows must have been formed in the past 30 years, the period during which deep ocean trawling has been conducted. A mapping program with a sidescan sonar system and a followup submersible survey would be necessary to understand the relationships in detail. A similar method of investigating the relative age of furrowing may be applied to submarine cables that occur in iceberg furrowed areas of the seabed.

Because some of the iceberg furrows occur in very hard seabed materials above the low sea level stand (lag gravels overlying semi-consolidated Tertiary "bedrock"), we feel that once formed, these furrows would persist and not be degraded beyond recognition at times when dynamic conditions were developed at the seabed. Some mobility of the thin sand is indicated from the sonograms and bottom photographs and in these areas the furrows may only partially be preserved. If this is to be accepted, then the number of iceberg furrows that presently occur at the seabed in the Hibernia area represent the total number of furrows formed in the last 10 000-12 000 years.

Sediment Stability

In depths of water less than 110-120 m, the lag gravel surfaces and below are highly stable and uniform and are interpreted as products of a relict environment. The semi-consolidated "bedrock" surface is defined by an extensive well-developed unconformity with little relief on its surface. Buried channels which may represent an engineering hazard below the seabed are virtually absent at the "bedrock" surface on the northern Grand Banks, and indicate stability at depth, unlike other areas of the Grand Banks to the south and west (Fig. 9.5, G-H) where such features do occur. In contrast the thin surficial sands which overlie the lag gravels are less stable and the distribution of the sand waves (Fig. 9.11) and the small scale ripples (Fig. 9.10b) indicate some degree of modern activity. Some characteristics of the sand deposits may in part be relict such as colour, the occurrence of bedforms associated with the pre-Holocene shoreline, and the high degree of sediment sorting above the low sea level stand at 110-120 m. It is difficult to clearly differentiate the modern and relict aspects of the environment for the sand cover.

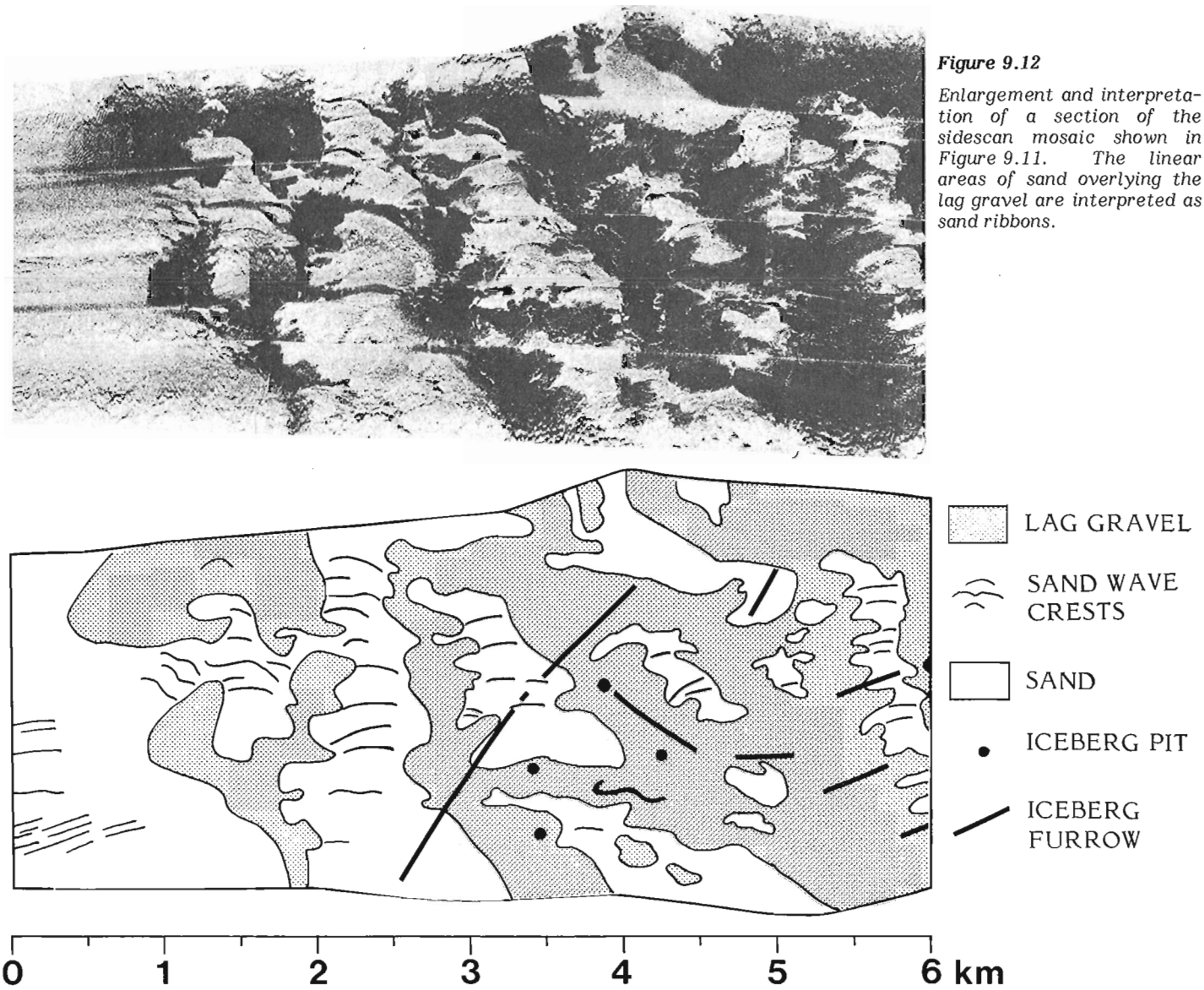

Figure 9.12

Enlargement and interpretation of a section of the sidescan mosaic shown in Figure 9.11. The linear areas of sand overlying the lag gravel are interpreted as sand ribbons.

Acknowledgments

We thank the Captain, Ship's Officers and Crew of **CSS Hudson** and the technical staff of the Atlantic Geoscience Centre for their co-operation during field operations. Sediment analyses were carried out by D.A. Clattenburg, and R.O. Miller assisted in field compilation and laboratory assessment of the data. Helpful comments were given by M. Latremouille, R. Parrott, and C.L. Amos.

References

Fader, G.B., King, L.H., and Josenhans, H.J.
Surficial geology of the Laurentian Channel and Western Grand Banks of Newfoundland; Marine Sciences Branch, Department of Energy, Mines and Resources, Ottawa, Ontario. (in press)

Hutchins, R.W., McKeown, D.L., and King, L.H.
1976: A deep tow high resolution seismic system for continental shelf mapping; Geoscience Canada, v. 3, p. 95-100.

King, L.H.
1970: Surficial geology of the Halifax-Sable Island map area; Department of Energy, Mines and Resources, Ottawa, Ontario, Marine Sciences Branch Paper 1.

King, L.H. and Fader, G.B.
1976: Application of the Huntec deep tow high-resolution seismic system to surficial and bedrock studies – Grand Banks of Newfoundland; in Report of Activities, Part C, Geological Survey of Canada, Paper 76-1C, p. 5-7.

Milliman, J.D. and Emery, K.O.
1968: Sea levels during the past 35 000 years; Science v. 162, p. 1121-1123.

Parrott, D.R., Dodds, D.J., King, L.H., and Simpkin, P.G.
1980: Measurement and evaluation of the acoustic reflectivity of the sea floor; Canadian Journal of Earth Sciences, v. 17, p. 722-737.

10.

CONTRIBUTION TO THE DIATOM FLORA OF ARCTIC CANADA: REPORT 2. ARCTIC REPRESENTATIVES OF THE GENUS NAVICULA

Project 720078

Sigrid Lichti-Federovich
Terrain Sciences Division

Lichti-Federovich, Sigrid, Contribution to the diatom flora of Arctic Canada: Report 2. Arctic representatives of the genus ***Navicula****; in Current Research, Part A, Geological Survey of Canada, Paper 81-1A, p. 57-62, 1981.*

Abstract

The second contribution to this series presents scanning electron micrographs of ***Navicula algida*** *Grun.,* ***Navicula trigonocephala*** *Cl., and* ***Navicula trigonocephala*** *fo.* ***minor*** *Østr. Information on distributional aspects of these marine diatom taxa establishes their ice-associated arctic habitat and confirms their endemic nature.*

Introduction

This contribution is part of a comprehensive taxonomic and ecologic evaluation of various diatom taxa of arctic regions (see Lichti-Federovich, 1979). Scanning electron images provide an invaluable aid in ascertaining and clarifying structural detail used in diatom systematics.

Electron optical analysis is of special importance in resolving some of the taxonomic ambiguities of arctic marine littoral and planktonic forms. Difficulties in the morphologic evaluation and systematic delineation of marine arctic **Navicula** species are mainly due to the wealth of transitional forms. For example, the form cycle of **Navicula transitans** Cl. and allied species exhibits close affinity to **Navicula directa** W. Sm. as noted by Cleve (1883) and stated by Heimdal (1970). Not only does the latitude of structural variability manifest at the specific and intraspecific levels, but in some naviculoid diatoms, particularly those endemic to arctic regions, structural differences occur even between the two valves of the same frustule.

Aside from uncertainties arising from partial or tentative identification, it is the diagnosis of as yet undescribed forms that most urgently requires electron analytical techniques.

Fukushima (1965), for example, in his analysis of a coloured sea ice sample from Point Barrow, Alaska, recognized about 40 taxa of diatoms of which 15 forms had to remain undetermined. Similar identification problems were encountered by Bunt (1966) in his investigations of the antarctic pack ice zone at Mawson and at McMurdo Sound.

Several naviculoid forms in a sample from Rosse Bay off Ellesmere Island also defied attempts at identification and could not be assigned to any previously published taxa. These diatoms will be the subject of further contributions to this series.

Acknowledgments

Once again I wish to express my appreciation to W. Blake, Jr. who collected the sample material and to D.A. Walker who took the scanning electron micrographs. Thanks are also extended to W.E. Podolak for his assistance with various salinity determination methods and to M.R. Sreenivasa, University of New Brunswick, Fredericton, for critically reading the manuscript.

Materials and Methods

The diatoms illustrated (Plates 10.1-10.3) originated from material collected by W. Blake, Jr. during his glacial geological studies in eastern Ellesmere Island. The collection was obtained on May 27, 1978 at Rosse Bay, between Cape Herschel peninsula and Neptune Island (78°36.7'N, 74°37'W).

The sample was taken roughly 200 m offshore from a crack in the sea ice. The lead was at least 50 cm wide, the ice thickness estimated at 0.5 to 1.5 m, and the depth of water more than 50 m. Since this account is based on a purely incidental collection (W. Blake, Jr., personal communication, 1980), physical indices are only approximate. The seawater sample scooped from the surface is characterized by its soup-like consistency and yellowish brown coloration. Salinity, ascertained as 20 ‰, was determined by conductance measurements in June 1978.

Sample preparation followed the method introduced by Van der Werff (1955) using hydrogen peroxide and potassium dichromate as oxidizing agents. Techniques employed in scanning electron analysis have been described previously (Lichti-Federovich, 1979).

Discussion

Arctic marine diatoms were described by Cleve (1873, 1883, 1896), Cleve and Grunow (1881), Østrup (1895, 1910), and Gran (1904a, b, 1908). More recent floristic studies of sea ice and plankton populations have been largely stimulated by investigations of primary productivity and by the importance of ice-associated diatoms as agents or initiators of primary production in arctic (Meguro et al., 1967; Alexander, 1974) and antarctic waters (Bunt, 1963, 1968; Burkholder and Mandelli, 1965; Fukushima and Meguro, 1966). The diatom sample from Rosse Bay, Ellesmere Island appears to represent just such an initiation phase.

It is characterized by an exceedingly high abundance of diatoms as denoted by its colour and consistency. Similar mucilagenous diatomaceous aggregates have been reported by Usachev (1946) from ice projection – seawater boundaries and from channels between ice floes in the eastern Soviet Arctic. He concluded that during ice melt with the formation of cavities, algae in the form of dirty brown accumulations or loose clumps of slimy masses drop into the water and float to the surface in the channels and cracks between ice floes.

Prolific growth of diatoms supported by the loosely aggregated bottom layer of sea ice and their subsequent release into the surrounding waters have also been documented by Bunt (1963) and Meguro et al. (1967). Furthermore, it is of interest to note that ice algae have been found in large concentrations in June on young winter ice in northern Ellesmere Island at the edge of the Arctic Ocean (Apollonio, 1965).

Compositional analysis of the surficial plankton sample from Rosse Bay discloses as its most salient feature the abundance and predominance of epontic elements, i.e., littoral forms such as **Pleurosigma, Amphiprora, Navicula, Gomphonema, Fragilaria, Nitzschia** which spend part of their

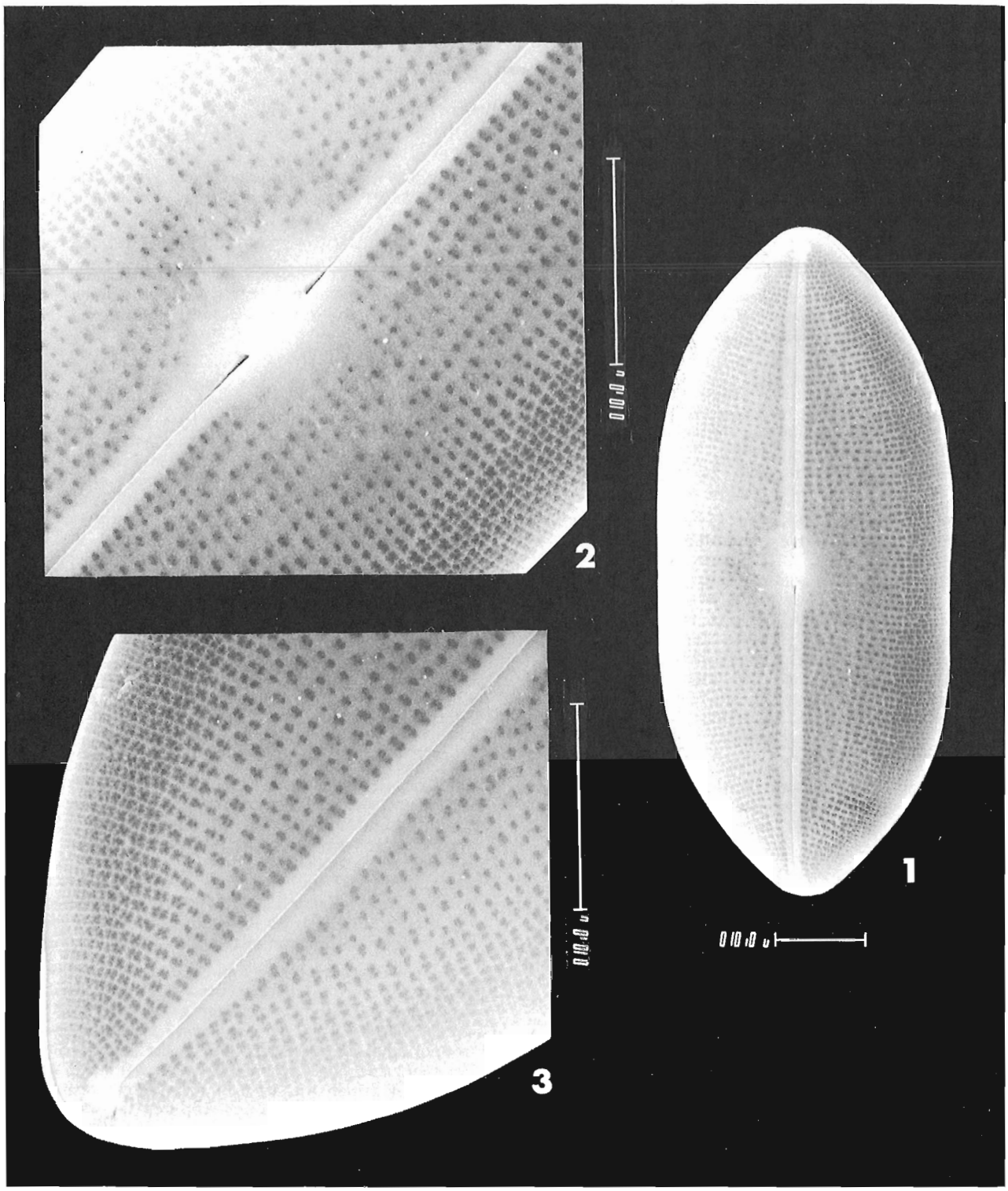

Plate 10.1

Figure 1. Scanning electron micrograph (GSC-97652): Outside view of valve (magnification x1500, tilt 20°).

Figure 2. Scanning electron micrograph (GSC-97652): Magnified central area showing central raphe fissure ending (magnification x3500, tilt 20°).

Figure 3. Scanning electron micrograph (GSC-97652): Magnification of valve apex illustrating deflection of polar raphe fissure ending (magnification x3500, tilt 20°).

life cycle attached to or frozen into the bottom layer of sea ice. This epontic constituent displays close floristic similarity to the diatom population in the plankton-coloured layer at the bottom of arctic sea ice off Point Barrow (Fukushima, 1965; Meguro et al., 1966, 1967).

The Rosse Bay algal bloom, including its small planktonic component (Thalassiosira, Melosira) also reveals a striking resemblance to a collection made in March from the ice of Karajakfjord, West Greenland, and to a sample taken in May from the surrounding water (Gran, 1899). Whether the centric diatoms were frozen into the ice together with the pennate forms of the ice algal community (Grant and Horner, 1976) and then released into the sea by the melting ice or whether they represent spring plankton forms present in the water column could not be determined. Nevertheless, this admixture of epontic and planktonic forms appears to represent an early spring successional phase of the seasonal phytoplankton cycle and is similar to that described by Saito and Taniguchi (1978) from the Bering Sea shelf region and the Chukchi Sea.

Aside from the distinctive dominance of epontic forms, the Rosse Bay diatom population is characterized by its strong endemic nature, succinctly expressed by the absence of bipolar distribution of its cryophilic species. This pronounced endemism, according to Fukushima (1965), is one of the features differentiating arctic and antarctic diatom floras.

Plate 10.1

Navicula algida Grunow

Denkschr. Akad. Wiss. Wien, math.-naturw. Kl. 48, p. 56, Pl. 1, Fig. 31, 1884.

Synonymy: See Van Landingham 1975, p. 2397.

Ecology: Arctic-marine, ice plankton, littoral, tychopelagic, psychrophilic, epontic, cryophilic, epicryotic, endocryotic.

Occurrence and Distribution: Hustedt (1971) characterized **Navicula algida** as an arctic marine form frequenting coastal areas and ice boundaries of the Arctic Ocean. Usachev (1946) included this species among those most often found in polar ice of local origin. Its circumpolar distribution and ice-associated occurrences have been clearly documented by the following finds:

In the sector of the Arctic Ocean bordering the Soviet Union, **Navicula algida** has been isolated from ice floe samples collected during the Vega Expedition (1878-1880) near Cape Wankarema, Chukchi Sea (Cleve, 1883). It has been found in Laptev sea ice and in ice from the region of Scott-Nansen Island, Kara Sea. This taxon has also been reported by Grunow (1884) from the under surface of an ice floe west of Novaya Zemlya in the Barents Sea.

Arctic occurrences in the waters surrounding Greenland include two plankton samples, one near Jan Mayen (Gran, 1908) and one from Cape Eglinton, Baffin Bay which may have originated from melted sea ice (Cleve, 1896). The occurrence of **Navicula algida** in East Greenland waters, connected with drift ice, has been reported by Østrup (1895) and in ice floes and in ice lumps in open channels, by Gran (1904b). Østrup (1897) also established its presence in western Greenland.

During the Canadian Arctic Expedition (1913-1918) exploring the waters bordering Yukon and Alaska, **Navicula algida** was encountered in dredgings off Cockburn point in Union Strait, Northwest Territories and north of Blossom shoals, Alaska. It has also been found at 150 fathoms in a vertical plankton net haul in ice, northeast of the Alaska – Yukon Territory International Boundary (Mann, 1925). From a plankton layer at the bottom of arctic sea ice off Point Barrow, Alaska, it has been recorded by Fukushima (1965) and Meguro et al. (1966, 1967).

Cleve's (1883) find of **Navicula algida** at the East Cape of Amchitka Island in the Bering Sea completes the circumpolar distribution of this endemic species.

Plate 10.2

Navicula trigonocephala Cleve

Vega Exped. vetensk, Iakttag., v. 3, p. 468, Pl. 36, Fig. 29, 1883.

Synonymy: See Van Landingham 1975, p. 2856.

Ecology: Arctic-marine, ice plankton, littoral, tychopelagic, psychrophilic, epontic, cryophilic, epicryotic, endocryotic.

Occurrence and Distribution: Similarity of the distributional pattern of **Navicula trigonocephala** to that of **Navicula algida** reflects the arctic nature of this species. It is found in nearly all collections listing **N. algida** and other endemic taxa; but whereas **N. algida**, according to Usachev (1946), exhibits close affinity to arctic ice of local origin, **N. trigonocephala** appears to be a common member of the drift ice flora. It has been discovered in samples associated with drifting ice near Cape Wankarema (Cleve, 1883), from East Greenland (Østrup, 1895), and Cape Eglinton, Baffin Bay (Cleve, 1896). Østrup (1910) listed **N. trigonocephala** from pack-ice samples at 75°14'N, 11°15'W and from samples from the outer margin of pack ice at 75°14'N, 4°34'W collected by the Danmark Expedition (1906-1908) from northeast Greenland. The latter occurrence appears to confirm Usachev's (1946) statement that **N. trigonocephala** is almost always found in samples of slimy aggregations on ice walls. **Navicula trigonocephala** has also been found in West Greenland near Umanarsuakat at 60°28'N (Østrup, 1897).

Additional ice-linked occurrences of **N. trigonocephala** in the polar seas were found by Gran (1904b) from samples collected during the North Polar Expedition (1893-1896) from the ice foot and from ice lumps in open channels between ice floes in the Arctic Ocean east of Greenland.

Navicula trigonocephala is also included in the diatom enumerations from the Beaufort Sea plankton haul sample taken northeast of the Alaska – Yukon Territory International Boundary (Mann, 1925) and from the bottom layer sample of sea ice off Point Barrow, Alaska (Fukushima, 1965; Meguro et al., 1966, 1967).

Plate 10.3

Navicula trigonocephala Cleve
fo. **minor** Østrup

Mar. diat. fra Østgrønl., p. 429, Pl. IV, Fig. 45, 1895.

Synonymy: See Van Landingham 1975, p. 2856.

Ecology: Arctic-marine, ice plankton, littoral, tychopelagic, psychrophilic, epontic, cryophilic, epicryotic, endocryotic.

Occurrence and Distribution: The distribution is the same as that for type species. It may be reasonably assumed that in most species listings differentiation between fo. **typica** and fo. **minor** has been omitted. Identification and a descriptive account of fo. **minor** by Østrup (1895) were based on a collection from ice floes drifting along the east coast of Greenland. It has also been recorded by Cleve (1896) from a plankton sample at Cape Eglinton, Baffin Bay, which may have been derived from melted ice.

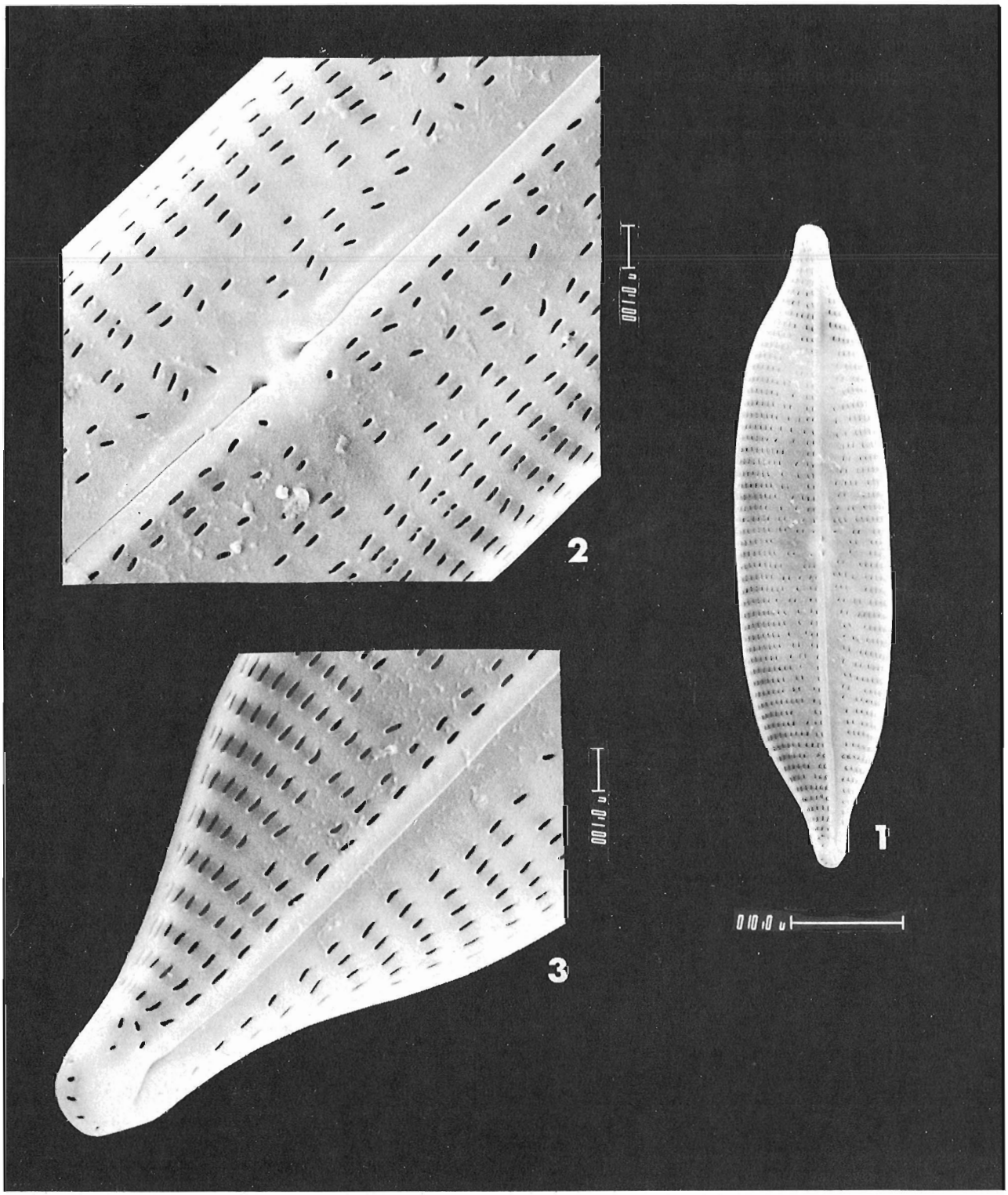

Plate 10.2

Figure 1. Scanning electron micrograph (GSC-97653): Exterior view of valve (magnification x1900, tilt 20°).

Figure 2. Scanning electron micrograph (GSC-97653): Enlarged central region displaying structural detail (magnification x7000, tilt 20°).

Figure 3. Scanning electron micrograph (GSC-97653): Magnified valve end showing polar raphe fissure deflection (magnification x7000, tilt 20°).

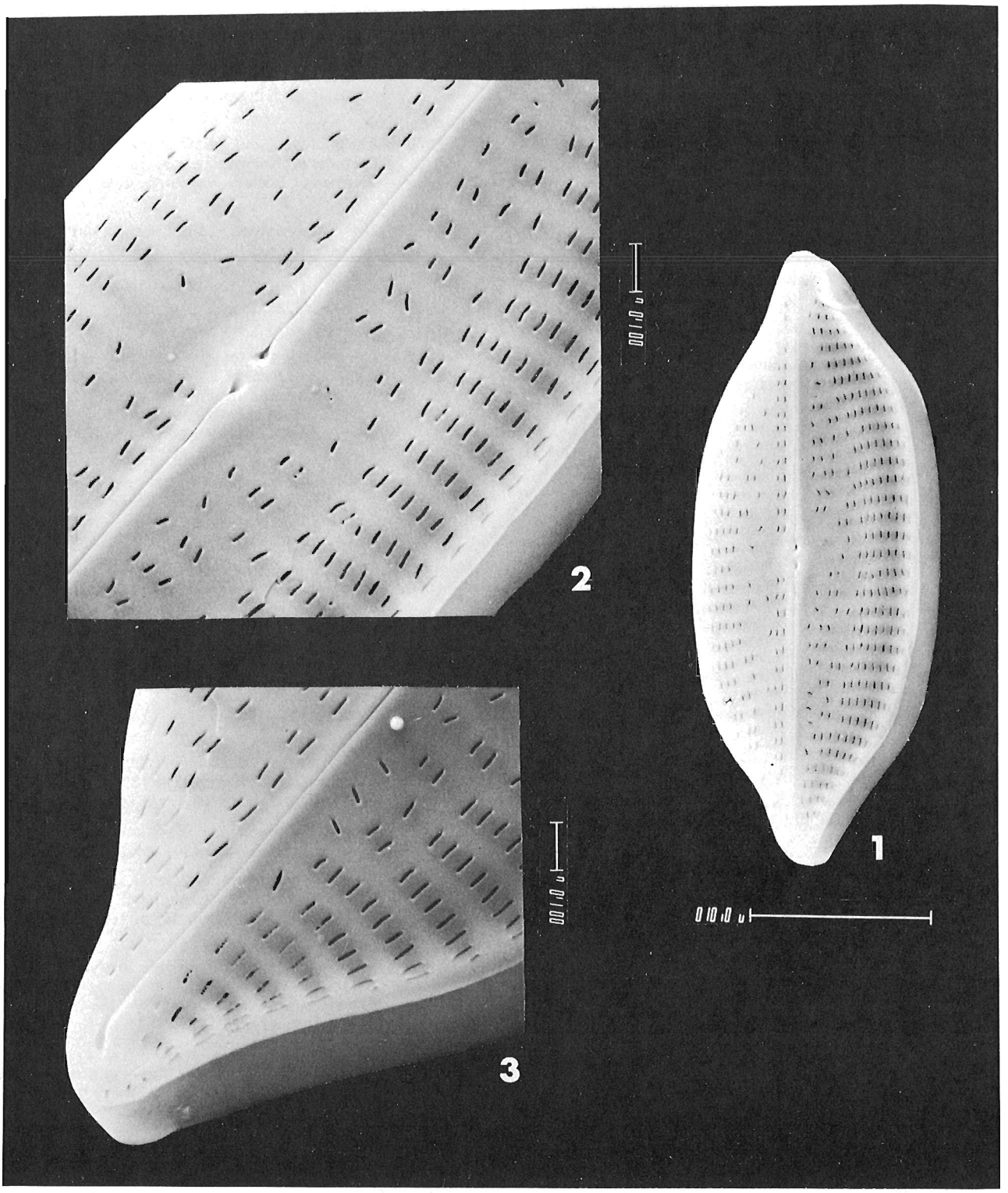

Plate 10.3

Figure 1. Scanning electron micrograph (GSC-97654): Exterior view of valve (magnification x3100, tilt 30°).

Figure 2. Scanning electron micrograph (GSC-97654): Magnification of valve centre showing external raphe fissure endings (magnification x8000, tilt 30°).

Figure 3. Scanning electron micrograph (GSC-97654): Enlarged apical region displaying polar external raphe fissure ending (magnification x8000, tilt 30°).

References

Alexander, V.
1974: Primary productivity regimes of the nearshore Beaufort Sea, with reference to potential roles of ice biota; The Coast and Shelf of the Beaufort Sea, ed. J.C. Reed and J.E. Slater; Arctic Institute of North America, p. 609-635.

Apollonio, S.
1965: Chlorophyll in Arctic sea ice; Arctic, v. 18, no. 2, p. 118-122.

Bunt, J.S.
1963: Diatoms of Antarctic sea ice as agents of primary production; Nature, v. 199, no. 4900, p. 1255-1257.

1968: Microalgae of the Antarctic pack ice zone; Symposium on Antarctic Oceanography (Santiago, Chile), Cambridge, Scott Polar Research Institute for Scientific Committee on Antarctic Research, p. 198-218.

Burkholder, P.R. and Mandelli, E.F.
1965: Productivity of microalgae in Antarctic sea ice; Science, v. 149, no. 3686, p. 872-874.

Cleve, P.T.
1873: On diatoms from the Arctic Sea; Bihang till kunkliga Svenska Vetenskaps-Akademiens Handlingar, v. 1, no. 13, p. 3-28.

1883: Diatoms collected during the expedition of the Vega; in Nordenskiolds, N.A.E., Vega Expeditionens vetenskapliga Iakttagelser, v. 3, p. 457-517.

1896: Diatoms from Baffins Bay and Davis Strait; Collected by M.E. Nilsson; Bihang till kungliga Svenska Vetenskaps-Akademiens Handlingar, v. 22, no. 4, p. 3-22.

Cleve, P.T. and Grunow, A.
1881: Beiträge zur Kenntnis der arktischen Diatomeen (1879); Kungliga Svenska Vetenskaps-Akademiens Handlingar, v. 17, no. 2, p. 3-121.

Fukushima, H.
1965: Preliminary report on diatoms from colored sea ice in Point Barrow, Alaska; Antarctic Record, v. 24, p. 31-35.

Fukushima, H. and Meguro, H.
1966: The plankton ice as basic factor of the primary production in the Antarctic Ocean; Antarctic Record, v. 27, p. 99-101.

Gran, H.H.
1899: Bacillariaceen vom kleinen Karajakfjord; Bibliotheca Botanica, v. 8, p. 13-24.

1904a: Diatomeen der arktischen Meere; Fauna Arctica, v. 3, no. 8, p. 509-554.

1904b: Diatomaceae from the ice-floes and plankton of the Arctic Ocean, Volume IV; in The Norwegian North Polar Expedition, 1893-1896, Scientific Results, ed. F. Nansen; v. 4, no. 11, Longmans, Green, and Co., London, New York, p. 3-74.

1908: Diatomeen; Nordisches Plankton XIX, ed. K. Brandt and C. Apstein; Kiel and Leipzig, Verlag von Lipsius and Tischer, p. 1-146.

Grant, W.S. and Horner, R.A.
1976: Growth responses to salinity variations in four arctic ice diatoms; Journal of Phycology, v. 12, p. 180-185.

Grunow, A.
1884: Die Diatomeen von Franz Josephs-Land; Denkschriften der kaiserlichen Akademie der Wissenschaften. Mathematisch-naturwissenschaftliche Klasse, 48, p. 53-112.

Heimdal, B.R.
1970: Morphology and distribution of two **Navicula** species in Norwegian coastal waters; Norwegian Journal of Botany, v. 17, no. 2, p. 65-75.

Hustedt, F.
1971: Die Kieselalgen, VII. Band; in Rabenhorsts Kryptogamen-Flora von Deutschland, Österreich und der Schweiz, v. 7 (1961-1966), Geest & Portig, K.-G., Leipzig, Johnson Reprint Corporation, New York, London.

Lichti-Federovich, S.
1979: Contributions to the diatom flora of Arctic Canada: Report 1. Scanning electron micrographs of some freshwater species from Ellesmere Island; in Current Research, Part B, Geological Survey of Canada, Paper 79-1B, p. 71-82.

Mann, A.
1925: The marine diatoms of the Canadian Arctic Expedition 1913-1918; in Report of the Canadian Arctic Expedition 1913-18, v. 4: Botany; F.A. Acland, Ottawa, p. 1-33.

Meguro, H., Ito, K., and Fukushima, H.
1966: Diatoms and the ecological conditions on their growth in sea ice in the Arctic Ocean; Science, v. 152, no. 3725, p. 1089-1090.

1967: Ice flora (bottom type): A mechanism of primary production in polar seas and the growth of diatoms in sea ice; Arctic, v. 20, no. 2, p. 114-133.

Østrup, E.
1895: VI. Marine diatoméer fra Østgrønland; Den østgrønlandske Expedition 1891-1892; Meddelelser om Grønland, Band 18, no. 6, p. 397-476.

1897: Kyst-Diatoméer fra Grønland; Meddelelser om Grønland, Band 15, p. 305-362.

1910: X. Diatoms from north-east Greenland; collected by the "Danmark-Expedition"; Meddelelser om Grønland, Band 43, no. 10, p. 195-256.

Saito, K. and Taniguchi, A.
1978: Phytoplankton communities in the Bering Sea and adjacent seas. II. Spring and summer communities in seasonally ice-covered areas; Astarte, v. 11, no. 1, p. 27-35.

Usachev, P.I.
1946: Biological indicators of the origin of the ice-floes in the Kara Sea and of Brothers Laptev and the Straits of the Franz-Josef-Land Archipelago; Akademiya Nauk SSSR, Institut Okeanologii, Trudy, v. 1, p. 113-150.

Van der Werff, A.
1955: A new method of concentrating and cleaning diatoms and other organisms; International Association of Theoretical and Applied Limnology, Proceedings, v. 12, p. 276-277.

Van Landingham, S.L.
1975: Catalogue of the Fossil and Recent Genera and Species of Diatoms and their Synonyms. Part V. **Navicula**; J. Cramer, Lehre, p. 2386-2963.

11.

AN EXPERIMENT IN LAKE DRAINAGE, RICHARDS ISLAND, NORTHWEST TERRITORIES: A PROGRESS REPORT

Project 680047

J. Ross Mackay[1]
Terrain Sciences Division

Mackay, Ross J., An experiment in lake drainage, Richards Island, Northwest Territories: A progress report; in Current Research, Part A, Geological Survey of Canada, Paper 81-1A, p. 63-68, 1981.

Abstract

In the Tuktoyaktuk Peninsula and Richards Island region, Northwest Territories, some thousands of lakes have drained naturally, either in whole or in part, in the past few thousand years. The present drainage rate is about one lake per year. Most lakes have drained by channel erosion of ice-wedge systems. Since the region lies in the zone of continuous permafrost, lake drainage and permafrost growth have produced a complex three dimensional permafrost distribution. In order to understand better the processes associated with permafrost growth in drained lakes, a lake 600 m long, 300 m wide, and up to 5 m deep was artificially drained by channel flow along an ice-wedge system in order to simulate natural drainage.

Following drainage on 13 August 1978, the outlet has widened by thaw of ice-rich permafrost to produce a greatly oversized canyon similar to many natural channels and indicative of catastrophic drainage. Probing of the lake bottom immediately after drainage showed that the permafrost surface dipped steeply lakeward where water depths had exceeded 1.5 m. Temperature measurements show that in nearshore areas, where permafrost was less than 10 m deep, freeze-through from the lake bottom to permafrost at depth was completed from 1978 to 1980 by both downward and upward freezing. Where permafrost was much deeper (e.g. more than 20 m), only 5 to 6 m of the lake bottom froze from 1978 to 1980. Accurate levelling of numerous lake bottom bench marks 2 to 23 m deep has shown that frozen ground has continued to heave after the temperature was below 0°C.

Introduction

In the Tuktoyaktuk Peninsula and Richards Island region, Northwest Territories (Fig. 11.1), lakes cover from 20 to 40 per cent of the total area. The region lies in the zone of continuous permafrost with mean annual undisturbed ground temperatures in the range of -7° to -10°C. Since 1950, when complete airphoto coverage of the region became available, photo interpretation and field studies have shown that at least 30 lakes have drained naturally, either in whole or in part, for a drainage rate of about one lake per year. In deep lakes where water depth exceeds 1 to 1.5 m, the mean annual lake bottom temperature is positive; therefore, when these deep lakes become drained, permafrost commences to grow on the exposed lake bottoms. Consequently, the three dimensional distribution of permafrost is extremely complex, because lake drainage has been taking place for thousands of years and the lakes grade in every conceivable combination from large to small, deep to shallow, old to young, and undrained to completely drained. As the time of natural drainage cannot be forecast, it seemed evident that if a lake were artificially drained, detailed before-and-after permafrost studies could make important short and long term contributions to our knowledge of permafrost. Towards this end, several lakes on the verge of natural drainage were selected for study, and land and water use permits for artificial drainage were obtained.

The first lake selected for drainage was "Illisarvik", located 60 km due west of Tuktoyaktuk, Northwest Territories (Fig. 11.1). (The name "Illisarvik", meaning "place of learning", is not yet officially approved but is used herein for convenience). The project has been a co-operative endeavour involving personnel from government and universities. Illisarvik was drained on 13 August 1978 (Fig. 11.2). In November 1978, a session dealing with Illisarvik was presented at a Symposium on Permafrost Geophysics, sponsored by the National Research Council of

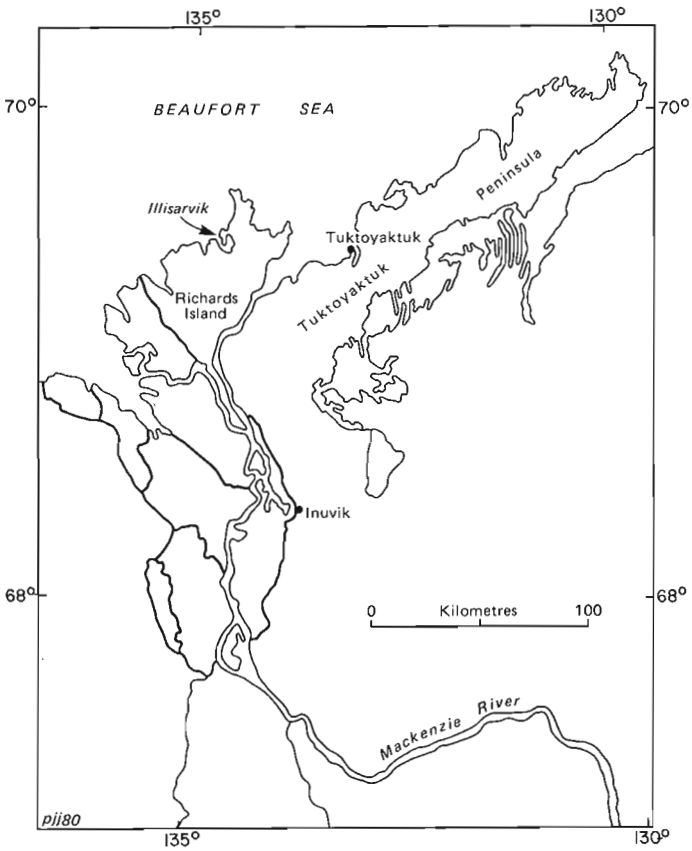

Figure 11.1. *Location map showing study area.*

[1]Department of Geography, University of British Columbia, Vancouver, B.C., V6T 1W5

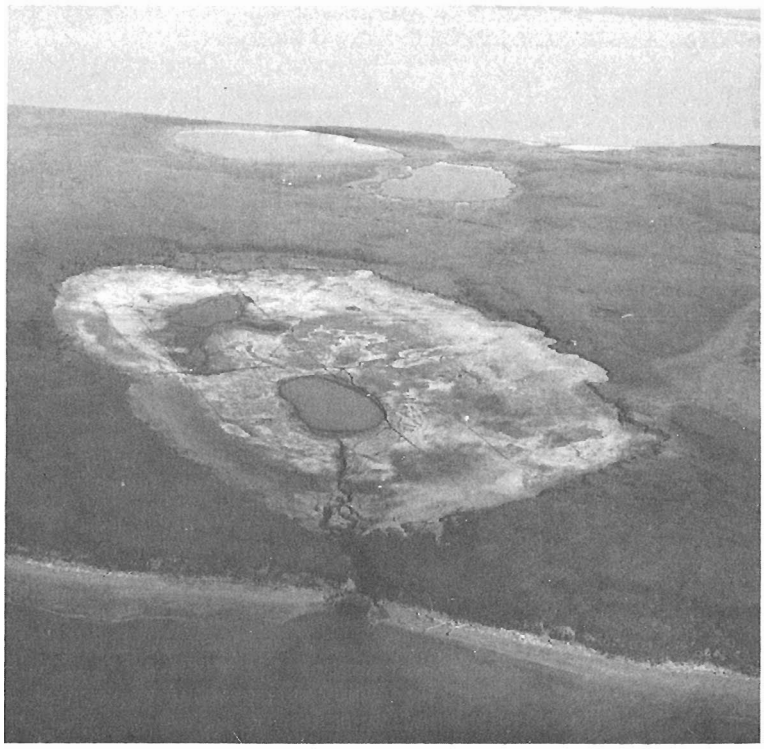

Figure 11.2. *Photograph of Illisarvik in August 1979 showing the two residual ponds, the outlet, and the plunge pool at the seaward end of the outlet.*

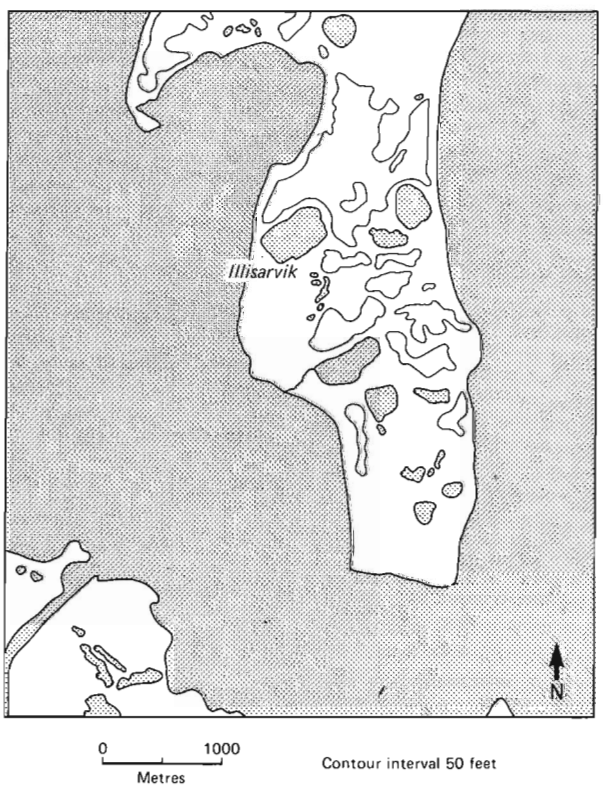

Figure 11.3. *Location map for Illisarvik (cf. Fig. 1). Stippled areas are water.*

Canada and held at Calgary, Alberta. In view of the interest created by the lake drainage experiment, and its potential for long term permafrost research, this paper gives a brief progress report on lake drainage, permafrost growth, and heave of permafrost.

Acknowledgments

The drained lake experiment has involved collaboration by personnel from the Department of Indian and Northern Affairs (Inuvik Scientific Resource Centre); Department of the Environment (Northern Hydrology Section); Earth Physics Branch and the Geological Survey of Canada, Department of Energy, Mines and Resources; University of Toronto; University of Waterloo; and University of British Columbia. Much help has been provided by the Polar Continental Shelf Project (Department of Energy, Mines and Resources), and research support has been received from the Natural Sciences and Engineering Research Council of Canada. The drainage experiment has been carried out under Land Use Permit N77N714.

Lake Drainage

Illisarvik Lake, prior to drainage, was 600 m long and 300 m wide (Fig. 11.3). The shortest distance between lake and sea was 45 m. The lake level was about 7.2 m above sea level and the maximum lake depth, about 5 m. The lake lacked a drainage channel but in the runoff period of June 1978 water overflowed by way of a sedgy draw to a drained lake to the south. The 45 m strip of land between the lake and the coastal bluff was in an area of ice-wedge polygons with the highest point along a potential channel being only 0.4 m above lake level. Since the majority of naturally drained lakes in the Richards Island and Tuktoyaktuk Peninsula area have drained along ice-wedge systems (Mackay, 1979), the drainage plan for Illisarvik was to channel lake water along an ice-wedge system to the coastal bluff and thus simulate natural drainage.

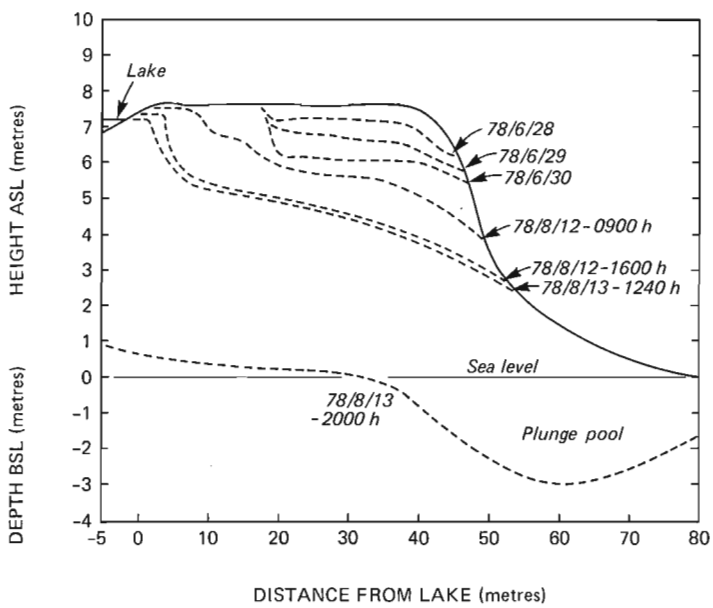

Figure 11.4. *A cross profile from the lake to the coastal bluff showing, by dashed lines, the various stages in the development of the drainage channel.*

Figure 11.5.

Photograph looking to the sea along the drainage channel in late June 1978. The peat has been removed to the frost table.

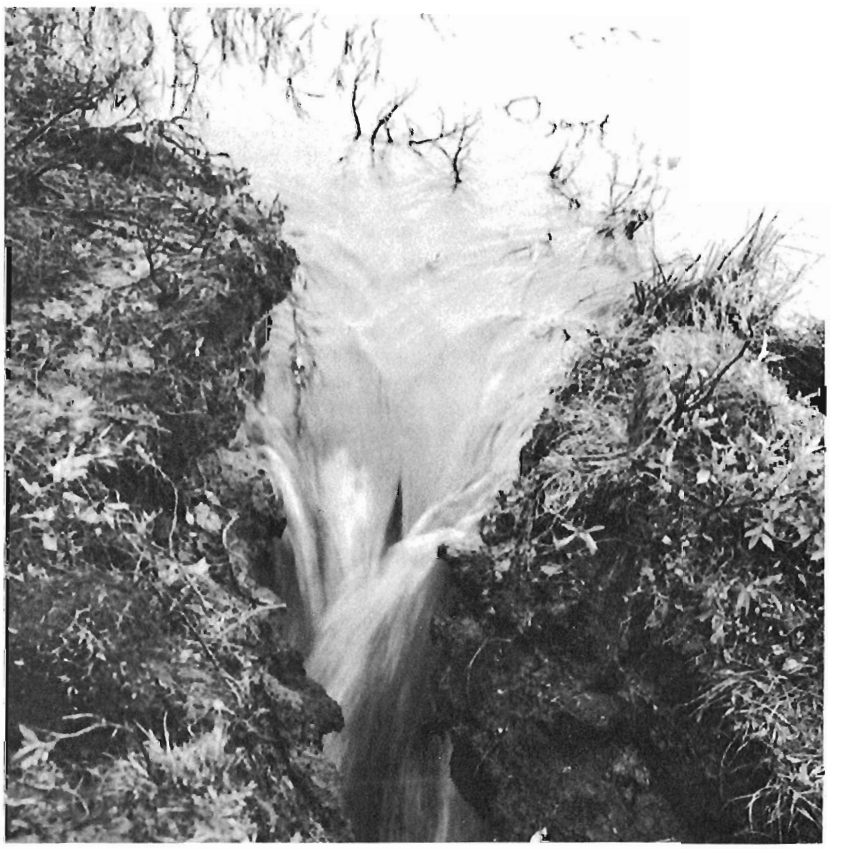

Figure 11.6.

The waterfall of the drainage channel eroding headward into the lake about one hour after flow had started. As soon as the falls began eroding into the soft active layer, headward erosion was exceedingly rapid.

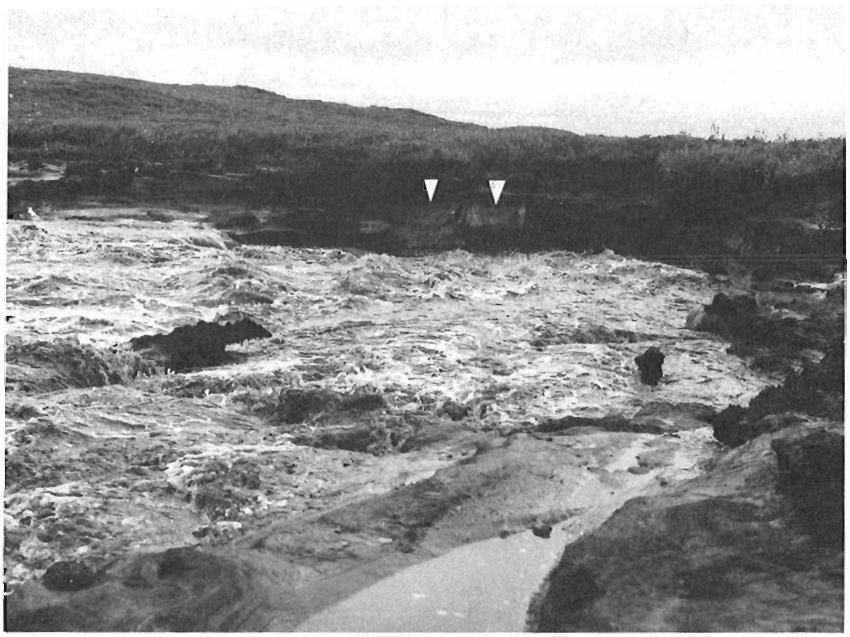

Figure 11.7.

The photograph shows the drawdown and rapids four hours after flow started. The lake is to the left, the outlet to the right. The water level had been lowered about 1 m and large blocks of eroded lake bottom sediments were being carried seaward. Exposed ice wedges are marked with arrows.

Ditching

Ditching along the 45 m drainage channel commenced on 20 June 1978. First the thawed organic matter was dug out from the 20 to 45 m mark with distances measured from the lakeshore (Fig. 11.4). On 21 June, a portable pump (Wajax Mark III) was used to flush lake water down the channel (Fig. 11.5). Even though the lake water was just above 0°C, erosion was rapid as soon as wedge ice was encountered. The flow was concentrated along fresh 1978 winter ice-wedge cracks, many of which were not yet infilled with ice. By 30 June, the channel had been enlarged to about 1.5 m deep and 20 to 30 cm wide. Most of the channel was incised into wedge ice. The channel was left undisturbed from 30 June to 5 August by which time the top width had increased by thaw and slumping to between 2.5 and 3.5 m. The pump was used again in early August to clean out the channel debris and deepen the seaward section to about 4 m. On 12 and 13 August, the unchannelled portion of the ice-wedge system close to the lake was stripped of peat to the frost table and a channel eroded with the pump. At the time when the channel was ready for breaching to the lake, the gradient was about 1:10 and there was a 1.5 m drop near the lakeshore. The purpose of creating a potential waterfall was to ensure rapid headward (lakeward) erosion once the channel was breached.

Drainage

At 1240 h on 13 August, a channel several centimetres deep was dug into frozen peat to permit throughflow from the lake to the sea. By 1400 h a waterfall had eroded 2 m lakewards (Fig. 11.6). The waterfall was 1.5 m high, 0.8 m wide, the water about 0.5 m deep, and the flow rate from lake to sea about 1 m/s. Once the unfrozen lake bottom sediments were exposed to erosion, the waterfall eroded lakeward in an ever enlarging crescent, concave to the outlet. By 1700 h the mean channel velocity from lake to sea was 2 m/s. The drawdown at the outlet (i.e. water depth below lake level) increased to at least 1 m and large blocks of lake bottom peat were swept downstream (Fig. 11.7). At all times the drainage was underground, first in a narrow box canyon, and then as the channel widened and deepened, in a 45 m long keyhole-shaped tunnel with the slot open to the sky. A 3 m-deep plunge pool developed at the landward edge of the coastal bluff (Fig. 11.4). By 1935 h the lake bottom for a distance of 50 m from the outlet was scoured into a typical badland topography. The erosion was along a rectangular ice-wedge channel system, inherited from thermokarst truncation of ice wedges during a post hypsithermal period of lake enlargement. By 2000 h the water level had dropped about 2 m (Fig. 11.8) leaving two large residual ponds and many smaller ponds on the soggy lake bottom. Accurate measurements of water level were impossible after 2000 h because the lake bottom was too soft

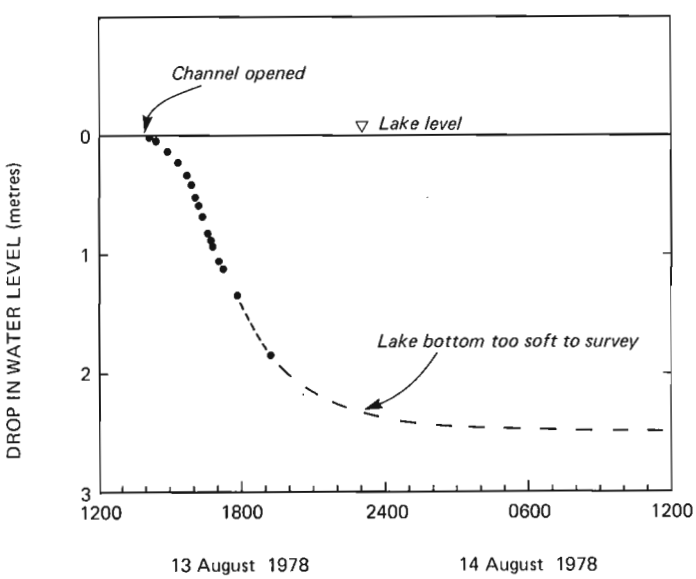

Figure 11.8. *The graph shows the drop in lake level following diversion of lake flow down the artificial channel to the sea.*

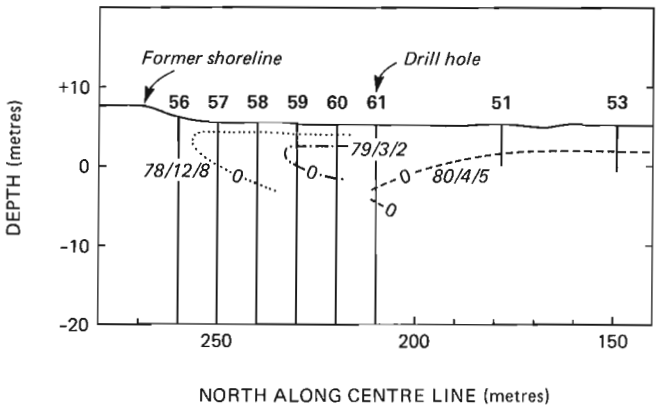

Figure 11.9. *A cross-profile of the northeast end of Illisarvik after drainage. The zero datum is sea level, as in Figure 11.8. The approximate location of the 0 C isotherm is shown for 8 December 1978; 2 March 1979; and 5 April 1980. Note that by 8 December 1978, drillhole 56 was entirely in frozen ground; by 2 March 1979, drillholes 57 and 58 were entirely in frozen ground; and by 5 April 1980, drillholes 59 and 60 were also in frozen ground. Even so, the 23 m-long bench marks installed at drillholes 56, 57, 58, 59, and 60 have continued to heave after the entire sections, except for the active layer, are frozen. As heave continued in the summer of 1980, heave of permafrost, not the active layer, was involved.*

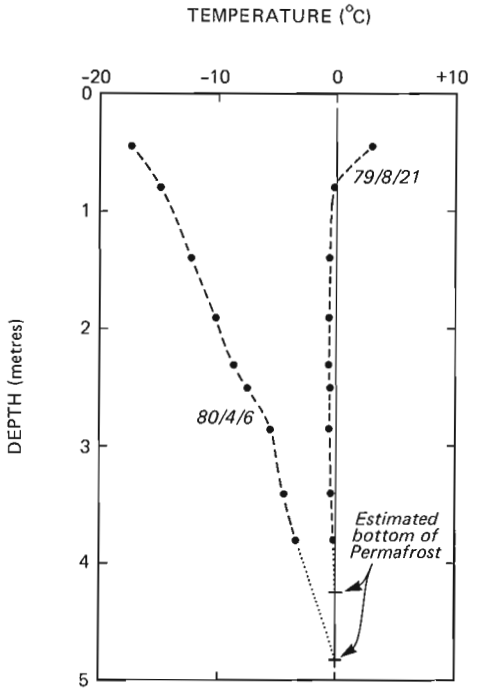

Figure 11.10. *The curves show temperatures on the lake bottom for 21 August 1979 and 6 April 1980. The ground had frozen during the winter of 1978-79, but in the summer of 1979 the newly frozen ground warmed almost to 0 C. The ground then cooled in the winter of 1979-80, and in the summer of 1980 it warmed again (data not plotted) nearly to 0 C as in the summer of 1979. The warming was due to heat conduction from the active layer and the talik beneath.*

to permit placement of measurement stakes. By 0800 h, 14 August, the lake level had been lowered about 2.5 m (Fig. 11.8) and the discharge was about 1 m^3/s. From 1200 h, 14 August to 23 August, the last full day spent at the site, the flow declined erratically, the discharge varying from about 0.3 m^3/s to about 0.025 m^3/s.

Prior to drainage Illisarvik had an area of about 170 000 m^2. The lake lowering from 1300 h to 2000 h on 13 August was about 2 m to give a mean discharge of about 10 m^3/s. As the mean flow rate was about 2 m/s through a tunnel of mean diameter of less than 5 m, the discharge flow was then 1 to 2 m deep.

Outlet

As mentioned earlier, field studies have shown that most of the lakes in the Tuktoyaktuk Peninsula and Richards Island area that have drained have done so by erosion along an ice-wedge system (Mackay, 1979, p. 31). Frequently, an underground channel that develops along an ice-wedge system will self-heal by infreezing of the channel before the lake can be drained. The resulting "pool" ice, which is frozen from bulk water, contrasts with the vertically foliated ice-wedge ice, which results from infilling of vertical thermal contraction cracks. It is not surprising, therefore, that "pool" ice was abundant in ice wedges exposed along the drainage channel, indicating that Illisarvik had nearly drained by natural means at least once previously.

The tunnel roof collapsed by the time of freeze-back in November 1978. Deep snow filled the outlet in winter. By early June 1979 the overhangs which were stabilized by the freeze-back of 1978 began to collapse. By mid-June 1979 the width at the top measured 7 to 10 m and by mid-August 1979 had increased to 10 to 12 m. The widening was from thaw of ice-rich permafrost along the sides of the channel and not from stream erosion, because there was little to no flow most of the summer. Even the plunge pool of 13 August 1978 remained unfilled in August 1979 (Fig. 11.2). The outlet continued to widen in the summer of 1980. By September 1980, the top width varied from 11 to 15 m. The channel was V-shaped, 4 to 6 m deep, and partially infilled with sediment transported by spring runoff from the exposed lake bottom.

After two years the drainage outlet is greatly oversized for the maximum flow; during early summer and after a rain, there may be slight flow, but at other times, the channel is dry. The oversized developing box canyon of Illisarvik, like that of hundreds of other drained lakes in the region, has formed by catastrophic flow and subsequent widening by thaw in ice-rich permafrost. The magnitude of the flow indicates the potential danger of artificial disturbances of drainage in ice-rich permafrost.

Permafrost Growth

The lakeward dip of the upper permafrost surface immediately after drainage was mapped by probing at the southwest end of the lake by the outlet and at the opposite northeast end. The permafrost surface plunged steeply lakeward at both ends of the lake where water depths had exceeded about 1.5 m. At the northeast end of the lake, five holes were drilled at 10 m intervals and 10 m-long cables, each with 10 thermistors, were installed in the holes in mid-August 1978. Additional and deeper holes were drilled in 1979 and 1980 (Fig. 11.9). Temperatures were measured in December 1978; March, June, and August 1979; and April, June, August, and September 1980. Two distinct freezing patterns have emerged. First, at the nearshore sites, where the permafrost below the lake bottom plunged steeply

lakewards and was less than about 10 m deep, rapid two-sided freezing has occurred, downwards from the ground surface and upwards from permafrost at depth. Second, at sites remote from shore, where permafrost is at depths of about 20 m or more, permafrost growth appears to be primarily downwards and the newly frozen ground is thin.

In the nearshore area, where the upper permafrost surface prior to drainage was at a depth of about 4 m, the downward-penetrating 0°C isotherm had merged with permafrost beneath by mid-March 1979 (Fig. 11.9). During the winter of 1980, the ground froze through to where permafrost was formerly at a depth of about 10 m. Thus, where permafrost was at a relatively shallow depth, such as 10 m or less, freeze-back was completed within one summer and two winters. By way of contrast, at sites more distant from shore where permafrost was at a depth in the order of 20 m, freezing was to a depth of only about 1 m by mid-December 1978; to about 2.25 m by March 1979; to about 3.5 m by March 1980; and to about 5 to 6 m by August 1980. It is evident, therefore, that upward freezing has played an important role in the growth of new permafrost at Illisarvik in the nearshore areas. During the summer of 1979, sites with thin newly frozen ground warmed up to nearly 0°C (Fig. 11.10); the same was repeated in the summer of 1980.

Permafrost Heave

Before and after the drainage of Illisarvik, a considerable number of holes were jet (water) drilled by other researchers collaborating in the Illisarvik experiment, and the holes were cased with one inch (2.54 cm) steel waterpipe in which temperature cables were inserted. In addition, numerous holes were drilled and cased by the writer after drainage. These pipes have been used as bench marks for accurate levelling of the lake bottom. The datum bench marks are three long pipes drilled to depths of 53, 58, and 66 m, located a few metres inland from the former shoreline and therefore in permafrost probably at least several hundred metres deep, as temperature measurements suggest. The datum bench marks were tied together by accurate levelling in the summers of 1979 and 1980, the height differences among them not exceeding ± 1 mm. By way of contrast, four 10 m-long bench marks installed parallel to and 2 m distant from bench marks 56, 57, 58, and 59 (Fig. 11.9) heaved 0.2, 1.2, 5.3, and 7.5 cm from 1979 to 1980, even though the ground remained frozen, except for summer active layer thaw. The heave of the 10 m-long bench marks continued through the summer of 1980, when the active layer was thawing, as did the 23 m-long bench marks of 56, 57, 58, and 59 (Fig. 11.9); so the heave represented a general lake bottom heave and not uplift by frost heaving of the active layer. The results of 1979 to 1980 levelling, and summer levelling in 1980, show rather conclusively that appreciable heave can occur in frozen ground if there is a temperature change.

Conclusion

1. The lake drainage experiment illustrates the catastrophic nature of natural drainage and the origin of the oversized box canyons which are so common in the western arctic coastal region.
2. The permafrost surface of Illisarvik dipped steeply lakewards where water depths had exceeded 1.5 m. In nearshore areas, development of new permafrost has been very rapid because of downward freezing from the ground surface and upward freezing from permafrost at depth. Where permafrost is at a considerable depth (e.g. more than 20 m), freezing is predominantly from the surface downwards. In areas with only a few metres of newly frozen ground, temperatures in the first two summers after drainage approached 0°C.
3. In growing permafrost, appreciable heave can occur for at least one year after the ground is below 0°C. This may have engineering implications.

Reference

Mackay, J.R.
1979: Pingos of the Tuktoyaktuk Peninsula area, Northwest Territories; Géographie physique et quaternaire, v. 23, p. 3-61.

GEOLOGY OF HOPEDALE BLOCK AND ADJACENT AREAS, LABRADOR: REPORT 3

Project 780025

Ingo Ermanovics and John A. Korstgård[1]
Precambrian Geology Division

Ermanovics Ingo and Korstgård, John A., Geology of Hopedale block and adjacent areas, Labrador: Report 3; in Current Research, Part A, Geological Survey of Canada, Paper 81-1A, p. 69-76, 1981.

Abstract

Migmatite gneiss in Hopedale block may represent a plutonic episode between the earlier Hunt River and later Florence Lake volcano-plutonic episodes. Rocks in Hopedale block and reworked equivalents in adjacent Makkovik subprovince are characterized by four structural trends.

Mapping has revealed that the Hunt River volcanic belt extends 32 km farther northeastward than previously recognized.

The Island Harbour (Bay of Islands) granite in Makkovik subprovince intrudes amphibolite facies gneiss thought to have been reworked during the Proterozoic.

A succession of Proterozoic mafic lavas and coarse grained volcanic sediments 1100 to 2000 m thick (Ingrid group) marks approximately the Nain-Churchill boundary in the study area. The volcanic rocks are mylonitized in the west; intensity of deformation wanes from west to east across the group.

Introduction

This report presents some results of 1980 field work in Hopedale block and adjacent areas. The main lithological units were defined by Ermanovics and Raudsepp (1979) and preliminary structural information was provided by Ermanovics (1980). A number of special projects were undertaken by visitors and members of the field party: geology of intrusive relationship between rocks of the Elsonian intrusive complex and Archean rocks of Nain Province (K. Downing, B.Sc. project, University of Western Ontario); geology of Proterozoic volcanic rocks of Ingrid group (R. Knight and J. Pearson, B.Sc. projects, University of Western Ontario and Lakehead University, respectively); petrology of Island Harbour (Bay of Islands) Proterozoic granite (A. Lalonde); structural analysis of Archean and Proterozoic rocks at Kanairiktok Bay and Hopedale area (J. Korstgård, NSERC Visiting Fellow); Rb-Sr isotope, rare earth and trace element geochemistry of felsic rocks in Nain Province and Makkovik subprovince in the area of Kanairiktok Bay (Professors N. Grant and M. Hickman, M.Sc. and Ph.D. theses project supervisors, Miami University of Oxford, Ohio).

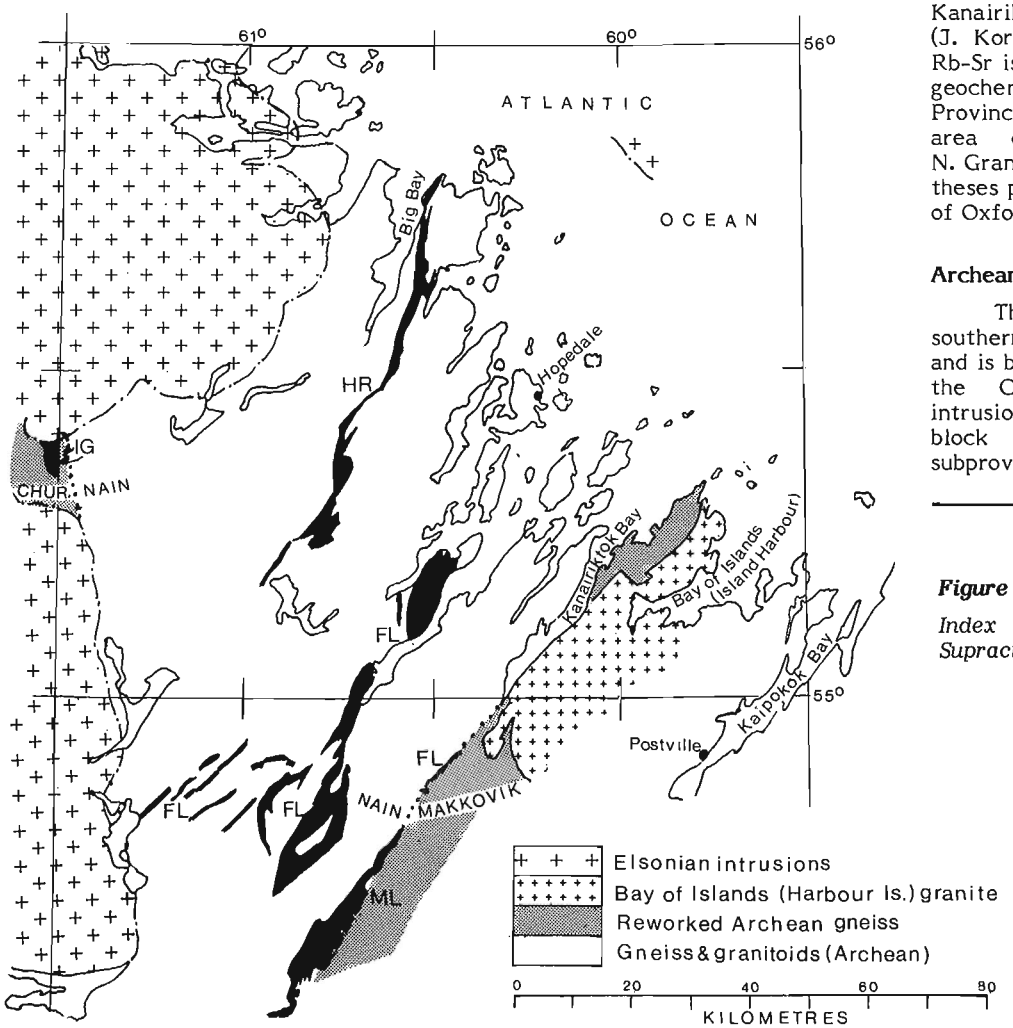

Archean Rocks

The Hopedale block forms the southern part of the Archean Nain Province and is bounded to the west and northwest by the Churchill Province and Elsonian intrusions. To the south and southeast the block is bounded by the Makkovik subprovince (Taylor, 1971).

Figure 12.1.

Index to areas discussed in text. Supracrustal rocks (black shading):

IG = Ingrid group (Proterozoic)
HR = Hunt River belt (Archean)
FL = Florence Lake group (Archean)
ML = Moran Lake Group (Proterozoic)
CHUR. = Churchill Province

[1] Department of Geology, Aarhus University, 8000 Aarhus, Denmark.


A

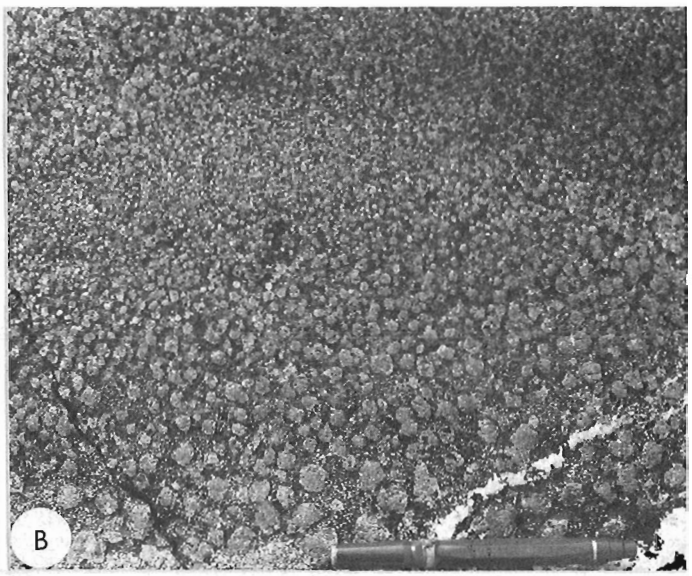
B

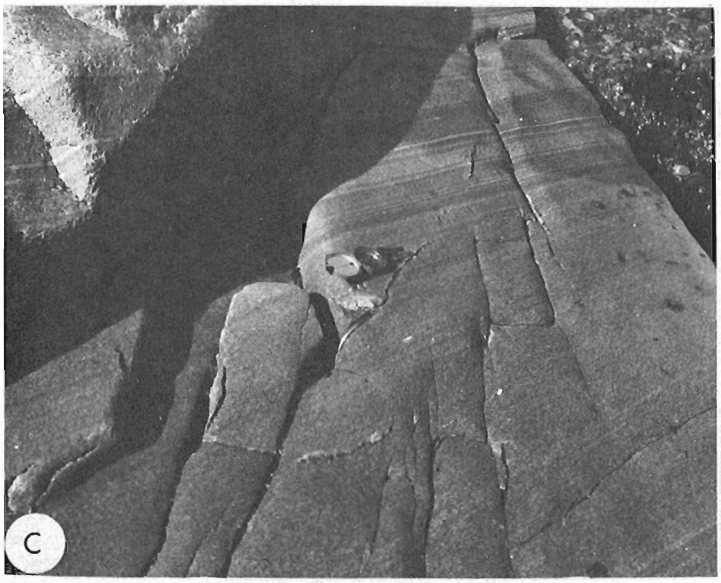
C


D


E

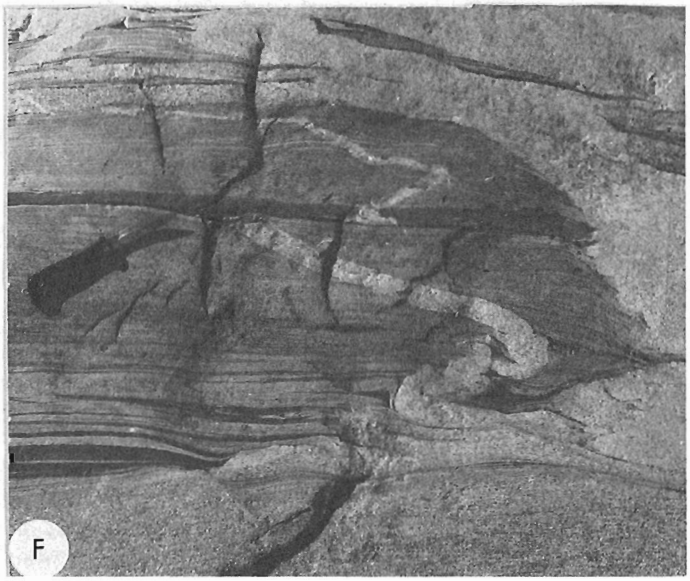
F

The rocks of the Hopedale block are mainly amphibolite facies quartzofeldspathic gneisses with rafts of layered amphibolite and inclusions of metadolerite(?) pods. Granitoids and pegmatities of various ages intrude the gneisses and their inclusions. Rocks of the Hopedale block have been named collectively Hopedale Gneiss (Kranck, 1953, Taylor, 1977a). Subdivisions of Hopedale Gneiss and their relationship to supracrustal rocks are as follows:

Hopedale Gneisses	Volcanic Rocks
Kanairiktok intrusions	
	Florence Lake
..... unconformity (inferred).....	
Migmatitic gneiss	
Maggo gneiss (≡ layered orthogneiss associated with Hunt River)	
Weekes amphibolite	Hunt River

Hunt River Volcanic Rocks

The Hunt River belt of volcanic rocks, initially mapped by Taylor (1977a), has been shown to extend 32 km farther northeastward to the mouth of Big Bay (Fig. 12.1). Rocks in this part of the belt occupy low lying areas, in contrast to the southwestern part where they form a prominent ridge. Rocks in the southwestern part are mainly homogeneous metabasalts at upper amphibolite facies (Jesseau, 1976). Rocks in the northeastern part are prominently layered and comprise intercalated amphibolite, variegated schist, felsic gneiss and ultramafic rocks. They differ from rocks of the southwestern part by their prominent layering and more felsic compositions.

Hopedale Gneisses

Previous reports have stressed a simple two-fold division of Archean gneiss in Hopedale block based on texture and grade of metamorphism (Ermanovics and Raudsepp, 1979; Ermanovics, 1980). An older suite of felsic granoblastic gneiss and associated layered amphibolite gneisses were termed Maggo gneiss and Weekes amphibolite, respectively. Weekes amphibolite is tentatively correlated with Hunt River volcanic rocks; Maggo gneiss is similarly correlated with layered felsic orthogneiss along the western contact of the Hunt River volcanic belt. This contact is sharp and sheared and the relationship of the orthogneiss to the volcanic rocks is not clear. However, Maggo gneiss intrudes Weekes amphibolite. Hence, if the correlation with Hunt River is correct, layered orthogneiss may also intrude Hunt River volcanics. A preliminary U-Pb zircon concordia intercept age for the felsic orthogneiss is about 3000 Ma (D. Loveridge, Geological Survey of Canada, personal communication 1980), which may be a minimum age for Hunt River volcanics.

Plutons of tonalite, granodiorite and minor granite (Kanairiktok intrusive suite; Ermanovics and Raudsepp, 1979) intrude the older gneiss suite and Florence Lake group volcanic rocks, and are metamorphosed to lower amphibolite facies. These granitoids are the youngest major intrusions in Hopedale block (Nain Province). A preliminary U-Pb zircon concordia intercept age for a metatonalite of the Kanairiktok intrusions is about 2830 Ma (D. Loveridge, personal communication, 1980) and provides a minimum age for Florence Lake volcanics.

Much of Hopedale block is underlain by migmatitic gneiss, previously referred to in part as Kanairiktok gneiss (Ermanovics, 1980, Fig. 2.2, p. 14), and interpreted as a mixture of the late Kanairiktok intrusive rocks and earlier gneiss. However, inclusions of this migmatitic gneiss were discovered this year in tonalite of the Kanairiktok intrusive suite. This seems to establish an earlier episode of migmatite formation that predates the emplacement of the Kanairiktok intrusions and the migmatite formation that accompanied them.

Proterozoic Rocks in Makkovik Subprovince

Island Harbour Granite

Various aspects of the Island Harbour granite (formerly Bay of Islands granite, Ermanovics, 1979) have been reported previously. Three major intrusive units define the granite: an early grey phase, a pink porphyritic phase, and a late grey aplitic phase. Central to any hypothesis of its emplacement is whether the granite intruded Proterozoic amphibolite facies gneiss (i.e. Hopedale gneisses reworked during Proterozoic) or Archean amphibolite facies gneiss (i.e. unaltered Hopedale gneiss). It is assumed here that basement gneisses in Makkovik subprovince were reworked at amphibolite facies in Proterozoic time, although a late Archean age cannot be precluded. A Proterozoic age for amphibolite facies metamorphism may be suggested by a K-Ar biotite age of 1728 ± 32 Ma in Kaipokok Bay, which is considerably younger than the 2400-2600 Ma K-Ar ages in Hopedale block (Taylor, 1979 and 1977b).

The northern part of the granite intrudes gneiss of Makkovik subprovince* that exhibits a degree of flattening (gneissosity and banding) and upgraded amphibolite facies metamorphism not present in the retrograded (greenschist) amphibolite facies gneiss immediately west of Kanairiktok Bay (Nain Province). Xenoliths of this gneiss lie in the early grey phase of the granite that exhibits magmatic banding (Fig. 12.2C, D, E, F). The granite develops a weak foliation peripheral to the xenoliths. Contacts between granite and gneiss in the southwestern part of the granite are gradational over large areas and the original nature of the gneiss there is obscured by discordant and concordant granitic mobilizate.

In an area 20 to 30 km southwest of the Island Harbour granite, a schistosity and greenschist facies metamorphism is recognized as the first Proterozoic deformation in basement rocks and Aphebian Moran Lake Group (Fig. 12.1). This deformation overprints amphibolite facies basement gneiss thought to have been metamorphosed to amphibolite facies during the Archean (Ryan, 1979). A Proterozoic age for amphibolite facies metamorphism is preferred by the present authors since these gneisses, like those intruded by Island

***Figure 12.2** (opposite)*

Archean Maggo gneiss (A,B). Proterozoic gneiss of Makkovik subprovince intruded by an early grey phase of Island Harbour (Bay of Islands) granite (C,D,E,F).

A. Layering in Maggo gneiss partly disrupted by late white granitic mobilizate. Photo 8-32-80.

B. Garnet-rich layer (hornblende-quartz matrix) from near an ultramafic layer associated with gneiss of Figure A. Photo 9-9-80.

C. Early grey phase of Island Harbour granite showing magmatic banding. Photo 17-8-80.

D. Complex xenolith of gneiss, amphibolite and mafic phase of granite in foliated less mafic granite. Photo 17-9-80.

E. Xenolith of complexly folded gneiss forming agmatite in granite. Photo 17-10-80.

F. Detail of Figure E showing magmatic resorption of gneiss in granite. Photo 17-11-80.

* Hopedale Gneiss of Taylor, 1979, and Hopedale Complex of Sutton, 1972, which actually includes Island Harbour granite, Fig. 1, p. 1678.

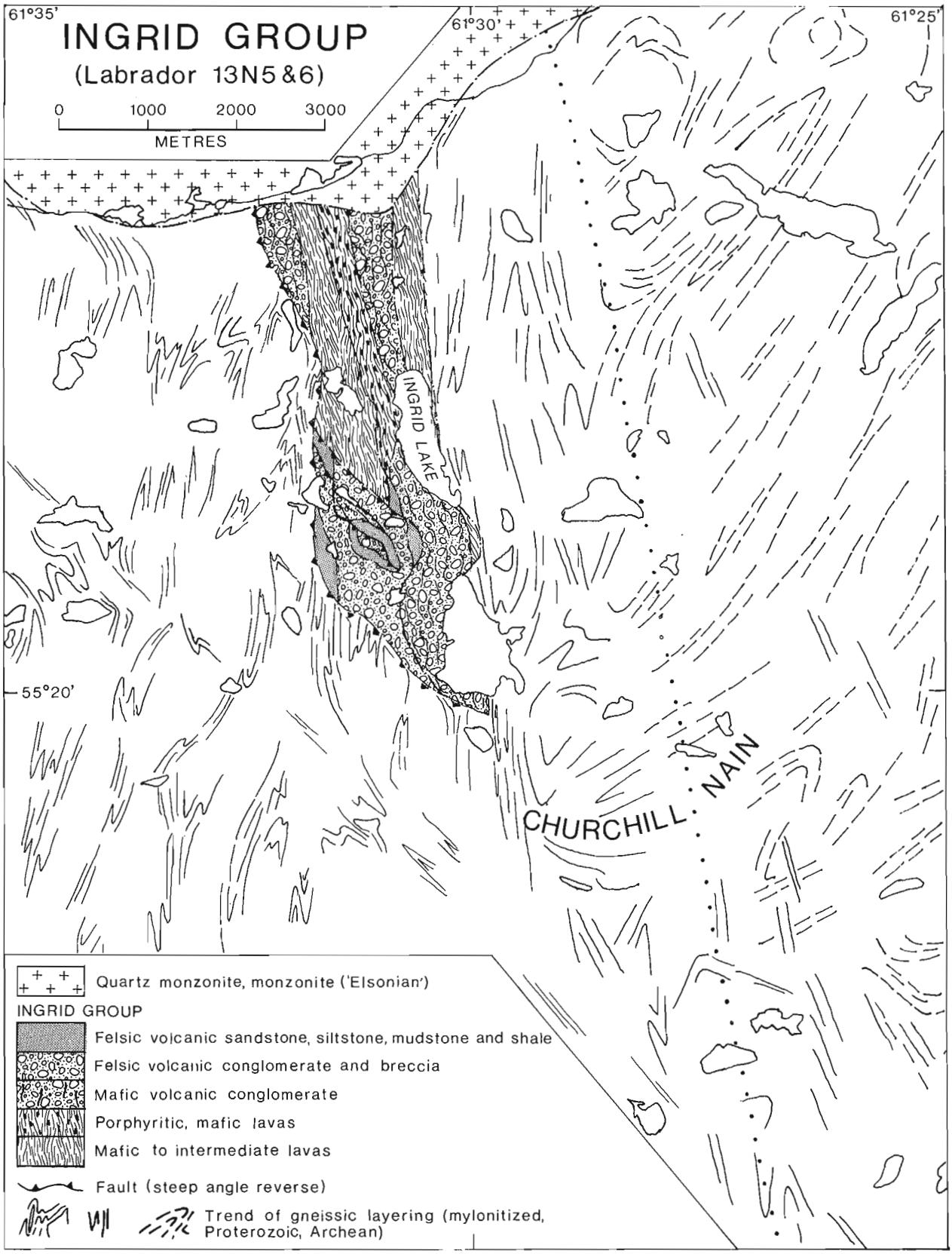
61°35'
INGRID GROUP
(Labrador 13N5&6)
0 1000 2000 3000
METRES
61°30'
61°25'
INGRID LAKE
55°20'
CHURCHILL
NAIN
Quartz monzonite, monzonite ('Elsonian')
INGRID GROUP
Felsic volcanic sandstone, siltstone, mudstone and shale
Felsic volcanic conglomerate and breccia
Mafic volcanic conglomerate
Porphyritic, mafic lavas
Mafic to intermediate lavas
Fault (steep angle reverse)
Trend of gneissic layering (mylonitized, Proterozoic, Archean)

Figure 12.3

Harbour granite, exhibit structural fabrics typical of Makkovik subprovince rather than Nain Province. If, as the northern exposures indicate, the granite intrudes Proterozoic gneisses, and if these are the same gneisses that underlie Moran Lake Group, then it follows that Moran Lake Group may have been deposited upon a Proterozoic craton.

Proterozoic Rocks in Churchill Province

Ingrid Group

An occurrence of andesite of Neohelikian age was reported by Taylor (1977a, 1979) just west of longitude 61°30, and immediately north of latitude 55°20, in map sheet 13 N/5. Mapping (scale 1:12 500) this year showed an area of 11 km^2 to be underlain by mafic lavas and volcaniclastic rocks that antedate Hudsonian mylonitization. The age of the rocks is therefore probably Aphebian. The rocks are foliated and metamorphosed to lower greenschist facies (chlorite, epidote). This succession is herein informally named Ingrid group, and formations from oldest to youngest are as follows (Fig. 12.3):

Mafic to intermediate lavas; minor porphyritic basalt and mafic volcanic conglomerate; rare pillowed lavas; maximum thickness 500 m.

Porphyritic basalt; minor mafic to intermediate lavas and mafic volcanic conglomerate; maximum thickness 200 m.

Mafic volcanic conglomerate; minor felsic volcanic conglomerate, breccia, sandstone, siltstone (possible tuffs) and mafic lavas; 200 to 800 m thick.

Felsic volcanic conglomerate; minor volcanic breccia, sandstone, siltstone and mafic conglomerate (possible tuffs); 100 to 400 m thick.

Felsic volcanic sandstone, siltstone, mudstone, shale (possible tuffs); minor volcanic conglomerate; maximum thickness 100 m.

Lavas are dominantly subaerial basalts and andesites intercalated with mafic volcanic conglomerate. Individual flows were not recognized. Porphyritic basalt is characterized by 10 to 30 per cent plagioclase phenocrysts (1 to 2 cm) developed in discontinuous 'cumulus' horizons. Mafic conglomerate members in this formation include clasts of porphyritic lavas (Fig. 12.4A). Volcanic conglomerates are unsorted, rarely bedded and comprise angular volcanic rock fragments (1 to 15 cm, 4 cm average), including basalt, gabbro, felsic aphanites, porphyritic aphanites and rare bedded shales (Fig. 12.4C, D). Basement gneiss and granitoid clasts are rare but occur as angular cobbles and boulders 10 to 50 cm in diameter in both mafic and felsic conglomerate formations (Fig. 12.4A, B). The uppermost formation comprises felsic volcanic sandstone, siltstone and mudstone in poorly sorted graded beds that have indistinct, gradational bed boundaries. Dropstones, intraformational rip-ups and soft sediment slumps are common (Fig. 12.4E). Coarse detritus lies unsorted in beds of felsic sandstones. These depositional features suggest debris slide deposits or, in a more general sense, unstable depositional conditions in which, perhaps, pyroclastic materials were reworked. Petrographic analyses are in progress to determine the source and composition of the sediments.

Ingrid group is intruded (contact not exposed) by Elsonian granitoids ("adamellite") along its northern contact. Everywhere else the succession is bounded by rocks that have been deformed and metamorphosed during mylonitization typical of parts of eastern Churchill Province, forming the contact with Nain Province (Taylor, 1979). Greenstone inclusions in foliated granodiorite increase in size and abundance toward the eastern contact with Ingrid group. Country gneiss, contact migmatite gneiss and marginal volcanic rocks on the west side are mylonitized (Fig. 12.4F). Mylonite is well developed in gneisses west of Ingrid group, but becomes increasingly less so eastward across the group, and is manifest as a weak north-south trending chlorite-epidote schistosity in the eastern gneisses.

Formations of Ingrid group appear to be folded to a gently flexed anticline, and were subsequently folded and faulted along steep, west dipping thrust faults. Foliations and bedding strike 140° to 190° and generally dip steeply west. Rare determinations in sparsely bedded horizons indicate overturned bedding tops. Post-consolidation mesoscopic structures are restricted to minor drag and kink folds in fine grained rocks near the western margin and are attributable to mylonite deformation.

Layered gneisses of Nain Province (NE-trending Fiord trend, see below) east of Ingrid group were rotated to north-south trends at amphibolite facies. The easternmost extent of the chlorite-epidote fabric, related to the Hudsonian mylonitization, approximately coincides with the first occurrence of reoriented gneiss. Accordingly, the Churchill-Nain boundary is placed along a line (Fig. 12.3) where the youngest structural trend in Nain is reoriented north-south and accompanied by low greenschist metamorphism.

Mylonite in granulite facies rocks in Churchill Province east of Mistastin Lake is seen as a late deformation that produced shallow north or south plunging folds (axial planes dip steeply west). Mylonitization occurred at amphibolite facies and co-axially overprinted the earlier tectonite (J. Hill, Newfoundland Department of Mines and Energy, personal communication 1980). The age of granulite metamorphism north of Mistastin Lake is interpreted as Aphebian (Taylor, in Wanless and Loveridge, 1978). It is likely that amphibolite facies metamorphism accompanying NS structural reorientation 2 km east of Ingrid group is also of Aphebian age. It is suggested that Ingrid group may have been deposited on an unstable Proterozoic 'craton' and was subsequently deformed by regional cataclasis whose intensity decreased from west to east across the area underlain by Ingrid group and adjacent eastern basement rocks.

Structural Trends

In the following a simplified structural framework for the Hopedale region is outlined as a basis for further detailed structural analysis.

Structural Elements

Most of the structural data were obtained at coastal exposures where waterwashed surfaces provide ample opportunity for detailed structural observations. Data collected were mostly recordings of the orientation of penetrative linear and planar structures related to the latest pervasive structural and metamorphic event in the rocks.

The penetrative planar structures in the gneisses are mainly of two types: (i) A schistosity defined by preferred habit orientation of mafic minerals (micas, hornblende and epidote). In some cases elongated felsic minerals (quartz and feldspars) or elongated aggregates of felsic minerals contribute to the schistosity. (ii) A compositional layering (banding) defined by alternating concentrations of mafic and felsic minerals. The compositional layering is commonly accentuated by lit-par-lit pegmatoids. The schistosity is parallel to the compositional layering and occurs within dominantly felsic as well as mafic layers.

The penetrative linear structures in the gneisses are mainly of three types: (i) A mineral lineation defined by preferred habit orientation, mostly of hornblende. (ii) An aggregate lineation (stretching lineation) defined by aggregates of granular grains; a linear structure created by intersecting leucocratic veins commonly appears as an aggregate lineation. (iii) Axes of minor crenulations or corrugations of planar surfaces (crenulation lineation).

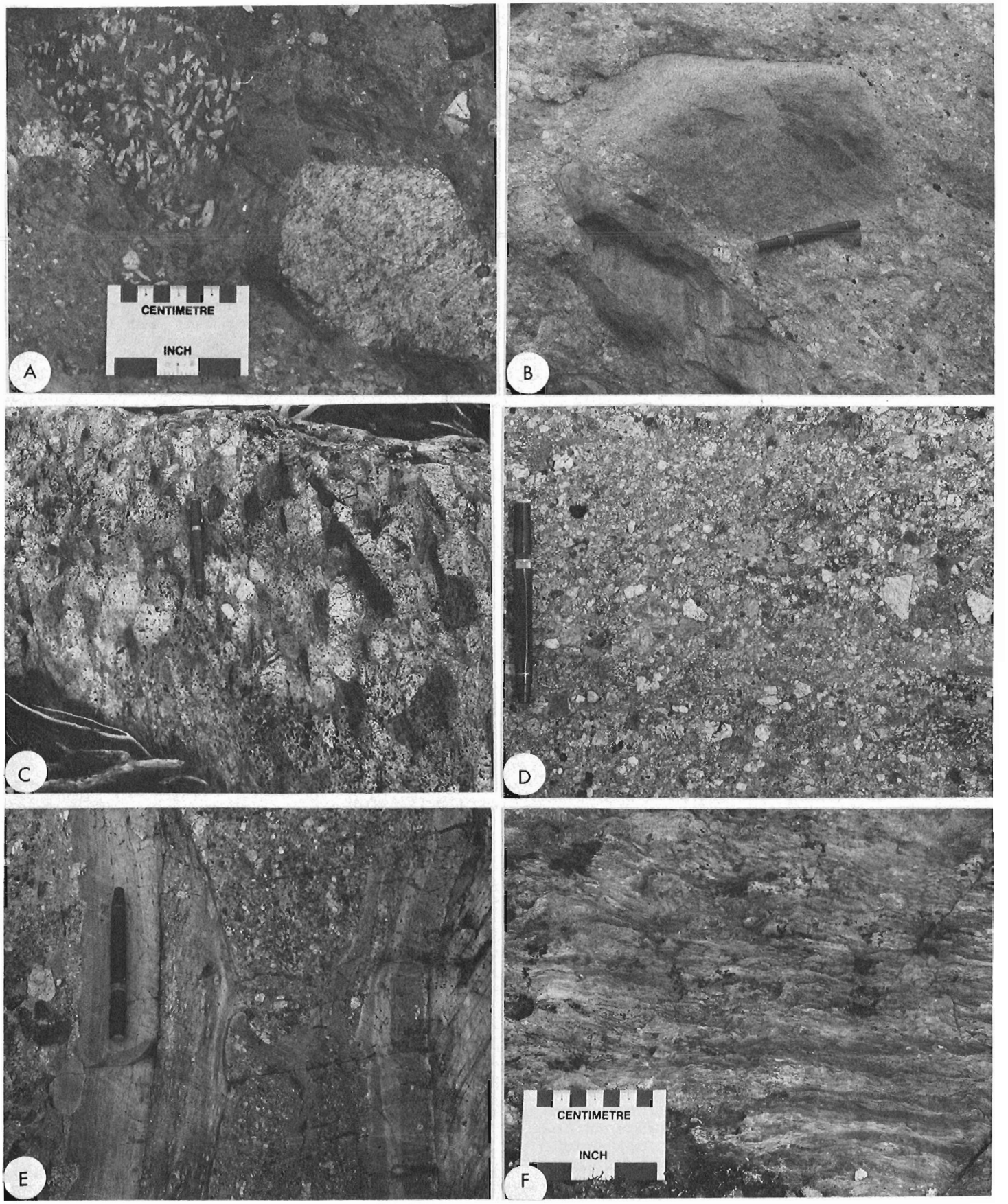
CENTIMETRE
INCH
A
B
C
D
E
CENTIMETRE
INCH
F

Figure 12.4 *(opposite)*

Volcanic sediments of Ingrid group.

A. Boulder of porphyritic basalt and gneissose granodiorite in mafic volcanic conglomerate. Photo 13-2-80.

B. Boulder of massive granodiorite and gneiss of possible Proterozoic age in felsic volcanic conglomerate. Photo 2-1-80.

C. Foliated felsic volcanic conglomerate with minor dark grey shale clasts. Photo 2-12-80.

D. Felsic volcanic breccia. Photo 1-19-80.

E. Graded beds, crossbed and load casts in felsic volcanic sediments; tops face left. Photo 1-10-80.

F. Schistose (mylonitized) felsic volcanic sediments from near the western margin of Ingrid group. Photo 13-6-80.

The linear structures are usually contained within the plane of the schistosity/compositional layering of the rocks. Mineral lineations are best developed in homogeneous coarse grained rocks, whereas aggregate lineations and crenulation lineations predominate in banded and highly schistose rocks. Most quartzofeldspathic gneisses in the Hopedale block are LS-tectonites and it is quite unusual to encounter rocks without an observable linear structure. Rocks without an observable planar structure, but with a good mineral lineation (i.e. L-tectonites), however, are not uncommon and in many cases the orientation of the planar structure at an outcrop is so variable or inconsistent that the linear structure, mostly aggregate and crenulation lineation, becomes the dominant structural element in the rock.

The structural trend areas described below are defined mainly on the basis of directional homogeneity of planar and/or linear structures within the trend areas. Age relations between trend areas are determined on the basis of deflection of structures, structural discordances or discontinuities, and intervening plutonic events.

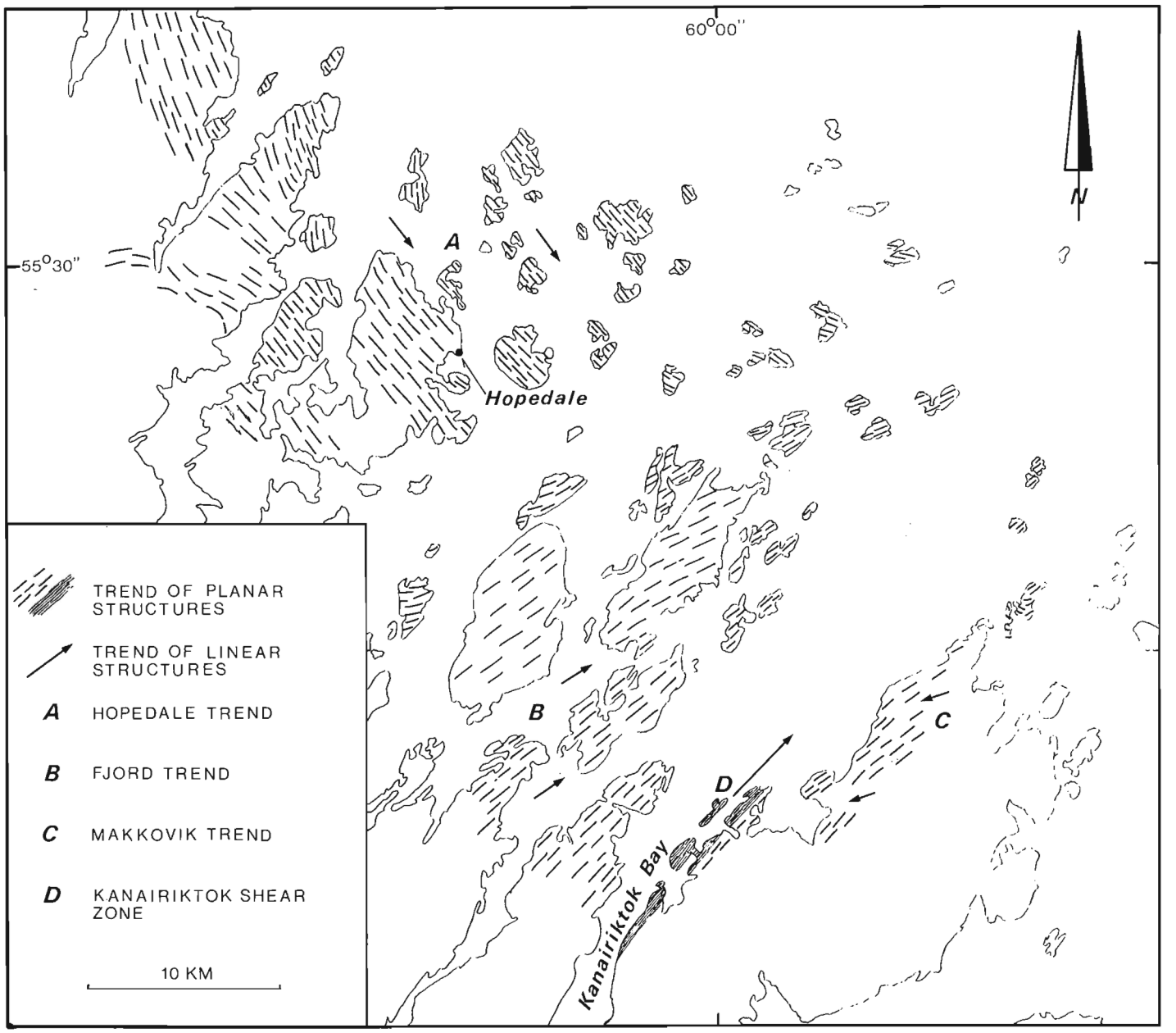

Figure 12.5. *Major planar and linear structural trends in Hopedale block and adjacent Makkovik subprovince.*

Major Structural Trends

The Hopedale Trend The earliest recognizable regional trend in the Hopedale block is a NW-SE striking steeply NE dipping planar trend combined with a SE plunging linear trend. This trend characterizes the gneisses in the vicinity of Hopedale (Fig. 12.5A) which are mainly banded, migmatitic gneisses at amphibolite grade.

The Fiord Trend North of Kanairiktok Bay the NW-SE planar Hopedale trend is deflected into a NE-SW subvertical orientation and the SE plunging linear trend is turned into a moderately steep NE plunging direction (Fig. 12.5B). However, prior to this change in regional structure, part of the area between Hopedale and Kanairiktok Bay was intruded by the Kanairiktok intrusive suite and these rocks show evidence of being affected only by the deformation responsible for the Fiord trend. The Fiord trend can also be found locally around Hopedale as crosscutting shears.

The Makkovik Trend The gneisses south of Kanairiktok Bay are dark grey tonalites tentatively considered to be thoroughly deformed equivalents of the Kanairiktok meta-intrusives and their inclusions. They are structurally characterized by a NE-SW striking subvertical planar trend (Fig. 12.5C) roughly parallel to the Fiord trend, but their linear structures plunge steeply WSW. So far the Makkovik trend is poorly defined, mainly on account of the extent of the Island Harbour granite and further data are needed to establish this trend firmly.

The Kanairiktok Shear Zone Along the southeast coast of Kanairiktok Bay earlier gneisses are found strongly deformed in a narrow, subvertical zone trending NNE-SSW. Linear structures in this zone plunge shallowly to the NNE (Fig. 12.5D). Deflection of older planar structures into the Kanairiktok shear zone shows a sinistral sense of movement and the geometry is consistent with a simple shear deformation.

Shearing along Kanairiktok Bay involved most earlier rock types and produced a variety of mylonitic rocks. A porphyritic granite confined to the immediate vicinity of the shear zone is also affected by and only by the shearing and may be related to the Island Harbour granite found southeast of Kanairiktok Bay.

Relative Chronology

At this stage of investigation we propose the following relative chronology for the Hopedale block:

Deposition of Hunt River belt volcanics, emplacement of granitoids (layered orthogneiss), and subsequent deformation and metamorphism at amphibolite facies grade.

Widespread migmatization and deformation resulted in formation of banded migmatitic gneisses and establishment of the Hopedale structural trend. Hunt River volcanics and layered orthogneiss can be recognized in the migmatitic gneisses as inclusions and rafts of Weekes amphibolite and Maggo gneiss respectively.

Florence Lake volcanics were deposited upon migmatitic gneisses and later intruded by the Kanairiktok granitoids. These meta-intrusives occur as large, elongate bodies parallel to the Fiord trend and may have been emplaced late during the establishment of the Fiord trend, as evidenced by the relatively limited amount of deformation they have suffered. The deformation following the emplacement of the Kanairiktok granitoids took place under low (epidote) amphibolite facies conditions.

Dolerite and large gabbro dykes striking NE-SW intrude all rocks north of Kanairiktok Bay. The dolerites are mostly unaltered, but may locally show evidence of cataclasis. Along the east coast of Kanairiktok Bay, in the gneisses bordering the Kanairiktok shear zone, unaltered dolerites are rare, whereas metadolerites aligned parallel to the planar structure in the gneisses are common. The metadolerites may represent the above-mentioned dolerite dykes deformed and metamorphosed during the establishment of the Makkovik trend, but clear-cut transitions from dolerite to metadolerite have not been observed.

Along the south coast of Kanairiktok Bay a pink, porphyritic phase of the Island Harbour granite intrudes the banded migmatitic gneisses and the metadolerites. Several generations of pegmatoid veins intruded the porphyritic granite prior to the Kanairiktok shearing.

The latest igneous event in the area was the intrusion of dioritic sills and dykes which are also a typical feature in the Island Harbour granite farther south.

Acknowledgments

We are indebted to our field assistants Karen Downing (University of Western Ontario), Ross Knight (University of Western Ontario), André Lalonde (McGill University), Siew Tin Ooi (Concordia), John Pearson (Lakehead), Lesia Zalusky (Concordia) and Ken Steel (Universal Helicopters) for a successful field season during 1980 in spite of adverse weather conditions. We thank A. Davidson for improvements made in manuscript.

References

Ermanovics, Ingo
1980: Geology of the Hopedale block of Nain Province, Labrador: Report 2, Nain-Makkovik boundary zone; in Current Research, Part B, Geological Survey of Canada, Paper 80-1B, p. 11-15.

Ermanovics, Ingo and Raudsepp, M.
1979: Geology of the Hopedale block of Nain Province, Labrador: Report 1; in Current Research, Part B, Geological Survey of Canada, Paper 79-1B, p. 341-348.

Jesseau, C.W.
1976: A structural-metamorphic and geochemical study of the Hunt River supracrustal belt, Nain Province, Labrador; unpublished M.Sc. thesis, Memorial University of Newfoundland, 211 p.

Kranck, E.H.
1953: Bedrock geology of the Seaboard of Labrador between Domino Run and Hopedale, Newfoundland; Geological Survey of Canada, Bulletin 26, 45 p.

Ryan, A.B.
1979: Kaipokok River, Newfoundland Department of Mines and Energy, Map 7949.

Sutton, J.S.
1972: The Precambrian gneisses and supracrustal rocks of the western shore of Kaipokok Bay, Labrador, Newfoundland; Canadian Journal of Earth Sciences, v. 9, p. 1677-1692.

Taylor, F.C.
1971: A revision of Precambrian structural provinces in northeastern Quebec and northern Labrador; Canadian Journal of Earth Sciences, v. 8, p. 579-584.

1977a: Geology – Hopedale, Newfoundland; Geological Survey of Canada, Map 1443A.

1977b: Geology – Makkovik, Newfoundland; Geological Survey of Canada, Map 1444A.

1978: Granulites of Northeastern Quebec and Northern Labrador; in Wanless, R.K. and Loveridge, W.D., 1978, Rubidium-Strontrium Isochron Age Studies, Report 2, Geological Survey of Canada, Paper 77-14, p. 52.

1979: Reconnaissance geology of a part of the Precambrian Shield, Northeastern Quebec, Northern Labrador and Northwest Territories; Geological Survey of Canada, Memoir 393, 99 p.

13.

PROGRESS REPORT ON REGIONAL GEOLOGICAL SYNTHESIS, CENTRAL SUPERIOR PROVINCE

Project 770070

K.D. Card, John A. Percival[1], J. Lafleur[2], and D.D. Hogarth[2]
Precambrian Geology Division

Card, K.D., Percival, John A., Lafleur, J., and Hogarth, D.D., Progress report on regional geological synthesis, central Superior Province; in Current Research, Part A, Geological Survey of Canada, Paper 81-1A, p. 77-93, 1981.

Abstract

Reconnaissance field work, combined with existing geological data, indicates that the region north of the Abitibi subprovince in northeastern Ontario and northwestern Québec can be subdivided into several lithotectonic domains that represent the eastward continuations of the Quetico, Wabigoon, and English River subprovinces of northwestern Ontario. There has apparently been little lateral offset of these domains across the Kapuskasing structural zone. The rock types, metamorphic patterns, and structure of the Quetico and Pontiac gneiss belts are described. It is noted that the two belts have many common features, including rock types, metamorphic and structural patterns, and position relative to neighbouring metavolcanic belts. The genesis of the Preissac-Lacorne batholith of the Abitibi volcanic belt is discussed, and it is suggested that the granitic parts of this intrusion, and the associated pegmatites, were formed by anatexis of Pontiac-type metasediments lying beneath the volcanic pile. A preliminary chemical-petrographic classification of diabase dykes in northeastern Ontario and northwestern Québec is given.

Northeast-striking belts of granulite facies paragneiss, mafic gneiss, tonalitic gneiss and anorthositic rocks in the Kapuskasing structural zone contrast sharply with low-grade metavolcanic and associated plutonic rocks of the Abitibi subprovince to the east and with orthogneiss domes and plutons in the Wawa subprovince to the west. Domes of the Wawa terrane consist of weakly foliated quartz monzonite-granodiorite cores and mantling xenolithic and gneissic tonalite-granodiorite. Granulite-facies mafic gneiss and paragneiss, similar in composition and metamorphic grade to Kapuskasing zone rocks, are exposed in a few domes, probably as the result of upwarping of the granulite-amphibolite isograd in the structurally lowest units. Regional block tilting (east side up) of possible Keweenawan age can account for the exposure of progressively higher grade Archean rocks from low greenschist near Lake Superior to granulite in the Kapuskasing zone.

The Round Lake batholith is a late Archean composite intrusion consisting of cataclastically foliated, gneissic granodiorite, and massive to foliated granitic and dioritic bodies. The batholith intrudes metavolcanic rocks of the Abitibi Supergroup and appears to have been emplaced as a magmatic diapir, cooling and partly solidifying while still moving upward in the dense mafic metavolcanic sequence.

Introduction

The program of reconnaissance field work in the central Superior Province (Card, 1979, 1980; Card et al., 1980) was continued during 1980. Data were gathered, using road access for the most part, in northeastern Ontario and northwestern Québec in the region bounded by 48°N to 52°N and 74°W to 88°W. A traverse was made along the highway extending from Matagami, Québec to the Québec Hydro development project at La Grande River. A number of granitic, gabbroic, and gabbro-anorthosite intrusions within and bordering the Abitibi volcanic belt were examined in the region between Lake Abitibi and Chibougamau, Québec. The rocks of the Pontiac gneiss belt south of Cadillac and Val d'Or, Québec and of the Quetico subprovince in the region between Lake Nipigon and Kapuskasing, Ontario were examined. Sampling and investigation of the chemistry and petrography of the diabase dykes that form several swarms in this part of the Shield were continued.

Field work by J.A. Percival on part of the Kapuskasing structural zone in the Chapleau-Foleyet area, and by J. Lafleur on the Round Lake batholith of the Kirkland Lake area was completed in 1980. The preliminary results of their investigations form parts of this report.

Acknowledgments

The authors were capably assisted in the field by R. Valenta, R. Buchanan, and P. Henshaw. The senior author wishes to acknowledge the assistance of the Societé de Baie James for allowing use of its road and other facilities in the Matagami-La Grande River region and of the Spruce Falls Pulp and Paper Company for allowing use of its bush roads in the Kapuskasing area. The authors also acknowledge assistance and information from R.P. Sage, L.S. Jensen and G. Johns, Ontario Geological Survey, D.G. Innes, consulting geologist, Sudbury, H. Lovell, Resident Geologist, Ontario Ministry of Natural Resources, Kirkland Lake, C. Pride, University of Ottawa, and Ontario Ministry of Natural Resources staff, Hearst, Kapuskasing, and Chapleau districts.

[1] Department of Geology, Queen's University, Kingston, Ontario.

[2] Department of Geology, University of Ottawa, Ottawa, Ontario.

PART 1. RESULTS OF RECONNAISSANCE INVESTIGATIONS AND STUDIES OF IGNEOUS INTRUSIONS

K.D. Card

Reconnaissance Investigations

A tentative outline of the major rock units and lithotectonic subdivisions of part of the Superior Province in the region bounded by 48°N to 52°N and 76°W to 82°W is shown in Figure 13.1. The delineation of rock units and structure east of the Kapuskasing structural zone and north of the Abitibi volcanic belt is hampered by extreme paucity of outcrop and by lack of detailed mapping. The present interpretation is based on data gathered during reconnaissance traverses combined with information published by the Québec Ministère des Richesses Naturelles and the Ontario Ministry of Natural Resources.

North of the Abitibi volcanic belt there are from south to north:

1. foliated felsic to intermediate plutonic rocks, including hornblende granodiorite, hornblende-biotite diorite, hornblende monzonite, and tonalitic and mafic gneiss. These rocks are considered to be part of the Abitibi subprovince;
2. a thin belt of paragneiss and associated migmatitic and granitic rocks;
3. a domain consisting of tonalite-granodiorite gneiss, massive to foliated plutons of dioritic to granitic composition and narrow, sinuous metavolcanic-metasedimentary belts;
4. a wide area consisting mainly of paragneiss and associated granitic and pegmatitic rocks with several narrow metavolcanic units. This domain continues north of the present map area to near the Eastmain River where it is in turn succeeded by metavolcanic and associated plutonic rocks.

The last three domains outlined are tentatively considered to represent the eastward extensions of the Quetico, Wabigoon, and English River subprovinces, respectively. If this interpretation is generally correct, it would appear that there has been relatively little lateral displacement across the Kapuskasing structural zone and that the major component of movement on the Kapuskasing fault was vertical rather than strike-slip.

Granite-greenstone domains display dome and basin structural patterns and greenschist to low amphibolite facies metamorphism. Paragneiss domains consist mainly of immature clastic sediments (quartz wacke, pelite, and minor calc-silicate rocks) metamorphosed under various conditions ranging from greenschist to upper amphibolite facies to a variety of biotite-garnet paragneiss and migmatitic paragneiss. Bedding, graded bedding and ripple cross-laminations are preserved locally where metamorphism and deformation were less intense. There are numerous granitic and pegmatitic bodies, probably mainly of anatectic origin. Granitic rocks contain paragneiss inclusions at various stages of digestion, and have minerals such as muscovite, biotite, and garnet. Pegmatites, which are particularly abundant in the northern paragneiss domain, typically contain muscovite, biotite, garnet, beryl, tourmaline, and allanite. Locally there are bodies of tonalite-granodiorite gneiss and mafic gneiss, presumably derived from mafic metavolcanic and intrusive rocks.

Quetico Subprovince

Figure 13.2 shows the general geology of the Quetico subprovince in the region between Lake Nipigon and the Kapuskasing structural zone. In the western part of the area there is a general increase in metamorphic grade inward from both the northern and southern margins of the belt. Low grade (chlorite and biotite grade) metasediments are succeeded inward by nonmigmatitic paragneiss with biotite + garnet ± staurolite ± andalusite ± cordierite assemblages and abundant pegmatite dykes and sheets. Pegmatites typically contain paragneiss xenoliths and abundant muscovite, biotite, and garnet. Many have beryl and tourmaline, and some also contain spodumene, columbite, and cassiterite.

The west-central part of the Quetico subprovince consists mainly of migmatitic paragneiss and granitic rocks (diatexite) with biotite ± garnet ± cordierite ± pyroxene assemblages. Both clinopyroxene and orthopyroxene are present in rocks of metasedimentary origin in several areas, indicating that granulite facies metamorphic conditions were attained locally within a background of mid- to upper amphibolite facies regional metamorphism.

The eastern part of the Quetico subprovince shown in Figure 13.2 consists of migmatitic paragneiss and granitic rocks (diatexite) with mineral assemblages indicative of amphibolite and lower granulite facies conditions. However, there are several areas of relatively well preserved metasediments with mineral assemblages indicative of greenschist facies conditions (chlorite, biotite ± garnet). These rocks are mainly quartz wacke with interbedded pelitic units and minor amounts of calcareous wacke and siltstone, and sulphide facies iron formation. Beds in the wacke sequences are generally 15 to 30 cm thick but locally reach 90 to 150 cm. Graded beds, parallel lamination, ripple cross-lamination, slump structures, and flames are present, indicating that these sediments are turbidites. There are also well preserved metavolcanic rocks in this area, mainly pillowed and amygdaloidal metabasalt.

South and east of the Quetico metasediments in the northern part of Wawa subprovince and in the Kapuskasing structural zone there are extensive areas of xenolithic gneiss. This rock consists of tonalitic gneiss with abundant (commonly 15 to 20 per cent; locally up to 70 per cent) mafic, amphibole-rich inclusions. Both layered and massive inclusions ranging in composition from amphibolite to diorite are present. The inclusions are generally 15 to 60 cm in maximum dimensions, but much larger blocks are common. Some inclusions display rotated foliation and minor folds that trend at high angles to the regional foliation in the enclosing tonalitic gneiss. Although the xenolithic gneiss would appear to represent breccia formed by the tectonic disruption of metavolcanic rocks, mafic dykes, and tonalite, the origin of these rocks and the significance of the structural relationships described remain unresolved problems.

Pontiac Gneiss Belt

Figure 13.3 shows the general geology of the Pontiac gneiss belt and adjacent parts of the Abitibi volcanic belt in the Cadillac-Val d'Or area, Québec. The Pontiac and Quetico belts share many common features. Both are situated south of dominantly volcanic terranes, the Abitibi and Wabigoon volcanic belts respectively. The rock types of the two gneiss belts are similar, consisting originally of quartz wacke and pelitic rocks with lesser amounts of calc-silicate and mafic igneous rocks. These have been metamorphosed under various conditions to paragneiss and migmatite, and invaded by granite and pegmatite bodies, most of which are of anatectic origin. In both, the grade of metamorphism increases toward the interior parts of the belts.

There are also some differences between the Pontiac and Quetico belts. The Quetico metasediments contain cordierite commonly, pyroxenes locally, and kyanite is apparently absent. The Pontiac metasediments contain kyanite, but lack cordierite and pyroxenes. These mineralogical differences indicate that metamorphism in the Pontiac belt occurred at somewhat higher pressure but lower temperature than in the Quetico belt.

The Pontiac gneiss belt can be subdivided into several east-west-trending zones on the basis of metamorphic grade and relative proportions of granitic rocks and metasediments (Fig. 13.3). In the north, there are low grade (chlorite, biotite) metasediments with relatively well preserved primary textures and structures such as bedding, graded bedding, crosslamination, and slump structures. Metamorphic grade increases rapidly southward, as shown by the successive

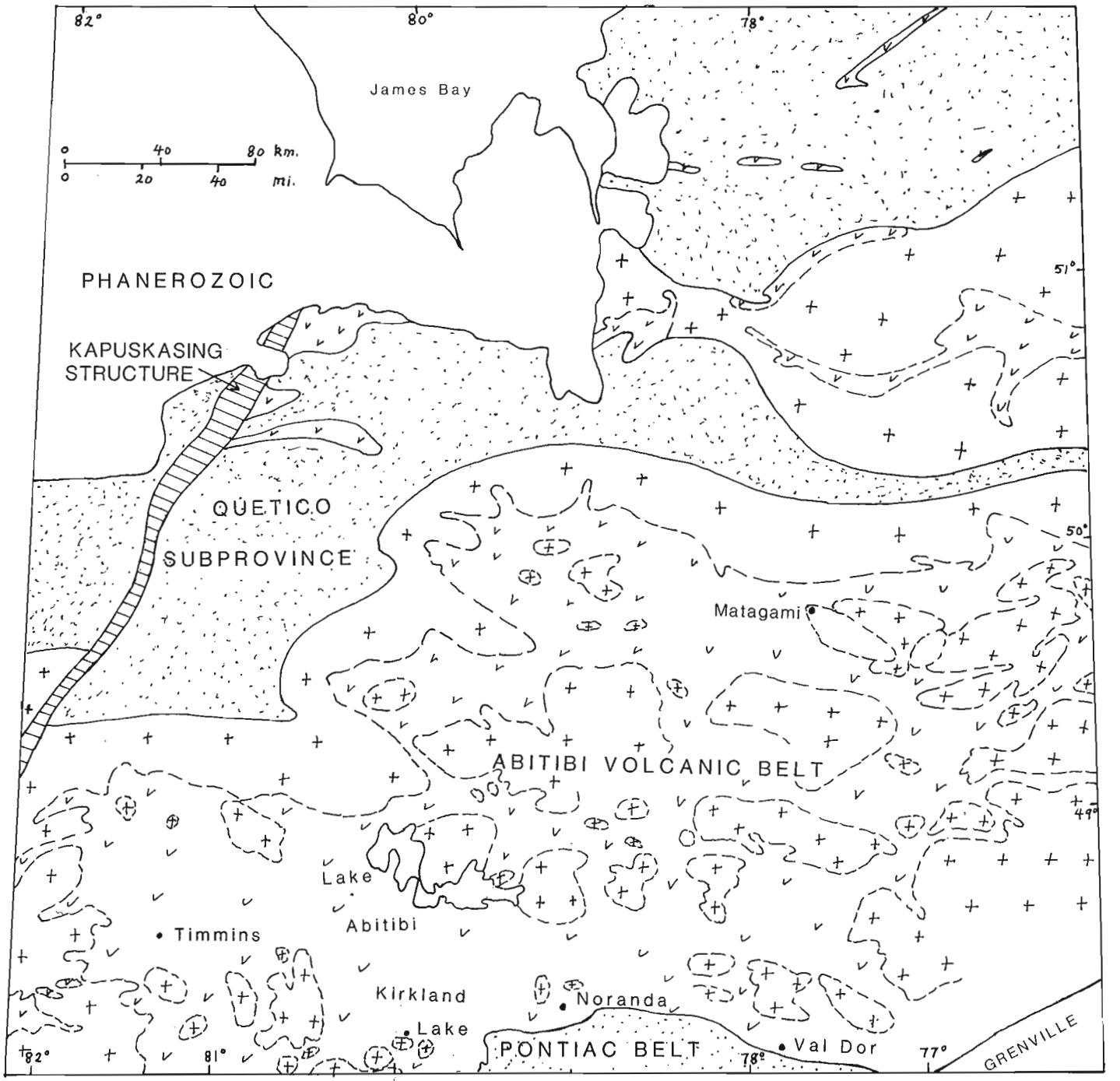

Massive to gneissic felsic and intermediate plutonic rocks = +
Metavolcanic-metasedimentary rocks = v
Paragneiss and associated migmatitic and granitic rocks = ⁘

Figure 13.1. *Distribution of major rock units and lithotectonic subdivisions of part of the Superior Province in northeastern Ontario and northwestern Québec.*

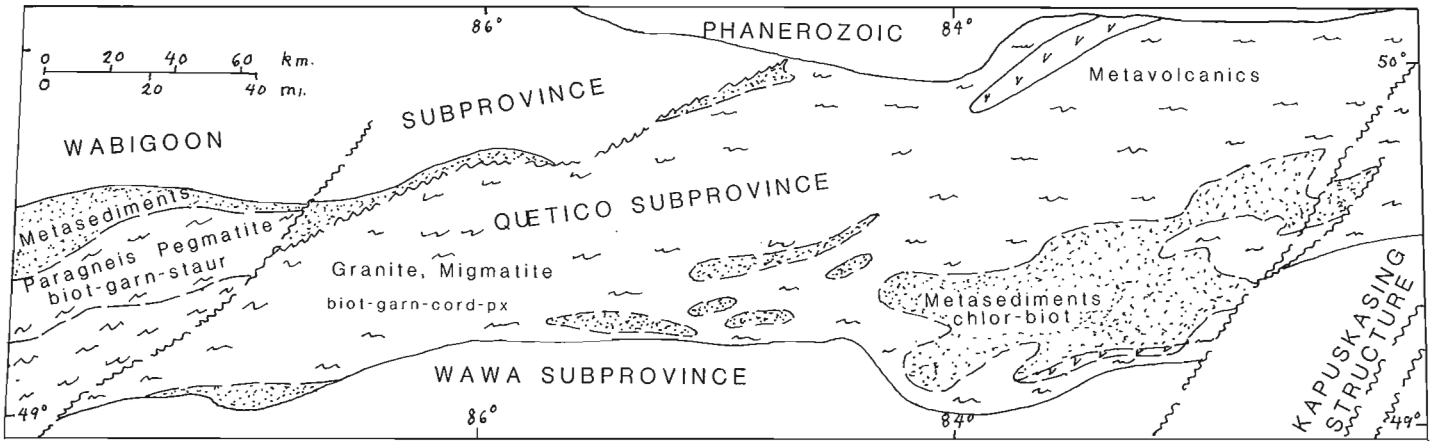

Figure 13.2. *General geology of the Quetico subprovince in the Lake Nipigon-Kapuskasing, Ontario region.*

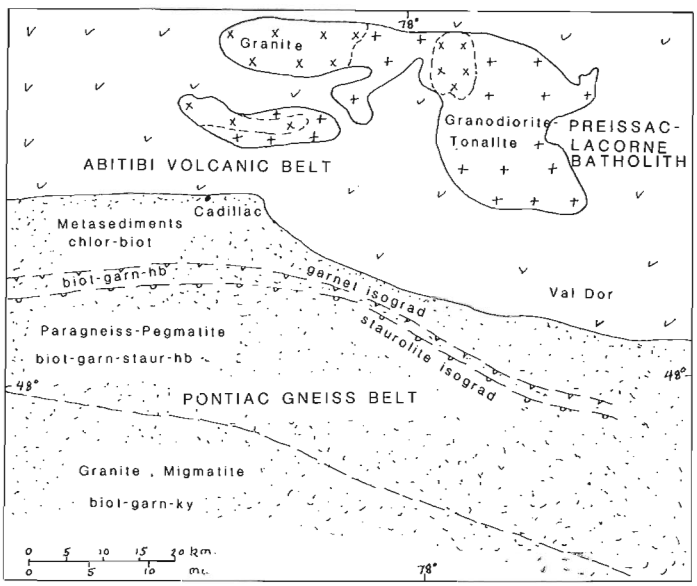

Figure 13.3. *General geology of the Pontiac gneiss belt and adjacent parts of the Abitibi volcanic belt, Cadillac-Val d'Or area, Québec.*

appearance of garnet, hornblende, staurolite, and kyanite. There is a wide central zone consisting of generally non-migmatitic biotite + garnet ± staurolite ± hornblende paragneiss, with abundant pegmatite and granite dykes and sheets. Most of the granitic rocks contain paragneiss inclusions and are mineralogically complex, containing muscovite, biotite, and garnet; beryl, tourmaline, and lepidolite are common minor constituents in the pegmatite. The southern part of the Pontiac belt consists mainly of migmatitic granitic rocks (diatexite) with abundant paragneiss inclusions and screens.

The structure of the Pontiac belt is complex. Foliation, both cleavage and gneissosity, is the dominant structural element. In the north, foliation is generally east-west and steeply dipping; in the south, low angle dips on foliation are prevalent, reflecting the presence of domal structures and recumbent folds. Primary bedding is recognizable only in the north. In the few places where top determinations could be made, the beds dip and face northward, suggesting that the Pontiac metasediments lie beneath and are older than the Abitibi metavolcanic rocks to the north.

Preissac-Lacorne Batholith

The Preissac-Lacorne batholith is located within the Abitibi volcanic belt some 20 km north of the Pontiac gneiss belt (Fig. 13.3). The batholith is described by Dawson (1966) as consisting of three main intrusions and a number of smaller stocks that intrude mafic metavolcanics, ultramafic rocks (komatiites in part), and metasediments. The intrusions consist of granite (leucoadamellite of Dawson, 1966), biotite-hornblende granodiorite and tonalite, and minor hornblende monzonite, syenodiorite, and diorite. Dawson suggested that the foregoing rock types resulted from normal crystallization differentiation of a granodioritic magma.

Part of the intrusion, the granite (leucoadamellite) is characterized by abundant accessory minerals, notably garnet, zircon and molybdenite, by abrupt, erratic variations in grain size, by the presence of paragneiss inclusions at various stages of digestion, and by associated, mineralogically complex pegmatites. The pegmatites contain abundant muscovite and garnet and some have beryl, spodumene, lithium micas, and columbite-tantalite. The granite and its associated pegmatites are consequently atypical of greenstone belt intrusions, but are much more akin to intrusions found within the paragneiss belts, for example, within the Pontiac belt immediately to the south. According to chemical and mineralogical data presented by Dawson (1966), the granite (leucoadamellite) falls within the minimum melting composition – thermal valley of the nepheline – kaliophyllite – quartz phase diagram. The granodiorite and tonalite fall outside this composition and would appear to represent typical greenstone belt intrusions.

It is speculated herein that the granite and granodiorite-tonalite are genetically different, and that the granite was not derived by differentiation of a granodiorite magma. The granite and associated pegmatites were probably formed by anatexis of metasediments at depth and intruded into the overlying metavolcanics, fortuitously in the same area as the granodiorite-tonalite. If the structural relationships suggested previously are valid, that is, that the Pontiac metasediments underlie the Abitibi metavolcanics, anatexis of these rocks would represent a possible source for the granitic magma.

Chemistry and Petrography of Diabase Dyke Swarms

Figure 13.4 is a sketch map showing the distribution of diabase dykes that cut the rocks of the Superior and Southern provinces in northeastern Ontario and northwestern Québec. Within this region there are a number of diabase dyke swarms of differing trends, ages, and chemical-mineralogical

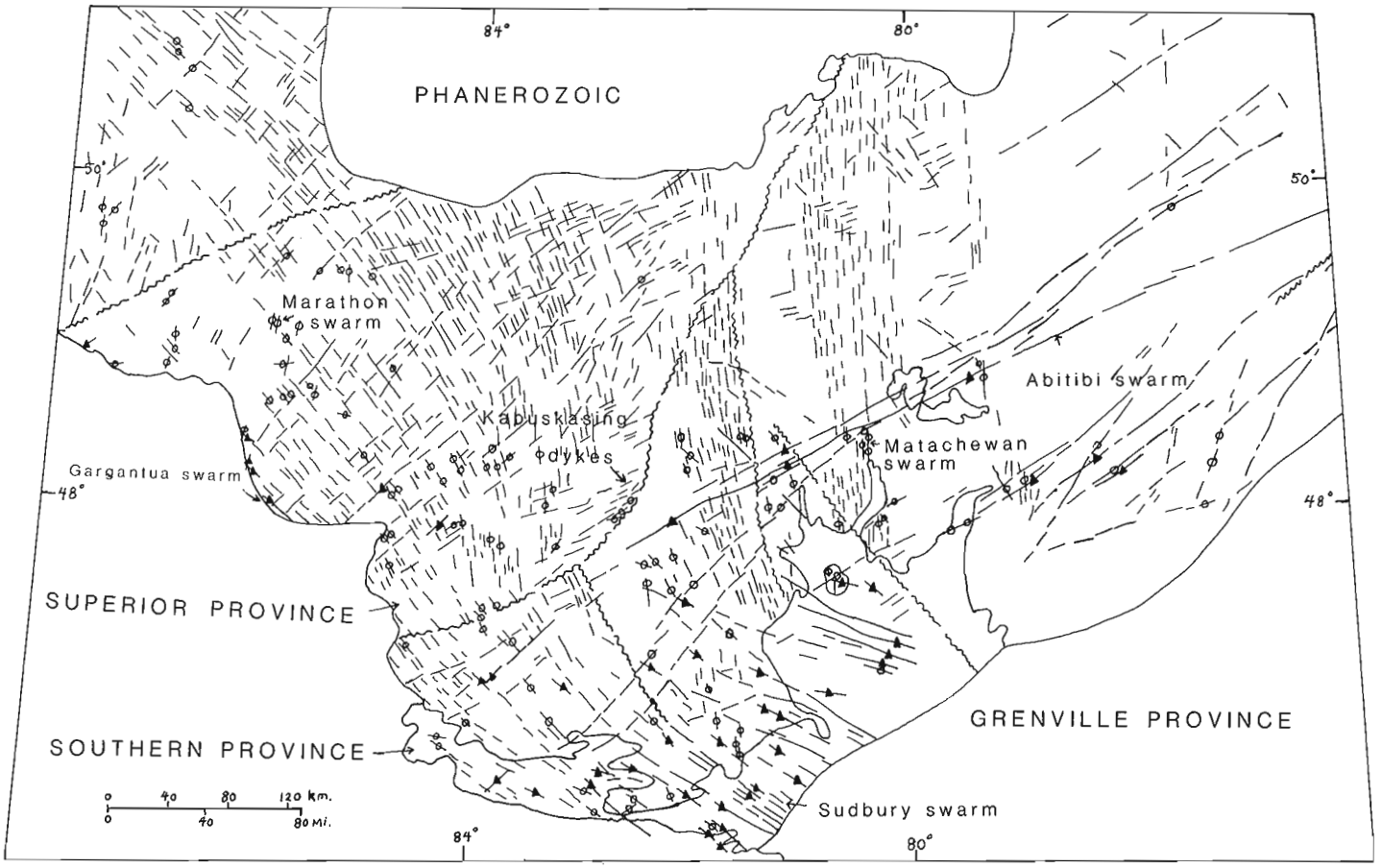

Sample site, tholeiitic diabase dyke = ϕ *Sample site, alkali olivine diabase dyke = ▲*

Figure 13.4. *Distribution and chemistry of diabase dykes in parts of the Superior and Southern provinces.*

characteristics. Dyke swarms of both the tholeiitic and alkali olivine basalt suites are present and they range in age from about 1100 Ma to over 2600 Ma. Assignment of individual dykes to one swarm or another is difficult and can only be done confidently with knowledge of several parameters, including orientation, chemistry, petrography, absolute age, and paleomagnetic characteristics. Assignment on the basis of orientation alone is not infallible as dykes of distinctly different ages and chemistry commonly have similar trends and occur in close proximity.

In Figure 13.4, the sample sites and dykes that have been classified as tholeiitic or alkali olivine basalt suite are shown. Chemical analyses for many of the sites were obtained from W.F. Fahrig, Geological Survey of Canada. Some of the analyses and petrographic descriptions were obtained from publications of the Ontario Geological Survey and the Québec Ministère des Richesses Naturelles. The remainder were collected by the writer.

On the basis of chemistry, it is evident that two major groups of dykes are present: tholeiitic and alkali olivine basalt. A simple silica versus alkalies plot (Irvine and Baragar, 1971) serves to distinguish between the two groups (Fig. 13.5). However, neither this plot nor any other plot attempted by the writer to date serves to distinguish the several dyke swarms included in each of the two major chemical groups.

The olivine diabase dykes are of remarkably constant mineralogical composition, consisting of plagioclase (labradorite), augite (commonly titaniferous), olivine, iron-titanium oxides, and accessory apatite and red biotite. These rocks are generally fresh, with only minor secondary chlorite and serpentine minerals, and display ophitic textures. The olivine diabase dykes, including those of the Abitibi (east-northeast), Sudbury (northwest) and Gargantua (northwest) swarms (Fig. 13.4) yield K-Ar mineral and whole rock radiometric ages in the range 1100 to 1250 Ma (Fahrig et al., 1965). However, Gates and Hurley (1973) have determined a Rb-Sr whole rock age of 2147 ± 68 Ma for olivine diabase dykes of the Abitibi swarm in the Lake Abitibi region.

The tholeiitic dykes are variable in mineralogy, chemistry, texture, and age. They consist of labradoritic plagioclase, commonly saussuritized, pyroxene, commonly uralitized, quartz, generally in amounts of less than 5 per cent and commonly forming myrmekitic intergrowths with feldspar, iron-titanium oxides, and accessory apatite, zircon, and sulphide minerals. Many dykes contain only one pyroxene, augite, but a number have two pyroxenes, either augite and pigeonite, or augite and hypersthene. The alteration products of the foregoing minerals include uralitic amphibole, epidote, biotite, chlorite, magnetite, and leucoxene. The texture of the tholeiitic dykes varies from subophitic to hypidiomorphic granular and many, notably those of the Matachewan swarm, are porphyritic. Some Matachewan dykes contain 30 to 50 per cent plagioclase phenocrysts and glomerocrysts up to 15 cm in maximum dimension. However, the phenocryst content of individual dykes can vary greatly over short distances and some

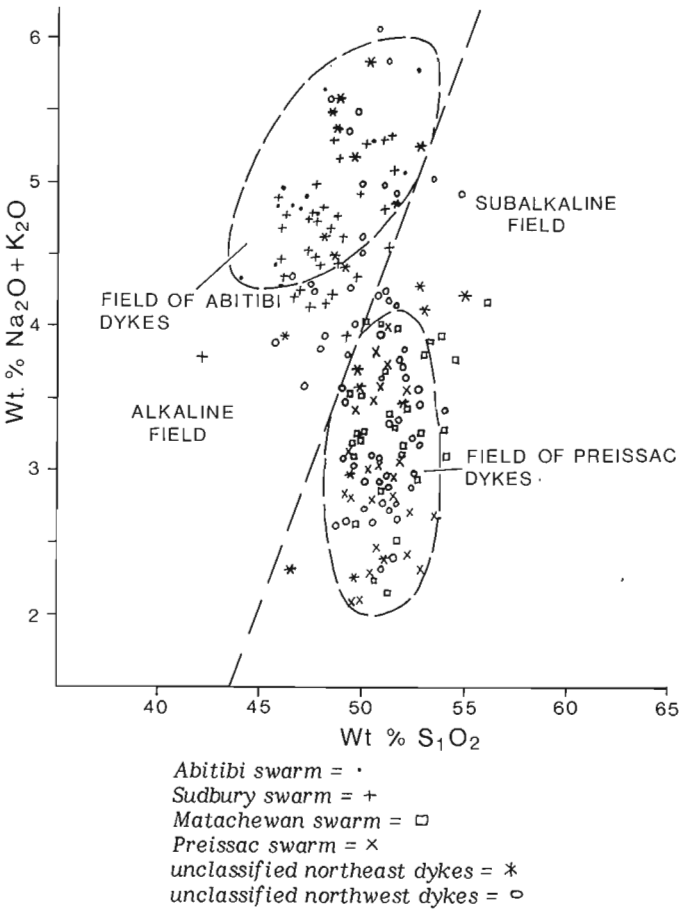

Figure 13.5. *Silica versus alkalies plot for diabase dykes.*

Matachewan dykes contain few or no phenocrysts. To date, no consistent mineralogical, textural, or alteration characteristics have been found that would serve to distinguish uniquely the tholeiitic dykes of one swarm or another.

The oldest tholeiitic dykes, the north to north-northwest Matachewan swarm, are of late Archean age (K-Ar – 2485 Ma; Rb-Sr – 2590 Ma, Goodwin et al., 1972; Rb-Sr – 2690 Ma, Gates and Hurley, 1973). The north-trending Marathon dykes in the west have a K-Ar age of about 1800 Ma (Goodwin et al., 1972), and are similar in trend and petrography to the Matachewan dykes. The arcuate northwest-trending tholeiitic dyke swarm in the western part of the area contains dykes of both Archean and Proterozoic ages; some cut the early Proterozoic Huronian Supergroup; others are unconformably overlain by the Huronian. Some of these dykes yield K-Ar mineral and whole rock ages in the range 2000 Ma to 2495 Ma and are probably equivalent to the Matachewan swarm of late Archean age (Ernst and Halls, 1980). On the basis of K-Ar ages of 1450 Ma to 1600 Ma, others are probably Proterozoic. Northwest-trending Proterozoic tholeiitic dykes within the Southern Province in the Sudbury region cut the Nipissing intrusions and have been affected by early Proterozoic deformation and metamorphism; they are probably about 1900 ± 100 Ma old. East-northeast tholeiitic dykes in and adjacent to the Kapuskasing structure (herein termed Kapuskasing dykes, Fig. 13.4) cut the high rank metamorphic gneiss of this zone, cut some of the northwest tholeiitic dykes, and are cut by faults associated with the Kapuskasing structure. One fresh east-northeast dyke yielded a K-Ar whole rock age of 1475 ± 75 Ma (R.D. Stevens, written communication, 1980).

In the Abitibi region in the eastern part of the area (Fig. 13.4), there are several subparallel northeast to east-northeast trending diabase dyke swarms of differing paleomagnetic and chemical characteristics. Larochelle (1966) has defined three such swarms on the basis of paleomagnetics:

1. ENEW dykes; magnetic declination 264°; inclination +61°;
2. ENEN dykes; magnetic declination 354°; inclination -32°;
3. NNE dykes; magnetic declination 221°; inclination +19°.

The ENEW dykes are olivine diabase and yield K-Ar ages of 1100 Ma to 1200 Ma and a Rb-Sr whole rock age of 2147 ± 68 Ma (Gates and Hurley, 1973). They are part of the Abitibi swarm as defined by Fahrig et al. (1965). The ENEN dykes are tholeiitic and have also yielded ages of about 2150 Ma (Rb-Sr – 2262 ± 279 Ma, Gates and Hurley, 1973; $^{39}Ar/^{40}Ar$ – 2150, Hanes and York, 1979). The NNE dykes yield K-Ar biotite and whole rock ages in the range 1485 Ma to 1935 Ma and a Rb-Sr whole rock age of 2227 ± 125 Ma (Gates and Hurley, 1973). These dykes have been termed Preissac by Fahrig in Goodwin et al. (1972). Consequently, although the three dyke sets are different in chemistry and paleomagnetic character, implying differences in age, their apparent radiometric ages are similar. Further paleomagnetic and geochronologic investigations, closely integrated with chemical and petrographic studies, are required to resolve the Abitibi dyke problem.

PART 2. STRATIGRAPHIC, STRUCTURAL AND METAMORPHIC RELATIONS BETWEEN THE WAWA AND ABITIBI SUBPROVINCES AND THE KAPUSKASING STRUCTURAL ZONE NEAR CHAPLEAU, ONTARIO

John A. Percival

Introduction

This report summarizes results of field studies in the Kapuskasing structural zone (KSZ) and surrounding rocks in the Chapleau-Foleyet area of Ontario. The KSZ is structurally discordant with respect to the adjacent Wawa and Abitibi subprovinces and is characterized by high grade metamorphism and positive gravity and aeromagnetic anomalies (Innes, 1960; Gaucher, 1966; Gibb, 1978). The structural zone separates the east-trending metavolcanic rocks of the Abitibi subprovince (Stockwell, 1970) to the east from gneissic terrane of the Wawa subprovince to the west. Studies were initiated in 1979 (Percival and Coe, 1980) to investigate relationships among the three subprovinces and to establish a tectonic framework for the area as a part of a regional reconnaissance and synthesis program (Card, 1979; Card et al., 1980). The results of the project will form the basis of a doctoral thesis by the writer at Queen's University.

General Geology

Figure 13.6 shows the general geology of parts of the eastern Wawa subprovince, the western Abitibi subprovince, and the southern Kapuskasing structural zone. The Abitibi subprovince (AS) is characterized by metavolcanic and associated metasedimentary rocks with upright structural elements. Intrusive into these supracrustal rocks are massive to locally gneissic quartz monzonite to tonalite bodies. The Kapuskasing structural zone (KSZ) consists of northeast-striking, northwest-dipping units of paragneiss, mafic orthogneiss, tonalite-granodiorite gneiss and anorthosite-suite rocks. The Wawa subprovince (WS) is made up dominantly of tonalite-granodiorite orthogneiss and massive to foliated tonalite to quartz monzonite bodies. Gneissic layering defines gneiss domes as well as east-striking units. Metamorphic grade is low in the Abitibi portion of the study area and increases abruptly to granulite facies within the KSZ across a cataclastic zone on the eastern margin of the structure. Metamorphic grade is intermediate in the Wawa subprovince and increases gradually through the domal gneiss terrane into the KSZ.

Abitibi Subprovince

Archean supracrustal rocks of the Abitibi and Swayze metavolcanic belts of the Abitibi subprovince consist dominantly of pillowed and massive flows and tuffaceous mafic volcanic rocks. Pyroclastic felsic metavolcanic rocks are present as discrete units and interlayered with mafic rocks. Ultramafic bodies in the metavolcanic sequence are probably intrusive, although ultramafic flows are present in the Abitibi belt to the east (Pyke et al., 1973). Metasedimentary rocks, interlayered with metavolcanics, occur as narrow units up to 15 km long.

Weakly foliated to gneissic tonalite northeast of Foleyet is the earliest recognized felsic plutonic body in the area. Posttectonic quartz monzonite bodies (not distinguished on Fig. 13.1) are variable in composition and texture. Near Ivanhoe Lake, quartz monzonite is weakly foliated to massive, medium grained, sparsely xenolithic and contains up to 15 per cent hornblende and biotite. South of Ivanhoe Lake, these rocks are massive, leucocratic and contain K-feldspar phenocrysts to 2 cm. North of Foleyet, quartz monzonite is weakly foliated, leucocratic to aplitic and contains up to 50 per cent pegmatite. Contacts with metavolcanic rocks are transitional zones less than 100 m wide of lit-par-lit migmatite. Similar contact relations between quartz monzonite and mafic gneiss of the KSZ are present at the southern end of Ivanhoe Lake. A north-trending intrusive body of monzonite and diorite, with rare pyroxenitic zones, is subparallel to the KSZ-AS boundary (Fig. 13.6). The northern portion of the body is strongly lineated, foliated and metamorphosed, whereas the southern part is weakly deformed and slightly altered to greenschist facies. Amphibole from a metavolcanic rock west of Foleyet has been dated by the $^{40}Ar/^{39}Ar$ method at 2567 Ma (D. Archibald, personal communication, 1980). No zircon ages are available for this part of the Abitibi subprovince. However, in the Kirkland Lake-Timmins area, Nunes et al. (1978) found volcanic rocks ranging from 2725 to 2700 Ma.

Folds in the supracrustal rocks of the Abitibi belt are upright, commonly with gentle to moderate westerly plunges. Planar fabrics, mainly mineral alignment, are common, whereas lineation (mineral, rodding, minor fold axes) are less pronounced. Polyphase deformation is evident in the fine-grained metasediments which display as many as three foliations.

In most areas of the Abitibi belt, metavolcanics are metamorphosed to greenschist facies assemblages of albite, epidote, chlorite, and actinolite. Near intrusive bodies, hornblende-plagioclase ± garnet assemblages are common. In a thin metavolcanic unit approximately 1 km east of the main cataclastic zone that marks the eastern boundary of the KSZ, the assemblage garnet-clinopyroxene-hornblende-plagioclase is present. Original textures and structures are commonly preserved in metasedimentary rocks. Slates consist of fine muscovite, chlorite, albite and quartz; low greenschist facies slate occurs in the AS less than 2 km east of granulite facies paragneiss in the KSZ across Ivanhoe Lake. It is probable that major faults separate these areas of contrasting metamorphic grade. Mafic minerals in granitic rocks are commonly altered to epidote.

Wawa Subprovince

Supracrustal rocks are not abundant in the Wawa terrane within the study area. Layered rocks of basaltic composition, interlayered with metasedimentary rocks at Borden Lake, are considered to be metavolcanic. Mafic gneiss of the Robson Lake dome (Fig. 13.6), although recrystallized to granulite facies, has conspicuous layering and is associated with paragneiss and thus may be of volcanic origin. Amphibolitic enclaves in xenolithic gneiss are possibly also of volcanic origin.

Metasedimentary rocks (paragneiss) occur as discrete narrow units as well as schlieren in orthogneiss. Primary features are rarely preserved; one example of primary features is at Borden Lake, where stretched-pebble metaconglomerate, containing amphibolite, felsic metavolcanic, metasedimentary, tonalite, quartz monzonite and metagabbro cobbles occurs in association with paragneiss. In general paragneiss is garnet-biotite-plagioclase-quartz rock (Table 13.1) which contains up to 20 per cent vein migmatite of tonalitic composition. West of the Como Lake fault, leucosome layers contain muscovite and K-feldspar. Rounded mafic enclaves are rare constituents of some paragneiss outcrops. The paragneiss units here may be traced into the KSZ.

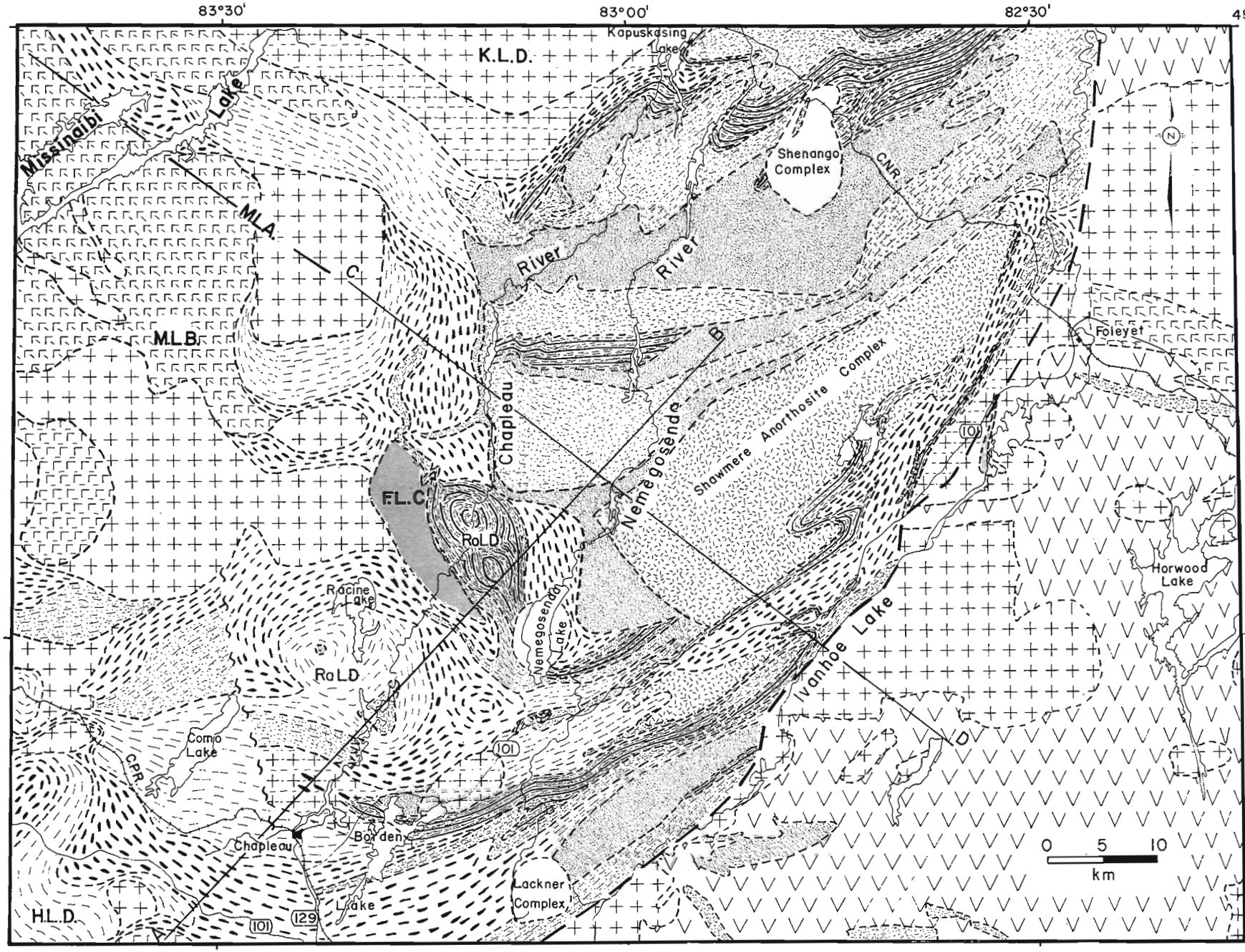

KLD = Kapuskasing Lake Dome; MLB = Missinaibi Lake batholith; RoLD = Robson Lake Dome; HLD = Highbrush Lake Dome. MLA = Missinaibi Lake arch; FLC = Floranna Lake complex; RaLD = Racine Lake Dome;

Figure 13.6. *Generalized geological map of the Chapleau-Foleyet area. Patterned symbols reflect measured structural trends. See Figure 13.7 for cross-sections AB and CE; Figure 13.8 for explanation of symbols.*

Table 13.1

Mineralogy of representative rock types in Abitibi, Wawa and Kapuskasing terrains.

	Wawa	Kapuskasing zone	Abitibi
Supracrustal			
Mafic:	Gt-Cpx-Hb-Pg-Qz Hb-Pg Cpx-Hb-Pg	Gt-Cpx-Hb-Pg-Qz Gt-Cpx-Pg-Qz Hb-Pg Gt-Opx-Cpx-Hb-Pg-Qz Opx-Cpx-Hb Gt-Opx-Hb-Bt	Hb-Pg Gt-Hb-Pg Ac-Ab-Ch-Ep-Qz Gt-Cpx-Hb-Pg
Metasedimentary:	Gt-Bt-Pg-Qz Gt-Bt-Ms-Pg-Qz Gt-Cpx-Pg-Qz Bt-Ms-Pg-Qz Gt-Hb-Bt-Pg-Qz	St-Ms-Pg-Qz Gt-Bt-Pg-Qz Gt-Opx-Bt-Pg-Qz Gt-Opx-Bt-Ksp-Pg-Qz Gt-Cpx-Bt-Pg-Qz Opx-Cpx-Bt-Ksp-Pg-Qz Gt-Bt-Ms-Pg-Qz Sl-Gt-Bt-Pg-Qz	Pg-Qz Ch-Ms Ch-Ms-Pg-Qz
Intrusive			
	Cpx-Hb Cpx-Hb-Pg-Qz Hb-Bt-Pg-Qz Cpx-Hb-Bt-Pg Cpx-Hb-Ksp-Pg	Opx-Cpx-Pg Opx-Cpx-Hb Opx-Cpx-Hb-Bt-Pg Gt-Opx-Hb-Sa-Pg-Sp Gt-Cpx-Hb-Pg Gt-Cpx-Hb-Pg-Qz Cpx-Hb-Bt-Pg ± Qz Gt-Hb-Bt-Pg-Qz Hb-Bt-Pg-Qz Ol-Opx-Gt-Hb-Pg	Hb-Bt-Pg-Qz Bt-Ksp-Pg-Qz Opx-Ta-Se-Ac

Ab: albite; Ac: actinolite; Bt: biotite; Ch: chlorite; Cpx: clinopyroxene; Ep: epidote; Gt: garnet; Hb: hornblende; Ksp: K-feldspar; Ms: muscovite; Ol: olivine; Opx: orthopyroxene; Pg: plagioclase; Qz: quartz; Sa: sapphirine; Se: serpentine; Sl: sillimanite; Sp: spinel; St: staurolite; Ta: talc.

Gneissic, foliated and massive plutonic bodies underlie most of the area west of Chapleau River (Fig. 13.6). Massive quartz monzonite, aplite, and pegmatite are ubiquitous in gneissic and foliated rocks; only the larger areas of quartz monzonite are shown on Figure 13.6. Probably the oldest intrusive rock is foliated mafic tonalite of the Missinaibi Lake batholith; inclusions of this foliated tonalite, along with amphibolitic enclaves, are present within tonalite gneiss that is in contact with the rocks of the Missinaibi Lake batholith. The batholith is made up of medium- to coarse-grained rocks of variable composition. The most abundant rock type is hornblende-biotite tonalite; however, hornblende porphyritic tonalite, biotite tonalite and mafic hornblende tonalite are also common. Outcrop-scale diorite, gabbro and hornblende clinopyroxenite lenses and layers are rare components. The body is cut by deformed gabbro to diorite dykes that are transected by still later intrusions. Concordant, weakly foliated, fine grained grey granodiorite to tonalite is cut by massive pink pegmatite and aplite. Local patches of very coarse tonalite pegmatite (hornblende crystals to 10 cm) resemble late tonalite associated with the Shawmere anorthosite complex (Simmons et al., 1980).

An arbitrary cutoff value of 5 per cent xenoliths has been used to distinguish xenolithic from gneissic tonalite-granodiorite. Layering in these rocks is hornblende and/or biotite concentrations in a felsic matrix. Xenolithic varieties contain up to 50 per cent rounded hornblende-plagioclase enclaves up to 1 m in size as well as elongate mafic schlieren. Clinopyroxene is a common constituent of mafic xenoliths.

The Floranna Lake complex (Fig. 13.6) is a layered, strongly lineated and foliated body of intermediate composition that intrudes mafic granulites of the Robson Lake dome. The margins are granitic in composition whereas the core is monzonite and diorite with local gabbro layers. Relict igneous clinopyroxene and feldspar phenocrysts to 1 cm are preserved in the least-deformed portions of the complex. Migmatitic quartz monzonite layers constitute up to 10 per cent of some outcrops.

Massive to weakly foliated, leucocratic, xenolith-free quartz monzonite and granodiorite, associated with pegmatite, occur in the crests of domes or antiforms as well as in structural basins. Gradational contacts between weakly foliated and gneissic rocks are common.

Amphibole from metaconglomerate matrix near Borden Lake yields a K-Ar age of 2594 Ma and biotite from the same rock 2263 Ma (R.D. Stevens, written communication, 1980). Zircons from metavolcanic rocks near Wawa, 80 km west of the study area, indicate volcanism at ∿2750 Ma (Krogh and Davis, 1971).

The structure of the Wawa terrane is dominated by gently dipping and plunging fabric elements. Domes, basins, antiforms and synforms are defined on the basis of fabric orientation in gneiss and foliated plutonic rocks. A composite section (Fig. 13.6, 13.7) shows that in general gneissic rocks structurally overlie and mantle plutonic bodies, suggesting that gneissic units were horizontal, probably laterally discontinuous sheets, prior to doming. This structural-stratigraphic sequence can be followed in a general way into the KSZ.

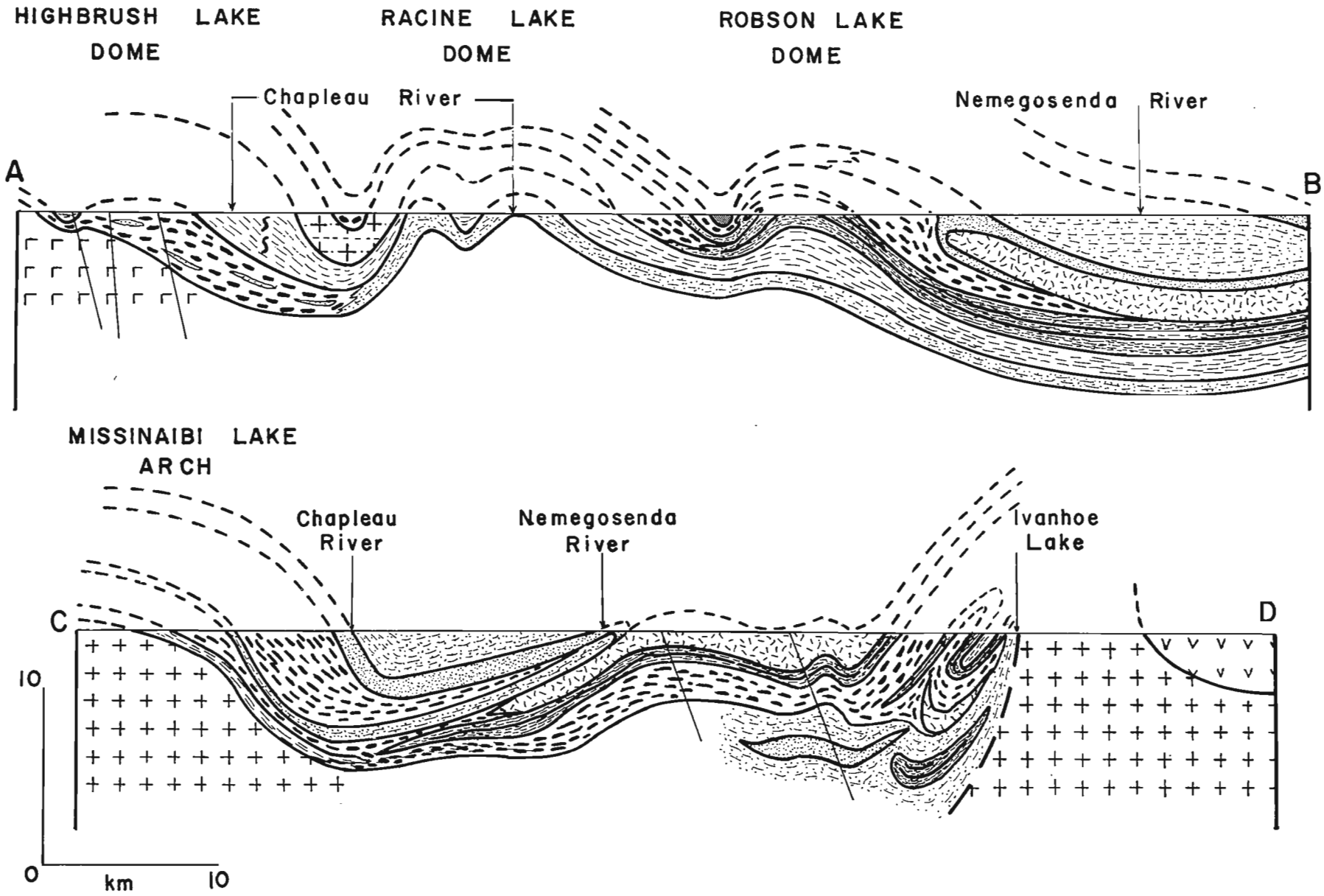

Figure 13.7. *Schematic cross-sections showing structural and stratigraphic relationships between the Wawa and Kapuskasing terrains (AB) and among Wawa, Kapuskasing and Abitibi belts (CD). Legend as for Figure 13.6.*

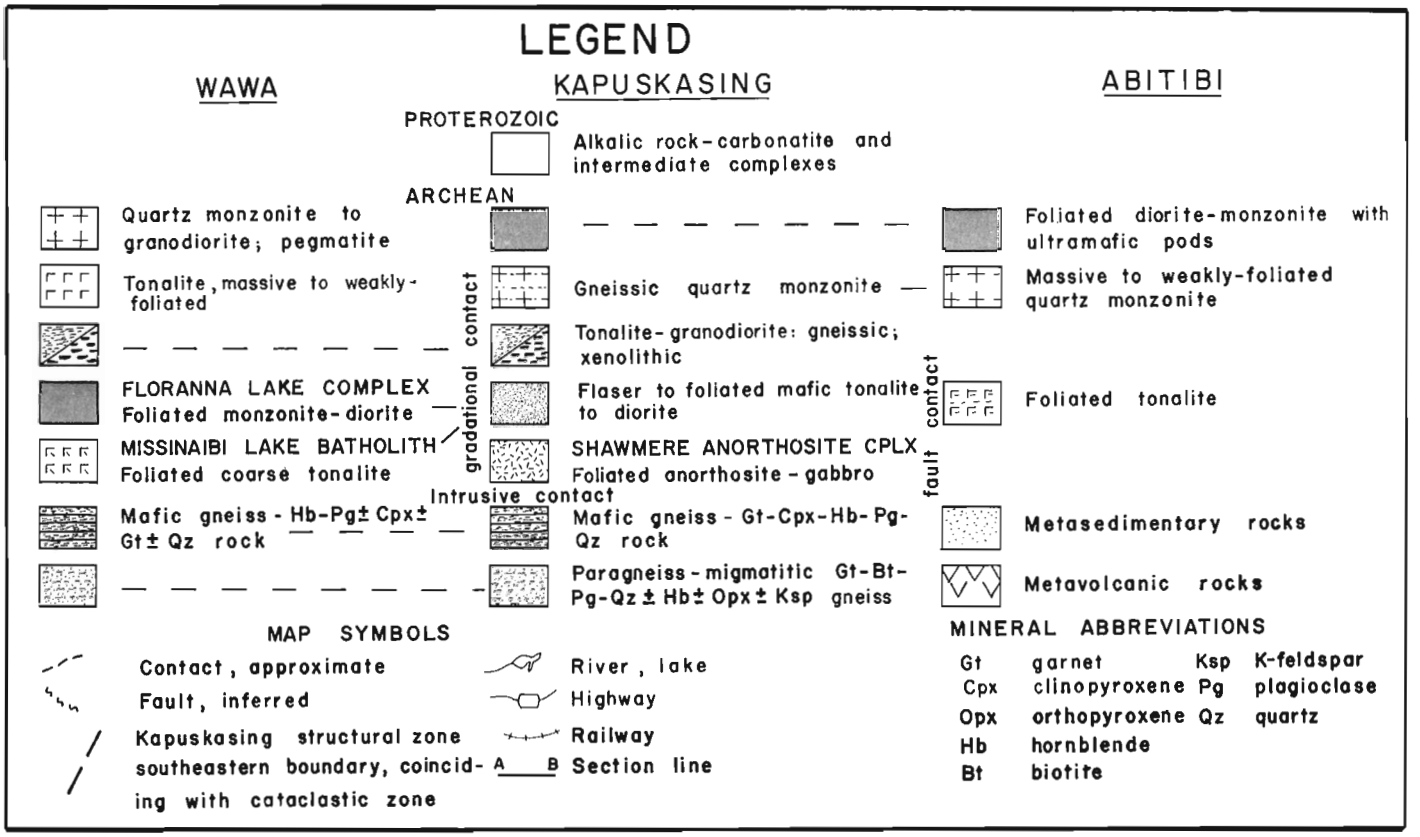

Figure 13.8. *Legend to accompany Figures 13.6 and 13.7. Dashed lines indicate probable lithological correlations between adjacent terrains.*

Small folds in gneiss near dome crests generally plunge away from culminations. Axial planes of small folds are gently-dipping, parallel to foliation in gneiss. Where foliation dips less than 10 degrees, small folds are chaotic in orientation and asymmetry, suggesting vertical compression of previously upright fabrics.

The Missinaibi Lake arch is a major antiformal structure defined by northwest-striking, gently southwest or northeast-dipping foliations. The flanks consist of tonalitic rocks of the Missinaibi Lake batholith, intruded in the core by xenolithic tonalite at Missinaibi Lake and by massive quartz monzonite to the southeast. Nappe-like minor folds of foliation are refolded about horizontal northeast-trending axes. The Racine Lake dome is mantled by xenolithic gneiss with both amphibolite and paragneiss enclaves that form a connection between paragneiss in the KSZ and the east-striking paragneiss unit southwest of the dome. The Robson Lake dome is underlain by garnet-clinopyroxene mafic granulite and gneissic tonalite. The Kapuskasing Lake dome has a quartz monzonite core and is mantled by gneissic quartz monzonite that intrudes rocks of the Missinaibi Lake batholith on the west and gneiss of the KSZ on the east.

Metamorphic grade in the Wawa terrane is generally in the amphibolite facies. Xenolithic gneiss contains mafic inclusions composed mainly of hornblende and plagioclase; clinopyroxene is a common accessory. Garnet-clinopyroxene-plagioclase-quartz assemblages occur at several locations near domal culminations and in metavolcanics west of Borden Lake. In xenolithic gneiss the mafic inclusions are commonly zoned with clinopyroxene-bearing cores and hornblende-plagioclase rims. Epidote replacing mafic minerals and late epidote veinlets are ubiquitous in the gneissic and plutonic rocks, as well as in some of the northwest mafic dykes.

Paragneiss of the WS is either garnet-biotite-plagioclase-quartz or biotite-plagioclase-quartz gneiss; south and southwest of Racine Lake, mafic enclaves in paragneiss have garnet-clinopyroxene-plagioclase-quartz ± hornblende assemblages. Leucosome is tonalitic east of Racine Lake but contains muscovite and K-feldspar to the west. Two thin paragneiss units that extend westward into the WS from their main outcrop areas in the KSZ exhibit transitions from layered migmatitic paragneiss in the KSZ to garnet-free, homogeneous diatexite in the WS. The transition is in a prograde direction in a textural sense toward increased grain size and homogeneity, but retrograde in terms of converting anhydrous to hydrous metamorphic mineral assemblages.

Kapuskasing Structural Zone

The rocks of the Kapuskasing structural zone have been highly deformed and metamorphosed with the result that original features are almost totally obliterated. Paragneiss is recognized by its mineralogy, generally garnet-biotite-plagioclase-quartz. Orthopyroxene, clinopyroxene, hornblende, muscovite, K-feldspar, sillimanite and graphite are additional constituents (Table 13.1). Migmatitic meta-iron formation, made up of garnet, quartz and magnetite, is located east of the Chapleau River. Paragneiss in many localities contains mafic granulite enclaves which are probably boudins of dykes or layers of metavolcanic origin.

The Shawmere anorthosite complex, a metamorphosed, deformed intrusion of Archean age (Watkinson et al., 1972; Thurston et al., 1977) is exposed north of Highway 101 and in a smaller body to the south (Fig. 13.6). These bodies consist mainly of gabbroic anorthosite to anorthosite, with outcrop-scale gabbro and melagabbro layers. Plagioclase megacrysts and clinopyroxene and orthopyroxene of possible igneous

origin are commonly preserved in low-strain areas. Corona structures, garnet and amphibole rimming ortho- and clinopyroxenes are common. As much as 5% quartz occurs in gabbroic anorthosite. Ultramafic rocks and tonalite are subordinate (Simmons et al., 1980; Riccio, 1979).

Foliated and gneissic mafic tonalite and diorite occur in four units. In the Chapleau-Nemegosenda Rivers area these rocks have relict layering and igneous clinopyroxene crystals to 1 cm, overgrown by hornblende. Gabbro and hornblendite layers are common close to contacts with paragneiss, suggesting that the bodies are layered sills with basal mafic accumulations. Rare ultramafic (orthopyroxene-clinopyroxene-hornblende) layers and lenses occur within the unit north of the Shawmere complex. Clinopyroxene-bearing quartz monzonite veinlets constitute up to 15 per cent of these rocks.

Gneissic and xenolithic tonalite-granodiorite units have been distinguished on the basis of proportion of xenoliths. The fabric comprises hornblende and/or biotite alignment and layering. Enclaves in xenolithic rocks are mafic (hornblende + plagioclase ± garnet ± clinopyroxene ± quartz), ultramafic (hornblende ± garnet ± clinopyroxene ± orthopyroxene) and rarely, paragneiss. Mafic granulite xenoliths commonly have amphibolitic rims. The xenolithic body south of the Shawmere anorthosite is garnetiferous; other bodies are hornblende-biotite-plagioclase-quartz gneiss.

Hornblende from mafic gneiss west of Foleyet yields a $^{40}Ar/^{39}Ar$ age of 2549 (D. Archibald, personal communication, 1980). Hornblende from mafic tonalite southeast of Kapuskasing Lake is dated at 2627 Ma by K-Ar and biotite from the same rock is 2544 Ma (R.D. Stevens, written communication, 1980).

The structure of the Kapuskasing zone is dominated by northeast-trending elongate lithologic units; lithologic contacts, gneissosity, and migmatitic layering strike northeast and dip moderately northwest. Gneissosity, defined by compositional layering and mineral alignment, is the earliest recognizable fabric.

In some areas the early gneissic fabrics are isoclinally folded about northeast-striking folds with northwest-dipping axial planes and gently northeast or southwest-plunging axes. Hinge areas of large-scale, northeast-plunging folds in the northern part of the KSZ near Kapuskasing Lake are characterized by northwest-striking, gently northeast-dipping foliation and northeast-plunging lineation. In the southern part of the KSZ within and southeast of the Shawmere anorthosite complex, rodding, small fold axes, and mineral lineations generally plunge southwest. Between the regions of dominant southwest and northeast plunges is a zone of horizontal lineation (0° to 10° plunge). The regional southwest plunge in the southern part of the KSZ suggests that the structurally lowest rocks are exposed on the east side of the structural zone. Northeast regional plunges in the northern segment indicate that the structurally lowest rocks are in the Wawa domal terrane (Fig. 13.7).

Metamorphic grade in the Kapuskasing structural zone is generally granulite facies. An isograd for the lower boundary of the granulite facies in mafic rocks is marked by the first appearance of garnet and clinopyroxene together and is based on the reaction (Carmichael, 1974):

hornblende + anorthite + quartz =
clinopyroxene + garnet + albite + H_2O

At the eastern margin of the KSZ, this isograd approximately coincides with the cataclastic zone, although in one locality metavolcanics with garnet-clinopyroxene assemblages occur approximately 1 km east of this zone. In the west, the metamorphic grade decreases from granulite facies in the KSZ to amphibolite facies in WS across a zone 20 to 30 km wide in the domal terrane.

Mafic gneiss in the KSZ is characterized by prominent compositional layers 1 to 10 cm thick composed of varying proportions of garnet, clinopyroxene, hornblende, plagioclase, and quartz. Orthopyroxene-plagioclase symplectitic coronas overgrow garnet and clinopyroxene in mafic gneiss at one locality.

Paragneiss contains concordant tonalite layers constituting up to 20 per cent of the rock. The paragneiss matrix is composed of garnet, biotite, plagioclase and quartz. Orthopyroxene and K-feldspar (Table 13.1) are also present in quantities up to 5 per cent and are probably the product of a reaction consuming biotite:

biotite + quartz = orthopyroxene + K-feldspar + H_2O

Mafic tonalite is hornblende-biotite-plagioclase-quartz rock, commonly with clinopyroxene crystals overgrown by hornblende. Rocks containing ortho- and clinopyroxene are present in this unit, particularly in ultramafic compositions, in an area southeast of the Shenango complex.

Mafic rocks of the Shawmere complex have mineralogy similar to country rock mafic gneiss and are veined by leucotonalite layers. Melagabbro of the anorthosite suite contains relict(?) phenocrysts of ortho- and clinopyroxene as well as hornblende and plagioclase. Rare relict olivine is present in the cores of orthopyroxene-hornblende-garnet (inside to out) coronas.

Metamorphic pressure-temperature conditions for rocks of the KSZ have been estimated using microprobe analyses and appropriate mineral equilibria. Estimates of T by Fe-Mg exchange equilibrium between garnet and clinopyroxene (Ellis and Green, 1979) in mafic gneiss are 700-1125°C but are more commonly in the range 730-800°C. The anomalously high value is from a rock 2 km east of the Nemegosenda Lake complex, with 28 mol% andradite in its garnet. Garnet-biotite Fe-Mg exchange thermometry (Ferry and Spear, 1978) on paragneiss shows a wider range of conditions (550-840°C). Pressure estimates based on Al solubility in orthopyroxene (Wood, 1974) are 4.5-13 kb; values of 5 to 12 kb are indicated by the Ghent et al. (1979) garnet-plagioclase geobarometer.

Retrograde metamorphism of granulites, first to amphibolite and later to greenschist facies, is common in the KSZ. Mafic granulites in contact with tonalite gneiss and tonalite dykes contain hornblende-plagioclase selvedges. The retrogression of relatively anhydrous to hydrous assemblages can be attributed to introduction of water by the tonalitic magma. The large xenolithic tonalite body south of the Shawmere complex (Fig. 13.6) contains marginally retrograded granulite xenoliths but is itself gneissic and garnetiferous (metamorphosed). This relationship suggests that either tonalite has intruded granulites of an earlier cycle of metamorphism, and was then metamorphosed by a subsequent event, or that syn-metamorphic tonalite magma introduced water into the granulite terrane after the peak of metamorphism.

Relationships Among Terranes

The relationship between the KSZ and AS has been discussed in some detail (Percival and Coe, 1980). Lithological, structural and metamorphic characteristics that define each domain change within a boundary zone some 1-2 km wide. Cataclastic veinlets crosscut rocks within and adjacent to the boundary zone. Intermittent ductile and brittle reactivation within the KSZ, limited by and concentrated along the eastern margin of the zone, could account for the eastern boundary characteristics (Percival, 1980).

The boundary between the KSZ and WS has been described as gradational (Bennett et al., 1967; Thurston et al., 1977; Percival and Coe, 1980). Lithological changes are gradational; paragneiss units characteristic of

the KSZ continue into the WS domal terrane as discreet units and migmatite zones. Mafic tonalite-diorite is a characteristic rock type of the KSZ and extends approximately to the western margin of this zone as defined on the basis of structural grounds. However, equivalents may be found in the Floranna Lake complex and Missinaibi Lake batholith (Fig. 13.7), which are weakly layered and of similar composition, texture and grain size. Mafic granulites are generally restricted to the KSZ; however identical rocks are exposed in the Robson Lake dome of the WS. Mafic inclusions in tonalite-granodiorite gneiss of the WS are possibly equivalent to mafic granulites of the KSZ. Xenolithic tonalite-granodiorite gneiss units are apparently continuous between the two terranes northeast of Chapleau; mafic granulite xenoliths are more common in the KSZ than to the west.

Structural patterns of the two terranes are different but appear to be related and inter-gradational; antiformal axes are continuous from domal culminations in the WS into gently northeast-plunging antiforms in the northern portion of the KSZ. Inter-dome synforms can also be traced from WS into KSZ. In the southern part of the KSZ, where plunges are generally southwest, structural and lithologic patterns are continuous with those of the WS across basinal depressions. Possibly the best criteria for distinguishing the two terranes are structural style and orientation. Although these criteria cannot be strictly applied, nor a sharp boundary drawn between the two structural domains, WS has dominantly gently-dipping fabrics with widely variable strike reflecting the domal structures, whereas KSZ has moderately-dipping fabrics with relatively constant northeast strike.

The western amphibolite-granulite isograd is a wide zone; textural relations of granulites exposed in WS suggest that retrograde metamorphism, associated with the intrusion of plutonic rocks, is partly responsible for the diffuse nature of the metamorphic boundary. However, the occurrence of granulites in domal culminations of the WS suggests that the garnet-clinopyroxene isograd was flat prior to doming.

The cross-sections of Figure 13.7 show structural and implied age relations between the KSZ and WS. Both sections show xenolithic rocks and mafic granulite associated with paragneiss to be structurally low. Paragneiss located structurally above anorthosite is highest in the section and may be correlative, across domal and batholithic terrane, with metavolcanic rocks of the Wawa belt west of the study area.

Mafic Dykes

The Archean rocks of the Kapuskasing structural zone and adjacent Abitibi and Wawa subprovinces are cut by several mafic dyke swarms of Archean and Proterozoic ages. Dykes of the late Archean Matachewan swarm (Rb-Sr – 2690, Gates and Hurley, 1973) strike north to north-northwest in the Abitibi subprovince and northwest to north-northwest in the Wawa subprovince (Ernst and Halls, 1980; Watson, 1980). Matachewan dykes are not present within the KSZ (Bennett et al., 1967; Thurston et al., 1977). Along roadcuts in the eastern part of the WS the Matachewan dykes dip consistently eastward at 75° to 85°.

At least two, and probably three, Proterozoic dyke swarms intrude Archean rocks in the region. Tholeiitic, sparsely plagioclase porphyritic tholeiitic mafic dykes, herein termed "Kapuskasing dykes" occur in the KSZ. These dykes are up to 10 m wide and strike consistently 070° and dip 70° to 80° southeast. Whole rock K-Ar ages range up to 3650 Ma (R.D. Stevens, written communication, 1980), indicating the presence of excess argon in at least some of the dykes. A vertical, fine grained, very fresh 070° dyke near the eastern margin of the KSZ yielded a K-Ar whole rock age of 1475 Ma (R.D. Stevens, written communication, 1980). Northwest-striking tholeiitic dykes in the WS west of the KSZ have been correlated with the Mackenzie III swarm by Thurston et al. (1977). Several olivine diabase dykes, possibly belonging to the Abitibi swarm, are present in the KSZ.

Mylonitic Rocks

Mylonitic rocks have previously been noted along the eastern boundary of the KSZ (Bennett et al., 1967; Thurston et al., 1977). In the Ivanhoe Lake area, the migmatitic contact zone between quartz monzonite and mafic granulite is crosscut by late pseudotachylite-type mylonitic veinlets. No preferred orientation of the mylonitic veinlets is obvious on the outcrop; rather, the veinlets crosscut one another and give the host rock a chaotic, shattered appearance. However, areal mapping shows that the zone of extreme cataclasis is approximately 1 to 2 km wide and strikes in a north-northeast direction (Fig. 13.6). North-northeast striking alteration veinlets consisting of quartz, chlorite, and paragonite occur in the Shawmere anorthosite complex and these may have originated as cataclastic veinlets.

Two ages of brittle deformation are indicated by the textures and crosscutting relationships of mylonitic veinlets; an early set is overgrown by epidote, chlorite and carbonate; a later set consists of unrecrystallized cryptocrystalline rock flour. A whole-rock $^{40}Ar/^{39}Ar$ date on one of the late, unrecrystallized mylonitic veinlets is 1732 Ma (D. Archibald, personal communication, 1980).

Alkalic Rock-Carbonatite Complexes

Three alkalic rock-carbonatite intrusions of late Proterozoic age (1100-1000 Ma) are shown on Figure 13.6. The Lackner Lake and Nemegosenda Lake complexes are composed of alkalic rock and carbonatite. The Shenango Complex is of dioritic to monzonitic composition. Zones of fenite alteration and lamprophyre-carbonatite dykes cut Archean rocks in the area between Lackner Lake and Nemegosenda Lake. Lamprophyre dykes up to 0.5 m wide are common in the KSZ and in the WS in the Chapleau area. Biotite from one such dyke yielded a K-Ar whole rock age of 1144 Ma (R.D. Stevens, written communication, 1980).

Discussion

Near Lake Superior, some 80 km west of the study area, supracrustal rocks of the Wawa metavolcanic belt are metamorphosed to low greenschist (Fraser et al., 1978); metamorphic grade increases to the east and the amphibolite-granulite facies transition is exposed in the area under investigation. The geometry of the amphibolite-granulite boundary is partly explained by ductile arching of metamorphic isograds in the domal terrane of the western WS. However, the large areal extent of granulite exposed in the KSZ, apparently unrelated to diapiric processes, suggests a different mechanism of uplift.

Northwest Matachewan dykes west of the KSZ dip northeast and ENE dykes in the KSZ dip southeast. If these dykes intruded vertical fractures then post-dyke regional block rotation may be responsible for their present orientation. To rotate both dyke sets back to vertical, the crustal block containing them must be rotated clockwise about a horizontal hinge line bisecting the dyke trends. This hypothetical hinge line is parallel to the cataclastic eastern margin of the KSZ. If post-dyke counterclockwise rotational movement has tilted the block, listric reverse movement along the eastern cataclastic boundary zone of the KSZ is required (Fig. 13.7, section C-D).

Preliminary $^{40}Ar/^{39}Ar$ studies of rocks in the cataclastic zone indicate disturbances at 1730 and 1100 Ma (D. Archibald, personal communication, 1980). Brittle movements along the zone may have been contemporaneous with Proterozoic events in nearby parts of the Shield, for example, Penokean-Hudsonian events in the Southern Province or Keweenawan rifting and volcanism in the Lake Superior basin.

The ages of Proterozoic igneous complexes (1100-1000 Ma K-Ar ages; Gittens et al., 1967; Thurston et al., 1977) are similar to the age of Keweenawan volcanism (1140-1120 Ma; Silver and Green, 1972). Based on the similarity of ages of these igneous events, the regional tilt implied by dyke dips, and the regional easterly increase in metamorphic grade from Lake Superior toward the KSZ, a Keweenawan age for tilting and uplift of granulites is suggested. Brittle fractures formed during this event would provide conduits for mantle-derived alkalic and carbonatite magmas. Regional tilting could result from crustal loading in the Lake Superior basin as a result of Keweenawan mafic volcanism.

The evidence thus supports the original contention of Innes (1960) that the KSZ gravity high is related to the mid-continent gravity high. However, rather than resulting from crustal thickening in a graben, the KSZ gravity high may result from crustal attenuation caused by erosion of the tilted block. This interpretation is in contrast to that of Watson (1980) who suggested that uplift of granulites predated intrusion of the Matachewan dyke swarm.

In the Chapleau-Foleyet area the positive gravity anomaly associated with the KSZ has a higher gradient on the east than on the west. Although this may simply be a function of grid spacing, it would also support the regional tilting hypothesis. The various lines of evidence given above suggest that the crust underlying the KSZ may be thinner than normal continental crust. For example, metamorphic pressures of the order of 10 kb suggest that up to 30 km of crust has been eroded. A seismic survey could indicate the extent to which the Moho has been affected by uplift of granulites in the structural zone.

PART 3. GEOLOGY OF THE ROUND LAKE BATHOLITH, KIRKLAND LAKE AREA, ONTARIO

J. Lafleur and D.D. Hogarth

Introduction

The Round Lake batholith has an exposed area of about 1900 km^2 south of Kirkland Lake, Ontario (Fig. 13.9). Granitic rocks of this batholith are Archean and apparently intrude metavolcanics and metasediments of the Abitibi Supergroup. The batholith is intruded by late Archean mafic dykes of the Matachewan swarm and by syenitic rocks of the Otto Stock. It is overlain unconformably by early Proterozoic sedimentary rocks of the Huronian Supergroup.

Parts of the batholith have been studied in the past, notably by Lawton (1957), Lovell (1972), and Ridler (1975). Lawton and Lovell regarded the batholith as magmatic and intrusive into the Abitibi Supergroup. In contrast, Ridler concluded that the batholith, or parts of it, represents the diapirically mobilized basement upon which the Abitibi supracrustal rocks were deposited.

The present study was undertaken to define the lithological and structural characteristics of the entire batholith, and insofar as possible, to determine its age, origin, mechanism of emplacement, and relationship to the tectonic evolution of the region.

General Geology

The Round Lake batholith is composite, consisting of cataclastically foliated and marginally gneissic granodiorite (granodiorite and tonalite) and several massive to foliated granitic (granite and quartz monzonite) and dioritic (diorite to syenite) bodies. An east-northeast-trending massive granitic stock (B – Indian Chute Stock; Fig. 13.9) in the central part of the batholith contains xenoliths of granodiorite and of the surrounding supracrustal rocks. Two smaller granitic stocks (A – Crooked Creek Stock; C – Hope Lake Stock; Fig. 13.9) occur in the north-central and south-central extremities of the batholith. Several foliated dioritic stocks occur along the western contact zone of the batholith.

The batholith is surrounded by supracrustal rocks of the Archean Abitibi Supergroup. These consist of:

1. ultramafic metavolcanic rocks with olivine and pyroxene spinifex textures and polysutured flows.
2. massive, pillowed, variolitic, and amygdaloidal mafic metavolcanic rocks.
3. finely laminated, aphanitic, intermediate to felsic metavolcanic rocks, mainly tuff, which are interbedded with chert, iron formation, and agglomerate.
4. clastic and chemical metasediments, including greywacke, conglomerate, and iron formation.
5. gabbroic and dioritic sills that occur with, and are probably related to, the metavolcanic sequence.

Metamorphism of the Abitibi Supergroup ranges from prehnite-pumpellyite to lower greenschist facies (Jolly, 1978). Near the contact with the Round Lake batholith, the metavolcanics and metasediments are apparently in the amphibolite facies.

The supracrustal rocks surrounding the batholith have a stratiform foliation subparallel to primary layering. This foliation is generally concordant with, and dips steeply away from, the batholith contact. However, between the Otto and Hope Lake stocks (1 and C, Fig. 13.9) the stratiform foliation dips steeply southward toward the batholith contact. There is extensive shearing and flattening of pillows in a plane parallel to the batholith contact in this area. East-west kink folds and quartz-carbonate shear zones, possibly representing a second deformational event (D_2), are present in the country rocks in the northeastern part of the study area.

The intrusion of five syenite stocks (1, Cairo; 2, Holmes; 3, Otto; 4, Lebel; 5, McElroy) deformed and metamorphosed the supracrustal rocks north of the batholith. One of these, the Otto Stock (3, Fig. 13.1) intrudes the batholith along its northern margin.

North-trending diabase dykes of the Matachewan swarm dated at 2690 Ma (Gates and Hurley, 1973) crosscut all previously described rocks.

Comparatively flat-lying Proterozoic rocks, quartzite, arkose and conglomerate of the Huronian Supergroup, with associated Nipissing Diabase intrusions, extend into the area from the south.

Major northwest-trending lineaments (CLF, Cross Lake Fault; MRF, Montreal River Fault), part of the Timiskaming fault system (Lovell and Caine, 1970), transect the central part of the study area with significant lateral displacement of the batholithic phases. Normal movement along the Timiskaming faults resulted in the preservation of Phanerozoic sediments in the southeastern part of the area.

Description of the Batholith

Foliated granodiorite is a greyish white, coarse grained, equigranular and feldspar porphyritic rock composed of plagioclase (interstitial and as phenocrysts), quartz, microcline, biotite, hornblende, chlorite, muscovite, epidote, allanite, and opaque minerals. The granodiorite contains a few mafic xenoliths and grey feldspar porphyry dykes. Cataclastic foliation is defined by oriented biotite-hornblende-epidote aggregates and by a granulated quartz-feldspar fabric. The main east-west cataclastic foliation of the granodiorite coincides with the D_2 fabric of the adjacent supracrustal rocks.

Dykes of granodiorite extending into the country rocks are rare. However, there is evidence for crosscutting relationships along the eastern contact zone. The intermediate to felsic metavolcanic unit adjacent to the batholith in the northeast and east is truncated at the southeastern margin. Furthermore, the supracrustal rocks at the batholith contact are overprinted by a narrow contact aureole of amphibolite facies (actinolite-epidote) metamorphism, best developed east of Tarzwell.

Eastward the foliated grey granodiorite seems to grade into a lineated reddish granodiorite characterized by 10 to 15 per cent microcline and an almost total lack of cataclastic foliation. The red coloration may be due to iron oxide staining of the primary minerals.

To the north and east, the foliated granodiorite passes gradationally into two distinct rock types – inhomogeneous xenolithic gneiss and cataclastic augen gneiss of granodioritic to tonalitic composition. The xenolithic gneiss occurs along the northern border of the batholith from west of Tarzwell to the Matachewan area. The rock is characterized by moderate cataclasis, by mafic metavolcanic xenoliths, and by a variety of granitic dykes, including granite offshoots from the Crooked Creek stock. Xenoliths are concentrated at or near the batholith contacts. They are generally sharp-bordered and unaltered, although partly assimilated and deformed inclusions are present. They range in length from a few metres to possibly a kilometre and are commonly oriented with their long dimensions parallel to the batholith contact.

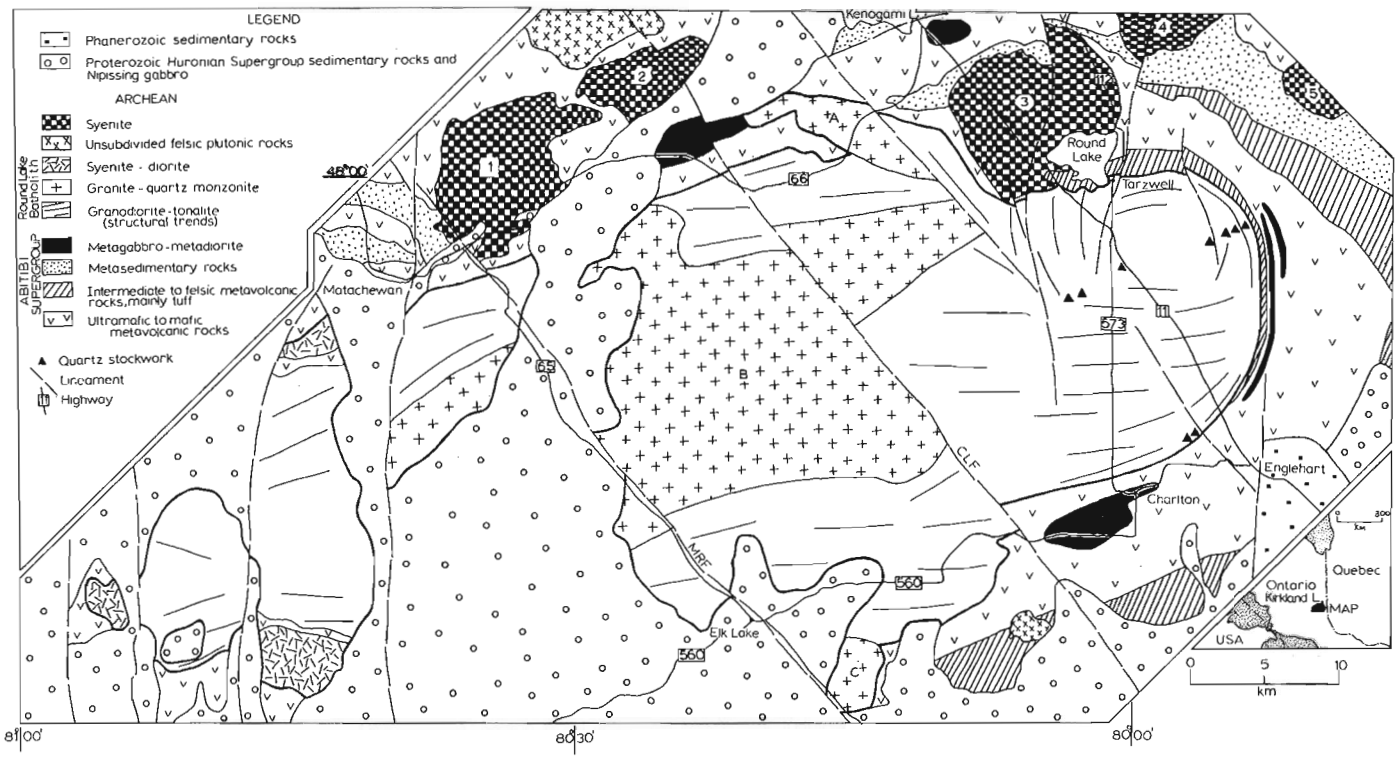

CLF	= *Cross Lake fault*	*1*	= *Cairo stock*
MRF	= *Montreal River fault*	*2*	= *Holmes stock*
A	= *Crooked Creek stock*	*3*	= *Otto stock*
B	= *Indian Chute stock*	*4*	= *Lebel stock*
C	= *Hope Lake stock*	*5*	= *McElroy stock*

Figure 13.9. *General geology of the Round Lake batholith area (modified from Pyke et al., 1973).*

The cataclastic augen gneiss occurs east and south of Tarzwell to the Cross Lake Fault and features flattened, granulated quartz-feldspar aggregates, chlorite-rich layers 1 to 5 cm thick, and rounded quartz and feldspar fragments with chloritic rims. Along the southeastern edge of the batholith the augen gneiss is black, a result of extreme cataclasis.

The marginal xenolithic gneiss and augen gneiss have a steep to moderate inward-dipping gneissic foliation which is generally parallel to the perimeter of the batholith, except at the southern end of Round Lake where this structure curves northerly.

The granite that occurs as stocks is massive, medium- to coarse-grained, red in colour, and composed of microcline (interstitial and as phenocrysts), plagioclase, biotite, hornblende, epidote, and opaque minerals. Xenoliths of supracrustal and felsic plutonic rocks are present, and include rounded, granitized felsic hornfels fragments (sediments or felsic volcanics originally), recrystallized ultramafic and mafic metavolcanic fragments, and foliated granodiorite fragments.

The granitic stocks display both concordant and discordant intrusive relationships toward the foliated and gneissic granodiorite. Near contacts, numerous granitic dykes, offshoots from the stocks, cut the older foliated and gneissic phases. The Hope Lake and Crooked Creek stocks also intrude the metavolcanic-metasedimentary country rocks. Adjacent to the Hope Lake stock, predominantly east-trending structures in the metavolcanics have been reoriented northerly.

Dioritic stocks form part of the batholith west of the Cross Lake Fault. The rocks, ranging in composition from diorite to syenite, are coarse grained, massive to foliated, red to white in colour, and consist essentially of plagioclase, microcline, and hornblende. The diorite intrudes the metavolcanic-metasedimentary country rocks, producing spectacular zones of agmatite consisting of foliated and pillowed mafic metavolcanics permeated by dioritic material. The contacts between the dioritic bodies and the foliated granodiorite were not observed.

Two northeast-trending quartz stockworks transect the batholith. The stockwork zones are approximately 60 m wide and 2 km long, and consist of massive white quartz and a breccia composed of granodiorite and altered mafic metavolcanic(?) fragments in quartz with pyrite, chalcopyrite, chlorite, sericite and hematite-bearing fractures, and pervasive hematite, kaolinite, and sericitic alteration. Several occurrences of gold are present in this zone (H. Lovell, personal communication, 1980).

Discussion

The Round Lake batholith appears to represent a late Archean, post-Abitibi Supergroup intrusion that was emplaced as a magmatic diapir. The intrusion cooled and partly solidified while still moving upward in the dense mafic volcanic sequence. This mechanism would explain the cataclastic nature of the early, solidified or partly solidified, granodiorite and the massive character of the late granite bodies which remained liquid, or were emplaced after movement ceased. Preliminary chemical and petrographic studies indicate that the two phases would represent differentiates of a common parental magma.

Furthermore, this model could explain the presence of both assimilated and unaltered xenoliths in the granodiorite, the narrowness of the contact metamorphic aureole, the paucity of granodiorite dykes in the country rocks, and the general conformity of foliation within the batholith to the structures within the adjacent country rocks.

References

Bennett, G., Brown, D.D., George, P.T., and Leahy, E.J.
1967: Operation Kapuskasing; Ontario Department of Mines, Miscellaneous Paper 10, 98 p.

Card, K.D.
1979: Regional geological synthesis, central Superior Province; in Current Research, Part A, Geological Survey of Canada, Paper 79-1A, p. 87-90.

1980: Preliminary maps, central Superior Province compilation – Sudbury (41I), Blind River (41J), Gogama (41P), Chapleau (41O); Geological Survey of Canada, Open File 690.

Card, K.D., Percival, John A., and Coe, Kenneth
1980: Progress report on regional geological synthesis, central Superior Province; in Current Research, Part A, Geological Survey of Canada, Paper 80-1A, p. 61-68.

Carmichael, D.M.
1974: Mineral equilibria in mafic granulites (abstract); Canadian Mineralogist, v. 12, p. 429-430.

Dawson, K.R.
1966: A comprehensive study of the Preissac-Lacorne batholith, Abitibi County, Québec; Geological Survey of Canada, Bulletin 142, 76 p.

Ellis, D.J. and Green, D.H.
1979: An experimental study of the effect of Ca upon garnet-clinopyroxene Fe-Mg exchange equilibria; Contributions to Mineralogy and Petrology, v. 71, p. 13-22.

Ernst, R. and Halls, H.C.
1980: Extension of the Matachewan and Abitibi diabase dike swarms west of the Kapuskasing structural zone, northern Ontario (abstract); EOS, v. 61, no. 17, p. 215.

Fahrig, W.F., Gaucher, E.H., and Larochelle, A.
1965: Paleomagnetism of diabase dykes of the Canadian Shield; Canadian Journal of Earth Sciences, v. 2, p. 278-298.

Ferry, J.M. and Spear, F.S.
1978: Experimental calibration of the partitioning of Fe and Mg between biotite and garnet; Contributions to Mineralogy and Petrology, v. 71, p. 113-117.

Fraser, J.A., Heywood, W.W., and Mazurski, M.
1978: Metamorphic map of the Canadian Shield; Geological Survey of Canada, Map 1475A.

Gates, T.M. and Hurley, P.
1973: Evaluation of Rb-Sr dating methods applied to the Matachewan, Abitibi, Mackenzie and Sudbury dike swarms in Canada; Canadian Journal of Earth Sciences, v. 10, p. 900-919.

Gaucher, E.H.
1966: Elsas-Kapuskasing-Moosonee magnetic highs; Geological Survey of Canada, Paper 66-1, p. 263-338.

Ghent, E.O., Robbins, B., and Stout, M.Z.
1979: Geothermometry, geobarometry and fluid compositions of metamorphosed calc-silicates and pelites, Mica Creek, British Columbia; American Mineralogist, v. 64, p. 874-885.

Gibb, R.A.
1978: A gravity survey of James Bay and its bearing on the Kapuskasing gneiss belt, Ontario; Tectonophysics, 45, p. T7-T13.

Gittins, J., MacIntyre, R.M., and York, D.
1967: The ages of carbonatite complexes in eastern Canada; Canadian Journal of Earth Sciences, v. 4, p. 651-655.

Goodwin, A.M., Innes, M.J.S., Gibb, R.A., Hall, D.H., MacLaren, A.S., Pettijohn, F.J., Norris, A.W., Clifford, P.M., Currie, K.L., Fahrig, W.F., Irvine, T.N., Ridler, R.H., Ayres, L.D., Ermanovics, I.F., and Ambrose, J.W.
1972: The Superior Province; in Variations in Tectonic Styles in Canada, R.A. Price and R.J.W. Douglas (eds.), Geological Association of Canada, Special Paper No. 11, p. 571-574.

Hanes, J.A. and York, Derek
1979: A detailed $^{40}Ar/^{39}Ar$ age study of an Abitibi dyke from the Canadian Superior Province; Canadian Journal of Earth Sciences, v. 16, p. 1060-1070.

Innes, M.J.S.
1960: Gravity and isostasy in Manitoba and northern Ontario; Dominion Observatory Publications 21, p. 263-338.

Irvine, T.N. and Baragar, W.R.A.
1971: A guide to the chemical classification of the common volcanic rocks; Canadian Journal of Earth Sciences, v. 8, p. 523-548.

Jolly, W.T.
1978: Metamorphic history of the Archean Abitibi Belt; in Metamorphism in the Canadian Shield, J.A. Fraser and W.W. Heywood (eds.), Geological Survey of Canada, Paper 78-10, p. 63-78.

Krogh, T.E. and Davis, G.L.
1971: Zircon U-Pb ages of Archean meta-volcanic rocks in the Canadian Shield; Yearbook, Carnegie Institute, Washington, 70, p. 241-242.

Larochelle, A.
1966: Paleomagnetism of the Abitibi dyke swarm; Canadian Journal of Earth Sciences, v. 3, p. 671-683.

Lawton, K.D.
1957: Geology of Boston Township and part of Pacaud Township; Ontario Department of Mines, v. LXVI, Pt. 5, p. 1-55.

Lovell, H.
1972: Geology of the Eby and Otto area, District of Timiskaming, Ontario; Ontario Department of Mines and Natural Resources, Geological Report 99.

Lovell, H. and Caine, T.W.
1970: Lake Timiskaming rift valley; Ontario Department of Mines, Miscellaneous Paper 39, 16 p.

Nunes, P.D., Pyke, D.R., and Jensen, L.S.
1978: Toward an absolute age stratigraphy for the Abitibi greenstone belt, eastern Ontario – zircon ages from the Timmins and Kirkland Lake areas (abstract); Geological Association of Canada, Program with Abstracts, 3, p. 464-465.

Percival, J.A.
1980: Archean tectonic evolution of the Kapuskasing structural zone, central Superior Province, Ontario (abstract); Geological Association of Canada, Program with Abstracts, 5, p. 75.

Percival, J.A. and Coe, K.
1980: Geology of the Kapuskasing structural zone in the Chapleau-Foleyet area, Ontario; in Card, K.D., Percival, J.A., Coe, K., Progress report on regional geological synthesis, central Superior Province; in Current Research, Part A, Geological Survey of Canada, Paper 80-1A, p. 61-68.

Pyke, D.R., Ayres, L.D., and Innes, D.G.
1973: Timmins-Kirkland Lake sheet, Cochrane, Sudbury and Timiskaming Districts; Ontario Division of Mines, Geological Compilation Series, Map 2205.

Pyke, D.R., Naldrett, A.J., and Eckstrand, O.R.
1973: Archean ultramafic flows in Munro Township, Ontario; Geological Society of America Bulletin, v. 84, p. 955-978.

Riccio, L.
1979: Shawmere anorthosite; in Summary of field work, 1979, Ontario Geological Survey, Miscellaneous Paper 90, p. 100-103.

Ridler, R.H.
1975: Regional metallogeny and volcanic stratigraphy of the Superior Province; in Report of Activities, Part A, Geological Survey of Canada, Paper 75-1A, p. 353-358.

Silver, L.T. and Green, J.C.
1972: Time constants for Keweenawan igneous activity (abstract); Geological Society of America, Abstracts with Program, 4, p. 665-666.

Simmons, E.C., Hanson, G.N., and Lumbers, S.B.
1980: Geochemistry of the Shawmere anorthosite complex, Kapuskasing structural zone, Ontario; Precambrian Research, v. 11, p. 43-71.

Stockwell, C.H.
1970: Geology of the Canadian Shield – Introduction; in Geology and Economic minerals of Canada, R.J.W. Douglas (ed.), Geological Survey of Canada, Economic Geology Report 1 (5th Edition), p. 44-54.

Thurston, P.C., Siragusa, G.M., and Sage, R.P.
1977: Geology of the Chapleau area, districts of Algoma, Sudbury and Cochrane; Ontario Division of Mines, Geoscience report 157, 293 p.

Watkinson, D.H., Thurston, P.C., and Shafiquilah, M.
1972: The Shawmere anorthosite complex of Archean age in the Kapuskasing belt, Ontario; Journal of Geology, v. 80, p. 736-739.

Watson, J.
1980: The origin and history of the Kapuskasing structural zone, Ontario, Canada; Canadian Journal of Earth Sciences, v. 17, p. 866-876.

Wood, B.J.
1974: The solubility of alumina in orthopyroxene coexisting with garnet; Contributions to Mineralogy and Petrology, v. 46, p. 1-15.

14.

MESOZOIC STRATIGRAPHY IN THE BLUE MOUNTAINS AND KRIEGER MOUNTAINS, NORTHERN ELLESMERE ISLAND, ARCTIC CANADA: A PRELIMINARY ACCOUNT

Project 750092

P.R. Moore[1]
Institute of Sedimentary and Petroleum Geology, Calgary

Moore, P.R., Mesozoic stratigraphy in the Blue Mountains and Krieger Mountains, northern Ellesmere Island, Arctic Canada: a preliminary account; in Current Research, Part A, Geological Survey of Canada, Paper 81-1A, p. 95-101, 1981.

Abstract

Five Mesozoic sections in the central part of northern Ellesmere Island are described. Triassic formations thin significantly to the northeast, where shallow-water, nearshore facies are preserved. Shallowing in the more axial parts of the basin occurred in the late Scythian (early Triassic), late Karnian (late Triassic) and Valanginian (early Cretaceous). Truly terrestrial conditions existed only in latest Triassic (Norian-Rhaetian) and Early Cretaceous (late Valanginian to early Aptian) times. Mesozoic sediments were largely deposited in a shallow to marginal marine environment.

New fossil collections indicate a possible Bathonian age, in part, for sediments of the Jurassic Savik Formation.

Introduction

Mesozoic sedimentary rocks in the Blue Mountains and Krieger Mountains were deposited near the northeastern margin of Sverdrup Basin, close to the southern end of the Grantland Uplift (Kerr, in press, Fig. 11). Isopach and facies maps (Thorsteinsson and Tozer, 1970, Figs. 10, 12) suggest that Triassic sediments accumulated near the axis of the subsiding basin, whereas overlying Jurassic and Lower Cretaceous strata probably occupied a more marginal position. The overall stratigraphic and structural setting of Sverdrup Basin has recently been summarized by Balkwill (1978) and Kerr (in press).

In June and July 1979 the writer studied a series of Mesozoic sections on northern Ellesmere Island as part of a wider project being undertaken by A.F. Embry. The five measured sections described here lie roughly along strike from one another, and span a distance of nearly 100 km (Fig. 14.1). Several of these sections have previously been described by Tozer (1963).

This paper provides a preliminary account of the content, thickness, age and inferred environment of deposition of Mesozoic formations in part of northern Ellesmere Island. It is anticipated that a comprehensive report will be presented at a future date.

Blind Fiord Formation

In its type section northwest of Blind Fiord, Ellesmere Island, the formation consists of green and grey, partly micaceous siltstone (Tozer, 1961). In the Blue Mountains (Section 1, Fig. 14.2) only the lower part of the formation is dominated by siltstone; the upper part comprises mainly fine sandstone and shale.

An upward change from siltstone to more sandy sediment is also evident in the Krieger Mountain and Hare Fiord sections (Sections 4, 5; Fig. 14.2). Thick, quartzose sandstone units first appear lower down in the formation at these localities, reflecting greater proximity to the basin margin and laterally equivalent Bjorne sandstone (Tozer, 1961) facies. Shell (bioclastic) limestones are also common.

The base of the formation is clearly exposed in the Krieger Mountains section (Fig. 14.3). Here bedded chert of Degerbols Formation (Upper Permian) is abruptly overlain by 2 m of green-grey shale which grades upward into laminated grey siltstone with thin sandstone beds. In the Blue Mountains section (Section 1) the base is not exposed but probably lies a few metres above the upper of two thin grey chert beds within hard grey-black shale of Van Hauen Formation (Lower Permian). At Hare Fiord (Section 5, Fig. 14.2) a thick gabbro sill lies along or close to the contact with the underlying Trold Fiord Formation (Thorsteinsson and Trettin, 1972).

The upper contact with Blaa Mountain Formation is well defined in the Krieger Mountains section where black shale abruptly overlies hard quartzose sandstone. In the Blue Mountain and Hare Fiord sections the contact is obscured, but there is an abrupt change from a sandstone – dominated sequence into black shale.

Although allowance must be made for imprecise measurement, and structural complications in the Blue Mountains section, the formation thins significantly to the east. The 1240 m thick section in the Blue Mountains is reduced to 830 m in the Krieger Mountains, and to 600 m at Hare Fiord. Whether or not there is a progressively greater truncation of the formation by the overlying Blaa Mountain Formation toward the east is an open question. Certainly, if correlation is correct, a prominent sandstone unit in the upper part of Blind Fiord Formation appears to be cut out between the Krieger Mountains and Hare Fiord sections (Fig. 14.2).

Age

No further refinement of the Lower Triassic, Scythian age determined by Tozer (1961) is possible at this time.

Environment of Deposition

The abundant ripple marks, trace fossils, cross-laminated sands, and scattered shellbeds in Blind Fiord Formation suggest an open shelf environment. The lower part of the formation, exposed 4 km north of Section 1, contains beds with features typical of turbidites (graded bedding, flame structures, flute casts), and several zones of intraformational slump folds. Slumps could have resulted from rapid deposition of sediment on a slight slope, such as on a delta front, but otherwise might indicate tectonic instability within the basin of sedimentation.

The upward increase in sandstone within Blind Fiord Formation implies a general shallowing of the basin. In the Blue Mountains section siltstone grades up into a sequence of wavy-laminated, bioturbated, sparsely fossiliferous fine

[1]N.Z. Geological Survey, P.O. Box 30-368, Lower Hutt, New Zealand.

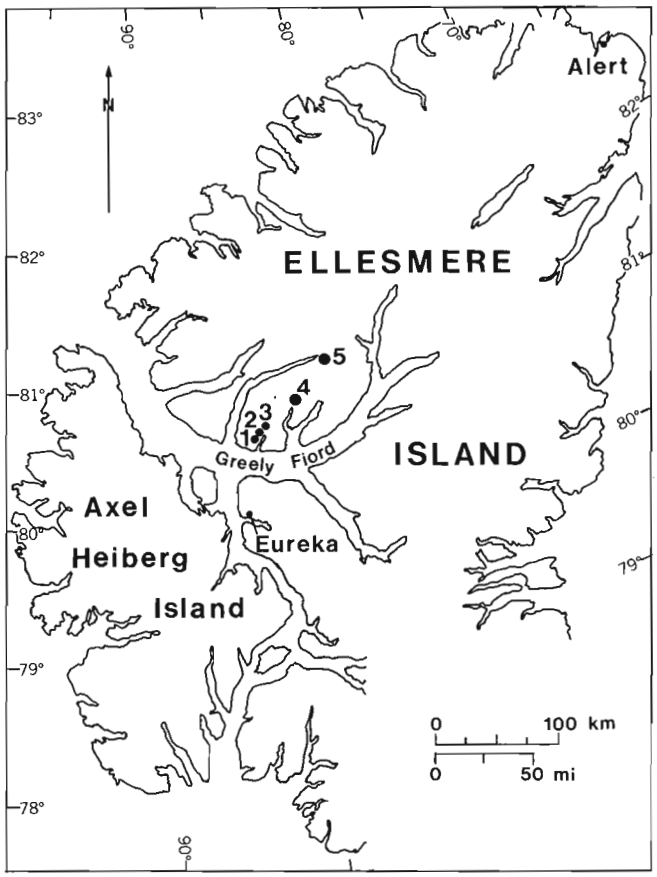

Figure 14.1. *Location of Mesozoic sections studied: Blue Mountains (Sections 1-3), Krieger Mountains (Section 4), and head of Hare Fiord (Section 5).*

sandstone and interbedded siltstone and dark shale. Scour casts and channelling occur at the base of some sandstone beds. Shallowing is even more evident in the Krieger Mountains section where the sequence contains common shellbeds, shelly limestones and a thick quartzose sandstone member with vertical burrows of the **Skolithos** type.

Blaa Mountain Formation

Blaa Mountain Formation was subdivided into five members by Tozer (1961): Lower Shale, Lower Calcareous, Middle Shale, Upper Calcareous, and Upper Shale. All five members (totalling 1530 m) are present in the Blue Mountains section, but the sequence is greatly reduced to the northeast and the Middle Shale and Lower Calcareous members are absent in the Hare Fiord section (Section.5, Fig. 14.2).

In the Blue Mountains, Blaa Mountain Formation consists predominantly of moderately soft black shale with concretionary bands and minor sandstone beds, bioclastic limestone and shell beds. The Lower and Upper Calcareous members consist of hard, dark grey calcareous siltstone, shale and very fine sandstone. These units apparently represent tongues of the laterally equivalent Schei Point facies (Tozer, 1961, p. 19). To the east, where the formation is markedly reduced in thickness, pebbly sandstone and limestone beds are present. Red-brown and green-grey shale occurs immediately below the Upper Calcareous member in the Krieger Mountains, over a distance of at least 18 km.

The base of the formation is not exposed in the Blue Mountains section, but is marked by the appearance of thick black shale containing concretionary beds and abundant ammonite impressions. In the Krieger Mountains section there is a sharp contact between Blind Fiord quartzose sandstone and the Lower Shale of Blaa Mountain Formation. At Hare Fiord the base of the formation is arbitrarily drawn between wavy-bedded sandstone and alternating sandstone and siltstone beds 15 m below the Upper Calcareous member (or **Gryphaea** bed of the laterally equivalent Schei Point Formation; Tozer, 1963, p. 12).

The upper contact with Heiberg Formation is well defined in the Blue Mountains and Hare Fiord sections. In the former, the upper 50 m of Blaa Mountain Formation consists of thin bedded, fine sandstone and shale containing a 5 m thick, large-scale crossbedded quartzose sandstone bed. This sequence essentially represents a gradation into the overlying Heiberg Formation, and theoretically the top of Blaa Mountain Formation could be drawn at the base of the quartzose sandstone bed. However, 35 m higher a thick carbonaceous quartzose sandstone with conglomerate at the base sharply overlies thin bedded sandstone and shale, and the upper boundary is taken at this point (Fig. 14.4). There appears to be a slight truncation of beds below the contact.

A similar transitional sandy zone occurs in the upper 4 m of the formation in Hare Fiord section, and the top is drawn at a sharp, iron-stained contact between convolute-laminated sandstone beds and overlying soft grey sandstone containing thin coaly shale.

Blaa Mountain Formation is only 100 m thick in the Hare Fiord section. Between the Blue Mountains and Krieger Mountains, the Middle Shale is greatly reduced in thickness, thinning from about 1000 m to only 180 m due to truncation beneath the Upper Calcareous. At Hare Fiord the Middle Shale and Lower Calcareous members are absent, and the Upper Calcareous member unconformably rests on the Lower Shale member (Fig. 14.2).

Although the Upper Calcareous and Upper Shale members also thin to the northeast, they are persistent. The Upper Calcareous becomes more sandy and shelly eastward and in the Hare Fiord section contains abundant **Gryphaea.** The Upper Shale also changes character, so that in the east it consists predominantly of thin bedded, alternating sandstone and shale.

Judging by the abrupt change in lithology between the Blind Fiord and Blaa Mountain formations, and by the sharp contact observed in the Krieger Mountains section, there may be a significant disconformity at the base of Blaa Mountain Formation. The break might not be as important in the Blue Mountains section, which represents a more basinward sequence, as it is in the more marginal sections to the northeast.

Age

The formation spans the Anisian to Karnian (Middle to Upper Triassic) according to Tozer (1961, 1963). The Upper Shale may be as young as Norian (A. Embry, personal communication, 1979).

Environment of Deposition

The bulk of Blaa Mountain Formation appears to have been deposited in a relatively quiet environment, perhaps in a shallow, partially enclosed basin with restricted current activity. Bioclastic limestones, and sparse sandy beds with parallel, wavy, ripple and low-angle crosslamination, indicate brief periods of stronger current action. Local instability is

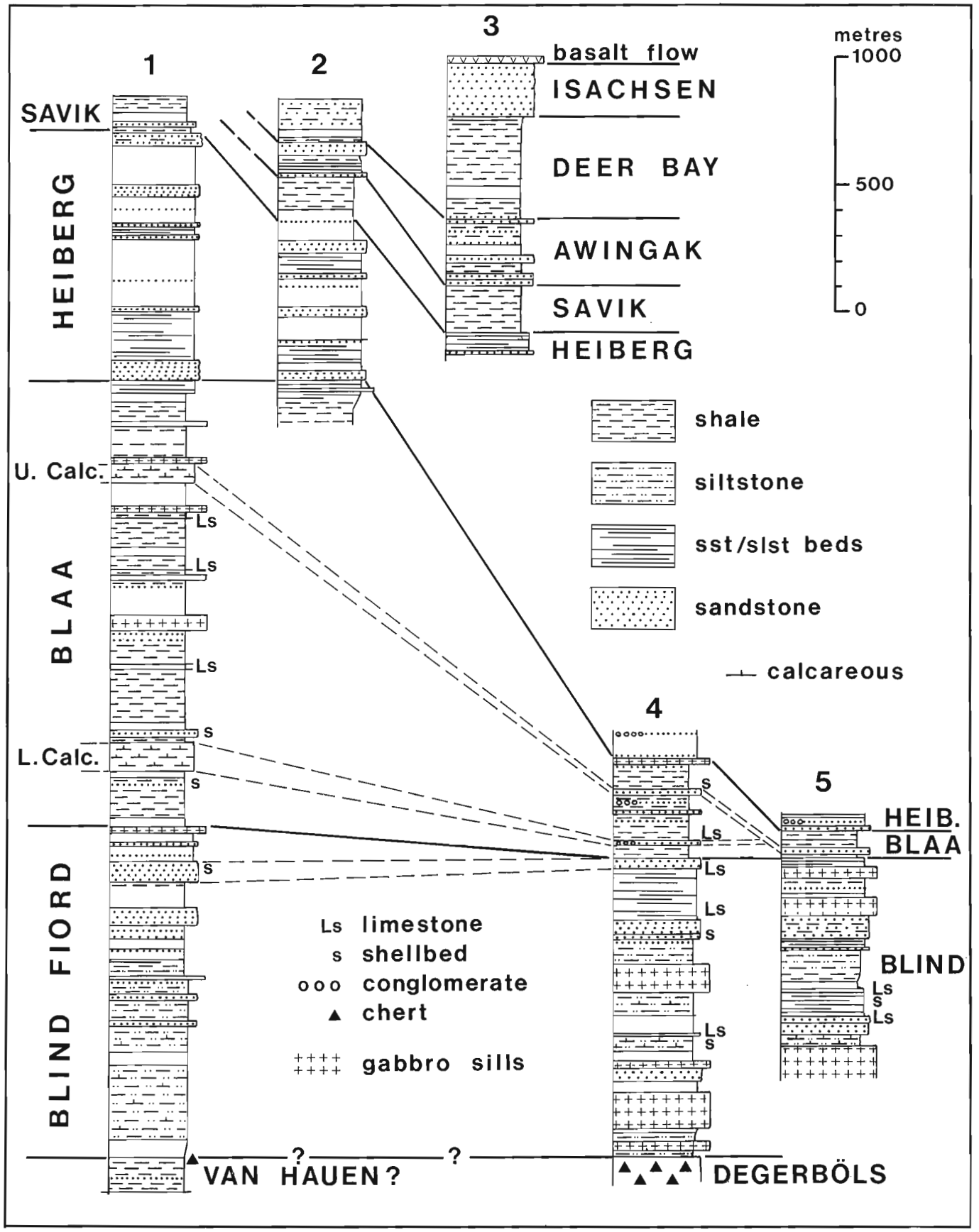

Figure 14.2. *Stratigraphic columns for Triassic to Lower Cretaceous formations. The location of measured sections is shown in Figure 14.1.*

reflected by the occurrence of large-scale intraformational(?) folds in the lower part of the formation, in the Blue Mountains section (although it is possible the folds result from ice-thrusting; see also Balkwill, in press, p. 30). Towards the basin margin, to the northeast, pebble bands appear and the sediments contain more sand, indicating proximity to the source area. The uppermost part of the formation, which is somewhat transitional into the partly nonmarine Heiberg Formation, was probably deposited in very shallow water, close inshore.

Heiberg Formation

Heiberg Formation consists primarily of quartzose fine sandstone, interbedded sandstone and shale, and minor coal. Two informal members have been recognized (Tozer, 1961): a lower, partly marine, thin bedded, sandstone and shale unit, and an upper, largely nonmarine member of thick, crossbedded sandstone and minor coal. Both members are present in the Blue Mountains, where the formation ranges from 640 m to 960 m thick (Sections 1 and 2, Fig. 14.2).

The lower 180 m of the formation is well-exposed in Section 1 and consists of at least three cyclic units of thick, crossbedded, quartzose sandstone together with thin bedded sandstone and shale. These are overlain by 100 m of thin bedded sandstone and minor black shale containing some thicker, fining-upward beds in the upper part. The first coal (2 cm thick) occurs 130 m above the base.

Scattered exposures in the upper part of the formation comprise thick, quartzose, fine sandstone beds with coaly laminae, thin bedded sandstone and shale, and a single, 3 m thick, coal seam. The upper 15-20 m is composed of three fining-upward quartzose sandstone beds, with black carbonaceous shale at the top of each cycle. These three beds are also present in Sections 2 and 3. In Section 3, 68 m of poorly bedded sandstone with ironstone bands, large pieces of wood and rare bivalves overlie the upper Heiberg cycles and have previously been mapped as Borden Island Formation (Tozer, 1963, p. 16; Thorsteinsson, 1971). In this paper these beds are included in Heiberg Formation because correlative beds from the uppermost part of the type section of the Heiberg Formation (A. Embry, personal communication, 1980).

The lower part of Heiberg Formation in the Hare Fiord section is similar to that in the Blue Mountains. A 2 m thick shelly conglomerate is a notable lithology observed in the lower Heiberg in the Krieger Mountains section.

The base of the formation is well-exposed in the Blue Mountains (Section 1), as shown in Figure 14.4. The contact is sharp, and underlying beds of the Blaa Mountain Formation appear to be slightly truncated. A similar, sharp contact is exposed in the Hare Fiord section. The upper contact is not well-exposed, although in Section 3 the lower Savik shale probably abruptly overlies the Heiberg.

Age

Heiberg Formation ranges in age from Norian (late Triassic) to Pliensbachian (early Jurassic) (A. Embry, personal communication, 1980). Further chronostratigraphic subdivision of the formation is not yet possible.

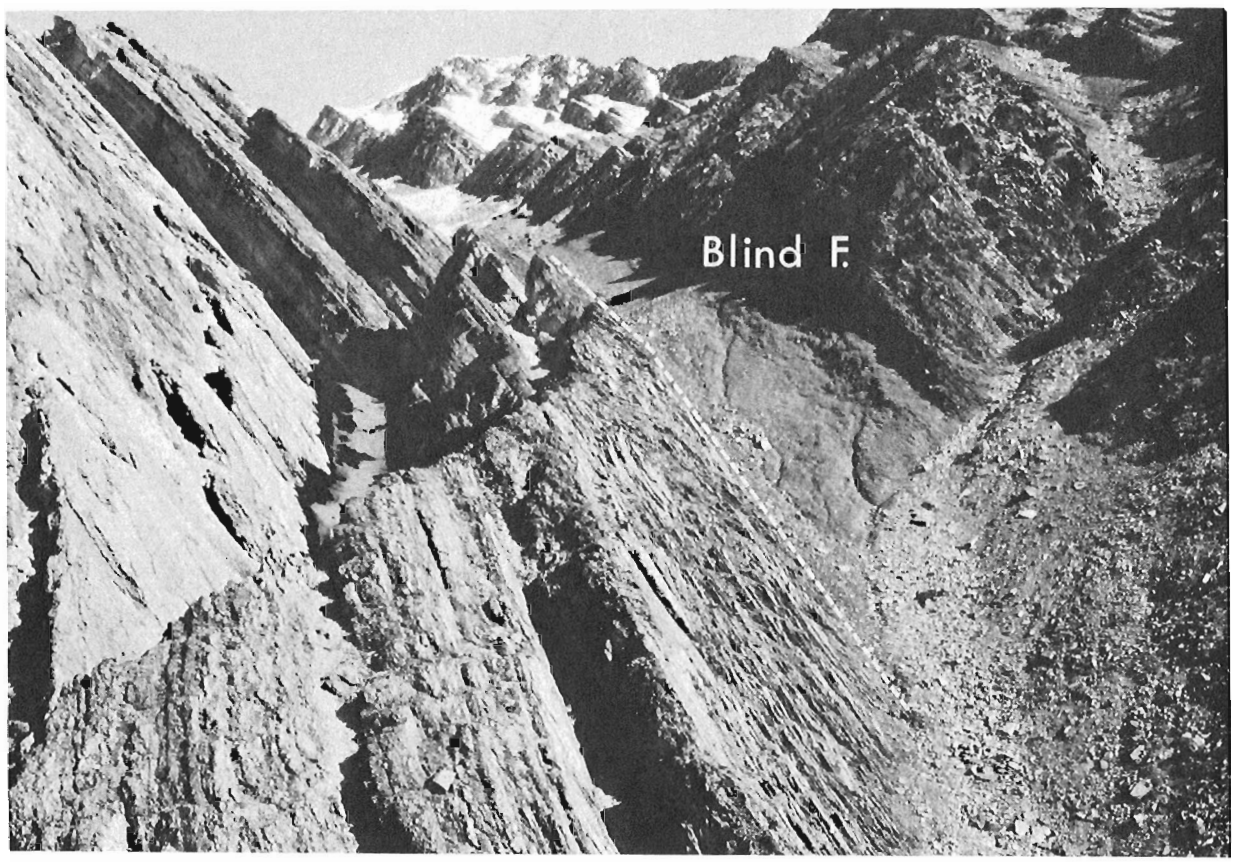

Figure 14.3. *Base of Blind Fiord Formation (Lower Triassic) in the Krieger Mountains. Contact between the basal Blind Fiord shale and underlying Degerböls Formation (Upper Permian) is abrupt, and probably disconformable.*

Environment of Deposition

As noted by Tozer (1961, p. 25) the lower member of the Heiberg is partly marine, although just how much of the sequence this represents is uncertain. At least the lower 60 m in Section 1 was probably deposited in a marine or marginal marine environment. The thick, strongly crossbedded quartzose sandstone beds could represent bar-finger or channel sands. The upper apart of the formation, containing thin coal beds, is probably mainly nonmarine. Poorly bedded, bioturbated carbonaceous sandstone in the upper 60 m contains sparse marine fossils and may have been deposited in somewhat stagnant, inner shelf environment.

Savik Formation

The formation was examined only in the Blue Mountains where it is 180-190 m thick. These measurements are consistent with the 600 feet (180 m) estimated by Tozer (1963, p. 22). Tozer (1963) divided the formation into three members – Lower Savik shale, Jaeger Member, and Upper Savik shale.

In the Blue Mountains (Sections 1-3, Fig. 14.2) the grey Lower Savik shale is poorly exposed, and no more than 10 to 20 m thick. The Jaeger sandstone, which is only 1 to 3 m thick, provides a useful marker between the Lower and Upper shales. In Section 2 the Jaeger consists of moderately hard, highly bioturbated, glauconitic, fine sandstone with belemnite moulds. The overlying Upper Savik shale is soft, sandy and black to dark grey-brown. It contains a few thin, poorly bedded sandstone beds and lenses, particularly in the upper part, concretionary bands, "hedgehogs" (Kemper and Schmitz, 1975), and some large petrified logs. Sedimentary dykes occur in the lower part of the shale in Section 1.

The basal contact with Heiberg Formation, as noted earlier, appears to be abrupt. In Section 3 a sharp contact between light grey shale and a prominent ironstone bed may represent the base of the formation. The top of the formation is taken at the base of the lowest, thick quartzose sandstone of the overlying Awingak Formation. The contact appears transitional.

Age

Savik Formation ranges from Toarcian to Lower Oxfordian (Lower to Upper Jurassic) in age (Tozer, 1963). Specimens of **Inoceramus (Petroceramus)** sp. collected from the lower part of the Upper Savik (C82116, C82911) indicate a Lower Bajocian to Callovian age for the middle of the formation (T.P. Poulton, personal communication, 1980). A Bathonian age, in part, for the Upper Savik is therefore a possibility.

Environment of Deposition

The nature of the Jaeger Member and Upper Savik shale suggest deposition in moderately shallow water, perhaps inner shelf. "Hedgehogs" or calcitic "euhedral aggregates" are considered to be indicative of cold water (Kemper and Schmitz, 1975) and imply that generally cool conditions existed during deposition of the Upper Savik shale.

Awingak Formation

The Awingak consists of interbedded thick, quartzose, fine to medium sandstone and black shale. In the Blue Mountains thickness ranges from a minimum 130 m (Section 2) to 260 m (Section 3).

Figure 14.4. *Sharp (unconformable?) contact between Blaa Mountain Formation (left) and overlying Heiberg Formation in the Blue Mountains (Section 1). Note the cyclic nature of sandstone (light coloured) and shaly beds (dark) in lower part of the Heiberg.*

Approximately half of Awingak Formation consists of quartzose sandstone beds up to 40 m thick which are cross-bedded, highly bioturbated, and contain wood fragments, coaly laminae, and sparse marine(?) bivalves. A distinctive feature of these sandstones is the huge "pillow" concretions, forming all or part of a bed. Intervening shales are black, sandy, and contain concretionary bands.

The base of the formation appears gradational into the underlying Upper Savik shale; no clear contact was observed. The upper boundary with Deer Bay Formation is drawn at the highest thick sandstone, and in both measured sections this is a prominent "pillow" concretionary bed containing the bivalve **Camptonectes (Boretonectes)** sp. cf. **C. (B) praecinctus** Spath (T.P. Poulton, personal communication, 1980).

Age

Fossils collected in the Blue Mountains sections have been assigned an Upper Oxfordian – Lower Kimmeridgian age for the lower part of the formation, and a Lower Volgian age for the uppermost sandstone (T.P. Poulton, personal communication, 1980). This age range agrees with that established by Tozer (1963).

Environment of Deposition

Despite the occurrence of coaly laminae in some sandstones, much of the Awingak is interpreted as marine, though probably marginal marine. No undoubtedly terrestrial beds were identified. Several of the thick sandstone beds are extensively bioturbated and contain poorly preserved bivalves, including **Camptonectes** sp.

Deer Bay Formation

In the Blue Mountains (Section 3), Deer Bay Formation consists of 400 m of black sandy shale with some sandy beds and scattered concretions. "Hedgehogs" (Kemper and Schmitz, 1975) occur in the upper part. The basal sediments are sandy and contain thin quartzose beds, suggesting a transitional boundary with the underlying Awingak. The upper contact with Isachsen Formation is well-exposed in this section and is also clearly transitional. Black, sandy micaceous shale, containing patches of small bivalves, including specimens of **Pinna** sp. in life position, becomes increasingly sandy upward and passes into a zone (10 m thick) of wavy and ripple-laminated fine sandstone with thin interbeds of black shale. A highly quartzose, coarse, gritty, crossbedded sandstone on top of this zone marks the base of the overlying Isachsen.

Age

The formation is well-dated and ranges from Portlandian (Upper Volgian) to Upper Valanginian (Tozer, 1960; Kemper, 1975). Much of the Berriasian, however, may be missing in the Blue Mountains section (cf. Kemper, 1975, Fig. 2).

Environment of Deposition

The bulk of Deer Bay Formation was most likely deposited in an open marine, shelf environment. Sandy beds near the top of the formation represent a shallowing, and were probably deposited under near-shore, subtidal conditions. According to Kemper (1975) the occurrence of "hedgehogs" in the Valanginian part of the Deer Bay is indicative of cold water.

Isachsen Formation

A well-exposed section through Isachsen Formation is present in the Blue Mountains (Section 3). Here the formation, about 200 m thick, consists predominantly of fine to coarse, highly quartzose sandstone with minor shale and thin coal beds. Some sandstones, particularly higher in the section, are strongly crossbedded and contain quartz pebbles up to 1-2 cm diameter. Channelling and ripple marks were also observed.

The lower boundary of the formation, as noted earlier, is taken at the base of a 1 m thick, crossbedded coarse quartzose sandstone overlying transitional Deer Bay beds. The upper contact, with a 20 m thick subaerial basalt flow is probably disconformable.

Twenty-five kilometres to the southeast, in a section on the east limb of the Troelsen Anticline, near Atwood Point, the Isachsen is only 110 m thick, and finer grained. There is a coarsening upward of the underlying Deer Bay Formation and abrupt contact with thick, quartzose sandstone of the Isachsen. Basalt is absent in this section, and Isachsen Formation is overlain directly by soft sandy shale of Christopher Formation.

Age

The formation ranges from Upper Valanginian to Aptian (Tozer, 1963; Thorsteinsson and Tozer, 1976).

Environment of Deposition

The large scale crossbedding, coal beds and coarse nature of Isachsen sediments suggest that a large part of the formation was deposited in a fluviolacustrine environment. Coal beds are more common and thicker in the upper part, and there is an overall coarsening upward of the sequence, presumably indicating infilling of the basin. A soil horizon is developed at the top of the formation, beneath the overlying basalt flow.

Conclusions

Detailed study of well-exposed Mesozoic sections in the Blue Mountains and Krieger Mountains has largely confirmed the established stratigraphic framework. At the same time, some significant features of the succession have been revealed, the most notable of which are:

1. A coarsening upward, and marked eastward shallowing and thinning of Blind Fiord Formation.
2. Very rapid thinning of Blaa Mountain Formation to the northeast, particularly of the Middle Shale member, accompanied by a facies change.
3. A sharp contact, probably a low-angle unconformity, at the base of Heiberg Formation.
4. Evidence of cold water conditions during deposition of upper Savik Formation (Mid-Upper Jurassic).
5. Deposition of a large part of Awingak Formation in a marine and marginal marine environment.
6. A transitional marine facies in the upper part of Deer Bay Formation and sharp contact with the overlying, nonmarine Isachsen Formation at the top of this transitional facies.
7. Confirmation of the subaerial nature of a basalt flow locally overlying the Isachsen.

Acknowledgments

I am grateful to A.F. Embry and to D.F. Stott, for the opportunity to study Mesozoic sections on Ellesmere Island. L. Heerze and C. Henderson assisted in the field, and T.P. Poulton identified macrofossils. The manuscript benefited from information and advice provided by A.F. Embry.

References

Balkwill, H.R.
1978: Evolution of Sverdrup Basin, Arctic Canada; American Association of Petroleum Geologists Bulletin, v. 62, p. 1004-1028.

Geology of Amund Ringnes, Cornwall, and Haig-Thomas Islands, District of Franklin (parts 59 C, 59 F, 69 D, 69 E); Geological Survey of Canada, Memoir 390. (in press)

Kemper, E.
1975: Upper Deer Bay Formation (Berriasian-Valanginian) of Sverdrup Basin and biostratigraphy of the Arctic Valanginian; in Current Research Part B, Geological Survey of Canada, Paper 75-1B.

Kemper, E. and Schmitz, H.H.
1975: Stellate nodules form the upper Deer Bay Formation (Valanginian) of Arctic Canada; in Current Research part C, Geological Survey of Canada, Paper 75-1C.

Kerr, J.W.
Evolution of the Canadian Arctic Islands – a transition between the Atlantic and Arctic Oceans in The Ocean Basins and Margins, Plenum Press Publishing Co. (in press)

Thorsteinsson, R.
1971: Greely Fiord West; Geological Survey of Canada, Map 1311A.

Thorsteinsson, R. and Tozer, E.T.
1970: Geology of the Arctic Archipelago in Geology and Economic Minerals of Canada, 5th ed. (R.J.W. Douglas, ed.), Geological Survey of Canada, Economic Geology Report 1, p. 548-590.

Thorsteinsson, R. and Trettin, H.P.
1972: Otto Fiord; Geological Survey of Canada, Map 1309A.

Tozer, E.T.
1960: Summary account of Mesozoic and Tertiary stratigraphy, Canadian Arctic Archipelago; Geological Survey of Canada, Paper 60-5.

1961: Triassic stratigraphy and faunas, Queen Elizabeth Islands, Arctic Archipelago; Geological Survey of Canada, Memoir 316.

1963: Mesozoic and Tertiary stratigraphy, western Ellesmere Island and Axel Heiberg Island, District of Franklin; Geological Survey of Canada, Paper 63-30.

15.

A TENNANTITE DEPOSIT IN THE M'CLINTOCK INLET AREA, NORTHERN ELLESMERE ISLAND, DISTRICT OF FRANKLIN

Project 730051

H.P. Trettin
Institute of Sedimentary and Petroleum Geology, Calgary

Trettin, H.P., A Tennantite deposit in the M'Clintock Inlet area, northern Ellesmere Island, District of Franklin; in Current Research, Part A, Geological Survey of Canada, Paper 81-1A, p. 103-106, 1981.

Abstract

A replacement deposit of zincian tennantite east of M'Clintock Inlet is the first reported metallic mineral deposit in the eugeosynclinal terrane of the Innuitian Orogen. It is too small to be of economic value but could serve as a guide for exploration. Significant features appear to be (1) occurrence in an Upper Ordovician shelf dolostone, deposited fairly close to the northwestern margin of the Hazen Trough, and (2) proximity to a repeatedly active fault zone that locally contains ophiolite slices.

Introduction

A small tennantite deposit found 30 km due east of an unnamed bay on upper M'Clintock Inlet (Fig. 15.1, 15.5) at 73°20' West, 82°37.3' North (NTS 340 E; UTM zone 18X, 9174400 N, 524000 E) is the first reported occurrence of that mineral in the Arctic Islands and the first reported metallic mineral deposit in the eugeosynclinal belt of the Innuitian Orogen. The discovery was made on the afternoon of the last day of field work of the 1980 season, a season intended to complete the geological reconnaissance of northern Ellesmere Island, and only four hours could be spent in the vicinity of the deposit. More detailed work is desirable to check the local geology and search for other deposits but was not feasible at the time.

I am indebted to pilot B. Russel of Okanagan Helicopters; to B.S. Norford for the fossil identifications; to A.G. Heinrich (Calgary) and A.G. Plant (Ottawa) for mineral analyses; and to A.V. Okulitch for critical reading of the manuscript.

Areal Geology

The geology shown in Figure 15.2 is based on three short traverses (dotted lines a, b, c), airphoto interpretation, and widely spaced foot traverses and helicopter landings in adjacent areas.

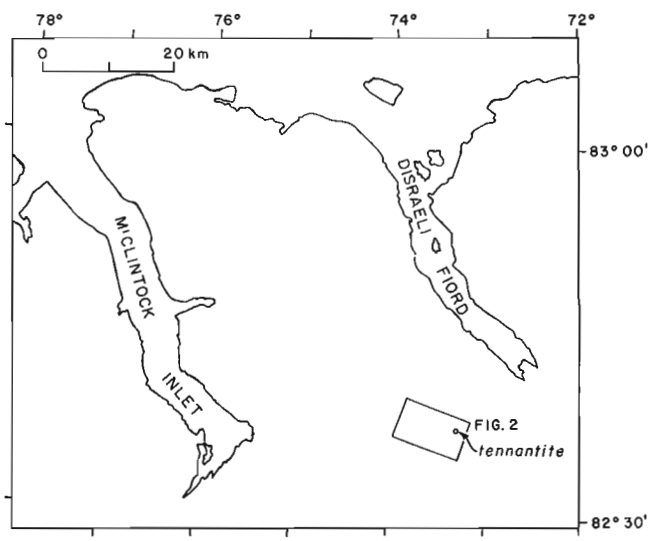

Figure 15.1. *Index map.*

Stratigraphy

Six major units are distinguished in Figure 15.2. Although several are identical with established formations they are here referred to as numbered map-units. Comprehensive reports on the very complex lower and upper Paleozoic stratigraphy of the region are presently being prepared by the writer and U. Mayr, respectively.

Map unit 1 is composed of compositionally immature sandstone, mudrock[1] and lesser amounts of granule to boulder conglomerate and carbonate rocks. The clastic sediments are red, green and grey. Fossil collections from other parts of the M'Clintock Inlet area indicate a Late Ordovician (Ashgillian) age. The unit probably is identical with the Taconite River Formation established west of M'Clintock Inlet (Trettin, 1969). At the head of M'Clintock Inlet it overlies Proterozoic metamorphic rocks with angular unconformity but farther north it lies on the Ordovician M'Clintock and Ayles formations. Its thickness varies from less than 10 m at the head of M'Clintock Inlet to probably thousands of metres in the present area but could not be established here because of structural complexities. The unit appears to be mainly shallow marine in origin with some nonmarine sediments.

Map unit 2 overlies map unit 1 with conformable contact, but the contact is not exposed in this area. The unit consists of variable proportions of limestone and dolostone, locally with some sandstone, mudrock, and granule to pebble conglomerate. The area containing the mineral deposit is underlain mainly by dolostone with less abundant dolomitic limestone. The limestones contain a diverse and fairly abundant benthonic fauna of Late Ordovician (Ashgillian) age. Fossils collected from talus at three localities along traverse b (Fig. 15.2) include **Catenipora** sp., **Paleophyllum** sp., ?**Austinella** sp., **Dicoelosia** sp., ?**Lepidocyclus** sp., aff. **Rhynobulus** sp., ?**Maclurites** sp., along with strophomenid, sowerbyellid and orthid brachiopods and unidentified gastropods, pelecypods, bryozoans, echinoderms, etc. The unit is identical with Members A and B of the original Zebra Cliffs Formation (Trettin, 1969), the original Member C now being regarded as a tongue of the upper Hazen Formation (Trettin and Balkwill, 1979). Lithology and fauna indicate predominantly subtidal shelf environments of deposition.

The overlying map unit 3 consists of compositionally immature sandstone and mudrock with small amounts of granule and pebble conglomerate and limestone. Most clastic rocks are conspicuously red, but green and grey strata also are common. East of the head of M'Clintock Inlet, map unit 3 overlies map unit 2 with low angular unconformity.

[1] The term mudrock is used here for all silt and clay-grade clastic sediments containing less than 50 per cent carbonate minerals. Some are fissile and most relatively fine grained rocks have a slaty cleavage.

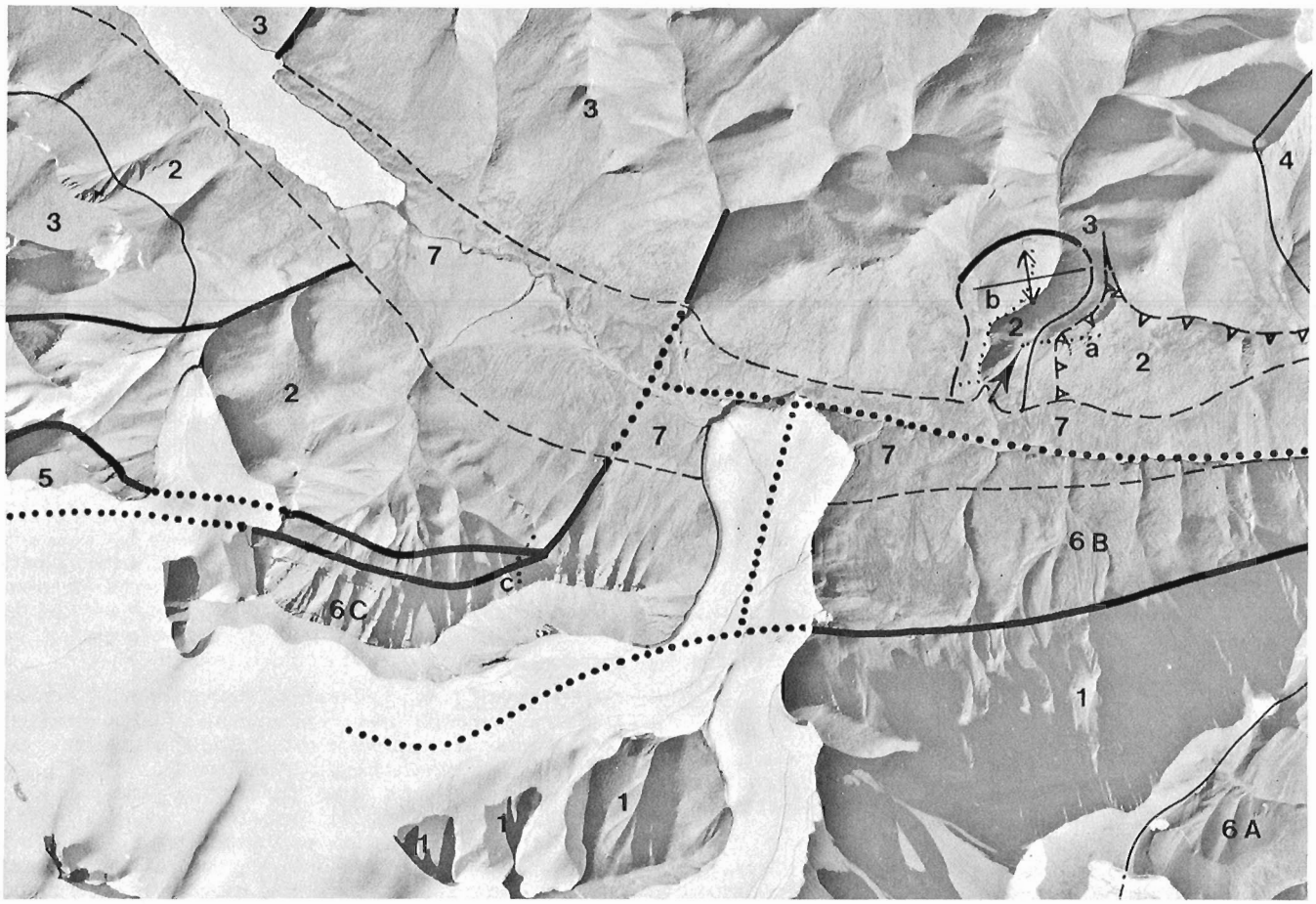

7 QUATERNARY
unconsolidated sediments (obscuring bedrock geology)

6C PENNSYLVANIAN AND/OR PERMIAN
dolostone

6B gypsum-anhydrite, clastic sediments, carbonate rocks (?) (not examined on the ground)

6A PENNSYLVANIAN
sandstone, conglomerate; minor dolostone

5 LOWER DEVONIAN OR OLDER
stratified igneous complex, ultramafic to granitic

4 UPPER ORDOVICIAN AND/OR SILURIAN
conglomerate, sandstone; minor mudrock

3 UPPER ORDOVICIAN
sandstone, mudrock; minor conglomerate, limestone

2 dolostone, limestone; locally minor sandstone, conglomerate, mudrock

1 sandstone, mudrock; minor conglomerate, carbonate rocks

Geological boundary (located, approximate, projected through ice)

Fault (located, projected through ice or overburden)

Probable thrust fault (teeth on hanging wall)

Anticline

b Foot traverse

Figure 15.2. *Geology in the vicinity of mineral deposit; deposit is at tip of arrow. (Part of vertical air photograph A-16708-14).*

The hiatus, however, must be small because benthonic fossils in this unit also are Late Ordovician (Ashgillian) in age. In the present area the contact relationships are uncertain. The sediments appear to be mainly or entirely of shallow marine origin. Map unit 3 is overlain at some localities by map unit 4 and at others by the Upper Silurian (Ludlovian) Marvin Formation. Both contacts probably are disconformable. Southeast of the head of Disraeli Fiord, where map unit 3 is overlain by the Marvin Formation, it has a thickness of about 770 m.

Map unit 4, composed mainly of resistant granule to pebble conglomerate and compositionally immature sandstone with lesser amounts of mudrock has been examined only at a few localities. The conglomerate beds appeared to be of nonmarine (braided river?) origin. It is tentatively regarded as latest Ordovician and/or Early Silurian in age.

Map unit 5 is a tabular body of stratified igneous rocks ranging in composition from ultramafic to granitic. It dips south and lies between map units 2 and 6C. Both contacts are covered but interpreted as faults. Three sets of samples collected along traverse c (Fig. 15.2) from south to north (i.e. structurally from top to bottom) represent (1) slightly serpentinized clinopyroxenite; (2) hornblende-rich diorite with coarse phenocrysts of hornblende; and (3) fine grained, leucocratic granitic rocks that are sheared, altered, and partly metamorphosed in the greenschist facies. The compositional trend is opposite to that normally observed in layered intrusions, suggesting that the body is overturned; it also appears to be incomplete on the ultramafic (south) side. The present body lies on strike with the M'Clintock East ultramafic massif (Frisch, 1974) from which it is separated by a glacier and volcanic rocks. Petrology and structural setting

suggest that both are fault slices derived from the cumulate part of an ophiolite (cf. Coleman, 1977). Both probably are related in age, origin, and structural setting to the larger M'Clintock West massif, which is unconformably overlain by middle Pennsylvanian strata and has a K/Ar (hornblende) age of 390 ± 20 Ma (Trettin, 1969; Frisch, 1974). All three igneous bodies are regarded as Early Devonian or older in age.

Three upper Paleozoic units occur as separate fault blocks in the southern part of the area. The oldest (map unit 6A), composed mainly of sandstone and conglomerate with some dolostone, overlies map unit 1 with angular unconformity and probably is early or middle Pennsylvanian in age. The age of the other two, composed of gypsum-anhydrite with clastic and (?) carbonate sediments (map unit 6B, not examined on the ground) and dolostone (map unit 6C) respectively, has not yet been determined but probably also is Pennsylvanian (U. Mayr, personal communication, 1980).

Structure

The lower Paleozoic strata are involved in complex and tight folds, which are better exposed immediately to the east than in the present area. The upper Paleozoic strata are faulted and tilted but not folded.

The most significant structural feature of the present area is the fault that separates map units 6B and 6C in the south from map units 2 and 3 in the north. It generally trends westerly, but is offset by poorly exposed, north-trending faults in the vicinity of the mineral deposit. The western branch of the fault bifurcates and encloses between its two branches the igneous rocks of map unit 5. If this ophiolite slice was tectonically emplaced in pre-Middle Pennsylvanian time (as inferred for the M'Clintock West massif) then the fault zone must have had at least two major phases of movement in pre-and post-Pennsylvanian times, respectively.

The Tennantite Deposit

The mineral deposit occurs on the southern limb of a west-trending asymmetrical anticline, in the upper part of map unit 2, close to the contact with map unit 3. The clastic strata of that unit are overlain by another set of dolomitic carbonate rocks, interpreted as a thrust slice of map unit 2.

The surface area of the deposit, perhaps 10 m to a few tens of metres in diameter, is strewn with fragments of dolostone weathered in place that contain scattered crystals, or lumps of crystals, of tennantite, surrounded by haloes of malachite and minor azurite. The tennantite content of the specimens collected varies from trace amounts to an estimated 5-10 per cent by volume. The crystals are euhedral, mostly tetrahedral in habit (Fig. 15.3), and vary in edge length from 0.7 mm to about 3 cm.

Semiquantitative X-ray fluorescence analysis by A.G. Heinrich revealed the following composition:

major elements (>2%)	minor elements (0.1 - 2%)	trace elements (<0.1%)
Sb	Ca	Ag
As	Al	Cd
Zn		
Cu		
Fe		
S		

As is considerably more abundant than Sb, and Zn is fairly common.

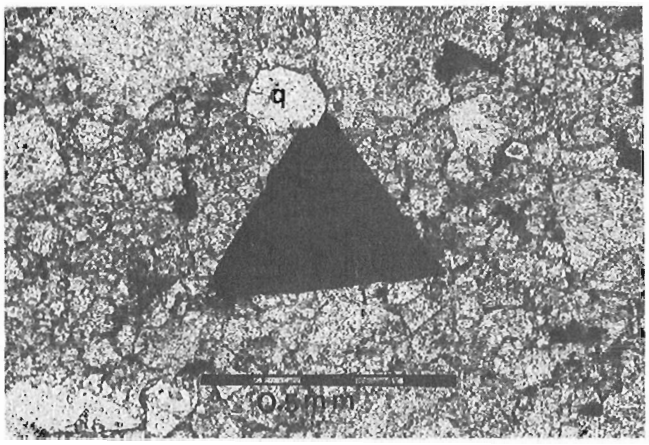

Figure 15.3. *Tennantite (dark) in matrix of dolomite and quartz (q) displays characteristic tetrahedral habit; photomicrograph, ordinary light.*

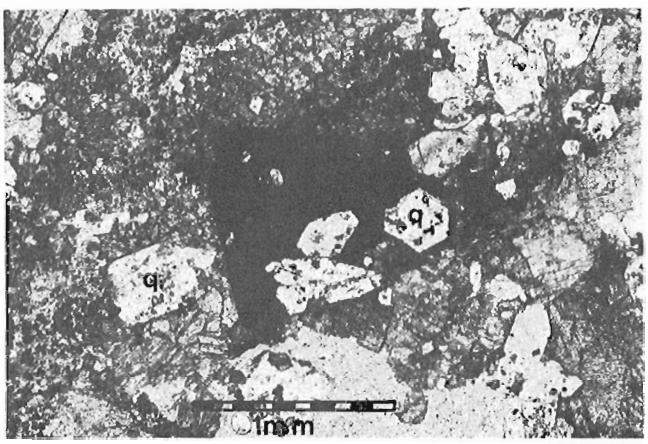

Figure 15.4. *Tennantite (dark) with inclusions of quartz (q), which contain inclusions of dolomite (very small dark rhombs); photomicrograph, ordinary light.*

The host rock of the tennantite is dolomite, ranging in crystal size approximately from 0.01 to 1.6 mm, with coarser crystals present in veinlets. The micritic texture of the limestone predecessor is apparent under crossed nicol prisms in the extinction position. Organic matter is concentrated in small, irregular solution zones. Scattered euhedral quartz crystals, about 0.08-1.44 mm long with very small inclusions of euhedral dolomite, make up perhaps 10-15 per cent of the rock. Such quartz is absent from normal dolostone of map unit 2 in this area and evidently related to the metallic mineralization. The tennantite has replaced the dolomite but not the quartz, which impinges on it (Fig. 15.3) or forms inclusions (Fig. 15.4). The paragenesis, therefore, is (1) calcite, (2) dolomite, (3) quartz, (4) tennantite.

Discussion

The eugeosynclinal belt of the Innuitian Orogen, exposed in northern Ellesmere and Axel Heiberg islands, has the ingredients for a variety of mineral deposits – siliceous to mafic volcanic rocks, granitic to ultramafic intrusions, various types of carbonate and clastic sediments, unconformities, and innumerable faults. That mineral deposits have not been found earlier in the region reflects the

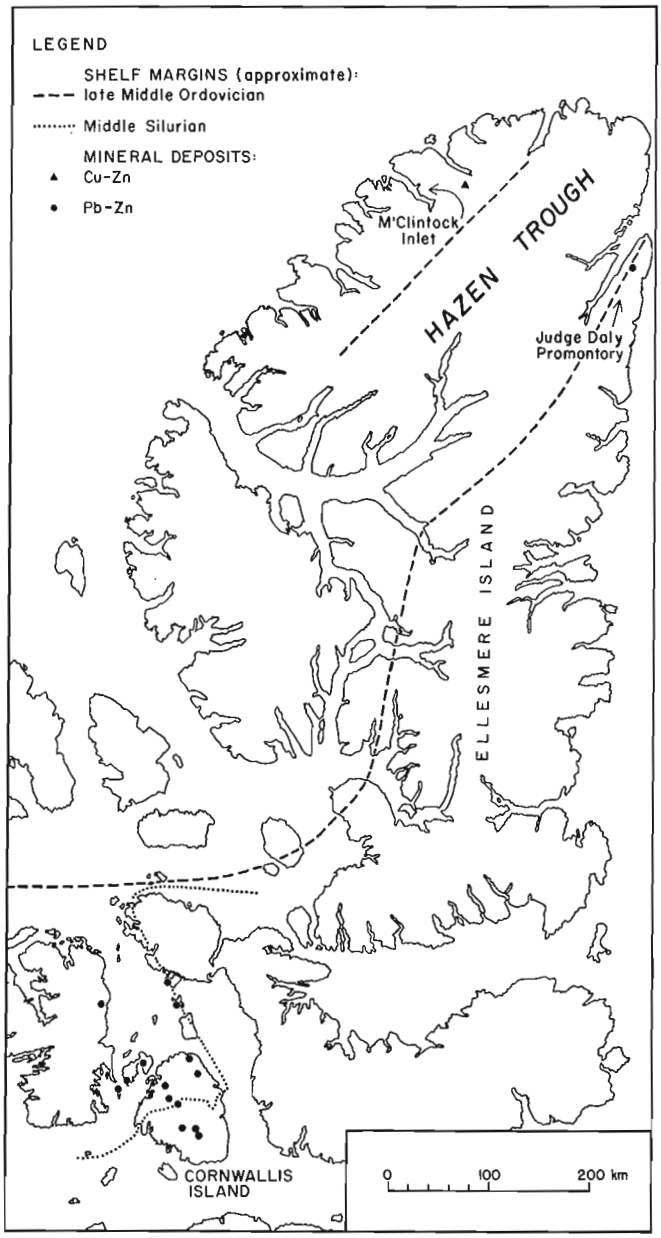

Figure 15.5. *Mineral deposits in eastern Queen Elizabeth Islands and their relationship with Hazen Trough. For outcrop control see Trettin and Balkwill, 1979, Fig. 4, 5. Mineral deposits of Cornwallis region after Kerr, 1977, Fig. 1.*

reconnaissance nature of the geological work and the lack of prospecting. This lack, of course, is due to the poor accessibility of this belt, which is flanked by the permanent ice pack of the Arctic Ocean on the northwest, and major mountain ranges on the southeast. These logistic and economic handicaps, however, are ignored in the following discussion in view of probable increases in metal demand and possible advances in Arctic exploration and exploitation technology.

The present deposit is too small to be of economic value but could be used as a guide for initial exploration. Two characteristics may be significant:

1. It occurs in a dolomitized shelf carbonate unit of Late Ordovician age, deposited probably fairly close to the northwestern margin of the Hazen Trough during the later part of the Ordovician (Fig. 15.5). It is interesting to note that the major deposits of the Cornwallis Pb-Zn district, which occur in the upper Middle Ordovician Thumb Mountain Formation (Kerr, 1977), occupy a comparable position on the southeastern margin of the Hazen Trough (if the southeastward migration of the trough margin is taken into consideration). The same applies to a small Pb-Zn deposit on northeastern Judge Daly Promontory (Fig. 15.5), presently owned by Norcen Energy Resources Limited and examined by the writer in 1980. It occurs in dolostone of the lower Copes Bay Formation (latest Cambrian to earliest Ordovician), less than 10 km southeast of the early Ordovician shelf margin. Connate waters, expelled from organic carbon-rich pelitic sediments of the Hazen Trough are a possible source for base metal deposits in both adjacent shelf areas (cf. Jackson and Beales, 1967). This hypothesis, however, seems more appropriate for the deposits of the southeastern shelf, which are far from any known igneous source than for the present deposit. The difference in mineralogy – galena and sphalerite in the Cornwallis district and on Judge Daly Promontory versus tennantite in the present area – also suggests a different origin.
2. The deposit is close to a major fault zone that locally contains ophiolite slices and appears to have been active repeatedly. It could have been an avenue of migration for fluids derived from various igneous or sedimentary sources.

In summary, initial prospecting could focus on (a) Ordovician shelf carbonate deposits such as the Zebra Cliffs Formation (original Members A and B) or Member B of the Cape Discovery Formation; and (b) on the present fault zone or comparable major fault zones involving ophiolite slices. Finally, it would be worthwhile investigating whether the unconformity between map units 2 and 3, seen east of the head of M'Clintock Inlet, extends into the present area and whether or not any mineralization may be associated with it.

References

Coleman, R.G.
1977: Ophiolites. Ancient lithosphere?; Springer Verlag, Berlin, Heidelberg, New York, 229 p.

Frisch, T.O.
1974: Metamorphic and plutonic rocks of northernmost Ellesmere Island, Canadian Arctic Archipelago; Geological Survey of Canada, Bulletin 229.

Jackson, S.A., and Beales, F.W.
1967: An aspect of sedimentary basin evolution: the concentration of Mississippi Valley-type ores during late stages of diagenesis; Bulletin of Canadian Petroleum Geology, v. 15, p. 383-433.

Kerr, J.Wm.
1977: Cornwallis Lead-Zinc District; Mississippi Valley-type deposits controlled by stratigraphy and tectonics; Canadian Journal of Earth Sciences, v. 14, p. 1402-1426.

Trettin, H.P.
1969: Geology of Ordovician to Pennsylvanian rocks, M'Clintock Inlet, north coast of Ellesmere Island, Canadian Arctic Archipelago; Geological Survey of Canada, Bulletin 183.

Trettin, H.P. and Balkwill, H.R.
1979: Contributions to the tectonic history of the Innuitian Province, Arctic Canada; Canadian Journal of Earth Sciences, v. 16, p. 748-769.

16.

THE EARLY TO MIDDLE DEVONIAN BEAR ROCK FORMATION IN THE TYPE SECTION AND IN OTHER SURFACE SECTIONS, DISTRICT OF MACKENZIE

Project 750085

D.W. Morrow and N.C. Meijer-Drees
Institute of Sedimentary and Petroleum Geology, Calgary

Morrow, D.W. and Meijer-Drees, N.C., The Early to Middle Devonian Bear Rock Formation in the type section and in other surface sections, District of Mackenzie; in Current Research, Part A, Geological Survey of Canada, Paper 81-1A, p. 107-114, 1981.

Abstract

Exposures of the Devonian Bear Rock Formation in the Franklin Mountains, including the type section at Bear Rock near Fort Norman, that were examined during Operation Canol, have been re-examined in more detail. The Bear Rock Formation at the type section is composed of a lower brecciated interval 154.0 m thick and an upper, incompletely exposed interval of bedded, nonbrecciated and unfossiliferous limestone. This upper interval was not mentioned in previous reports but appears to be the surface counterpart of the upper pellet limestone member of the Gossage Formation mapped in the adjacent subsurface and also of the Landry Formation mapped in the Mackenzie Mountains.

An intermediate stage in the solution-collapse origin of the Bear Rock breccias was observed north of Great Bear River where mosaic breccias of angular greyish brown dolomite fragments are cemented with coarsely crystalline white gypsum. A new threefold classification of breccia fabrics developed for this study aided in the description of the Bear Rock breccia.

Introduction

The Bear Rock Formation has been the object of comprehensive subsurface investigations near the type area around Fort Norman (e.g. Tassonyi, 1969). But the surface exposures along the Franklin Mountains, including the type area at Bear Rock, have not been examined in as much detail as the subsurface. Correlation between the surface and subsurface Bear Rock strata is hampered because of the lack of requisite detail in the existing descriptions of the Bear Rock surface sections. The main sources of published data concerning surface exposures are the unpublished reports of the Canol Project (e.g. Stelck, 1944) which were summarized by Hume and Link (1945) and later by Hume (1954). Other data pertaining to surface exposures of Bear Rock strata in the Franklin Mountains is contained in Bassett (1961).

In this report we provide some detailed descriptions of the type section and sections from a few surrounding localities (Fig. 16.1). Correlations between the Bear Rock in these surface sections and in the subsurface are described and some problems of stratigraphic nomenclature involving the Bear Rock interval are discussed, particularly with regard to the type section. Regional variations in the lithology of the Bear Rock Formation and the origin of the Bear Rock breccias are also briefly discussed. In addition, we propose a purely descriptive classification of breccia fabrics which we found useful in describing the Bear Rock breccias.

The data for this report were gathered between September 2 and 8, 1980 while the authors were based at Norman Wells, N.W.T. Transportation to the localities studied was provided by a Bell 206B Jet Ranger piloted by Lee Sexsmith of Okanagan Helicopters Ltd. based in Norman Wells.

The Type Section of the Bear Rock Formation at Bear Rock, N.W.T.

History of Nomenclature

The term Bear Rock was applied by Hume and Link (1945) and Hume (1954) to strata which were described previously by Stelck (1944) in an unpublished report submitted to the Government of Canada as part of the Canol Project. Hume (ibid.) based his description of the Bear Rock Formation at the type section on Stelck's measured section across Bear Rock at the junction of the Mackenzie and Great Bear rivers (Fig. 16.1). Stelck (1944) and Hume and Link (1945) regarded the Bear Rock Formation as resting disconformably on underlying Silurian strata of the Ronning Group, a view that has come to be generally accepted (e.g. Aitken and Cook, 1974), and to be conformably overlain by limestones of the Ramparts Formation.

Hume and Link (1945) and Hume (1954, p. 20-22) described the Bear Rock Formation as being almost entirely composed of limestone and dolomite breccia containing little or no bedded strata. They defined the upper contact of the Bear Rock to occur precisely where brecciated strata passes upward to bedded, nonbrecciated strata of their overlying Ramparts Formation. In a later report, Bassett (1961) renamed the three members of the Ramparts Formation, and

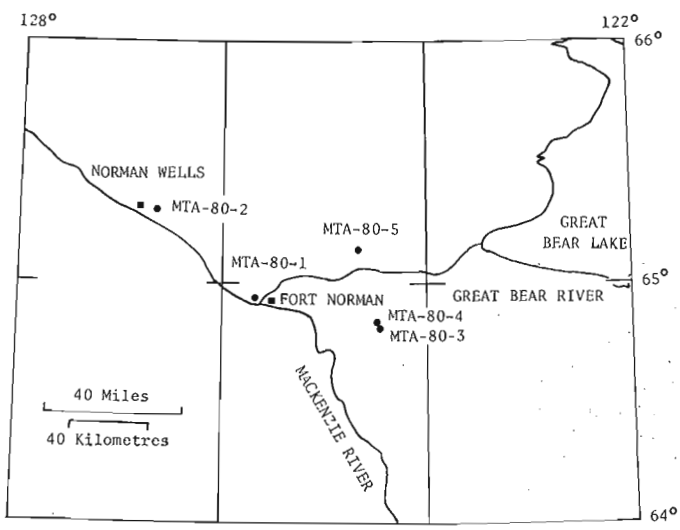

Figure 16.1. *Location map of the area west of Great Bear Lake and east of the Mackenzie Mountains showing the location of Bear Rock Sections (MTA-80-1, 2, 3 and 4) and places where Bear Rock strata were examined (MTA-80-5).*

Figure 16.2. *Type section of the Bear Rock Formation. The original type section description is shown for comparison. The legend shown here applies also to the other measured sections.*

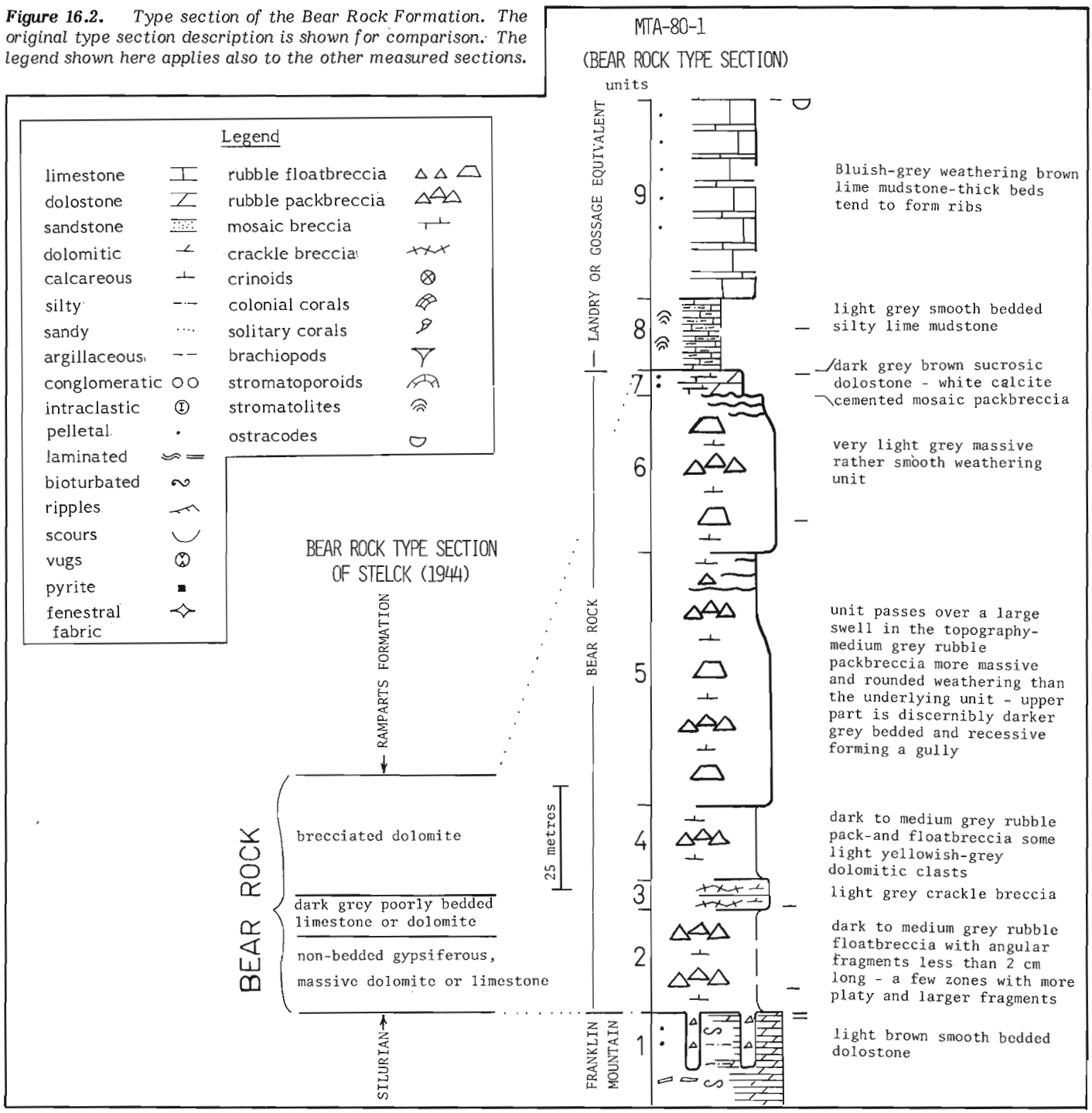

applied the name Hume Formation to the lowermost member directly overlying the Bear Rock Formation, both in, and around the Norman Wells area and throughout the central Mackenzie District. Bassett (1961) was the first to recognize that much of the Bear Rock Formation mapped by Hume and Link (1945) and Hume (1954) is not breccia but is, instead bedded limestone containing only small amounts of breccia. He pointed out the difficulty in determining the upper contact of the Bear Rock Formation, as distinct from the Bear Rock breccia, in those places where "the upper Bear Rock beds are composed of bedded limestone" (Bassett, 1961, p. 484). The fact that the Bear Rock Formation is not coincident with the Bear Rock breccias has led to inconsistencies in the stratigraphic nomenclature of this sequence.

Geological Setting

Stelck's original description of the type section of the Bear Rock Formation at Bear Rock is reproduced alongside our measured section in Figure 16.2. The brecciated Bear Rock strata of Stelck's section are underlain disconformably by thin bedded Silurian limestones and are overlain by shaly and fossiliferous limestones of the Ramparts Formation, the lower part of which has been renamed the Hume Formation. The beds in the type section dip ~30 to 60 degrees northwest and are exposed in the hanging wall of a west-dipping thrust fault that has formed a broad north-trending hump in the topography (Fig. 16.3). The line of section follows the top of the south-facing cliffs that extend down to the Mackenzie River (Fig. 16.3, 16.4). Exposure is only fair and the upper part is not completely exposed.

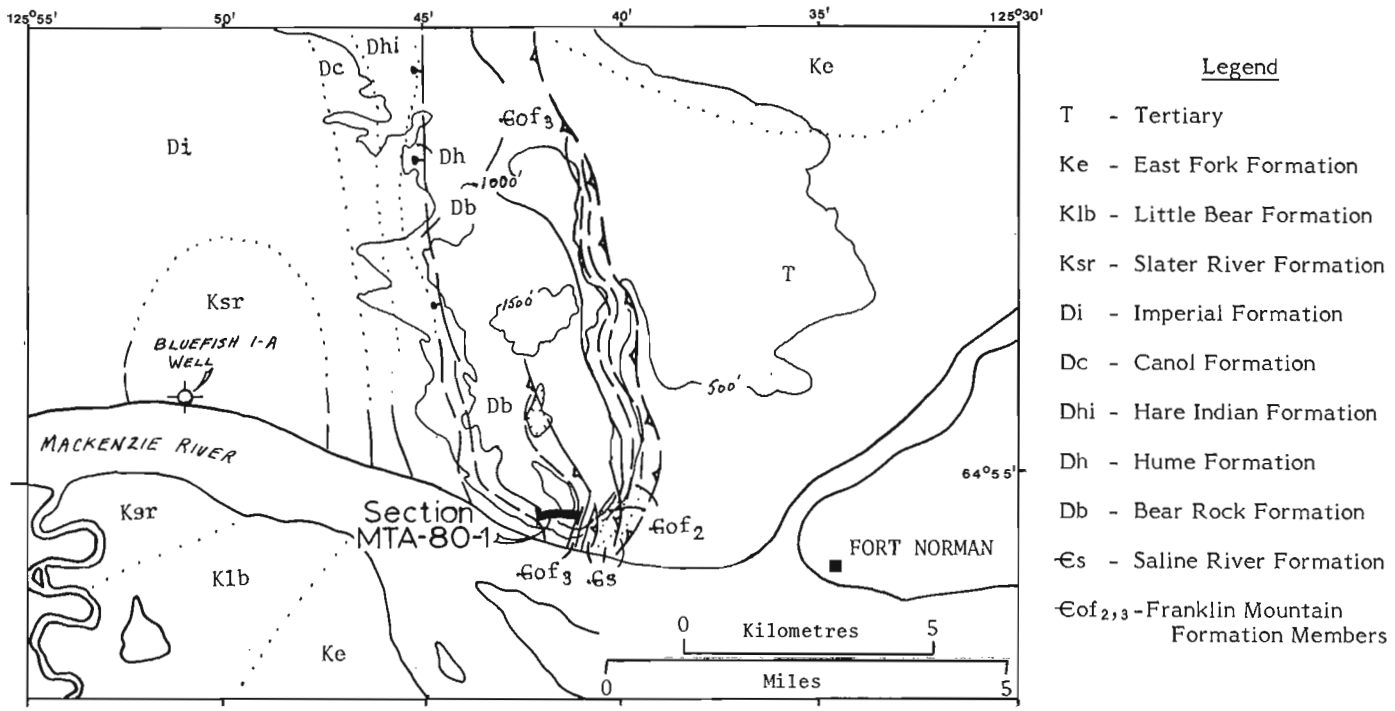

Figure 16.3. *Geological sketch map of Bear Rock and its environs near Fort Norman. The type section of the Bear Rock Formation (MTA-80-1) at the south end of Bear Rock. The Bear Rock Formation is exposed in the hanging wall of a thrust fault. All symbols are standard and the map is adapted from Cook and Aitken (1976).*

Section Description

The section (Fig. 16.2) begins in the uppermost member of the Ordovician-Franklin Mountain Formation ($\in Of_3$ of Cook and Aitken, 1976). Intervals about one metre thick of buff or light greyish- or yellowish-brown, thin and smooth bedded dolomicrite alternate with intervals of slightly darker brown, finely crystalline, thin to medium, irregularly bedded bioturbated dolostone imparting a colour-banded appearance to the uppermost part of the Franklin Mountain at Bear Rock. The basal contact of the Bear Rock Formation is not well exposed because it is much more recessive weathering than the underlying Franklin Mountain (Fig. 16.5). In detail, the contact appears to be somewhat irregular over a range of several metres and masses of Bear Rock breccia extend several metres down into the well bedded Franklin Mountain (Fig. 16.2). The most completely exposed examples of this phenomenon were observed 1.5 km north of the type section where near-tabular bodies of breccia 1-2 m thick extend downward perpendicular to bedding from the Bear Rock into the Franklin Mountain (Fig. 16.6, 16.7). These bodies become thinner downwards. Like the overlying Bear Rock breccias, these breccia 'dykes' are formed of particulate rubble pack- and floatbreccia[1] (Fig. 16.5). Many of the angular clasts in these breccias are yellow dolostone and may have been derived locally from the Franklin Mountain (Fig. 16.7) and the remainder are darker Bear Rock fragments. The inter-fragment matrix is finely crystalline grey calcite that appears to be a recrystallized lime mudstone.

The brecciated part of the Bear Rock, units 2 to 7 inclusive (Fig. 16.2), extends across the high point of the south end of Bear Rock and is formed mostly of massive weathering, particulate rubble pack- and floatbreccias. The fragments are very poorly sorted, dolomitic, finely crystalline calcite and are set in a finely crystalline grey recrystallized lime mud or lime silt matrix (Fig. 16.8). Fragments in the lower part of the breccia (units 2, 3 and 4) tend to be smaller than those in the upper part (units 5 and 6) which contains some fragments several metres across. Also a few beds of relatively undisturbed crackle breccia occur in the lower part (Fig. 16.2). Units 5 and 6 are separated by a gully which is eroded into an interval of less massive weathering and more well bedded breccia. Unit 7 is a transitional unit of cemented mosaic packbreccia between the underlying typical Bear Rock breccia and the overlying bedded limestones.

Unit 8 is a very recessive (Fig. 16.9) and very thin, smooth bedded silty lime mudstone that contains some definite stromatolites (Fig. 16.2). The overlying unit 9 is medium smooth bedded unfossiliferous pelletal lime mudstone although ostracodes of an unknown, smooth-shelled type were collected at the top (Fig. 16.2). No nearby exposure of higher beds are present east of Unit 9, although east-facing hogbacks of the Hume Formation (Fig. 16.9) appear somewhat farther east (Cook and Aitken, 1976). It seems likely that the top of our section is close to the recessive base of the Hume Formation. The geological map shown in Figure 16.3 is modified slightly from Cook and Aitken (in press) because they appear to have placed units 8 and 9 of this section in the fossiliferous Hume Formation. But the rocks in units 8 and 9 are similar to the unfossiliferous Landry Formation beneath the Hume Formation of the Mackenzie Mountains, and so we have excluded them from the Hume Formation.

Discussion

A comparison of the original section description of Stelck (1944) with our section description reveals several anomalies (Fig. 16.2). The total thickness of Stelck's section (~280 ft or 85 m) is a mere fraction of our section thickness (154.0 m of breccia) and the bedded sequence above the breccias in our section does appear to have a counterpart in Stelck's section. We can only speculate that the beds he

[1] See section entitled classification of breccia fabrics.

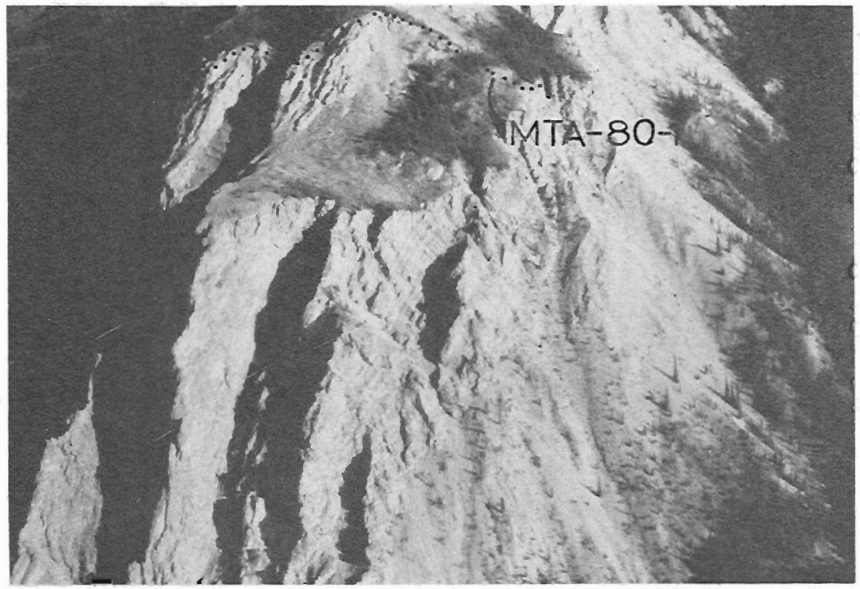

Figure 16.4. *View of the south end of Bear Rock. Our remeasurement of the type section (MTA-80-1) proceeded along the ridge crest as shown. The uppermost part of the section is in shadow.*

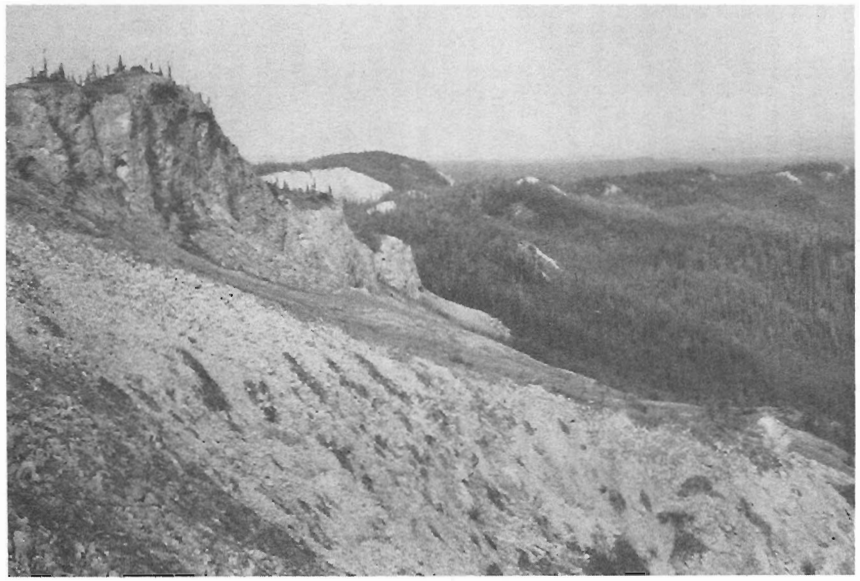

Figure 16.5. *View looking north of massive, grey weathering Bear Rock breccia over light coloured Franklin Mountain 2.4 km north of Section MTA-80-1.*

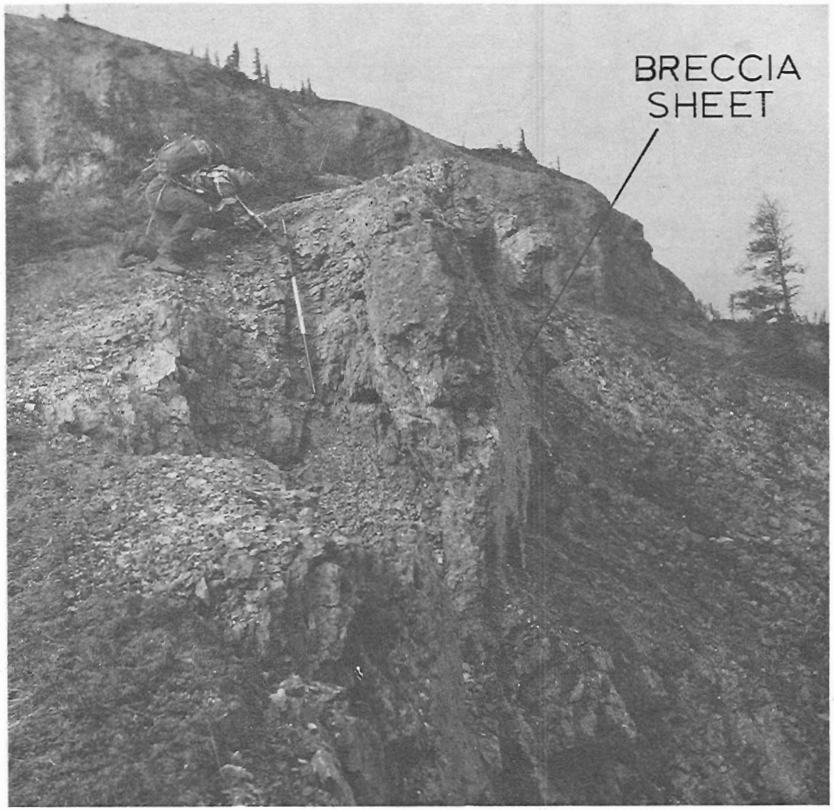

Figure 16.6. *View looking northwest at the same locality as in Figure 16.5. A breccia sheet or dyke extends downward from the overlying Bear Rock into the underlying Franklin Mountain beds.*

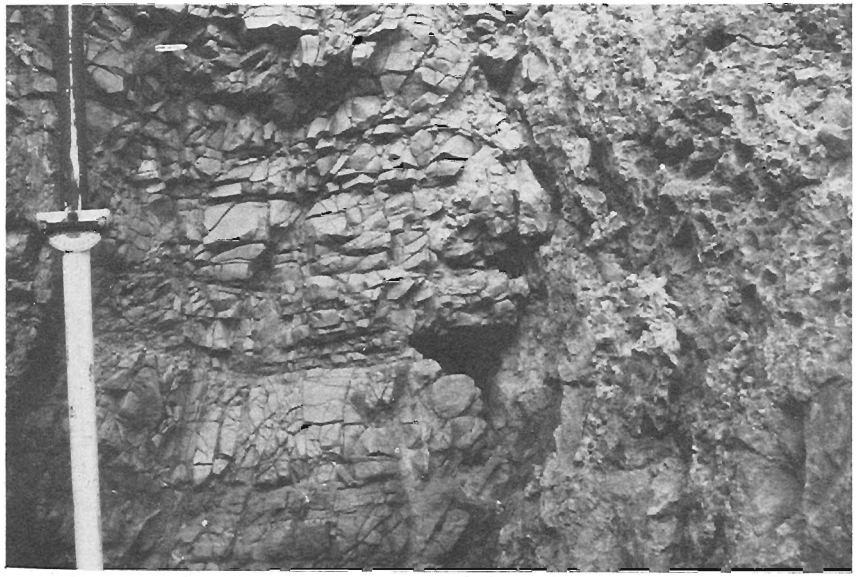

Figure 16.7. *A closer view of the contact between the breccia sheet and the bedded Franklin Mountain dolostone shown in Figure 16.6.*

Figure 16.8. *Outcrop view of particulate rubble packbreccia in the Bear Rock exposure shown in the foreground of Figure 16.5.*

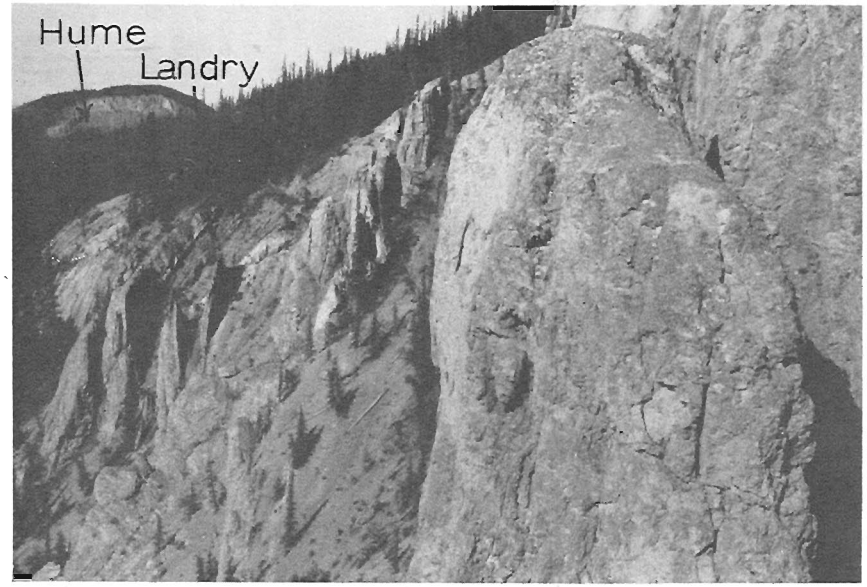

Figure 16.9. *View towards the northwest of the bedded Landry-like interval above the Bear Rock breccias at Section MTA-80-1.*

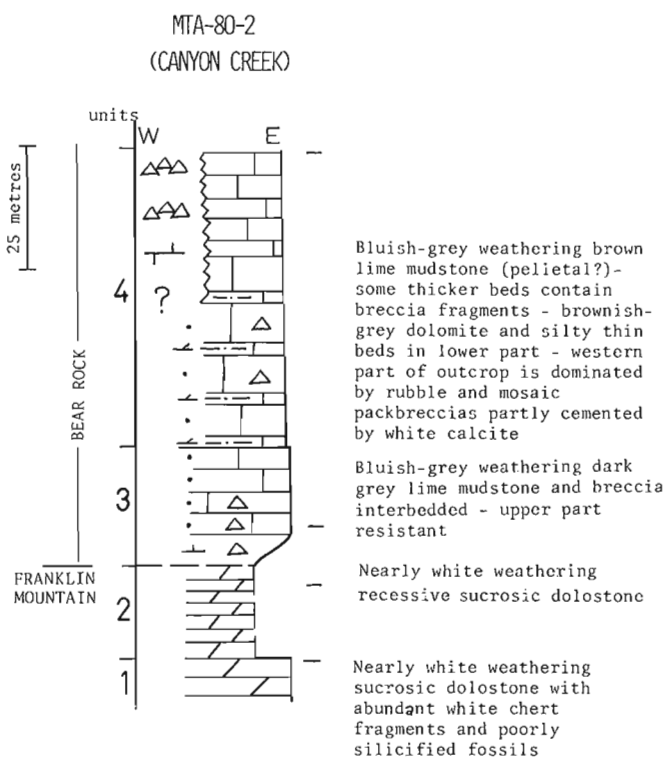

Figure 16.10. *The Landry-like Bear Rock Formation at Canyon Creek.*

included in his Ramparts Formation contained the bedded sequence in the upper part of our section. But the lack of fossils in our bedded sequence implies it is unlike the fossiliferous lower Ramparts member described by Stelck (1944, p. 21).

One possible explanation for these differences is that Stelck's section may be a composite of several subsections joined along strike. Perhaps the ties between these component sections were not along strike and some beds were omitted. We emphasize that this is purely speculation. Stelck (1944, p. 14) mentions only that his Silurian section is a composite section.

The Imperial Canol Bluefish 1-A well, which is only 8 km west of Bear Rock (Fig. 16.3) contains a 430 foot (131 m) thick Bear Rock sequence according to Stelck (1944) but later Tassonyi (1969) revised this to 619+ feet (189+ m) and suggested that the well bottomed in the Bear Rock Formation. Also, Tassonyi assigned a sequence of unfossiliferous pelletal limestones beneath the Hume and above the Bear Rock Formation in this well to the Gossage Formation. These limestones are probably equivalent to units 8 and 9 of our section. Tassonyi has also suggested that the upper limestone beds of Bassett's Bear Rock Formation should be considered as a limestone wedge of the Gossage Formation.

Recent stratigraphic practice has been to subdivide the Gossage Formation into the pelletal limestone of the Landry Formation, the dolostone of the Arnica Formation and the detrital strata beneath the Arnica Formation and above the Mount Kindle Formation (Pugh, in press; Aitken and Cook, 1974). This suggests that units 8 and 9 could also be assigned to the Landry Formation. In the Mackenzie Mountains west of Norman Wells, Aitken and Cook (1974) found that the Landry Formation is the uppermost of the lithologic units that pass laterally into the Bear Rock. Like Bassett (1961), Aitken and Cook (1974) regarded the bedded unfossiliferous limestones above the Bear Rock breccia and beneath the Hume to be part of the Bear Rock Formation.

The Landry interval has already been mapped in the subsurface as the pelletal limestone member of the Gossage or as the Landry Formation (Tassonyi, 1969; Pugh, in press). The equivalent strata in outcrop, such as at the Bear Rock type section, is also readily mappable as part of the Landry Formation, although perhaps not at the common 1:250 000 scale of regional mapping.

Other Outcrop Localities of the Bear Rock

In addition to the type section, we examined Bear Rock strata at four other widely separated localities (Fig. 16.1). Incomplete sections were measured at three places (MTA-80-2, 3 and 4) and observations were made at the fourth locality (MTA-80-5).

Canyon Creek

A short section 126.5 m thick near Canyon Creek on the west side of the Discovery range near Norman Wells through strata mapped as Bear Rock (Cook and Aitken, 1976) proved to be composed mainly of bedded Landry-like strata, although the extreme western part of the ridge is brecciated (Fig. 16.10). This breccia is largely a cemented mosaic packbreccia, unlike the particulate rubble floatbreccias of the Bear Rock breccias at the type section.

South of Mt. St. Charles

Sections MTA-80-3 and 4 are two closely spaced partial Bear Rock sections that were measured in an unnamed range of low mountains 25 km south of Mount Charles (Fig. 16.1). In these sections the Bear Rock may be divided into three parts. The lower subdivision (units 7, 8 and 9 of Section MTA-80-3; and units 1, 2 and 3 of Section MTA-80-4) is predominantly recessive yellow weathering silty and sandy dolomite with some chert pebble lenses (Fig. 16.11). It is 52.0 m thick in Section MTA-80-3 and 31.5 m thick at Section MTA-80-4. This subdivision which is not present at the type section of the Bear Rock was not identified by earlier workers but by definition was included in the Bear Rock interval above the Ronning Group. Later it was mapped as a separate unnamed Silurian-Devonian (SD) map unit beneath the Bear Rock by Cook and Aitken (1976) and N.C. Meijer-Drees (in prep.) recently proposed the name Tsetso Formation. This interval disconformably overlies the Mount Kindle Formation (Fig. 16.11).

Overlying this basal part is a resistant cliff-forming, crudely bedded division composed of units 9, 10, 11 and 12 of Section MTA-80-3 and units 4, 5, 6, 7 and 8 of Section MTA-80-4 (Fig. 16.11). A complete exposure of this division in Section MTA-80-4 is 105.0 m thick. Medium- to thin-bedded intervals of brownish-grey calcareous dolostone and dolomitic limestone grade up to and are abruptly overlain by medium to light grey weathering intervals of particulate rubble packbreccia and floatbreccia. The interfragment matrix of these breccia bodies is grey very finely crystalline calcite that appears to have recrystallized from a carbonate silt. The angular subequant fragments are brownish-grey finely crystalline dolomitic limestone and calcareous dolostone that resemble the dolostone in the bedded intervals. Individual beds of white, fine to medium quartzarenite sandstone separate some bedded intervals from overlying and underlying brecciated intervals (Fig. 16.11).

The uppermost division of the Bear Rock Formation is a light brown to yellowish-brown weathering nonbedded, more or less homogeneous breccia formed of very poorly sorted

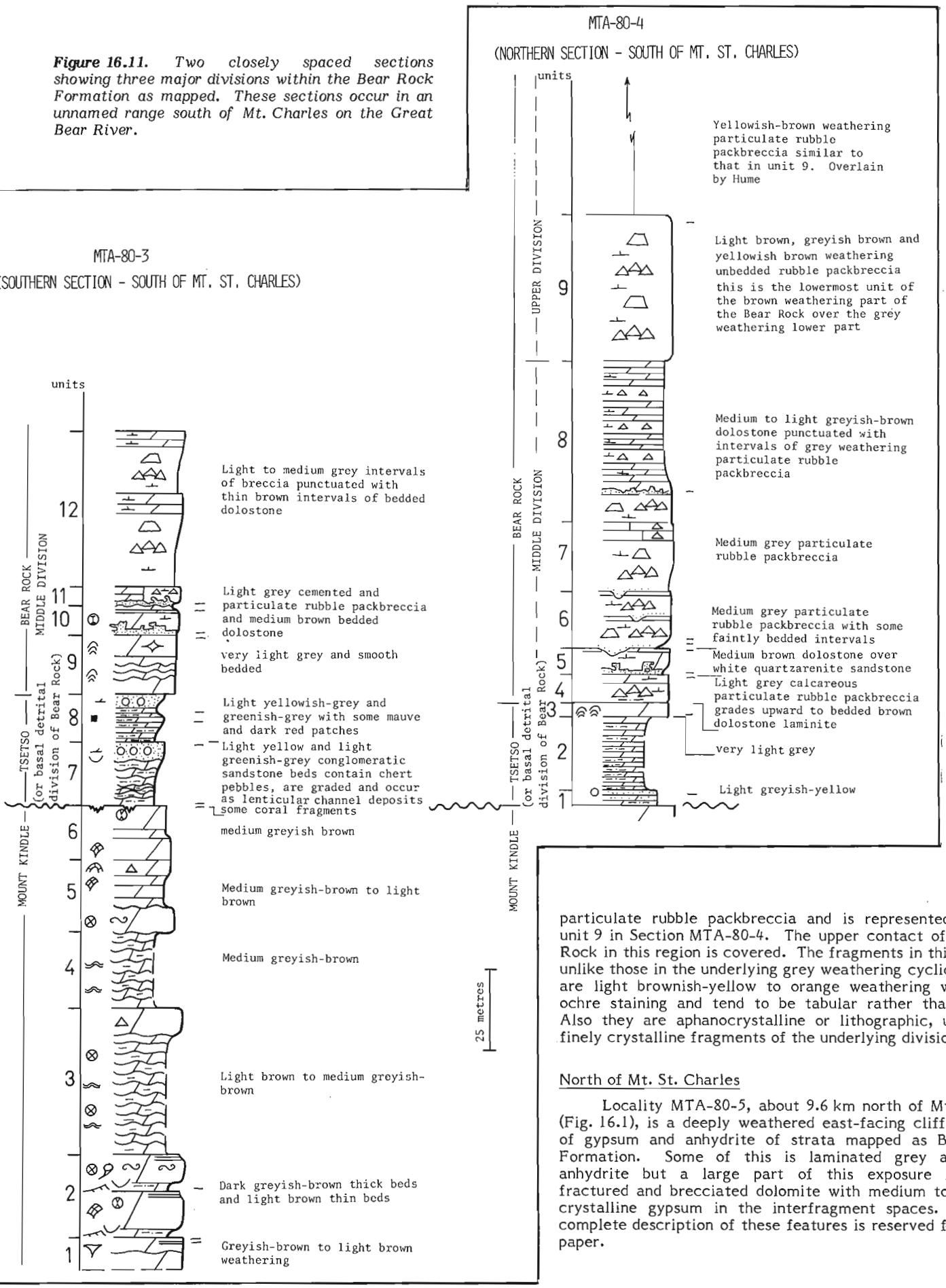

Figure 16.11. *Two closely spaced sections showing three major divisions within the Bear Rock Formation as mapped. These sections occur in an unnamed range south of Mt. Charles on the Great Bear River.*

particulate rubble packbreccia and is represented only by unit 9 in Section MTA-80-4. The upper contact of the Bear Rock in this region is covered. The fragments in this breccia, unlike those in the underlying grey weathering cyclic division, are light brownish-yellow to orange weathering with some ochre staining and tend to be tabular rather than equant. Also they are aphanocrystalline or lithographic, unlike the finely crystalline fragments of the underlying division.

North of Mt. St. Charles

Locality MTA-80-5, about 9.6 km north of Mt. Charles (Fig. 16.1), is a deeply weathered east-facing cliff exposure of gypsum and anhydrite of strata mapped as Bear Rock Formation. Some of this is laminated grey and white anhydrite but a large part of this exposure is brown, fractured and brecciated dolomite with medium to coarsely crystalline gypsum in the interfragment spaces. A more complete description of these features is reserved for a later paper.

Table 16.1

Descriptive Classification of Breccia Fabrics

Interfragment space	Spatial relationship of fragments – mutual orientation	Mutual Proximity of Fragments
1. open	1. crackle	1. packbreccia
2. cemented	2. mosaic	
3. particulate	3. rubble	2. floatbreccia

Origin of the Bear Rock Breccias

We will not discuss here the origin of the breccia fabrics in detail. The fact that all surface exposures of Bear Rock are brecciated and are generally lacking in evaporite minerals whereas adjacent subsurface Bear Rock well sections are composed of bedded anhydrite and dolomite is compelling evidence that dissolution of evaporite minerals played the dominant role in brecciation of the Bear Rock. We regard the exposure at MTA-80-5 as representing an intermediate step in the formation of these breccias. The vertical breccia sheets extending downwards from the Bear Rock into Franklin Mountain strata may, in part, be passive gravity fillings of fractures that opened during Laramide deformation and during the period of solution-collapse of the overlying Bear Rock.

Classification of Breccia Fabrics

The simple, nongenetic descriptive classification proposed here is an outgrowth of the existing descriptive terms crackle, mosaic and rubble that are presently used to describe breccia fabrics (Ridge, 1968). These terms reflect, to some degree, the spatial relationship of fragments to one another primarily through their degree of mutual orientation. A crackle breccia denotes a fabric in which there is little relative displacement of fragments; a mosaic breccia is characterized by fragments that are largely but not wholly displaced; and the term rubble breccia signifies a fabric in which no fragments match.

We feel that some additional variables could reasonably be included in this classification. Two other important variables from a purely descriptive standpoint involve the mutual proximity of the fragments and the character of the interfragment space (Table 16.1). Other variables are, of course, important, but we feel that the listed attributes are the most accessible to an often cursory visual examination.

The interfragment space of a breccia may be in one of three possible states; it may be unfilled void space, and hence open, it may be filled by chemically precipitated crystalline minerals, and hence cemented, or, it may be filled with discrete grains of subgranule size, and hence particulate. The degree of mutual proximity of fragments may be characterized by two conditions; either the fragments are largely in contact in which case the term packbreccia may be used, or they are not in contact in which case the term floatbreccia may be applied. An example of breccia fabric completely classified by this system would be a particulate rubble floatbreccia indicating a fabric in which fragments of chaotic orientation are suspended in fine grained fragmental matrix. All or part of this classification may be used depending on circumstances such as the degree or quality of exposure. It may be difficult to determine, for example, if the breccia fabric displayed on a strongly weathered surface is that of a packbreccia or a floatbreccia. Also other attributes, such as composition of fragments, may be used to more fully describe a particular breccia (e.g. oligomictic vs. polymictic), but in most cases, these attributes entail investigations beyond a simple field examination. For this reason we regard such attributes as adjuncts to, rather than as part of, the classification proposed here.

Concluding Remarks

1. We have substantially revised the description of the type section of the Bear Rock Formation from the original description by Stelck (1944). We propose that the section description provided here be used as the type section description in the future.
2. The bedded strata above the Bear Rock breccias in the type section are equivalent to the pelletal limestone member of the Gossage Formation and therefore also to the Landry Formation.
3. The Bear Rock breccias themselves are due to the solution removal of evaporite minerals on exposure to the vadose zone. The exact processes of brecciation remain to be defined.
4. Description of breccia fabrics in the Bear Rock Formation was aided by the use of a new three-fold descriptive classification of breccia fabrics.

References

Aitken, J.D. and Cook, D.G.
1974: Carcajou Canyon map-area, District of Mackenzie, Northwest Territories; Geological Survey of Canada, Paper 74-13.

Bassett, H.G.
1961: Devonian stratigraphy, Central Mackenzie River region, Northwest Territories, Canada; in Geology of the Arctic, Volume 1, Raasch, G.O. (ed.), Alberta Society of Petroleum Geology, and University of Toronto Press, p. 481-495.

Cook, D.G. and Aitken, J.D.
1976: Geological maps of Blackwater Lake (96B) and Fort Norman (96C), District of Mackenzie; Geological Survey of Canada, Open File 402.

Hume, G.S.
1954: The lower Mackenzie River area, Northwest Territories and Yukon; Geological Survey of Canada, Memoir 273.

Hume, G.S. and Link, T.A.
1945: Canol Geological Investigations in the Mackenzie River area, Northwest Territories and Yukon; Geological Survey of Canada, Paper 45-16.

Meijer-Drees, N.C.
Devonian evaporitic carbonate rocks in the subsurface of the Great Slave and Great Bear Plains, Northwest Territories; Geological Survey of Canada, Paper. (in prep.)

Pugh, D.C.
Pre-Mesozoic geology in the subsurface of Peel River map-area, Yukon Territory and District of Mackenzie; Geological Survey of Canada, Memoir. (in prep.)

Ridge, J.D.
1968: Comments on the development of the ore-bearing structures of the Mascot-Jefferson City district and on the genesis of the ores contained in them; Institution of Mining and Metallurgy, Transactions, v. 77, Sec. B, p. B6-B17.

Stelck, C.R.
1944: Bear Rock-Bluefish area; Imperial Oil Ltd., Canol Project; Geological Survey of Canada, unpublished report.

Tassonyi, E.J.
1969: Subsurface geology, Lower Mackenzie River and Anderson River area, District of Mackenzie; Geological Survey of Canada, Paper 68-25.

17. PETROCHEMICAL AND MINERALOGICAL EVOLUTION OF RADIOACTIVE ROCKS IN THE BAIE-JOHAN-BEETZ AREA, QUÉBEC: A PRELIMINARY REPORT

Project 770061

J. Rimsaite
Economic Geology Division

Rimsaite, J., Petrochemical and mineralogical evolution of radioactive rocks in the Baie-Johan-Beetz area, Québec: a preliminary report; in Current Research, Part A, Geological Survey of Canada, Paper 81-1A, p. 115-131, 1981.

Abstract

This report summarizes results of field and laboratory studies of specimens collected in 1978 and 1979 in the Baie-Johan-Beetz area, Quebec. The radioactive syenitic and granitic rocks are characterized by their heterogeneous character, namely, variable grain size, petrochemistry, mineralogical composition, size and nature of xenoliths, and by abundance and distribution of radioactive ore and rare-earth elements (REE) minerals.

The study of the relationship between mode of occurrence of radioactive ore minerals and the petrochemical evolution of the host rocks indicates apparent associations between early plagioclase- and biotite-bearing syenitic phases and uraninite and phosphate minerals, and between later microcline-quartz phases and REE-bearing minerals. Two types of favourable host rocks for uranium mineralization studied are (1) white syenitic pegmatites, characterized by relatively low silica content, high concentrations of alumina and the ratio $Fe^{II}/Fe^{III} > 1$; and (2) pink to red granite pegmatites, characterized by variable proportions of plagioclase, microcline, albite and quartz, the ratio $Fe^{II}/Fe^{III} < 1$, and by alteration of primary iron- and uranium-bearing minerals. The uranium mineralization is a factor of geochemical evolution of host rocks and of the nature of paleosome remnants. Most of the uraninite grains alter during late stages of pegmatitic activity. The U/Th ratio in the Baie-Johan-Beetz area is relatively high, the average being 4, but varies from 0.3 to 10 depending on the abundance of secondary uranyl-bearing minerals in the rock, and on redistribution and losses of uranium during deuteric alteration and weathering.

Introduction

Radioactive pegmatites and occurrences of Rare Earth Elements (REE)-bearing minerals north of the Gulf of St. Lawrence, Québec, have been reported by Blais (1955), Baldwin (1970) and Rose (1979). In 1978, 1979 and 1980, the author visited scattered radioactive occurrences in an area of 1200 km^2 between Baie-Johan-Beetz (50°16'N, 62°30'W), Turgeon Lake (50°24'N, 62°57'W), Costebelle Lake (50°23'N, 62°25'W), and Baie Pontbriand (50°16'N, 62°30'W), NTS sheets 12 L/7 and 12 L/8, and collected samples for laboratory studies. The radioactive occurrences examined in 1978 and 1979, sampling localities, and concentration range and the highest uranium values are given in Figure 17.1. The visited trenches "A", "AB", "B" and "Grandroy Deposit" are north of Turgeon Lake; "C" is east of Little Piashti Lake; "D" and "D1" are between Roston Lake and Little Piashti Lake; and "E", "F", "G" are near Johan Beetz village.

Blais (1955) mapped the area east and north of Pontbriand. Cooper (1957) mapped the area east of Pontbriand, covering Baie-Johan-Beetz, Little Piashti Lake and Turgeon Lake granite. The mapping was done before exploration for uranium started in 1956. Hauseux (1976) reviewed the history of exploration and studied petrology and mineralogy of radioactive granitic rocks near Baie-Johan-Beetz. Schimann (1978) studied radioactive minerals by electron microprobe.

This paper summarizes preliminary laboratory results and the author's field observations in an attempt to establish criteria for locating favourable lithologies for uranium and REE mineralizations in vast areas of granitic rocks. The scope of this report includes the following discussions:

1. Petrographic description and chemical composition of the principal rock units, with special emphasis on pegmatitic differentiation and evolution of radioactive rocks.
2. List of rock-forming, accessory and radioactive ore minerals and unidentified secondary mineral aggregates from the area studied.
3. Mode of occurrence of radioactive and accessory minerals in relation to the petrochemical evolution of host rocks.
4. Alteration of accessory and radioactive ore minerals and fixation of mobilized uranium in secondary radioactive mineral aggregates.

The report is based on preliminary results of the following laboratory studies: optical examination of thin and polished thin sections under the petrographic microscope; chemical, spectrographic and neutron activation analyses of the principal rock types (Table 17.1, 17.2); scanning electron microscope (SEM) and energy dispersive spectrometer (EDS) studies of radioactive minerals in polished thin sections and of small chips mounted on a rod; and X-ray identification of minerals. The type of heterogeneous feldspars is identified by symbols and references to the pertinent illustrations in Rimsaite (1967). Textural relationships between accessory and radioactive ore minerals are illustrated in electron micrographs, as for samples from the Bancroft area (Rimsaite, 1980a).

Most of the minerals have been identified by optical and X-ray diffractometer studies during concentration of minerals for chemical and isotopic analyses. Metamict minerals have been selected for X-ray identification using a powder camera and samples have been prepared for electron microprobe and isotopic analyses. These analyses have not yet been completed and will be discussed in subsequent reports.

Some results of these studies have been presented at the last International Geological Congress (Rimsaite, 1980b).

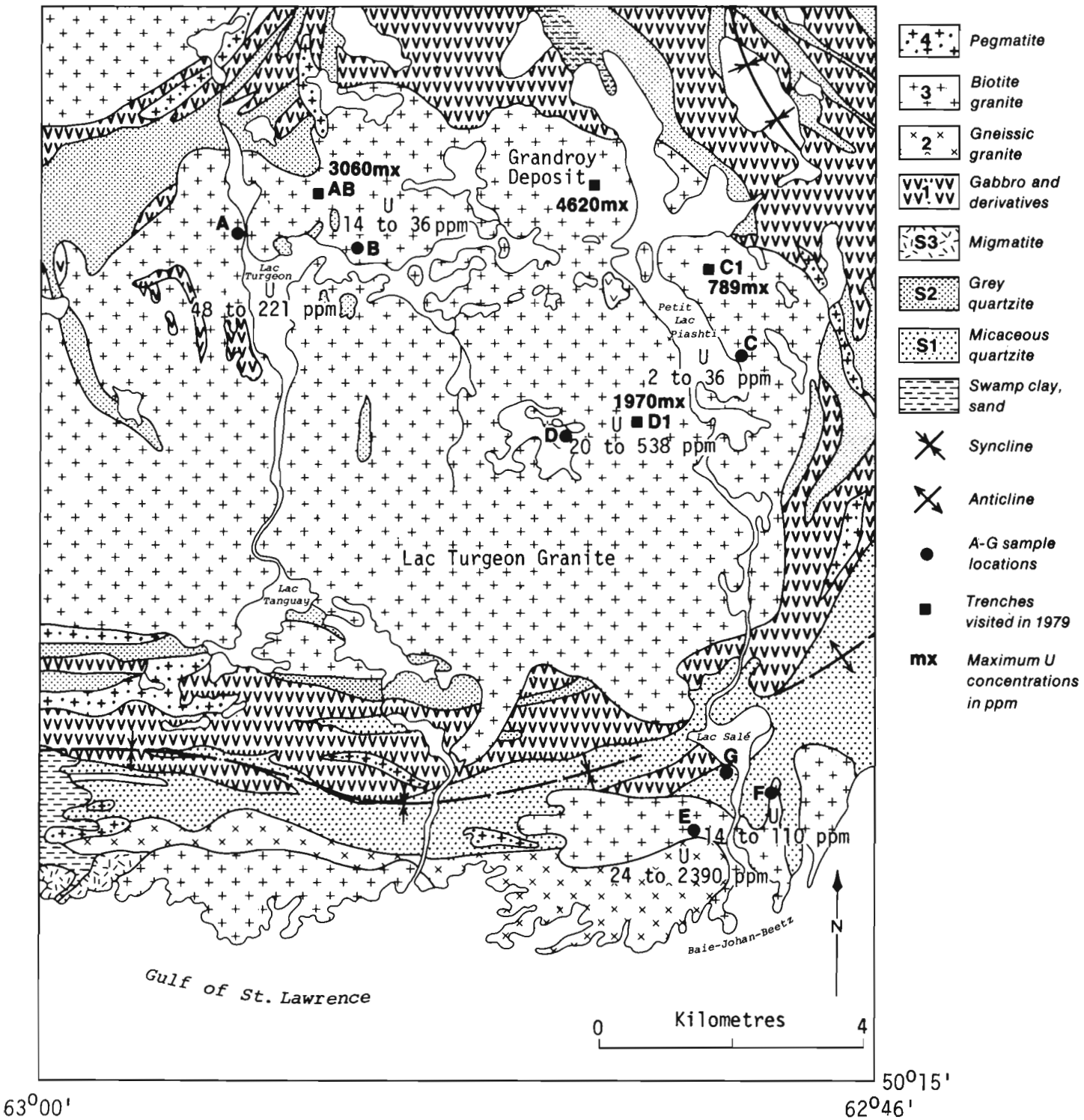

Figure 17.1. *Geological sketch map showing location of samples in the Baie-Johan-Beetz area, Québec (geology after Cooper, 1957).*

Table 17.1.

Chemical composition of the principal rock types in the Baie-Johan-Beetz area, Québec*,**

Analysis No.	Rock type***	U (ppm)**	Weight per cent											
			SiO_2	TiO_2	Al_2O_3	Fe_2O_3	FeO	MnO	MgO	CaO	Na_2O	K_2O	P_2O_5	H_2O
1****	S 1, G	3.6	92.8	0.3	2.4	1.3	0.1	0.02	0.4	0.1	0.1	0.4	0.04	0.4
2	S 2, G	2.3	90.9	0.4	3.8	0.7	1.5	0.07	0.6	0.3	1.2	0.5	0.06	0.3
3	S 3, E	11.7	66.0	0.8	14.6	0.4	5.0	0.10	1.2	1.4	3.2	4.1	0.13	0.9
4	1, G	1.0	44.1	3.9	13.3	6.8	9.3	0.25	5.3	10.6	1.3	1.3	0.70	2.7
5	2, E	16.1	73.1	0.1	14.0	0.2	0.8	0.02	0.3	1.2	3.2	4.5	0.05	0.5
6	2, E	26.8	67.9	0.5	15.1	0.2	3.3	0.06	0.9	1.4	3.6	4.1	0.12	0.6
7	3-4, E	4.2	66.7	1.3	12.6	1.0	6.2	0.12	3.1	1.6	2.0	3.4	0.18	1.3
8	3-4, E	2390	55.1	1.2	19.5	2.3	5.7	0.13	2.2	1.8	4.7	3.7	0.23	1.3
9	4, E	8.6	73.0	0.0	14.0	0.0	0.5	0.00	0.1	0.0	2.0	8.0	0.00	0.5
10	3, E	1363	77.4	0.1	11.9	0.0	0.8	0.01	0.4	1.0	3.6	2.1	0.03	0.6
11	4, E	285	76.6	0.1	12.6	0.3	0.5	0.02	0.4	1.1	3.4	2.6	0.01	0.5
12	4, E	951	77.5	0.6	8.7	1.0	2.4	0.05	1.1	0.8	1.5	2.8	1.00	0.6
13	3-4, D	538	82.8	0.0	8.9	0.8	0.3	0.01	0.2	0.8	2.1	2.3	0.04	0.3
14	4, B	2.8	77.8	0.1	13.3	0.1	0.0	0.00	0.0	0.3	4.8	3.0	0.00	0.3
15	4, G	9.5	77.1	0.1	13.1	0.8	0.2	0.01	0.3	0.2	4.5	2.1	0.06	0.6

* Chemical analyses by the staff of the Central Laboratories and Technical Services, Geological Survey of Canada.

** Uranium determined by neutron activation analysis at the Atomic Energy of Canada, Ltd.

*** Rock unit and sampling location on the map in Figure 17.1.

**** Specimens, their petrographic names, field numbers and characteristic properties:

1. Quartzite, RT-78-38: mainly quartz, minor altered feldspar and biotite.
2. Quartzite, RT-78-6: similar to RT-78-38 but less altered.
3. Migmatite, RT-78-46: biotite-plagioclase layers interbanded with microcline granite.
4. Amphibole-rich metagabbro, RT-78-39 transected by epidote-filled veins.
5. Gneissic granite, RT-78-44A: contains abundant microcline porphyroblasts.
6. Biotite-bearing groundmass, RT-78-44B surrounding feldspathic portion RT-78-44A.
7. Biotite-rich xenolith, RT-78-15 in pegmatitic biotite syenite RT-78-14.
8. Pegmatitic biotite syenite RT-78-14 adjacent to biotite-rich xenolith RT-78-15.
9. Microcline-rich pegmatite RT-78-17 adjacent to biotite syenite RT-78-14.
10. White gneissic biotite granite RT-78-19 containing secondary U minerals.
11. Pegmatite RT-78-18: coarse grained portion in gneissic granite RT-78-19.
12. Pegmatite RT-78-21 containing secondary U phosphates, adjacent to RT-78-19.
13. Red mineralized pegmatite granite RTT-78-29g grading to quartz pegmatite.
14. White albite-quartz pegmatite RT-78-1: late pegmatitic phase.
15. Red albite-rich pegmatite RT-78-43 transecting metagabbro RT-78-39.

Table 17.2.

Chemical composition of selected minerals and radioactive rocks in Baie-Johan-Beetz area, Québec*,**,***

Elements and oxides	Rock units and sampling localities: 4, AB			3-4, E 4, AB		3-4, D1								
	Specimen No.*****													
	16	17	18	19	20	21	22	23	24	25	26	27	28	29
U**	ND****	ND	ND	100	3060	50.3	789	4620	1490	607	530	470	1970	287
Th***	ND	ND	ND	10	617	41	229	586	546	116	142	117	339	896
SiO_2*	68.3	37.3	44.3	35.3	61.0	53.4	59.7	62.8	70.4	83.3	72.9	72.0	72.2	65.3
Al_2O_3	20.0	17.6	33.7	17.2	15.0	12.7	16.1	21.8	14.9	6.8	14.9	15.1	11.9	15.8
TiO_2	0.0	2.7	0.4	3.2	0.7	2.1	0.5	0.0	0.1	0.6	0.0	0.1	1.7	1.5
Fe_2O_3	0.2	4.4	4.2	7.1	2.0	3.5	7.5	0.1	2.5	1.9	1.6	0.4	1.1	2.8
FeO	0.0	16.6	1.2	16.9	3.1	11.7	0.0	0.2	0.7	1.3	0.6	0.3	1.7	1.5
MgO	0.0	7.9	1.0	6.8	1.0	4.9	1.3	0.0	0.2	0.5	0.1	0.2	0.6	0.4
MnO	0.0	0.6	0.1	0.3	0.1	0.5	0.1	0.0	0.0	0.0	0.0	0.0	0.0	0.0
CaO	2.2	0.1	0.0	0.0	1.0	0.1	0.8	2.8	1.5	0.5	1.0	0.4	1.0	1.7
Na_2O	8.6	0.5	0.7	0.0	6.0	0.8	5.8	9.3	5.0	1.4	4.0	2.6	2.6	7.2
K_2O	0.4	8.4	10.1	8.5	1.0	7.1	2.3	0.7	2.9	2.7	4.9	8.5	5.0	0.8
P_2O_5	0.0	0.0	0.0	0.0	0.2	0.0	0.2	0.2	0.2	0.1	0.1	0.1	0.1	0.3
S	0.1	0.1	0.1	0.0	0.1	0.1	3.0	0.0	0.0	0.0	0.0	0.0	0.0	0.0
CO_2	0.1	0.2	0.1	0.0	0.2	0.2	0.1	0.1	0.2	0.1	0.1	0.1	0.4	0.1
H_2O	0.4	4.1	4.4	3.9	2.0	2.4	1.7	0.9	1.0	1.0	1.0	0.7	0.8	1.5
F	0.0	1.1	0.2	0.5	0.1	0.5	0.2	0.0	0.0	0.0	0.0	0.0	0.1	0.0
Cl	0.1	0.1	0.0	0.2	0.1	0.1	0.0	0.1	0.1	0.0	0.0	0.0	0.0	0.1
Ba (ppm)	400	200	100	ND	0	100	70	90	190	150	190	490	250	50
Cs (ppm)	2	102	93	ND	6	82	18	25	22	20	40	30	25	22
Li (ppm)	7	608	330	ND	67	200	75	15	15	22	8	20	75	18
Rb (ppm)	30	1580	2125	1300	114	1270	325	90	75	125	225	425	275	112
Zn (ppm)	20	450	60	59	0	390	90	80	50	70	20	30	100	20

* Chemical analyses (wt. %) by the staff of the Analytical Section, Central Laboratories and Technical Services Division, Geological Survey of Canada.

** Uranium (ppm) determined by neutron activation analysis at the Atomic Energy of Canada, Ltd.

*** Th (ppm) determined by X-ray fluorescence analysis by Bondar-Clegg & Co., Ltd.

**** ND = not determined.

***** Specimens, their petrographic names, field numbers and descriptions:

16, 17, 18: green plagioclase, biotite and muscovite from two-mica pegmatite RT-79-110.

19: biotite from radioactive pegmatite RT-78-14; secondary U minerals on biotite.

20: red pegmatite RT-79-125, contains plagioclase, biotite and secondary U minerals.

21: red pegmatite RT-79-126, porphyroblastic microcline overgrown by biotite, adjacent to plagioclase pegmatite RT-79-125.

22: red pegmatite RT-79-130, contains partly oxidized sulphides and U phosphates and niobates.

23: white radioactive syenite pegmatite from Grandroy mine, RT-79-141, contains zircon and secondary U minerals (see Fig. 17.2).

24, 25, 26, 27: adjacent specimens RT-79-159, RT-79-158, RT-79-157 and RT-79-155 representing transition from peristerite to microcline pegmatites.

28: red microcline pegmatite RT-79-160 containing pyrochlore.

29: red pegmatite RT-79-164 containing oxidized Fe and Ti minerals and altered feldspar.

Acknowledgments

Petrographic and X-ray diffractometer studies by the author were supported by neutron activation analysis for U by the Atomic Energy of Canada Limited; X-ray fluorescence determinations of Th by Bondar-Clegg and Company Ltd.; chemical and spectrographic analyses by the staff of the Analytical Chemistry Section, scanning electron microscope and energy dispersive spectrometer analyses by D.A. Walker and X-ray identification of minerals by A.C. Roberts of the Mineralogy Section, Central Laboratories and Technical Services Division at the Geological Survey of Canada. Their contributions are gratefully acknowledged. Special thanks are due to Dr. L.P. Tremblay of the Geological Survey of Canada for specimens RTT-78-22 and RTT-78-33, and to Dr. L. Kish and his field party of the Ministère de l'Energie et des Ressources, Québec, for providing base camp facilities, airplane flying time and valuable suggestions during field studies in 1979.

General Geology

Cooper's (1957) geological map of the Johan Beetz area, scale 1:63 360, distinguished seven rock units. Blais (1955) mapped the adjacent eastern region and subdivided the rocks into 12 petrographic units in his preliminary map. Cooper's map has been used as a base may by many authors, and for the present report (Fig. 17.1). The granitic rocks are surrounded by metasedimentary rocks, migmatites and metagabbro. Cooper identified four intrusive contacts: between metasedimentary rocks and gabbro; between gabbro and gneissic granite; between gneissic granite and biotite granite; and between biotite granite and pegmatite. To the author's knowledge, the age relationships between these rock units have not been determined by radiometric methods and the time difference between the deposition of metasediments and late pegmatites is still unknown. However, the younger granitic rocks appear to be more radioactive. In the Massif Central in France the time span between the formation of Hercynian early granitic rocks (350-360 Ma ago) and precipitation of pitchblende (275-280 Ma ago) is at least 70 Ma (Leroy, 1978). Because the youngest granitic rocks in the Grenville structural subprovince contain xenoliths (ranging in size from a few centimetres to several hundred metres) of preexisting rocks which might have contributed radioactive elements, this report summarizes petrochemical features of all rock units. Hauseux (1977), Mackie (1978) and Schimann (1978) favour an anatectic hypothesis for the Lake Turgeon granite rather than an origin from the upper mantle. Hauseux (1976) concluded that the most important source of uranium is zircon, with some contribution from uraninite, whereas Schimann (1978), who calculated uranium, thorium and REE content in seven types of radioactive minerals on the basis of electron microprobe analyses, showed that the major contributor of uranium is uraninite. Schimann (ibid.) used electron microprobe data to calculate "chemical ages", using the formula $t = \frac{Pb \times 10^{10}\ y}{1.612U + 0.495Th}$, and, assuming that no gains or losses of these elements occurred from the time of crystallization, obtained two groups of uraninite ages, 1152 Ma and 1317 Ma.

Petrography and Petrochemistry of the Principal Rock Units

Unit S1: Micaceous Quartzite, Table 17.1.1

The micaceous quartzite underlies swampy areas around the Johan Beetz village. A specimen collected south of La Salé Lake consists dominantly of quartz (90%), small interstitial grains of altered plagioclase and a few biotite laths. Quartz grains are angular, strained and recrystallized to larger units, engulfing remnants of plagioclase and biotite. Plagioclase, clouded by fine grained sericitic alteration in the centre, occurs in intergrowths with biotite, representing relicts of detrital rock fragments. The accessory minerals apatite, magnetite, rutile, zircon and one small grain of uraninite in a prominent yellow rim, cluster in and around biotite laths or are disseminated throughout the rock. Fractures traversing biotite and quartz are coated with red and black iron oxides. This quartzite contains 3.6 ppm U.

Unit S2: Grey Quartzite, Table 17.1.2

Grey quartzite collected east of Little Piashti Lake has a mineralogical composition similar to that of quartzite S1, but the rock-forming minerals are coarser grained and remnant plagioclase-biotite fragments are larger, suggesting a closer source of detrital minerals and fragments. Altered biotite, partly replaced by muscovite and chlorite, contains pleochroic haloes surrounding inclusions of zircon and epidote. Scarce accessory minerals i.e. apatite, rounded zircon grains, allanite-epidote intergrowths, magnetite and green tourmaline, are disseminated in feldspar. Chloritized biotite and patchy replacements of plagioclase by muscovite indicate effects of retrograde metamorphism in this area. The quartzite contains only 2.3 ppm U.

Unit S3: Migmatite, Table 17.1.3

Migmatite east of Johan Beetz village consists of melanocratic biotite-rich paleosome bands enclosed in leucocratic, microcline-rich granite. Biotite laths contain abundant radioactive inclusions surrounded by pleochroic haloes and lie in a groundmass of plagioclase and quartz. Plagioclase, partly clouded by muscovite alteration, contains disseminated grains of apatite and minute, rimmed uraninite. Large apatite grains crystallized between paleosome and neosome portions of the rock. The leucocratic portion of the migmatite consists of poikilitic microcline porphyroblasts, strained quartz and irregular remnants of altered biotite, stretched between microcline and quartz. The migmatite is more radioactive (11.7 ppm U) than quartzites S1 and S2, and possibly reflects first stage of uranium concentration.

Unit 1: Gabbro and Derivatives, Table 17.1.4

Metagabbro forms irregular bands and patches in metasediments and is transected by red quartz-feldspar veins. A sample collected at the south shore of La Salé Lake is made up of hornblende crystals in a groundmass of altered plagioclase. The alteration of plagioclase to clay and sericite is accompanied by losses of calcium which recrystallizes in epidote aggregates. Epidote-filled veins transect the rock. The hornblende is poikilitic, strongly pleochroic, dark green to pale olive yellow, and contains inclusions of quartz, pyrite, magnetite, apatite and titanite. Xenoliths of metagabbro occur in granite and can be a potential source of Fe, Ti, Ca, Mg and P.

Unit 2: Gneissic Granite, Table 17.1.5, 6

Gneissic granite with abundant bands and xenoliths of biotite gneiss was sampled west of Johan Beetz village. The biotite bands are elongated in an east-west direction, parallel to the shore of the Gulf of St. Lawrence. The granite varies from various shades of red to grey, depending on its content and degree of recrystallization and oxidation of mafic minerals. Biotite contains numerous pleochroic haloes and occurs in roughly parallel streaks in a groundmass of oligoclase and quartz. Leucocratic bands consist mainly of porphyroblastic microcline that overgrows zoned grains of plagioclase and a few laths of altered biotite. Quartz and microcline are poikilitic with irregular contacts, embayments and micrographic margins. Biotite bands and streaks contain more Al, Fe, Mg, P, Ti and U than the porphyroblastic

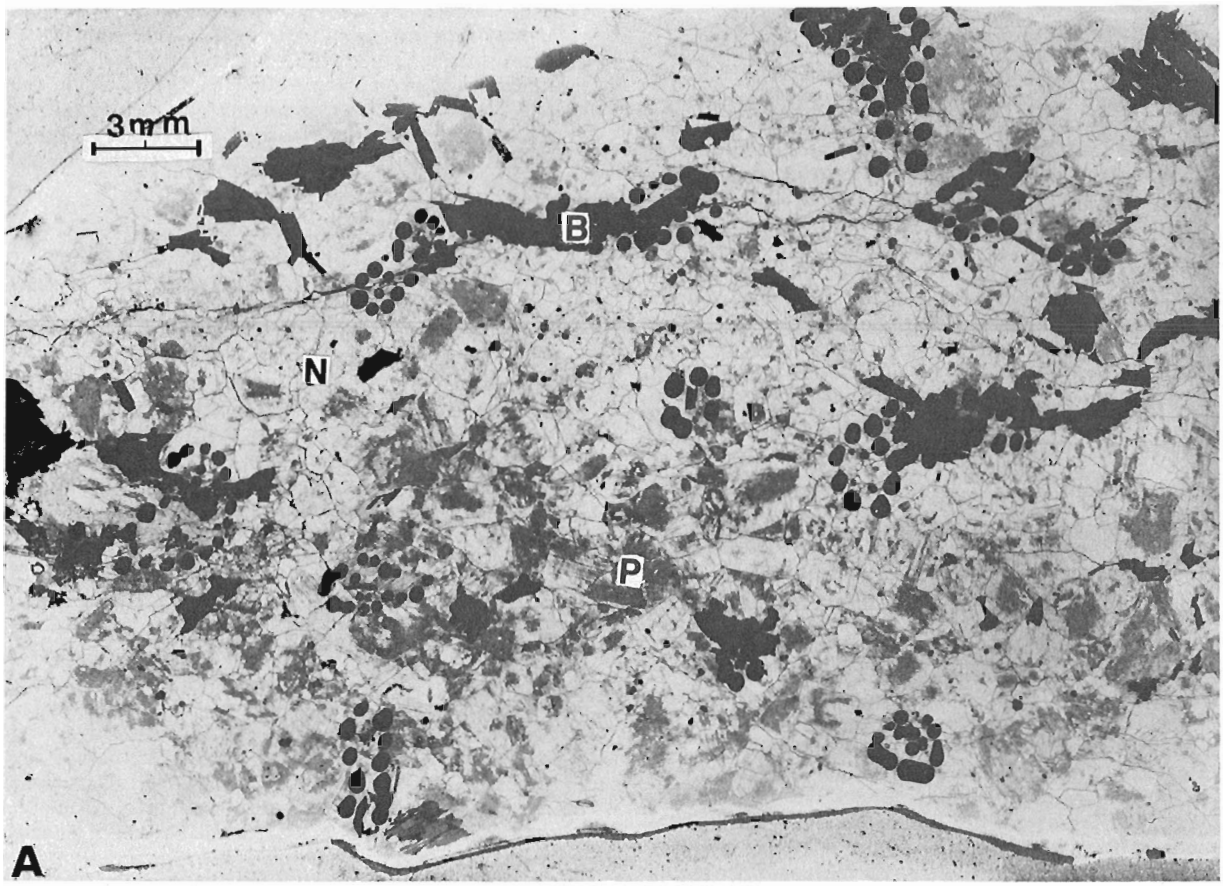

Figure 17.2A. *Polished thin section of radioactive rock from the Grandroy mine. The rock consists of clouded older, or paleosome, areas (P), including elongated flakes of biotite (B) and clear younger, or neosome areas (N). Black ink circles mark areas analyzed by scanning electron microscope.*

quartz-microcline intergrowths (Table 17.1, analyses 5 and 6). Accessory minerals are apatite, monazite, zircon and rare pyrochlore grains concentrate mainly in biotite-rich streaks and bands. Secondary minerals are calcite, chlorite and sericite and replace biotite laths along (001) fractures. Because of porphyroblastic growth of feldspar, gneissic granite varies from medium grained to coarse grained pegmatitic or porphyroblastic patches. The feldspar porphyroblasts are commonly surrounded by a zone of intersecting blades of biotite. The gneissic granite contains more uranium than migmatite, probably as a result of the second stage of U enrichment.

Unit 3-4: Biotite Granite-syenite and Xenoliths, Grading to Pegmatite. Biotite-rich Xenoliths, Table 17.1.7

Banded biotite-rich xenoliths trend in N80°E direction. Melanocratic bands of a xenolith consist of biotite, plagioclase, clouded by sericite and clay alteration, and quartz. Leucocratic bands are made up of arkosic quartzite. The original small quartz grains are intergrown to form much larger quartzitic patches that enclose fine grained remnants of clouded plagioclase crystals. Accessory minerals in decreasing order of abundance are apatite, titanite and zircon. Biotite has radioactive inclusions surrounded by pleochroic haloes and rims of quartz and K-feldspar along (001) cleavage planes, similar to those illustrated in Rimsaite (1967, Pl. III, VII-19, VII-21). The xenolith contains concentration of uranium (4.2 ppm) similar to that in quartzite S1.

Unit 3-4: Biotite Syenite and Granite Grading to Pegmatite, Table 17.1.8

Biotite granite and syenite that host the xenolith of biotite quartzite vary in grain size and in distribution of biotite, plagioclase, microcline, quartz, albite and radioactive minerals. Fine- and medium-grained portions made up of grains <2 mm in size are referred to as granite or syenite. Coarse grained portions having grain size >2 mm, or variable grain size in an area of a thin section, are referred to as pegmatite or pegmatitic granite. Rocks made up predominantly of plagioclase and albite, and containing <65 weight per cent silica are referred to as syenite. However, the presence of biotite lowers considerably the silica content of the host rock; therefore the biotite content should be considered when choosing a proper name for these hybrid rocks (compare biotite analysis in Table 17.2.17).

The biotite-rich portion of syenite adjacent to the south side of the xenolith is made up of biotite, lamellar plagioclase, type IIKn:FP (Rimsaite, 1967, Pl. I, II-6), interstitial twinned microcline and anhedral quartz. Biotite is partly replaced by muscovite and contains inclusions of apatite, uraninite, xenotime, monazite and titanite. Uraninite in bright red rims occurs also in feldspar. Patches of coarse grained phosphates, titanite and molybdenite cluster around biotite. Secondary quartz and uranyl-bearing minerals crystallized in numerous fractures. This biotite syenite has a chemical composition similar to that of the adjacent xenolith, but contains less silica and more alumina, ferric

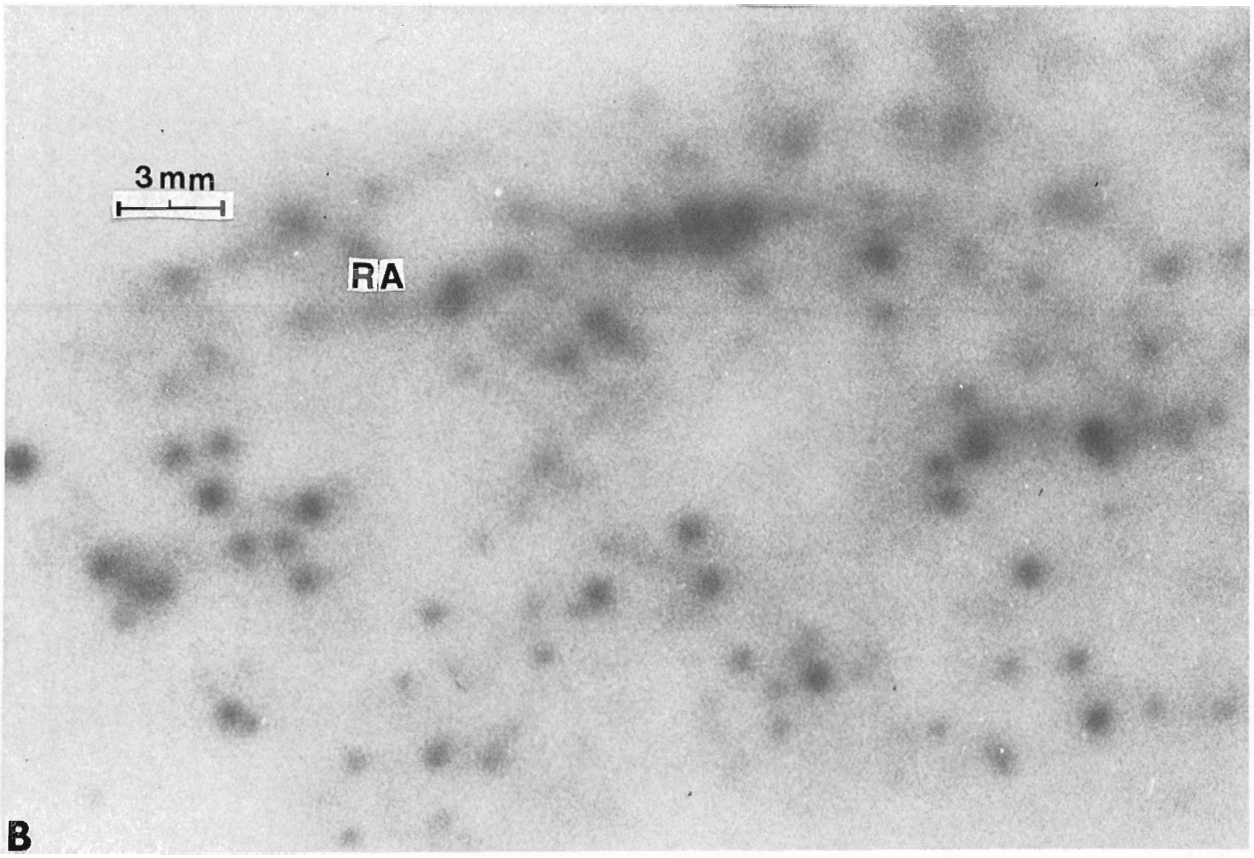

Figure 17.2B. *Autoradiograph of polished thin section in Figure 17.2A, showing distribution of single strongly and moderately radioactive spots (black and grey); clusters of strongly and weakly radioactive spots; and of fractures filled with secondary mineral aggregates (RA).*

iron and sodium, due to abundant biotite, plagioclase and albite. The syenite contains 2390 ppm U, apparently reflecting the third stage of uranium enrichment.

Unit 4: Microcline Pegmatite, Table 17.1.9

South of the xenolith, the pegmatitic biotite syenite grades within a few metres to coarse grained leucocratic pegmatite. The microcline has a patchy appearance, encloses partly resorbed plagioclase grains and is veined by irregular bands of albite, types V-13 and V-14 (Rimsaite, 1967, Pl. II). Locally, albite grains are replaced by quartz and/or muscovite and grade to myrmekite towards their edges. One grain of uraninite was found at the grain boundaries between microcline and quartz. The pegmatite differs from the adjacent syenite by the higher content of potassium and silica and by lower concentrations of alumina, calcium, iron, phosphorus, uranium and water. The porphyroblastic microcline pegmatite is biotite-poor and contains only 8.6 ppm U.

Unit 3-4: White Quartz-feldspar Granite and Pegmatites, Table 17.1.10, 11, 12

On the north side of the xenolith, the adjacent pegmatitic granite is made up of altered plagioclase and disseminated biotite that represent paleosome or older parts of the rock, partly replaced by patches and veins of quartz and interstitial microcline that represent neosome or younger parts of the rock. Plagioclase is coated and partly replaced by green chlorite and muscovite. Biotite is overgrown by muscovite. Accessory and radioactive minerals crystallized at the contact of paleosome and neosome portions of the rock. Uraninite grains in orange rims alter to secondary uranyl-bearing minerals. Coarse grained pegmatitic patches are similar in chemical composition to the finer grained host biotite granite but contain less uranium. Paleosome portions of the rock consist of altered lamellar plagioclase, type IIKn:FP, the coarser lamellae being replaced by green chlorite aggregates, derived from decomposed ferromagnesian minerals. The neosome portions that engulf the paleosome are made up of microcline perthite porphyroblasts and quartz. Biotite laths are almost entirely replaced by muscovite and most of the uraninite grains are replaced by alteration products. Remnants of characteristic brightly coloured rims that commonly surround uraninite and uranothorite, provide evidence of the original presence of the primary radioactive ore minerals. The partly destroyed biotite and uraninite grains indicate that early formed minerals alter and much of the uranium is liberated during crystallization of late pegmatitic phases. Depending on the proportions of paleosome and neosome components in the pegmatite, ratios of K/Na and Na/Ca vary. Neosome minerals, listed in approximate order of crystallization are: microcline, quartz, muscovite, chlorite, sericite and albite. Depending on the differentiation stage of the pegmatite, the dominant pegmatitic mineral is plagioclase, microcline, quartz or albite. The albite has Na/Ca ratio of ten or more and replaces preexisting minerals. Similar petrochemical and mineralogical trends in evolution of pegmatites have been described for other zoned pegmatites in the Grenville structural province (Rimsaite, 1968). However, in the Baie-Johan-Beetz area, the pegmatitic differentiation is less

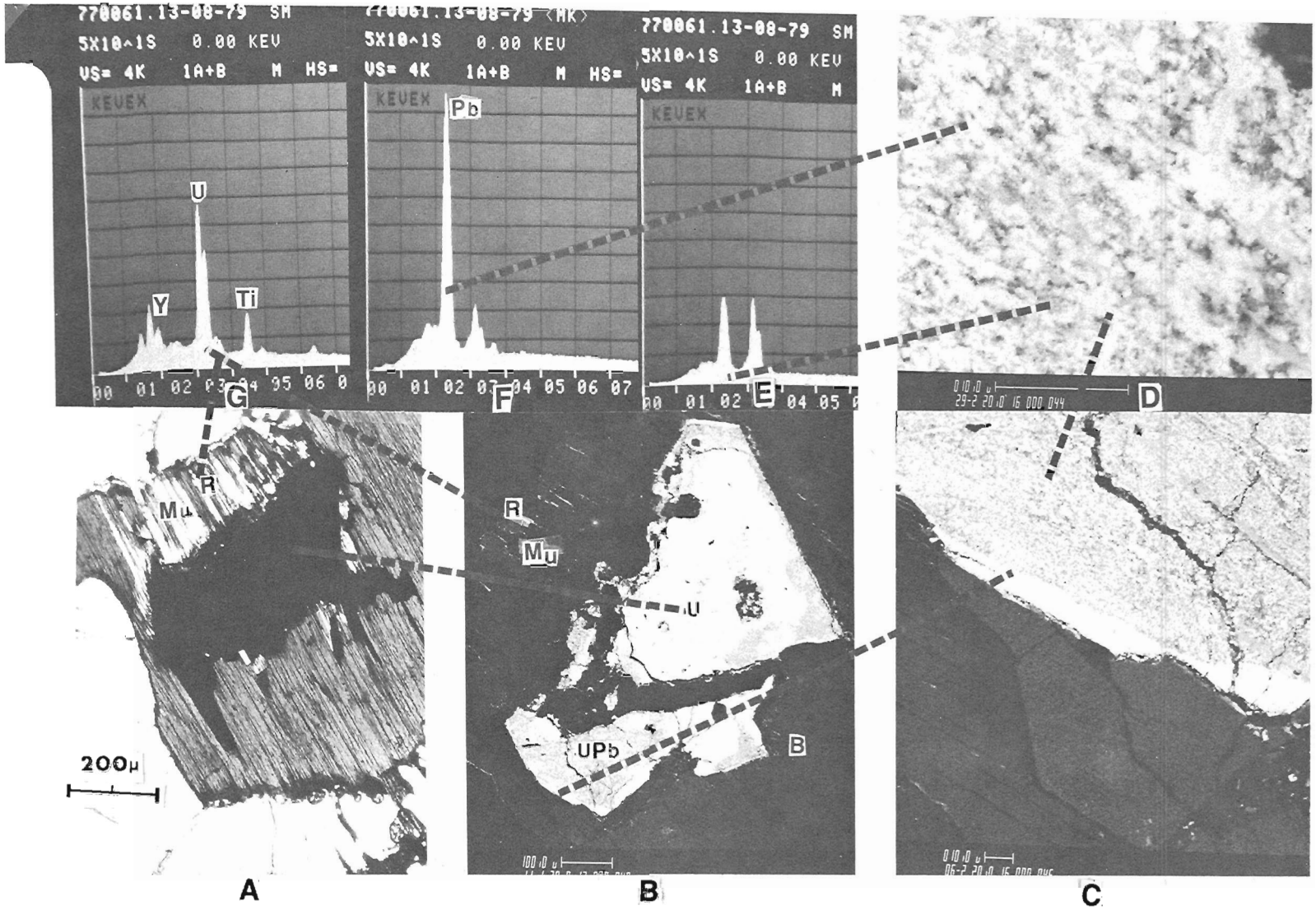

A. *Photomicrograph of uraninite grain (black) in biotite (streaky grey). The biotite is partly replaced by muscovite (Mu) along 001 fractures. Radioactive coatings (R) crystallize at the biotite-muscovite contact.*

B. *Backscattered electron image (BEI) of uraninite in Figure 17.3A. The uraninite (U) is replaced along the periphery by unidentified uranium-lead compounds (UPb).*

C. *BEI of the altered edge of uraninite at the ten times higher magnification than in Figure 17.3B.*

D. *Mottled unidentified U-Pb and Pb-rich phases replacing uraninite.*

E and F. *Energy dispersive spectra of spots in Figure 17.3D. Enlarged area from Figure 17.3C.*

G. *ED spectrum of U, Ti, Y-bearing fracture fillings at the contact between biotite and muscovite in Figure 17.3A. Dashed lines connect the spot analyzed and corresponding spectrum.*

Figure 17.3. *Illustration of uraninite at the contact between biotite and muscovite. GSC 203532-T*

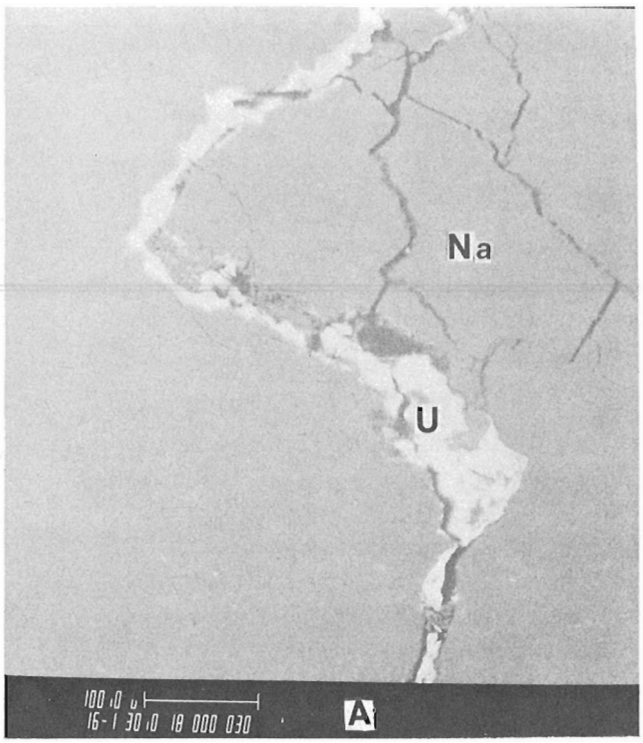

A. *BEI of uranophane (U) at the contact of plagioclase (Na) and quartz (black).*

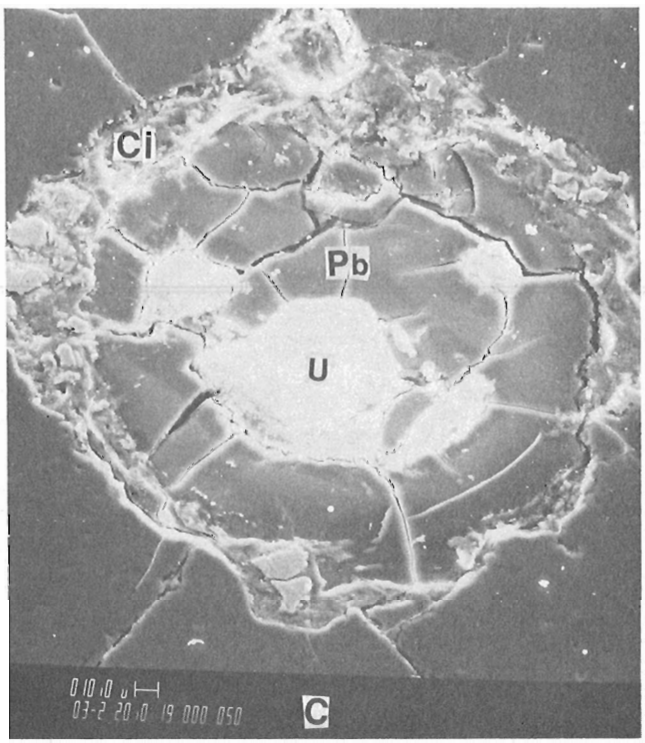

C. *BEI of uraninite remnants (white) replaced by anglesite (Pb) traversed by mudcracks, all surrounded by chlorite-like rim (Cl).*

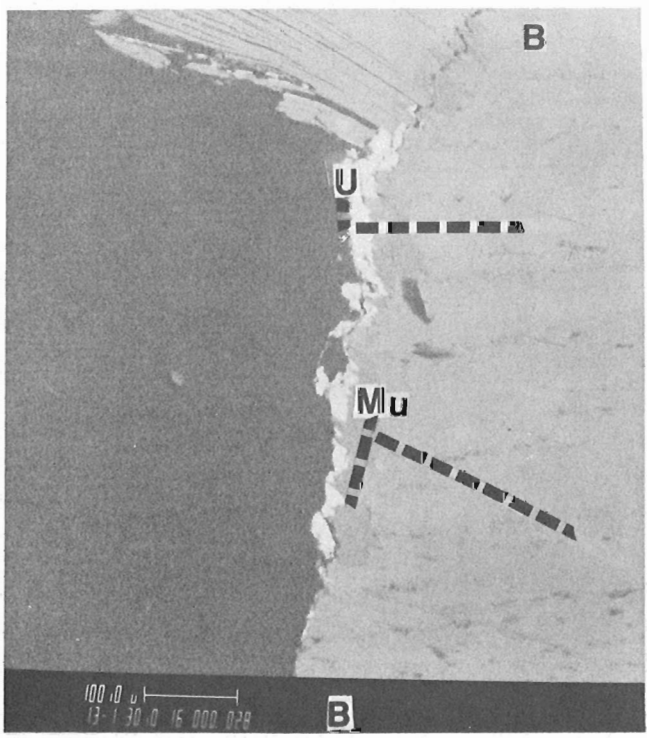

B. *BEI of uraniferous fracture fillings at the contact between biotite (B) and quartz (black). The uraniferous material is surrounded by muscovite (Mu). Analyzed grains are marked with a dotted line.*

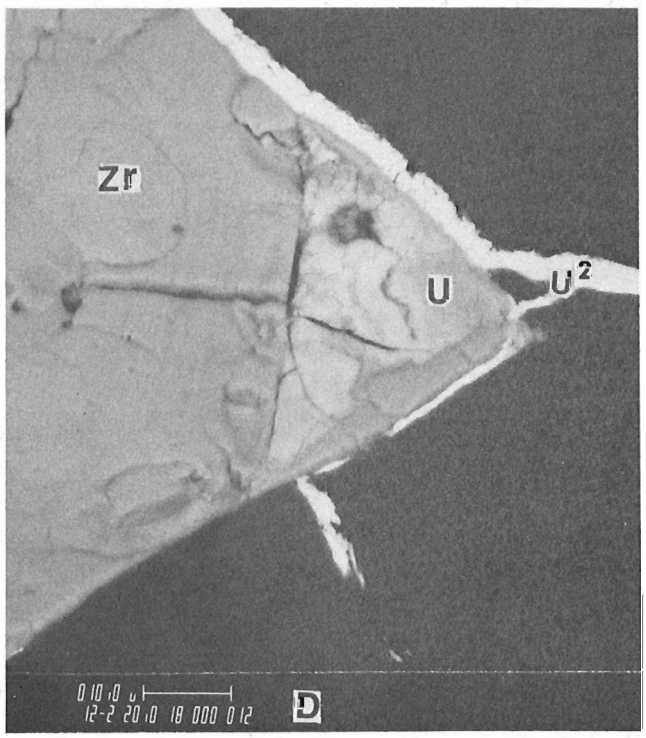

D. *BEI of zircon (Zr) overgrown by uraniferous phase (U) in fractures filled by secondary uranyl-bearing aggregates (U^2).*

Figure 17.4. *Radioactive fracture fillings, reactions between altered zircon and uranium and remnants of uraninite replaced and surrounded by anglesite and chlorite. GSC 203577-Y*

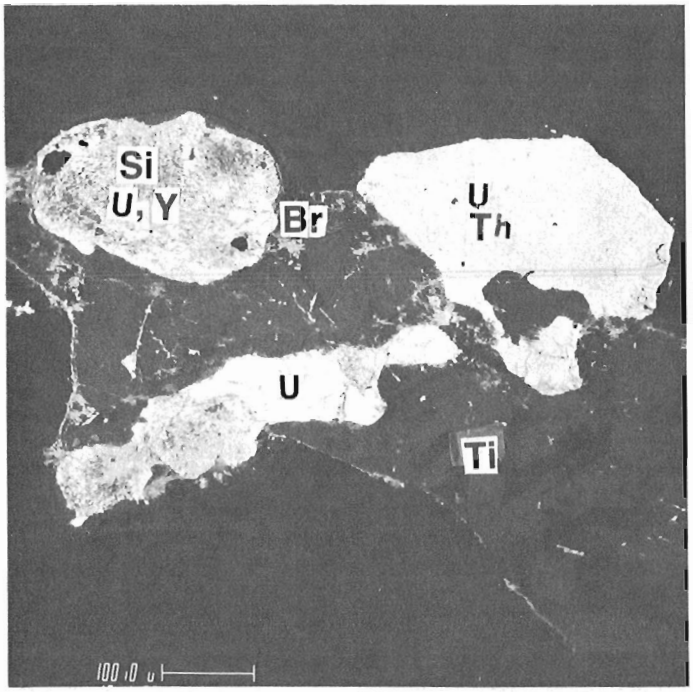
Si
U, Y
Br
U
Th
U
Ti

A

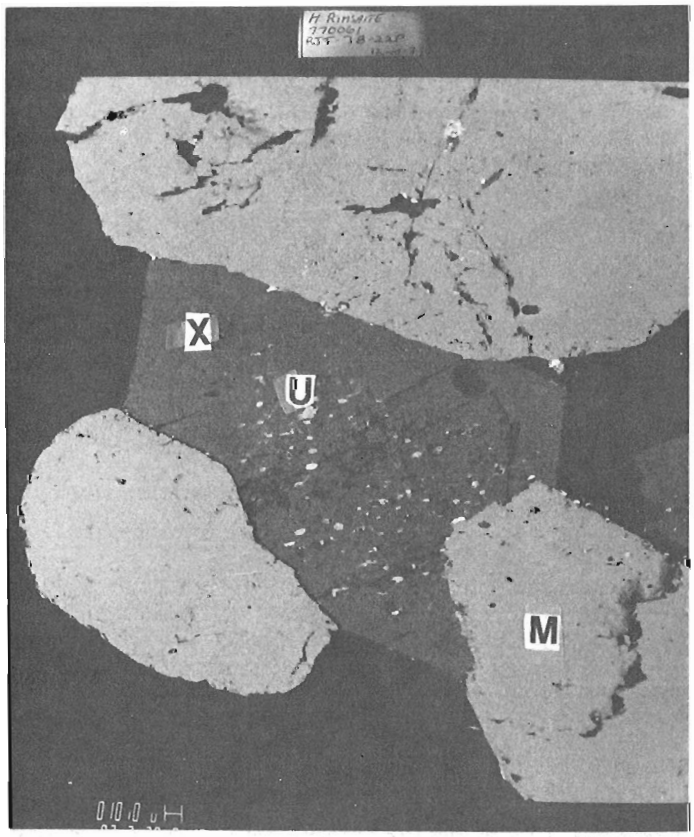
X
U
M

B

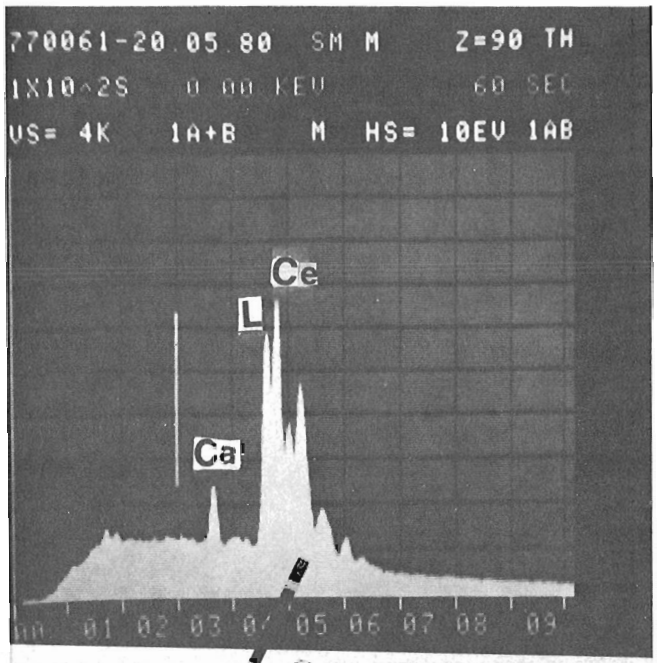
770061-20.05.80 SM M Z=90 TH
1X10^2S 0.00 KEV 60 SEC
VS= 4K 1A+B M HS= 10EV 1AB
Ce
L
Ca
01 02 03 04 05 06 07 08 09

D

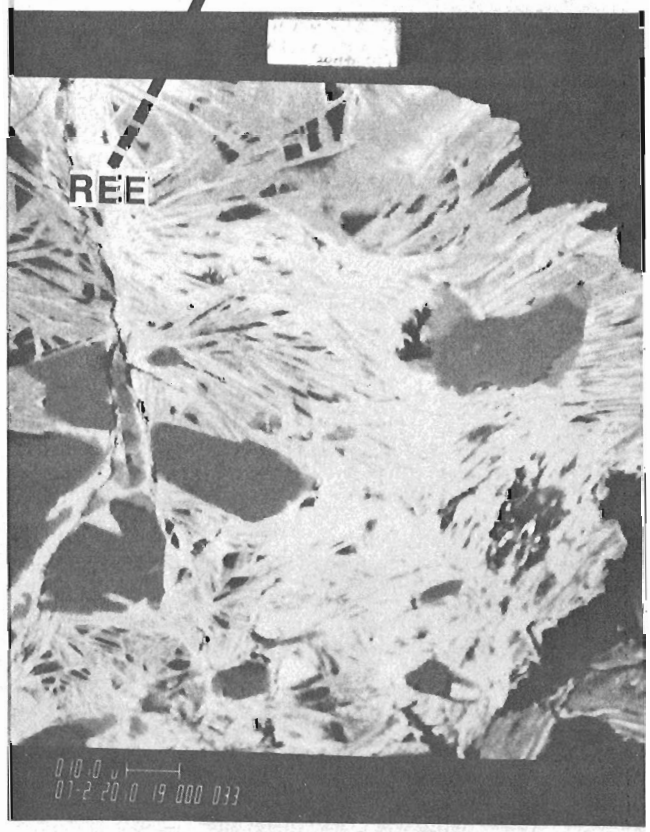
REE

C

obvious because of the presence of paleosome remnants and several generations of feldspars and quartz in the same rock. Quartz occurs in several generations, the youngest being represented by micrographic and poikilitic intergrowths with albite, type VIQ:FP (Rimsaite, 1967, Pl. VI-16) and by quartz veins transecting all minerals. During the replacement of paleosome components by microcline, muscovite, chlorite, albite and quartz, some of the uraninite crystals also alter and the liberated uranium either remains in altered grains, being fixed in secondary minerals, or is removed. Examples of quartz-rich radioactive pegmatites having variable proportions of paleosome and neosome components, variable K/Na and Na/Ca ratios, and abundant secondary uranyl-bearing phosphates and silicates, provide analyses 11 and 12 in Table 17.1, and analyses in Table 17.2.

Unit 4: Quartz-rich Granite Pegmatite, Table 17.1.13

The rock represents the quartz-rich portion of the pegmatite (SiO_2 = 82.8 wt. %). The paleosome remnants are made up of altered lamellar plagioclase, Type II, and neosome of porphyroblastic microcline perthite, enclosed in quartz. Biotite is altered to chlorite and muscovite, and locally coated with iron oxides. The ratio K/Na is close to 1, and Fe^{III}/Fe^{II} is 2.7. Ferric iron crystallized in mineral fractures giving this rock red coloration. Most of the original uraninite grains are altered and part of liberated uranium is fixed in secondary uranium minerals that crystallize in altered biotite. Rims enclosing remnants of uraninite grains consist of Fe-rich chlorite-like aggregates and uraniferous clays enclosing disseminated specks enriched in several metals: Cu, Mn, Ni, Fe, Sn and Zn. Although some of the uranium was lost, this altered quartz pegmatite contains 538 ppm U.

Unit 4: Late Albite Pegmatites, Table 17.1.14, 15

Coarse grained leucocratic pegmatites occupy large areas north of Turgeon Lake. Red pegmatite transecting metagabbro is similar in chemical composition to the leucocratic albite pegmatite but contains more ferric iron that gives a red colour to the clouded feldspar crystals. The leucocratic pegmatite is made up almost entirely of neosome minerals: albite-veined microcline perthite, enclosed in quartz and albite, and a few remnants of plagioclase, feldspar Type IV (Rimsaite, 1967, Pl. II, IV-10, IV-12). Muscovite replaces biotite and is in turn replaced by iron and titanium oxides. This late stage pegmatitic phase has only 2.8 ppm U.

The red pegmatite has a few mineralogical features related to host metagabbro, namely, patches of epidote, apatite and titanite and abundant specks of iron and titanium oxides in feldspar and quartz. Patches of red albitized plagioclase and remnants of chloritized biotite are replaced by muscovite. The red pegmatite veins, up to ten centimetres wide, contain more uranium (9.5 ppm) than the host metagabbro (1 ppm U).

Rocks Containing More Than 250 ppm U (Potential Ore Grade Mineralization)

White and red pegmatitic syenites and granites locally contain marked concentrations of uranium. The first type, white radioactive syenite pegmatites, crop out in N80°E direction from swampy terrains underlain by quartzite, Figure 17.1, area E. These pegmatites contain biotite-rich xenoliths and vary in grain size, grading from gneissic biotite syenite to leucocratic pegmatite. The leucocratic pegmatites studied include those east of Johan Beetz village, in Grandroy mine, northeast of Turgeon Lake, and north of Baie Pontbriand. The plagioclase-rich radioactive pegmatites grade to less radioactive microcline-quartz-albite pegmatites (compare analyses 8 and 9 in Table 17.1 and analyses 20 and 21 in Table 17.2). The characteristic petrochemical and mineralogical properties of these syenitic rocks are: high proportion of plagioclase resulting in moderate silica and high alumina concentrations, the ratio Na/Ca of 6 or less and Na/K of > 1 (Table. 17.1.8, 10, 11, 12 and Table 17.2.20, 24). In these rocks, iron is present mainly in biotite and the high Fe^{II}/Fe^{III} ratio of > 2 and scarce disseminated iron oxides result in their leucocratic appearance. Radioactive minerals crystallized in biotite and at the contact between paleosome (older parts) and neosome (younger parts) of the rock, Figure 17.2a.

The other type of radioactive pegmatite, ranging in width from 20 cm to 5 m, occurs within the Turgeon Lake granite (Fig. 17.1). These red granitic rocks are made up of variable proportions of neosome and paleosome components and consequently differ in the abundance of plagioclase, microcline, quartz and albite. In the red pegmatites much of the iron is dispersed as ferric oxide throughout the altered paleosome portions and in fractures, and their Fe^{II}/Fe^{III} ratio is commonly < 1. Red radioactive rocks, made up of plagioclase, blue-red peristerite, less abundant microcline and quartz, and variable quantities of biotite, muscovite, pyrite, magnetite and titanium oxides, occur northwest of Turgeon Lake and east of Roston Lake (not named in Fig. 17.1), and areas A, AB, D and D1 (Fig. 17.1). In the Turgeon Lake granite, between Roston Lake and Little Piashti Lake, radioactive rocks reflect redistribution of elements during evolution of the pegmatite and, with increasing differentiation and increasing proportion of neosome components, show the following petrochemical trends: peristerite-rich pegmatitic granite grades to microcline pegmatites and to quartz- and albite-rich rocks (compare analyses of adjacent rocks: 24, 26, 27 and 28 in Table 17.2, and analysis of quartz-rich rock 13 in Table 17.1). Radioactive minerals commonly occur at the contact between paleosome and neosome portions of the rock and their U/Th ratio depends on the degree of alteration of the original minerals and on fixation of uranium and lead in secondary minerals. The red radioactive rocks and their primary radioactive minerals are partly to completely altered. The last two analyses in Table 17.2 represent Ti-rich pegmatites. In potassium-rich microcline pegmatite most of the uranium is in pyrochlore. The Na-rich pegmatite consists of altered feldspar, accessory magnetite, recrystallized TiO_2 aggregates and patches of monazite. Remnants of characteristic rims around the altered uraninite or uranothorite grains are scattered near magnetite crystals. This pegmatite contains more thorium than uranium. The uraninite grains became altered and the uranium was removed during sericitization and albitization of plagioclase. The thorium-rich monazite apparently survived the alteration and retained its thorium (last analysis in Table 17.2; note relatively high water content in this altered rock).

Figure 17.5

Relationships between uranium, thorium and titanium minerals; monazite and xenotime with radioactive minerals in the core, and secondary REE minerals. GSC 203414-M

A. *BEI of acicular titanium oxide aggregates (Ti) in intergrowths with uraninite (U), uranothorite (UTh) and altered Si, U, Y-bearing grains. Fine grained, needle-like aggregates consist of U and Ti and resemble in chemical composition brannerite (Br). White coatings on Ti blades consist also of Ti-U compounds.*

B. *BEI of monazite (M) and xenotime (X) intergrowths. The xenotime contains disseminated U (U) and Th grains in the centre.*

C. *BEI of radiating secondary REE aggregates formed from altered monazite and xenotime.*

D. *ED spectrum of REE mineral aggregates in Figure 17.5C.*

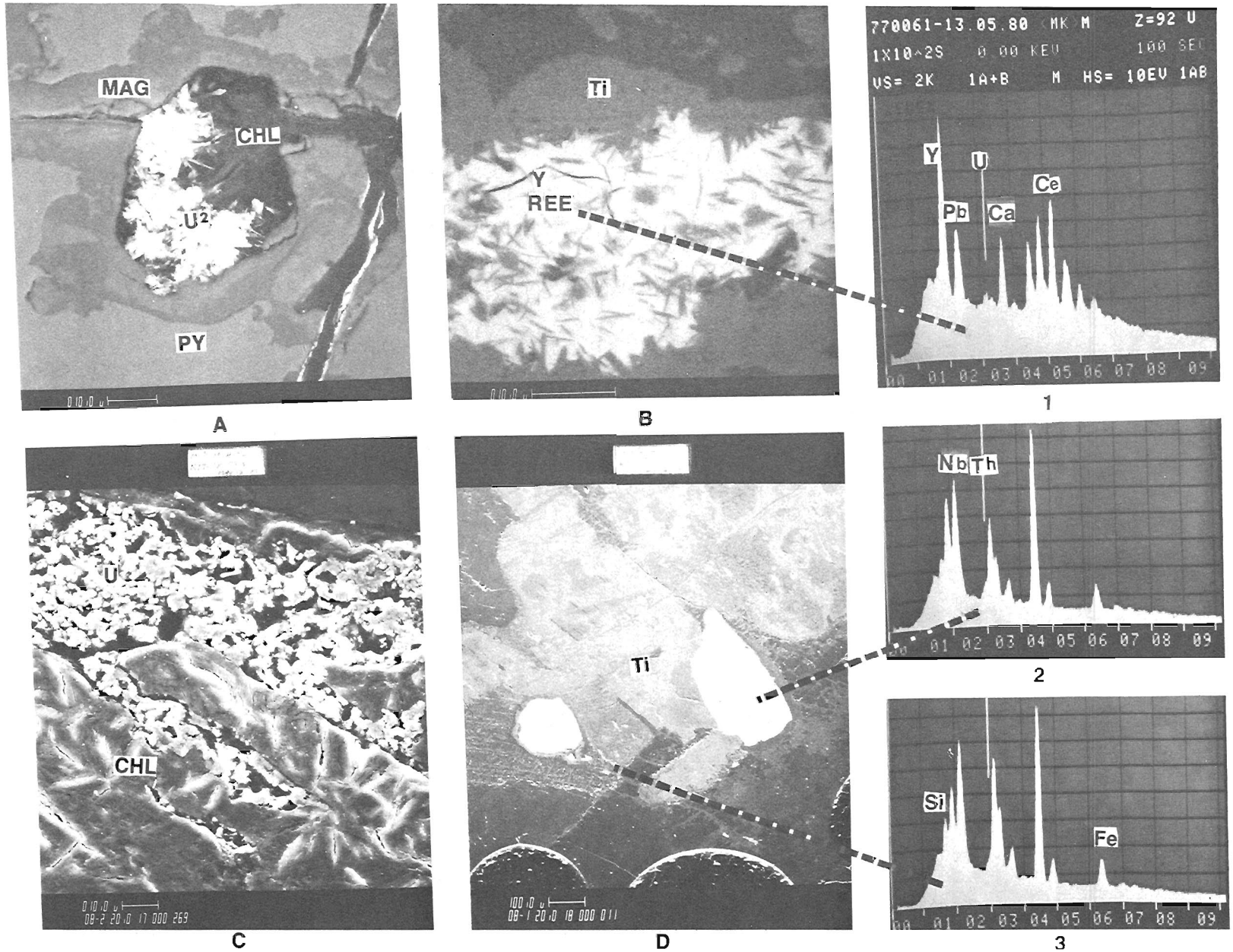

A. BEI of altered pyrite (PY) replaced by magnetite (MAG), chlorite (CHL) and secondary uranyl-bearing aggregates (U^2) along fractures.

B. BEI of altered acicular REE-bearing mineral (Y, REE, spectrum 1) in altered Ti-bearing grains (Ti).

C. BEI of altered uraninite (U) that crumbles into small white fragments and is partly replaced by chlorite (CHL).

D. Altered prisms of Ti minerals associated with white titaniferous pyrochlore-like grains (ED spectra 2 and 3).

Figure 17.6. *Relationships between iron, titanium, uranium and secondary REE minerals. GSC 203577-N*

Mineralogy

Minerals identified in the present study, listed in order of apparent sequence of crystallization, are as follows:

Rock-forming minerals: hornblende; biotite (Fig. 17.3a); plagioclase (Fig. 17.4a); antiperthite; perthite; microcline; quartz; albite; myrmekite; muscovite. The complex feldspar intergrowths and replacement textures observed in the present study are referred to similar heterogeneous feldspars described and illustrated by Rimsaite (1967).

Fracture-fillings and secondary minerals: epidote; chlorite; serpentine; stilpnomelane; sericite; quartz; kaolinite; hematite; goethite; calcite; barite; anglesite; fluorite.

Accessory and radioactive ore minerals: Pyrite, FeS_2; chalcopyrite $(Cu,Fe)S_2$; molybdenite, MoS_2; arsenopyrite, FeAsS; magnetite, $FeO{\cdot}Fe_2O_3$ (Fig. 6a); ilmenite, $FeO{\cdot}TiO_2$; titanite, $CaO{\cdot}TiO_2{\cdot}SiO_2$; rutile and other Ti oxides, TiO_2; galena, PbS; sphalerite, ZnS; apatite, $(Ca,F)Ca_4(PO_4)_3$; monazite $(Ce,La,Di,Th){\cdot}PO_4$; xenotime, YPO_4; garnet, $(Mn,Fe)_3Al_2(SiO_4)_3$; tourmaline $(Mg,Fe,Ca)(B{\cdot}OH)_2Si_4O_{19}$; zircon, var. cyrtolite, $ZrSiO_4$; allanite, $(Ca,Fe)_2(Al,OH)(Al,REE,Fe)_2(SiO_4)_3$.

Radioactive ore minerals: uraninite, UO_2; uranothorite, $(U,Th)SiO_4$; thorite, $ThSiO_4$; thorianite, $(Th,U)O_2$; pyrochlore $(Na,Ca,U)(Nb,Ta,Ti)_2O_6(OH,F,O)$; brannerite, $(U,Th,Ca,REE)(Ti,Fe^{II})_2O_6$ (Fig. 6a); samarskite, $(Fe,Ca,UO_2)(Y,Ce)Nb_6O_{21}$; coffinite, $USiO_4$; kasolite, $Pb(UO_2)SiO_4$; uranophane, $CaO{\cdot}2UO_3{\cdot}2SiO_2{\cdot}7H_2O$; boltwoodite, $K_2H_2(UO_2)(SiO_4)_2{\cdot}4H_2O$ (Fig. 7); autunite, $Ca(UO_2)_2(PO_4)_2{\cdot}10H_2O$; torbernite $Cu(UO_2)_2(PO_4)_2{\cdot}8\text{-}12H_2O$; phosphuranylite $Ca(UO_2)_3(PO_4)_2{\cdot}6H_2O$.

Unidentified secondary radioactive compounds in mineral and fracture coatings, recorded in energy dispersive (ED) spectra and listed in order of decreasing intensities of element peaks:

In rims of uraninite:

1. U = Pb (around uraninite remnants, ED spectrum in Fig. 17.3E);
2. Fe, Si, trace Al, Mg (common rims on uraninite and in magnetite fractures);
3. U = Th, Si, Y, trace Pb;
4. specks within rims around uraninite containing high concentrations of the following elements: As, Ba, Mn, Mo, REE, Sn, Th, U, W, Zn, Ni, V.

Fracture coatings:

1. U, Ti, Si, Y, Al, Fe (between muscovite and biotite, ED spectrum in Fig. 17.3G);
2. U, Si, P, Fe, Ca (in uraninite fractures);
3. Pb, U, Si (in biotite fractures);
4. U = Si, Y, Th, Pb (in uraninite fractures);
5. Ti, U = Si, Pb, Fe = Ca (in rutile fractures);
6. Th, U, Si, P (in Fe-rich crusts);
7. U, Si, Zr = Fe, Th, Ca (in fractures of Fe-rich "thorogummite");
8. U = Th, Si, Zr, Pb, Fe (in fractures surrounding altered zircon grains);
9. U, Si, Pb = Ti, Th = Zr, Al = Fe (in biotite adjacent to uraninite and zircon).

Pseudomorphous replacements of U, Th and REE minerals:

1. Si, Y = Th = U;
2. Y, Si, U;
3. Th, Si, U;
4. U = Pb, Si, Fe, Al, P (ED spectrum in Fig. 17.7D);
5. Y, Ce, Ca = Pb, Ti (ED spectrum in Fig. 17.6.1);
6. Si, Zr, U (uraniferous compound replaces zircon along the edges, Fig. 4D).

These secondary compounds provide information on the chemical environment and associated elements during fixation of uranium liberated from primary minerals and its reactions with other liberated ions, such as Ti, Zr, REE, Si and others.

Mode of Occurrence of Radioactive and Accessory Minerals in Relation to the Petrochemical Evolution of Host Rocks

Autoradiographs of mineralized rocks show the following five types of radioactive ore minerals, Figure 17.2b:

1. strongly radioactive minerals (black single spots);
2. moderately radioactive minerals (grey single spots);
3. associations of strongly and moderately radioactive minerals;
4. radioactive fracture fillings (grey streaks); and
5. secondary radioactive minerals (grey hazy areas).

1. Strongly Radioactive Minerals (Fig. 17.3, 4)

In white pegmatites made up predominantly of plagioclase and less abundant microcline, quartz, albite, biotite and muscovite, uraninite crystals occur in biotite at the boundary with muscovite that replaces the biotite (Fig. 17.3A). Round uraninite grains, surrounded by prominent orange coloured rims, commonly all enclosed in muscovite, occur singly in fractures and interstices between clouded plagioclase-rich paleosome and clear neosome portions of the syenite, Figure 17.2a. The transition stage biotite-muscovite represents an important change in composition of mineralizing solutions, apparently coinciding with the marked decrease of fluorine content. The biotite contains five times more fluorine than does associated muscovite (Table 17.2.17, 18), indicating increase of hydrous activity and decrease of fluorine during crystallization of the muscovite. The uraninite crystallized after the biotite and before muscovite. The fluorine that might have kept uraninite in solution was consumed by the biotite, and the change in pH apparently was sufficient to precipitate uranium as uraninite. Biotite and part of uraninite grains were affected by alteration during latest stages of pegmatitic activity. Biotite altered to chlorite and uraninite grains were partly replaced by REE, Pb-rich or Th-bearing phases.

2. Moderately Radioactive Minerals (Fig. 17.5)

In Baie-Johan-Beetz area, xenotime, monazite, allanite and pyrochlore contain variable quantities of U and Th in their structures and in minute inclusions (Fig. 17.5B). The phosphates crystallized in biotite and/or around biotite and plagioclase crystals. Pyrochlore grains in prominent black or orange rims commonly occur in microcline and quartz-rich granite pegmatites, Table 17.1.13 and Table 17.2.28. The major stage of pyrochlore crystallization coincides with the transition of microcline to albite during the late phase of pegmatitic evolution. The pyrochlore is surrounded by albite envelopes. Similar relationship between microcline, albite and euxenite exists in the Wakefield pegmatite, Quebec (Robinson et al., 1963).

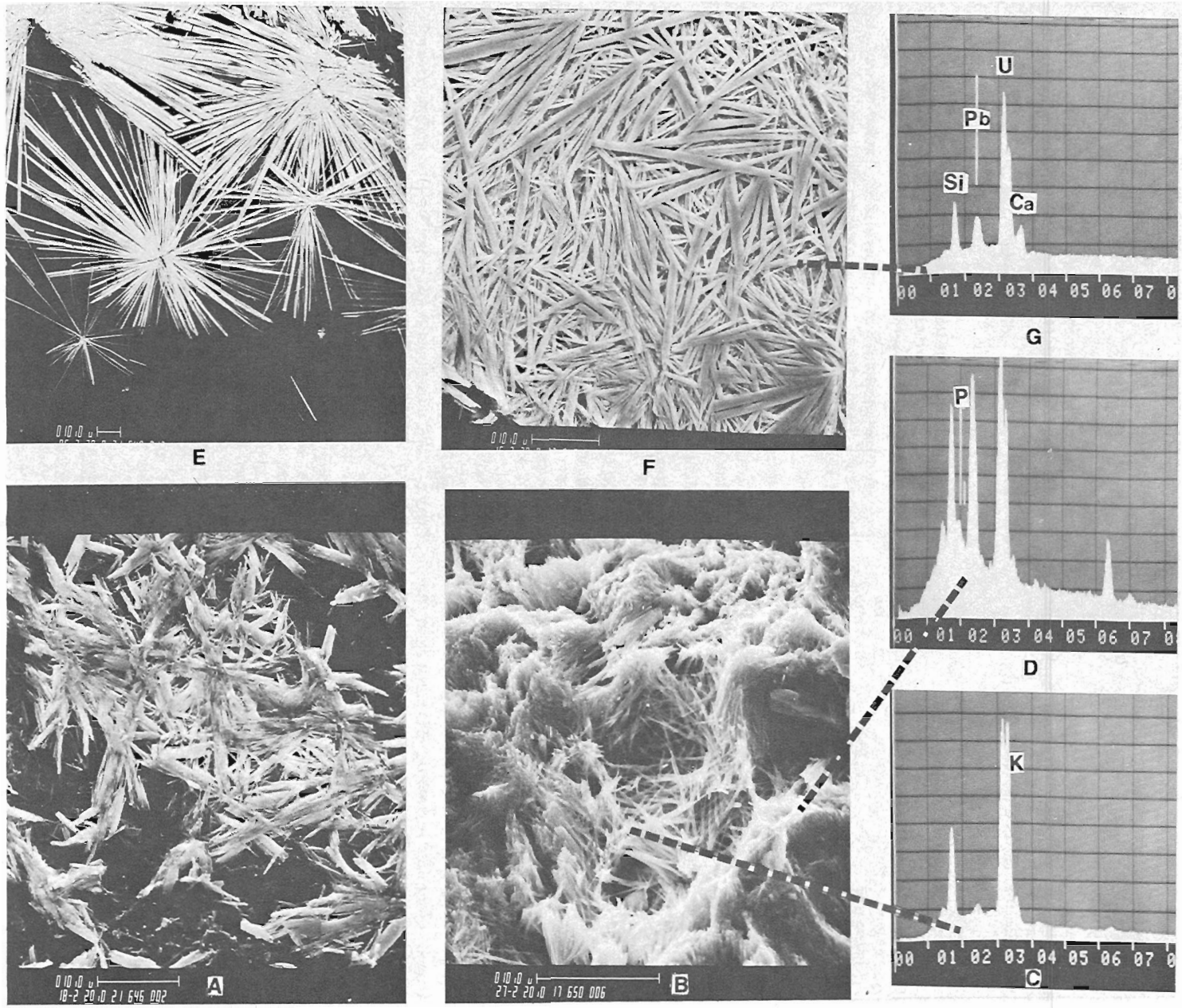

A and B: *BEI of boltwoodite (ED spectrum in Fig. C) in intergrowths with unidentified Pb-rich fibrous aggregates (ED spectrum in Fig. D).*

E and F: *BEI of radiating uranophane aggregates (ED spectrum in Fig. G).*

Figure 17.7. *Secondary uranyl-bearing mineral aggregates. GSC 203577-D*

3. Associations of Strongly and Moderately Radioactive Minerals (Fig. 17.5, 6)

Strongly and moderately radioactive minerals occur in groups surrounding biotite, magnetite, Ti-oxides or altered plagioclase-rich paleosome portions of the pegmatite. The common mineral associations of uraninite and uranothorite are with phosphates, zirconium, iron sulphides and oxides, titanium and REE-bearing minerals. Figure 17.5A provides an example of an association of accessory and radioactive ore minerals. Ti-oxide aggregates recrystallized in quartz are intergrown with uraninite, uranothorite, zircon and altered unidentified (Si,U,Y)-bearing grains. All minerals are partly altered. The uraninite is veined and partly replaced by a complex (U, Si, Pb, Ce, Fe, La, Y)-bearing phase. The replacement of uraninite along fractures results in liberation and partial loss of the uranium.

4. Radioactive Fracture Fillings (Fig. 17.4)

Early crystallized minerals become unstable during crystallization of late pegmatitic minerals. Biotite alters and is partly replaced by muscovite, deuteric(?) chlorite and quartz. Plagioclase becomes clouded by fine grained aggregates of sericite, chlorite, epidote and iron oxides, and is partly replaced by patches of microcline, quartz, muscovite and albite. Clear albite and myrmekite rims overgrow and partly replace altered plagioclase. Uraninite grains are veined by late Th- and REE-bearing phases and locally are replaced by muscovite, chlorite or uraniferous clay (Fig. 17.6C). Part of the uranium and radiogenic lead, liberated during these replacements, recrystallized in mineral fractures or along the boundaries between neosome and paleosome portions of the radioactive rock (Fig. 17.4A,B,D). The uranium reacts with lead, silica, titanium, phosphorus and other liberated ions and reprecipitates in complex secondary compounds in a chemically favourable environment. Partly altered micas provide suitable conditions for crystallization of U, Ti, Si, Y and Zr compounds (Fig. 17.3G); the interstices and fractures between early crystallized biotite or plagioclase and late formed quartz provide a favourable environment for crystallization of uranyl-bearing silicates (Fig. 17.4A,B,D); and interstices between rutile and quartz are filled with (Ti, U, Si, Pb, Fe, Ca)-bearing crusts. Coffinite, kasolite, uranophane and autunite are the most common fracture fillings between neosome and paleosome portions of the rock. Qualitative compositions of fracture coatings identified in this study are summarized in the previous section on "fracture coatings".

5. Secondary Radioactive Aggregates (Fig. 17.6, 7)

Most of the strongly radioactive spots on the autoradiograph are surrounded by hazy haloes produced by secondary radioactive mineral aggregates. The secondary radioactive minerals include uranyl- and REE-bearing compounds formed in an oxidizing environment (Fig. 17.6, 7). Depending on weathering conditions and on type and nature of ions available for reactions with mobilized uranium, the uranium reprecipitates as kasolite, uranophane, boltwoodite or Pb-rich unidentified mineral aggregates in form of radiating needles or acicular crystals (Fig. 17.7). The secondary uranyl-bearing aggregates pseudomorphously replace original grains of uraninite, zircon and other minerals, or precipitate in fractures and vugs (Fig. 17.4D, 17.6A). The phosphates also alter to acicular mineral aggregates that consist of Y, Ce, Pb, Ca and U, or predominantly of REE and Ca (Fig. 17.5C, spectrum 5D; Fig. 17.6B, spectrum 1).

Alteration of Radioactive and Accessory Minerals and Complex Secondary Compounds

In the thin sections (Fig. 17.4, 5, 6 and 7) examined, early-formed minerals are partly to completely altered to secondary mineral aggregates during the late stage of pegmatitic differentiation and/or in the oxidizing environment during weathering. The most prominent chemical trend of alteration of strongly radioactive samples is the enrichment in radiogenic lead resulting from the replacement of uraninite by Pb-rich secondary compounds. The uraninite grain in Figure 17.3 is corroded and partly replaced by unidentified Pb-rich and Pb-U intergrowths. At least half of the uraninite grain is replaced by Pb-rich material. Uraninite in Figure 17.4C also altered to Pb-rich material, anglesite and unidentified U-Pb compounds that are transected by shrinkage cracks. Only about 20% of the original uraninite remained after the replacement. Isotopic analysis of uraninite from the Baie-Johan-Beetz area yielded the following isotopic ratios: $^{207}Pb/^{235}U = 1.922$; $^{206}Pb/^{238}U = 0.1931$; $^{208}Pb/^{232}Th = 0.04109$ which fall above the concordia curve and provide the corresponding apparent discordant ages of 1138 Ma, 1088.8 Ma and 813.9 Ma (Cumming, 1979). This uraninite contains 0.39% common Pb, indicating that the excess of radiogenic lead accounts for the high Pb/U isotopic ratios.

Partly altered U-Th and Ti-bearing grains in Figure 17.5A released U, Ti, and Th which reacted together and formed acicular aggregates that yielded ED spectra of U and Ti similar to brannerite. The "Pronto reaction", or reaction between U and Ti, suggested by Ramdohr (1957), was recently studied by Ruhlmann (1980) in rocks from metamorphic terranes using the scanning electron microscope. Ruhlmann found that brannerite is unstable under anatectic conditions and at high temperature breaks down to uranium and titanium oxides. In the example from the Baie-Johan-Beetz area, the brannerite-like acicular aggregates are secondary and account only for a small proportion of the uranium and titanium liberated from adjacent altered uraninite and rutile. Other reactions between U and Ti result in formation of complex Ti, U, Si, Pb, Zr, Th, Fe, Ca compounds discussed in the section on "fracture fillings".

Secondary uraniferous phosphates are abundant in Baie-Johan-Beetz area "E" and north of Turgeon Lake, area "AB". Torbernite, autunite and phosphuranylite form within and around altered intergrowths of monazite, xenotime, uraninite and uranothorite. Apatite is more resistant to alteration than monazite and xenotime, which commonly alter to acicular aggregates made up of REE and Ca, thus releasing phosphoric acid (Fig. 17.5C, 5D).

Pyrochlore and Ti, Nb, U, Si, Ta, Fe-bearing grains, associated with TiO_2 aggregates are illustrated in Figure 17.6D, spectra 6-2 and 6-3.

Zirconium-uranium reactions are illustrated in samples from Grandroy mine, northeast of Turgeon Lake (Fig. 17.4D). The euhedral zircon, made up of a core of several zoned crystals overgrown by a Zr-Si-U phase, occurs in fractures filled with uranophane and with Pb-rich kasolite-like mineral aggregates. The uraniferous zircons occur in fractured and altered portions of radioactive rock.

Red radioactive pegmatites are common in Turgeon Lake granite, in areas "AB", D and D1. These rocks contain pyrite, magnetite and titanite that oxidize and alter to hematite, Fe-rich chlorite, chert and Ti oxides, giving the rock a bright red and green appearance. The relationship between pyrite, magnetite, chlorite and secondary uranium mineral aggregates is depicted in Figure 17.6A. Pyrite oxidizes to magnetite; magnetite is fractured and alters to red iron oxides and green chlorite. Secondary uranium minerals crystallize in fractures and vugs, precipitating on

chlorite. The apparent association of iron oxides and uranium minerals in red pegmatites results from oxidation of the Fe-bearing minerals biotite, pyrite, magnetite and ilmenite. In such oxidized rocks, uraninite crystals are partly to completely replaced by secondary uranium minerals that are associated with secondary iron oxides. Part of the uranium is removed by aqueous solutions during oxidation, and this may result in an apparent enrichment in Th, which remains mainly in monazite, see last analysis in Table 17.2.

The Baie-Johan-Beetz area is characterized generally by a relatively high U/Th ratio in radioactive rocks (Table 17.2). The high U/Th ratio results from the abundance of pure uraninite and of Th-poor secondary uranyl-bearing minerals. The thorium is present in uranothorite, in monazite and in complex U-Th-REE compounds that replaced uraninite during late stages of pegmatitic activity.

Summary and Conclusions

The field observations and preliminary results of petrochemical and mineralogical studies of a few specimens from several sample collecting areas in Figure 17.1 can be summarized as follows:

1. The radioactive rocks containing more than 250 ppm U are scarce and widely dispersed in waste areas of less radioactive granitic rocks. The favourable rock types are:
   (a) white syenite pegmatites made up of predominant plagioclase and less abundant microcline, quartz and biotite, containing biotite-rich xenoliths and underlain by quartzite; and
   (b) red peristerite-bearing granitic rocks made up of variable proportions of plagioclase, K-feldspar, quartz and albite. Their U and Th content depends on preservation of primary radioactive grains in the paleosome component during crystallization of late pegmatitic phases and under weathering conditions.
2. The radioactivity results from the presence of primary and secondary radioactive minerals which are related to the petrochemical and mineralogical evolution of syenitic and granitic rocks and to the U and Th contribution by xenoliths and other preexisting rocks. The pegmatites are heterogeneous in grain size, mineralogical composition, type and size of xenoliths and in radioactivity. The poikilitic and granoblastic replacement textures and mineral associations suggest the following mineralogical evolution and petrochemical differentiation of the pegmatites, from the biotitic xenolith: radioactive fine- to medium-grained syenitic, plagioclase-rich biotite-bearing phase, followed by microcline porphyroblasts, grades to quartz- and albite-rich phases represented by albite-veined perthite and clear rims of albite and myrmekite on remnant plagioclase.
3. Crystallization of uraninite coincides with the transition of fluorine-bearing biotite to fluorine-poor muscovite, which suggests that the fluorine-rich phase has contributed to the enrichment and transportation of uranium in pegmatitic solution. The phosphate minerals are temporally and spatially related to uraninite. The pyrochlore crystallizes in association with microcline and albite, following crystallization of the uraninite. Primary radioactive minerals alter during late pegmatitic phases.
4. Many types of secondary radioactive compounds crystallize during chloritic (deuteric?) alteration and oxidation. The alterations involve replacements of uraninite by Th, REE and Pb-rich phases and by hydrous silicates, accompanied by losses of uranium and of radiogenic lead. The secondary mineral aggregates formed by reaction of the liberated uranium with other ions include U-Pb; U-Zr; U-Ti ("brannerite"); U-Ti-Si; U-P and many other complex unidentified compounds.
5. Pegmatitic differentiation and redistribution of elements during late hydrothermal phases and under weathering conditions account for variations in the U/Th ratio.
6. Textures and petrochemistry of original rocks are modified and masked by replacements and redistribution of elements during metamorphism and evolution of granitic and syenitic rocks. The hybrid rocks, made up of paleosome and neosome components within the "younger" syenites and granites are favourable lithological types for uranium mineralization. However, radioactivity markedly decreases in late porphyroblastic microcline-quartz-albite phases (Table 17.1.9). The source of radioactive elements could be biotite-rich xenoliths and reworked gneissic granite (Table 17.1.6).
7. Because of the excess of radiogenic lead indicated by the point above the concordia curve, the "chemical dating" using U/Pb ratios is not applicable to the Baie-Johan-Beetz area. More detailed isotopic dating is required to establish age relationships between various granitic rocks and diverse generations of radioactive minerals.

References

Baldwin, A.B.
1970: Uranium and thorium occurrences on the north shore of the Gulf of St. Lawrence; Canadian Mining and Metallurgical Bulletin, v. 63, p. 699-707.

Blais, R.
1955: Pashashibou area, Dracourt and Costebelle Townships, Saguenay County, Quebec; Quebec Department of Mines, Preliminary Report 316, 8 p.; map No. 1114.

Cooper, G.E.
1957: Johan Beetz area, Electoral District of Saguenay; Department of Mines, Quebec, Geological Report 74, 54 p.; map No. 1099.

Cumming, G.L.
1979: Isotope analyses for Geological Survey of Canada, Contract No. OSU78-00319. Final Report, March 15, 1979, 21 p. (Available from the author.)

Hauseux, M.A.
1976: Petrology and mineralogy of radioactive granitic rocks near Baie Johan Beetz, Quebec; unpublished M.Sc. thesis, McGill University, Montréal, Québec, 85 p.

1977: Mode of uranium occurrences in migmatite granite terrain, Baie Johan Beetz, Quebec; Canadian Mining and Metallurgical Bulletin, v. 70, No. 780, p. 110-116.

Leroy, J.
1978: The Margnac and Fanay uranium deposits of the La Crouzille District (Western Massif Central, France): Geologic and Fluid Inclusion Studies; Economic Geology, v. 73, p. 1611-1634.

Mackie, B.
1978: Petrogenesis of the Lac Turgeon Granite and associated uranium occurrences near Baie Johan Beetz, Quebec (Abstract); Economic Geology, v. 73, p. 1408.

Ramdohr, P.
1957: Die Pronto-Reaktion; Neujes Jahrbuch – Mineralogie Monatshefte, p. 217-222.

Rimsaite, J.
1967: Optical heterogeneity of feldspars observed in diverse Canadian rocks; Schweizerische Mineralogische und Petrographische Mitteilungen, v. 47/1, p. 61-74.

1968: Geochemistry, mineralogy and petrology of polymica rocks; XXIII International Geological Congress, v. 6, p. 45-66.

Rimsaite, J. (cont.)
1980a: Mineralogy of radioactive occurrences in the Grenville structural province, Bancroft area, Ontario: A Progress Report; in Current Research, Part A, Geological Survey of Canada, Paper 80-1A, p. 253-264.

1980b: Selected mineral suites and evolution of radioactive pegmatites in the Grenville structural province, Canada; 26^{e} Congrès Géologique International, Abstracts, v. III, p. 999.

Robinson, S.C., Loveridge, W.D., Rimsaite, J., and van Peteghem, J.
1963: Factors involved in discordant ages of euxenite from a Grenville pegmatite; Canadian Mineralogist, v. 7, part 3, p. 533-546.

Rose, E.R.
1979: Rare-earth prospects in Canada; Canadian Mining Metallurgical Bulletin, v. 72, No. 805, p. 110-116.

Ruhlmann, F.
1980: Quelques examples de relation uranium-titane; Bulletin Minéralogie, v. 103, p. 240-244.

Schimann (Cameron-Schimann), M.
1978: Electron microprobe study of uranium minerals and its application to some Canadian deposits; unpublished Ph.D. thesis, University of Alberta, Edmonton, Canada, 337 p.

18. **STUDIES ON URANIUM IN CANADA, 1980**

Project 750010

V. Ruzicka and A.L. Littlejohn[1]
Economic Geology Division

Ruzicka, V. and Littlejohn, A.L., Studies on uranium in Canada, 1980; in Current Research, Part A, Geological Survey of Canada, Paper 81-1A, p. 133-144, 1981.

Abstract

Research on and exploration for uranium in Canada during 1980 encompassed almost all environments thought to be favourable for uranium mineralization. The main attention was in areas favourable for occurrence of the unconformity-related deposits in Saskatchewan, Northwest Territories, and Quebec.

Preliminary results of the authors' own field and laboratory investigations indicate that certain mineral and elemental associations are characteristic for certain geological units rather than for conventionally classified types of uranium deposits. It appears, for instance, that the uranium-titanium aggregates, generally described as brannerite, are relatively common in several types of deposits in a certain geological environment rather than in certain types in different geological units.

Introduction

Studies on uranium mineralization in Canada conducted during 1980 by the Uranium Resource Evaluation Section of the Geological Survey of Canada encompassed almost all areas believed to be favourable for uranium mineralization in Canada (Fig. 18.1).

The senior author conducted field and/or laboratory studies (the latter with co-operation of the co-author) to evaluate the uranium and thorium resources of some of these regions and areas. This paper outlines some results of these investigations.

Northern Saskatchewan

About 60 per cent of the total expenditures for uranium exploration in Canada in 1980 are estimated to have been spent in northern Saskatchewan and almost 70 per cent of exploration drilling in Canada was carried out there.

Identified uranium resources occur in this area in several types of deposits (Fig. 18.2): (a) in podiform orebodies spatially related to the pre-Athabasca unconformity; (b) in mineralized veins spatially related to major faults, such as the orebodies in the Beaverlodge segment; (c) in deposits of, apparently, diagenetic origin with subsequent redistribution of mineralization (e.g. Duddridge Lake deposit); and (d) in disseminations in granitoid rocks. Notes from current research on selected deposit types are included here.

Studies on selected ore samples collected from deposits of the unconformity-related type, namely Key Lake, Collins Bay, Midwest Lake and Maurice Bay, are summarized as follows:

The uranium mineralization in the Key Lake deposit (9 samples studied) occurs in at least four main generations: (i) as thorium-free euhedral crystals of uraninite (Ruzicka, 1977); (ii) as massive pitchblende, commonly in botryoidal form (Fig. 18.3); (iii) as pitchblende-coffinite aggregates (Fig. 18.4); and (iv) as pitchblende in sooty form. The thorium-free euhedral crystals of uraninite may be tetragonal α-U_3O_7 reported by Dahlkamp (1978).

The most common mineral assemblages of the deposits consist of pitchblende-coffinite aggregates + millerite + gersdorffite and massive pitchblende + gersdorffite + sooty pitchblende. The pitchblende contains minor amounts of Si, Ca, and Pb and trace amounts of P, Ti, and Fe. Calcite or siderite occur as gangue minerals.

The whole rock spectrochemical analyses of selected samples containing uranium mineralization showed high contents of As, Ni, Co, Ag, Pb, Cu, Sr, Zr, and V (Table 18.1). Samples 3 to 8 in Table 18.1 contained regolithic (?) clay material associated with high grade uranium mineralization.

The uranium mineralization of the Collins Bay 'A' and 'B' zones (13 samples studied) is, as in the Key Lake deposits, associated with regolithic(?) clay material, that is spatially related to the pre-Athabasca unconformity. At least three generations of uranium minerals have been identified in the drill core samples: (i) massive, commonly spherulitic, pitchblende; (ii) pitchblende-coffinite aggregates; and (iii) sooty pitchblende. The uranium minerals commonly occur in an assemblage with millerite, gersdorffite (Fig. 18.5), rammelsbergite, pararammelsbergite, nickeline, and locally with galena and/or sphalerite.

The high grade uranium mineralization of the 'A' zone, analyzed for U, Ni, Pb, and Au, showed positive correlations with Pb (r=0.96) and Au (r=0.83). Weak statistical correlations were observed between U and Ni (r=-0.21), U and Ag (r=-0.13), Ag and Au (r=-0.11). No correlation was found between Ni and Pb and Ni and Au. These results may indicate that U and Au were apparently governed by similar geochemical processes during the formation of the ore; that Pb is apparently of radiogenic origin; and that U and Ni mineralization might be coeval but not necessarily cogenetic.

Samples containing uranium collected from the alteration and/or regolithic portion of the 'B' zone were analyzed for selected elemental constituents. The results showed that As, Ni, Pb, Ti and Cu are commonly associated with U (Table 18.2).

The uranium mineralization of the Midwest Lake deposit (17 samples studied) is represented by pitchblende and coffinite. As in the Key Lake and Collins Bay deposits, the pitchblende occurs in at least three generations: (i) in a massive form; (ii) in a mixture with coffinite; and (iii) in a sooty form. Associated nonradioactive minerals are nickeline, millerite, maucherite, rammelsbergite, gersdorffite, nickel-hexahydrite, retgersite, calcite, chlorite, halloysite, hematite, and goethite.

A generalized conceptual mineral succession for the Midwest Lake deposit (Fig. 18.6) postulates five stages of mineralization: (1) first generation of pitchblende (massive, spherulitic) (Fig. 18.7); (2) first generation of nickel arsenides and sulphides; (3) second generation of nickel arsenides, first generation of nickel sulpharsenides, aggregates of second

[1] Central Laboratories and Technical Services Division

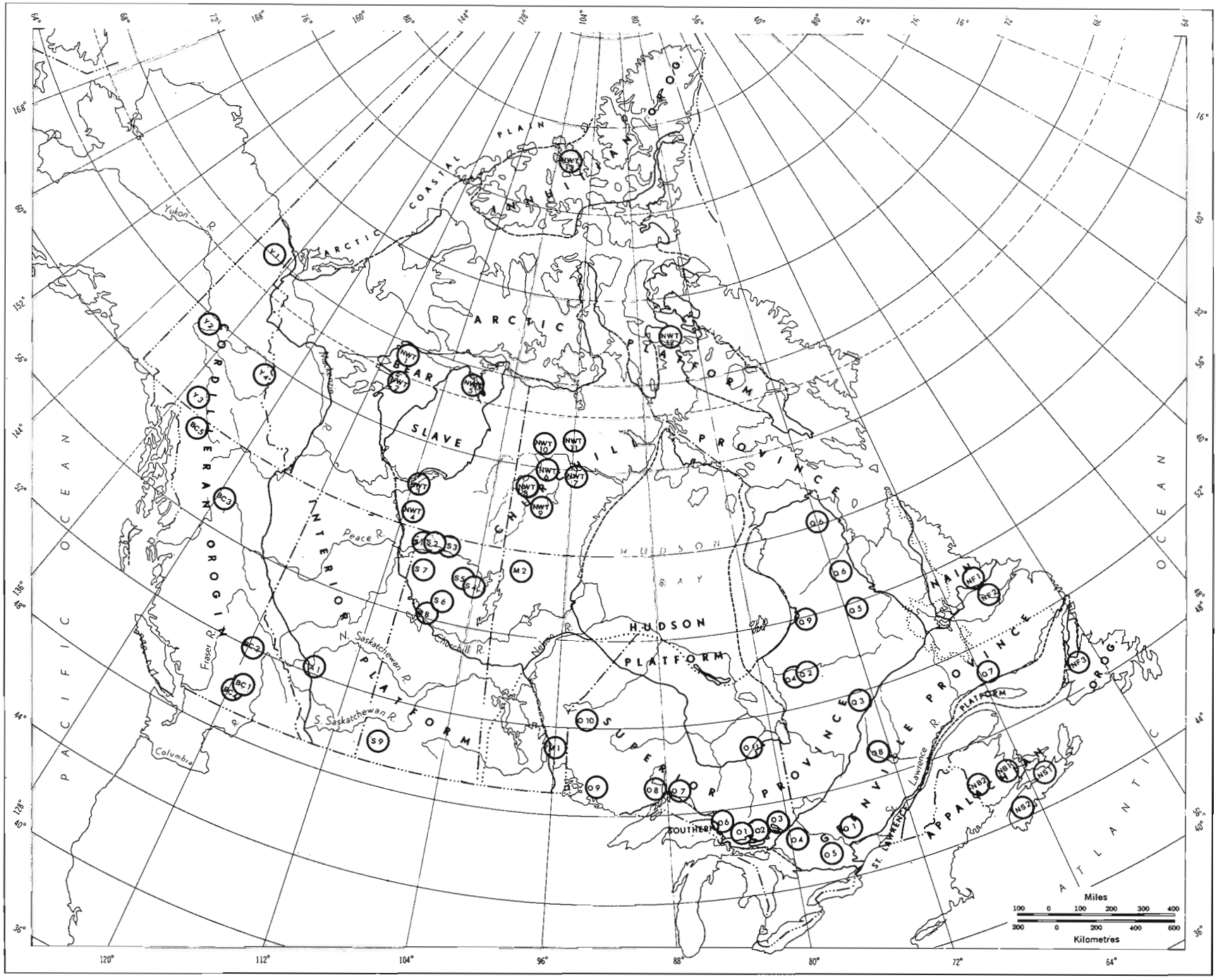
PACIFIC OCEAN
ATLANTIC OCEAN
ARCTIC COASTAL PLAIN
ARCTIC PLATFORM
ARCTIC OROGEN
SLAVE PROVINCE
CHURCHILL PROVINCE
INTERIOR PLATFORM
CORDILLERAN OROGEN
HUDSON BAY
HUDSON PLATFORM
SUPERIOR PROVINCE
GRENVILLE PROVINCE
APPALACHIAN OROGEN
NAIN PLATFORM
SOUTHERN PLATFORM
Yukon R.
Mackenzie R.
Peace R.
Fraser R.
N. Saskatchewan R.
S. Saskatchewan R.
Columbia R.
Churchill R.
Nelson R.
St. Lawrence R.
Miles
Kilometres

LEGEND

Area:					
A 1	Alberta Basin	NWT 6	Schultz Lake	Q 2	James Bay
BC 1	Kelowna-Beaverdell	NWT 7	Baker Lake	Q 3	Otish Mountains
BC 2	Birch Island (Rexspar)	NWT 8	Dubawnt Lake	Q 4	Sakami Lake
BC 3	Sustut Basin	NWT 9	Angikuni-Yathkyed	Q 5	Dieter Lake (Lac Gayot)
BC 4	Summerland	NWT 10	Thelon Basin	Q 6	Labrador Trough
BC 5	Atlin	NWT 11	Amer Lake	Q 7	Johan Beetz
M 1	Bissett	NWT 12	Fury and Hecla Strait	Q 8	Crevier
M 2	Kasmere Lake	NWT 13	Arctic Islands	Q 9	Richmond Gulf
NB 1	New Brunswick Basins	O 1	Elliot Lake	S 1	West Rim of Athabasca Basin
NB 2	New Brunswick Other	O 2	Agnew Lake	S 2	Area North of Athabasca Basin
NF 1	Makkovik-Seal Lake	O 3	Cobalt Embayment	S 3	North Rim of Athabasca Basin
NF 2	Melville Lake	O 4	Lake Nipissing	S 4	East Rim of Athabasca Basin
NF 3	Deer Lake Basin	O 5	Bancroft-Sharbot Lake	S 5	Midwest Lake-McClean Lake
NS 1	Nova Scotia Basins	O 6	Sault Ste. Marie-Montreal River-Chapleau	S 6	South Rim of Athabasca Basin
NS 2	Nova Scotia Other	O 7	Prairie Lake	S 7	Carswell Structure
NWT 1	Hornby Bay-Dismal Lakes	O 8	Nipigon	S 8	Wollaston Lake Belt
NWT 2	W. Bear Province	O 9	Kenora-Dryden	Y 1	Northern Yukon
NWT 3	East Arm of Great Slave Lake	O 10	Favourable Lake	Y 2	Central Yukon
NWT 4	Nonacho Lake	Q 1	Mont Laurier	Y 3	Southwestern Yukon
NWT 5	Bathurst Inlet			Y 4	Selwyn Basin

Figure 18.1. *Areas studied by members of the Uranium Resource Evaluation Section in 1980.*

generation of pitchblende and coffinite; (4) sulpharsenides and third generation of pitchblende (sooty); (5) gangue and post-ore minerals.

The mineralized successions at the Key Lake and Collins Bay and at Midwest Lake appear to be similar, with some minor modifications.

As in the other above mentioned deposits, the highest uranium contents in the Midwest Lake deposit are commonly associated with the regolithic(?) clay material (see Table 18.3, analyses of samples 3, 5, and 6) and the suite of elements associated with uranium mineralization, including As, Ni, Co, Ag, Pb, Cu, Sr, Zr, and V, is similar.

On the other hand the Maurice Bay deposit, at the northwest rim of the Athabasca Basin (Fig. 18.2), also spatially related to the pre-Athabasca unconformity, contains (according to a study of 10 samples) rather simple monometallic and one stage uranium (pitchblende-coffinite) mineralization intimately associated with chlorite and/or iron oxides (Fig. 18.8, 18.9); the corresponding spectrochemical analyses of the samples for selected elements are shown in Table 18.4 (samples 1 and 2 respectively). The Fond du Lac deposit contains a similar suite of minerals.

All the above mentioned unconformity-related deposits were formed by epigenetic processes; however their elemental and mineral assemblages indicate that the metal-bearing solutions participating in formation of the deposits in the southeastern part of the Athabasca Basin (i.e. Key Lake, Collins Bay, Midwest Lake, McClean Lake and Eagle Point) were apparently derived from geologically different sources than those in the northern part of the basin (i.e. Maurice Bay and Fond du Lac).

Microscopic and X-ray examination of a sample of the vein-type mineralization from the Ace-Fay mine of Eldorado Nuclear Limited at Beaverlodge, Saskatchewan (Fig. 18.2), revealed uranium-titanium oxides (brannerite) intergrown with, or adjacent to, acicular ilmenite and embedded in chlorite and calcite (Fig. 18.10). In addition to uranium and titanium this mineral assemblage contains Fe (>3.0%), Si (15.0%), Ca (>20.0%), Pb (0.2%), V (0.3%), Cu (>0.3%), and P (0.5%). The occurrence of uranium-titanium aggregates (brannerite) is apparently restricted to deeper portions of the orebodies and may indicate zoning of mineralization in the veins.

Ontario

Estimated expenditures for uranium exploration in Ontario during 1980 amounted to approximately 2 per cent of Canada's total.

Laboratory examination of 11 samples collected by the senior author from uranium occurrences in the Kirkland Lake-Larder Lake and Cobalt areas revealed:

1. The mineralization in trachytic rocks from the Kirkland Lake-Larder Lake area (Ruzicka, 1977, 1979) is represented by metamict uranium-titanium compounds resembling brannerite. The uranium-bearing minerals replace quartz and feldspar in the chlorite-sericite-carbonate host rock (Fig. 18.11). The mineralization is apparently a result of late metasomatism related to the volcanic activity.
2. The mineralization at the Silvermaque property near Cobalt (Ruzicka, 1979, p. 147) is also of a metasomatic type. There is in addition to pitchblende, unidentified uranium mineralization intimately associated with chlorite and spatially with carbonate that replaces the earlier rock-forming minerals.

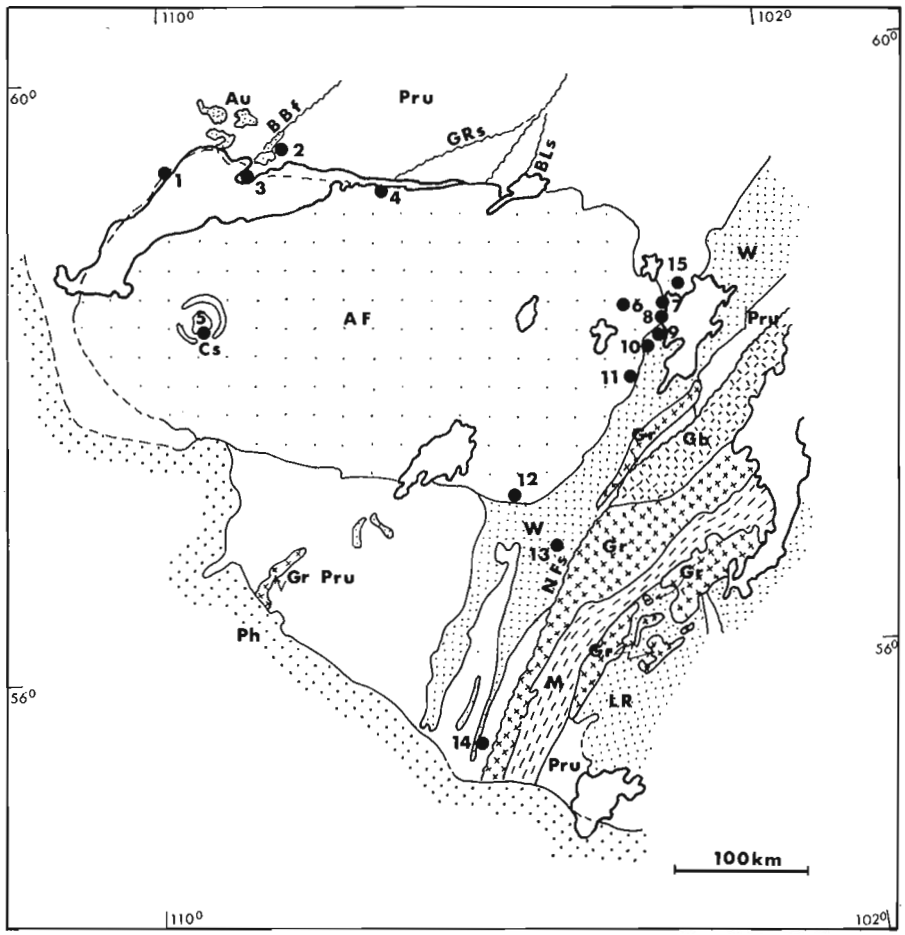

LEGEND

Ph = Phanerozoic rocks
AF = Athabasca Formation
Au = Aphebian rocks, undivided
W = Wollaston Domain
LR = La Ronge Domain
Cs = Carswell structure
Pru = Precambrian rocks, undivided (including Archean)
M = Migmatites of the Rottenstone Domain
Gr = Granitic rocks (Hudsonian)
Gb = Gabbro and associated gneiss
BBf = Black Bay fault
GRs = Grease River shear
BLs = Black Lake shear
NFs = Needle Falls shear

Uranium Deposits

1 = Maurice Bay
2 = Fay – Ace – Verna
3 = Gunnar
4 = Fond du Lac
5 = Cluff Lake ("D", "NR", "OP", Claude)
6 = Midwest Lake
7 = Collins Bay A
8 = Collins Bay B
9 = Rabbit Lake
10 = Raven and Horseshoe
11 = West Bear
12 = Key Lake
13 = Burbidge Lake
14 = Duddridge Lake
15 = Eagle Point

(Adapted from Ruzicka, 1979)

Figure 18.2. *Uranium deposits in northern Saskatchewan.*

Figure 18.3. *Autoradioluxograph of massive botryoidal pitchblende from Gärtner orebody, Key Lake deposit, Saskatchewan. Positive image.*

Manitoba

Estimated expenditures for uranium exploration in Manitoba during 1980 amounted to about 0.2 per cent of Canada's totals. In addition to the northwestern part of the province the occurrences in the Bissett area, southeastern Manitoba, were evaluated.

Microscopic and chemical analyses of 4 samples of the uranium mineralization from Bissett area (Ruzicka, 1979, p. 147), which is confined to conglomerate and quartzite of the Proterozoic (?) San Antonio Formation (Fig. 18.12), showed that the main uraniferous mineral is coffinite associated with limonite (Fig. 18.3). The Fe_2O_3:FeO ratio in the mineralized parts of the sediments is 3.3:1. The mineralogical composition attests to oxidizing conditions and epigenetic processes involved in the formation of the mineralization. This feature makes the mineralization different from that in the Matinenda Formation in the Elliot Lake area, Ontario.

Quebec

The exploration for uranium in Quebec amounted in 1980 to about 6 per cent of Canada's total. Most of it was in the Mistassini and Otish homoclines and Lac Gayot area. Interesting mineralization in rocks of the Labrador Fold Belt also has been explored.

Rocks of the Mistassini and Otish homoclines contain uranium mineralization in various environments. At the base of the Papaskwasati Formation, uranium mineralization

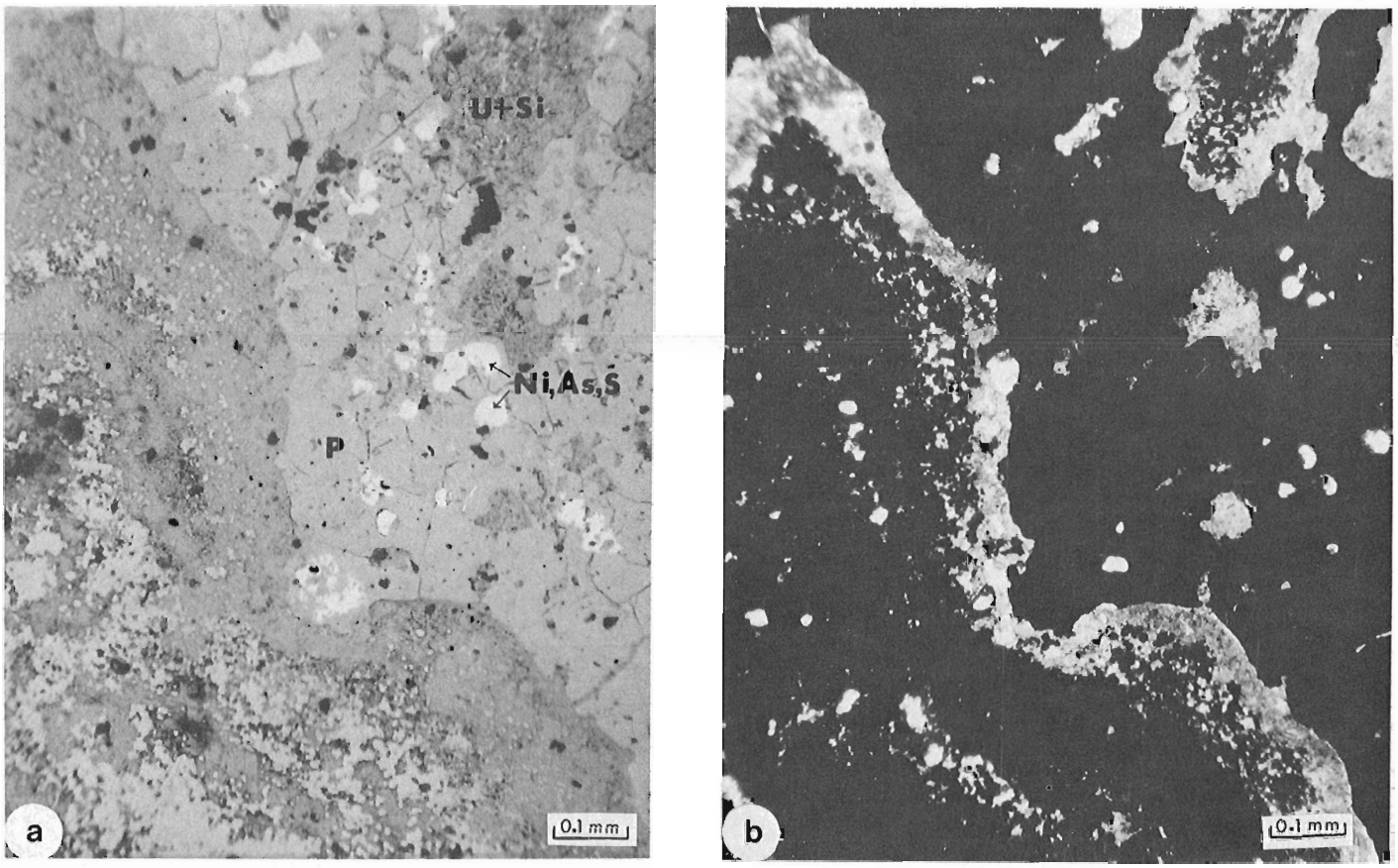

Figure 18.4. *Pitchblende (P), pitchblende-coffinite aggregates (U+Si), and nickel sulpharsenides (Ni,As,S) from the Gärtner orebody, Key Lake deposit, Saskatchewan. (a) reflected light; (b) transmitted light.*

Table 18.1

Selected elemental constituents in selected drill core samples from the Key Lake deposit, Saskatchewan

	Constituents in per cent							
Sample	1)	1)	2)	2)	2)	2)	2)	2)
Element	1	2	3	4	5	6	7	8
Ag	< 0.0005	< 0.0005	n.d.	< 0.001	0.03	0.03	0.03	0.02
As	< 0.20	< 0.2	2.0	0.7	3.0	>10.0	>10.0	>10.0
Ca	0.073	0.017	10.0	3.0	10.0	1.5	1.5	10.0
Co	0.002	< 0.001	0.1	0.2	0.07	0.3	0.3	0.1
Cr	0.017	< 0.0005	< 0.001	< 0.001	< 0.001	< 0.001	0.03	< 0.001
Cu	0.0014	< 0.0007	0.05	0.02	0.07	0.2	0.07	0.03
Mn	0.011	0.002	0.5	0.3	0.3	0.05	0.02	0.2
Mo	< 0.005	< 0.005	n.a.	n.a.	n.a.	n.a.	n.a.	n.a.
Ni	0.019	0.0022	> 0.7	> 0.7	> 0.7	> 0.7	> 0.7	> 0.7
Pb	< 0.07	< 0.07	2.0	1.0	3.0	3.0	1.5	5.0
Sr	0.03	0.005	0.1	0.03	0.07	0.02	< 0.001	0.15
Ti	0.90	0.029	0.2	0.15	0.2	0.2	0.15	0.17
U 3)	0.0048	0.0155	23.0	20.4	31.6	30.8	32.1	26.9
V	0.033	< 0.002	0.1	0.07	0.1	0.07	0.15	0.07
Zn	< 0.02	< 0.02	< 0.1	< 0.1	< 0.1	< 0.1	< 0.1	< 0.1
Zr	0.058	0.0055	< 0.005	< 0.005	< 0.005	< 0.005	< 0.005	< 0.005

Location of Samples:

1: DDH 1962 (Deilmann): graphitic schist
2: DDH 1967 (Deilmann): sandstone
3: DDH 5052 (Gärtner): regolith with pitchblende
4: DDH 5052 (Gärtner): regolith with pitchblende
5: DDH 5057 (Gärtner): regolith with pitchblende
6: DDH 5062 (Gärtner): regolith with pitchblende
7: DDH 5050 (Gärtner): regolith with pitchblende
8: DDH 5057 (Gärtner): regolith with pitchblende

n.a. = analysis not available
n.d. = not detected (i.e. below the detection limit)
Th was not detected in any sample

1) Analyzed by K.A. Church and using 12B-DR
2) Analyzed by K.A. Church and W.H. Champ using 5Q-23
3) Analyzed by Atomic Energy Canada Ltd. by Neutron Activation

Table 18.2

Selected elemental constituents in selected drill core samples from the Collins Bay "B" zone, Saskatchewan

	Constituents in per cent					
Sample	2)	1)	1)	1)	1)	2)
Element	1	2	3	4	5	6
Ag	0.015	< 0.0005	< 0.0005	< 0.0005	< 0.0005	0.015
As	>10.0	0.55	0.56	< 0.2	< 0.2	>10.0
B	n.a.	0.023	0.078	0.0098	0.014	n.a.
Ba	n.a.	0.0083	0.014	0.003	0.0089	n.a.
Be	n.a.	< 0.0003	< 0.0003	< 0.0003	< 0.0003	n.a.
Co	0.1	0.0062	0.0044	< 0.001	< 0.001	0.1
Cr	0.01	< 0.0005	0.001	< 0.0005	< 0.0005	0.01
Cu	> 0.3	0.058	0.0034	0.001	< 0.0007	0.2
Mo	n.a.	0.0062	0.0091	< 0.005	< 0.005	n.a.
Ni	> 0.7	0.37	0.32	0.0039	0.010	> 0.7
Pb	2.0	< 0.07	< 0.07	< 0.07	< 0.07	5.0
Sr	n.d.	0.026	0.11	0.0093	0.0039	n.d.
Ti	0.15	0.31	0.84	0.13	0.17	0.2
U 3)	21.4	0.004	0.046	0.005	0.009	17.6
V	0.02	0.004	0.16	< 0.002	0.0024	0.05
Zn	n.d.	< 0.02	< 0.02	< 0.02	< 0.02	n.d.
Zr	< 0.005	0.11	0.30	0.035	0.10	< 0.005

Location of Samples:

1: DDH 241 (CAB): regolith with pitchblende
2: DDH 253 (CAB): altered sandstone
3: DDH 241 (CAB): regolithic clay
4: DDH 241 (CAB): regolith
5: DDH 241 (CAB): altered gneiss
6: DDH 253 (CAB): regolith with pitchblende

n.a. = analysis not available
n.d. = not detected (i.e. below the detection limit)
Th was not detected in any sample

1) Analyzed by K.A. Church using 12B-DR
2) Analyzed by K.A. Church and W.H. Champ using 5Q-23
3) Analyzed by Atomic Energy Canada Ltd. by Neutron Activation

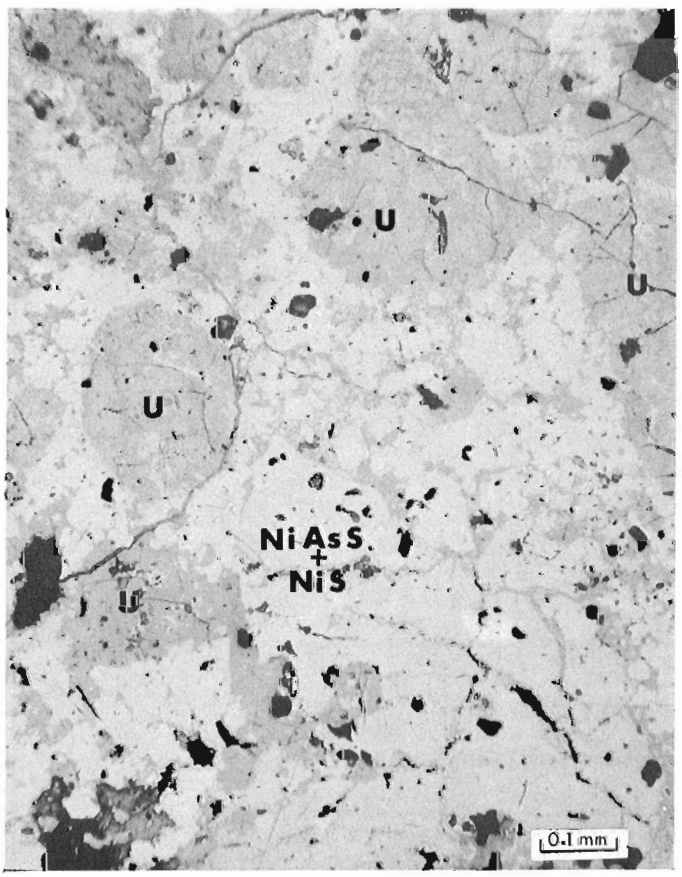

Figure 18.5. (opposite) Massive pitchblende (U) associated with nickel sulpharsenides (NiAs S+NiS) from Collins Bay 'B' zone. Reflected light.

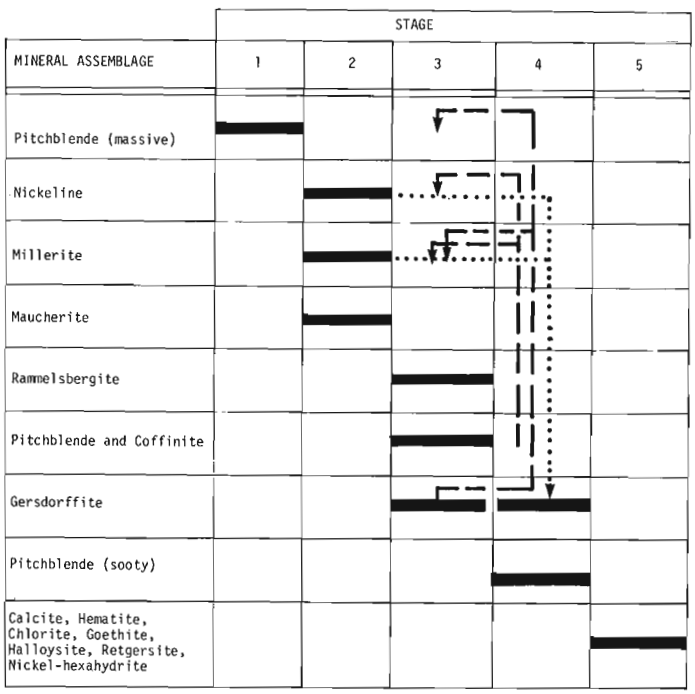

Figure 18.6. (above) Generalized mineral succession in the Midwest Lake deposit, Saskatchewan. Dashed line (---) indicates replacement process; dotted line (...) indicates that the younger mineral has been derived from another mineral(s).

Table 18.3

Selected elemental constituents in selected drill core samples from the Midwest Lake deposit, Saskatchewan

Element \ Sample	1) 1	1) 2	2) 3	2) 4	2) 5	1) 6	2) 7	2) 8	1) 9
	Constituents in per cent								
Ag	0.0068	< 0.0005	0.015	n.d.	0.003	< 0.0005	0.0015	n.d.	< 0.0005
As	7.2	< 0.20	>10.0	n.d.	3.0	0.23	5.0	n.d.	0.35
B	0.0068	0.024	n.a.	n.a.	n.a.	0.068	n.a.	n.a.	0.0085
Ba	< 0.0005	0.0082	n.a.	n.a.	n.a.	0.0078	n.a.	n.a.	0.0033
Be	< 0.0003	0.0004	n.a.	n.a.	n.a.	0.0016	n.a.	n.a.	< 0.0003
Bi	n.a.	n.a.	n.a.	n.d.	0.1	n.a.	0.15	n.d.	n.a.
Co	0.22	0.013	1.0	0.3	0.5	0.003	0.2	< 0.05	0.29
Cr	< 0.0005	0.019	0.015	0.003	0.015	0.033	0.01	0.02	< 0.0005
Cu	0.033	0.0024	0.15	0.007	0.007	0.0014	0.15	0.02	0.00073
Mo	0.49	< 0.005	n.a.	n.a.	n.a.	< 0.005	n.a.	n.a.	< 0.005
Ni	> 2.0	0.02	> 0.7	0.2	> 1.5	0.35	> 1.5	< 0.005	0.12
Pb	0.082	< 0.07	3.0	n.d.	n.d.	< 0.07	n.d.	n.d.	< 0.07
Sr	0.0028	0.0052	n.d.	n.d.	0.007	0.0029	0.003	n.d.	< 0.001
Ti	0.24	0.93	0.2	0.05	2.0	0.66	1.0	0.7	0.066
U 3)	0.02	0.007	27.2	4.8	2.2	0.14	14.4	17.3	0.009
V	0.014	0.062	0.3	0.015	0.3	0.49	0.3	0.1	0.0055
Zn	< 0.02	< 0.02	n.d.	n.d.	n.d.	< 0.02	n.d.	n.d.	< 0.02
Zr	0.025	0.032	< 0.005	0.03	0.3	0.02	0.5	0.15	0.014

Location of Samples:

1: DDH 78-40; sandstone
2: 58°18'N, 104°06'W: chloritized basement rock
3: DDH 78-42: regolith
4: DDH 78-40: sandstone
5: DDH 78-18: regolith
6: DDH 78-18: regolith
7: DDH 78-18: sandstone
8: DDH 78-70: sandstone
9: DDH 78-15: sandstone

n.a. = analysis not available
n.d. = not detected (i.e. below the detection limit)
Th was not detected in any sample

1) Analyzed by K.A. Church using 12B-DR
2) Analyzed by K.A. Church and W.H. Champ using 5Q-23
3) Analyzed by Atomic Energy Canada Ltd. by Neutron Activation

Table 18.4

Selected constituents of selected drill core samples from Maurice Bay deposit, Saskatchewan

Element \ Sample	1) 1	1) 2	2) 3	1) 4	1) 5
	Constituents in per cent				
Ag	n.d.	n.d.	< 0.005	n.d.	n.d.
As	n.d.	n.d.	< 0.2	n.d.	n.d.
Co	n.d.	n.d.	< 0.001	n.d.	n.d.
Cr	0.01	0.03	< 0.0005	n.d.	n.d.
Cu	< 0.001	0.05	< 0.0007	0.005	0.007
Mo	n.a.	n.a.	< 0.005	n.a.	n.a.
Ni	0.02	< 0.0015	< 0.001	0.02	< 0.0015
Pb	0.2	1.5	< 0.7	n.d.	n.d.
Sc	n.d.	< 0.0007	n.a.	n.d.	n.d.
Ti	0.3	0.3	0.48	0.1	0.1
U 3)	5.84	32.5	0.14	7.70	11.1
V	0.01	0.07	< 0.002	0.005	n.d.
Zn	n.d.	n.d.	0.11	n.d.	n.d.
Zr	0.015	< 0.005	0.0096	n.d.	n.d.

Location of Samples:

1: DDH MB-21: sandstone
2: DDH MB-87: regolith
3: DDH MB-24: altered sandstone
4: DDH MB-46: regolith
5: DDH MB-98: regolith

n.a. = not available
n.d. = not detected (i.e. below the detection limit)
Th was not detected in any sample
Tr. = traces

1) Analyzed by K.A. Church and W.H. Champ by 5Q-23
2) Analyzed by K.A. Church by 12B-DR
3) Analyzed by Atomic Energy Canada Ltd. by Neutron Activation

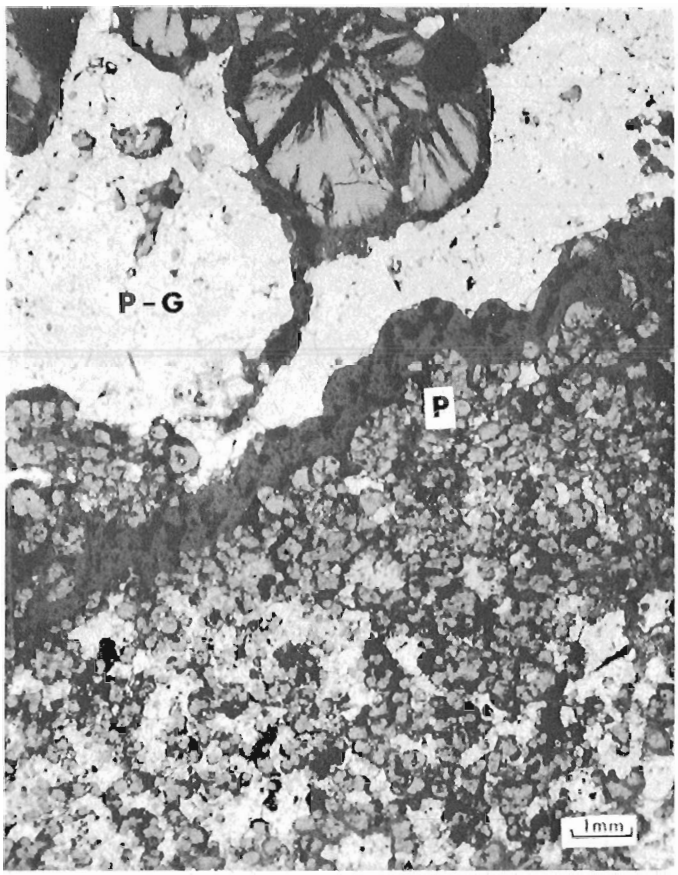

Figure 18.7. *Spherulitic pitchblende (P) and pitchblende-gersdorffite (P-G) aggregates from Midwest Lake deposit, Saskatchewan. Reflected light.*

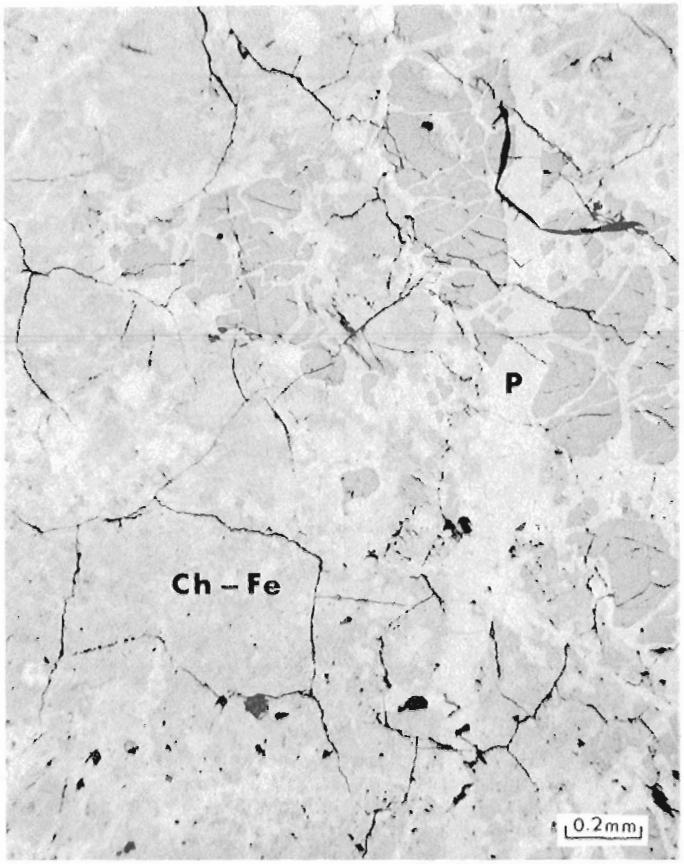

Figure 18.8. *Pitchblende (P) associated with chlorite (Ch) and iron oxides (Fe) from Maurice Bay deposit, Saskatchewan. (Spectrochemical analysis of the same sample is in Table 6, No. 1). Reflected light.*

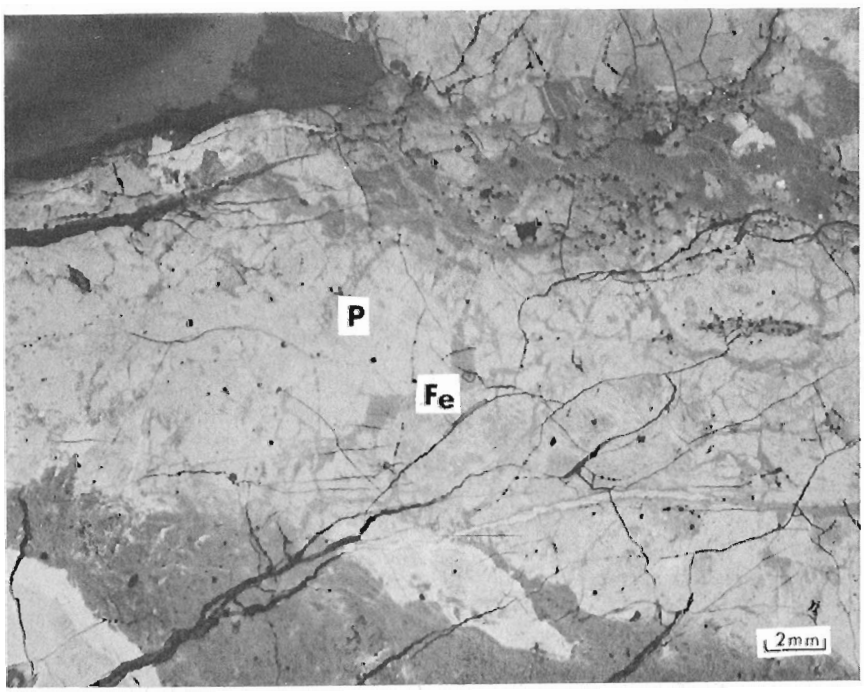

Figure 18.9

Pitchblende (P) intergrown with iron oxides (Fe) from Maurice Bay deposit, Saskatchewan. (Spectrochemical analysis of the same sample is in Table 6, No. 1). Reflected light.

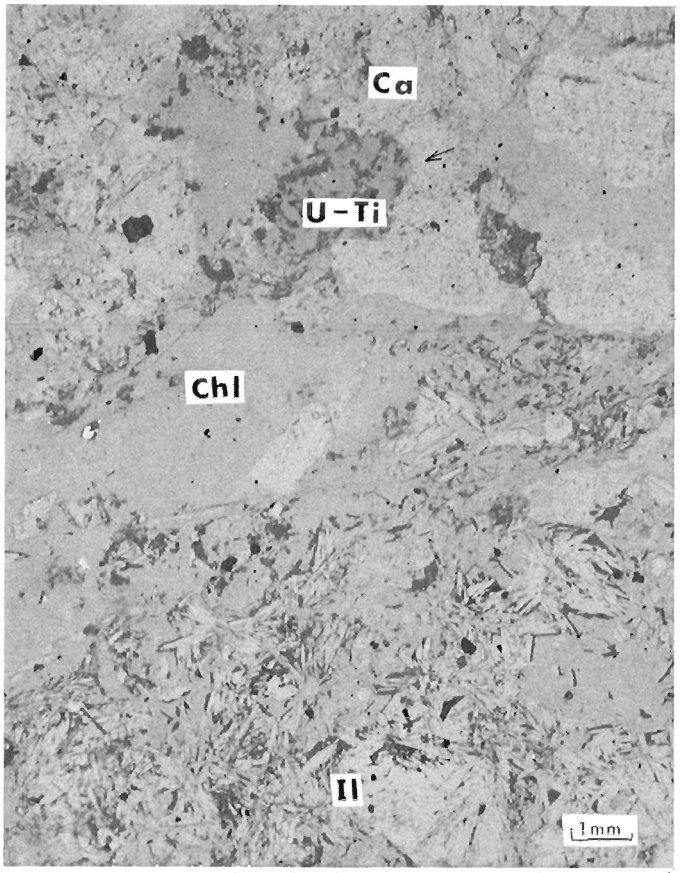

Figure 18.10. *Uranium-titanium aggregate (brannerite?) (U-Ti) in an assemblage with calcite (Ca), chlorite (Chl), and ilmenite (Il) from 29th level, drift 3092, Ace-Fay mine, Eldorado Nuclear Limited, Beaverlodge, Saskatchewan. Reflected and transmitted light.*

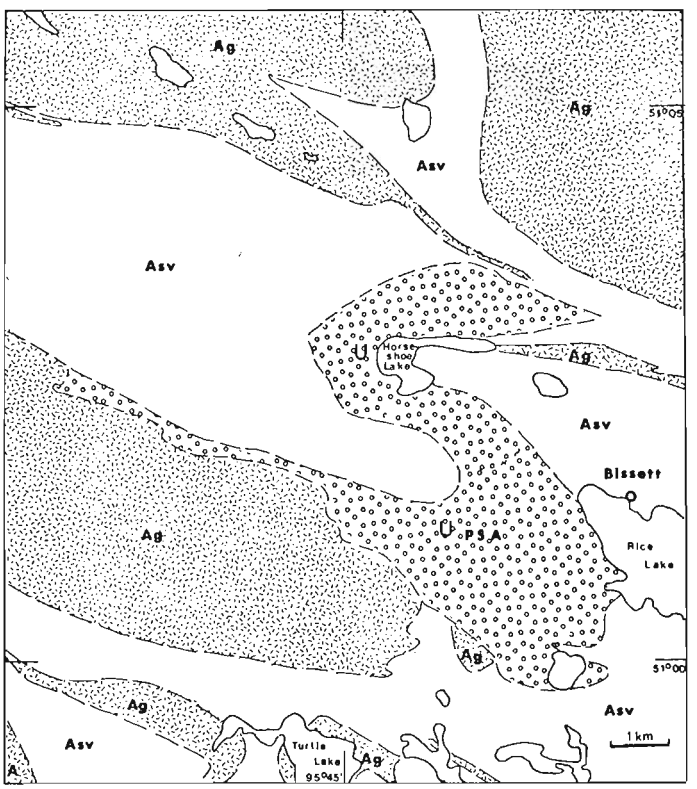

Figure 18.12. *Uranium occurrences (U) at Bissett, Manitoba. Asv = Archean sedimentary and volcanic rocks; Ag = Archean granitic rocks; PSA = Proterozoic (?) San Antonio Formation.*

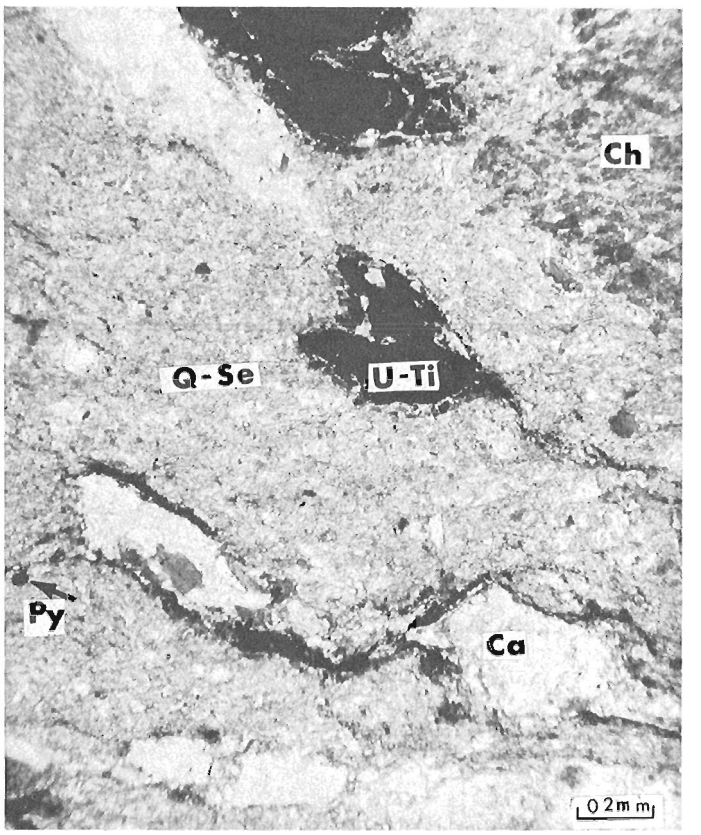

Figure 18.11. *Metamict uranium-titanium mineralization resembling brannerite (U-Ti) in a chlorite-sericite-carbonate host-rock from locality KL-7 (Ruzicka, 1978), Kirkland Lake area, Ontario. Q-Se = quartz and sericite; Ca = calcite; Py = pyrite; Ch = chlorite. Transmitted light.*

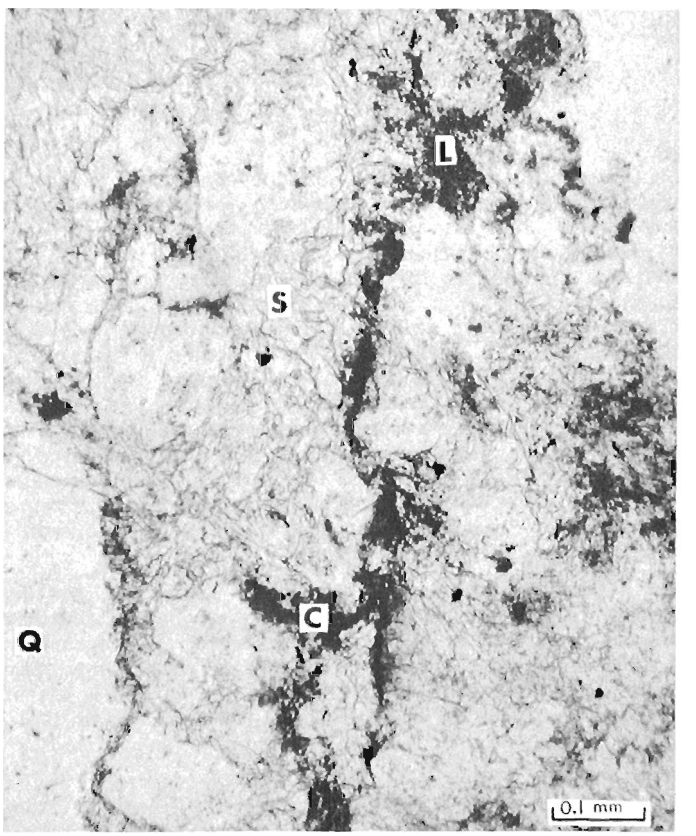

Figure 18.13. *Uranium mineralization from sedimentary rocks, San Antonio Formation, Bissett area, Manitoba. C = coffinite, L = limonite, Q = quartz, S = sericite. Transmitted light.*

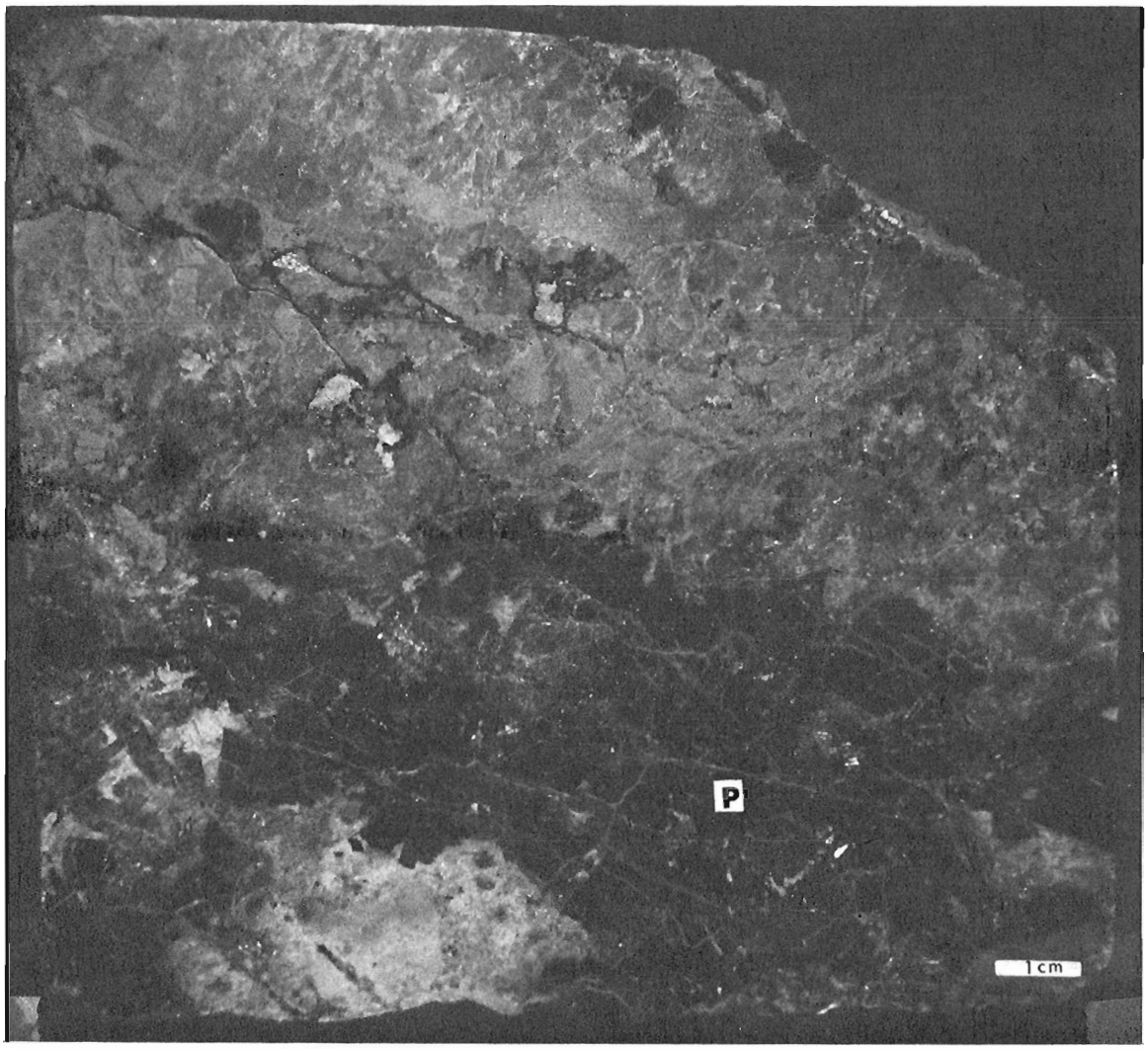

Figure 18.14. *Pitchblende (P) mineralization filling a fracture; Lake Mistamisk area, Quebec.*

occurs erratically in gritty sandstone commonly associated with thorium and locally with copper. This type of mineralization resembles that occurring in the upper Huronian rocks of the Sault Ste. Marie-Cobalt area, Ontario. It is unlikely that this environment contains large uranium deposits similar to those of the lower Huronian of the Elliot Lake mining district of the above mentioned area in Ontario. However a possibility that the Papaskwasati Formation hosts mineralization similar to that of Key Lake or Maurice Bay deposits cannot be excluded. In the Peribonca Formation, uranium occurs locally in brecciated stromatolitic dolomite. This type of mineralization is not common in Canada and deserves more study. In quartzite of the Indicator Formation, uranium mineralization occurs in scattered nodule-like concentrations surrounded by limonite haloes. This type of uranium mineralization is also uncommon in Canada.

The Lac Gayot area in the James Bay region contains uranium mineralization (Kish and Tremblay-Clark, 1979) that has been explored by drilling in a joint venture program by Uranerz Exploration and Mining Limited and James Bay Development Corporation. The mineralization occurs within sedimentary rocks of the Sakami Formation (Eade, 1966, p. 48) and is apparently spatially related to an unconformity.

Kish and Tremblay-Clark (1978, 1979) reported uranium mineralization from rocks of the Labrador Trough at Lake Mistamisk. The main uranium mineral is pitchblende forming large crystals in calcite and chlorite gangue that fill fractures and replace rock-forming minerals of the granitic country rocks (Fig. 18.14). L. Kish of the Quebec Department of Natural Resources (personal communication) detected three zones, surrounding the pitchblende, containing Te, Ni, and Pb respectively.

New Brunswick

Exploration for uranium in New Brunswick amounted in 1980 to about 1 per cent of Canada's totals.

Following the discovery of uranium mineralization at the Lake George mine by the senior author and H.E. Dunsmore of the Geological Survey of Canada, the Mactaquac and adjacent areas near Fredericton became one of the most attractive targets for uranium exploration in New Brunswick.

The uranium mineralization in the Lake George antimony mine (10 samples studied) occurs as fracture filling in Silurian shale, greywacke, and quartzite that are intruded by Devonian granitic rocks of the Pokiok pluton. The uranium occurs: (a) as uranoan hydrocarbon, a thorium-free mixture of hydrocarbons, pitchblende, coffinite and iron oxides (a sample of this material contained 11.2% C, 1.0% S, about 9.9% H_2O, 2.37% U, 13.6% FeO, 9.4% Fe_2O_3, and 44.3% SiO_2); (b) as coffinite containing minor amounts of Fe,

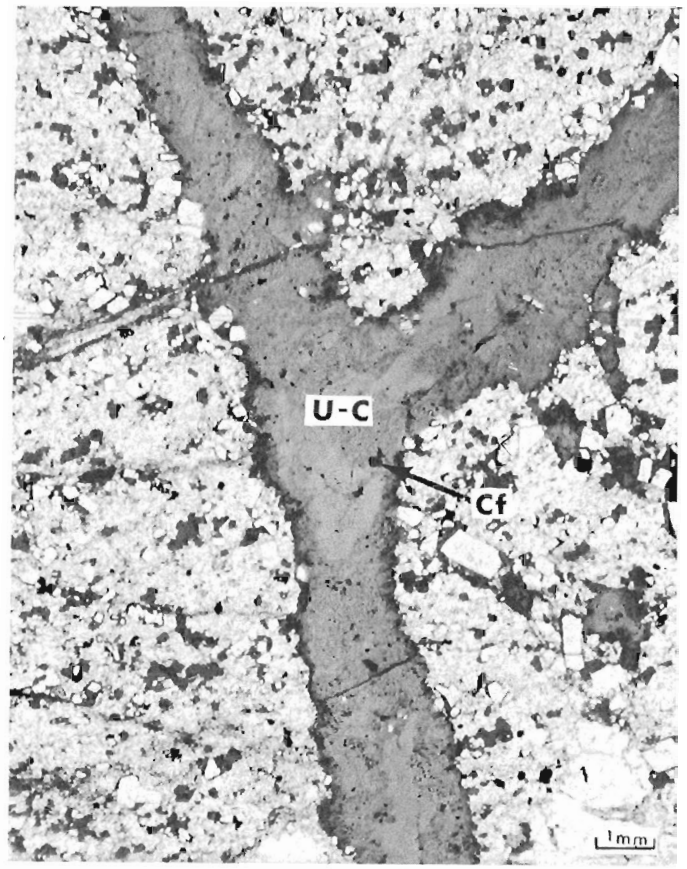

Figure 18.15. *Uranium hydrocarbon (U-C), containing grains of coffinite (Cf) in fractured altered quartzite from Lake George Mine, New Brunswick.*

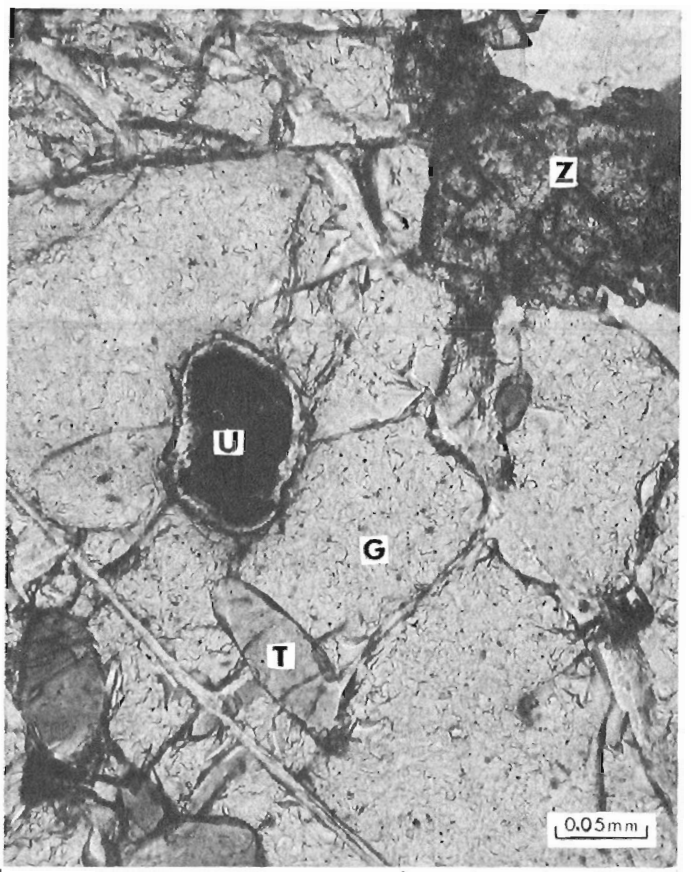

Figure 18.16. *Photomicrograph of uranium mineralization from Hellroaring Creek occurrence, British Columbia. U = thorium-free uraninite; G = garnet; T = tourmaline; Z = zircon. Transmitted light.*

Pb, Al, and Ca; and (c) as pitchblende, commonly intimately associated with chlorite. In addition to Sb, elements commonly associated with uranium are Si, S, Al, Fe, Pb, Ti, Ca, and V. Native antimony is more frequently associated with uranium mineralization than stibnite is.

Although information on absolute age of this uranium mineralization is not available, ground waters appear to have played an important role.

A conceptual genetic model, based on the field and laboratory observations, postulates: (1) introduction of uranium by pre-Devonian granitic rocks (xenoliths of these older granites occur in the marginal facies of the Pokiok granites); (2) concentration of uranium in Silurian pelitic rocks (reduzates) derived from granites; (3) intrusion of Devonian granites; (4) formation of the sulphidic antimony and associated Fe ± Cu ± Pb ± As mineralization in several stages (Abbot and Watson, 1975); (5) liberation of hydrocarbons, sulphur and uranium from the environment and their transportation by ground water; this process was accompanied by clay alteration of the sedimentary rocks, desulphurisation of stibnite and formation of native antimony, and by crystallization of coffinite and pitchblende; (6) deposition of the uranoan hydrocarbon (Fig. 18.15).

Remaining Atlantic Provinces

In 1980 exploration for uranium in Nova Scotia, Newfoundland and Labrador and Prince Edward Island, amounted to about 5 per cent of Canada's total. The main exploration targets were Devonian granitic and sedimentary peribatholithic rocks in Nova Scotia, sedimentary rocks of Deer Lake basin in Newfoundland, and Proterozoic rocks of the Makkovik-Seal Lake area in Labrador.

Northwest Territories and Yukon

The exploration for uranium in Northwest Territories and Yukon in 1980 amounted to about 24 per cent of Canada's total. The main exploration targets were in the Baker Lake-Thelon area, Coppermine homocline, Nonacho basin, Tombstone Mountains, and Fury and Hecla Strait area.

British Columbia

Only a limited amount of exploration had been carried on in British Columbia during 1980 prior to British Columbia government's seven year moratorium on uranium exploration and mining.

Office and laboratory investigations were carried on by the authors on 5 samples from the Hellroaring Creek occurrences, Purcell Mountains, discovered by the senior author and R.T. Bell of the Geological Survey before the imposed moratorium.

The Hellroaring Creek occurrences (located 49°34.4'N, 116°10.9'W) are confined to Precambrian granodiorite pegmatite (Leech, 1962, p. 3; Ryan and Blenkinsop, 1971). Locally the pegmatite contains abundant tourmaline, muscovite, garnet and zircon. Arsenopyrite is an accessory mineral. Uranium occurs: (a) as hypidiomorphic inclusions of thorium-free uraninite in garnet (Fig. 18.16), arsenopyrite,

and zircon; (b) as fracture fillings of uraniferous goethite; (c) as meta-autunite in fractures in association with goethite; and (d) in a metamict compound containing Si, Fe, Al, Th, Pb, Ca, and P.

The uranium mineralization in the Hellroaring Creek occurrences appears to have formed during formation of the pegmatite from thorium-deficient residual uraniferous solutions.

Discussion

Combined mineralogical-chemical studies are useful complementary tools for refinement of conceptual genetic models simulating formation of individual types of uranium deposits and for delineation of uranium subprovinces. For instance the differences between the mineralogical and chemical compositions of the unconformity-related deposits at the south-southeast and the north-northwest margins of the Athabasca Basin, may reflect differences in source environments.

Certain mineral and elemental assemblages, for example the uranium-titanium associations, occur in several types of deposits. This feature is apparently related to the geological character of the source and/or host rocks.

Clay and mica minerals, such as illite, chlorite and sericite, developed as a result of alteration of aluminosilicate minerals in the host rocks, are commonly associated with pitchblende and/or coffinite not only in the unconformity-related deposits but also in the vein deposits, sandstone-hosted deposits, and deposits containing disseminated mineralization. Thus the geochemical environment indicated by this association of alteration and uranium mineralization is common to several deposit types.

Acknowledgments

The authors acknowledge the co-operation of professionals working for companies in the areas studied, especially for Gulf Minerals Canada Limited, Canada Wide Mines, Uranerz Exploration and Mining Limited, Eldorado Nuclear Limited, Urangesellschaft Canada Limited, Key Lake Mining Corporation, SOQUEM, and Consolidated Durham Mines and Resources Limited. The authors also acknowledge assistance of J.A. Kerswill in preparation of samples for mineralogical and chemical analyses and of A.C. Roberts in mineral identification by XRD. G. MacDonald assisted in some microscopic investigations.

References

Abbott, D. and Watson, D.
1975: Mineralogy of the Lake George Antimony Deposit, New Brunswick; Canadian Institute of Mining Bulletin, July 1975, p. 111-113.

Dahlkamp, F.J.
1978: Geologic Appraisal of the Key Lake U-Ni Deposits, Northern Saskatchewan; Economic Geology, v. 73, p. 1430-1449.

Eade, K.E.
1966: Fort George River and Kaniapiskau River (West Half) map-areas, New Quebec; Geological Survey of Canada, Memoir 339, 83 p.

Kish, L. and Tremblay-Clark, P.
1978: Geochemistry and radioactivity in the Labrador Trough (56°11'-58°30'); Quebec Ministère des richesses naturelles, Report DPV-567.

1979: Géochimie et radioactivité dans la Fosse du Labrador; Quebec Ministère des richesses naturelles, Report DPV-666.

Leech, G.B.
1962: Metamorphism and granite intrusions of Precambrian age in southeastern British Columbia; Geological Survey of Canada, Paper 62-13, 8 p.

Roscoe, S.M.
1969: Huronian rocks and uraniferous conglomerates in the Canadian Shield; Geological Survey of Canada, Paper 68-40, 205 p.

Ruzicka, V.
1977: Assessment of selected uranium occurrences and areas favourable for uranium mineralization in Canada; in Report of Activities, Part A, Geological Survey of Canada, Paper 77-1A, p. 27-29.

1979: Uranium and thorium in Canada, 1978; in Current Research, Part A, Geological Survey of Canada, Paper 79-1A, p. 139-155.

Ryan, B.D. and Blenkinsop, J.
1971: Geology and geochronology of the Hellroaring Creek Stock, British Columbia; Canadian Journal of Earth Sciences, v. 8, no. 1, p. 85-95.

19.

TWO CAMBRIAN STRATIGRAPHIC SECTIONS, EASTERN NAHANNI MAP AREA, MACKENZIE MOUNTAINS, DISTRICT OF MACKENZIE

Project 650024

W.H. Fritz
Institute of Sedimentary and Petroleum Geology, Ottawa

Fritz, W.H., Two Cambrian stratigraphic sections, eastern Nahanni map area, Mackenzie Mountains, District of Mackenzie; in Current Research, Part A, Geological Survey of Canada, Paper 81-1A, p. 145-156, 1981.

Abstract

Two new sections (sections 2 and 3) are described in detail and are compared with a nearby section (section 1) of an earlier publication. Unnamed early Lower Cambrian strata that are in part equivalent to the upper member of the Backbone Ranges Formation and in part equivalent to map unit 13 of Blusson underlie and extend into the three sections. The lower half of the overlying Sekwi Formation (Lower Cambrian) at the three sections contains four regional rock types that extend far north of the map area. Orange dolomite and dolomitic siltstone in the upper half of the Sekwi Formation are presently known to extend only a short distance to the north. Above the Sekwi Formation the Middle Cambrian Rockslide and Avalanche formations overlap each other at sections 1 and 2, whereas only the Rockslide is present at section 3.

A regional "sub-Franconian" (sub-medial Upper Cambrian) unconformity is diminished or absent at the expected position between the Rockslide and overlying Rabbitkettle Formation at section 3. Here the late Middle Cambrian ***Bolaspidella*** *Zone extends to the top of the Rockslide and fossils of the early Upper Cambrian* ***Cedaria-Crepicephalus*** *Zone are present 36.5 m above the base of the Rabbitkettle. At section 3 the Rabbitkettle spans most of the Upper Cambrian and may be equivalent to a large part of the Broken Skull Formation that overlies the Avalanche Formation at sections 1 and 2. The lower Broken Skull is barren of fossils at sections 1 and 2, therefore a previously predicted minor unconformity at its base could not be tested.*

Introduction

In 1978 the writer assisted S.P. Gordey on Operation Nahanni by measuring and describing a Cambrian stratigraphic section northeast of the South Nahanni River (Fig. 19.1, section 1, see Fritz, 1979a). The present report describes two more sections (Fig. 19.1, sections 2, 3) that are the result of additional field work in 1979.

The described strata were first mapped by Green and Roddick (1961) and then by Green et al., (1967). They were assigned to informal, numbered map units and discussed briefly on the margin of both maps. The locations of some stratigraphic sections were plotted on one map (Green et al., 1967), but no stratigraphic sections were drafted or described on either.

Gabrielse et al. (1973) assigned formal names and provided type sections for Cambrian strata in the adjoining map areas to the southeast (Flat River), east (Glacier Lake), and northeast (Wrigley Lake). Gordey has introduced this formal nomenclature into the Nahanni map area by illustrating the formations in large scale stratigraphic sections (1979, 1980a), and by plotting them on an open file geological map (1980b).

The Cambrian stratigraphic work accomplished thus far has highlighted two problems which will demand close future attention. The first is establishing control across rapid facies changes in the early Lower, Middle, and Upper Cambrian. The second is evaluating regional unconformities, many of which serve as formational boundaries at type sections east of the Nahanni area. To the east Gabrielse et al. (1973) have reported unconformities at the following positions in type sections for Cambrian formations: top of Backbone Ranges, base of Avalanche, base and top of Rockslide, base and top of Rabbitkettle (in type area, no type section), and base of Broken Skull. The type section for the Sekwi Formation, extended into the Nahanni area from the adjacent map area to the north, has an erosional unconformity a few metres above the top (Handfield, 1968; Fritz, 1976, section 10).

Stratigraphic section 2

Unnamed formation (318 m+)

Only the upper part of this formation was measured between a fault at the base of section 2 and the overlying Sekwi Formation (Fig. 19.1). Above the fault, the lowest unit (unit 1, 99 m+) is predominantly rust weathering siltstone that is dark grey on fresh surface. Interbedded with the siltstone is a subordinate amount (25 per cent) of rust to medium light brownish grey weathering quartzite that is very fine grained. The beds are medium to thick and fresh surfaces are medium grey. Quartzite forming ball and pillow structures is present 28.5 m above the base of the section.

Siltstone like that in unit 1 and siltstone that is light greenish grey weathering with medium greenish grey fresh surfaces comprise most of unit 2 (161 m). Some (15 per cent) quartzite is present in medium light greenish grey weathering beds that are medium grey on fresh surface. The quartzite is thin to thick bedded and very fine grained. Burrows are present 4, 23.5, 28, and 59.5 m above the base and microripples are exposed 4, 23.5, 62.5, and 128.5 m above the base.

Unit 3 (40 m) is composed of resistant, thick bedded quartzite. The basal 10.5 m is white on both weathered and fresh surfaces, and is fine to very fine grained. Quartzite in the interval 10.5 to 21 m above the base weathers rust, medium greenish grey and orange, and is light greenish grey on fresh surfaces. The upper half of the unit (21 to 40 m) weathers rust to light orange and fresh surfaces are light brown. The quartzite is very fine grained in the upper two intervals. Interbedded in the upper half is siltstone (33 per cent) that is rust weathering and olive grey on fresh surface.

At the top of the unnamed formation is a unit (unit 4, 18 m) of medium light brownish grey weathering siltstone in thick parting beds that are olive grey on unweathered surfaces.

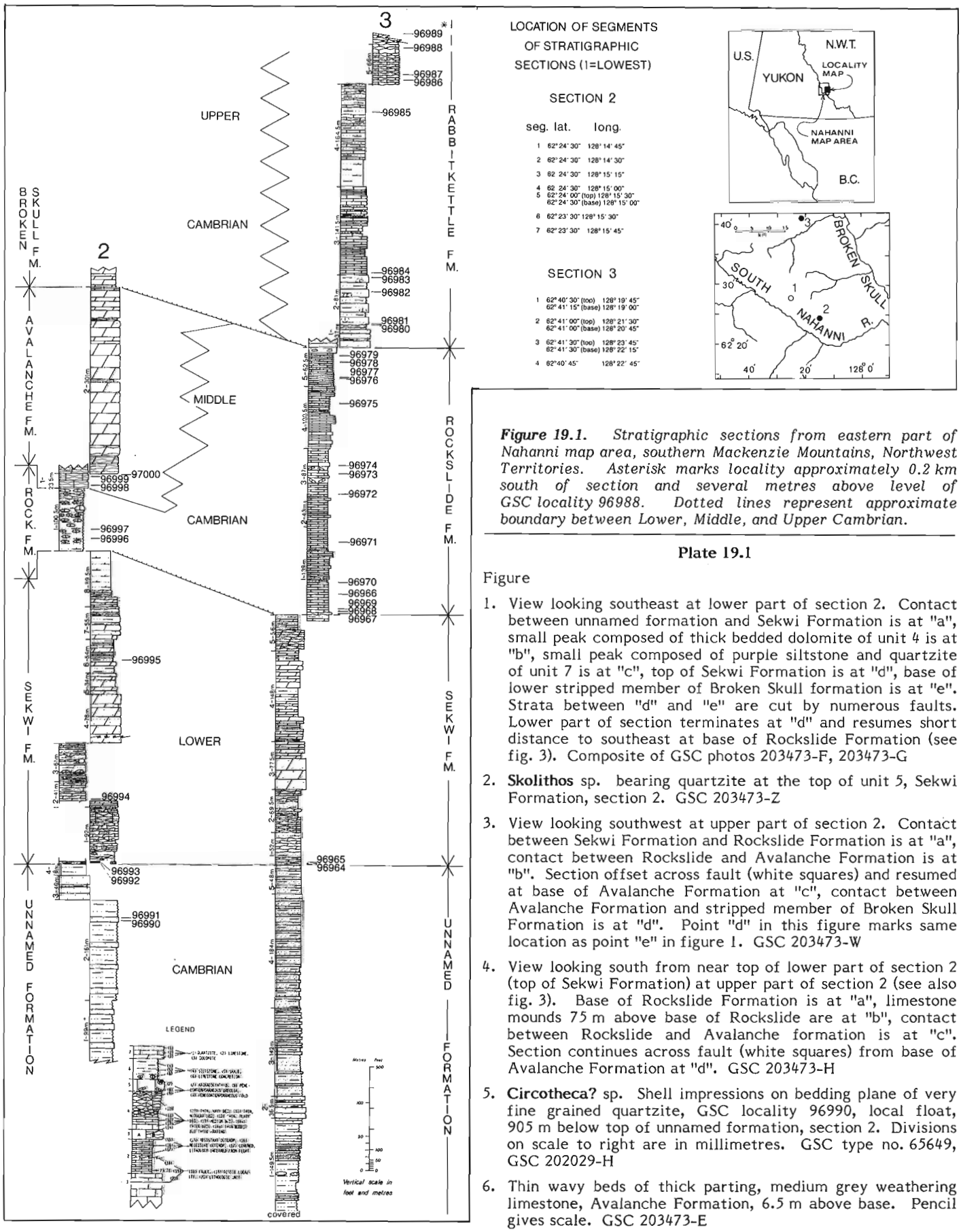

Figure 19.1. *Stratigraphic sections from eastern part of Nahanni map area, southern Mackenzie Mountains, Northwest Territories. Asterisk marks locality approximately 0.2 km south of section and several metres above level of GSC locality 96988. Dotted lines represent approximate boundary between Lower, Middle, and Upper Cambrian.*

Plate 19.1

Figure

1. View looking southeast at lower part of section 2. Contact between unnamed formation and Sekwi Formation is at "a", small peak composed of thick bedded dolomite of unit 4 is at "b", small peak composed of purple siltstone and quartzite of unit 7 is at "c", top of Sekwi Formation is at "d", base of lower stripped member of Broken Skull formation is at "e". Strata between "d" and "e" are cut by numerous faults. Lower part of section terminates at "d" and resumes short distance to southeast at base of Rockslide Formation (see fig. 3). Composite of GSC photos 203473-F, 203473-G
2. **Skolithos** sp. bearing quartzite at the top of unit 5, Sekwi Formation, section 2. GSC 203473-Z
3. View looking southwest at upper part of section 2. Contact between Sekwi Formation and Rockslide Formation is at "a", contact between Rockslide and Avalanche Formation is at "b". Section offset across fault (white squares) and resumed at base of Avalanche Formation at "c", contact between Avalanche Formation and stripped member of Broken Skull Formation is at "d". Point "d" in this figure marks same location as point "e" in figure 1. GSC 203473-W
4. View looking south from near top of lower part of section 2 (top of Sekwi Formation) at upper part of section 2 (see also fig. 3). Base of Rockslide Formation is at "a", limestone mounds 75 m above base of Rockslide are at "b", contact between Rockslide and Avalanche formation is at "c". Section continues across fault (white squares) from base of Avalanche Formation at "d". GSC 203473-H
5. **Circotheca?** sp. Shell impressions on bedding plane of very fine grained quartzite, GSC locality 96990, local float, 905 m below top of unnamed formation, section 2. Divisions on scale to right are in millimetres. GSC type no. 65649, GSC 202029-H
6. Thin wavy beds of thick parting, medium grey weathering limestone, Avalanche Formation, 6.5 m above base. Pencil gives scale. GSC 203473-E

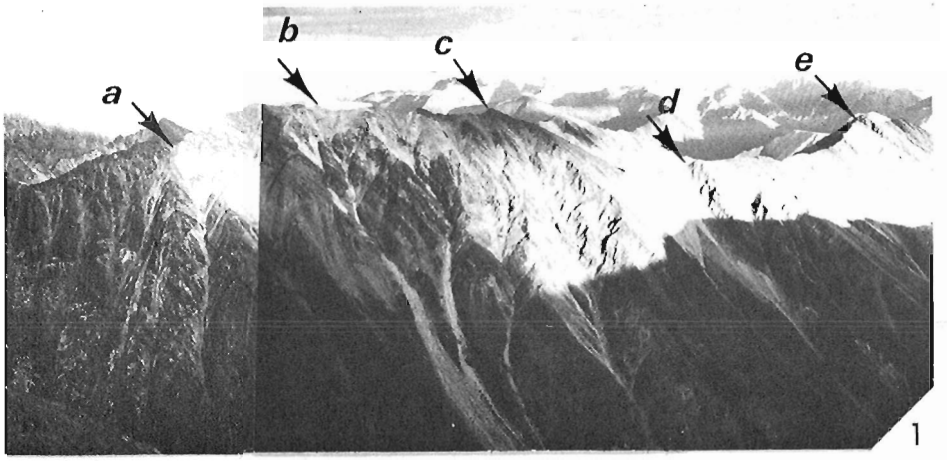

1

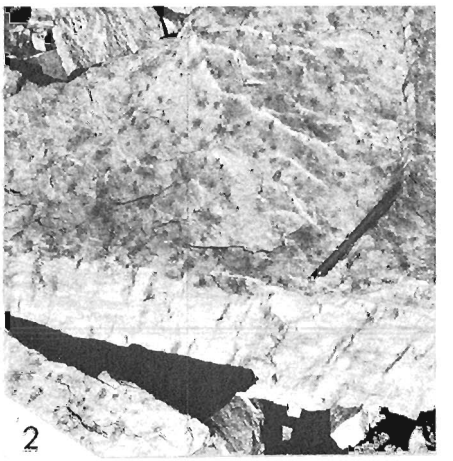

2

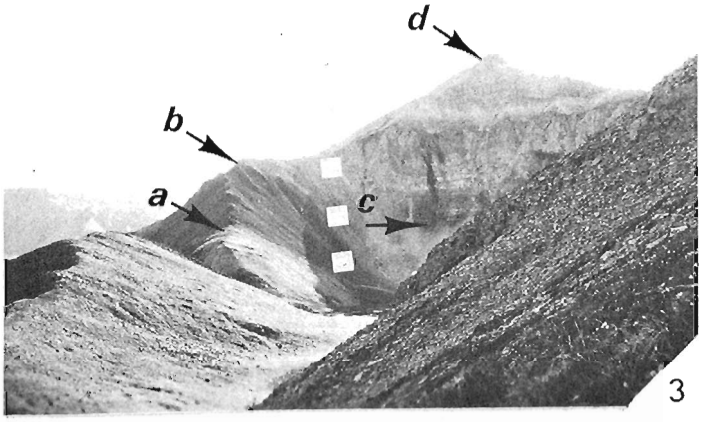

3

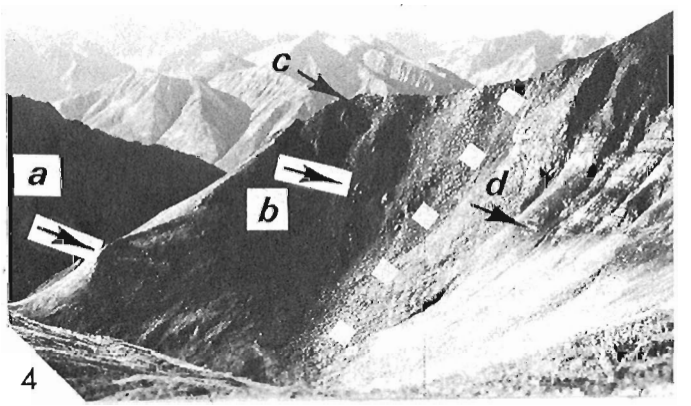

4

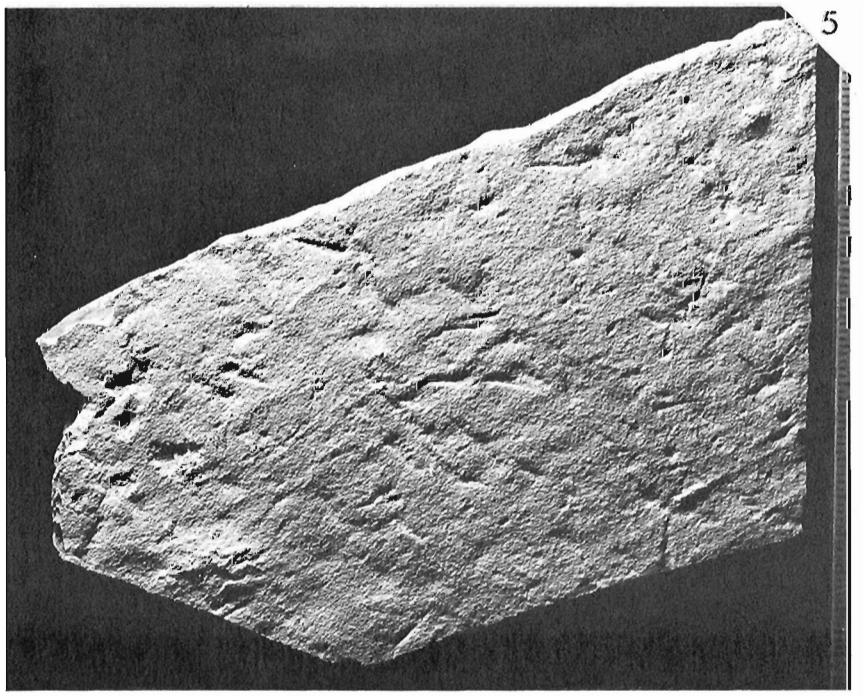

5

6

Sekwi Formation (504.5 m)

The basal unit (unit 1, 92 m) in the Sekwi Formation is mainly composed of thin, wavy bedded limestone that is thin to thick parting, weathers medium grey to medium blue grey, and is medium dark grey and finely crystalline on fresh surfaces. Beds of this limestone have been locally altered to medium grey weathering, finely crystalline dolomite. At the base of the unit is 5 m of light yellow to orange brown weathering siltstone with sparse, orange weathering limestone nodules. A similar, but less resistant siltstone occupies the interval 5 to 21 m above the base. Within this interval are limestone nodules that increase in number and coalesce up section into thin, wavy beds of medium grey limestone constituting 50 per cent of the strata near the top. At the top of the unit is 0.5 m of medium dark brown weathering shale. Penecontemporaneous limestone breccia is present 28.5 to 29 m and 83.5 to 84.5 m above the base of the unit.

Medium grey weathering dolomite in thin, broadly wavy beds predominate in unit 2 (41 m). Fresh surfaces are medium dark grey and finely crystalline. Dolomitic quartz sandstone that is fine to medium grained is present in the basal 2 m of the unit and orange weathering siltstone with dark grey fresh surfaces is present in the interval 27.5 to 32 m above the base.

Unit 3 (61 m) is composed of dolomitic siltstone and silty dolomite. The siltstone is medium brownish grey weathering and is medium grey to medium dark grey on fresh surface. The dolomite is in orange weathering thin to thick irregular beds and in pods that are up to 0.5 m high, all of which have fresh surfaces that are medium dark grey and are finely crystalline. A thick bed of fine to coarse grained quartzite is present 26 to 27 m above the base of the unit. In the interval 51 to 61 m above the base are thin beds of both medium grey dolomitic sandstone that is fine and very fine grained and orange weathering dolomite.

Cream weathering and fresh dolomite in thick, resistant beds distinguishes this unit (unit 4, 78 m) from other, darker strata in the formation. The dolomite is finely crystalline and is mixed with fine to coarse quartz sand that is "floating" or is in sandy dolomite beds at various horizons.

Unit 5 (34 m) is half medium light brownish orange weathering dolomite in medium and thick beds that are light brown and finely crystalline on fresh surfaces, and half light grey weathering and unweathered quartzite that is fine to coarse grained. At the top of the unit is 5.5 m of fine to coarse grained quartzite in thick beds that are white on weathered and fresh surfaces. **Skolithos** sp. is present in these upper quartzite beds (Plate 19.1, fig. 2).

Unit 6 (54 m) contains a mixture of siltstone, dolomite, and quartzite. At the base of the unit (0 to 12 m) is medium brown to orange weathering siltstone that is medium dark grey on fresh surface. This is overlain (12 to 18 m) by orange weathering, thin and medium bedded dolomite which in turn is overlain (18 to 25.5 m) by orange to medium brown weathering siltstone containing sparse trilobites. The upper half of the unit (25.5 to 54 m) contains mostly medium light orange brown and bright orange weathering dolomite in thin and medium beds. **Skolithos** sp. bearing quartzite is present in the interval 25.5 to 30 m above the base of the unit and 5 m or orange to medium brown weathering siltstone is present at the top.

Strata of Unit 7 (55 m) are equally as resistant as those of unit 4 and the two units form small peaks (Plate 19.1, fig. 1) on the ridge crest used as the measuring route for the Sekwi Formation. The basal 22.5 m is composed of orange weathering dolomite and light brown weathering, fine and medium grained quartzite. Interval 22.5 to 55 m contains maroon and purple weathering siltstone and sandstone in thin to thick beds. The sandstone is mainly concentrated at the top of the unit where it is fine to coarse grained.

The highest unit (unit 8, 89.5 m) in the Sekwi Formation is composed of dolomite and siltstone. Light orange weathering (0-15.5 m) and light brownish grey weathering (19.5 to 25.5 m) dolomite in thin and medium, broadly wavy beds are concentrated in the lower part of the unit. Orange weathering platy dolomitic siltstone occupies the remainder or the unit.

Rockslide Formation (100.5 m)

Medium brownish grey weathering siltstone predominates in the one unit (unit 1, 100.5 m) of this formation. The siltstone weathers to irregular slabs and fresh surfaces are medium grey. Above the 13 m level, limestone is present in lenses averaging 8 cm thick and 30 cm long. The limestone is medium grey weathering and fresh surfaces are medium dark grey and finely crystalline. At the 75 m level limestone mounds that are 4 m high are present (Plate 19.1, fig. 4). Two beds of maroon weathering siltstone 0.5 m thick are located 30 m and 50 m above the base of the unit.

Avalanche Formation (324.5 m)

Unit 1 (23.5 m) consists of medium grey weathering limestone in thin wavy, thick parting beds (Plate 19.1, fig. 6). Fresh surfaces are medium dark grey and finely crystalline. Except for the change from lenses to thin beds and the lack of shale and siltstone interbeds, the limestone in this unit resembles that in the Rockslide Formation below.

Plate 19.2

Figure

1. View looking east at lower part of section 3. Top of unit 2 in unnamed formation is at "a", base of Sekwi Formation is at "b", base of **Skolithos** bearing quartzite (16 m above base of unit 4) is at "c", contact between Sekwi and Rockslide formations is at "d". Composite of photos 203473-P, 203473-R, 203473-Q
2. View looking west at Rockslide Formation in section 3. Contact between Sekwi and Rockslide formations is at "a", base of unit 4 is at "b", and contact between Rockslide and Rabbitkettle formations is at "c". GSC 203473-N
3. View looking west at lower part (units 1 to 3) of Rabbitkettle Formation in section 3. Base of Rabbitkettle is at "a", base of bright orange weathering dolomite-bearing interval (61 to 79 m above base of unit 3) is at "knickpoint" at "b", top of unit 3 is at "c". See figure 7 for second view of this part of section. GSC 203473-K
4. Abundant burrows and small cross ripple marks in local float 63.5 m above base of unit 3, unnamed formation, section 3. Pencil located left of centre gives scale. GSC 203473-O
5. Interbedded medium brownish grey weathering, platy limestone and rust weathering (black on unweathered surface) siltstone, 94 m above base of Rockslide Formation, section 3. GSC 203473-L
6. View looking west at Rabbitkettle Formation, section 3, base of unit 5 is at "a". Black squares locate fault. Steep face below "a" is on strike (slightly offset by fault) with unit 4 measured along route with less relief to right of photo (see fig. 7). "Swiss cheese" texture in unit 4 is exposed below "a". GSC 203473-I
7. View looking northwest at Rabbitkettle Formation in section 3. Base of Rabbitkettle Formation is at "a", base of bright orange weathering dolomite-bearing interval (61 to 79 m above base of unit 3) is at "knickpoint" marked "b", top of unit 3 is at "c", top of unit 4 is approximately at "d". GSC 203473-J

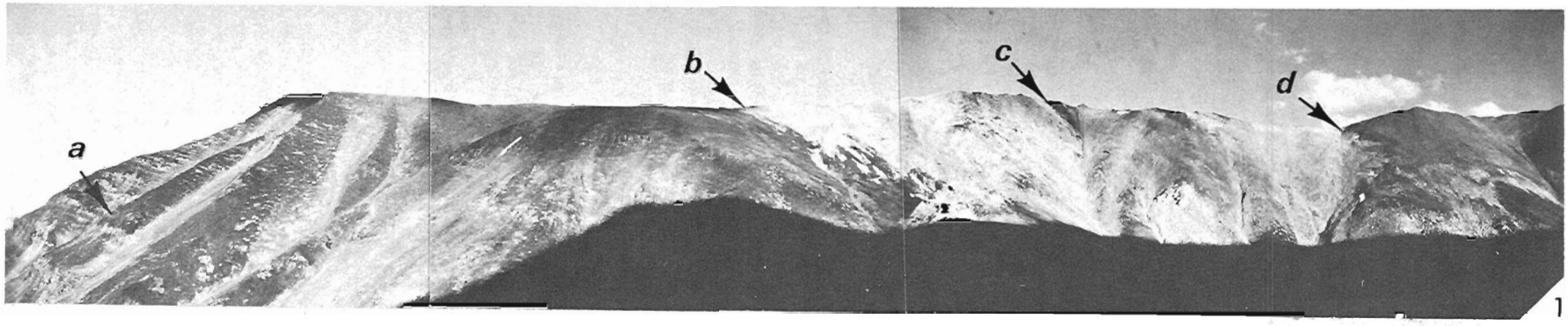

1

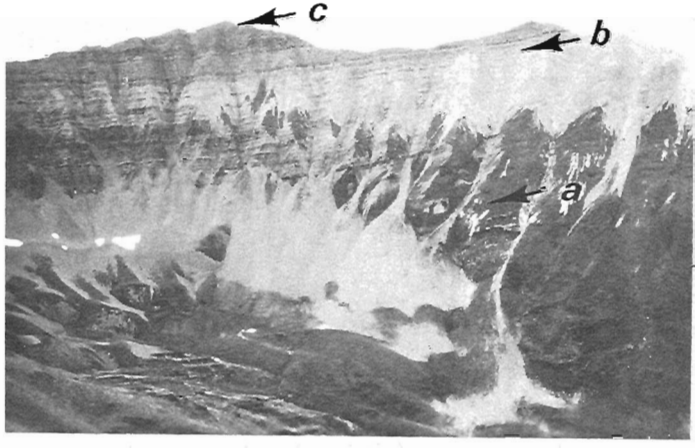

2

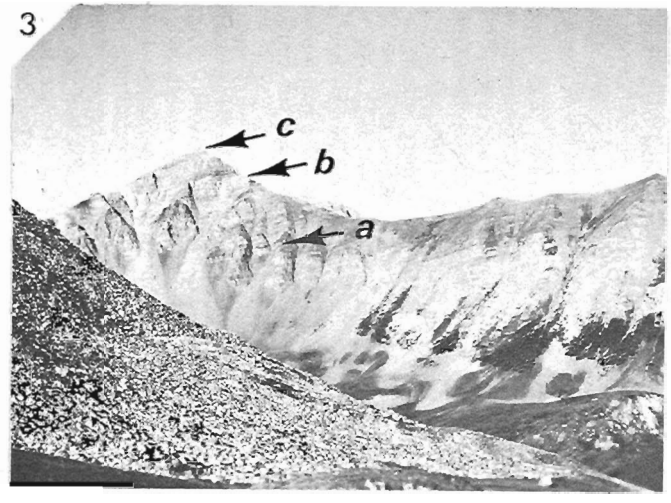

3

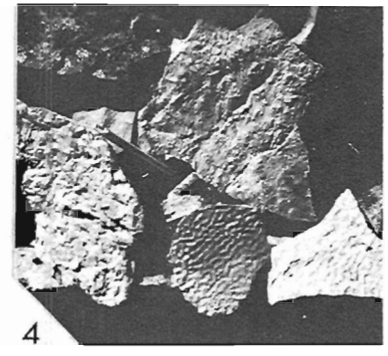

4

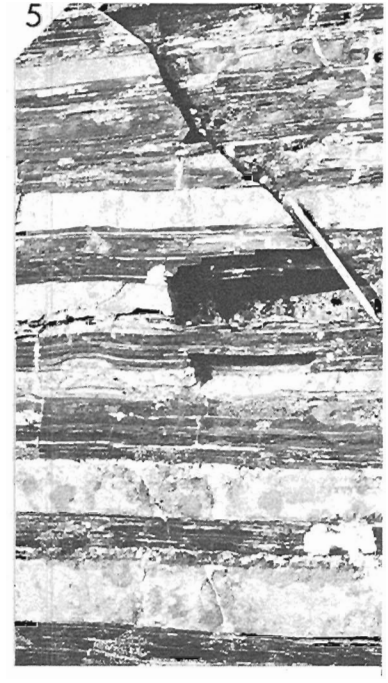

5

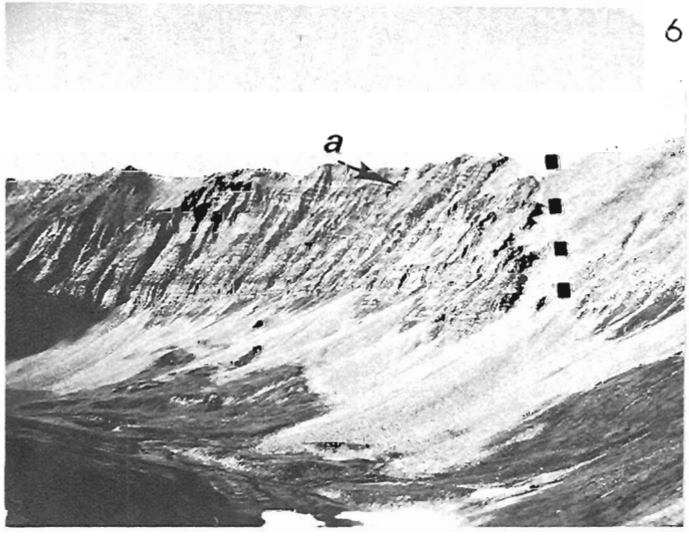

6

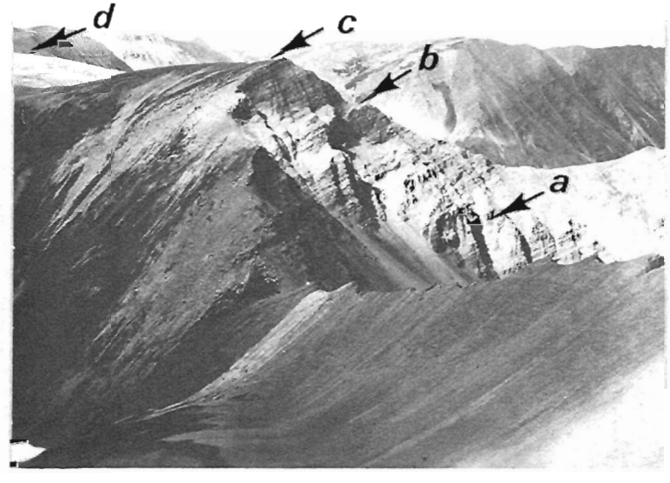

7

Resistant, medium light grey to cream weathering dolomite in thick beds comprise the upper unit (unit 2, 301 m) of this formation. At various levels faint outlines of thin wavy beds suggest that at least part of the unit was originally limestone similar to that in unit 1. Some fine to coarse "floating" grains of quartz sand are present 17.5 m below the top of the unit, and the uppermost 5.5 m is composed of cream weathering and unweathered dolomite in thin planar laminated beds.

Lower stripped member, Broken Skull Formation

Overlying the Rockslide Formation is an unmeasured succession of varicoloured strata that are here referred to as the lower stripped member of the Broken Skull Formation. At the base of the succession is dolomite in bright, light orange and brick red weathering interbeds. The dolomite is thin to thick bedded and is planar laminated. Some maroon layers of silty dolomite are present, many of which display mudcracks. Higher in the section are beds containing "floating" quartz sand and minor white sandstone interbeds are present. In these beds quartz grains are mainly in the fine range, but sparse coarse grains were seen.

Stratigraphic Section 3

Unnamed Formation (560+ m)

Above the covered base of section 3, unit 1 (149.5+ m) is composed of rust to medium brownish grey siltstone (30 per cent) and very fine grained quartzite (70 per cent) in thin (5 mm), planar laminated plates. Fresh surfaces of the siltstone and of half of the quartzite are light greenish grey and those of the remaining quartzite are light brownish grey. Lenses of quartzite 0.7 m thick and 2 m long are present 60 m above the base of the section and trace fossils 5 mm wide are present near the same horizon.

Unit 2 (36.5 m) contains white weathering and unweathered quartzite in thin to thick beds that are fine to coarse grained. Intervals 17.5 to 22.5 m and 26.5 to 30 m above the base contain highly burrowed, very fine grained quartzite and siltstone that are similar to that in unit 1.

Interbedded siltstone and very fine grained sandstone in approximately equal proportions comprise unit 3 (142 m). In the lower part (0-67 m) the siltstone and sandstone weather medium dark grey, medium dark brownish grey, and rust and they are in plates that are dark grey on fresh surfaces. In the upper part (67 m to 142 m) half of the strata is like that below and half is rust to light brownish grey, very fine grained quartzite in medium and thin beds that are medium to dark grey on unweathered surfaces. The trace fossil **Didymaulichnus** sp. is present 29 m above the base, burrows and mud cracks are present at 63.5 m, and cross ripples and burrows are present in float at 120 m.

Unit 4 (184 m) is composed of silty very fine grained sandstone and sandy siltstone in thin plates that weather medium grey, medium reddish brown and are medium dark grey on fresh surfaces. In the interval 65 to 173 m above the base rust weathering sandstone (25 per cent) is interbedded with the strata just described. Resistant, thick bedded quartzite in the top 11 m of the unit weathers light grey and is light brown on unweathered surfaces. Trace fossils and cross ripples are present in local float 14 m above the base of the unit.

The highest unit (unit 5, 48 m) contains siltstone and sandstone as in the 65 to 173 m interval of unit 4, but also contains khaki shale in various intervals throughout the unit. Large (2 cm wide), abundant burrows are present 0.5 m above the base.

Sekwi Formation (403 m)

The basal unit (unit 1, 52 m) in this formation comprises 40 per cent orange to orange brown weathering siltstone and 60 per cent thin, wavy bedded dolomite. Half of the dolomite is cream weathering with fresh surfaces that are light grey, and the other half is medium grey on both weathered and unweathered surfaces.

Unit 2 (69.5 m) contains dolomite (60 per cent) in thin, broadly wavy beds that are light grey on fresh surfaces, except in the top 13.5 m where the dolomite is pink to cream weathering. Between the dolomite exposures are covered intervals (40 per cent) that probably are underlain by siltstone similar to that in unit 1.

Unit 3 (77.5 m) is composed of dolomite in thick beds (0 to 50 m) and in thin to thick beds (50 to 77.5 m) that are cream coloured on both weathered and fresh surfaces. The dolomite is finely crystalline and contains fine to coarse quartz grains that are "floating" in a dolomite matrix and are also concentrated in planar and crossbedded laminae.

Dolomite that is orange on weathered and fresh surfaces predominates in unit 4 (148 m). The dolomite is in thin, platy beds except for thin to thick beds 29 to 40 m above the base and medium and thin beds 85.5 to 130 m above the base. Interval 16 to 20.5 m contains thick beds of medium grained quartzite that is white on weathered and fresh surfaces and contains **Skolithos** sp. Fine to coarse quartz grains that are "floating" and are in planar and crossbedded laminae are abundant 20.5 to 63 m above the base. Interval 63 to 85.5 m contains dolomite as mentioned and siltstone (66 per cent) that weathers purple, maroon and light brown.

Unit 5 (56 m) is composed of dolomite and a subordinate amount of siltstone. The lower 30 m is composed of light brownish grey weathering dolomite in thin wavy beds with thin to thick partings. Fresh surfaces are medium light grey and finely crystalline. The upper 26 m of unit 5 contains orange weathering siltstone and dolomite in thin plates. The top of this unit and the top of the Sekwi Formation is placed at an abrupt change from orange weathering siltstone and dolomite to medium grey weathering limestone.

Rockslide Formation (432 m)

Thin bedded, platy limestone with medium brownish grey, light yellow grey, and some light orange parting surfaces comprise the basal unit (unit 1, 139 m) of the Rockslide Formation. The limestone is planar laminated, finely crystalline, and fresh surfaces are dark grey. Interval 0 to 3.5 m contains medium blue grey weathering limestone in thin, wavy beds. Some rust weathering, dark grey siltstone is present in the upper one-fourth of the unit. Penecontemporaneous folds 0.5 m high are exposed 60.5 m above the base of the unit, and sponge spicules in local float were noted 59 m above the base.

From a distance, unit 2 (43 m) is a medium brown band between medium grey units above and below. It is composed of thin (7.5 mm) plates that weather medium brown to medium brownish grey and are medium grey to medium dark grey on fresh surfaces. A distinctive orange weathering bed 0.3 m thick is present 19.5 m above the base and sponge spicules were observed 38.5 m above the base.

Very thin to thin (6 mm to 36 mm), platy beds that weather medium grey, light orange and light orange brown comprise this unit (unit 3, 87 m). The limestone is planar laminated, finely crystalline, and fresh surfaces are dark grey. Penecontemporaneous slump structures are present 36 m (folds 0.5 m high), 51.5 m (breccia bed 1.5 m thick), and 65 m (breccia bed 0.25 m thick) above the base.

Unit 4 (100.5 m) is mainly limestone in very thin (6 mm), platy beds, many of which combine to weather in thick parting "books". The remaining limestone is thin bedded and platy. Limestone of both types are medium grey, light grey, and medium grey brown on weathered surfaces and are medium and dark grey on fresh surfaces. Minor interbeds of rust weathering siltstone that is black on fresh surface are present in the upper half of the unit. A thin bed of very fine grained quartzite is present 72 m above the base of the unit.

An abundance of very fine grained quartz sand is present in this uppermost unit (unit 5, 62.5 m) of the Rockslide Formation. The lowermost 22 m is medium brownish grey to rust weathering silty sandstone in very thin plates that are medium light grey on fresh surface. This is overlain by 31.5 m of medium grey to medium grey brown limestone containing varying amounts of quartz sand. At the top of the unit is 9 m of greenish grey weathering, limy siltstone with limestone nodules (33 per cent) both of which are medium light grey on fresh surfaces.

Rabbitkettle Formation, 490+ m

Orange to brownish grey weathering quartzite in medium and thick beds predominates in the basal unit (unit 1, 37 m) of this formation. Fresh surfaces are light grey and the quartzite is very fine to fine grained. Interbedded with the quartzite is medium greenish grey siltstone (25 per cent) that is medium grey on fresh surface. At the top of the unit is 4 m of limy quartz sandstone in thin, wavy beds that weather the same colour as the quartzite below.

Unit 2 (81 m) is composed of medium brownish grey weathering, limy siltstone in thick to thin parting, planar laminated beds that are medium grey to medium dark grey on fresh surface. Orange weathering lenses and nodules of siltstone that is slightly more limy than the surrounding matrix are common.

Thin bedded, platy limestone comprises most of unit 3 (141.5 m). In interval 0 to 61 m is limestone weathering medium grey (0 to 29 m), medium brownish grey (29 to 43 m), and light brownish to yellowish grey (43 to 61 m) that is medium to dark grey on fresh surfaces. An interval (61 m to 79 m) containing bright orange weathering limestone (33 per cent) is present in the middle of unit 3. This limestone, together with medium blue grey weathering limestone (33 per cent) and medium brownish grey siltstone (33 per cent) forms a recessive "knick point" in the middle of the unit (Plate 19.2, fig. 7). Interval 79 to 141.5 m contains medium light grey, brownish grey, and medium brown weathering limestone in thin to very thin plates. Subinterval 84 to 112.5 m has some (33 per cent) interbedded light brownish grey weathering siltstone.

An abundance of limy shale and siltstone in unit 4 (164.5 m) is responsible for the weak topographic expression of this unit. The lower 43.5 m comprises siltstone and shale that weather light brown and is medium grey on fresh surfaces. The upper 121 m contains siltstone (50 per cent) that weathers light grey and is medium grey on fresh surfaces, and limestone (50 per cent) in thin plates, thin wavy beds, and nodules. The limestone weathers medium light grey with orange mottled parting surfaces, and fresh surfaces are medium dark grey. One bed of penecontemporaneous breccia 0.5 m thick was noted 0.5 km south of the section and 86.5 m above the base of the unit.

Unit 5 (66 m) is composed of medium grey weathering limestone in thin, wavy beds that are medium grey to medium dark grey on fresh surfaces and finely crystalline. Parting surfaces 0 to 24 m above the base are mottled bright red and those 42 to 66 m above the base are mottled bright orange. Limestone (siliceous?) in the latter interval produces a tinkling sound under foot.

Overlying unit 5 and a short distance below a fault at the top of the section (Plate 19.2, fig. 6) is light grey weathering and unweathered dolomite in thin wavy beds that are medium and thick parting. It was not determined whether this dolomite is widespread or whether it represents local alteration related to the nearby fault.

Age and Correlation

Unnamed formation

Gordey (1979, Fig. 2.1, section C) assigned the strata immediately below the Sekwi Formation in section 1 to the Backbone Ranges Formation, while in the same year the writer (Fritz, 1979a, p. 123) retained the original assignment (Green and Roddick, 1961) of map unit 3. The writer was then uncertain as to the relationship of these strata to the type Backbone Ranges Formation and to map unit 13 of Blusson (1971) and therefore favoured a delay in reassignment.

In the type area immediately to the north, map unit 13 overlies the lithological equivalent (map unit 12 of Blusson, 1971) of the upper member of the Backbone Ranges Formation and underlies the Sekwi Formation. Despite proximity, no southern extension of map unit 13 into the Nahanni area has been proposed. Twenty-six sections in the Sekwi Mountain map area and farther to the north that include parts or all of map unit 13 have been briefly described (Fritz, 1976, 1978, 1979b), and in all of the sections the map unit is remarkably uniform, consisting of medium to dark brownish grey or rust weathering siltstone and very fine grained quartzite. Unweathered siltstone and thin bedded quartzite surfaces of map unit 13 are dark grey whereas those of thicker bedded quartzite are medium brownish grey.

At the type section of the Backbone Ranges Formation (1440 m) located 40 km east of the Nahanni map area, the formation comprises an upper and lower member of light coloured, fine to coarse grained quartzite separated by a middle member of thin bedded dolomite (Gabrielse et al., 1973, section 12). Here a sub-Avalanche Formation disconformity records the removal of the Sekwi Formation, possibly map unit 13, and an unknown thickness of light coloured quartzite that would otherwise be included in the Backbone Ranges Formation. Gabrielse et al. (1973, Fig. 7) have placed the base of the Cambrian at the base of the Backbone Ranges Formation, and Blusson (1971, p. 9) has placed the base at the bottom of map unit 12 (bottom of upper member of Backbone Ranges Formation). In 1980 the international Precambrian/Cambrian Boundary Working Group tentatively placed the boundary within map unit 12 (Fritz, 1980, Fig. 7.3).

At sections 2 and 3 the measured strata in the unnamed formation are believed to belong to the early Lower Cambrian because they contain an abundance of trace fossils and because the shelly fossil **Circotheca?** sp. (Fig. 19.1, GSC locs. 96990, 96991; Plate 19.1, fig. 5) was collected at section 2. The considerable thickness of early Lower Cambrian strata in the upper part of the unnamed formation implies the absence of an unconformity between the formation and the overlying Sekwi Formation, which is in agreement with the gradational contact noted between the two formations at section 1 (Fritz, 1979a, p. 121) and section 2 (contact at section 3 not exposed). Faunal evidence in the Nahanni area indicates that Sekwi strata immediately above the contact are the same age as those reported (Fritz, 1976, 1978, 1979b) in the basal Sekwi that immediately overlies map unit 13 to the north.

The boundary between the **Fallotaspis** Zone and the **Nevadella** Zone in section 3 is a short distance above the formational contact and between **Parafallotaspis grata** Fritz in local float (GSC loc. 96964) 1 m above the base of the formation and **Nevadella** sp. in local float (GSC loc. 96965) 2.5 m above the base. At section 1 fossils (GSC loc. 95668) questionably assigned (Fritz, 1979a, p. 121) to the **Fallotaspis** Zone are 6.5 m above the base, and at section 2 **Parafallotaspis grata** is 4.7 m above the base (GSC loc. 96992) and **Parafallotaspis** sp. is 5 m above base (GSC loc. 96993).

After considering the above data and after inspecting in 1980 the type Backbone Ranges Formation and equivalent strata in the southeastern part of the Nahanni Anticline, it is the writer's conclusion that the strata here described as belonging to the "unnamed formation" should ultimately be placed in a new formation. A suggested location for a type section is the southeastern end of the Nahanni Anticline where the base could be placed at the top of the middle member of the Backbone Ranges Formation (top of dolomite) and the top at the base of the Sekwi Formation. Given these vertical limits, the dark siltstone and interbedded quartzite of the new formation would correlate temporally with the light coloured quartzite in the upper member of the type Backbone Ranges Formation plus an unknown amount of early Lower Cambrian strata removed there by erosion. Unit 13 could be considered as part of the new formation, as it is a physical northward extension of the same lithology and is overlain by the same (Sekwi) formation. Action on this consideration would require recognition of a diachronous base, for at the proposed type section the new formation would directly overlie the middle member of the Backbone Ranges Formation and in the Sekwi Mountain map area it would overlie the upper member in the Backbone Ranges Formation (map unit 12).

Sekwi Formation

Strata at the type section (Handfield, 1968; Fritz, 1972) of the Sekwi Formation belong to the Lower Cambrian **Fallotaspis, Nevadella,** and **Bonnia-Olenellus** Zones. The boundary between the **Fallotaspis** and **Nevadella** Zones is a short distance above the base of the formation and the Lower-Middle Cambrian boundary is a short distance above the top.

The fossils near the base of the Sekwi Formation in the Nahanni area have been mentioned above. Higher in sections 2 and 3 fossils are rare but at one locality (GSC loc. 96994) **Holmiella** sp., **Keeleaspis** sp., **Kootenia?** sp., **Nevadella** sp., and **Sekwiaspis** sp. were collected in the lower part of the formation, and a second locality (GSC loc. 96995) in the upper one-third of the formation produced **Olenellus** sp. These localities belong to the **Nevadella** Zone and to the **Bonnia-Olenellus** Zone, respectively. The presence of **Poliella** sp. (GSC loc. 96967) 3.5 m above the top of the Sekwi at section 3 indicates the presence of the oldest Middle Cambrian zone at that level, and therefore suggests that the top of the Sekwi there is close to the boundary between the Lower and Middle Cambrian.

In an earlier description of section 1, Fritz (1979a, p. 123) mentioned that the strata in the lower half of the Sekwi Formation closely resemble those in the lower Sekwi at numerous sections to the north (Fritz, 1976, 1978, 1979b; total of 36 sections). The succession in ascending order in this half of the Sekwi in sections 1 to 3 and over the wide area to the north is as follows: (1) orange-brown or pink weathering limy siltstone with nodules, sparse glauconite, upper **Fallotaspis** and lower **Nevedalla** Zone; (2) blue grey weathering limestone in thin wavy beds (dolomitized at section 3) and light brown weathering limy siltstone with abundant nodules (Swiss cheese), some penecontemporaneous slump folds and breccias, **Nevadella** Zone; (3) light grey to light orange weathering, thick bedded dolomite with "floating" quartz grains, **Nevadella** Zone; (4) medium and thick bedded quartzite with **Skolithos** sp., top of **Nevadella** Zone-base of **Bonnia-Olenellus** Zone.

The upper half of the Sekwi Formation (above the lowest **Skolithos**-bearing quartzite) contains abundant orange weathering dolomite and dolomitic siltstone with minor maroon and purple beds at all three sections in the Nahanni map area. Strata of this type were noted in the upper half of the Sekwi in a section just north of the map area (Fritz, 1979b, section 36, units 8-16), but are absent in all other sections measured by the writer farther north. Similar strata, but with a higher proportion of maroon, calcareous siltstone, have been reported in sections located 47 km (Gabrielse et al., 1973, section 14, units 21, 22) and 46 km (op. cit., section 18, units 1, 2) northeast of the Nahanni map area. Although these strata were assigned to the Backbone Ranges Formation, the lithology plus the presence of fossils belonging to the **Bonnia-Olenellus** Zone indicate they belong to the Sekwi Formation.

Rockslide Formation

The type section for the Rockslide Formation (Gabrielse et al., 1973, section 16) lies 45 km northeast of the Nahanni map area and comprises dark, platy limestone and calcareous siltstone. Despite a disconformity at the base and an angular unconformity at the top, the formation is reported to contain all of the Middle Cambrian zones except the **Bolaspidella** Zone, and this zone is present in a Rockslide section a short distance away (op. cit., section 19).

At section 3 all of the Middle Cambrian zones are present. Rockslide fossils in section 3 are listed below.

GSC locality	Fossils and zone	Metres above base of formation
96967	**Kochaspis?** sp. **Pachyaspis** sp. **Poliella** sp.	3.5
	Plagiura-Poliella Zone	
	Albertella Zone	
96968	**Amecephalus** sp. **Helcionella** sp. **Oryctocephalus** sp. **Pagetia clytia** Walcott **Yohoaspis** sp.	6
96969	**Pagetia clytia?** Walcott aff. **Pagetia mucrogena** Fritz	9.5
	Albertella Zone	
	----------?----------?----------?----------	
	Glossopleura Zone	

GSC locality	Fossils and zone	Metres above base of formation
96966	**Alokistocare** sp. **Bathyuriscus** sp. **Pachyaspis** sp. **Peronopsis** sp. **Ptychagnostus** sp. **Spencia** sp.	35
	Glossopleura Zone	
	----------?----------?----------?----------	
	Bathyuriscus-Elrathina Zone	
96970	**Elrathina** sp. **Peronopsis** sp. **Ptychagnostus richmondensis?** (Walcott) **Zacanthoides?** sp.	52
96971	**Protospongia?** sp.	177.5
	Bathyuriscus-Elrathina Zone	
	----------?----------?----------?----------	
	Bolaspidella Zone	
96972	**Ptychagnostus punctuosus affinis** (Brögger)	196
96973	**Hypagnostus?** sp. **Modocia** sp.	227.5
96974	**Bolaspidella** sp. **Hemirhodon** sp. **Modocia** sp. **Ptychagnostus** sp.	241
96975	**Lejopyge calva** Robison **Diplagnostus** sp.	341
96976	**Baltagnostus** sp. **Eldoradia** sp. **Hypagnostus** sp. **Lejopyge** sp. **Modocia** sp.	381
96977	**Eldoradia** sp. **Hypagnostus** sp. cf. **Ptychangostus (Ptychagnostus) aculeatus** (Angelin) **Modocia** sp.	383
96978	**Eldoradia** sp. **Hypagnostus** sp. **Modocia** sp.	408
96979	**Baltagnostus** sp. **Elrathia** sp. **Hypagnostus** sp. **Modocia** sp. cf. **Ptychagnostus (Ptychagnostus) aculeatus** (Angelin)	418.5

At section 2 only the lower part of the Rockslide Formation is present as the upper part has been displaced by the Avalanche Formation. Rockslide fossils at section 2 are as follows:

GSC locality	Fossils and zone	Metres above base of formation
96996	**Amecephalus** sp. **Caborcella?** sp. **Kochiella?** sp. **Ogygopsis** sp. **Pagetia clytia?** Walcott **Zacanthoides** sp.	19
	Plagiura-Poliella Zone	
	----------?----------?----------?----------	
	Albertella Zone	
96997	**Amecephalus** sp. **Kootenia** sp. **Pachyaspis** sp. **Pagetia resseri?** Kobayashi **Poliella** sp. **Ptarmiganoides?** sp. **Yohoaspis?** sp.	36.5

The lithology and fossils of the Rockslide Formation at section 3 are in close agreement with the description given for the type section, the most significant difference between the two sections being the nature of the upper contact. In their description of this contact Gabrielse et al. (1973, p. 38) stated "Erosion prior to deposition of the Upper Cambrian rocks has been partly responsible for the marked changes in thickness of Middle Cambrian rocks from place to place. For example, in 3 miles south-southeast of the type section the formation is reduced from more than 1,640 to 680 feet [500 m to 207 m] in thickness".

At section 3 the top of the Rockslide is drawn at the base of a sandstone unit (Rabbitkettle Formation, unit 1, 37 m) that is believed to be an early depositional record of the mentioned erosion elsewhere. The **Cedaria-Crepicephalus** Zone boundary probably extends to the base of the sandstone unit and is first documented 36.5 m (GSC loc. 96980) above the base of the formation. This thickness suggests little or no erosion has taken place at the Rockslide-Rabbitkettle boundary at section 3.

A lithological correlation of the upper part of the Sekwi Formation to section 3 suggests that most if not all of the latest Lower Cambrian is present below the Rockslide-Sekwi contact at the base of the formation. Above this contact are fossils (GSC loc. 96967) belonging to the earliest Middle Cambrian **Plagiura-Poliella** Zone.

Avalanche Formation

At the type section (Gabrielse et al., 1973, section 20) located 34 km east of the Nahanni map area, an erosional unconformity separates the Avalanche Formation from the underlying Backbone Ranges Formation. Fossils a short distance above the base of the formation (21 m to 25.6 m, loc. cit.) belong to the earliest Middle Cambrian **Plagiura-Poliella** Zone. No fossils were found higher in the type section and the top has been placed (op. cit., p. 39) "...somewhat arbitrarily, at the base of the first significant influx of sand into the dolomite sequence."

The highly coloured, platy dolomite and dolomitic siltstone at the type section does not closely resemble the light to medium grey, thick bedded dolomite at section 2, but the two sections are probably part of the same carbonate body. A second Avalanche section described by Gabrielse et al. (1973, section 21) located 14 km north of the type section, is intermediate between the type section and section 2 in that it contains an abundance of light coloured dolomite. The difference between the three mentioned sections may reflect a different position across the middle carbonate belt, with the type section occupying a position on the inner edge near the contact with the inner detrital belt, the intermediate section being positioned within the middle carbonate belt, and section 2 occupying a position near the outer edge of the middle carbonate belt and near the transition with the outer detrital (Rockslide Formation) belt.

Concerning the age of the Avalanche and Rockslide formations, Gabrielse et al. (1973, p. 45) stated that the basal strata of the two formations are "essentially correlative", but equating the higher strata "is tenuous, however, because faunal control is lacking in the upper Avalanche Formation". At section 2 the following fossils were collected in the Avalanche Formation:

GSC locality	Fossils and zone	Metres above base of formation
96998	**Caborcells** sp. **Kootenia** sp. **Pachyaspis** sp. **Pagetia resseri?** Kobayashi	5.5 m
96999	**Achlysopsis** sp. **Paralbertella?** sp. **Kootenia** sp. **Pagetia** sp.	20 m
96700	**Amecephalus** sp. **Kootenia** sp. **Oryctocephalus** sp. **Pachyaspis** sp. **Zacanthoides** sp.	23.2 m

In addition to the above fossils, the following 1978 collections are available from a thin Avalanche tongue that displaces uppermost strata of the Rockslide Formation at section 1. These fossils were previously (wrongly) assigned to the Rockslide Formation (Fritz, 1979a, Fig. 15.1, unit 14).

GSC locality	Fossils and zone	Metres above base of formation
95686	**Hypagnostus?** sp. **Modocia** sp.	0.5 m
95687	**Bolaspidella?** sp. **Modocia** sp.	14.5 m
95688	**Baltagnostus?** sp. **Hemirhodon?** sp. **Hypagnostus** sp. **Modocia** sp.	46.5 m

The fossils in localities 96998 to 96700 are tentatively assigned to the early Middle Cambrian **Albertella** Zone and those in localities 95686 to 95688 to the late Middle Cambrian **Bolaspidella** Zone. If the Avalanche tongue at section 1 is correlated to the barren upper Avalanche strata in section 2, then it can be assumed that the Avalanche Formation at section 2 spans all of the Middle Cambrian except for the earliest zone, the **Plagiura-Poliella** Zone. Since this latter zone is known from the type section, both the Avalanche and Rockslide formations have a regional age that spans the Middle Cambrian.

Rabbitkettle Formation

In terms of a type section or faunal collections, the Rabbitkettle Formation is the least known of the formations described thus far. Gabrielse et al. (1973, p. 48) designated a type area rather than a type section for the formation "near the headwaters of Rabbitkettle River", which is an outcrop area extending westward from the adjacent Glacier Lake map area into the southeastern part of the Nahanni map area. No fossils were reported from this (loc. cit.) "relatively uniform sequence of interbedded limestones, silty limestones, and siltstones" that are estimated to be more than 1220 m thick, nor are they known from an upper member of finely laminated, dark grey to black limestone and calcareous shale that is more than 305 m thick. Gabrielse et al. (1973, p. 51, 52) have tentatively suggested that the Rabbitkettle correlates with the Broken Skull Formation and that both formations overlie a regional sub-Franconian erosion surface. In the type area an angular unconformity separates the Rabbitkettle Formation from the underlying Sekwi Formation and the overlying Road River Formation (op. cit.). Prior to formal description, the Rabbitkettle Formation was described by Gabrielse et al. (1965) as map unit 18 and by Blusson (1968) as map unit 9.

The following fossils were collected from the Rabbitkettle Formation at section 3:

GSC locality	Fossils and zone	Metres above base of formation
96980	**Agnostus** sp. **Blountia** sp. **Kingstonia** sp. **Kormagnostus** sp.	36.5
96981	**Agnostus** sp. **Cedaria** sp. **Kormagnostus** sp. **Welleraspis** sp.	37
96982	**Coosells** ap. **Crepicephalus** sp. **Kormagnostus** sp.	90.5
	Cedaria-Crepicephalus Zone	
	Aphelaspis Zone	
96983	**Aphelaspis** sp. **Olenaspella** sp. **Ptychagnostus** sp.	113.5
96984	**Olenaspella** sp.	121

Dunderhergia Zone, **Elvania** Zone, **Conaspis** Zone, part **Ptychaspis-Prosaukia** Zones barren or absent.

GSC locality	Fossils and zone	Metres above base of formation
	part? **Ptychaspis-Prosaukia** Zone and **Saukia** Zone	
96985	**Rasettia** sp.	378.5
96986	**Eurekia** sp.	431.5
96987	**Eurekia** sp.	440.5
96988	**Eurekia?** sp.	482.5
96989	**Eurekia?** sp. **Leiocoryphe?** sp.	along strike and several metres above 96988 level.

In addition to the fossils mentioned above, a collection made by S.P. Gordey 2 km north of the top of section 3 (GSC loc. C-81817; lat. 62°42'10", long. 128°23'45") and approximately 30 m below the top of the Rabbitkettle Formation contains the following fossils identified by B.S. Norford: **Bowmania** sp., **Euptychaspis** sp. **Eurekia** sp., **Leiocoryphe** sp., and **Pseudagnostus?** sp. These fossils belong to the late Upper Cambrian **Saukia** Zone.

The unconformities and bounding formations that delineate the Rabbitkettle Formation in the type area are not useful in delineating the formation at section 3, and no fossils are known from the type area for faunal correlation. The present correlation (Gordey, 1980a, Fig. 1, section D; 1980b) is therefore based upon lithological similarities and areal mapping. The high proportion of clastic material (clay to very fine quartz sand) distinguishes the Rabbitkettle at section 3 from the formations above and below. Also present at section 3 is the (Gabrielse et al., 1973, p. 48) "typical 'Swiss-cheese' texture [that] results from the weathering of limestone pods in a more resistant anastomosing network of silty beds". This texture is present at section 3 in unit 2 and in unit 4 at outcrops along strike a short distance to the south and on the steep surface of an east facing valley wall (Plate 19.2, fig. 6).

Fossils from section 3 indicate a large overlap in the age of the Rabbitkettle and Broken Skull formations. At section 3 the Rabbitkettle Formation spans most of Late Cambrian, whereas the Broken Skull Formation has been reported (Gabrielse et al., 1973, p. 51) to range from medial Late Cambrian (Franconian) into the early Ordovician.

Goodfellow et al. (1980, p. 153) have reported the Rabbitkettle as far as 190 km north of the Nahanni map area where it is described as consisting of "as much as 750 m of thin bedded yellowish weathering light to medium grey silty limestone." Here the reported SiO_2 and Al_2O_3 content is surprisingly low as compared to what might be expected in the type are or at section 3.

Broken Skull Formation

At the type section (Gabrielse et al., 1973, section 20) located 35 km east of the Nahanni map area, this formation consists of 820 m of mainly thick bedded, light grey, yellow grey weathering dolomite and limestone. A thin unit (13.4 m) containing quartz silt and sand mixed with dolomite and purple, mudcracked siltstone is present at the base. Trilobites belonging to the medial Upper Cambrian **Ptychapis-Prosaukia** Zone are located 185 m above the base of the formation.

Gordey (1980b) has mapped the strata overlying the Avalanche Formation at sections 1 and 2 as the "Broken Skull; minor Sunblood and Whittaker?" formations. A lower stripped member of this combined map unit was briefly inspected at the two sections, and it was noted that this member is overlain by a thick succession of thick bedded, light grey dolomite. The lower stripped member is composed of siltstone, dolomite and quartzite in mainly medium beds. At section 2 the member is especially colourful, as there the dolomite weathers bright orange, the siltstone maroon or purple, and the quartzite white. No physical evidence of an unconformity was seen at the base or within the member, although mudcracks are common in the siltstone. Gordey (1980a, section C; 1980b) showed a slight erosional unconformity in the area of sections 1 and 2, and Gabrielse et al. (1973, section 15) reported that an angular unconformity separates the Broken Skull from the underlying Sekwi Formation 22 km southeast of section 2. At the latter locality the medial Upper Cambrian trilobite **Conaspis** sp. is present 33.5 to 35 m above the base of the Broken Skull Formation.

References

Blusson, S.L.

1968: Geology and tungsten deposits near the headwaters of Flat River, Yukon Territory and southwestern District of Mackenzie, Canada; Geological Survey of Canada, Paper 67-22.

1971: Sekwi Mountain map-area, Yukon Territory and District of Mackenzie; Geological Survey of Canada, Paper 71-22.

Fritz, W.H.

1972: Lower Cambrian trilobites from the Sekwi Formation type section, Mackenzie Mountains, northwestern Canada; Geological Survey of Canada, Bulletin 212.

1976: Ten stratigraphic sections from the Lower Cambrian Sekwi Formation, Mackenzie Mountains, northwestern Canada; Geological Survey of Canada, Paper 76-22.

1978: Fifteen stratigraphic sections from the Lower Cambrian of the Mackenzie Mountains, northwestern Canada; Geological Survey of Canada, Paper 77-33.

1979a: Cambrian stratigraphic section between South Nahanni and Broken Skull Rivers, southern Mackenzie Mountains; in Current Research, Part B, Geological Survey of Canada, Paper 79-1B, p. 121-125.

1979b: Eleven stratigraphic sections from the Lower Cambrian of the Mackenzie Mountains, northwestern Canada; Geological Survey of Canada, Paper 78-23.

1980: International Precambrian-Cambrian Boundary Working Group's 1979 field study to Mackenzie Mountains, Northwest Territories, Canada; in Current Research, Part A, Geological Survey of Canada, Paper 80-1A, p. 41-45.

Gabrielse, H., Roddick, J.A., and Blusson, S.L.
1965: Flat River, Glacier Lake, and Wrigley Lake, District of Mackenzie and Yukon Territory 95E, 95L, and 95M; Geological Survey of Canada, Paper 64-52.

Gabrielse, H., Blusson, S.L., and Roddick, J.A.
1973: Geology of Flat River, Glacier Lake, and Wrigley Lake map-areas, District of Mackenzie and Yukon Territory; Geological Survey of Canada, Memoir 366.

Goodfellow, W.D., Jonasson, I.R., and Cecile, M.P.
1980: Nahanni Integrated Multidisciplinary Pilot Project. Geochemical studies part 1: geochemistry and mineralogy of shales, cherts, carbonates and volcanic rocks from the Road River Formation, Misty Creek Embayment, Northwest Territories; in Current Research, Part B, Geological Survey of Canda, Paper 80-1B, p. 149-161.

Gordey, S.P.
1979: Stratigraphy of southeastern Selwyn Basin in the Summit Lake area, Yukon Territory and Northwest Territories; in Current Research, Part A, Geological Survey of Canada, Paper 79-1A, p. 13-16.

Gordey, S.P. (cont.)
1980a: Stratigraphic cross-section, Selwyn Basin to Mackenzie Platform, Nahanni map area, Yukon Territory and District of Mackenzie; in current Research, Part A, Geological Survey of Canada, Paper 80-1A, p. 353-355.

1980b: Nahanni map area, Yukon Territory and Northwest Territories (NTS 105 I); Geological Survey of Canada, Open File Report 689.

Green, L.H. and Roddick, J.A.
1961: Nahanni, Yukon Territory and District of Mackenzie; Geological Survey of Canada, Map 14-1961.

Green L.H., Roddick, J.A., and Blusson, S.L.
1967: Nahanni, District of Mackenzie and Yukon Territory; Geological Survey of Canada, Map 8-1967.

Handfield, R.C.
1968: Sekwi Formation, a new Lower Cambrian formation in the southern Mackenzie Mountains, District of Mackenzie (95L, 105 I, 105 P); Geological Survey of Canada, Paper 68-47.

20. BEDROCK HEAVE IN THE CENTRAL CANADIAN ARCTIC

Project 770036

Larry D. Dyke
Terrain Sciences Division

Dyke, Larry D., Bedrock heave in the central Canadian Arctic; in Current Research, Part A, Geological Survey of Canada, Paper 81-1A, p. 157-167, 1981.

Abstract

Resurveys of sites established for the measurement of rock heave has shown that yearly movement of up to at least 5 cm takes place where pressures accompanying the freezing of water in soil bodies associated with rock (till deposits, fracture fillings, weathering products) can be transmitted to rock. Movement is less where pressure is developed in free water that becomes trapped between downward-advancing freezing fronts and permafrost, but pressures in this confined water have been shown in the field and laboratory to reach at least 400 kPa. These two processes give rise to a variety of rock heave features.

Introduction

Frost heave of bedrock is a process that results in the displacement of bedrock blocks due to forces produced by the freezing of water. It is expressed by a variety of geomorphic forms ranging from barely opened cracks to domes and uplifted blocks having relief measured in metres. The purpose of studying this process is to determine how fast and by what mechanisms frost heave takes place. The results may be of importance to engineering endeavours in permafrost regions where horizontal or vertical bedrock movement would be intolerable for a given foundation or buried structure.

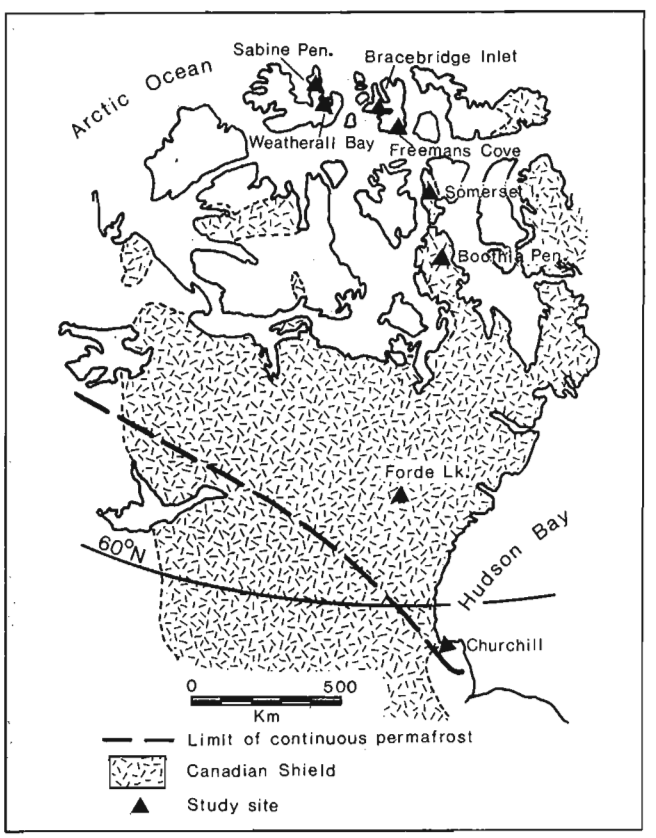

Figure 20.1. *Map of central Canadian Arctic showing location of rock heave study sites.*

Acknowledgments

Thanks are extended to Dr. Chris Mathewson and Ms. Terry Mayer of the Department of Geology, Texas A & M University for considerable assistance in the field. In the Arctic Islands the kind of support that is becoming almost legendary in its quality was provided by Polar Continental Shelf Project. Dr. Alan Judge was kind enough to supply thermal conductivity measurements on several rock samples. The Churchill Northern Studies Center provided logistical support to the author while in Churchill and Urangesellschaft Canada Limited provided transportation for a visit to Forde Lake.

Approach to the Problem

Studies of frost heave and formation of segregated ice in soils have, in part, been aided by the appropriateness of dealing with soils as homogeneous materials. Much of the behaviour of freezing soils depends on the properties of water in soil pores; these pores may be assumed to be evenly distributed throughout a soil element. Pore space is also present in rock, but it must usually be thought of as the openings bounded by fractures and bedding surfaces. These openings will separate to accomodate ice, and once this happens, an avenue is open for features to form similar to those seen in soils. This discontinuous nature of pore space, however, rules out the treatment of rock as a continuum. To understand rock heave it thus becomes necessary to determine the conditions under which pressures generated by the freezing of water can be transmitted to bedrock.

The recognition of features produced by the growth of ice in rock is of prime importance in establishing the form and extent of ice and the conditions under which it grows, as well as the rate of growth of these features or at least the rate of movement of bedrock blocks. Processes that have known rates and that interact with frost heaving in such a way as to enable rates to be inferred for progressively exposed features offer a hope; otherwise, direct observations over known time intervals must be made.

Two summers have been spent studying bedrock features from the fringe of the continuous permafrost zone to the central Arctic Islands. It was felt that an effective way to approach this relatively unstudied process was to examine rock heave in as wide a range of climatic, hydrologic, and geologic conditions as possible in one field season. Eight sites were chosen in areas of coarsely crystalline rocks of the Canadian Shield and sedimentary rocks of the western Arctic Islands (Fig. 20.1). Although each site was picked for a particular lithology or climatic regime, further subdivisions have been made based on

Table 20.1

Summary of horizontal movements of survey markers for selected frost heave features after one year of observation

Locality (see Fig. 1)	Description of Feature	Maximum Horizontal Movement (cm)	Average Horizontal Movement and Standard Deviation (cm)	No. of Markers Measured
Forde Lake	Blocks bounded by water-filled cracks	0.8	0.3 ± 0.2	27
Boothia Peninsula	Blocks surrounding soil upwellings	1.3	0.5 ± 0.3	22
Somerset Island	Blocks surrounding soil upwellings	4.5	1.1 ± 1.2	12
Weatherall Bay	Blocks bounding soil-filled cracks	4.5	0.6 ± 0.9	25
Weatherall Bay	Rims of ice wedge furrow	1.2	0.6 ± 0.3	12
Freemans Cove	Rims of ice wedge furrow	0.5	0.2 ± 0.1	11
Freemans Cove	Blocks in bedding plane exposures on shallowly sloping ridge top	1.0	0.3 ± 0.3	16
Sabine Peninsula	Marker array across anticlinal feature	3.3	1.8 ± 1.1	12

apparent local behaviour of the rock or on hydrologic conditions. The study sites are in areas having little or no topographic relief in order to reduce the influence of gravity-related processes. At all sites survey markers were placed on bedrock features thought to have been produced by frost heave. Levelling and triangulation were carried out for each feature from three set-up positions located over markers installed in apparently undisturbed bedrock. The average and maximum horizontal movements for selected sites are shown in Table 20.1. From these measurements and observations, hypotheses for heaving mechanisms can be proposed. Measurements of conditions that should exist according to these hypotheses are also being made, and laboratory experiments have been carried out to verify the existence of other necessary conditions.

Geomorphology of Rock Heave

Between Churchill, Manitoba, and the central Arctic Islands, little difficulty was encountered in locating outcrops disturbed by frost heaving. Movement due to glacial scouring can be discounted where bedrock features present too much of a vertical obstacle to have survived ice movement or where horizontal dilation of an outcrop to produce a radial movement pattern is not compatible with a single flow direction. Based on the sense of movement, rock heave features can be categorized as originating from primarily vertical or horizontal motion. Which predominates appears to depend upon the mechanism by which heaving forces are developed. It must be recognized that many factors determine this dominance, so to confine certain heaving styles to particular geographic areas is not necessarily characteristic. On the other hand, rock heave as a widespread process seems to be characteristic of the continuous permafrost zone. This is true because of the opportunity presented by the permafrost either for closed hydrologic systems to form or for the continuous existence of frozen soils in which segregated ice growth can take place.

The continuous permafrost zone along the west side of Hudson Bay and northward into the Arctic Islands covers two broad geological provinces: (1) the generally coarsely crystalline metamorphic rocks of the Canadian Shield and (2) the unmetamorphosed deposits of the Arctic Islands sedimentary basins. Within this area seven sites for detailed study were established in 1978, and a description of the features at each are given by Dyke (1979). An additional site at Churchill, Manitoba, has been added to include the southern extent of the continuous permafrost zone and the most spectacular examples of rock heave seen to date.

At the Churchill site a broad, glacially smoothed ridge in Precambrian quartzite stands 30 m above the surrounding peatlands. Virtually the only discontinuities in this material are two sets of vertical or steeply dipping fractures. Panels of rock bounded by relatively closely spaced fractures have been heaved along the vertical fracture set. The panels, from 1 to 5 m wide and up to 30 m long, stand as much as 3 m above the surrounding essentially flat bedrock ridge surface (Fig. 20.2, 20.3). They are cut by the other set of fractures, along which separation occurs. In some cases wide cracks separate discrete blocks. Uplift of these panels has undoubtedly left spaces into which other blocks have fallen; such jamming of blocks was originally observed by Tyrrell (1896).

Long narrow ridges in otherwise flat-lying Paleozoic carbonate bedrock were seen in the wide valley bottom of Lord Lindsay River on southern Boothia Peninsula. These ridges have formed where the sides of vertical fractures have been upturned to form two sloping surfaces separated by a V-shaped trench (Fig. 20.4, 20.6). At this particular site they stand up to 3 m high. Where undisturbed, the carbonate bedrock is veneered by till, probably less than 0.5 m thick. Other examples of less impressive size were seen on other flat-lying carbonate outcrops on Boothia Peninsula. A cross-section of one of these smaller examples was exposed and revealed ice interbedded with upturned flags of carbonate rock (Fig. 20.5). Although the full depth of the disturbance could not be reached, it was apparent that a considerable volume of ice must have accumulated to produce the observed ridges.

Mechanisms of Bedrock Frost Heave

While it can be assumed that some freezing will take place each year in the permafrost region, the frequency of rock movements will be dependent on how effective a particular ice growth mechanism is in producing a heaving force. Any situation whereby growing ice produces a direct application of force to rock will probably result in the most frequent movement. It is possible to consider the study sites according to the means by which an expansive force is applied to rock:

1. The freezing of free water in bedrock cracks: The downward growth of ice into any system of water-filled openings will result in the expulsion of water in response to the volume increase that accompanies freezing of water. If all routes for the release of this water are blocked by ice-filled cracks and permafrost, then the confinement of the remaining water in an enclosed saturated zone will produce a force for heaving.

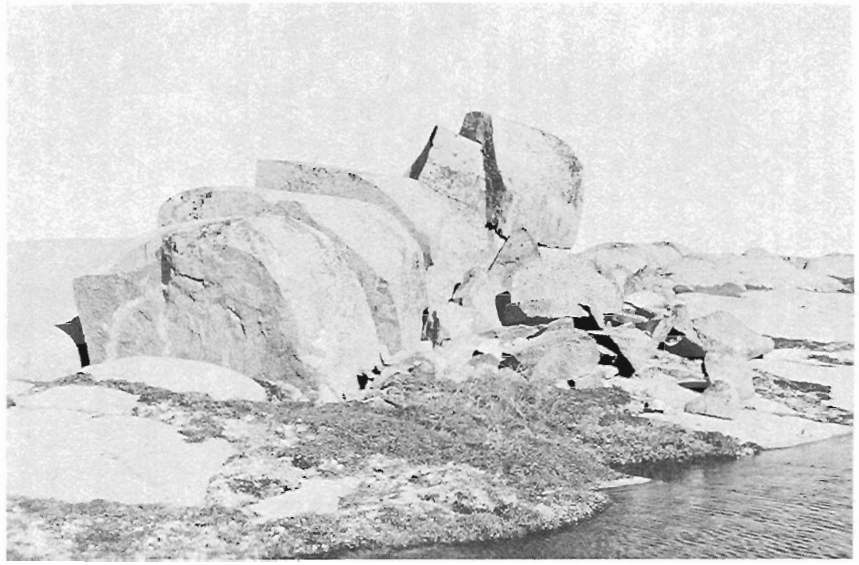

Figure 20.2. *Frost heaved panel in Precambrian quartzite at Churchill, Manitoba. Panel stands up to 3 m above undisturbed bedrock surface. GSC 203603-C*

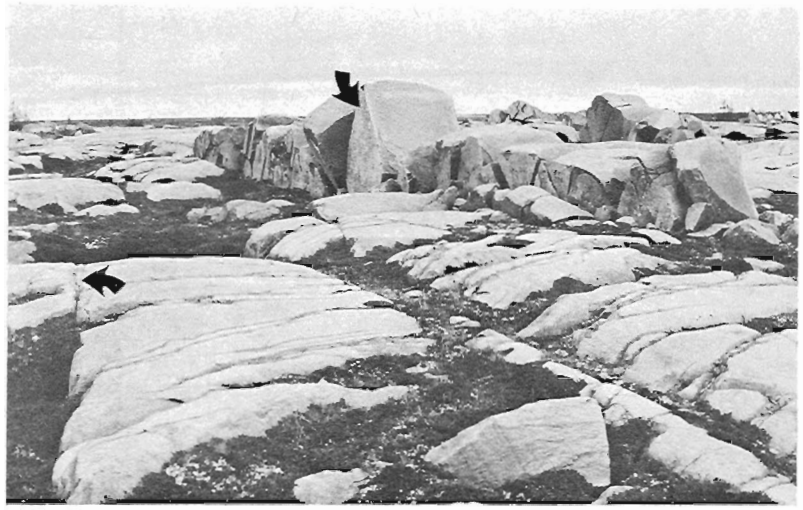

Figure 20.3. *Feature similar to that shown in Figure 20.2; note that heaving has occurred along pronounced vertical fractures (arrows). GSC 203603-A*

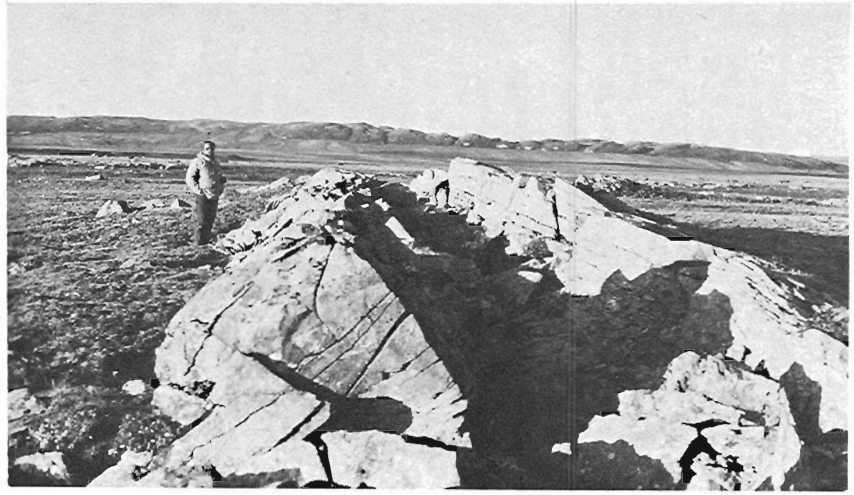

Figure 20.4. *Originally flat-lying beds of limestone, upturned along a vertical fracture, southern Boothia Peninsula. GSC 203603-J*

Figure 20.5. *Cross-section through thin-bedded carbonates, Boothia Peninsula, showing upturning on a smaller scale that that seen in Figure 20.4. GSC 203603-H*

Figure 20.6. *Oblique aerial view from a height of 200 m showing frost heaved bedrock ridges similar to the ridge shown in Figure 20.4. GSC 203603-B*

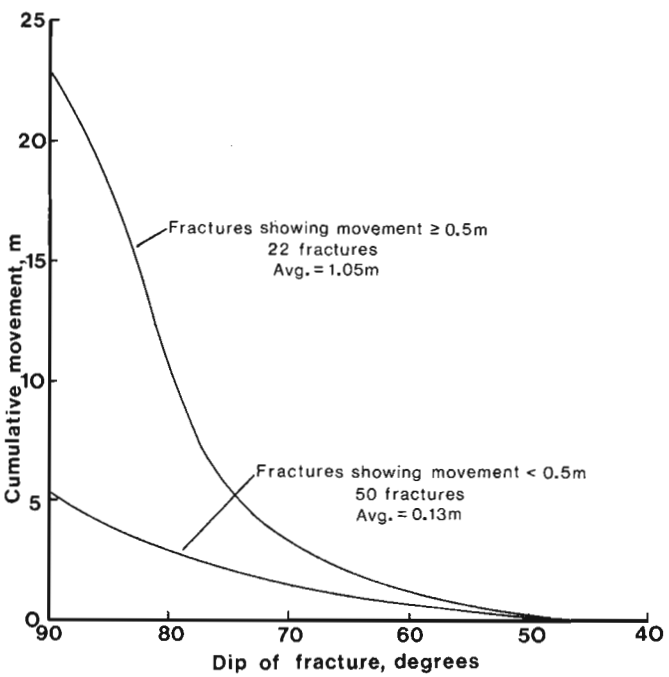

Figure 20.7. *Curves showing cumulative movement along fractures having dips less than or equal to a given value at the Churchill site.*

2. The freezing of water in soil associated with bedrock: The formation of segregated ice in soil is the commonest cause of frost heaving. That the pressure accompanying the freezing of water in soil can be transferred to rock is a known fact, but the position of the soil relative to bedrock will determine how effective the transfer will be. Work by Mackay and Burrous (1979) suggests that a version of this mechanism may allow the growth of ice to widen a bedrock crack rather than simply fill the initial opening. Fine pores or the presence of a surface roughness fine enough to permit the existence of unfrozen water below 0°C would permit water to migrate laterally along the crack or through rock to the crack.

Apparent Mechanisms of Rock Heave and Survey Results

At the Churchill site and in central District of Keewatin bedrock heave appears to result solely from the freezing of free water occupying cracks. Although no observations have been made in the intervening region, heaving does appear to be associated with that part of an outcrop at or near the water table – an association of topography and hydrology that is widespread. The most noteworthy displacements commonly involve the upward movement of discrete blocks. To achieve this, pressure is probably applied over an area larger than the cross-section of the block. This would be possible if excess pressure developed in zones of water confined between permafrost and the downward-advancing freezing front.

The origin of the heaving force may be similar to one of the mechanisms responsible for the growth of pingos (Mackay, 1973). For the growth of ice due to a matric potential,

$$P_i - P_w = 2\frac{\sigma_{iw}}{r_i}$$

where P_i-P_w is the pressure difference between ice and water, σ_{iw} is the interfacial energy (surface tension) of the ice-water interface, and r_i is the radius of curvature of ice in a soil pore. For relatively large pore sizes (i.e., as in a sand), r_i is large and the term on the right approaches zero; barring capillary effects, for ice to grow beyond the initial volume afforded by a crack, the pressure of water must be at least equal to that of the ice (i.e. overlying soil, rock, and ice).

The crack system in a given volume of rock can be considered a form of porosity. If excess water pressure is developed in this crack system, a doming of the rock above the zone of excess pressure will take place if a detachment surface, such as a near-horizontal crack, is available. Alternatively, expansion may be most easily accommodated by the uplift of a few blocks or even a single block. To predict an actual heaving event would require that the heaving force and the resistance provided by weight, friction, and the deformation of ice be known. Thus the occurrence of a heave event can be thought of as an attainment of limiting equilibrium whereby the heaving force on a given block overcomes all the resistances holding it in place. It may be readily appreciated how difficult determining the two could be. It is more practical to identify heaving processes and the conditions that favour them so that environments conducive to heaving may be found.

Churchill, Manitoba. Although survey data for the Churchill locality are still being reduced, the well developed nature of heaving allows inferences to be made about mechanisms. Even a casual inspection shows that by far the greatest displacements have taken place along one set of approximately north-south trending vertical fractures. Figure 20.7 shows that the greatest movements have taken

place on fractures dipping at 80 degrees or more; no movements greater than 1 m are seen on fractures inclined at less than 80°. The fractures accommodating the largest movements are remarkably planar. The other major fracture set trends northeasterly to easterly, and members of this set have undulating, irregular surfaces. Because most movement occurs along planar, near vertical fractures, it is possible that a dilation of a rock mass takes place as the first step in the heaving process. If zones within the saturated fracture porosity can be sealed off by advancing freezing fronts, the resulting excess water pressures may produce heaving. This may at first express itself as a doming during which extension tangential to the dome takes place. Vertical cracks will be most quickly opened by this extension, and once this happens, blocks are free to be uplifted. Figure 20.8 shows a family of curves indicating how much extension will take place for a given amount of doming for different sizes of domes. The curves show that for a given amount of uplift, extension is greatest for the smallest dome. Figure 20.9, a map of an area of outcrop about 0.5 km east of the public terminal at Churchill airport, shows the typical heaving pattern. The heaved panels are aligned in groups that belong to pairs of bounding fractures. The fact that the panels are generally discrete rather than continuous heaved ridges suggests that doming, if it is indeed the process, is occurring over relatively small areas.

Individual blocks can be found whose tops lie as much as 3 m above the surrounding rock surface (Fig. 20.2, 20.3). North-trending glacial striae on the tops of heaved blocks show that heaving has occurred since the onset of the last continental glaciation. Somewhat more information on the rate of heave is offered by lichen growth, specifically that of **Rhizocarpon geographicum.** In places encrustations of lichens dense enough to hide the rock are seen to end abruptly along a horizontal fringe, suggesting that a block has been displaced relatively recently to expose the bare surface below. More common are faces on which there is a trend from small to larger diameter individuals; for several of these, the diameter of the largest individual and its height above the undisturbed rock surface was measured and plotted (Fig. 20.10). The graph contains almost a random scatter except for the lack of observations of large thalli at low heights. Assuming that these lichens began to grow shortly after exposure of the rock face and that the growth rate was constant, this distribution could indicate that heaving was a gradual process. The fact that the lichens do not exceed a diameter of 5 cm may be due to a decrease in growth rate as a given lichen becomes more exposed to the abrasive action of wind-borne particles. Curves have been plotted showing growth rates of **R. geographicum** of 50 and 5 mm/1000 years for localities in Sweden (Karlén, 1973) and Baffin Island (Miller and Andrews, 1972), respectively. The variation in rates makes it impractical to compare the observations from Churchill. It can only be said safely that the greatest amount of gradual heave at the Churchill site has probably taken at least 1000 years to complete. On the other hand, comparatively rapid heave of up to 30 cm, as suggested by lichen fringes, may take place.

Forde Lake, District of Keewatin. At the outlet of Forde Lake, located about 100 km southwest of Baker Lake settlement, glacially smoothed ridges in coarse grained granite gneisses are interspersed with till-filled low areas. The relief rarely exceeds 50 m over an area of 1 km^2. Although frost heaving in bedrock is not as spectacular as that seen near Churchill, possible influences of topography and the availability of water can be seen.

It was observed in 1978 that heaving is most apparent along the flanks of outcrops adjacent to till deposits (Fig. 20.11) whereas on bedrock hilltops it is very rare.

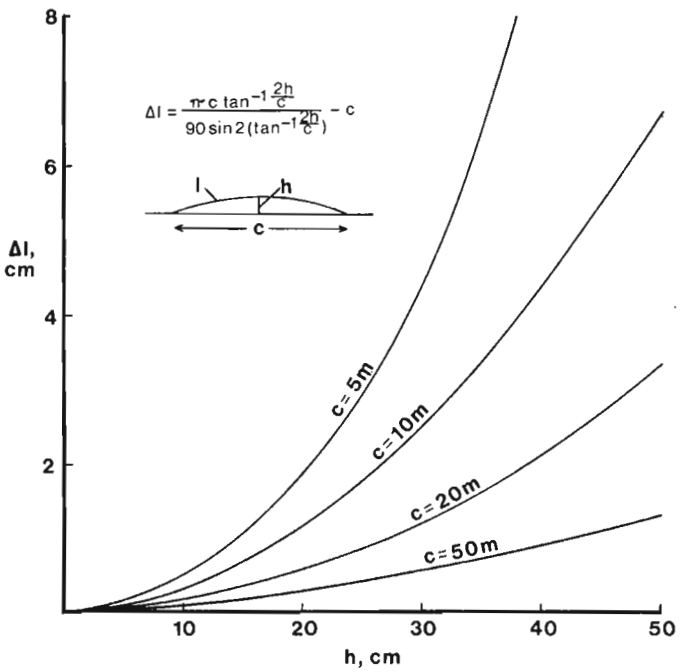

Figure 20.8. Curves showing the change in arc length (Δl) for a hypothetical dome, given the diameter of the incipient dome (c) and the amount of uplift (h).

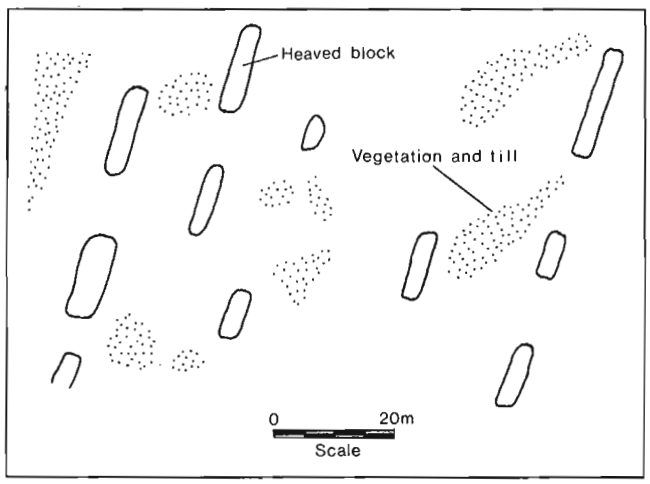

Figure 20.9. Plan view of a portion of outcrop near Churchill airport showing arrangement of heaved blocks.

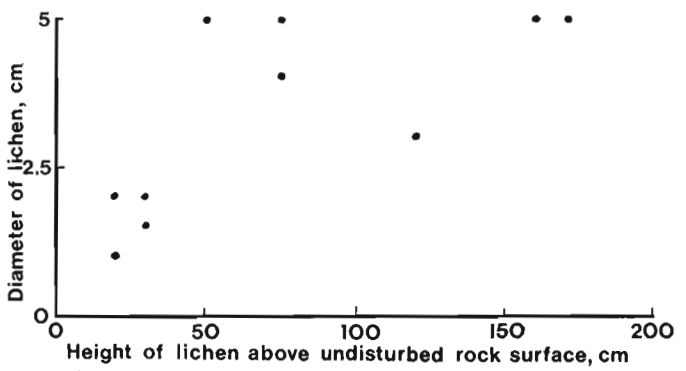

*Figure 20.10. Graph showing diameter vs. height above the undisturbed bedrock surface of the largest **R. geographicum** thallus found on the sides of each of several heaved blocks.*

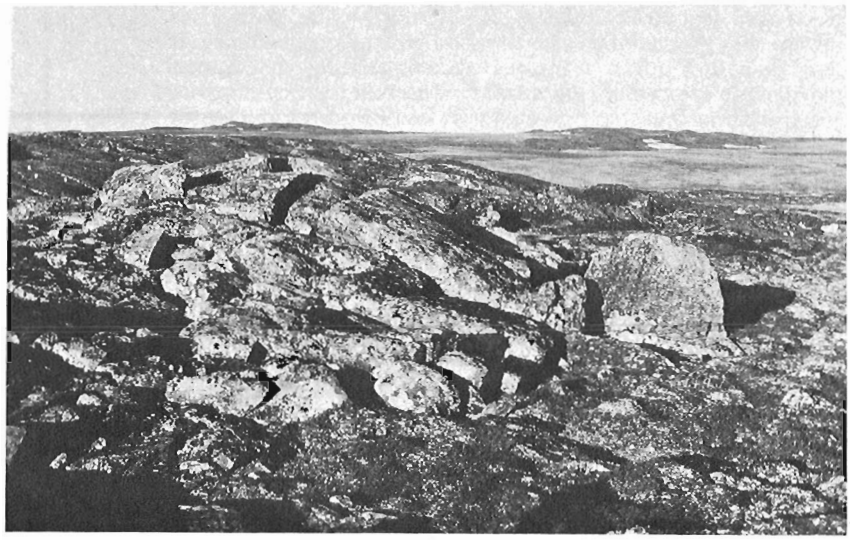

Figure 20.11

Dome-shaped rock heave feature on the flank of an outcrop of the north end of Forde Lake, District of Keewatin. GSC 203603-E

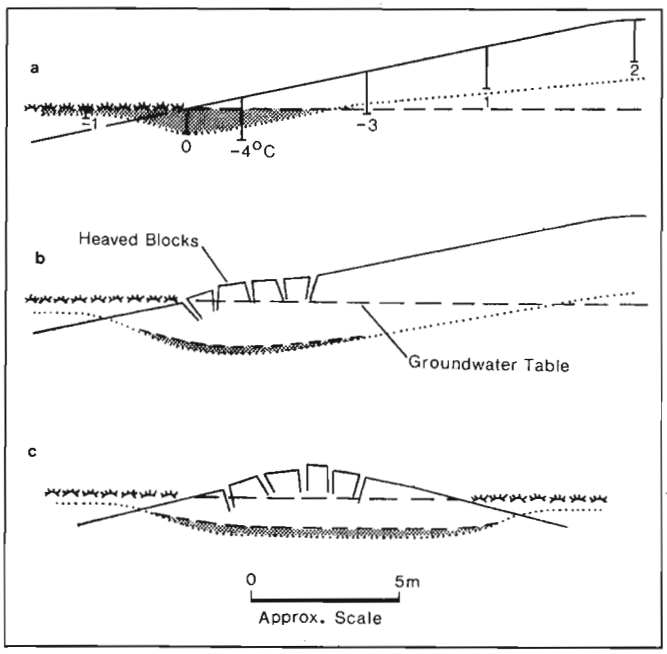

(a) Numbers show temperatures measured at the bottom of drillholes in late June 1979. The dotted line is the 0°C isotherm which also forms the lower boundary of the saturated zone (shaded).

(b) The same cross-section during fall freeze-back, with the dotted line now showing the configuration of the active layer and the shaded zone now representing a zone of trapped water where freeze-back has been retarded.

(c) Small isolated outcrop showing an alternative configuration for the formation of a zone of trapped water during freeze-back.

Figure 20.12. *Cross-sections of outcrops flanked by till deposits*

A comparatively abrupt deepening of the active layer must exist beneath the flanks of outcrops due to the contrast in thermal conductivity between this rock and the vegetated till. Any abrupt depression in the active layer provides an opportunity for a zone of trapped water to form during fall freeze-back. In central District of Keewatin the water table normally coincides with the surface of the till and organic cover. It presumably extends into bedrock outcrops via open fractures so that the hypothesized depression in the active layer is saturated (Fig. 20.12a). Freeze-back of the saturated zone is retarded relative to higher, dry parts of the outcrop due to the extra heat dissipated as the water-filled cracks freeze. A localized confined, unfrozen zone will be temporarily formed if a seal can be effected by ice-filled cracks. As freezing continues downwards, the attempted expulsion of water results in heaving at the surface (Fig. 20.12b).

To test for the existence of a deepening of the active layer, temperature measurements were made at the bottom of holes placed in a line on the flank of an outcrop (Fig. 20 12a). By tracing the 0°C isotherm, a depression coincident with the flank of the outcrop is evident. Any isolated area of outcrop that allows the active layer to remain at least partly within the saturated zone may be susceptible to heave (Fig. 20.12c). Differences in thermal conductivity of different lithologies may also result in variations in the active layer thickness; for example, active layer freeze-back is retarded below the water table in a rock body of relatively low thermal conductivity (such as a mafic volcanic dyke).

In general the greater the thickness of the saturated active layer in rock, the greater the heave. The maximum vertical component of heave in the Forde Lake area is about half that at Churchill. This observation may reflect the corresponding ratio for the thicknesses of the saturated active layer at the two places as reflected in thermal gradient measurements reported by Brown (1978). Climatic differences account in part for differences in active layer thickness, but the major factor is probably the contrast in thermal conductivities of the rock: 14.3 millical/cm·s·°C for the Churchill quartzite compared to 7.6 for the Forde Lake granite gneiss (A. Judge, written communication, 1979). Thermal conductivities generally are relatively high for quartz-rich rock (e.g., Clark, 1966), and so the active layer will be correspondingly thick. A conductivity of 6.2 millical/cm·s·°C was determined for a diabase typical of dykes in the Forde Lake area. This value does not differ greatly from that for granite gneiss, but local variations in quartz content for the gneiss could result in contrasts great enough to influence rates of freeze-back.

Mackay (1973) found that certain pingos in the Mackenzie Delta are currently growing several centimetres per year and that growth of some has continued for several hundreds of years. If the mechanisms are similar, the average movement rate of individual heaved blocks will be much less considering that 1) the zone of thaw may be much

thinner than that associated with a large incipient pingo and 2) the mechanical stiffness of the frozen layer at a site of rock heaving will be much greater. The relatively small size of a rock heave feature may determine that growth is an intermittent event, taking place when certain components of the resistance to growth are overcome, such as frictional force along the contacts. A pingo is generally a much larger feature, and deformation can be considered as taking place in a continuum so that each increment of pressure produces an increment of upward movement.

At Forde Lake, survey markers were placed on several features having the appearance of domes or mounds of heaved blocks and on individual heaved blocks surrounded by otherwise undisturbed bedrock. While the measured movements for Forde Lake (Table 20.1) are barely larger than the standard deviation of error for sightings up to 30 m (±0.3 cm), other much larger movements are evident in the area. Foot traverses within a radius of 1 km revealed heaved blocks every few hundred metres. These relatively recent movements of the order of 10 cm vertically were indicated by the exposure of a fresh, lichen-free bedrock surface. Several occurrences of such movements likely would exist per square kilometre of bedrock exposure in this area.

Northernmost Canadian Mainland and Arctic Islands. Continuing northward, the character of rock heave responds to the increasing shortness of thaw and relative lack of water. At least equally important is the geology, for weathering products from the unmetamorphosed sediments of the Arctic islands have provided sites for ice segretation. Where free water is not commonly available but the bedrock is relatively susceptible to physical weathering or where till deposits are present, a distinct class of rock heave features can be developed. Their form depends on the structural fabric of the rock and the degree to which a given terrain has been affected by other geomorphic processes.

The sites established in this northern region (Fig. 20.1) exhibit frost heave features that can be divided into three categories.

1. Fields of loose blocks containing scattered circular deposits of poorly sorted soil (till). Fields of blocks are especially common in the Precambrian gneiss areas of western Somerset Island and north-central Boothia Peninsula. There seems to be a diversity of ways in which these fields have originated.

Block fields associated with the development of tors are prominent on the highest parts of the gneiss terrane of Somerset Island (Dyke, 1976). They are thought to have developed during an extended period of weathering when this area remained ice free during the most recent glaciation. This weathering has left aprons of blocks about the tors, together with accumulations of grus in the spaces between blocks. With increasing distance from the tors, the concentration of blocks decreases until all that remains is soil consisting almost entirely of granule and smaller sized particles.

The broad valley extending north from Stanwell-Fletcher Lake, southern Somerset Island, was glaciated during the last glaciation (Dyke, 1978). Ice flow here has enhanced the north-south structural grain of the gneiss, resulting in long narrow ridges of 10 to 300 m relief. Between these ridges are low-lying areas covered with a variety of materials ranging from sandy silt deposits to block fields consisting of blocks up to 2 m in size. Unlike the tor areas, fines and blocks seem to be of separate origin: the fines are perhaps a glacial outwash deposit whereas blocks have originated either by mechanical weathering of steep ridge flanks or by frost heaving.

Figure 20.13. *Outcrop of gneiss on Somerset Island with flanking talus slope. Mudboils (dashed lines) in foreground have presumably developed from buried till.*

Block fields are characterized by an absence of soil fillings between blocks with the notable exception of circular patches of stony soil that appear to be a form of mudboil. These soil accumulations, which can be up to 2 m in diameter, are rimmed with blocks; the largest ones extend at least 1 m below the surface. This soil probably has originated as a till, considering its diverse content of metamorphic and igneous clasts. Most blocks are angular and show no intermediate stages of weathering. Accepting this, it is then necessary to explain the incorporation of till into the block field.

Frost heaving in a manner similar to that hypothesized for central District of Keewatin may have initiated the development of the block fields; however, the extent of disruption at certain places at the site on Somerset Island is far advanced over the Forde Lake example. This maturity may be encouraged by the structural fabric of the gneiss. A prominent set of near-vertically dipping fractures parallels compositional layering, providing a weaknes along which blocks may break free and become incorporated in the adjacent till deposit.

The incorporation of blocks of rock in till is a common feature at the Somerset Island site. Talus slopes at the base of bedrock ridges commonly grade farther downslope to distinct mudboils with rock rims (Fig. 20.13). In this case mechanical weathering of the ridges has resulted in the burial of till. Trails of blocks occurring downslope from isolated outcrops confirms that discrete frost heaved blocks have moved downslope through frost creep (Fig. 20.14). The water table is virtually coincident with the soil surface around these outcrops. During thaw the water table will transect a small outcrop; lenses of water could be trapped during freeze-up, providing a mechanism for the initial disruption (see Fig. 20.12c) and the eventual separation of rock blocks. The blocks then move downslope by frost creep (Davison, 1889; Fig. 20.14).

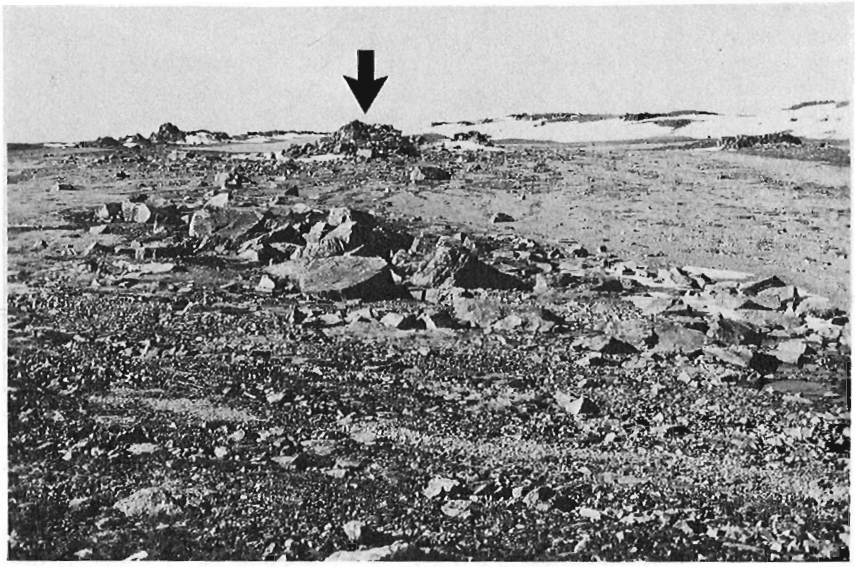

Figure 20.14.

Isolated outcrops surrounded by silty sand deposits on Somerset Island. The blocks in foreground have been moved downslope from the outcrop at top centre (arrow) through a combination of frost heave and frost creep. GSC 203603-G

Block fields containing soil upwellings may form because insufficient soil exists to enable the transport of blocks by frost creep. Around soil upwellings net movements measured over one year vary from nil to about 5 cm laterally. The greatest movements are seen for blocks adjacent to upwellings, although movements are not necessarily radially away from the centres of the upwellings. The cumulative movement over many seasons is undoubtedly in part radially outward, produced by a horizontal component of the heaving force developed in the till. The freezing front in a soil upwelling will likely be curved downward close to the block rim because of the loss of heat through the surrounding blocks being more rapid than through frozen till. If heaving takes place perpendicular to this front, then a horizontal component will exist close to any block.

2. Bedrock cracks containing soil infillings. The comparative ease with which the sedimentary rocks of the Arctic Islands weather, together with a much lower average precipitation than farther south in the District of Keewatin, produces a characteristic style of rock heave. Outcrops commonly are limited to hill or ridge tops where water is least likely to collect. The presence of soils derived from weathering in cracks and openings in bedrock appears to be the major cause of heaving in this environment. Soil deposits, whatever their origin, have the ability to store water. Given the right texture, soils may host the formation of segregated ice, especially if a subsurface source of water is available. Expansion accompanying freezing will produce heave and may constitute one stage in the production of the regolith.

Along the south side of Bracebridge Inlet, Bathurst Island (Fig. 20.1) thin bedded siltstone of the Stuart Bay Formation is exposed on well drained hilltops and yet is rich in segregated ice which is interlayered with individual beds. The growth of this ice presumably has aided in the degradation of bedrock as individual bedding plates rest at odd angles or groups of beds stand dilated into fan-shaped arrangments. Essentially the same process, but on a much broader scale, is exhibited in outcrops of flat-lying, massive bedded sandstone of the Griper Formation on a plateau adjacent Weatherall Bay, Melville Island. Vertical fractures within the sandstone have widened to become cracks filled with a silty sand derived directly from the sandstone. Resurveying of markers placed in one outcrop to detect changes in crack width has shown that a range of movements has taken place. The outcrop forms a cap to a broad hilltop. The outcrop is essentially intact on the top, and blocks have shifted at most a few millimetres. Cracks up to almost 1 m wide are present away from the top, and movements up to 5 cm were measured.

The freezing of water contained in the soil infilling of a vertical crack may produce lateral heave by two mechanisms. As was hypothesized for soil upwellings surrounded by blocks, a concave-downward freezing front will form due to the most rapid loss of heat through the crack walls. Secondly, while the bulk of the volume will be expressed as a movement upwards, this will be resisted by adhesion between the soil and the crack walls. Ice growing from free water in a crack is at liberty to grow downwards and so no lateral pressure is exerted; however a freezing soil can be treated as an elastic body in which vertical compression will also have a horizontal component. Whatever the mechanism, the results of lateral heave appear to be cumulative because with increasing distance from the most intact part of many outcrops, blocks become more widely spread.

The soil that is generated by the weathering of the sandstone, while sandy, contains 15 to 25 per cent silt and clay. It is evidently frost susceptible (i.e., capable of hosting segregated ice), considering the existence of a nearby solifluction lobe that is transporting blocks with dimensions of up to 3 m. The front of the lobe is supported by a rim of blocks 1 m high; immediately behind this, the surface is covered with a net of block polygons. Because the snout of the lobe is at the base of a hill, the water table here was within 0.1 m of the surface in late July 1980. A heave recorder installed in a large block and anchored to a block immediately below showed a maximum vertical heave of 5 cm and a recession of 3 cm. Heaving and recessions of about half this amount were seen on two recorders installed in thin bedded sandstone outcrops nearby.

Mackay and Burrous (1979) have produced uplift accompanied by pressures of at least a few tenths of a megapascal (1 megapascal = 10 bars) using pieces of porous tile and ceramic plate immersed in a container of water. A freezing temperature was applied from the bottom so that the porous object permitted water to migrate from above to the freezing front on the bottom side. A natural counterpart of this process may occur in the Stuart Bay or Griper formations if the bedrock surrounding cracks acts in the same manner as the porous plate. A natural counterpart would be horizontal cracks in sandstone where ice would supposedly form in the crack provided the whole system was saturated. The growth of ice would occur on a much smaller scale and probably

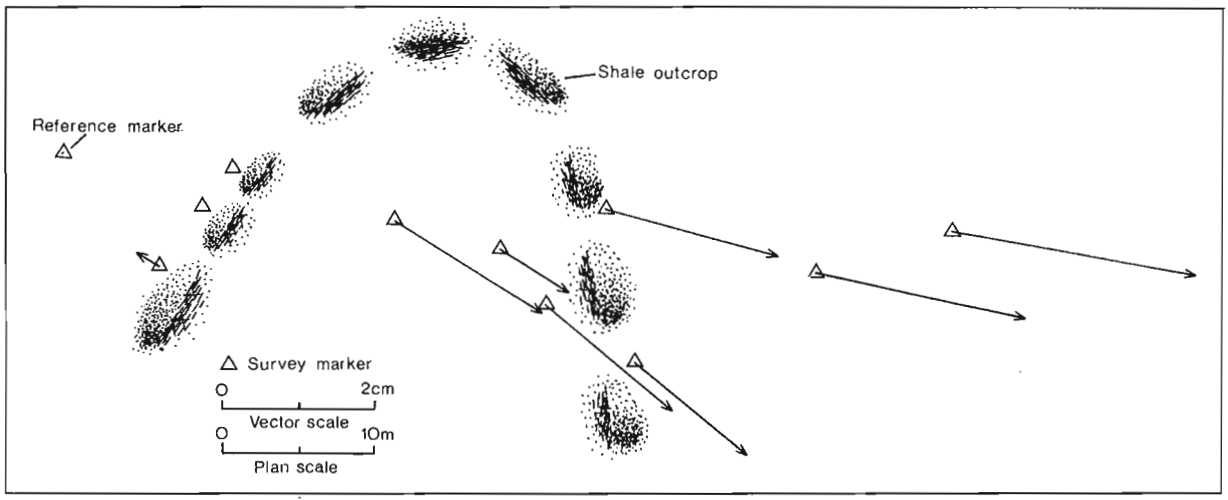

Figure 20.15. *Plan view of a study site in the Kanguk shale on Sabine Peninsula, Melville Island. Markers are located across an anticlinal structure.*

much more slowly in the case of siltstone beds. Were the beds vertical, it would depend on heat being conducted most readily up individual plates so that the lateral component of heat flow at the edges of a plate would permit some lateral growth of ice.

3. Ice Wedges in Bedrock. Several features have been found that point to the growth of ice wedges in bedrock. Deformation of bedrock due to frost heaving is indicated by the presence of linear furrows at least 10 m long or is observed where uplift along either side of a fracture has produced a ridge-like feature, in cross-section having a V-shaped trough through the centre (Fig. 20.4). These features are rare but so are outcrops in areas where water would be expected to collect. Where observed they occur singly or as an array having a few branches. Although little excavation has been done to search for ice, its presence and growth are suggested by the resemblance to ice-wedge features in soils and the apparent tendency for uplifted blocks on the rims to slump inward. It is thought that ice wedges form in bedrock by the same thermal contraction process as proposed by Leffingwell (1919) for soil ice wedges. According to Lachenbruch (1962), the thermally induced tensions in the soil that cause the initial crack are greatest at the surface and fall off rapidly with depth. This will also be true for rock, but contraction will widen pre-existing fractures. Values of the thermal coefficient of expansion for rocks given by Skinner (1966) are about an order of magnitude smaller than the value used by Lachenbruch for frozen soil. Consequently ice wedges in rock would be expected to grow relatively slowly and/or be relatively widely spaced. Moreover, yearly fluctuations in temperature would decrease rapidly with an increase in the thickness of the soil covering, further inhibiting ice-wedge growth in rock.

Survey markers established on either side of furrows in the Griper sandstone at Weatherall Bay and the Disappointment Bay dolomite at Freemans Cove on Bathurst Island indicated furrow widening over one year. Marked blocks on the edges did show movements inwards of a few millimetres, suggestive of slumping. In general these results are taken as an indication that ice-wedge growth in mechanically stiff sedimentary rocks is one of the slowest forms of rock heave.

A notable exception is seen in the thinly laminated shale of the Kanguk Formation on Sabine Peninsula, Melville Island. Ice wedges up to 50 cm thick and at least 2 m deep were encountered in shallow boreholes. It is not known how this ice accumulates. The active layer is very shallow, the depth of thaw measuring 10 to 30 cm in early August. No water appears to be available except during snowmelt. Presumably meltwater may be admitted below the frost table by contraction cracks, but ice lenses and veins of various shapes and sizes suggest that other avenues are available. It is possible that partings of shale act as conduits for water within the permafrost. As a rock type, shale may be particularly efficient in making water available below the permafrost table due to the high surface area provided by its thin bedded structure. Regionally, the formation is essentially flat-lying but on the scale of a few tens of metres, outcrops display tight anticlinal folds. Markers were installed along a line of about 30 m length, perpendicular to the axis of one of these folds. Resurveying after one year shows a horizontal expansion of the outcrop perpendicular to the axis. Movements of up to 3 cm have taken place with the amount of movement increasing with distance from a reference marker on one flank (Fig. 20.15). The heaved ridge-like features cut by a V-shaped trough found in thin bedded carbonates on Boothia Peninsula may be formed by the growth of ice between bedding planes. A 60 cm-deep trench was dug across one of these and revealed a continuation of the surface form of the structure with depth (Fig. 20.5). Interlayed with the carbonate strata were layers of ice. While the feature did not appear to contain an ice wedge, its formation may still be related to thermal contraction. Water available during thaw presumably gains access to the subsurface via the vertical fracture along which the features are aligned. This fracture may well be widened by thermal contraction, but the presence of horizontal bedding partings also permits the lateral flow of water. If the water freezes, vertical expansion may occur along the vertical fracture. Although the ice that is formed each year may melt completely, that ice has probably caused separation along bedding planes which will be partly permanent. The frost heaved ridge may then result from the accumulated expansion from yearly ice formation.

Experiments

If rock heave due to excess water pressures is to take place, water-tight seals must form around ice-filled cracks. At the Churchill, Manitoba, and Forde Lake, central District of Keewatin sites, pressure sensors capable of recording an approximate maximum water pressure were placed in water-filled cavities below heaved blocks. A small balloon filled

with antifreeze was connected to the sealed cylinder of a syringe, via a length of Tygon (brand name) tubing. Excess water pressure at the balloon then forces the piston along the syringe to a position in equilibrium with air pressure. The farthest point of travel is then recorded by a sliding ring moved by the piston. At Forde Lake, these devices have recorded pressures as high as 400 kPa at depths of about 2 m. It is evident that pressures are available that at least balance the weight of overlying material.

Laboratory experiments have verified that excess water pressure can be maintained by ice-plugged cracks. A square concrete box with walls 10 cm thick, 20 cm high, and 45 cm long was constructed using 1 cm diameter threaded steel rod for reinforcement (Fig. 20.16). A square concrete block was then placed in the box such that a space of a few centimetres remained beneath the bottom and on all sides of the block. This space was filled with water, the outside insulated with 5 cm of styrofoam, and the whole assembly placed in a cold room. Freezing temperatures could therefore be applied to

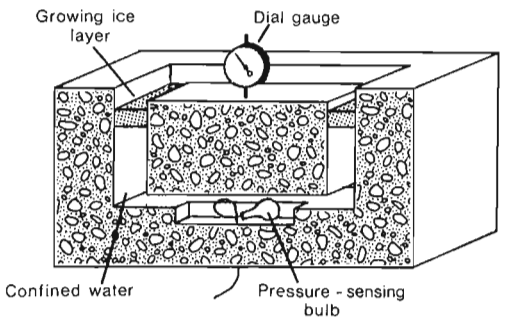

Figure 20.16. Cutaway view of frost heaving apparatus. See text for description.

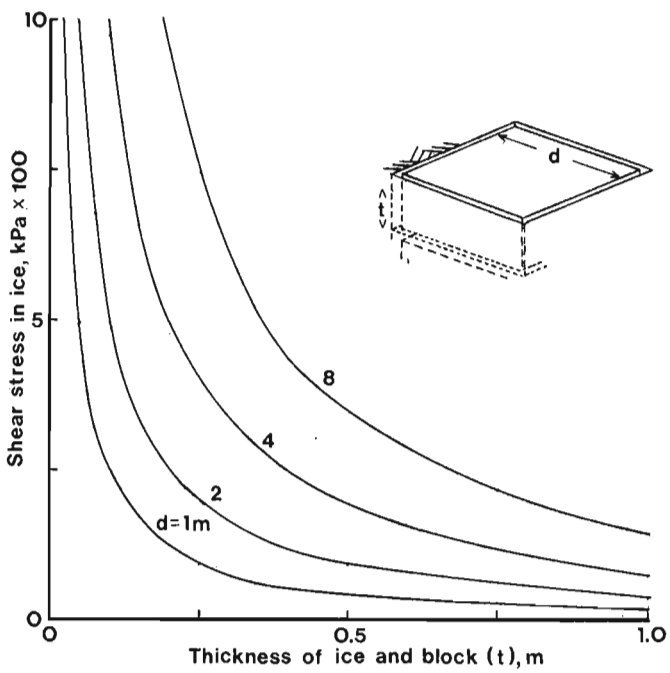

Figure 20.17. Curves showing shear stress exerted in a layer of ice surrounding a hypothetical block, assuming a water pressure of 100 kPa. Curves are plotted for a block of square cross-section and it is assumed that a horizontal crack exists at the base of the ice layer, whatever the thickness of the layer. The change in shape of the curves would be negligible if the block was assumed to be 1 m thick.

the top, allowing ice to form in the gap. A pressure sensor was installed in the bottom and a dial gauge used to measure heave of the block.

The pressure of the remaining water was observed to rise once ice had grown to a thickness of about half the depth of the box. The greatest pressures, in excess of 100 kPa, were produced at an air temperature of -10°C. A second set of tests was carried out at -2°C for which the maximum pressure never exceeded about 20 kPa. In all cases the amount of heave was small, in part because of the limited time available (i.e., about one day) before all the water had frozen. At -2°C, upward movement of approximately 0.2 mm took place whereas at -10°C movement was less than 0.1 mm. These movements may seem negligible but in addition to the short duration of the experiment, it must be remembered that the block is relatively highly constrained compared to a representative block in nature. As the size of the block increases, the area on which excess water pressure has to act will increase exponentially while the length of the ice-filled crack constraining it will only increase linearly. This effect is most pronounced for a block having a roughly square horizontal cross-section. Also, as the thickness of ice in the bounding crack increases, the shear stress between the block and the ice decreases proportionally for a given water pressure. This effect is shown in Figure 20.17 for blocks of different dimensins. It is apparent that as the ice thickness increses, the shear stress available to move the block falls off rapidly. Excess water pressures are not likely to reach a value capable of producing rock heave until a considerable thickness of ice has formed. Consequently the heaving of individual blocks becomes unlikely and uplift of an area many times larger than an individual block is favoured. The common occurrence of roughly circular piles of angular blocks and dome-shaped uplifts in the District of Keewatin may be explained by this observation.

The experiments also suggest that a more rapid rate of heaving is accomplished at temperatures closest to 0°C. It is difficult to judge if this result is significant in a natural situation. It is not known during what part of the winter freezing cycle heaving takes place. The possibility exists that heaving takes place before the ice fillings reach temperatures much below 0°C but have the ability to maintain a water tight seal. No account has been taken of rock to rock friction, but this may be removed if dilation or doming occurs.

Conclusions

Bedrock frost heave is essentially the result of two processes (Dyke, 1979): 1) the freezing of water in open cracks in rock and 2) the freezing of water in soil associated with bedrock. It must be understood that no mechanisms have been proven, rather they have been verified by the measurement of anticipated conditions or the detection of movement where movements were expected. The study is far from being advanced enough to predict absolute probabilities of heaving, heaving amounts, or pressures. Some suggestions can be made, however, as to where heaving due to various processes is most likely to occur.

Rock heave due to excess water pressures can be expected where bedrock cracks are saturated and a relatively abrupt local thickening of the active layer is present. Observations at Churchill, Manitoba, and in District of Keewatin show that the amount of vertical heave may be directly proportional to the thickness of the saturated zone within the active layer. In a stricter sense the amount of heave may be proportional to the thickness of the zone of water confined between the top of the permafrost table and the downward-advancing freezing front, once the zone is formed.

As a geologic hazard, rock heave by the excess water pressure mechanism can best be anticipated by locating geologic situations which promote local deepenings in the active layer or local variations in the rate of freeze-back. Favourable situations appear to be small in area, such as the flanks of bedrock outcrops or small rock bodies of contrasting thermal conductivity. Rock heave due to frost heaving in soils is likely to be a slower but steadier process. It will occur wherever soil containing silt and clay has access to water and is situated in a position that allows expansive forces to be transmitted to adjacent rock. To hold this in abeyance would require methods similar to those used in the treatment of engineering problems related to permafrost, i.e., removal of frost-susceptible soils or insulation of these soils to prevent freeze-thaw cycles from taking place in them.

Frost heaving of bedrock results in a variety of distinctive landforms. As a geomorphic process it is relatively common in the permafrost region and appears to be capable of producing forces and movements similar to those associated with other periglacial phenomena.

References

Brown, R.J.E.
1978: Influence of climate and terrain on ground temperatures at three locations in the permafrost region of Canada; in Permafrost, North American Contributions, Second International Conference (Yakutsk, USSR), National Academy of Sciences, p. 27-34.

Clark, S.P., Jr.
1966: Thermal Conductivity; in Handbook of Physical Constants, ed. S.P. Clark, Jr.; Geological Society of America, Memoir 97, p. 459.

Davison, C.
1889: On the creeping of the soil-cap through the action of frost; Geological Magazine, v. 6, p. 255.

Dyke, A.S.
1976: Tors and associated weathering phenomena, Somerset Island, District of Franklin; in Report of Activities, Part B; Geological Survey of Canada, Paper 76-1B, p. 209-216.

Dyke, A.S. (cont.)
1978: Glacial history of and marine limits on southern Somerset Island, District of Franklin; in Current Research, Part B; Geological Survey of Canada, Paper 78-1b, p. 218-224.

Dyke, L.D.
1979: Bedrock heave in the central Canadian Arctic; in Current Research, Part A; Geological Survey of Canada, Paper 79-1A, p. 241-246.

Karlén, W.
1973: Holocene glacier and climatic variations, Kebnekaise Mountains, Swedish Lapland; Geografiska Annaler, Series A, v. 55A, p. 29-63.

Lachenbruch, A.H.
1962: Mechanics of thermal contraction cracks and ice-wedge polygons in permafrost; Geolgical Society of America, Special Paper no. 70, 69 p.

Leffingwell, E. de K.
1919: The Canning River Region, northern Alaska; United States Geological Survey, Professional Paper 109, 251 p.

Mackay, J.R.
1973: The growth of pingos, western Arctic coast, Canada; Canadian Journal of Earth Sciences, v. 10, no. 6, p. 979-1004.

Mackay, J.R. and Burrous, C.
1979: Uplift of objects by an upfreezing ice surface; Canadian Journal of Earth Science, v. 16, no. 3, p. 609-613.

Miller, G.H. and Andrews, J.T.
1972: Quaternary history of northern Cumberland Peninsula, east Baffin Island, N.W.T., Canada. Part VI: Preliminary lichen growth curve for **Rhizocarpon geographicum**; Geological Society of America, Bulletin, v. 83, p. 1133-1138.

Skinner, B.J.
1966: Thermal expansion; in Handbook of Physical Constants, ed. S.P. Clark, Jr.; Geological Society of America, Memoir 97, p. 75.

Tyrrell, J.B.
1896: Report on the Dubawnt, Kazan and Ferguson Rivers and the Northwest Coast of Hudson Bay; Geological Survey of Canada, Annual Report, v. IX, Part F, 205 p.

21.

STRATIGRAPHY AND STRUCTURE: NORTHERN HALF OF THOR-ODIN NAPPE, VERNON EAST-HALF MAP AREA, SOUTHERN BRITISH COLUMBIA

EMR Contract OSB80-00117

Peter B. Read[1] and David W. Klepacki[1]
Cordilleran Geology Division, Vancouver

Read, Peter B. and Klepacki, David W., Stratigraphy and structure: northern half of Thor-Odin nappe, Vernon east-half map area, southern British Columbia; in Current Research, Part A, Geological Survey of Canada, Paper 81-1A, p. 169-173, 1981.

Abstract

Because of facies changes, stratigraphy of the Mantling Zone varies southward along the east side of Thor-Odin nappe. The basal quartzite thins southward to 10 m or less, the immediately overlying calcite-bearing calc-silicate gneiss outcrops very locally southwards, and the presence of the "white marble" is uncertain in the south.

Three phases of isoclinal folding combine to create the complexly folded Thor-Odin nappe which is folded about a late northerly trending warp. Two second phase anticlines and an intervening syncline plunge west-southwesterly on the west side of the Core Zone and east-northeasterly on the east side. Third phase folds trending northwesterly and the late warp change the plunge of second phase structures and allow their partial preservation in the footwall of the gently eastward dipping Columbia River fault zone on the west bank of the Columbia River. First phase folds probably trend northerly, form west dipping antiformal anticlines on the west side of the Core Zone and east dipping synformal anticlines on the east side.

Introduction

A month was devoted to unravelling the stratigraphy and structure of the stratified metamorphic rocks forming the northern half of Thor-Odin nappe in the Shuswap Metamorphic Complex. This study is a continuation of earlier work (Read, 1979a, b, 1980) and supplements the published work of Reesor (1973) and unpublished investigations of Craig (1966), Hill (1975) and Mutti (1978).

Four structural culminations constitute the eastern part of the Shuswap Metamorphic Complex from Frenchman Cap dome northwest of Revelstoke to Valhalla dome southeast of Nakusp (Fig. 21.1). Frenchman Cap and Thor-Odin immediately to the south, expose paragneiss and orthogneiss of the Core Zone beneath a basal quartzite and overlying schist and gneiss of the Mantling Zone. Reesor and Moore's (1971) and Read's (1980) investigations show that the isoclinally folded Core and Mantling zones of Thor-Odin form a complexly folded nappe. East of Thor-Odin nappe, the Columbia River fault zone sets Clachnacudainn and Selkirk allochthons against the eastern margin of the Shuswap Metamorphic Complex.

Stratigraphy of the Shuswap Metamorphic Complex

Schist and gneiss of the Shuswap Metamorphic Complex are divided into Core and Mantling zones by an intervening quartzite. The base of the lowest persistent quartzite (Q1) defines the contact between the Core and Mantling zone. Within the map area, a few thousand metres of stratified rocks of the amphibolite facies form the northern half of Thor-Odin nappe. The rocks are mostly of sedimentary origin, lie mainly in the sillimanite zone, and on the western and southern side of the nappe contain abundant pegmatites and leucogranitic intrusions.

The present investigation substantiates the stratigraphy of the Mantling Zone detailed by Read (1980). In the following stratigraphic summary, facies changes that develop southward along Thor-Odin nappe are emphasized. Biotite-quartz-feldspar paragneiss, locally with sillimanite, forms the Core Zone; calc-silicate gneiss is absent. Southward along the east side of Thor-Odin nappe, biotite paragneiss replaces the biotite-muscovite gneiss and schist which characterize the top 100 m of the Core Zone. On the east side of the nappe, well layered, muscovite- and tourmaline-bearing basal quartzite abruptly thins south of Blanket Creek. North of the creek, it is 100 to 500 m thick but southward it diminishes to 10 m or less. A white, calcite-bearing calc-silicate gneiss up to 30 m thick, usually present immediately above the basal quartzite north of Blanket Creek, only locally exists south of the creek. Here and there within 100 m of the top of the basal quartzite is a white marble but the presence of this marble south of Blanket Creek is uncertain. Higher in the section are one to several thin, white quartzites which lack tourmaline and are locally biotitic. West of Englishman Creek, these quartzites thin to less than 20 m and are discontinuous. Biotite ± sillimanite ± garnet gneiss and calc-silicate gneiss host the quartzite and marble horizons, and constitute unit S which extends from the top of the basal quartzite to the top of the uppermost quartzite. In unfaulted succession above unit S are psammitic and some pelitic gneisses with abundant pegmatite and leucogranitic intrusions which compose unit H of unknown but considerable thickness. It outcrops mainly on the west side of Thor-Odin nappe west of Victor Creek fault.

Deformation

At least three phases of tight to isoclinal folds combine to form Thor-Odin nappe. Late warps and subvertical faulting add to the structural complexities. Widespread, second phase fold axes and lineations plunge gently to the west-southwest to the west of the Core Zone and east-northeast to the east of the zone. They pass through the horizontal across the Core Zone. On the west side, thick basal quartzite outlines two reclined anticlines and an intervening syncline which plunge west-southwest (Fig. 21.2, 21.3). To the southwest these are Begbie anticline, Mulvehill syncline and Tilley anticline. Within the map area, only the trace of the axial plane of Begbie anticline extends eastward across the Core Zone to the Columbia River where the Columbia River fault zone cuts it (Fig. 21.3). The southwesterly dipping axial planes of Mulvehill syncline and Tilley anticline lie in the western part of the Core Zone where they leave the map area at its southern limit. The third phase Wetask fold and a late, northerly trending warp may bring these second phase axial planes down on the east side of the Core Zone near the Columbia River south of Revelstoke, as tentatively shown (Fig. 21.3). Isoclinal, second phase folds

[1] Consulting geologists; Geotex Consultants Limited, No. 1000 – 100 W. Pender St., Vancouver, B.C., V6B 1R8

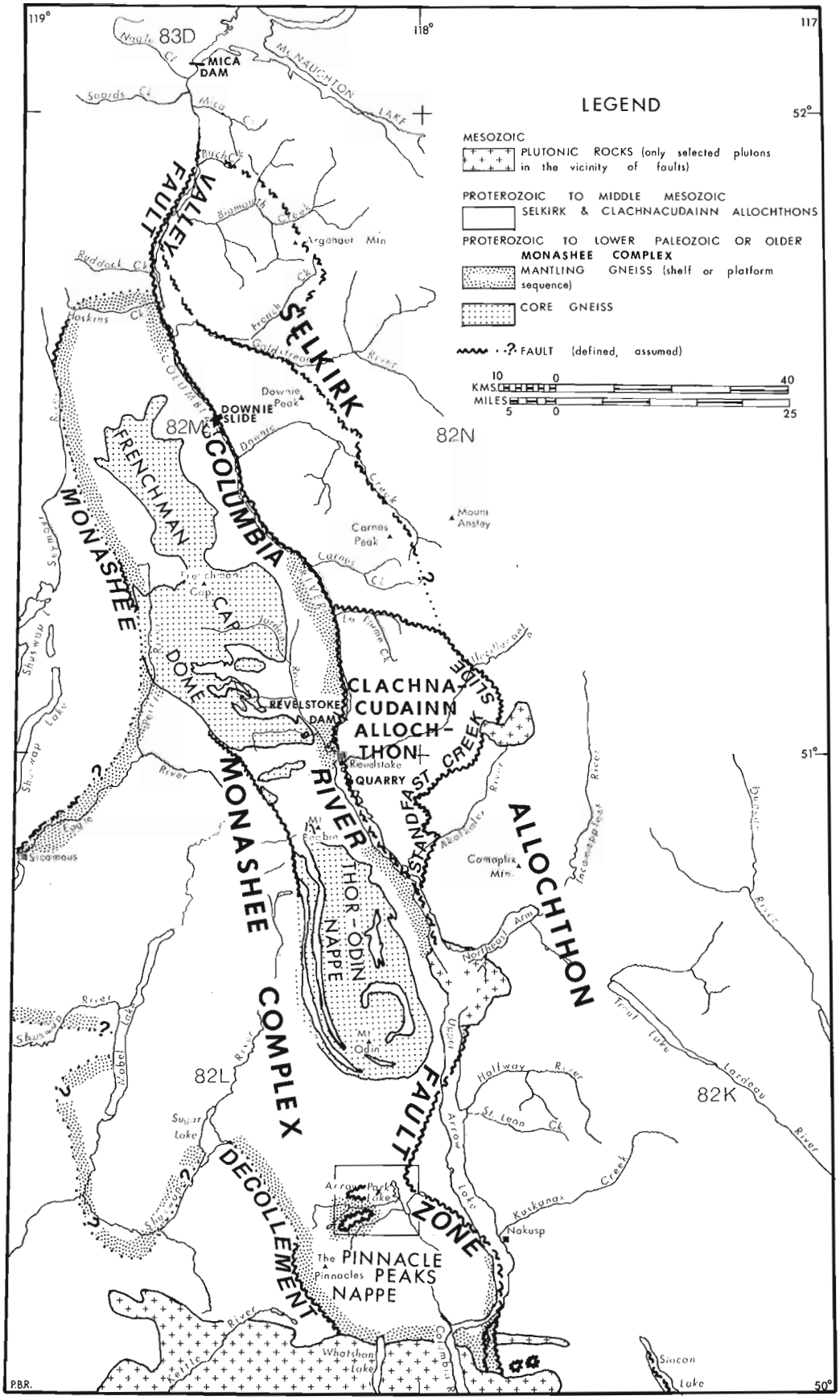

Figure 21.1. *Regional map of the Shuswap Metamorphic Complex and Selkirk and Clachnacudainn allochthons showing major faults, the structural culminations in the eastern part of the complex, and the distribution of core gneiss.*

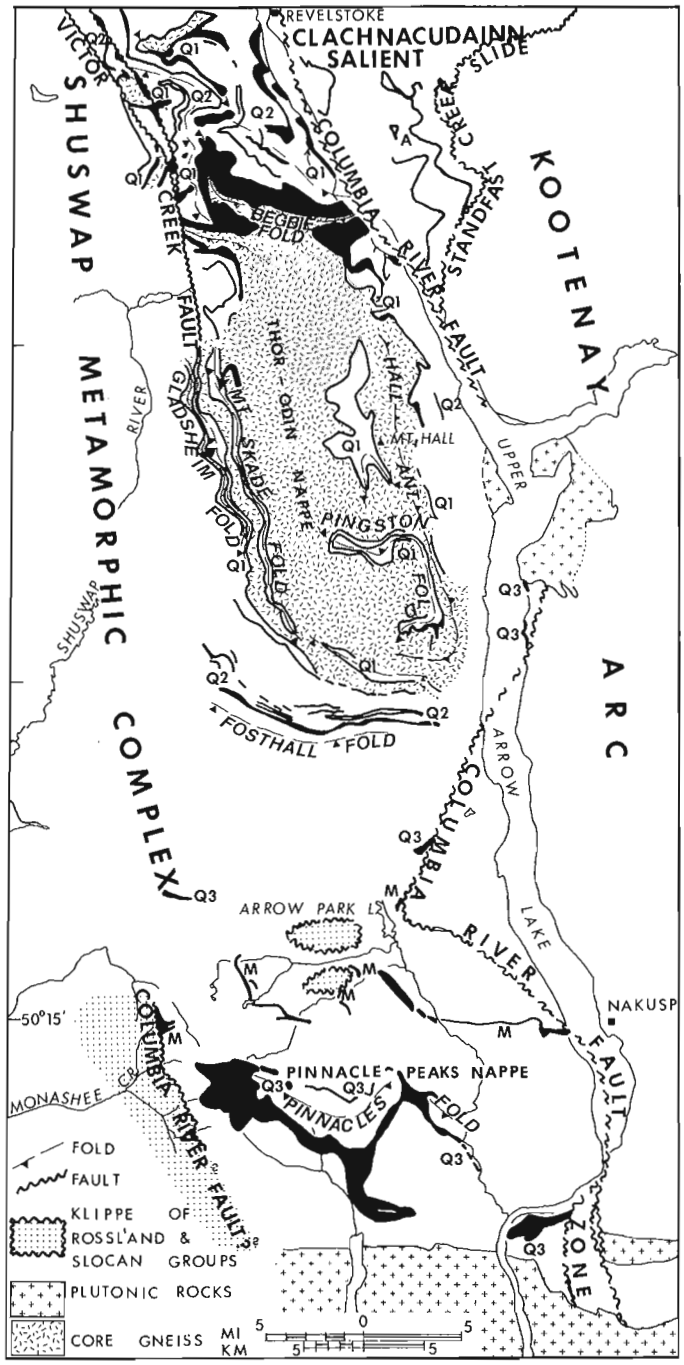

Q = quartzite undifferentiated *Q2 = second quartzite*
Q1 = basal quartzite *Q3 = quartzite in Pinnacle Peaks nappe*

Figure 21.2. *Distribution of quartzite and marble units on the southeastern side of the Shuswap Metamorphic Complex, amphibolite (A) in the Clachnacudainn Allochthon, klippen of the Rossland and Slocan groups lying on the southern edge of the complex, and the distribution of major folds.*

apparently persist west of Englishman Creek and cross Victor Creek fault. A west dipping, northwest plunging syncline-anticline pair are suggested in Figure 21.3. The traces of their axial planes would be truncated by the Columbia River fault zone east of the Core Zone.

Third phase folding trends and plunges gently northwestward north of Mount Begbie and southeastward southeast of Mount Begbie. it is restricted to the northeastern part of Thor-Odin nappe and continues northward along the east side of Frenchman Cap dome (Brown and Psutka, 1980). North of the Trans-Canada highway near Clanwilliam, basal quartzite outlines the noncylindrical Wetask fold. The fold amplitude increases southeastward from Clanwilliam to the Columbia River where the fold is cut by the Columbia River fault zone.

East of Davis Peak, west-southwest plunging, upright folds deform second phase folds. Although designated as "fourth phase?", their relationship to third phase is unknown.

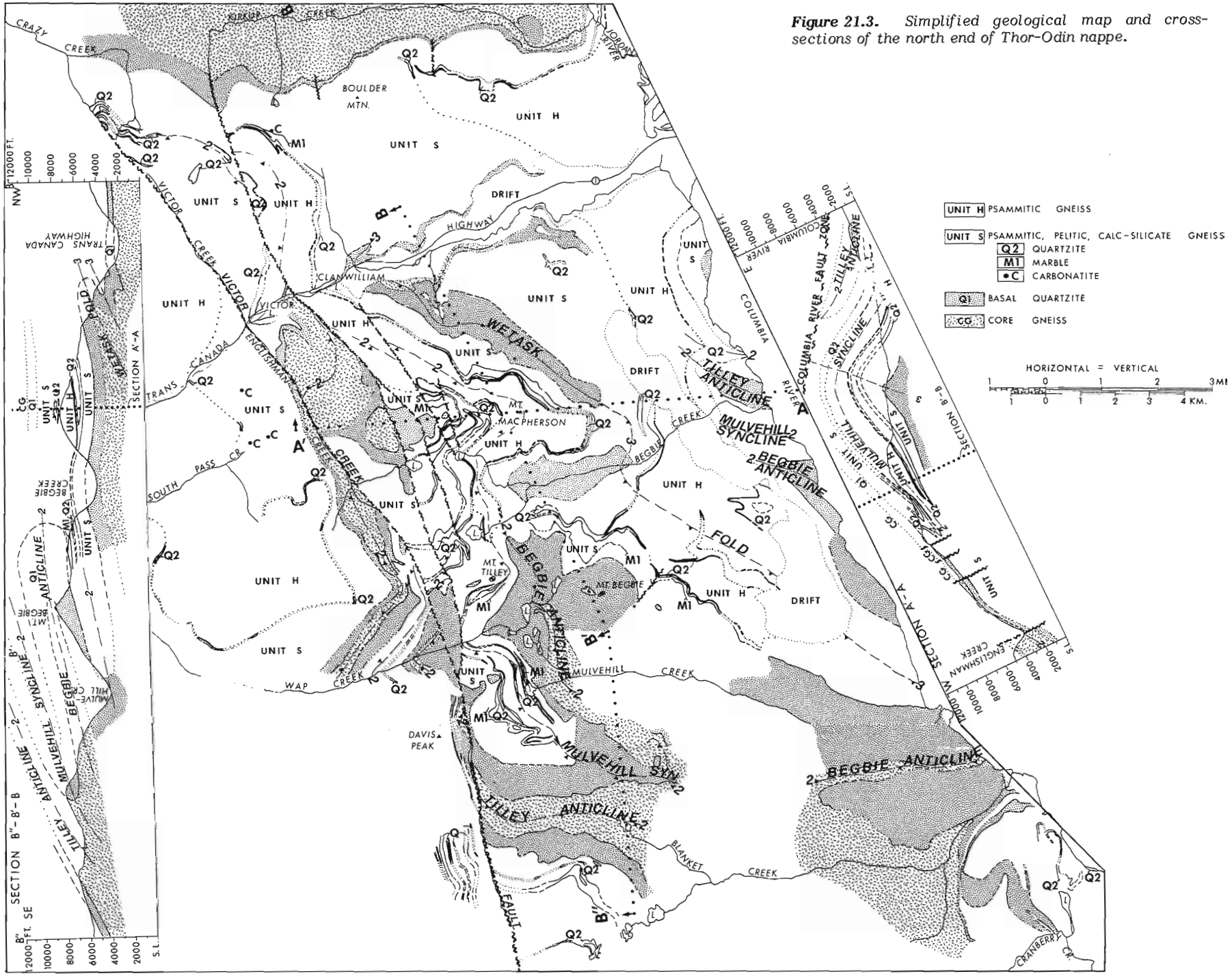

Figure 21.3. *Simplified geological map and cross-sections of the north end of Thor-Odin nappe.*

First phase folding produced large isoclinal folds, but mesoscopic structures are rarely preserved. On the west side of Thor-Odin nappe, northerly striking, basal quartzite outlines two synclines named the Mount Skade and Gladsheim folds, and intervening anticlines (Fig. 21.2). These folds trend northerly, have westerly dipping axial planes, and anticlines which close eastward as antiformal anticlines. On the east side of Thor-Odin nappe, Pingston fold and its northward extension west of Mount Hall are parts of a northerly trending antiformal syncline with a northeast to easterly dipping axial plane (Fig. 21.2). Hall anticline, centred by Core Gneiss, overlies Pingston Fold and closes eastward as a synformal anticline. Northerly trending first phase folds on the west side may become east-west across the Core Zone before returning to the northerly trend on the east side. Westerly dipping antiformal anticlines on the west side of Thor-Odin nappe become easterly dipping synformal anticlines on the east, but more precise correlations of first phase folds across the Core Zone remain speculative.

A late, northerly trending warp causes foliations to dip east on the east side of Thor-Odin nappe and west on the west side. Small subsidiary warps of similar trend complicate the map pattern in the lower part of Cranberry Creek west of Highway 23.

On the several, late, subvertical faults which strike north-northwesterly across Trans-Canada highway, only Victor Creek fault extends as far south as Wap Creek. There the fault has a displacement of less than 700 m right lateral oblique-slip and offsets Tilley anticline and an unnamed syncline-anticline pair on the west (Fig. 21.3).

References

Brown, R.L. and Psutka, J.F.
1980: Structural and stratigraphic setting of the Downie slide, Columbia River valley, British Columbia; Canadian Journal of Earth Sciences, v. 17, p. 698-709.

Craig, D.B.
1966: Structure and petrology within Shuswap Metamorphic Complex, Revelstoke, British Columbia; unpublished Ph.D. thesis, Department of Geology, University of Wisconsin, 130 p.

Hill, R.P.
1975: Structural and petrological studies in the Shuswap Metamorphic Complex near Revelstoke, British Columbia; unpublished M.Sc. thesis, Department of Geology, University of Calgary, 147 p.

Mutti, L.J.
1978: Structure and metamorphism of the Cranberry region, Thor-Odin gneiss dome, Shuswap Metamorphic Complex, British Columbia; unpublished Ph.D. thesis, Department of Geological Sciences, Harvard University, 109 p.

Read, P.B.
1979a: Relationship between the Shuswap Metamorphic Complex and Kootenay Arc, Vernon east-half, southern British Columbia; in Current Research, Part A, Geological Survey of Canada, Paper 79-1A, p. 37-40.

1979b: Geology and mineral deposits, eastern part of Vernon east-half, British Columbia; Geological Survey of Canada, Open File 658.

1980: Stratigraphy and structure: Thor-Odin to Frenchman Cap "domes", Vernon east-half map area, southern British Columbia; in Current Research, Part A, Geological Survey of Canada, Paper 80-1A, p. 19-25.

Reesor, J.E.
1973: Blanket Mountain area, British Columbia; in Report of Activities, Part A, Geological Survey of Canada, Paper 73-1A, p. 38.

Reesor, J.E. and Moore, J.M.
1971: Petrology and structure of Thor-Odin gneiss dome, Shuswap Metamorphic Complex, British Columbia; Geological Survey of Canada, Bulletin 195, 149 p.

22.

THE HEALEY LAKE MAP AREA AND THE ENIGMATIC THELON FRONT, DISTRICT OF MACKENZIE

Project 780009

John B. Henderson and Peter H. Thompson
Precambrian Geology Division

Henderson, John B. and Thompson, Peter H. The Healey Lake map area and the enigmatic Thelon Front, District of Mackenzie; in Current Research, Part A, Geological Survey of Canada, Paper 81-1A, p. 175-180, 1981.

Abstract

The Yellowknife Supergroup, consisting mainly of metasedimentary rocks, occurs throughout the area. Metavolcanic rocks dominated by intermediate fragmental deposits occur in four major centres. The supracrustal rocks are intruded by intermediate to felsic, commonly metamorphosed and foliated plutons. A heterogeneous complex of massive granitoids, gneisses and migmatitic granitoids, part of which may be older than the Yellowknife, extends across the area. Archean structural trends are curvilinear in the west half of the area and have a consistent northerly trend in the east half. Intermediate pressure amphibolite facies Proterozoic metamorphism in the east half of the area is superimposed on Archean low pressure series metamorphism that increases in grade from greenschist to granulite to the southeast. A Proterozoic "straight zone" of cataclastic Yellowknife rocks that formed intermediate in time between the two metamorphisms is a candidate for the Thelon Front – the boundary between the Slave and Churchill Provinces.

Introduction

Part of the Thelon Front, the boundary between the Slave Structural Province and the Queen Maude Block of the Churchill Structural Province, occurs within the Healey Lake map area. It was defined on the basis of the change from the relatively well preserved, low grade supracrustal rocks with irregular structural trends intruded by massive granitoid bodies of the Slave, to the generally higher grade, consistently north-northeasterly trending gneisses in the Queen Maude Block (Wright, 1967). Previous mapping at 1:250 000 scale in the northern part of the area has revealed the transition from the complex curvilinear structural style in the Yellowknife Supergroup rocks in the western part of the area to a pronounced northerly trend that involves both Yellowknife and granitoid units. However, no significant change in lithology, metamorphic grade or structural style in the area previously defined as the Thelon Front was recognized (Henderson and Thompson, 1980). Mapping in the summer of 1980 was concentrated in the southern half of the area and has resulted in the recognition of a tectonic "straight zone" in the southeast part of the area that coincides with a linear aeromagnetic trough and a major inflection in the gravity field. The straight zone is a good candidate for the enigmatic Thelon Front.

General Geology

The geology of the southern portion of the area is, in many respects, similar to that in the north reported previously by Henderson and Thompson (1980) (Fig. 22.1). The Archean Yellowknife Supergroup rocks occur throughout the area and can be traced almost continuously from the minimally deformed, low metamorphic grade, well preserved volcanic complex in the northwest corner into a tectonic straight zone that transects the southeast corner of the map area. The transition, as in the northern part of the area, from irregular-curvilinear structural trends in the supracrustal and associated massive, lobate, intrusive bodies changes rather sharply to a linear northerly trend involving both Yellowknife and granitoid rocks east of 107°W longitude. The metamorphic grade increases to the east where there is evidence of an additional post-Archean metamorphic event.

Yellowknife Supergroup

As is typical of most of the Slave Province, sedimentary rocks of the Yellowknife Supergroup are more abundant than volcanic rocks. The sediments consist almost entirely of metamorphosed greywacke-mudstone turbidites and vary only in the proportion of pelitic to psammitic components. In the western part of the area where the rocks are at a relatively low grade, primary structures are locally preserved. To the east, with increasing grade of metamorphism and degree of deformation, all primary features other than compositional layering are lost as the rocks become migmatitic. In the north-northeasterly trending cataclastic straight zone west of Moraine Lake, the Yellowknife metasediments are recognizable as the milled equivalent of the metasedimentary migmatites. The high grade terrane east of the straight zone is incompletely mapped and although metasedimentary rocks do occur, it is not certain that they are equivalent to the Yellowknife Supergroup.

Several volcanic centres have been mapped in the southern part of the area although none is as large as the major felsic complex at Back River. They are similar to that complex in being dominated by intermediate to felsic compositions. The more completely mapped and probably largest occurs at Healey Lake. The most mafic rocks occur on the large peninsula in the centre of the lake and consist of both pillowed, massive, and fragmental units of probable basalt-andesite composition. Most of the complex to the north, south and west is compositionally heterogeneous, ranging from dark green andesites through grey dacites to white rhyolite. Carbonate in thin laminae to units locally up to several metres thick are commonly associated with the more felsic volcanics. The volcanics are mainly layered, fine grained, fragmental units with coarser breccia units locally preserved. South-southeast of Healey Lake two thick sequences of dominantly dacitic metavolcanics are separated by a thin septum of metasediments. To the east and separated from it by about 10 km of granitoid gneiss terrane are more metavolcanics that occur mainly within the straight zone. These metavolcanics, also mainly of intermediate composition, may represent the southern extension of the major metavolcanic sequence north of Tourgis Lake (Henderson and Thompson, 1980). Like them, these rocks are

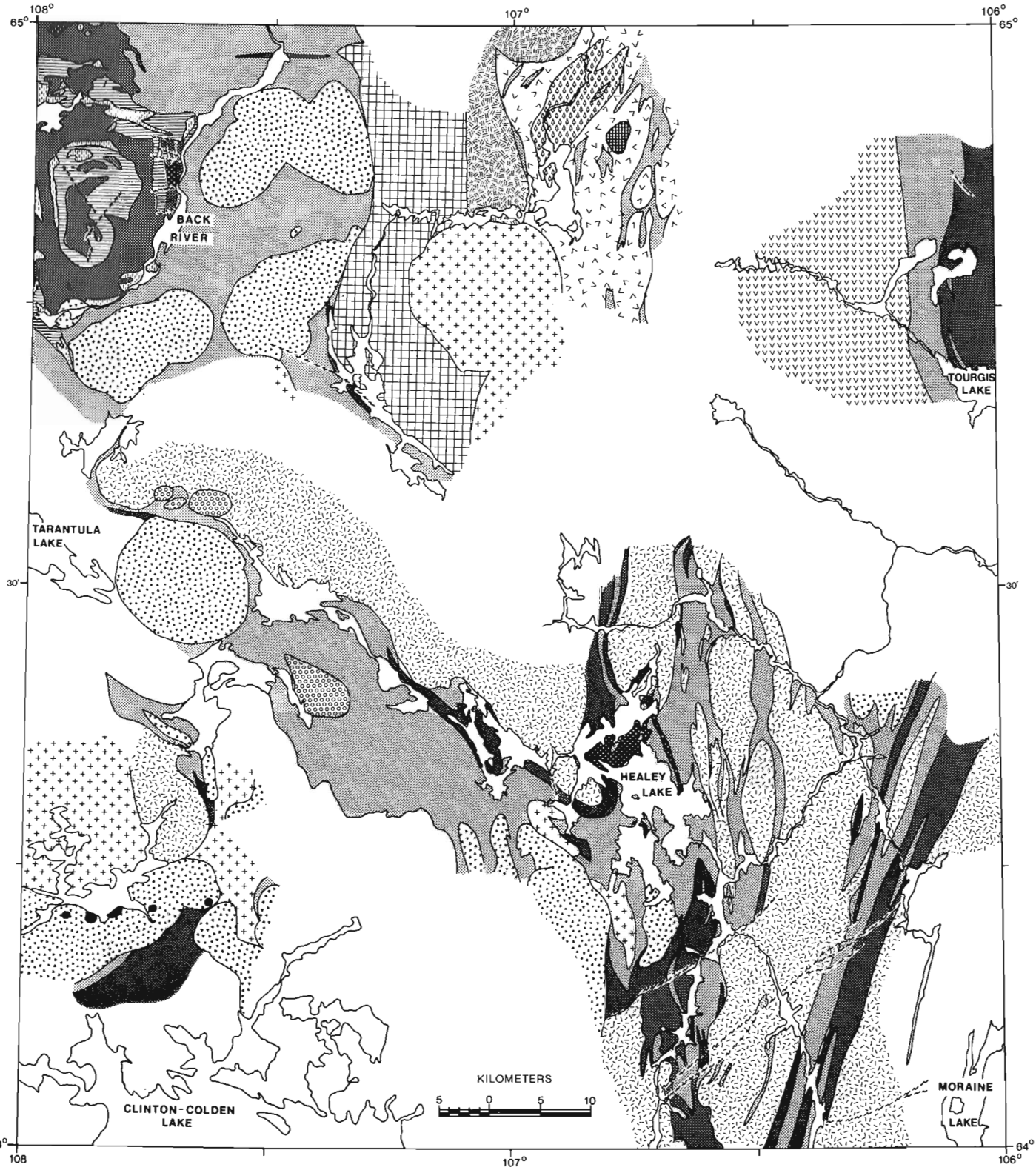

Figure 22.1. *General geology of parts of the Healey Lake map area (76 B).*

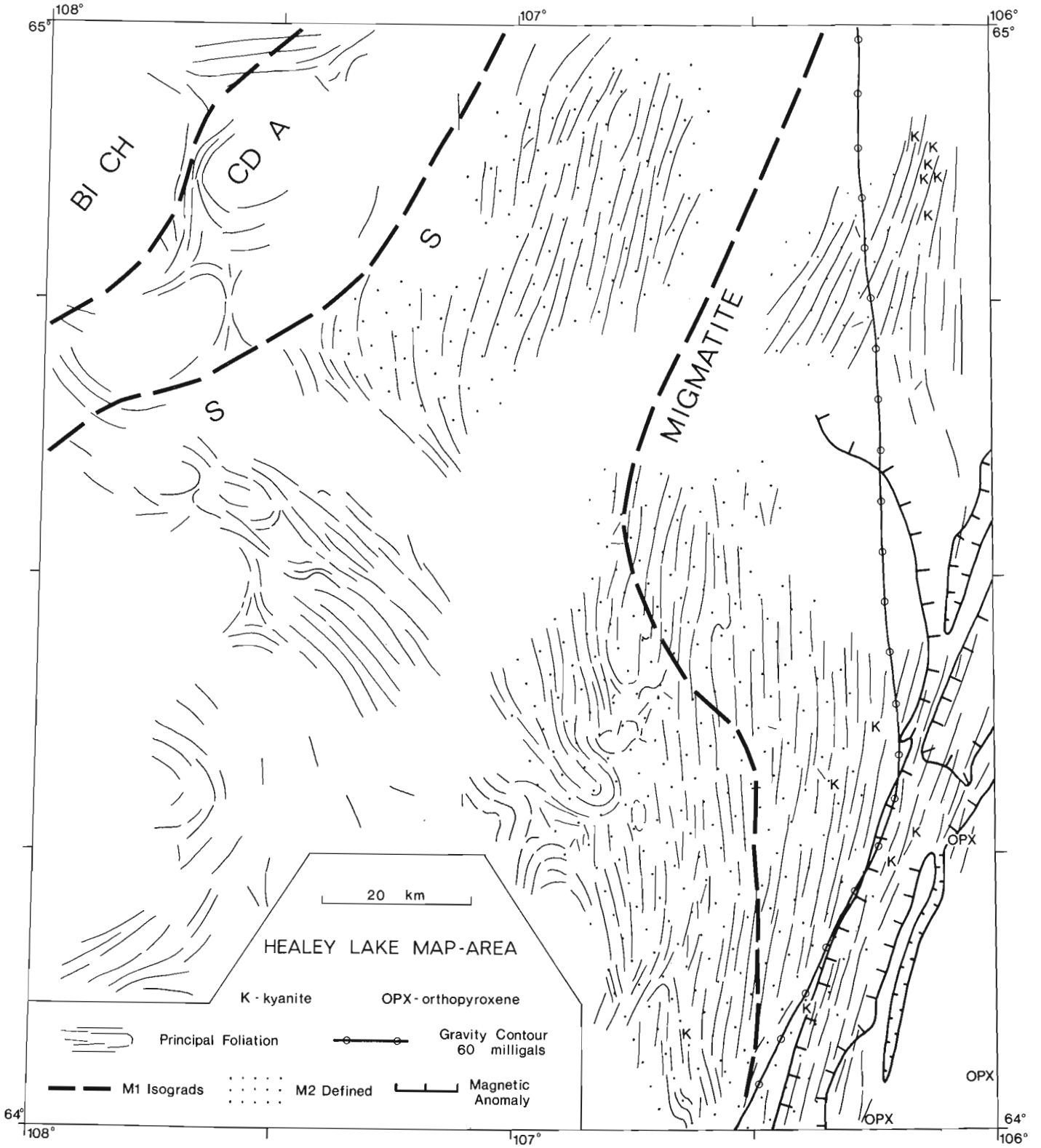

Figure 22.2. *Metamorphic and structural trend map for the Healey Lake area. The heavy dashed lines are Archean cordierite-andalusite, sillimanite and migmatite metamorphic isograds (BI = biotite, CH = chlorite, CD = cordierite, A = andalusite, S = sillimanite). The dot pattern approximates the amphibolite facies of a Proterozoic metamorphism. The orientation of the principal foliation is given by the light line segments. The magnetic anomaly outlined in the southeast corner is a prominent trough that corresponds to the tectonic straight zone. The -60 milligal contour corresponds to the inflection between major negative and positive Bouguer gravity anomalies which is coincidental with the straight zone.*

locally migmatitic but are more commonly deformed into a featureless, fine grained, pinkish grey to greenish grey quartzofeldspathic (hornblende) rock. The third major volcanic centre north of Clinton-Colden Lake has been incompletely mapped. It is better preserved than the volcanics to the east and consists of well layered fragmental andesite-dacite in the northwest, while the southeastern part is dominated by andesitic pillowed volcanics.

Intrusive and Gneissic Rocks

Several of the intrusive units previously mapped in the northern part of the area also occur in the southern part. Although not as pronounced as in the north, the proportion of more mafic granodiorite, tonalite and diorite is high with respect to more felsic granites.

Figure 22.3. *Legend to accompany Figure 22.1 – General geology of the Healey Lake area. The order of the units in the legend for the most part has no stratigraphic or age implication.*

The suite of large tonalitic to dioritic plutons southeast of the Back River occurs throughout the western third of the area. These plutons are typically massive, medium grained, equigranular, dark grey to pink, and contain hornblende as the dominant mafic mineral. Although mainly massive, the southernmost body northwest of Clinton-Colden Lake has a moderately strong westerly foliation. Included with this diorite map unit are several diorite plutons southwest of Healey Lake. These plutons are intruded by two mica granite-granodiorite.

Two mica granite-granodiorite underlies a large part of the area between Tarantula and Clinton-Colden Lake. It occurs as a leucocratic, massive, medium grained equigranular rock devoid of pegmatite and with highly variable amounts and proportions of biotite and muscovite. A somewhat similar rock occurs southwest of Healey Lake where it is generally foliated and contains abundant inclusions, to screens, of metasediment. Between Healey Lake and the major areas of the unit as shown in Figure 22.1, are abundant small stocks intruding the metasediments.

Twenty kilometres southeast and 10 km northeast of Tarantula Lake are plutons of a massive, medium grained, even grained, pink to white biotite granite.

The most extensive granitoid unit in the southern half of the area as presently mapped extends almost completely across the map area. It is a highly complex heterogeneous unit that cannot be subdivided at 1:250 000 scale. Composition ranges from metadiorite to granite and the rocks are texturally diverse. Within the unit are massive granitoid bodies, complexly folded compositionally layered gneisses, and granitoid migmatites. Much of the unit is extensively recrystallized, as for example near the west end of the complex, where an originally coarse augen granodiorite now occurs as a medium grained equigranular rock, its original coarse texture evident only by the distribution of biotite. The unit differs from the other granitoids of the Healey Lake area in that layered gneisses and migmatites form part of the unit in the western as well as in the eastern parts of the map area. At Healey Lake and to the east, massive phases are no longer present and all facies of the unit are foliated. Granitoid rocks within, and east of, the straight zone are included in this unit (Fig. 22.1). They are highly heterogeneous, commonly intruded by mafic bodies and locally contain granulite grade metamorphic mineral assemblages. Throughout the area contacts between this unit and the supracrustal units are tectonic or intrusive. Parts of this unit may be older than the Yellowknife Supergroup, as suggested by the lithological and structural complexity of the unit, particularly in the west where it contrasts strongly with the relatively simple structural style and intermediate metamorphic grade of the Yellowknife rocks.

An east-west line of five small, massive, coarse grained, metamorphosed ultramafic stocks occurs north of Clinton-Colden Lake. Only the second most westerly was observed in outcrop. Three were recognized from their distinctive aeromagnetic pattern while the easternmost one was recognized from a concentration of coarse, rather altered blocks. It does not have a magnetic expression.

At least three sets of post-Archean mafic dykes occur in the area mapped. The north-northwesterly trending Mackenzie dykes are unaltered throughout the area, while in the eastern part of the area both an east-west set and a northeasterly trending set are metamorphosed and foliated although their trend is not disturbed. With one exception no dykes have been recognized within or east of the straight zone although in this area there are abundant mafic intrusions, generally parallel to the regional foliation.

Structural Geology

The change from a complex curvilinear structural pattern to a north or north-northeast striking, mainly east-dipping linear pattern mapped in the north half of the area (Henderson and Thompson, 1980) continues across the south half (Fig. 22.2). The zone of transition from one to the other is shaped like an open S with the curvilinear pattern persisting farther east in the south. The "principal foliation" in Figure 22.2 is the dominant schistosity, foliation or gneissosity in outcrop. Near Back River it represents a second phase of deformation in that the foliation is axial planar to isoclinal folds that deform an older foliation and bedding. To the east and at higher metamorphic grade, the principal foliation generally has a northerly orientation but scattered M-shaped minor folds involving the principal foliation and local changes in attitude indicate this surface has been folded into its present attitude during a later deformation. The undeflected trends of three sets of Proterozoic diabase dykes that cut across the regional structural pattern in both western and eastern structural zones suggests that the pattern (Fig. 22.2) is Archean.

Although the regional structural pattern appears to be Archean, later deformation has affected the eastern part of the area. Two of the Proterozoic diabase dyke sets within this part of the area are metamorphosed to amphibolite (see below) with the metamorphic amphibole forming a foliation parallel to the principal foliation in the rocks they intrude. Southeasternmost dykes are commonly broken into segments along surfaces parallel to the regional foliation. Individual segments maintain their original orientation. Reactivation by shear along the pre-dyke structure could account for the foliation and displacement.

A striking feature in the southeastern part of the area is a north-northeasterly trending "straight zone" (in the sense of Hepworth, 1967 and Watson, 1973) up to 5 km wide. This prominent feature has a pronounced topographic expression, with lakes within it being very long and narrow. It corresponds closely to a magnetic "trough" on the aero-magnetic map (Geological Survey of Canada, 1968) that separates the relatively flat magnetic topography to the west from the much higher and very irregular magnetic topography to the east (Fig. 22.2). The inflection zone between a prominent negative Bouguer gravity anomaly to the west and a positive anomaly to the east (60 milligals over 100 km) (Gibb and Thomas, 1977) also coincides with the straight zone (Fig. 22.2). The rocks within the zone are predominantly cataclastically deformed and metamorphosed members of the Yellowknife Supergroup whose trend differs significantly from the more northerly trend of the Yellowknife rocks to the west (Fig. 22.1). However, if the principal foliations in granitoid as well as supracrustal rocks are considered, there is a gradual convergence of the foliations inside and outside the zone (Fig. 22.2). If the less deformed supracrustal rocks north of Tourgis Lake are correlative with those in the straight zone, the straight zone probably diverges from this supracrustal belt as the magnetic trough (presumed to correspond to the straight zone) can be traced 75 km to the north-northeast as far as the Bathurst Fault, although it becomes broader and more diffuse. The magnetic trough can also be traced about 75 km to the south-southwest beyond the map area. Similar north-northeasterly structural trends of Archean age are present in the north-central part of the area although there the rocks are not deformed in the same style. As a large part of the deformed rocks in the straight zone consist of the crushed equivalent of the Yellowknife migmatites, the shearing in this zone indicates significant deformation after the peak of the early metamorphism. However, the medium grade metamorphic assemblage (kyanite-biotite-muscovite) in the shear zone implies deformation was older than or synchronous with the later metamorphism.

Regional Metamorphism

Field observations and limited petrography indicate two phases of regional metamorphism have altered the Yellowknife Supergroup and some of the granitoid rocks (Fig. 22.2). The predominant early phase, Archean in age, is represented by isograds in metasedimentary rocks, indicating metamorphic grade increases southeastward. Superimposed on the early phase is a second metamorphic gradient that is most easily recognized in the field by metamorphism of Proterozoic diabase dykes.

The early metamorphism is the low pressure type characteristic of the 2600 Ma event in the Slave Province (Thompson, 1978). In Figure 22.2, cordierite, sillimanite and migmatite (>10% leucosome) isograds are extrapolated across masses of plutonic rock both older and younger than the metamorphism. In pelitic schist and metagreywacke, chlorite-biotite occurs at lowest grade and cordierite-biotite, cordierite-biotite-andalusite and staurolite-biotite-andalusite at medium grade, with sillimanite appearing as grade increases. Ultimately these rocks become biotite-garnet-sillimanite migmatites, locally containing kyanite. Orthopyroxene is present east of the straight zone. Commonly, textural relations between porphyroblasts and microstructures indicate porphyroblastic growth outlasted the main phases of deformation but some rocks contain evidence of significant deformation after growth ceased and the leucosome in migmatitic rocks can be intensely folded. Although it can be inferred that early metamorphism temperatures peaked during or after the main phases of deformation, the presence of kyanite in migmatite suggests maximum pressures may have been reached in the highest grade rocks before the temperature maximum (Henderson and Thompson, 1980). In metasedimentary rocks in the north-central part of the map area in particular, but also elsewhere downgrade of the migmatite isograd, white mica and chlorite occur in the matrix and coarse white mica or white mica and chlorite have replaced the porphyroblasts. These retrograde textures and mineral assemblages may be related to cooling after the thermal maximum or to low grade conditions during the later metamorphism.

The influence of the later metamorphism (Fig. 22.2) is most obvious in the Proterozoic (pre-Mackenzie) diabase dykes which change eastward from brown-weathering dykes with diabasic textures to black-weathering, foliated and lineated amphibolites in which the amphibole is seen in thin section to change from blue-green to yellow or brown-green. Garnet poikiloblasts are present in the easternmost samples. Clinopyroxene was not observed. In pelitic rocks later metamorphism is expressed as muscovite-rich seams containing chlorite and euhedral staurolite which cut across the leucosome of biotite-garnet migmatite, and by a chlorite-kyanite-euhedral staurolite assemblage superimposed on an older staurolite-biotite-andalusite-sillimanite assemblage. Mineral assemblages attributed to later metamorphism are typical of the lower to middle amphibolite facies. Kyanite related to the later metamorphism suggests that at least in the southern part of the area the later metamorphism was the intermediate pressure type, that is, was at a higher pressure than the pressure during the temperature maximum of the earlier metamorphism.

Several occurrences of orthopyroxene-bearing metamorphic assemblages have been found east of the straight zone. The easternmost occurrence is one of several in the region discussed by Fraser (1978). The other two, a biotite-quartz-plagioclase-microcline paragneiss and a more mafic gneiss with hornblende and clinopyroxene, occur in a terrane dominated by biotite- and hornblende-bearing quartzo-feldspathic gneisses. These rocks may represent either a prograde transition to granulite facies metamorphism or granulites retrogressed, for the most part, to amphibolite

facies, or both. Granulites would be a smooth continuation of the southeastward increasing grade of the early metamorphism. If retrogression has occurred, the metamorphic conditions attributed to the later metamorphism accompanied by deformation and some water would be adequate for the process.

Except for the small granite pluton 40 km northwest of Tourgis Lake, and possibly the two mica granite-granodiorite north of Clinton-Colden Lake, the granitoid rocks in the map area (Fig. 22.1) show varying degrees of metamorphic recrystallization and deformation. For example, dioritic plutons known to intrude the Yellowknife Supergroup east of Back River exhibit textures and mineral assemblages compatible with the regional metamorphic grade of the adjacent metasediments, suggesting they are older than the metamorphism. In the central part of the map area leucocratic muscovite-biotite granite-granodiorite has intruded regionally metamorphosed rocks and are themselves foliated and recrystallized. The undifferentiated granitoid unit is in part composed of isoclinally-folded, partially-migmatized granitoid rocks.

Discussion

"Fronts" in the sense of boundaries separate the Churchill and Slave Provinces (Thelon), the Churchill and Superior Provinces (Nelson) and the Grenville Province and older provinces to the north (Grenville). As has been recently discussed for the eastern Grenville (Gower et al., 1980), changes across a front may be related to lithology, metamorphism, structure, various geophysical parameters, or some combination of these. Commonly, a front defined on the basis of one aspect does not correspond with that for another, and indeed the criteria may change along strike. The enigmatic aspect of the Thelon Front is not unique.

With this in mind, what is the current status of the Thelon Front? Wright (1967) originally thought of the front as ". . .gradational, probably over some miles. . ." across which occurred a change in lithology, metamorphic grade or structural style. Mapping in both the northern and southern parts of the area has failed to locate such a zone of the scale implied by Wright in the region he suggested. Both metamorphic gradients are on the scale of many tens of kilometres with no discontinuous changes in grade recognized in the areas mapped to date. In the southern half of the area the change in structural trend approximately corresponds to Wright's zone, although they diverge widely in the northern part of the area. Similar supracrustal, granitoid and gneissic rocks occur throughout the area mapped. The Thelon Front is commonly thought to be a Proterozoic feature (Wright, 1967; Davidson, 1972) yet at present it appears that the main metamorphic gradient and major change in structural style are Archean.

Is the straight zone in the southeast corner the Thelon Front? This zone is expressed in the presently exposed rocks within the map area as a probable Proterozoic metamorphosed zone of cataclasis in previously metamorphosed Yellowknife supracrustal rocks that has a magnetic expression traceable for at least 200 km along strike. Its correspondence with the zone of inflection between a large positive and negative Bouguer gravity anomaly (Gibb and Thomas, 1977) suggests this feature is of more than surficial importance. Little is known of the terrane southeast of the zone. Its granulite facies metamorphic assemblages are compatible with the high grade rocks produced by the Archean metamorphism to the northwest. Its generally retrogressed state could be related to the later metamorphism that also affects the straight zone. The straight zone may be only the largest and westernmost of a series of similar cataclastic zones to the southeast. Until more is known about this terrane, both within and beyond the Healey Lake area, the straight zone can be thought of only as a candidate for the Thelon Front, if indeed a particular feature is to be chosen.

Acknowledgments

Marc St. Martin, Luc Plante and Wolf Schnittker greatly facilitated the field work with their enthusiastic assistance and good company. The Geology Office of the Department of Indian and Northern Affairs at Yellowknife provided an expediting service and assisted the party in many ways. The report was reviewed by W.F. Fahrig and J.C. McGlynn.

References

Davidson, A.
1972: The Churchill Province; in Variations in tectonic styles in Canada, Geological Association of Canada, Special Paper 11, p. 382-433.

Fraser, J.A.
1978: Metamorphism in the Churchill Province, District of Mackenzie; in Metamorphism in the Canadian Shield, Geological Survey of Canada, Paper 78-10, p. 195-202.

Geological Survey of Canada
1968: Healey Lake, Northwest Territories; Geological Survey of Canada, Geophysics Paper 7198.

Gower, C.F., Ryan, A.B., Bailey, D.G., and Thomas, A.
1980: The position of the Grenville Front in eastern and central Labrador; Canadian Journal of Earth Sciences, v. 17, p. 784-788.

Gibb, R.A. and Thomas, M.D.
1977: The Thelon Front: a cryptic suture in the Canadian Shield?; Tectonophysics, v. 38, p. 211-212.

Henderson, J.B. and Thompson, P.H.
1980: The Healey Lake map area (northern part) and the enigmatic Thelon Front, District of Mackenzie; in Current Research, Part A, Geological Survey of Canada, Paper 80-1A, p. 165-169.

Hepworth, J.V.
1967: The photogeological recognition of ancient orogenic belts in Africa; Quarterly Journal of the Geological Society of London, v. 123, p. 253-292.

Thompson, P.H.
1978: Archean regional metamorphism in the Slave Structural Province – a new perspective on some old rocks; in Metamorphism in the Canadian Shield, Geological Survey of Canada, Paper 78-10, p. 95-102.

Watson, J.V.
1973: Effects of reworking on high-grade gneiss complexes; Philosophical Transactions of the Royal Society of London, Series A, v. 273, p. 443-455.

Wright, G.M.
1967: Geology of the southeastern barren grounds, parts of the Districts of Mackenzie and Keewatin (Operations Keewatin, Baker, Thelon); Geological Survey of Canada, Memoir 350.

23.

BASEMENT GNEISSES OF THE WESTERN ROCKY MOUNTAINS, HUGH ALLAN CREEK AREA, BRITISH COLUMBIA

EMR Research Agreement 86-4-80

Christopher Oke[1] and P.S. Simony[1]
Cordilleran Geology Division, Vancouver

Oke, Christopher and Simony, P.S., Basement gneisses of the western Rocky Mountains, Hugh Allan Creek area, British Columbia; in Current Research, Part A, Geological Survey of Canada, Paper 81-1A, p. 181-184, 1981.

Abstract

Granitoid gneisses constituting Mount Blackman form the core of a large anticline on the northeast flank of which is a complete Hadrynian Miette to Lower Cambrian sequence. the gneiss forming the ridge south and west of Hugh Allan Creek and east of the Rocky Mountain Trench is separated from the Mount Blackman Gneiss by the Purcell Thrust.

The Hadrynian Miette Group is about 2500 m thick and consists of a basal quartzite followed by grit, pelite, carbonate, and sandstone in a sequence similar to Miette sequences elsewhere on the west flank of the Rockies. It is overlain by the Lower Cambrian Gog Group. The granitoid gneiss immediately underlying the basal Miette quartzite is strongly sheared and probably represents a folded décollement zone.

Introduction

Since the mid sixties granitoid gneiss has been known on the west flank of the Rocky Mountains in the vicinity of Hugh Allan Creek (83 D/7) (Giovanella, 1967, 1968; Campbell, 1968; Chamberlain et al., 1978). The gneiss has generally been interpreted as being carried by the Purcell Thrust over the Hadrynian to Middle Cambrian metasediments of the Western Rocky Mountains (Price and Mountjoy, 1970; Wheeler et al., 1972). Chamberlain et al. (1978) showed it to be Precambrian basement but its relationship to the Malton Gneiss exposed west of the Rocky Mountain Trench and to the Canadian Shield basement of the Rocky Mountains was unclear.

In summer 1980 the gneiss and the adjacent Hadrynian and Cambrian formations were mapped in detail on a scale of 1:12 000. The gneiss north and east of Hugh Allan Creek was found to underlie a complete, upright succession extending from the base of the Miette to the Lower Cambrian McNaughton quartzite.

Stratigraphy

Most of the gneiss in the study area is granitoid. In most locations a foliation consisting of biotite, muscovite and elongated quartz is present. Garnets ranging from 2 mm to more than 10 mm occur in laterally discontinuous layers. The biotite content of the gneiss is variable, ranging from biotite-poor near the contact with the overlying quartzite to biotite-rich in occasional thin layers. Away from the contact with the overlying quartzite the gneiss is migmatitic. Both foliated and unfoliated leucosome is present suggesting two periods of leucosome development.

Along the ridge south of Hugh Allan Creek and in several other locations is a felsic hornblende gneiss (Fig. 23.1). The felsic gneiss generally is lineated, parallel to fold axes in the area, and in places is also foliated. The foliation is parallel to that in the surrounding rocks. The felsic gneiss occurs only in the hanging wall of the thrust fault.

Bodies of amphibolite appear in the gneiss throughout the study area, commonly forming layers parallel to the foliation. These amphibolite layers are interpreted as mafic intrusions.

North and east of Hugh Allan Creek the gneiss is overlain by muscovitic quartzite which is separated from the pelite and grit of the lower Miette by a thin (3-10 m) layer of biotite schist. The actual contact between the gneiss and quartzite is difficult to locate because the two rocks are essentially identical at the contact. For the purposes of field mapping the contact was placed at the appearance of biotite. Preliminary petrographic work suggests that this is reasonable.

East of Hugh Allan Creek the gneiss becomes very platy in the vicinity of the contact with the quartzite. This platiness is indicative of a zone of shear. The biotite schist layer may also be a shear zone. The presence of shear zones suggests that the Miette stratigraphy has slid over the basement gneiss along a zone of décollement. Because the gneiss/quartzite contact now appears gradational, this thrusting presumably predated metamorphism.

The contact between the gneiss and cover rocks on the ridge south of the mouth of Hugh Allan Creek is somewhat different. The thick quartzite layer is absent and biotite schist forms only thin laterally discontinuous layers. Near the contact felsic hornblende gneiss is interlayered with pelite and quartzite.

In the area east of Hugh Allan Creek a complete package of the Hadrynian metasediments is present between the gneiss of Mount Blackman and the Lower Cambrian McNaughton Formation of the Gog Group. The main characteristics of the Hadrynian succession are summarized in Table 23.1.

The quartzite in contact with the gneiss is not a tectonized sliver of Gog as suggested by the earlier interpretation but is, instead, a muscovitic foliated quartzite, some 200 m thick, at the base of the Hadrynian package. It is overlain by the 3-10 m thick layer of black biotite schist (with quartz blebs) which forms a continuous marker. South of Blackman Creek approximately 40 m of quartzite-pebble conglomerate in pelitic matrix intervenes between the quartzite and the black biotite schist.

More than 1000 m of granule conglomerate ("grit"), interbedded with pelite and psammite, overlie the biotite schist. It is in this unit that graded bedding, showing that the sequence is upright, was found in 10 localities south and east of the gneiss.

Only the upper and lower part of the aluminum-silicate-rich pelite unit is well exposed but from cross-sections the thickness can be estimated to be nearly 1000 m.

[1]Department of Geology, University of Calgary

The upper part of the Miette succession emerges from underneath the 170 m thick, basal McNaughton, white quartzite at the south end of the map area. Some 200 m of metasandstone, pelite, quartzite and some marble beds, constituting the Upper Clastic Division (Craw, 1978), overlie the grey marble, pelite and quartzite of the Carbonate Division.

The lithologic succession and the thicknesses of the units are about the same as those recorded by Craw (1978) some 25 km along strike to the southeast. This and the fact that the succession was crossed going down plunge along the trend, strongly suggest that the Miette succession described here is complete and unfaulted even though it is not continously exposed.

Structure

The major structural elements of the area are illustrated by the composite cross-section of Figure 23.2. Data from different ridges have been combined by axial projection to show more clearly the interrelationship of the structural elements.

The major structure is the large overturned anticline with the gneiss of Mount Blackman in its core, surrounded by the unbroken band of the basal-Miette quartzite. North of Mount Blackman the overturned northeast limb is well exposed and the Miette cover is upsidedown, under the gneiss.

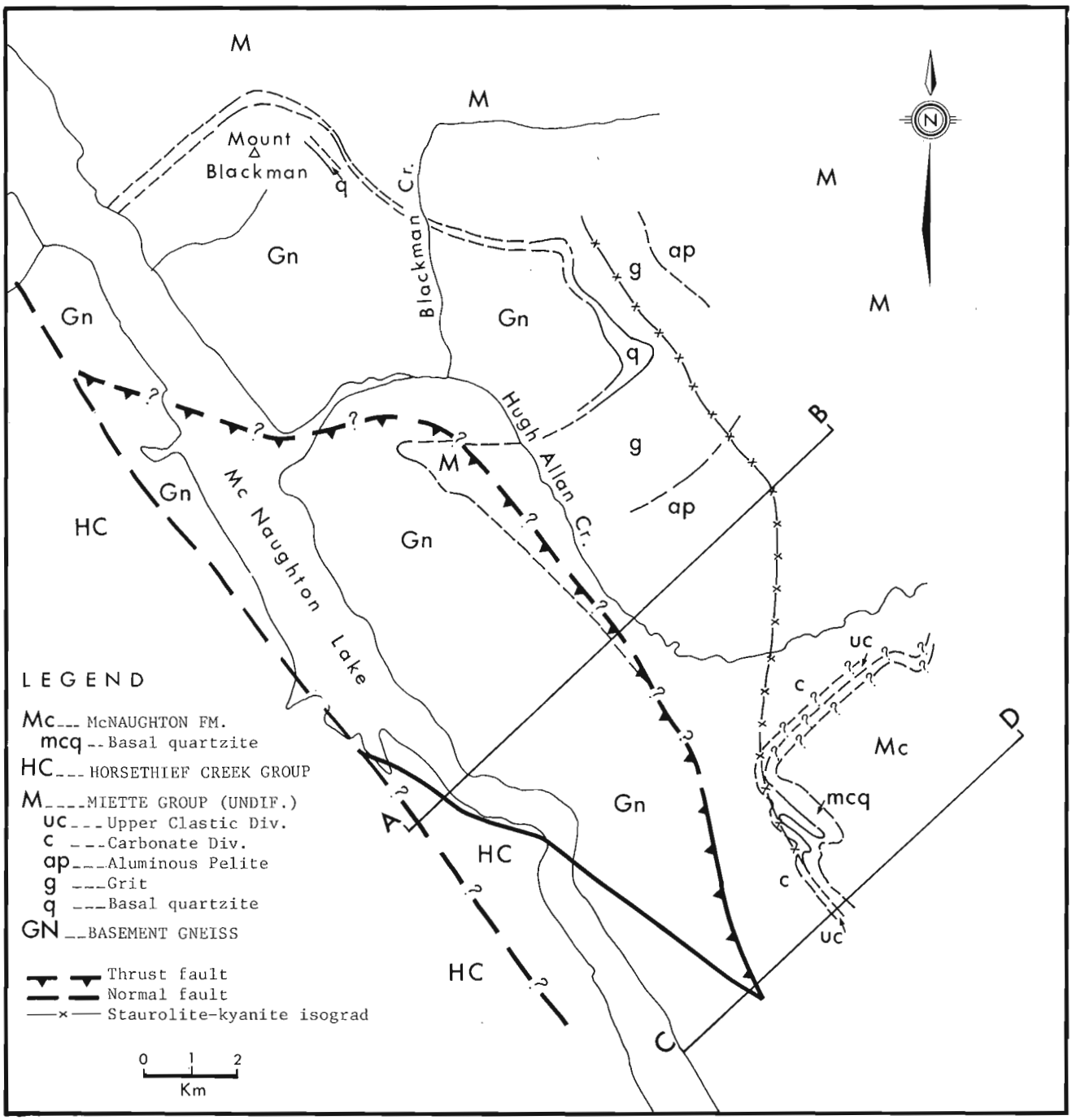

Figure 23.1. *Geology of the Hugh Allan Creek area. Co-ordinates of Mount Blackman are 52°29', 118°42'.*

As the quartzite is traced southward it becomes upright and then wraps over the gneiss which plunges southeastward under the Miette and the Gog. The anticline has a southeastward plunge of 15 to 20° and, at the level of the basal-Miette quartzite, the hinge is sharp and the axial surface dips southwest at about 50°. Mesoscopic folds and crenulations, congruent with the major anticline, are common but on a larger scale the anticline is quite simple. The anticline is flanked on the northeast by a very complex synclinal zone consisting of "bundles" of large mesoscopic folds with wavelengths of 50 to 200 m and with axial planes that are vertical or dip steeply to the northeast.

The mesoscopic folds and crenulations, congruent with the large anticline, fold a pre-existing foliation of biotite, muscovite, and flattened quartz. They also refold small folds to which the early foliation is axial planar. This suggests that formation of the large anticline is not the earliest deformation event; however, no large folds have been found associated with the early mesoscopic structures. A similar situation was described by Craw (1978) for the Mount Dainard area some 25 km to the southeast.

In the migmatized portion of the gneiss folding is very complex with no consistent orientation to either the fold axes or axial planes. Pre-existing foliation is folded, perhaps a result of deformation under very ductile conditions. Whether such folding is first or second phase is not known.

Striated fault-surfaces are present just above the biotite schist at the north end of the map area. The surfaces of many of the quartz blebs within the biotite-schist layer are also striated. These striated surfaces indicate that postmetamorphic movement has occurred along this zone. This movement could conceivably have been a result of flexural slip during the folding of the major anticline.

The contact of the gneiss that forms the ridge south and west of Hugh Allan Creek with the overlying Hadrynian cover, as described earlier, is somewhat different from the contact north and east of Hugh Allan Creek. The gneiss must be juxtaposed against the upper Miette and Gog strata, in the southern portion of the map area, by a fault, perhaps the northern continuation of the Purcell Thrust. One possible fault trace is shown on the map (Fig. 23.1). In that interpretation, the Purcell Thrust places the Hugh Allan Creek gneiss over the large anticline cored by the Mount Blackman gneiss.

The southwestern contact of the Hugh Allan Creek gneiss body is a near-vertical normal fault. Where polished fault surfaces are present their fresh appearance indicates that faulting is postmetamorphic. The fault puts psammites and pelites of the Horsethief Creek Group down against the gneiss. Gouges on the fault surfaces plunge approximately 10° to the east indicating a substantial component of strike-slip motion.

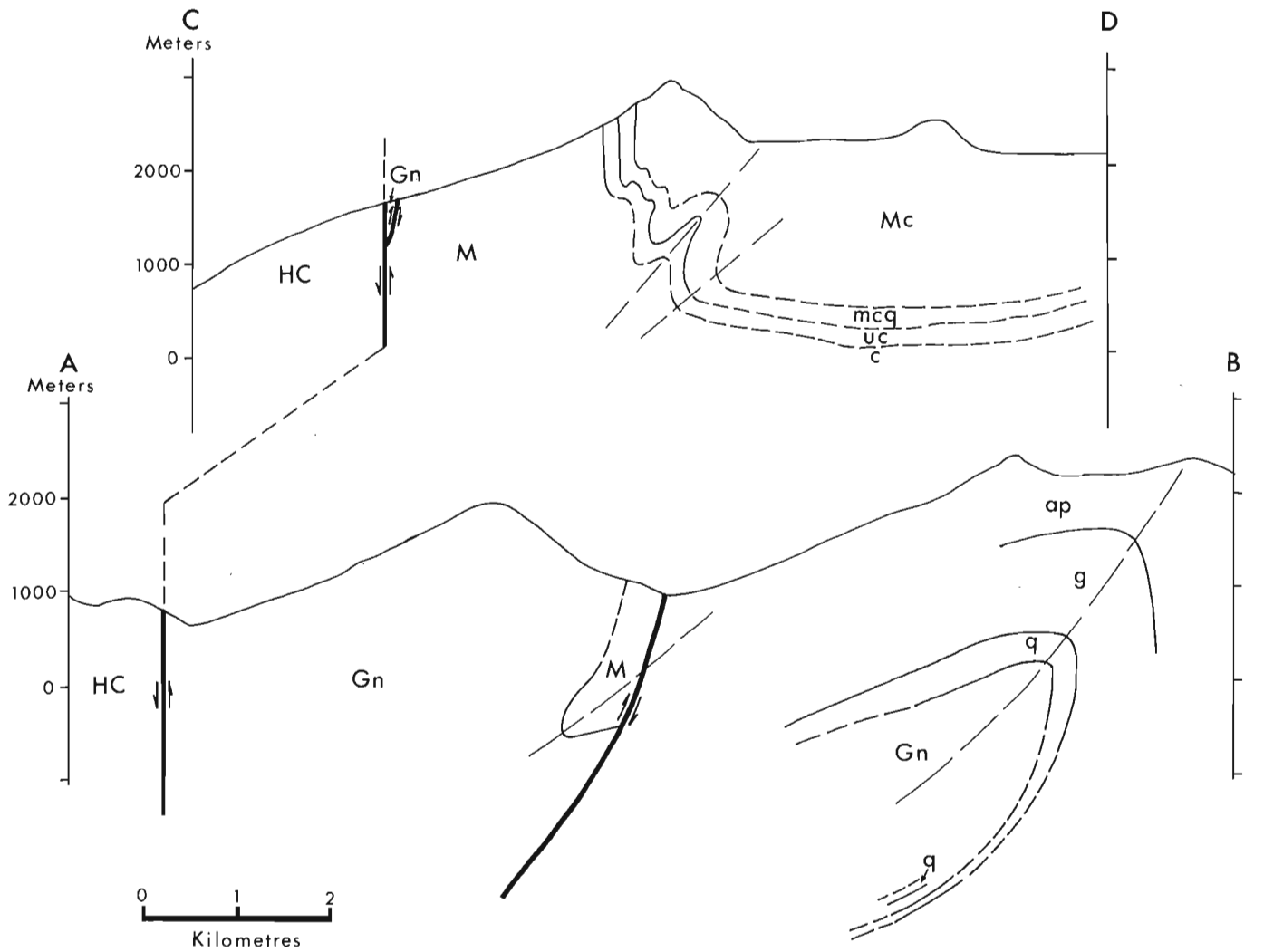

Figure 23.2. Compilation cross-section. Legend same as Figure 23.1.

Table 23.1

Stratigraphy of the Hugh Allan Creek area

Unit	Thickness (in metres)	Description
Gog Group		
McNaughton	570 m	Medium to coarse grained, white quartzite at the base (170 m thick), overlain by quartzite with pelitic interbeds.
Miette Group		
Upper Clastic	220 m	Pelitic schist and fine grained quartzite interbedded. Local lenses of sandy carbonate and granule conglomerate ("grit").
Carbonate	200 m	Grey marble lenses in interbedded pelite and quartzite.
Aluminous Pelite	1000 m	Interbedded pelitic schist and psammite. Grit interbeds near base.
Grit	1000 m	Grit with pelitic interbeds.
Biotite Schist	3-10 m	Black biotite schist with quartz blebs.
Basal Quartzite	250 m	Foliated muscovitic quartzite.
Basement Gneiss	----	Foliated biotite muscovite gneiss, may contain garnet. Contains amphibolite layers.

The western contact is a normal fault (Campbell, 1968). The gneiss exposed on the western shore of McNaughton Lake corresponds more closely to the gneiss east of the lake than to the Malton Gneiss to the west (Morrison, personal communication, 1980). Thus the major normal fault must be west of the lake and hence farther west than shown by Campbell (1968).

Metamorphism

The staurolite-kyanite isograd was located at five places in the map area (see Fig. 23.1). Because the presence of the index minerals is controlled by the bulk composition of the rock as well as by the metamorphic conditions the isograd as shown on the map represents the easternmost appearance of staurolite and kyanite. Consequently the isograd may be located even farther east than shown. Campbell (1968) showed the isograd cutting through the eastern part of the gneiss body; however, the isograd as shown in Figure 23.1 passes to the east of the gneiss. In the northeast part of the map area the isograd is in the lower part of the Miette. Towards the south the isograd cuts upsection and appears at the top of the Miette in the southeast. This suggests that either the Miette strata were not horizontal at the time of metamorphism or that the isograd had an original dip reflecting a dipping isothermal surface.

References

Campbell, R.B.
1968: Canoe River (83 D), British Columbia; Geological Survey of Canada, Map 15-1967.

Chamberlain, V.E., Lambert, R. St. J., and Holland, J.G.
1978: Preliminary subdivisions of the Malton Gneiss Complex, British Columbia; in Current Research, Part A, Geological Survey of Canada, Paper 78-1A, p. 491-492.

Craw, D.
1978: Metamorphism, structure and stratigraphy in the Southern Park Ranges, British Columbia; Canadian Journal Earth Sciences, v. 15, p. 86-98.

Giovanella, C.A.
1967: Structural relationships of the metamorphic rocks along the Rocky Mountain Trench at Canoe River; in Report of Activities, Part A, Geological Survey of Canada, Paper 67-1A, p. 60-61.

Giovanella, C.A.
1968: Structural studies of the metamorphic rocks along the Rocky Mountain Trench at Canoe River, British Columbia; in Report of Activities, Part A, Geological Survey of Canada, Paper 68-1A, p. 27-30.

Price, R.A. and Mountjoy, E.W.
1970: Geologic structure of the Canadian Rocky Mountains between Bow and Athabasca Rivers – a progress report; Geological Association of Canada, Special Paper 6, p. 7-26.

Wheeler, J.O., Campbell, R.B., Reesor, J.E., and Mountjoy, E.W.
1972: Structural style of the southern Canadian Cordillera; Guidebook, XXIV International Geological Congress, Montreal, Quebec, 1972.

24.

GEOLOGY OF PARTS OF WESTERN ASHCROFT MAP AREA, SOUTHWESTERN BRITISH COLUMBIA

Project 800029

J.W.H. Monger
Cordilleran Geology Division, Vancouver

Monger, J.W.H., Geology of parts of western Ashcroft map area, southwestern British Columbia; in Current Research, Part A, Geological Survey of Canada, Paper 81-1A, p. 185-189, 1981.

Abstract

Dominant structures in western Ashcroft map area are 140-150° trending and due north-trending steep faults that involve rocks probably as young as early Oligocene. The Late Pennsylvanian to Late Triassic Cache Creek Group, the eastern one third of which appears to be melange, is partly coeval and probably partly stratigraphically overlain by the Upper Triassic Nicola Group. Oldest continental rocks are sandstone and conglomerate of mid-Cretaceous (Upper Albian-Cenomanian) age, that are possibly older than the continental acidic to basic volcanics of the "Kingsvale-Spences Bridge Group".

Introduction

Project 800029 involves remapping of Ashcroft (92 I) and Hope (92 H) 1:250 000 sheets, which are bounded by latitudes 49° and 51° and longitudes 120° and 122°. The region was mapped formerly on a scale of 4 miles to 1 inch as the Princeton (Rice, 1947), Nicola (Cockfield, 1948) and Ashcroft (Duffell and McTaggart, 1952) map areas; Hope map area was compiled on a scale of 1:250 000 (Monger, 1970). Detailed local and topical studies carried out since, mainly by geologists with the British Columbia Ministry of Energy, Mines and Petroleum Resources and the University of British Columbia, indicated the need for revisions in the regional mapping.

During 1980, the area mainly east of the Fraser River and west and north of the Thompson River as far east as Kamloops Lake was mapped. Rocks of the Cache Creek Group and contiguous units near the settlement of Cache Creek were studied in more detail by Shannon (1981) as part of the project. Earlier detailed work in this area by Church (1975), Grette (1978), Ladd (1978), Travers (1978) and Trettin (1961, 1980) proved to be invaluable. W.R. Danner (University of British Columbia), who for many years has studied the carbonate rocks of the Cache Creek Group, and W.B. Travers (Cornell University), who examined relationships between the Ashcroft Formation and contiguous beds, guided Shannon and the writer on short field trips.

General Structure

The region mapped forms the westernmost part of the Intermontane Belt at these latitudes. It is bounded on the west by the north and northwest striking Fraser fault system, west of which again is the predominantly granitic Coast Plutonic Complex. Steeply dipping faults, parallel and subparallel with those of the Fraser fault system, are the dominant structural features. They are observed or inferred to form most boundaries between rock units, including some that are probably as young as lower Oligocene. The faults have two dominant trends, one at between 140° and 150° and the other due north, with the latter at least locally offsetting the former. The regional strike of bedding, and of schistosity where developed in rocks the late Paleozoic and early Mesozoic rocks, parallels the northwest trending faults, although those faults clearly involve Cretaceous and Early Tertiary strata as well.

Stratigraphic Units

Cache Creek Group

The Cache Creek Group is divisible into western, central and eastern belts, each of different character (Fig. 24.1). The western belt comprises mainly silicified argillite and siltstone, some radiolarian chert and minor limestone. Limestone beds at Pavilion Lake contain Lower Triassic and Upper Triassic conodonts (M. Orchard, personal communication) and Trettin (1980, p. 8) collected mid-Permian fusulinids from this belt, north of the map area. The central belt, the Marble Canyon Formation of Duffell and McTaggart (1952), is dominated by massive carbonate containing mid- and Upper Permian fusulinids, and interbedded and interfolded chert, argillite, tuff and basalt. Although the limestone at Marble Canyon gives an impression of great thickness, bedding is near vertical and the canyon runs more-or-less along strike. The true thickness of the limestone is probably about 300 m, on the same order as that suggested by Trettin (1980) for contiguous rocks in the Marble Range, north of Ashcroft map area. The western contact is either a thrust, shown in Figure 24.1 or an overturned stratigraphic contact, for the Lower Triassic strata of the western belt dip steeply towards topographically higher carbonate of the Marble Canyon Formation at Pavilion Lake. The eastern contact of the central belt is probably a steeply dipping fault, more-or-less parallel with bedding. The writer concurs with the suggestion made by Trettin (1980) from the area to the north, that thrust faulting may be responsible for juxtaposing all or part of the massive carbonate with other units of the Cache Creek Group, and that the thrust was later folded about a mainly 140° trend. The eastern belt, described by Shannon (1981) comprises mélange, basalt, volcaniclastics, gabbro and serpentinite. Limestone blocks in the mélange contain Upper Pennsylvanian and Lower Permian conodonts or fusulinids, and the matrix contains "Permian" and Upper Triassic radiolarians (W.R. Danner, D.L. Jones, M. Orchard, personal communication).

Nicola Group; "Pavilion Beds"

Strata correlated with the Nicola Group (Duffell and McTaggart, 1952; Morrison, 1980) and the "Pavilion beds" (Trettin, 1980) are closely associated with rocks of the Cache Creek Group in, respectively, the eastern and western belts. They comprise predominantly sand-sized intermediate volcaniclastic rocks, local mafic volcanics, distinctive quartz crystal tuff, local argillite and limestone. In many places these rocks are not penetratively deformed, but in a 140°-trending zone that crosses the Thompson River approximately 10 km south-southwest of Ashcroft, the rocks are schistose and comprise mafic and "quartz-eye" sericite schist. In places these rocks are so highly disrupted and broken that they resemble the mélange of the eastern belt of the Cache Creek Group. Middle Norian (Travers, 1978) and Karnian (Grette, 1978) fossils have been obtained from rocks associated with the eastern belt, and Middle or Late Triassic fossils from the western belt (Trettin, 1980).

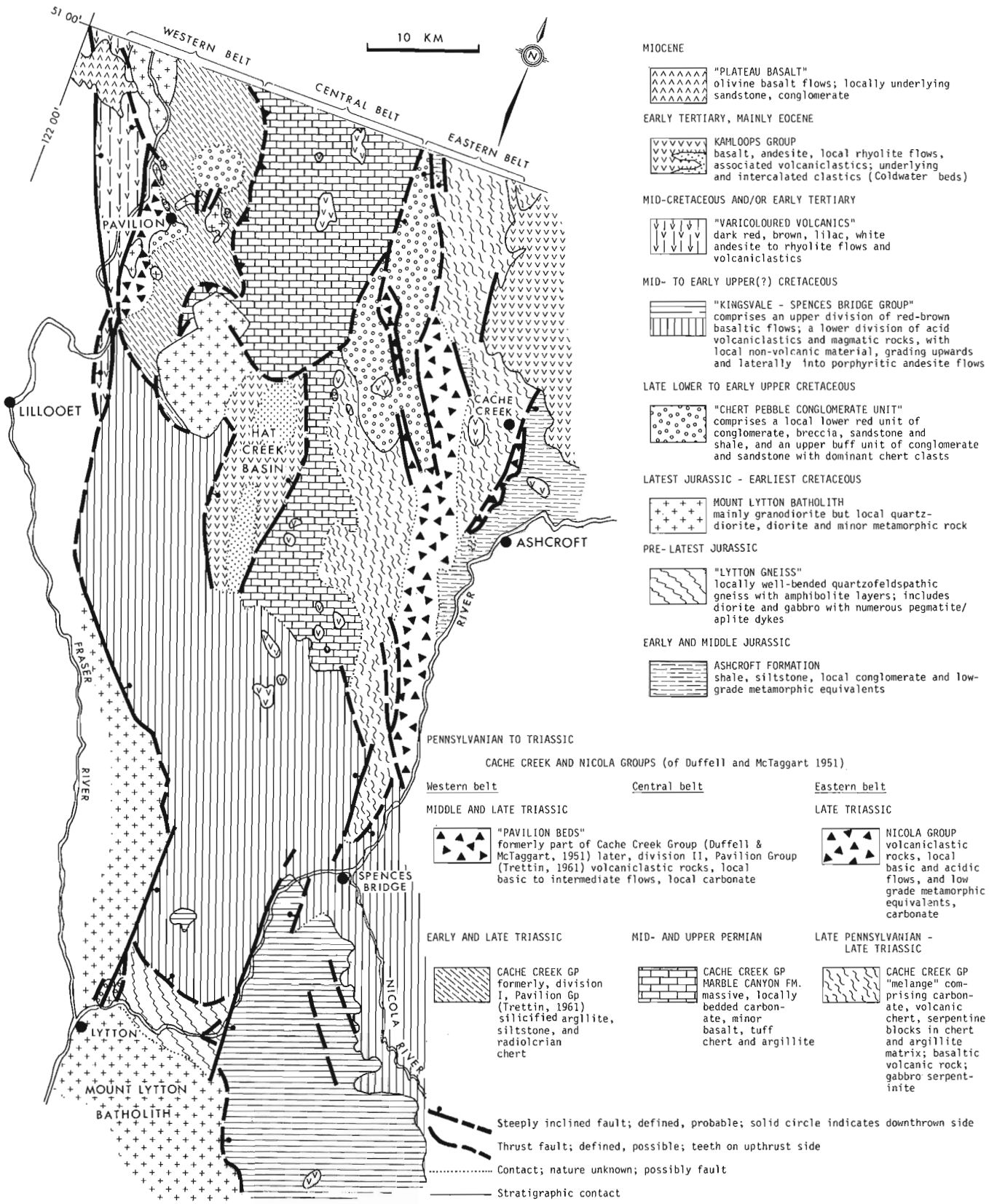

Figure 24.1. *Geological sketch map of the western part of Ashcroft map area, southwestern British Columbia.*

In most cases this sequence is in probable fault contact with Cache Creek strata. However, the presence in it of fragments of radiolarian chert near the contact with the Cache Creek Group, near Cache Creek, suggests that the contact is a faulted stratigraphic contact. The rocks are clearly stratigraphically overlain by Lower Jurassic strata of the Ashcroft Formation (Grette, 1978; Travers, 1978).

Rocks similar to the Nicola Group and Pavilion beds are associated with the Cache Creek Group for much of the length of the Cordillera. In northern British Columbia, near Cry Lake, such rocks have been called the "Kutcho sequence" (Monger and Thorstad, 1978), and are associated with copper-zinc sulphide mineralization. In central British Columbia, at Takla Lake, comparable schistose mafic and acidic rocks are known as the Sitlika assemblage (Paterson, 1974).

"Lytton Gneiss"

Foliated quartzofeldspathic gneiss with conformable amphibolite layers, together with massive "quartzite", massive amphibolite and gabbroic intrusions are exposed east of Lytton along the Thompson River valley and locally about 15 km north of Lytton along the Fraser River valley. These rocks are discordantly cut by the Mount Lytton batholith and by dykes that probably are feeders to the "Kingsvale-Spences Bridge" volcanics. In the steep valley walls on the north side of the Thompson River, northeast of Lytton, sedimentary rocks of the lower part of the "Kingsvale-Spences Bridge Group" lie above the gneissic rocks, although the contact between the two is a fault that at least locally dips steeply northwards. Bedding in the "Kingsvale-Spences Bridge" sediments is roughly conformable with that of layering of the foliated gneissic part of the "Lytton gneiss".

Mount Lytton Batholith and Related (?) Intrusions

Granodiorite, local diorite and gabbro of the Mount Lytton gneiss is mainly in fault contact with other units. The probable southern extension of the Mount Lytton Batholith, known as the Eagle granodiorite, is dated at about 104 Ma (Roddick and Farrar, 1972) although Geological Survey dates are as old as 143 Ma (Leech et al., 1963). The possibly equivalent, lithologically similar, Mount Martley stock, near Pavilion, is dated at 141 Ma (Preto et al., 1979). Both the Mount Lytton batholith and Mount Martley stock locally underlie late Lower and early Upper Cretaceous continental clastic rocks and carry the characteristic red staining associated with these sedimentary rocks. The Mount Martley stock produced foliation in enclosing rocks of the Cache Creek Group.

"Chert-pebble Conglomerate"

The unit is of considerable regional significance, as it probably represents the earliest known continental deposits in the region. It consists, typically, of two units. The lower is generally red-stained and comprises conglomerate and breccia, whose clasts strongly reflect local older lithologies, together with sandstone and mudstone. Where this unit lies on older rocks, as near Lytton and west of Pavilion Lake, the underlying unit is strongly red-stained. The upper unit is typically buff-weathering sandstone and chert pebble conglomerate and is probably more voluminous than the lower one. From preliminary observations of these rocks along Hat Creek road, D.G.F. Long (personal communication) suggested that the lower unit is an arid-region(?) alluvial fan deposit, with an easterly source; whereas the upper unit is interpreted as a braided stream deposit with a northern and (?) western source (personal communication).

Near Lytton, the lower unit contains Albian flora (Duffell and McTaggart, 1952). Preliminary investigation of plant material collected by Shannon (1981) from the Hat Creek beds was identified independently by W.S. Hopkins (G.S.C.) and G.E. Rouse (University of British Columbia) as upper Albian or Cenomanian.

This unit is probably correlative with rocks exposed north of Kamloops Lake (unit 7 of Cockfield, 1948) and with the Pasayten Group in Manning Park area (Coates, 1974).

"Kingsvale-Spences Bridge group"

The Kingsvale and Spences Bridge groups of Duffell and McTaggart (1952) appear to be a single stratigraphic package. Until nomenclature is revised to take this into account, the informal term "Kingsvale-Spences Bridge group" is used. It is the most extensive unit in the area mapped, and comprises subaerial flows and volcaniclastics that show a general change upwards from acidic to basic composition and contains a locally abundant nonvolcanic clastic component near the base.

Most contacts of this group with other units are faults, although the basal contact, developed apparently on rough topography, is exposed about 25 km south of Ashcroft near Martel on the Trans-Canada Highway, and can be approached closely, but is not exposed, at the southern limit of exposure of the Marble Canyon Formation. As mentioned above, the largely nonvolcanic "Kingsvale-Spences Bridge group" may overlie the "Lytton gneiss" stratigraphically, but where seen the contact is a fault. Although the relationship between the "Kingsvale-Spences Bridge group" and the "chert pebble conglomerate unit" is not known, some nonvolcanic sandstones in the lowermost "Kingsvale-Spences Bridge group" northwest of Lytton superficially resemble sandstone in the "chert pebble conglomerate", which therefore may be older and gradational upwards into the "Kingsvale-Spences Bridge group".

The lower part of the "Kingsvale-Spences Bridge group" is dominantly buff-olive green volcaniclastic sandstone, tuff, local breccia and shale with notable massive ignimbrite members and local rhyolite intrusions and flows. In the upper part of this section, pale green to grey, intermediate feldspar porphyry sills and flows are common, particularly west of Thompson River. Uppermost are red, brown and grey pyroxene andesites. The upper part of the group, forming most of the Kingsvale Group of Duffell and McTaggart (1952), is red brown, mainly aphanitic but locally coarsely amygdaloidal basalt. This upper unit is juxtaposed with the lower unit, across a north-trending fault zone along the Thompson River valley south of Spences Bridge and which has an east-side downthrow of at least 1200 m.

On the basis of plant fossils the "Kingsvale-Spences Bridge group" is late Lower Cretaceous, according to Duffell and McTaggart (1952). They assigned their lower unit (Spences Bridge Group) to the Aptian, and their upper unit (Kingsvale Group) to the Albian. The writer re-examined the localities from which these plant fossils were obtained and found they apparently are in the same rock unit. Church (1975, 1979) obtained from Spences Bridge volcanics an age of 91.6 Ma, which is early Late Cretaceous or Turonian, on the revised time scale of Armstrong (1978), Preto et al. (1979) obtained a whole rock Rb-Sr isochron of 112 Ma (that is late Early Cretaceous or Albian) from southwest of the map area near Princeton, British Columbia. Currently, plant material collected from the "Kingsvale-Spences Bridge group" is being re-examined by W.S. Hopkins.

"Varicoloured Volcanics"

A belt of red, brown, lilac and white volcanic rocks, ranging from basalt to rhyolite, is exposed along the Fraser River, in the northwestern part of the map area. These rocks were included in the Spences Bridge group by Duffell and McTaggart (1952), although Trettin (1961) separated some of them out as his Fountain Creek and Ward Creek assemblages of post-mid Early Cretaceous and pre-Oligocene age. Some red and grey volcaniclastics were reported by Trettin (1961) to contain a post-Aptian, probably Albian flora and Trettin correlated these rocks with the Kingsvale Group in the Nicola River area. Other, mainly volcanic, rocks can be traced more-or-less continuously to the north-northwest into Bonaparte and Taseko Lakes map area, where Tipper (Campbell and Tipper, 1971) obtained an early Oligocene fauna. Thus, two rock units with superficially similar, strong coloration may be present. That rocks apparently as young as early Oligocene are involved in strong deformation along the Fraser River fault zone is regionally significant, as it shows that there were very late, strong moments on this fault zone.

Kamloops Group

These rocks were examined in the area northeast of Cache Creek and in Hat Creek valley, where they have been mapped in detail by Church (1975). They comprise mainly dark andesite and local rhyolite flows, with abundant and characteristic breccia and finer volcaniclastics, which near Hat Creek overlie a thick section of coal-bearing sedimentary rocks. Church obtained ages of 51 Ma (Eocene) from these rocks in Hat Creek area.

The Kamloops Group lies unconformably on the Cache Creek Group but in places is faulted against it.

Miocene

Brown weathering, olivine basalt flows are exposed in the northwestern part of the map area, where they overlie semiconsolidated breccia and sandstone tentatively correlated with the Deadman Creek Formation of Campbell and Tipper (1971). Both sedimentary and volcanic units clearly lie across, and are unaffected by, the faults that displaced the "varicoloured volcanics".

Conclusions

1. The Cache Creek Group appears to be stratigraphically overlain by rocks that have been correlated with the Nicola Group by Duffell and McTaggart, 1952, and Morrison, 1980. If this correlation is correct, then the Cache Creek Group, with its exotic Permian faunas (Monger and Ross, 1971) was emplaced against the so-called Cache Creek Group at Kamloops, with its very different lithology and Permian faunas, by the end of Triassic time.
2. The fact that parts of the Cache Creek Group are coeval with parts of the Nicola Group supports the idea, put forward by several workers, that the Cache Creek Group represents an early Mesozoic subduction complex and the Nicola Group its corresponding volcanic arc.
3. Oldest continental rocks are probably the mid-Cretaceous (Upper Albian to Cenomanian) chert pebble conglomerate, which probably correlate with the Pasayten Group farther south.
4. Dominant structures in the area are steep faults trending either 140° to 150° or due north, which affect rock units probably as young as early Oligocene.

References

Armstrong, R.L.
1978: Pre-Cenozoic Phanerozoic time-scale-computer file of critical dates and consequences of new and in-progress decay-constant revisions; in Contributions to the geologic time scale, G.V. Cohee, M.F. Glaessner and H.D. Hedberg, editors, studies in geology No. 6, American Association of Petroleum Geologists, p. 73-91.

Campbell, R.B. and Tipper, H.W.
1971: Geology of Bonaparte Lake map-area, British Columbia; Geological Survey of Canada, Memoir 363, 100 p.

Church, B.N.
1975: Geology of the Hat Creek coal basin (93I, 13E); in Geology in British Columbia; British Columbia Ministry of Mines and Petroleum Resources, p. G99-G118.

Church, B.N., Matheson, A., and Hora, Z.D.
1979: Combustion metamorphism in the Hat Creek area, British Columbia; Canadian Journal of Earth Sciences, v. 16, p. 1882-1887.

Coates, J.A.
1974: Geology of the Manning Park area, British Columbia; Geological Survey of Canada, Bulletin 238, 117 p.

Cockfield, W.E.
1948: Geology and mineral deposits of Nicola map-area, British Columbia; Geological Survey of Canada, Memoir 249, 164 p.

Duffell, S. and McTaggart, K.C.
1952: Ashcroft map-area, British Columbia; Geological Survey of Canada, Memoir 262, 122 p.

Grette, J.F.
1978: Cache Creek and Nicola Group near Ashcroft, British Columbia; University of British Columbia, unpublished M.Sc. thesis, 88 p.

Ladd, J.H.
1978: Mesozoic overthrusting of oceanic crust in south-central British Columbia; Cornell University, unpublished M.Sc. thesis, 96 p.

Leech, G.B., Lowdon, J.A., Stockwell, C.H., and Wanless, R.K.
1963: Age determinations and geological studies; Geological Survey of Canada, Paper 63-17, 140 p.

Monger, J.W.H.
1970: Hope map-area (west half), British Columbia; Geological Survey of Canada, Paper 69-47, 75 p.

Monger, J.W.H. and Ross, C.A.
1971: Distribution of fusulinaceous in the western Canadian Cordillera; Canadian Journal of Earth Sciences, v. 8, p. 259-278.

Monger, J.W.H. and Thorstad, L.
1978: Lower Mesozoic stratigraphy, Cry Lake and Spatzizi map-areas, British Columbia; in Current Research, Part A, Geological Survey of Canada, Paper 78-1A, p. 21-24.

Morrison, G.W.
1980: Stratigraphic control of Cu-Fe skarn ore distribution and genesis at Craigmont, British Columbia; Canadian Mining and Metallurgical Bulletin, v. 73, no. 820, p. 109-123.

Paterson, I.A.
1974: Geology of the Cache Creek Group and Mesozoic rocks at the northern end of the Stuart Lake belt, British Columbia; in Report of Activities, Part B, Geological Survey of Canada, Paper 74-1B, p. 31-42.

Preto, V.A., Osatenko, M.J., McMillan, W.J., and Armstrong, R.L.
1979: Isotopic dates and strontium isotopic ratios for plutonic and volcanic rocks in the Quesnel Trough and Nicola Belt, south-central British Columbia; Canadian Journal of Earth Sciences, v. 16, p. 1658-1672.

Roddick, J.C. and Farrar, E.
1972: Potassium-argon ages of the Eagle Granodiorite, southern British Columbia; Canadian Journal of Earth Sciences, v. 9, p. 596-599.

Rice, H.M.A.
1947: Geology and mineral deposits of the Princeton map-area, British Columbia; Geological Survey of Canada, Memoir 243, 136 p.

Shannon, K.R.
1981: The Cache Creek Group and contiguous rocks near Cache Creek, British Columbia; in Current Research, Part A, Geological Survey of Canada, Paper 81-1A, report 29.

Travers, W.B.
1961: Overturned Nicola Group and Ashcroft strata and their relation to the Cache Creek Group, south-western Intermontane Belt, British Columbia; Canadian Journal of Earth Sciences, v. 15, p. 99-116.

Trettin, H.P.
1961: Geology of the Fraser River valley between Lillooet and Big Bar Creek; British Columbia Department of Mines and Petroleum Resources, Bulletin 44, 109 p.

1980: Permian rocks of the Cache Creek Group in the Marble Range, Clinton area, British Columbia; Geological Survey of Canada, Paper 79-17, 17 p.

25.

LAKE SEDIMENT CORING ALONG SMITH SOUND, ELLESMERE ISLAND AND GREENLAND

Project 750063

W. Blake, Jr.
Terrain Sciences Division

Blake, W. Jr., Lake sediment coring along Smith Sound, Ellesmere Island and Greenland; in Current Research, Part A, Geological Survey of Canada, Paper 81-1A, p. 191-200, 1981.

Abstract

During the 1979 and 1980 field seasons, cores of bottom sediments have been recovered from six lakes on the Ellesmere Island side of Smith Sound and from three lakes in Inglefield Land, northwestern Greenland. Radiocarbon age determinations on basal organic material from a lake at 390 m on Pim Island and from a lake at 295 m above Ekblaw Glacier, innermost Baird Inlet, indicate that both areas were free of glacier ice by 9000 years ago. The basal moss-rich sediment from a pond at 300 m in a moraine above Baird Inlet is slightly younger, perhaps because dead ice may have persisted at that locality.

Introduction

Studies of lake sediments in the Canadian Arctic Archipelago are few and far between, especially those carried out with the specific purpose of establishing absolute chronologies by radiocarbon dating or other means. The scattered investigations that have been undertaken over this vast area have all been done during the last two decades. The earliest attempts at recovering lake sediment samples for ^{14}C age determinations were those in northern Ellesmere Island of G. Hattersley-Smith (Defence Research Board) and staff of the Smithsonian Institution (Long and Mielke, 1967; Hattersley-Smith, 1969; Mielke and Long, 1969). Caflisch (1972) cored lakes, including an ice-dammed lake, on Axel Heiberg Island, and Barnett (1977) cored Generator Lake, an ice-dammed lake in central Baffin Island. More recently, J.C. Ritchie and R.J. Mott have, independently, cored organic lake sediments on Banks Island, and ^{14}C ages have been obtained from five sites (see Vincent, 1980). Bradley and England (1977) have recovered four cores from a lake near the Mer de Glace Agassiz in northeastern Ellesmere Island, and Davis (1978, 1980a, b) has carried out an extensive lake coring program in southern Cumberland Peninsula, Baffin Island.

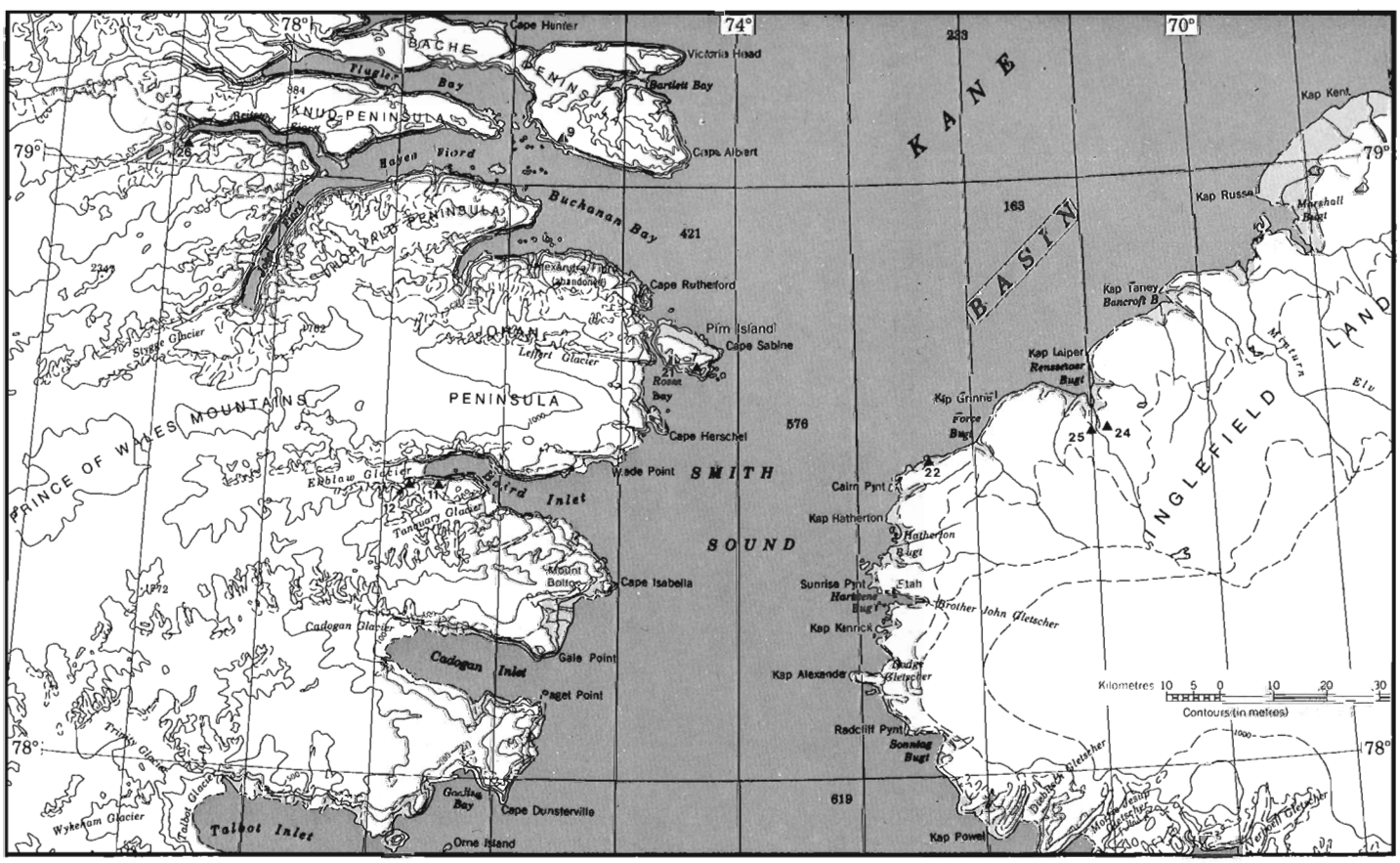

Figure 25.1. *Location map of eastern Ellesmere Island and northwestern Greenland showing lakes cored. Numbers beside triangles correspond to sites in Table 25.1. Contours, spot elevations, and depths are in metres.*

Blake (1978) described the technique of recovering cores of sediments from shallow ponds that freeze to the bottom each winter on Cape Herschel peninsula, eastern Ellesmere Island (Fig. 25.1). This work, which was continued successfully in 1979 and 1980, was carried out primarily to obtain data bearing on the rate of Holocene emergence, and nearly all the ponds cored are situated below the Holocene marine limit, which is at approximately 90 m a.s.l. on the north side of Cape Herschel. Now the emphasis has shifted to larger and deeper lakes, utilizing conventional coring equipment, i.e., a modified Livingstone corer. The present report is a preliminary account of the lake coring program, the main purpose of which is to obtain chronological data bearing on glacial history. It is also hoped that study of the cores will provide information on changes in climate through time by means of analysis of the sediments themselves as well as by investigations of the contained pollen, diatoms, and plant macrofossils.

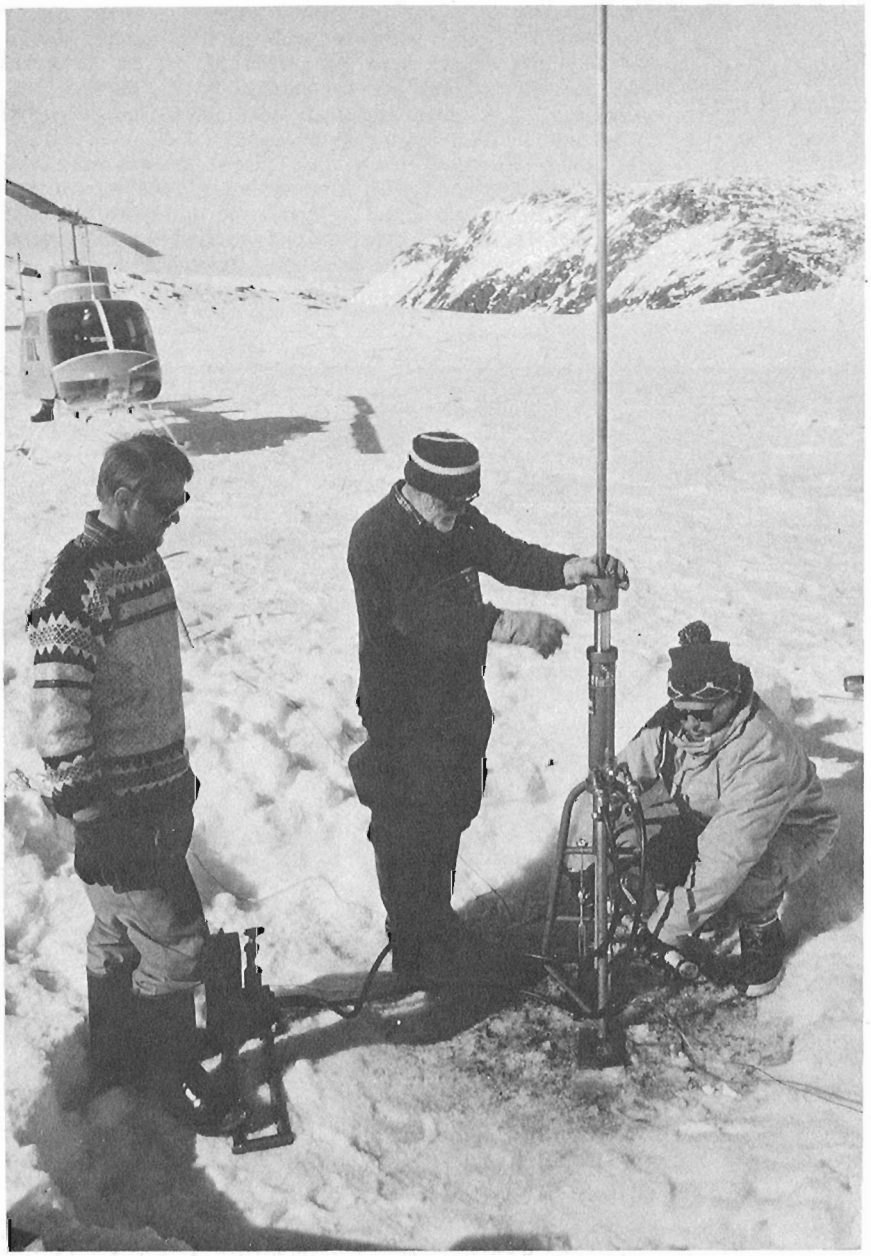

Figure 25.2. *Detail of the hydraulic unit and the foot-operated pump and reservoir used for jacking the plastic coring tubes into the lake sediments. View northwest toward the highest part of Pim Island from lake no. 7 at 390 m. June 12, 1980. GSC 202823-H*

Coring was carried out in June, between the 12th and the 19th in 1979 and between the 3rd and the 16th in 1980. By that time air temperatures were close to 0°C and yet the intact ice cover on the lakes provided a stable platform to operate from. Another advantage to coring at this time of year is that the bays and fiords along the coast are still frozen. The presence of the ice permits the helicopter, necessary to reach the coring sites, to be equipped with skids rather than floats, thus allowing faster travel and heavier loads.

Methods

Three or four people participated in the coring. The first trip to each lake was to transport personnel, the second trip was to bring in the bulk of the equipment. On most occasions the equipment was transported in a cargo net, but in 1980 the Bell 206B helicopter (supplied by Okanagan Helicopters, Ltd., through the Polar Continental Shelf Project) could be converted easily into an ambulance. In this configuration the front left seat folds to the side towards the pilot, permitting the storage of coring tubes (2.4 m long), rods, and casing lengthwise inside. Elimination of the cargo net on long distance flights, such as to Inglefield Land or to the head of Beitstad Fiord (Fig. 25.1), simplified transport and saved flying time, especially in windy conditions.

In 1979 a 6 inch (15 cm) diameter and 41 inch (105 cm) long hand auger (manufactured by K.J. Eriksson's Knivfabrik, Mora, Sweden) was used for drilling through the ice. This tool, designed primarily for use as an aid to ice fishing in more southerly latitudes, worked well on lakes where the ice was of the order of 150 cm thick. Once the ice thickness exceeded 150 cm, it proved difficult to continue augering because of the accumulation of chips in the hole; the auger is flighted only for the first 50 cm of its length, and the extension rods are not flighted. The problem was solved by utilizing an empty plastic coring tube equipped with a cutting edge and a core retriever on the lower end, a coring head and extension rods on the top. The tube was jammed into the hole and the ice chips were forced inside where they were held by the retriever, then the head was removed, the chips were emptied out, and the process was repeated until the hole was cleared, after which augering could proceed. In this way it proved possible to core through more than 3 m of ice at the high level lake on Pim Island.

In 1980, in addition to the hand auger, a power-driven 8 inch (20 cm) diameter auger (Model 51, manufactured by General Equipment Co., Owatonna, Minnesota) was tried. Attachments included a 48 in (122 cm) long auger, flighted for 46 inches (117 cm) of its length, two flighted extensions, each 36 inches (91 cm) long, and a non-flighted extension of the same length. A few holes were drilled successfully with this unit, most of them at the lake with the thickest ice at ca. 390 m elevation on Pim Island (Locality 7 in Fig. 25.1). However, difficulties were encountered with both the cutting edge and with the operation of the

power unit itself; the latter ultimately refused to start despite all efforts at repair. For the rest of the 1980 season most holes were drilled with the same 6 inch (15 cm) diameter hand auger that had been used in 1979.

Although complete recovery of the basal organic material in each lake sampled in 1979 was achieved, it had not proved possible to penetrate more than a few centimetres into the underlying inorganic sediment. For this reason a hydraulic unit to aid in driving down the coring tubes was employed in 1980. The device used, a Portasampler Model DR-2000 (manufactured by Soiltest, Inc., Evanston, Illinois), is made up of two components (Fig. 25.2): (1) a hydraulic cylinder mounted on a tripod, and (2) a foot-operated pump and reservoir which are connected to the cylinder by rubber hoses (these can be disconnected from the cylinder for transport). The complete unit weighs 45 kg, stands about 120 cm high, and the piston has a play of 30 cm. Direction of movement of the piston within the cylinder is controlled by a valve. The hollow piston, which is clamped onto the rods attached to the coring tube by means of four large bolts, can accommodate rods up to 3.5 cm in diameter; those used were a magnesium/zirconium alloy 1.5 m long and 2.7 cm in diameter.

The hydraulic unit, which was anchored to the underside of the ice by means of two deadmen attached to opposite sides of its frame by 3 mm steel cables, worked well. The use of this equipment saved a great deal of effort and allowed somewhat deeper penetration into the inorganic sediments, although lower suites of organic deposits (if, in fact, such materials exist) were not reached. Perhaps the rods utilized need to be stronger, for on a few occasions the casing broke (or became cross-threaded at the joints) as a result of the pressure exerted by bending of the rods as the corer was jacked downward.

Most of the core tubing was 8 foot (2.4 m)-long cellulose acetate butyrate tubing having an outside diameter (O.D.) of 2 7/8 inches (7.3 cm) and an inside diameter (I.D.) of 2 5/8 inches (6.7 cm). In 1979 some slightly smaller diameter tubing also was tried – O.D. 2 1/2 inches (6.4 cm), I.D. 2 1/4 inches (5.7 cm). The advantage of using clear plastic tubing is that it is not necessary to extrude a core in the field in order to see what has been obtained; in fact extrusion would not have been possible in many cases because of the watery nature of the uppermost organic sediments as well as the lack of cohesiveness in sand.

For casing ABS plastic drainpipe was used, cut into 6 foot (1.8 m) lengths. In 1979 the casing was 3 inches (7.6 cm) I.D., but as this was too small to use with the larger diameter plastic core tubes, in 1980 the next size larger was tried. The 4 inch (10.2 cm) I.D. casing could still be accommodated in the hole drilled with the 6 inch (15 cm) auger, together with the cables necessary to anchor the hydraulic tripod.

Results

Two of four lakes cored in 1979 were revisited in 1980 to obtain new cores, and in addition five other lakes were cored during the second season. The locations of the lakes are indicated in Figure 25.1, and details of snow thickness, ice thickness, water depth, and maximum amount of sediment recovered are summarized in Table 25.1. With the exception of the sites on Bache Peninsula (No. 9) and near Kap Inglefield (No. 22), coring has been restricted to areas underlain by granite or gneiss to avoid the 'hard water effect' characteristic of lakes on carbonate terrane.

A great variety of sediments has been encountered in the lakes, and the thickness of organic sediment has proved to be equally variable. For example, at the high level lake (No. 7) on Pim Island only 50 to 60 cm of gyttja and moss was obtained above inorganic material, but in the lower lake (No. 21) 179 cm of organic-bearing sediment was recovered above grey sand and silt. Concentrations of mosses occur at

Table 25.1

Data on lake coring, Smith Sound

	Year	Baird Inlet		Pim Island		Bache Peninsula	Beitstad Fiord	Kap Inglefield	Rensselaer Bugt	
Lake/pond designation (Fig. 25.1)		11	12	7	21	9	26	22	24	25
Approximate elevation m a.s.l.*		300	295	390	260	415	200	250	220	220
Maximum snow thickness at coring sites (cm)	1979	36	40	< 25		40				
	1980	70		32	>20		25	25	30	30
Maximum ice thickness at coring sites (cm)	1979	89	101	304		143				
	1980	91		290	220		140	165	200	190
Depth to sediment/water interface from ice surface (m)	1979	2.7	15.6	10.9						
	1980	2.6		8.1	9.8	6.3	12.8	3.95	2.9	8.0
Number of coring drives attempted	1979	4	3	12		4				
	1980	5		7	2		1	1	1	2
Maximum amount of sediment recovered (cm)	1979	122	95	80		84				
	1980	165		85	255		64	132	19**	209
Sample designations	1979	BS-79-45	BS-79-47	BS-79-27		BS-79-38				
	1980	BS-80-17		BS-80-16	BS-80-21		BS-80-46	BS-80-18	BS-80-24	BS-80-25

* Altimeter determinations, rounded off to the nearest 5 m. Most elevations are based on more than one reading (helicopter traverses), but are uncorrected for temperature or pressure changes.

** Only slight penetration achieved, as sediments were frozen at shallow depth.

Table 25.2

Radiocarbon age determinations, basal organic sediment

Location	Lake number (Fig. 1, Table 1)	Sample No. of core	Depth below sediment/water interface (cm)	Laboratory dating no.	Uncorrected age[1]	$\delta^{13}C$	Corrected age[1]	Organic carbon content (%)[2]	Inorganic carbon content (%)[2]	Dry sample weight (g)	Gas yield, CO_2 (cm)	Counter (L)	Pressure (atm)	Counting time (days)	Comments
Southeastern Pim Island	7	BS-79-27 Core 2	45-50	GSC-2934	9060 ± 190	-30.8	8970 ± 190	25.38	-	5.0	6.1	2	2	4	Only moss utilized for dating.[3]
	7	BS-79-27 Core 12	50-53	GSC-3042	8600 ± 90	-26.1	8580 ± 90	5.44	0.54	34.1	25.2	2	2	3	Basal gyttja – moss (much less common here than in Core 2) was not utilized.[4]
Inner south side of Baird Inlet	11	BS-79-45 Core 2	98-102	GSC-3009	8530 ± 170	-24.3	8540 ± 170	6.00	1.36	14.8	7.5	2	2	3	Moss-rich peaty sediment.
Above Ekblaw Glacier	12	BS-79-47 Core 3	46-51	GSC-3051	9070 ± 160	-31.2	8970 ± 160	3.85	0.43	24.7	13.4	2	2	4	Laminated sediment.[4]

[1] All age determinations from the Radiocarbon Dating Laboratory, Geological Survey of Canada, are based on a ^{14}C half-life of 5568 ± 30 years and 0.95 of the activity of the NBS oxalic acid standard. Ages are quoted in conventional radiocarbon years before present (B.P.) where 'present' is taken to be 1950. All finite age determinations from this laboratory are based on the 2σ criterion; i.e., there is a 95% probability that the correct age in conventional radiocarbon years lies within the stated limits of error. $^{13}C/^{12}C$ ratios were determined at the Department of Earth Sciences, University of Waterloo, under the direction of Professor P. Fritz and R.J. Drimmie (DSS contract OSU79-0045) and by Waterloo Isotope Analysts, Inc. (R.J. Drimmie; DSS contract OSQ80-00018).

[2] The carbon determinations were carried out by W.E. Podolak on a Leco IR12 carbon determinator. Two separate runs were made for each sample, and each run is the average of 2 or 3 determinations. The first run is to determine total carbon on the untreated sample; the second run is on a portion of the original sample which has been digested in 10% HCl and dried – this gives the amount of organic carbon. Inorganic carbon content is the difference between these two values. For GSC-2934 the value obtained for total carbon was 25.42; i.e., essentially no inorganic carbon is present.

[3] The moss at the base of the cores from Pim Island has proved to be difficult to identify but is a member of the Amblystegiaceae (J.A. Janssens, personal communication, 1980). The basal organic material in the Baird Inlet cores contains **Drepanocladus lycopodioides** var. **brevifolius**, whereas the surface of the sediment today is characterized by **Drepanocladus exannulatus** (both determinations by J.A. Janssens; unpublished Bryological Reports JJ 409b, -410b, -411, and -412, Boreal Institute, University of Alberta).

[4] GSC-3042 is the only sample of the four which was not mixed with dead gas for counting. NaOH leach omitted in the pretreatment of GSC-3042 and -3051.

various horizons in a number of cores, and such concentrations appear to be especially prevalent near or at the base of a given organic sequence. Similar basal moss layers have been observed by Funder (1978) in two of five lakes that he sampled in central East Greenland, and data on mosses in lake sediment cores from southernmost Greenland and from Peary Land are given in Fredskild et al. (1975) and Fredskild (1977).

Radiocarbon age determinations on basal organic material are now available for three of the lakes along the western side of Smith Sound, as summarized in Table 25.2. The results indicate that the lake basin at ca. 390 m in the southern part of Pim Island was ice free by approximately 9000 years ago, for the basal moss in one of the cores is 8970 ± 190 years old (GSC-2934). This lake (No. 7), situated in a rock basin with abundant evidence of scouring by south-flowing ice (cf. Blake, 1977), is one of the highest on the island (Fig. 25.3); within 1.5 km to the east-northeast is a patch of dead ice at the head of a col, and 2 km to the northwest is a small (and presumably thin) ice cap which is in a lee position relative to moisture-laden southerly winds blowing across the highest part of the Pim Island plateau. The dimensions of this carapace ice cap 9000 years ago are unknown. Dating the basal organic sediment from the lake (No. 21) at ca. 260 m, together with future coring and dating of other lakes on Pim Island, should make it possible to define the glacier boundaries in early Holocene time more precisely.

Equally interesting to the results from Pim Island is the age of the basal organic sediment (8970 ± 160 years; GSC-3051) from a rock basin lake (No. 12) above Ekblaw Glacier, some 3 km west of the head of Baird Inlet and 50 km west of Cape Herschel (Fig. 25.4). A somewhat younger age than that obtained for the basal moss from Pim Island was expected, since the lake (elevation 295 m) occupies a deep basin excavated by glacier ice in the middle of a rock bastion surrounded by valley glaciers. The rock surfaces 40 m and more above the level of the lake show unmistakable signs of overriding by ice (Fig. 25.5). Thinning of an enlarged Ekblaw Glacier apparently proceeded rapidly enough that organic accumulation could commence at approximately the same time as it did at the higher and much more exposed Pim Island site. Today the south-facing ledges above the rock basin lake are characterized by rather lush vegetation for this latitude, including **Empetrum nigrum** and **Vaccinium uliginosum** in addition to the more widespread **Cassiope tetragona.** The changes in vegetation from the outer coast (Pim Island and Cape Herschel, where the first two plants do not occur) to the innermost fiord areas (Baird Inlet and Beitstad Fiord) mirror those reported long ago from Svalbard (Elton, 1925; Summerhayes and Elton, 1928).

The third water body for which an age determination is available is a small pond (No. 11), elevation 300 m, situated in the moraine (Fig. 25.6) that occupies a col above Baird Inlet, about 5.5 km east of the rock basin lake just described. The age obtained for basal organic material from this pond is 8540 ± 170 years (GSC-3009). Well developed moraines, such as the one in which this pond lies, are rather rare in the Queen Elizabeth Islands, and it is even more unusual to find one that contains a pond or lake suitable for coring. The configuration of the moraine shows that it formed in an interlobate situation, between ice in the valley (Fig. 25.4), now occupied by a northern branch of Tanquary Glacier, and an enlarged Ekblaw Glacier which formerly extended farther east in Baird Inlet. The position of the moraine in the col shows that the major push must have come from Ekblaw Glacier, which was, and is, one of the main outlet glaciers from the ice cap to the west. The crest of the moraine, which now forms the drainage divide in the col, rises 13 m above the level of the adjacent pond. An interlobate moraine is forming nearby today (Fig. 25.4), but at a lower elevation, in the same way as is envisaged for the moraine above Baird Inlet.

Figure 25.3. *Aerial view north at lake no. 7 at 390 m elevation, southeastern Pim Island. Coring in both 1979 and 1980 was carried out in the northwestern part of the lake (arrow). June 19, 1979. GSC 202823-O*

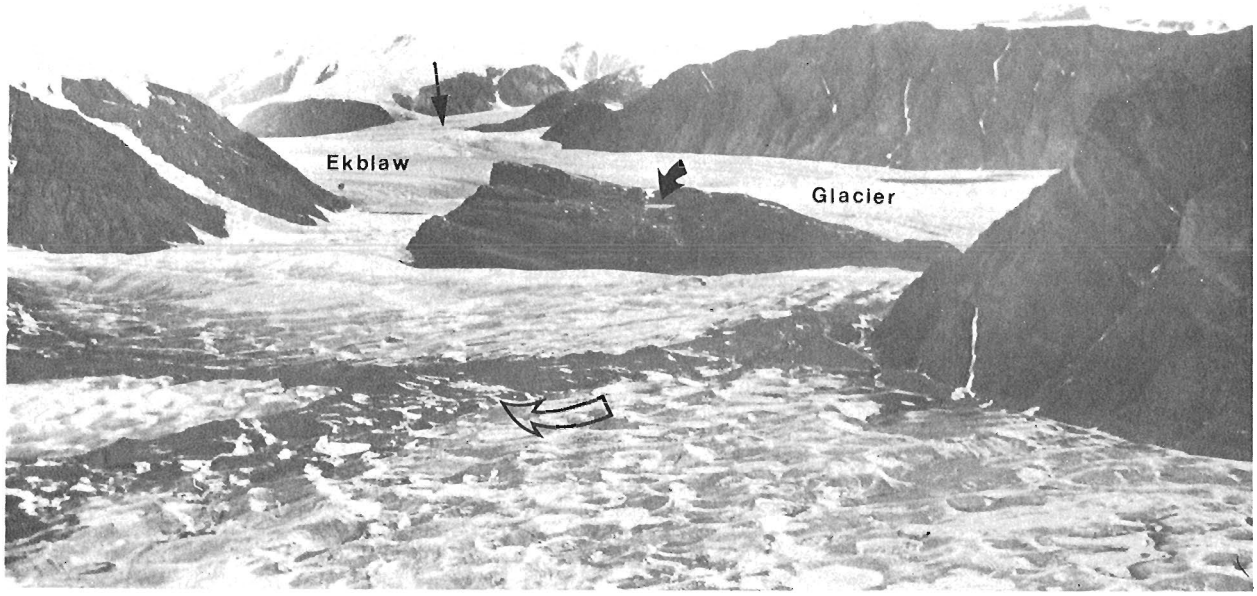

Figure 25.4. *Aerial view northwest at the rock basin lake (no. 12 – curved black arrow) at 295 m elevation, above Ekblaw Glacier. Glacier in foreground is a northern arm of Tanquary Glacier; note the interlobate moraine (open arrow) between it and an unnamed glacier descending from the ice cap to the south (left of photo). In the distance (straight black arrow) Isachsen Glacier joins the main outlet, Ekblaw Glacier. July 25, 1977. GSC 174432*

Discussion

Although there is no reason to doubt, as yet, the validity of the few ^{14}C ages available on lake sediments from the west side of Smith Sound, investigations elsewhere have shown that severe difficulties may arise with the dating of basal organic materials or of sediments containing finely disseminated organic matter (e.g., see Lundqvist, 1973; Donner and Jungner, 1974; Mott, 1975; Karrow and Anderson, 1975; Schroeder and Bada, 1978). Recently, the papers of Lowe and Walker (1980) and Sutherland (1980) treated the dating of basal organic sediments, especially as related to the chronology of deglaciation in Scotland, and Davis and Davis (1980) described problems encountered with attempts to date basal bog and pond-bottom sediments in Maine. In addition, the significance of $\delta^{13}C$ values with regard to source of organic matter has been touched on briefly by Funder (1978). A detailed discussion is beyond the scope of the present paper and would be premature until additional age determinaitons have been obtained, but a few points are worth emphasizing.

The two age determinations from the Pim Island lake (cf. Table 25.2), carried out on separate cores, are in proper sequence, for the gyttja stratigraphically overlies the moss in Core 2. At this site the inorganic sediment underlying the organic layers contains an average (8 determinations) of 1.65% inorganic carbon, a value equivalent to 13.8% $CaCO_3$. This value is similar to the values for carbonate content obtained on a number of till samples from the Cape Herschel – Pim Island area. The moss unit at the base of the core does not suffer from the problem of low organic content (Table 25.2) which often characterizes basal organic sediments in newly deglaciated terrain (cf. Olsson, 1979; Sutherland, 1980), and the $\delta^{13}C$ value of -30.8‰ falls in the general range of terrestrial plants (Olsson and Osadebe, 1974; Stuiver, 1975). If the moss is of terrestrial origin, rather than being a submerged aquatic species, and its $\delta^{13}C$ value is well outside the typical range (-18.3 to -8.6 ‰) of submerged aquatic plants such as **Chara, Potamogeton, Myriophyllum,** and **Nitella** (cf. Stuiver, 1975)[1], it seems curious that it is such a pure layer. If it had been washed into the lake basin from the adjacent slopes one would expect detritus derived from vascular plants or fragments of other mosses to be present as well. Pertinent evidence is also provided by the diatoms present in the same increment of Core 2 that was used for dating. The assemblage is characterized by distinct bloom of **Fragilaria construens** var. **venter;** other species present are **F. construens, F. pinnata,** and **F. pinnata** var. **intercedens.** The dominance of **F. construens** var. **venter** "strongly reflects a well-oxygenated, cool water biotope and the presence of aquatic vegetation" (S. Lichti-Federovich, unpublished GSC Diatom Reports 79-2 and 79-3).

In the case of the coring sites above Baird Inlet and Ekblaw Glacier the inorganic carbon content of the sediments beneath the dated basal organic horizons is even lower than on Pim Island – 0.01% for the moraine pond and 0.11% for the rock basin lake. The bedrock in the vicinity is dominantly granulite gneiss, and carbonate rocks were not observed in the area drained by Ekblaw Glacier (cf. Frisch et al., 1978; T. Frisch, personal communication, 1980). Two samples of bedrock from above the rock basin, however, were analyzed for their carbon content, and small amounts are indeed present. The untreated samples contained an average of 0.085% carbon, and after treatment with 10% HCl an average value of 0.06% was obtained. Thus it is clear that the potential for a small amount of contamination by 'old' carbon exists at all three lakes, but whether or not contamination has actually occurred is another question. For the time being it seems reasonable to accept the dates as valid ages for the basal increments (5 cm or less) of the organic sediments.

[1] A recent $\delta^{13}C$ determination on **Drepanocladus exannulatus,** a submerged moss collected from holes in the ice of the moraine pond above Baird Inlet, gave a value of -21.0‰ (GSC-3128).

At the time that the moraine in the col above Baird Inlet was being constructed, ice must have covered the 'up-glacier' site of the rock basin lake. At the coring site the elevation of the moraine is above 300 m, and it rises up the mountain slope to the west (Fig. 25.6). If a gradient similar to that of the present-day Ekblaw Glacier were maintained, then the ice would have been roughly 150 m higher in elevation at the site of the rock basin lake (Fig. 25.4) than at the moraine pond. This amount would be sufficient to inundate the bedrock knobs that surround the lake (cf. Fig. 25.5).

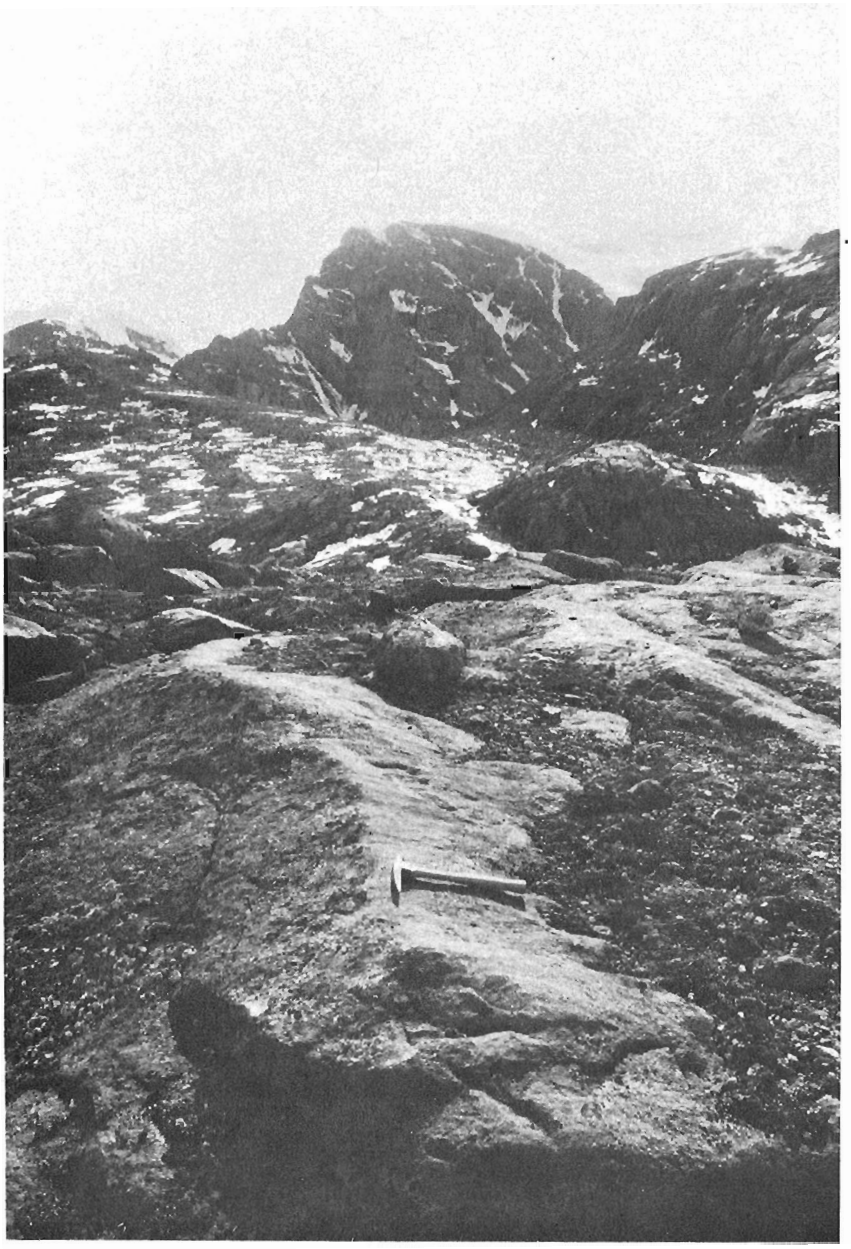

Figure 25.5. *Detail of glacially sculptured surface on hilltop (gneiss) to the east of the rock basin lake (no. 12). View toward the southwest. Ice flowed across this hill from west to east (right to left in the photograph). Note the form of the highest part of the bastion, showing how an enlarged Ekblaw Glacier once flowed eastward through the valley shown in Figure 25.4 (the reverse direction to today). July 20, 1979. GSC 202823-F*

Several explanations may help to account for the younger age of the basal organic material in the moraine pond:

1. The depression now occupied by the pond is assumed to have originated by the melting in situ of a block of ice that had become isolated from the main ice mass. The melting process would have taken a period of time, perhaps several hundred years, thus delaying the start of organic accumulation.
2. Vegetation was slower to invade this area, more exposed as it is, and today its environs are not characterized by the rich vegetation found around the rock basin lake. Also, the morainic substrate was unstable as the ice melted away.
3. Fortuitously the oldest organic sediment was obtained from the rock basin lake but not from the much smaller moraine pond. In neither case were soundings taken nor is any sort of bathymetric map available; coring was attempted as near to the middle of the lake and the pond as possible, and air photographs show that the pond is deepest in the middle.
4. The peaty, moss-rich material used for dating in the moraine pond consisted of distinct layers that could be clearly seen to extend right across the core. The same moss-rich material extended 3 cm lower on one side of the core but this material was not used for dating as it was feared it might be an artifact of the coring process; possibly it merely reflected an uneven bottom, and had this lowermost organic material been dated, an older age would have been obtained.
5. The ice surface may still have been above the level of the rock basin lake but the surrounding rock bastion prevented the ice from filling the basin; i.e., the lake was originally deeper in an early phase when ice blocked its outlet and when ice still covered the site of the moraine pond to the east.

The sequence of events at this pond is further complicated by the fact that the moss, **Drepanocladus lycopodioides** var. **brevifolius**, at the base of the core is not a true aquatic species (J.A. Janssens, personal communication, 1980). Unlike the luxurious growth of **Drepanocladus exannulatus** (aquatic modification) which is present in the centre of this 2.6 m-deep pond today, **D. lycopodioides** var. **brevifolius** is a typical fen species; it appears to develop especially well on calcareous substrates. **Drepanocladus brevifolius** (synonymous with **D. lycopodioides** var. **brevifolius** (Ireland et al., 1980)) is common, for example, in hummocky sedge-moss meadows and wet sedge-moss meadows on the Truelove Lowland, northern Devon Island (Muc and Bliss, 1977; Vitt and Pakarinen, 1977), and in central Bathurst Island it is widespread at the edges of ponds and pools and in wet tundra meadows (Miller and Ireland, 1978). Both areas are characterized by Paleozoic carbonate rocks

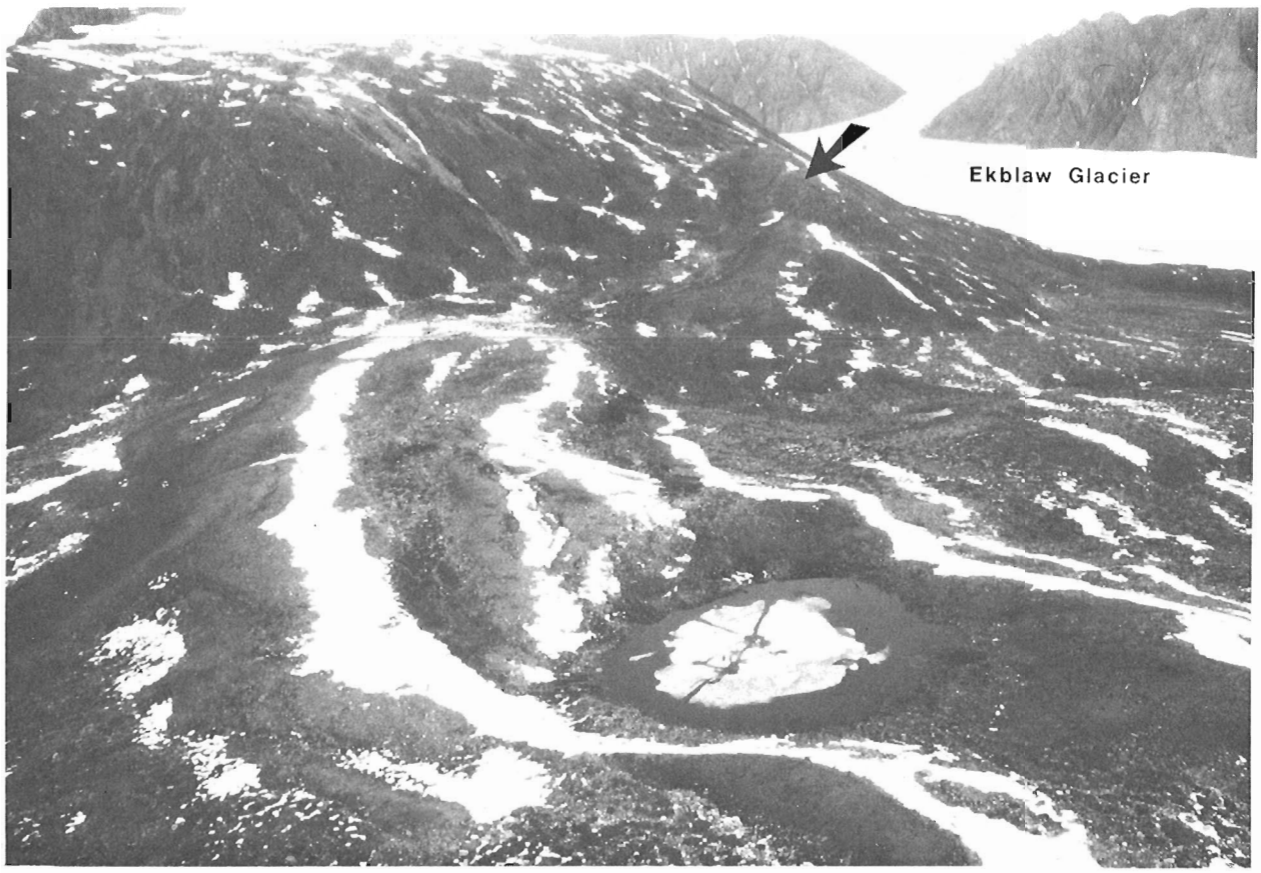

Figure 25.6. *Aerial view west at the moraine pond (no. 11) at an elevation of 300 m on the south side of Baird Inlet. The hole in the centre of the ice is where coring was carried out June 18, 1979. Note how the moraine ascends the mountain slope (arrow) on the far side of the pond (in an up-glacier direction). July 20, 1979. GSC 202823-M*

outcropping nearby, and the same is true in Peary Land, North Greenland, where Holmen (1960, p. 78) cited it as "a very important species in calcareous marshes and meadows. . ." (cf. also Brassard (1971) for data on this moss community in northern Ellesmere Island). Although, as noted earlier, no carbonate rocks are known to exist at the head of Baird Inlet (T. Frisch, personal communication, 1980), and the underlying inorganic material does not react with dilute HCl, at the level of the dated sample in Core 2 from this pond 1.36% of inorganic (carbonate) carbon is present.

The presence of **Drepanocladus lycopodioides** var. **brevifolius** indicates that shallower water conditions prevailed 8700 to 8400 years ago, for this species does not live in 2+ m-deep water such as exists in this pond today. As mentioned earlier the basin containing the moraine pond was created by the melting of a block of ice. Although the presence of dead ice would have resulted in shallower water, it is by no means certain that the moss grew in this environment. Alternatively, if the permafrost table was originally lower, drainage through the bouldery, morainic debris to the north may have occurred in early postglacial time. As the outlet gradually became blocked by fines derived from the moraine ridges on the other sides of the pond, by the growth of vegetation, and by a rise in the permafrost table, the pond that we see today could have developed from what was originally a meadow-bordered pool. This alternative would explain the change in moss species without the necessity of washing material in at an early stage in the pond's history.

Although the correct explanation may be a combination of several of the factors mentioned, it is interesting to note that in a comparative situation at Nakervare in Swedish Lapland, Karlén (1979) appeared to favour the interpretation that a moss peat/gyttja sequence could result if peat had accumulated in shallow water above ice; then, as the ice melted, a deeper body of water would be formed, and gyttja would be deposited. Wright (1980), too, has stressed the importance of dead ice as a way of explaining similar sequences – coarse organic detritus overlain by deep-water organic lake mud – that are common in Minnesota; cf. also Florin and Wright (1969), Rampton (1970), and Watson (1980) for illustrations of the development of a cover of vegetation on top of dead ice.

The age determinations from innermost Baird Inlet also bear on the question of ice cap symmetry, a topic that has been discussed by Koerner (1977) as a result of his studies of mass balance and ice thickness on several ice caps in the eastern Queen Elizabeth Islands. He presented a series of profiles, based on radio echo sounding, which showed that the ice is significantly thicker on the eastern and southern sides of the Devon Island and central Ellesmere Island ice caps, the latter being the one from which Ekblaw Glacier drains (Fig. 25.1). The present asymmetry of these ice caps is primarily a result of the greater accumulation of snow on the slopes towards Baffin Bay (Koerner, 1966, 1970). Questions posed by Koerner (1977) were: when had the asymmetry developed and was the ice now as thick as, or thicker than, in late Wisconsinan time?

Although the period of time during which the moraine was being constructed cannot be determined precisely on the basis of the available data, there is no reason to doubt that it represents a marginal position of Ekblaw Glacier in late Wisconsinan time, or possibly even in the earliest Holocene as well. Ekblaw Glacier has not reattained the position occupied by the moraine since the inception of organic sedimentation.

Finally, the two oldest age determinations, those from the rock basin above Ekblaw Glacier and from the lake at 390 m on Pim Island, are nearly identical with one in a similar situation on the plateau of Nordvestø, the main island in the Carey Øer, 225 km to the south-southeast of Pim Island. There, although the coring site was a frozen peat mound instead of a lake, and the elevation was lower (ca. 124 m a.s.l.), the basal peat was 8940 ± 90 years old (GSC-2440, at 99-104 cm depth; Brassard and Blake, 1978). It will be of interest to see if age determinations on the basal organic sediment in any of the other lakes sampled fall into the same period of time, and whether any ages are obtained to match the oldest obtained so far on lake sediments from Greenland, i.e., 10 050 ± 150 years (K-2034) from Scoresby Sund, East Greenland, and 9840 ± 170 years (K-1149) in southern West Greenland (Kelly and Funder, 1974).

Acknowledgments

Logistical support was provided by the Polar Continental Shelf Project (G.D. Hobson, Director), and thanks are extended to the staff of that organization in Resolute for expediting our work in every way possible. Assistance with the coring program in 1979 was provided by R.J. Richardson (GSC), R.N. McNeely (on secondment from the Water Quality Branch, Inland Waters Directorate, Environment Canada; responsible for chemical analysis of water samples), and H. Hyvärinen (University of Helsinki; palynology of the cores from Pim Island and Baird Inlet). In 1980 the coring group consisted of T.W. Anderson and I.M. Robertson (both GSC), and S. Funder (University of Copenhagen; palynology of the cores from Greenland); J.P. Bridgland served as general assistant in addition to conducting his own studies of the present-day moss flora at Cape Herschel. The carbon content of the rocks and sediments was analyzed by W.E. Podolak and the radiocarbon age determinations were carried out under the supervision of J.A. Lowdon. J.A. Janssens (University of Alberta) determined the mosses, and S. Lichti-Federovich (GSC) identified the diatoms. T.W. Anderson provided a most helpful critical review of the manuscript.

References

Barnett, D.M.
1977: Glacial geomorphology in a sub-polar proglacial lake basin: a process-response model; unpublished Ph.D. dissertation, University of Western Ontario, London, 302 p.

Blake, W., Jr.
1977: Glacial sculpture along the east-central coast of Ellesmere Island, Arctic Archipelago; in Report of Activities, Part C, Geological Survey of Canada, Paper 77-1C, p. 107-115.

1978: Coring of Holocene pond sediments at Cape Herschel, Ellesmere Island, Arctic Archipelago; in Current Research, Part C; Geological Survey of Canada, Paper 78-1C, p. 119-122.

Bradley, R.S. and England, J.
1977: Postglacial activity in the High Arctic; Department of Geology and Geography, University of Massachusetts, Amherst, Contribution No. 31, 184 p.

Brassard, G.R.
1971: The mosses of northern Ellesmere Island, Arctic Canada. I. Ecology and phytogeography, with an analysis for the Queen Elizabeth Islands; The Bryologist, v. 74, p. 233-281.

Brassard, G.R. and Blake, W., Jr.
1978: An extensive subfossil deposit of the arctic moss **Aplodon wormskioldii**; Canadian Journal of Botany, v. 56, p. 1852-1859.

Caflisch, T.
1972: Limnological investigations on Colour and Phantom Lakes; in 22nd International Geographical Congress (Montreal), Guidebook to Field Tour Ea2, ed. F. Müller; Axel Heiberg Island Research Reports, McGill University, Miscellaneous Papers, p. 49-56.

Davis, P.T.
1978: Pangnirtung and Kingnait Fiord area; The Canadian Alpine Journal, v. 61, p. 73-76.

1980a: Holocene vegetation and climate record from Iglutalik Lake, Cumberland Sound, Baffin Island, N.W.T., Canada; American Quaternary Association, 6th Biennial meeting (Orono, Maine) Abstracts, p. 61.

1980b: Late Holocene glacial, vegetational, and climatic history of Pangnirtung and Kingnait Fiord area, Baffin Island, N.W.T., Canada; unpublished Ph.D. dissertation, University of Colorado, Boulder, 366 p.

Davis, P.T. and Davis, R.B.
1980: Interpretation of minimum-limiting radiocarbon dates for deglaciation of Mount Katahdin area, Maine; Geology, v. 8, p. 396-400.

Donner, J.J. and Jungner, H.
1974: Errors in the radiocarbon dating of deposits in Finland from the time of deglaciation; Bulletin of the Geological Society of Finland, No. 46, Part 2, p. 139-144.

Elton, C.S.
1925: The biology in relation to the geography; Appendix I in The Oxford University Arctic Expedition, 1924; Geographical Journal, v. 66, p. 111-113.

Florin, M-B. and Wright, H.E., Jr.
1969: Diatom evidence for the persistence of stagnant glacial ice in Minnesota; Geological Society of America Bulletin, v. 80, p. 695-704.

Fredskild, B.
1977: The development of the Greenland lakes since the last glaciation; in Danish Limnology – Reviews and Perspectives, ed. C. Hunding; Folia Limnologica Scandinavica, v. 17, p. 101-106.

Fredskild, B., Jacobsen, N., and Roen, U.
1975: Remains of mosses and freshwater animals in some Holocene lake and bog sediments from Greenland; Meddelelser om Grønland, Band 198, Nr. 5, 44 p.

Frisch, T., Morgan, W.C., and Dunning, G.R.
1978: Reconnaissance geology of the Precambrian Shield on Ellesmere and Coburg Islands, Canadian Arctic Archipelago; in Current Research, Part A; Geological Survey of Canada, Paper 78-1A, p. 135-138.

Funder, S.
1978: Holocene stratigraphy and vegetation history in the Scoresby Sund area, East Greenland; Grønlands Geologiske Undersøgelse, Bulletin 129, 66 p.

Hattersley-Smith, G.
1969: Glacial features of Tanquary Fiord and adjoining areas of northern Ellesmere Island, N.W.T.; Journal of Glaciology, v. 8, no. 52, p. 23-50.

Holmen, K.
1960: The mosses of Peary Land, North Greenland; Meddelelser om Grønland, Band 163, Nr. 2, 96 p.

Ireland, R.R., Bird, C.D., Brassard, G.R., Schofield, W.B., and Vitt, D.M.
1980: Checklist of the Mosses of Canada; National Museum of Natural Sciences, Publications in Botany, No. 8, 75 p.

Karlén, W.
1979: Deglaciation dates from northern Swedish Lappland; Geografiska Annaler, v. 61A, p. 203-210.

Karrow, P.F. and Anderson, T.W.
1975: Palynological study of lake sediment profiles from southwestern New Brunswick: Discussion; Canadian Journal of Earth Sciences, v. 12, p. 1808-1812.

Kelly, M. and Funder, S.
1974: The pollen stratigraphy of late Quaternary lake sediments of South-West Greenland; Grønlands Geologiske Undersøgelse, Rapport Nr. 64, 26 p.

Koerner, R.M.
1966: Accumulation on the Devon Island ice cap, Northwest Territories, Canada; Journal of Glaciology, v. 6, p. 383-392.

1970: The mass balance of the Devon Island ice cap, Northwest Territories, Canada, 1961-66; Journal of Glaciology, v. 9, p. 325-336.

1977: Ice thickness measurements and their implications with respect to past and present ice volumes in the Canadian High Arctic ice caps; Canadian Journal of Earth Sciences, v. 14, p. 2697-2705.

Long, A. and Mielke, J.E.
1967: Smithsonian Institution radiocarbon measurements IV; Radiocarbon, v. 9, p. 368-381.

Lowe, J.J. and Walker, M.J.C.
1980: Problems associated with radiocarbon dating of the close of the Lateglacial period in the Rannoch Moor area, Scotland; in Studies in the Lateglacial of North-West Europe, ed. J.J. Lowe, J.M. Gray, and J.E. Robinson; Pergamon Press, Oxford, p. 123-137.

Lundqvist, J.
1973: Isavsmältningens förlopp i Jämtlands Län; Sveriges Geologiska Undersökning, Series C, Nr. 681, Årsbok 66, Nr. 12, 187 p.

Mielke, J.E. and Long, A.
1969: Smithsonian Institution radiocarbon measurements V: Radiocarbon, v. 11, p. 163-182.

Miller, N.G. and Ireland, R.R.
1978: A floristic account of the bryophytes of Bathurst Island, Arctic Canada; Occasional Papers of the Farlow Herbarium of Harvard University, No. 13, 38 p.

Mott, R.J.
1975: Palynological studies of lake sediment profiles from southwestern New Brunswick; Canadian Journal of Earth Sciences, v. 12, p. 273-288.

Muc, M. and Bliss, L.C.
1977: Plant communities of Truelove Lowland; in Truelove Lowland, Devon Island, Canada: A High Arctic Ecosystem, ed. L.C. Bliss; The University of Alberta Press, Edmonton, p. 143-154.

Olsson, I.U.
1979: A warning against radiocarbon dating of samples containing too little carbon; Boreas, v. 8, p. 203-207.

Olsson, I.U. and Osadebe, F.A.N.
1974: Carbon isotope variations and fractionation corrections in ^{14}C dating; Boreas, v. 3, p. 139-146.

Rampton, V.N.
1970: Neoglacial fluctuations of the Natazhat and Klutlan Glaciers, Yukon Territory, Canada; Canadian Journal of Earth Sciences, v. 7, p. 1236-1263.

Schroeder, R.A. and Bada, J.L.
1978: Aspartic acid racemization in Late Wisconsin Lake Ontario sediments; Quaternary Research, v. 9, p. 193-204.

Stuiver, M.
1975: Climate versus changes in ^{13}C content of the organic component of lake sediments during the Late Quaternary; Quaternary Research, v. 5, p. 251-262.

Summerhayes, V.S. and Elton, C.S.
1928: Further contributions to the ecology of Spitsbergen; Journal of Ecology, v. 16, p. 193-268.

Sutherland, D.G.
1980; Problems of radiocarbon dating deposits from newly deglaciated terrain: examples from the Scottish Lateglacial; in Studies in the Lateglacial of North-West Europe, ed. J.J. Lowe, J.M. Gray, and J.E. Robinson; Pergamon Press, Oxford, p. 139-149.

Vincent, J-S.
1980: Les glaciations quaternaires de l'île de Banks, Arctique canadien; thèse de doctorat non-publiée, Université de Bruxelles, 248 p.

Vitt, D.H. and Pakarinen, P.
1977: The bryophyte vegetation, production, and organic components of Truelove Lowland; in Truelove Lowland, Devon Island, Canada: A High Arctic Ecosystem, ed. L.C. Bliss; The University of Alberta Press, Edmonton, p. 225-244.

Watson, R.A.
1980: Landform development in moraines of the Klutlan Glacier, Yukon Territory, Canada; Quaternary Research, v. 14, p. 50-59.

Wright, H.E., Jr.
1980: Surge moraines of the Klutlan Glacier, Yukon Territory, Canada: Origin, wastage, vegetation succession, lake development, and application to the Late-Glacial of Minnesota; Quaternary Research, v. 14, p. 2-18.

26. STRATIGRAPHY AND STRUCTURE OF ROAD RIVER AND ASSOCIATED STRATA IN WARE (WEST HALF) MAP AREA, NORTHERN ROCKY MOUNTAINS, BRITISH COLUMBIA

Project 700047

H. Gabrielse
Cordilleran Geology Division, Vancouver

Gabrielse, H., Stratigraphy and structure of Road River and associated strata in Ware (west half) map area, northern Rocky Mountains, British Columbia; in Current Research, Part A, Geological Survey of Canada, Paper 81-1A, p. 201-207, 1981.

Abstract

Asymmetrical folds and related easterly directed thrust faults of relatively small displacement are typical of the structural style involving Road River and associated strata. The character and distribution of facies indicate that the depositional basin southwest and west of the carbonate shelf margin was differentiated at various times during the early Paleozoic into northwesterly trending troughs or subbasins and ridges or platforms.

Introduction

The stratigraphy of lower Paleozoic rocks transitional from basin to platform facies in Ware and Trutch map areas has been described by Cecile and Norford (1979). This report deals mainly with basinal facies of Ordovician and Silurian strata in the region between Akie and Kwadacha rivers in the west half of Ware map area. The object of this ongoing study is to define variations of sedimentation and structural style within the basin facies so as to better understand the paleogeography and deformational history. Ultimately studies of this type may help provide insight into the localization of lead-zinc-barite deposits in Upper Devonian shales, the prime target of current exploration in the region.

Acknowledgments

The author is grateful for the assistance of C.A. Evenchick during the 1979 field season and to W.J. Roberts of Cyprus Anvil Mining Corporation and his staff for stimulating discussions and logistic support during the 1980 field season.

Stratigraphy

Brief accounts of stratigraphy presented herein are supplemental to those provided by Cecile and Norford (1979). In general, the thickness of Road River rocks appears to decrease markedly as distance from the margin of the platform increases. Northwest of Akie River near the headwaters of Truncate Creek typical black graptolitic shale of Ordovician age is thin or absent (Fig. 26.1). Near the headwaters of Del Creek, Ordovician shale is intensely deformed but estimated thicknesses do not exceed 100 m. East of Paul River in the belt including Middle Ordovician volcanic rocks the Ordovician succession may be more than 500 m thick. Silurian dolomitic siltstone does not show as marked a change in thickness as do Ordovician rocks. It appears to be as much as 600 m thick near the upper reaches of Kwadacha River but elsewhere is probably closer to 200 m thick.

Kechika Group

Upper Cambrian and Lower Ordovician strata of the Kechika Group were not examined in detail. Southeast of the headwaters of Del Creek the uppermost beds comprise characteristic nodular, wavy banded silty limestone and calcareous shale. Cleavage is strongly and penetratively developed and produces a glossy surface on fragments that comprise the typical glistening buff and silvery grey weathering talus of the Kechika Group. Olistostromes as much as 8 m thick occur locally. They consist of angular to subrounded fragments of light and dark grey limestone, in

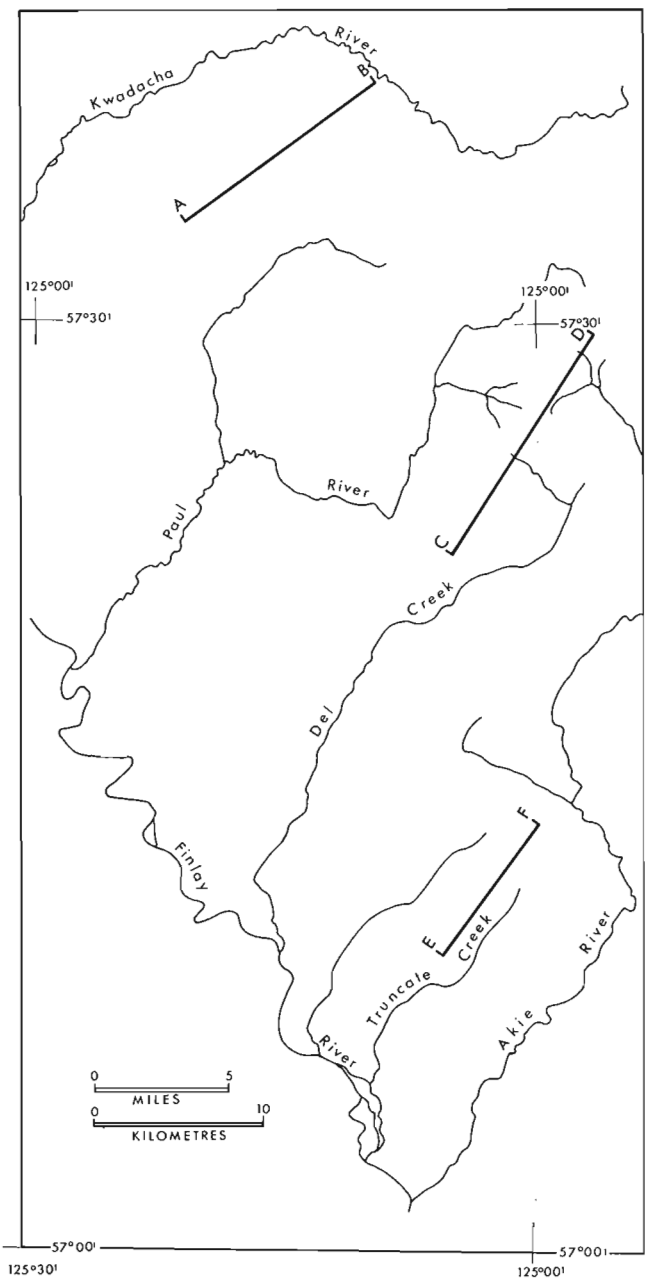

Figure 26.1. *Index map showing locations of structural cross-sections.*

Figure 26.2

Argillaceous rocks with beds, lenses and nodules of limestone directly underlying Silurian siltstone near headwaters of Truncate Creek.

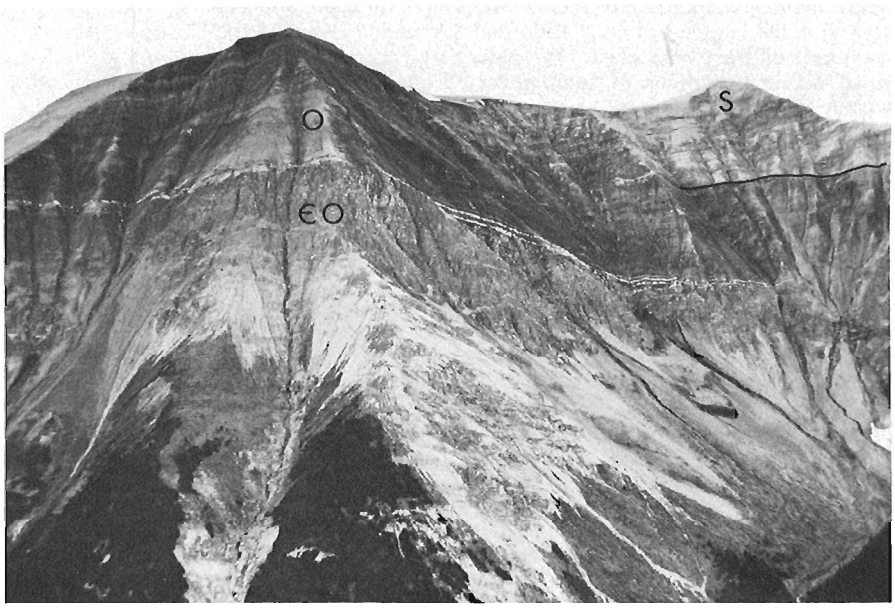

Figure 26.3

View southwesterly to Kechika Group (CO) Ordovician shale units (O) and Silurian siltstone unit (S) southeast of headwaters of Paul River. Note conspicuous carbonate beds in basal part of Ordovician shale unit which is highly folded and faulted.

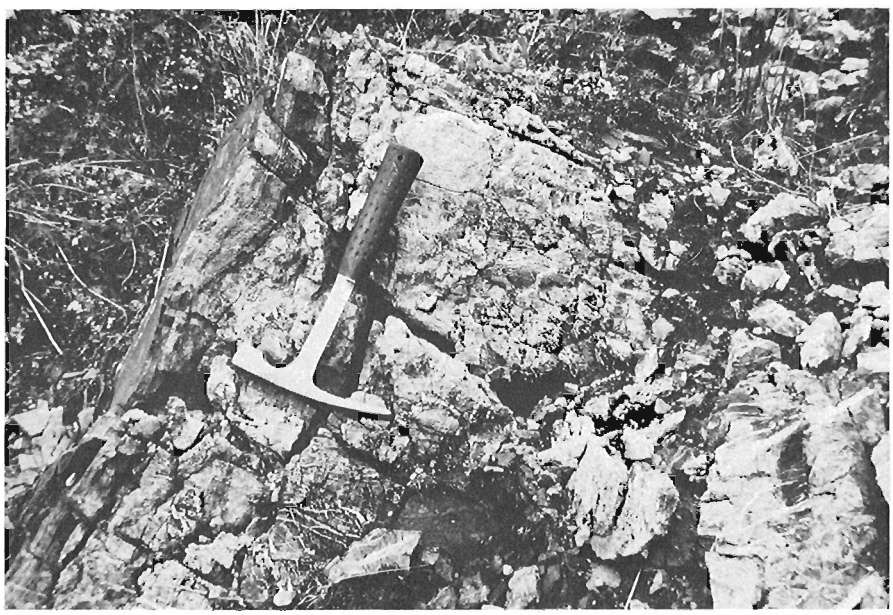

Figure 26.4

Olistostromal dolomite capped by graded sandstone to left of hammer. Silurian siltstone unit southeast of headwaters of Del Creek.

part well laminated and rare black chert as much as 20 cm long in a buff grey weathering limestone matrix. In places the uppermost strata are dark grey weathering and resistant and from a distance are not easily distinguished from the Silurian siltstone formation if the commonly intervening black Ordovician shale unit is thin or absent.

At the headwaters of Truncate Creek strata directly underlying the Silurian siltstone unit comprise well laminated light to dark grey weathering shale, phyllitic slate and silty shale with pods and lenses of blue grey limestone (Fig. 26.2). A blocky grey limestone bed 1 m thick forms a conspicuous member, and a strong striping is imparted to outcrops by several bright orange weathering limestone beds about 5 cm thick. If the rocks are part of the Kechika Group, or a basal Road River unit (OR_1 unit of Cecile and Norford, 1979), the typical black shale of the Ordovician is missing, probably because of an unconformity below the Silurian siltstone (see Fig. 26.8).

Road River Strata, Ordovician Shale Unit

In the report area the Ordovician shale unit is intensely deformed and commonly only the uppermost part is preserved in the hanging walls of thrust faults. Even where the base and top of the unit are observable in a continuous sequence, for example, southeast of the headwaters of Paul River, internal folding and faulting make stratigraphic study difficult.

A basal unit of black calcareous shale, slate and siltstone ranges from 20 to 40 m thick and is overlain by a distinctive member of buff orange to cream weathering well bedded platy limestone interbedded with platy silty slate and shale (Fig. 26.3). The limestone is distinctly layered with alternating units of blue-grey weathering limestone in beds 1 to 2 cm thick and buff orange weathering limestone 2 to 4 m thick. Southeast of the headwaters of Paul River several carbonate beds are present. Some are continuous for more than 1 km whereas others extend for no more than a few hundred metres along trend. Thickness of the limestone and shale unit ranges up to 25 m. Northwest of Paul River only one limestone rib, less than 1 m thick, was observed in this interval.

The remainder of the Ordovician shale unit in the southern and southwestern parts of the area is predominantly black graptolitic shale and platy calcareous slate. Near the headwaters of Paul River a volcanic member 50 to 60 m thick occurs low in the sequence. McIntyre (1980) has described one occurrence as comprising a greenish grey weathering massive micro-dioritic flow up to 50 m thick overlain by interbedded shale and orange- and brown-weathering vitric crystal and lapilli tuff.

Road River, Silurian Siltstone Unit

Resistant, well blended, platy dolomitic siltstone and silty dolomite of Silurian age underlie many of the higher peaks in the region. Commonly they cap ridges with dip slopes to the southwest and steep slopes or cliffs to the northeast (Fig. 26.3). Apparent great thicknesses in the southern parts of the area result from imbricate thrusts and tight folds.

Southeast of the headwaters of Paul River the basal part of the unit overlying jet black shale of the Ordovician shale unit is as follows from the base upward:

1. well bedded blue-grey weathering dark grey limestone with laminated beds in the upper part; 20 m thick
2. platy, argillaceous dark grey siltstone; 5-10 m thick
3. tan weathering platy dolomitic siltstone with black silty shale and siltstone in the lower part; 30 m thick
4. black porcellanite and chert with silty black shale; 15 m thick.

Similar rocks form the base of the Silurian siltstone unit elsewhere but the thickness of member 4 decreases to the south. Typically most of the unit consists of tan weathering, platy, well laminated, dolomitic siltstone. Generally sequences of very platy beds alternate with sequences of bioturbated beds in which partings parallel with bedding are spaced very irregularly. The platy beds are locally richly graptolitic whereas the bioturbated beds contain only abundant feeding trails.

An olistostromal member southeast of the headwaters of Del Creek is about 12 m thick and consists of angular to subangular fragments and blocks of medium grey dolomite and black chert in a sandy dolomite matrix. The top of the olistostrome is marked by a graded bed of laminated even grained sandstone about 8 cm thick (Fig. 26.4). The member is similar to olistostromes noted in Silurian siltstones in the east half of Fort Grahame map area to the southeast (Gabrielse, 1975).

The Silurian siltstone unit between the headwaters of Paul River and Kwadacha River is thicker and contains thicker bedded sequences than farther south and west. There too, however, platy siltstone is the dominant lithology.

Devonian Limestone

Devonian limestone as much as 100 m thick occurs in a belt 5 to 6 km wide between Kwadacha River and the head of Paul River. The rocks can be traced for a considerable distance to the southeast but pinch out to the northwest about 3 km north of Kwadacha River (Gabrielse et al., 1977). The limestone is generally medium to thick bedded, commonly fetid and locally very fossiliferous. In places breccia is abundant with fossils in both fragments and matrix. Sandy and cherty beds have been noted in several places. Unlike most of the other formations described above the limestone was clearly deposited in shallow water. It has not been observed farther southwest in the west half of Ware map area, even where younger rocks are known to be present. Fossils indicate an Early Devonian (Emsian) to Middle Devonian age.

Devonian Shale Unit

Overlying the Devonian limestone in the northeastern part of the report area, or the Silurian siltstone unit farther southwest, is a sequence of black shale or slate, locally with barite, siltstone, siliceous shale and porcellanite and chert pebble conglomerate. Regionally, chert pebble conglomerate occurs high in the clastic sequence but in a tight syncline northwest of the head of Paul River the conglomerate lies almost directly on Devonian limestone suggesting a significant unconformity. Elsewhere black melanteritic shale commonly overlies the limestone or the Silurian siltstone unit. A graptolitic argillaceous Lower Devonian unit has been noted in a number of places above Silurian siltstone but where the Devonian limestone is absent the strata are difficult to separate from Upper Devonian clastic rocks.

Structure

Throughout the report area strata are tightly folded and thrust faulted (Fig. 26.5). In general the intensity of folding and faulting increases from northeast to southwest. Folds and thrust faults are clearly related and, typically, northeasterly directed thrust faults of relatively small displacement have broken through the back limbs of asymmetrical folds (Fig. 26.6). Thus the thrust panels commonly comprise a synclinal core of Silurian siltstone with variable thicknesses of the underlying Ordovician shale unit in the hanging wall adjacent to the faults.

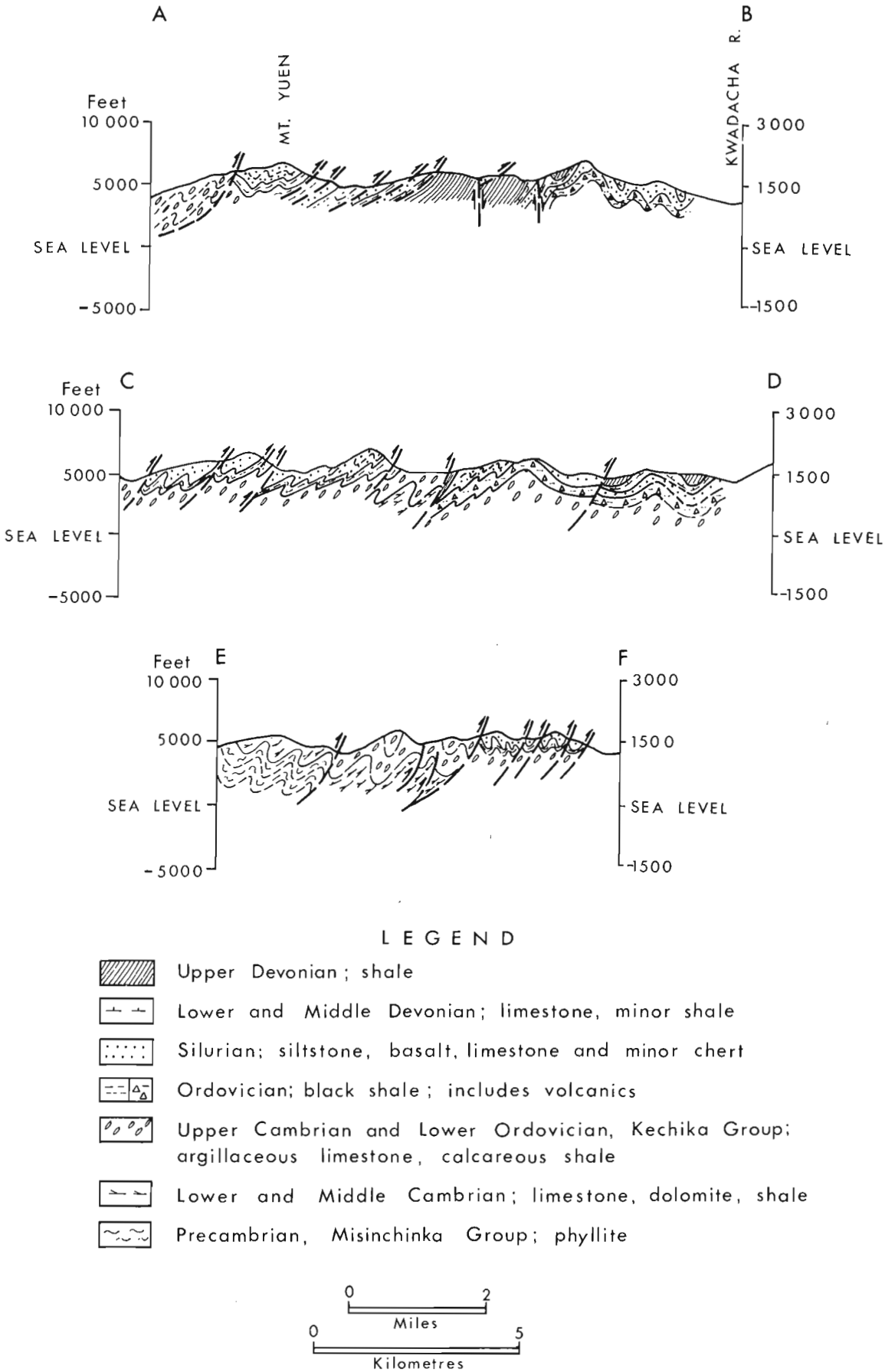

Figure 26.5. *Structural cross-sections between Akie and Kwadacha rivers. See Figure 26.1 for location.*

Figure 26.6

Fold and related thrust fault in Silurian siltstone unit. View southerly to ridge south-southeast of Mt. Yuen.

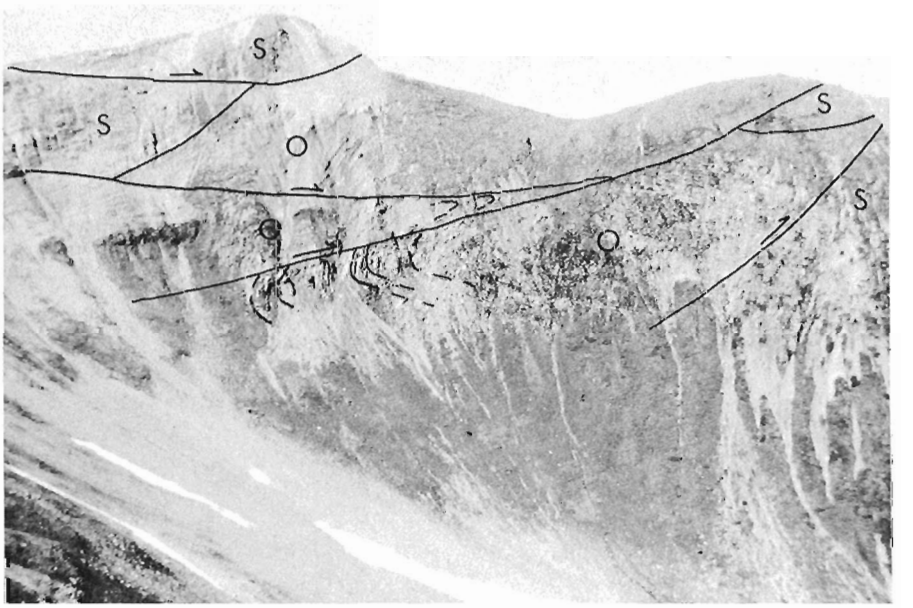

Figure 26.7

View northwesterly to shallow dipping thrust faults cutting Ordovician shale (O) and Silurian siltstone (S) southeast of Quadacha River (see Section A-B, Fig. 26.5.).

Near the headwaters of Truncate Creek axial planes of synclines within thrust panels and cleavage in underlying strata of the Kechika Group dip steeply to the northeast although thrust faults are directed northeasterly (see Fig. 26.2, section E-F). This relationship is probably the result of rotation above thrust faults that are concave upward.

Northeast of Mt. Yuen a set of shallow west-dipping thrust faults involves Ordovician and Silurian strata (see Fig. 26.5, section A-B; Fig. 26.7). There the thrust panels are offset by a steep northerly trending fault similar in attitude to several other faults noted farther south.

Paleogeography

Much more study is required to determine the paleogeographic evolution of the region. Regional mapping and local studies (See Taylor, 1979; Taylor et al., 1979; Fritz, 1979; McIntyre, 1980) show, however, that during early Paleozoic time the basin west and southwest of the various shale-out boundaries was not a simple homogeneous element (Fig. 26.8). Strong differentiation took place in Middle Cambrian time with the development of northerly to northwesterly trending facies belts characterized by the following lithologies and interpreted environments from northeast to southwest:

1. shale, siltstone, sandstone (clastic basinal)
2. olistostromes, debris flows and shale (block faulted basin?)
3. carbonate, siltstone, shale, platy limestone (starved basin in upper part)
4. massive limestone (linear reef and ? intrabasin platform)
5. siltstone, shale, platy, carbonate (starved basin)
6. dolomite, sandy dolomite (platform)

Upper Cambrian and Lower Ordovician rocks are progressively more argillaceous to the southwest but no distinct facies belts have been recognized. Olistostromes are conspicuous in the Ordovician shale unit in northeastern part of the study area but are much less important farther south and west, probably reflecting relative distance from the eastern shelf margin. A deep-seated fracture or system of

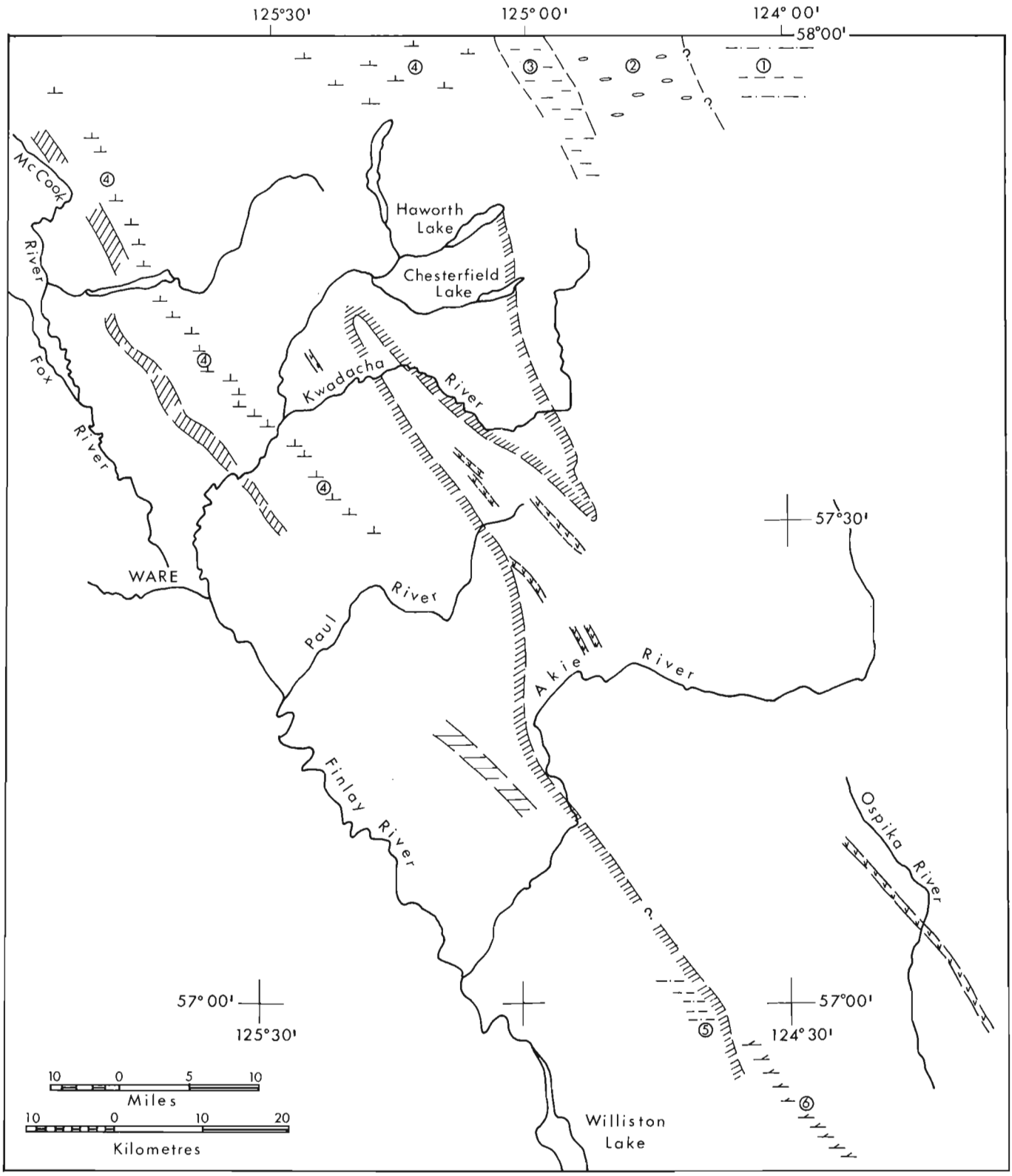

Figure 26.8. *Various lower Paleozoic paleogeographic elements in Ware map area.*

fractures in mid-Ordovician time is indicated by a narrow belt of volcanic rocks that can be traced discontinuously from northwest of Kwadacha River to northeastern Fort Grahame map area and beyond. The Ordovician shale unit appears to thin depositionally to the southwest but the effects of a pre-Silurian siltstone unconformity are not yet fully known.

Thicknesses of the Silurian siltstone unit near Chesterfield and Haworth lakes in the study area suggest a depocentre probably near the shelf margin. Generally, the unit is fairly consistent in facies throughout the region although more silty and less dolomitic to the southwest. An important exception is, however, the southwesternmost belt of exposures trending northwesterly from Mt. Haworth to northeast of McCook River (see Gabrielse et al., 1977; and Fig. 26.8). There, rocks correlative with the Silurian siltstone unit comprise clean, crossbedded white sandstone, sandstone, and chert pebble conglomerate with slate chips and interbedded graptolitic siltstone. These lithologies and the lack of typical Ordovician shale point to a northwesterly trending, relatively elevated belt during early and mid-Silurian time.

The original distribution of Lower and Middle Devonian carbonate strata is equivocal because of possible removal by postcarbonate erosion. Either the belt of carbonate as now exposed represents approximately the depositional limit of these rocks on a paleogeographic high or the belt was relatively low in immediate postcarbonate time and protected from erosion. In either case differential uplift or depression of the belt is indicated. On the basis of regional facies and stratigraphic relationships the writer favours the hypothesis of deposition on a local northwest-trending high area within the basin.

The cursory discussion on paleogeographic elements given above suggests considerable complexity of the lower Paleozoic basin west of the carbonate shelf margin. Further studies will refine the concepts presented herein and ultimately should provide a much better idea of the evolution of the basin that preceded and accompanied late Devonian mineralization.

References

Cecile, M.P. and Norford, B.S.
1979: Basin to Platform Transition, lower Paleozoic strata of Ware and Trutch map areas, Northeastern British Columbia; in Current Research, Part A, Geological Survey of Canada, Paper 79-1A.

Fritz, W.H.
1979: Cambrian stratigraphy in the northern Rocky Mountains, British Columbia; in Current Research, Part B, Geological Survey of Canada, Paper 79-1B.

Gabrielse, H.
1975: Geology of Fort Grahame E½ map-area, British Columbia; Geological Survey of Canada, Paper 75-33.

Gabrielse, H., Dodds, C.J., and Mansy, J.L.
1977: Geological map of Ware W½ and Toodoggone River map-areas; Geological Survey of Canada, Open File Report 483.

McIntyre, D.G.
1980: Driftpile Creek – Akie River project; in British Columbia Ministry of Energy, Mines and Petroleum Resources, Geological Fieldwork 1979, Paper 1980-1.

Taylor, G.C.
1979: Trutch and Ware east half map-areas; Geological Survey of Canada, Open File Report 606.

Taylor, G.C., Cecile, M.P., Jefferson, C.W., and Norford, B.S.
1979: Stratigraphy of the Ware E½ map area; in Current Research, Part A, Geological Survey of Canada, Paper 79-1A.

27.

JURASSIC BIOSTRATIGRAPHY, STRATIGRAPHY AND RELATED HYDROCARBON OCCURRENCES OF QUEEN CHARLOTTE ISLANDS, BRITISH COLUMBIA

Project 750035

B.E.B. Cameron and H.W. Tipper
Cordilleran Geology Division, Vancouver

Cameron, B.E.B. and Tipper, H.W., Jurassic biostratigraphy, stratigraphy and related hydrocarbon occurrences of Queen Charlotte Islands, British Columbia; in Current Research, Part A, Geological Survey of Canada, Paper 81-1A, p. 209-212, 1981.

Abstract

The Jurassic formations of Queen Charlotte Islands yield many prolific microfaunal assemblages. When studied in conjunction with well dated ammonites, they permit the recognition of previously unknown rock units. Detailed study of the stratigraphy has contributed new information on the source and occurrence of hydrocarbons.

Introduction

In 1974 biostratigraphic studies were undertaken in Queen Charlotte Islands with the intent of working out the sequence of Jurassic ammonite faunas. Field work has continued each year subsequently except for 1977 (Tipper, 1975, 1976, 1977; Tipper and Cameron, 1979, 1980). Although many faunas were known from previous studies (McLearn, 1927, 1929, 1949; Sutherland Brown, 1968) thorough collecting from known sections and the discovery of new, commonly recessive, sections produced a fairly complete Jurassic sequence from Lower Sinemurian to Lower Callovian with varied and well preserved faunas. In addition, some Triassic and Cretaceous sections were examined.

Many beds yielded a prolific microfauna including foraminifera, radiolaria, ostracoda, fish teeth, and other skeletal debris, and the study of the microfauna subsequently became a vital part of the project. With ammonites providing stratigraphic control, it is possible to work out the faunal succession and to present eventually a useful microfaunal zonation. Foraminifera have received the most attention so far but other microfauna are potentially useful index fossils.

Ammonite Faunas

The ammonite faunas are of increasing value. Each field season provides faunas new to Queen Charlotte Islands and provides a more complete Jurassic succession. Faunas are varied, generally prolific, and excellently preserved in the main. Study of the ammonite faunas is in progress, particularly by Hans Frebold, who has published one report on the Bathonian **Iniskinites** fauna (Frebold, 1979). The ammonites listed in Table 27.1 are only those genera that are most characteristic and abundant, but are associated with several other well represented genera. They potentially are useful as zonal index fossils. Correlation with the standard zonation of Europe is difficult as only a few European zonal species have been recognized. Many of the genera have strong affinities to Mediterranean genera, particularly in Pliensbachian and Toarcian beds.

Jurassic Microfaunas

In addition to detailed descriptions of stratigraphic units and methodical collection of ammonite and pelecypod faunas, sedimentary units have been extensively sampled for microfauna. The rich and highly varied foraminifers, ostracods and radiolaria are currently under intensive study and will eventually prove to be excellent index faunas especially insofar as their stratigraphic distribution is so well controlled by diagnostic ammonite faunas. Seventeen highly distinctive microfaunal assemblages are listed for purposes of this initial report (Table 27.1). It is expected that this number will increase as detailed analyses continue and new stratigraphic sequences are found.

A few preliminary notes on the microfaunas are included here.

MF 1. **Pseudolamarckina** fauna, see Tipper and Cameron, 1980

MF 2. **Reinholdella** fauna, see Tipper and Cameron, 1980

MF 3. foraminifers and ostracods were recovered from sandy shales exposed in Richardson Bay, Maude Island in association with middle Bajocian **Stephanoceras.** Equivalent strata in the Yakoun River area yielded well preserved radiolaria. Species of **Lenticulina, Marginulina, Astacolus, Citharina** and **Marginulinopsis** are distinctive elements of the foraminiferal fauna.

MF 4 and 5. new middle and Lower Bajocian shales and limestones in the vicinity of the Yakoun River, Graham Island have yielded distinctive species of **Lenticulina, Marginulina** and others. Associated limestones have produced good radiolarian assemblages.

MF 6 to MF 10. Toarcian foraminiferal assemblages are highly varied and include many distinctive forms. Included are species of **Lenticulina, Citharina, Falsopalmula, Nodosaria, Astacolus,** and many others. Radiolaria are abundant in the shales but are generally poorly preserved. A few limestone samples from the late Toarcian have yielded excellent radiolaria.

MF 11 to MF 14. Pliensbachian foraminifers are generally small but can readily be differentiated on the basis of **Lingulaina (tenera** group), **Frondicularia, Gaudryina, Ammobaculites,** and others. In general, well preserved radiolaria were obtained from limestone of Pliensbachian age.

MF 15. Good radiolarian faunas have been recovered from the Late Sinemurian part of the Kunga Formation. Much of this part of the Kunga has not been studied in detail for other microfauna.

MF 16. The true stratigraphic position of this microfauna is uncertain. It has been recovered from only one locality on Moresby Island, where it appears to be equivalent to the Late Triassic (Norian) although no specimens of **Monotis** were found in direct association.

MF 17. Excellent radiolaria were recovered from limestone samples associated with **Halobia** on Sandilands Island, Skidegate Inlet.

Table 27.1

Stratigraphic distribution of Jurassic fossils and related hydrocarbons

Stages		Lithology and Formations	Notes	Ammonite and Pelecypod Faunas	Micro-fauna: Faunal Assemb.	Forams	Radiolaria	Ostracods	Hydrocarbons: bitumen/dead oil	Porosity P_F, P_G	Source Beds
Callovian	U	Yakoun Formation (Upper)									
	M		A	Kepplerites spinosum	MF 1	X	X_S	X			X
	L			Seymourites Fauna	MF 2	X	X_S	X		P_G	X
Bathonian	U			Iniskinites Fauna							
	M		B								
	L	absent ?									
Bajocian	U	Yakoun Formation (Lower)	C								
	M		D	Stephanoceras	MF 3	X	X_L	X	X	P_F	
			E	sonninids	MF 4	X	X_L				
			F	sonninids							
	L	Maude Formation	G	Graphoceras	MF 5	X	X				X
			H	Tmetoceras							
Toarcian	U		I	Hammatoceras	MF 6	X	X_L				
				Haugia	MF 7	X	X_S	X			
	M			Phymatoceras	MF 8		X_L		X	P_F	
				Dactylioceras	MF 9	X		X			
	L		J	harpoceratids	MF 10	X	X_S	X			
Pliensbachian	U		K	Arieticeras	MF 11	X	X_L				
			L	Fanninoceras	MF 12	X	X_L		X	P_F	X
			M	Dayiceras	MF 13	X	X_L				
	L		N	Tropidoceras	MF 14	X	X_L		X		X
				Tetraspidoceras							
Sinemurian	U	Kunga Formation	O	Entolium baltiatum	MF 15		X_L		X	P_F	X
				Paltechioceras							
				Gleviceras	not studied						
	L		P	Asteroceras							
			Q	Arnioceras							
				Microderoceras							
Hettangian	U		R	not recognized							
	L										
Norian	U										
	M		S	Monotis subcircularis	MF 16	X	X_S	X			X
		not recognized	T								
	L										
Karnian	U		U	Halobia	MF 17		X_L			P_F	
	L	not recognized	V								

Table 27.1 cont.

 shale, limy siltstone, thin limestone

 sandstone, fine grit

 massive limestone

 tuff, volcanic breccia, volcanogenic sediments

 conglomerate

NOTES

A. previously discussed (Tipper and Cameron 1980)
B. base of this section may be much older
C. top of this section may be younger
D. this fauna studied in detail recently by Hall (1975) and by Hall and Westermann (1980)
E. associated with Docidoceras
F. this unconformity involved deep erosion but no apparent angular discordance
G. preliminary field identification; associated with other genera
H. these sections are fault bounded
I. these beds have a rich fauna associated with dicoelitid belemnites
J. possible hiatus as suggested by macrofossils and microfossils
K. unconformity indicated; no latest Pliensbachian ammonites found
L. Fanninoceras ranges up to Harpoceras; a single specimen of Amaltheus is associated
M. slight angular discordance, erosion
N. Dayiceras was previously identified as Uptonia
O. wherever position of this pelecypod is well established it is at top of Sinemurian
P. thinly interbedded fine tuff and siltstone
Q. may extend lower
R. reportedly represented by unfossiliferous beds (Sutherland Brown, 1968, p. 60)
S. associated with ammonites
T. may be present
U. massive grey limestone
V. probably represented by Karmutsen volcanics

Radiolaria X_S = generally poorly preserved specimens recovered from shales

X_L = well preserved specimens recovered from acidization of limestones

Porosity P_G = intergranular porosity

P_F = fracture or vuggy porosity

Stratigraphy of the Maude Formation

The Maude Formation subsequent to its original, rather liberal, definition by MacKenzie (1916) has also been interpreted by McLearn (1949) and Sutherland Brown (1968). The most restricted interpretation, as proposed by Sutherland Brown will serve as the nucleus for this discussion.

In 1968 the Maude Formation in its type locality included beds of Pliensbachian and Lower Toarcian age. This sequence contains the ammonite faunas in this sequence range from the occurrence of **Tetraspidoceras** to that of the harpoceratids (Table 27.1). During the 1978 field season the authors collected ammonites from recessive grey shale stratigraphically above the harpoceratid beds, which have subsequently been assigned Middle and Late Toarcian ages. Contacts between this shale and other parts of the Maude and Yakoun formations are best exposed on the banks of small stream which run onto the tidal flats of southern Maude Island and indicate at least in the type area that the upper part of the Maude Formation is highly faulted. Similar occurrences of Upper Toarcian grey shale are exposed on the tidal flats of Whiteaves Bay on Moresby Island, and are very well exposed on the banks of the Yakoun River on Graham Island.

Additional field work in 1979 and 1980 on Graham Island on the Yakoun River and the prominent bluff 0.5 km east of there necessitates the expansion of the Maude Formation to include beds of later Toarcian, Early Bajocian and early Middle Bajocian ages. The **Hammatoceras** and belemnite sandstone, which conformably overlies the Upper Toarcian grey shale, is well exposed in several localities on and near Yakoun River. About 100 m of dark grey shale, thin sandstone and limestone occur above the **Hammatoceras** beds in stream-cut exposures on the western face of a prominent bluff 0.5 km east of Yakoun River. Ammonite faunas recovered from the latter have been tentatively assigned Lower and early Middle Bajocian age. Stratigraphic relationships to the underlying Toarcian beds and the overlying Yakoun Formation appear to be unconformable, but contacts are somewhat obscured by faulting.

Hydrocarbons

During the course of field and laboratory examination of strata and rock samples many occurrences of bitumen and oil stain were noted. Bitumen has been observed in fractures and cavities or vugs in the upper Kunga Formation, the lower

and upper Maude Formation, and the Yakoun volcanogenic rocks. Minor seeps have also been observed in both the Kunga and Maude formations. Possible source beds of these hydrocarbons are outlined in Table 27.1, in this case reflecting the stratigraphic distribution of dark organic-rich shales. Most of the hydrocarbon occurrences observed in the field were in the form of fracture or vug infill. Jurassic sandstones, although thin in outcrop and showing no visible evidence of oil stain, indicate some intergranular porosity in field observations. It is possible that these sands could prove to be potential reservoir rocks in subsurface to the east, especially if a more proximal facies equivalent were encountered.

Similar occurrences of bitumen and oil stain have been noted in younger rocks of the Queen Charlotte Islands and vicinity. These include tar occurrences in the Tertiary Masset volcanics (MacKenzie, 1916) and oil stain in subsurface of the Tertiary Skonum Formation (Sutherland Brown, 1968; Shouldice, 1971). Oil stain and bitumen have also been noted by various geologists in the Cretaceous Haida and Honna formations.

It appears therefore that the entire sedimentary sequence from Late Triassic to Late Tertiary of the Queen Charlotte Islands and vicinity show one or more of the necessary characteristics of a petroliferous basin, namely source beds, oil show and/or bitumen, or porosity. Further exploration in the area will indicate whether the hydrocarbons have been entrapped, whether the entrapping medium has acceptable porosity and permeability and whether any accumulated hydrocarbons can be considered to be economically recoverable.

References

Frebold, H.
1979: Occurrence of the Upper Bathonian ammonite genus **Iniskinites** in the Queen Charlotte Islands, British Columbia; in Current Research, Part C, Geological Survey of Canada, Paper 79-1C, p. 63-66.

Hall, R.L.
1975: Sexual Dimorphism in Jurassic ammonites from the Queen Charlotte Islands; Geoscience Canada, v. 2, no. 1, p. 21.

Hall, R.L. and Westermann, G.E.G.
1980: Lower Bajocian (Jurassic) cephalopod faunas from Western Canada and proposed assemblage zones for the Lower Bajocian of North America; Palaeontographica Americana, v. 9, no. 52.

Mackenzie, J.D.
1916: Geology of Graham Island; Geological Survey of Canada, Memoir 88.

McLearn, F.H.
1927: Some Canadian Jurassic Faunas; Royal Society Canada, Transactions 3rd Ser., v. 21, sec. IV, p. 61-73.

1929: Contributions to the Stratigraphy and Paleontology of Skidegate Inlet, Queen Charlotte Islands, B.C.; National Museum of Canada, Bulletin 54.

1949: Jurassic Formations of Maude Island and Alliford Bay, Skidegate Inlet, Queen Charlotte Islands, British Columbia; Geological Survey of Canada, Bulletin 12.

Shouldice, D.H.
1971: Geology of the Western Canadian Continental Shelf; Bulletin of Canadian Petroleum Geology, v. 19, no. 2, p. 405-436.

Sutherland Brown, A.
1968: Geology of the Queen Charlotte Islands; British Columbia Department of Mines and Petroleum Resources, Bulletin 54.

Tipper, H.W.
1975: Taseko Lakes (92C) and Smithers (93L) map-areas, British Columbia; in Report of Activities, Part A, Geological Survey of Canada, Paper 75-1A.

1976: Biostratigraphic Study of Mesozoic Rocks in Intermontane and Insular Belts of the Canadian Cordillera, British Columbia; in Report of Activities, Part A, Geological Survey of Canada, Paper 76-1A.

1977: Jurassic studies in Queen Charlotte Islands, Harbledown Island and Taseko Lakes area, British Columbia; in Report of Activities, Part A, Geological Survey of Canada, Paper 77-1A.

Tipper, H.W. and Cameron, B.E.B.
1979: Jurassic biostratigraphy of Skidegate Inlet, Queen Charlotte Islands; in Current Research, Part A, Geological Survey of Canada, Paper 79-1A.

1980: Stratigraphy and Paleontology of the Upper Yakoun Formation (Jurassic) in Alliford Bay Syncline, Queen Charlotte Islands, British Columbia; in Current Research, Part C, Geological Survey of Canada, Paper 80-1C.

28. SNOWSHOE FORMATION, CENTRAL BRITISH COLUMBIA

Project 680066

L.C. Struik
Cordilleran Geology Division, Vancouver

Struik, L.C., Snowshoe Formation, central British Columbia; in Current Research, Part A, Geological Survey of Canada, Paper 81-1A, p. 213-216, 1981.

Abstract

Re-examination of the area underlain by the Snowshoe Formation in the Wells map area (93 H/4), has resulted in a revamping of the stratigraphy of the Snowshoe and related formations. The present stratigraphic interpretation suggests that the Antler Formation is para-autochthonous with respect to the Snowshoe Formation and that the Snowshoe Formation is older than parts of the Antler Formation.

Introduction

The area underlain by the Snowshoe Formation is being remapped because previous interpretations have not agreed on the age of these rocks, nor their stratigraphic relationship to surrounding areas, nor their internal stratigraphy, nor the nature of their major structures. The primary purpose of this project is to clarify these uncertainties, explain aspects of the evolution of the Canadian Cordillera, and provide stratigraphic information which can be used in mineral exploration. The following preliminary information is from two months of field work in the summer of 1980.

Stratigraphy

The map area shown in Figure 28.1 is underlain by nine major units, including the following five previously defined formations: (1) the Snowshoe Formation as defined by Holland (1954) and Sutherland Brown (1957) or the Kaza Group of Campbell et al. (1973); (2) the Midas Formation of Sutherland Brown (1957) or the Isaac Formation of Campbell et al. (1973); (3) the Guyet Formation of Struik (1980); (4) the Antler Formation of Sutherland Brown (1957), Campbell et al. (1973) and Struik (1980) and (5) unnamed Triassic strata of Campbell et al. (1973). Of these five formations, only the Antler Formation and the unnamed Triassic strata are mapped as originally defined. Figure 28.4 is an approximate stratigraphic cross-section showing the lateral variation of units 1 to 6.

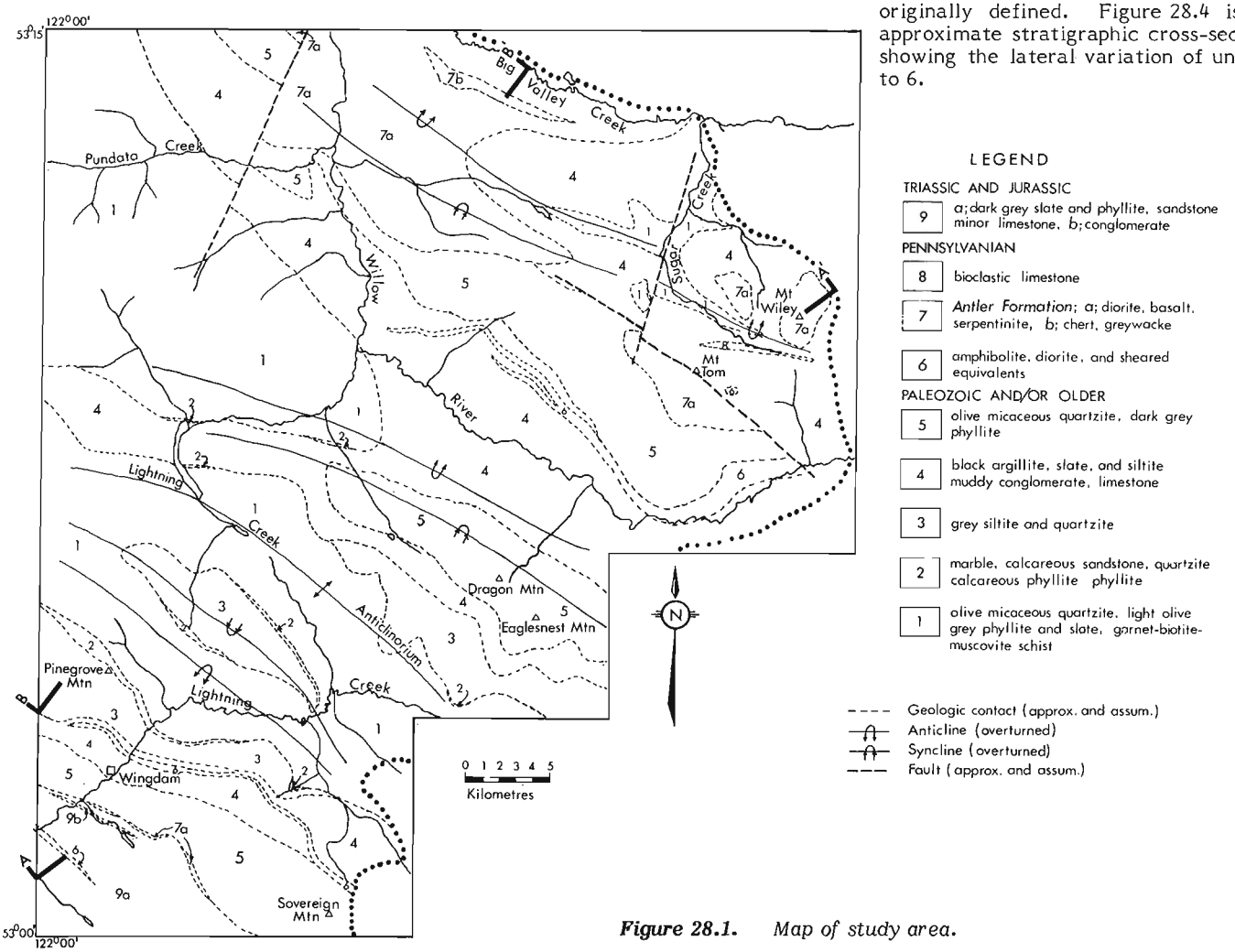

Figure 28.1. *Map of study area.*

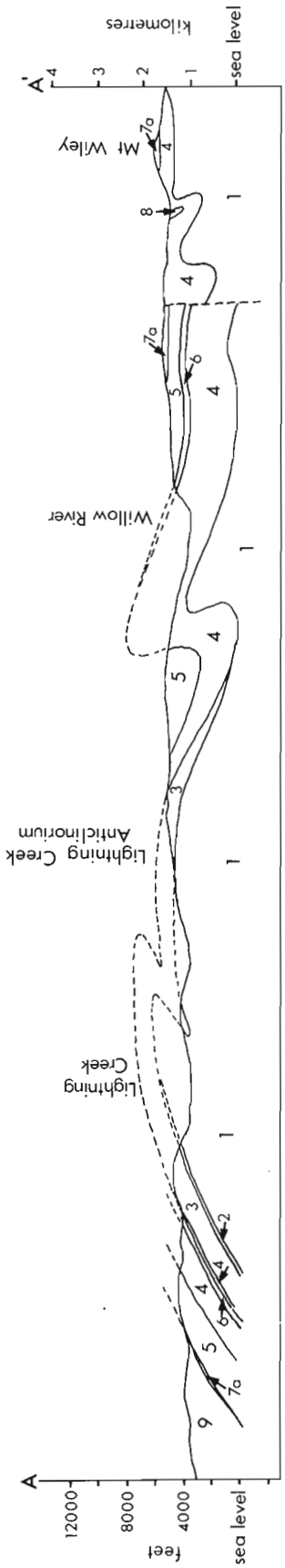

Figure 28.2. Cross-section A-A'. Stratigraphic units and location of section are described in Figure 28.1. Vertical equals horizontal scale.

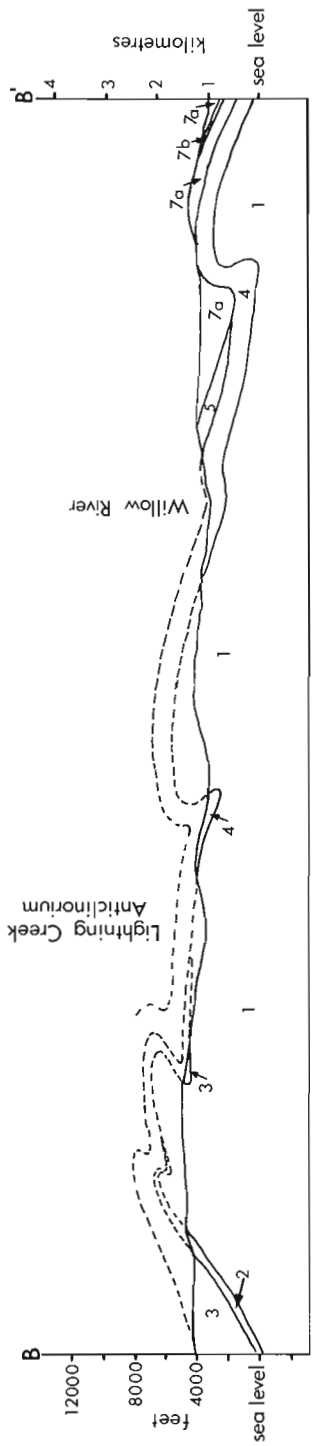

Figure 28.3. Cross-section B-B'. Stratigraphic units and location of section are described in Figure 28.1. Vertical equals horizontal scale.

Unit 1

These rocks were originally included in the Snowshoe Formation as defined by Holland (1954) and Sutherland Brown (1957) or the Kaza Group as defined by Campbell et al. (1973). They consist of micaceous, poorly-sorted quartzite, various metamorphic grades of pelite, and conglomerate. Most of these rock types weather brown to olive grey and are olive to olive grey on fresh surfaces. Dark grey pelite is limited, occurring near the top of the unit. The quartzite and conglomerate both have clasts of glassy light grey, and minor blue quartz and some feldspar. In addition the conglomerate has white quartzite clasts which outnumber other clast types. The conglomerate occurs near the top of the unit. The quartzite and pelite are interbedded on a 0.5 to 2.5 m scale throughout the unit's estimated minimum thickness of 300 m.

Unit 2

Rocks of unit 2 have been previously mapped as Snowshoe Formation or Kaza Group. Marble, calcareous clastics and pelite form this thin, discontinuous unit. Limy sandstones, with quartz clasts similar in composition to those in the quartzites of unit 1, and interbedded limy, brown weathering green phyllite are the most common constituents of the unit. Light grey weathering, white to grey marble occurs as 1 m to 20 m bands in some localities, such as, at Pinegrove Mountain and at the head of Kee Khan Creek. At Pinegrove Mountain, where the unit is approximately 100 m or more thick, marble bands are interbedded with dark grey and green slates.

Unit 3

This southwestward thickening unit consists of quartzite, micaceous quartzite, siltite and pelite. It has been previously included in the Kaza Group of Campbell et al. (1973). Green or chrome-green phyllite is gradational with the calcareous phyllite of unit 2. At the headwaters of Dilman Creek, this green phyllite contains 1 to 4 per cent fine magnetite crystals. The phyllite is gradational to olive grey micaceous siltite which in turn grades upsection to light grey clean fine- to moderately coarse-grained quartzite. The western facies of this unit, as shown in section A of Figure 28.4 is much thicker than the eastern facies.

Unit 4

The black rocks of this unit have been previously included in the Isaac Formation by Campbell et al. (1973). Correlatives of this unit, in the gold-bearing rocks, around the towns of Wells and Barkerville, were mapped as Midas Formation by Sutherland Brown (1957). The unit is dominated by black pelite, siltite and muddy conglomerate. Minor components include grey-weathering, light grey marble and quartzites and pelites similar to those in unit 5.

Muddy conglomerate, found mostly at the base of the unit, has grey, dark grey and minor blue glassy quartz clasts supported in a black pelite matrix. Clast sizes range from coarse sand to granule and vary from 10 to 60 per cent of the rock volume. The majority of the unit consists of thin-bedded siltite, argillite, slate and phyllite. These rocks interdigitate with micaceous quartzites in the area of Pinegrove Mountain and Devils Canyon. Thin light grey marble horizons occur near the top of the unit. These marbles are interlayered with dark grey pelite which distinguishes them from the green pelite-bearing marbles of unit 2.

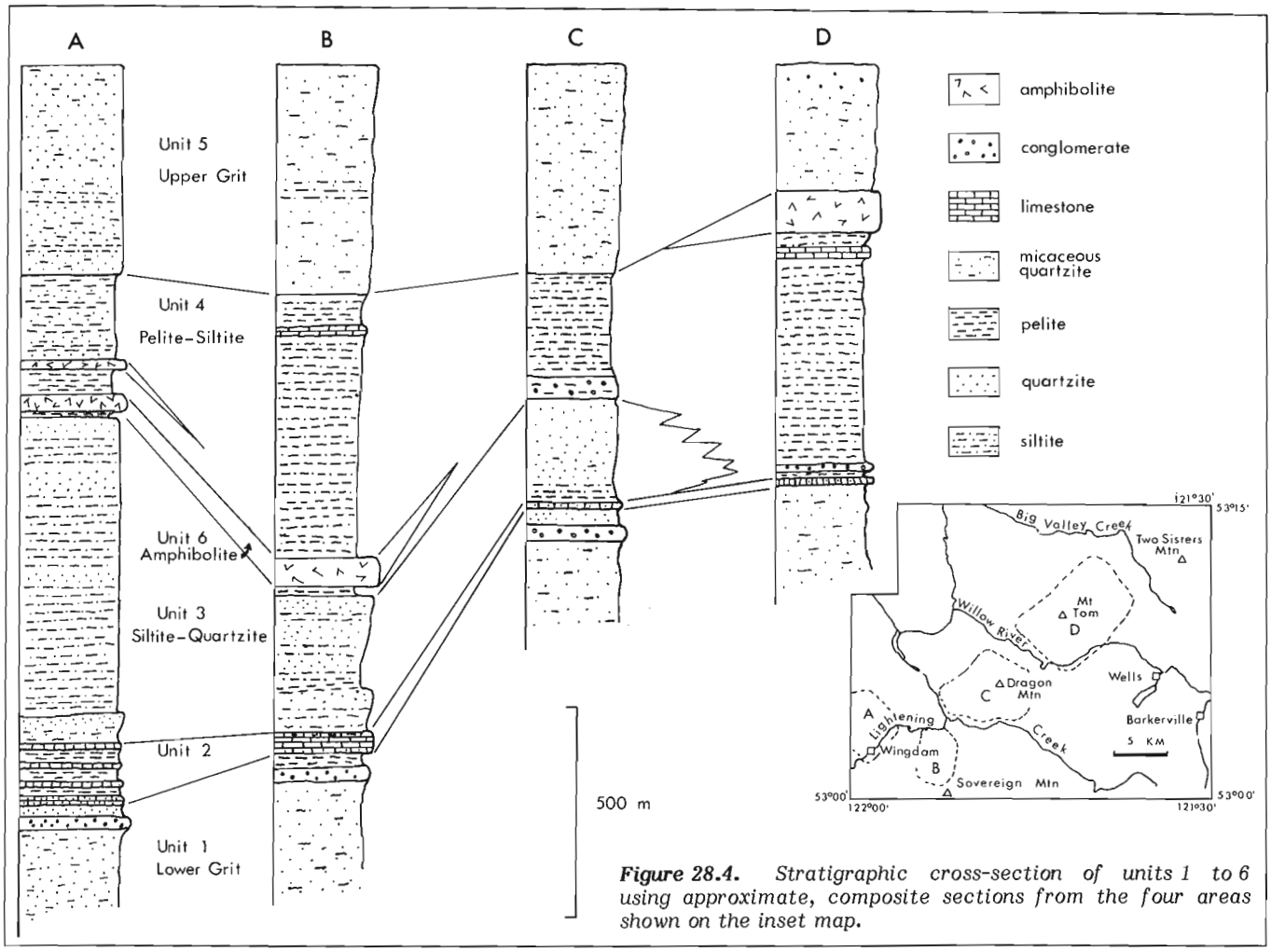

Figure 28.4. *Stratigraphic cross-section of units 1 to 6 using approximate, composite sections from the four areas shown on the inset map.*

Unit 5

Previously mapped as Snowshoe Formation by Sutherland Brown (1957) and as Kaza Group by Campbell et al. (1973), unit 5 consists of micaceous quartzite, mylonite, siltite and dark grey pelite. Olive grit, similar to grit within unit 1, is interbedded with grey siltite to moderately coarse grained quartzite and dark grey and olive phyllite and slate. The grit has clasts of glassy grey and minor blue quartz and some white quartz and feldspar. Bedding within the unit is thinner and more obvious than in unit 1 (Fig. 28.6). The mylonite occurs at the contact with unit 7.

Unit 6

Amphibolite and diorite of unit 6 may be intrusive into units 3, 4 and 5 and resemble rocks of the Antler Formation. The unit has been previously mapped as Kaza Group by Campbell et al. (1973). Diorite of the unit is gradational to well foliated equivalents, resembling the finer grained amphibolite. Coarse-grained amphibolite has 0.5 to 1.5 cm knots of partly chloritized amphibole in a well foliated chlorite and feldspar matrix. Commonly the well foliated amphibolite has glassy grey and opaque white quartz veinlets parallel to the foliation.

Thin amphibolite bands appear intrusive where seen in contact with rocks of unit 5 in the Ramos and Yuzkli Creek area. This implies that the amphibolites are younger than units 3, 4 and 5 which they intrude. If the rocks of unit 6 are feeders to, or are otherwise correlative with the Antler Formation, units 1 to 5 are older than the Antler Formation. The total time span of the Antler Formation is unknown, but it is in part Pennsylvanian.

Unit 7

Unit 7 includes the Antler Formation, which has been described by Sutherland Brown (1957), Campbell et al. (1973) and Struik (1980). Much of the lower contact of the Antler Formation is sheared as displayed by cherty mylonite, serpentinite, foliated diorite and amphibolite.

Unit 8

The bioclastic limestone of unit 8 is part of the Pennsylvanian bioclastic unit of the Greenberry Limestone Member of the Guyet Formation (Struik, 1980). It is in contact with unit 4 but the nature of this contact is unresolved.

Unit 9

Dark grey slate dominates this unit of slate, siltstone, sandstone, conglomerate and minor limestone. The unit outcrops only in the southwest corner of the map area, but is reported to be part of a major belt of rock following the western margin of the Omineca Belt (Campbell et al., 1973, p. 60, and Tipper, personal communication, 1980). In the area of Wingdam a conglomerate near the base of the unit consists of pebbles and cobbles of quartzite, phyllite and minor granitic rocks in a matrix of quartz sandstone which grades

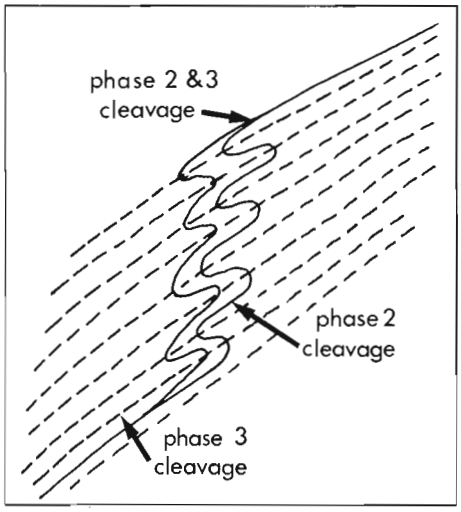

Figure 28.5. *The relationship between phase 2 and 3 cleavage.*

Figure 28.6 *Bedding style characteristic of unit 5.*

laterally to dolomitic fine, dark, muddy sandstone. The conglomerate grades upsection to limy, muddy siltstone and this is overlain by dark grey slate. Thin beds of slate are defined by alternating dark grey and biscuit weathering colours. Local deformation has produced phyllite within the slate belt. Light olive brown, medium-grained sandstone and a darker, muscovite, quartz sandstone are found locally near underlying Antler Formation serpentinite. Fossil fragments within the light olive-brown sandstone have been preliminarily identified by H.W. Tipper as aptyki and belemnite. Tipper believes the assemblage is indicative of the Lower Jurassic. The overlying slate, however, is considered Upper Triassic in age and the relationship would imply thrust faulting.

Structure

All folds trend northwest-southeast and are open, tight or isoclinal. The dominant structural feature is the Lightning Creek Anticlinorium (Fig. 28.1). The stratigraphic interpretation presented here shows the fold is anticlinal (Fig. 28.2, 28.3). Overturned folds on either side of the axis verge towards the axis. The axial planar cleavage associated with these flanking folds appears to become bedding parallel through the core of the Lightning Creek anticline, such that the cleavage forms an arch rather than a fan.

There are at least four phases of cleavage development, the last three of which are associated with recorded folds. Cleavages of the different phases are seen to merge into each other such that they cannot be differentiated. Figure 28.5 shows this relationship for the second and third phase of cleavage. The coincidence of all phases of cleavage, in a composite sense, may be the result of a common stress system which was either constantly or periodically active over considerable geologic time.

The detachment zone at the base of the Antler Formation is the largest fault of the area. It predates high-angle strike faults which are cut by late transverse faults.

Discussion

The stratigraphic succession between units 1 and 5 appears to be continuous, however, the possibility of large scale thrusting cannot be discounted. Indeed, it is recognized that many small scale strike and transcurrent faults have been overlooked due to the poor bedrock exposure and nature of the mapping. Accepting the stratigraphy as given in Figure 28.4, the Snowshoe Formation includes the Midas Formation as defined by Holland (1954). Similarly within the definitions of Campbell et al. (1973) the Kaza Group (Snowshoe) includes within it the Isaac Formation (Midas).

The age of units 1 to 5 is as yet uncertain. They are probably older than parts of the Antler Formation because they are intruded by the rocks of unit 6 which may be feeder horizons to the Antler Formation. The Antler Formation is in part Pennsylvanian but may also include older or younger rocks.

The Antler Formation may be thrust eastward but perhaps only in a para-autochthonous sense. The correlation of unit 6 with the Antler Formation would link older units with the Antler. Thrusting of the Antler Formation is older than the major folding event which involved the lower Antler contact in the Yuzkli Creek area (Fig. 28.3).

References

Campbell, R.B., Mountjoy, E.W., and Young, F.G.
1973: Geology of McBride map-area, British Columbia; Geological Survey of Canada, Paper 72-35.

Holland, S.S.
1954: Yanks Peak – Roundtop Mountain area, British Columbia; British Columbia Department of Mines, Bulletin 34.

Struik, L.C.
1980: Geology of the Barkerville-Cariboo River area, central British Columbia; unpublished Ph.D. thesis, University of Calgary.

Sutherland Brown, A.
1957: Geology of the Antler Creek Area, Cariboo District, British Columbia; British Columbia Department of Mines, Bulletin 38.

29. THE CACHE CREEK GROUP AND CONTIGUOUS ROCKS NEAR CACHE CREEK, BRITISH COLUMBIA

Project 800029

K.R. Shannon[1]
Cordilleran Geology Division, Vancouver

Shannon, K.R., The Cache Creek Group and contiguous rocks near Cache Creek, British Columbia, in Current Research, Part A, Geological Survey of Canada, Paper 81-1A, p. 217-221, 1981.

Abstract

The Cache Creek Group near Cache Creek, British Columbia is divided into a mélange unit and an overlying greenstone unit. The mélange probably formed by sedimentary processes but was modified by later tectonism. The Cache Creek Group is stratigraphically overlain by the Upper Triassic Nicola (?) Group, with the contact between the two modified by later faulting.

Introduction

This report describes the geology of the Cache Creek Group and associated rocks near Bonaparte River from Ashcroft Manor to 20 Mile House (Fig. 29.1), is a continuation of earlier work to the south by Ladd (1978) and Grette (1978) and was done concurrently with regional mapping in the Ashcroft area (Monger, 1981). The Cache Creek Group as described by Duffell and McTaggart (1952) consists of an eastern, central and western belt. Work on this project was mainly in the eastern belt and the east margin of the central belt (Marble Canyon Formation).

The Cache Creek Group described in this study is divided into three major units: (1) a mélange of blocks of limestone, chert, greenstone and tuff in a variably sheared chert-argillite matrix; (2) a greenstone unit with vesicular basalt flows, pillowed basalt, gabbro and basalt breccias, and (3) the Marble Canyon Formation, composed of limestone, bedded radiolarian chert, tuff, argillite and greenstone. Results from this study combined with known ages from earlier work indicate a Pennsylvanian to Triassic age for these rocks (Danner and Nestell, 1966; Danner, 1968; Travers, 1978; and Orchard, M. personal communication).

Acknowledgments

Contributions to mapping were made by Derek Brown and Barry Devlin; their assistance was much appreciated. The author wuld also like to thank W.B. Travers, W.R. Danner and J.W.H. Monger for invaluable discussion in the field.

Lithologic Units

Cache Creek Group

1. Mélange Unit This unit comprises blocks of limestone, greenstone, tuffs, bedded radiolarian chert, and siliceous volcanics in a variably sheared matrix of carbonaceous argillites, phyllites, and chert (Fig. 29.2). The blocks range in length from centimetres to hundreds of metres. Commonly the matrix of the mélange is highly sheared, but locally (especially chert-rich zones) it is almost undeformed; deformation in the mélange unit seems in large part to be related to its structural incompetency. All blocks in the mélange correspond to lithologies common in the Cache Creek Group and thus do not appear to be "exotic".

Serpentinites in the mélange unit outcrop mainly along large lineaments visible on airphotos and trending 140° and 360°. Intense shearing and abundant slickensides are characteristic of the serpentinites and indicate their association with fault activity. Crosscutting gabbro dykes in the serpentinite are commonly altered to rodingite.

Chert forms layers 1-5 cm thick, with thin argillaceous partings (ribbon chert), and commonly ranges from grey to black, with minor green, red, and brown varieties. Radiolaria are locally abundant in hand specimens, but are usually visible only in light grey cherts, wherein they form clear glassy spheres <1 mm in diameter. Intense folding is common in the chert (Fig. 29.3), and appears to be due partly to sediment slumping and partly to brittle deformation.

Intensive recrystallization obliterated most original textures in the limestone blocks, leaving a grey and white, mottled, coarsely crystalline rock with rare fusulinids and crinoid columnals. Some blocks are slightly dolomitized (up to 10 per cent) and may give a strong bituminous odour on fresh surfaces.

2. Greenstone Unit This unit appears to stratigraphically overlie the mélange unit and comprises pillowed basalt, vesicular basalt flows, gabbro, and basalt breccia (Fig. 29.4). Basalt breccias are common, with light green clasts often speckled with dark green phenocrysts (augite?) or more often green to black amygdaloidal chlorite splotches. Pillowed basalt is in stratigraphic contact with ribbon chert of the mélange unit north of Carquile (Loc. 1); the contact is parallel to bedding in the chert and is marked by a 10-20 cm bed of dense black fetid limestone.

3. Marble Canyon Formation The Marble Canyon Formation was mapped by Duffell and McTaggart (1952) as mostly limestone. Remapping revealed a wide variety of lithologies, including bedded radiolarian chert, tuff, argillite, and greenstone, and in the map area this unit is probably less than 50 per cent limestone; these limestones do not appear to attain thicknesses greater than 100 m.

One of the most fossiliferous rocks in the Marble Canyon Formation is a clastic limestone with fragments of micrite, fusulinids, crinoid columnals and other fossil debris (bryozoans, bivalves, and echinoderm plates) in a fine grained tuffaceous (?) matrix. Abrasive rounding of the fusulinids and other fossils indicates transport of the fossil debris to the site of deposition.

Nicola (?) Group

Intimately associated with the Cache Creek Group rocks is a siliceous, mainly volcaniclastic unit which was mapped as Nicola Group by Ladd (1978) and Grette (1978). It was assigned an Upper Triassic age by Travers (1978) and Grette (1978). This unit ranges from dark green to blue-green, with locally abundant quartz phenocrysts (1-3 cm across). Most units in this package are distinctively siliceous. North of Cache Creek the predominant lithology is a blue-green siliceous tuff, with minor grey and white banded limestone beds. South of Cache Creek (Loc. 2) Nicola (?) volcaniclastic rocks appear to be in fault contact with serpentine of the Cache Creek Group; chert clasts in this volcaniclastic unit contain radiolaria (Fig. 29.5). On the

[1]Department of Geological Sciences, University of British Columbia.

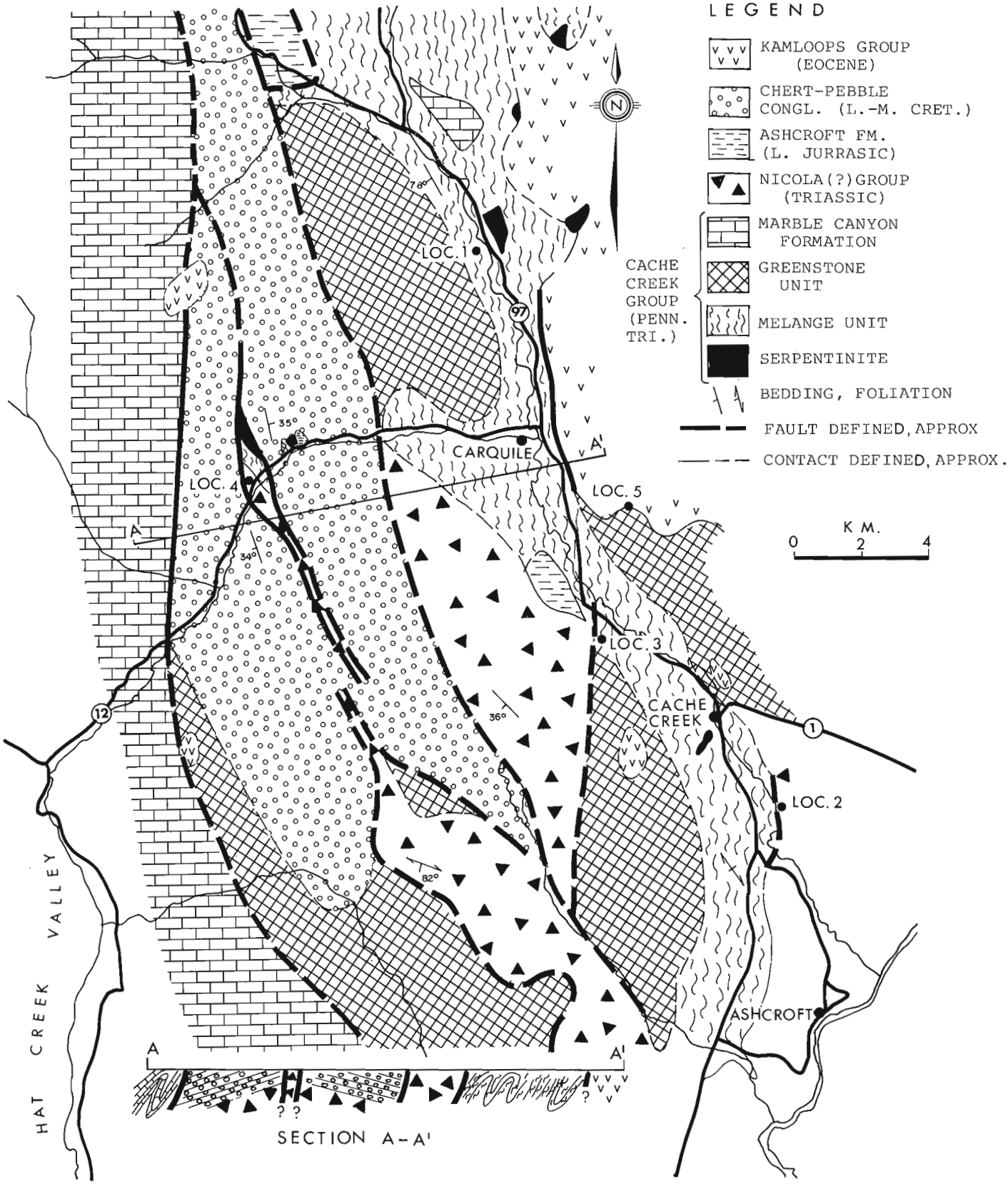

Figure 29.1. *Geological map and cross-section of the area between Cache Creek and Hat Creek valley.*

Figure 29.2. *Block of Pennsylvanian limestone in a sheared matrix of Permo-Triassic chert-argillite, at Cache Creek.*

Figure 29.3. *Highly folded ribbon cherts, north of Carquile.*

Bonaparte Indian Reserve (Loc. 3) a large (>30 m across) outcrop of quartz-eye porphyry apparently forms a block in the Cache Creek mélange unit.

Sediments become more and more common towards the top of the Nicola (?) section. South of Cache Creek the boundary between upper Nicola (?) sediments and Lower Jurassic Ashcroft Formation appears to be gradational (W.B. Travers, personal communication). The narrow outcrop of Nicola (?) Group along Hat Creek road (Loc. 4) includes both volcaniclastics and siltstone and claystones.

Ashcroft Formation

North of the Bonaparte Indian Reserve is a large area of brown to grey conglomerate and siltstone. Clasts of the conglomerate are mostly granitic, porphyritic volcanics and limestone with some chert, argillite and greenstone (Fig. 29.6). Clasts are well rounded to subrounded and the sand matrix commonly forms more than ten per cent of the rock. Poorly developed foliation is common in the interbedded siltstones. This sedimentary unit outcrops in several other localities in the map area, and on lithological grounds is correlated with the Lower Jurassic Ashcroft Formation; no fossils were found in it.

Chert-Pebble Conglomerate Unit

Two conglomerate-sandstone units that outcrop along Hat Creek road were mapped by Duffell and McTaggart (1952) as Coldwater Formation of Eocene age. The lowest unit is a red calcareous conglomerate in which clast lithology depends on the nature of the Cache Creek Group bedrock. Near the Marble Canyon Formation the clasts are commonly limestone, some with visible fusulinids. However, in another locality (near the gravel pit on Hat Creek road) the red conglomerate contains no limestone clasts but is predominantly greenstone. Clasts are quite angular, range up to 20 cm across, and are usually set in a white calcite matrix. One feature of this conglomerate is locally abundant red chert clasts, a colour variety known, but not common, in Cache Creek Group cherts. The age of this conglomerate is unknown, although the large angular clasts and direct relationship of clast lithology to adjacent bedrock suggest that the unit formed on the Cache Creek Group paleosurface, with little subsequent transport of material.

Overlying this unit is a second, commonly buff, conglomerate-sandstone member. This unit is more mature both lithologically and texturally than the red conglomerate-sandstone. Predominant lithology is grey to black chert pebbles (usually >50%); other clasts include aphanitic volcanics, fine grained sediments and greenstone. Clasts are well rounded and most are less than 3 cm across. Sandstones interbedded with the conglomerates appear to be composed chiefly of small chert fragments. Palynomorphs examined both by G. Rouse (University of British Columbia), and by W.S. Hopkins (Geological Survey) show the age to be Upper Albian or Cenomanian.

Kamloops Group

This is the youngest unit in the map area and has been assigned an Eocene age by Duffell and McTaggart (1952) and Church (1975). It consists mainly of agglomerates, lahars and vesicular basalt-andesite, with some sandstone and ashfall tuff units. Kamloops Group sandstone unconformably overlies Cache Creek Group greenstones at Locality 5, but in most other places it was in fault contact.

Figure 29.4

Pillowed basalt with common dark grey inter-pillow limestone, north of Carquile. Note pencil at left centre for scale.

Figure 29.5

Nicola (?) volcaniclastic unit with radiolarian chert clasts probably derived from Cache Creek Group strata. South of Cache Creek.

Figure 29.6

Lower Jurassic Ashcroft conglomerate from north of Cache Creek. Dark clasts are chert, large light clast is limestone.

Conclusions

1. The association of radiolarian ribbon chert, pillowed basalt gabbro, ultramafic rock and limestone indicate an "oceanic" environment for deposition of the Cache Creek Group. Landmasses were either a long distance away or separated by a sediment trap, as the Cache Creek Group contains little terrigenous material. Parts of the depositional basin must have been shallow enough to allow the formation of small carbonate banks with abundant growth of crinoids and fusulinids. There was enough relief in the basin to cause formation of limestone turbidites. Deeper parts of the basin and its margins were characterized by deposition of black muds and radiolarian cherts; however, several outcrops in the map area have radiolarian chert interbedded with limestone, indicating that the chert had a wider range of depositional environments. There was abundant volcanism in the basin, mostly pillowed basalt, basalt breccia and vesicular basalt flows; aphanitic basalt is not common.

2. Thinly laminated chert-argillite of the mélange unit is interpreted as representing a deeper water environment because of lack of carbonate (except as blocks) and evidence of pelagic sedimentation (radiolaria and thin rhythmic bedding). Limestone blocks in the mélange unit contain fusulinids and algal structures (W.R. Danner, personal communication) indicating their shallow water provenance. Greenstones in the mélange unit contain clasts of fusulinid limestone as well as interpillow carbonate (but no chert-argillite), again indicating deposition in relatively shallow water. Therefore the mélange probably formed by blocks of shallow water facies rocks sliding into deeper water where deposition of chert and argillite was predominant. A term for mélange formed in this manner would be talus mélange. Olistostrome would imply transport of the chert-argillite matrix, which has not occurred. Tectonism has sheared the mélange unit and caused rotation of blocks in the mélange; this is thought to be a later event, as the Triassic Nicola (?) Group near Martel, south of the map area, is also extensively sheared in a manner similar to the mélange unit.

3. The widespread association of Cache Creek Group rocks and Nicola (?) Group rocks, discovery of radiolarian chert clasts in the Nicola (?) volcaniclastic unit and occurrence of Nicola (?) quartz-eye porphyries as blocks in the mélange unit suggests that the Cache Creek Group was in stratigraphic contact with the Nicola (?) Group in the Upper Triassic; contacts between the two have been modified by later faulting.

References

Church, B.N.
1975: Geology of the Hat Creek coal basin (93I 13E) ; in Geology in British Columbia; British Columbia Ministry of Mines and Petroleum Resources, p. G99-G118.

Danner, W.R. and Nestell, M.K.
1966: Biostratigraphy of the Cache Creek Group, Pennsylvanian-Permian, in the type area, British Columbia, Canada; (Abstract), in Geological Society of America Annual Meeting in San Francisco, 1966, p. 49-50.

Danner, W.R.
1968: The Cache Creek Complex in southern British Columbia and northern Washington; (Abstract), in Geological Association of Canada Annual Meeting in Vancouver, 1968, p. 10-11.

Duffell, S. and McTaggart, K.C.
1952: Ashcroft map-area, British Columbia; Geological Survey of Canada, Memoir 262, 122 p.

Grette, J.F.
1978: Cache Creek and Nicola Group near Ashcroft, British Columbia; University of British Columbia, unpublished M.Sc. thesis, 88 p.

Ladd, J.H.
1978: Mesozoic overthrusting of oceanic crust in south-central British Columbia; Cornell University unpublished M.Sc. thesis, 96 p.

Monger, J.W.H.
1981: Geology of parts of western Ashcroft map area, southwestern British Columbia; in Current Research, Part A, Geological Survey of Canada, Paper 81-1A, Report 24.

Travers, W.B.
1978: Overturned Nicola and Ashcroft strata and their relation to the Cache Creek Group, southwestern Intermontane Belt, British Columbia; Canadian Journal of Earth Sciences, v. 15, p. 99-116.

30. **WESTERN MARGIN OF THE OMINECA BELT AT QUESNEL LAKE, BRITISH COLUMBIA**

EMR Research Agreement 84-4-80

C.J. Rees[1]
Cordilleran Geology Division, Vancouver

Rees, C.J., Western margin of the Omineca Belt at Quesnel Lake, British Columbia; in Current Research, Part A, Geological Survey of Canada, Paper 81-1A, p. 223-226, 1981.

Abstract

Field mapping of the boundary between the Omineca Belt and the Intermontane Belt has revealed evidence of a major shear zone, marked by mylonized sedimentary and plutonic rocks immediately east of the boundary, and larger-scale tectonic imbrication on both sides. Immediately overlying the shear zone to its west are mafic and ultramafic rocks and argillites of the Intermontane Belt which are interpreted as representing oceanic terrane. The inferred major thrusting of the Intermontane Belt rocks eastwards over the older Omineca terrane is compatible with recent interpretations of the same boundary in Yukon.

Introduction

The area straddles the boundary between the Omineca Belt and the Intermontane Belt to its west, and is included in the reconnaissance map of Campbell (1978).

The boundary is usually drawn on tectonic maps as a major fault, although on less direct evidence in the southern Canadian Cordillera than to the north. The western boundary of the Omineca Belt in Yukon was recently described by Tempelman-Kluit (1979); he found impressive evidence for major telescoping at the boundary and concluded that Intermontane terrane has been obducted onto Omineca terrane.

The boundary in question is comparatively well-defined and exposed in the Quesnel Lake area, and the writer spent the 1980 field season studying contact relations and evidence for major shearing and a possible suture.

This work forms the basis of a Ph.D. program begun this year at Carleton University. The writer is grateful to Dr. R.L. Brown and Dr. J.M. Moore of Carleton University for their support, supervision and advice during field visits. Thanks are also expressed to Jim Connelly for cheerful and competent assistance in the field. The project and the area of study were suggested by Dr. R.B. Campbell of the Geological Survey of Canada.

Figure 30.1, which summarizes the geology of the area, is based on Campbell (1978) and Tipper et al. (1979), with minor modifications as a result of the summer's mapping. All the geological contacts in the simplified cross-section are regarded as tectonic; no evidence for stratigraphic continuity between any of the major units has been found in either the Omineca Belt or the Intermontane Belt. The section is described from west to east.

Takla Group

The westernmost rocks in the section are designated Upper Triassic to Lower Jurassic Takla Group, following Tipper et al. (1979). These comprise mainly volcaniclastic and volcanic rocks of basaltic to andesitic composition (Campbell, 1971; Bailey, 1976; Morton, 1976), with subordinate conglomerate, sandstone, shale and limestone. Plant remains found in shale may permit more precise dating of the sediments. No mature continentally derived clastic lithologies were found, and the overall assemblage is compatible with formation in an island-arc environment (see Wheeler and Gabrielse, 1972) or possibly an intraplate rift setting (Morton, 1976).

The rocks are fractured on all scales, mainly along discrete shear zones and faults, where there has been low grade alteration. Some are steeply dipping, but the rocks lack penetrative fabric. The metamorphic grade is very low (zeolite facies: Morton, 1976).

Black Phyllite

The informal name describes the dominant lithology of this comparatively uniform unit; minor rock types include siltstone, volcaniclastics, carbonate and impure chert. The age of these rocks is unknown, but is thought to be Upper Triassic on the basis of meagre fossils in presumably equivalent rocks outside this area (Campbell, 1971; Campbell and Tipper, 1971).

Because of the fine grain size, low metamorphic grade and virtual absence of stratigraphic markers, the internal structure of the Black Phyllite is obscure. Locally, three cleavages are visible; usually two are present. Bedding is indicated by very fine discontinuous compositional laminations and locally by beds of carbonate or siltstone, but both indicators are probably transposed within the dominant cleavage. The trends of the two main cleavages are similar, being about 130°; the earlier cleavage commonly dips southwest.

Antler Formation

Previous workers correlated this unit with mafic rocks in the Mississippian Slide Mountain Group of the McBride and Bonaparte River areas, on the basis of lithological and chemical similarities (Campbell, 1971; Campbell and Tipper, 1971; Campbell et al., 1973). In the Quesnel Lake area the unit mainly comprises green to green-grey, fine- to medium-grained 'greenstone'. Subtle compositional banding over a few centimetres is typical, parallel to the dominant cleavage. Concordant quartz-carbonate-epidote-magnetite veins and lenses are present locally. Important but uncommon varieties of this unit include coarse grained metagabbro-like lithologies: variably altered ultramafic rocks, now chlorite-talc-serpentine-carbonate and actinolite-tremolite 'schists', and serpentinite breccia. The unit is usually strongly folded and foliated, especially near its margins; structures have a similar style and trend to those in the Black Phyllite.

[1]Department of Geology, Carleton University, Ottawa, Ontario, K1S 5B6

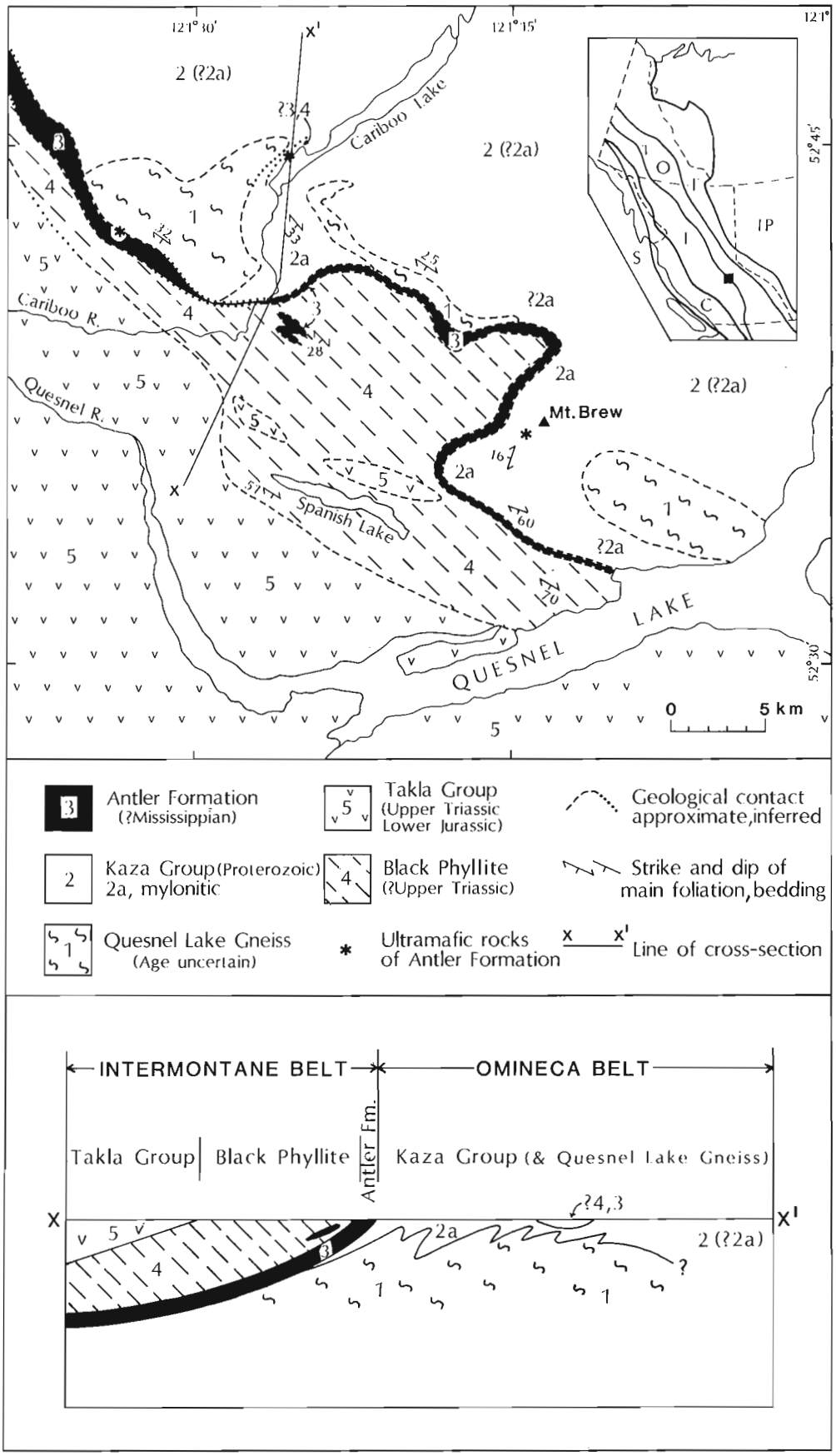

Figure 30.1. *Simplified geological map of the study area and schematic cross-section. Inset shows location of area (black square) in terms of structural provinces of Canadian Cordillera: IP, Interior Platform; F, Foreland Thrust and Fold Belt; O, Omineca Belt; I, Intermontane Belt; C, Coast Plutonic Complex; S, St. Elias and Insular Belt; T, Teslin Suture Zone, where defined by Tempelman-Kluit (1979).*

Higher metamorphic grade equivalents of the Antler Formation are present southeast of Quesnel Lake in the Crooked Lake area (Campbell, 1971) and the Lake Dunford area (Montgomery, 1978). In the latter it forms a klippen within the Omineca terrane and comprises a basically intact section of variably altered dunite, peridotite with cumulate layering, metagabbro and amphibole schist.

Kaza Group

The age of these rocks is speculative, there being no apparent stratigraphic continuity with Proterozoic or Paleozoic strata as defined to the northeast; they are, however, designated Kaza Group following Tipper et al. (1979) (see also Campbell and Campbell, 1970; Campbell and Tipper, 1971; Campbell et al., 1973). In the map area the rocks comprise blue quartz feldspathic grits, psammites, phyllites and semipelitic to pelitic metasediments. Generally, greenschist grade is inferred from hand specimen examination, although localized retrograde alteration of garnet suggests that peak metamorphic grade was higher in the east of the area. Two distinct 'bodies' of felsic orthogneiss occur within the Kaza outcrop, termed the Quesnel Lake Gneiss by Campbell and Campbell (1970); their age is under investigation by Dr. R.L. Armstrong of the University of British Columbia.

Of importance is that nearly all rocks so far mapped in this unit display evidence of mylonization, such as local fine to cryptocrystalline mylonitic fabrics in siliceous and quartzofeldspathic rocks. The mylonization is generally more widespread and more intense towards the unit's southwestern margin with the Antler Formation, which also shows signs of mylonization. The mylonitic fabric forms the dominant structure in the rocks and in most places dips southwest; it is commonly deformed by at least one major phase of later folds. The writer's preliminary impression is that the trend and style of the shear fabric and later minor folds correlate with structures in the Antler Formation and Black Phyllite to the west.

The mylonized Kaza is well exposed around Mount Brew where it extends eastwards from the Antler Formation for at least 3 km; its true thickness may be indeterminate because of later folding or imbrication. Several discontinuous and variously sized lenses of greenstone and meta-ultramafic schists occur within the mylonitic rocks; both are identical to those described within the Antler Formation.

Discussion

The thickness and intensity of the mylonite zone in the westernmost part of the Omineca Belt in the study area seems to indicate a major shear zone adjacent to the lowest unit of the Intermontane Belt, the Antler Formation. Its existence has not previously been emphasized, probably because farther southeast recrystallization has disguised mylonitic textures; Campbell (1971) mentioned cataclastic rocks but inferred localized thrusting of an originally stratigraphic contact.

If the Antler Formation has the composition of primitive tholeiitic basalt (Campbell, 1971), this and the evidence of (metamorphosed) ultramafic and mafic cumulate rocks suggest that the Antler is part of a layer of oceanic crust, and has been thrust eastwards over the western margin of the Omineca Belt. The serpentinite breccia may be some kind of trench mélange, and will be examined for fragments of blueschists. Montgomery (1978) called this association in the Lake Dunford area an obducted ophiolite; there too it overlies a "well defined, west-dipping thrust of unknown displacement" (Montgomery, 1978). If this interpretation is correct, and assuming that the Antler Formation in this area is correlative with the type-Antler Formation in the Black Stuart Synclinorium (in the McBride area to the north; Campbell et al., 1973), it follows that the Slide Mountain Group there is also allochthonous, at least in part.

At its contact with the Black Phyllite in the Cariboo River the Antler greenstone is strongly altered and streaked with orange-brown ankeritic veinlets concordant with the main cleavage, which is subparallel to that in the Black Phyllite. The Black Phyllite may represent hemipelagic carbonaceous mud deposited on oceanic crust; the original contact features are now masked or obliterated by shearing and hydrothermal alteration resulting from the same thrusting and deformation that affected the Antler and the underlying Kaza Group rocks. Carbonate and siltstone within the Black Phyllite may represent distal derivatives of shelf-slope deposits in the Takla volcanic complex to the west, or conceivably from the Omineca shelf-slope to the east. The Takla Group rocks themselves must be in fault contact with the Black Phyllite in the study area, possibly another easterly directed thrust, or a strike-slip fault. Only this can account for the contrast in strain between the two units, which can be observed over a few metres in the field.

Northeast of the mylonite zone the Kaza rocks may be tectonically imbricated, which might explain why previous attempts to define their stratigraphy have been inconclusive. In this connection, the transition between this Kaza terrane and the Windermere-Paleozoic succession north of Cariboo Lake (the southwest limb of the Black Stuart Synclinorium) has important implications, depending on whether it is stratigraphic or whether it is another tectonic contact, perhaps directly related to the 'Antler allochthon'. That this allochthon does extend northeast of its main contact with the Kaza is suggested by an outcrop exposed on Cariboo Lake (Fig. 30.1) which closely resembles Black Phyllite and which includes strongly deformed and altered ultramafic schists and possibly mylonized greenstone. This might be a klippen of Intermontane Belt rocks, although it was originally mapped by Campbell (1978) as Lower Cambrian Midas Formation.

Preliminary impressions are that the dominant fabric is subparallel in all the rocks in the area (except the Takla Group), and is genetically related to horizontal translation and eastward thrusting (obduction) of the Intermontane Belt relative to the Omineca terrane. A process of progressive deformation is envisaged in which primary structures and early formed fold elements are partly reoriented and transposed within the contemporaneous cleavage. Tectonic imbrication probably accounts for complex structural repetitions, especially within the main shear zone, but may also be applicable to the Kaza terrane on a larger scale.

The mylonitic and related cleavages are refolded about commonly steep axial surfaces. This is thought to reflect compression of the shear fabric after mylonization ceased; it may or may not be related to the large regional Z-fold visible in Figure 30.1. Hand specimen examination indicates that garnet crystals are incorporated within the mylonitic fabric and appear to be moderately to severely altered; mica growth is synchronous with the later folds. This implies that mylonization outlasted the peak of metamorphism, which probably correlates with the regional Middle Jurassic event. The significance of the younger, lower grade recrystallization has yet to be determined.

In conclusion, Tempelman-Kluit's (1979) suggestion that the Teslin Suture Zone may be extrapolated southeast to the western margin of the Shuswap terrane is compatible with the writer's observations in the Quesnel Lake area. The horizontal movements involved in the evolution of this boundary zone may be directly related to major décollement structures in the core zone of the Omineca Belt to the east (R.L. Brown, personal communication).

References

Bailey, David G.
1976: Geology of the Morehead Lake area, central British Columbia; Notes to accompany preliminary map no. 20; British Columbia Department of Mines and Petroleum Resources, July 1976, 6 p.

Campbell, K.V.
1971: Metamorphic petrology and structural geology of the Crooked Lake area, Cariboo Mountains, British Columbia; unpublished Ph.D. thesis, University of Washington, 192 p.

Campbell, K.V. and Campbell, R.B.
1970: Quesnel Lake map area, British Columbia (93A); in Report of Activities, April to October, 1969, Geological Survey of Canada, Paper 70-1, Pt. A, p. 32-35.

Campbell, R.B.
1978: Quesnel Lake, British Columbia; Geological Survey of Canada, Open File 574.

Campbell, R.B. and Tipper, H.W.
1971: Geology of Bonaparte Lake map-area, British Columbia; Geological Survey of Canada, Memoir 363, 100 p.

Campbell, R.B., Mountjoy, E.W., and Young, F.G.
1973: Geology of McBride map area, British Columbia; Geological Survey of Canada, Paper 72-35, 104 p.

Montgomery, Scott L.
1978: Structural and metamorphic history of the Lake Dunford map area, Cariboo Mountains, British Columbia: ophiolite obduction in the southeastern Canadian Cordillera; unpublished M.Sc. thesis, Cornell University, 170 p.

Morton, R.L.
1976: Alkalic volcanism and copper deposits of the Horsefly area, central British Columbia; unpublished Ph.D. thesis, Carleton University, 196 p.

Tempelman-Kluit, D.J.
1979: Transported cataclasite, ophiolite and granodiorite in Yukon: evidence of arc-continent collision; Geological Survey of Canada, Paper 79-14, 27 p.

Tipper, H.W., Campbell, R.B., Taylor, G.C., and Stott, D.F.
1979: Parsnip River, British Columbia (Sheet 93); Geological Survey of Canada, Map 1424A (1:1 000 000).

Wheeler, J.O. and Gabrielse, H.
1972: The Cordilleran Structural Province; in Variations in Tectonic Styles in Canada, ed. R.A. Price and R.J.W. Douglas; Geological Association of Canada, Special Paper no. 11, p. 1-81.

31.

STRATIGRAPHY, STRUCTURE, AND METAMORPHISM IN THE SOUTHERN CARIBOO MOUNTAINS, BRITISH COLUMBIA

EMR Research Agreement 86-4-80

Jennifer Pell[1] and P. Simony[1]
Cordilleran Geology Division, Vancouver

Pell, Jennifer and Simony, P., Stratigraphy, structure, and metamorphism in the southern Cariboo Mountains, British Columbia; in Current Research, Part A, Geological Survey of Canada, Paper 81-1A, p. 227-230, 1981.

Abstract

The Hadrynian metasedimentary rocks of the Blue River area, British Columbia, are stratigraphically equivalent to the upper three divisions of the Horsethief Creek Group, in the northern Selkirks. The major mappable structures in the area are folds with steep southwesterly dipping axial surfaces, and with a shallow southeasterly axial plunge. These folds are outlined by an upright stratigraphy. Metamorphism increases from garnet grade in the north to sillimanite grade in the south, with steep isogradic surfaces striking subparallel to major structures. Pressures and temperatures of approximately 4.5 kb[2] and 550°C have been estimated for the sillimanite isograd. To the east of the west-side-down, North Thompson normal fault, metamorphic temperature and pressures at the sillimanite isograd were approximately 50°C and 1.5 kb greater, respectively, implying a throw of about 4 km.

Introduction

During the summer of 1980, Hadrynian metasedimentary rocks of the Southern Cariboo Mountains, which border on the Shuswap Metamorphic Complex, were mapped at a scale of 1:12 000. These metasedimentary rocks were originally mapped by Campbell (1968) as part of the Hadrynian Kaza Group, as they appear to pass westward under rocks clearly belonging to the Kaza, and they include lithologies, such as feldspathic granule conglomerate ("grit"), and mica schist, which are typical of the Kaza Group.

The Hadrynian metasedimentary strata of the Northern Monashee Mountains, on the east side of the North Thompson – Albreda Valley were previously shown to belong to the Horsethief Creek Group (Ghent et al., 1977; Morrison, 1979; Poulton and Simony, in press) and to correlate well with the Horsethief Creek strata of the northern Selkirks (Brown et al., 1978) (Table 31.1). Brown et al. (1978) proposed that the higher units of the Horsethief Creek Group in the Selkirks are correlative with the Cariboo Group, whereas the lowest unit is correlative with the Kaza Group of the Cariboo Mountains.

A major west-side-down normal fault, the North Thompson Fault, forms a structural and metamorphic discontinuity between the Cariboo Mountains and the Monashee Mountains to the east. It was important, therefore, to try and establish the correct stratigraphic position of the Hadrynian rocks in the Blue River area of the Cariboo Mountains.

Stratigraphy

Three separate stratigraphic units exist within the study area (Fig. 31.1), as follows: the Semipelite-Amphibolite division; the Middle Marble division; and the Upper Clastic division. Semipelite-Amphibolite division can be subdivided into three zones. The lowest zone observed consists of thinly interbedded semipelites and aluminum-silicate-poor pelites, with both layers and lenses of

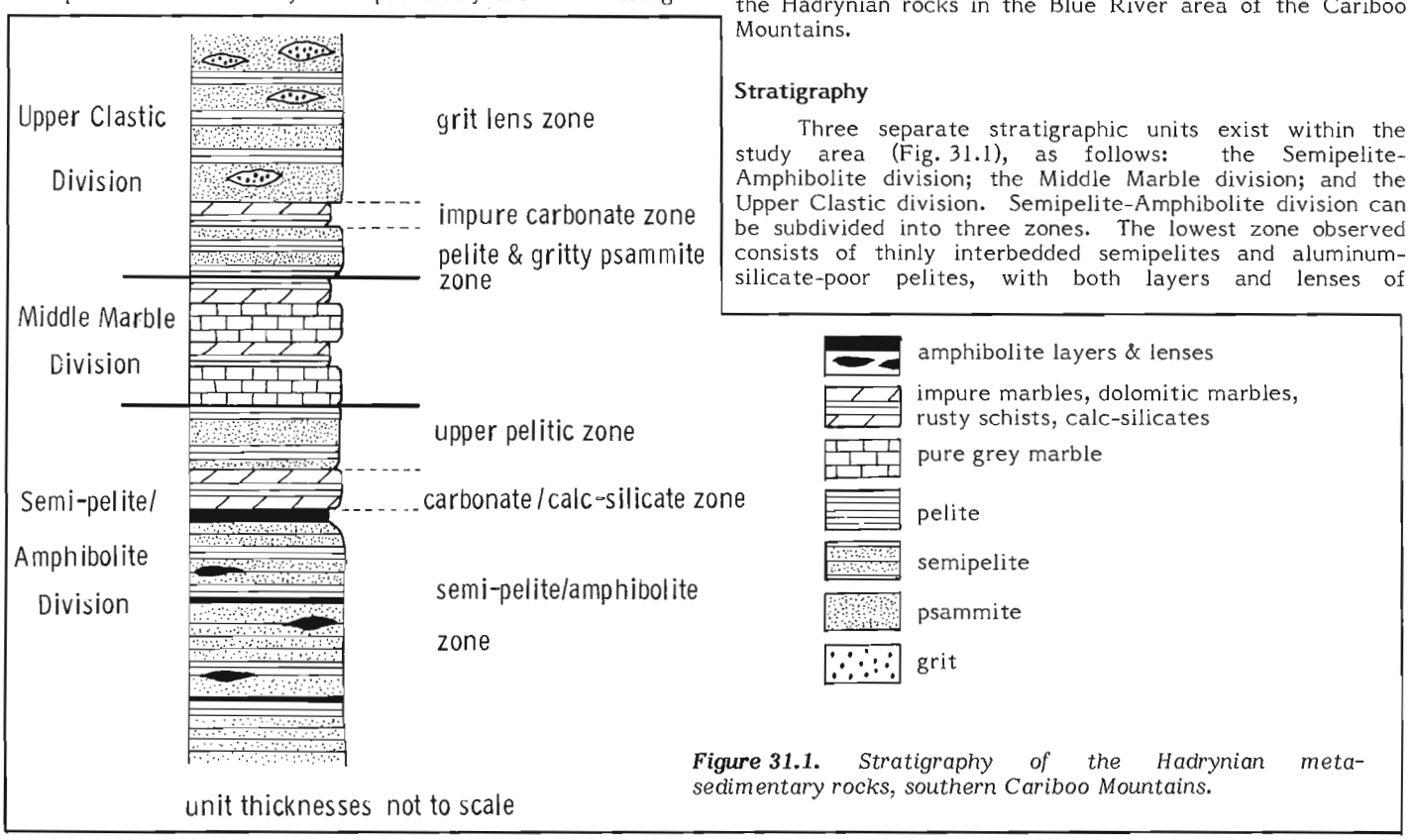

Figure 31.1. *Stratigraphy of the Hadrynian metasedimentary rocks, southern Cariboo Mountains.*

[1] Department of Geology, University of Calgary.

[2] 1 kilobar = 10^5 kPa.

amphibolite. Pure marbles, impure marbles, rusty pelitic schists, garnet hornblende calc-silicates, actinolite tremolite calc-silicates, and minor amphibolite make up the middle zone, which is highly variable along strike. The upper zone is composed of thinly interbedded aluminous pelites and psammites. Two massive grey marble bands, with intermediate and overlying layers of buff dolomitic marble, rusty muscovite schist, gritty psammite and quartzite constitute the Middle Marble division. The Upper Clastic division, where well exposed, can also be divided into three zones. The lower zone is largely psammite and gritty psammite, thinly interbedded with iron and aluminum-rich pelites. Minor garnet hornblende calc-silicate lenses are present. A thin (approximately 5 m) unit of brown dolomitic marble and rusty schist lies between the lower and upper zones of the Upper Clastic division. The upper zone is similar to the lower zone, except that grit lenses, the frequency of which increases up section, are better developed than in the lower zone. Several graded beds with sharp erosional bases on both flanks of the Mount Ste. Anne antiform, give the correct stratigraphic order for this unit. The total stratigraphic thickness is unknown, as neither the base of the Semipelite-Amphibolite division, nor the top of the Upper Clastic division are exposed within the area studied.

The entire sequence of Semipelite-Amphibolite, Middle Marble, and Upper Clastic divisions correlates very well with the upper divisions of the Horsethief Creek Group in the Selkirk and Monashee mountains (Table 31.1), and there can be little doubt that the Horsethief Creek Group extends into the Cariboo Mountains.

The identification of the Hadrynian strata in the Blue River area as Kaza Group, by Campbell (1968), and the correlations between the Selkirk and Cariboo mountains proposed by Brown et al. (1978) can obviously not both be right. A helicopter reconnaissance traverse made westward from Blue River, into the Cariboo Mountains, by R.B. Campbell, R.L. Brown, and P. Simony in the summer of 1980, suggests that Horsethief Creek strata are, in fact, beneath those of Kaza Group, as well as those of the Cariboo Group. The true relationship between the Horsethief Creek and Kaza groups will have to be established by extending detailed mapping westward from the present area.

Structure

The dominant structures in the area, which fold an upright stratigraphy, are two antiform-synform pairs with southeast-striking, subvertical- to southwest-dipping, axial surfaces and a southeasterly axial plunge that averages about 5° (Fig. 31.2, 31.3). The axial surfaces are fanned to some degree. The orientation of fold axes is variable, and although both mode and mean indicate a southeast plunge. locally, the axes may have as much as a 30° plunge to the northwest. Although the individual smaller macroscopic folds cannot be traced for more than 2 or 3 km, large compound structures, like the Mount Ste. Anne antiform, are approximately cylindrical and can be traced for as much as 20 km.

The cross-section of Figure 31.3 shows that the Mount Ste. Anne antiform and associated folds are characterized by broad hinge zones, made up of several large parasitic folds.

The major folds of the Mount Ste. Anne type are of at least a second generation. Their axial planar fabric ranges from crenulation to strain-slip cleavage superimposed on a previous foliation. The earlier foliation is locally parallel with the axial planes of nearly isoclinal folds, which are coaxially refolded by the Mount Ste. Anne-type folds.

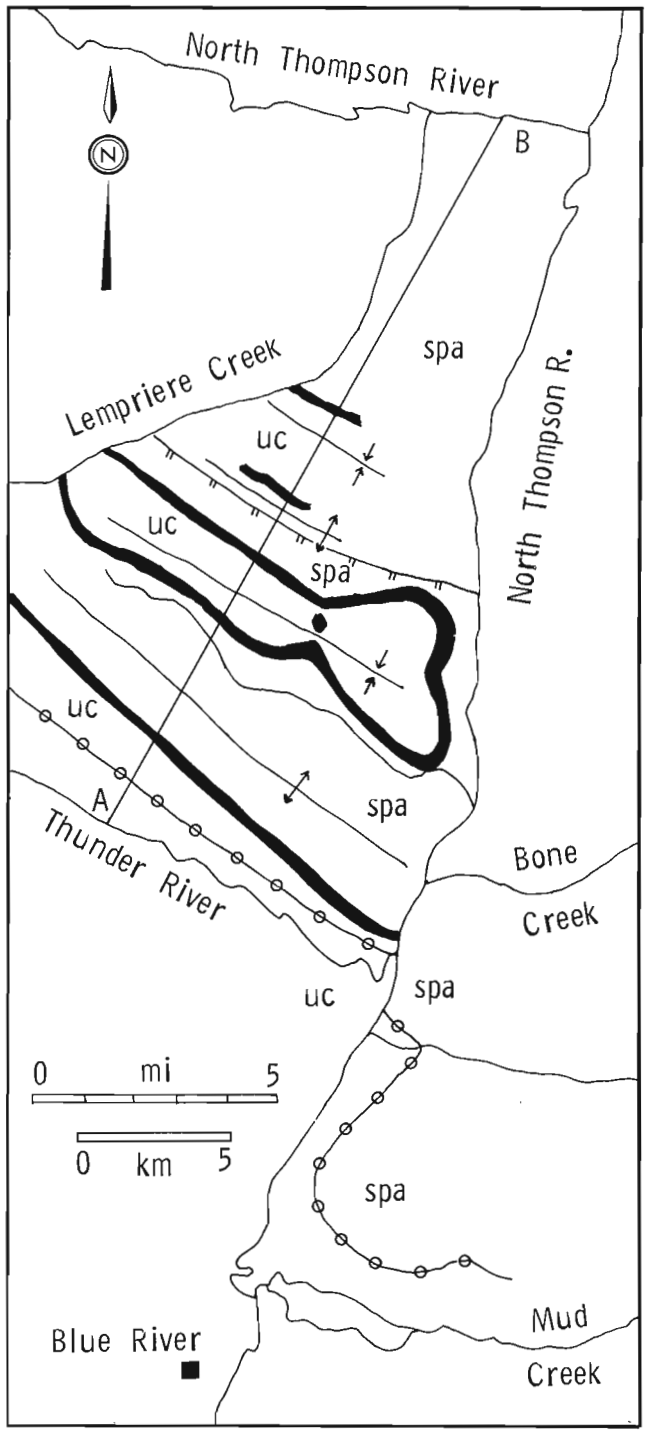

Figure 31.2. *Geology of the southern Cariboo Mountains, near Blue River, British Columbia.*

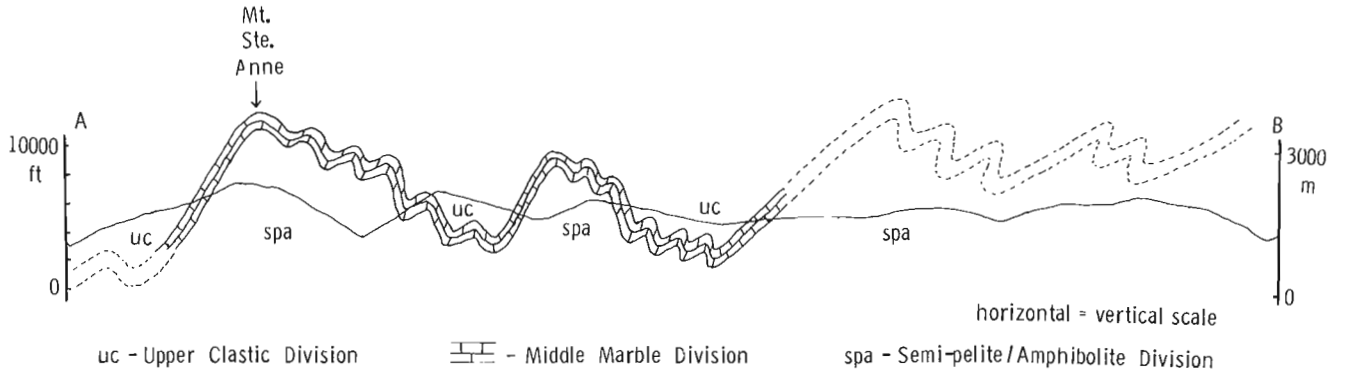

Figure 31.3. *Diagrammatic cross-section, AB. See Figure 31.2 for location of the line of section.*

Table 31.1.

Stratigraphic correlation

Rogers Pass Selkirks	Downie/Sorcerer Creek Northern Selkirks	Mica Dam Northern Selkirks	Mount Ste. Anne Southern Cariboos
Poulton and Simony in press	Brown et al., 1978	Poulton and Simony in press	this paper
Upper Clastic Division; semipelite and grit lenses	Upper Pelitic Member; a) pelites b) grits c) pelites	Upper Clastic Division; pelite, semipelite; carbonate and minor amphibolite	Upper Clastic Division; pelite and psammite with grit lenses impure carbonates pelite and psammite
Carbonate Division	Middle Marble Member	Carbonate Division	Middle Marble Division
Slate Division (Upper Part) semipelite and calc-phyllite	Lower Pelitic Member	Semipelite-Amphibolite Division; semipelite; aluminous pelite and minor amphibolite semipelite, amphibolite and calc-silicates	Semipelite-Amphibolite Division; alluminous pelite and psammite carbonate, calc-silicate platy semipelite, pelite and amphibolite

The exposed succession, which outlines the major folds, is entirely upright, but the possibility exists that the great thickness of Semipelite-Amphibolite division, which forms the lower exposed levels, and within which there are zones with abundant early mesoscopic isoclines, may harbour the axial surface of a large early recumbent fold.

Late deformation events manifest themselves as crenulations and mesoscopic folds in both the foliation and bedding, but no associated megascopic structures have been recognized.

Postdating all folding and metamorphism, was a period of extension, during which the northeast-trending North Thompson Fault was formed.

Metamorphism

Metamorphic grade within the region studied increases from garnet grade in the north, to sillimanite grade in the south, near Thunder River (Fig. 31.2). The isogradic surfaces are subparallel to the main structures, and apparently quite steep; their traces are unaffected by topography. At the sillimanite isograd, kyanite, staurolite, and sillimanite coexist along with biotite, garnet, and plagioclase. Garnet-biotite geothermometry (Thompson, 1976; Ferry and Spear, 1977) and garnet-plagioclase geobarometry (Ghent, 1976) suggest that at the sillimanite isograd, pressures and temperatures of approximately 4.5 kb and 550°C were attained.

Metamorphic isograds are offset by the North Thompson Fault. Also, both the orientation and nature of the sillimanite isograd are quite different east of the fault. In the eastern terrane the isogradic surface is shallowly dipping and folded. A very broad staurolite-free upper kyanite zone exists, and migmatization is common. Pressures and temperatures calculated for the sillimanite isograd farther east, near Mica Creek (Knitter, 1979; Ghent et al., 1979) are approximately 600°C and 6.0 kb. The nature of the sillimanite isograd near Mica Creek is similar to that immediately east of the fault, suggesting a difference of about 1.5 kb across the fault.

The mineralogical contrast across the North Thompson Fault is similar to the one described by Craw (1978) across the Purcell Thrust east of Mica Creek. There, a high-pressure terrane with a broad staurolite-free upper kyanite zone in which migmatite is developed, is juxtaposed against a lower pressure terrane where staurolite persists to the sillimanite isograd, and no migmatite is formed. Such a mineralogical contrast, along with the pressure determinations, is consistent with a west-side-down throw on the North Thompson Fault of at least 4 km.

Conclusions

The Horsethief Creek stratigraphy typical of the allochthonous cover of the Malton Gneiss in the northern Monashees (Morrison, 1979; Ghent et al., 1977) continues into the Cariboo Mountains where it is now at a tectonic level some 4 km higher than in the Monashee Mountains. It is involved in at least two generations of folding, the later of which, has a wavelength of more than 5 km and dominates the map pattern.

References

Brown, R.L., Perkins, M.J., and Lane, L.S.
1978: Stratigraphy, facies changes, and correlations in the northern Selkirk Mountains, southern Canadian Cordillera; Canadian Journal of Earth Sciences, v. 15, p. 1129-1140.

Campbell, R.B.
1968: Geology of Canoe River, British Columbia; Geological Survey of Canada, Map 15-1967.

Craw, D.
1978: Metamorphism, structure and stratigrpahy in the southern Park Ranges, British Columbia; Canadian Journal of Earth Sciences, v. 15, p. 86 98.

Ferry, J.M. and Spear, F.S.
1977: Experimental calibration of the partitioning of Fe and Mg between biotite and garnet; Carnegie Institute, Washington Yearbook 76, p. 579-581.

Ghent, E.D.
1976: Plagioclase-garnet-Al_2SiO_5-quartz: a potential geobarometer-geothermometer; American Mineralogist, v. 61, p. 710-774.

Ghent, E.D., Simony, S.P., Mitchel, W., Perry, J., Robbins, D., and Wagner, J.
1977: Structure and metamorphism in the southeast Canoe River area, British Columbia; in Report of Activities, Part C, Geological Survey of Canada, Paper 77-1C, p. 13-17.

Ghent, E.D., Robbins, D.B., and Stout, M.Z.
1979: Geobarometery, geothermometery, and fluid compositions of metamorphosed calc-silicates and pelites, Mica Creek, British Columbia; American Mineralogist, v. 64, p. 874-885.

Knitter, C.C.
1979: Metamorphism and structure of the Soards Creek area, British Columbia; M.Sc. thesis, University of Calgary.

Morrison, M.L.
1979: Structure and petrology of the southern portion of the Malton Gneiss, British Columbia; in Current Research, Part B, Geological Survey of Canada, Paper 79-1B, p. 407-410.

Poulton, T. and Simony, P.
Stratigraphy, sedimentology and regional correlation of the Horsethief Creek Group (Hadrynian, late Precambrian) in the northern Purcell and Selkirk Mountains, British Columbia; Canadian Journal of Earth Sciences. (in press)

Thompson, A.B.
1976: Mineral reactions in pelitic rocks: II. Calculations of some P-T-X (Fe-Mg) phase relations; American Journal of Science, v. 276, p. 425-454.

32. GEOLOGY OF THE WEST HALF OF THE KAMILUKUAK LAKE MAP AREA, DISTRICT OF KEEWATIN: A PART OF THE CHURCHILL STRUCTURAL PROVINCE

Project 790009

Subhas Tella, K.E. Eade, A.R. Miller[1], and C.G. Lamontagne[2]
Precambrian Geology Division

Tella, Subhas, Eade, K.E., Miller, A.R., and Lamontagne, C.G., Geology of the west half of the Kamilukuak Lake map area, District of Keewatin: a part of the Churchill structural province; in Current Research, Part A, Geological Survey of Canada, Paper 81-1A, p. 231-240, 1981.

Abstract

The area is underlain by an Archean and/or Aphebian granitoid complex intruded by quartz monzonite and diorite and by late Aphebian or Helikian sedimentary, volcaniclastic, and volcanic rocks of the Dubawnt Group intruded by syenite and granite-quartz monzonite. The basal unit of the Dubawnt Group is a poorly sorted and locally sheared, polymictic sharpstone conglomerate which is disconformably to unconformably overlain by a sequence of interbedded mafic and felsic lavas, volcaniclastic sediments, pyroclastics, wacke, siltstone, and chert, succeeded by quartz-feldspar porphyry flows, welded tuff, and breccia. These units of the Dubawnt Group make up the Christopher Island Formation. A red clastic succession of calcareous shale, sandstone, and polymictic boulder conglomerate unconformably overlies the Christopher Island Formation. Intrusions of syenite, biotite lamprophyre, and diabase, cut the granitoid complex and the Dubawnt Group.

The basal unit of the Dubawnt Group is interpreted as a possible regolith or an immature fluvial deposit. The basal sedimentary and volcaniclastic rocks of the Christopher Island Formation are interpreted as distal fluvial deposits, whereas the upper massive and stratified volcaniclastic rocks are interpreted as mass flow and fluvial deposits respectively. These upper and lower sedimentary sequences are separated by cycles of trachytic volcanism. Interbedded chert and lava sequences suggest local subaqueous extrusion of lavas into ephemeral lakes, with precipitation of chert reflecting intermittent periods of quiescence.

Northeast trending cataclastic to mylonitic zones are present in the basement complex, and four sets of faults transect both the basement complex and the cover rocks. Uranium mineralization was noted in the basement complex and the Christopher Island Formation.

Introduction

Mapping in the west half of the Kamlukuak Lake map area (65K), at a scale of 1:250 000, was completed during the 1980 field season. Preliminary results of the mapping in the east half were reported previously (Tella and Eade, 1980). The area is part of a region previously mapped by Wright (1955, 1967) at a scale of one inch to eight miles. A.R. Miller spent six weeks in this map area as part of a regional study of uranium mineralization, concentrating on mapping Dubawnt Group rocks and uranium occurrences in the south half of the map area.

Archean and/or Aphebian Basement Complex

The basement complex (units 1 to 4, Fig. 32.1) is widely exposed throughout the map area. Unit 1 is a mixed unit consisting of well foliated, porphyroblastic, potash feldspar augen gneiss, and a medium- to coarse-grained, layered, hornblende-biotite orthogneiss (1A). Inclusions of amphibolite and minor garnetiferous, biotite paragneiss layers are present within unit 1A. The augen gneiss, containing subhedral, white to pink feldspar crystals (up to 6 cm long), is of granodiorite to quartz monzonite composition, and corresponds to the augen gneiss unit previously described in the area to the east (unit 4, Fig. 5.1, Tella and Eade, 1980). The augen gneiss outcrops are abundant north of Kamilukuak River, and they are less abundant in areas to the south of the Kamilukuak Lake. Locally preserved massive and porphyritic phases of the unit in otherwise highly deformed parts suggest an igenous protolith for the augen gneiss. Exposures of hornblende-biotite orthogneiss (unit 1A; corresponding to unit 2, Fig. 5.1 of Tella and Eade, 1980) are predominant in the southern half of the map sheet, and commonly show compositional variations from granodiorite to quartz monzonite. Migmatitic banding is locally present in several places. Rare east trending, weakly metamorphosed and altered basic dykes of probable Aphebian age cut the unit.

A belt of cataclastic to mylonitic rocks (unit 2) of quartz monzonite to granite composition is well exposed to the southeast of Kamilukuak River. Isolated bodies of medium- to coarse-grained, well foliated, pink monzonite to syenodiorite occur within this unit. Unit 3, occurring south of Nowleye Lake, consists of fine- to medium-grained, well foliated pink syenite. Rocks of both units 2 and 3 are less deformed that those of unit 1. Hence, although the relative age of units 2 and 3 is uncertain, both are considered to be younger than unit 1.

Unit 4 consists of medium- to coarse-grained, massive to weakly foliated diorite, quartz diorite, and minor gabbro with some inclusions of feldspar augen gneiss and orthogneiss.

Field relations and structural data indicate that rocks of unit 1 have undergone at least three periods of deformation and an event of regional metamorphism. East to northeast trending regional foliation, the most penetrative planar fabric element, represents a syntectonic metamorphic fabric development during the first period of deformation. A mineral (hornblende) lineation is locally developed in rocks of this unit at a few localities. First generation folds have not been identified in the area. The second generation structures are characterized by mesoscopic to macroscopic, upright, open to tight folds with east to east-northeast trending axial planes. Associated minor folds commonly plunge to the west or to the west-southwest at shallow angles (20°-30°). Local reversals to the east and to the east-northeast are common. The third generation structures are marked by open, upright folds with northwest trending axial planes that plunge either to the northwest or to the southeast at shallow angles (10°-15°). No minor folds have been recognized in units 2 to 4, but a regionally pervasive, east to northeast trending foliation is present in these units. The regional metamorphic grade in the basement complex is within the amphibolite facies, and the mineral assemblages have been partially retrograded to chlorite and epidote bearing assemblages.

[1] Economic Geology Division
[2] Department of Geology, Université de Laval, Ste-Foy, Québec, G1K 7P4

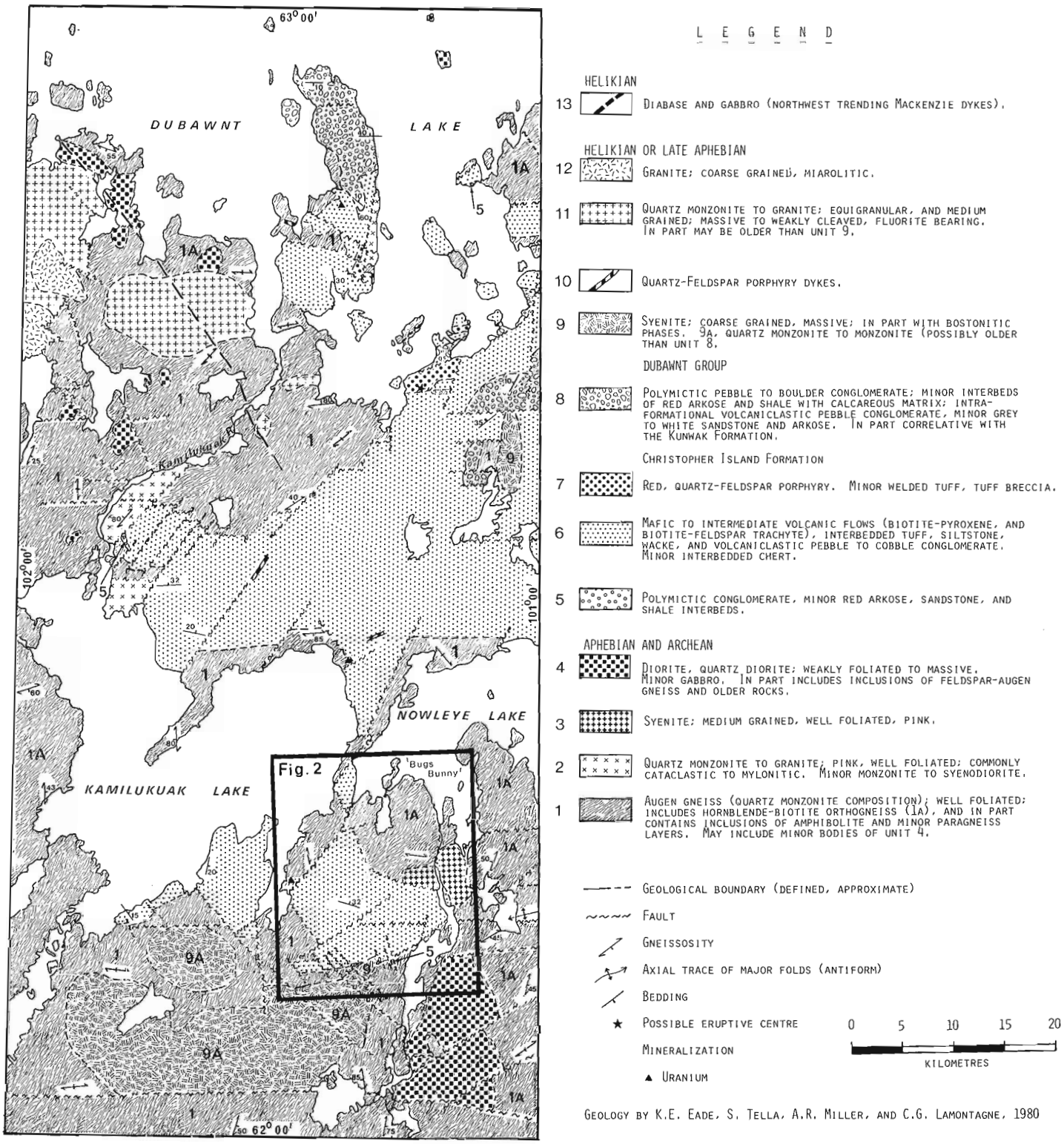

Figure 32.1. *Geological sketch map of Kamilukuak Lake map area (65K, west half).*

The structural and metamorphic history of the basement complex is consistent with that described in the adjacent area to the east (Tella and Eade, 1980).

Late Aphebian or Helikian

Dubawnt Group

The Dubawnt Group rocks (units 5 to 8) unconformably overlie or are in fault contact with the basement complex. They are predominantly exposed in the central part of the map area and south of Kamilukuak and Nowleye lakes. A part of this latter area, which encompasses the Dubawnt Group rocks and adjacent basement complex (Fig. 32.2), is informally referred to here as the "Bugs Bunny" area. Detailed descriptions and the environment of deposition of the Dubawnt Group rocks in the "Bugs Bunny" area will be presented in a later section.

Basal Polymictic Conglomerate (unit 5). Rocks of this unit (Fig. 32.1) consist of locally derived and poorly sorted, angular to rounded, pebble to boulder size clasts of basement granitoid gneisses, feldspar crystals, and vein quartz. Matrix of the conglomerate, commonly sheared, is composed of sand, silt and clay size fractions. Interbedded red arkose and shale are present. In one locality, south of Kamilukuak River, the conglomerate represents a thin regolith separating the granitoid basement from the overlying Christopher Island Formation. The conglomerate unit is correlated with the South Channel Formation (Donaldson, 1965) on the basis of lithological similarities and stratigraphic position.

Christopher Island Formation (units 6 and 7). A sequence of mafic and felsic lavas, interbedded volcaniclastic pebble to cobble conglomerate, pyroclastic rocks, agglomerate, tuff, siltstone, wacke, and chert (unit 6) overlies, unconformably to disconformably or is in fault contact with, the basement complex and the basal conglomerate (unit 5). Discontinuous wedges of immature, poorly sorted, maroon coloured, pebble conglomerate (basement and volcanic clasts) occur in the basal parts, and less commonly in the upper parts of the sequence. Mafic trachyte lavas are typically porphyritic, containing phenocrysts (3 mm to 1 cm) of phlogopite, clinopyroxene, and alkali feldspar. The less common felsic trachytes normally contain alkali feldspar and rare phlogopite phenocrysts. Rocks within this sequence (unit 6) form a north to northeast dipping (10°-35°) and faulted homoclinal succession, and are overlain by a sequence of red feldspar porphyry flows, welded tuff, and breccia (unit 7*). In one area (south of Dubawnt Lake) the rocks of unit 7 are characterized by highly contorted and brecciated volcanic fragments mixed with welded tuff and quartz-feldspar porphyry, and may represent volcanic debris associated with an eruptive centre. The character of the Christopher Island Formation is similar to that described in adjacent areas by Blake (1980), Eade (1976), Eade and Blake (1977), LeCheminant et al. (1979a, b; 1980), and Tella and Eade (1980). One possible addition to the rock types in the present map area is thin interbeds of chert occurring with mafic trachyte lavas in the lower parts of the Christopher Island Formation.

The rocks of units 6 and 7 are cut by discontinuous, east trending and southeast trending biotite lamprophyre and hornblende syenite sills and dykes which are probably cogenetic with the alkaline lavas. Anomalously radioactive bostonite dykes cut the Christopher Island rocks.

Red clastic succession (unit 8). The unit consists of a variety of conglomerates possibly reflecting different provenances, environments of deposition, and age. In one locality, along the east shore of the north trending peninsula in Dubawnt Lake, a 150 m thick discontinuous succession of fine grained redbeds (Fig. 32.3) unconformably overlies the Christopher Island Formation. The red shale-sandstone beds, containing abundant carbonate cement, are interbedded with grey-green sandstone and locally developed volcaniclastic pebble conglomerate. Primary structures include crossbedding, laminations, load features, rare graded bedding, and desiccation cracks, indicating shallow water deposition and subaerial exposure. The fine grained redbeds are conformably overlain by a thick blanket of coarse polymictic (pebble to boulder) conglomerate (Fig. 32.4) containing poorly sorted, subangular to subrounded clasts of basement granitoid gneisses (80%), mafic to felsic trachyte and red quartz-feldspar porphyry (15%), and angular boulders of redbeds (5%). Crossbedded calcareous and arkosic sandstone occurs as thin (5 cm to 1 m) interbeds within the polymictic conglomerate. Although the above redbed succession is lithologically similar to the Kunwak Formation (LeCheminant et al, 1979b), the presence of red quartz-feldspar porphyry clasts (possibly representing the Pitz Formation) indicates that the succession may be even younger than the Kunwak Formation.

Similar conglomerates but with a low basement clast content, occur in isolated areas to the southeast of Dubawnt Lake at the same stratigraphic level. They contain fine- to medium-grained, grey to white, gritty sandstone interbeds that are absent in the succession described above. Although the relative age of these conglomerates is uncertain, the presence of white, gritty sandstone beds (some of which show minor kaolinization) suggests that they may, in part, be correlative with the Thelon Formation (Donaldson, 1965).

"Bugs Bunny" Area (Fig. 32.2)

Basal Sedimentary Sequence. The basal unit of the Dubawnt Group is a locally developed massive, polymictic, clast supported, sharpstone conglomerate containing angular to subangular clasts (up to 25 cm in longest dimension) of potassic feldspar augen gneiss, layered biotite gneiss, cataclastic granitoid gneisses, and minor white quartz (see Fig. 32.5, 32.6). The angular, coarse sand to silt sized detritus comprising the matrix is unsorted and massive, and contains no volcanic material. The unit, the South Channel equivalent, unconformably overlies the basement, and is estimated to be 5 to 10 m thick.

Christopher Island Formation. Mafic and felsic lavas, pyroclastics, and a variety of volcaniclastic sediments, unconformably overlie or are in fault contact with the basement complex. The formation unconformably or disconformably overlies the basal sedimentary sequence. Lavas have been classified in the field as mafic or felsic trachytes based on phenocryst populations and are similar to those described by Blake (1980), and LeCheminant et al. (1979). The Christopher Island Formation is divided into four subunits based on lithological abundances and the character of the associated volcaniclastic sediments (Fig. 32.5).

Basal volcaniclastic sediments. This unit overlies the basement and the South Channel equivalent rocks along the southern and southeastern portion of the Dubawnt basin (Fig. 32.2), and is characterized by black, dark green to grey-green, and locally maroon volcaniclastic siltstone, fine- to medium-grained wacke, granulestone, and minor conglomerate. This unit displays even-parallel beds and laminae, from less than 5 mm to 3 cm in thickness. In thin section, the siltstone and wacke show angular to subrounded strained quartz and trachyte clasts (up to 2 mm in size). Biotite- and pyroxene-phyric lavas are intercalated with the clastic sediments, and increase in abundance towards the overlying mafic trachyte volcanic sequence.

* Although the rocks within unit 7 are included in the Christopher Island Formation, the red quartz feldspar porphyry flows are lithologically similar to the rhyolite flows of the Pitz Formation (Donaldson, 1965) and may postdate the Christopher Island Formation.

Figure 32.2

Geology of the "Bugs Bunny" area (65K/3, 6).

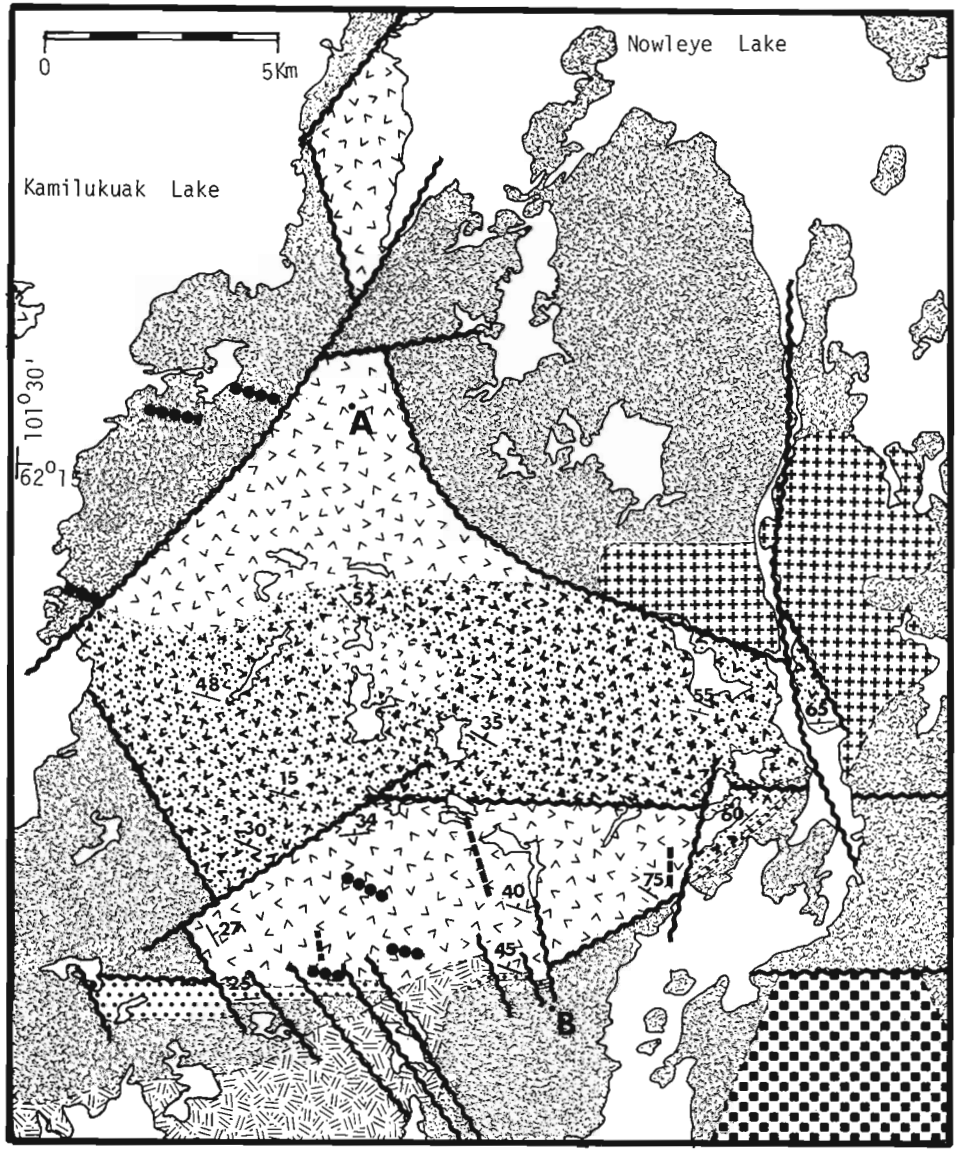

HELIKIAN

Diabase and gabbro (Mackenzie dykes)

HELIKIAN OR LATE APHEBIAN

Dubawnt Group

Christopher Island Formation

Syenite massive

Bostonite dykes

Felsic trachyte lavas with interflow conglomerate, wacke, siltstone

Mafic trachyte lavas with equal portion of interflow conglomerate, wacke, siltstone, minor chert.

Mafic trachyte lavas and tuff with minor interflow conglomerate, wacke, siltstone and chert

Tuffaceous wacke, siltstone, volcaniclastic conglomerate with minor intercalated mafic lavas

South Channel Formation (equivalent)

Polymictic sharpstone conglomerate

APHEBIAN and ARCHEAN

Diorite, quartz diorite and gabbro; foliated to massive

Syenite; medium grained, well foliated, pink

Augen gneiss (quartz monzonite composition) well foliated; includes hornblende-biotite orthogneiss and in part inclusions of amphibolite and minor biotite paragneiss layers

Figure 32.3

Interbedded shale and sandstone of the redbed succession, unit 8, showing discontinuous grey-green sandstone layers. GSC 183793

Figure 32.4

Polyictic boulder conglomerate (unit 8) consisting of assorted basement granitoid gneiss and the Christopher Island volcanic clasts. GSC 183801

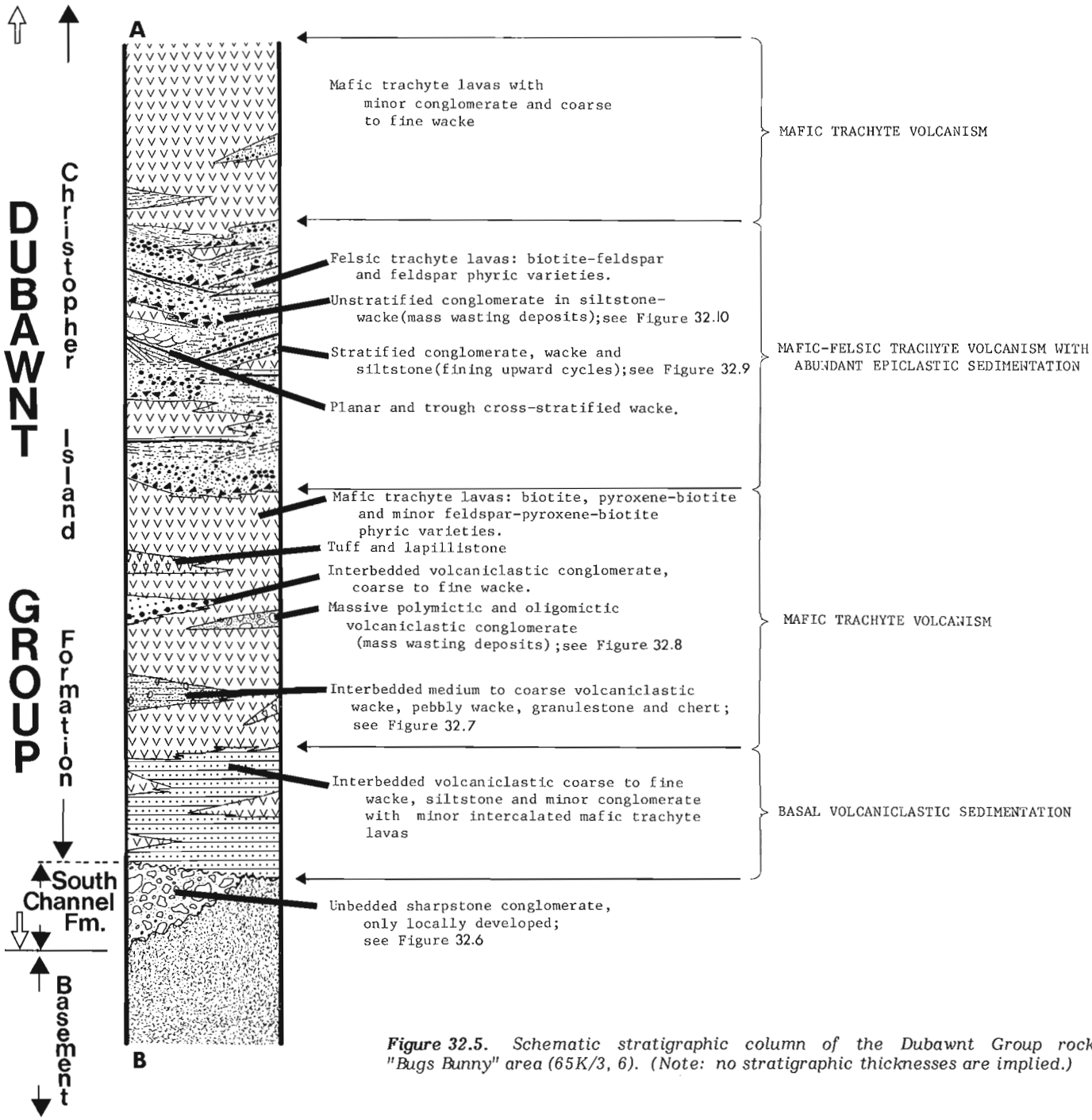

Figure 32.5. *Schematic stratigraphic column of the Dubawnt Group rocks, "Bugs Bunny" area (65K/3, 6). (Note: no stratigraphic thicknesses are implied.)*

Mafic trachyte volcanic sequence. The mafic trachyte sequence is dominated by the abundance of lava and pyroclastic units with subordinate epiclastic deposits. The varicoloured mafic lavas are characteristically porphyritic, displaying a range of phenocryst populations: black biotite-rich, black to maroon pyroxene-biotite phyric, and minor maroon feldspar-pyroxene-biotite phyric types. Lithic crystal tuff and lapillistone are interstratified with the lavas. In spite of excellent textural preservation, phenocrysts and groundmass are locally altered to chlorite, carbonate (both calcite and dolomite), and opaques (probably hematite).

A variety of epiclastic sediments are present that have limited lateral continuity within this lava sequence. Massive polymictic to oligomictic volcaniclastic conglomerates contain subrounded to rounded volcanic clasts (up to 20 cm in longest dimension; see Fig. 32.8). Minor maroon to red, stratified volcaniclastic conglomerate, coarse to fine lithic wacke and siltstone are intercalated with the lava. Bedded units are characteristically even parallel to even nonparallel with thicknesses of 1 cm to 10 cm. The third and most distinctive rock unit is interbedded, brown to maroon chert and volcaniclastic granulestone, coarse lithic wacke, and siltstone. The intercalated clastic and chemical beds are parallel, even bedded, and the laminae range in thickness from 5 mm to 10 cm (Fig. 32.5, 32.7). These epiclastic wacke and siltstone deposits undoubtedly include a tuffaceous component.

Figure 32.6

Sharpstone conglomerate, South Channel equivalent, consisting of angular gneiss clasts in an unbedded arkosic material. GSC 203179-W

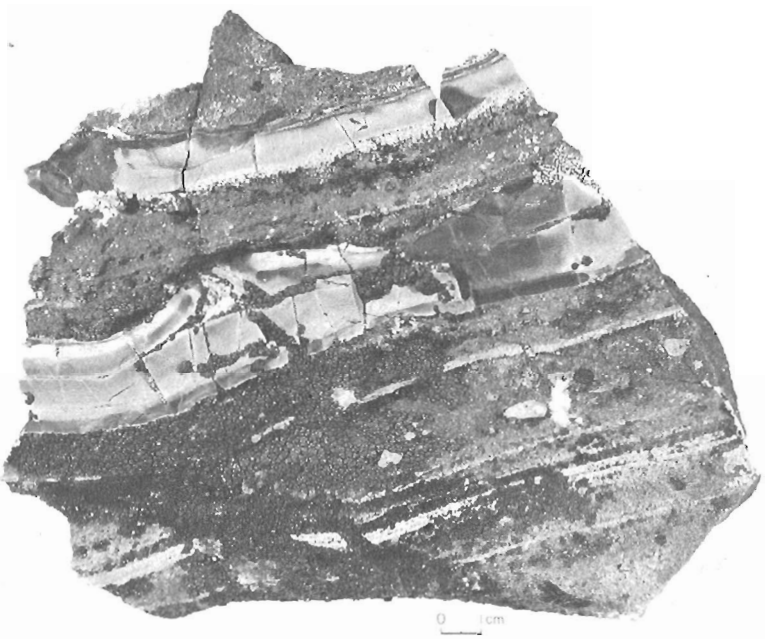

Figure 32.7

Interbedded, massive, granular to coarse volcaniclastic wacke and maroon to brown chert, Christopher Island Formation, "Bugs Bunny" area. GSC 203592-R

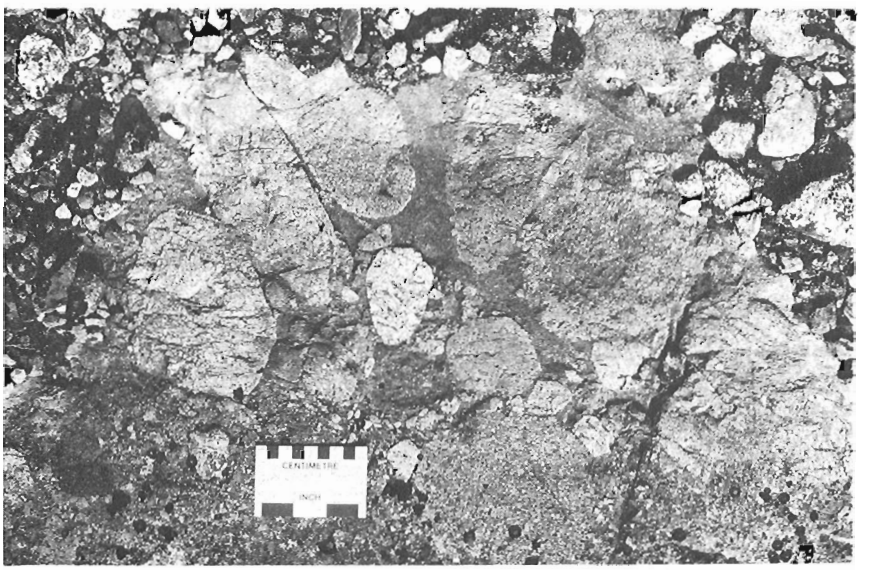

Figure 32.8

Polymictic paraconglomerate with massive volcaniclastic matrix, Christopher Island Formation. GSC 203179-V

Figure 32.9. *Stratified fluvial volcaniclastic wacke-siltstone, Christopher Island Formation, "Bugs Bunny" area. GSC 203592-Q*

Mafic trachyte lava and interflow sediment sequence. This sequence is distinguished from the mafic trachyte lava sequence by the presence of equal proportions of lava and interflow sediments. Lavas are dominantly maroon mafic (pyroxene-biotite and biotite phyric) varieties, with local occurrences of maroon to grey felsic (pyroxene-biotite-feldspar, biotite-feldspar, and feldspar phyric) varieties. Minor pyroclastic layers occur within the sequence. In areas of relatively continuous outcrop, flow units were found to vary locally from 3 m to 100 m, with an average true thickness of 10-20 m.

Intercalated sediments range from coarse conglomerates and granulestone to coarse to fine lithic, possibly tuffaceous, wacke and siltstone. The finer grained sand to silt sized rocks are typically red to maroon with rare diagenetically altered drab green beds. Coarser sediments, conglomerate to granulestone, are composed of angular to subrounded volcanic detritus up to 30 cm in size with rare, well rounded basement gneiss clasts with a maximum size of 5 cm. Bedding is commonly even parallel with beds up to 30 cm thick in the conglomerate-granulestone, and 1-10 cm thick in the wacke-siltstone. Wacke and siltstone, in some places, contain crystal and lithic clasts, suggesting a tuffaceous origin in part. Interflow sediments, typically in fining upward cycles, commonly range from 3 m to 50 m in thickness although thicker successions are present (Fig. 32.9). Locally, trough and planar crossbedding, channel scours, asymmetrical and symmetrical ripple marks are present, all suggesting a transport direction from the east and southeast.

The typical sedimentary lithologies observed in a flow-interflow sediment sequence are as follows: overlying the flow a coarse, angular to subrounded, commonly monolithic (similar to the underlying flow), immature, clast surrounded conglomerate with a red to maroon, massive to finely bedded, or locally contorted, silt-fine sand matrix (Fig. 32.10). These rocks represent mass waste deposits of either mass flow origin, the infiltration of fine debritus amongst coarse detritus, or dumping of coarse detritus from proximal flow fronts into well bedded siltstone-fine wacke deposits. These rock types are overlain by fining upward cycles of conglomerate-granulestone to wacke-siltstone displaying a variety of sedimentary structures that suggest a fluvial environment. In one locality, 10-60 m thick biotite phyric lavas are interbedded with 2-10 cm thick maroon chert bands.

Felsic trachyte and interflow sediments. Locally, felsic, maroon to grey biotite-feldspar and feldspar phyric lavas are interlayered with fluvial clastic sediments.

Intrusive Rocks. A variety of intrusions cut the Christopher Island Formation in the "Bugs Bunny" area: lamprophyre, biotite-feldspar porphyry, bostonite dykes, and diabase. Lamprophyre dykes, normally black but grading to maroon, are typically porphyritic with phenocrysts of biotite and pyroxene-biotite. The dykes are most recognizable where they transect interflow sediments, and are interpreted as feeder dykes to overlying flows. Biotite-feldspar (monzonitic) porphyries comprise a dyke swarm trending 280° and small circular to ellipsoidal stocks intruding the Christopher Island Formation. The dykes range from 3 m to 30 m in width and stocks up to 0.4 km across. These intrusions may be related to the syenite, quartz monzonite to monzonite exposed to the south of the "Bugs Bunny" area (unit 9, 9A; Fig. 32.1). Bostonite dykes, trending east to east-southeast, cut the basement complex and the lower stratigraphic levels of the Christopher Island Formation. The dykes are interpreted to represent the last phase of alkalic magmatism because, in one locality, they cut a monzonite porphyry which itself intrudes mafic trachyte. Northwest trending diabase dykes (Mackenzie dykes) are the youngest intrusions in the area.

Environment of Deposition of the Dubawnt Group. A schematic stratigraphic column representing the interfingering of lithologies in a rapidly changing volcanic environment is illustrated in Figure 32.5. The basal polymictic conglomerate (South Channel Formation equivalent) is interpreted as a possible, locally preserved regolithic deposit or an immature fluvial deposit formed during initial faulting that preceded volcanism. The basal volcaniclastic deposits, tuffaceous wacke-siltstone, granulestone and minor conglomerate of the Christopher Island Formation, resting unconformably to disconformably on the South Channel equivalent, are interpreted as distal fluvial deposits with minor volcanic intercalations. The presence of significant quartz and lithic quartz-feldspar detritus in these sediments reflects, in part, a basement provenance.

The basal volcaniclastic sediments grade into the mafic lava-pyroclastic unit, implying the onset of major trachytic volcanism in, or adjacent to, the basin. This major volcanic influx is represented in a variety of stratified and massive volcaniclastic deposits. Massive units are interpreted as mass flow deposits, whereas stratified conglomerate to siltstone are interpreted as fluvial deposits. The interstratified volcaniclastic granulestone, coarse to medium wacke, and chert are interpreted as possible ephemeral lake deposits. The lava-chemical sediment interbeds suggest local subaqueous extrusion of trachyte lavas into ephemeral lakes with accompanying chert deposition during periods of quiescence. Massive epiclastic beds may represent debris flows (Walker, 1979), with chert (possibly due to fumarolic activity) being precipitated during quiescent periods. This

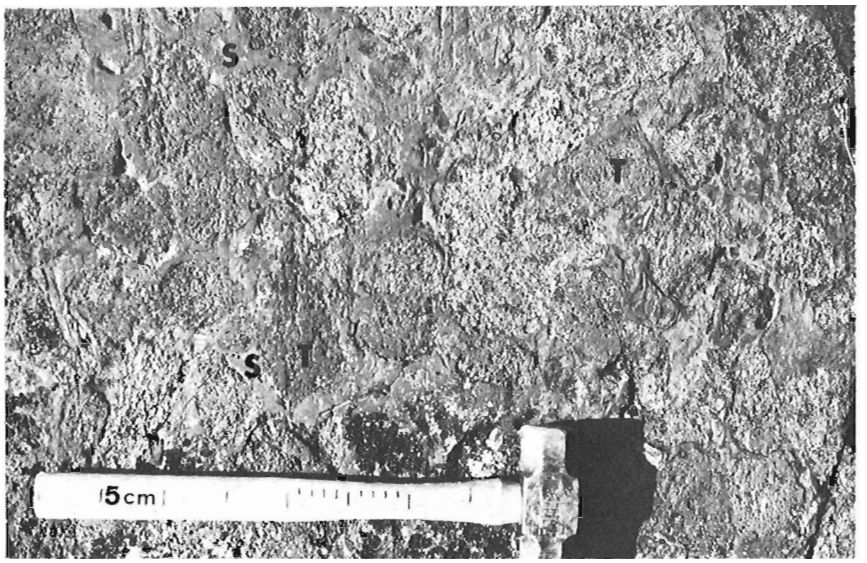

Figure 32.10

Angular to subrounded pyroxene-biotite trachyte clasts (T) in a maroon siltstone matrix (S). Photograph of a bedding surface of an orthoconglomerate resting directly on massive pyroxene-biotite trachyte. GSC 203179-U

volcanic-dominated unit is apparently succeeded by an interstratified sequence of fluvial volcaniclastic sediments and mafic to felsic trachyte lavas. This change to approximately equal proportions of volcanic and sedimentary rocks may reflect a waning phase of volcanism or perhaps a shift in the eruptive centre(s), resulting in more distal rock assemblages.

Post Dubawnt Group Intrusions

North of Nowleye Lake and in the "Bugs Bunny" area (Fig. 32.1), a coarse grained, massive, equigranular, pink hornblende syenite (unit 9) intrudes the Christopher Island rocks. A medium- to coarse-grained, massive, and equigranular monzonite to quartz monzonite (unit 9A) pluton is exposed in the southern part of the map sheet. The syenite of unit 9 in the "Bugs Bunny" area is marginal to the monzonite to quartz monzonite pluton and may represent a border phase. Dykes of red quartz-feldspar porphyry (unit 10) cut the Christopher Island Formation in several places. The dykes range in thickness from 1 to 20 m and, in some places, follow local faults. The above rock types do not appear to intrude the red clastic sequence (unit 8) and may predate this unit.

A medium- to coarse-grained, massive to weakly cleaved, equigranular, fluorite-bearing quartz monzonite to granite (unit 11) intrudes the basement granitoid gneiss in the northwestern portion of the map area. Mafic minerals (mostly biotite) represent less than 5 per cent of the total mineral constituents. Accessory minerals include fluorite, muscovite, sphene, apatite, zircon and opaques. Two stocks of coarse grained, massive, and miarolitic granite (unit 12) are exposed to the northwest of Kamilukuak River. The granite is fresh and locally contains fluorite. Units 11 and 12 are similar in composition but differ in grain size, and probably are comagmatic. The assigned post-Dubawnt Group age for the two units is uncertain because they do not appear to cut the Dubawnt Group rocks. However, the above plutonic rocks have similarities to the fluorite-bearing porphyritic granite which intrudes the Christopher Island volcanics in adjacent area (65K east half, Tella and Eade, 1980). Fine grained aplite veins and coarse grained pink pegmatites of different age cut the basement complex.

Helikian

Northwest trending, fine- to coarse-grained diabase and gabbro dykes (10 m – 30 m thick) related to the Mackenzie Swarm cut the basement complex, the cover rocks, and the younger plutons.

Faults

Northeast trending shear zones, as well as east, northeast, north, and northwest trending faults transect the area. Numerous northeast trending cataclastic to mylonitic zones are present within the basement complex, and may have acted as zones of weakness for subsequent brittle faulting. Most faults probably have a history of multiple movements.

Economic Geology

Epigenetic uranium mineralization is present within the basement complex of Dubawnt Group rocks. Potassic feldspar augen gneiss boulders containing fracture controlled uranium mineralization occur in an area of extensive Pleistocene cover but proximal to the faulted basal Dubawnt unconformity in the 'Bugs Bunny' area. Uranium mineralization, northwest of Nowleye Lake (Fig. 32.1), is hosted in hematitic and chloritic augen gneiss. Intense faulting of the Dubawnt Basin indicate that the basal unconformity-fault, or fault-fault intersections are favourable sites for Beaverlodge-type epigenetic uranium mineralization (Miller, 1980).

Two varieties of uranium-thorium bearing bostonites intrude the basement complex and Christopher Island Formation in the 'Bugs Bunny' area. The 'Nutarawit Lake type' is cherry red, leucocratic and fine grained. In thin section it is characterized by well aligned mats of feldspars with interstitial radioactive phases and desseminated hematite (Miller, 1979). The 'Kamilukuak Lake type' is fine grained with rare phenocrysts of plagioclase and anorthoclase. It is characterized by hackly fractured and mottled red-brown fresh surface containing 1 – 2 mm black knots. In thin section fresh hornblende, biotite and sphene are aligned in a feldspathic groundmass. The mafic minerals are disseminated and clustered in mafic knots. Disseminated metamict radioactive phases and uraniferous zircon are rimmed by hematite.

Uranium contents range from 200 to 475 ppm (neutron activation, Atomic Energy of Canada Ltd. and thorium to uranium ratios range from 2 to 3 (semi-quantitative X-ray fluorescence, Analytical Chemistry Section, Geological Survey of Canada).

Fracture controlled uranium mineralization located on the peninsula that projects into Dubawnt Lake just north of Kamilukuak River (65K/14) is hosted in Christopher Island trachyte near an unconformably overlying conglomerate-sandstone succession. The Christopher Island Formation – redbed succession (units 6 and 8) contact represents a favourable horizon for uranium exploration in the west half of the Kamilukuak Lake map area.

References

Blake, D.H.
1980: Volcanic rocks of the Paleohelikian Dubawnt Group in the Baker Lake-Angikuni Lake areas, District of Keewatin, N.W.T.; Geological Survey of Canada, Bulletin 309, 50 p.

Donaldson, J.A.
1965: The Dubawnt Group, Districts of Keewatin and Mackenzie; Geological Survey of Canada, Paper 64-20.

Eade, K.E. and Blake, D.H.
1977: Geology of the Tulemalu lake map area, District of Keewatin; in Report of Activities, Part A, Geological Survey of Canada, Paper 77-1A, p. 209-211.

Eade, K.E.
1976: Geology of the Tulemalu Lake map area (65J), District of Keewatin; in Report of Activities, Part A, Geological Survey of Canada, Paper 76-1A, p. 379-381.

LeCheminant, A.N., Lambert, M.B., Miller, A.R., and Booth G.W.
1979a: Geological studies: Tebesjuak Lake map area, District of Keewatin; in Current Research, Part A, Geological Survey of Canada, Paper 79-1A, p. 179-186.

LeCheminant, A.N., Leatherbarrow, R.W., and Miller, A.R.
1979b: Thirty Mile Lake map area, District of Keewatin; in Current Research, Part B, Geological Survey of Canada, Paper 79-1B, p. 319-327.

LeCheminant, A.N., Miller, A.R., Booth, G.W., Murray, M.J., and Jenner, G.A.
1980: Geology of the Tebesjuak Lake map area, District of Keewatin: A Progress Report with notes on uranium and base metal mineralization; in Current Research, Part A, Geological Survey of Canada, Paper 80-1A, p. 339-346.

Miller, A.R.
1979: Uranium geology in the central Baker Lake Basin, District of Keewatin; in Current Research, Part A, Geological Survey of Canada, Paper 79-1A, p. 57-59.

1980: Uranium geology of the eastern Baker Lake Basin, District of Keewatin, Northwest Territories; Geological Survey of Canada, Bulletin 330, 63 p.

Tella, Subhas and Eade, K.E.
1980: Geology of the Kamilukuak Lake map area, District of Keewatin, A part of the Churchill Structural Province; in Current Research, Part B, Geological Survey of Canada, Paper 80-1B, p. 39-45.

Walker, R.G.
1979: Turbidites and associated coarse clastic deposits; in Facies Models, R.G. Walker, ed., Geoscience Canada Reprint Series No. 1, p. 91-103.

Wright, G.M.
1955: Geological notes on central District of Keewatin; Geological Survey of Canada, Paper 55-17.

1967: Geology of the southestern barren grounds, parts of the Districts of Mackenzie and Keewatin (Operation Keewatin, Baker, Thelon); Geological Survey of Canada, Memoir 350.

33. PRELIMINARY EVALUATION OF URANIUM IN SUSTUT AND BOWSER SUCCESSOR BASINS, BRITISH COLUMBIA

Project 750069

R.T. Bell
Economic Geology Division

Bell, R.T., Preliminary evaluation of uranium in Sustut and Bowser successor basins, British Columbia; in Current Research, Part A, Geological Survey of Canada, Paper 81-1A, p. 241-246, 1981.

Abstract

Uranium occurrences are confirmed for the Late Mesozoic-Paleogene basins in central British Columbia. One occurrence is in conglomerates and sandstones of the lower part of the Sustut Group. Widespread tuffaceous rocks in the upper part of the Sustut Group are anomalously radioactive; uranium content at one locality is 380 ppm. The source of uranium is interpreted to be dominantly from Paleogene Sloko and Ootsa volcanic centres. Black pelites in the lower part of the Bowser assemblage are anomalously radioactive.

Introduction

Late orogenic basins, both successor basins (epieugeosynclines) and foreland basins (exogeosynclines) host a large part of the world's known uranium reserves, notably those in sandstone, volcaniclastic, and volcanic regimes. Such basins possess some of the most favourable conditions for uranium deposit formation: erosion of felsic rocks (granitic, gneissic, and volcanic) of adjacent uplift areas, accumulation of compositionally immature clastic rocks, terrestrial conditions for both basin sedimentation and attendant groundwaters, and closed-basin morphology, particularly for successor basins.

During part of the summers of 1979 and 1980 the author examined parts of the Bowser and Sustut successor basins (Fig. 33.1). Late in 1978 Aquitaine discovered mineralization near Mount Helvecker. The deposit was visited briefly in July 1979 at the start of Aquitaine's investigations. At present their investigations are suspended. Also in 1979 the author inspected and discovered uranium anomalies in the basal zone of the Bowser assemblage near the Dunwell mine, near Stewart, B.C., an Au-Ag-Pb-Zn property briefly mined in 1927 (Grove, 1971). Anomalous radioactivity was detected in specimens from Anyox, B.C. that are part of the Geological Survey's collections (Ruzicka, 1979). The Anyox material comes from just below the basal zone of the Bowser sequence, in a screen of Hazelton-Bowser rocks within Coast Intrusions.

In early February 1980, the author found radioactive specimens in material collected by G.H. Eisbacher during his Sustut, Sifton and Bowser basin studies. Accordingly the type sections of Sustut were investigated in the field and further occurrences were discovered. This paper summarizes the regional geological setting, describes the occurrences and speculates on the uranium potential of the region.

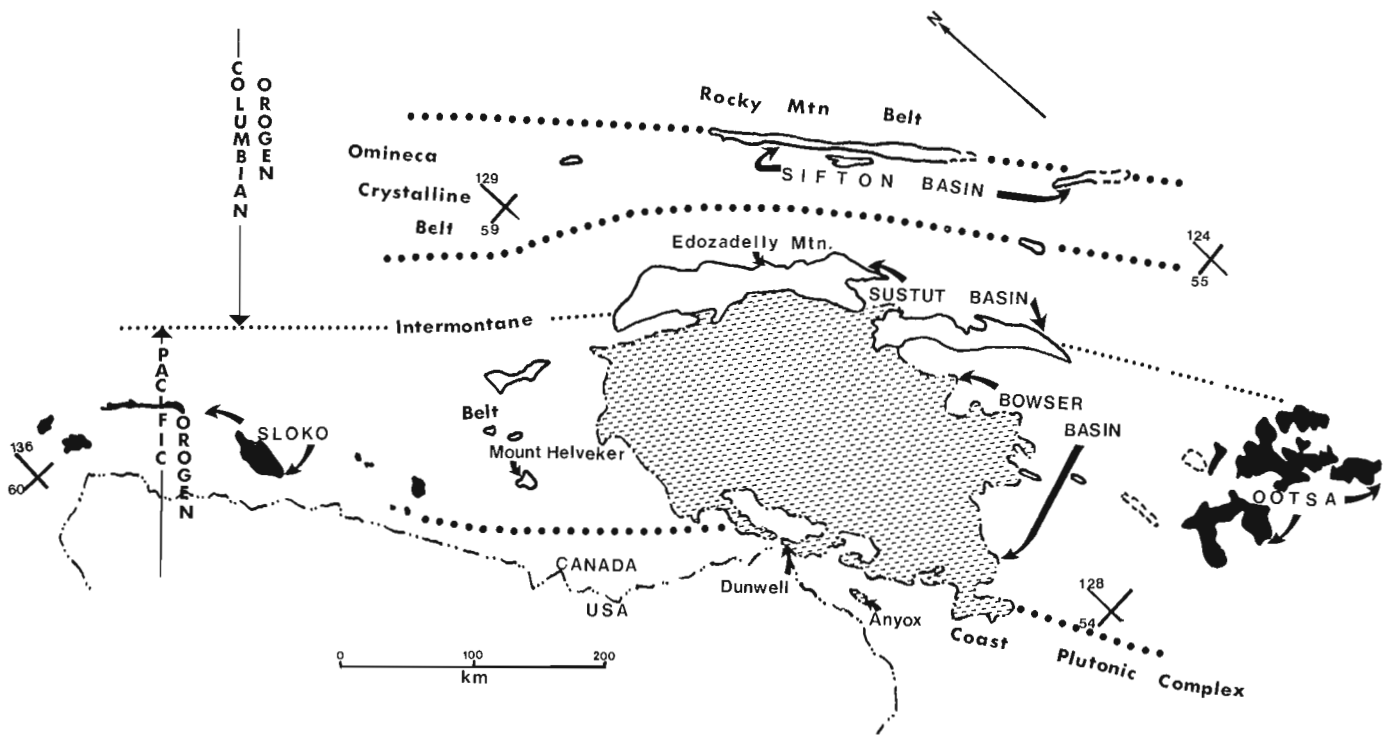

Figure 33.1. *Regional setting of Sustut and Bowser successor basins.*

Regional Geological Setting

Rocks to the east

East of the main successor basins is the Omineca Crystalline Belt which comprises late Proterozoic and Paleozoic feldspathic grits, phyllites, slates, quartzites and carbonates of the Cordilleran miogeocline. During Middle and Late Mesozoic time these rocks were deformed extensively, metamorphosed, and intruded by granitic rocks. The Sifton Basin lies on the eastern border of the Omineca Crystalline Belt (Fig. 33.1).

Basement rocks

The Cache Creek assemblage is a Permo-Carboniferous eugeosynclinal succession of chert, argillite, limestone, volcaniclastic rocks and intrusive mafic igneous rocks. Gabrielse (1976) and Souther (1977) suggested that these were deposited on oceanic crust. They are overlain unconformably by the Asitka Group of felsic to intermediate volcanic rocks. These in turn are overlain by Upper Triassic to Middle Jurassic andesitic and basaltic rocks with local shallow-level granodiorite stocks. These rocks, with associated redbeds and limestones probably represent an island arc volcanic suite (Gabrielse, 1976; Souther, 1977). The Upper Triassic to Middle Jurassic rocks are referred to informally as Hazelton-Takla assemblage.

Bowser assemblage

In the northeastern and central part of the Bowser Basin three facies (Eisbacher, 1974b) make up this assemblage. Facies A is the product of a prograding, delta system typified by coarsening-upwards cycles deposited by southwesterly flowing streams. Just west of the present Sustut Basin, marine-dominated delta and prodelta sediments occur and are successively succeeded to the southwest by sea-fan, turbidite, and shale subfacies. The basal zone near the Dunwell occurrence may represent the most distal shale subfacies of facies A or a transitional facies with uppermost Hazelton. Facies B and C apparently occur only in the centre of the Bowser Basin. The former was deposited during Late Jurassic and perhaps Early Cretaceous time by southward flowing stream systems in deltaic-alluvial fan environments including coal swamps. Facies C was probably deposited in Early Cretaceous time by westerly flowing streams and comprises entirely continental, fine grained clastics, and carbonates.

Sustut Group

Lord (1948) recognized and mapped a belt of Upper Cretaceous and Lower Tertiary continental clastic sedimentary rocks in McConnell Creek map area which he named Sustut Group. The northern extension of this belt and small isolated outliers were identified in succeeding years. Eisbacher (1974a, 1974b) made a definitive study of the Sustut Group as well as reporting on the adjacent Bowser assemblage. He formally subdivided the group into two formations, the Tango Creek and the overlying Brothers Peak, and each of these into two informal members. This summary follows Eisbacher's excellent studies on the Sustut Basin.

The lower member of the Tango Creek Formation, the Niven member, comprises a drab-coloured sandstone-mudstone succession. Drab sandstones predominate and are subquartzose, feldspathic arenites. A few thin maroon and maroon-mottled mudstones in an otherwise green-grey mudstone and drab quartz-pebble conglomerate beds provide useful stratigraphic markers. In many localities a polymict conglomerate is present at the base. The upper member of the Tango Creek Formation, the Tatlatui member, comprises dark grey mudstones, with subordinate chert-pebble-bearing arenites.

The thickness of the Tango Creek Formation ranges from 500 m on the east side to 1400 m on the west side of the basin. Eisbacher concluded that during deposition of the Niven member drainage was southwest, with a transition to northerly longitudinal drainage during Tatlatui time. the Tango Creek Formation was probably deposited during Late Cretaceous and Paleocene time.

The lower member of the Brothers Peak Formation, the Lasuli member, rests apparently conformably on the Tango Creek Formation although local angular unconformities may exist. The Lasuli member comprises coarse, grey, polymictic conglomerate and arenites interbedded with grey, green, and rarely varicoloured ash tuffs and tuffaceous mudstones and siltstones. Eisbacher chose the upper boundary of the Lasuli where there is a sharp decrease in conglomerate beds and change in paleocurrents. The upper member, the Spatsizi, comprises drab, pebbly arenites interbedded with grey tuffs and tuffaceous mudstones. Eisbacher concluded that the drainage system for the Lasuli member was longitudinal to the southeast with principal clastic input along an apron on the western edge of the north part of the Sustut Basin and joined by drainage from the east in the southern part of the basin. In the Spatsizi member main sediment imput appeared to be from the northwest. Eisbacher concluded that the drainage system in Spatsizi time was probably erosional in the southwest.

Figure 33.2 summarizes clast composition and paleocurrents for the Sustut Group.

Between 10 and 30 per cent of the Brothers Peak Formation is ash tuff and highly tuffaceous pelites. Overall thicknesses are related to the amount of conglomerate present; total thicknesses range up to 900 m. Eisbacher concluded the Brothers Peak Formation is largely Eocene in age, therefore coeval with the Sloko Group volcanics to the northwest. It is likely coeval with the Ootsa Lake volcanics (Souther, 1977) to the south as well (Fig. 33.1).

Of note are zeolites described by Read and Eisbacher (1974). Heulandite and analcime are found in altered tuffs and tuffaceous sedimentary rocks (Brothers Peak Formation), while laumontite is found mainly in the Tango Creek Formation and sparsely in nontuffaceous sedimentary rocks of the Brothers Peak Formation. They concluded that the tuffs were altered within a few million years after deposition under inferred conditions of temperature and pressure not exceeding 65°C and 0.4 kb, respectively.

Folding and faulting preceded, accompanied, and outlived deposition of the Sustut (and Sifton) rocks. Eisbacher (1974a, p. 49) concluded that the Sustut Basin represents the 'molasse facies' of both the Columbian Orogen (Tango Creek Formation) and the Pacific Orogen (Brothers Peak Formation).

Sifton Formation

The Sifton Formation occurs in the northern Rocky Mountain Trench. Exposure is poor and structurally complicated. Boulder conglomerate, breccias, sandstone, and mudstone of probable Late Cretaceous to Eocene time represent an intramontane molasse that was separated from Sustut by an uplift area that contained the most metamorphosed part of the Omineca Crystalline Belt.

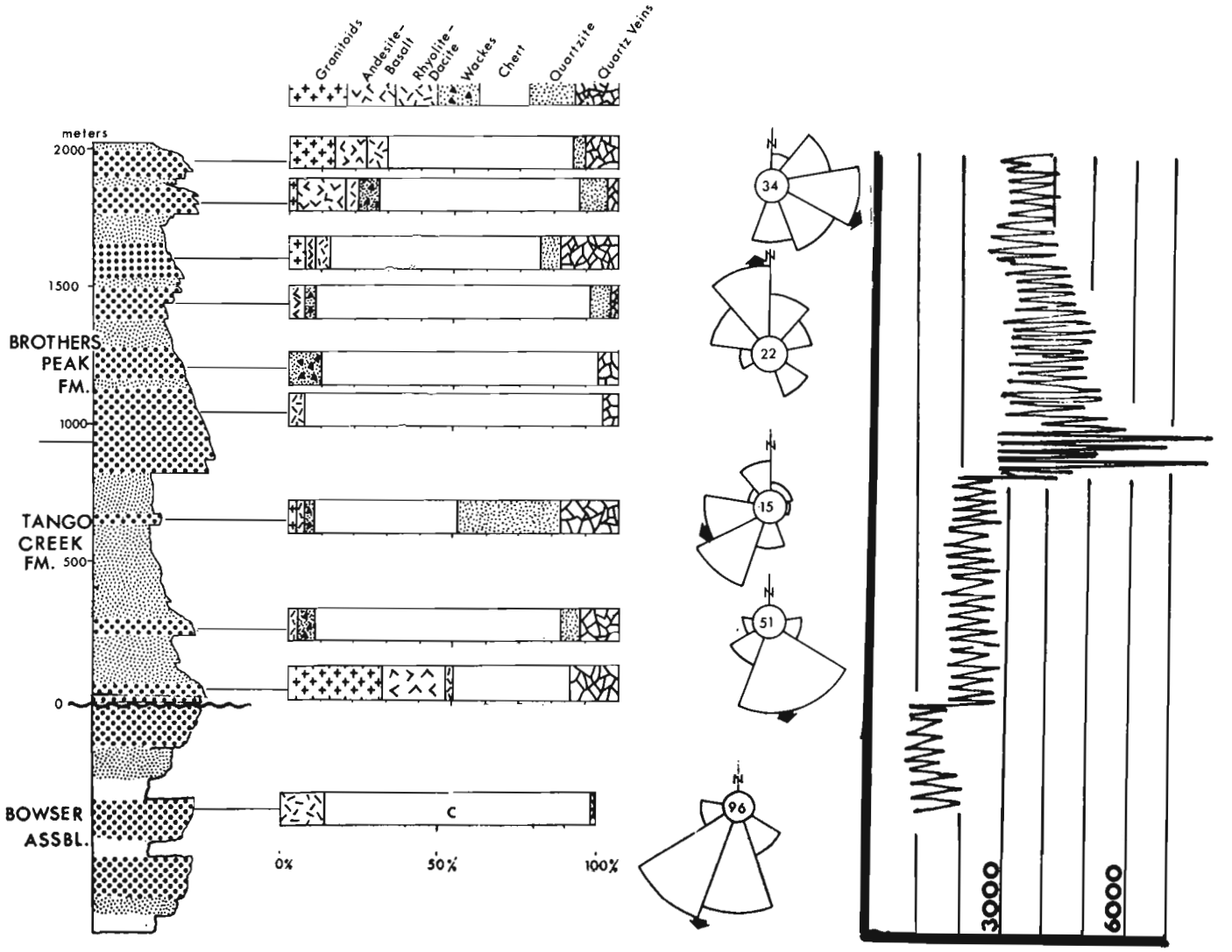

Figure 33.2. *Generalized paleocurrents and clast composition of Bowser assemblage and Sustut Group (after Eisbacher et al. 1974) and generalized radiometric response, using McPhar TV-1A Scintillometer, T-1 scale, in counts per minute).*

Uranium Occurrences

Mount Helvecker (HEL Prospect)

The sedimentary section at Mount Helvecker comprises about 300 m of poorly consolidated, green-grey, pebbly, feldspathic and quartzose arenites with subordinate pebble and cobble conglomerates. A few thin coal seams are also present. It is interpreted to be Sustut Group (Souther, 1972) and, lacking internal pyroclastic units, is tentatively correlated with the Tango Creek Formation. It overlies both the Bowser assemblage and Upper Triassic volcanics and is overlain by grey and green trachytic and rhyolitic flows and pyroclastic rocks of the Sloko Group (Souther, ibid).

Mineralization occurs in three forms. The most important is in rusty-weathering, chert-, and volcanic-pebble conglomerates underlying coal seams (themselves not notably radioactive). The conglomerates contain secondary uranium minerals (mainly of the autunite group). At the original discovery, mineralization of the order of one-half per cent U persists for several metres along strike in a zone up to 30 cm thick.

A second form of mineralization is in disperse coal fragments within pebbly sandstones where the coaly material is strongly radioactive and marked by a pink alteration halo.

A third form (not observed in situ) comprises anomalously (six times background) radioactive trachyte in talus, presumed to come from overlying Sloko Group.

In summary three points should be stressed:

a. the sedimentary rocks are poorly consolidated and no mudstones were observed, both features in contrast to the Sustut Group of Tango Creek-Brothers Peaks-Edozadelly Mountain area;

b. the coal seams are not notably radioactive, but the underlying coarse grained clastic rocks are;

c. anomalously radioactive volcanics are present.

The mineralization is probably epigenetic, primarily fixed by organically dominated materials. Humic acids likely played an important role. The observed occurrences have been weathered, consequently only secondary minerals have been identified. The uranium was probably derived from felsic igneous rocks in nearby areas; the Paleogene volcanic rocks (Sloko) providing most of the uranium by means of downwards percolating groundwaters.

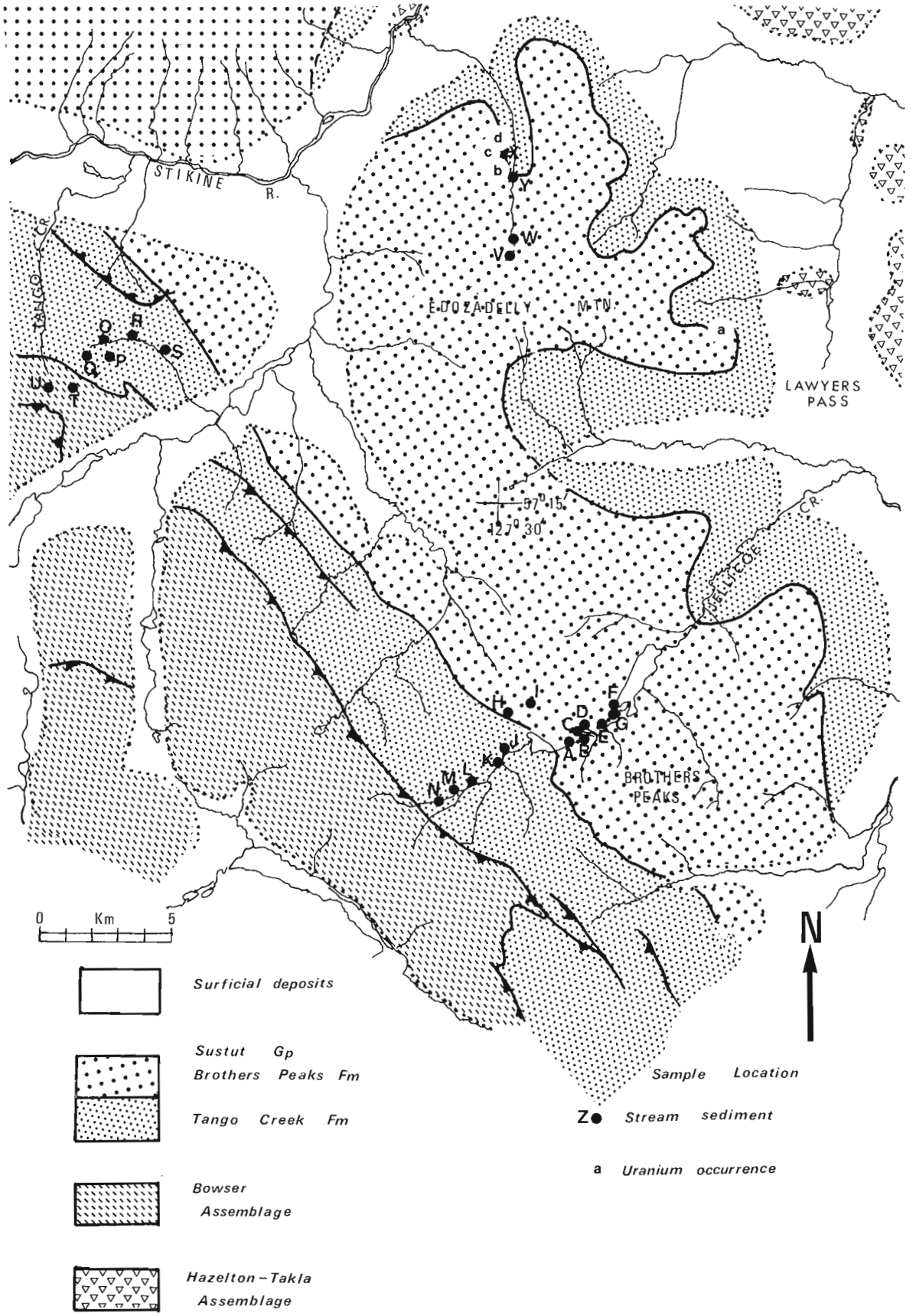

Figure 33.3. *Generalized geology (after Eisbacher, 1974a), of Edozadelly Mountain area, with location of uranium occurrences and stream sediment sample sites.*

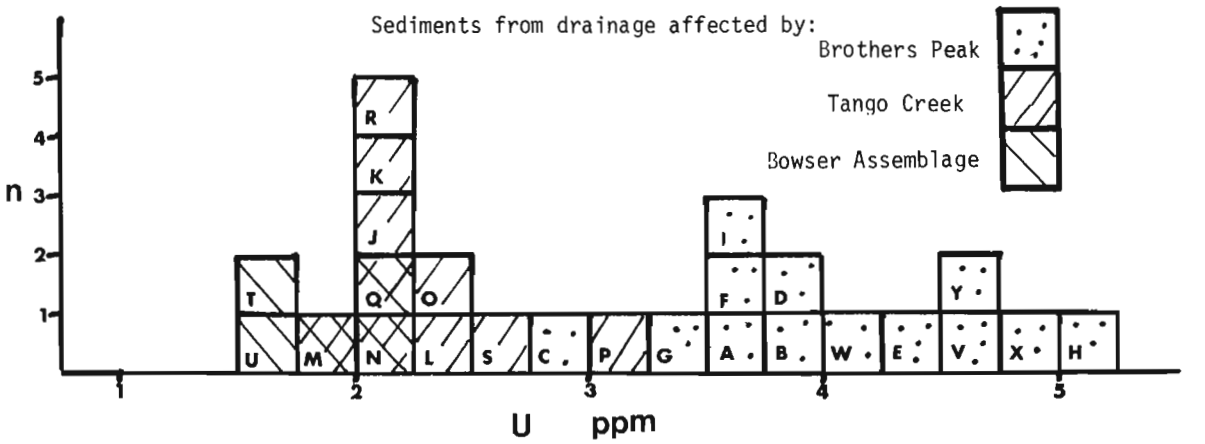

Figure 33.4. *Distribution of uranium in stream sediment samples from Edozadelly Mountain area.*

Edozadelly Mountain Area

Figure 33.2 illustrates the stratigraphy in this area as well as a generalized, radiometric response of rocks in the section, as measured during 1980 field season using a McPhar TV-1A. All radiometric values would be correspondingly higher along cliffs and lower along ridge tops.

Tuffaceous rocks of the Brothers Peak Formation, notably the lowermost 6 or 7 ash-tuff units are found to be anomalous throughout the area illustrated in Figure 33.3. These tuffs generally are laminated, greenish grey, porcelaneous and hard, and weather cream-coloured to pale brown. The more radioactive tuffs and tuffaceous mudstones are marked by pink layers or mottles (locations b and d). The most radioactive (locations a and c) are altered to a bright red, contain coaly fragments, and are within sequences containing white spherules and coalescent spherules of analcime. The specimen from Eisbacher's collection (in Fig. 10, Read and Eisbacher, 1974) contains about 380 ppm U over a 2 cm-thick layer.

The tuffaceous material in the Brothers Peak Formation is very fine grained. The ash was likely carried by high-altitude west winds from Sloko and south winds from Ootsa irruptive centres, deposited and preserved in shallow lakes and covered by episodic floods of coarse grained alluvial fans. There is evidence that most of the tuffs were reworked to varying degrees by flowing water. Eisbacher (1974a) suggested that at least 50 to 100 volcanic events were necessary to supply the Brothers Peak tuffs.

All the tuffs and tuffaceous mudstones in the Lasuli member are at least slightly radioactive and were probably lithified very early in their history. Those in the Spatsizi member are, in general, less radioactive. This may reflect either a lower initial uranium content in these later volcanic materials or longer periods of sedimentary reworking that permitted greater leaching of uranium and allowed dilution by other materials. The latter reason is preferred because reworking is more strongly evident in these rocks and there is a gradual increase in nontuffaceous mudstones up section.

The tuffaceous units are relatively impermeable. Diagenetic alteration (including zeolitization) probably freed some of the uranium which in turn was refixed in adjacent layers having slightly higher permeability and containing slightly greater amounts of organic matter. Layers containing randomly oriented vegetation fragments are scarcely affected; layers with fragments subparallel with bedding are considerably more radioactive.

Radioactive inspection suggests that all tuffs in the Lasuli member contain about 20 to 60 ppm uranium; some zones 2 to 10 cm thick over 500 m strike length contain more than 100 ppm.

Uranium mineralization is interpreted as being early diagenetic, but essentially syngenetic within water-laid tuffs. Inspection for U of the source-area volcanics and associated intrusions is strongly recommended. No other occurrences nor anomalous radioactivity was detected in this area.

Bowser Assemblage-Dunwell

During examination of the west flank of Sustut Basin in 1980, marine-dominated, coal-bearing, deltaic sedimentary rocks of Facies A of the Bowser assemblage were inspected briefly. No uranium occurrences or anomalies were detected; radiometric response was very low.

During the summer of 1979 while investigating the Stewart area, anomalously radioactive, black, cherty siltstones and argillites within 30 m of the base of Bowser assemblage were found on the road to the Dunwell mine. These contain about 30 ppm uranium. They may be related to the Anyox occurrence (Ruzicka, 1979), and lie in the distal, entirely marine, facies of the Bowser Basin.

Such anomalies are common in black, shaly rocks in many parts of the world (Bell, 1978).

Stream Sediment Geochemistry Orientation Survey

Figures 33.3 and 33.4 and Table 33.1 summarize uranium content in 25 stream sediment samples collected during the course of investigation of the type sections of the Sustut Group. All samples are from first-order tributaries, usually at least 15 m upstream from the main, higher order streams except samples N, T, U, V, W and Y. Samples I and E are from the same tributary. Collection of carbonaceous sediments was avoided. At the time of sampling all streams were flowing, although the streams at H, I and X, almost certainly, are dry most of the summer during some years. The samples were dried and the minus-80 mesh-size fractions were assayed using the neutron activation method.

The number of samples is too small for meaningful statistical treatment. The samples do indicate (Fig. 33.4) a distinct response to the bedrock and suggest this method could be useful in the Sustut and Bowser basins.

Table 33.1

Stream sediment analyses

Sample No.	Bedrock at Sample Site	Additional Units Upstream	U ppm
A	Brothers Peak Fm.		3.7
B	" " "		3.9
C	" " "		2 9
D	" " "		4.0
E	" " "		4.4
F	" " "		3.7
G	" " "		3.5
H*	" " "		5.2
I*	" " "		3.7
J	Tango Creek Fm.		2.1
K	" " "		2.1
L	" " "		2.3
M	" " "	Bowser assemblage	1.8
N	" " "	Bowser assemblage	2.1
O	" " "		2.5
P	" " "		3.1
Q	" " "	Bowser assemblage	2.1
R	" " "		2.2
S	" " "		2.6
T*	Bowser assemblage		1.7
U*	" "		1.6
V*	Brothers Peak Fm.		4.6
W*	" " "		4.2
X*	" " "		5.0
Y*	" " "		4.9

* Stream sediment probably unaffected by glacially transported material from other units.

Analyses by neutron activation by AECL.

Conclusion

Uranium occurrences have been found in the Sustut Basin in both coarse grained clastic rocks and in fine grained volcaniclastic rocks, those in the latter being widespread, albeit very low grade. The author favours Paleogene volcanic rocks as a prime source for the uranium. Accordingly, relatively undeformed areas of the Tango Creek Formation would probably be most favourable, especially where poorly consolidated. Tuffaceous horizons of the Brothers Peak Formation merit more detailed inspection. Most definitely, Sloko and Ootsa Lake volcanics and associated high level Paleogene intrusions warrant special attention.

Acknowledgments

I wish to thank J. Carne, N. Carter, G. Eisbacher, H. Gabrielse, R. Kirkham, and T. Schroeter for many useful discussions and guidance concerning regional geology and local field logistics. D.J.R. Bell gave exemplary field assistance in 1980. Stream sediment preparation was done by Terrain Sciences Division.

References

Bell, R.T.
1978: Uranium in black shales – a review; in Kimberly, M.M. (ed.), short course in uranium deposits, their mineralogy and origin; Mineralogical Association of Canada, October 1978, p. 307-329.

Eisbacher, G.H.
1974a: Sedimentary history and tectonic evolution of the Sustut and Sifton basins, north-central British Columbia; Geological Survey of Canada, Paper 73-31, 57 p.

1974b: Deltaic sedimentation in the northeastern Bowser basin, British Columbia; Geological Survey of Canada, Paper 73-33, 13 p.

Eisbacher, G.H., Carrigy, M.A., and Campbell, R.B.
1974: Paleodrainage pattern and late-orogenic basins of the Canadian Cordillera; in Dickinson, W.R. (ed.) Tectonics and Sedimentation, Society of Economic Paleontologists and Mineralogists, Special Publication, No. 22, p. 143-166.

Eisbacher, G.H. and Gabrielse, H.
1975: The molasse facies of the Columbian orogen, Canadian Cordillera; Geologische Rundschau, Band 64, p. 85-100.

Gabrielse, H.
1976: Environments of Canadian Cordillera depositional basins; in Circum-Pacific Energy and Mineral Resources, American Association of Petroleum Geologists, Memoir 25, p. 492-502.

Grove, E.W.
1971: Geology and mineral deposits of the Stewart area, British Columbia; British Columbia Department of Mines and Petroleum Resources, Bulletin 58, 217 p.

Lord, C.S.
1948: McConnell Creek map area, Cassiar District, British Columbia; Geological Survey of Canada, Memoir 251, 72 p.

Read, P.B. and Eisbacher, G.H.
1974: Regional zeolite alteration of the Sustut Group, north-central British Columbia; Canadian Mineralogist, v. 12, p. 527-541.

Ruzicka, V.
1979: Uranium and thorium in Canada, 1978; in Current Research, Part A, Geological Survey of Canada, Paper 79-1A, p. 139-155.

Souther, J.G.
1972: Telegraph Creek map area, British Columbia; Geological Survey of Canada, Paper 71-44, 38 p.

1977: Volcanism and tectonic environments in the Canadian Cordillera – a second look; in Baragar, W.R.A. et al. (eds.) Volcanic Regimes in Canada; Geological Association of Canada, Special Paper No.16, p. 3-24.

34. REVISION OF STRATIGRAPHIC NOMENCLATURE, FORELAND THRUST-FOLD BELT OF WOPMAY OROGEN, DISTRICT OF MACKENZIE

Project 770019

P.F. Hoffman
Precambrian Geology Division

Hoffman, P.F., Revision of stratigraphic nomenclature, foreland thrust-fold belt of Wopmay Orogen, District of Mackenzie; in Current Research, Part A, Geological Survey of Canada, Paper 81-1A, p. 247-250, 1981.

Abstract

Certain revisions of stratigraphic nomenclature for the foreland of Wopmay Orogen are proposed to better reflect the main lithologic divisions and their tectonic settings. The "Recluse Formation", which consists of dark marine foredeep deposits, is elevated to a group consisting of three formations: the Tree River Formation, cratogenic siltstone; the Fontano Formation, hemipelagic shale; and the Asiak Formation, orogenic greywacke. It is proposed that the term "Epworth Group" be confined to the Odjick and Rocknest formations, thereby returning to its original stratigraphic definition. As thus defined, the Epworth Group comprises the passive-margin sedimentary prism of the orogen. The Akaitcho Group, an epicontinental rift-fill assemblage, underlies the Epworth Group. All three groups, plus two formations above the Recluse Group, the Cowles Lake and Takiyuak formations, may be collectively referred to as the Coronation Supergroup. Regional correlations are presented between the Coronation Supergroup, the Great Slave Supergroup and the Goulburn Group, thus linking the three major Aphebian basins marginal to the Slave Province.

Introduction

The foreland thrust-fold belt of Wopmay Orogen (Coronation Geosyncline) that is the part of the orogen east of Wopmay Fault is being studied as an example of a passive continental margin of early Proterozoic age that was destroyed by collisional orogeny (Hoffman, 1979, in press) at about 1.9 Ga (Van Schmus and Bowring, 1980). Systematic 1:100 000 scale geological mapping is virtually complete north of 66 degrees latitude for the internal, or western, part of the belt (see Hoffman and St-Onge, 1981). This work is complimented by earlier preliminary stratigraphic studies in the external part (Hoffman, 1970, 1973, 1975). It is now desirable to make certain refinements to the existing stratigraphic nomenclature, which evolved mainly during the era of reconnaissance mapping. This note briefly outlines the need for certain refinements in the nomenclature and makes some proposals. The stratigraphy will be described formally and in some detail later.

Evolution of the Existing Stratigraphic Nomenclature

O'Neill (1924) introduced the name "Epworth formation" to the formal stratigraphic literature. His type locality is the folded synclinal sequence of cherty dolomites with a basal member of terrigenous clastics that rest unconformably on Archean granite around Port Epworth, at the mouth of the Tree River on the south side of Coronation Gulf. In the current nomenclature (Fraser, 1974), this "Epworth formation" is equivalent to both the Odjick Formation, comprising the basal clastics which are relatively thin at Port Epworth, and the Rocknest Formation, the cherty dolomite (Table 34.1).

During helicopter-traverse mapping, the "Epworth formation", later "Epworth Group", was extended to include virtually all the early Proterozoic rocks of low metamorphic grade between Hepburn Batholith and the Archean Shield of the Slave Province (Fraser et al., 1960). Thus, the name "Epworth" came to be associated with strata far above and below those of O'Neill's type section, and it came to be used as much with an areal as a stratigraphic meaning. This usage also diverged from Phanerozoic practice in that inclusion was not based on common lithological features.

The internal stratigraphy of the enlarged "Epworth Group" was established for the external part of the belt during ground-traverse mapping by Fraser (1974). The group was divided into five formations (Table 34.1), of which only the three oldest are preserved in the thrust-fold belt proper, as distinct from the autochthonous Takijuq Basin to the east. They are, in ascending order: (1) Odjick Formation, composed of mature quartz arenite, minor subfeldspathic arenite, and pelite, (2) Rocknest Formation, cherty stromatolitic dolomite and marly pelite, and (3) Recluse Formation, immature feldspathic-lithic wacke and pelite.

Work in the internal zone has revealed a thick complex of submature clastic sedimentary rocks, and bimodal (basalt-rhyolite) volcanic and shallow-intrusive rocks (Hoffman et al., 1978). The top of this complex, named Akaitcho Group, is essentially conformable with the overlying Odjick Formation (Easton, 1980). The group has been divided into formations and subgroups (Easton, in press). In Cloos Anticline, the internal-external transition zone, two formations occur below the Odjick Formation that are tentatively correlated with the Akaitcho Group (Hoffman et al., 1978). The Vaillant Formation, composed of basaltic-eruptive rocks, is overlain with some intercalation by the Stanbridge Formation, composed of cherty stromatolitic dolomite (Table 34.1). The Akaitcho Group is interpreted as an epicontinental rift-fill deposit prior to the onset of seafloor spreading in the initial development of the passive continental margin (Easton, in press).

No changes in nomenclature are needed for the Odjick and Rocknest formations. The Odjick Formation is easily recognized in the internal zone by its quartzite beds. Major but gradational changes in sedimentary facies from east to west are interpreted in terms of a prograding continental shelf in the external zone, a continental slope near Cloos Anticline, and a continental rise in the internal zone. The Rocknest Formation is a 1-km-thick blanket of peritidal deposits atop the shelf sequence. It passes through a high-energy shelf-edge facies and then thins abruptly into a starved submarine-slope facies just east of Cloos Anticline. It is not recognizable in the internal zone. The Odjick and Rocknest Formations together are interpreted as an Atlantic-type marginal sedimentary prism deposited following the onset of seafloor spreading (Fraser et al., 1972; Hoffman, 1973, in press).

The Recluse Formation, on the other hand, requires subdivision as it comprises three distinct lithologic units of differing environmental and tectonic significance. In the

Table 34.1.

Evolution of stratigraphic nomenclature in the foreland of Wopmay Orogen.

O'NEILL (1924)	FRASER (1974)		THIS PAPER	
EPWORTH FM.	EPWORTH GROUP	Takiyuak Fm.	CORONATION SUPERGROUP	Takiyuak Fm.
		Cowles Lake Fm.		Cowles Lake Fm.
		Recluse Fm.	RECLUSE GROUP	Asiak Fm.
				Fontano Fm.
				Tree River Fm.
		Rocknest Fm.	EPWORTH GROUP	Rocknest Fm.
		Odjick Fm.		Odjick Fm.
			AKAITCHO GROUP	Stanbridge Fm.
				Vaillant Fm.
				many other formations see Easton (in press)

Table 34.2.

Regional correlation chart.

WOPMAY OROGEN			EAST ARM THRUST BELT		KILOHIGOK BASIN	
CORONATION SUPERGROUP		Takiyuak Fm.	GREAT SLAVE SUPERGROUP	CHRISTIE BAY GROUP	unnamed fm.	GOULBURN GROUP	Amagok Fm.
		unnamed breccia			Pearson Fm.		Brown Sound Fm.
		Cowles Lake Fm.			Portage Inlet Fm.		
	RECLUSE GROUP	Asiak Fm.			Tochatwi Fm.		Omingmaktook breccia
		Fontano Fm.			Stark breccia		Kuuvik Fm.
		Tree River Fm.		PETHEI GROUP			Peacock Hills Fm.
	EPWORTH GROUP	Rocknest Fm.		KAHOCHELLA GROUP			Quadyuk Fm.
		Odjick Fm.		SOSAN GROUP	unnamed mbr.		Mara Fm.
	AKAITCHO GROUP				Akaitcho River Fm.		Burnside River Fm.
					Kluziai Fm.		Western River Fm.
					Duhamel Fm.		
					Hornby Channel Fm.		
				UNION ISLAND GROUP			

internal zone, more than 1.5 km of carbonaceous pelite with varve-like laminations, named Fontano Formation (Hoffman et al., 1978) is gradationally overlain by turbidites of highly-immature feldspathic-lithic wacke. The same two units occur in the external zone, but the laminated pelite is generally less than 100 m thick and is overlain sharply by more than 1.5 km of thick bedded wackes. Locally, steep-walled canyons, filled by abnormally thick Fontano pelite bordered in part by canyon-wall breccias, were cut down through the Rocknest Formation and into the upper Odjick Formation. This and major submarine-slide breccias, composed of debris derived from the Stanbridge Formation, occurring in the lower Fontano Formation along Lupin Fault on the west limb of Cloos Anticline, attest to an episode of block faulting and canyon cutting as the continental shelf foundered and was draped by the hemipelagic Fontano Formation. The foundering of the shelf and subsequent backfilling of the deepwater trough by immature wackes are interpreted mobilistically as resulting from descent of the passive margin into a west-dipping subduction zone (Hoffman, in press). In this model, the trough in which these units were deposited was an oceanic trench that evolved into a collisional foredeep. The autochthonous basins east of the thrust-fold belt have a thin unit of dark quartzose siltstone above the Rocknest Formation and below the Fontano Formation. This minor spurt of cratogenic clastics into the foredeep is tentatively correlated with the much thicker and coarser clastics of the Burnside River and Mara formations of Kilohigok Basin (Campbell and Cecile, in press). All three of the units are sufficiently important to warrant formational rank.

Proposed Revision of the Stratigraphic Nomenclature

It is proposed to elevate the rank of the "Recluse Formation" (Fraser, 1974) to that of a group (Table 34.1), retaining its original stratigraphic limits. It would be divided into three formations: (1) Fontano Formation, as defined previously, (2) Asiak Formation, the feldspathic-lithic wackes named for the Asiak River along which they are well exposed, and (3) Tree River Formation, the quartzose siltstones. The three formations are appropriately grouped as all are dark-coloured submarine deposits, and deserve to be separated from the underlying passive-margin sequence for reasons of lithology, tectonic setting and evidence of local disconformity between them. The formations can be symbolized "Rf", "Ra", and "Rt" on maps.

Instead of elevating the rank of the venerable name "Epworth" to a supergroup, it is proposed that we return to O'Neill's well-described original definition (O'Neill, 1924, p. 21-2, 45-7), that is the Odjick and Rocknest formations, but retain its current rank as Epworth Group (Table 34.1). The lithological common denominator is that both formations, in the external zone, are shallow-marine shelf deposits, and they are mutually conformable and intergradational. The two formations can be symbolized "Eo" and "Er".

It is recommended that the two highest formations, Cowles Lake and Takiyuak formations (Table 34.1), remain ungrouped at least until their contact relations have been more thoroughly studied. The entire succession, from the Akaitcho Group through to the Takiyuak Formation, may be referred to as the Coronation Supergroup (Table 34.1), thereby reviving that name in substantially its original meaning (Hoffman et al., 1970; Hoffman, 1973). The Cowles Lake and Takiyuak formations could then be symbolized "Cc" and "Ct".

Regional stratigraphic correlations with the East Arm of Great Slave Lake and the Bathurst Inlet area are shown in Table 34.2. These correlations have remained essentially unchanged since they were first proposed more than a decade ago (Fraser and Tremblay, 1969; Hoffman, 1970).

Summary

Revision of the existing stratigraphic nomenclature of the foreland thrust-fold belt of Wopmay Orogen into three groups would better reflect the principal lithologic and tectonic divisions of the succession. The proposed groups, each of which comprises two or more formations, are in ascending order: (1) Akaitcho Group, the clastic sedimentary and bimodal igneous rocks of an initial rift environment, (2) Epworth Group, a passive-margin sedimentary prism, and (3) Recluse Group, the deepwater clastics of a collisional foredeep. These three groups, plus two additional formations that overlie the Recluse Group in an autochthonous basin east of the thrust-fold belt, may be collectively referred to as the Coronation Supergroup.

References

Campbell, F.H.A. and Cecile, M.P.
Evolution of the early Proterozoic Kilohigok Basin, Bathurst Inlet – Victoria Island, N.W.T.; in Proterozoic Basins of Canada, ed., F.H.A. Campbell; Geological Survey of Canada, Paper 81-10. (in press)

Easton, R.M.
1980: Stratigraphy and geochemistry of the Akaitcho Group, Hepburn Lake map area, District of Mackenzie: An initial rift succession in Wopmay Orogen (early Proterozoic); in Current Research, Part B, Geological Survey of Canada, Paper 80-1B, p. 47-57.

Stratigraphy of the Akaitcho Group and the development of an early Proterozoic continental margin, Wopmay Orogen, N.W.T.; in Proterozoic Basins of Canada, ed., F.H.A. Campbell; Geological Survey of Canada, Paper 81-10. (in press)

Fraser, J.A.
1974: The Epworth Group, Rocknest Lake area, District of Mackenzie; Geological Survey of Canada, Paper 73-39, 23 p.

Fraser, J.A. and Tremblay, L.P.
1969: Correlation of Proterozoic strata in the northwestern Canadian Shield; Canadian Journal of Earth Sciences, v. 6, p. 1-9.

Fraser, J.A., Craig, B.G., Davison, W.L., Fulton, R.J., Heywood, W.W., and Irvine, T.N.
1960: North-central District of Mackenzie, Northwest Territories; Geological Survey of Canada, Map 18-1960.

Fraser, J.A., Hoffman, P.F., Irvine, T.N., and Mursky, G.
1972: The Bear Province; in Variations in Tectonic Styles in Canada, ed. R.A. Price and R.J.W. Douglas; Geological Association of Canada, Special Paper No. 11, p. 453-503.

Hoffman, P.F.
1970: Study of the Epworth Group, Coppermine River area, District of Mackenzie; in Report of Activities, Part A, Geological Survey of Canada, Paper 70-1A, p. 144-149.

1973: Evolution of an early Proterozoic continental margin: the Coronation geosyncline and associated aulacogens of the northwestern Canadian Shield; Philosophical Transactions of the Royal Society of London Series A, v. 273, p. 547-581.

Hoffman, P.F. (cont.)
1975: Shoaling-upward shale-to-dolomite cycles in the Rocknest Formation (Lower Proterozoic), Northwest Territories, Canada; in Tidal Deposits: A Casebook of Recent Examples and Fossil Counterparts, ed., R.N. Ginsburg; Springer-Verlag, New York, p. 257-265.

1979: Wopmay Orogen: continent-microcontinent-continent collision of early Proterozoic age, Bear Province, Canadian Shield; in Program with Abstracts; Geological Association of Canada, v. 4, p. 58.

Beyond basin analysis: the East Arm Thrust Belt of Great Slave Lake and its tectonic relation to Wopmay Orogen and the Churchill Province; in Proterozoic Basins of Canada, ed., F.H.A. Campbell; Geological Survey of Canada, Paper 81-10. (in press)

Hoffman, P.F. and St-Onge, M.R.
1981: Contemporaneous thrusting and conjugate transcurrent faulting during the second collision in Wopmay Orogen: implications for the subsurface structure of Hornby Bay Group outliers; in Current Research, Part A, Geological Survey of Canada, Paper 81-1A, Report 35.

Hoffman, P.F., Fraser, J.A., and McGlynn, J.C.
1970: The Coronation Geosyncline of Aphebian age, District of Mackenzie; in Symposium on Basins and Geosynclines of the Canadian Shield, ed. A.J. Baer; Geological Survey of Canada, Paper 70-40, p. 200-212.

Hoffman, P.F., St-Onge, M.R., Carmichael, D.M., and Bie, I. de
1978: Geology of the Coronation Geosyncline (Aphebian), Hepburn Lake sheet, Bear Province, District of Mackenzie; in Current Research, Part A, Geological Survey of Canada, Paper 78-1A, p. 147-151.

O'Neill, J.J.
1924: The geology of the Arctic Coast of Canada, west of the Kent Peninsula; in Report of the Canadian Arctic Expedition 1913-18, Volume XI, Part A; King's Printer, Ottawa, 107 p.

Van Schmus, W.R. and Bowring, S.A.
1980: Chronology of igneous events in the Wopmay Orogen, Northwest Territories, Canada; in Abstracts with Programs, Geological Society of America, v. 12, no. 7.

35. CONTEMPORANEOUS THRUSTING AND CONJUGATE TRANSCURRENT FAULTING DURING THE SECOND COLLISION IN WOPMAY OROGEN: IMPLICATIONS FOR THE SUBSURFACE STRUCTURE OF POST-OROGENIC OUTLIERS

Project 770019

P.F. Hoffman and M.R. St-Onge[1]
Precambrian Geology Division

Hoffman, P.F., and St-Onge, M.R., Contemporaneous thrusting and conjugate transcurrent faulting during the second collision in Wopmay Orogen: implications for the subsurface structure of post-orogenic outliers; in Current Research, Part A, Geological Survey of Canada, Paper 81-1A, p. 251-257, 1981.

Abstract

The north-central part of Wopmay Orogen has been segmented into crudely hexagonal fault-blocks, about 75 km in diameter, that appear to have overriden each other from west to east and have relative displacements measured in kilometres both laterally and vertically. Block thrusting appears to have been superimposed on an ongoing system of conjugate transcurrent faulting in relieving east-west compression. The unusual fault system dates from the second of two collisional orogenies affecting this early Proterozoic continental margin and it deforms an earlier thrust-fold belt, more familiar in style, that formed during the first collision. Backsliding on the hexagonal block-margin thrusts during post-orogenic extension could account for the graben-like outliers of post-orogenic clastics that have been a focus of uranium exploration in the area.

Introduction

Wopmay Orogen is the north-south Aphebian belt on the west flank of the Archean Slave craton in the northwest corner of the Canadian Shield. One of the remarkable features of the orogen is its system of late northeast- and northwest-trending faults. These have been interpreted as a system of conjugate transcurrent faults (Freund, 1974), dating from the second of two collisional orogenies affecting the orogen (Hoffman, 1979, 1980, in press). Recent mapping of the eastern part of Hepburn Lake (86 J) map area suggests that significant thrusting occurred more-or-less simultaneously with transcurrent faulting. The result is a segmentation of the orogen into crudely-hexagonal imbricate thrust-blocks, about 75 km in diameter. Graben-like outliers of post-orogenic clasts, being explored for uranium, occur intermittently along the thrust-block margins.

Tectonic Setting and Timing

The foreland thrust-fold belt of Wopmay Orogen, that is the part of the orogen east of Wopmay Fault (Fig. 35.1), is interpreted as a passive continental margin of early Proterozoic age that became involved in two collisions (Hoffman, 1979, in press) between about 1.90 and 1.85 Ga (Van Schmus and Bowring, 1980). In the first collision, the passive margin was drawn into a west-dipping subduction zone, where it was sheared and compressed into a north-south belt of west-dipping thrusts and folds (Fig. 35.2). This belt was, before the second collision, similar in scale and style to thrust-fold belts in many other orogenic forelands (eg. Mountjoy, 1980; Price, in press). The thrusts (solid teeth in Fig. 35.2) appear to be relatively thin-skinned and terminate in folds along strike. Some of the folding no doubt accompanied the thrusting but much of it is younger, certain of the thrusts being tightly folded (St-Onge, in press). The westward change from relatively short (about 30 km), closely-spaced thrusts in the external zone to long (more than 100 km), widely-spaced thrusts in the internal zone coincide with the change in sedimentary facies from quartzite and dolomite of the continental shelf into pelites of the continental slope and rise.

The internal zone is intruded by batholiths of the Hepburn Intrusive Suite (Fig. 35.2), composed mostly of more-or-less foliated granites and tonalites of generally peraluminous mineralogy (Hoffman et al., 1980; Hoffman, 1980). Metamorphic conditions were raised from regional greenschist- to local granulite-facies at a depth of about 12 km by the magmatic heat of these batholiths (St-Onge and Carmichael, 1979; St-Onge, 1979, 1980, in press). The metamorphism postdates adjacent thrusts.

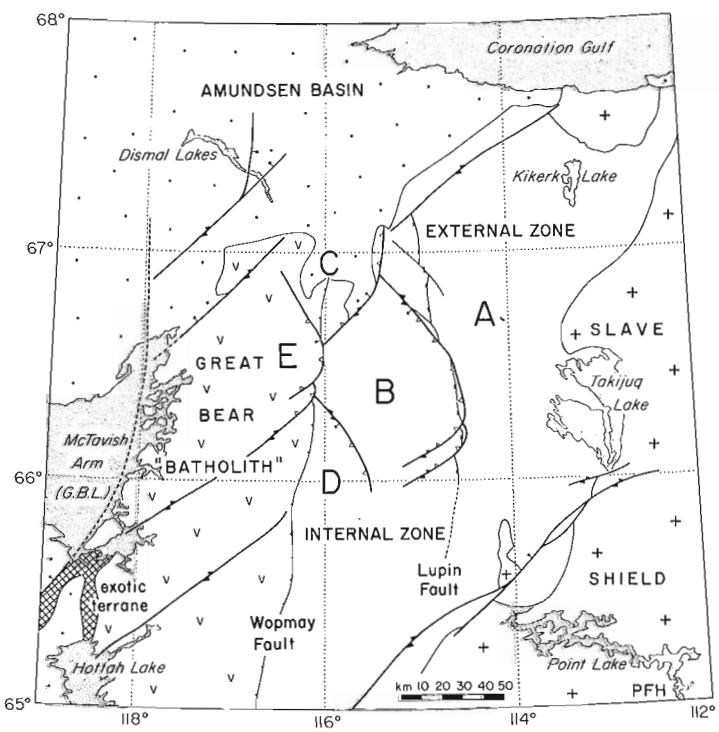

Figure 35.1. *Major faults and structural blocks (A-E) in the northern part of Wopmay Orogen. Amundsen Basin consists of Helikian post-orogenic cover. The "external zone" and "internal zone" comprise the foreland thrust-fold belt related to the first collision. The Slave Shield exposes middle and late Archean rocks. The extent of the "exotic terrane" is based on observations by R.S. Hildebrand. The exotic terrane reappears around the southern half of Hottah Lake (McGlynn, 1976, 1979) and in both areas is largely engulfed by younger intrusions of the Great Bear "Batholith". Fault symbolism is explained in Figure 35.2.*

[1] Department of Geological Sciences, Queen's University, Kingston, Ontario K7L 3N6

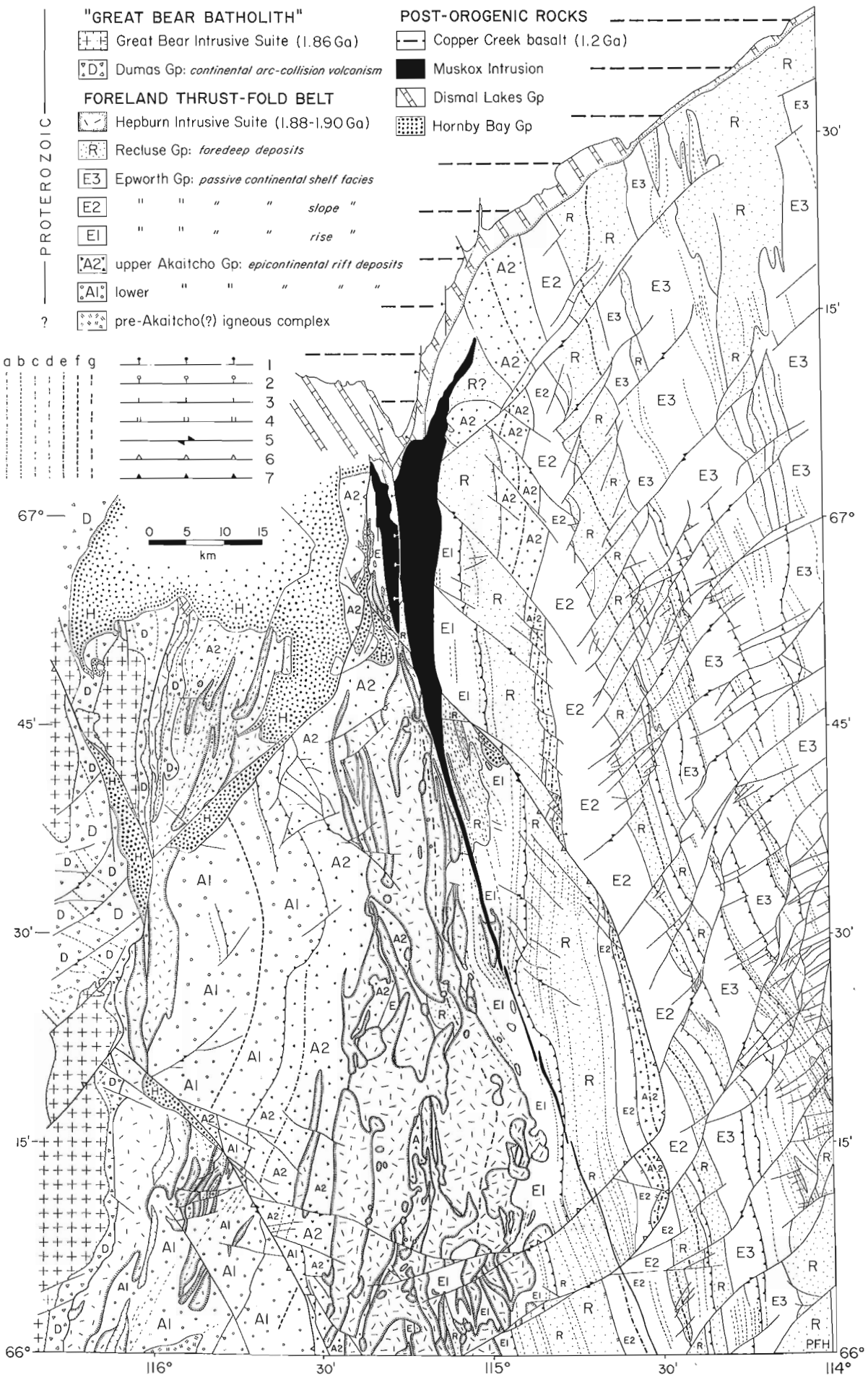
"GREAT BEAR BATHOLITH"
Great Bear Intrusive Suite (1.86 Ga)
Dumas Gp: continental arc-collision volcanism
FORELAND THRUST-FOLD BELT
Hepburn Intrusive Suite (1.88-1.90 Ga)
Recluse Gp: foredeep deposits
Epworth Gp: passive continental shelf facies
" " " " slope "
" " " " rise "
upper Akaitcho Gp: epicontinental rift deposits
lower " " " " "
pre-Akaitcho(?) igneous complex
PROTEROZOIC
POST-OROGENIC ROCKS
Copper Creek basalt (1.2 Ga)
Muskox Intrusion
Dismal Lakes Gp
Hornby Bay Gp
a b c d e f g
1
2
3
4
5
6
7
0 5 10 15
km
67°
45'
30'
15'
66°
116°
30'
115°
30'
114°
PFH

Different plutons of the Hepburn Intrusive Suite range in age from 1.90 to 1.88 Ga (Van Schmus and Bowring, 1980) and they were already exposed at the surface when the Dumas Group (continental volcanics and clastics) in outliers east of Wopmay Fault (Fig. 35.2) was deposited, not later than 1.86 Ga (Van Schmus and Bowring, 1980).

Remnants of an exotic terrane (Fig. 35.1), perhaps accreted in the first collision, are exposed for 75 km along the westernmost edge of Shield (McGlynn, 1976, 1979, Hildebrand, personal communication). They comprise a metamorphic complex and a variety of foliated granitoids, which have a SSW-NNE foliation that is distinctly older than the Great Bear Intrusive Suite, which almost engulfs the exotic terrane. An age of 1.92 ± .01 Ga (Van Schmus and Bowring, 1980) for one of the foliated intrusions suggests that they may be part of a magmatic arc generated above the west-dipping subduction zone that led to the first collision. The origin of the metamorphic complex and the nature of its basement remain to be determined.

The second collision is interpreted as resulting from an oblique, shallow, east-dipping, subduction that consumed oceanic lithosphere west of the exotic terrane accreted in the first collision. Most of the volcanic and plutonic rocks between Wopmay Fault and the accreted terrane, the "Great Bear Batholith" (Fig. 35.1) of Hoffman and McGlynn (1977), belong to the magmatic are above this subduction zone. Arc volcanism and plutonism began with the LaBine Group (Hildebrand, in press), at least 1.875 Ga (Van Schmus and Bowring, 1980), which overlies the accreted terrane (Hildebrand, personal communication). Arc magmatism appears to have migrated eastward with time, ending with the Dumas Group, which straddles Wopmay Fault (Fig. 35.2), at about 1.86 Ga (Van Schmus and Bowring, 1980). At about this time, the general arc-like character of the magmatism changed with the emplacement of high-potash, high-silica granites. This may signal the onset of collision, far to the west. The system of conjugate faults and thrusts that produced the hexagonal block-structure of the orogen post-dates virtually all these magmatic rocks (Hoffman, 1978).

Figure 35.2

Structural detail and major litho-stratigraphic units in north-central Wopmay Orogen. Area south of latitude 67 was mapped in this project and the geology north of 67 is adapted from Baragar and Donaldson (1973). Symbolism for faults (see legend):

1. *normal fault related to post-orogenic extension;*
2. *Kapvik Fault, a shallow-dipping normal fault, possibly a denudation fault related to thrusting of "Block D";*
3. *Wopmay Fault, a west-side-down and probable right-lateral transcurrent fault active during Dumas Group deposition;*
4. *Lupin Fault, a west-side-down normal fault active during early Recluse Group sedimentation;*
5. *conjugate transcurrent faults, some with minor components of dip slip;*
6. *thrust faults outlining the hexagonal block-structure and active more-or-less simultaneously with the conjugate transcurrent faults;*
7. *thrust faults related to the first collisional orogeny.*

Symbolism for folds:

a. *minor anticline,*
b. *minor syncline,*
c. *minor antiform (folded gneissic foliation),*
d. *minor synform,*
e. *major anticlinorium,*
f. *major synclinorium,*
g. *major synform.*

The fault system is the result of east-west compression, probably related to continent-continent convergence during the collision. It appears to be the youngest compressional event in the orogen.

Evidence that the Hexagonal Crustal Blocks are Bounded by Thrusts

A structural map of north-central Wopmay Orogen is shown in Figure 35.2. The stratigraphic nomenclature follows the revisions suggested in Hoffman (1981). The inferred crustal block-structure is shown in Figure 35.1. Evidence of west-over-east thrust displacements between the various crudely-hexagonal blocks falls into three categories: (1) truncation of transcurrent faults at block boundaries, (2) regional variation in metamorphic pressure (ie. in post-metamorphic uplift), (3) occurrence of otherwise-unexplained denudation faults.

Evidence of truncation, or structural overlap, of transcurrent faults can be seen especially along the meridional boundaries of all the blocks (Fig. 35.2). The east boundary of "Block B" truncates a transcurrent fault in "Block A" that has 10 km right-slip. The east boundary of "Block C" truncates the northeast boundary-fault of "Block B", which has a sinistral strike-separation of 10 km. Similarly, the southeast boundary of "Block E" truncates the northeast boundary-fault of "Block D". As the truncated faults do not reappear on the adjacent block (ie. they are not merely offset), geometry demands some sort of structural overlap. In general, blocks to the east are truncated by blocks to the west, suggesting that the blocks override

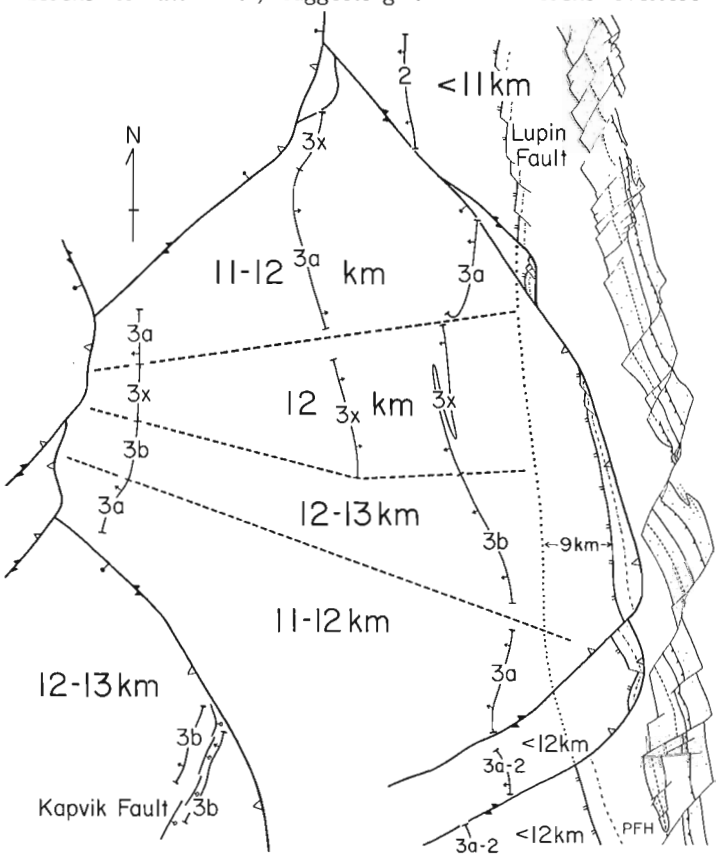

Figure 35.3. *Bathozonal control and depths of postmetamorphic erosion in and around "Block B", based on the P-T petrogenetic grid for pelites (St-Onge and Hoffman, 1980). Also indicated are the lateral displacement of Lupin Fault and the continuity of the Recluse Group syncline east of "Block B". Fault symbolism is explained in Figure 35.2.*

each other from west to east. Displacement of Lupin Fault (Fig. 35.3) indicates 8-10 km of lateral convergence between "Block B" and "Block A", but how much of this is the result of thrusting and how much to pure strike-slip before thrusting is not known.

Regional variation in metamorphic pressure serves as a measure of vertical displacements between the structural blocks. Metamorphic pressure may be estimated from reaction isograds using the bathozonal scheme of Carmichael (1978) as modified by St-Onge and Carmichael (1979), or from microprobe analyses of certain mineral pairs (St-Onge, 1979). Microprobe analyses of samples from all the blocks except "Block E", in which no metamorphic rocks from the first collision are exposed, are now being processed and will be reported elsewhere. The bathozonal results (Fig. 35.3) are useful mainly in "Block B" and its relation to "Block A". "Block B" is entirely in bathozone 3, except possibly at its southern tip, where control is lacking. It has a well-documented WNW-ESE medial arch, where the depth of erosion since the thermal peak is 12-13 km. "Block A", adjacent to the north end of "Block B", is in bathozone 2 and has thus been eroded less than 11 km. Although there is no bathozonal control directly east of "Block B", the remarkable continuity of the Recluse Group syncline there (Fig. 35.3) appears to rule out any projection of the medial arch of "Block B" into "Block A". Therefore, "Block B" has been arched and uplifted at least 1-2 km relative to "Block A".

Bathozonal data limit the vertical displacement of "Block B" relative to either "Block C" or "Block D" to less than 2 km and also indicate that "Block D" has moved up relative to "Block B". Both "Block C" and "Block D" have generally higher peak-metamorphic temperatures than "Block B", and it would be consistent with hot-side-down metamorphism related to Wentzel Batholith (St-Onge, in press) if these blocks are more deeply-eroded than "Block B". Conversely, the juxtaposition of low-grade Akaitcho Group in "Block C" and high-grade Epworth Group in "Block A" (Fig. 35.2) is consistent with "Block C" being relatively uplifted because the metamorphism related to Hepburn Batholith is hot-side-up (St-Onge, in press). To conclude, "Block C" and "Block D" are structurally up relative to "Block B", which is up relative to "Block A". This is consistent with the west-over-east sense of overriding deduced from fault truncations.

The peculiar Kapvik Fault (Fig. 35.3) repeats a metamorphic sequence in such a manner that geometry dictates a gently-dipping fault plane and normal (ie. extensional) displacement (St-Onge, in press). Previously inexplicable, this fault could be the up-dip trace of a low-angle denudation fault developed along the leading edge of "Block D" during thrusting.

Mechanism

To our knowledge, this style of thrusting has not been described before. Areas where fault-maps resemble those in Wopmay Orogen include the mid-Proterozoic Mount Isa Orogen of Australia (Wilson and Derrick, 1976), the Pan-African orogen of the Hoggar Shield in West Africa (Bertrand and Caby, 1978), and the Tertiary orogen between the Lut Block of Baluchistan and the Farah Block of Afghanistan (Freund, 1970). All of these areas have been interpreted in terms of conjugate transcurrent (ie. strike-slip) faulting alone, as has Wopmay Orogen (Hoffman, 1980). We now interpret the faulting in Wopmay Orogen as having evolved in three, perhaps somewhat overlapping, stages (Fig. 35.4): (1) initial development of a conjugate system of presumably near-vertical transcurrent faults (WSW-ENE right-slip and WNW-ESE left-slip) as a result of a horizontally-directed east-west compression (Freund, 1974;

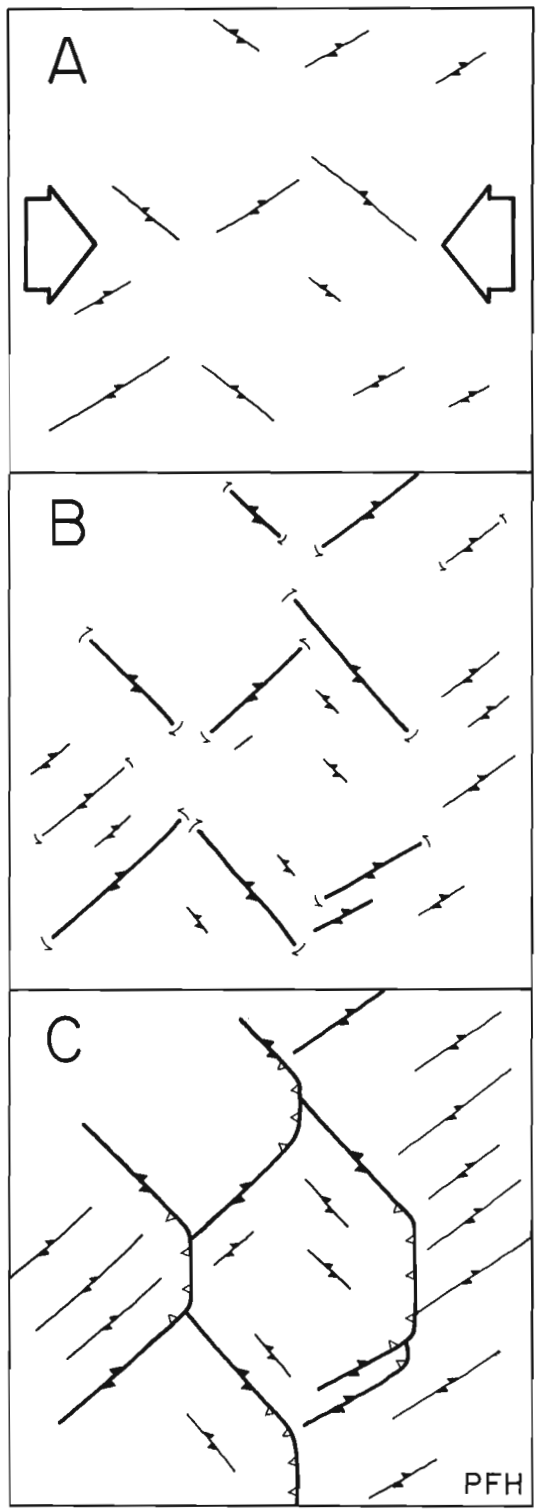

Figure 35.4. *Possible sequential development of the hexagonal thrust-block structure.*

A. Conjugate transcurrent faults develop in response to lateral compression.

B. With continued compression, the transcurrent faults rotate away from the direction of maximum compression.

C. Thrusts develop to accommodate continued lateral compression without more lateral extension. Fault symbolism explained in Figure 35.2.

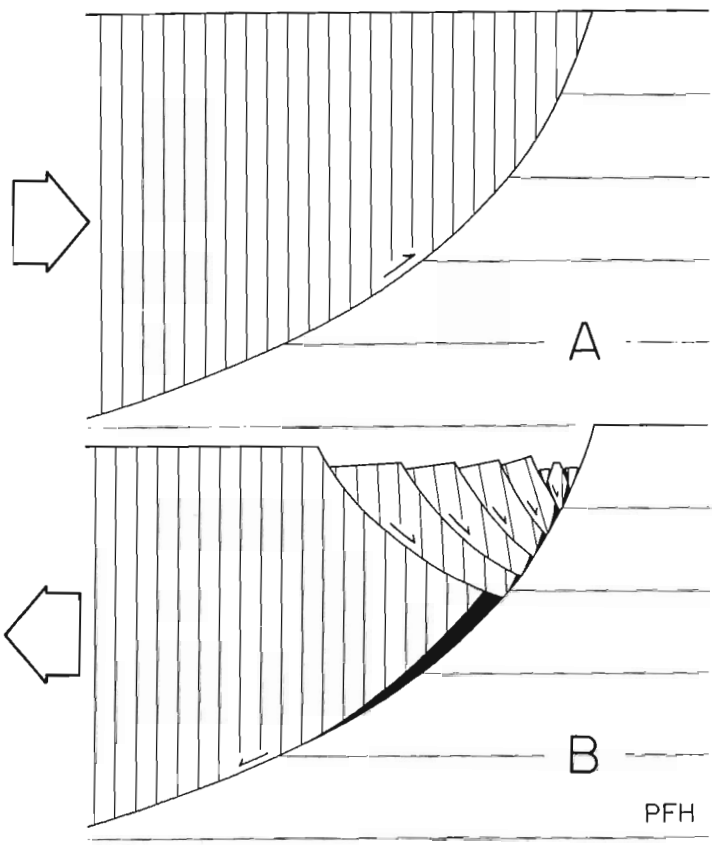

Figure 35.5. *Brittle-medium (paper-and-scissors) model illustrating the development of a graben controlled by back-sliding on a listric thrust fault. Note the rotation of fault-blocks, the predicted void spaces (black), and the fact that the graben is underlain by fault-blocks of the hanging wall of the thrust. A. thrusting, B. extension.*

Dubey, 1980), (2) continued compression with rotation about vertical axes of the transcurrent faults away from the direction of maximum compressive stress (Cloos, 1955; Freund, 1970), and (3) as continued compression exceeds the ability of the transcurrent faults and the rocks between them to withstand rotational deformation, thrust faults develop linking the major transcurrent faults. The onset of thrusting allows the compressive stress to be relieved by vertical thickening rather than north-south lengthening of the crust. This scenario is very tentative and should be scrutinized by clay-model studies.

The effect of rotations is well shown by the anticline of Akaitcho Group and syncline of Recluse Group east of Muskox Intrusion (Fig. 35.2), where the folds have been rotated clockwise in zones of left-slip faulting and counter-clockwise in zones of right-slip faulting. The main megascopic cleavage in these zones systematically transects the rotated folds and has an orientation closer to the regional tectonic strike. This may imply that the cleavage postdates the onset of the rotation stage. If so, it is much younger than the main microscopic foliation in the higher-grade rocks to the west, which developed during the prograde metamorphism of the first collision.

The transition from transcurrent faulting to thrusting must greatly deform the margins of the hexagonal blocks. The oblique margins must change from presumably near-vertical strike-slip faults to oblique-slip reverse faults. Perhaps the distortion and crescentic segmentation of the fault system directly east of "Block B" (Fig. 35.2) is a reflection of this. Deformations accompanying the onset of thrusting may also contribute to smoothing of the east-convex thrust-traces of the block margins. The pattern of overlapping east-convex arcs gives an overall impression of eastward vergence to the fault system.

The thrust system related to the second collision in Wopmay Orogen is very different in style to that developed during the first collision (Fig. 35.2). On the basis of their regional tectonic setting, two fundamentally different mechanisms may be responsible. In the first collision, thrusting is synthetic to lithospheric subduction. The under-thrusting element, the Archean craton, is being driven by the gravitational descent of the lithospheric slab of which it is a part. The stresses being relieved by thrusting are primarily those of shear. In contrast, thrusting in the second collision is antithetic to the proposed subduction zone. No sinking slabs are directly involved in the thrusting and the main stress is a near-horizontal compression emanating from the zone of continental impaction.

Implications for the Structure of Hornby Bay Group Outliers

During and after deposition of the post-orogenic non-marine clastics of the Hornby Bay Group, the region underwent intermittent east-west extension, causing dip-slip reactivation of basement (ie. Wopmay Orogen) faults (Hoffman, 1980). All of the Hornby Bay Group outliers occur in graben-like structures along the margins of the main hexagonal blocks (Fig. 35.2). In the majority of cases, the outliers rest on the upthrust block, indicating that extension has reversed the sense of vertical movement. If the block margins are thrusts, then the sense of dip-slip has been reversed and the thrust planes have become normal faults. The thrusts of the first collision cannot do this because they are folded and will not slip. The changes in metamorphic pressures across block boundaries (Fig. 35.3) are net displacements and represent only a minimum for thrusting. The outlier on the northeast margin of "Block B" is 1.2 km thick (G.M Ross, personal communication), so "Block B" must have dropped at least that much relative to "Block A" during post-orogenic extension. As "Block B" is nevertheless 1-2 km more deeply eroded according to the metamorphic pressure data, it must originally have been uplifted 2-3 km or more relative to "Block A". Note that it is incorrect to use the outliers to determine the net sense of dip-slip, as was done for the northeast margin of "Block B" (Hoffman, in press; St-Onge and Hoffman, 1980). The correct solution is in St-Onge (in press).

The subsurface structure of the outliers, some of which are being explored by the drill for uranium, may well be controlled by the form of the basement thrusts. The development of grabens along the thrust traces could be explained by backsliding on a listric thrust plane (Fig. 35.5). This model predicts that basement blocks within the graben will belong to the hanging wall of the thrust and not the footwall. This is true for the graben on the east margin of "Block C", in which basement horsts are all composed of low-grade Akaitcho Group rocks of "Block C", not the adjacent granitoids and high-grade rocks of "Block A".

Discussion

Conjugate transcurrent faulting with simultaneous thrusting is not a geologically well-known phenomenon. There are also numerous geometrical difficulties to be overcome.

Clay-model experiments have been very useful in understanding conjugate transcurrent faulting and consequent fault rotations (Cloos, 1955; Freund, 1970, 1974) and experiments involving simultaneous folding (Dubey, 1980) are

especially enlightening. It would be interesting to see what would happen in such experiments if constraints on lengthening of the model were imposed. It may be wise also to dissect the models to check for fault-plane rotations about nonvertical axes.

That simultaneous thrusting and conjugate transcurrent faulting can and do occur in the same region is indicated by earthquake first-motion studies in south-central Asia (Molnar and Tapponnier, 1978; Sengor and Kidd, 1979). It is surely no accident that the gross tectonic environment there is virtually the same as that already proposed for the event in Wopmay Orogen – the rigid subcontinents of Arabia and India, still part of the subducting Arabian-Indian-Australian plate, continue to converge with the thermally-weakened overriding Eurasian plate long after continental impingement.

Acknowledgments

It is a pleasure to acknowledge R.S. Hildebrand (Memorial University) for the exciting new information concerning the possible "exotic terrane" and its unconformity with the overlying LaBine Group. P.A. Geiser (University of Connecticut and Lamont-Doherty), who worked with us in the field for one month in 1980, first observed that many of the folds are transected by cleavage. We are grateful to the Geology Office, Department of Indian Affairs and Northern Development Yellowknife, N.W.T., for essential aircraft and logistical support.

References

Baragar, W.R.A. and Donaldson, J.A.
1973: Coppermine and Dismal Lakes map-areas; Geological Survey of Canada, Paper 71-39, 20 p.

Bertrand, J.M.L. and Caby, R.
1978: Geodynamic evolution of the Pan-African orogenic belt: a new interpretation of the Hoggar Shield (Algerian Sahara); Geologische Rundschau, v. 67, p. 357-383.

Carmichael, D.M.
1978: Metamorphic bathozones and bathograds: a measure of the depth of post-metamorphic uplift and erosion on the regional scale; American Journal of Science, v. 278, p. 769-797.

Cloos, E.
1955: Experimental analysis of fracture patterns; Geological Society of America Bulletin, v. 66, p. 241-256.

Dubey, A.K.
1980: Model experiments showing simulataneous development of folds and transcurrent faults; Tectonophysics, v. 65, p. 69-84.

Freund, R.
1970: Rotation of strike-slip faults in Sistan, southeast Iran; Journal of Geology, v. 78, p. 188-200.

1974: Kinematics of transform and transcurrent faults; Tectonophysics, v. 21, p. 93-134.

Hildebrand, R.S.
LaBine Group, Echo Bay to Hornby Bay, Great Bear Lake, Northwest Territories: remnant of an early Proterozoic continental volcanic arc; in Proterozoic Basins in Canada, ed. F.H.A. Campbell, Geological Survey of Canada, Paper 81-10. (in press)

Hoffman, P.F.
1978: Geology of the Sloan River map area, District of Mackenzie; Geological Survey of Canada, Open File Map 535.

Hoffman, P.F. (cont.)
1979: Wopmay Orogen: continent-microcontinent-continent collision of early Proterozoic age, Bear Province, Canadian Shield; in Program with Abstracts, Geological Association of Canada, v. 4, p. 58.

1980: Conjugate transcurrent faults in north-central Wopmay Orogen and their dip-slip reactivation during post-orogenic extension, Hepburn Lake map area, District of Mackenzie; in Current Research, Part A, Geological Survey of Canada, Paper 80-1A, p. 183-185.

1981: Revision of stratigraphic nomenclature, foreland thrust-fold belt of Wopmay Orogen, District of Mackenzie; in Current Research, Part A, Geological Survey of Canada, Paper 81-1A, Report 34.

Wopmay Orogen: a Wilson Cycle of early Proterozoic age in the northwest of the Canadian Shield; in The Crust of the Earth and Its Mineral Resources, ed. D.W. Strangway, Geological Association of Canada, Special Paper 20. (in press)

Hoffman, P.F. and McGlynn, J.C.
1977: Great Bear Batholith: a volcano-plutonic depression; in Volcanic Regimes in Canada, ed. W.R.A. Baragar, L.C. Coleman, and J.M. Hall, Geological Association of Canada, Special Paper 16, p. 170-192.

Hoffman, P.F., St-Onge, M.R., Easton, R.M., Grotzinger, J., and Schulze, D.E.
1980: Syntectonic plutonism in north-central Wopmay Orogen, Hepburn Lake map area, District of Mackenzie; in Current Research, Part A, Geological Survey of Canada, Paper 80-1A, p. 171-177.

McGlynn, J.C.
1976: Geology of the Calder River and Leith Peninsula map-areas, District of Mackenzie; in Report of Activities, Part A, Geological Survey of Canada, Paper 76-1A, p. 359-361.

1979: Geology of the Precambrian rocks of the Riviere Grandin and in part of the Marian River map areas, District of Mackenzie; in Current Research, Part A, Geological Survey of Canada, Paper 79-1A, p. 127-131.

Molnar, P. and Tapponnier, P.
1978: Active tectonics of Tibet; Journal of Geophysical Research, v. 83, p. 5361-5375.

Mountjoy, E.W.
1980: Geology of Mount Robson map area, Alberta-British Columbia; Geological Survey of Canada, Map 1499A.

Price, R.A.
The Cordilleran foreland thrust and fold belt in the southern Canadian Rocky Mountains; in Thrust and Nappe Tectonics, Geological Society of London, Special Volume. (in press)

Sengor, A.M.C. and Kidd, W.S.F.
1979: Post-collisional tectonics of the Turkish-Iranian Plateau and a comparison with Tibet; Tectonophysics, v. 55, p. 361-376.

St-Onge, M.R.
1979: The assemblage garnet-andalusite/sillimanite-biotite-plagioclase-quartz as a measure of metamorphic pressure and temperature in the Wopmay Orogen, Bear Province, Northwest Territories; in Abstracts with Programs, Geological Society of America, v. 11, p. 509.

1980: "Hot-side-up" and "hot-side-down" metamorphic isograds and the shape of Wopmay Orogen batholiths; in Program with Abstracts, Geological Association of Canada, v. 5, p. 83.

"Hot-side-up" and "hot-side-down" metamorphic isograds and their relation to syntectonic Proterozoic batholiths in the Wopmay Orogen, Northwest Territories, Canada; Tectonophysics. (in press)

St-Onge, M.R. and Carmichael, D.M.
1979: Metamorphic conditions, northern Wopmay Orogen, N.W.T. Aureole de contact de l'intrusion du Muskox, T.N.W.; in Program with Abstracts, Geologicial Association of Canada, v. 4, p. 81.

St-Onge, M.R. and Hoffman, P.F.
1980: "Hot-side-up" and "hot-side-down" metamorphic isograds in north-central Wopmay Orogen, Hepburn Lake map area, District of Mackenzie; in Current Research, Part A, Geological Survey of Canada, Paper 80-1A, p. 179-182.

Wilson, I.H. and Derrick, G.M.
1976: Precambrian geology of the Mount Isa region, northwest Queensland; International Geological Congress, 25th, Sydney, Excursion Guide 5A, 5C.

Van Schmus, W.R. and Bowring, S.A.
1980: Chronology of igneous events in the Wopmay Orogen, Northwest Territories, Canada; in Abstracts with Programs, Geological Society of America, v. 12, p. 540.

36. GEOLOGY OF BAKER LAKE REGION, DISTRICT OF KEEWATIN

Project 800008

W.W. Heywood and Mikkel Schau
Precambrian Geology Division

Heywood, W.W. and Schau, Mikkel, Geology of Baker Lake region, District of Keewatin; in Current Research, Part A, Geological Survey of Canada, Paper 81-1A, p. 259-264, 1981.

Abstract

The west half of the Baker Lake map sheet is divided into five domains based on characteristic rock suites and their style of deformation. An east to north striking metasedimentary belt contains quartzites, conglomerates, slates and minor volcanics, iron formation and carbonate. North of the sedimentary belt a large granitoid complex is emplaced in the sediments and gently dipping medium to high grade metamorphic rocks mantle cores of granite. South of the sedimentary belt a gently to steeply dipping fault contact or rarely, intrusive contact, forms the boundary with a deformed plutonic complex characterized by low dipping foliations. Along the north shore of Baker Lake the plutonic rocks are cut by a 15 km wide steeply dipping east-west trending fault zone in which plutonic rocks and dykes have been emplaced. Along the north shore of Baker Lake gently deformed and locally faulted rocks of the Dubawnt Group rest unconformably on, or cut, the older foliated rocks.

Introduction

The geology of the west half of the Baker Lake map sheet (56 D, W 1/2) was mapped at a scale of 1:250 000 during this field season, upgrading part of the previous 1 inch to 8 mile map (Wright, 1967).

The area is divided into five geologically distinct regions, each with a typical pattern of deformation and a characteristic suite of rock units (Fig. 36.1). An east to northeast striking metasedimentary belt (A) located east of Whitehills Lake contains the oldest rocks in the area. To the south, in fault and intrusive contact with metasediments, is a deformed plutonic complex (B). These complexes are cut to the south, near the north shore of Baker Lake, by a wide east-west trending fault shear and/or mylonite zone in which plutonic rocks and hypabyssal dykes have been emplaced (C). This zone is probably part of the Chesterfield Fault Zone (Heywood and Schau, 1978). North of the metasedimentary belt a large intrusive complex centred on Tehek Lake is in intrusive contact with the metasediments (D). South of the Chesterfield Fault Zone the Dubawnt Group unconformably overlies the older foliated rocks (E).

Sedimentary Group (A)

Sedimentary rocks underlie the middle part of the region (56 D/11, 12) in a broad belt which trends northeasterly in the east and is complexly deformed to the west and north, near Whitehills Lake.

The sedimentary group consists of quartzites, metasiltstones, slates, phyllites, metagreywackes, greenstones, greenschists, metavolcanic rocks, paraconglomerates, graphitic slates, iron formations, minor carbonate beds, and locally to the north, higher grade equivalents of these rock types. The quartzites are exceedingly pure, although thicker sections are commonly muscovite-rich and chromian muscovite-rich. The paraconglomerate may be used as a marker in the slates and phyllites, but the deformation of the clasts ranges from relatively undeformed cobbles to thick (0.5 cm thick, 15 cm long) flattened cobbles that render the rock into a lenticular phyllite. The clasts, which rarely touch one another, are medium grained granitoid cobbles, quartzite cobbles and greywacke cobbles, with rare dolomite boulders set in a quartzose, locally phyllitic matrix. The finer grained rocks such as the metasiltstones, metagreywackes, phyllites and slates, are very fine grained, variably cleaved, in places layered, light grey to black rocks which are generally poorly exposed. The metavolcanic rocks retain the textures and structures of tuffs, breccias, flows and pillows, whereas the greenstones are massive, fine grained, locally gabbroic rocks; the greenschists are similar, however they contain abundant carbonate fragments which in places are of tectonic origin. The iron formations are layered, consist of magnetite and quartz, and grade along strike into carbonate-rich beds, and locally carbonated chlorite schist. Near the scarce carbonate layers, which are generally less than 3 m thick, the host rock is calcareous phyllite or siltstone.

A stratigraphic section has not been established since primary structures are rare and the fold patterns complex. The main structure of the region is unknown. On the north shore of Whitehills Lake crossbedded shallow south-dipping quartzite is overlain by slate. Farther north, steeply north-dipping metavolcanic rocks are immediately overlain by iron formation, and still farther north, by slate. It is possible that the quartzite is an easterly trending anticlinal core and the fine grained sediments are disposed in synclinal troughs to the north and south. However, the fine grained sediments may not be equivalent, although carbonate beds are present in both regions, iron formations were observed only north of the quartzites and the paraconglomerate only to the south. Near the eastern border, a greenstone unit is situated within the finer grained metasediments. These metasediments structurally overlie quartzites and apparently underlie the paraconglomerate, but iron formations and carbonate beds are not present.

Metamorphic grade in the belt is generally of low grade. Chlorite, white mica and rarely biotite form the fine grained phyllosilicates; porphyroblasts are extremely rare. This grade is maintained to the south where contact metamorphism with the now sheared plutonic complex is not at all obvious, although coarsening of grain does occur locally. In comparison, to the north, sillimanite-bearing quartzites, partially melted arkosic quartzites, and calc-silicate marbles, indicate the high grade metamorphism of the sediments near Tehek Lake Plutonic Complex.

The age of the sedimentary belt is unknown, but it is probably the oldest group in the region. Wright (1967) assigned these rocks to the Lower Proterozoic Hurwitz Group because of their lithologic similarity to the Hurwitz Group in central Keewatin. The rocks are also similar to the nearby "Woodburn Group", and to the upper Archean Prince Albert Group to the north. The unit is thus early Proterozoic or late Archean in age, depending on which long range correlation is chosen.

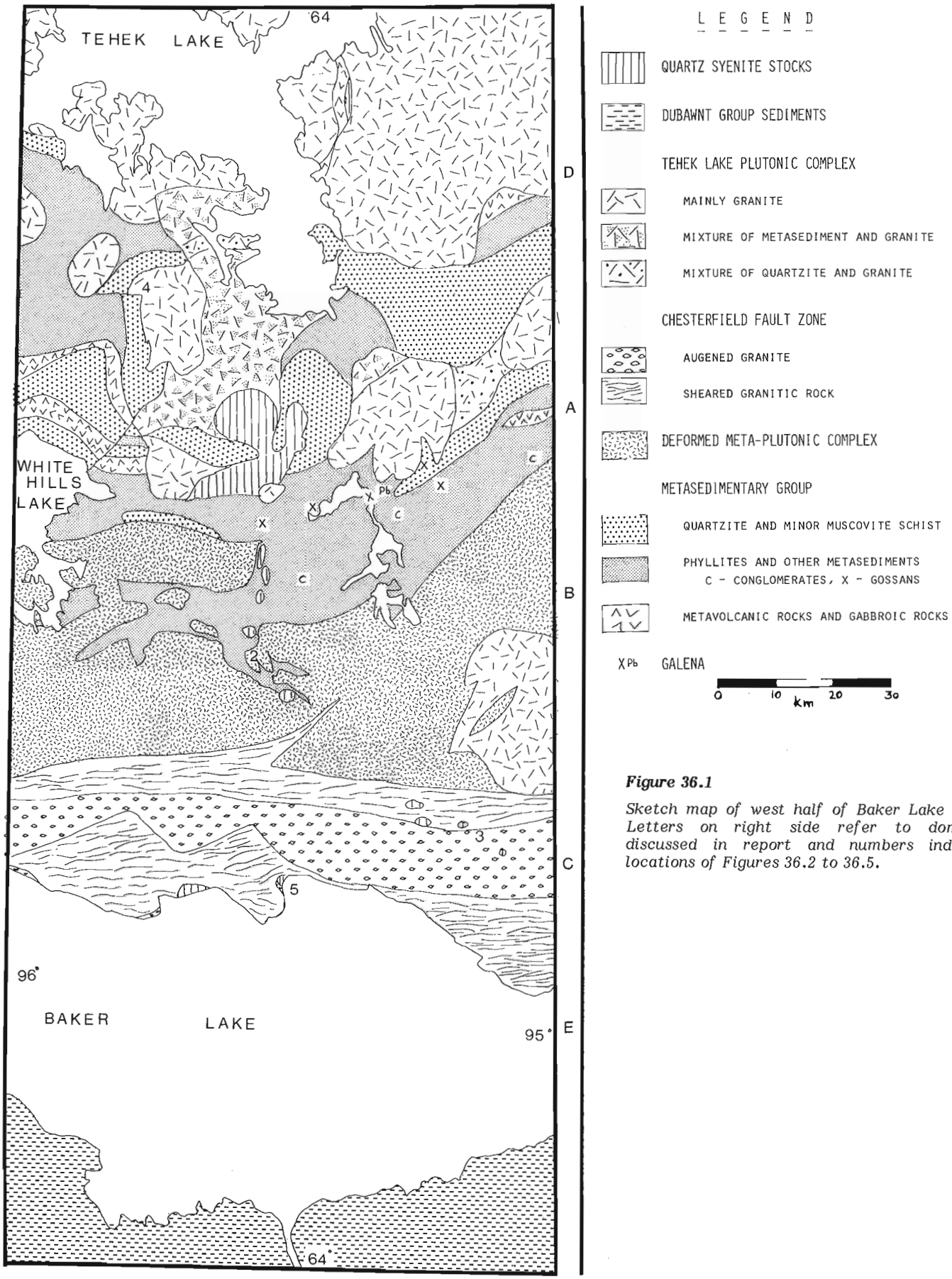

Figure 36.1

Sketch map of west half of Baker Lake area. Letters on right side refer to domains discussed in report and numbers indicate locations of Figures 36.2 to 36.5.

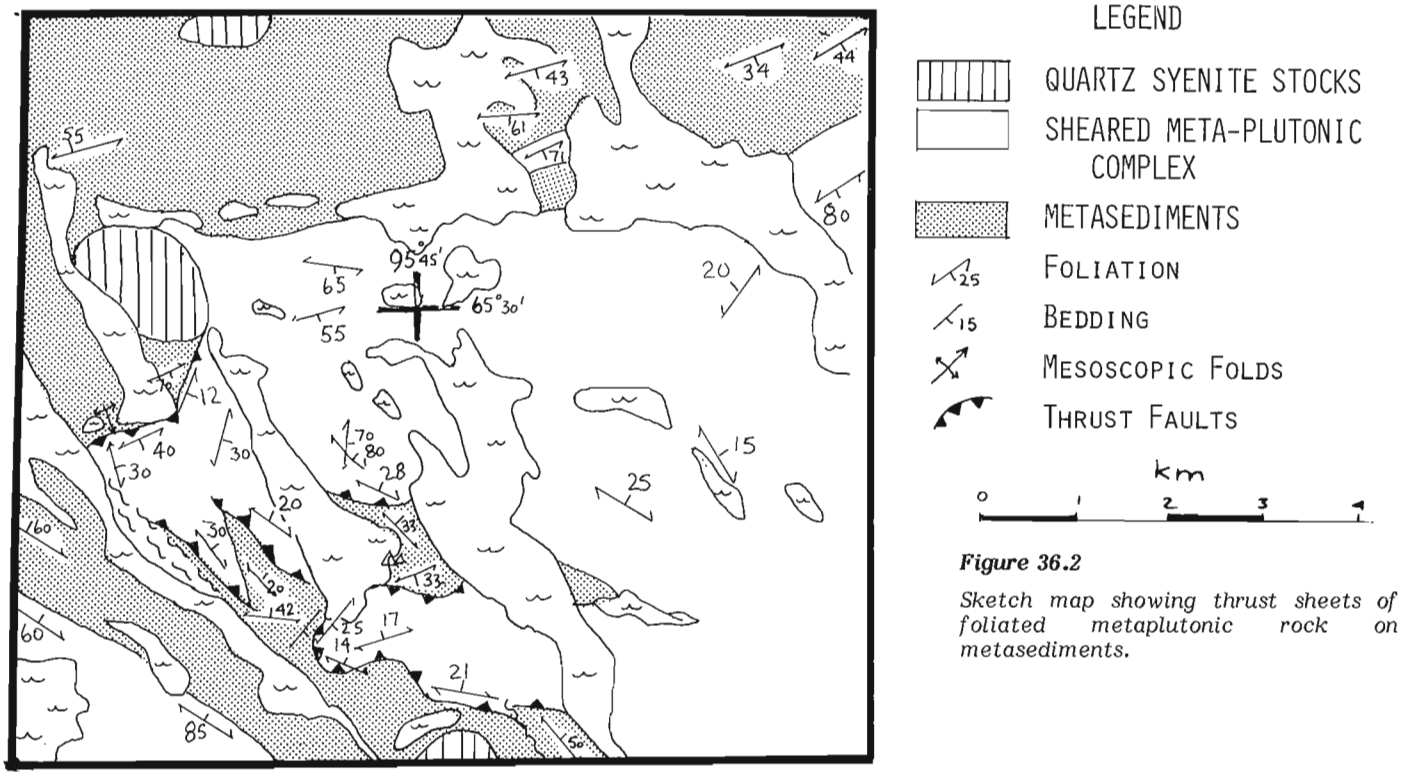

Figure 36.2

Sketch map showing thrust sheets of foliated metaplutonic rock on metasediments.

Deformed Plutonic Complex (B)

The sheared plutonic complex outcrops south of the sedimentary belt and underlies a triangular portion of the map area mainly within 56 D/5, 6, and 11. It is terminated to the south by an east-west fault zone.

The complex is characterized by foliated, sheared and locally degraded rocks ranging from grey quartz diorite to biotite granodiorite. Thin slivers and blocks of gneiss and amphibolite are present within the pluton. Near the borders the complex has been finely foliated and contains rare plagioclase augen; these rocks have been crinkled and, locally, contain abundant quartz veins. Along the northwestern border of the map area phyllonitic rocks are composed of slivers of sheared metasediments and sheared plutonic rocks. In the southeastern part of the region white weathering locally foliated hornblende biotite granodiorite intrudes the grey foliated pluton. The granodiorite is in turn intruded by an orange weathering massive biotite granite which underlies the eastern part of this region. Mafic-rich syenite plugs and stocks intrude the rocks with no apparent pattern.

The structures within this region are complex. They include very gently-dipping foliations and faults, steep northeast trending shear zones and vertical north striking fault zones. Their relations are shown in Figure 36.2. The northern boundary of the zone is quite irregular since sheared plutonic rocks have been thrust over the metasediments along gently-dipping faults. These relations are obscured by northeast trending shear zones but accentuated by the north-south faults which locally show small, apparent, west-side-down, displacement.

The complex has been variably degraded and contains typical greenschist grade minerals. The low grade approximates that of the nearby sedimentary belt to the north. Even near the few granitoid dykes in the sediments there is no obvious widespread metamorphism. The gneissic enclaves and the metasediments are the oldest rocks of this region. They were intruded by the grey biotite quartz diorite followed by the white hornblende biotite granodiorite. The flat foliations and faults, the northeast foliations and the east-west shear zone were imposed during an interval prior to the emplacement of the orange biotite granite and the movement along steep north and northwest striking faults. The syenite stocks are probably the last intrusive event, although no syenite was seen to cut the orange granite.

The correlation and age of this complex awaits further work but a wide range in the age of the various components is apparent. Gneisses in 56 D/1, similar to the gneissic enclaves, are 2675 Ma (U-Pb dating of zircons, Schau and Ashton, 1980). The syenites are probably related to the Dubawnt Group.

Chesterfield Fault Zone (C)

The Chesterfield Fault Zone extends from Baker Lake to about 15 km north of Baker Lake. Within it are a variety of foliated plutonic rocks, spectacular mylonite zones, abundant faults and many sets of generally east-west trending dykes.

The best exposed rocks form bald hills of pink to red weathering coarse grained augened porphyroblastic granitoid rocks containing biotite, minor garnet and hornblende (CI=20-30) and abundant K-feldspar porphyroblasts (as much as 3 cm and commonly rimmed by another feldspar) in a matrix of quartz and feldspar. This unit grades to the north into more sparsely porphyroblastic and medium grained biotite granodiorite, and to the south into a white weathering, layered, biotite hornblende granite. The southern part of the zone is marked by a fault or shear zone in which granitic rocks are rendered pink by introduction of hematite and quartz. This southern zone includes: extremely degraded arkose-like rocks that contain decomposed feldspars; tectonic breccias consisting of hematite carbonate and largely replaced breccia fragments; and well foliated and jointed granite. The northern edge is less distinct; it is

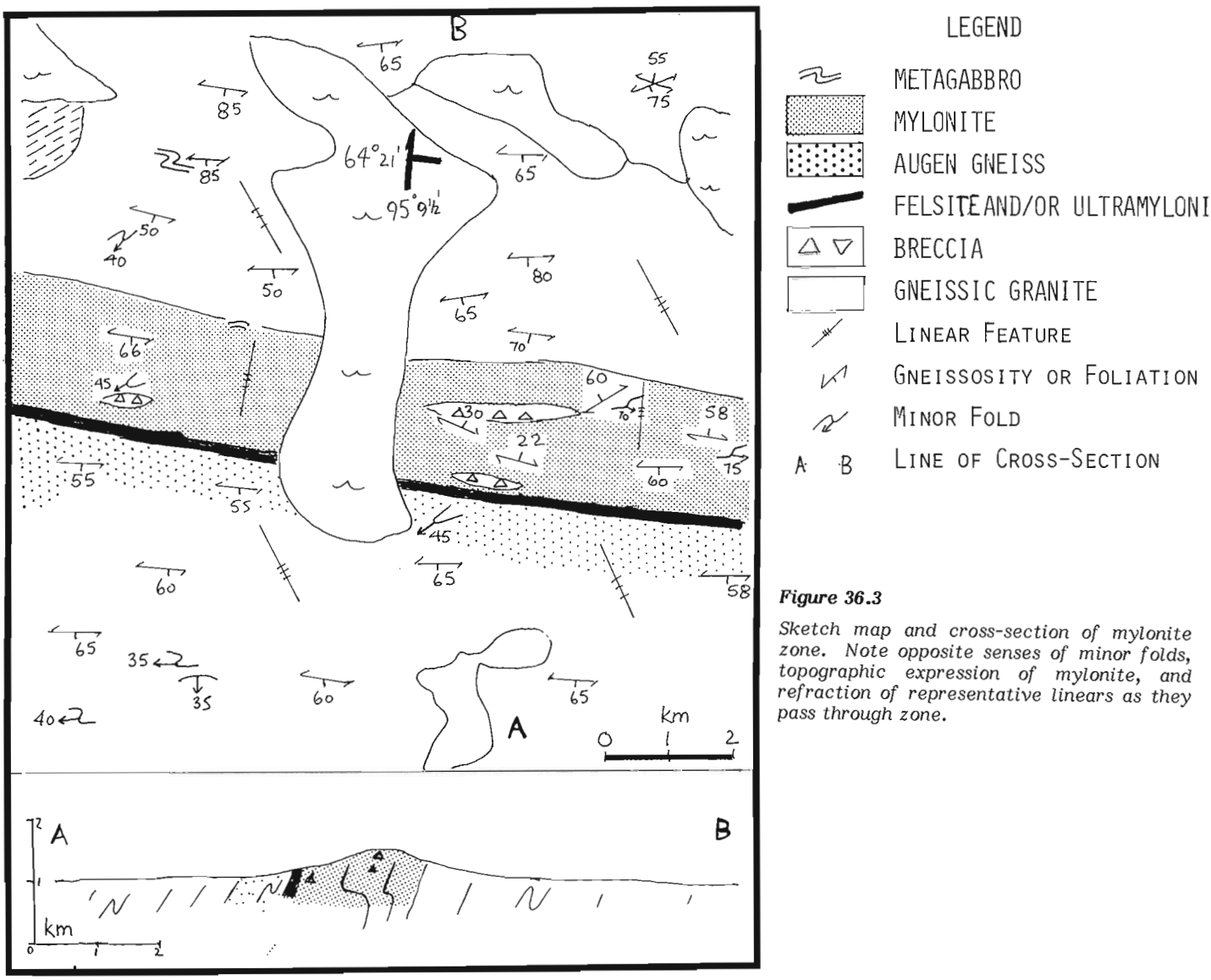

Figure 36.3

Sketch map and cross-section of mylonite zone. Note opposite senses of minor folds, topographic expression of mylonite, and refraction of representative linears as they pass through zone.

marked by steeply dipping east-west foliated rocks and a broad east-west valley with rare exposures of fault breccias or crushed rocks. Easterly trending mylonite zones form an anastomosing array within the Chesterfield Fault Zone. Spectacular exposures of mylonite that outcrop on a high hill (Fig. 36.3) are bounded on either side by progressively sheared plutonic rocks. They were intruded by gabbro dykes which were subsequently folded in an opposing sense to the minor structures within the zone, suggesting that the zone has a complex history.

The rocks of the zone are degraded. The mineral assemblage of garnet, hornblende, biotite, potassium feldspar, quartz plagioclase and oxide in the granite, indicates moderate pressure and temperature conditions (Froese, 1980). This long tabular granite body lies completely within the fault zone and its genesis may be related to movements along the fault zone.

Later gabbro plugs and dykes, locally extensively folded, were followed by a variety of biotite and/or pyroxene porphyry dykes possibly associated with the Dubawnt Group. These porphyry dykes are generally fresh, but some are carbonated and sheared along steep east-west and northwest trends.

The fault zone obviously has a long history. Possibly granitic plutons formed as a result of stress release within the zone; later, and nearer the surface, gabbro dykes were emplaced, only to be deformed in the continuously deforming rocks, and much nearer the surface, presumably when the zone was active as the northern fault margin of the Baker Lake Basin (or graben?) the porphyry dykes were emplaced and cut. Plugs of Dubawnt Group are undeformed in the northern part of the zone, whereas in the south, dykes of the same age are sheared. The patterns of deformation and the location of the fault zone suggests it is continuous with the Chesterfield Fault Zone as mapped at the mouth of the Quoich River (Schau, 1980). There the fault zone was active prior to the end of the Archean and intrusions and local deformation continued into middle Proterozoic times.

Tehek Plutonic Complex (D)

In the northern part of the region near Tehek Lake (56 D/13, 14) a plutonic complex is emplaced in the sedimentary rocks. Part of the complex is composed of granitic rocks and other portions are intricate mixtures of metasedimentary slices and low dipping granitic dykes and sills. These mixtures are easily recognized where metasediments are quartzite or carbonate. However, poorly

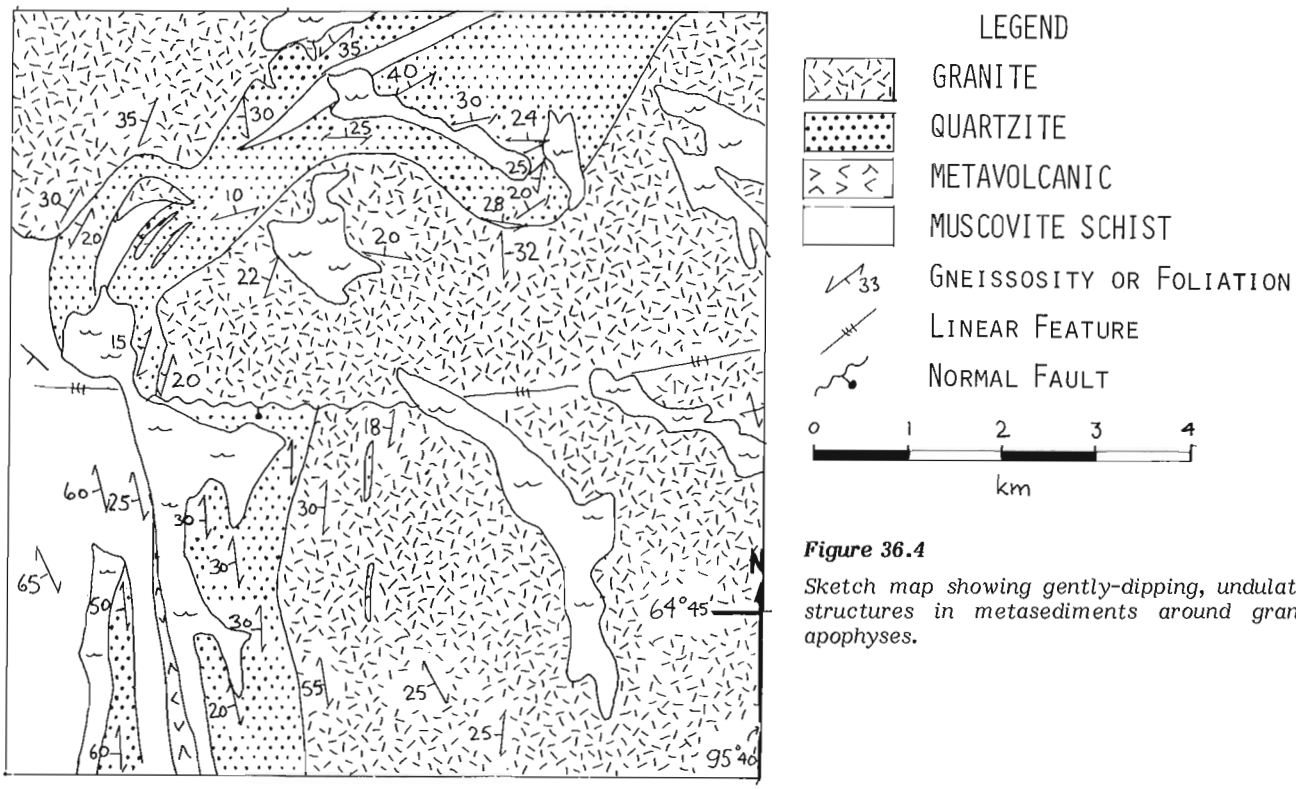

Figure 36.4

Sketch map showing gently-dipping, undulating structures in metasediments around granite apophyses.

layered to massive biotite-rich fine grained metasediments and fine grained biotite granite sills are difficult to distinguish. The complex is divided into three units: those where the main rock type is clearly granite, those where biotite-rich metasediments and granite are intermixed, and those in which quartzites are also intermixed.

The map pattern indicates that several plutonic apophyses have risen into the sedimentary mass, each to a different level. The grade of the associated sediments varies but near the granite, sillimanite or partially melted metasediments are present. The annular nature and low dips of the bedding suggest that the deformation occurred near the roof of the granite apophyses (Fig. 36.4).

The geologic patterns in the region near Tehek Lake suggest that the area is near the roof of a batholith. This interpretation is supported by the presence of a negative gravity anomaly, suggestive of a large granitic body at depth.

The age of the Tehek complex is not known but it intrudes deformed metasediments. Syenite, aerially associated with the intruded metasediments, locally appears to cut the granitic mass and is in turn cut by pegmatite. Within the complex different ages and fabrics associated with the various apophyses are probably coeval.

Dubawnt Group (E)

The Dubawnt Group in the Baker Lake region has been recently reviewed by Blake (1980). The group is mainly exposed south of the lake but small slivers are preserved along the north shore.

The Dubawnt Group along the north shore consists of basal, pebbly, crossbedded arkose containing red siltstone layers. East of Ingilik Point the bleached arkoses are cut by a biotite porphyry dyke; farther north a thin, vesicular, fine grained, pyroxene porphyry flow apparently overlies the arkoses. These relations are shown in Figure 36.5. Basal conglomerate and pebbly arkose have been reported along the shore west of the Prince River. Although the conglomerates are basal, they contain quartzite cobbles and fragments similar to Christopher Island volcanics present farther east in 56 D/1, 2, but do not contain clasts of the distinctive augen granites that outcrop immediately north of the Dubawnt sediments.

Elsewhere, pyroxene porphyry stocks outcrop along the shore, usually in fault zones, and in one place (Fig. 36.5) an intrusive breccia occurs near the contact. These stocks are cut by northwest faults, and slickensides on one fault suggest dextral movement. Pyroxene porphyry dykes found throughout the region generally trend easterly. Most dykes are fresh, but near the shore they are sheared, carbonated and hematitized.

The age of the group is early to middle Proterozoic (Blake, 1980). It clearly postdates most of the deformation of the mylonite zone and sheared plutonic rocks. The emplacement of igneous rocks of the group and quartz syenitic stocks may be coeval. The placement of the conglomerate and pebbly arkose within the Dubawnt section is uncertain, but they are not South Channel conglomerate. They are a later conglomerate that was formed on the northern edge of the developing basin since they contain clasts of Christopher Island volcanic rocks.

Quartz Syenite Complex

Quartz syenite dykes, sills and stocks are found throughout the area and are most concentrated near 95°30'W.

The rock is fine- to coarse-grained and consists of biotite, hornblende, potash feldspar, and may contain minor quartz. Variations in grain size and in mineral proportions occur within a single body and over short distances.

The quartz syenites occur as stocks, dykes, low dipping dykes and sills. The unit is massive and resistant to erosion. In the region southwest of Tehek Lake quartz syenite sills and dykes form the hill tops and country rocks are present in the valleys.

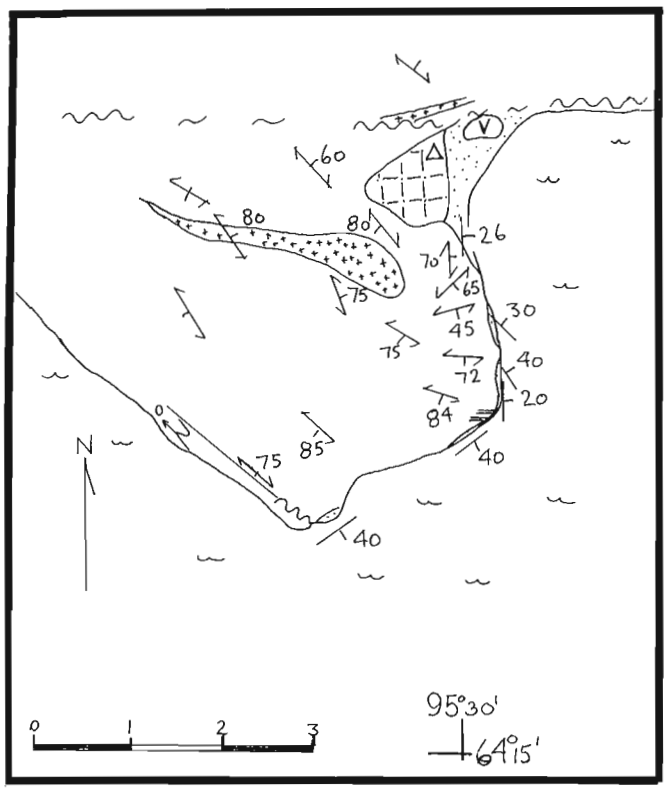

LEGEND

DUBAWNT GROUP

SYENITE STOCK

BRECCIA

VESICULAR FLOW

ARKOSE AND CONGLOMERATE

UNCONFORMITY

METAGABBRO

GNEISSIC GRANITE

GNEISSOSITY

MINOR FOLD

BEDDING

FAULT ZONE

DYKES

Figure 36.5. *Sketch map showing warped Dubawnt metasediments unconformably overlying sheared and gneissic granites and metagabbro.*

The rocks are generally fresh in hand specimen but locally are epidotized. Their age is not known but they may be correlated with Dubawnt syenites and/or with syenites in the Amer Lake region dated at 1849 ± 18 Ma by U-Pb on zircon and 1834 ± 32 Ma by K-Ar on hornblende.

Economic Geology and Regional Considerations

A zone of rusty slates trend eastward from Whitehills Lake and gossans (Fig. 36.1) are locally well developed near granitic contacts. At one such locality (Fig. 36.1) small amounts of galena are present in a metre-thick pyritic layer associated with complexly folded quartzite and slate.

The unconformity beneath the Dubawnt Group is exposed on the east side of Ingilik Point but routine monitoring of natural radioactivity levels in this vicinity yielded no anomalous values.

The importance of the gently-dipping reverse faults is difficult to assess. Most apparently dip to the southeast, but the exact direction may be an artifact of later warping. Thrust faulting has been documented in the Amer sheet (65 H) to the northeast (Tippett and Heywood, 1978) where the thrusts dip southwesterly. The gently-dipping foliations and layers in the vicinity of the Tehek pluton are thought to be local manifestations near the roof of a large granitic batholith but examination of orientations of gneissosities from other parts of the Armit block show that flat foliations are relatively common in this block (Heywood, 1967). It is apparent that gently-dipping structures are widespread in this Precambrian metamorphic terrane.

Acknowledgments

We thank L. Nadeau, senior assistant, S. Babcock, D. McNulty and A. Malnasi, junior assistants, L. Haack, cook, and W. Clifford, pilot-engineer of Liftair, for their efforts during the summer. Dr. F.C. Taylor and I. Annesley provided much help at start and end of season. The camp was ably delivered by B. Kolelewitz. Supplies were provided by Hudson Bay Company and Nunamuit Company, Baker Lake.

References

Blake, D.H.
1980: Volcanic rocks of the Paleohelikian Dubawnt Group in the Baker Lake Angikuni Lake area, District of Keewatin, N.W.T.; Geological Survey of Canada, Bulletin 309, 39 p.

Froese, E.
1980: Reaction grid for medium grade mafic rocks; in Current Research, Part A, Geological Survey of Canada, Paper 80-1A, p. 53-55.

Heywood, W.W.
1967: Geological notes, northeastern District of Keewatin and southern Melville Peninsula, District of Franklin, N.W.T., Parts of 46, 47, 56, 57; Geological Survey of Canada, Paper 66-40.

Heywood, W.W. and Schau, Mikkel
1978: A subdivision of the northern Churchill Structural Province; in Current Research, Part A, Geological Survey of Canada, Paper 78-1A, p. 139-143.

Schau, Mikkel
1980: Geological History of Anorthosites and Granulites at the edge of the Armit Lake Block, northern Churchill Structural Province, Canada; Geological Association of Canada, Program with Abstracts, v. 5, p. 79.

Schau, Mikkel and Ashton, K.E.
1980: Preliminary map of 56 D/1 and 56 C/4; Geological Survey of Canada, Open File 712.

Tippett, C.R. and Heywood, W.W.
1978: Stratigraphy and Structure of the northern Amer Group (Aphebian), Churchill Structural Province, District of Keewatin; in Current Research, Part B, Geological Survey of Canada, Paper 78-1B, p. 7-11.

Wright, G.M.
1967: Geology of the southeastern barren grounds, parts of the Districts of Mackenzie and Keewatin; Geological Survey of Canada, Memoir 350.

37.

THE GEOLOGY OF WHITEHILLS LAKE MAP AREA, DISTRICT OF KEEWATIN

Project 800008

Léopold Nadeau[1]
Precambrian Geology Division

Nadeau, L., The geology of Whitehills Lake map area, District of Keewatin; in Current Research, Part A, Geological Survey of Canada, Paper 81-1A, p. 265-268, 1981.

Abstract

The Whitehills Lake map area is underlain by a wide variety of sedimentary, volcanic and plutonic rocks and shows various structural styles.

In the northeast quarter, the vertical tectonism and the high grade metamorphism of the supracrustal rocks is caused by the intrusive Tehek Lake plutonic complex. The northwest quarter is underlain by refolded quartzite, slates and metavolcanic rocks. The southern half is characterized by thrust slices of low grade meta-igneous, metavolcanic and metasedimentary rocks.

General Geology

A variety of metasedimentary, meta-igneous and igneous rocks underlie the eastern Whitehills Lake region (56 D/12). The metasedimentary rocks include slates, phyllites, quartzites, quartz muscovite schists with minor iron formations, paragneiss, quartz biotite schists, and meta-volcanic rocks. The meta-igneous rocks include a syenitic complex and the granitic rocks of the "Tehek Lake plutonic complex".[2]

Metamorphosed Supracrustal Rocks

Three types of volcanogenic sediments are recognized. In the northwestern quadrant pillowed and fragmental structures are preserved. In the Tehek Lake plutonic complex area they are fine grained, well layered (<1 cm), light to dark green on both fresh and weathered surfaces, and amphibole-rich. They are locally in contact with iron formation, quartzite and paragneiss. The third type is generally a featureless aphanitic to fine grained dark greenish grey rock that contains variable proportions (0-30%) of carbonate and quartz filled cavities and, locally, on weathered surface, it shows a thin primary layering (<1 cm). A few tuffaceous and brecciated horizons are recognized. The south-central greenstone area is bordered on the north and south by meta-igneous rocks; to the east it seems to interfinger with slates and phyllites. One band is within the quartzite, and another, south of the northeast fault, is in contact with slates and paragneiss.

A few quartz magnetite (<1 cm) iron formations (probably <50 m thick by 1-2 km long) are in contact with quartzite, well layered volcanogenic sediments, and paragneiss.

North of Whitehills Lake, a weakly foliated, locally massive, white recrystallized orthoquartzite containing muscovite forms large ridges. East of Whitehills Lake orthoquartzites commonly overlie quartz muscovite schist. Although the schists are poorly exposed and hence are not mappable, they may be widespread. Elsewhere in the area, the massive to weakly foliated muscovite bearing quartzite is common. Primary sedimentary structures such as bedding, crossbedding, and quartz-pebble conglomerate lenses(?) are locally preserved. Light green chromian mica is present in trace quantities throughout the area and sillimanite is locally abundant near the Tehek Lake plutonic complex. The number and the variety of lithologic associations suggest that there is probably more than one quartzite unit.

Light greenish to dark grey slates and phyllites are exposed east of Whitehills Lake and in the southeast corner of the area. They show a weak primary layering at an angle to the principal foliation and, locally, they contain up to 25 per cent discontinuous thin quartz ribbons (flattened pebbles?) aligned parallel to the foliation plane. No contacts are exposed with the other sediments. In spite of the resemblance of the two regions there is no evidence for a common stratigraphic position.

The east-central part of the area comprises an assemblage of biotite schist and fine to medium grained biotitic paragneiss containing some dark grey to black slate and, to the south, minor quartzite. This unit also contains rusty weathering pyrite and, locally, some well developed gossan zones. No contact with the other metasediments has been observed.

In the Tehek Plutonic Complex area an appreciable amount of quartz-biotite, locally with amphibole, schist is associated with the quartzites.

Several small occurrences of fine to medium grained biotite paragneiss associated with other metasediments are irregularly distributed in the map area. They contain a few discontinuous small quartz ribbons parallel to the foliation and, locally, some quartz layers.

Basic and Ultrabasic Intrusions

Several small, medium- to coarse-grained metagabbro dykes and sills are near or within the volcanogenic sediments. In the southwest corner of the map area, a small metamorphosed(?) ultramafic sheet (a few metres thick and few hundred metres long) of unknown stratigraphic position is associated with the phyllonite.

Meta-igneous Rocks

A broad belt of meta-igneous rocks underlie most of the southern half of the map area. The northern part is a medium- to coarse-grained, pink, locally grey, foliated feldspathic porphyritic granodioritic unit containing 10 to 30 per cent biotite. Near Whitehills Lake it structurally overlies metasediments.

The southern part of the belt is composed of a fine grained inequigranular, irregularly layered, lightly coloured hornblende biotite gneiss. The contact with the northern part is sharp and at one place it forms a thin (<1 m) sheared epidotized zone. Locally, along the southern contact with

[1] Department of Geology, Carleton University, Ottawa, Ontario, K1S 2X9

[2] An informal name introduced by Heywood and Schau (1981)

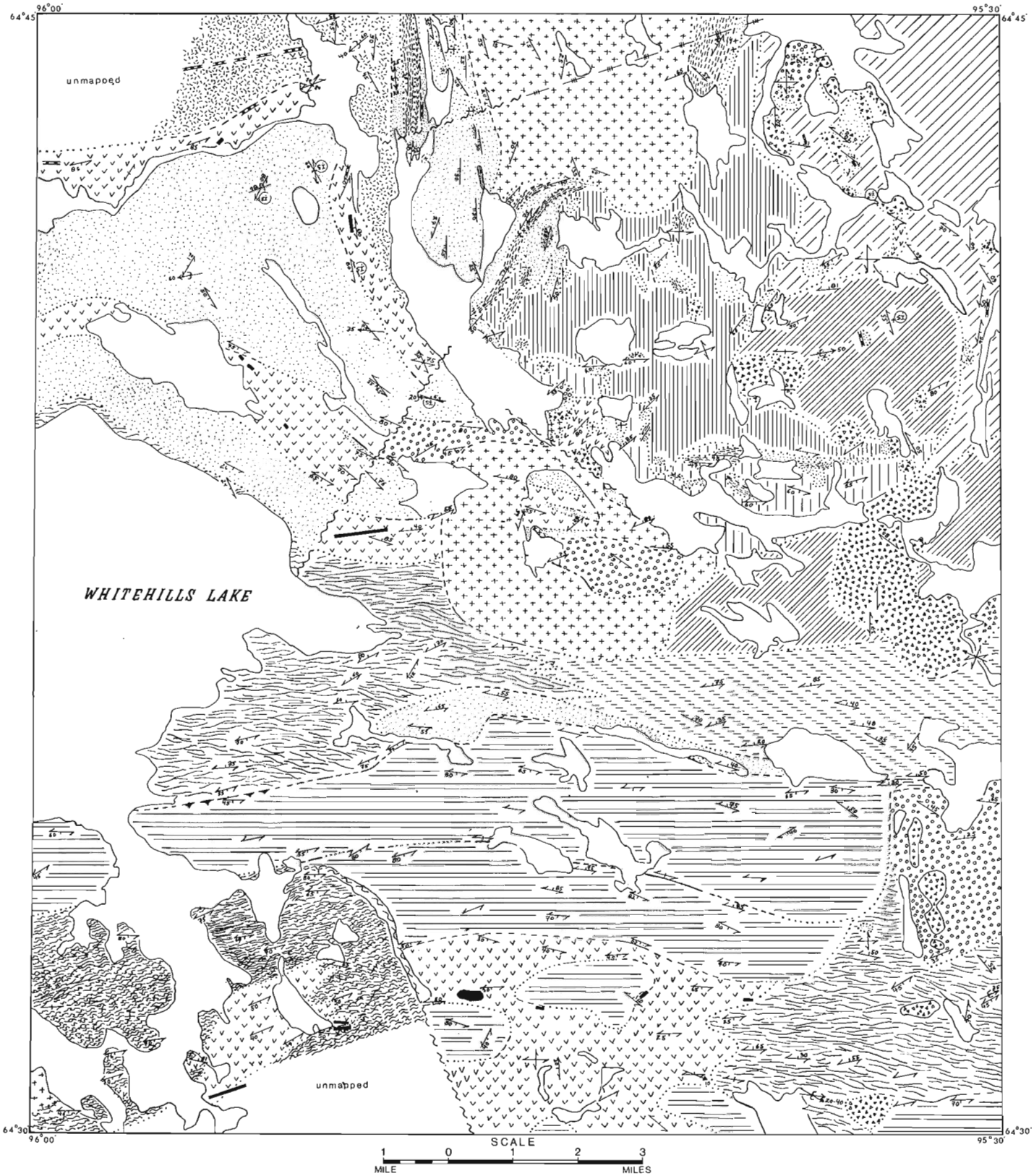

Figure 37.1. *Geology of the Whitehills Lake map area.*

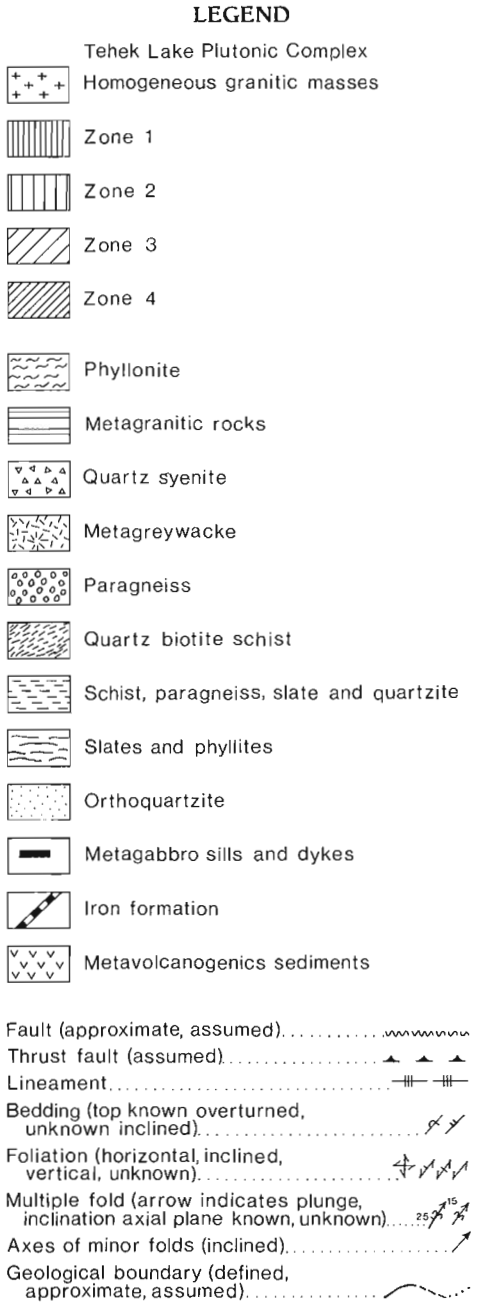

greenstone, a thin band of garnet porphyroblastic biotite schist suggests an intrusive relationship. It has many similarities to the igneous masses that intrude the southern greenstone.

Quartz Syenite Complex

Several quartz syenite masses occur along the eastern border of the area. They are typically massive to weakly foliated, medium grained, equigranular, granulated, pink, contain 30 to 50 per cent, rarely 80 per cent biotite and hornblende. The southern masses form small rounded plug-like bodies with a well marked topographic expression, whereas the northern masses are larger, show no topographic expression, and seem to form plug-like bodies and sills. These intrusions cut across the metasediments and the linear distribution in the southeast corner suggests a post-regional deformation emplacement. They are intruded by pegmatite dykes.

Tehek Lake Plutonic Complex

An irregular distribution of plutonic rock units characterizes the northeast quarter of the map area. The large mappable patches of the different units are shown on Figure 37.1. This pattern results from the near coincidence of the erosional surface with the contact between the metasedimentary and plutonic rocks.

The northern homogeneous granitic mass is composed of two distinct foliated phases, a pink medium grained to pegmatitic felsic granite phase that contains less than 5 per cent mafic minerals, and a mafic phase that is finer grained and contains more than 5 per cent of mafic minerals.

Zones 1 to 4 of the Tehek Lake complex are characterized by erosional remnants of the supracrustal and syenitic rocks in a region of pegmatitic and granitic rocks. On the basis of the kind and the proportion of the rock units, this area of mixed rocks is subdivided into four different zones. Zone 1 is mainly the massive white to pinkish southern type granite and minor quartzite, biotite schist and paragneiss. In zone 2 the metasediments are predominant. Zone 3 is mainly quartzite, biotite schist, paragneiss and minor iron formation intruded by pegmatite, granite and quartz syenite. In zone 4 the quartz syenite is predominant.

Phyllonite

This unit, restricted to the southwest corner of the map area, contains a medium grained chloritic quartz-rich phyllonite that, to the north, grades into a fine grained greenish grey calcareous gneissic rock. The distribution and stratigraphic position of this unit is unknown.

Giant Quartz Veins

In the southern half of the map area sinuous, white, glassy quartz layers are interpreted as giant quartz veins. One vein is continuous from slate to greenstone, and another is present in the porphyritic granodiorite.

Structural Geology

There is a striking change in the structural style across the map area. The orientation of the principal foliation and major lithologic contacts change from an east-west linear pattern in the southern half to a wide-open folded pattern north of Whitehills Lake to an irregular, low to moderate dip pattern in the Tehek Lake plutonic complex area.

North of Whitehills Lake, the lithologic distribution, the top indications, and the minor structures affecting the main foliation, suggest that the present pattern results from superposed folds. The fold axes of the minor folds produced at the end of the deformation show a gentle west plunge. To the east, in the Tehek Lake plutonic complex area, the irregular distribution of the rock units, the divergence in the trend, and the gentle to flat dips of the principal foliation resulted from vertical deformation generated by the emplacement of the intrusive masses.

In the southern half, no major folds have been recognized. In the slates and phyllites the minor folds are common and show a gentle eastern plunge. South of Whitehills Lake, the porphyritic granodiorite is structurally above the slates and phyllites. That, with the irregular distribution of the rock units in the southwest corner and the sharp break in the rock units in the eastern one, suggests thrust faulting.

Metamorphism

Field observations suggest a regional greenschist facies metamorphism in the southern half of the area. An increase in grade in the eastern corner coincides with lithologic contacts. The slates and phyllites are biotite-free whereas the paragneiss is biotite-rich and locally garnet bearing.

North of the porphyritic granodiorite, the grade increases from the chlorite to the biotite zone in an easterly and northeasterly direction. To the north, the presence of well developed sillimanite rosettes in the foliation plane results from contact metamorphism associated with the Tehek Lake plutonic complex.

Acknowledgments

This work was undertaken by the author as part of the Geological Survey of Canada reconnaissance mapping of the Baker Lake map area in 1980 under the direction of W.W. Heywood and Mikkel Schau. The author is grateful for their supervision during the field season and for their criticisms and suggestions in the preparation of this report.

Reference

Heywood, W.W. and Schau, M.
1981: Geology of the Baker Lake region, District of Keewatin; in Current Research, Part A, Geological Survey of Canada, Paper 81-1A, Report 36.

38. PRELIMINARY REPORT ON GEOLOGICAL STUDIES OF THE "WOODBURN LAKE GROUP" NORTHWEST OF TEHEK LAKE, DISTRICT OF KEEWATIN

Contract 1147740

K.E. Ashton[1]
Precambrian Geology Division

Ashton, K.E., Preliminary report on geological studies of the "Woodburn Lake Group" northwest of Tehek Lake, District of Keewatin; in Current Research, Part A, Geological Survey of Canada, Paper 81-1A, p. 269-274, 1981.

Abstract

Northwest of Tehek Lake, the "Woodburn Lake Group" is exposed in several northeast-trending bands of metamorphosed volcanic, plutonic, and sedimentary rocks. The volcanic rocks consist largely of felsic to mafic volcanic breccias and tuffs with minor mafic flows. Massive and spinifex-textured ultramafic flows occur within intermediate volcanic rocks and are particularly common in the western part of the area. Magnetite-quartz iron formation is associated with the metavolcanic rocks but was probably also deposited at other stratigraphic horizons (within the metasediments). Massive to porphyroblastic hornblende metagabbro and metadiorite intrude the metavolcanic sequence.

Extensive, white orthoquartzite is exposed in long, thin ridges and hills in the eastern part of the area. Thin, conglomeratic horizons containing orthoquartzite pebbles in a matrix of the same composition occur at several localities within the orthoquartzite. Green chromian(?) mica is disseminated throughout the orthoquartzite (including both the pebbles and the matrix of the pebbly horizons) and locally forms thin, green horizons within it. Thin bands of white mica-quartz schist and black phyllite are present within the orthoquartzite. A separate horizon of black phyllite locally contains pebbles of orthoquartzite.

Extensive bodies of pink, foliated and/or sheared granitic rocks intrude the metavolcanic and gabbroic rocks. Contact relationships between the granitic and the metasedimentary rocks are unknown.

Late biotite porphyry dykes cross cut the regional northeast-trending foliation and the older granitic and metavolcanic rocks.

Introduction

The 1980 field season initiated a two-year project to map metamorphosed volcanic, sedimentary and plutonic rocks in the southeast corner (66 H/1) of the Amer Lake map area (located about 80 km north of the settlement of Baker Lake), District of Keewatin.

The southern half of the Amer Lake map sheet was mapped by W.W. Heywood, S. Tella, and I. Annesley during the summer of 1978. At that time, the informal name "Woodburn Lake Group" was assigned to a sequence of metavolcanic rocks (including ultramafic flows), associated greywacke, iron formation and quartzite. These supracrustal rocks were thought to unconformably overlie an extensive granitic basement and to be intruded by a late, fluorite-bearing granite. The southern half of the study area was mapped during the summer of 1980 (Fig. 38.1).

The project is being carried out under contract with the Geological Survey of Canada and will form the basis of a doctoral thesis to be completed at Queen's University in Kingston, Ontario. The author wishes to express gratitude for the support provided by the Geological Survey of Canada and, in particular, to WW. Heywood and M. Schau. Many helpful insights into the geology of this and adjacent areas have been provided by D. Carmichael, M. Schau, W.W. Heywood, and I. Annesley. The able assistance of G. Baragar during the course of the field work was greatly appreciated.

General Geology

Metavolcanic rocks are exposed in several northeast- to east-trending bands and consist mainly of greenschist to amphibolite facies flows and fragmental rocks. Most appear to be intermediate in composition but felsic, mafic and ultramafic volcanic rocks were also distinguished. Spinifex textures and polyhedral jointing are well preserved in some of the ultramafic flows. Thin, locally traceable bands of magnetite-quartz iron formation and minor greywacke occur in the greenstone sequence.

Chlorite schists are common in the southeast corner of the area. Many contain millimetre to centimetre scale fragments of pink, fine grained felsic rocks. Thin lenses and beds of marble are present within other chlorite schists and Heywood (personal communication, 1980) reported thin limestone horizons within chlorite schists near the northeast corner of "Third Portage Lake".

Several large gabbroic masses occur within the metavolcanics and appear to display intrusive relationships. Inclusions of similar gabbro are locally common in the granitic rocks.

Orthoquartzite, minor greywacke and phyllite are exposed in the eastern part of the area. The relationship of these rocks to the metavolcanic sequence is not clear.

Pink, foliated to sheared granite intrudes the metavolcanic sequence and the gabbroic rocks. Granite-orthoquartzite contacts were not observed.

Several, late, north trending biotite porphyry dykes crosscut the metavolcanic and granitic rocks as well as the regional, northeast trending foliation.

Metavolcanic Rocks

Metavolcanic rocks are abundant in the area and occur in several northeast- to east-trending belts. Mafic to intermediate flows, breccias and tuffs weather dark green to black but are locally rusty due to the presence of disseminated iron sulphides. Layering in the fragmental rocks is locally discernible on a millimetre to centimetre scale and most rocks exhibit a strong schistosity parallel to

[1]Department of Geological Sciences, Queen's University, Kingston, Ontario

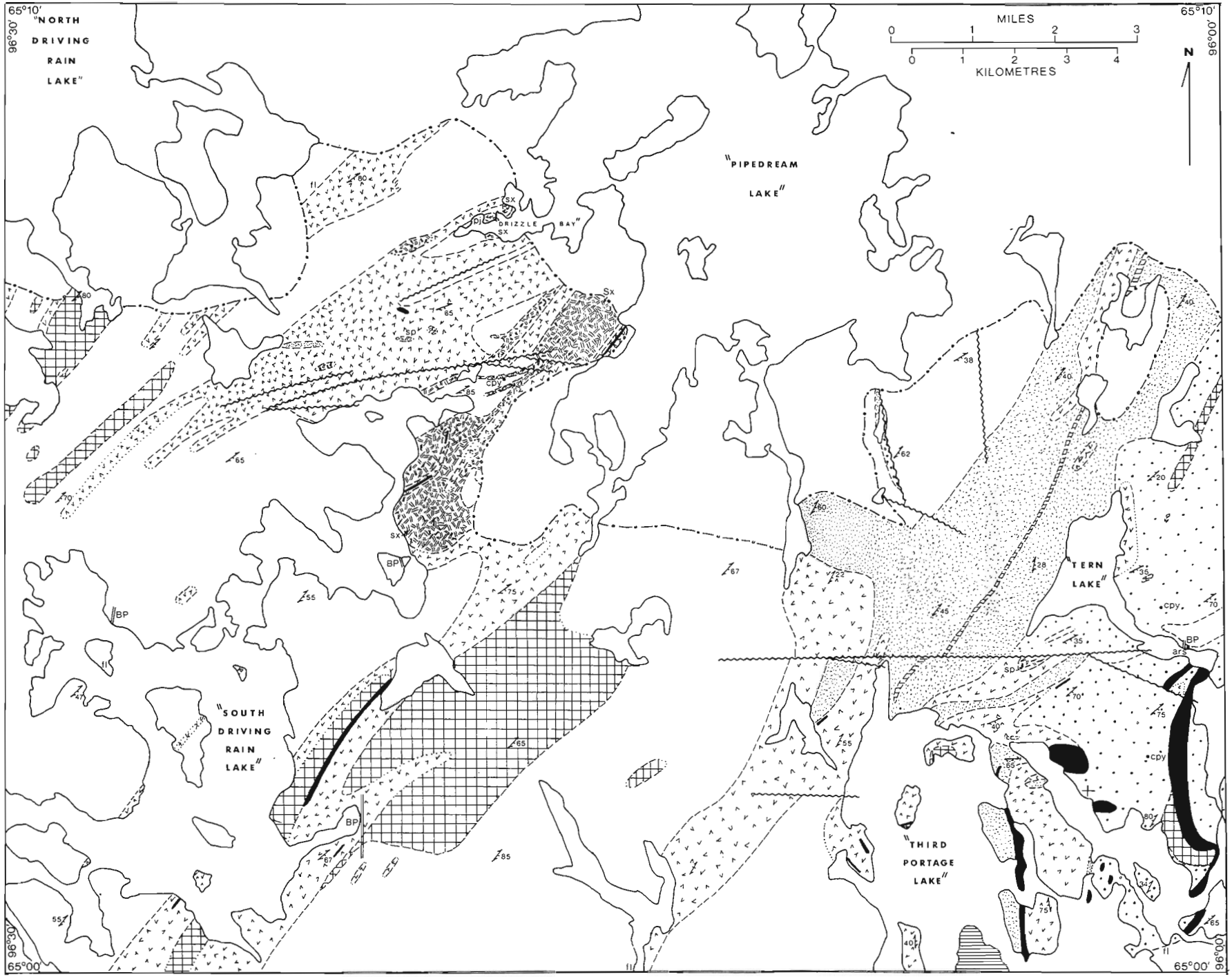
65°10'
96°30'
"NORTH DRIVING RAIN LAKE"
"PIPEDREAM LAKE"
"DRIZZLE BAY"
"SOUTH DRIVING RAIN LAKE"
"TERN LAKE"
"THIRD PORTAGE LAKE"
MILES
0 1 2 3
0 1 2 3 4
KILOMETRES
N
65°00'
96°00'
BP
SX
SD
CDY

layering. Chlorite, biotite, hornblende, actinolite and epidote are the most common mafic minerals and typically form 30-50 per cent of these rocks. Plagioclase phenocrysts (up to 1 mm) and epidote-bearing amygdules can be discerned locally. Quartz and feldspar crystal tuffs are particularly abundant in the western part of the area, and display striking centimetre to metre scale, white, pink and grey-green colour banding. In well-exposed outcrops many of these apparently banded rocks are lensoidal in nature and are probably extremely flattened volcanic breccias. Minor medium- to coarse-grained felsic rocks observed at the eastern end of "Tern Lake" may represent quartz porphyry.

Iron Formation

Iron Formation was observed within intermediate metavolcanic tuffs, chlorite schists, orthoquartzite and at the contact between the metavolcanics and chlorite schists. It occurs as thin, recessive, conformable bands which are traceable for as much as 4 km. Because of repetition due to folding, thicknesses were not determined. The iron formation consists of alternating millimetre to centimetre scale bands of very fine grained magnetite and quartz. Individual laminae are traceable for tens of metres. As well as quartz and magnetite, some bands of iron formation contain chlorite with or without amphibole as thin, dark green laminae. Scattered pyrite grains locally replace magnetite.

The spatial distribution of iron formation suggests that it was deposited at more than one stratigraphic horizon.

Ultramafic Rocks

Ultramafic rocks appear to be spatially and genetically related to the metavolcanic rocks previously described. Many occur as light grey to apple green, soft tremolite-talc-serpentine rocks which locally grade into soapstone.

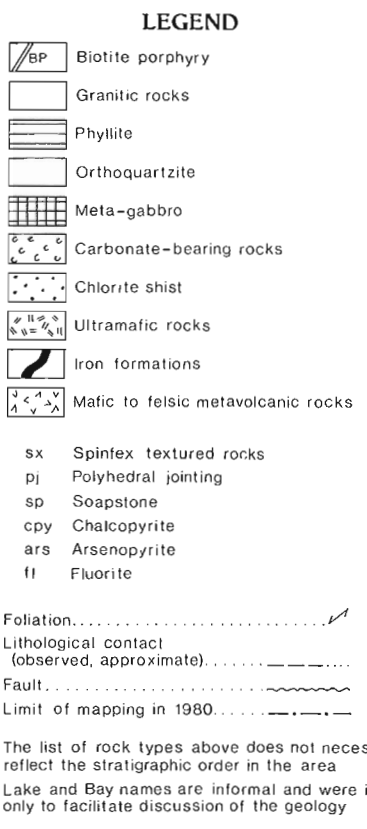

Figure 38.1. *Geology of study area, northwest of Tehek Lake.*

However, primary textures have been preserved in some ultramafic rocks in the central part of the area. The best-exposed of these outcrop immediately west of southern "Pipedream Lake". There, alternating zones of green, spinifex-textured rocks and rust coloured, cumulate zones, 1-3 m thick, mark the presence of komatiitic flows. Flow tops (A1 zones of Pyke et al., 1973) and foliated, skeletal olivine (B1 zone) are discernible in some outcrops. A representative suite of these rocks has been chemically analyzed by I. Annesley as part of an M.Sc. thesis at the University of Windsor.

Chocolate brown weathering ultramafic rocks in the "Drizzle Bay" area are characterized by extensive polyhedral jointing and rare spinifex textures. Arndt et al. (1979) have described similar rocks as massive ultramafic flows.

Contacts between the ultramafics and other rock types in the area are generally not exposed. Most occurrences, however, are within bands of metavolcanic rocks suggesting that they are part of a complex extrusive event. At the eastern end of the "Pipedream Lake" occurrence, spinifex-textured flows are cut by a thin, granitic dyke.

Chlorite Schists

Chlorite schists are exposed over a wide region in the southeast corner of the area. They are generally fine grained, phyllitic, grey-green rocks which contain various proportions of chlorite, quartz, feldspar and, locally, biotite and carbonate. Many also contain scattered, fine grained, pink inclusions up to several centimetres in size. Thin, discontinuous horizons contain as much as 30 per cent felsic inclusions but scattered, millimetre-scale fragments are more common. These inclusions are generally elliptical in shape and are very fine grained although some contain scattered quartz and feldspar grains up to 1 mm in size. Whether these inclusions are flattened granitic pebbles or felsic metavolcanic fragments is not known.

Contacts between the chlorite schists and the iron formation and carbonate-bearing rocks are conformable and some interlayering of the three rock types was observed. Metavolcanic rocks are interlayered with the chlorite schists in the "Tern Lake" area. Orthoquartzite was not observed in contact with the chlorite schist.

Carbonate-Bearing Rocks

Several, small exposures of carbonate-bearing rocks in the southeastern corner of the area consist of fine- to medium-grained calcite (dolomite in thickest horizons) marble beds alternating on a centimetre to metre scale with chlorite schists. Thin lenses, pods and veins of carbonate within adjacent chlorite schists and metavolcanic and ultramafic rocks indicate that substantial remobilization of the primary carbonate has taken place. W.W. Heywood (personal communication, 1980) reported a thin layer of limestone near the northeast corner of "Third Portage Lake".

Metagabbro

Several small bodies of metamorphosed diorite and gabbro were observed within metavolcanic and chloritic rocks. Contacts are generally not exposed but intrusive relationships observed at several outcrops indicate that the metagabbro postdates the metavolcanic rocks. Contact relationships between the metagabbro and iron formation are unknown. More extensive occurrences of metagabbro were found within the large, granitic mass east of "South Driving Rain Lake". There, agmatite is common in which centimetre to outcrop scale blocks of amphibolite and metagabbro are present within the granite and within hybridized rocks (presumably resulting from the assimilation of minor metagabbro by the granite).

The gabbro has been deformed and altered to varying degrees. It ranges from massive and porphyroblastic in its freshest state to fine grained, sheared amphibolite which can be easily confused with mafic and ultramafic metavolcanic rocks. Most weathers dark green to black and contains 30-50 per cent porphyroblastic hornblende. Individual porphyroblasts are as much as 1 cm in size and are partially altered to biotite and chlorite. Plagioclase in the metagabbro is typically fine grained and is cataclastic in some of the sheared rocks.

Compositional variations from diorite to gabbro are generally gradational but a porphyroblastic metadiorite phase cuts the medium grained metagabbro at the south end of "North Driving Rain Lake". The diorite contains about 20 per cent pink to white feldspar porphyroblasts in a matrix which resembles the metagabbro.

Orthoquartzite

Remarkably clean, white orthoquartzite, common in the eastern part of the area, outcrops as long, narrow, resistant ridges and extensive plateaus; it is fine grained and recrystallized. Bedding and other primary textures are rare. Typical samples contain only trace amounts of white micas and/or clay minerals and chromian mica in an almost monomineralic quartz matrix. Locally, thin, metre-scale bands of white mica (and/or clay minerals) – quartz schist and centimetre-scale bands of green, chromian mica-rich quartzite within the quartzite were not mappable. Thin, centimetre-scale layers of magnetite are present in the quartzite along the eastern shore of "Third Portage Lake".

Thin beds (1-3 m thick) of intraformational conglomerate occur within the orthoquartzite at three localities in the "Third Portage Lake" area. Both pebbles and matrix are orthoquartzite and locally contain chromian mica, although the matrix in most samples appears to be somewhat richer in white mica and/or clay minerals. At one occurrence, orthoquartzite pebbles are present in a small outcrop of greywacke, separated from a quartzite pebble conglomerate by a thin band of iron formation.

A thin veneer of white mica-chlorite-quartz schist typically occurs between the orthoquartzite and the metavolcanic and granitic rocks.

Phyllite

Dark grey to black phyllite is exposed in a thin band extending from "Third Portage Lake" to the northeast corner of the map area and on a large island in "Third Portage Lake" along the southern map boundary. The only observed contact is immediately north of "Third Portage Lake" where phyllite is interbanded with orthoquartzite on a scale of metres to tens of metres. Pebbles of orthoquartzite are present within the phyllite at several localities.

The spatial distribution of the two phyllite occurrences may indicate that they were deposited at different stratigraphic levels.

Granitic Rocks

Pink, foliated and locally sheared granitic rocks are exposed in several areas. Most are medium- to coarse-grained, pink granites but thin, unmappable bands of porphyroblastic to augen granodiorites and small pods of pink aplite are common. Typical granite contains about 10 per cent partially chloritized biotite aggregates and 30 per cent flattened blue to white quartz. Minor purple fluorite was observed in several outcrops. Granitic dykes intrude metavolcanic rocks in several localities and large metavolcanic xenoliths are exposed within the granite at some contacts between the two rock types. Along the western edge of the central granitic mass, in a belt between "Pipedream Lake" and "South Driving Rain Lake", agmatites and other hybrid rocks were produced by the emplacement of the granite within gabbroic and volcanic rocks.

Granitic rocks in the "South Driving Rain Lake" and "Drizzle Bay" areas appear somewhat more deformed than those in the central part of the area. Penetrative deformation has affected them to a greater extent and quartz is generally white rather than blue. Locally, brick red weathering indicates sheared and cataclastic rocks, some of which appear to be quartz depleted.

The granitic rocks southeast of "Pipedream Lake" are mostly of the red-weathering, cataclastic variety. Contacts with the orthoquartzite are not exposed but a thin mylonite zone is present at the contact with chlorite schists near the southwestern boundary of the intrusive body. Granitic rocks to the west of that fault weather pink and are generally fresher and less deformed than the granitic rocks in the eastern block. Relatively fresh, pink granitic rocks are also found adjacent to red, cataclastic granite immediately west of "Third Portage Lake". Extensive shearing in both granites suggests that the two are in fault contact.

Intrusive relationships suggest that the granite post-dates the volcanic, ultramafic and gabbroic rocks but the contact relationships between the granite and the chlorite schists, iron formation, orthoquartzites and phyllites are unknown.

Biotite Porphyry

At several localities (east of "Tern Lake" and around "South Driving Rain Lake"), discontinuous, north-trending, biotite porphyry dykes cut across the regional foliation. They are generally 1-7 m wide but widths vary significantly along strike. The rocks are very fine grained, pink to grey and contain 5-10 per cent biotite with or without pyroxene(?) phenocrysts up to 1 cm in size. The dykes may be part of an extensive network of lamprophyres which are related to the Dubawnt Group volcanics in the Baker Lake area (Schau and Hulbert, 1977).

Glacial Features

Bedrock surfaces and glacial debris in the area show evidence of polishing and other glacial erosional features. In general, striae and grooves trend north-south in the eastern part of the area and northwest-southeast in the west. Some of these striae and a few roches moutonnées indicate a northwestward movement of ice in the western part of the area. At several outcrops, two sets of striae were observed, one trending north-northwest, the other west-northwest.

Structure

The regional foliation in the area generally trends northeast and dips moderately to steeply southeast. Micaceous minerals define this foliation in most rocks but it is defined by flattened quartz in some of the more "massive" granitic rocks. The orthoquartzites are characterized by a pervasive cleavage.

Bedding, as defined by pebbly horizons in the ortho-quartzite, has been folded about gently northeastward-plunging fold axes. The regional foliation appears to be axial planar to these folds. A second set of northeast-trending, doubly plunging folds has, in turn, deformed the regional foliation. Axial planes dip moderately to steeply south-eastward and suggest that the folds are overturned to the northwest. A third set of folds is responsible for doubly-plunging, northwest-trending minor folds in the southeast corner of the area and for deviations in the regional foliation in that region.

Local shearing and cataclasis, particularly in the granitic rocks, is parallel to the regional foliation and is probably related to the first or second set of folds. An east-west set of dextral faults is common in the eastern half of the area. Large offsets have been demonstrated only at the north end of "Third Portage Lake". The eastern "domain" also contains a set of north-south faults and lineaments. The offset on these is not clear but movement appears to have been mainly dip-slip.

In the western half of the area, two sets of faults and lineaments were recognized. A major set of sinistral, east-northeast-trending faults was mapped near the north end of "South Driving Rain Lake". Offsets of at least tens of metres were observed in northeast-trending rocks near "Pipedream Lake" but much of the movement on the western portion of these faults also appears to be dip-slip. A second set of northwest-trending lineaments is present in the western half of the area.

Late quartz veins, dipping steeply to the southeast were observed throughout the area.

Metamorphism

Macroscopic mineral assemblages indicate a range in metamorphic grade from lower greenschist facies (in the phyllites, chlorite schists and some of the orthoquartzites and metavolcanics) to middle amphibolite facies (in the metavolcanic and metagabbroic rocks).

Economic Potential

No economically significant mineral occurrences were noted. Disseminated pyrite was observed throughout the metavolcanic rocks and at scattered localities in the chlorite schists (where pyrite crystals are up to 8 mm in size) and in orthoquartzite. Trace occurrences of chalcopyrite and arsenopyrite found at several localities are plotted on the map. A small outcrop on the northeastern shore of "Tern Lake" contains 20 per cent arsenopyrite up to 8 mm in grain size.

Magnetite-quartz iron formation is abundant in the area but thicknesses are difficult to determine due to tight folding and the shallow dips encountered at many occurrences.

Minor amounts of soapstone are present at several localities within altered ultramafic rocks.

Purple fluorite occurs in granitic rocks at several localities.

References

Arndt, N.T., Francis, D., and Hynes, A.J.
1979: The field characteristics and petrology of Archean and Proterozoic komatiites; Canadian Mineralogist, v. 17, No. 2, p. 147-163.

Pyke, D.R., Naldrett, A.J., and Eckstrand O.R.
1973: Archean ultramafic flows in Munro Township, Ontario. Geological Society of America Bulletin, v. 84, p. 955-978.

Schau, Mikkel and Hubert, L.
1977: Granulites, anorthosites, and cover rocks northeast of Baker Lake, District of Keewatin; in Report of Activities , Part A, Geological Survey of Canada, Paper 77-1A, p. 399-407.

39.

FIELD CHARACTERISTICS, PETROLOGY, AND GEOCHEMISTRY OF THE AMER LAKE ULTRAMAFIC METAVOLCANICS, DISTRICT OF KEEWATIN

Project 760025

I.R. Annesley[1]
Precambrian Geology Division

Annesley, I.R., Field characteristics, petrology, and geochemistry of the Amer Lake ultramafic metavolcanics, District of Keewatin; in Current Research, Part A, Geological Survey of Canada, Paper 81-1A, p. 275-279, 1981.

Abstract

Metakomatiites in association with serpentinized peridotites occur in metavolcanic-metasedimentary belts in the Amer Lake area. In one locality 25-30 ultramafic flow units have a stratigraphic thickness of 75 m. The komatiites are peridotitic in composition (MgO > 20%) and occur as spinifex-textured and massive flows; individual flows range in thickness from 0.5 – 10 m. Most flows contain a spinifex zone which has finer grained tops. Other massive flows are characterized by distinct polyhedral jointing. The Amer Lake komatiites are assumed to be Archean in age.

Introduction

Reconnaissance mapping of Operation Baker in 1954 (Wright, 1967) outlined linear belts of mafic to ultramafic rocks in the Amer Lake area. Subsequent mapping in 1976 (Heywood, 1977) and 1978 (Heywood, personal communication) defined these belts and noted the occurrence of spinifex textured komatiites in the southernmost belt (Fig. 39.1). In 1980, K.E. Ashton (Ashton, 1981) commenced detailed mapping of the southeast corner (NTS 66 H/1) of the Amer Lake map area and described the geology in the vicinity of the komatiites. Most of the ultramafic rocks present in the southern area are of extrusive origin and are of similar mineralogy, morphology, and textures to ultramafic flows of other worldwide occurrences. Two other belts consist of featureless fine grained mafic to ultramafic rocks containing minor sulphides. The investigation of the spinifex-texture komatiites is the subject of an M.Sc. thesis in preparation at the University of Windsor.

Regional Geology

The study area is within the Churchill Structural Province. It is characterized by metavolcanic-metasedimentary greenstone belts that are typical of those assumed to be of Archean age. In this area they consist of metaquartzites, metakomatiites, mafic to felsic metavolcanics, iron formations, and granitoid intrusions which overlie a basement complex (Tippett and Heywood, 1978). The rocks are isoclinally folded with vertical axial planes parallel to the axes of the belts. Abundant thrust faulting has occurred throughout the region. Metamorphic grade varies from lower greenschist to upper amphibolite (Tella and Heywood, 1978) with major deformation and metamorphism occurring during the Hudsonian Orogeny. The stratigraphy of the area is not clearly understood due to the effects of metamorphism and deformation.

History and Classification of Komatiites

Komatiites, a relatively new class of igneous rocks established by Viljoen and Viljoen (1969a, b) are characterized by high Ca/Al and Fe/Mg ratios, low alkali content, low TiO_2, and typical extrusive textures. They have been redefined by Brooks and Hart (1974), Arndt et al. (1977), and others, hence at present there is no universally accepted definition of the term komatiite. Field, mineralogical, petrologic, and chemical data of the Amer Lake ultramafic metavolcanics classify them as ultramafic or peridotitic komatiites (Arndt et al., 1979).

Table 39.1

Average composition (mean and standard deviation) of 26 komatiite samples from the study area. Analyses by author using XRF with all oxides recalculated on a dry basis using loss on ignition for 1 hour at 1000°C.

	Mean (wt. %)	St. Dev.
SiO_2	44.465	1.175
Al_2O_3	6.599	2.337
TiO_2	0.284	0.100
Fe_2O_3	11.678	1.096
MnO	0.156	0.042
MgO	32.431	5.927
CaO	4.230	2.492
Na_2O	0.116	0.125
K_2O	0.040	0.027
P_2O_5	0.010	0.009

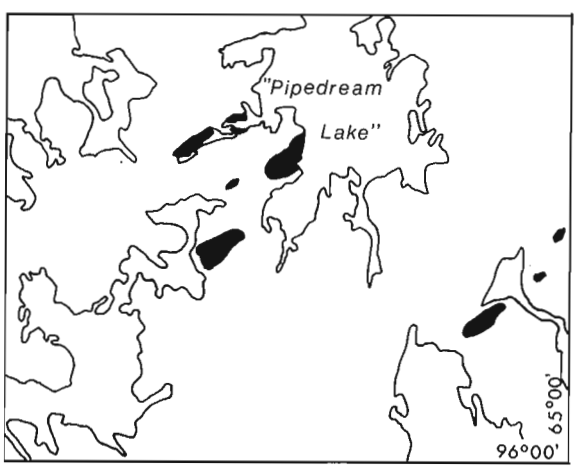

Figure 39.1. *A map showing the distribution of ultramafic rocks in the southeast corner of the Amer Lake map area. From data by Heywood (1977) and from field work by Heywood in 1976 and 1978, Ashton in 1980, and Annesley in 1980.*

[1] Department of Geology, University of Windsor, Windsor, Ontario, N9B 3P4

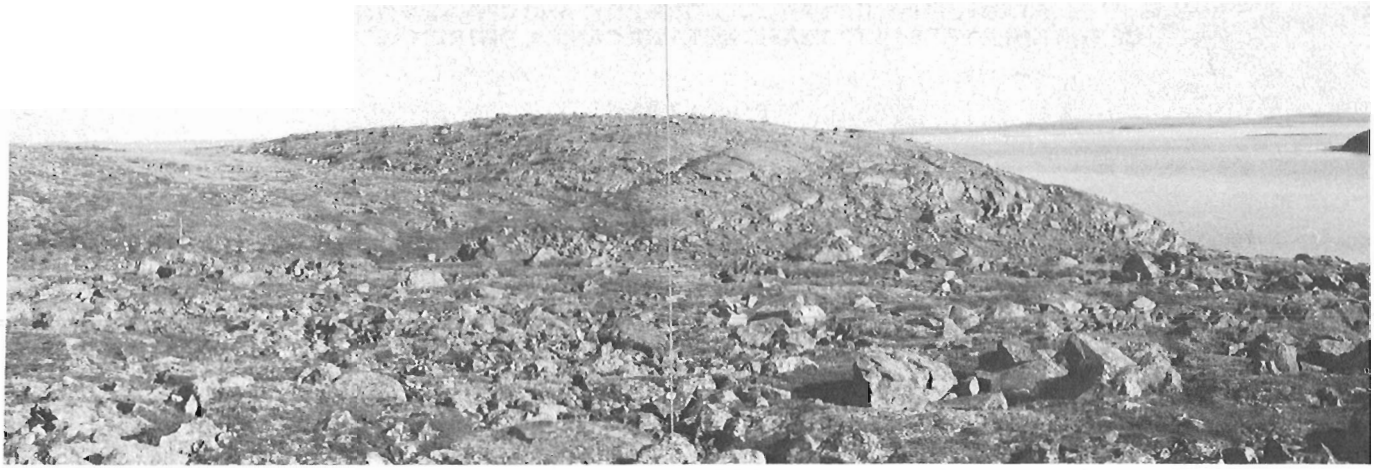

Figure 39.2. *View north of large outcrop of komatiites in predominantly spinifex-textured flows of southern belt. GSC 203652A and B*

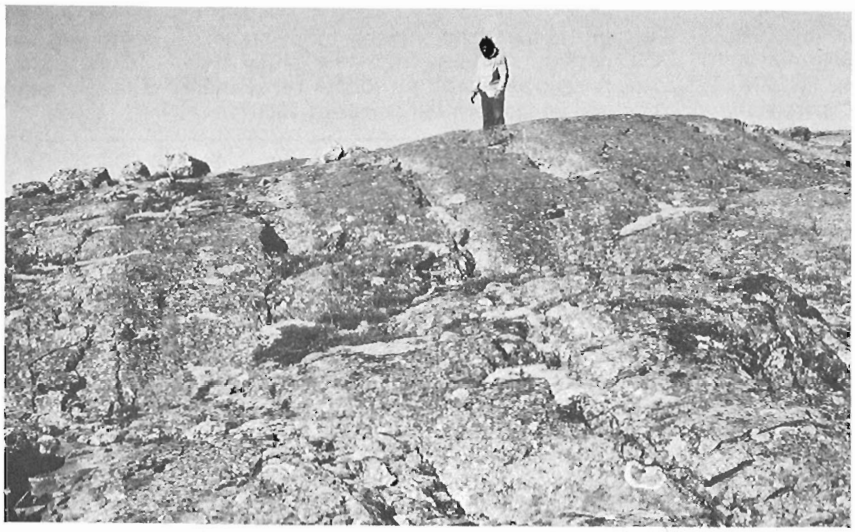

Figure 39.3. *Ultramafic flows of peridotitic komatiitic composition. Lighter coloured zones are cumulate layers and darker coloured zones are spinifex-textured layers. GSC 201634N*

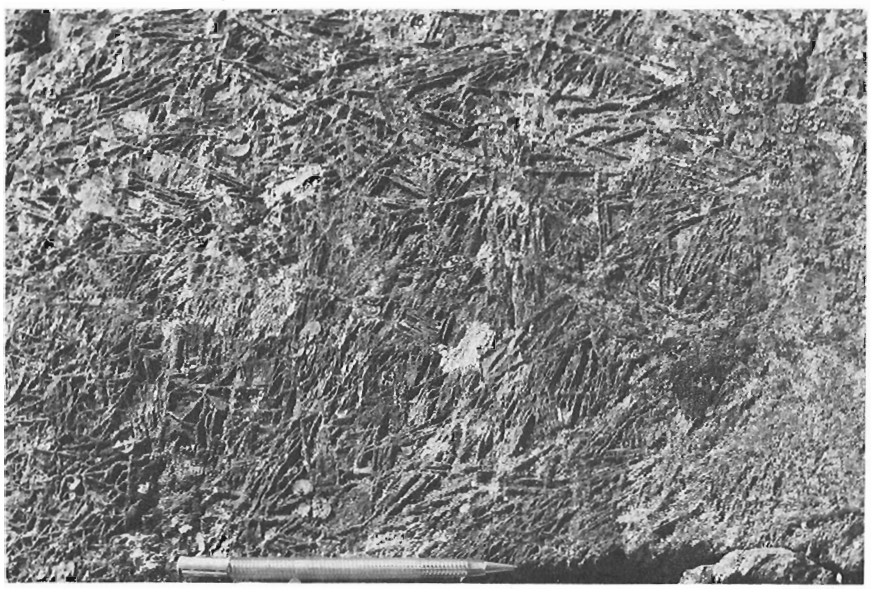

Figure 39.4. *Spinifex-textured komatiite. GSC 203652*

Field Characteristics

The Amer Lake ultramafics are best exposed in the southern belt (Fig. 39.2, 39.3) where they are associated with mafic metavolcanics (either tholeiites or mafic komatiites). The ultramafic rocks are predominantly extrusive (peridotitic komatiites) but local small sill-like outcrops of peridotite are present. No contacts were observed between the komatiites and the adjacent supracrustal rocks. The stratigraphic thickness of the steeply dipping flows is not known. In places massive and spinifex-textured flows are interlayered but the latter are most common. Individual flows range from less than 0.5 m to 10 m thick and are identified as flows by the following field criteria: flow top hyaloclastite and breccia, vesicular tops, distinct contacts between flows, spinifex textures and polyhedral jointing. The flows can be traced for as much as 300 m, but their full extent could not be determined. Both flow types show distinct development of polyhedral cooling joints, as much as 8 cm in diameter in the quenched flow tops.

The spinifex-textured flows consist of dull greenish grey weathering spinifex layers and reddish brown weathering cumulate layers. The proportion of spinifex layers to cumulate layers varies from flow to flow as well as laterally along the strike in individual flows. The contact between the spinifex-textured zone and the cumulate zone is distinct, sharp, and relatively planar. Spinifex blades are small in thin flows and large in thick flows (up to 50 cm long and 10 cm wide). The spinifex blades are commonly planar (Fig. 39.4) but some are curved. Most of the spinifex layers have finer grained tops although coarsening upward does occur. The grain size within a spinifex-textured flow generally increases downwards to the middle part of the cumulate zone and then decreases to the base which is commonly brecciated. Vesicular flow tops are preserved in some of the flows.

Massive flows are very fine grained to fine grained. They contain rounded or polyhedral shaped serpentinized olivine grains in an augite-glass matrix altered to chlorite and fibrous

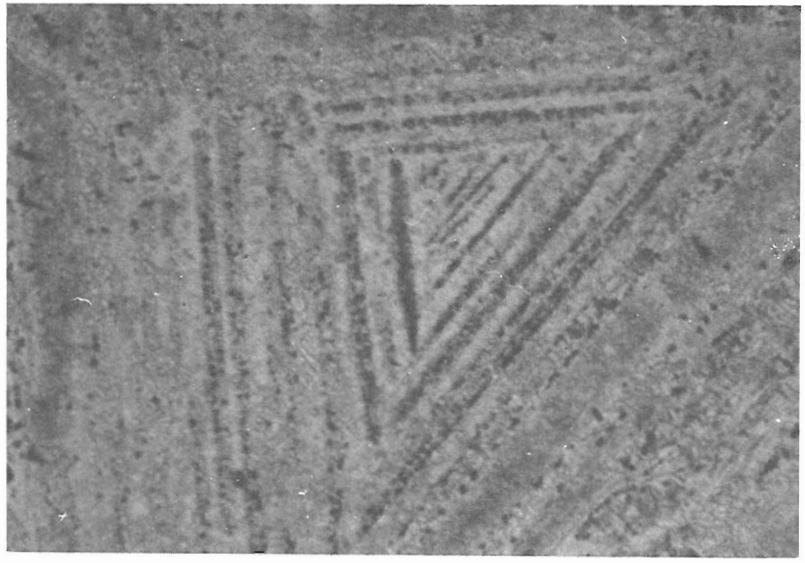

Figure 39.5. *Photomicrograph of the lower part of a spinifex-textured zone of peridotitic komatiitic flow. Blades and plates of pseudomorphic serpentine are set in a groundmass of chlorite, uralite, and opaque oxides (Plane Light – 25X).*

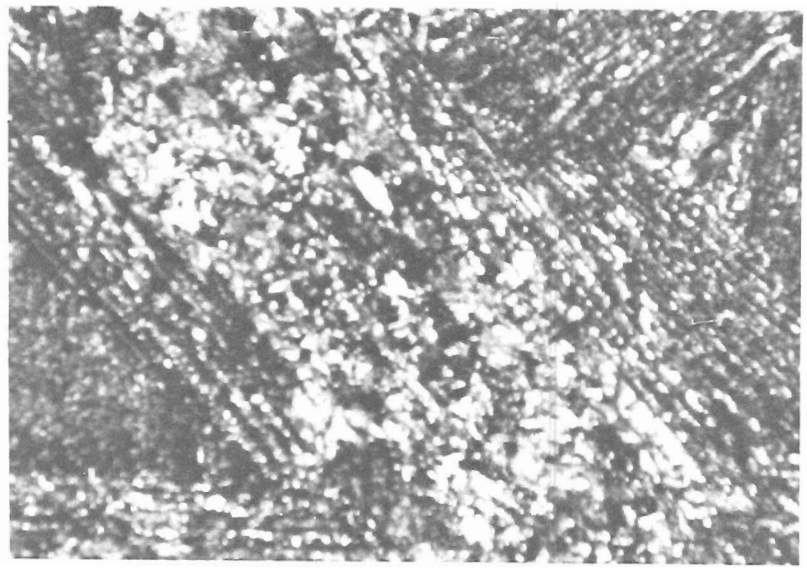

Figure 39.6. *Photomicrograph of the middle lower part of a pseudomorphed spinifex-textured zone of a peridotitic komatiitic flow (Plane Polarized Light – 25X).*

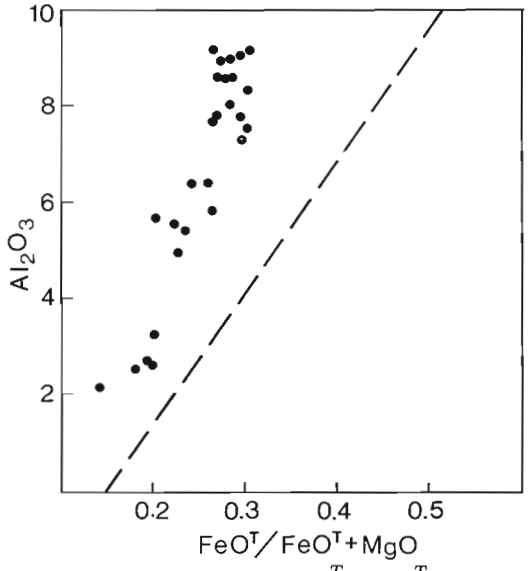

Figure 39.7. *Al_2O_3 vs. $FeO^T/(FeO^T + MgO)$ diagram from Arndt et al. (1977) which shows that the Amer Lake ultramafic rocks are komatiitic in composition.*

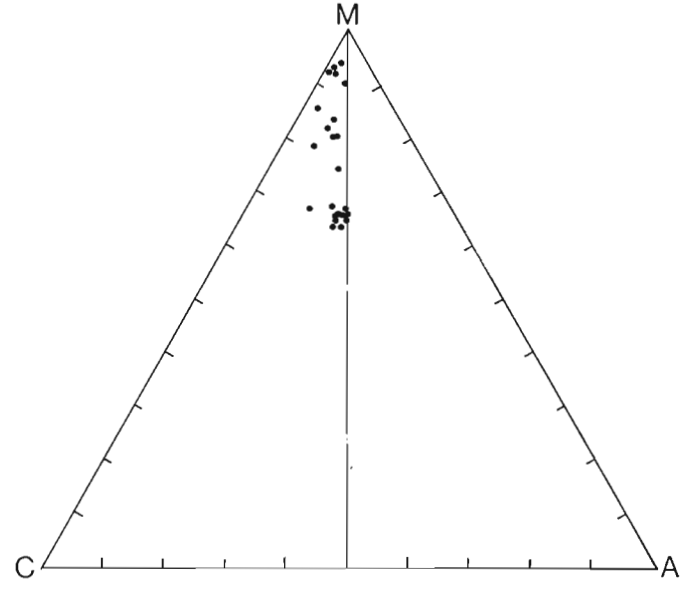

Figure 39.8. *AMC ternary diagram; C = CaO, M = MgO, and A = Al_2O_3. A continuous spread of MgO vs. CaO/Al_2O_3 is shown thus implying the importance of olivine fractionation in the formation of komatiites.*

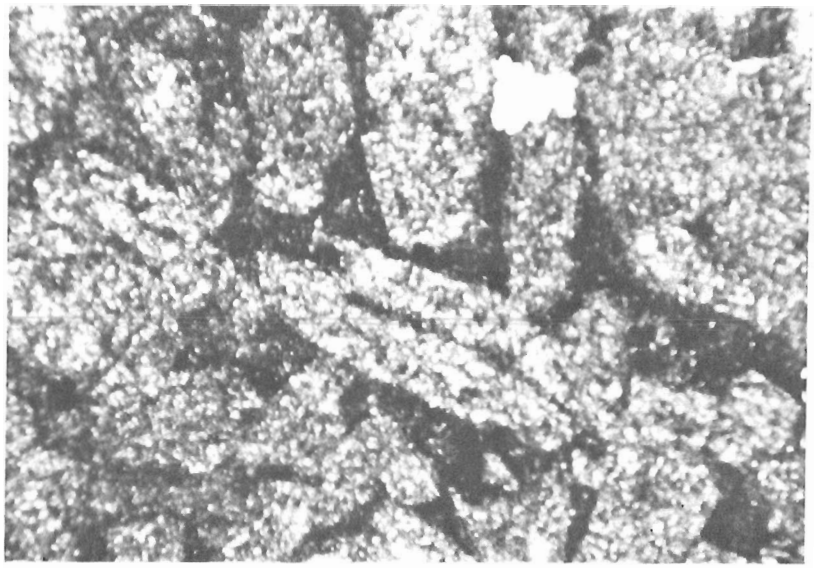

Figure 39.9. *Photomicrograph of the cumulate zone within a peridotitic komatiite. Solid serpentinized olivine grains are set in a chloritized and uralitized matrix of clinopyroxene and glass (PPL – 25X).*

amphiboles; a texture similar to the rubbly cumulate layers of spinifex-textured flows. An outstanding feature of these flows is the polyhedral jointing which is fine at the flow margins and coarse at the flow centre.

Petrography

The primary minerals of the spinifex-textured rocks are replaced by serpentine, tremolite, chlorite, and magnetite. Parallel to subparallel blades of primary olivine are pseudomorphed by serpentine (in places partly altered to chlorite and tremolite) and the groundmass is now composed of very fine grains of chlorite and fibrous amphibole (uralite) (Fig. 39.5, 39.6). Finely disseminated magnetite is present between the spinifex blades. The spinifex-textured layer grades sharply to the underlying cumulate layer. The equant primary olivine crystals of the cumulate layer have been pseudomorphed by serpentine and the groundmass clinopyroxene, chromite and glass has been hydrously altered to a fine grained felty matrix of chlorite, fibrous amphiboles, and magnetite (Fig. 39.9).

It is apparent from thin section examination that although grain sizes and the proportions of various minerals change greatly across individual flows, the mineral assemblages remain consistent.

Massive flows show a rubbly texture similar to that of the cumulate zones of the spinifex textured flows but contained less closely packed olivine grains. The olivine grains were coarser and more concentrated towards the centre and base of flows whereas the quench margins were depleted in olivine. As in the cumulate layers, primary olivine crystals are pseudomorphed by serpentine and the groundmass of clinopyroxene and glass are replaced by fine grained tremolite, chlorite, and magnetite.

Geochemical Results

Primary minerals are not preserved in the komatiites therefore whole rock analyses rather than mineral analyses were conducted. The results from the analyzed samples clearly show the Amer Lake rocks to be komatiites (Table 39.1). Calculations of the norm indicate a consistent mineral assemblage across individual flows and between flows, but mineral proportions are variable. The magnesian nature of the rocks with respect to Al_2O_3, CaO, and FeO^T is an important criterion in identifying komatiites and Figures 39.7 and 39.8 illustrate the komatiitic affinity of the Amer Lake rocks.

Conclusions

Field, textural, mineralogical, and chemical evidence suggest that the Amer Lake ultramafic rocks erupted as a family of lava flows and high level ultrabasic intrusions. The volume of lava was small but of widespread distribution. The komatiites present in the Amer Lake region are predominantly peridotitic and occur mainly as spinifex-textured flows. In general, the range of composition of these komatiitic rocks is not as variable as that of Munro Township (Arndt et al., 1977).

Acknowledgments

The author acknowledges the co-operation and assistance of W.W. Heywood, M. Schau and F.C. Taylor of the Geological Survey of Canada in providing samples and field support in 1978 and 1980. Special thanks are directed to T.E. Smith, University of Windsor, who has supervised the thesis and offered many constructive criticisms. W.W. Heywood and M. Schau critically read the manuscript; their comments are gratefully acknowledged.

References

Arndt, N.T., Francis, D., and Hynes, A.J.
1979: The field characteristics and petrology of Archean and Proterozoic komatiites; Canadian Mineralogist, v. 17, p. 147-163.

Arndt, N.T., Naldrett, A.J., and Pyke, D.R.
1977: Komatiitic and iron rich tholeiitic lavas of Munro Township, northeast Ontario; Journal of Petrology 18, p. 319-369.

Ashton, K.E.
1981: Preliminary Report on geological studies of the "Woodborn Lake Group" northwest of Tehek Lake, District of Keewatin, Northwest Territories; Geological Survey of Canada, Paper 81-1A, report 38.

Brooks, C. and Hart, S.R.
1974: On the significance of komatiite; Geology, v. 2, p. 107-110.

Heywood, W.W.
1977: Geology of the Amer Lake map area, District of Keewatin; in Report of Activities, Part A, Geological Survey of Canada, Paper 77-1A, p. 409-410.

Nesbitt, R.W., Sun, S.S., and Purvis, A.C.
1979: Komatiites: geochemistry and genesis; Canadian Mineralogist, v. 17, p. 165-186.

Schau, M.
1977: Komatiites and quartzites in the Archean Prince Albert Group. In Volcanic Regimes in Canada (W.R.A. Baragar, L.S. Coleman and J.M. Hall, eds.), Geological Association of Canada, Special Publication 16, p. 341-354.

Tella, S. and Heywood, W.W.
1978: The structural history of the Amer Mylonite Zone, Churchill Structural Province, District of Keewatin; in Report of Activities, Part C, Geological Survey of Canada, Paper 78-1C, p. 79-88.

Tippett, C.R. and Heywood, W.W.
1978: Stratigraphy and structure of the northern Amer Group (Aphebian), Churchill Structural Province, District of Keewatin, N.W.T.; in Report of Activities, Part B, Geological Survey of Canada, Paper 78-1B, p. 7-11.

Viljoen, M.J. and Viljoen, R.P.
1969a: Evidence for the existence of a mobile extrusive peridotitic magma from the Komati Formation of the Onverwacht Group, in Upper Mantle Project: Geological Society South Africa, Special Publication No. 2, p. 87-112.

1969b: The geology and geochemistry of the lower ultramafic unit of the Onverwacht Group and a proposed new class of igneous rock, in Upper Mantle Project: Geological Society of South Africa, Special Publication No. 2, p. 55-85.

Wright, G.M.
1967: Geology of the southern barren grounds, parts of the Districts of MacKenzie and Keewatin, N.W.T.; Geological Survey of Canada, Memoir 350.

40.

OCCURRENCE OF OLDHAMIA AND OTHER TRACE FOSSILS IN LOWER CAMBRIAN(?) ARGILLITES, NIDDERY LAKE MAP AREA, SELWYN MOUNTAINS, YUKON TERRITORY

Project 770044

H.J. Hofmann[1] and M.P. Cecile
Institute of Sedimentary and Petroleum Geology, Calgary

Hofmann, H.J. and Cecile, M.P., Occurrence of ***Oldhamia*** *and other trace fossils in Lower Cambrian(?) argillites, Niddery Lake map area, Selwyn Mountains, Yukon Territory; in Current Research, Part A, Geological Survey of Canada, Paper 81-1A, p. 281-290, 1981.*

Abstract

Oldhamia radiata*, together with* ***Oldhamia****? sp.,* ***Gordia****? sp.,* ***Planolites*** *sp., and unidentified large trails are reported from equivalents of the upper maroon shale of the Grit unit in east central Yukon. About 150 km southeast of these new fossil localities the maroon shale is directly overlain by debris flow deposits of Early Cambrian age. The maroon shale unit is correlated with Lower Cambrian* ***Oldhamia****-bearing beds in Alaska.*

Introduction

The age of certain clastic rocks underlying fossiliferous Cambrian sediments in the Selwyn Mountains (northeast Niddery Lake map area, 105 O) of southeastern Yukon is problematic. Gordey (1980) provisionally assigned strata underlying archaeocyathid-bearing, buff-weathering shale to the Hadrynian. These Hadrynian strata are informally referred to as the Grit unit and consist of a succession of interstratified siltstone, shale and sandstone (Gordey, 1980). At the top of the Grit unit Gordey recognized a distinct unit of maroon shale. An equivalent maroon argillite unit northwest of Gordey's study area has since yielded trace fossils which include **Oldhamia radiata,** characteristic of beds generally assigned to the Lower Cambrian, but possibly ranging from Late Hadrynian to Middle Cambrian (Fig. 40.2-40.4). We document this new occurrence to call attention to a characteristic trace fossil and its possible role in defining the Cambrian-Precambrian boundary, and the age of the upper Grit unit in the Selwyn basin.

Geological Setting

The new trace fossil occurrences are from strata associated with Hadrynian to Middle Paleozoic chert and argillite facies of the Selwyn basin located southwest of the Selwyn Valley in northeastern Niddery Lake map area (Fig. 40.2). Three localities have been discovered to date and are: N1 at 63°52'N, 130°58'W; N2 at 63°48'N, 130°50'W; and the best locality N3 at 63°47'N, 130°48'W (Fig. 40.4-40.5, Table 40.1).

These trace fossils all occur in approximately the same stratigraphic position about 50 m below the top of a distinct 100 m thick succession of maroon and apple green weathering argillites (H€ma Fig. 40.2, 40.3) tentatively correlated with Gordey's (1980) maroon shale (approximately 400 m thick) at the top of the Hadrynian Grit unit (Fig. 40.3). In the area of the fossil occurrences the maroon and green argillites are overlain by green and buff argillites (L€a, Fig. 40.2, 40.3) that can be mapped laterally northeast into a transitional argillite facies of the Lower Cambrian Sekwi Formation. This Sekwi transitional facies is a succession of green and buff argillites, black shale and grey platy limestone, and platy limestone breccia, with a prominent upper platy limestone unit, all of which underlie Lower Ordovician cherts and shales. This transition facies can be followed across the Selwyn Valley (Fig. 40.2) into a recognizable Sekwi Formation described by Fritz (1976, Sec. 6).

The maroon and green argillites (H€ma) of northeast Niddery Lake map-area are underlain by a 390 m thick succession of green and black argillites with thick units of buff or white weathering very coarse to pebbly quartz sandstone, and minor limestone and arenaceous limestone (H€g, Fig. 40.2, 40.3).

Paleontology

Oldhamia radiata Forbes, 1849

Fig. 40.4A-D, F

Description. Stellate to plumose patterns of small club-shaped ridges on bedding planes; patterns 1-2 cm across, composed of rectilinear to gently curving rays of generally subequal length, but slightly broadening distally, and ending in bluntly rounded termini; rays up to 10 mm long, 0.2-0.8 mm wide, very closely spaced, emanating from a common central burrow; individual stellate patterns often overlapping adjoining ones.

Remarks. The structures are indistinguishable from typical **O. radiata** from the Bray Group of southeastern Ireland (e.g. Sollas, 1900) and from specimens reported from Alaska (Churkin and Brabb, 1965). The genus **Oldhamia** is known from more than a dozen localities in Europe and North America, always in rocks now regarded as Late Hadrynian to Middle Cambrian, but mostly Early Cambrian (Fig. 40.1; Table 40.1). It is, therefore, a useful guide fossil for this time interval (Churkin and Brabb, 1965, p. D123); Häntzschel, 1975, p. W85; Crimes et al., 1977, p. 121). Following Ruedemann (1942a, p. 9), we regard **Oldhamia** as a radiating feeding structure made by a small worm-like organism.

Oldhamia? sp.

Fig. 40.4C, E

Description. Fragmentary specimens showing bundles of gently curving, radiating furrows along bedding plane of red and olive shale; furrows 2 mm wide, up to at least 3 cm long, terminating in bluntly rounded end; interspersed with **Oldhamia radiata.**

Remarks. The structures are much larger and more irregular than the associated **O. radiata,** but could be envisaged to have been made by unusually large individuals of the same species, if the abundant smaller structures are made by immature individuals. The larger structures, however, also resemble **Chondrites** and **Phycodes,** and they may possibly belong to one of these feeding burrows. Complete specimens will have to be found to resolve this problem.

[1] Department of Geology, University of Montreal, Montreal, Quebec, H3C 3J7

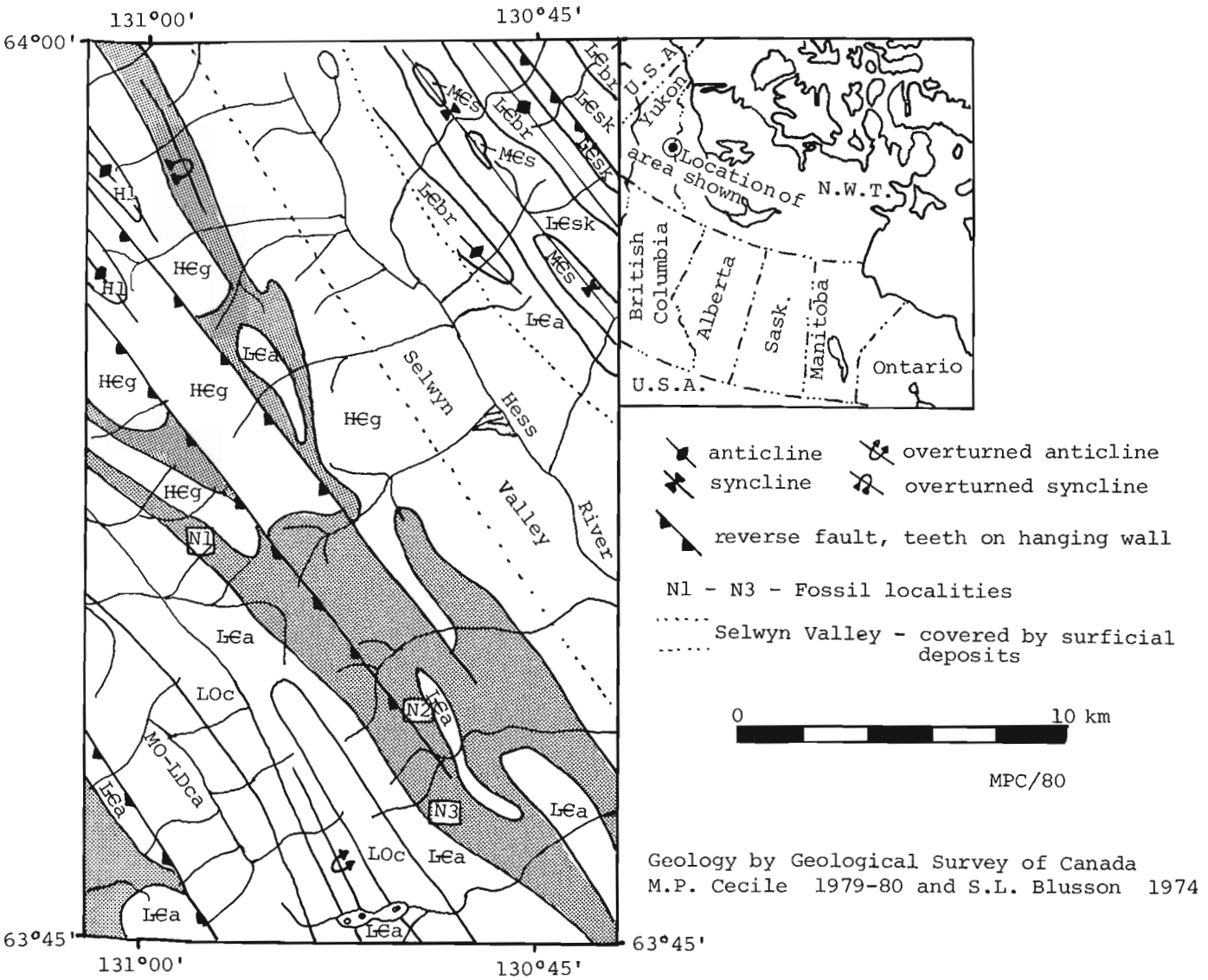

MO-LDca	Middle Ordovician to Lower Devonian black chert, shale and rusty green argillite
LOc	Lower Ordovician chert
Lea	Lower Cambrian, green argillite, black shale; minor platy limestone
Hema	Hadrynian to Cambrian maroon and apple green argillite; minor quartz sandstone
Heg	Hadrynian to Cambrian lower Grit unit - green and black argillite; minor quartz sandstone, pebbly quartz sandstone and limestone
Hl	Hadrynian arenaceous limestone and limestone

Mes	Middle Cambrian black shale; includes minor exposures of younger limestone
Lesk	Sekwi Fm. - platy limestone with units of black shale and orange siltstone
Lebr	Backbone Ranges Fm. - maroon and green quartzite

Figure 40.1. *Location and geological map. Heg, Hema, and Lea are extensively open to tightly shear-folded and LOc and MO-LDca units are extensively tight to isoclinally concentrically folded. Fold hinges in both types are spaced at intervals of only a few hundred metres.*

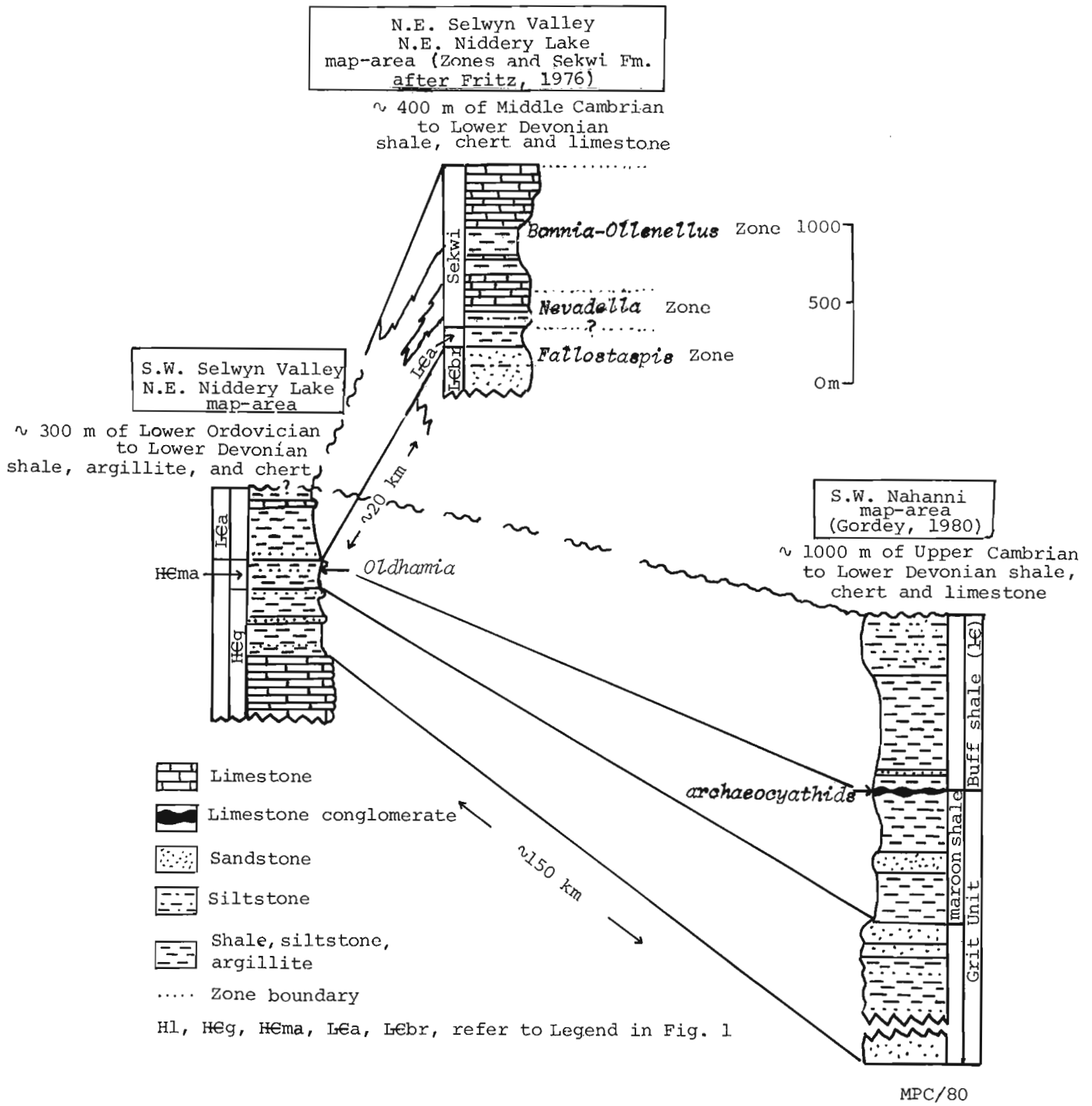

Figure 40.2. *Tentative lithostratigraphic correlation of map units in northeastern Niddery Lake map area and southwestern Nahanni map area. Sections are arranged as a fence but horizontal distances are not to scale.*

Gordia? sp.

Fig. 40.4B, G

Description. Unbranched, sinuous furrows of uniform width parallel to bedding, about 2 mm wide and several centimetres long, in places cutting across individuals of **O. radiata.**

Remarks. The structures are either trails assignable to **Gordia,** or they are impressions of **Planolites** burrows from the immediately overlying layer, now removed. Inasmuch as the overlying layer is now lost, the structures cannot be assigned with confidence.

Planolites sp.

Fig. 40.5A, B

Description. Gently curving, criss-crossing, subhorizontal and oblique cylindrical burrows, 1-7 mm wide, with elliptical cross-section (due to flattening?), sand-filled, occurring at the base of 1-2 cm thick, ripple-laminated sand layers that grade upward into maroon, parallel laminated siltstone and shale with **O. radiata.** Portions of some burrows show oblique, posteriorly directed, lobate irregularities suggesting backstoping by the burrowing animal.

Table 40.1

Tabular summary of selected data on **Oldhamia**

Occurrence	Taxon	Locality	Stratigraphic unit and age	Lithology	Selected references	Figured types
1	**Oldhamia** sp.	Vicinity of Mount Schwatka, Alaska	Lower Cambrian (originally reported as Mississippian)		Mertie 1937, p. 121, Plate 9A Churkin and Brabb 1965, p. D123	
2	**Oldhamia** sp.	Crazy Mountains, Alaska 65°43'N, 145°43'W	unnamed formation Lower Cambrian	interbedded mudstone and quartzite	Churkin and Brabb 1965, p. D123, Fig. 4	BP Exploration Co. (Alaska) Inc.
3	**Oldhamia** sp.	Kandik and Nation River area, Charley River quadrangle, Alaska a) 65°20.2'N 141°46.0'W b) 65°20.0'N 141°45.7'W c) 65°19.4'N 141°50.1'W d) 65°19.7'N 141°43.4'W	unnamed formation Lower Cambrian	thinly bedded and crosslaminated pale olive quartzose siltstone, and light olive grey silty argillite	Churkin and Brabb 1965, p. D120-121, Fig. 2	USNM 146373 USNM 146374
4	**Oldhamia** sp.	Nation River area, Alaska 65°13.4'N 141°37.0'W	unnamed formation Lower Cambrian	(same as for occurrence 3)	Churkin and Brabb 1965, p. D121	
5	**Oldhamia radiata** **Oldhamia**? sp.	Selwyn Mountains, Yukon N1-63°52'N 130°58'W N2-63°48'N 130°50'W N3-63°47'N 130°48'W	Grit Unit (here considered to be Lower Cambrian)	interbedded maroon and apple green argillite and fine grained greenish grey sandstone with ripple lamination	new (this paper)	GSC 64731 64732 64733 64734a 64735 64736
6	**Oldhamia occidens**	Rensselaer Co., N.Y. a) 42°43.7'N 73°38.8'W b) 42°34.2'N 73°33.6'W c) 42°33.3'N 73°34.6'W d) 42°31.5'N 73°36.2'W e) 42°31.0'N 73°35.6'W f) 42°33.0'N 73°41.8'W	Nassau Fm. Lower Cambrian or Hadrynian (below beds with Early Cambrian trilobites)	reddish and green shales, interbedded with quartzite	Walcott 1895, p. 314 Dale 1904, p. 13 Ruedemann 1929, p. 47 Ruedemann 1942a, p. 5	NYSM 33669
7	**Oldhamia antiqua**	Pearl Street, Weymouth, near Boston, Mass.	Weymouth Fm. Lower Cambrian	purple shales	Howell 1922, p. 198-199	
8	**Oldhamia smithi**	East branch of Penobscot River, Twp. 5 Rge. 8, Penobscot Co., Maine a) Bowlin Falls b) Grand Arch	Grand Pitch Fm. Late Precambrian to Early Ordovician	red slate	Smith 1928, p. 484 Ruedemann 1942a, p. 8; Fig. 1, pt. 3; Fig. 3, pt. 5 Neuman 1962, p. 794	USNM 139806 NYSM
9	**Oldhamia antiqua** **Oldhamia radiata**	Ireland a) Bray Head, County Wicklow b) Howth Head, Dublin area c) County Wexford	Bray Gp. Lower Cambrian	red and green shales interbedded with quartzose sandstone	Sollas 1900, p. 273-284 Dhonau and Holland 1974, p. 161	NMI G2:1969 NMI G4:1969 USNM 25003
10	**Oldhamia radiata**	Oisquerq, Brabant, Belgium 50°40'N 4°13'E	Oisquerq Beds (Devilien) Middle Cambrian	variegated green and purple shale	Waterlot 1956, p. 178	
11	**Oldhamia radiata**	Stavelot Massif, Ardennes, Belgium 50°23'N 5°56'E	Grand-Halleux Beds, Middle Cambrian	green and bluish-grey shale	Waterlot 1956, p. 164-172	
12	**Oldhamia radiata**	Rocroi Massif, Ardennes 49°46'N 4°30'E	Fumay Fm. (Devilien) Middle Cambrian	greenish and purple shale interbedded with light quartzite	Waterlot 1956, p. 167, 168	
13	**Oldhamia radiata**	Cabeza de Campo, west of Ponferrada, Leon, Spain	Vegadeo Limestone top of Lower Cambrian	shallow water sandy limestone	Crimes et al. 1977, p. 121	

Numerals refer to occurrences considered valid; letters refer to dubious occurrences, or occurrences reported as **Oldhamia** but now considered not to belong to this ichnogenus

Table 40.1 cont.

Occurrence	Taxon	Locality	Stratigraphic unit and age	Lithology	Selected references	Figured types
A	**Oldhamia** (not described or illustrated)	Wisconsin	Potsdam Ss. Upper Cambrian		Barrois 1888, p. 157 Sollas 1900, p. 274	
B	**Oldhamia? fruticosa** (not illustrated, nor described in detail; not **Oldhamia** according to Walcott 1895, p. 313)	Platteville, Wisconsin	Trenton Limestone Middle Ordovician	shaly beds	Hall 1965, p. 49-50, Walcott 1895, p. 313	
C	**Oldhamia** sp. (not described or illustrated)	near Farnham, Quebec	Sillery Gp. Cambrian	purple slates	Walcott 1895, p. 313 Smith 1928, p. 484	
D	**Oldhamia keithi** (appears to be mineralic pseudofossil resembling **Sewardiella**)	Méchins Point, Gaspé, Quebec	Lower Ordovician (with graptolites)	dark grey, calcareous shale	Ruedemann 1942b, p. 19	GSC 13603
E	**Oldhamia** sp. (fragment of 1 specimen, orientation unknown)	Catons Island, in St. John River, New Brunswick	St. John Gp. Lower Cambrian (associated with **Botsfordia pulchra**)	olive grey argillaceous sandstone	Matthew 1902, p. 231-232 Smith 1928, p. 484	
F	**Oldhamia** cf. **occidens** (=mechanical pseudofossils according to Ruedemann 1942a, p. 6-7; here considered probably **Oldhamia**)	Old Chatham area, Columbia County, N.Y. a) 42°26.5'N 73°33.7'W b) 42°27.2'N 73°33.3'W c) 42°29.0'N 73°31.8'W	Rensselaer Greywacke Lower Cambrian, or Hadrynian according to Fisher 1977, p. 13	in red and green shale interbedded with greywacke	Vaughan and Wilson 1934, p. 461-462 Ruedemann 1942a Fig. 1, pt. 7, Fig. 2, pts. 3, 4	NYSM
G	**Oldhamia** (chemical pseudofossils Hofmann 1971, p. 14)	near St. John's, Newfoundland	upper part of Conception Group Hadrynian	green slate	Hofmann 1971, p. 14 Pl. 4, fig. 10	
H	?**Oldhamia pedemontana** (specimens now kown to be bryozoans: **Hallopora**)	Empozada River, Las Heras, Mendoza Prov., Argentina	Empozadense Fm. Middle Ordovician	fossiliferous crystalline limestone	Rusconi 1956 Fritz 1965 p. 141	MHNM 19309 NHNM 19309a NHNM 19309b NHNM 87207
I	**Oldhamia** (no figures or descriptions)	Oslo Graben, Norway	'Blue Quartz' Middle Cambrian (associated with **Paradoxides**)	terrigenous sediments	Kjerulf 1880 **fide** Sollas 1900, p. 273, Dhonau and Holland 1974, p. 161	
J	**Oldhamia hovelacquei** (has features of **Chondrites**, according to Ruedemann 1942a, p. 10; assignment to **Oldhamia** is questionable; Häntzschel 1965, p. 63)	Ravine of Montmédan-Majou near Juravielle, Haute Garonne, France			Barrois 1888, p. 154 Ruedemann 1942a, p. 10	

Abbreviations: GSC Geological Survey of Canada; MHNM Museo de Historia Natural de Mendoza; NMI National Museum of Ireland; NYSM New York State Museum; USNM United States National Museum

Figure 40.3

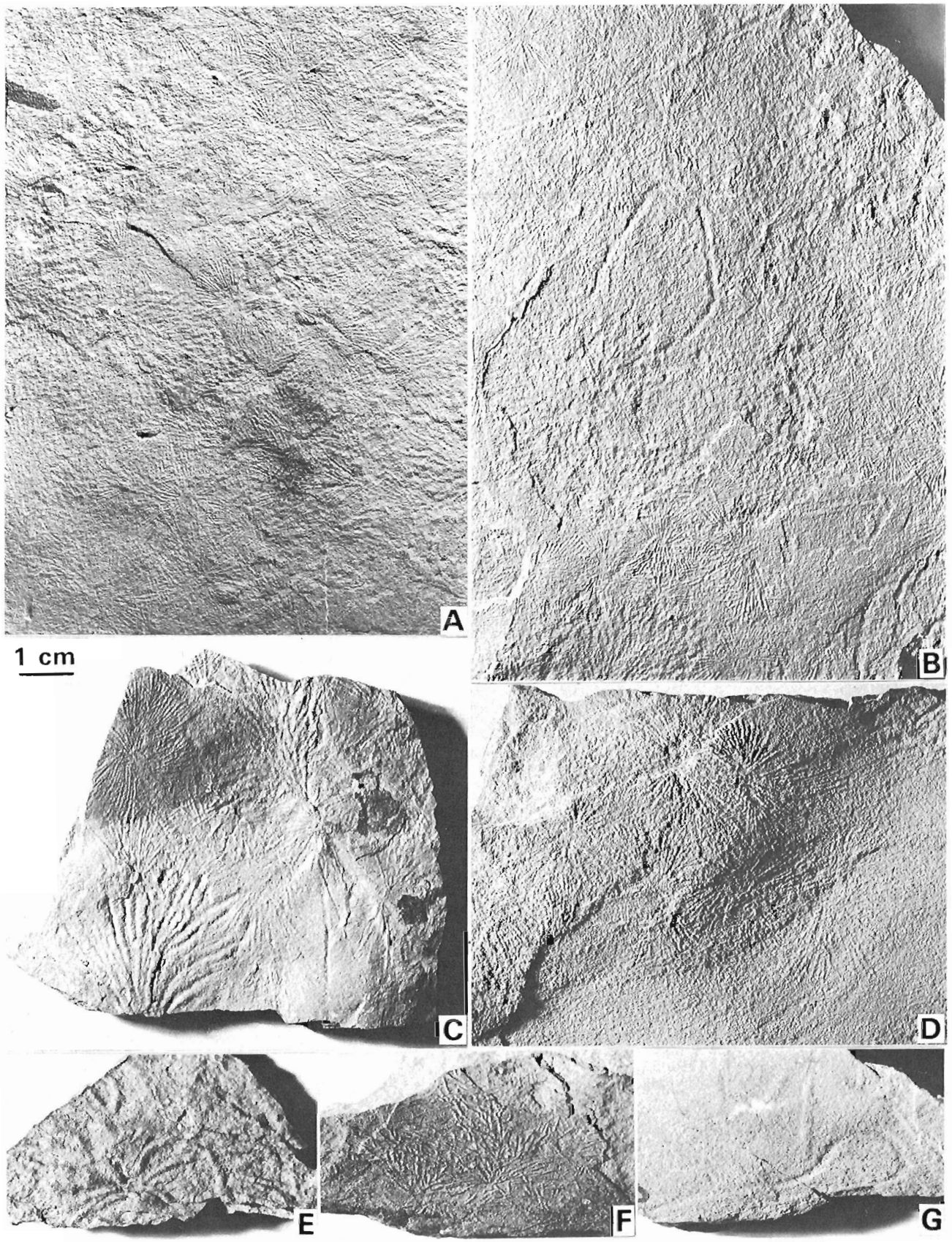

Figure 40.3

Trace fossils from the Lower Cambrian(?) Grit unit, Selwyn Mountains, Yukon. Same scale for all parts of figure.

A - ***Oldhamia radiata**; epirelief on maroon silty shale. Locality C-84632; GSC type 64731.*

B - ***Oldhamia radiata** and **Gordia**? sp.; epirelief on maroon siltstone. Locality C-84632; GSC type 64732.*

C - ***Oldhamia radiata** and **Oldhamia**? sp.; epirelief on red and olive siltstone. Locality C-84632. GSC type 64733.*

D - ***Oldhamia radiata**; epirelief on fine grained maroon sandstone; upper surface of specimen shown in Figure 40.5B. Locality C-84632; GSC type 64734a.*

E - ***Oldhamia**? sp.; epirelief on greenish grey siltstone. Locality C-89067; GSC type 64735.*

F - ***Oldhamia radiata**; epirelief on very fine grained greenish grey sandstone; structures are more irregular than those in parts A-D, and resemble the "**Ichnium Watsii**" variety of **Oldhamia** (see Sollas 1900, Pl. XVII, Fig. 1). Locality C-89067; GSC type 64736.*

G - ***Gordia**? sp.; epirelief on greenish grey siltstone. Locality C-89067; GSC type 64737.*

Remarks. The structures are probably due to worm-like animals. They appear to be larger and more robust than **Planolites** burrows generally found in the Precambrian, and similar to those in Cambrian and younger rocks.

Unidentified trails

Fig. 40.5C

Description. Simple criss-crossing traces parallel to bedding, 15-18 mm wide, 6-7 mm deep, more than 20 cm long, without distinct regular longitudinal or transverse ornamentation, but with irregular low humps of up to 1.5 mm relief along crestal surface of ridge that forms convex hyporelief; structures preserved by fine grained, cross-laminated sandstone, filling furrows made on surface of subjacent maroon mudstone.

Remarks. These relatively large structures superficially resemble **Palaeophycus**. However, they appear not to be cylindrical burrows, but surface trails, unless they were made as burrows which were subsequently truncated by erosion before the deposition of the succeeding bed. Cross-sections show the features to be depressions filled with cross-laminated fine grained sandstone that is part of the overlying layer. The lack of distinct longitudinal and transverse markings and the humpy nature of the relief suggest that the traces were made by animals not dragging a shell and without legs, perhaps primitive mollusks, or soft-bodied organisms. The irregular humps (depressions in the actual furrows) could be related to unsteady advance of the originators. Randomly located, millimetre-sized monticules on the casted trails are similar to those found beside the trails and are secondary burrows attributed to small **Planolites**-producing burrowers.

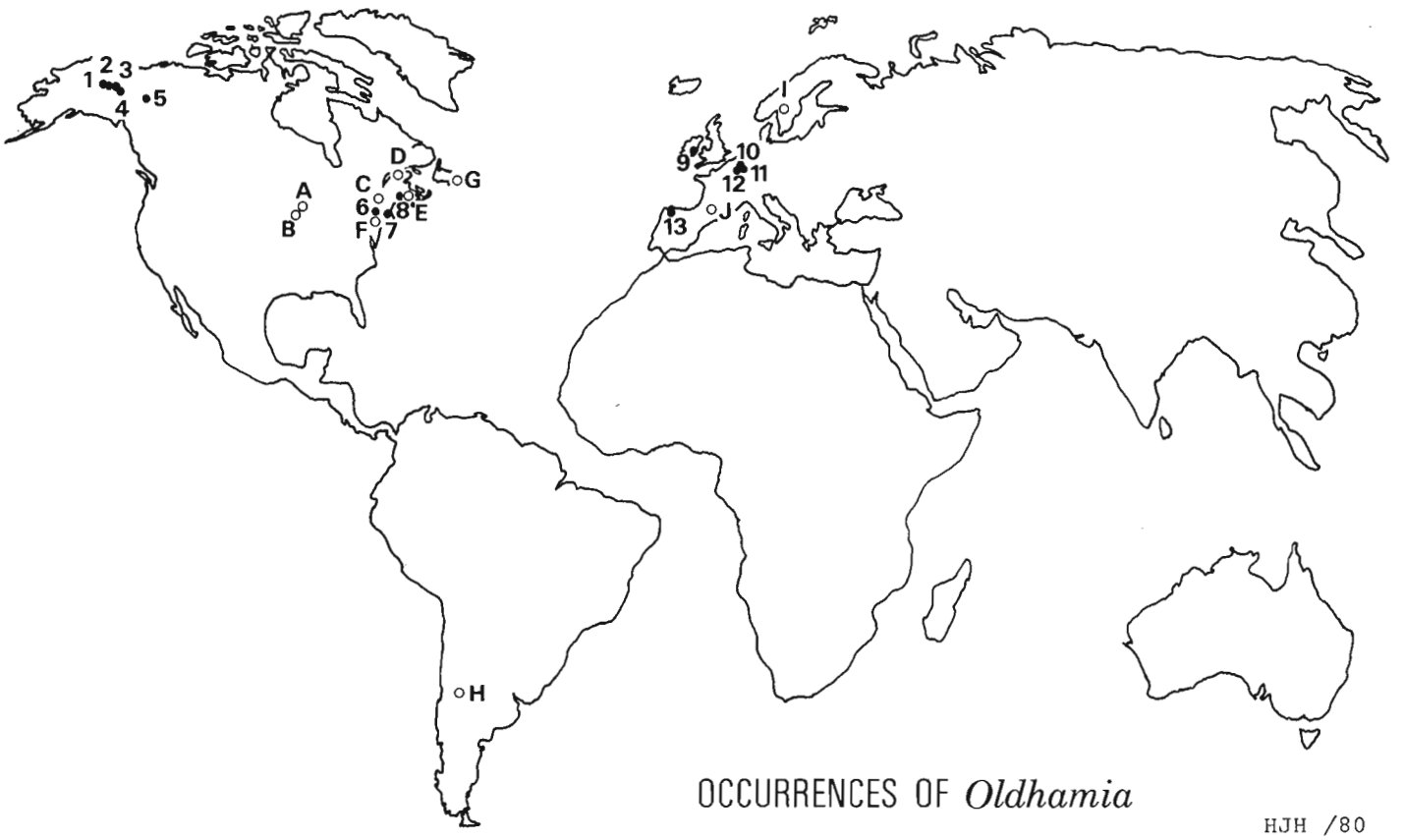

Figure 40.4. *World occurrences of **Oldhamia** (for details see Table 40.1). Numbered black dots refer to 13 occurrences considered valid; open circles identified by letters refer to another 10 occurrences reported as **Oldhamia**, but here considered as dubious, or as definitely not belonging to this ichnogenus.*

A - ***Planolites*** *sp.; hyporelief. Locality C-84632; GSC type 64738.*

B - ***Planolites*** *sp.; hyporelief; this is lower surface of specimen shown in Figure 3D. Locality C-84632; GSC type 64734b.*

C - *Unidentified trails and small* ***Planolites*** *sp.; hyporelief; reverse side of specimen bears* ***Oldhamia radiata****. Locality C-89076; GSC type 64739.*

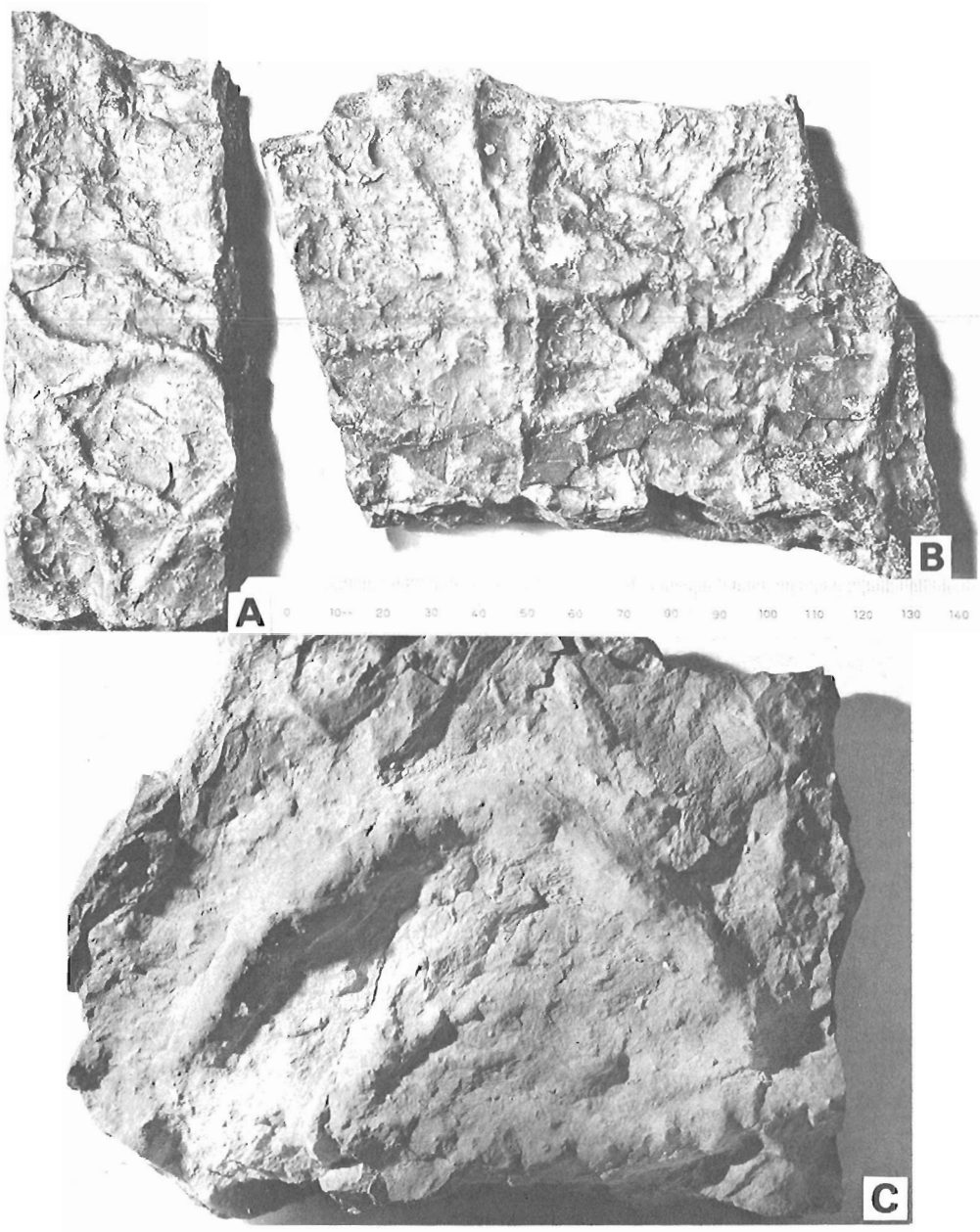

Figure 40.5. *Trace fossils from the Lower Cambrian(?) Grit unit, Selwyn Mountains, Yukon. Same scale for all parts of figure.*

Discussion

Although **Oldhamia** is considered to be a guide fossil to the Lower Cambrian, it is rarely found associated with other fossils that could date the containing beds independently. In some localities it occurs below beds with Early Cambrian shelly fossils. At several localities cited in Table 40.1, rocks are assigned to the Lower Cambrian solely on the presence of **Oldhamia;** others are dated indirectly on the basis of field relationships. In New York State the two units with **Oldhamia** (Rensselaer Greywacke and Nassau Formation) are now assigned to the Hadrynian (Fisher, 1977, p. 13), and some others could also be Precambrian. The ichnogenus **Oldhamia** thus assumes importance for the problem of the Precambrian-Cambrian boundary. It should receive more attention in view of its apparent occurrence on both sides of this boundary, and consequently its possible role in defining the base of the Cambrian. It has a distinctive morphology and is easily recognized in the field, making it a useful tool for the field geologists. The occurrences reported here are particularly significant considering that a tentative Cambrian/Precambrian boundary interval has recently been selected within a sub-Sekwi Formation map unit of quartzite, siltstone, shale and minor carbonate about 50 km east of the new N1-N3 occurrences (see Fritz, 1980).

On the basis of lithology, similar sequence, and the presence of **Oldhamia,** we here correlate the maroon shale at the top of the Grit unit with **Oldhamia**-bearing rocks in Alaska, which in turn are correlated with archaeocyathid-bearing Lower Cambrian beds (Churkin and Brabb, 1965, p. D122). Similar variegated clastic units in the Mackenzie Mountains to the east (e.g. Backbone Ranges Formation) should be examined with the aim of finding **Oldhamia** and other trace fossils.

The frequent occurrence of **Oldhamia** with maroon, red and purple fine grained clastic rocks, and the infrequent occurrence of this trace fossil with other fauna has led J.D. Aitken (personal communication, 1980) to speculate on their occurrence in a deep ocean environment. An environment with oxidizing conditions (open ocean circulation) and slow rates of precipitation, would allow full development of these fossil traces. We concur that the maroon and apple green argillites (HCma) are in succession with Early Paleozoic cherts, lack any features suggesting shallow water, and are thin bedded and graded.

Acknowledgments

We thank W.W. Nassichuk and J.D. Aitken for their critical reading and helpful comments.

M.P. Cecile would like to thank Rob Gibsun and Brian Fischer for the field assistance in 1979 and 1980. Rob's keen eye discovered the first **Oldhamia** in 1979. Hilde King patiently typed our final manuscript.

References

Barrois, C.
1888: Note sur l'existence du genre **Oldhamia** dans les Pyrénées; Annales de la Société geologique du Nord (Lille), v. 15, p. 154-157.

Churkin, M. Jr. and Brabb, E.E.
1965: Occurrence and stratigraphic significance of **Oldhamia**, a Cambrian trace fossil, in east-central Alaska; U.S. Geological Survey, Professional Paper 525-D, p. D120-D124.

Crimes, T.P., Legg, I., Marcos, A. and Arboleya, M.
1977: ?Late Precambrian-Lower Cambrian trace fossils from Spain; in Trace Fossils 2, T.P. Crimes and J.C. Harper (ed.), Geological Journal Special Issue No. 9, Seel House Press, Liverpool, p. 91-138.

Dale, T.N.
1904: Geology of the Hudson Valley between the Hoosic and the Kinderhook; U.S. Geological Survey, Bulletin 242, p. 13-14, 27, 28-29.

Dhonau, N.B. and Holland, C.H.
1974: The Cambrian of Ireland; in Cambrian of the British Isles, Norden, and Spitsbergen, C.H. Holland (ed.), John Wiley and Sons, New York, London, p. 157-176.

Fisher, D.W.
1977: Correlation of the Hadrynian, Cambrian and Ordovician rocks in New York State; New York State Museum, Map and Chart Series No. 25, 75 p.

Forbes, E.
1848-1850: On **Oldhamia**, a new genus of Silurian fossils; Journal of the Geological Society of Dublin, v. 4, p. 20.

Fritz, M.A.
1965: Bryozoan fauna from the Middle Ordovician of Mendoza, Argentina; Journal of Paleontology, v. 39, no. 1, p. 141-142.

Fritz, W.H.
1976: Ten stratigraphic sections from the Lower Cambrian Sekwi Formation, Mackenzie Mountains, northwestern Canada; Geological Survey of Canada, Paper 76-22.

1980: International Precambrian-Cambrian Boundary Working Groups' 1979 Field Study to Mackenzie Mountains, Northwest Territories, Canada; in Current Research, Part A, Geological Survey of Canada, Paper 80-1A, p. 41-45.

Gordey, S.P.
1980: Stratigraphic cross-section, Selwyn Basin to Mackenzie Platform, Nahanni map area, Yukon Territory and District of Mackenzie; in Current Research, Part A, Geological Survey of Canada, Paper 80-1A, p. 353-355.

Hall, J.
1865: Graptolites of the Quebec Group, Canadian Organic Remains, Decade II, 151 p. (49-50).

Häntzschel, W.
1965: Vestigia invertebratorum et Problematica; Fossilium Catalogus, 1: Animalia, pars 108, s'Gravenhage, Junk., 142 p.

Hantzschel, W. (cont.)
1975: Miscellanea; Supplement 1, Trace fossils and problematica, Treatise on Invertebrate Paleontology, Part W; Geological Society of America and University of Kansas, Boulder and Lawrence, 269 p.

Hofmann, H.J.
1971: Precambrian fossils, pseudofossils, and problematica in Canada; Geological Survey of Canada, Bulletin 189, 146 p.

Howell, B.F.
1922: **Oldhamia** in the Lower Cambrian of Massachusetts; (abst.), Geological Society of America, Bulletin, v. 33, p. 198-199.

Kjerulf, Th.
1880: Die Geologie des südlichen und mittleren Norwegen; A. Gurlt, Bonn, p. 66, 133, 195-196.

Matthew, G.F.
1902: **Oldhamia**; Canadian Record of Science, v. 8, p. 228-232.

Mertie, J.B. Jr.
1937: The Yukon-Tanana region, Alaska; U.S. Geological Survey, Bulletin 872, 276 p.

Neuman, R.B.
1962: The Grand Pitch Formation: new name for the Grand Falls Formation (Cambrian?) in northeastern Maine; American Journal of Science, v. 260, p. 794-797.

Ruedemann, R.
1929: Note on **Oldhamia (Murchisonites) occidens** (Walcott); New York State Museum, Bulletin 281, p. 47-50.

1942a: **Oldhamia** and the Rensselaer Grit problem; New York State Museum, Bulletin 327, p. 5-17.

1942b: Cambrian and Ordovician fossils; New York State Museum, Bulletin 327, p. 19-32.

Rusconi, C.
1956: Oldhamias Ordovicicas de Mendoza; Revista del Museo de Historia Natural (Mendoza), v. 9 – Entragas 1-2, p. 47-53.

Smith, E.S.C.
1928: The Cambrian in northern Maine; American Journal of Science, v. 215, p. 484-486.

Sollas, W.J.
1900: Fossils in the Oxford University Museum, – III. **Ichnium Wattsii**, a worm-like track from the slates of Bray Head: with observations on the genus **Oldhamia**; Geological Society of London, Quarterly Journal, v. 56, p. 273-286.

Vaughan, H. and Wilson, T.Y.
1934: The age of the Rensselaer Graywacke; American Journal of Science, v. 227, p. 460-462.

Walcott, C.D.
1895: Discovery of the genus **Oldhamia** in America; U.S. National Museum, Proceedings, v. 17, p. 313-315.

Waterlot, G.
1956: Le Cambrien de l'Ardenne; in El Sistema Cámbrico, su paleogeografía y el problema de su base, J. Rodgers (ed.), International Geological Congress, 20th Session, Mexico, Symposium, Part 1, p. 161-183.

41.

PRELIMINARY NOTES ON THE GEOLOGY EAST OF GEORGIAN BAY, GRENVILLE STRUCTURAL PROVINCE, ONTARIO

Project 760061

A. Davidson and W.C. Morgan
Precambrian Geology Division

Davidson, A. and Morgan, W.C., Preliminary notes on the geology east of Georgian Bay, Grenville Structural Province, Ontario; in Current Research, Part A, Geological Survey of Canada, Paper 81-1A, p. 291-298, 1980.

Abstract

Reconnaissance mapping was initiated in 1980 in a 24 000 km² area east of Georgian Bay in a previously poorly mapped part of the Central Gneiss Belt, Grenville Province of Ontario. Three previously unreported anorthositic bodies were discovered, and the region was found to be divisible into several domains on the basis of structure and lithology. Several zones of blastomylonite and tectonite gneiss were identified; their significance with respect to development of a thick crust during orogeny is discussed.

Introduction

Much attention has been given to certain restricted aspects of Grenville Province geology for many years. A search of the geological literature pertaining to the Grenville of Ontario and western Quebec reveals that effort has been most concentrated on features and problems associated with either the Grenville Front or the Central Metasedimentary Belt (Wynne-Edwards, 1972). This is hardly surprising when one considers the exceptional and interest-arousing nature of the geology in these two separate regions – the one containing a zone of marked change where east-trending Archean and lower Aphebian (Huronian) rocks abut against northeast-trending, commonly cataclastic Grenville gneiss, and the other displaying features such as recognizable sedimentary and volcanic rocks at low metamorphic grade, rapid metamorphic grade changes, well-exposed complex structures, many small and varied plutonic bodies, unusual alkaline rocks, and numerous if small mineral deposits, to name a few. In contrast, the intervening region, part of the Central Gneiss Belt (Wynne-Edwards, 1972; Davidson et al., 1979, Fig. 19.1), has been considered by many to be, for the most part, an intractable "sea of gneiss", monotonous and at fairly uniform high metamorphic grade, of far less rewarding prospect for study, and certainly of little economic interest.

Most of the Quebec segment of the Central Gneiss Belt has been mapped at scales suitable for compilation at 1:250 000 scale, but parts of the Ontario segment have never been systematically mapped, despite relative ease of access and, in the coastal region of Georgian Bay, superb rock exposure; only compilation maps at very small scale are available (Baer et al., 1977; Freeman, 1978; Lumbers, 1980). Therefore, as a precursor to attempting to make a geological synthesis of the whole southwest part of the exposed Grenville Province, a reconnaissance mapping program was initiated last season in that part of Ontario (shaded in Fig. 41.1) south of latitude 46°N and northwest of the Central Metasedimentary Belt. Also indicated in Figure 41.1 are areas that have been mapped adjacent to and within this region. Apart from recently completed mapping in Renfrew County (Lumbers, 1980), other maps within the region need re-evaluation for various reasons, in particular because they do not have comparable map legends either among themselves or with that developed in adjacent map areas.

Field work in 1980 was carried out in two phases: reconnaissance mapping by helicopter for the first six weeks, and more detailed ground-based work for the rest of the season. Beginning in mid-April, helicopter traversing enabled aerial observations of rocks and structures to be made throughout this 24 000 km² area during the short period between the disappearance of winter's snow and leaf-out of deciduous vegetation. Over 750 landings for sampling and measurement were made during this time, mainly in otherwise inaccessible places. Groundwork began in June and was confined to that part of the area west of Ontario highway 11. W.C. Morgan was associated with the project during the helicopter mapping phase; able assistance was provided by A. Leclair, A. Moravec and N. Fraser during the remainder of the season. The authors are particularly grateful for the many courtesies extended by the managing staff at Parry Sound, Pembroke, Bancroft and South River air fields, and by Ontario Ministry of Natural Resources personnel at Huntsville, Parry Sound and Grundy Lake Provincial Park.

Subdivision of the Ontario Segment, Central Gneiss Belt

Examination of structural trends compiled from airphotos, satellite imagery, aeromagnetic maps and what little published information is available reveals that the Central Gneiss Belt is far from being a uniform structural entity. The initial helicopter traversing served to enhance this impression by allowing recognition that certain rock assemblages are associated with particular structural domains, tentatively outlined in Figure 41.2. Although the combinations of characteristics that set apart one domain from another are quite apparent in the field, it is not necessarily clear where boundaries between them should be placed. Ill-defined boundaries, dotted in Figure 41.2, appear to be zones of gradual change; subsequent work, however, may identify specific criteria that can be used for more definite delineation. Well defined boundaries are shown in Figure 41.2 as dashed lines. The domains and features of their mutual boundaries are characterized in a simplified way below.

Britt Domain

The Britt Domain is underlain by highly deformed ortho- and paragneiss, cut by a suite of younger granitoid plutonic rocks, and subsequently has been deformed and metamorphosed again. Dominant structural grain in a zone 30 km wide parallel to the coast of Georgian Bay is northwesterly, and is due to late major folds that become more open northeastward. Within Britt domain are a number of tracts of highly leucocratic, pink, fine grained, sugary textured quartzofeldspathic gneiss with variably developed layering. Rare, thin but locally continuous interlayers of impure quartzite, muscovite-sillimanite quartzofeldspathic gneiss and epidote-hornblende feldspathic gneiss poor in quartz attest to a sedimentary origin, and the leucocratic quartz-feldspar gneiss is best interpreted as having been

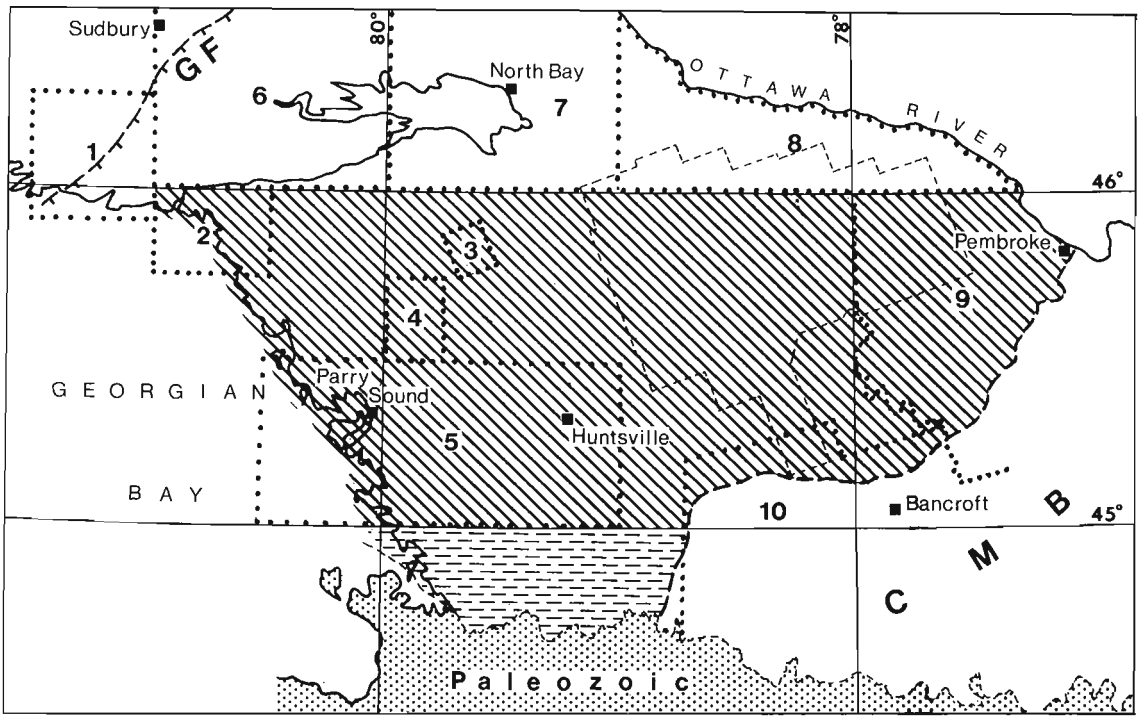

Figure 41.1. *Status of geological mapping between the Grenville Front (GF) and the Central Metasedimentary Belt (CMB) in the Grenville Province of Ontario. Current study area for this project is ruled diagonally; dash pattern shows area under study by the Department of Geology, University of Toronto, under contract. Existing maps are numbered: 1 – Quirke and Collins, 1930; Frarey and Cannon, 1969; 2 – Quirke, 1930; 3 – Satterly, 1955; 4 – Lacy, 1960; 5 – Hewitt, 1967; 6, 7, 8, 9 – Lumbers, 1975, 1971, 1976, 1980; 10 – Ontario Department of Mines, 1957 (compilation). Algonquin Provincial Park is outlined.*

arkose, a conclusion reached by Lumbers (1975) for the area immediately to the north. Some tracts of 'meta-arkose', however, are so weakly layered, if at all, and so uniform in composition that one's first impulse is to map them as leucogranite orthogneiss, implying plutonic parentage. Despite the facts that relict igneous textures are absent, that modal analyses show from 35 to 50 per cent quartz content and colour indices less than 2, and that contacts with well-layered gneiss of undoubted supracrustal origin are gradational, the problem of interpretation of parentage is a very real one, especially where a leucosome has developed. The problem is even more acute for certain tracts of grey, monotonous, partly migmatitic hornblende-biotite gneiss. On the other hand, the younger plutonic suite, despite the fact that its plutons have been, for the most part, moderately to severely flattened and folded (Fig. 41.3), is readily distinguished from its country rock envelope, and contacts can usually be mapped with confidence. Primary features are remarkably well-preserved in a few structurally sheltered places (Plate 41.1, fig. A). Where such places are at or close to a contact, the country rock can be observed to have been migmatitic gneiss prior to intrusion. The extent to which some of these plutons have been flattened, however, is just as remarkable as the state of preservation of the non-deformed parts. For example, a single sheet-like unit of distinctive, grey hornblende-biotite granitoid orthogneiss with augen or lenticles of granular, pink K-feldspar can be traced for 30 km along the northeast limb of the antiform mapped among the shoals and islands along the coast of Georgian Bay west of Britt (shown as a dashed lined in Fig. 41.3), yet does not exceed 750 m in thickness. The internal homogeneity of these plutons (not considering the varied degree of migmatization) and the fact that the type of country rocks varies along contacts suggest that these plutons were originally discordant, although now structurally concordant at any one place. Where preserved, sharp contacts, lack of contact migmatite or veining of the wall rock, and marginal zones of both cognate and country rock xenoliths are more suggestive of a high level of crustal emplacement than of deep-seated plutonism.

Metamorphic grade within Britt domain ranges from middle through upper amphibolite facies (sillimanite – K-feldspar). Hypersthene-bearing orthogneiss occurs along highway 522 some 25 km west of Arnstein (Fig. 41.3).

The boundary between Britt domain and the Grenville Front Tectonic Zone is one of structural deflection to northeast trend, characterized closer to the Grenville Front itself by zones of superimposed cataclasis (Lumbers, 1978a). The boundary with Parry Sound domain is a relatively abrupt change in lithology, from predominantly quartzofeldspathic gneiss and migmatite to predominantly mafic gneiss. The boundary itself has been placed at the east side of a narrow but notably continuous belt of deformed granitoid orthogneiss whose foliation dips moderately beneath the layered gneiss of Parry Sound domain. Structurally below these granitoid lenses, foliation and layering become shallower and less regular in trend.

Parry Sound Domain

A preponderance of relatively mafic rocks characterizes Parry Sound domain, although in detail rock types and assemblages are asymmetrically distributed. In Figure 41.2 a dotted line has been drawn between a western zone of well-layered and continuously north- to northeast-trending supracrustal gneiss in amphibolite facies, enclosing sharply defined bodies of gabbroic anorthosite, and an eastern zone of less

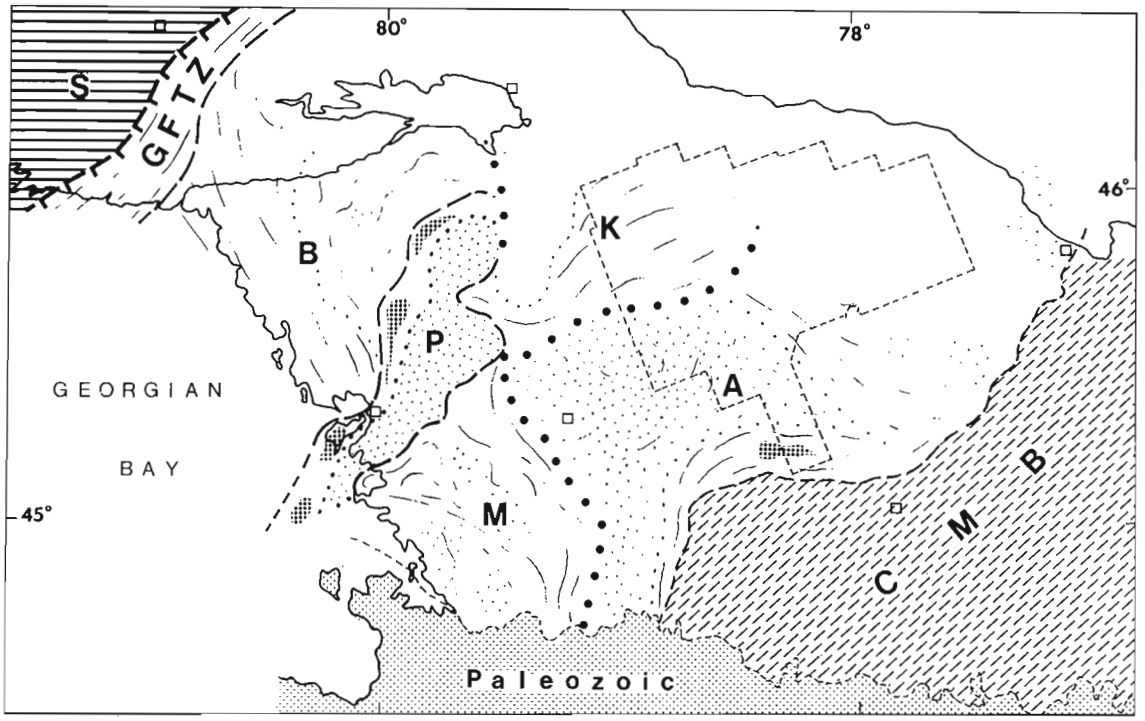

Figure 41.2. Tentative subdivision, southwest part of the Ontario Gneiss Segment, Central Gneiss Belt. B – Britt, P– Parry Sound, M – Muskoka, K – Kiosk, A – Algonquin domains; S – Southern Province, GFTZ – Grenville Front Tectonic Zone, CMB – Central Metasedimentary Belt. Dominant regional trends, areas of granulite facies (stipple) and main bodies of gabbroic anorthosite (close dot pattern) are shown.

regularly trending gneiss, including marble, at granulite facies that encloses bodies of hypersthene diorite, enderbite and charnockite whose contacts are commonly nebulous. If the nature of the contact between these two zones, described and discussed below, can be shown to be a continuous and fundamental structural feature, then separate domain status may be warranted.

Lying structurally above the granitoid orthogneiss belt that marks the west boundary of Parry Sound domain, well-layered gneiss has a grossly continuous stratigraphy, at least in the southern half of the western subdomain, namely: hornblende and/or biotite quartzofeldspathic gneiss, in places with 'meta-arkose' and quartzite layers close to the 'base'; darker gneiss, usually hornblende-bearing with or without red garnet, and enclosing zones of pelitic gneiss characterized by kyanite, muscovite and pink-violet garnet; hornblende gneiss and amphibolite with rusty-weathering pyritic gneiss, scattered pelitic gneiss, and rare lenses of marble and quartzite, the latter accompanied by lean iron formation. Within the lowest unit, metaconglomerate has been identified positively at one locality (Plate 41.1, fig. B), tentatively at two other places along the same zone. Four major bodies of gabbroic anorthosite lie within the hornblende gneiss and amphibolite zone (Fig. 41.3). The northernmost body, near Arnstein, and the southernmost, in the Western Islands, have not been described before. The other two, the Whitestone and Parry Island 'anorthosites', respectively north and southwest of Parry Sound, have been known for some time (Walker, 1913; Satterly, 1943; Lacy, 1960), and the Whitestone body has been studied extensively (Mason, 1969). In addition to these, a narrow conformable anorthositic layer intersected by highway 69, 1.5 km north of its junction with highway 124 has been traced 4 km southwest to the shore of Parry Sound and 20 km to the north; its width does not exceed 400 m. Another narrow anorthosite body is exposed among the islands west of the Parry Island body; it pinches out northeastward, but small anorthosite lenses, apparently tectonic slivers, occur along its projected strike line. The 'tail' of the Whitestone body has now been traced continuously southward for 26 km, linking it directly with previously reported anorthositic gabro occurrences at Mill Lake and Five Mile Bay (Hewitt, 1967). The preservation of primary features in these anorthositic bodies is highly variable. Primary igneous texture and, locally, structure are recognizable in the Whitestone body (Mason, 1969), but most of the Parry Island and Arnstein bodies are thoroughly deformed and recrystallized. Folds in the foliation of the derived anorthositic orthogneiss are cut by mafic dykes, themselves boudinaged and recrystallized. The narrow bodies and 'tails' of the larger bodies are even more highly deformed, commonly displaying an internal, mesoscopic lenticular structure in which lenses with deformed relict igneous texture are separated by intensely streaked-out and comminuted anorthositic material. This structure appears to be the advanced equivalent of the 'block structure' found in the Whitestone body (Mason, 1969) and also in other Grenville anorthosites (Mawdsley, 1927; Balk, 1931).

East of the line of gabbroic anorthosite bodies, Parry Sound domain is underlain by a very complex mixture of mafic, intermediate and feldspathic gneiss with some marble and minor pelitic units, and hypersthene-bearing plutonic rocks. The whole of this eastern zone is in granulite facies, or has retrograded from it. The rocks are characteristically granular and fine grained. Mineral assemblages in supracrustal rocks indicative of high metamorphic rank are: in mafic gneiss, hypersthene + augite + almandine + ilmenite + antiperthite ± hornblende ± quartz; in pelitic gneiss, quartz + perthite + hypersthene + almandine + sillimanite ± biotite; in marble, diopside + grossularite + wollastonite ± plagioclase + either calcite or quartz. Several of the thin

sections so far examined show that cataclastic granulation has followed formation of hypersthene and antiperthite, and has been accompanied or followed by growth of minerals indicative of amphibolite facies. In the field, fresh plagioclase-rich rocks with hypersthene are usually some shade of olive colour, but where retrograde are grey with a distinct bluish cast.

In a narrow zone that to date has been traced approximately 10 km north-northeast and 20 km southwest of Parry Sound (Fig. 41.3), well-layered, fine grained, grey gneiss is found within or at the eastern margin of the 'tail' of the Whitestone gabbroic anorthosite (Plate 41.1, fig. C). It is characterized by scattered feldspar ovoids up to 4 cm in diameter and by smaller megacrysts of garnet and hornblende. Feldspar ovoids commonly show sigmoidal structure (Plate 41.1, fig. D) and are connected by thin seams of granulated feldspar. In the Parry Sound vicinity, this gneiss can be demonstrated conclusively to have been derived from anorthositic gabbro by intense cataclasis. Subangular to rounded and locally spindle-shaped clasts of the parent rock, some of them several metres across, are found within this gneiss. Complete disaggregation of coarse pegmatite dykes, which crosscut the adjacent anorthositic gabbro, appears to have been the mechanism whereby the feldspar ovoids developed. Partial disaggregation (Plate 41.1, fig. E) is locally common throughout the map area. The fine grained grey gneiss has many hallmarks of mylonite, but is in fact blastomylonite; thin sections reveal it to have completely recrystallized, eliminating all evidence of former strain in mineral grains and producing granoblastic assemblages of plagioclase, hornblende, garnet and biotite, and locally with K-feldspar, quartz, and epidote, all indicative of amphibolite facies conditions for recrystallization. This zone of mylonitization is many tens of metres thick and dips moderately beneath the granulite facies rocks of the eastern subdomain. It may thus be the locus of relatively deep crustal thrusting whereby granulite facies rocks have moved northwesterly up and over the amphibolite facies rocks to the west and northwest. It remains to be seen if this zone can be traced northward and continues to separate the two subdomains of Parry Sound domain.

At the southeast side of Parry Sound domain, granulite facies rocks are structurally overlain by coarser grained, more leucocratic, commonly migmatitic, amphibolite facies gneiss of Muskoka domain. An important feature along part, if not all, of this boundary is the occurrence of highly tectonized rock that contains blocks, slivers and isolated boudins in a gneiss matrix. Several hundred metres thick, this 'tectonoclastic' gneiss is conformable and gradational with structurally overlying gneiss and, in a gross sense, is unconformable with trends in Parry Sound domain. Figure F of Plate 41.1 illustrates the age relationships quite clearly; Parry Sound domain gneiss with granulite facies minerals is enclosed in tectonite gneiss recrystallized at amphibolite facies. Does this mean that there is another deep crustal dislocation zone along the southeast side of Parry Sound domain, and is it too the site of northwest directed thrusting?

Farther north, the boundary with Kiosk domain is chiefly against a large metaplutonic massif, the southward extension of the Powassan batholith (Lumbers, 1971), except that south of this massif, amphibolite facies gneiss, the Ahmic gneiss of Lacy (1960), forms an antiform that plunges westward beneath mafic granulite gneiss and marble of Parry Sound domain.

Muskoka Domain

Muskoka domain extends from the southeast side of Parry Sound domain southeastward to the edge of the exposed Shield, and is bounded to the east by Algonquin domain. It is characterized by parallel, northwest-trending belts of relatively straight-layered gneiss in amphibolite facies, separated by terranes with less regular structural trend, higher metamorphic grade and a higher proportion of orthogneiss, some of which is charnockitic. The central of the three belts contains the Moon River synform, studied by Waddington (1973); this synform and an adjacent, major antiform-synform pair to the northeast make up what is here termed the Moon River structure. The other two belts, one of which is barely exposed on islands off the coast of Georgian Bay, appear to be synformal also, but overturned to the southwest. These belts consist predominantly of well-layered, migmatitic gneiss, including 'meta-arkose', but also contain sheet-like masses of orthogneiss. In the Moon River structure, for example, a thin layer of highly tectonized anorthositic gneiss has been traced for 15 km around the northwest closure of the Moon River synform (Fig. 41.3). Similar narrow anorthositic layers are known in the intervening terranes, for example east and southeast of Rosseau Lake (Bennett, 1975).

An intriguing feature of the Moon River structure is that it appears to be circumscribed by a zone of 'tectonoclastic' gneiss, separating it not only from Parry Sound domain but also from adjacent terranes. The zone along the south side has been traced continuously for more than 35 km (from Twelve Mile Bay to Bala), and is notable for containing thin, discontinuous sheets of anorthositic gneiss as well as smaller chunks and lenses of gneissic anorthosite, gabbro and amphibolite. The latter have been taken as evidence that "...the gneissic host is metatonalite." (Schwerdtner and Waddington, 1978, p. 204), implying that the clasts represent xenoliths of plutonic origin. These rocks, however, also contain sigmoidal feldspars just like those in

---

Plate 41.1

Figure A. Angular xenoliths in nondeformed part of meta-granitoid pluton, Britt domain, 10 km southwest of Britt. Matchstick lies on xenolith with earlier metamorphic foliation. GSC 100461-R

Figure B. Coarse metaconglomerate in east-dipping metasedimentary gneiss sequence at west side of Parry Sound domain, 15 km north of Parry Sound. Granitic clast at top is 22 cm long. GSC 200461-V

Figure C. Thinly layered mylonite gneiss derived from meta-anorthositic gabbro with pegmatite veins; road cut on Parry Sound bypass, Ontario highway 69. GSC 200461-T

Figure D. Sigmoidal K-feldspar augen connected by thin seam of fine granular, K-feldspar, in mylonite gneiss derived from metagabbro, road cut 0.5 km east of bridge to Parry Island. GSC 200461-P

Figure E. Disaggregated pegmatite dyke in deformed migmatitic gneiss, Britt domain. GSC 200461-S

Figure F. Block of granulite-facies layered gneiss (foreground) enclosed by xenolithic tectonic gneiss, Woods Bay, at juncture between Parry Sound domain and Moon River structure of Muskoka domain. Tectonite gneiss is in amphibolite facies. GSC 200461-Q

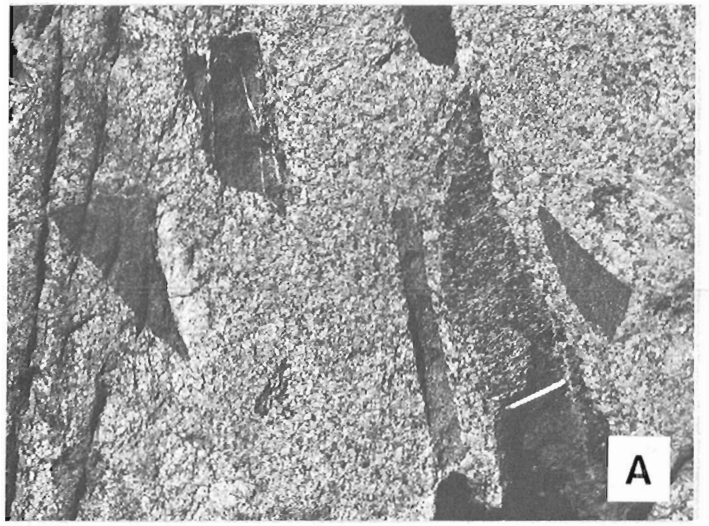
A


B

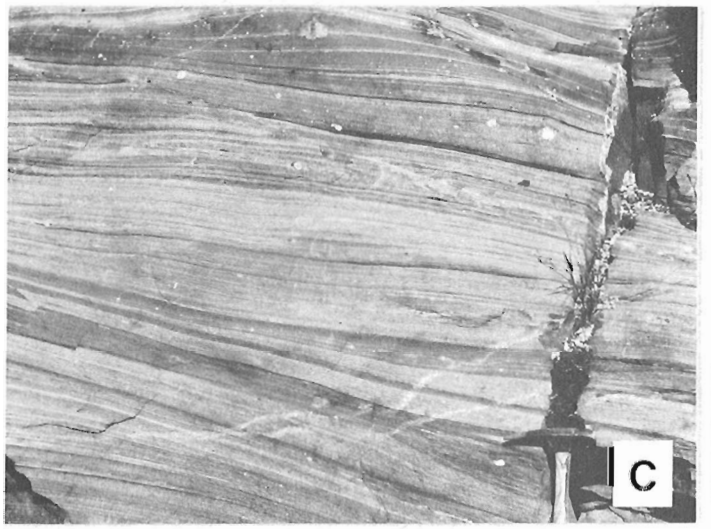
C

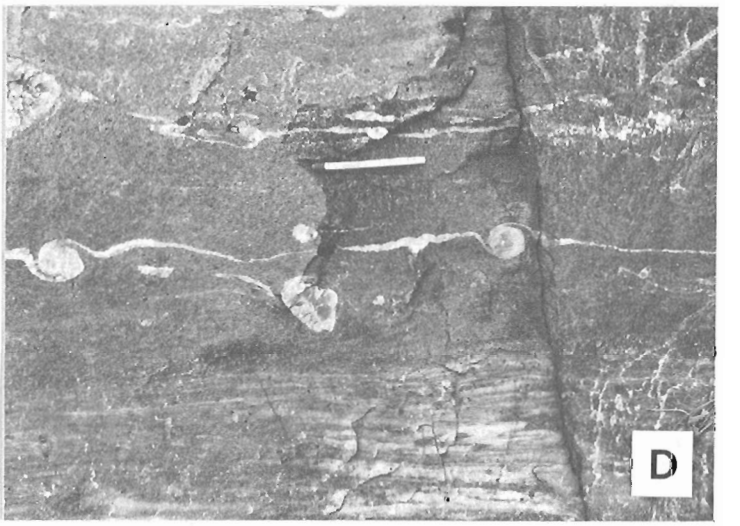
D


E

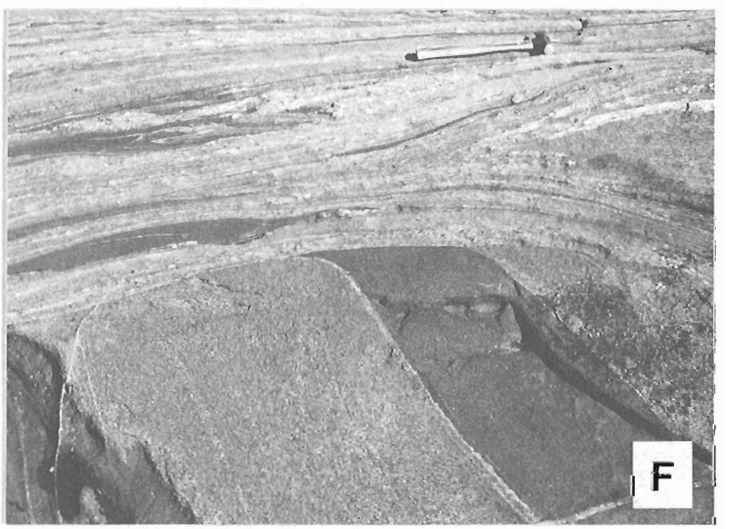
F

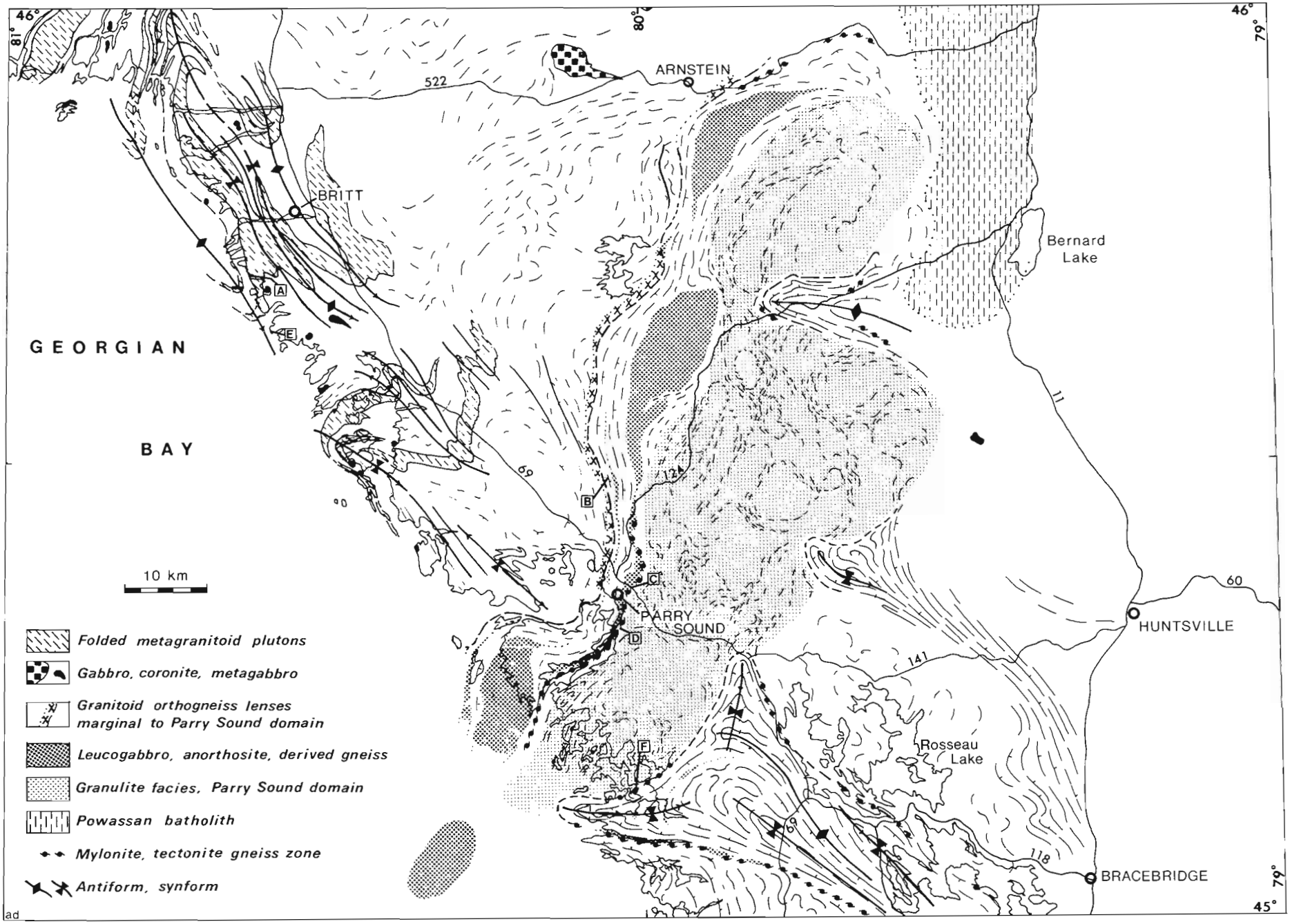

Figure 41.3. *Some characteristic geological features between Georgian Bay and Ontario highway 11. Areas in which structural trends are drawn are underlain by varieties of gneiss, in places migmatitic, of both supracrustal and plutonic derivation. Boxed letters indicate locations of figures in Plate 41.1. Numbered lines are main highways.*

the Parry Sound blastomylonite and lie in a zone that is discordant with structural trends to the south, and therefore may be equally well explained on a tectonic basis. Wherever observed, these peculiar rocks dip toward the core of the Moon River structure. Is this gneiss belt, then, allochthonous with respect to both Parry Sound domain and to the adjacent terranes in Muskoka domain? It is not yet known whether the other two gneiss belts are similarly circumscribed. The boundary between Muskoka and Algonquin domains to the east has not been studied on the ground, but appears to be a zone of change to irregular structural trends and to higher metamorphic grade.

Kiosk Domain

Structural trend in this domain is predominantly east-northeasterly; gneissosity dips moderately southeast and strongly developed, penetrative mineral lineation plunges down dip. At the northern edge of the map area (latitude 46°N) structures swing abruptly through north to northwest. At the western margin with Parry Sound domain, the weakly structured Powassan batholith seems an anachronism in this domain, but its inclusion is justified on the basis that similar metaplutonic rocks occur for a long way to the east, where they become progressively more flattened and acquire charnockitic affinity. This is, for the most part, a poorly exposed domain, but its structural grain is well displayed by the pattern of aeromagnetic anomalies. The metaplutonic rocks of Kiosk domain include a characteristic cream to pale salmon pink hornblende metamonzonite to metaquartz monzonite with conspicuous, wine-red garnet porphyroblasts. More highly deformed equivalents of this rock type become progressively finer grained and change colour to yellowish green, locally containing metamorphic hypersthene. Interpluton layered gneiss, however, does not appear to be in granulite facies. Like the eastern boundary of Muskoka domain, the southern boundary of Kiosk domain appears to be one of change to less regular structural trend and to higher metamorphic grade in Algonquin domain.

Algonquin Domain

This domain is heterogeneous in its make-up and may subsequently be further subdivided. In its northwestern part, rapidly changing structural trends in relatively low-dipping gneiss contrast strongly with regular trends in adjacent domains. Metamorphic grade is uniformly in two-pyroxene granulite facies over a large area east-northeast of Huntsville. Farther to the east and also to the south, small, isolated terranes have granulite facies assemblages, but on the whole amphibolite facies, in part retrograde in origin, prevails. An arcuate subdomain of pink and grey quartzo-feldspathic gneiss, in large measure of plutonic origin, skirts the western part of the Central Metasedimentary Belt, and includes a relatively large body of deformed gabbroic anorthosite (Fig. 41.2). Eastern Algonquin Park and the area west and southwest of Pembroke are also underlain mainly by varieties of orthogneiss, recently mapped by Lumbers (1980) and referred to collectively by him as the Algonquin batholith.

Close to the boundary with the Central Metasedimentary Belt in this region, here taken as the northwestern limit of marble and syenitic gneiss, outcrops of grey gneiss have many features in common with the 'tectonoclastic' gneiss found in Muskoka domain, and also with the tectonite gneiss that is disposed parallel to the Grenville Front in the Tectonic Zone (see Davidson et al., 1979, Plate 19.1). This rock is considered by Lumbers (1978b, 1980) to have been derived from coarse clastic sediments that were laid down unconformably on the Algonquin batholith, and as such is relegated to the basal unit of the Late Precambrian supracrustal sequence (Grenville Supergroup) of the Central Metasedimentary Belt. There is little doubt, however, that the structural features of this rock (boudins and clasts with twisted internal foliation, streaked-out aggregates of mafic minerals, flattened quartz and disaggregated pegmatite) are of tectonic origin, even though now recrystallized, and the rock may have an entirely different parentage. An alternative interpretation, the same as that already advocated for 'tectonoclastic' gneiss elsewhere, should be entertained, namely that these rocks are markers of dislocation zones of considerable magnitude, and likely originated deep in the crust. If this is so, it leads to the suggestion that the Central Metasedimentary Belt has moved as a block in relation to Algonquin domain.

Another zone of tectonite gneiss within Algonquin domain occurs along parts of the boundary between the arcuate subdomain mentioned above and the higher grade region towards Huntsville (Fig. 41.2); its extent is not yet known.

Possible Significance of Tectonite Gneiss Zones

Mapping has shown that various types of rock whose origin is ascribable to tectonism occur in zones that can be traced for many kilometres, and that they are seemingly associated with regional changes in structural trend, lithologic assemblage and metamorphic grade. Preliminary observations reported above suggest that, with further study in the map area, it may be possible to illustrate a complete gradation from mylonite to 'tectonoclastic' gneiss, with intermediate stages involving increasing degree of blastesis. On the whole, 'tectonoclastic' gneiss zones are many hundred, maybe even a few thousand metres wide, and have broad gradational boundaries with 'normal' gneiss. Blastomylonite zones are of the order of a few tens of metres wide, rarely exceeding 100 m, although several zones may occur in close proximity. They tend to branch around large blocks of less disturbed rock, and either have gradational boundaries over a few metres or are sharply defined. True mylonite and ultramylonite are even more restricted; narrow mylonite zones crosscut adjacent structures and are usually mapped as faults. These variations in width and in the type of tectonite developed are likely related to the depth at which they formed. A study of the metamorphic mineral assemblages in these rocks, provided it can be shown that they developed at the time of or immediately following tectonism, may help to determine depth of tectonism.

If it is subsequently shown that zones of rock interpreted as having tectonic origin can be used to delineate specific domains in this part of the Grenville Province, that they do represent loci of considerable differential movement between domains, and that thrusting is the predominant sense of transport, then we have a mechanism to explain the surface exposure of high grade metamorphic rocks in crust of normal thickness (approximately 35 km according to Mereu and Jobidon, 1971). Conditions for granulite facies metamorphism require that the exposed rocks were once covered by an additional 20 to 25 km of crust, maybe more. In a regime of crustal shortening, stacking of thrust slices can produce the implied 55 to 60 km crustal thickness. A thrusting mechanism can also bring deep-seated rocks to higher crustal levels where they can subsequently be unroofed by erosion. It is possible that a model for crustal evolution involving a combination of these effects may emerge from continuing studies in this part of the Grenville Province.

References

Baer, A.J., Poole, W.H., and Sanford, B.V.
1977: Rivière Gatineau; Geological Survey of Canada, Map 1334A.

Balk, R.
1931: Structural geology of the Adirondack anorthosite; Mineralogische und Petrographische Mitteilungen, v. 41, p. 308-434.

Bennett, P.J.
1975: The deformation of the northern half of the Brandy Lake complex, Port Carling, Ontario; unpublished M.Sc. thesis, University of Toronto, Toronto, Ontario.

Davidson, A., Britten, J.M., Bell, K., and Blenkinsop, J.
1979: Regional synthesis of the Grenville Province of Ontario and western Quebec; in Current Research, Part B, Geological Survey of Canada, Paper 79-1B, p. 153-172.

Frarey, M.J. and Cannon, R.T.
1969: Notes to accompany a map of the geology of the Proterozoic rocks of Lake Panache – Collins Inlet map-areas, Ontario; Geological Survey of Canada, Paper 68-43, 5 p. and Map 21-1968.

Freeman, E.B., ed.
1978: Geological highway map, southern Ontario; Ontario Geological Survey, Map 2418.

Hewitt, D.F.
1967: Geology and mineral deposits of the Parry Sound – Huntsville area; Ontario Department of Mines, Geological Report 52, 65 p. and Map 2118.

Lacy, W.C.
1960: Geology of the Dunchurch area, Ontario; Geological Society of America Bulletin, v. 71, p. 1713-1718.

Lumbers, S.B.
1971: Geology of the North Bay area, Districts of Nipissing and Parry Sound; Ontario Department of Mines and Northern Affairs, Geological Report 94, 104 p. and Map 2216.

1975: Geology of the Burwash area, Districts of Nipissing, Parry Sound, and Sudbury; Ontario Division of Mines, Geological Report 116, 158 p. and Map 2271.

1976: Mattawa – Deep River area, District of Nipissing and County of Renfrew; Ontario Division of Mines, Preliminary Maps P.1196 and P.1197, Geological Series.

1978a: Geology of the Grenville Front Tectonic Zone in Ontario; in Toronto '78, Field Trip Guidebook, ed. A.L. Currie and W.O. Mackasey; Geological Association of Canada, p. 347-361.

1978b: Southern Renfrew County; in Summary of Field Work, 1978, ed. V.G. Milne, O.L. White, R.B. Barlow, and J.A. Robertson; Ontario Geological Survey, Miscellaneous Paper 82, p. 125-127.

Lumbers, S.B. (cont.)
1980: Geology of Renfrew County, southern Ontario; Ontario Geological Survey, Open File Report 5282, 118 p. and Preliminary Maps P.1838, P.2355, P.2356, P.2357, Geological Series.

Mason, I.M.
1969: Petrology of the Whitestone anorthosite; unpublished Ph.D. thesis, University of Toronto, Toronto, Ontario, 299 p.

Mawdsley, J.B.
1927: St. Urbain area, Charlevoix District, Quebec; Geological Survey of Canada, Memoir 152.

Mereu, R.F. and Jobidon, G.
1971: A seismic investigation of the crust and Moho on a line perpendicular to the Grenville Front; Canadian Journal of Earth Sciences, v. 8, p. 1553-1583.

Ontario Department of Mines
1957: Haliburton-Bancroft area, Map 1957b.

Quirke, T.T.
1930: Key Harbour Sheet; Geological Survey of Canada, Map 239A.

Quirke, T.T. and Collins, W.H.
1930: The disappearance of the Huronian; Geological Survey of Canada, Memoir 160, 129 p. and Maps 220A and 221A.

Satterly, J.
1943: Mineral occurrences in Parry Sound District; Ontario Department of Mines, Annual Report for 1942, v. 51, part 2, 86 p. and Map 51a.

1956: Geology of Lount Township; Ontario Department of Mines, Annual Report for 1955, v. 64, part 6, 46 p. and Map 1955-4.

Schwerdtner, W.M. and Waddington, D.H.
1978: Structure and lithology of Muskoka – southern Georgian Bay region, central Ontario; in Toronto '78, Field Trips Guidebook, ed. A.L. Currie and W.O. Mackasey; Geological Association of Canada, p. 204-212.

Waddington, D.H.
1973: Foliation and lineation in Moon River synform, Grenville Structural Province, Ontario; unpublished M.Sc. thesis, University of Toronto, Toronto, Ontario.

Walker, T.L.
1913: The Precambrian of Parry Island and vicinity; Geological Survey of Canada, Guide Book No. 5, p. 98-100.

Wynne-Edwards, H.R.
1972: The Grenville Province; in Variations in Tectonic Styles in Canada, ed. R.A. Price and R.J.W. Douglas; Geological Association of Canada, Special Paper 11, p. 263-334.

42.

THE IMPACT OF DISTURBANCE ON MUDBOIL ACTIVITY, NORTH HENIK LAKE, DISTRICT OF KEEWATIN

Project 770035

P.A. Egginton
Terrain Sciences Division

Egginton, P.A., The impact of disturbance on mudboil activity, north Henik Lake, District of Keewatin; in Current Research, Part A, Geological Survey of Canada, Paper 81-1A, p. 299-303, 1981.

Abstract

The construction of an airstrip at North Henik Lake, District of Keewatin has led to a localized disruption of the familiar mudboil pattern. The pattern has since been re-established on the peripheral areas of strip, which were bulldozed during initial construction, and to a lesser extent on the main airstrip. At the disturbed sites the vegetation and the carapace have been removed exposing the underlying thawed mud substrate. The mud within these areas, eleven years after the initial disturbance, is considerably more active than in an adjacent undisturbed area; maximum recorded rates of yearly displacement of the surface mud are 14.5 and 2.0 cm/a, respectively.

Introduction

Mudboils, a patterned ground form, are common on the fine grained glacial and marine muds of central District of Keewatin. The pattern is formed by a heavy vegetation ring, typically lichens, mosses, and willows, around a central area of bare or sparsely vegetated mud. Some frost sorting occurs, however, and the mud in the central portion of the mudboil commonly contains a higher proportion of fines than the mud in the vicinity of the vegetated border. The mud is further differentiated in that the upper 30 to 45 cm forms a rigid covering (carapace), as it dries out during summer, over the thawed mud substrate (TMS). The TMS has a higher percentage of fines than the carapace and is at or near saturation throughout the thaw season (Shilts, 1978).

The mud has a low liquid limit and plasticity index and is rigid or slightly plastic under normal field conditions. The mud in the central portion of the mudboils liquefies during spring melt but is generally contained by the vegetated border. Occasionally, when conditions are favourable, the mud may burst through or flow over the vegetated border (Fig. 42.1).

Figure 42.1. *Mudflow originating from a mudboil and flowing through and over the vegetated border (dashed line). Note that the flow occurs immediately upslope of a late lying snow patch. The 5 cm² targets (arrow) give scale. GSC 203502-O*

This paper describes some problems encountered in the construction of an airstrip at North Henik Lake, District of Keewatin and gives rates of surface movements of mud in both disturbed and undisturbed mudboils along the sides of the airstrip. These data were collected as part of a larger study of mudboils in central District of Keewatin (Egginton, 1979).

Acknowledgments

I would like to thank the owner and personnel of Henik Lake Lodge (Grand Domain Retreats) for the support they provided during the 1978 and 1979 field seasons. A. Reid provided the details of airstrip construction.

North Henik Lake Airstrip

An airstrip some 1500 m long has been constructed at North Henik Lake, District of Keewatin (Fig. 42.2) to provide access to a fishing lodge. The strip, located on the crest of a drumlinoid feature, was constructed over a two-year period commencing in 1968. It was built by pushing vegetation and excess material to the sides of the strip (A, Fig. 42.3) and grading the cleared area continually over a two-year period with a D4 Caterpillar. During the construction period some permafrost degradation occurred. Low points were brought up to grade by as much as 0.8 m in the first year but by the second year they had subsided to 0.3 m below grade. Today, thaw depressions up to 1 m deep are found on the abandoned southern portion of the airstrip. In addition to permafrost degradation, the builder encountered many other problems during construction. Vibration from the idling bulldozer caused the underlying mud to liquefy causing the machine to sink to the bottom of the thaw zone; as a result the bulldozer was mired down on many occasions. The mud (till) on which the airstrip was built, when subjected to vibration, behaves like a fluid. During construction, the moving bulldozer generated surge waves in the muds 30 m or more in front of the vehicle.

The removal of the vegetation and carapace exposed the underlying thawed mud substrate. Eventually, during the two years of construction an equilibrium active layer depth was reached and the mud stabilized. Continual grading of the strip, which allowed some fines to be removed by washing and deflation, as well as the addition of

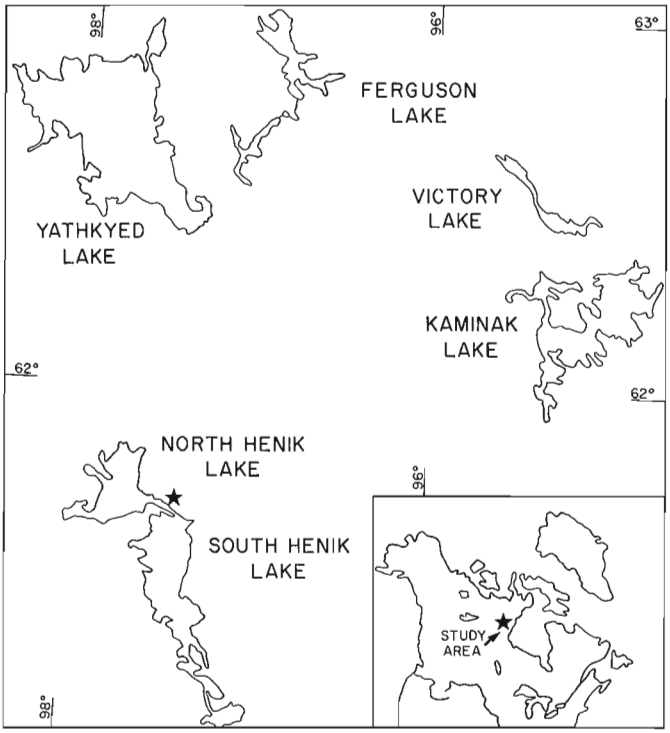

Figure 42.2. The location of the study site at North Henik Lake.

beach sand and gravel to the strip, contributed to stabilization. The resulting surface is consequently much less prone to deformation or liquefaction than the unmodified thawed mud substrate which is still exposed along the periphery of the airstrip (A, Fig. 42.3).

Mudflow and Mudboil Activity

Although present maintenance operations on the airstrip are limited as it is not used until the mud is at least moderately dry, infrequent and irregular patching is required. In spring 1978, a 0.2 km-long winding path was bulldozed through a large snowdrift from the airstrip to North Henik Lake. The path concentrated runoff at a critical period when the mud was first melting. Several days later surface mudflows of 10 cm per hour were measured in one area in the vicinity of the snow patch. For comparison, over the 1977 to 1978 period, nearby unaffected mud in mudboil centres was displaced downslope less than 4.5 cm per year (Egginton, 1979).

In the eleven years since construction a mudboil pattern is slowly evolving on parts of the main airstrip. Some sorting is occurring with coarse gravel being concentrated in the border areas of the patterned form (Fig. 42.4). At the unused southern end of the strip recent mud surges, associated with thaw depressions, can be seen (Fig. 42.5).

Along the periphery of the airstrip in areas stripped of vegetation but not excessively graded, a mudboil pattern has re-established and the borders again are vegetated (Fig. 42.6). The new mudboils are essentially flat, the grasses bordering the mudboils provide the only relief. These young mudboils appear more active than adjacent undisturbed boils which are almost completely vegetated by lichens and mosses and have slightly raised centres (Fig. 42.8).

In order to assess relative rates of deformation and movement in disturbed and undisturbed areas, aluminum tags were spaced at known intervals and patterns on selected mudboils. The distances between the tags were measured over time to provide rates of relative movement. In plan view the disturbed mudboils (1 and 2, Fig. 42.7) as outlined by vegetation, are larger than the undisturbed mudboils (3 and 4, Fig. 42.7). Areas of movement over the period June 12, 1978 to June 10, 1979 are shown schematically in Figure 42.7. Only certain areas of each mudboil are active. These zones of relatively high activity may be associated with diapirism (Shilts, 1978) and/or with areas of differential heaving (Egginton, 1979).

Tag movements for two intervals June 12, 1978 to June 10, 1979 and June 10, 1979 to August 1, 1980 are presented in histogram form (Fig. 42.9). The data are based upon 83 tag measurements for each period. At the undisturbed sites maximum recorded movements were 2 cm/a; displacements of up to 14.5 cm/a were recorded at disturbed sites.

Discussion

Field and laboratory tests indicate that the mud, if unconfined, will flow when porewater pressures are equal to or greater than overburden pressures. Differential hydrostatic pressure, simple spring melt, or vibration from a moving vehicle can create this condition.

When segregated ice forms in the active layer of mudboils during freezeup, accumulations are usually high in the upper few centimetres of the soil or at the bottom of the active layer (Egginton, 1979). Through this process moisture is locally concentrated so that when the ice melts, local porewater pressure is equal to overburden pressure and the mud may liquefy. For example, Egginton (1979) has reported the liquefaction of surface mud experiencing diurnal freeze-thaw cycles. Generally the vegetation border around the mudboils helps to stabilize the features, both because of the strength and binding characteristics of the vegetation and roots and because of the thermal insulative properties of the vegetation. The border areas thaw much more slowly than the bare mud in the centre with the result that, early in the thaw season, the mud is thereby contained by a rigid border. Removal of the vegetation net thus can lead to instability in both the thermal and geotechnical sense. For this reason and because of the exposure of the TMS, mud surges and rapid surface displacements are common in the disturbed zones associated with the North Henik Lake airstrip.

Surface mud is most sensitive to disturbance in the early spring when ground thaw commences, but sensitivity is increased if the mud lies immediately upslope of a snow patch. Water moving downslope as seepage is forced to the surface as the thawed zone thins towards the upslope side of a snow patch (Egginton, 1979). The frozen ground under the snow patch essentially acts as a dam, and water moving through the active layer is forced upward producing positive porewater pressures and mudflow (Fig. 42.1). Similar conditions existed at North Henik Lake when a path was bulldozed through a snow patch routing surface water and seepage down the slope. Where the depth of thaw thinned in the vicinity of the snow patch, seepage was forced upward, positive pore pressures were generated, and rapid downslope displacements of the surface mud resulted.

If the mud is near saturation, such as during the early thaw season, vibrating the soil can cause the internal soil structure to collapse producing a "quick" condition. Where the mud is unconfined, mudflow may result. Airstrip construction at North Henik Lake was difficult because of the quick nature of the materials. The critical factors determining whether the mud will liquefy are the nature and magnitude of the force applied and soil moisture conditions. When the soils dry, a substantial force is required to make them liquefy. In the vicinity of the airstrip the till is well drained and typically by July 1, bearing strengths, determined by pocket penetrometer, are 5.0×10^4 kg/m^2. The movement of a D4 Caterpillar at this time causes little detectable disturbance.

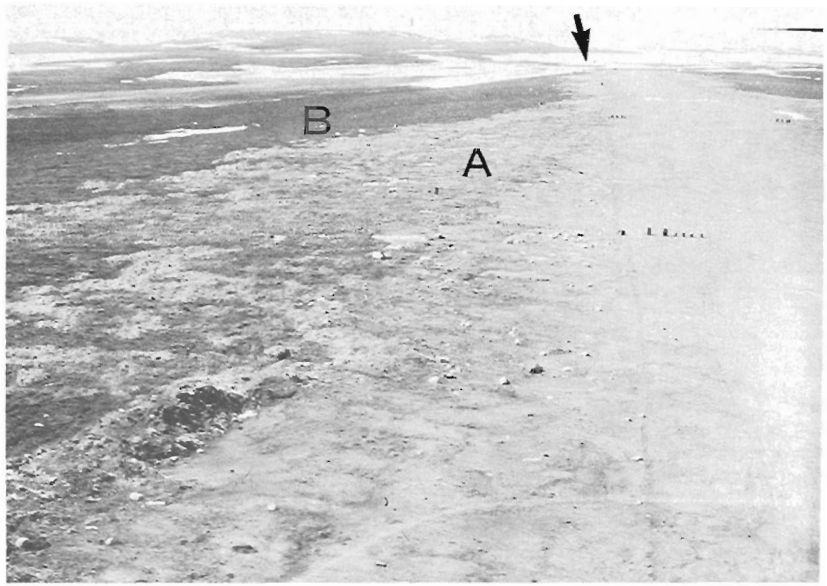

Figure 42.3. *Oblique photograph of the airstrip at North Henik Lake. The view is from the unused southern portion of the strip towards Henik Lake Lodge, located some 1.5 km away (arrow). The area peripheral to the airstrip (A) was cleared during construction. Mudboils just outside of this zone are undisturbed (B). The 45 gallon drums give scale. GSC 203502*

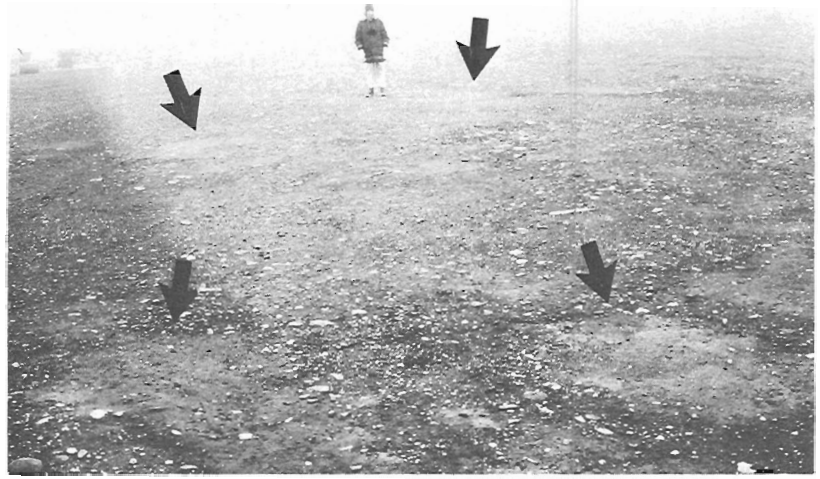

Figure 42.4. *Mudboil pattern re-establishing on the main airstrip, North Henik Lake. The pattern is most clearly visible immediately after a rainfall and during overcast conditions. GSC 203503-E*

Figure 42.5. *Mud flowing into the central thaw depression on an unused portion of the airstrip. GSC 203502-D*

Figure 42.6. *Mudboils located in the disturbed zone along the edge of the airstrip (cf. A of Fig. 42.3); only the border of the boils are vegetated. GSC 203502-N*

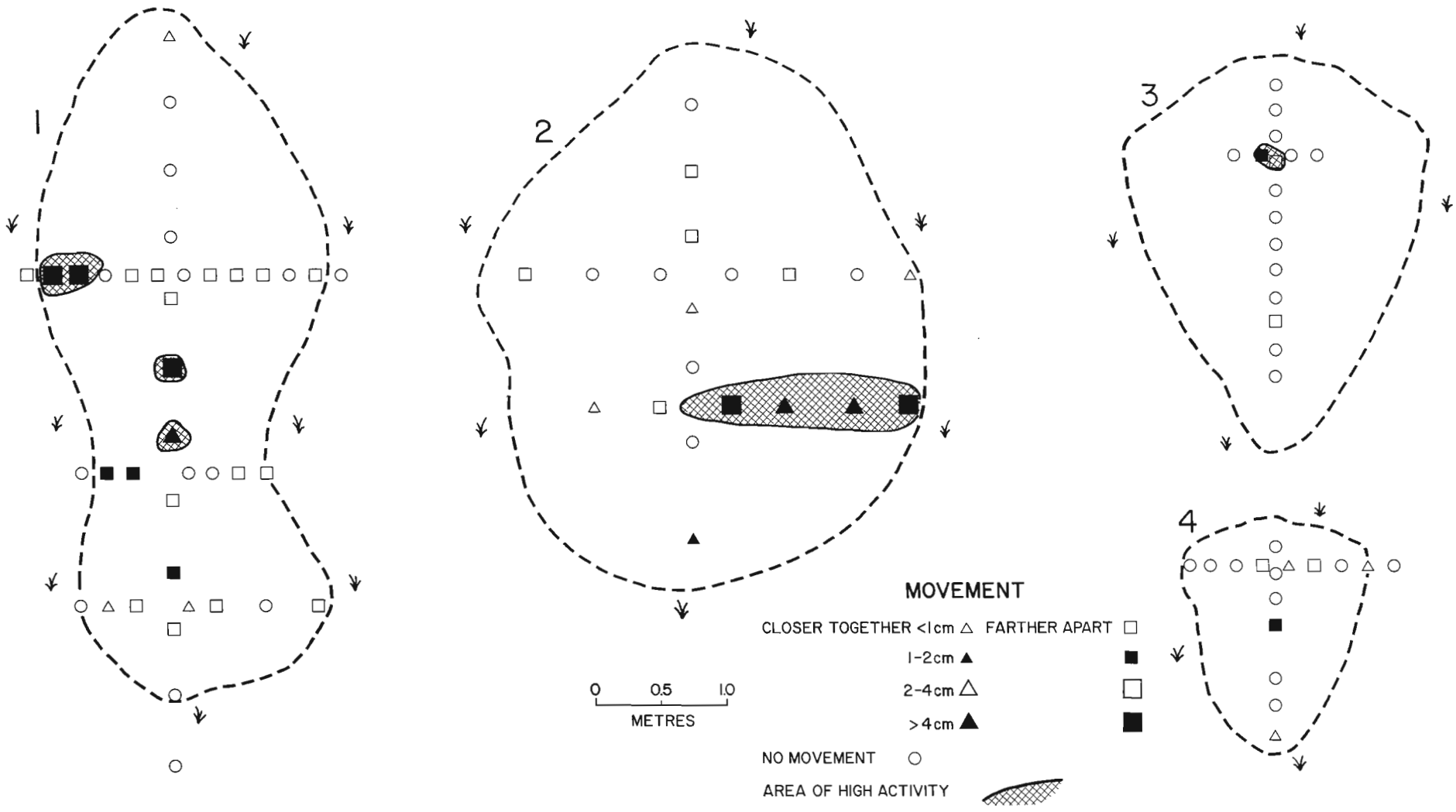

Figure 42.7. *Plan view of mudboils with vegetated borders in disturbed areas adjacent to the strip (mudboils 1 and 2) and undisturbed areas (mudboils 3 and 4) showing surface displacement (June 1978 to June 1979) of marker tags placed on the mudboils.*

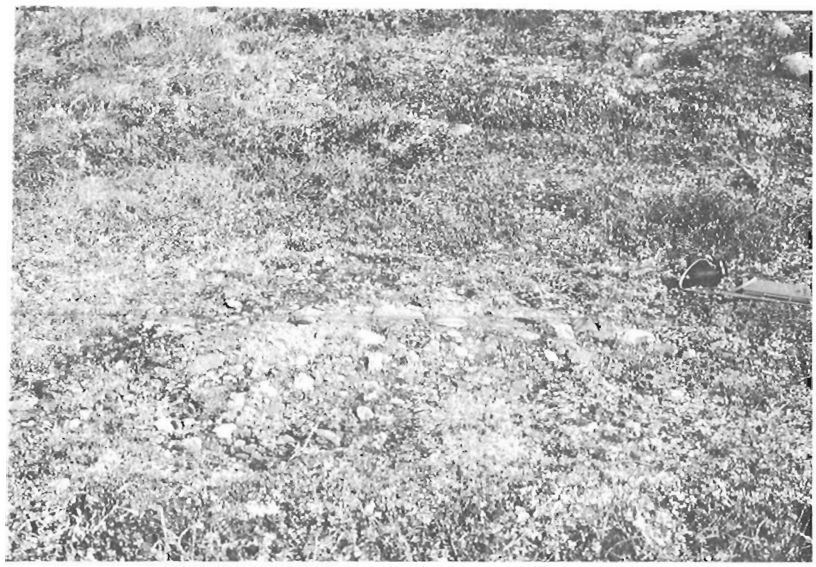

Figure 42.8

Undisturbed mudboil adjacent to the airstrip (B of Fig. 42.3). Notebook gives scale. Only a small area in the centre is devoid of vegetation; the borders are densely vegetated. (GSC 203502-F)

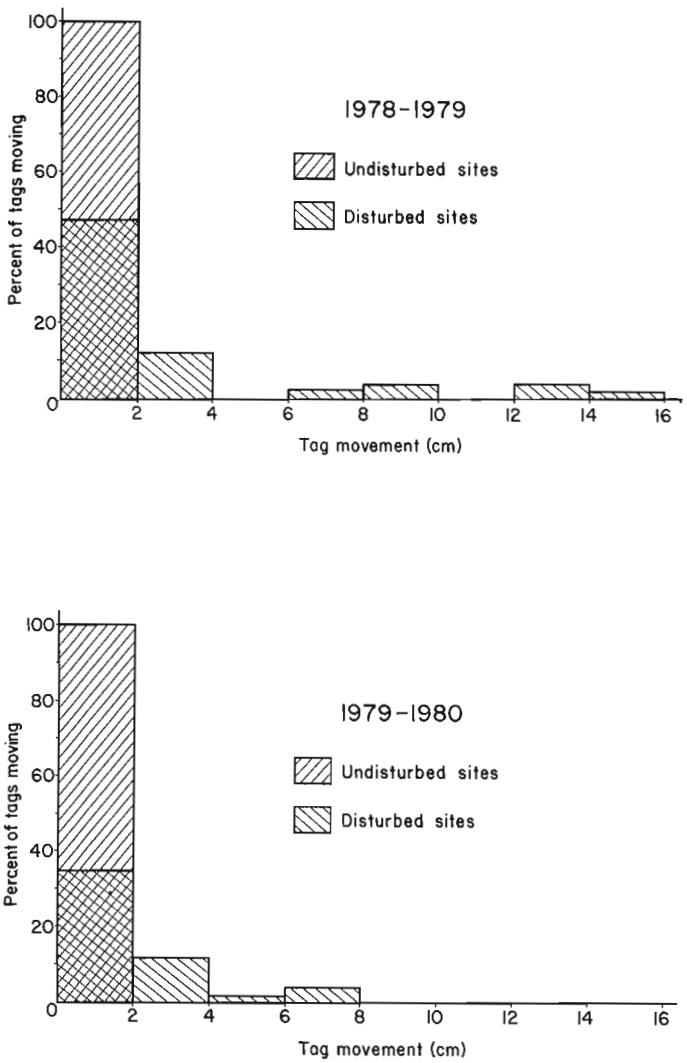

Figure 42.9. *Surface displacement of marker tags located on mudboils in disturbed and undisturbed areas.*

Summary

The construction of an airstrip at North Henik Lake in 1968 and 1969 induced minor subsidence and mudflow. This disturbance, however, is highly localized. Construction difficulties were encountered because of the physical properties of the till which is most sensitive to disturbance in the early spring. At present, maintenance activities at the Henik Lake airstrip are limited as the strip receives little use until it dries.

The stripping of the vegetation from the peripheral areas of the airstrip during construction and exposing the TMS have caused the surface mud to become active. A mudboil pattern is re-establishing both in the peripheral areas of the airstrip and on the airstrip proper. Rates of displacement of surface mud associated with mudboils in the disturbed terrain are still substantially higher than in undisturbed sites eleven years after the initial disturbance.

References

Egginton, P.A.
1979: Mudboil activity, central District of Keewatin; in Current Research, Part B, Geological Survey of Canada, Paper 79-1B, p. 349-356.

Shilts, W.W.
1978: Nature and genesis of mudboils, central Keewatin; Canadian Journal of Earth Sciences, v. 15, no. 7, p. 1053-1068.

43. STRATIGRAPHY OF A PROTEROZOIC VOLCANIC COMPLEX AT TUERTOK LAKE, WOPMAY OROGEN, DISTRICT OF MACKENZIE

EMR Contract 23233-0-0057

R.M. Easton[1]
Precambrian Geology Division

Easton, R.M., Stratigraphy of a Proterozoic volcanic complex at Tuertok Lake, Wopmay Orogen, District of Mackenzie; in Current Research, Part A, Geological Survey of Canada, Paper 81-1A, p. 305-309, 1981.

Abstract

The Tuertok Lake Volcanic Complex is one of the best exposed of several volcanic complexes present in the early Proterozoic Akaitcho Group. The complex consists of a 3 km thick basal sequence of mainly pillowed basalt, overlain by several rhyolite volcanic domes. The basalts have been divided into nine stratigraphic "units". The lowest unit shows evidence of a brief period of erosion before deposition of the later units. A glomeroporphyritic gabbro intrudes the central part of the volcanic complex and may represent a sub-volcanic magma chamber.

Introduction

The Tuertok Lake Volcanic Complex exposed in parts of map areas 86 J/11, 12, is one of the best exposed of several volcanic complexes present in the Akaitcho Group (Proterozoic). The area was previously mapped at 1:100 000 scale (Hoffman et al., 1978), and was sampled for geochemical studies by Easton (1980). Preliminary REE studies (Easton, in preparation and unpublished data) revealed a transition from continental tholeiite to ocean tholeiite in basalts of the Tuertok Complex. Detailed sampling for geochemistry and geochronology and detailed mapping were carried out in the Tuertok Lake area during three weeks of the 1980 field season in order to better document the geochemical transition present in the Tuertok basalts and to obtain a better understanding of the stratigraphy of an Akaitcho Group volcanic complex.

General Geology

The Akaitcho Group is located in the metamorphic core (Zone 3) of Wopmay Orogen (Hoffman, 1980a). The sequence is intruded on the east by the Hepburn Batholith and on the west by Wentzel Batholith. Regional metamorphism of the Akaitcho Group ranges from chlorite grade (lower greenschist) to above sillimanite breakdown (granulite) and is spatially related to the two batholiths (St-Onge and Carmichael, 1979; Hoffman et al., 1980). Volcanic rocks of the Tuertok Lake area are in the chlorite zone, although metamorphic grade rises abruptly to above muscovite breakdown in the pelites 5 km east and northeast of Tuertok Lake (St-Onge, unpublished data) (Fig. 43.1).

The Akaitcho Group consists of a lower basaltic unit with interbedded pelites (Ipiutak Subgroup) overlain by arkosic turbidites (Zephyr Formation) intruded by sills of rhyolite porphyry (Okrark sills). Basalt and rhyolite volcanic complexes, including the Tuertok Volcanic Complex, of the Nasittok Subgroup overlie the Zephyr Formation. Volcaniclastic sediments and pelites of the Aglerok Formation interfinger with, and overlie the volcanic complexes. Locally, abundant basaltic extrusive and intrusive rocks are present in the upper part of the Aglerok Formation. The Ipiutak Subgroup is not present in the Tuertok Lake area. The west dipping Okrark Thrust juxtaposes rocks of the Zephyr Formation and the Okrark sills against the Nasittok Subgroup in the western part of the Tuertok Lake area (Fig. 43.1); Easton, 1980).

The volcanic complexes of the Nassitok Subgroup typically have a 2 km or greater thick base of green to dark green weathering, plagioclase-phyric and aphyric pillowed and massive metabasalts locally with thin beds of basalt metatuffs. The basal metabasalts are capped by 1 to 1.5 km of pink and grey weathering, plagioclase-quartz- and orthoclase-phyric metarhyolites. The metarhyolites have been interpreted to be remanents of volcanic domes (Easton, 1980). Wedges of metasandstone and siliceous metasiltstone are typically present on the north side of the metarhyolite domes. Intraformational metaconglomerates, volcanic breccias, quartzites and marbles are commonly found on the south side of the metarhyolite domes. In addition, beds of rhyolite metatuff can be traced for many kilometres south of the metarhyolite domes.

Volcanic Stratigraphy

Only the volcanic lithologies of the Nasittok Subgroup shown in Figure 43.1 are described. Descriptions of other Akaitcho Group units are given in Easton (1980). The Hepburn Batholith has been described by Hoffman et al. (1980).

It was not possible to map individual flow units for any distance in the Tuertok Volcanic Complex because of much late faulting, lack of marker horizons, prolific lichen cover and lack of outcrop in critical areas. Nevertheless, it was possible to map several distinctive groups of flows (units 3 to 11, Fig. 43.1).

The oldest "unit" (unit 3) consists of dark grey, brown-green and green massive flows and sills of phyric basalt and gabbro. The basalts contain mainly mafic phenocrysts, now completely altered to chlorite and only minor plagioclase phenocrysts. Locally unit 3 basalts are cut by former channels up to 100 m across and 10 m deep which are filled with volcaniclastic sediments, basaltic tuffs and fine grained rhyolite, possibly air fall tuff.

A distinctive glomerophyric gabbro body about 500 m thick (unit 4) intrudes units 3 and 5. This gabbro is a coarse feldspathic rock spotted with rounded feldspar aggregates up to 10 cm in diameter. The gabbro is relatively homogeneous along its length, although there is some variation in grain size. The gabbro is finer grained on its upper contact where it resembles plagioclase-phyric flows and feldspathic gabbros present in the overlying unit 5. The shape of the body could not be determined fully because of complications of late faulting, but it appears to lens out to the north and south. The gabbro is thickest in the Tuertok Lake area, which is also where the thickest accumulation of basalt occurs.

Dense, pale green, 4 to 6 m thick basalt flows, commonly pillowed with 10-15 mm selvages, and some feldspar-rich, 5 to 7 m thick massive flows and sills form the bulk of unit 5. Phyric flows make up 15 to 25 per cent of this unit. Plagioclase-phyric flows are most abundant, but

[1] Department of Geology, Memorial University, St. John's, Newfoundland, A1B 3X5

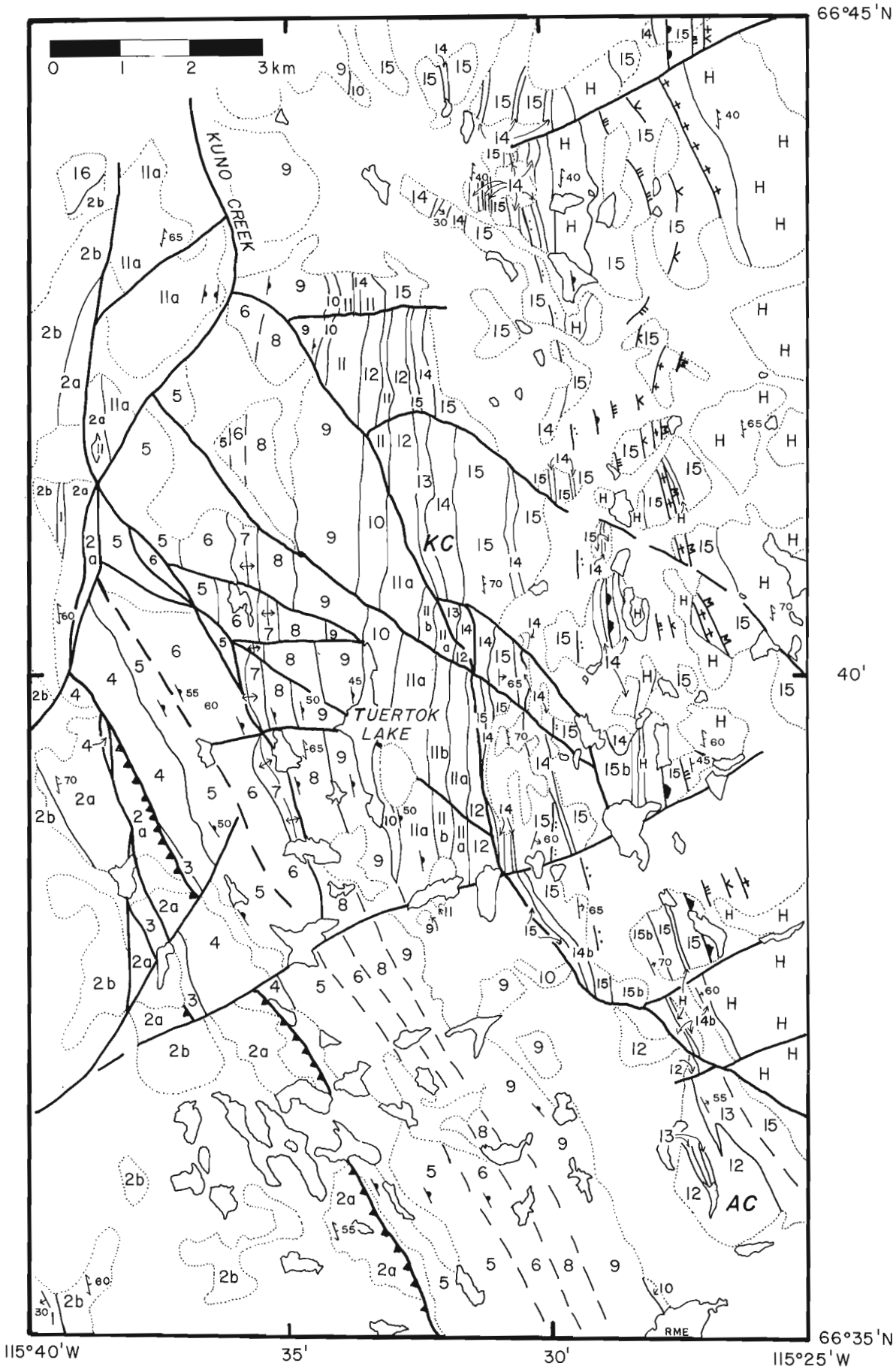
66°45'N
0 1 2 3km
KUNO CREEK
KC
TUERTOK LAKE
AC
40'
66°35'N
115°40'W
35'
30'
115°25'W

Legend

16 HORNBY BAY GROUP sandstone

H tonalite and granite of HEPBURN BATHOLITH

AKAITCHO GROUP

15 AGLEROK fm. pelites,
15b sandstone

NASITTOK SUB-GROUP

14 porphyritic rhyolite flows and tuffs,
14b mainly bedded tuff, minor pelite

13 pelite, carbonate, rhyolite tuffs

12 crystal-rich porphyritic rhyolite

11 pillowed, massive, tuffaceous dark green basalt, minor rhyolite,
11b much interbedded rhyolite

10 dark, fine grained rhyolites

9 pillow basalt

8 pillow basalt, thin selvages

7 breccia, tuffs, thin flows, strongly cleaved basalt

6 as Unit 5 but with dark green basalt dykes

5 pale green pillowed and massive basalts, commonly feldspathic, minor chert, black shale

4 glomeroporphyritic feldspathic gabbro

3 mafic basalts, minor black shale

2 OKRARK rhyolite sills,
2a plagioclase porphyritic,
2b orthoclase porphyritic

1 ZEPHYR fm. arkosic turbidites

METAMORPHIC ISOGRADS

(ornament on high T side, data courtesy of M.R. ST-ONGE)

bi biotite

st staurolite

sill sillimanite

ms muscovite breakdown

+ granite pods

M migmatite (> 30% granite)

fault, known, assumed

OKRARK thrust fault

contact, known approximate

bedding, tops known, unknown

pillow tops

foliation

AC Aklak centre

KC Kuno centre

Figure 43.1. *Geological map of the Tuertok Lake area. Mackenzie Set III diabase dykes have been omitted for clarity.*

plagioclase-phyric flows with chlorite clots after mafic phenocrysts, and flows containing only chlorite clots are also common. The plagioclase-phyric flows may be extrusive equivalents of unit 4. The flows are more abundant in the upper (easterly) part of unit 5. Minor volcaniclastic sediments, black shales, flow and pillow breccias are present locally in unit 5. All flows and sediments dip 45 to 50° east and tops are to the east. A 10 to 50 cm thick felsite band caps unit 5. This felsite may be a chert or air fall tuff.

Unit 6 contains basalts similar to those present in unit 5. This "unit" differs from unit 5 in that it is cut by a sill and dyke swarm of green to dark green medium grained basalt, similar in appearance to the units 8 and 11 basalts. As the sills and dykes cannot be traced through unit 9, they may have served as feeders for the unit 8 flows.

Unit 7 consists of strongly cleaved basalt breccias. Some 50 cm thick pillowed flows, with abundant pillow breccia, and some bedded mafic tuffs and lapilli tuff are also present. Unit 7 is cored by a small, north-south trending anticlinal structure which folds cleavage and bedding. It is the only unit which shows evidence of minor folding, perhaps because of the less competent nature of the breccias and tuffs present in this unit.

Dark green to green, 3 to 6 m thick flows of pillowed basalt with extremely thin (5 mm or less) selvages characterize unit 8. On most outcrop surfaces, the selvages weather out and appear as arcuate fractures which cut across the cleavage present in the rocks. Only on relatively polished surfaces, or surfaces cut near perpendicular to bedding are the selvages distinct.

Green, 3 to 6 m thick pillowed basalt flows (unit 9) with thicker (5 to 10 mm), more obvious selvages overlie unit 8. Pillow breccia is minor in both units 8 and 9. Units 8 and 9 flows dip 45 to 55° east and tops are to the east.

Dark weathering, dark grey, fine grained to flinty, bedded rhyolite tuffs, flows and spherulitic rhyolite flows constitute the 150 to 200 m thick unit 10. This unit represents the first major appearance of rhyolite in the Tuertok Volcanic Complex. The rhyolites, in contrast to later rhyolites, are a darker colour and fine grained to aphanitic. Some of the unit 10 rhyolites contain microphenocrysts of orthoclase and quartz. No chemical difference has yet been detected between these rhyolites and overlying, phyric rhyolites (Easton, unpublished, 1980).

Dark green weathering, dark green, 2 to 4 m thick, commonly pillowed basalt flows (unit 11) appear again in the volcanic pile above unit 10 in a 1 km thick sequence. Minor dark, fine grained rhyolite, mafic crystal tuffs and volcaniclastic sediment beds are present throughout unit 11. Abundant dark, fine grained rhyolite horizons 1 to 5 m thick, commonly containing quartz and orthoclase microphenocrysts interbedded with pillowed and massive basalts, form a distinctive zone (unit 11b) within unit 11.

Units 3 to 11 represent the basal, mainly basalt portion of the Akaitcho Group volcanic complexes (unit 3c, Easton, 1980).

Unit 12 overlies the basal of the Tuertok Volcanic Complex and consists of a crystal-rich (60 to 70 per cent crystal) quartz-orthoclase-phyric rhyolite. This unit has been rotated and displaced along the east branch of the Kuno Creek Fault (Fig. 43.1) and is severely dismembered. Unit 12 probably represents the proximal portion of a volcanic dome. Mudstone with interbeds of carbonate lutite (unit 13) and 5-25 cm thick rhyolite tuff beds cap unit 12 and can be traced south of the main mass of this rhyolite. The carbonate does not extend to the north. Unit 13 grades

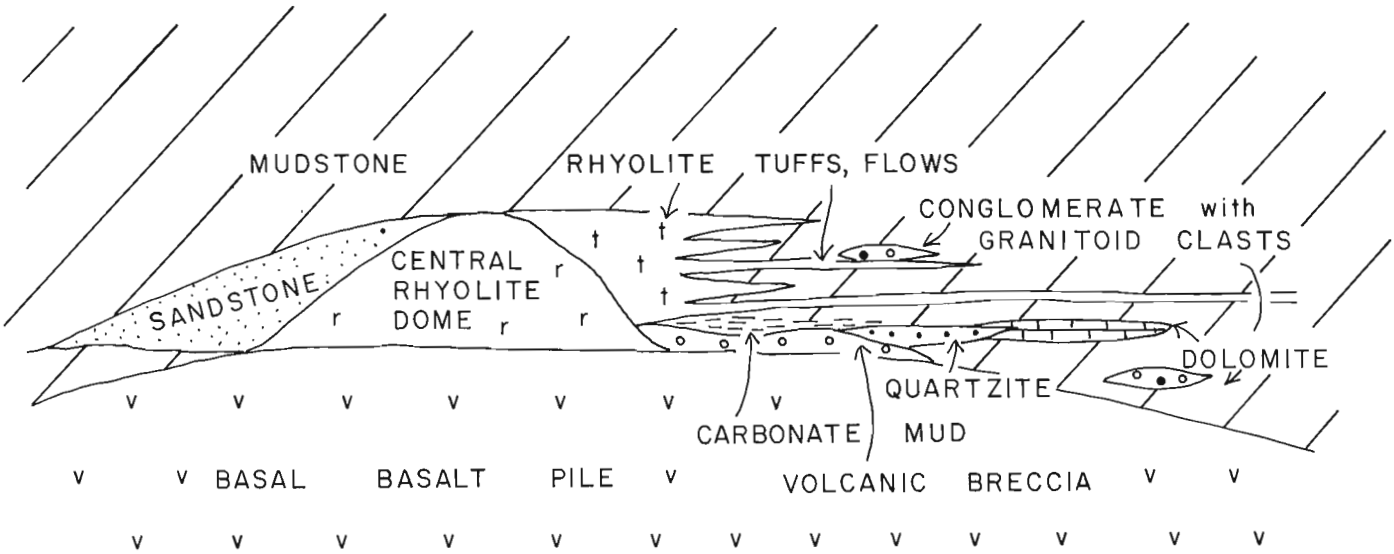

Figure 43.2. *Generalized facies relationships in rhyolite centres overlying the Tuertok Lake Volcanic Complex.*

upsection (to the east) into unit 15 mudstones, which contain bands of quartz and orthoclase-phyric rhyolite ranging from 50 to 200 m thick (unit 14). Some of the rhyolite bands (unit 14) north of the Kuno centre are probably derived from the Sinister Volcanic Complex to the north. Bands of rhyolite south of the Kuno centre are probably related to the centre.

Units 12 to 14 are interpreted to be the remanents of a volcanic dome, similar to the Aklak centre, but which has been dismembered by later faulting. Unit 15 represents the basal portion of the Aglerok Formation.

Basalts north of the west branch of the Kuno Creek Fault have been assigned to unit 11, the unit which they most closely resemble, although the structural position of these basalts is not fully understood.

The overall stratigraphy of the Tuertok Volcanic Complex is described by Easton (1980). Important details to note are the presence of a series of distinctive flows near the base of the complex which show some evidence for local erosion (unit 3) and the presence of a glomerophyric gabbro body in the core of the complex (unit 4) which could represent a shallow level intrusion or a subvolcanic magma chamber. Rhyolites appear late in the volcanic sequence, consistent with the geochemical evidence (Easton, in press) that they are related to crustal melting. Much of the rhyolite appears to have been extruded during waning and after cesation of the basaltic volcanism. The volcanic units thin to the south away from the Tuertok centre, and units 3, 4, 6, 7, and 10 thin abruptly and/or pinch out.

The Kuno Rhyolite Centre is the third volcanic dome to be found in the Tuertok Complex, and it has the same stratigraphic relations as do the other centres (Fig. 43.2). Sandstone wedges, consisting of detritus shed off of the rhyolite pile are present on the north side of the domes. Volcanic breccias, conglomerates containing granitoid clasts, quartzites, and carbonate, occurred on the south side of the domes. The consistent reappearance of these facies relations (Fig. 43.2) suggests that they reflect on the environment of deposition. One interpretation is that deeper water lay to the north of the domes. Extrusion of the domes resulted in a barrier to the north, producing a protected basin to the south where carbonates and quartzites were deposited.

Structure

The volcanic sequences, with the exception of unit 7, are all east facing and dip 45 to 60° east. All Akaitcho Group lithologies are cut by a strong north-south trending steeply east dipping cleavage. The cleavage is most intense in the bedded units adjacent to late faults.

The dominant structures in the area are late northeast and northwest trending transcurrent faults and the Kuno Creek Fault System (Fig. 43.1) which may have subsequent dip-slip (Hoffman, 1980b). Only faults with recognizable offset are shown in Figure 43.1. Many other lineaments and rubble zones are present in the area, and these may be related to additional faults. Rubbly weathering zones and an intensification of cleavage are common in basalts and rhyolites adjacent to the faults. The north-south trending portion of the Kuno Creek Fault in the north part of the Tuertok area is on strike with the west boundary fault of the Mouse Graben (Hoffman, 1980b) and may be related to that structure. Along the west branch of Kuno Creek, late faulting has obscured relations along a west dipping thrust (Fig. 43.1). In places, the Okrark porphyry sills have been strongly brecciated along these late faults. Brecciation has been intense enough to produce rounded clasts in a fine, mylonitic matrix, and these breccias may be mistaken for conglomerates. The restriction of these breccia units to areas of known faulting strongly suggests that they are fault related, and not deformed conglomerates. The Tuertok Volcanic Complex appears to have acted as a rigid block during faulting, as the Kuno Creek Fault System wraps around the basalt core of the Tuertok Volcanic Complex, and the volcanic complex is cut by many small, northwest trending faults. The intense fracturing of the volcanic complex is important with regard to dating the Tuertok Volcanic Complex by Rb-Sr techniques. The fractures may have served as conduits for introducing fluids into the volcanic pile well after extrusion of the basalts. If the volume of fluids introduced into the pile was large, resetting of the Rb-Sr system may have occurred.

Acknowledgments

This paper has benefited from discussions in the field with B.J. Fryer. Geochemical and geochronological studies of samples collected during this project constitute part of a doctoral dissertation at Memorial University by the author.

Laboratory work is supported by an N.S.E.R.C. operating grant to B.J. Fryer and a Memorial University of Newfoundland Fellowship to the author. Aircraft support and expediting services provided by the Geology Office, D.I.A.N.D., Yellowknife, were indispensible and are gratefully acknowledged. Peter de Bie provided able assistance in the field. B.J. Fryer reviewed an earlier version of this paper.

References

Easton, R.M.
1980: Stratigraphy and geochemistry of the Akaitcho Group, Hepburn Lake map area, District of Mackenzie: An initial rift succession in Wopmay Orogen (Early Proterozoic); in Current Research, Part B, Geological Survey of Canada, Paper 80-1B, p. 47-57.

Stratigraphy of the Akaitcho Group and the development of an Early Proterozoic continental margin, Wopmay Orogen, N.W.T.; in Proterozoic Basins in Canada, F.H.A. Campbell, ed., Geological Survey of Canada Paper. (in preparation)

Hoffman, P.F.
1980a: Wopmay Orogen: A Wilson Cycle of Early Proterozoic Age in the Northwest of the Canadian Shield; in The Continental Crust and its Mineral Deposits, D.W. Strangway, ed., Geological Association of Canada, Special Paper 20, p. 523-549.

Hoffman, P.F. (cont.)
1980b: Conjugate transcurrent faults in north-central Wopmay Orogen (Early Proterozoic) and their dip-slip reactivation during post-orogenic extension, Hepburn Lake map area, District of Mackenzie; in Current Research, Part A, Geological Survey of Canada, Paper 80-1A, p. 183-185.

Hoffman, P.F., St-Onge, M.R., Carmichael, D.M., and de Bie, I.
1978: Geology of the Coronation Geosyncline (Aphebian), Hepburn Lake Sheet, Bear Province, District of Mackenzie; in Current Research, Part A, Geological Survey of Canada, Paper 78-1A, p. 147-151.

Hoffman, P.F., St-Onge, M.R., Easton, R.M., Grotzinger, J., and Schulze, D.E.
1980: Syntectonic plutonism in north-central Wopmay Orogen (Early Proterozoic), Hepburn Lake map area, District of Mackenzie; in Current Research, Part A, Geological Survey of Canada, Paper 80-1A, p. 171-177.

St-Onge, M.R. and Carmichael, D.M.
1979: Metamorphic Conditions, Northern Wopmay Orogen, N.W.T.; Geological Association of Canada, Program with Abstracts, v. 4, p. 81.

44. GEOLOGY OF THE EASTERN VICINITY OF KISSEYNEW LAKE, MANITOBA

Project 800007

E. Froese and Q. Gall[1]
Precambrian Geology Division

Froese, E. and Gall, Q., Geology of the eastern vicinity of Kisseynew Lake, Manitoba; in Current Research, Part A, Geological Survey of Canada, Paper 81-1A, p. 311-313, 1981.

Abstract

In the area surrounding the eastern half of Kisseynew Lake, the boundary betwen the Flin Flon volcanic belt and the Kisseynew gneiss belt appears to be an unconformity along which quartz-rich Kisseynew gneisses overlie Amisk volcanic rocks. An elongated dome of quartzofeldspathic gneisses within the volcanic belt probably represents a diapiric uprise of lighter supracrustal rocks of uncertain stratigraphic position. Several sulphide occurrences, some associated with anthophyllite rocks, are present in volcanic rocks of felsic to intermediate composition.

Since the earliest mapping in the Flin Flon region, the boundary between volcanic and sedimentary rocks of the Amisk Group and Kisseynew gneisses has presented a stratigraphic, structural, and metamorphic problem. During the summer of 1980, a segment of this controversial boundary was examined in the area shown in Figure 44.1. The area lies near the junction of four one-mile map areas (Bateman and Harrison, 1945; Kalliokoski, 1952; Frarey, 1961; Pollock, 1964) and straddles three of these. An area in the immediate vicinity of the junction was mapped in 1980 by McRitchie (1980).

The dominant rock type of the Amisk Group is a fine grained amphibolite, probably derived from volcanic flow rocks. South of Weldon Bay, a unit of fine grained, granular biotite garnet schist and a unit of fine to medium grained amphibolite are shown (Fig. 44.1). Although included in the Amisk Group of volcanic and sedimentary rock by Wright (1929), these rocks became the object of much controversy in later mapping. Robertson (1951) regarded the biotite-garnet schist as a metasediment. Kalliokoski (1952) conceded such origin to some rocks in this unit but thought that others were mylonitized granitic rocks. The presence of fragments in a few places suggests that the rocks are metamorphosed volcaniclastic rocks of felsic to intermediate composition. A few lensey layers of garnet anthophyllite rock are present in this unit. Interlayering of amphibolites along the contact with biotite-garnet schist convinced Kalliokoski (1952) that at least some of the amphibolites were of sedimentary origin. Kalliokoski (1952) recognized hornblende gabbro as a separate map unit. However, the gabbro grades into fine grained amphibolite which could be a sedimentary gneiss (Robertson, 1951). Layers and lenses of calc-silicate rocks occur within the fine grained and medium grained amphibolite. Because of the close association of amphibolites and biotite-garnet schist, it is suggested that this unit of amphibolites represents a sequence of mafic, in part calcareous, volcaniclastic rocks. The rocks of the Amisk Group are intruded by medium grained granodiorite.

The main rock type of the Kisseynew gneisses is a grey, medium grained, quartz-rich gneiss. Within this gneiss, there is a unit of fine grained, pink, leucocratic rock, which was mapped as an alaskitic granodiorite by Kalliokoski (1952). However, the transitional contact with grey gneisses and the stratigraphic persistence suggest a sedimentary origin. East of Weldon Bay, a variety of fragments of cherty and felsic to mafic composition occur in layers of calc-silicate rocks interbedded with the pink, fine grained gneiss. Northwest of Weldon Bay, biotite-garnet schist with characteristically euhedral garnets forms a separate map unit, which extends westward as a thin but very persistent layer just north of Kisseynew Lake (McRitchie, 1980). The biotite-garnet schist is separated from the main area of quartz-rich gneisses to the southeast by a unit of layered amphibolites and hornblende gneisses which probably are of sedimentary origin.

An elongated dome, the Defender Lake gneiss dome, composed mainly of grey, medium grained, quartzofeldspathic gneisses is present within the Flin Flon volcanic belt near its northern boundary. Originally these rocks were mapped as part of the Kisseynew gneisses (Bateman and Harrison, 1945) but, although they bear a close resemblance to the unit of quartz-rich gneisses, they are somewhat more mafic and include small layers of amphibolite. A characteristic feature of this amphibolite is the alternation, measureable in centimetres, of mafic layers with felsic layers displaying remarkably straight and sharp contacts. Another unit within the gneiss dome is composed of pink granitoid gneiss having gradational contacts with the grey quartzofeldspathic gneiss. The heterogeneous nature of associated rock types suggests a derivation from supracrustal rocks of uncertain stratigraphic position.

All rocks display one prominent foliation parallel to the lithologic contacts, possibly originating as an axial plane schistosity during early recumbent folding, as postulated in other areas of the Kisseynew gneisses (Pearson, 1972). The present complex pattern of the foliation apparently resulted from an interference of at least two other fold systems.

The nature of the contact between Amisk volcanic rocks and Kisseynew gneisses has been controversial. Bruce (1918) and Wright (1929) thought that the Kisseynew gneisses stratigraphically overlie the Amisk volcanic rocks along a transitional contact. Bateman and Harrison (1945) agreed with the stratigraphic succession but suggested an erosional unconformity at the contact. Kalliokoski (1952) proposed a fault separating the Amisk Group from the Kisseynew gneisses and included the biotite-garnet schist and amphibolite south of Weldon Bay in the Kisseynew gneisses. The present mapping indicates a sharp contact of quartz-rich gneisses with units of the Amisk Group to the south, possibly representing an unconformity. As Bateman and Harrison (1945) noted there is a lithologic similarity between quartz-rich gneisses and rocks of the Missi Group, a sequence of arenites unconformably overlying the Amisk Group near Flin Flon. In the present area, the contact is not a metamorphic boundary because Amisk volcanic rocks and Kisseynew gneisses have been metamorphosed to about the same grade, corresponding to the upper part of medium grade metamorphism (Winkler, 1979). The presence of the assemblage biotite-garnet-sillimanite in some rocks and the common occurrence of muscovite, bracket metamorphic conditions between the decomposition curves of staurolite + muscovite + quartz and of muscovite + plagioclase + quartz.

[1] Department of Geology, Carleton University, Ottawa.

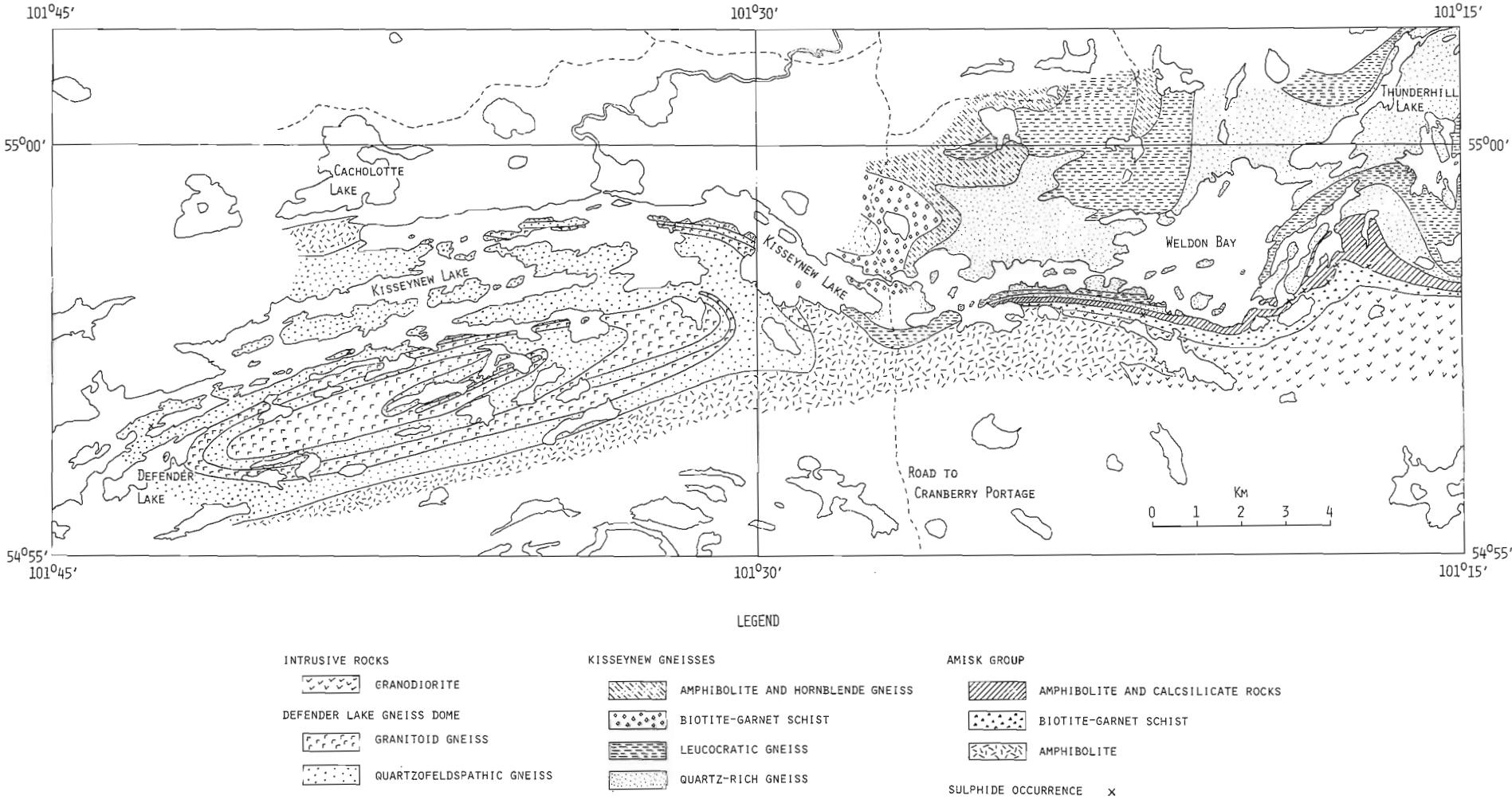

Figure 44.1. *Geological sketch map of the eastern vicinity of Kisseynew Lake.*

Sulphide mineralization has been known in the area for some time (Wright, 1931; Kalliokoski, 1952) and various deposits were recently investigated by Gale (1980). Of particular interest are several sulphide occurrences along the contact between the biotite-garnet schist and amphibolite south and southeast of Weldon Bay. Mineralization consists of disseminated and massive pyrite, pyrrhotite, chalcopyrite, and sphalerite in biotite-garnet gneiss. Anthophyllite was noted in two prospecting pits. Lensey layers of garnet-anthophyllite rock are also present in the biotite-garnet schist without associated mineralization. They probably represent metamorphosed hydrothermally altered rocks. The deposit south of Weldon Bay occurs in finely layered, very siliceous rock. The presence of quartz phenocrysts in some layers suggests a rhyolitic tuff although other layers could be cherty sediments (Gale, 1980). The geological setting suggests that the sulphide occurrences represent volcanogenic mineralization in felsic to intermediate volcaniclastic rocks of the Amisk Group.

Acknowledgment

We are much obliged to D.P. Price for alerting us to the presence of fragmental rocks in the unit of biotite-garnet schist south of Weldon Bay.

References

Bateman, J.D. and Harrison, J.M.
1945: Mikanagan Lake, Manitoba; Geological Survey of Canada, Map 832A with descriptive notes.

Bruce, E.L.
1918: Amisk-Athapapuskow Lake district; Geological Survey of Canada, Memoir 105.

Frarey, M.J.
1961: Collins Point, Manitoba; Geological Survey of Canada, Map 1068A with descriptive notes.

Gale, G.H.
1980: Mineral deposit studies – Flin Flon/Kisseynew; Manitoba Mineral Resources Division, Report of Field Activities 1980, Paper GS-10, p. 51-64.

Kalliokoski, J.
1952: Weldon Bay map-area, Manitoba; Geological Survey of Canada, Memoir 270.

McRitchie, W.D.
1980: Cacholotte Lake (parts of 63 K/13,14 and 63N/3,4); Manitoba Mineral Resources Division, Report of Field Activities 1980, Paper GS-11, p. 65-69.

Pearson, D.E.
1972: The location and structure of the Precambrian Kisseynew gneiss domain of northern Saskatchewan; Canadian Journal of Earth Sciences, v. 9, p. 1235-1249.

Pollock, G.D.
1964: Geology of the Duval Lake area; Manitoba Mines Branch, Publication 61-6.

Robertson, D.S.
1951: The Kisseynew lineament, northern Manitoba; The Precambrian, v. 24, p. 8-11, 13, 23.

Winkler, H.G.F.
1979: Petrogenesis of metamorphic rocks, fifth edition; Springer-Verlag, New York.

Wright, J.F.
1929: Kississing Lake area, Manitoba; Geological Survey of Canada, Summary Report 1928, part B, p. 73-104.

1931: Geology and mineral deposits of a part of northwestern Manitoba; Geological Survey of Canada, Summary Report 1930, part C, p. 1-124.

45. METAMORPHISM IN THE CROWDUCK BAY AREA, MANITOBA

Project 800014

T.M. Gordon
Precambrian Geology Division

Gordon, T.M., Metamorphism in the Crowduck Bay area, Manitoba; in Current Research, Part A, Geological Survey of Canada, Paper 81-1A, p. 315-316, 1981.

Abstract

Isograds previously mapped in the Snow Lake area have been extended eastward where they are cut by a northeast trending fault.

Mapping and petrologic studies by Froese and Gasparrini (1975) and Froese and Moore (1980) have documented the regional metamorphism in the Snow Lake area of the Aphebian Flin Flon volcanic-sedimentary belt. The current project is intended to extend their work eastward and elucidate the history and metamorphism of rocks near the eastern end of the belt.

The area under study extends from Wekusko Lake to longitude 99°30'W and from latitude 54°45'N to 55°00'N. A 1:250 000 geological map published by Bell (1980) covers this region and incorporates the 1:63 360 mapping of Armstrong (1941) and Frarey (1950). Detailed studies within the area are those of Stockwell (1937) and Shanks and Bailes (1977). Adjacent areas have been mapped at 1:50 000 scale by Bailes (1975, 1976), and Lenton (1978).

The general geology of the eastern end of the Flin Flon belt is concisely summarized in Bailes (1980). The main lithologic subdivisions are:

Intrusive rocks

Missi Group metavolcanic rocks

Missi Group metasedimentary rocks

Amisk Group metasedimentary rocks

Amisk Group metavolcanic and intrusive rocks.

Mapping during 1980 was restricted to areas accessible from Wekusko Lake and Grass River. Particular emphasis was given to Amisk and Missi metasedimentary rocks where they were sufficiently aluminous to record the isograds mapped to the west by Froese and Moore (op. cit.). Reconnaissance of Missi metavolcanic rocks was carried out to select areas for future detailed examination and chemical sampling.

Figure 45.1 shows the distribution of aluminous metasedimentary rocks and minerals identified in the field. Points west of Wekusko Lake are from Froese (personal communication). Although thin section petrography will be required to establish compatible mineral assemblages, a preliminary isograd pattern can be deduced. A northeast trending fault mapped by previous workers along the Grass River apparently offsets the isograds.

Samples collected for age determination studies from Missi quartz-feldspar porphyry bodies were unfortunately found to contain no zircon.

References

Armstrong, J.E.
1941: Wekusko (Herb) Lake, Manitoba; Geological Survey of Canada, Map 665A.

Bailes, A.H.
1975: Geology of the Guay-Wimapedi Lakes area; Manitoba Mineral Resources Division, Geological Services Branch, Publication 75-2.

1976: Saw Lake area (Grass River Project); in Report of Field Activities, 1976; Manitoba Mineral Resources Division, p. 45-50.

1980: Geology of the File Lake area; Manitoba Mineral Resources Division, Geological Report 78-1.

Bell, C.K.
1980: Geology, Wekusko Lake map area, Manitoba; Geological Survey of Canada, Memoir 384.

Frarey, M.J.
1950: Crowduck Bay, Manitoba; Geological Survey of Canada, Map 987A.

Froese, E. and Gasparrini, E.
1975: Metamorphic zones in Snow Lake area, Manitoba; Canadian Mineralogist, v. 13, p. 162-167.

Froese, E. and Moore, J.M.
1980: Metamorphism in the Snow Lake area, Manitoba; Geological Survey of Canada, Paper 78-27.

Lenton, P.G.
1978: Geology of the McNeill Lake – Pistol Lake area; in Report of Field Activities, 1978; Manitoba Mineral Resources Division, p. 40-42.

Shanks, R.J. and Bailes, A.H.
1977: "Missi Group" Rocks, Wekusko Lake Area; in Report of Field Activities, 1977; Manitoba Mineral Resources Division, p. 83-87.

Stockwell, C.H.
1936: Gold deposits of Herb Lake area, northern Manitoba; Geological Survey of Canada, Memoir 208.

***(Figure 45.1** over)*

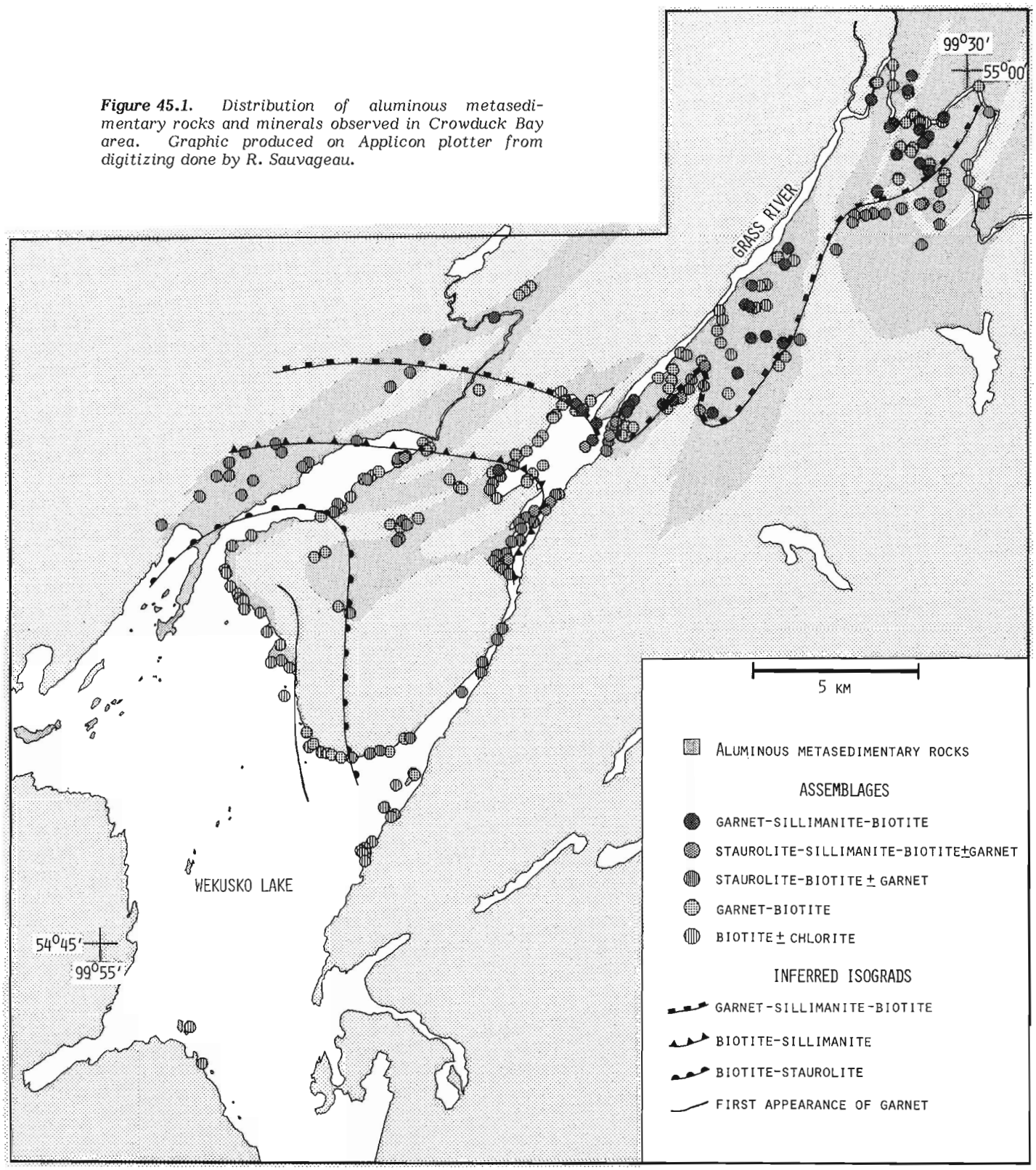

Figure 45.1. *Distribution of aluminous metasedimentary rocks and minerals observed in Crowduck Bay area. Graphic produced on Applicon plotter from digitizing done by R. Sauvageau.*

46. # ASPECTS OF THE GLACIAL HISTORY OF BYLOT ISLAND, DISTRICT OF FRANKLIN

Project 780018

R.A. Klassen
Terrain Sciences Division

Klassen, R.A., Aspects of the glacial history of Bylot Island, District of Franklin; in Current Research, Part A, Geological Survey of Canada, Paper 81-1A, p. 317-326, 1981.

Abstract

Erratics derived from north-central Baffin Island prove that large glaciers have moved onto Bylot Island across both the north and south coasts. The maximum elevation to which such debris has yet been found is about 1100 m a.s.l. and these high-level erratics are considered to have been emplaced prior to the 'last' glaciation. During the 'last' glaciation ice form offshore sources carried debris to maximum elevations of between 300 and 550 m a.s.l.; debris was carried by two glaciers – the first flowed northward through Admiralty Inlet and then eastward within Lancaster Sound, while the second flowed northward through Milne Inlet and then eastward within Pond Inlet. Both glaciers were grounded within the marine channels that they occupied. Shell fragments from glacial and derived deposits associated with that stade have minimum amino acid ratios (free) of about 0.3. Shells from material deposited after that event are more than 35 000 radiocarbon years old and have amino acid ratios of about 0.24. Subsequent to the maximum of the last glaciation, Bylot glaciers expanded 10 to 15 km beyond their present limits.

Introduction

Northern Baffin and Bylot islands have conceivably been traversed by ice originating from major independent ice sheets that converged within Lancaster Sound and flowed eastwards towards northern Baffin Bay during Pleistocene glaciations. Accumulation areas of those ice sheets may have been located to the north, over the islands of the Arctic Archipelago, and to the south, over Foxe Basin or the main part of the Canadian Shield. The location of Bylot Island within that area of convergence and outflow suggests that evidence of glaciation from there is key to the glacial history of the entire eastern Canadian Arctic. Despite this, little geologic information about the area has been available.

During the summers of 1978 and 1979, the Geological Survey of Canada conducted field studies of the Quaternary geology and glacial history of the Bylot Island region (Fig. 46.1). Those studies addressed the extent of former glacier ice cover, the source areas(s) of that ice, and the timing of ice movement(s). Most of the fieldwork was done on Bylot Island. This is a preliminary report on the evidence of movement onto Bylot Island by ice from offshore sources and of interaction of that ice with glaciers nourished there during what is interpreted to have been the maximum of the last glaciation. For this report, 'last glaciation' refers to glacial events of approximately the last 125 000 years and is used in a general sense.

In this paper the term 'foreign' is used to describe either glacier ice or debris carried onto Bylot Island, in contrast to 'native' ice or debris that is considered to have originated there. It may also refer to landforms created by foreign ice. The glacial history of Bylot Island is essentially one of interaction between foreign and native ice. Focus on this interaction is important. Bylot Island is physically isolated from Baffin Island, despite their proximity, by deep (> 500 m) marine channels (Fig. 46.1). Consequently, foreign ice deposits on Bylot Island must relate to major glacial events elsewhere. The extent of interaction between foreign and native ice is then a potentially unique measure of the dynamics of a large ice sheet and conditions of glacierization along a segment of its margin.

Because a variety of lithologically distinct areas of bedrock is found within the region, foreign erratics can be distinguished easily from those of local glaciers. In areas lying above the limits of marine submergence, the presence of such debris is compelling evidence of glaciation by foreign ice and, where their bedrock sources can be determined, net flow paths within that ice as well. Thus, erratics on Bylot Island form the principal evidence discussed here.

Only evidence related to the maximum advance of foreign ice and the extent to which it interacted with native ice during the last glaciation has been considered. I do not wish to imply by its omission that evidence of other glacial events, either foreign or native, does not exist.

Bedrock Geology

Bedrock geology of the study area has been mapped at a scale of 1:250 000, although the level of detail varies greatly between adjoining map sheets. Consequently, the definition of distinctive bedrock sources for purposes of boulder tracing is restricted by the most general scheme of mapping. Five rock suites have been defined on the basis of their lithologic and faunal characteristics with reference to published work (Fig. 46.1); they form source areas for the dispersal of glacial erratics.

A variety of igneous and metamorphic rock types of Archean and Aphebian ages comprises a basement complex that underlies much of Bylot Island and north-central and northeastern Baffin Island (Fig. 46.2). This suite of crystalline rocks has not been divided further and is considered as a single source area. No attempt has been made to differentiate crystalline debris from Baffin Island from that originating on Bylot Island. Crystalline erratics, however, are easily distinguished from the other rock suites.

Proterozoic volcanic rocks comprise a second physically and lithologically distinctive suite that outcrops near the northern shore of Fury and Hecla Strait, along the eastern shore of Admiralty Inlet, and on northern Bylot Island (Fig. 46.1). Exposures along Admiralty Inlet are areally the largest. On Borden Peninsula and on Bylot Island this rock type is mapped as part of the Nauyat Formation (Jackson et al., 1978). The rocks are fine grained, brown to reddish brown, and amygdaloidal. Amygdules are infilled with calcite and quartz, among other minerals (Fig. 46.2a).

A third suite is comprised of silica-cemented quartz arenites of the Proterozoic Nauyat, Adams Sound, and Arctic Bay formations which are mapped across Borden Peninsula and western Bylot Island (Jackson and Davidson, 1975; Jackson et al., 1978). Only the outcrop area of Adams Sound

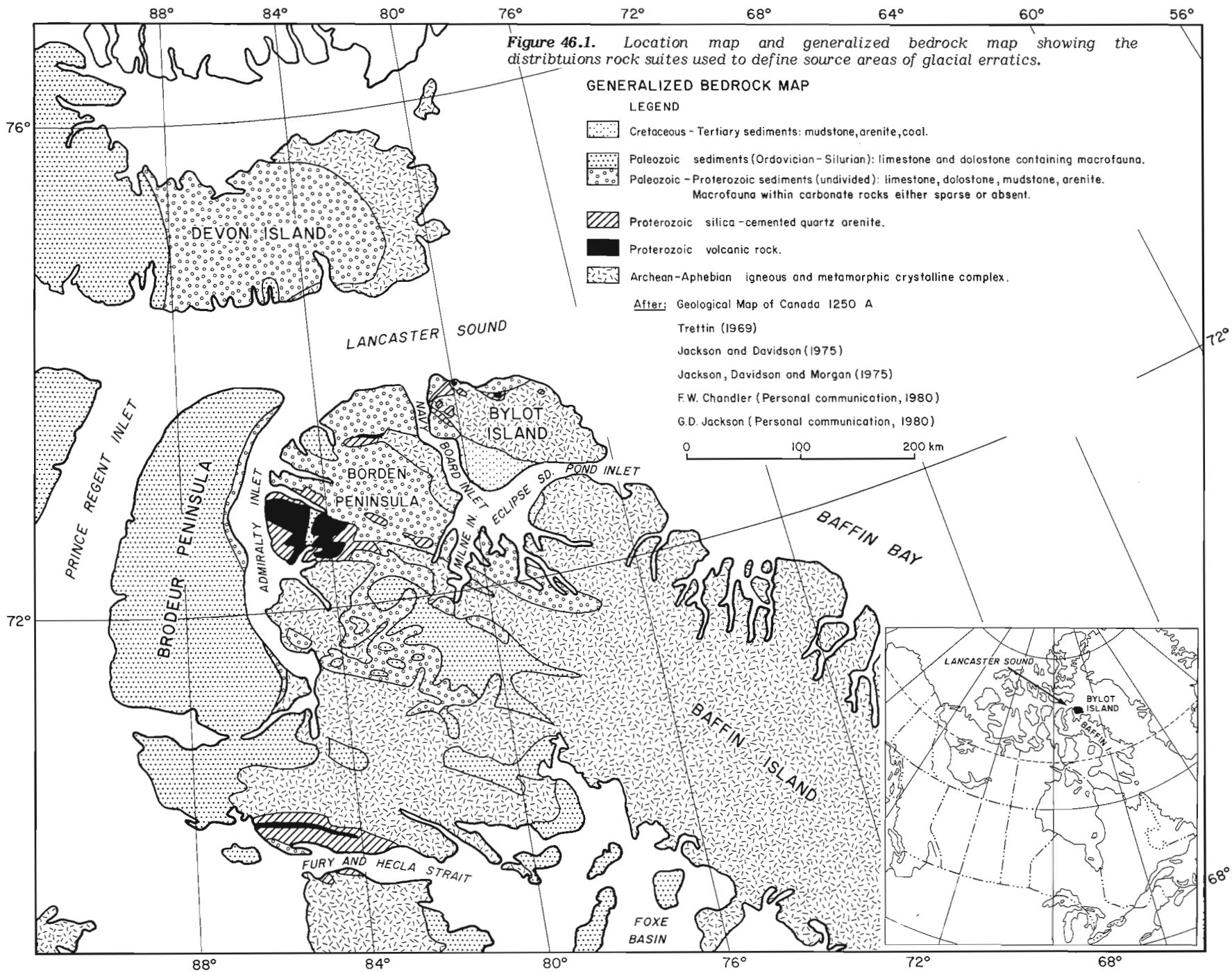

Figure 46.1. *Location map and generalized bedrock map showing the distribtuions rock suites used to define source areas of glacial erratics.*

Formation, the largest single source, is shown in Figure 46.1. Erratics found on Bylot Island are commonly pink and light brown and, in a few cases, are well rounded (Fig. 46.2b).

Proterozoic and Paleozoic sedimentary rocks that include diverse carbonate rock types, mudstones, and arenites underlie all of Brodeur and most of Borden peninsulas, much of western Bylot Island, and western Devon Island (Jackson et al., 1978; Trettin, 1969; Thorsteinsson, 1970) (Fig. 46.1). Although this suite represents several formations, only erratics containing abundant macrofauna can readily be matched to specific source areas, which lie on north-central Baffin Island south of Milne Inlet, on Borden Peninsula, and on westernmost Devon Island. Those erratics can be distinctive in appearance (Fig. 46.2c).

Poorly consolidated sedimentary rocks of Cretaceous-Tertiary age underlie the lowlands on southern Bylot Island and on Baffin Island to the south across Eclipse Sound (Fig. 46.1). The rocks of this fifth suite, which include mudstones, immature to mature arenites, and coal (Miall et al., 1980) are easily distinguished in the field from those of the Proterozoic and Paleozoic successions.

Most of the evidence presented here concerning glacier transport of debris onto Bylot Island refers to deposits located east of longitude 80°W on the island. East of that line the occurrence of either volcanic rocks or Proterozoic-Paleozoic sedimentary rocks as erratics can be taken as unequivocal evidence of onshore movement of foreign ice, excluding the lowland area near Maud Bight. Those erratic rock types stand in clear visual contrast with the underlying crystalline and Cretaceous-Tertiary sedimentary bedrock.

Distribution of Foreign Glacial Erratics

The distribution of foreign erratics has been mapped across both Bylot Island and the northern shore of Baffin Island along Eclipse Sound and Pond Inlet (Fig. 46.3). The maximum elevations to which this debris has been found vary around the margin of Bylot Island. Erratics of pink quartz arenite, thought to have been derived from either the Adams Sound or Nauyat formations, were found to 1130 m a.s.l. immediately west of Sermilik glacier, and erratics of other Proterozoic sedimentary rocks, including carbonates, were found at 820 m a.s.l. in the same area (Fig. 46.3). These are the highest elevations to which sedimentary erratics were found within the crystalline complex anywhere on the island.

The quartz arenites have, conceivably, an alternative native origin from small unmapped outliers of either Nauyat or Adams Sound formations within the Byam Martin Mountains. Although such outliers could exist, given the

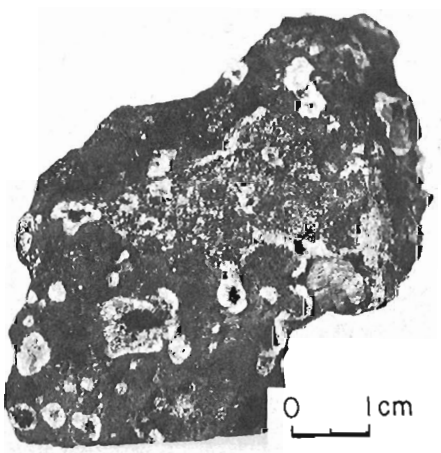

a

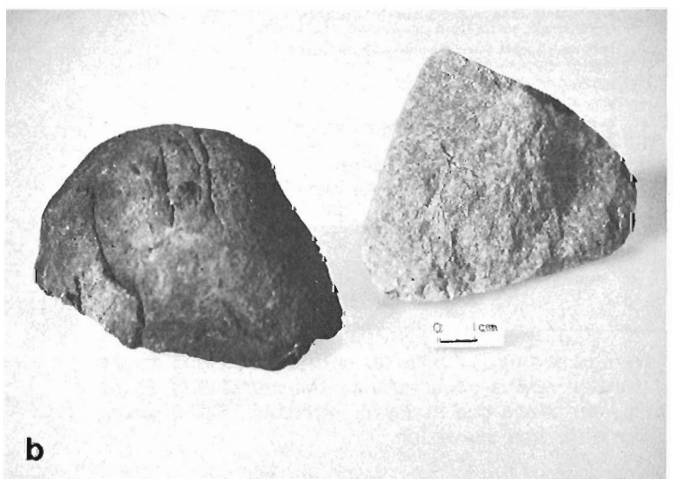

b

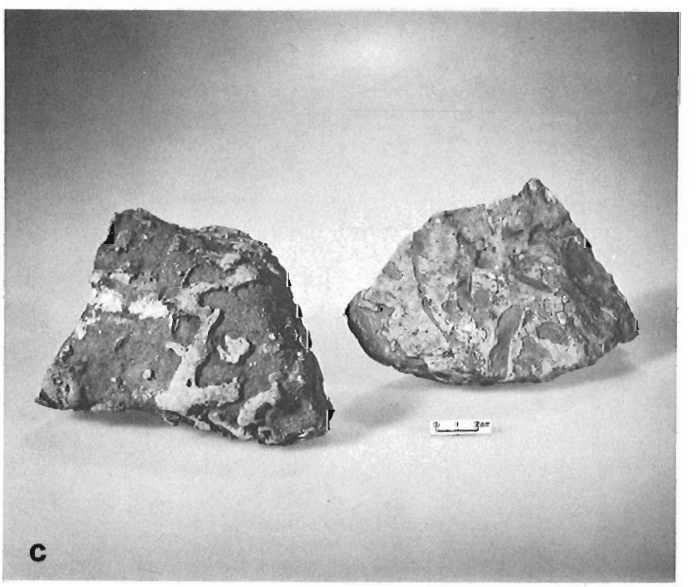

c

a. Amygdular volcanic rock found near Bathurst Bay at about 200 m a.s.l. GSC 203650-I ;

b. Pink and light brown quartz arenites, thought to have been derived from the Adams Sound Formation GSC 203650-A ;

c. Paleozoic carbonate rocks containing abundant macrofauna and typical of those types of erratics found within the outer foreign erratic zone. GSC 203650-F.

Figure 46.2. *Foreign glacial erratics found on Bylot Island.*

regional geologic setting described by Jackson et al. (1975), none are known anywhere within the eastern portion of the crystalline highlands, and consequently their interpretation as foreign erratic debris is favoured.

In general, the maximum elevations attained by foreign debris were higher along the southern side of the island. Although the site elevations reported above were exceptionally high, foreign debris was found commonly at elevations to 700 m a.s.l. along Pond Inlet. Maximum levels on the northern side were about 550 m a.s.l.

Foreign debris can be characterized both by its abundance and by it gross lithologic composition; a broad "foreign erratic" zone can be mapped around most of the outer margin of Bylot Island on the basis of those criteria (Fig. 46.3). This outer zone is characterized by abundant foreign debris and, in areas not situated in front of large modern glaciers, extends to elevations between 300 m a.s.l. and 550 m a.s.l.; in front of some modern glaciers the maximum elevations of the foreign erratic zone are lower than on adjacent valley walls or foreign debris may be

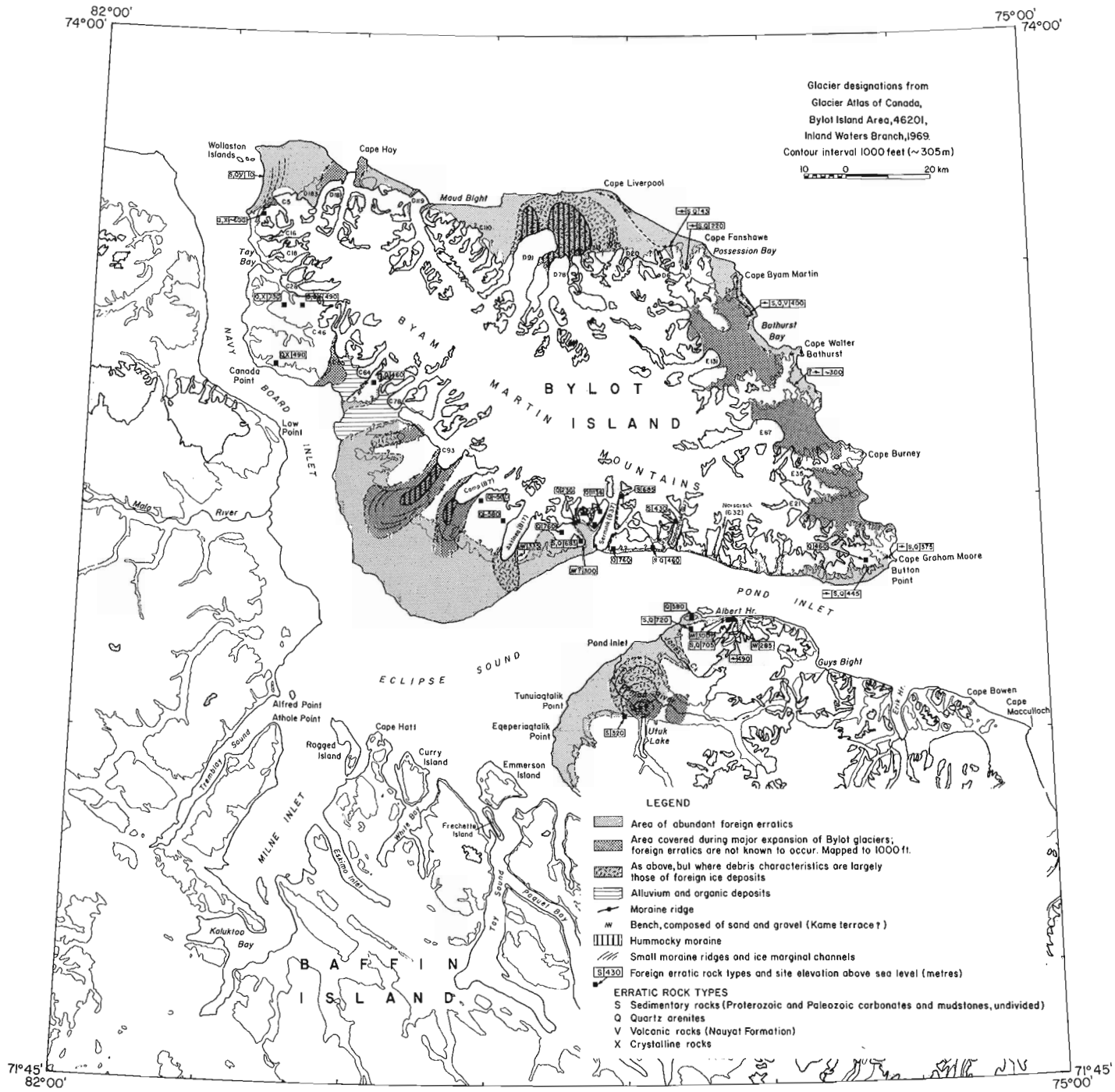

Figure 46.3. *Preliminary map showing the distribution of foreign and native erratics on Bylot Island and part of northern Baffin Island. Areas characterized by abundant foreign debris occur around the margins of Bylot Island and in places are bounded on their inland, distal side by moraines and by kame terraces. Sites where foreign erratics are found above that zone are also noted, along with their elevation.*

Figure 46.4

Moraine formed by foreign ice moving onto the northeastern coast of Bylot Island out of Lancaster Sound. The moraine contains a high proportion of carbonate sedimentary rocks and is consequently light toned in contrast to the crystalline bedrock. No foreign debris occurs distal to it. Note the tor-like features on the skyline. The clifftop position of this moraine, which lies between 350 and 400 m a.s.l., is shown more clearly in Figure 46.5. GSC 203639-K

altogether absent (e.g. glacier C93, glacier E67*). (The term 'abundant' is used here in a general sense to mean that such debris can be readily seen by examination of erratics in the field.) Farther inland and above the foreign erratic zone, the abundance of foreign debris is markedly lower, and in many transects made across the mapped boundary no such debris was found on the inland (distal) side. In those situations the abrupt change in lithologic composition is striking. It is important to note, however, that foreign debris can be found on the inland side of the mapped boundary in some places (Fig. 46.3).

Along the southern coast of Bylot Island the outer foreign erratic zone contains erratics clearly representative of three source areas: (1) Proterozoic and Paleozoic carbonate sedimentary rocks (undifferentiated); (2) quartz arenites; and (3) carbonate rocks containing abundant macrofauna, listed in decreasing order of abundance. Inland of that zone no sedimentary rocks with macrofauna have been found and quartz arenites appear to be the predominant foreign erratic type. The source areas of much of the foreign debris within the outer foreign erratic zone must lie on north-central Baffin Island south of Milne Inlet, a conclusion based primarily on the distribution of erratics of fossiliferous Paleozoic sedimentary rocks.

Along the northern coast, foreign erratics include representatives of all of the lithologic groups, with the possible exception of Cretaceous-Tertiary sedimentary rocks. Because of the diverse and scattered distribution of potential source areas of the sedimentary erratics, they can be used only to demonstrate flow of foreign ice onto the island without providing evidence of specific source areas.

The volcanic erratics, however, are of particular interest because of the more restricted extent of outcrop source areas. They have been found in glacial deposits along the northern coast of Bylot Island from its westernmost tip as far east as Bathurst Bay. Some of these erratics are fine grained and amygdular and are similar in appearance to outcrops described from Admiralty Inlet (Jackson et al., 1978; p. 4); outcrops of volcanic rocks on Bylot Island are thought to be coarser grained and lacking in amygdules (G.D. Jackson, personal communication, 1980). If the source area of the amygdular volcanic erratics is Admiralty Inlet, as it appears to be, then their presence in glacial deposits along the northern coast strongly indicates that they were carried there by a glacier that moved northward through Admiralty Inlet and eastward down Lancaster Sound.

Foreign Glacial Landforms

Foreign landforms and deposits coincident with the inland margin of the outer foreign erratic zone can be traced on air photographs around much of the island (Fig. 46.3). Across most of the southern lowland of Bylot Island the inland margin was defined at about 500 m a.s.l. by ground checking of the distribution of erratic types. A continuous morphologic boundary along that margin was not identified in that area, although as mapped the margin is associated with the headward limit of abundant small meltwater channels. East of Aktineq glacier (B17) a bench (kame terrace?) composed mostly of sand and gravel at about 335 m a.s.l. marks the inland boundary; a similar feature at a comparable elevation occurs above Sermilik glacier (B37) although it is not known if it too lies along the inland limit of the foreign erratic zone (Fig. 46.3). Between Sermilik glacier and Button Point the coast is fronted by steep cliffs that in places rise to more than 1000 m a.s.l.; consequently moraines either were not deposited or their position and elevation are difficult to determine. Along that section of coast, ice marginal positions are thought to lie between about 400 and 450 m a.s.l. based on the recognition of abundant foreign debris below those altitudes at a few sites and on the occurrence of trimlines and short segments of lateral moraines inland along the walls of valleys that intersect the coast. Above Button Point foreign moraines are draped across headlands between valleys and are coincident with the inland boundary of the foreign erratic zone. Neither the inland extension of those moraines nor any foreign debris was seen in that area more than 1 to 2 km inland beyond the valley mouths and at much lower elevations than the moraines.

Along the northeastern coast of Bylot Island, southeast of Cape Fanshawe, a foreign moraine follows closely along the edge of high (300 to 400 m) coastal cliffs (Fig. 46.3, 46.4). It is easily identified by virtue of its morphologic definition and 'perched' topographic position and, as first suggested by Hodgson and Haselton (1974, p. 7), probably represents a maximum ice-marginal position for a large glacier grounded within Lancaster Sound. This conclusion is further supported by observations of the considerable abundance of foreign debris which it contains and the apparent absence of foreign debris inland (distal) from it. The moraine varies in form along its length from a broad, thin (< 1 m thick) surface cover of foreign debris to a well defined sharply peaked ridge several metres high. It lies between 350 and 400 m a.s.l.,

*Glacier designations from the Glacier Atlas of Canada (1969).

based on topographic maps, and extends more or less continuously for about 20 km between Cape Byam Martin and Bathurst Bay. It turns inland and declines in elevation along the northern side of the valley that ends in Bathurst Bay, but does not appear to extend more than a few kilometres up the valley (Fig. 46.5). Southeast of that bay it is less clearly defined and generally decreases in overall elevation along the outer coast. It is not evident southeast of Cape Burney.

A second foreign moraine also occurs along the northeast coast, but at much lower elevations (≤ 50 m a.s.l.). It can be traced across the outer valley floors in areas where the higher moraine has been observed. The relationship between the two moraines is not clear, but based on their morphological relationship the lower system is either roughly contemporaneous with or younger than the higher moraine.

Glacial Maximum: The Extent of Foreign vs. Native Ice

During the maximum of the last glaciation, at least some of the major native Bylot glaciers, and possibly all, were in contact and interactive with foreign ice that filled offshore areas. Some of the large modern glaciers, for example Aktineq (B17), Sermilik (B37) and glacier D91, currently lie well below and extend outwards beyond the maximum inland limits of foreign debris. Because it does not seem likely that those glaciers are less extensive today than during conditions of full glaciation, they must have been contiguous with the foreign ice, although overpowered by it, at least in their lower reaches.

The distribution of foreign debris in areas in front of Bylot glaciers is variable, and no foreign debris has yet been found within either the zone of hummocky moraine in front of glaciers C93 and B7 or in the main parts of valleys along the northeastern coast at, and southeast of, Bathurst Bay (Fig. 46.3). Areas where foreign debris does not occur are probably zones where native ice successfully restricted the influx of foreign ice; this is supported by the observation that foreign debris occurs to higher elevations across headlands between valleys where it has not been found.

Between Cape Hay and Cape Fanshawe, till within modern end moraines of native glaciers differs lithologically from the older till that lies distal to them between the highlands and the coast. The older till contains a much higher component of sedimentary rocks. Although no debris that is unequivocally foreign has been found here above elevations of 50 m a.s.l., it seems reasonable to suggest that the older till was deposited by ice flowing along the mountain front, parallel to Lancaster Sound rather than into it. Thus, it would seem that native ice did not successfully restrict onshore movement of ice in the Cape Hay – Cape Fanshawe region.

Native Ice Advance

Landforms in front of large Bylot glaciers, including meltwater channels and both lateral and end moraines, demonstrate that at least one major expansion of native ice did occur subsequent to high level inundation of the island by foreign ice. This has also been noted by Hodgson and Haselton (1974). During that advance, native ice extended 10 to 15 km beyond its present limits. In some areas overridden by native ice during the major advance (e.g. in front of Aktineq (B17), Sermilik (B37), glacier (D91), however, glacial deposits contain abundant foreign debris and can be strikingly different in texture and lithology from material within modern moraines (Fig. 46.3). This suggests that little if any erosion or redistribution of drift occurred during that major expansion of native ice.

Timing of the Last Major Foreign Ice Advance

Evidence bearing on the timing of the maximum foreign ice advance of the last glaciation is derived from both ^{14}C analysis and ratios of the amino acids D-allo isoleucine to L-isoleucine from **Hiatella arctica** and **Mya truncata** found within Quaternary sediments. The amino acid ratios referred to here are based on the 'free' or naturally hydrolyzed protein

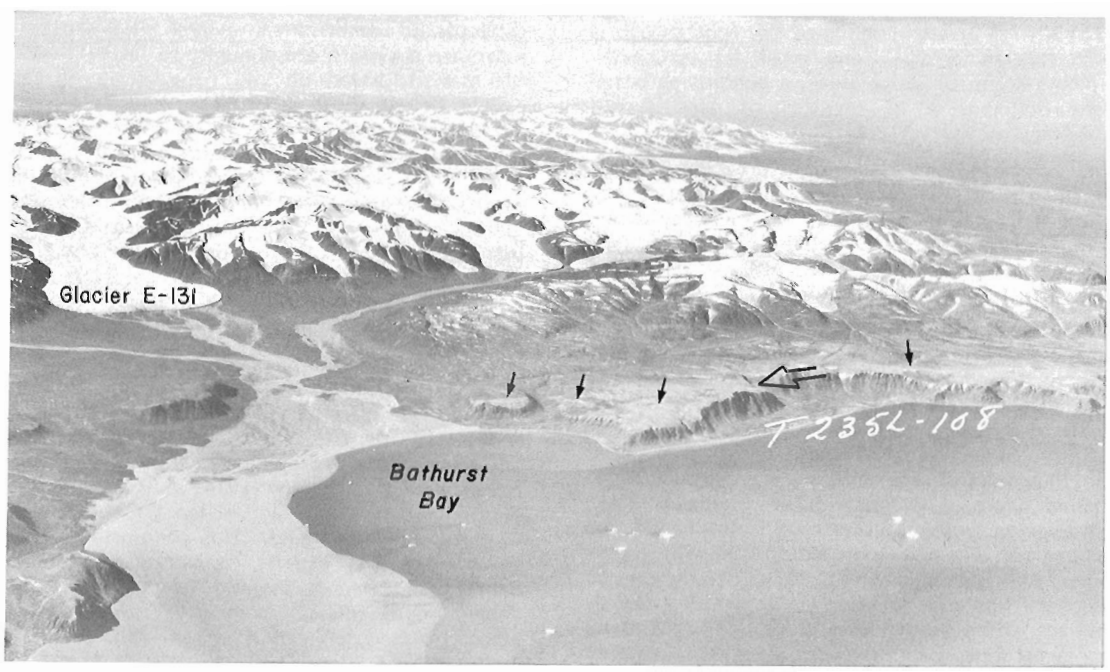

Figure 46.5. *Foreign moraine (black arrows) on northeastern Bylot Island along the southern coast of Lancaster Sound. The highest point along the cliff is 410 m a.s.l. The view shown in Figure 46.4 is indicated by an open arrow (EMR T23SL-108).*

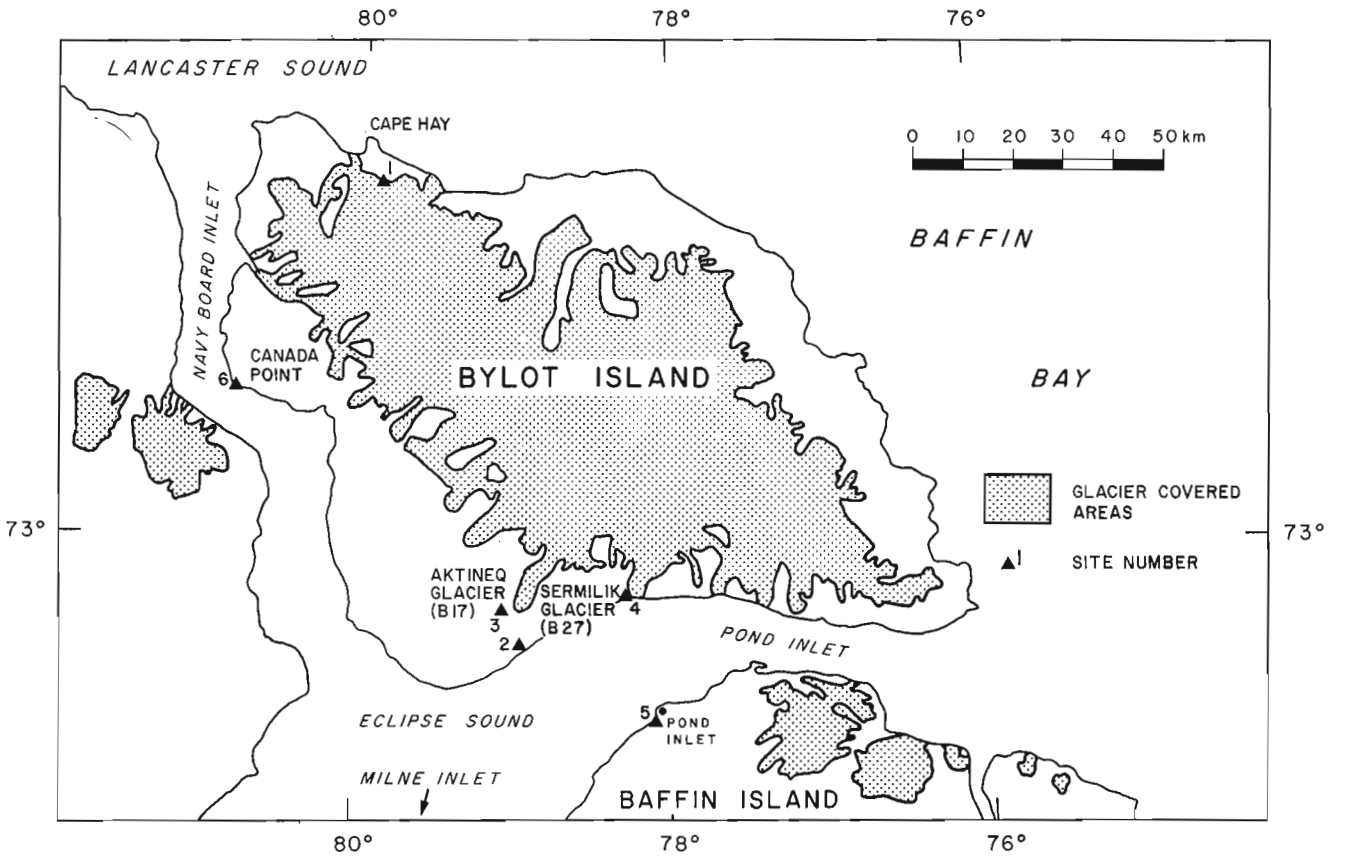

Figure 46.6. *Location map of shell collections referred to in Table 46.1.*

component of the shells (cf. Miller et al., 1977). Although amino acid ratios are not necessarily directly proportional to absolute shell ages, in this report that relationship will be assumed and the ratios will be referred to as though they can define a chronostratigraphic boundary. Few analyses are available, and, consequently, conclusions drawn from these must be considered as preliminary.

Small marine shell fragments have been found within deposits of foreign glacial debris at sites near Aktineq glacier (B17), Sermilik glacier (B37), and eastwards of Cape Hay (sites 1 to 4, Fig. 46.6). The shells are thought to have been transported onto the island by foreign ice either because they were found at altitudes above expected maximum marine limits or because they were collected from sediments thought to be of glacial origin. Although the fragments are clearly not in situ and consequently do not necessarily bear any close age relationship to the enclosing sediments, they can be used to provide a 'maximum' estimate for the age of the ice advance. In this case, the ratios ranged between 0.3 and 0.5 (Table 46.1). Thus, a minimum amino acid ratio 'dating' this advance is thought to be of the order of about 0.3. The small size of these fragments and problems of species determination require that caution be used in their interpretation, and they are presented here only as a guide.

In southeastern Baffin Island, amino acid ratios of at least 0.4 to 0.45 are associated with deposits of the last interglaciation (Brigham, 1980; Miller et al., 1977). Thus, it would appear that the last major advance of foreign ice onto Bylot Island occurred some time during the last glaciation, probably shortly after the last interglacial.

Estimates of the minimum age of the foreign ice advance are considered to be based on better evidence. At Canada Point, whole valves of **Mya truncata** were collected from a large deltaic complex that did not appear to have been modified or covered by glacier ice. Many shells were found paired and oriented with their siphuncle ends upward, and are consequently considered to have been found in situ. The shells were well preserved, most having retained either all or part of their periostracum, and no pitting or other alteration, apart from minor surface chalkiness, was observed. The shells were aragonitic (W. Blake, Jr., personal communication, 1980). They were estimated to be more than 35 000 (GSC-2916) radiocarbon years old and their amino acid ratios were about 0.24 (AAL-1218; Table 46.1). These determinations are considered to constitute an upper 'time' boundary of the last major advance of foreign ice onto Bylot Island.

The timing of the major expansion of native ice is not known. Based on ^{14}C analysis of peat buried beneath the end moraine of Aktineq glacier, that glacier "is as far advanced as it has been in the past 7000 to 8000 years, or longer." (DiLabio and Shilts, 1979, p. 148). Observations of advanced weathering of glacial erratics within the zone of former native ice cover suggest that the major native ice advance is much older than the ^{14}C date.

Discussion

Whether all of the observed foreign debris was emplaced during the last glaciation or not is currently unknown, although it seems clear that foreign ice did attain elevations between 300 and 550 m a.s.l. during the maximum stage of that event. This conclusion is based mainly on the amino acid ratios of ice-transported shell fragments. The only indication of more than one major inundation of Bylot Island by ice is based on the coincidence of moraines and

Table 46.1

Site No. (see Fig. 46.6)	Laboratory Sample No.[1]	Locality	Elevation (m a.s.l.)	Amino Acid Ratio[2]	^{14}C Age[3]	Species	Comments
1	AAL-1971	10 km east of Cape Hay	∿ 335	0.3	-	**Hiatella arctica**(?)	Small shell fragment within foreign glacial debris at surface. Only one amino acid determination.
2	AAL-1392	Near Aktineq Glacier (B17)	∿ 12	0.39	-	**Hiatella arctica**(?)	Small shell fragment within foreign glacial deposit that forms part of a stratigraphic section. Only one amino acid determination.
3	AAL-1470	Near Aktineq Glacier (B17)	∿ 230	0.41, 0.50	-	**Hiatella arctica**	Angular shell fragments from ice-contact fluvial deposit. Deposit partly stratified and contains abundant foreign debris.
				0.37, 0.50	-	**Mya truncata**	
4	AAL-1475	Near Sermilik Glacier (B37)	-	0.30, 0.29	-	**Mya truncata**(?)	Small shell fragments from foreign glacial deposit that forms part of a stratigraphic section.
5	GSC-1964	∿1.5 km southwest of Pond Inlet	65	-	33 300 ± 800	**Mya truncata**	Shell fragments from ice-contact fluvial deposits or marine deposits (from Hodgson and Haselton, 1974, p. 7).
	No AAL no. available	∿1.5 km southwest of Pond Inlet	65	0.27	-	**Mya truncata**	
6	GSC-2916	Canada Point	25	-	>35 000	**Mya truncata**	Shell in situ within a large delta complex. Valves intact and well preserved.
	AAL-1218	Canada Point	25	(0.23, 0.26), (0.13, 0.24), 0.22)		**Mya truncata**	

[1] AAL – Institute of Arctic and Alpine Research, Amino Acid Laboratory.
GSC – Geological Survey of Canada, Radiocarbon Dating Laboratory.

[2] Ratios of D-allo isoleucine to L-isoleucine in naturally hydrolyzed protein fraction.

[3] Radiocarbon years before present (B.P.)

other ice-contact deposits with the inland limits of abundant foreign debris (~300 to 550 m a.s.l.) well below the maximum elevations (800 to 1100 m a.s.l.) to which foreign debris has been found. That coincidence would appear to define an ice-marginal position attained by foreign ice during the maximum of the last glaciation; by implication then, this interpretation requires the existence of at least one earlier glacial event of greater magnitude to account for the high-level erratics.

At the time of emplacement of the high-level erratics, foreign ice must have crossed the topographic divide of Bylot Island at least in the few places where its elevation lies below about 1100 m a.s.l. From examination of topographic maps it is evident that during that event foreign ice flowing from the south probably contributed to northward-flowing native glaciers terminating at the western end of Maud Bight and to glaciers ending along the northeast coast between Cape Burney and Button Point. It is possible that the foreign ice was much thicker than the maximum elevations to which foreign erratics have been found and, in that case, more of the island would have been covered by foreign ice.

The glacial erratics found on Bylot Island demonstrate that during the maximum of the last glaciation foreign ice crossed onto the island from the north out of Lancaster Sound and from the south out of Eclipse Sound and carried debris to elevations of between 300 and 550 m a.s.l. That ice must have completely covered the marine channels and have been grounded within them. Because the maximum depths of those channels are about 1000 m (Canadian Hydrographic Services Chart 7220), a minimum estimate of ice thickness around Bylot Island is about 1500 m.

The volcanic erratics along the northern coast of Bylot Island indicate that the ice that carried them probably flowed northwards through Admiralty Inlet before turning eastwards towards Baffin Bay. The source of the ice was then either at or south of north-central Baffin Island. Because the glacier remained against the northern coast of Bylot Island and was at least 1500 m thick there, it is suggested here that it must have merged with a larger glacier within Lancaster Sound and held the status of a coalescent tributary glacier. The tributaries of that large glacier within Lancaster Sound probably included a north-flowing glacier within Prince Rupert Inlet to the west and ice from Devon Island to the north.

Across southern Bylot Island erratics of fossiliferous Paleozoic sedimentary rocks also indicate a source for foreign ice on or south of north-central Baffin Island. A direct route northwards through Milne Inlet and then eastwards towards Baffin Bay is the most reasonable path for the ice that carried them.

Interaction between native and foreign glaciers appears to have varied greatly in character around the margins of Bylot Island. In the south and possibly on the northern coast as well, foreign ice was dominant, whereas along the northeast coast native ice was dominant. The reasons for this are not known, although it seems likely that valley aspect relative to the direction of foreign ice flow, submarine topography, and overall decrease in surface elevation of the foreign ice sheet towards Baffin Bay all may have played a role.

Despite clear morphologic evidence of a major advance of Bylot glaciers after the major foreign advance, till in front of and beside some glaciers within the area covered during that advance is significantly different from that of modern end moraines (e.g. Aktineq (B17), Sermilik (B37) and glacier D91). This implies some sort of difference in ice flow compared with present conditions. It is possible that the ice of the older native advance was cold-based and consequently did not erode pre-existing deposits.

Conclusions

The main conclusions drawn from this work can be summarized as follows:

1. Ice from major ice sheets has moved northwards across Baffin Island and crossed onto Bylot Island. To date, the highest level demonstrated to have been attained by foreign ice is about 1130 m a.s.l. and this was probably achieved during a glaciation prior to the 'last'. During that 'maximum' event, foreign ice could have flowed northward across the topographic divide of Bylot Island.
2. During the last glaciation two major glaciers moved onto Bylot Island across both the north and south coasts and carried debris to elevations of about 300 to 550 m a.s.l., which was probably their maximum extent. One glacier moved northward across north-central Baffin Island and through Milne Inlet before turning eastward to Pond Inlet; the second flowed northward through Admiralty Inlet and then eastward down Lancaster Sound. The marine channels between Bylot and Baffin islands, as well as Lancaster Sound, were completely filled by grounded glacier ice when Bylot Island was so covered.
3. Some time after the inundation of Bylot Island by foreign ice, Bylot glaciers advanced 10 to 15 km beyond their present limits.
4. The channels between Bylot and Baffin islands have not been occupied by grounded glacier ice for at least 35 000 radiocarbon years.

Acknowledgments

I would like to acknowledge gratefully the support of the Polar Continental Shelf Project (G.D. Hobson, Director) through which invaluable logistical and aircraft support was provided. Mr. S. Lavender and Mr. R. Needham gave excellent assistance in the field during 1978 and 1979, respectively. Drs. W.W. Shilts, R.N.W. DiLabio, and W. Blake, Jr. are thanked for numerous discussions concerning this study, and their influence on ideas presented here is recognized. Drs. G.D. Jackson and F.W. Chandler have provided information and comments on bedrock geology. By permission of the Geological Survey, this project forms the basis of a Ph.D. thesis within the Department of Geology, University of Illinois at Urbana-Champaign with Dr. W.H. Johnson, thesis supervisor. Amino acid analyses have been done by the INSTAAR Amino Acid Laboratory at the University of Colorado, and thanks are extended to Dr. J.T. Andrews for his kind and generous assistance. D.A. Hodgson is thanked for permission to present an amino acid ratio from shells collected by him.

References

Brigham, J.
1980: Stratigraphy, amino acid geochronology, and genesis of Quaternary sediments, Broughton Island, E. Baffin Island, Canada; unpublished M.Sc. Thesis, University of Colorado, Boulder, 200 p.

DiLabio, R.N.W. and Shilts, W.W.
1979: Composition and dispersal of debris by modern glaciers, Bylot Island, Canada; in Moraines and Varves, ed. Ch. Schlüchter; Proceedings of an INQUA Symposium on Genesis and Lithology of Quaternary Deposits (Zurich), A.A. Balkema, Rotterdam, p. 145-155.

Glacier Atlas of Canada
1969: Bylot Island area 46201, Glacier Atlas of Canada; Inland Waters Branch, Environment Canada.

Hodgson, D.A. and Haselton, G.M.
1974: Reconnaissance glacial geology, northeastern Baffin Island; Geological Survey of Canada, Paper 74-20, 10 p.

Jackson, G.D. and Davidson, A.
1975: Bylot Island map-area, District of Franklin; Geological Survey of Canada, Paper 74-29, 12 p.

Jackson, G.D., Davidson, A., and Morgan, W.C.
1975: Geology of the Pond Inlet map area, Baffin Island, District of Franklin; Geological Survey of Canada, Paper 74-26, 33 p.

Jackson, G.D., Iannelli, T.R., Narbonne, G.M., and Wallace, P.J.
1978: Upper Proterozoic sedimentary and volcanic rocks of northwestern Baffin Island; Geological Survey of Canada, Paper 78-14, 15 p.

Miall, A.D., Balkwill, H.R., and Hopkins, W.S., Jr.
1980: Cretaceous and Tertiary sediments of Eclipse Trough, Bylot Island area, Arctic Canada, and their regional setting; Geological Survey of Canada, Paper 79-23, 20 p.

Miller, G.H., Andrews, J.T., and Short, S.K.
1977: The last interglacial-glacial cycle, Clyde foreland, Baffin Island, N.W.T.: stratigraphy, biostratigraphy, and chronology; Canadian Journal of Earth Sciences, v. 14, p. 2824-2857.

Thorsteinsson, R.
1970: Geology of the Arctic Archipelago; in Geology and Economic Minerals of Canada, ed. R.J.W. Douglas; Geological Survey of Canada, Economic Geology Report No. 1, p. 552-569.

Trettin, H.P.
1969: Lower Paleozoic sediments of northwestern Baffin Island, District of Franklin; Geological Survey of Canada, Bulletin 157, 70 p.

47.

ASPECTS OF THE DEGLACIATION OF THE COPPERMINE RIVER REGION, DISTRICT OF MACKENZIE

EMR Research Agreement 2-4-80

D.A. St-Onge[1], M.A. Geurts[1], F. Guay[1],
V. Dewez[2], F. Landriault[1], and P. Léveillé[1]
Terrain Sciences Division

St-Onge, D.A., Geurts, M.A., Guay, F., Dewez, V., Landriault, F., and Léveillé, P., Aspects of the deglaciation of the Coppermine River region, District of Mackenzie; in Current Research, Part A, Geological Survey of Canada, Paper 81-1A, p. 327-331, 1981.

Abstract

In late glacial time the disintegration of the Laurentide Ice Sheet resulted in the deposition of erratics, moraines, and various ice-contact sediments in the Hepburn Lake map area. During ice retreat, Coppermine River valley south of the mouth of Kendall River became ice free and was occupied by a high-level (370 m a.s.l.) glacial lake which drained through Kamut Lake channel and Sloan River valley into Great Bear Lake. As a result of further ice retreat, the glacial lake expanded into the valley of Dismal Lakes. This lower phase of glacial Lake Coppermine (approximately 310 m a.s.l.) drained westward through Dismal Lakes and Dease River valleys to Great Bear Lake. Preliminary palynological studies of a 4 m-thick sequence of organic-rich sediments show important vegetation changes between 8400 and 3200 years ago.

Introduction

This paper describes the distribution of Quaternary deposits within the Hepburn Lake map area (86 J); discusses outlets of glacial Lake Coppermine (St-Onge, 1980) outlets; and reports on preliminary pollen analysis of the 4 m organic-rich channel fill of the Quicksand Creek site (Fig. 47.1; St-Onge, 1980).

The area mapped lies between 66° and 67°N and 114°00' and 116°30'W. It is part of a plateau on Precambrian rocks with an average elevation of 500 m a.s.l. in the south and 615 m in the north. The plateau is deeply dissected by tributaries of either the north-flowing Coppermine River draining into Coronation Gulf or of the west-flowing Sloan River draining into McTavish Arm of Great Bear Lake (Fig. 47.1). Forest cover is found only in valley bottoms and is replaced by shrubs, lichens, and mosses on the plateau surface.

Acknowledgments

We are very grateful to the Resident Geologist, Department of Indian and Northern Affairs, Yellowknife, for logistical support. The Royal Canadian Geographical Society awarded a research grant to two undergraduate students who assisted on field traverses and carried out an ecological study of the forest zone in Coppermine River valley. Dr. Paul Hoffman (GSC) provided logistical support and contributed encouragement and stimulating discussion. We also wish to thank B.P. Minerals Limited (Eastern Canada) for providing field accommodation and transportation.

Surficial Materials[3]

The gently rounded topography bears numerous evidence to the former presence of active glacial ice. (Craig, 1960). The surficial materials discussed here can be divided into the following general groups:

1. Erratic strewn bedrock
2. Morainic deposits: thin till and ground moraine
3. Ice-contact deposits: Forcier Moraine
4. Glaciofluvial deposits: eskers and outwash
5. Glaciolacustrine deposits: glacial Lake Coppermine
6. Organic deposits (Dépôts organiques)

Erratic Strewn Bedrock

Erratic boulders are scattered throughout the area both in valleys and on plateau surfaces. They generally rest directly on bedrock. Although the limit between scattered erratics and thin bouldery till veneer is usually distinct, in places one unit gradually grades into the other. In some areas, because of contrasting rock colours, fields of isolated large boulders create a peculiar speckled landscape; for example, east of Coppermine River valley, along the Arctic Circle, whitish dolomites of the Rocknest Formation have been carried northwesterly onto the dark greywackes of the Recluse Group (Hoffman et al., 1980).

Morainic Deposits: Thin Till and Ground Moraine

Thin till, a veneer of bouldery till and rubble from 1 to 3 m thick, covers large areas in the west-central part of the map area (Fig. 47.1). Commonly the deposit is not thick enough to mask underlying bedrock structure. Fluting is rare on this unit which seems to result from deposition by a large dead ice mass and from the shattering of frost susceptible rocks of the Akaitcho Group and of the Hepburn Batholith (Hoffman et al., 1980). On the north side of Coppermine River a narrow north-south belt of thin till and rubble corresponds to thin bedded phyllites of the Odjich Formation (Hoffman et al., 1980). Although large expanses of this unit suggest the former presence of a decaying ice mass, smaller occurrences of the unit predominantly reflect lithology rather than ice activity or position.

Ground moraine is a till deposit of sufficient thickness to mask completely underlying bedrock structure. This unit, composed of bouldery till with a sand matrix, covers two sizeable areas on either side of Coppermine valley in the northwest part of the map area (Fig. 47.1). North of the river, gently rolling ground moraine covers the floor of Mouse Graben (Hoffman et al., 1980). This 15 by 10 km depression, with a long axis at nearly right angle to the direction of ice flow (Craig, 1960), was an area of glacial deposition. Except for two exposures of frost-shattered sandstone slabs, till completely blankets the down-faulted Hornby Bay Group (Hoffman et al., 1980). The depression is crossed by an esker, north of which ribbed moraine occurs (Prest, 1968, p. 5) and south of which hummocky moraine occurs – typical of a stagnating ice mass. Prairie mounds (Prest, 1968, p. 9) are abundant. South of Coppermine Valley fluted ground moraine

[1]Department of Geography, University of Ottawa, Ottawa, Ontario K1N 6N5
[2]Département de Géographie, Université de Louvain, Louvain-la-Neuve, Belgique
[3]by D.A. St-Onge, V. Dewez, F. Landriault, and P. Léveillé

Figure 47.1. *Location map showing generalized deglaciation pattern of the Coppermine River region.*

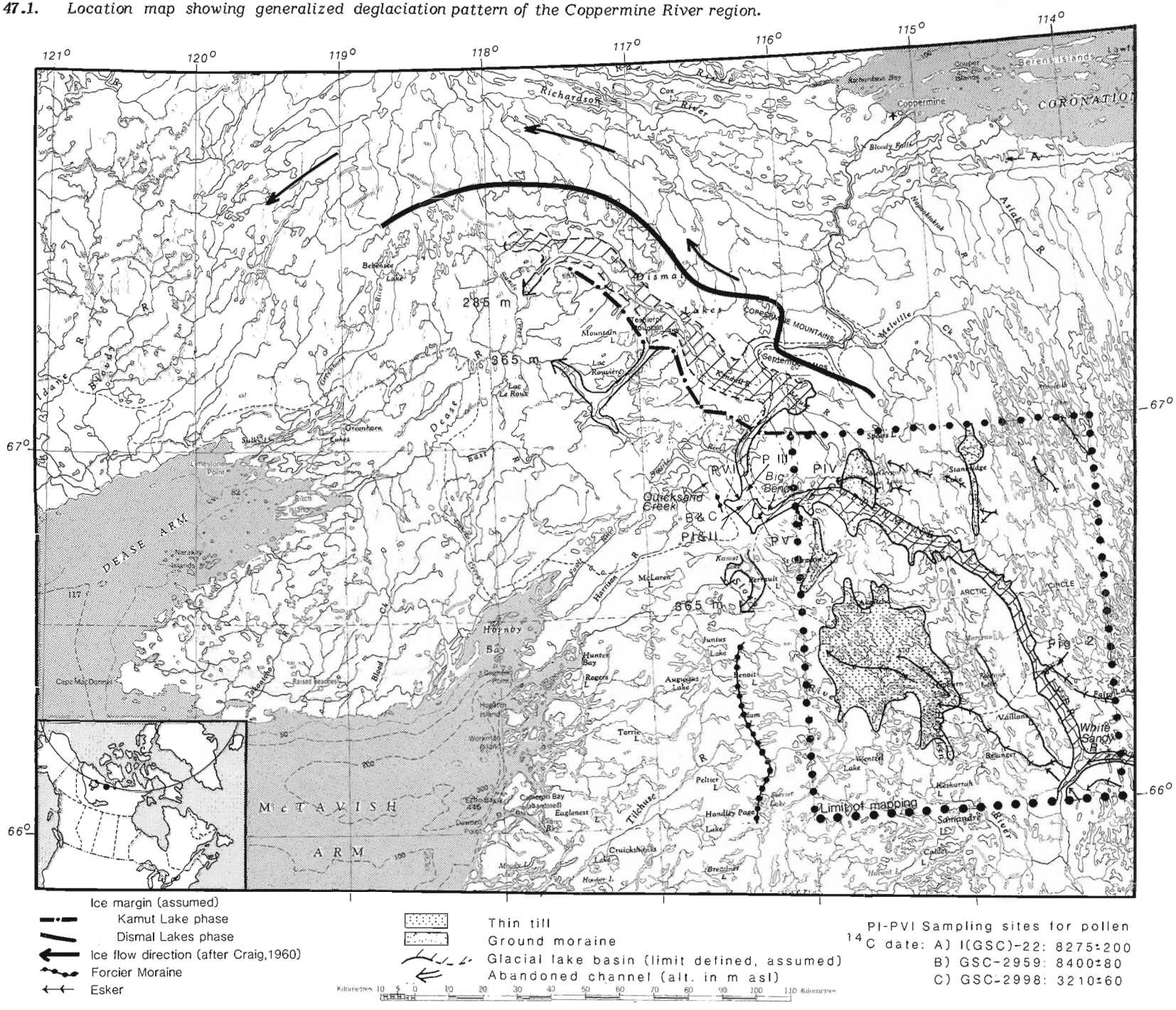

covers a 5 to 8 by 20 km belt of upland. The direction of ice flow measured on glacial fluting of till and on rock knobs in this area is N25°W; fluting does not occur on rock knobs in the immediate area northwest of this ground moraine.

Ice-contact Deposits: Forcier Moraine

Only one large morainic ridge has been identified just outside the map area (Fig. 47.1); its extension south of 66°N has not been mapped. The ridge was studied in the field at the western end of an unnamed rectangular lake 10 km north of Adam Lake. It is composed of large boulders, up to 3 m in diameter, in a sand-gravel matrix. The ridge is 5 to 20 m high with a steep 15° to 30° east slope and a more gentle 5° to 15° west slope. On the west side of the moraine small fans are found where the ridge was breached by meltwater. Some of these sand and gravel deposits are now covered by string bogs. Except for gaps carved by former meltwater streams, the moraine is continuous across valleys and plateau. The bedrock is essentially bare on either side of the moraine. It is proposed that this morainic ridge be called the Forcier Moraine after a lake on its eastern side, 5 km north of 66°N.

The steep eastern slope and the sand-gravel fans on the west side indicate that Forcier Moraine was constructed by west-flowing ice. It is not possible at this stage to determine the time or the duration of the ice frontal position that is responsible for its formation, nor is it possible to indicate whether or not other morainic ridges east and west of Big Bend are part of the Forcier Moraine.

Glaciofluvial Deposits: Eskers and Outwash

Glaciofluvial sand and gravel are abundant in the Hepburn Lake map area and occur typically as esker ridges flanked by outwash terraces up to 1 km wide (Fig. 47.2). Esker ridges generally trend southeast-northwest (Fig. 47.1), reflecting the glacial pattern (Craig, 1960) of the Amundsen Gulf lobe of the Laurentide Ice Sheet (Mackay, 1958, p. 35; Craig and Fyles, 1960, p. 7, 16).

A major esker system is located in the southern half of the map area. It follows White Sandy River valley and crosses Coppermine valley where erosion has reduced it to a boulder lag, creating rapids in the river. The esker then bifurcates with a northern arm towards Marceau Lake and a southern arm towards Hepburn Lake and beyond. It is impossible to say whether this system was active along all its length at a given time or whether it was constructed in segments. The fact that it crosses Coppermine valley and then runs uphill strongly suggests that, in its initial phase, the esker was formed in an ice cave.

Eskers are commonly interrupted by rocks ridges that have been washed clean of till and that on air photographs appear as a light strip joining two esker segments. On the ground, large boulders (3 m diameter) occur sporadically on the bare outcrop ridges. There is little doubt that these segments are local topographic highs that partially blocked the esker tunnel. Meltwater depositing the sand and gravel of the esker flowed over these obstacles and left them as "clean" surfaces.

The sand and gravel outwash terraces (Fig. 47.2) flanking the esker ridges represent a later phase in the evolution of the outwash system. The terraces are lower than the esker ridge and are covered by channel scars, indicating that at the time of their formation, the tunnel had collapsed and water was flowing subaerially. Numerous kettle lakes pit the terraces. Many esker ridge terrace complexes do not follow present drainage patterns but flow across numerous small valleys, such as the esker running northwestward from Fairy Lake River (Fig. 47.2). This pattern implies that, even at the time the outwash terraces were being formed, dead ice masses still covered large parts of the map area.

Although not shown in Figure 47.1, glaciofluvial sand and gravel deposits, including eskers, are found in Coppermine valley commonly protruding through younger deposits of glacial Lake Coppermine (St-Onge, 1980). In spite of subsequent erosion, a sufficient number of these esker segments have been preserved to suggest that during the esker building phase of late glacial time, long sections of Coppermine valley were occupied by meltwater tunnels.

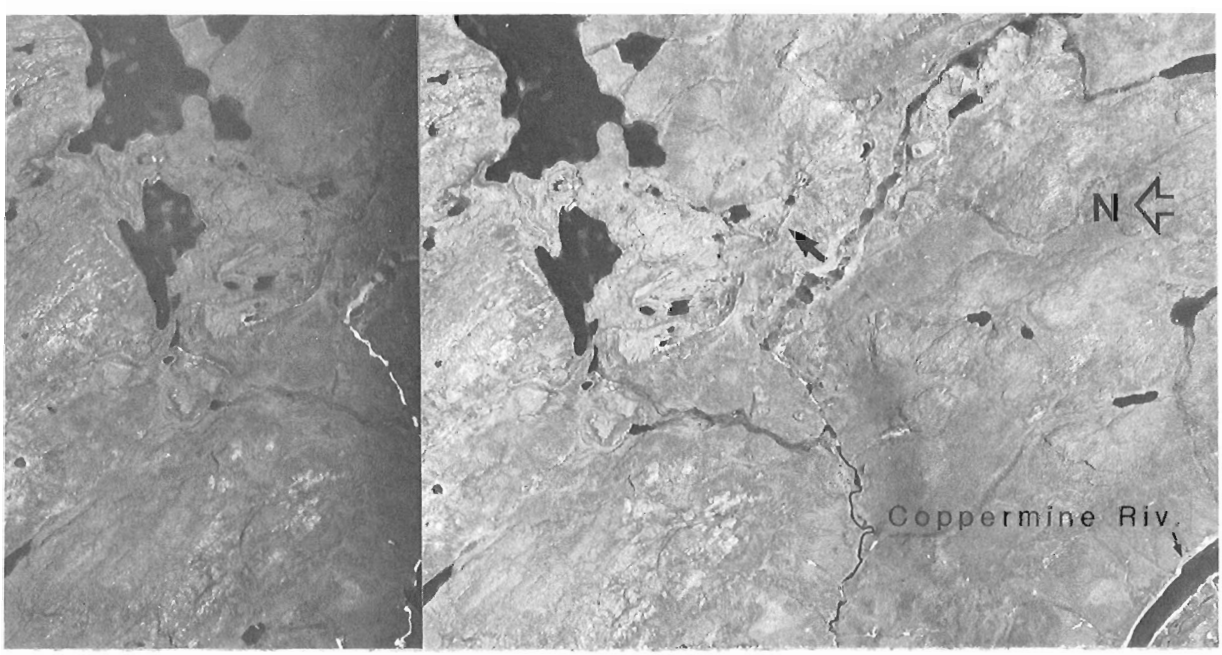

Figure 47.2. *Stereogram of terraced and pitted esker (arrow) east of Coppermine River along 66 20'N (see Fig. 47.1 for location).*

Glaciolacustrine Deposits: Glacial Lake Coppermine Sediments

Sediments related to glacial Lake Coppermine have been described by St-Onge (1980); phases of the glacial lake related to deglaciation of the Coppermine region will be discussed here.

A glacial lake (Kamut Lake phase) first appeared in Coppermine River valley as a result of glacier ice impounding the valley north of the mouth of Kendall River. The elevation of the lake was around 370 m a.s.l. and it drained via the Kamut Lake channel (elevation 365 m a.s.l., Fig. 47.1) to the present Sloan River and then to Great Bear Lake.

A massive gravel terrace occurs at 370 m. a.s.l., at the north end of Kamut Lake; its steep slope into the lake is ridged suggesting block slumping when the material was frozen. No important sand-gravel deposits exist where the bifurcated channel opens into Sloan River valley. This implies that, if Kamut Lake valley did function as a glacial lake outlet, the present lake must have already existed and was acting as a sediment trap. The steep terrace slope at the north end of Kamut Lake would have been an advancing delta front fed by south-flowing braided channels, the scars of which remain on the terrace surface. Kamut Lake now drains northward into the Coppermine via Hook River (not identified in Fig. 47.1).

A perched delta along Coppermine valley just north of the mouth of Bigtree River and terraces in Bigtree valley also suggest the former presence of a lake in Coppermine valley at a level of 360-370 m a.s.l. High deltas at similar elevations are found in Coppermine valley as far south as the Arctic Circle.

During the Kamut Lake phase glacier ice occupied the valley of Dismal Lakes. The channel at the western end of Dismal Lakes, being at 285 m a.s.l., could not have been the outlet for a glacial lake at 370 m a.s.l. Teshierpi River valley (south of Teshierpi Mountain in Fig. 47.1) was a major outwash channel during Kamut Lake phase. Meltwaters carried large quantities of sand and gravel south through Teshierpi valley to Lac Rouvière via a narrow valley which is in part occupied by an esker flanked by terraces. The sill elevation of this valley is between 360 and 370 m a.s.l. A large delta with an apex at 365 m a.s.l. was constructed into Lac Rouvière. This delta complex could not have been constructed unless Dismal Lakes valley was occupied by glacier ice from which meltwater fed directly into Teshierpi valley; a glacial lake, acting as a sediment trap, would have made this impossible.

Following retreat of the ice front to the north, the glacial lake extended into Dismal Lakes valley. A lower outlet at 285 m a.s.l. at the western end of Dismal Lakes drained this lower phase of glacial Lake Coppermine (St-Onge, 1980) via Dease River to Great Bear Lake (Fig. 47.1). The former level of this glacial lake phase is marked by large perched deltas located in tributary valleys on either side of Coppermine valley. Their channelled surfaces of coarse gravel are at approximately 290 m a.s.l. in the north part of the lake basin and 310 m in the southern part.

The deep water facies of glacial Lake Coppermine sediments is formed of varved fine sand and silt. The varves are exposed as 10 to 30 m-high white-grey bluffs along the valley; 1 km south of the mouth of White Sandy River at least 450 varves are present in a 27 m-high section.

As deglaciation progressed and the ice margin retreated from the lowlands north of Coppermine and September mountains, the postglacial Coppermine River drainage system was established to Coronation Gulf. This initiated a phase of downcutting through glacial lake and other sediments, resulting in the formation of numerous terraces. Organic material recovered from alluvial deposits on these terraces will make it possible to date this event.

Dépôts organiques[1]

En 1979, D.A. St-Onge découvre les dépôts d'un important lac glaciaire dans la vallée de la Coppermine (St-Onge, 1980). Dans une coupe près du ruisseau Quicksand, la partie supérieure des dépôts lacustres est entaillée par des chenaux remplis de sables riches en matière organique (fig. 47.1). Ceux-ci sont recouverts de tourbe.

Trois échantillons prélevés dans ce remplissage de chenal sont riches en grains de pollen. Les résultats de ces analyses polliniques préliminaires sont figurés par le diagramme Coppermine I (fig. 47.3). L'échantillon DS 79-19 provient de la base du chenal daté de 8400 ± 80 B.P. (GSC 2959). Le spectre pollinique est dominé par les pollens d'arbustes dont les pourcentages par rapport au total des espèces arborescentes, arbustives et herbacées sont répartis en 56.3% de Betula, 3.2% de Salix et 0.7% d'Alnus. Les conifères sont faiblement représentés, 12.3% de Picea, 1.6% de Pinus et 0.2% d'Abies. Les espèces herbacées sont dominées par les cypéracées et on note la présence des espèces aquatiques Potamogeton et Sparganium, ainsi que l'encombrement du spectre par des spores dont le pourcentage atteint 94.21% du total des AP + NAP.

La fréquence élevée des arbustes et le faible pourcentage des résineux suggèrent un paysage de toundra arbustive. La présence de Potamogeton et Sparganium confirme le milieu inondé identifié par l'analyse sédimentologique.

L'échantillon 7C est riche en coquilles et en oogones de characée. Le spectre pollinique indique une extension des cypéracées (30.3%), des graminées (10.7%) et d'Artemisia (2.7%). Les pourcentages des conifères régressent fortement ainsi que ceux de Betula. Salix et Alnus augmentent leurs fréquences mais ne traduisent sans doute qu'une colonisation locale de zones humides en bordure du chenal.

Ce spectre pollinique révèle un environnement de toundra herbeuse. Bien que le milieu soit toujours inondé comme l'indique la présence de Potamogeton, le climat semble plus sec, car Artemisia s'étend légèrement.

L'échantillon E provient de la tourbe compacte qui occupe le sommet du remplissage du chenal. Cet échantillon est daté de 3200 ± 60 B.P. (GSC-2998). Son spectre pollinique est caractérisé par l'extension de Picea (26.2%), Pinus, Populus, l'apparition de Larix, une légère croissance de Betula (34.8%) et le retrait de Salix. Les herbes n'atteignent plus que 20.7% du total des AP + NAP.

Ce spectre indique un retour à des conditions climatiques favorables au développement d'une toundra arbustive ou forestière comparable aux ensembles végétaux qui occupent la région actuellement.

Les résultats de ces analyses préliminaires sont prometteurs puisque dès l'abord ils indiquent des modifications végétales qui pourraient résulter des fluctuations climatiques survenues durant l'Holocène. De plus, il n'existe pas dans cette région un diagramme retraçant les stades précoces de la colonisation végétale. Les diagrammes de Nichols (1975) à Port Radium (Grand lac de l'Ours) et à Coppermine débutent bien plus tardivement. Ces raisons sont donc suffisantes pour entamer une étude palynologique systématique de la zone, dont la cartographie des dépôts meubles est réalisée par St-Onge (plus haut).

L'étude palynologique s'exerce sur deux thèmes: un échantillonnage de surface qui doit permettre de comprendre les relations entre les spectres polliniques et la végétation

[1]Par M.A. Geurts et F. Guay

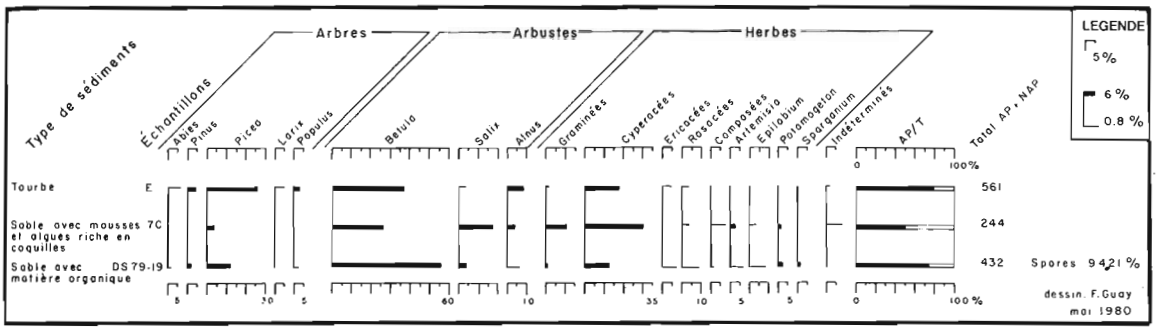

Figure 47.3. *Diagramme Coppermine I.*

actuelle, et, le prélèvement de profils dans des dépôts minéraux et organiques pour l'étude palynostratigraphique qui tend à retracer l'évolution du paysage végétal postglaciaire et ses relations avec le milieu et le climat. La première zone d'analyse systématique est celle du lac Qingaluk sise à l'ouest des rapides Big Bend le long de la rivière Coppermine, et au nord du cercle polaire (66°48'N, 116°19'W).

Palynologie de surface La limite des arbres atteint dans la vallée de la Coppermine la latitude de 67°20'N et l'altitude de 450 m dans la région du lac Qingaluk. Cependant dans le détail et le long de la vallée, la forêt d'épinettes occupe essentiellement les versants tandis que les replats bien drainés sur matériel sableux et graveleux sont colonisés par une végétation de toundra arbustive dominée par le bouleau nain et les éricacées. Les dépressions humides sur les replats sont envahies d'une végétation riche en cypéracées. Sur les lacs asséchés, ou sur les berges de lac, ainsi que sur les barres alluviales poussent des saules, parfois en peuplement purs.

Treize échantillons de surface ont été prélevés dans ces différents environnements afin de contrôler le contenu pollinique des mousses ou des sols de surface et leurs spectres polliniques avec les composantes de la végétation actuelle.

Palynostratigraphie Autour du lac Qingaluk 5 profils palynologiques ont été échantillonnés et numérotés de II à VI sur la figure 47.1. Le profil Coppermine II est un échantillonnage complet du remplissage de chenal qui a livré les premières analyses décrites ci-dessus et le profil Coppermine I.

Le profil Coppermine V (66°48'N, 116°15'W, altitude ±345 m a.n.m.) a été prélevé dans une tourbière réticulée édifiée sur la colline située entre le lac Qingaluk et la rivière Coppermine. La toubière est dominée au nord et au sud par des versants couverts de till et colonisés par une forêt d'épinette. L'altitude de cette tourbière, comprise entre 340 et 350 m a.n.m., place le site au-dessus de l'altitude des deltas lacustres du lac glaciaire Coppermine (St-Onge, 1980). Le site de la tourbière a donc constitué une île au milieu du lac Coppermine et devrait posséder des sédiments plus anciens que ceux du profil du chenal (Coppermine I et II). Malheureusement le profil Coppermine V n'atteint pas la base de la tourbière. Les analyses actuellement en cours révèlent un pourcentage relativement élevé d'Alnus ce qui semble indiquer un climat relativement chaud et un paysage végétal comparable à celui de l'échantillon E du profil Coppermine I.

Ainsi par un échantillonnage plus systématique réalisé durant l'été 1980, et rattaché à des surfaces topographiques identifiées par l'analyse géomorphologique et par l'étude des dépôts meubles, nous espérons retracer l'histoire végétale post-glaciaire de cette région, ses relations avec les variations climatiques et les environnements sédimentaires.

References/Références

Craig, B.G.
1960: Surficial geology of north-central District of Mackenzie, Northwest Territories; Geological Survey of Canada, Paper 60-18, 8 p., Map 24-1960.

Craig, B.G. and Fyles, J.G.
1960: Pleistocene geology of Arctic Canada; Geological Survey of Canada, Paper 60-10, 21 p.

Hoffman, P.F., St-Onge, M.R., Easton, R.M., Grotzinger, J., and Schulze, D.E.
1980: Syntectonic plutonism in north-central Wopmay Orogen (Early Proterozoic), Hepburn Lake map area, District of Mackenzie; in Current Research, Part A, Geological Survey of Canada, Paper 80-1A, p. 171-177.

Mackay, J.R.
1958: The Anderson River Map Area, N.W.T.; Geographical Branch, Memoir 5, p. 137.

Nichols, H.
1975: Palynological and paleoclimatic study of the late Quaternary displacement of the Boreal Forest Tundra Ecotone in Keewatin and Mackenzie, N.W.T., Canada; Institute of Arctic and Alpine Research, University of Colorado, Occasional Paper no. 15.

Prest, V.K.
1968: Nomenclature of moraines and ice-flow features as applied to the Glacial Map of Canada; Geologial Survey of Canada, Paper 67-57.

St-Onge, D.A.
1980: Glacial Lake Coppermine, north-central District of Mackenzie, Northwest Territories; Canadian Journal of Earth Sciences, v. 17, no. 9, p. 1310-1315.

48.

PRELIMINARY ACCOUNT OF THE GEOLOGY OF THE BEECHEY LAKE – DUGGAN LAKE MAP AREAS, DISTRICT OF MACKENZIE

Project 800006

R.A. Frith
Precambrian Geology Division

Frith, R.A., Preliminary account of the geology of the Beechey Lake – Duggan Lake map areas, District of Mackenzie; in Current Research, Part A, Geological Survey of Canada, Paper 81-1A, p. 333-339, 1981.

Abstract

Rocks of the Slave Province west of the Bathurst Fault System are typical of the Slave Province except for the presence of Proterozoic north-south cleavages. In the northern half of the area the north-south cleavage was found to cut the Goulburn Group and the northwest diabase dyke swarm that parallels the Bathurst Fault System, and is thought to be related to folding and deformation associated with the Bathurst Fault System. A similarly oriented shear-cleavage is present in the south half of the map area which is associated with a north-south muscovite schistosity that may be related to the Hudsonian orogeny. Both north-south structures postdate an early Proterozoic northeast cleavage which may have an analogy in the mylonites and aeromagnetic highs that parallel the Slave Province boundary (Thelon Front).

Introduction

The Beechey-Duggan Lakes map area (76 G, east half, 76 H, west half) is being remapped to try and better understand the nature of the boundary transition between the Churchill and Slave structural provinces. The boundary, in part, coincides with the Bathurst Fault System, a major left-lateral strike-slip structure that has a displacement estimated at 140 km (Campbell and Cecile, 1979). The fault separates the map area into two approximately equal parts. The west block contains the Thelon Front (Wright, 1967), a major structural transition zone between Archean Slave Province structures and Proterozoic Churchill Province structures.

This study builds on the earlier work of Tremblay (1971) which outlined the Goulburn Group and investigated some representative Archean areas in the western half of the map area. The first systematic mapping in the area was helicopter-assisted reconnaissance work compiled by Wright in 1967.

About one half of the Beechey-Duggan Lakes map area was mapped for a final publication scale of 1:250 000 during the 1980 field season, and the results are summarized in Figure 48.1.

The author was capably assisted by Raynald Lapointe, Kenneth Ellison, and Joachime Kosiusko. The report was reviewed by J.C. McGlynn.

General Geology

Beechey Lake Group (Unit 1)

Greywacke-mudstones and their metamorphosed equivalents are included as unit 1 (Fig. 48.1, Table 48.1). The unit is divided into 8 subunits based on varying degrees of metamorphism. In general, the least metamorphosed rocks are similar to the uniform turbidites of the Burwash Formation of the Yellowknife Supergroup which have been described in a type area near Yellowknife (Henderson, 1970). The rocks are part of the Beechey Lake Group described by Frith and Percival (1978) in the adjoining Nose-Beechey Lakes map area.

Rocks of subunit 1a include greywacke-mudstone turbidites that are metamorphosed up to and including biotite grade. Generally, primary sedimentary structures, particularly graded bedding, are well preserved. Minor banded iron formation and some thin carbonaceous mudstones occur locally. Isoclinal folding is common but hinges are rarely observed. Undifferentiated rocks of unit 1b are locally included in unit 1a, particularly around the granite intrusions (unit 7) around 'Propeller' Lake.

Subunit 1b consists of porphyroblastic schists derived from subunit 1a and the contact is placed at the staurolite-cordierite isograd. In the transition zone where cordierite and staurolite porphyroblasts first appear, primary bedding may still be evident. With increasing metamorphism, porphyroblasts become unstable, the rock becomes more schistose, and leucosome segregations become more abundant. The subunit may contain garnet and an aluminosilicate polymorph. Commonly andalusite is present, but sillimanite and kyanite are evident in the higher grade rocks, such as those along the 'Knot' Rapids and the lower Back River (Fig. 48.1). The subunit is intruded by coarse muscovite-bearing pegmatite granite of units 8 and 8p.

Subunit 1c consists of rusty weathering gneiss that contains biotite, plagioclase, quartz, and in places muscovite, but no potash feldspar. Thin-section control will be needed to differentiate some rocks of this unit from rocks of subunit 1d.

With increasing metamorphism these rocks grade to migmatitic gneiss of subunit 1d, which contains variable proportions of coarse discontinuous pegmatitic granite that both parallel and cut across existing foliations. The restite phase is similar to unit 1c but contains sillimanite, microcline, and in places, garnet. Locally, kyanite is present in place of sillimanite. Rocks of this subunit are found principally in the south-central part of the map area.

Subunit 1e comprises migmatites that contain more than 50 per cent leucosome phase with the remaining restite derived from units 1a-1d. The restite is usually a rusty colour, containing biotite, quartz plagioclase, and microcline. The microcline may be porphyroblastic, as in unit 3. The rocks are mostly well layered and compositionally banded. Locally, agmatitic and lit-par-lit phases are present. Contacts with other rock types, including unit 3, are usually gradational. Most of these rocks are found east of the Bathurst Fault System where they are associated with other migmatites of less certain origin.

Subunit 1f comprises poorly defined bodies of gneissic but homogeneous rusty granodiorite which are similar in mineralogy to subunit 1e. However, no remnant bedding is present and the rocks are presumed to have undergone some kind of remobilizaiton. Further study of these rocks is

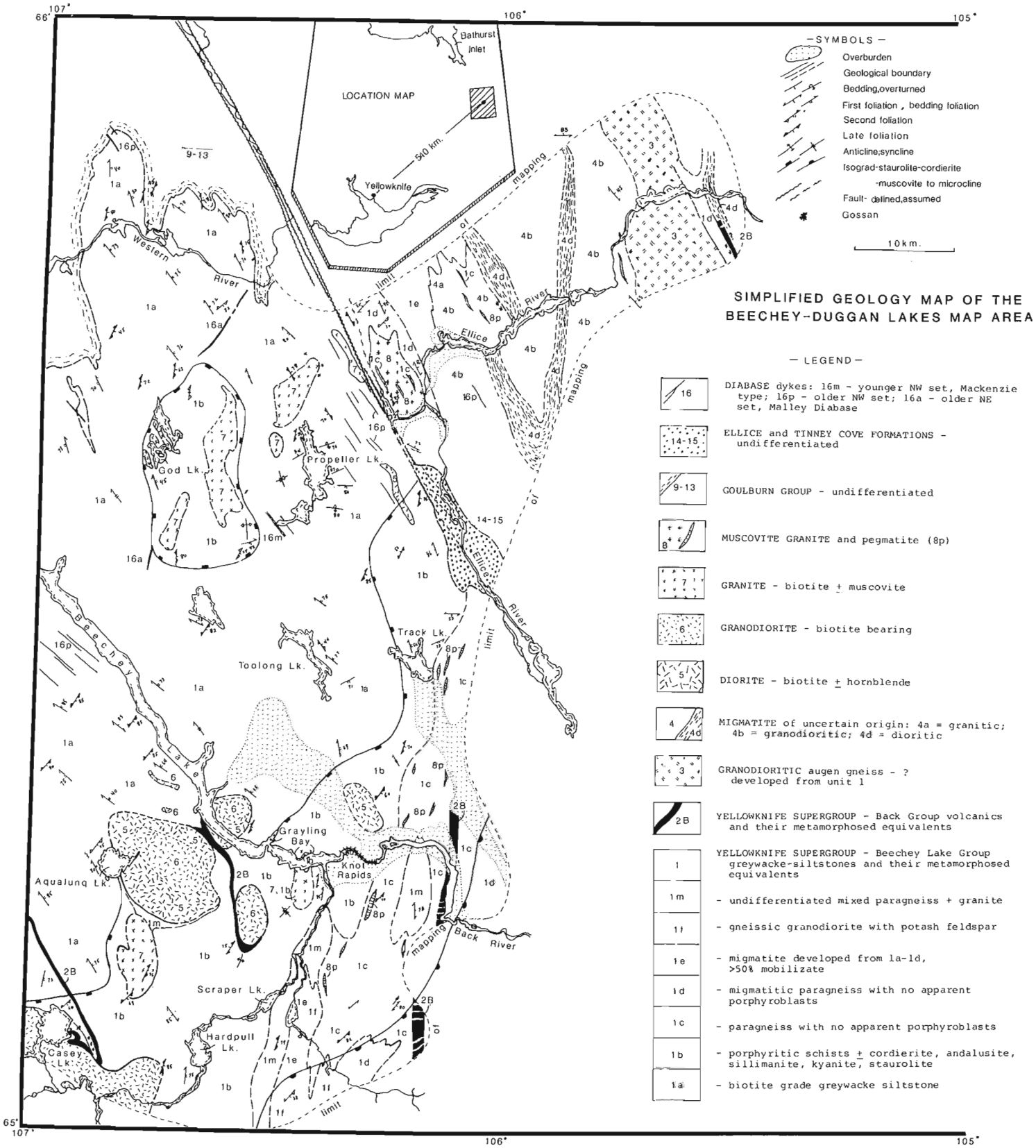

Figure 48.1. *Simplified geology map of the Beechey-Duggan Lakes map area. All the lake names other than Beechey Lake and Casey Lake are informal.*

needed, but in the field they appear to intrude other migmatites. They may be anatectites or partly melted rocks of unit 1. The contact regions contain abundant fish-shaped inclusions of biotite-rich rock that are subparallel to randomly oriented.

Due to poor exposure and lithological heterogeneity, some regions of mixed gneiss and granite could not be delineated and these are designated as subunit 1m. The subunit includes remnant paraschists, paragneiss and migmatite, interlayered or intruded by granitic rocks similar to units 7 or 8.

Volcanic Rocks (Unit 2)

Four volcanic belts were partly outlined during the course of the mapping. Two belts were less than 500 m wide. The Casey Lake belt is an extension of a previously mapped belt that can be traced to the Back River near the Malley Rapids (Frith et al., 1977a; Frith and Hill, 1975). The volcanics are principally pillowed or fragmented andesites with lesser amounts of dacitic tuff. The belt is both underlain and overlain by greywacke-mudstone of the Beechey Lake Group (unit 1) and is thought to be part of the Back Group (Frith and Percival, 1978).

A previously unmapped belt, referred to here as the 'Scraper' Lake belt, was outlined over a distance of 15 km. The belt is about the same width and has the same composition as the Casey Lake belt. The 'Scraper' Lake belt faces west and is intruded along the east side by a porphyritic granodiorite. The north part of the belt pinches out around the south side of a zoned granodiorite-diorite intrusion near the south end of Beechey Lake. The south part of the belt is folded in an anticlinal structural cored by a bounding granodiorite. Some andesitic volcanics occur north of 'Hardpull' Lake (not on Fig. 48.1), which may be part of the same belt.

Along the southeast margin of mapping highly metamorphosed volcanics, mostly of andesitic composition, were found as 'islands' in an area of extensive drift cover.

Table 48.1

Tentative table of formations, with estimates of age

Unit	Formation or lithology	Age
16	Diabase dykes – 16m Younger northwest set – Mackenzie 16p Older northwest set 16a Malley Diabase	1200 Ma ↶2000 Ma ↶2500-2000 Ma
	(intrusive)	
14-15	Ellice and Tinney Cove sediments	Helikian
	(unconformable)	
9-13	Goulburn Group sediments	Aphebian
	(unconformable)	
8	Muscovite granite with pegmatite, commonly tourmaline bearing	↶1750 Ma
	(intrusive)	
7	Regan Intrusive Suite Diorite – hornblende, biotite bearing	↶2500
6	Granodiorite – biotite bearing	
5	Granite – muscovite with or without biotite	
	(intrusive)	
4	Migmatites of uncertain origin – of granitic (4a), granodioritic (4b) and dioritic (4c) composition	?
3	Granodioritic augen gneiss developed from unit 1	?
	(gradational)	
2	Yellowknife Supergroup Back Group – volcanics and their metamorphosed equivalents	↶2670 Ma
	(conformable)	
1	Yellowknife Supergroup Beechey Lake Group – greywacke-mudstones and their metamorphosed equivalents	↶2670 Ma
	?	

The presence of overlying iron formation and remnant pillows suggests that the belt faces east. The belt disappears under glacial drift north of the Back River, but toward the south, appears to widen. Henderson and Thompson (1980) have outlined an amphibolite belt near Tourgis Lake that may be a southerly continuation of this belt.

To the east of the Bathurst Fault System (Fig. 48.1) a west-facing metavolcanic amphibolite was identified. Overlying the belt were gossan zones associated with cherty iron formation.

Granodiorite Augen Gneiss (Unit 3)

Extensive regions of biotite-potash feldspar augen granodioritic gneiss are present along parts of the Ellice River (Fig. 48.1). The rocks are relatively uniform, with local heterogeneities and interlayers of biotite-schlieren migmatite similar to unit 1e.

South of the Ellice River the gneiss is partly bounded by abrupt linears which may be faults. Other contacts grade or interlayer with migmatite of uncertain origin (unit 4). The rocks locally contain microcline megacrysts instead of augens, suggesting that metamorphic growth locally outlasted deformation. Other metamorphic minerals include garnet and hornblende.

Migmatites of uncertain origin (Unit 4)

Along the Ellice River are migmatites that cannot be readily related to the metasedimentary rocks of the Yellowknife Supergroup. Included in this unit are migmatites and gneiss of overall granitic composition (4a); granodioritic composition (4b); and hornblende diorite composition (4d). The rocks of the unit are too migmatized or granitized to identify the restite phase. Some of the dioritic gneiss may be metavolcanic.

Diorite (Unit 5) and Granodiorite (Unit 6)

Two zoned intrusions near the southeast corner of the map area have granodioritic cores and dioritic margins (Fig. 48.1). In addition, a discrete intrusion of diorite occurs just north of 'Knot' Rapids. The diorite is a buff to slightly rusty colour, medium even grained, and contains biotite and/or hornblende, and variable but minor amounts of quartz.

The contacts with the enclosing metasediments or metavolcanics are sharp, with a narrow metamorphic aureole locally evident. Some rounded inclusions of mafic gneiss occur locally in the diorite.

The diorite zone around the margins of the intrusions is of variable width, suggesting variable depths of erosion of zoned spherical intrusions.

The granodiorite both in the cores and in unzoned intrusions contain quartz, biotite, plagioclase, and microcline, in a generally medium, even grained texture. Near the margins of the intrusive bodies, faint conformable gneissosity may be present.

The diorites and the granodiorites are probably part of the Regan Intrusive Suite found in the Nose-Beechey Lakes map area (Frith and Hill, in preparation).

Biotite-Muscovite Granite (Unit 7)

On the west side of the Bathurst Fault System, biotite-muscovite granites are present as discrete large intrusive bodies that shoulder aside bedding foliations of the enclosing metasediments. The rocks are medium- to coarse-grained and are characterized by the presence of muscovite and biotite.

Near 'God' Lake irregular-shaped bodies of granite occur within a rather large metamorphic high. These granites may be the surface expression of a larger subsurface body that has not been completely unroofed. The biotite-muscovite granites are similar to those of the Regan Intrusive Suite (Frith and Hill, in preparation).

Pegmatitic Muscovite Granite (Unit 8)

The rock is a coarse grained pegmatitic rock present in most of the higher metamorphic grades of unit 1. These rocks generally contain muscovite, K-feldspar and quartz, and locally, tourmaline. Most commonly the unit forms small irregular pods that cannot be mapped at the scale of this study. However, some larger bodies and layers within abundant paraschist inclusions and layers are present just south of the 'Knot' Rapids and along the east side of the Bathurst Fault. Many small pods have been mapped in a belt extending from 'Track' Lake to 'Scraper' Lake.

Aphebian and Helikian Rocks (Units 9-15)

Sedimentary units of the Goulburn Group (units 9-13) and the Ellice and Tinney Cove formations (units 14-15) were not studied in detail, as previous workers (Tremblay, 1971; Campbell and Cecile, 1979) have treated these rocks quite thoroughly. However, some stratigraphic and structural relationships were re-examined and compared with the Archean basement rocks and the diabase dykes of unit 16p which intrude both the Goulburn Group (unit 9) and the Beechey Lake Group (unit 1). This is discussed in the following section.

Diabase and Gabbro Dykes and Sills (Unit 16)

Three sets of dykes and one intrusion are present in the map area. Northeast striking dykes (16a) are probably equivalents of the northeast trending Malley Diabase mapped in the Nose-Beechey Lakes map area (Frith and Hill, in preparation). These dykes have little or no magnetic expression and are far more extensive and numerous in the Nose-Beechey Lakes map area where they are linked with 2500-2000 Ma northeast cleavage.

The major northwest dyke swarm (16p) that parallels the Bathurst Fault System is similar to the Malley Diabase in composition and in the degree of post-intrusive metamorphism or alteration. This set has no obvious magnetic expression and is cut by a north-south fracture cleavage. Both 16a and 16p are altered and locally are cut by narrow quartz veins. These dykes intrude the base of the Goulburn and some may be feeders to the gabbro sills that are found at the base of the Goulburn, near Western River.

A third northwest set (16m) comprises little metamorphosed, rusty weathering, ophitic diabase and gabbro dykes of the Mackenzie swarm.

Structure and Metamorphism

Three phases of folding are found in the western part of the map area. The first is apparent only where the Casey and 'Scraper' Lake volcanic belts have been folded into large synclinal and anticlinal structures. However, early fold closures are rarely observed in the Beechey Lake Group sediments, but an early cleavage (S_1), commonly a bedding-cleavage, is thought to be axial planar to these northwest trending folds. Second folding into smaller scale isoclines is commonly parallel or subparallel to the earlier folding and the distinction in the field is not always observed. Only where fold hinge zones are encountered are these relationships readily perceived. Axial planar foliation (S_1) formed

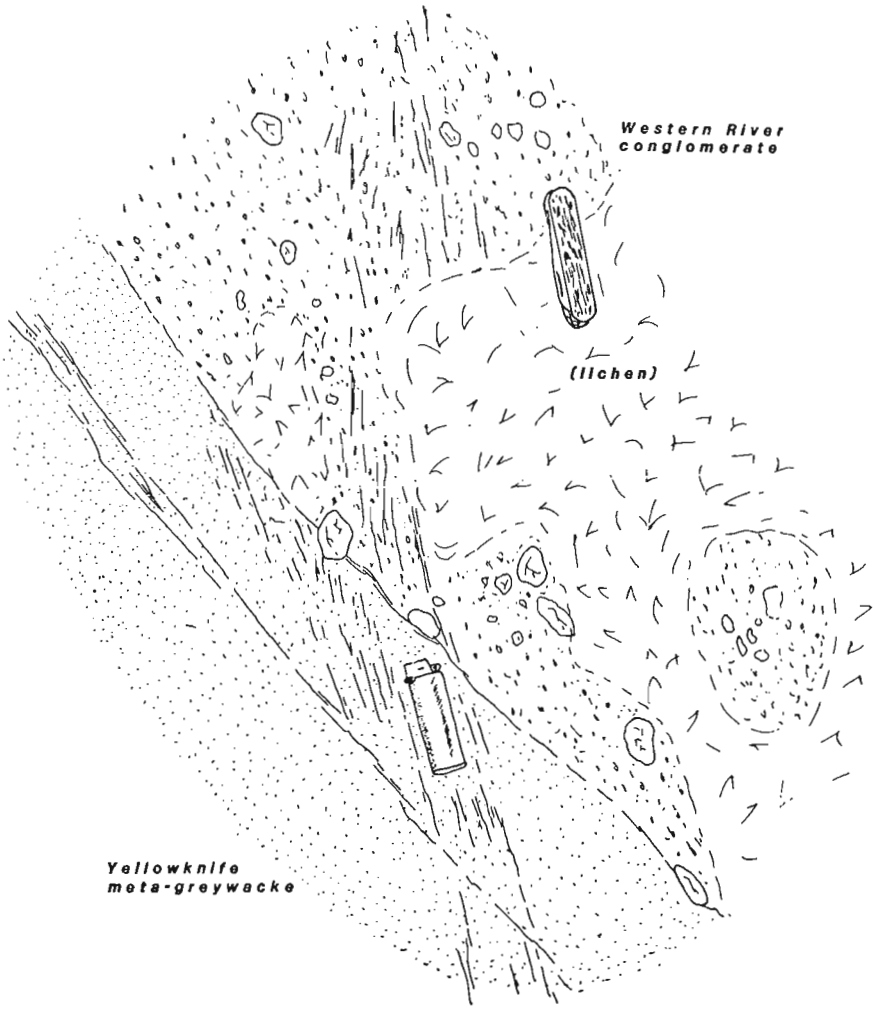

Figure 48.2. *A drawing from a photograph of a cleavage that cuts the unconformity between the Archean Beechey Lake Group, Yellowknife Supergroup metagreywackes and the Western River conglomerate of the Goulburn Group. The cleavage is axial planar to Goulburn folding in the Western River area.*

during the early folding may be seen to wrap around second fold hinges. This is especially apparent where both of these axial planar foliations (S_1 and S_2) have become more shallow dipping as a result of granite uplift, as in the 'God' Lake area. In the 'Propeller' Lake area, bedding and early fold axes trend east-west and are deformed by second generation north-northwest folding, making S_1 and S_2 easily discernible.

A third cleavage (S_3) related to undulating open upright folding is present. The cleavage commonly dips steeply to the east and in the western part of the map area strikes to the northeast. This is best documented in the rocks of subunit 1a south of Beechey Lake.

In the region south and northeast of the 'Knot' Rapids a strong north-south fracture cleavage (S_4) is present that cuts all rock types including the late muscovite granite pegmatites. The relative age of this cleavage is uncertain. It is similar in orientation to the S_5 cleavage that deforms the base of the Goulburn Group, but the latter cleavage is thought to be related to movement along the Bathurst Fault System, as discussed in the next section. However, in the 'Knot' Rapids region a muscovite schistosity is locally developed under temperature conditions that are too high for such a derivation. Conversely, the cleavage could be the same as the northeast cleavage (S_3) which Frith and Hill (in preparation) consider to be early Proterozoic in age, i.e. 2500-2600 Ma.

In the 'Propeller' Lake-Western River area late north trending cleavage (S_5) occurs that cuts the late Archean granite, the northwest trending diabase dykes and the basal parts of the Goulburn Group, Western River Formation. This late cleavage is mostly vertical to steeply dipping. At an unconformity between the Yellowknife metagreywacke and the overlying Western River conglomerate (Fig. 48.2) the S_5 cleavage is common to both. The same S_5 develops a slaty cleavage in the lower argillites of the Western River Formation and is axial planar to the undulating folds that warp the southernmost part of the Goulburn Group.

The metamorphism that affects the region is readily perceived in the more argillaceous metasediments of the Beechey Lake Group. Two isograds were mapped, namely the cordierite-staurolite and the isograd marking the breakdown of muscovite to potash feldspar and aluminosilicate. Thin section work is required to define chlorite grade rocks within subunit 1a. Previous work in the Nose-Beechey Lakes map area to the west outlined significant areas of subbiotite grade rocks (Frith and Hill, in preparation). Similarly, thin section control is needed to outline a third isograd which involves the breakdown of staurolite.

The Bathurst Fault System

Campbell and Cecile (1979) have estimated the left-lateral horizontal movement along the fault at 140 km. The movement was multi-staged as there are a number of unconformities preserved in the sedimentary record and different displacements of units of different stratigraphic age (Campbell and Cecile, in press). The older Aphebian rocks have moved much greater distances than the Helikian rocks. In this map area, horizontal displacement of the Ellice Formation is not apparent, but vertical movements have tilted strata to 70° or more. Deformation along the Bathurst Fault is thought to have continued episodically over an estimated 600 Ma, except for the cleavage (S_5) that also affects basal Goulburn units.

The effect of the fault on the Archean rocks east of 'Propeller' Lake is not dramatic. No mylonite zones were recognized. Instead, brecciated and fractured rock, commonly with carbonate infilling, was observed. The metamorphic grade jumps from biotite grade west of the fault to upper amphibolite on the east side. On the east side of the fault, sharp lithologic changes with some evidence of boundary faulting, suggest vertical movements within the block.

Campbell and Cecile (in preparation) liken the folds in Goulburn rocks to wrench-fault fold structures developed in an en echelon system at acute angles to the principal movement plane, as suggested by Wilcox et al. (1973). In the Wilcox model, folds formed by deep-seated compression that cause conjugate strike-slip, reverse and normal faulting.

Table 48.2

A tentative correlation of deformation in the Slave-Churchill boundary area

Deformation	Estimated age (Ma)	Northwest Beechey Lake area	Thelon Front area	Thelon Magnetic High area	Notes
D_1	2600 to	x	x	?	Compression and/or isoclinal folding of Yellowknife
D_2	2500	x	x	?	Supergroup
D_3	2200	x	x	?	NE cleavage in Slave ? mylonitization in the Churchill ? mylonitization is post-Wilson Is. Group, pre-Great Slave Supergroup
D_4	2000-1750		x	?	Retrograde mm at Slave margin ? Related to Hudsonian ? Retrograde mm of mylonite
D_5	1800-1500		x	?	Related to Bathurst Fault Movement

The Thelon Front

The Thelon Front separates the Slave and Churchill structural provinces. Wright (1967) defined the front as a boundary zone separating rocks of contrasting structure, lithology and metamorphic rank. In the present more detailed study, these characteristics were not readily observed. The difficulty in this map area lies mainly in the region south of the Thelon Front as mapped by Wright (1967), where the origin of the late north-south structures is ambiguous. In this study the cleavage is considered to be post-S_3, the northeast early Proterozoic cleavage and pre-S_5, the cleavage associated with the Bathurst Fault movement. The main reason for doing this is the presence of a muscovite fabric parallel to a north-south cleavage (S_4) which is more likely associated with renewed thermal metamorphism ("Hudsonian" Orogeny) than with Bathurst Fault and its associated folding.

Transitions in lithology and metamorphic rank are not distinctive on opposing sides of the Thelon Front. Yellowknife metasediments occur on both sides and the metamorphism that produced the various types of paragneiss, paraschist and migmatite, is likely of Archean age. It does not seem reasonable to use an Archean isograd to define a Proterozoic tectonic boundary.

The Thelon Front is far more impressive on a larger scale than on the present map scale. Gibb and Thomas (1977) using gravity, and Thomas et al. (1976) using aeromagnetics, have proposed various fault and plate tectonic interpretations of the gravity and magnetic anomalies that occur along and parallel to the Thelon Front. Whether or not their interpretations are accepted or not, the geophysical data suggest an important change in crustal structures along the Thelon Front.

A tentative correlation of the various deformations present in the map area with regions farther to the east is shown in Table 48.2. The S_3 and S_4 found in the map area may have analogues to the early and mid-Proterozoic tectonic events described to the west and south of the Slave Province (Frith et al., 1977b; Frith and Hill, in preparation). The early Proterozoic events are associated with basin formation in the Wopmay Orogen and along the west margin of the Slave Province (Frith et al., 1977b), where the craton has been affected by intrusion, low grade metamorphism and deformation recorded at about 2200 and 1900 Ma. Along the eastern margin of the Slave craton there are similarly related cleavages, but the presence of mylonite zones (Henderson and Thompson, 1981) suggests that the early tectonic events were of compression rather than dilation. The mylonites are probably of comparable age as they deform the Wilson Island Group yet are unconformably overlain by the mid-Proterozoic Great Slave Supergroup (Hoffman et al., 1977). It is not certain that the mylonites are tectonically related to S_3 structures found along the east margin of the Slave, but there is mounting evidence that these S_3 structures penetrate at least 90 km into the Slave craton, and relationships in the Nose Lake region suggest they too are early-Proterozoic (Frith and Hill, in preparation).

References

Campbell, F.H.A. and Cecile, M.P.
1979: The northeastern margin of the Aphebian Kilohigok Basin, Melville Sound, Victoria Island, District of Franklin; in Current Research, Part A, Geological Survey of Canada, Paper 79-1A, p. 91-94.

Campbell, F.H.A. and Cecile, M.P.
Evolution of the Early Proterozoic Kilohigok Basin, Bathurst Inlet-Victoria Island, N.W.T.; in Proterozoic Basins of Canada, Geological Survey of Canada, Paper 81-10. (in press)

Frith, R.A. and Hill, J.D.
1975: The geology of the Hackett-Back River Greenstone Belt – preliminary account; in Report of Activities, Part C, Geological Survey of Canada, Paper 75-1C, p. 367-370.

The geology of the Nose-Beechey Lakes map area, District of Mackenzie; Geological Survey of Canada. (in preparation)

Frith, R.A. and Percival, J.A.
1978: Stratigraphy of the Yellowknife Supergroup in the Mara-Back Rivers area, District of Mackenzie; in Current Research, Part C, Geological Survey of Canada, Paper 78-1C, p. 89-98.

Frith, R.A., Fyson, W.K., and Hill, J.D.
1977a: The geology of the Hackett-Back River Greenstone Belt – second preliminary report; in Report of Activities, Part C, Geological Survey of Canada, Paper 77-1A, p. 415-423.

Frith, Rosaline, Frith, R.A., and Doig, R.
1977b: The geochronology of the granitic rocks along the Bear-Slave Structural Province boundary, northwest Canadian Shield; Canadian Journal of Earth Sciences, v. 14, p. 1356-1373.

Fyson, W.K. and Frith, R.A.
1979: Regional deformation and emplacement of granitoid plutons in the Hackett River greenstone belt, Slave Province, Northwest Territories; Canadian Journal of Earth Sciences, v. 16, p. 1187-1195.

Gibb, R.A. and Thomas, M.D.
1977: The Thelon Front: A cryptic suture in the Canadian Shield; Tectonophysics, v. 38, p. 211-222.

Henderson, J.B.
1970: Stratigraphy of the Archean Yellowknife Supergroup, Yellowknife Bay-Prosperous Lake area, District of Mackenzie; Geological Survey of Canada, Paper 70-26.

Henderson, J.B. and Thompson, P.H.
1980: The Healey Lake map area (northern part) and the enigmatic Thelon Front, District of Mackenzie; in Current Research, Part A, Geological Survey of Canada, Paper 80-1A, p. 165-169.

1981: The Healey Lake map area and the enigmatic Thelon Front; in Current Research, Geological Survey of Canada Paper 81-1A, report 22.

Heywood, W.W. and Schau, M.
1978: A subdivision of the northern Churchill Structural Province; in Current Research, Part A, Geological Survey of Canada, Paper 78-1A, p. 139-143.

Hoffman, P.F., Bell, I.R., Hildebrand, R.S., and Thorstad, L.
1977: Geology of the Athapscow Aulacogen, East Arm of Great Slave Lake, District of Mackenzie; in Current Research, Geological Survey of Canada, Paper 77-1A, p. 117-129.

Thomas, M.D., Gibb, R.A., and Quince, J.R.
1976: New evidence from offset aeromagnetic anomalies for transcurrent faulting associated with the Bathurst and McDonald faults, Northwest Territories; Canadian Journal of Earth Sciences, v. 13, p. 1244-1250.

Tremblay, L.P.
1971: Geology of Beechey Lake map-area, District of Mackenzie; Geological Survey of Canada, Memoir 365.

Wilcox, R.E., Harding, T.P., and Seely, D.R.
1973: Basic Wrench Tectonics; American Association of Petroleum Geologists, Bulletin, v. 57, p. 74-96.

Wright, G.M.
1967: Geology of the southeastern barren grounds, parts of the Districts of Mackenzie and Keewatin (Operations Keewatin, Baker, Thelon); Geological Survey of Canada, Memoir 350.

CADOMIN FORMATION, FLATHEAD RIDGE VICINITY, SOUTHEASTERN BRITISH COLUMBIA

Project 750082

N.C. Ollerenshaw
Institute of Sedimentary and Petroleum Geology, Calgary

Ollerenshaw, N.C., Cadomin Formation, Flathead Ridge vicinity, southeastern British Columbia; in Current Research, Part A, Geological Survey of Canada, Paper 81-1A, p. 341-347, 1981.

Abstract

The Lower Cretaceous Cadomin Formation, on and in the vicinity of Flathead Ridge, in the Fernie basin region of southeastern British Columbia, is well exposed and consists of at least four conglomerate or conglomerate and sandstone units, separated by equally thick units of green and red mudstone (with some shale, siltstone and sandstone beds). Two sections, 5 km apart, one at least 45 m and the other 75.5 m thick, are described. Basal contacts with the underlying Elk Formation are well exposed, with conglomerate of the Cadomin variously resting on either Elk sandstone, or mudstone or siltstone. The contrast between this relatively thick, multiple-conglomerate sequence of the Cadomin and the single conglomerate unit to the northeast in the Alberta Foothills is emphasized. The alternation of conglomerate and mudstone units in the Cadomin of the Fernie basin reflects the interfingering of coarse into fine clastics eastwards in a proximal braided stream environment, on the outer periphery of an alluvial fan. A minor but regional association with micritic limestone is noted. The red colour of some mudstones suggests at least a semi-arid climate. Extensive, clean bedding surfaces, devoid of lichen greatly facilitate the study of the Cadomin conglomerates in this locality.

Introduction

The Cadomin is a conglomerate bearing formation which forms the lowest part of the Lower Cretaceous Blairmore Group.

This report is intended to outline and draw attention to the accessible exposures and good sections of Cadomin Formation in southeastern British Columbia. McLean (1977, p. 796), in a regional study of the Cadomin Formation, noted the scarcity of published data for the formation in this area. The only previously published section of the Cadomin in the Fernie basin is that of Newmarch (1953), on Coal Creek, near Fernie. It is intended that this paper will provide a more detailed outline of the Cadomin Formation in this area to promote further investigation, and an awareness of the relative differences between the stratigraphy and facies of this region and the better known sections to the northeast in Alberta. Geological mapping and investigation (1977-80) of the Dominion Coal Block, Parcel 82, east of Fernie, British Columbia, involved the examination of extensive outcrops of Cadomin Formation, along the north side of Flathead Ridge (Fig. 49.1). Two sections are discussed. They are about 5 km apart and located close to a gas pipeline, on the north side of Flathead Ridge, about 24 km southeast of Fernie.

Stratigraphy

The Cadomin Formation was first defined as the "Cadomin Conglomerate" by B.R. MacKay in 1929, with its type section in the railway cut at Cadomin, 85 km southwest of Edson, Alberta. This terminology has been gradually extended throughout southwestern Alberta and Crowsnest Pass, to replace the term "basal Blairmore conglomerate", or "Blairmore conglomerate", introduced by Rose (1917). For example, Glaister (1959) used the term "Cadomin Conglomerate Member", in the Crowsnest Pass region of southwestern Alberta. The general acceptance of the Cadomin as a formation rather than a member was noted by McLean (1977, p. 793).

Allan and Carr (1947, p. 32) suggested the possibility that the lower part of the Blairmore Group in southeastern British Columbia may correlate with their Pocaterra Creek Member, defined in southwestern Alberta and comprising a unit of the Blairmore Group between the Cadomin Formation and the underlying Kootenay Group. The Pocaterra Creek Member was defined by Allan and Carr as a local facies near Highwood Pass, Alberta, 140 km north-northwest of Flathead Ridge. It is 112 m thick on Pocaterra Creek but thins southward to lens out about 24 km in that direction. It consists of grey and olive grey shale, fine grained quartzitic sandstone, coarse grained cherty sandstone, including 4.3 m of interbedded sandstone and conglomerate at the base, with minor carbonaceous shale, maroon shale and limestone nodules. The basal conglomerate of the Pocaterra Creek Member was differentiated by Allan and Carr (1947, p. 28) from the Cadomin conglomerate by the absence of green pebbles and relative scarcity of white quartzite pebbles in the former, together with its finer grain size. Glaister (1959, p. 605) speculated that the Pocaterra Creek Member, "is probably lithologically equivalent to part of the Elk Formation in the Fernie area of British Columbia". Gibson (1977, p. 783), however, recognized the Pocaterra Creek Member in the Blairmore Group of the Fernie area, in his Sparwood, Fernie and Marten Ridge sections. For this reason, the writer has considered the basal Blairmore sequence in the vicinity of Flathead Ridge in terms of the Pocaterra Creek Member as described in the reports referenced above. The succession of conglomerate and sandstone units in the lower part of the Blairmore Group at this locality cannot be differentiated or subdivided on the basis of clast size or composition. In fact, lateral variation in these parameters within individual coarse clastic units is at least as great as vertical change from one of these units to another and all variations are comparable to those commonly seen in the established Cadomin Formation in the Foothills of southern Alberta. The separation of the coarse clastic units by mudstone units does not constitute grounds for correlation with the Pocaterra Creek Member. On this basis, the sections described in this report are positively identified as Cadomin Formation.

In the Fernie basin, the Cadomin Formation overlies the Elk Formation (the uppermost formation of the Kootenay Group). Both sequences are Lower Cretaceous and consist of nonmarine clastic sediments, ranging from shale and mudstone through siltstone and sandstone to conglomerate. Erosional relief at the contact between the formations is in the order of a few centimetres to about 0.5 m locally, with beds on either side essentially parallel. This relief could be

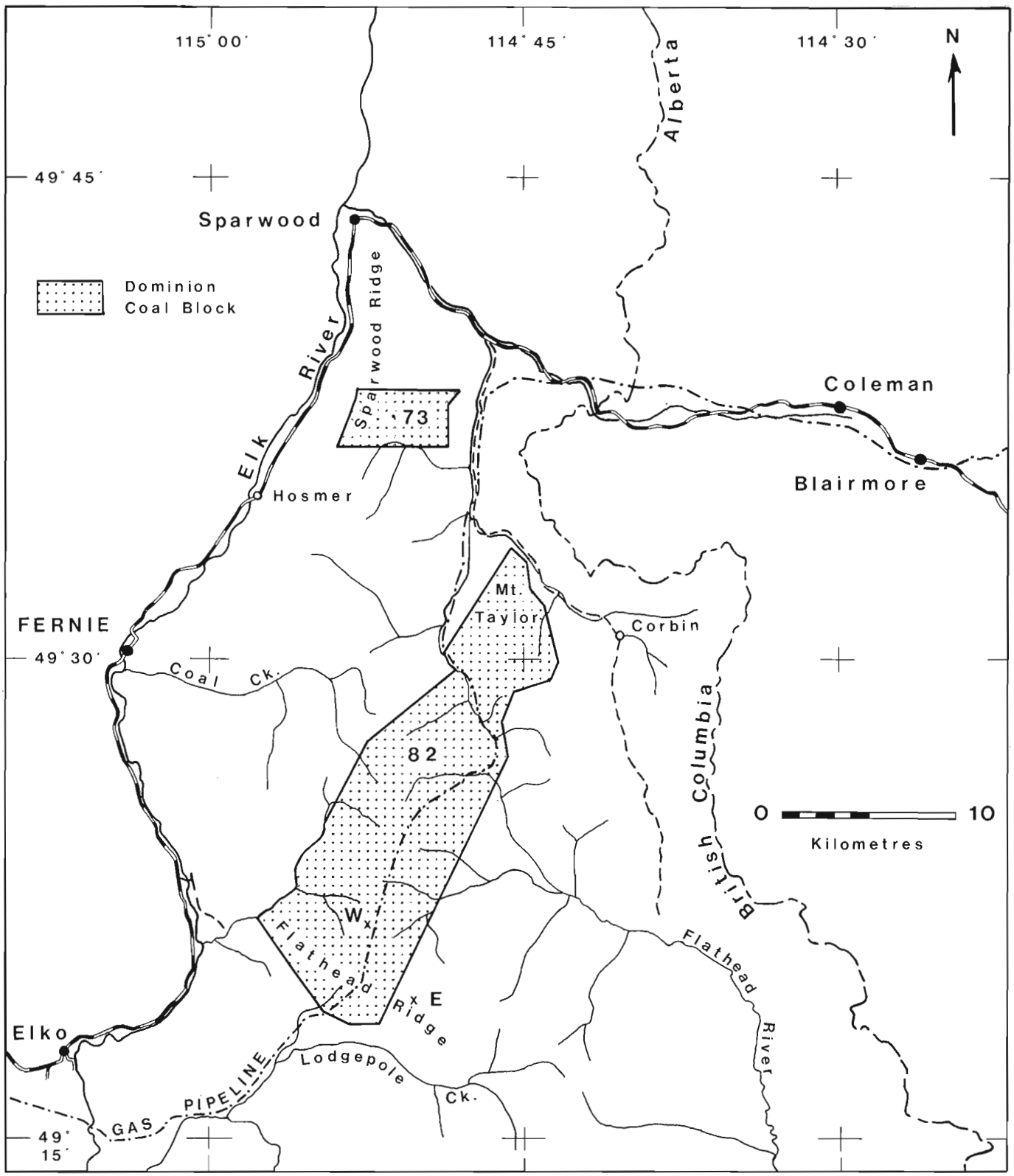

Figure 49.1. *The Fernie basin area, in southeastern British Columbia, and adjoining areas, showing the location of Cadomin Formation sections near Flathead Ridge. East section (E), West section (W).*

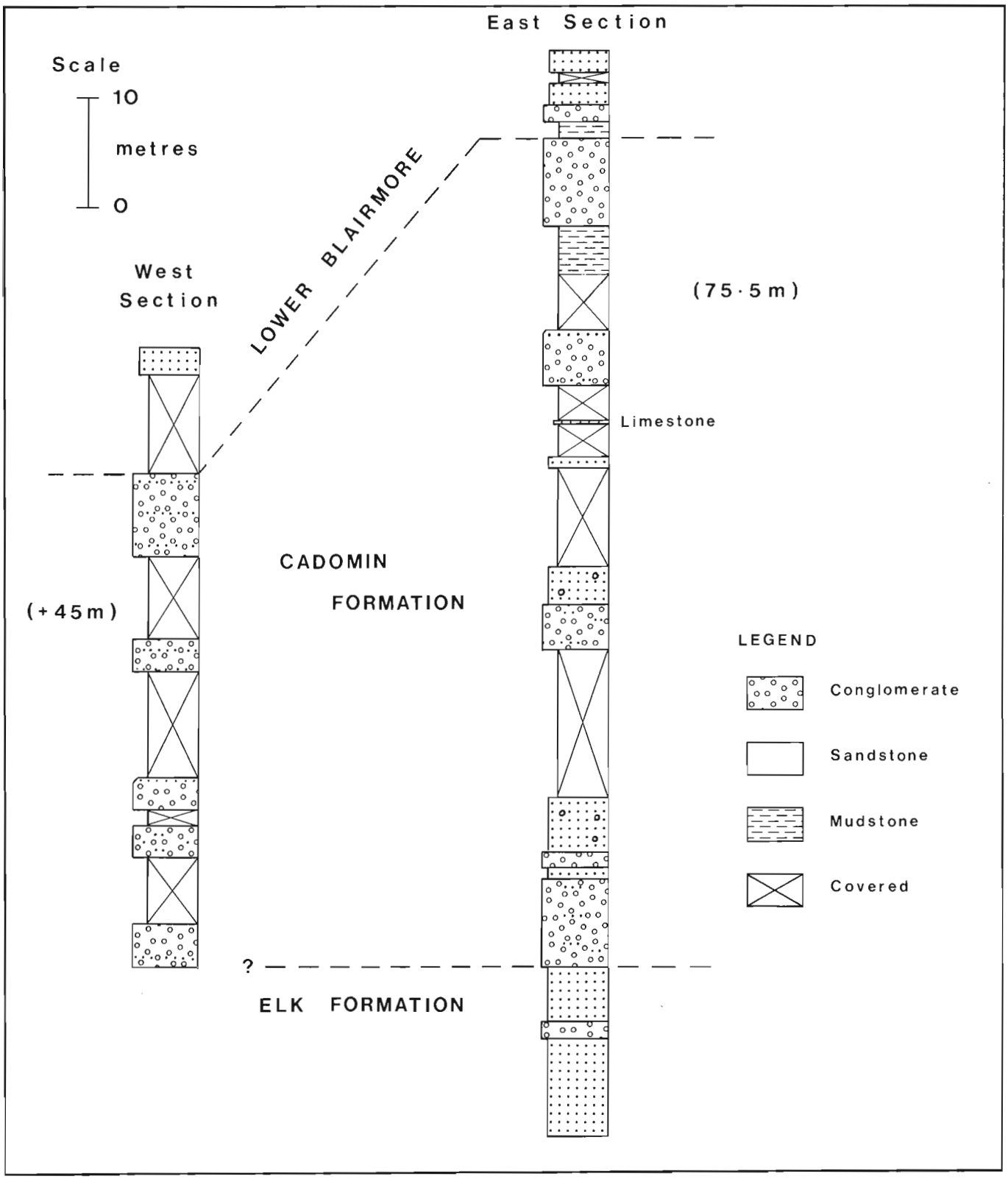

Figure 49.2. *Columnar sections of Cadomin Formation, on Flathead Ridge.*

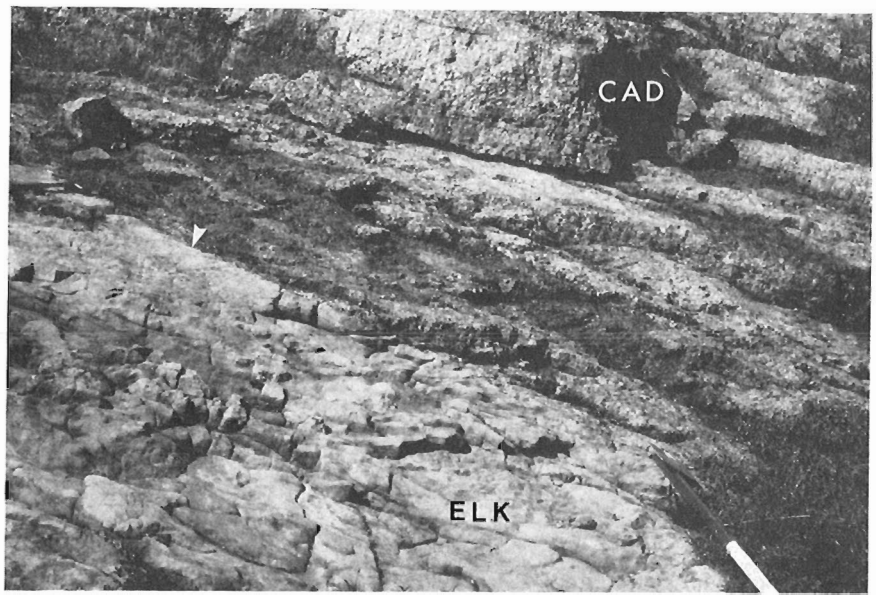

Figure 49.3

Contact between conglomerate (upper) of the Cadomin Formation and sandstone (lower) of the Elk Formation (hammer and end of pogo stick mark contact). East section, Flathead Ridge.

ascribed to local channelling, or it could reflect the regional erosional unconformity at this contact, documented in Alberta and northeastern British Columbia (see McLean, 1977, p. 799). The basal conglomerate of the Cadomin rests on shale at some locations and on mudstone or sandstone at others; a relationship which, at least on a local level, can be attributed to lateral facies variation in the Elk Formation. Where Elk sandstones are in direct contact with the basal Cadomin conglomerate, the two lithologies commonly form a single cliff, with the formation contact part way up.

The Elk Formation at its type section on Coal Creek, near Fernie (Newmarch, 1953), represents an alluvial fan margin (Gibson, 1977, p. 783), with abundant conglomerates, comparable to those of the Cadomin, indicating a fairly high energy environment. The Elk Formation rapidly changes to a distal facies away from Coal Creek, such that, 20 km south-southeast on Flathead Ridge, its strata have changed to predominantly sandstone and mudstone, with only minor conglomerate, the assemblage indicating a relatively lower energy environment. Between the same two points, the Cadomin shows little evidence of major facies change, and the alternation of several high energy conglomerate units with low energy mudstone sequences persists. The finer grained deposits probably reflect overbank, interlobe, or, locally, channel fill deposition.

Both the Elk and Cadomin display strong fining upward cycles, with conglomerates typically overlain by sandstones followed by mudstones, whereas coarse grained sandstones are overlain by finer grained sandstones capped, in turn, by shale or mudstone.

Individual conglomerate units of the Cadomin Formation in the Fernie basin commonly pass laterally within a short distance into conglomeratic sandstone to pebbly sandstone facies with individual units also thinning or lensing out laterally. As a result, the thickest and most dominant cliff-forming conglomerate in one section may be relatively inconspicuous in the next or adjacent section and vice-versa. The conglomerate units along Coal Creek just east of Fernie illustrate this lenticular lateral transition very well, particularly when viewed from the air.

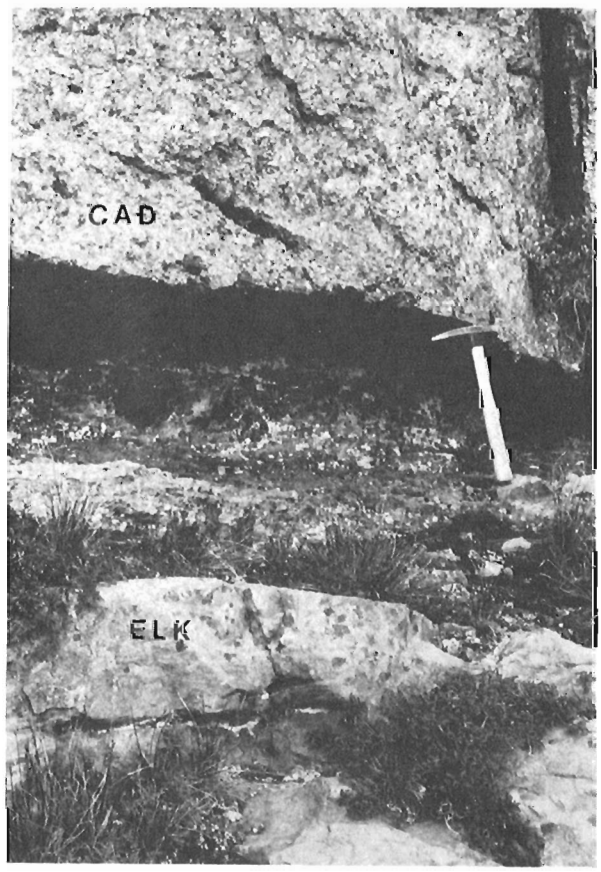

Figure 49.4. *Hammer head marks contact between conglomerate of the Cadomin Formation and very dark grey siltstone of the Elk Formation, near east section on Flathead Ridge.*

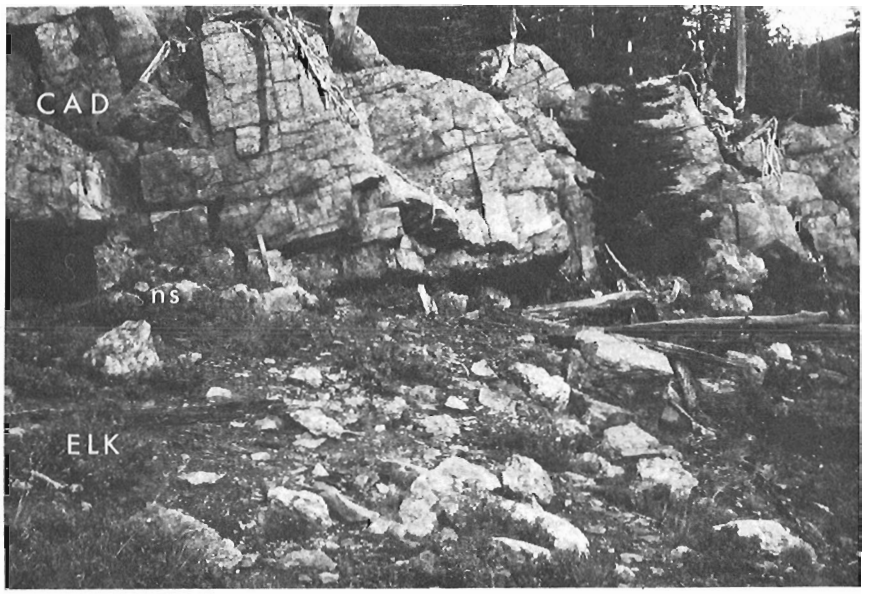

Figure 49.5

Hammer head rests on contact between Cadomin conglomerate (above) and Elk Formation blackish mudstones, one kilometre southeast of the east section. Top bed (ns) of Elk is an argillaceous siltstone containing scattered "needles" of algal coal.

In the general vicinity of Flathead Ridge, the Elk Formation is easily distinguishable from the Cadomin. The Elk sandstones tend to be darker (medium to very dark grey), more limonitic, more carbonaceous, and to contain more plant debris and coal material than the Cadomin sandstones. In addition, the upper part of the Elk Formation, as in other parts of the Fernie basin, includes thin to medium beds of "needle coal" (Newmarch, 1953, p. 41; Ollerenshaw, 1977, p. 157; and Gibson, 1977, p. 782). The needles are about the size and shape of pine-needles. They are completely coalified and have been identified as algal by Pearson and Grieve (1980, p. 93). Throughout the Fernie basin area, beds containing coal needles vary from thin beds of true "needle coal", to light grey weathering, argillaceous siltstones containing scattered coal needles. Only the "needle siltstones" have been observed in the vicinity of Flathead Ridge. Coal also occurs in the upper Elk, forming scattered lenses and small pockets, and there are thin seams of coal, 5-30 cm thick. Plant detritus is common and typically occurs as carbonized, macerated fragments or as coalified, small to medium sized, stem and branch fragments and impressions. Roots and rootlets, a few small, coalified tree trunk segments in growth position and a possible fossil soil profile with a leached zone on top have been observed locally. Current ripple marks in sandstones and one example of mudcracks in a siltstone bed are other features noted in the Elk Formation, but not in the Cadomin on Flathead Ridge. Dark grey to blackish mudstones and shales are typical of the Elk Formation and occur as only a minor, local component in the Cadomin, so that they are useful in differentiation. The green and maroon mudstones characteristic of the recessive and covered intervals between the conglomerate units in the Cadomin Formation have not been observed in the underlying Elk Formation, so that they can be used to positively differentiate the two formations.

Cadomin sandstones are light medium grey to medium grey, only slightly carbonaceous to noncarbonaceous, less limonitic and much cleaner than those in the Elk. Plant stem and or branch fragments are quite common in the Cadomin in both sandstones and conglomerates, usually occurring as slightly carbonaceous, crisscrossed impressions on bedding surfaces.

Light grey, very light grey weathering, micritic limestone occurs at many localities, in the upper part of and slightly above the Cadomin Formation. Only one bed has been noted at any one locality. The limestone is massive at some localities, nodular at others and up to 1.2 m thick. Similar micritic limestone occurs as scattered calcrete nodules in mudstones and as pebbles in conglomerates higher in the section, within the Lower Blairmore.

The contact between the Cadomin Formation and overlying Lower Blairmore strata in the Fernie basin is not everywhere obvious or easy to pick. It is a contact based on a vertical facies change, in which the same lithologies change only in relative proportions across the contact. Green and red mudstones and shales occur in both formations, but are clearly predominant in the Lower Blairmore. Conglomerates and coarse grained sandstones are a major component in the Cadomin and a minor one in the Lower Blairmore. Essentially, therefore, the size and spacing of the coarse clastic and fine clastic units determines the placing of the contact. This is a subjective rather than a precise designation. The writer does not, however, accept McLean's (1977, p. 796) working definition which incorporates all coarse clastic units in the Cadomin, "unless they are separated from the main body of the formation by a unit of finer sediments greater than 1.5 times the thickness of the overlying unit". This 1.5 times rule is too arbitrary and too inflexible. Until the facies relationships across this contact are more thoroughly understood its placement should remain moderately flexible. The writer would include in the Cadomin Formation all units of conglomerate and coarse-grained sandstone that are lithologically similar, form a major component of the sequence, and are in sufficient vertical proximity to constitute collectively the best mappable grouping of strata available.

Where the writer has also worked, approximately 140 to 315 km to the north of Flathead Ridge, in the southern Foothills of Alberta, from Turner Valley north to Ram River (Calgary Foothills), the Cadomin Formation is very different from the southeastern British Columbia occurrences. In the Calgary Foothills, the formation consists of one unit only, where observed. This unit is mainly conglomerate or sandy conglomerate but passes locally into sandstone. It ranges from 7 to 23 m in thickness, but is mainly 8 to 12 m thick. The Cadomin Formation in southeastern British Columbia differs from its counterpart in the Calgary Foothills region of Alberta in that it is thicker, and consists of multiple (instead of a single) conglomerate-sandstone units, which are interbedded with and overlain by quite different fine grained sedimentary rocks, notably green and red mudstone. There is obviously a pronounced facies change between the two areas

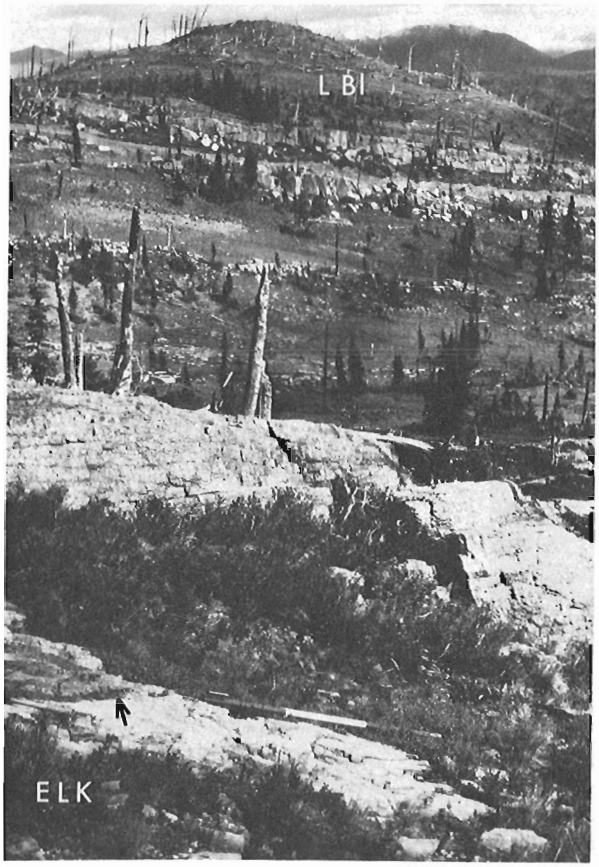

Figure 49.6. *East section of Cadomin Formation, north side of Flathead Ridge. Note four resistant conglomerate units. Hammer and pogo stick rest on Elk sandstone at the contact with overlying Cadomin conglomerate. Rounded hill in background is underlain by Lower Blairmore strata (LB1).*

and the Fernie basin Cadomin represents a more proximal environment than its distal counterpart in the Calgary Foothills.

Associated sedimentary rocks in the overlying Lower Blairmore of the Calgary Foothills area are shales, siltstones and sandstones, ranging from lighter to darker grey as grain size decreases. There are no green and red mudstones in the Cadomin or Lower Blairmore strata of this area. Green and minor red mudstones only appear much higher in the section, in the younger Beaver Mines Formation. In fact, the Lower Blairmore of the Turner Valley to Ram River part of the Foothills is more similar lithologically to some of the shales, siltstones and fine grained sandstones of the upper Elk Formation in Fernie basin than it is to the Lower Blairmore in that region.

A good section of the Cadomin Formation, here designated the east section, occurs on the north side of Flathead Ridge, approximately 700 m north of the crest, 1130 m east-southeast of Parcel 82 and 3 km east-southeast of a gas pipeline, at latitude 49°19'45"N and longitude 114°50'15"W (Fig. 49.1). Access is by 4-wheel drive vehicle along a 1980 exploration road east from the gas pipeline access road junction at the crest of Flathead Ridge. Exposure is approximately 55 per cent complete, but could be improved to 80 per cent or more by relatively minor trenching of the covered recessive units. Another fairly good section, designated the west section, is located 2.4 km north of Flathead Ridge about 300 m west of the pipeline at latitude 49°21'45"N and longitude 114°52'15"W (Fig. 49.1).

The main lithologic units are plotted on Figure 49.2, which illustrates the stratigraphy of the east and west sections. The figure shows some similarities and differences between the two sections, which are only 5 km apart. Both sections have four distinct conglomerate horizons, but differ in total formation thickness from 75.5 m in the east section, to at least 45 m in the west section. The base of the west section is not exposed, but probably not more than 1 to 10 m is missing.

The basal contact of the Cadomin Formation with the underlying Elk Formation is well exposed in the east section. There is a fairly rapid lateral change in the lithology of the strata underlying the contact. Where the section was measured, Cadomin conglomerate rests directly on Elk sandstone (see Fig. 49.3), but about 30 m east the conglomerate rests on a 30 cm thick bed of very dark grey, argillaceous siltstone (see Fig. 49.4) which separates the Cadomin conglomerate from the Elk sandstone. About 1 km southeast of the east section the upper part of the Elk consists of several metres of mainly very dark grey to black mudstone, the uppermost bed of which is a 25 cm-thick bed of light grey weathering argillaceous siltstone (see Fig. 49.5), containing scattered "needles" of algal coal. Erosional relief along the contact ranges from a few centimetres to one half metre at the most, probably the result of local channelling.

Figure 49.6 is a view of the entire east section showing the basal contact, the four resistant coarse clastic units, and the overlying Lower Blairmore strata.

The upper contact between the Cadomin Formation and overlying Lower Blairmore strata in the east section is moderately well exposed locally. The contact is placed at the top of the uppermost cliff-forming conglomerate unit (8 m thick). The upper surface of this conglomerate is slightly uneven and is overlain, apparently conformably by a 1.5 m thick unit of very dark grey, hard, silty mudstone containing minor thin beds of very fine grained sandstone. The mudstone is overlain by 1.5 m of granule to pebble conglomerate capped by 5 m of very fine to fine grained sandstone (with minor medium grained sandstone). Showings of green and red mudstone with local minor units of sandstone continue up the hillside for the next 25 m, clearly indicating that there are no more conglomerate units in sufficient vertical proximity to warrant their inclusion in the Cadomin Formation. The very dark grey mudstone and strata above it must be classified as Lower Blairmore.

In the west section, the upper contact between the Cadomin Formation, and overlying Lower Blairmore strata is covered but there are showings of green and red mudstones and local sandstone units in the overlying interval. In the interval 79.5 to 149 m above the top of the Cadomin Formation in the west section, several units of conglomerate (1 to 5.5 m thick) and coarse grained sandstone (1 to 7.5 m thick) occur within the Lower Blairmore. Apart from an increased content of, and association with sandstone, these conglomerates are very similar in composition and bedding characteristics to the Cadomin conglomerates below. Conglomerate deposition in the vicinity of Flathead Ridge commenced in the top 50 m of the Elk Formation, peaked in the Cadomin Formation and persisted into the upper part of the Lower Blairmore, across an interval of 250 m of section.

In both sections, conglomerates typically consist of well rounded to very well rounded chert and quartzitic sandstone phenoclasts, with fabrics ranging from clast-supported to matrix-supported. The long axes of phenoclasts range from 0.3 to 18 cm, mainly 0.5 to 2.5 cm; commonly 2.5 to 6.5 cm; and minor 6.5 to 14 cm, with rare to 18 cm. Scattered chert phenoclasts containing fossils, including one containing fusulinids and another containing part of a coral, were found in the topmost conglomerate of the east section. Medium to large scale crossbedding is very common, and is mainly planar

to curviplanar but with common trough sets. The crossbedding is mainly apparent in the sandy conglomerate and sandstone facies where foresets display conspicuous size differentiation with layers of very coarse sand size, granules and pebbles alternating with finer material. Conglomerate units locally pass laterally into more sandy facies. Lenticular beds of crossbedded sandstone, 10 to 75 cm thick and 15 cm to 1 m apart, separated by reactivation surfaces, are common in the conglomerate units. Conversely, similar pebbly and conglomeratic lenses occur in the sandstones. Conglomerate beds locally rest on channelled surfaces cut into underlying sandstones or mudstones.

Crisscrossing patterns of plant stem or branch fragment impressions occur on many surfaces or as scattered individuals in the conglomerate and sandstone units. Typically, these broken plant fragments are 0.5 to 3 cm wide and 10 to 25 cm long. A few larger fragments (up to 6 x 59 cm) occur locally. These impressions are similar to those commonly found in the Elk Formation but show only minor carbonaceous residues rather than the conspicuous coal lenses associated with the plant debris in the Elk.

Ashowing of distinctive nodular limestone, at least 30 cm thick, occurs 49.5 m above the base of the Cadomin Formation in the east section (Fig. 49.2). This limestone is micritic, medium grey and very light grey weathering.

Exposures along strike indicate that the covered intervals in the measured sections are mainly mudstones and shales which are typically greenish grey, with minor to common maroon colouration. Mudstone units have no obvious stratification, but do contain scattered thin to medium thick beds of very fine to fine grained sandstone.

A bedding surface in the lowermost conglomerate unit in the east section has the form of an embankment, and is possibly a relict channel margin terrace, as described by Williams and Rust (1969, p. 659). The base of the uppermost conglomerate unit in the east section locally displays a series of sub-parallel, discontinuous furrows and ridges along its basal surface (overlying mudstone). These structures are 3.5 to 6.5 cm deep and wide and at least 20 to 30 cm long. They could be obstacle-scour marks or rill marks but exposure is inadequate for valid identification.

Following the suggestion of McLean (1977, p. 814) for the Coal Creek section, the environment of deposition of these Cadomin sections may also be interpreted as a distal alluvial fan margin. Strata in the vicinity of Flathead Ridge suggest a braided river environment. The coarse grained sandstones and conglomerates represent channel and bar deposits, interdigitated with finer grained interlobe, overbank and flood-plain material, the latter including minor limestone of probable lacustrine origin. The maroon beds suggest at least a semi-arid climate.

Finally, it should be noted that, as a result of forest fires during the 1930s, subsequent local erosion to bedrock and the slow development of lichens, the conglomerate outcrops of the Cadomin Formation, in the vicinity of Flathead Ridge, are completely clean, stripped of all cover and devoid of lichens over wide areas. This greatly facilitates the study of clasts, matrix and extensive exhumed bedding surfaces.

References

Allan, J.A. and Carr, J.L.
1947: Geology of highwood-Elbow Area Alberta; Research Council of Alberta, Report no. 49, 74 p.

Gibson, D.W.
1977: Sedimentary facies in the Jura-Cretaceous Kootenay Formation, Crowsnest Pass Area, southwestern Alberta and southeastern British Columbia; Bulletin of Canadian Petroleum Geology, v. 25, no. 4, p. 767-791.

Glaister, R.P.
1959: Lower Cretaceous of southern Alberta and adjoining areas; American Association of Petroleum Geologists, Bulletin, v. 43, no. 3, p. 590-640.

MacKay, B.R.
1929: Cadomin; Geological Survey of Canada, Map 209A.

McLean, J.R.
1977: The Cadomin Formation: stratigraphy, sedimentology, and tectonic implications; Bulletin of Canadian Petroleum Geology, v. 25, no. 4, p. 792-827.

Newmarch, C.B.
1953: Geology of the Crowsnest coal basin, with special reference to the Fernie area; British Columbia Department of Mines, Bulletin no. 33, 107 p.

Ollerenshaw, N.C.
1977: Canadian Government Coal Block, Parcel 73, Fernie basin, British Columbia; in Report of Activities, Part A, Geological Survey of Canada, Paper 77-1A, p. 155-159.

Pearson D.E. and Grieve, D.A.
1980: Elk Valley coalfield; in Geological fieldwork, 1979, Ministry of Energy, Mines and Petroleum Resources, British Columbia, Paper 1980-1, p. 91-96.

Rose, B.
1917: Crowsnest coal field, Alberta; Geological Survey of Canada, Summary Report, 1916, p. 107-114.

Williams, P.F. and Rust, B.R.
1969: The sedimentology of a braided river; Journal of Sedimentary Petrology, v. 39, no. 2, p. 649-678.

50.

CHROMITE IN SOME ULTRAMAFIC ROCKS OF THE CACHE CREEK GROUP, BRITISH COLUMBIA

EMR Research Agreement 103-4-80

Peter J. Whittaker[1] and David H. Watkinson[1]
Economic Geology Division

Whittaker, Peter J. and Watkinson, David H., Chromite in some ultramafic rocks of the Cache Creek Group, British Columbia, in Current Research, Part A, Paper 81-1A, p. 349-355, 1981.

Abstract

The Anarchist and Bridon chromite occurrences in the Anarchist Group, the Nicola (Cameo Lake) deposit in the Chapperon Group, and the Scottie Creek and Murray Ridge deposits in the Cache Creek Group were among the chromite occurrences in British Columbia examined during the 1980 field season. Mapping was concentrated on Murray Ridge where the occurrence of chromite is ubiquitous in blocks of harzburgite and dunite. Chromite was observed to occur in three general forms; (a) disseminated chromite forming 2 to 3 modal per cent of the harzburgite and dunite, (b) wispy chromite layers 1 to 2 cm thick and discontinuous over lengths up to 20 cm, and (c) as irregularly shaped chromitite lenses. Chromite in harzburgite is anhedral, extensively fractured and embayed, whereas chromite in dunite layers in euhedral and weakly fractured. Electron microprobe analyses of chromite from Murray Ridge and Chrome Peak (43 km north of Mt. Sydney-Williams) indicate that crystal zoning is absent, chromium to iron ratios are high, and distinct differences exist in composition of chromite from harzburgite and dunite. Cryptic variation of Cr/Cr+Al, Mg/Mg+Fe and Mn values is observed.

Introduction

Mapping of chromite occurrences in ultramafic rocks of the Anarchist, Cache Creek, and Chapperon groups was initiated during the 1980 field season.

The Cache Creek Group represents a subduction complex, the youngest rocks of which are Early Triassic. Late Triassic rocks of the Nicola, Takla, and Stuhini groups flank the Cache Creek Group. The Cache Creek Group, Hozameen Group, and the Bridge River Group rocks, all representative of late Paleozoic and early Mesozoic Pacific Ocean crust, are thought to have accreted in Mesozoic time (Monger and Price, 1979).

Chromite occurrences are well known in British Columbia, principally through the work of geologists of the British Columbia Ministry of Energy, Mines and Petroleum Resources and the Geological Survey of Canada (Nichols, 1931; James, 1958; Armstrong, 1949; Sutherland Brown, 1958). Several chromite occurrences were mapped (Fig. 50.1, 1-5) including: (1) the Anarchist deposit, (2) the Bridon deposit, (3) the Nicola (Cameo Lake) deposit, (4) the Scottie Creek deposit, and (5) Murray Ridge. In preparation for future work on the Irish, Simpson, and Bob deposits (Armstrong, 1949) in the Trembleur ultramafic rocks of the Cache Creek Group, Murray Ridge, the southernmost of the Trembleur Intrusions, was examined in detail.

Geology of the Murray Ridge area

Murray Ridge is 10 km northeast of Fort St. James in central British Columbia (Fig. 50.1). A road suitable for four-wheel drive vehicles leaves the Fort St. James-Germansen Landing road and provides access to a fire tower on the southeast end of Murray Ridge.

Murray Ridge was included in a reconnaissance map sheet by Armstrong (1949) and was studied in greater detail by Paterson (1973, 1977). The ultramafic rocks were the subject of a structural study by Ross (1977) who concluded that internal structures showed two mantle transport fabrics, and a third fabric related to high-level emplacement.

The main structural feature in the Murray Ridge area is the Pinchi Fault Zone which trends northwest and separates the Late Paleozoic Cache Creek Group to the west from the Early Mesozoic Takla Group to the east.

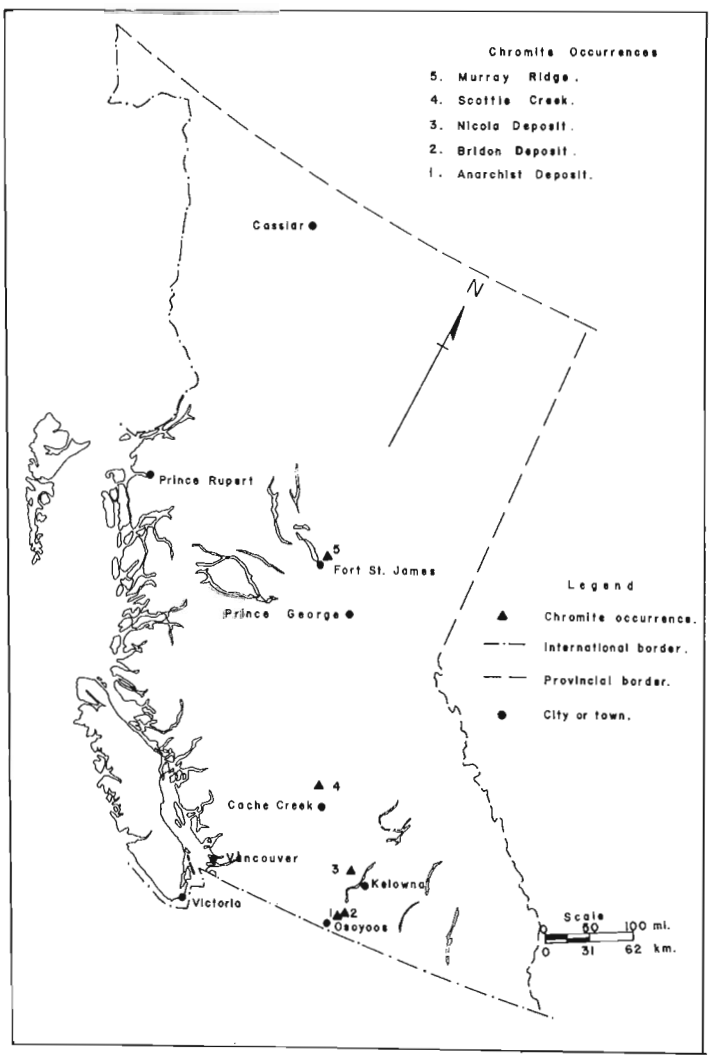

Figure 50.1. *Location of chromite occurrences examined in British Columbia.*

[1]Department of Geology, Carleton University, Ottawa K1S 5B6

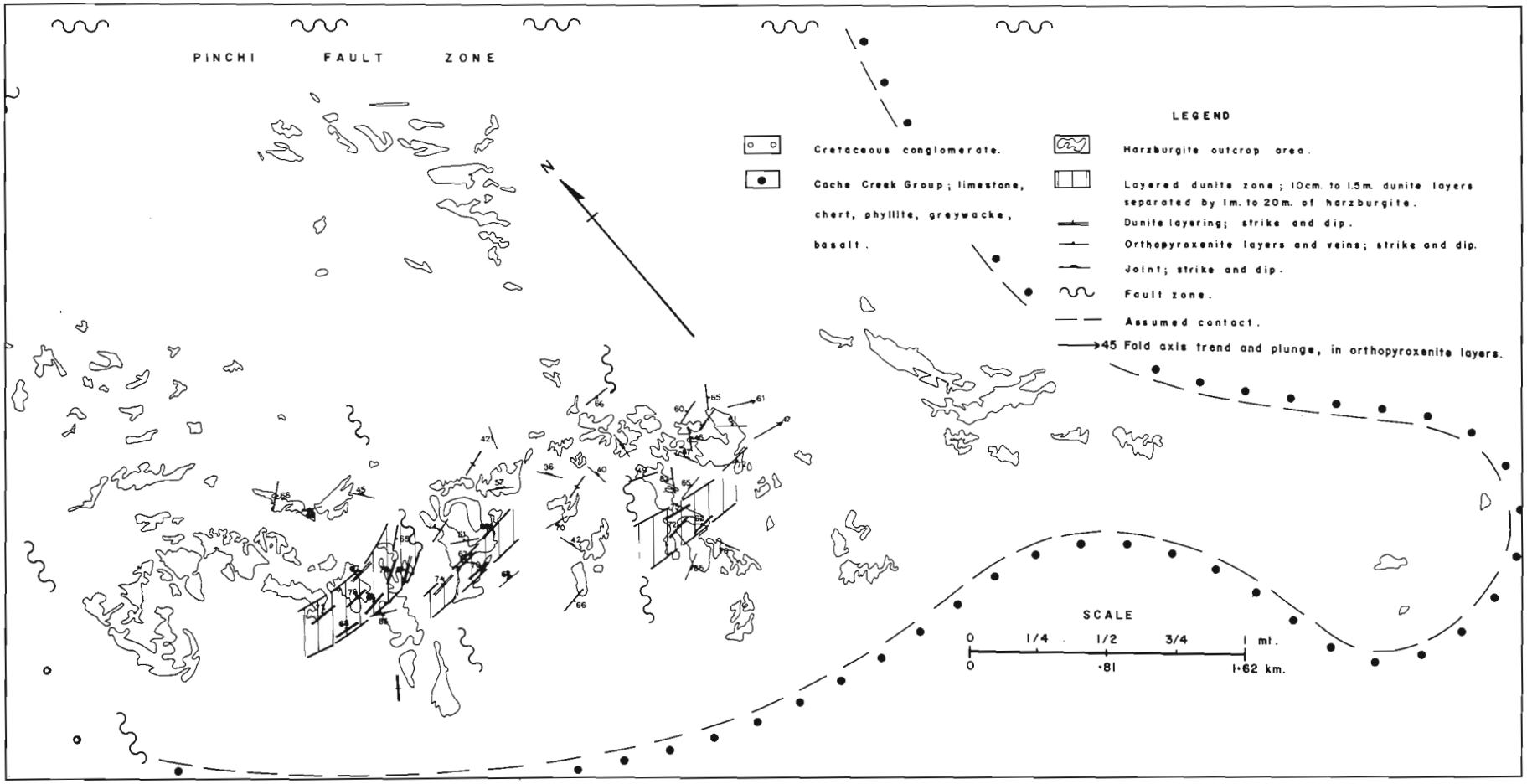

Figure 50.2. *Geological map of Murray Ridge*

Murray Ridge consists of a fault-bounded "alpine-type" ultramafic body, predominantly harzburgite with dunite occupying approximately 2 per cent of the outcrop area. The ultramafic body is considered to have been emplaced within the Cache Creek Group (Armstrong, 1949; Paterson, 1977), which includes biomicritic limestone, minor chert, thin siltstone beds, and volcanic rocks, prior to deposition of Upper Triassic Takla Group sediments. The Murray Ridge body plus ultramafic rocks on the north flank of Mount Pope 6 km to the west, and those which underlie Pinchi Mountain 20 km to the northwest, belong to the Trembleur Instrusions in the Fort St. James area (Armstrong, 1949).

Geology of Murray Ridge Ultramafic Rocks

Harzburgite

Murray Ridge (Fig. 50.2) is underlain by homogeneous, coarse grained harzburgite which forms 97 to 98 per cent of the outcrop area. Weathered surfaces are buff-brown with a coarse to hackly appearance caused by resistant orthopyroxene phenocrysts; fresh surfaces are very dark brownish green. Harzburgite outcrops exhibit brittle fracture planes in numerous orientations.

Dunite

Within the harzburgite on the southwest flank of Murray Ridge a layered dunite zone occurs which trends subparallel to the strike of the ridge. The layered dunite zone is approximately 200 m thick (Fig. 50.3) and dips steeply to the north. Individual dunite layers range in thickness from 10 cm to 1.5 m and may be traced in outcrop up to 30 m. The layered dunite zone appears to be offset and slightly rotated by minor faults which crosscut the trend of Murray Ridge. Dunite weathers pale buff-brown and has a smooth surface relative to the harzburgite. On a fresh surface it is black-green with a weathering rind 1 cm to 1.5 cm thick.

Orthopyroxenite

A third and minor unit is orthopyroxenite which occupies two distinct generations of planar structures. The early generation of orthopyroxenite forms cumulate layers within the harzburgite and these layers range in thickness from 3 cm to 10 cm, are very coarse grained, and occur singly or in zones of several layers. The layers are folded and exhibit both open and isoclinal structures possibly reflecting internal deformation. The later generation of orthopyroxenite occurs as veins. These veins range from 2 cm to 15 cm thick and crosscut both the folded orthopyroxenite layers and the enclosing harzburgite. The veins are planar and occur individually or in parallel groups.

Petrography of Ultramafic Rocks

Olivine within both the harzburgite and dunite is coarse grained and has been partially serpentinized resulting in a mosaic texture with cores of nonserpentinized olivine separated by lizardite ribbons. In areas where serpentinization has been more complete, mesh-textured lizardite is separated by ribbony lizardite.

Orthopyroxene, predominantly within harzburgite, is subhedral to anhedral. In a few grains faint exsolution lamellae of clinopyroxene occur. Serpentinization has affected the orthopyroxene, breaking it into groups of anhedral cores separated by ribbony lizardite. Where serpentinization has affected orthopyrozene and olivine, the remnant cores retain optical continuity which defines the original coarse grained texture.

Chromite is a ubiquitous phase throughout the ultramafic rocks, including the orthopyroxenite layers. Generally it occurs as fine to medium sized disseminated grains, but in widely scattered localities it forms thin 2 mm to 5 mm chains of individual grains which are usually proximal to or within dunite layers. The chain-like strings of chromite are up to 50 cm long and are conformable with the strike of dunite layers (Fig. 50.4a).

Chromite within the harzburgite contrasts strongly with chromite from dunite layers in form and texture. In both rock types deep red-brown and pale amber chromite may be found. Within harzburgite chromite is anhedral and is usually highly fractured with angular fragments separated by planar, and more rarely, by curved fractures. Chromite in harzburgite has embayments against partially serpentinized olivine and orthopyroxene. Embayments range from one third to one half the equivalent area of the host chromite grain. In sections where chromite has been cut perpendicular to an embayment, a doughnut form results (Fig. 50.4b). Reaction rims of magnetite are either absent or very thin and discontinuous.

In contrast to chromite in harzburgite, chromite in dunite is unfractured to weakly fractured. The grains are euhedral and in many cases exhibit well developed reaction rims (Fig. 50.4c). In reflected light, medium grey chromite is encased by white reaction rims which form a battlement-like texture with the surrounding partially serpentinized silicate matrix. The same reaction rim material fills fracture planes where it develops a comb texture.

Inclusions have been observed in chromite grains within the harzburgite and dunite. The inclusions in some cases are fluid-filled and exhibit a variety of forms ranging from spherical to tubular. Necked inclusions appear to have formed from tubular inclusions by thinning of the central portion which has left both ends slightly larger and bulbous (Fig. 50.4d). Inclusions appear to occur in trains in individual chromite grains whereas other chromite grains in the same thin section are devoid of inclusions.

The primary or secondary nature and compositions of fluid and solid inclusions as they relate to chromite genesis and the petrogenesis of these ultramafic rocks are being investigated. From this approach a greater understanding may be obtained of the conditions which control the formation of chromite.

Chemistry of Chromite from Murray Ridge and Chrome Peak

Electron microprobe analyses of chromite from Murray Ridge and from Chrome Peak, also one of the Trembleur Intrusions and located 43 km northwest of Trembleur Lake (Armstrong, 1949) indicate high chromium contents in all of the sections examined (Table 50.1). Analyses of the rims and cores of chromite grains show that individual crystals are virtually unzoned. There are marked compositional differences between the chromites from dunite as compared with those from harzburgite as exemplified by the two clusters formed on the plot of Cr/Cr+Al vs. Mg/Mg+Fe in Figure 50.5. All of the analyses, with the exception of one from the inclusion-rich part of a grain from the Irish deposit on Chrome Peak, plot within the field of alpine-type peridotite (Irvine and Findlay, 1972) and are thus compatible with the proposed ophiolitic nature of the ultramafic rocks of the Cache Creek Group. In the four harzburgite specimens, the chromite has a maximum of 48.1 weight per cent Cr_2O_3 whereas in the two dunite specimens the maximum is 59.9 weight per cent. The Cr/Fe ratios range from 2.47 to 3.28 and average 2.78. The average ratio in the dunite associated chromite is 3.06 whereas that in the harzburgite associated chromite is 2.56. A plot of Cr/Cr+Al and Mg/Mg+Fe ratios versus stratigraphic position in Figure 50.6 illustrates the inverse relationship between them as well as a moderate amount of cryptic variation across the section. The concentration of MnO in the harzburgite associated chromite increases upwards from the base of the section.

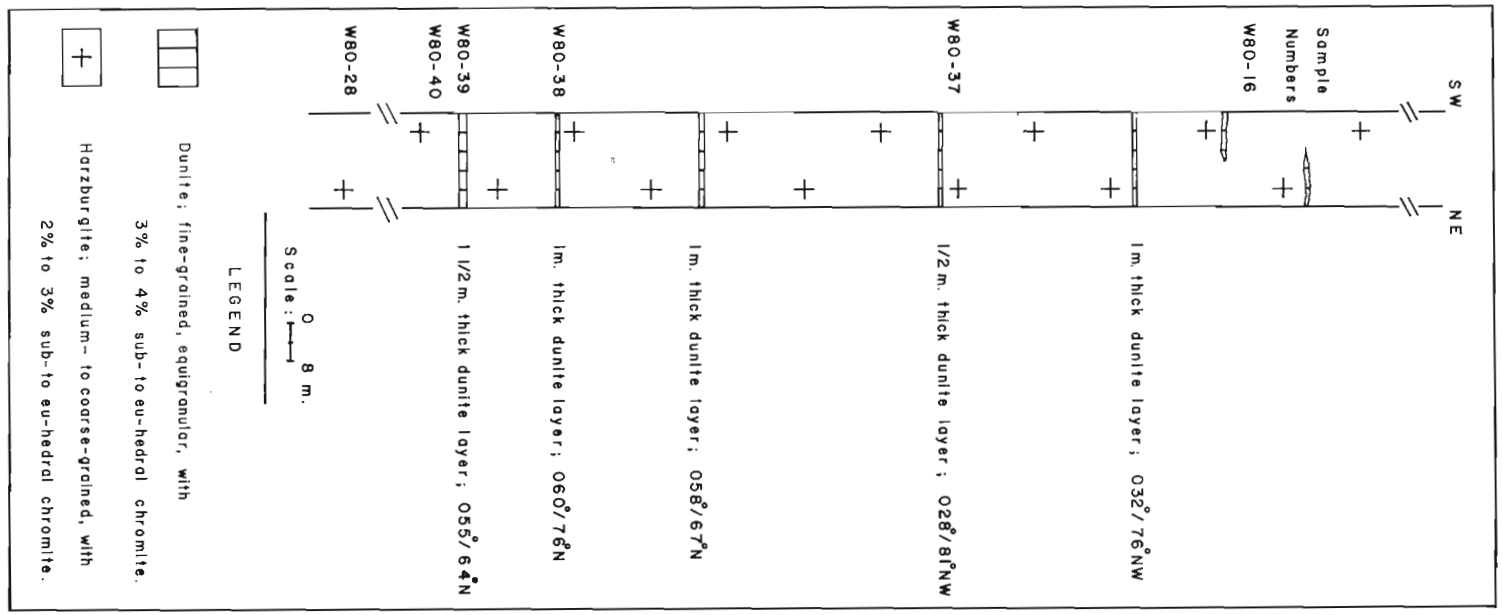

Figure 50.3. *Vertical section through the main dunite zone, Murray Ridge.*

Table 50.1

Electron Microprobe Analyses of chromite from Murray Ridge and Chrome Peak

Oxide	1.	2.	3.	4.	5.	6.	7.	8.	9.	10.	11.	12.	13.	14.
TiO_2	0.03	0.03	0.03	0.28	0.02	0.01	0.01	0.01	0.06	0.07	0.03	0.03	0.15	0.28
Al_2O_3	20.56	20.14	25.23	24.70	21.47	20.67	12.03	11.97	9.58	9.13	20.00	19.26	17.59	7.80
Cr_2O_3	46.54	47.69	43.24	43.91	46.96	48.02	57.69	57.85	59.51	59.86	47.27	48.13	51.87	59.19
Fe_2O_3	2.98	2.54	2.34	1.72	2.70	2.29	2.89	2.86	2.83	2.95	2.91	2.77	4.00	2.85
FeO	15.89	16.01	14.56	14.87	16.04	16.16	16.35	15.84	16.90	16.26	16.03	15.71	11.79	17.42
MgO	12.01	11.97	13.60	13.48	12.29	12.08	11.14	11.45	10.36	10.69	11.87	11.92	15.07	9.78
MnO	0.58	0.59	0.52	0.53	0.62	0.61	0.85	0.83	0.87	0.86	0.62	0.65	0.34	0.41
Total	98.59	98.97	99.52	99.49	100.10	99.84	100.96	100.81	100.11	99.82	98.73	98.47	100.81	97.93
Cr/Cr+Al	0.603	0.614	0.535	0.544	0.595	0.609	0.763	0.765	0.807	0.815	0.613	0.627	0.792	0.908
Mg/Mg+Fe	0.574	0.572	0.625	0.618	0.577	0.571	0.548	0.563	0.522	0.539	0.569	0.575	0.500	0.303
Fe^{3+}/ε^{3+}	0.036	0.030	0.027	0.020	0.032	0.027	0.035	0.035	0.036	0.037	0.035	0.034	0.059	0.043
N=	2	2	2	2	2	2	3	2	3	3	3	2	1	1

1, 2. Rim and core, W80-16 (harzburgite).
3, 4. Rim and core, W80-28 (harzburgite).
5, 6. Rim and core, W80-37 (harzburgite).
7, 8. Rim and core, W80-38 (dunite).
9, 10. Rim and core, W80-39 (dunite).
11, 12. Rim and core, W80-40 (harzburgite).
13, 14. Inclusion-rich and inclusion-free areas, Irish deposit chromitite.
N= number of analyses. See Figure 50.3 for location of samples.

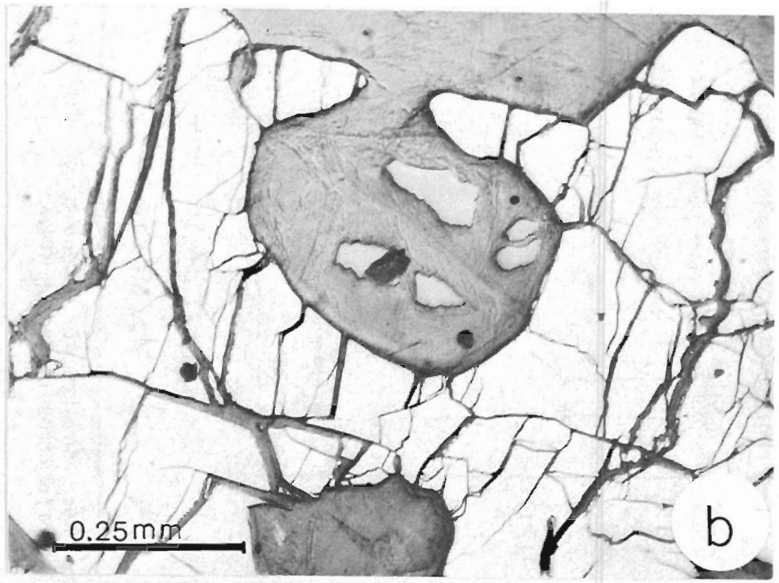

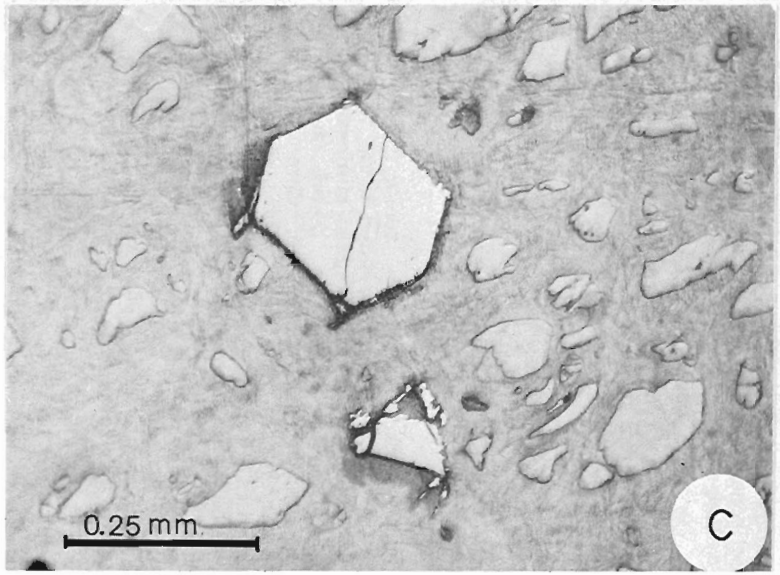

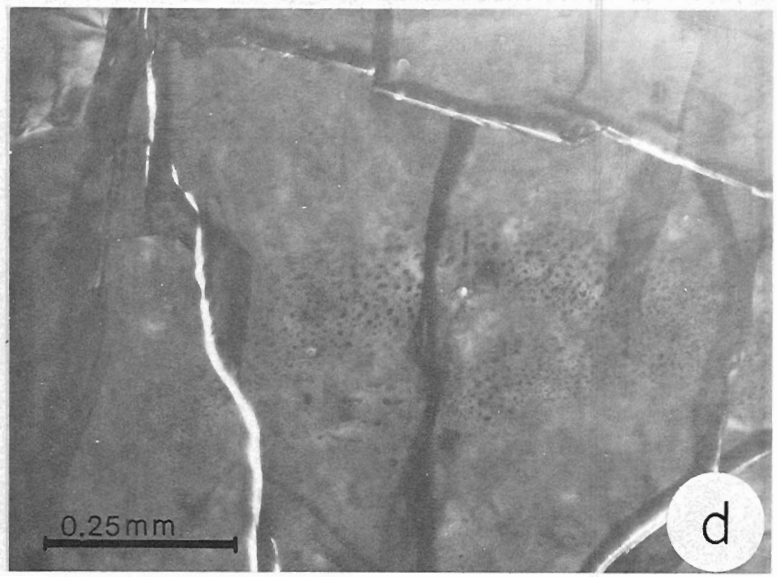

Figure 50.4a. *Chain-like string of medium grained chromite within and concordant to a dunite layer in harzburgite, Murray Ridge, B.C. Pen for scale.*

Figure 50.4b. *Fractured and embayed anhedral chromite in harzburgite, Murray Ridge, B.C. Reflected light.*

Figure 50.4c. *Euhedral chromite in dunite layer, Murray Ridge, B.C. Reflected light.*

Figure 50.4d. *Fluid inclusions in chromite from harzburgite. Plane light.*

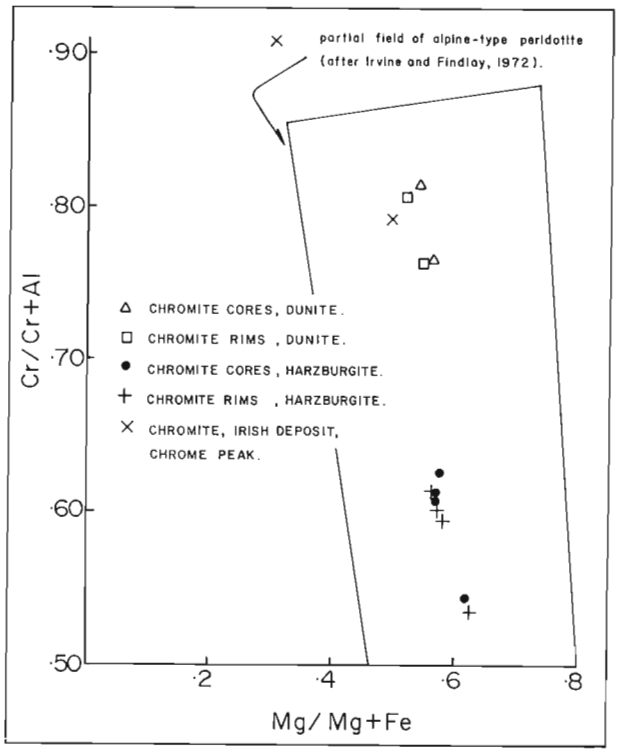

Figure 50.5. *Cr/Cr+Al versus Mg/Mg+Fe for chromite from Murray Ridge and Irish deposit.*

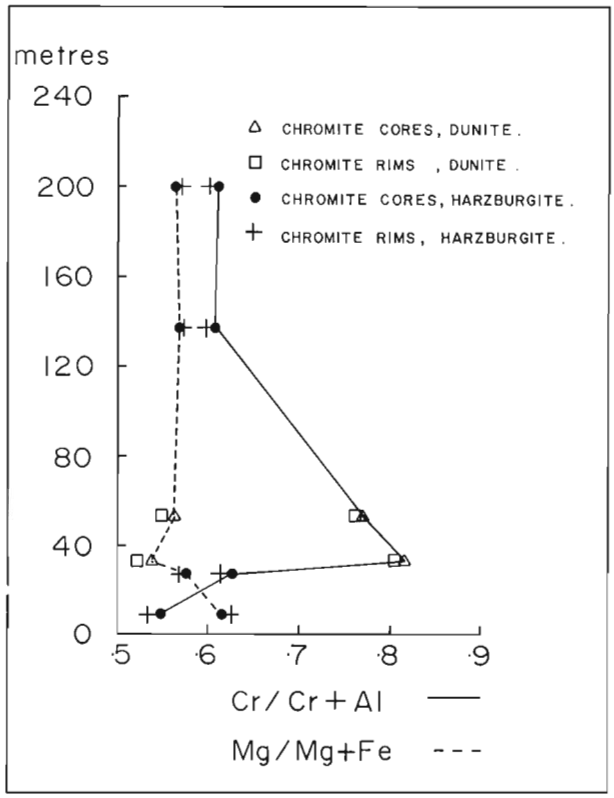

Figure 50.6. *Stratigraphic variation of Cr/Cr+Al and Mg/Mg+Fe for chromite, Murray Ridge.*

Two analyses of inclusion-rich and inclusion-poor parts of one chromite grain from the Irish deposit on Chrome Peak have Cr_2O_3 values of 51.9 and 59.2 weight per cent respectively. These concentrations are within the range defined by the Murray Ridge chromites.

The similarity of rim and core compositions of individual chromite grains and the differences in compositions of chromites from the dunite and harzburgite suggest that chromite compositions are primary and related to equilibration with the enclosing silicates.

Conclusions

Ultramafic rocks of the Cache Creek Group at Murray Ridge are fault emplaced and exhibit evidence of shearing and brittle deformation.

Chromite occurs within harzburgite, dunite, and orthopyroxenite. Orthopyroxenite layers are thin (3 cm to 10 cm) and have trace amounts of disseminated chromite whereas thicker dunite layers (10 cm to 1.5 m), and harzburgite have 3 to 5 modal per cent chromite. Chromite occurs as disseminated grains, in wispy layers, and in rarely observed chromitite lenses. Chromite in the harzburgite is anhedral, embayed, differing from chromite in dunite which is usually euhedral and finer grained.

Chromite analyses from Murray Ridge and Chrome Peak are high in chromium content and have primary compositions. Dunite associated chromite is distinctly chromium-rich compared to chromite from harzburgite.

Differences in chromite habit and chemistry are being examined further in this study. Of prime interest is the possibility that fluid and other inclusions are primary and that their compositions will permit a more complete understanding of the roles of fluids in the concentration of chromite in ultramafic rocks, as has been suggested for both stratiform and "alpine-type" or ophiolitic complexes (Johan, et al., 1980; Watkinson and Mainwaring, in press).

Acknowledgments

Field work for this study was funded by EMR Research Agreement 130-4-80 to D. Watkinson. Ken Booth ably assisted in the field, and discussions with G. Klein (Prince George) and G. White (Kamloops), district geologists, British Columbia Ministry of Energy, Mines and Petroleum Resources, were greatly appreciated. Additional information and aerial photographs for the Murray Ridge area were provided by J.V. Ross, University of British Columbia. Peter Jones performed most of the electron microprobe analyses. We also thank R. Anderson, Z. Johan, P. Mainwaring and J. Bloemraad for their contributions to this project.

References

Armstrong, J.E.
1949: Fort St. James map-area, Cassiar and Coast Districts, British Columbia; Geological Survey of Canada, Memoir 252, 210 p.

Irvine, T.N. and Findlay, T.C.
1972: Alpine-type peridotite with particular reference to the Bay of Islands Igneous Complex; Canada, Department of Energy, Mines and Resources, Earth Physics Branch Publications, v. 42, no. 3, p. 97-128.

James, A.R.C.
1958: Belchrome (Belair Mining Corporation Ltd.); in British Columbia Minister of Mines, Annual Report for 1957, p. 35-36.

Johan, Z., Lebel, L. and Watkinson, D.H.
1980: Gènese des couches et podes de chromite dans les complexes ophiolitiques et stratiformes; Paper presented in Section 13, 26^{e} Congres Geologique International.

Monger, J.W.H. and Price, R.A.
1979: Geodynamic evolution of the Canadian Cordillera – progress and problems; Canadian Journal of Earth Sciences, v. 16, p. 770-791.

Nichols, H.G.
1931: Central Mineral Survey District; in British Columbia Minister of Mines, Annual Report for 1930, p. 198-199.

Paterson, I.A.
1973: The geology of the Pinchi Lake area, central British Columbia; Unpublished Ph.D. thesis, University of British Columbia, Vancouver, B.C., 260 p.

1977: The geology and evolution of the Pinchi Fault Zone at Pinchi Lake, central British Columbia; Canadian Journal of Earth Sciences, v. 14, p. 1324-1342.

Ross, J.V.
1977: The internal fabric of an alpine peridotite near Pinchi Lake, central British Columbia; Canadian Journal of Earth Sciences, v. 14, p. 32-44.

Sutherland Brown, A.
1958: Anarchist Chrome; in British Columbia Minister of Mines, Annual Report for 1957, p. 35.

Watkinson, D.H. and Mainwaring, P.R.
1980: Chromite in Ontario; Geology of chromite zones, Puddy Lake – Chrome Lake and Chromite Chemistry; in Geoscience Research Grant Program, Summary of Research, Ontario Geological Survey. (in press)

51. TRIASSIC CONODONTS FROM THE CACHE CREEK GROUP, MARBLE CANYON, SOUTHERN BRITISH COLUMBIA

Project 790007

M.J. Orchard
Cordilleran Geology Division, Vancouver

Orchard, M.J., Triassic conodonts from the Cache Creek Group, Marble Canyon, southern British Columbia; in Current Research, Part A, Geological Survey of Canada, Paper 81-1A, p. 357-359, 1981.

Abstract

Triassic conodont faunas are recorded from the type area of the Cache Creek Group in southern British Columbia. Upper Triassic (late Carnian or early Norian) ***'Epigondolella' primitia*** *is recorded from one outcrop. Another outcrop nearby yielded platform elements of* ***Hindeodus***, ***'Neogondolella'*** *and* ***Neospathodus****. This fauna is dated as Lower Triassic (Dienerian) but it also includes a few elements of Upper Permian aspect which may have been derived from older rocks. This is the first record of Lower Triassic fossils from the Canadian Western Cordillera.*

Introduction

This paper provides a preliminary report on Triassic conodonts from the type area of the Cache Creek Group in the southwestern Intermontane Belt of British Columbia (92 I). Faunas of Early and Late Triassic age are recognized. Traditionally the Cache Creek Group has been regarded as wholly Permian but recent work has shown that some of the rocks contain Upper Triassic bivalves and Radiolaria (Travers, 1978, p. 116) and conodonts (Rafek, in Trettin, 1980, p. 16). Lower Triassic rocks have not been recognized previously in the Intermontane Belt of British Columbia although they are known from one locality in northern Washington State (Kuenzi, 1965).

A full taxonomic account of the Lower Triassic conodonts is in an advanced stage of preparation.

Localities and Faunas

Figure 51.1 indicates the location of the sections (MaCa 1-3) from which the conodonts were recovered. The outcrops are in roadcuts near the west end of Marble Canyon (Pavilion, map area, 92 I/ 13e, 5901E, 56344N).

MaCa 1

Siliceous rocks dominate the section at this locality, occurring both as thin beds and as massive units. The westernmost end of the outcrop (GSC Loc. C-087057) includes several metres of calcareous beds that produced a small poorly preserved but diagnostic fauna, including **'Epigondolella' primitia** Mosher, a species of late Carnian or early Norian age. This species has previously been reported from the Pavilion beds near Big Bar, about 45 km to the northwest (Rafek, in Trettin, 1980, p. 16) and I have also found it in limestone associated with chert and phyllite of the Bridge River Group about 70 km to the west, near Gold Bridge (GSC Loc. C-087058). Cameron (in Okulitch and Cameron, 1975; in Read and Okulitch, 1977, p. 636) also reported conodont faunas of this age from the Vernon and Penticton map areas of southern British Columbia.

MaCa 2

The section at MaCa 2 is predominantly of argillaceous strata but includes some thin chert and calcareous beds. The outcrop extends for about 150 m along the roadside but the stratigraphic thickness is uncertain. The argillaceous sequence at this locality yielded a single blade element of probable Triassic age.

MaCa 3

Section MaCa 3 comprises about 13 m of steeply dipping, fine grained, homogeneous limestone and shale strata apparently devoid of macrofossils. The eastern 3 m (MaCa 3a, b, c) is poorly bedded limestone which is recrystallized to a mosaic of dark and pale grey carbonate. Towards the west the overlying beds become less calcareous and at about 6 m pass into sheared, rusty weathering argillite. From 9 m, thin beds of dark limestone (MaCa 3d, e, f; MCW) are interbedded with the shale. This locality, the most prolific for conodonts, was discovered after processing a sample (MGW, GSC Loc. C-087055) collected early in 1980. On a later visit additional samples (MaCa a-f) were taken from the same outcrop. The eastern limestone beds (MaCa 3a, b, c) yielded small, poorly preserved faunas of early Triassic age. Each of the three species complete

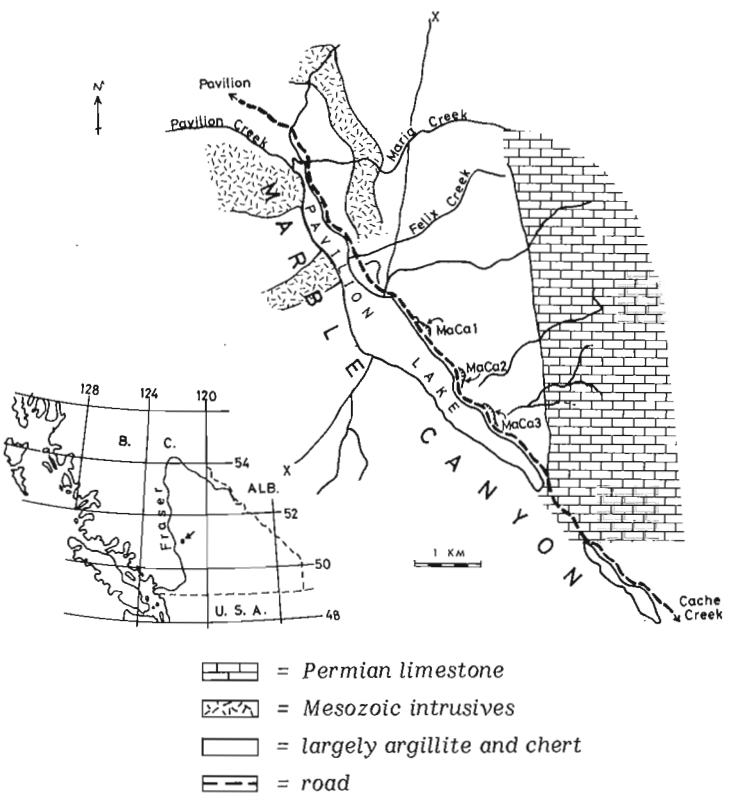

Figure 51.1. *Map showing location of Triassic conodont localities in Marble Canyon. X-X marks the western edge of the Marble Canyon Formation, based on Trettin, 1961.*

enough for determination is new: **Hindeodus** ? n. sp. A, **'Neogondolella'** n. sp. A and **Neospathodus** n. sp. A. Associated ramiform elements in these and the other collections are referable to species of **'Xaniognathus'** and **'Ellisonia'**, which I interpret as multi-element components of conodont assemblages that include the above named platform genera.

The higher beds at this locality are thin limestones (MaCa 3d, e, f; MCW) interbedded with shale, that yield an abundant, and diverse fauna, dominated by **Neospathodus dieneri** Sweet and including **'Neogondolella' carinata** (Clark) and **Neospathodus peculiaris** Sweet.

Comparisons with the data provided from sequences in the Tethys and the Western United States (Sweet, 1970a, b, 1979; Sweet et al., 1971; Collinson and Hasenmueller, 1978; Clark et al. 1979) suggest that the most significant feature for assessing the age of the fauna from MCW is the presence of abundant specimens of **Neospathodus dieneri** in association with **'Neogondolella' carinata. 'Neogondolella' carinata** appears in the Griesbachian but ranges no higher than early Dienerian. **Neospathodus dieneri** appears in the Dienerian and ranges as high as Smithian. The two overlap only in the Dienerian. A Dienerian age from the MCW fauna thus seems well established. More specifically the fauna evidently indicates a correlation with the **N. dieneri** Zone as recognized in the Salt Range by Sweet (1970b, p. 215). Tozer (1967) recognized two ammonoid zones within the Dienerian: Candidus followed by Sverdrupi. Mosher (1973) has described a few conodonts from beds representative of these zones. From the Candidus Zone (GSC Loc. 56181) Mosher has recorded **Neospathodus kummeli** Sweet, which characterizes the early Dienerian according to Sweet et al. (1971, p. 446) and Collinson and Hasenmueller (1978, p. 176). One faunule from the Sverdrupi zone (GSC Loc. 56205) has **Neospathodus dieneri** with **Neospathodus cristagalli** (Huckriede); the other (GSC Loc. 56224) has **Neospathodus cristagalli** without **N. dieneri.** In the Salt Range, according to Sweet et al. (1971, p. 446), **Neospathodus cristagalli** appears later in the Dienerian than **'Neogondolella' carinata.** The absence of **Neospathodus kummeli** and **Neospathodus cristagalli** in the fauna from MCW further supports the conclusion that it is of mid-Dienerian age, perhaps intermediate in age between that of the faunules from the Candidus and Sverdrupi Zones described by Mosher.

The occurrence of **Hindeodus** spp., **Sweetognathus** ? cf. **S. iranicus** Kozur, Mostler and Rahimi-Yazd, a possible element of the **'Neogondolella' serrata** complex and **Neostreptognathodus** ? sp. indet. represents anomalies in this Dienerian fauna.

Hindeodus is known from both the Upper Paleozoic and the basal Triassic (Griesbachian). The possible extension of its range to the Dienerian is not drastically anomalous.

The presence of the other elemets seems to require further explanation. No known early Triassic conodonts have comparable morphology, whereas counterparts do occur in Upper Permian faunas (although none are known at present from British Columbia). The most complete element is compared with **Sweetognathus** ? **iranicus,** a species known only from the early Upper Permian (Abadehian) of the Abadeh region of central Iran (Kozur et al., 1978, p. 107). A second platform fragment resembles some species of the Permian genus **Neostreptognathodus.** A single ornate gondolellid anterior platform fragment is similar to representatives of the Upper Permian **'Neogondolella' serrata** complex. Unless they represent rare holdovers from Permian stocks these three specimens are presumably reworked and derived from Upper Permian rocks. Such a phenomenon is not unknown among lower Triassic fossil assemblages: Teichert and Kummel (1972) reported Upper Permian macrofossils in ophiceratid-bearing Triassic strata of the Kap Stosch area of East Greenland. Furthermore, a break at this boundary is a world wide phenomenon. In the Marble Canyon area upper Permian rocks may have been removed by erosion and derived conodonts incorporated in Dienerian sediment.

Stratigraphic Context

The exposures from which Triassic conodonts are here recorded lie within the area mapped as Cache Creek Group by Duffell and McTaggart (1952) and Trettin (1961, Fig. 1, sheet C). The Cache Creek Group was originally established by Selwyn (1872) and has a long history of research; Monger (1975, p. 62) discussed this and restricted the scope of the group name. Between Cache Creek and Pavilion, British Columbia, the Cache Creek rocks comprise three north trending belts: an eastern belt in which rocks as old as mid-Pennsylvanian (Danner, in Trettin, 1980, p. 1) and as young as late Triassic (Pessagno, in Travers, 1978, p. 116) have been identified; a central belt, that comprises the Marble Canyon Formation (Duffel and McTaggart, 1952); and a western belt from which only one early to mid-Permian age determination has been made (Ross, in Trettin, 1980, p. 15). Ross (in Trettin, 1980, p. 1) regarded the fusulinaceans from the central belt (Marble Canyon Formation) as representative of the **Neoschwagerina margaritae** assemblage zone, that is Wordian (mid-Permian) in age. The Marble Canyon carbonates contain "Tethyan" faunas of verbeekinid fusulinaceans (Thompson et al., 1950; Bostwick and Nestell, 1967; Monger and Ross, 1971) which are unlike contemporary "North American" faunas known to the east near Kamloops, and to the southwest near Chilliwack, British Columbia. This anomaly in Cordilleran geology has been cited in support of current theory that regards the rock assemblages with "Tethyan" faunas as an exotic terrane accreted to cratonic North America during the early Mesozoic (Davis et al., 1978).

Trettin (1961) included the outcrop area of MaCa 1-3 within the Marble Canyon Formation of the Central Belt, specifically within his map-unit 2, an association of limestone, chert, argillite, tuff and volcanic flows. Areas to the west, and similar rocks south of Pavilion Lake were included in Division I of the Pavilion Group by Trettin (1961). Trettin (1980) now considers that Division I of the Pavilion Group is not separable from the western belt of the Cache Greek Group. On lithological grounds, map unit 2 of the Marble Canyon Formation and the rocks of the western belt of the Cache Creek Group may be indistinguishable.

References

Bostwick, D.A. and Nestell, M.K.
1967: Permian Tethyan fusulinid faunas of the northwestern United States; in Aspects of Tethyan Biogeography, Adams, C.G. and Ager, D.V., ed., Systematics Association Publication, no. 7, p. 93-102.

Clark, D.L., Paull, R.K., Solien, M.A., and Morgan, W.A.
1979: Triassic conodont biostratigraphy in the Great Basin; in Conodont Biostratigraphy of the Great Basin and Rocky Mountains, Sandberg, C.A. and Clark, D.L., ed., Brigham Young University Geology Studies, v. 26, p. 179-185.

Collinson, J.W. and Hasenmueller, W.A.
1978: Early Triassic paleogeography and biostratigraphy of the Cordilleran Miogeosyncline; in Mesozoic Paleogeography of the Western United States;, Pacific Coast Paleogeography Symposium 2, Howell, D.G. and McDougall, K.A., ed., Society of Economic Paleontologists and Mineralogists, p. 175-187.

Davis, G.A., Monger, J.W.H., and Burchfiel, B.C.
1978: Mesozoic construction of the Cordilleran collage, central British Columbia to central California; in Mesozoic Paleogeography of the Western United States, Pacific Coast Paleogeography Symposium 2, Howell, D.G. and McDougall, K.A., ed., Society of Economic Paleontologists and Mineralogists, p. 1-32.

Duffell, S. and McTaggart, K.C.
1952: Ashcroft map-area, British Columbia; Geological Survey of Canada, Memoir 262.

Kozur, H., Leven, E. Ya., Lozovskii, V.R., and Pyatakova, M.V.
1978: Raschlenenie po konodontam pogranichnykh sloev Permi i Triasa Zakavkazya; Byulleten Moskovskogo Osbshestva Ispytatelei Prirody (otdel geologicheskii), v. 53, p. 15-24.

Kuenzi, W.D.
1965: Early Triassic (Scythian) ammonoids from north-eastern Washington; Journl of Paleontology, v. 39, p. 365-378.

Monger, J.W.H.
1975: Upper Palaeozoic rocks of the Atlin Terrane, northwestern British Columbia and south-central Yukon; Geological Survey of Canada, Paper 74-77.

Monger, J.W.H. and Ross, C.A.
1971: Distribution of fusulinaceans in the western Canadian Cordillera; Canadian Journal of Earth Sciences, v. 8, p. 259-278.

Mosher, L.C.
1973: Triassic conodonts from British Columbia and the northern Arctic Islands; Geological Survey of Canada, Bulletin 222, p. 141-192.

Okulitch, A.V. and Cameron, B.E.B.
1975: Stratigraphic revisions of the Nicola, Cache Creek, and Mount Ida Groups, based on conodont collections from the western margin of the Shuswap Metamorphic Complex, south-central British Columbia; Canadian Journal of Earth Sciences, v. 13, p. 44-53.

Read, P.B. and Okulitch, A.V.
1977: The Triassic unconformity of south-central British Columbia; Canadian Journal of Earth Sciences, v. 14, p. 606-638.

Selwyn, A.R.C.
1872: Journal and report of preliminary explorations in British Columbia; Geological Survey of Canada, Report of Progress for 1871-72, p. 16-72.

Sweet, W.C.
1970a: Permian and Triassic conodonts from a section at Guryul Ravine, Vihi District, Kashmir; Kansas University Paleontology Contributions no. 49.

1970b: Uppermost Permian and Lower Triassic conodonts of the Salt Range and Trans-Indus Ranges, West Pakistan; in Stratigraphic Boundary Problems: Permian and Triassic of West Pakistan, Kummel, B. and Teichert, C., ed., Department of Geology, University of Kansas Special Publication no. 4, p. 207-275.

1979: Graphic correlation of Permo-Triassic Rocks in Kashmir, Pakistan and Iran; Geologica et Palaeontologica, v. 13, p. 239-248.

Sweet, W.C., Mosher, L.C., Clark, D.L., Collinson, J.W., and Hasenmueller
1971: Conodont Biostratigraphy of the Triassic; Geological Society of America, Memoir 127, p. 441-465.

Thompson, M.L., Wheeler, H.E. and Danner, W.R.
1950: Middle and Upper Permian fusulinids of Washington and British Columbia; Contributions to the Cushman Foundation for Foraminiferal Research, v. 1, p. 46-63.

Tozer, E.T.
1967: A Standard for Triassic Time; Geological Survey of Canada, Bulletin 156.

Travers, W.B.
1978: Overturned Nicola and Ashcroft strata and their relation to the Cache Creek Group, southwestern Intermontane Belt, British Columbia; Canadian Journal of Earth Sciences, v. 15, p. 99-116.

Teichert, C. and Kummel, B.
1972: Permian – Triassic boundary in the Kap Stosch Area, East Greenland; Bulletin of Canadian Petroleum Geology, v. 20, p. 659-675.

Trettin, H.P.
1961: Geology of the Fraser River Valley between Lillooet and Big Bar Creek; British Columbia Department of Mines and Petroleum Resources, Bulletin 44.

1980: Permian rocks of the Cache Creek Group in the Marble Range, Clinton Area, British Columbia; Geological Survey of Canada, Paper 79-17.

52.

THE CORRELATION OF "TUBE WAVE" EVENTS WITH OPEN FRACTURES IN FLUID-FILLED BOREHOLES

C.F. Huang[1] and J.A. Hunter[2]

Huang, C.F. and Hunter, J.A., The correlation of "tube wave" events with open fractures in fluid-filled boreholes; in Current Research, Part A, Geological Survey of Canada, Paper 81-1A, p. 361-376, 1981.

Abstract

Tube waves generated by incident compressional waves have been correlated with open fractures in a fluid-filled borehole. As part of the AECL radioactive waste disposal program to study the subsurface open fractures in impermeable igneous and/or metamorphic rock bodies, a 12 hydrophone array (crystal cable) employing a surface seismic source was used to measure variations in compressional wave velocities in boreholes. The records obtained also displayed many large amplitude, low velocity events identified as tube waves which originated at intervals in the hole. Tube waves appear to be generated by the incidence of compressional waves in the surrounding rock body onto fluid-filled zones intersecting the borehole. Correlations of positions and amplitudes of tube waves with TV logging, core logging and hydrogeology studies suggest that tube wave events can be used as reliable indicators of fractures open to fluid flow. The relative amplitudes of tube waves appear to be related to measured hydraulic conductivities.

Introduction

For the past few years, the disposal of nuclear radioactive waste has been of great concern. One of the possible solutions to this problem currently under study by Atomic Energy of Canada Limited (AECL) is an underground repository located in a highly impermeable crystalline rock body. In order to assure the success of isolating high level radioactive waste in the stable Precambrian Shield, the determination of the dependence of the permeability within a subsurface crystalline rock formation on the presence of interconnected open fractures is currently under study. This report presents the results of work done for AECL's Whiteshell Nuclear Research Establishment, Pinawa, Manitoba.

At present several methods are being used in identifying and characterizing open fractures which intersect with a borehole. They are, core logging, TV logging, standard logging and hydraulic conductivity studies. However, each method is subject to certain limitations in its own application. Recent borehole seismic studies have suggested that the identification of tube waves can be used as reliable indicators of fractures open to fluid flow. Correlations of positions and amplitudes of tube waves with TV logging, core logging and hydrogeology studies in borehole WN-1, Pinawa, Manitoba, suggest that some open fractures which are not observed by the TV method can be detected by both tube wave analysis and hydrogeology studies. In addition, the relative amplitudes of tube waves appear to be correlatable with measured hydraulic conductivities. Furthermore the low frequency of seismic waves employed in this study may possibly provide a way to improve estimations of fracture permeabilities for several metres surrounding the borehole wall.

Tube Wave Method

As part of the AECL radioactive waste disposal program, our original intention with the borehole seismic study was to investigate the first-arrival compressional waves (P-waves) for use in measurement of velocity variations in boreholes drilled at Chalk River, Ontario and Pinawa, Manitoba (Huang and Hunter, 1979). However in our records, we observed not only the P-waves, but also large amplitude, low velocity later events. These later events were subsequently identified as tube wave events. Hence efforts were directed towards recording these events wherever possible on digital tapes. On close examination of the records, it was found that in addition to the tube waves from the top of the borehole, and those reflected from the bottom of the hole, there were also many tube wave events apparently being generated at intervals in the borehole. Figure 52.1 is a typical example showing tube wave events for a record section between 400 and 422 m depths in borehole WN-1 at the Pinawa site. An event appears to be generated at 416.5 m depth which radiates a low velocity, large amplitude wave both down and up the borehole. This location corresponds to a large (16 mm) partly open fracture

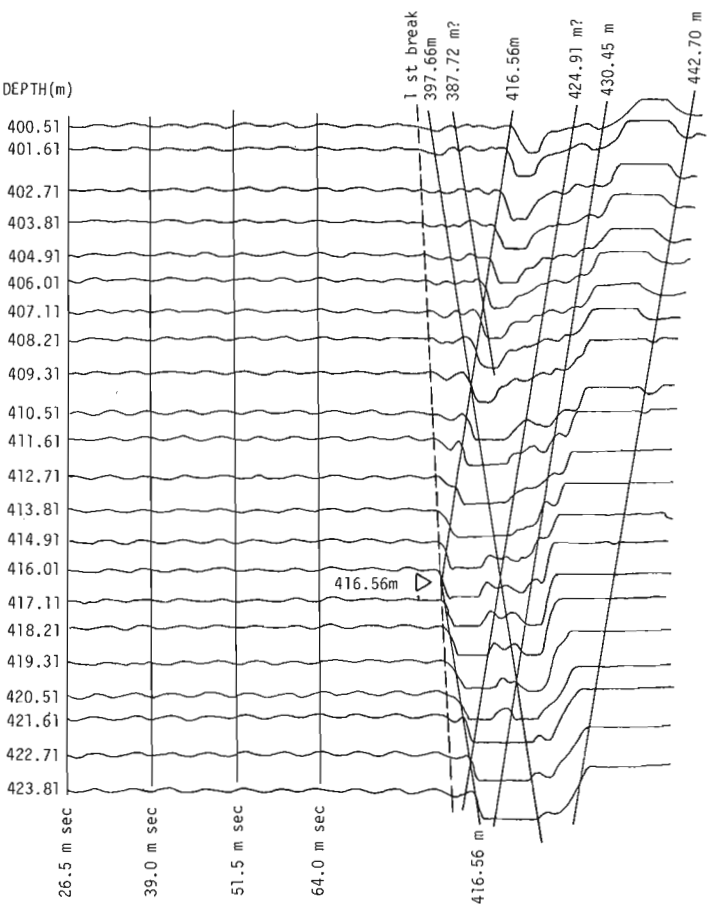

Figure 52.1. *A typical example showing the tube wave generated at 416.56 m in borehole WN-1, Pinawa, Manitoba.*

[1] Atomic Energy of Canada Ltd., 601 Booth St., Ottawa

[2] Resource Geophysics and Geochemistry Division

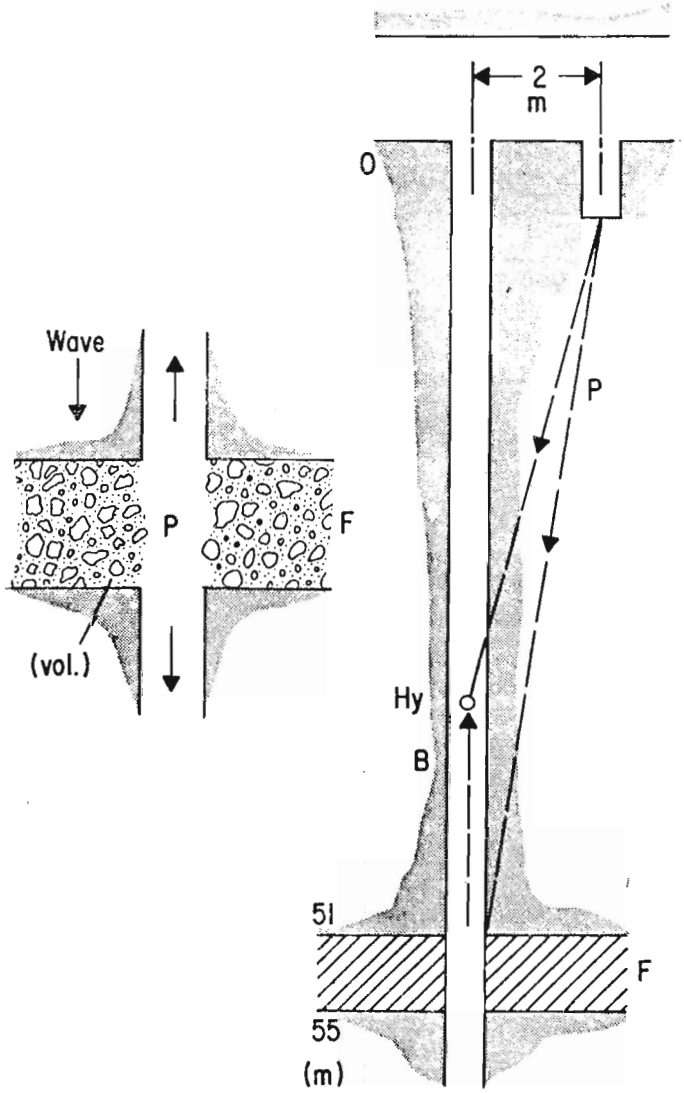

Figure 52.2. *Tube wave generated at a fractured zone by incidence of P-wave. Hy: Hydrophone, F: Fractured zone, Wall rock: Black schist (after C. Kitsunezaki, 1971, p. 124).*

registered on the TV log and to an equivalent single open fracture of 205-210 μm (micrometres) in aperture size recorded by hydrogeology study. Other tube wave events were also recorded which have been correlated with large permeability zones.

Tube waves, which have been considered a form of Stoneley waves (Sheriff, 1974), are low velocity, large amplitude events propagating along the interface between the borehole wall and the borehole fluid. They are generated by incident compressional wave energy from a surface source near the borehole or from a source within the borehole. Tube waves are also generated when a compressional wave in the surrounding solid passes any major discontinuity in the borehole (White, 1965, p. 148).

Tube wave measurements have been the subject of numerous investigations in borehole seismic studies for many years, because of their interfering effects in the identification of later events (shear waves and reflections). Studies have been made of the tube wave velocities by Ording and Redding (1953), Riggs (1955), White (1965), Biot (1952) and Kitsunezaki (1971). The velocity of the tube wave (≈1.30 km/s) depends upon the density contrast between the fluid and wall rock as well as the rigidity modulus of the wall rock.

Kitsunezaki (1971) showed that fractured zones in rock behave as effective sources of tube waves resulting from incident compressional wave energy. Figure 52.2 (after Kitsunezaki, 1971) shows the model; compressional wave pressure results in water contained in the fractured zone being forced into the borehole where the tube wave conversion takes place. Hence, if tube wave conversion zones can be mapped in the borehole, zones of high permeability (and open fractures) can be detected.

Of primary concern in the application of tube waves is the depth of penetration as well as spatial resolution of individual open fractures. It is difficult to estimate the volume of rock being sampled when the conversion of P-wave into tube wave occurs at fractured zones which intersect a borehole at the seismic frequency used. In our study (Huang and Hunter, 1980a) we suggested that a volume of rock circumjacent to the hole equal in radius to that of 1/2 seismic wavelength is sampled in the formation of the compressional wave. For a seismic pulse with a centre frequency of 200 Hz, this would represent a radius of about 8 to 15 m. Based on this assumption, a macroscopic bulk property of the rock mass containing open fractures is monitored at the time of incidence of the P-wave onto a fluid-filled fracture zone which intersects a borehole. Therefore, the tube wave records should provide information on rock properties for a penetration depth of several metres. In addition, the results can also be used to study the resolution of individual open fractures or open fractured zones.

Instrumentation

The crystal cable hydrophone array, designed for high resolution surveying, was reduced in scale compared to that used in the oil industry. Instead of a 12 hydrophone array with 15 m between hydrophones, the interval was reduced to approximately 1.13 m giving a 12.43 m "live" section. The hydrophones and preamplifiers are imbedded in "pods" which are connected in line with the cable and the interconnectors. The frequency response of the hydrophones is relatively broad-band, between 2 Hz and 1000 Hz. The centre-frequency of seismic energy currently used in this work is 200 Hz.

The crystal cable array is connected to a 28-conductor steel-cord cable 650 m in length. The cable is stored on a wooden spool mounted on a 3 hp electric winch and is used in conjunction with a large diameter well-head pulley. Figure 52.3 shows the crystal cable hydrophone array and Figure 52.4 shows the assemblage of cable, winch and well-head pulley used in our test set-up.

An SIE RS-49 digital recording system capable of 0.25 millisecond digital rate was used to record the entire seismic wave train. This unit consists of analog amplifiers, analog to digital conversion and stacking, and 9-track digital tape recording in standard seismic format. Figure 52.5 shows the recording unit.

Field Procedures

In the field, we lowered the array of hydrophones into the hole at various selected depths. At each location a small dynamite charge (~0.15 kg Forcite 75%) was detonated in a 2-metre deep shot hole tamped with water. The surface offsets between shot hole and well-head were 6 to ~29 m in our study. The array locations were arranged such that overlap of hydrophone positions occurred between successive locations as shown in Figure 52.6 (the amount of overlap varied with each hole record according to the number of active hydrophones available in each survey). Using the RS-49 recording system, amplifier gains were reduced in most cases so that the entire seismic wave train from the

Figure 52.3

An array of 12 crystal cable hydrophones and well-head pulley (CR-1, Chalk River, Ontario).

Figure 52.4

The assemblage of seismic cable, winch and well-head pulley at test site (WN-1, Pinawa, Manitoba).

12 channel array could be adequately recorded for future "tube" wave studies. Records were then played back on an electrostatic oscillograph and edited to form a record suite displaying seismic traces from all hydrophone locations in the hole. Sometimes, true amplitudes of later events could not be measured since the limited dynamic range of the RS-49 system resulted in amplifier saturation by large amplitude tube waves. However, on-scale portions of saturated events as well as the degree of saturation often give the interpreter a qualitative estimate of the relative strength of the tube wave.

Results

The record suites measured at the two holes (CR-1 and CR-9) in Chalk River and one hole (WN-1) in Pinawa were analyzed for tube wave generation. The relative amplitudes of tube waves were first visually estimated and thereafter normalized[1] to their corresponding travel distances. The generation-positions and the relative amplitudes of tube waves were then constructed to form bar-graphs (Fig. 52.7, 52.8, 52.9) over the entire survey depths of boreholes. The hydraulic conductivity studies were selectively done over certain depth intervals where isolated open fractures or open fracture zones had already been designated by TV logging in borehole WN-1. The positions and their calculated apertures of equivalent single open fractures per 2.97 m testing interval were also shown in bar-graph form over the surveyed depth intervals (WN-1 only; Davison, 1979). The number and the total widths of open fractures per metre interval were computed from the TV log. Similarly the number of naturally open fractures (both open and possibly open to fluid flow) per metre interval were obtained from the core log.

With the information cited above, figures showing the integration of TV, core, hydrogeology, and tube-wave data for each borehole were constructed. These composite bar-graphs not only show clearly the correlations of open fractures when compared amongst differing groups of

[1] Normalized tube wave relative amplitude = tube wave relative amplitude x travel distance by assuming that an equal amount of energy was generated for each record shot and the loss of energy is proportional to increasing travel distance.

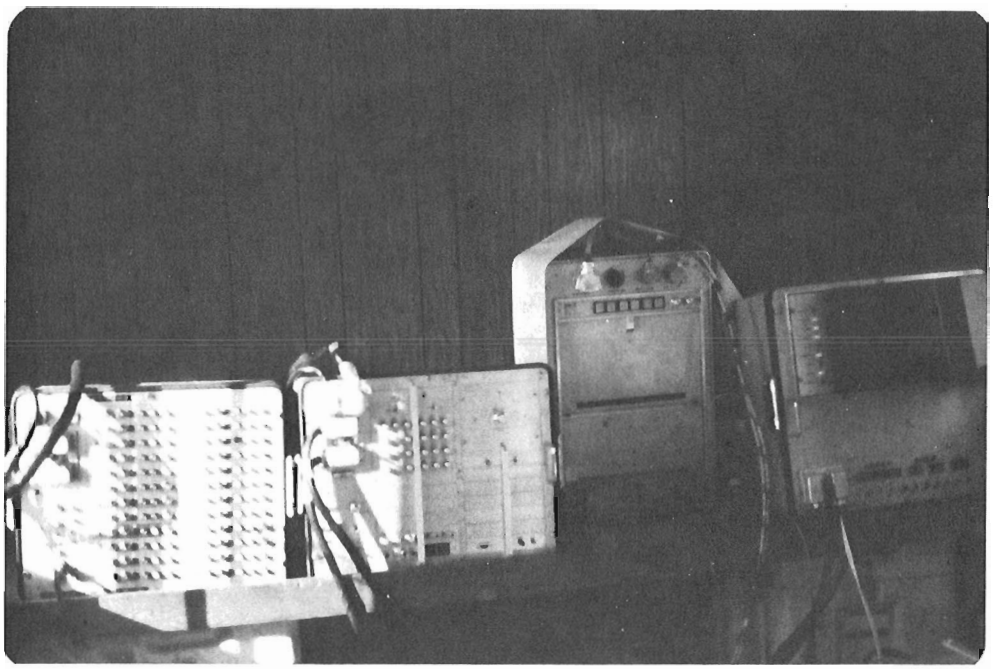

Figure 52.5

SIE RS-49 seismic recording system (from left to right: RA-49 analog amplifier, RM-49 analog to digital and stacking unit, ERC-10C oscillograph, and RU-49R9 9 track digital tape recorder).

borehole data, but also provide the most complete descriptions about fractures open to fluid flow in each borehole. The results of WN-1, CR-1 and CR-9 are displayed in Figure 52.7, 52.8, and 52.9, respectively. These figures follow the order right to left as described below.

1. Tube wave relative amplitudes (Tube wave analysis).
2. Normalized tube wave relative amplitudes (Tube wave analysis).
3. Hydraulic conductivities (Hydrology isolation and injection method, only available for WN-1).
4. Total number of naturally open fractures per metre (core log).
5. Total number of open, partly open and large (≥1.00 mm) closed fractures per metre (TV log).
6. Total number of open and partly open fractures per metre (TV log).
7. Total widths of open, partly open and large (≥1.00 mm) closed fractures per metre (TV log).
8. Total widths of open and partly open fractures per metre (TV log).

The symbols "X" and their corresponding length-bars in each individual plot depict not only the locations of recorded open fractures, but also the number or the total widths of open fractures within the depth interval surveyed by that particular method.

Pinawa WN-1

The results are presented in Figure 52.7 and Table 52.1. The following observations are noted:

1. In general there is good correlation with the occurrences of tube wave generating points and open fractures shown from the TV log, the core log and the hydrogeology study. In other words, all four methods of fracture characterization appear to give good indications for isolated open fractures, or isolated open fractured zones.
2. The relative amplitudes of tube waves appear to be correlatable with measured hydraulic conductivities (in terms of the aperture size of an equivalent single open fracture). Similar correlations are also noted between the relative tube wave amplitudes and the total widths of open, partly open, and large (≥1.0 mm) closed fractures per metre from the TV log. Consequently it appears that relative amplitudes of tube waves are direct indicators of fracture permeabilities.
3. Some open fractures which are not observed (or are indicated as large (≥1.00 mm) closed fractures) by the TV log are detected by both the tube wave analysis and the hydrogeology study. Open fractures, located at 22.26 m, 58.40 m, 92.70 m, 149.38 m and 303.0 m, are such examples. Hydraulic conductivity testings are sectionally carried out at selective locations which check those open fractures that have already been recorded by the TV log. Hence a complete comparison between the tube wave analysis and the hydrogeology study over all depths in WN-1 is not possible.
4. In general comparative studies of the TV log, core log and tube wave analysis indicate that more open fractures are identified by the tube wave analysis and the core log than by the TV log. Some examples are those open fractures positioned at 98.0 m, 102.24 m, 111.68 m, 115.53 m, 136.08 m, 149.38 m, 164.50 m, 191.61 m 303.0 m, 381.0 m and 387.72 m.
5. Comparisons between core log, hydrogeology study, and the tube wave analysis also suggest that the tube wave identification method and the hydrogeology studies could record more open fractures than are indicated by the core log. These open fractures are located at 22.26 m, 30.61 m, 32.81 m, 35.56 m, 58.40 m, 92.70 m and 466.0 m.
6. Points 3, 4 and 5 (above) indicate that each method is more or less limited in its own applications. However, the integration of different groups of borehole data could probably provide the most constructive and complete information about fracture permeability.

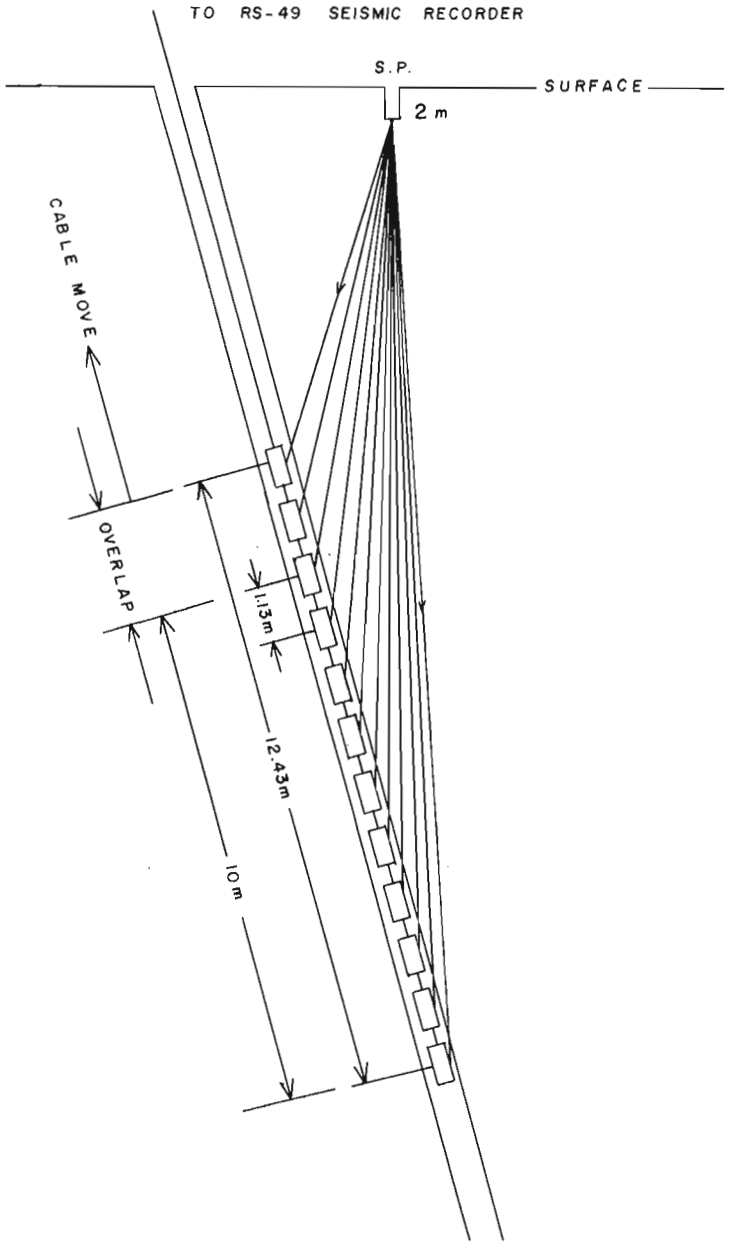

DOWN-HOLE SEISMIC RECORDING LAYOUT

Figure 52.6. *The crystal cable array shows the overlap-coverage between two successive shots.*

7. A study of the depth section between 380 to 460 m illustrates some interesting features. At certain locations there are corresponding increases among the tube wave amplitudes, the hydraulic conductivities, and the widths of open fractures. These are 395-400 m, 416.5 m, 430.45 m, 442.70 m, and 450.50 m (see Fig. 52.7 and Table 52.1 for a detailed comparison). These positive correlations may possibly provide evidence that the relative amplitudes of tube waves are associated with the degree of permeability of open fractures. The correlation can be seen by comparing the following two fracture zones, i.e., the upper one at 395-400 m (denoted zone A), and the lower one at 416 m (denoted zone B). By comparing the number of open fractures per metre in these two zones, one would consider zone A (37 naturally open fractures by core log and 9 open fractures by TV log) has much higher fracture permeability than zone B (6 naturally open fractures by core log and 1 open fracture by TV log). In spite of the heavily fractured nature of zone A with respect to that of zone B, the hydraulic injection tests however show the reverse results in permeabilities, i.e. 205-210 μms in aperture for zone B and 83-86 μms for zone A. These aperture figures are calculated by assuming that there is only one open fracture within the testing interval of 2.97 m since the injecting technique could not effectively isolate individual fractures in each testing interval (Davison, 1979). This differential in fracture permeability is supported by the tube wave relative amplitudes which show a very large increase in amplitudes for zone B in comparison with much smaller amplitudes for zone A (see Fig. 52.1, 52.7). These characterizations by relative amplitudes of tube waves do suggest that zone B is more hydrologically significant than any other open fractures in borehole WN-1. As a result, tube wave response seems to be more directly related to permeability than fracture data obtained from TV and core log.

Chalk River CR-1

To date, borehole CR-1 has been shot twice for tube wave analysis. A comparison of two record suites (1977 and 1979 data) shows that the results are reproducible regardless of the positions of the shot points. The shot locations in 1977 and 1979 are approximately on opposite sides of the borehole. The results are presented in Figure 52.8 and Table 52.2: From examining these borehole data the following observations are noted:

1. In general there is a good correlation with the occurrence of tube wave generation points and open fractures shown from both TV and core logging.
2. There appears to be a general relationship between the relative amplitudes of tube waves and the total widths of open fractures per metre from the TV log, as well as between tube wave relative amplitudes and the total number of open fractures per metre from the TV log.
3. The TV log indicates that depth intervals shallower than 140 m are heavily fractured. Standard logs also suggest the upper 150 m could be relatively more porous and electrically conductive. Similarly the tube waves record the same phenomenon distinctly.
4. Over the depth interval of 6-100 m, the TV log and tube wave analysis indicate more open fractures than given by the core log. The situation is reversed over the depth interval of 100-163 m, i.e., both the core log and tube wave analyses indicate more open fractures than does the TV log. Over the depth interval of 162-260 m, the TV log indicates four small open fractures located at 246-248 m whereas the core log shows no naturally open fracture at all. However, a number of weak tube wave events have been identified and their corresponding origins are as follows: 204.26 m, 217.91 m, 222.52 m, 225.34 m, 229.95 m, 233.0 m, 237.95 m, 240.40 m, 245.0 m, 247.08 m, and 258.5 m. Standard logs imply a basically competent rock unit over depth interval of 150-260 m with some possible porous sections located at 205-208 m, 222-238 m, 248-252 m and 256-258 m.

In general, the relative amplitudes of tube waves suggest the fracture permeabilities are relatively high over the depth intervals of 6-150 m. The record suite of CR-1 is presented in Appendix 1. On the record suite, open fractures detected by the tube wave analysis are divided into two groups: I) open fractures, which are also indicated as open or partly open fractures on the TV log, are marked with symbols "Δ", and II) open fractures, which are designated as (≥1.00 mm) large closed fractures on TV log, are represented by "▲".

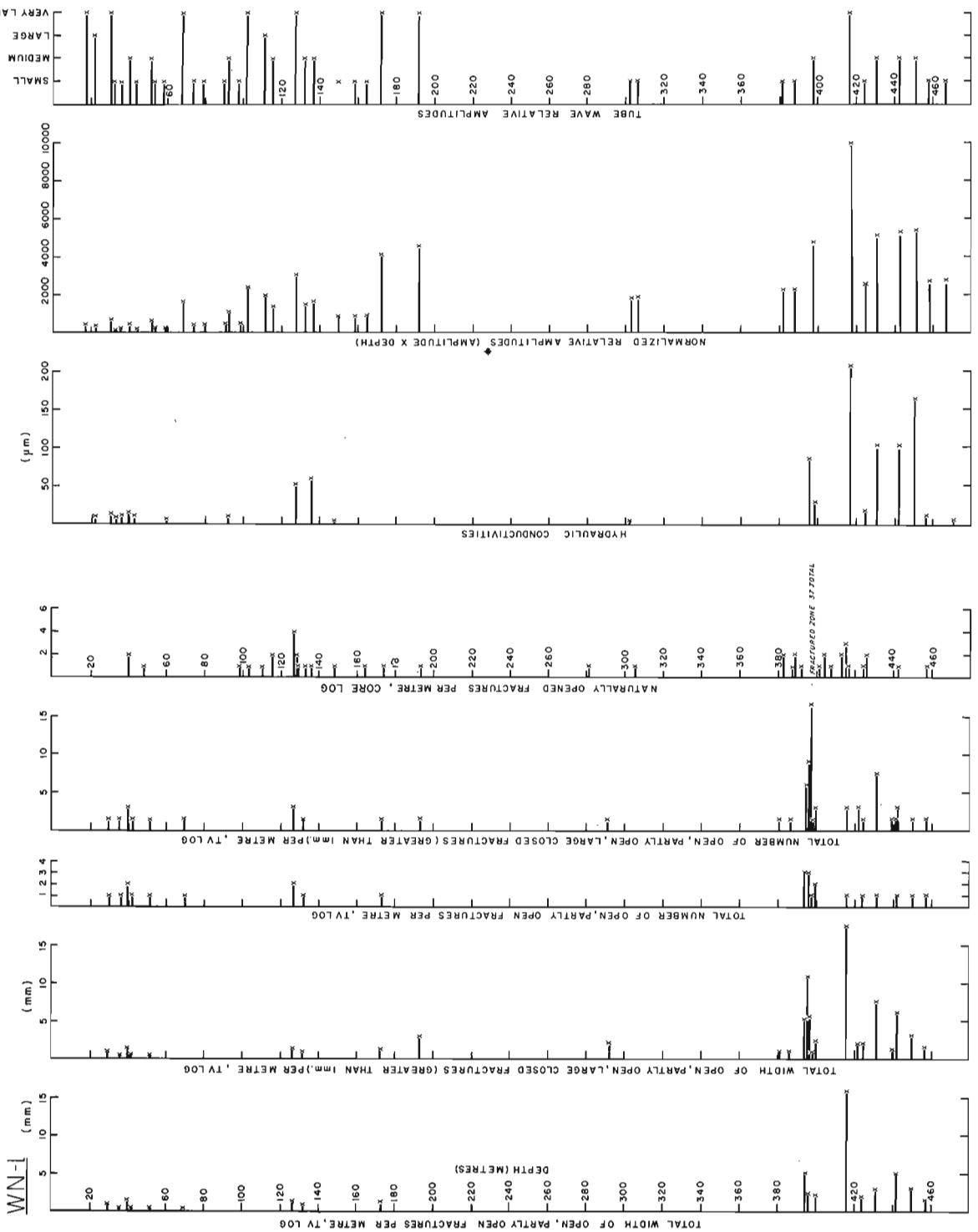

Figure 52.7. *Correlation of open fractures amongst tube wave, core logging, TV logging and hydrogeology study in hole WN-1.*

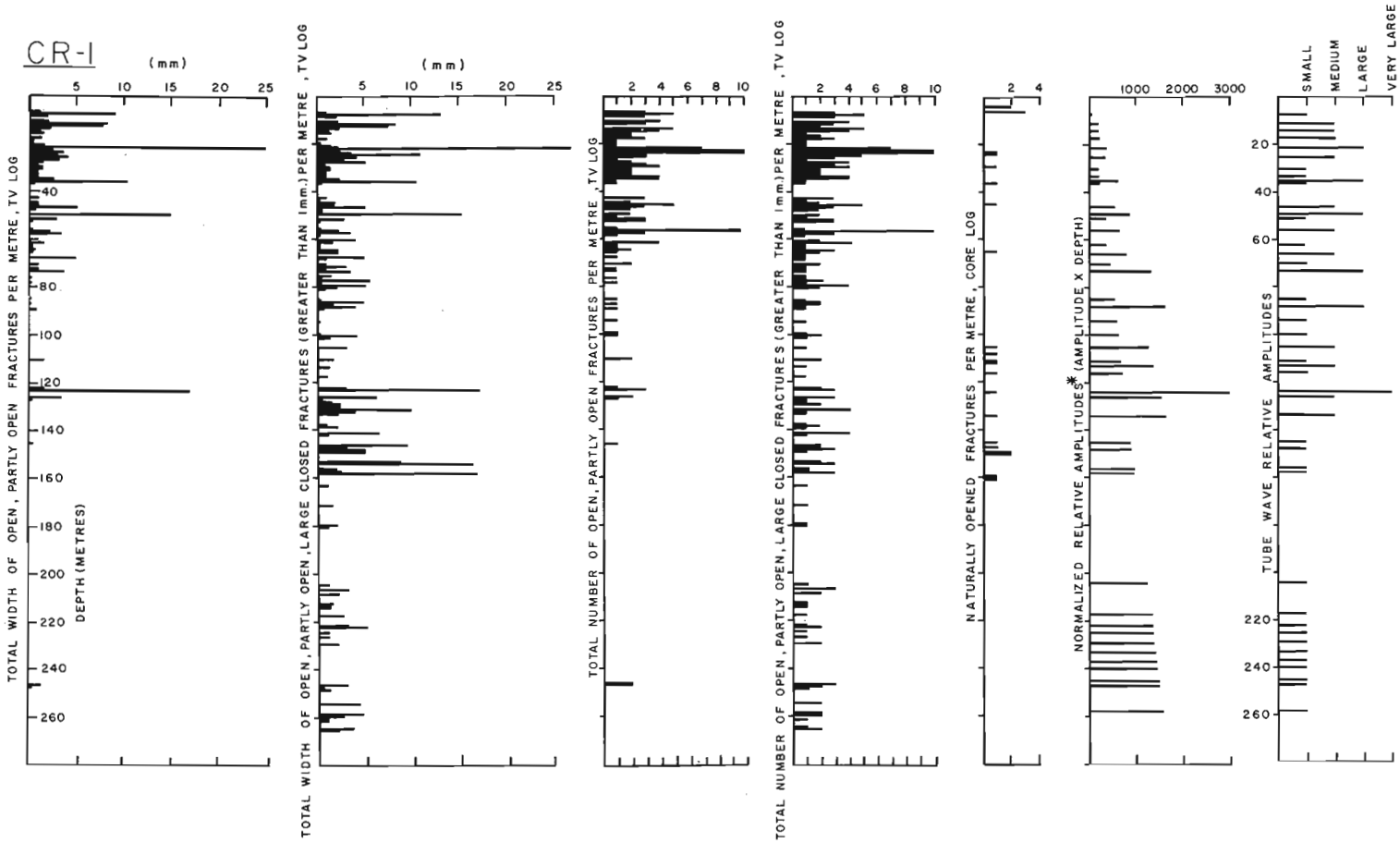

Figure 52.8. *Correlation of open fractures amongst tube wave, core logging and TV logging in hole CR-1.*

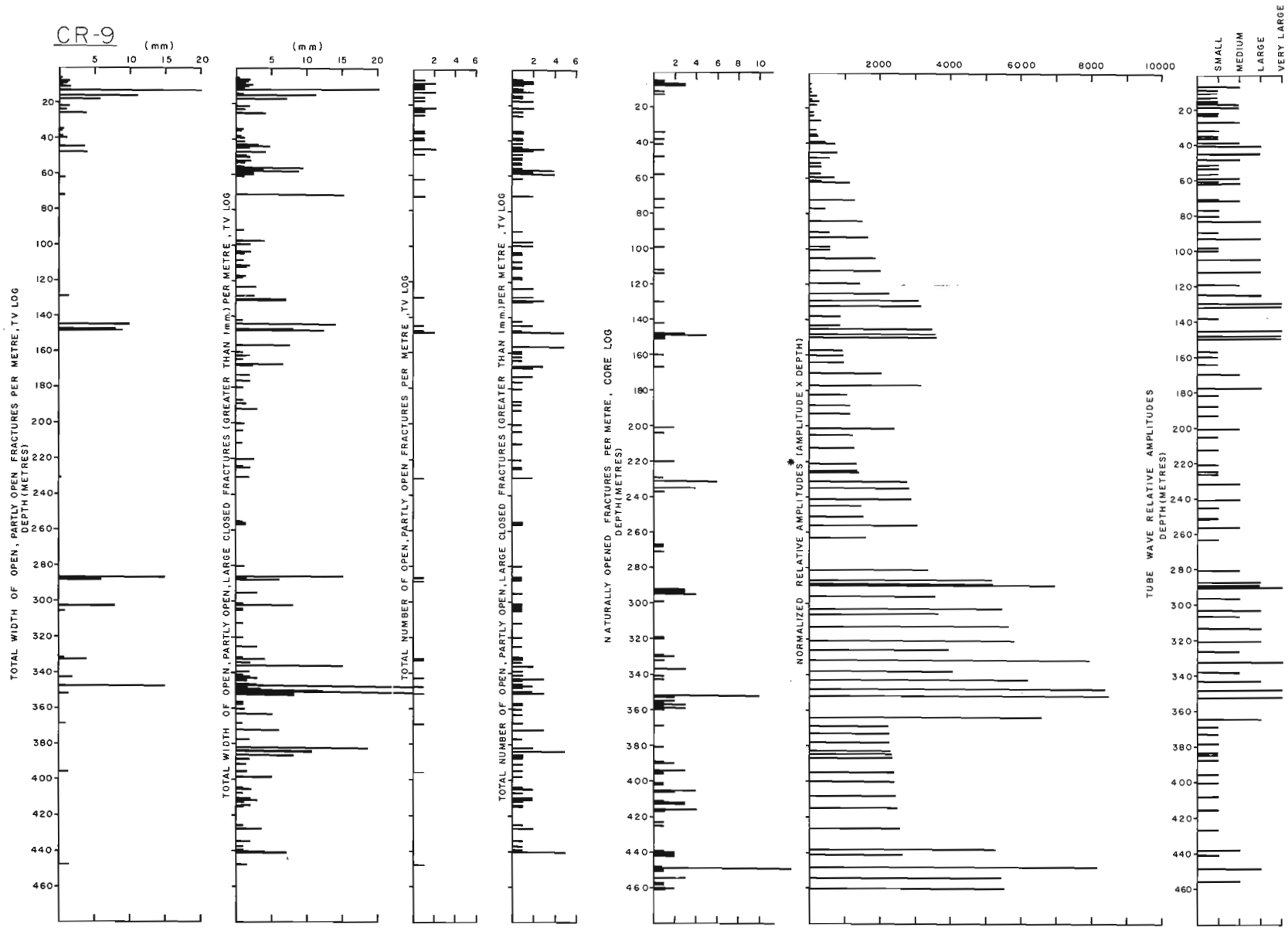

* *Normalized tube wave relative amplitude = Tube wave relative amplitude X Travel distance by assuming that an equal amount of energy was generated for each record shot and the loss of energy is proportional to increasing travel distance.*

Figure 52.9. *Correlation of open fractures amongst tube wave, core logging and TV logging in hole CR-9.*

Table 52.1

Correlations among tube wave, core log and hydrogeology study in WN-1

Tube wave originating depth (m)	Tube wave relative amplitude[1]	TV log: Total opening widths[2] of open fractures Depth in m (widths in mm)	TV log: No. of open fractures[3] Depth in m (numbers)	Core log: No. of naturally open fractures per meter[4] Depth in m (no. & type of fractures)	Hydraulic conductivity test: Calculated aperture in μm[5] Depth in m (aperture in μm)
17.80	VL				
22.26	L				21.0-23.97 (9-12)
30.61	VL	30.0-31.0 (0.8)	30.0-31.0 (1)		29.0-31.97 (12-14)
32.81	S				32.0-34.97 (8)
35.56	S	36.0-37.0 (0.5)	36.0-37.0 (1)		35.0-37.97 (20-30)
40.01	M	40.0-41.0 (1.4)	40.0-41.0 (2)	40.0-42.0 (2A & 2B)	38.0-40.97 (13-17)
43.35	S	42.0-43.0 (0.5)	42.0-43.0 (1)		41.0-43.97 (8-13)
51.70	M	52.0-53.0 (0.4)	52.0-53.0 (1)	48.0-49.0 (1 B)	
53.90	S				
58.40	S				56.93-62.47 (12,5-7,5-6)
68.35	VL	70.0-71.0 (0.2)	70.0-71.0 (1)		
74.10	S				
79.49	S				
90.59	S				89.58-94.44 (9-11,5-6,
92.70	M				3-4)
98.00	S			98.0-99.0 (1 B)	
102.24	VL			103.0-104.0 (1 B)	
111.68	L			110.0-111.0 (1 A)	
115.53	M			115.0-116.0 (2 B)	
127.19	VL	127.0-128.0 (1.3)	127.0-128.0 (2)	127.0-130.0 (5A&2B)	126.0-128.97 (33-70)
132.78	M	132.0-133.0 (0.8)	132.0-133.0 (1)	133.0-134.0 (1A)	
136.08	M			136.0-137.0 (1B)	
149.38	S			148.0-149.0 (1B)	
158.80	S				
164.50	S			164.0-165.0 (1B)	
172.73	VL	173.0-174.0 (1.2)	173.0-174.0 (1)	174.0-175.0 (1A)	
191.61	VL			193.0-194.0 (1B)	
				281.0-282.0 (1B)	
305.50	S			305.0-306.0 (1B)	
381.00	S			382.0-383.0 (1A&1B)	
387.72	S			387.0-389.0 (3B)	
				391.0-392.0 (1B)	
397.66	M	395.0-400.0 (10.5)	395.0-400.0 (9)	396.0-400.0 (37A&B)	394.5-397.47 (83-86)
				401.0-402.0 (1B)	397.5-400.47 (27-29)
				403.0-404.0 (2B)	
				407.0-408.0 (1B)	
				413.0-415.0 (5B)	
416.56	VL	416.0-417.0 (16.0)	416.0-417.0 (1)	416.0-417.0 (1B)	415.0-417.97 (205-210)
424.91	S	424.0-425.0 (2.0)	424.0-425.0 (1)	424.0-425.0 (1A&2B)	423.0-425.97 (17)
430.45	M	431.0-432.0 (3.0)	431.0-432.0 (1)		429.56-432.62 (103)
442.70	M	442.0-443.0 (5.0)	442.0-443.0 (1)	442.0-443.0 (1B)	441.0-443.97 (103)
450.50	M	450.0-451.0 (3.0)	450.0-451.0 (1)		448.96-451.93 (164)
457.50	S	457.0-458.0 (1.5)	457.0-458.0 (1)	457.5-458.5 (1B)	455.02-457.99 (10)
466.00	S				

(1) Tube wave relative amplitudes: Visually estimated and subdivided into small (S), medium (M), large (L), very large (VL).

(2) Total opening widths of open and partly open fractures on TV log (J. Lau).

(3) No. of open and partly open fractures on TV log (J. Lau).

(4) No. of naturally open fractures: type A = open to fluid flow & type B = maybe open to fluid flow, per meter on core log (J. Dugal).

(5) Calculated aperture in μm of single equivalent fracture per 2.97 m testing interval (C. Davison).

Chalk River CR-9

This is the best tube wave record suite yet obtained (see Appendix 2). The comparison of tube wave analysis, TV log and core log are shown in Figure 52.9 and Table 52.3. The following observations are noted:

1. As in WN-1 and CR-1 these three borehole logs show excellent correlations in positions of open fractures. However, the tube wave analysis and the core log appear to record more open fractures than the TV log.
2. Although good quality records assure confidence in identifying tube wave events, some observed weak events (not observed by core and TV logs) still remain questionable and need further justification by hydrogeology studies.
3. By examining the record suite, we suggest that some large (≥1.00 mm) closed fractures interpreted from the TV log are actually open to fluid flow since their associated tube waves are strong. Because of this, open fractures identified by tube wave events are subdivided into three groups according to the relative strength of amplitudes:

a) Definite open fractures, indicated by "▲" marks on the record suite. All the open fractures detected by the TV method fall into this group. The tube waves resulting from these open fractures show very strong amplitudes. Examples are those open fractures located at 128.78 m, 144.52 m, 147.91 m and 289.65 m, etc.

b) This group of open fractures is recorded as large (≥1.00 mm) closed fractures by TV log. They are distinguished by the symbol "▲" on the record suite. Tube waves generated by them are high amplitude, easily identified and indicate open fractures. Furthermore, the majority of open fractures within this group are correlatably recorded by the core log. Examples are the open fractures at 176.78 m, 320.0 m, 363.91 m, and 437.39 m.

Table 52.2

Correlation among tube wave, core log and TV log in CR-1

Tube wave originating depth (m)	Tube wave Relative amplitude(1)	TV log Total opening widths of open fractures(2) Depth in m (widths in mm)	TV log No. of open fractures(3) Depth in m (numbers)	Core log No. of naturally open fractures per meter(4) Depth in m (numbers)
		6.0- 7.0 (1.1)	6.0- 7.0 (3)	4.0- 5.0 (2)
7.69	S	7.0- 8.0 (9.2)	7.0- 8.0 (5)	6.0- 7.0 (3)
11.08	M	11.0-12.0 (8.4)	11.0-12.0 (3)	
14.47	M	14.0-16.0 (2.7)	14.0-16.0 (5)	
17.95	M	17.0-19.0 (1.5)	17.0-19.0 (4)	
21.34	L	21.0-22.0 (25.0)	21.0-22.0 (7)	
		22.0-23.0 (2.5)	22.0-23.0 (10)	
		23.0-24.0 (3.6)	23.0-24.0 (10)	23.0-24.0 (1)
25.39	M	24.0-26.0 (7.2)	24.0-26.0 (6)	24.0-25.0 (1)
30.52	S	29.0-31.0 (2.8)	29.0-31.0 (6)	29.0-30.0 (1)
33.00	S	33.0-34.0 (1.0)	33.0-34.0 (4)	
35.08	L	34.0-36.0 (13.0)	34.0-36.0 (5)	36.0-37.0 (1)
36.88	S	36.0-37.0 (0.5)	36.0-37.0 (1)	
46.52	M	45.0-47.0 (7.0)	45.0-47.0 (8)	45.0-46.0 (1)
49.39	L	49.0-50.0 (15.4)	49.0-50.0 (2)	
51.65	S	51.0-52.0 (3.0)	51.0-52.0 (3)	
56.82	M	56.0-58.0 (5.8)	56.0-58.0 (13)	
62.80	S	62.0-64.0 (0.8)	62.0-64.0 (2)	
66.52	M	67.0-68.0 (5.0)	67.0-68.0 (1)	65.0-66.0 (1)
70.47	S	70.0-71.0 (1.0)	70.0-71.0 (2)	
73.91	L	73.0-74.0 (3.5)	73.0-74.0 (1)	
85.34	S	85.0-86.0 (0.2)	85.0-86.0 (1)	
88.82	L	89.0-90.0 (0.7)	89.0-90.0 (1)	
94.52	S	94.0-95.0 (0.1)	94.0-95.0 (1)	
100.21	S	100.0-101.0 (0.1)	100.0-101.0 (1)	
105.30	M			105.0-106.0 (1)
				108.0-109.0 (1)
111.04	S	110.0-111.0 (1.7)	110.0-111.0 (2)	111.0-112.0 (1)
113.30	M			112.0-113.0 (1)
116.78	S			116.0-117.0 (1)
124.21	VL	122.0-124.0 (18.7)	122.0-124.0 (4)	124.0-125.0 (1)
126.47	M	126.0-128.0 (1.6)	126.0-128.0 (3)	
134.52	M			134.0-135.0 (1)
145.39	S	146.0-147.0 (0.5)	146.0-147.0 (1)	145.0-146.0 (1)
148.21	S			147.0-148.0 (1)
				149.0-150.0 (2)
				150.0-151.0 (2)
156.21	S			
158.26	S			159.0-160.0 (1)
				160.0-161.0 (1)
				161.0-162.0 (1)
204.26	S			
217.91	S			
222.52	S			
225.34	S			
229.95	S			
233.0	S			
237.95	S			
240.40	S			
245.0	S			
247.08	S	246.0-248.0 (1.8)	246.0-248.0 (2)	
258.50	S			

(1) Tube wave relative amplitudes: visually estimated and subdivided into small (S), medium (M), large (L), & very large (VL).

(2) Total opening widths of open and partly open fractures on TV log (J. Lau).

(3) No. of open and partly open fractures on TV log (J. Lau).

(4) No. of naturally open fractures per meter on core log (J. Dugal).

c) The symbol of an open triangle "Δ" is used to designate this group of open fractures. The characteristics of this group are: I) they are recorded as large (≥1.00 mm) closed fractures on the TV log, and II) they are very weak tube wave events. This is the group of open fractures which the authors regard as "questionable". Examples are the open fractures located at 99.34 m, 156.52 m, 181.08 m, and 225.69 m.

4. Table 52.4 shows the open fractures which are not observed (or are indicated as large (≥1.00 mm) closed fractures) by the TV log but have been identified by both the tube wave analysis and the core log.

5. Table 52.5 shows some open fractures which are not recorded by the core log but have been indicated by both the tube wave analysis and the TV log.

6. Table 52.6 shows the open fractures which are not recorded by the core log, but have been designated by tube wave identification as open fractures and by the TV log as large (≥1.00 mm) closed fractures.

From 3, 4, 5, and 6, it is suggested that tube wave analysis technique can detect more open fractures than can be indicated by the core log and TV log. There appears to be a positive correlation between the relative amplitudes of tube waves and the total opening widths of open fractures from the TV log, and also the number of naturally open fractures from core log.

Table 52.3

Correlations among tube waves, core log and TV log in CR-9

Tube wave originating depth (m)	Tube wave relative amplitude[1]	TV log: Total opening widths of open fractures[2] depth in m (widths in cm)	TV log: No. of open fractures[3] Depth in m (numbers)	Core log: No. of naturally open fractures per meter[4] Depth in m (numbers)
				4.0- 5.0 (1 B)
5.95	M	5.0- 6.0 (0.4)	5.0- 6.0 (1)	5.0- 6.0 (1 B)
		7.0- 8.0 (1.6)	7.0- 8.0 (2)	6.0- 7.0 (2A & 1B)
8.21	S	8.0- 9.0 (1.2)	8.0- 9.0 (1)	7.0- 8.0 (3B)
10.47	S	9.0-11.0 (2.4)	9.0-11.0 (2)	10.0-11.0 (1B)
12.52	L	12.0-13.0 (20.0)	12.0-13.0 (2)	12.0-13.0 (1A)
14.78	S			
15.91	L	15.0-16.0 (11.0)	15.0-16.0 (1)	
17.95	M	17.0-18.0 (6.0)	17.0-18.0 (1)	
21.13	S	21.0-22.0 (1.6)	21.0-22.0 (2)	
23.39	S	23.0-24.0 (1.2)	23.0-24.0 (1)	
26.21	M	25.0-26.0 (4.0)	25.0-26.0 (1)	
31.08	S			
34.47	S	34.0-35.0 (0.8)	34.0-35.0 (1)	33.0-34.0 (1B)
35.39	S	35.0-36.0 (0.6)	35.0-36.0 (1)	
38.21	M	38.0-39.0 (0.6)	38.0-39.0 (1)	37.0-38.0 (1B)
39.91	L	39.0-40.0 (1.0)	39.0-40.0 (1)	40.0-41.0 (1B)
44.21	L	44.0-45.0 (3.6)	44.0-45.0 (2)	
47.78	M	47.0-48.0 (4.0)	47.0-48.0 (1)	47.0-48.0 (1A)
50.78	S			
52.65	S			
56.21	S			
58.47	M			57.0-58.0 (1B)
60.52	S			
61.65	L	61.0-62.0 (1.0)	61.0-62.0 (1)	
71.39	L	71.0-72.0 (1.0)	71.0-72.0 (1)	71.0-72.0 (1B)
76.47	S			76.0-77.0 (1A)
83.04	L			
89.04	S			88.0-89.0 (1B)
92.21	L			
97.65	S			98.0-99.0 (1B)
99.34	S			
104.21	L			
111.34	L			111.0-112.0 (1A)
				113.0-114.0 (1A)
118.47	M			
124.10	L			
128.78	VL	128.0-129.0 (1.5)	128.0-129.0 (1)	
131.21	VL			129.0-130.0 (1A)
137.78	S			
142.50	S			141.0-142.0 (1A)
144.52	VL	144.0-145.0 (10.0)	144.0-145.0 (1)	
147.91	VL	147.0-148.0 (8.0)	147.0-148.0 (1)	147.0-148.0 (3A)
		148.0-149.0 (9.0)	148.0-149.0 (2)	148.0-149.0 (3A & 1B)
149.04	VL			149.0-150.0 (1A)
				150.0-151.0 (1A)
156.52	S			
159.34	S			159.0-160.0 (1A)
163.65	S			
169.08	M			166.0-167.0 (1B)
176.78	L			
181.08	S			
187.26	S			
192.52	S			
200.00	M			200.0-201.0 (1A&1B)
204.52	S			203.0-204.0 (1B)
211.82	S			
220.26	S			219.0-220.0 (2A)
224.00	S			
225.69	S			
				228.0-229.0 (1B)
230.78	M	230.0-231.0 (0.4)	230.0-231.0 (cavity)	230.0-231.0 (2A & 4B)
234.0	M			234.0-235.0 (4A)
240.52	M			236.0-237.0 (1A)
244.82	S			
250.82	S			
255.69	M			
262.82	S			
				266.0-267.0 (1B)
				267.0-268.0 (1B)
				270.0-271.0 (1B)
280.26	M			
286.82	L	286.0-287.0 (15.0)	286.0-287.0 (1)	
288.52	L	287.0-288.0 (1.5)	287.0-288.0 (1)	
289.65	VL	288.0-289.0 (6.0)	288.0-289.0 (1)	291.0-292.0 (3B)
				292.0-293.0 (3B)
				293.0-294.0 (3B)
295.65	M			294.0-295.0 (4B)
				298.0-299.0 (1B)
302.39	L	302.0-303.0 (8.0)	302.0-303.0 (1)	
305.95	M	305.0-306.0 (1.0)	305.0-306.0 (1)	
312.52	L			
				318.0-319.0 (1B)
				319.0-320.0 (1B)
320.39	L			
325.65	M			
				328.0-329.0 (1B)
				329.0-330.0 (2B)
331.82	VL	331.0-333.0 (4.9)	331.0-333.0 (2)	331.0-332.0 (1B)
337.08	M			336.0-337.0 (3B)
				340.0-341.0 (1B)
342.52	L	342.0-343.0 (2.0)	342.0-343.0 (1)	342.0-343.0 (1B)
347.95	VL	347.0-348.0 (15.0)	347.0-348.0 (1)	
351.69	VL	351.0-352.0 (1.5)	351.0-352.0 (1)	351.0-352.0 (3A & 7B)
				352.0-353.0 (1A & 1B)
				354.0-355.0 (2B)
				355.0-356.0 (1B)
				356.0-357.0 (3B)
				357.0-358.0 (1B)
				358.0-359.0 (3B)
				359.0-360.0 (1B)
363.91	L			
368.21	S	368.0-369.0 (1.0)	368.0-369.0 (1)	368.0-369.0 (1B)
372.52	S			
377.95	S			
382.65	S			380.0-381.0 (1B)
384.52	S			
386.78	S			
				388.0-389.0 (1B)
				389.0-390.0 (2B)
				393.0-394.0 (3B)
394.82	S			394.0-395.0 (1B)
		395.0-396.0 (1.5)	395.0-396.0 (1)	395.0-396.0 (1B)
399.34	S			400.0-401.0 (1B)
				401.0-402.0 (1B)
				404.0-405.0 (4B)
				405.0-406.0 (2B)
407.39	S			
				410.0-411.0 (1B)
				411.0-412.0 (3B)
414.52	S			412.0-413.0 (3B)
				415.0-416.0 (4B)
				416.0-417.0 (1B)
				422.0-423.0 (1B)
425.96	S			424.0-425.0 (1B)
437.39	M			438.0-439.0 (1B)
				439.0-440.0 (2B)
440.22	S			440.0-441.0 (2B)
				441.0-442.0 (2B)
447.91	L	447.0-448.0 (1.5)	447.0-448.0 (cavity)	447.0-448.0 (1B)
				448.0-449.0 (13B)
				450.0-451.0 (1B)
453.52	M			453.0-454.0 (1A & 2B)
				456.0-457.0 (1B)
				457.0-458.0 (1B)
459.50	M			459.0-460.0 (1A & 1B)
				460.0-461.0 (1A)

(1) Tube wave relative amplitudes: visually estimated and subdivided into small (S), medium (M), large (L), very large (VL).
(2) Total opening widths of open and partly open fractures on TV log (J. Lau).
(3) No. of open and partly open fractures on TV log (J. Lau).
(4) No. of naturally open fractures: type A = open to fluid flow & type B = Maybe open to fluid flow, per meter on core log (J. Dugal).

Table 52.4

Correlation among tube wave, TV log and core log in CR-9

Tube wave generating depth (m)	Tube wave relative amplitude[1]	TV log: Total widths of large closed fractures per m — Depth in m	(widths in mm)	Core log: Naturally open fractures: A and B[2] — Depth in m (no. of fractures)
56.21	S	56.0 - 57.0	(9.3)	
58.47	M	57.0 - 59.0	(12.4)	57.23 (1 B)
76.47	S	76.0 - 77.0	(0.5)	76.0 - 77.0 (1 A)
89.04	S	89.0 - 90.00		88.40 (1 B)
97.65	S	97.0 - 98.0	(4.0)	
99.34	S	99.0 - 100.0	(2.0)	98.89 (1 B)
111.34	L	111.0 - 112.0	(2.0)	111.503 (1 A)
		112.0 - 113.0	(1.5)	113.0 - 114.0 (1 A)
142.50	S	142.0 - 143.0	(1.0)	141.36 (1 A)
159.34	S	160.0 - 161.0	(1.0)	159.27 (1 A)
200.00	M	200.0 - 201.0	(1.2)	200.22 (1 B)
				200.44 (1 A)
204.52	S	204.0 - 205.0	(1.0)	203.73 (1 B)
220.26	M	220.0 - 221.0	(2.5)	219.55 (1 A)
				219.57 (1 A)
234.00	M	234.0 - 235.0	(0.9)	234.0 - 235.0 (4 A)
295.65	M	295.0 - 296.0	(3.0)	294.0 - 295.0 (4 B)
320.39	L	320.0 - 321.0	(1.0)	318.40 (1 B?)
				319.31 (1 B?)
337.08	M	336.0 - 337.0	(15.0)	336.0 - 337.0 (3 B)
382.65	S	382.0 - 383.0	(18.5)	380.0 - 381.0 (1 B)
399.34	S	398.0 - 399.0	(5.0)	400.29 (1 B)
407.39	S	407.0 - 408.0	(1.0)	404.0 - 406.0 (6 B)
414.52	S	414.0 - 415.0	(2.0)	415.0 - 416.0 (4 B)
		415.0 - 416.0	(1.0)	
425.96	S	425.0 - 426.0	(1.0)	424.19 (1 B)
437.39	M	437.0 - 438.0	(1.0)	438.83 (1 B)
440.22	S	440.0 - 441.0	(4.0)	440.30 (1 B)
				440.77 (1 B)
453.52	M	no information		453.0 - 454.0 (1 A & 2 B)
459.5	M	no information		459.0 - 460.0 (1 A & 1 B)
				460.0 - 461.0 (1 A)

[1] Tube wave relative amplitude: visually estimated and subdivided into small (S), medium (M), large (L), very large (VL).

[2] Naturally open fractures: A = open to fluid flow; B = maybe open to fluid flow

Tube Wave Velocities

An attempt was made to study the velocity variations of tube waves as they propagate along the borehole in hole CR-1. In theory the tube wave velocity is a function of the rigidity of the borehole wall. The following equations describe the relationship:

$$V_T = \frac{V_w\sqrt{\mu}}{\sqrt{\rho_w V_w^2 + \mu}}$$

where V_T = tube wave velocity

V_w = fluid velocity

ρ_w = fluid density

μ = rigidity

Since $V_s = \frac{\sqrt{\mu}}{\rho}$, substituted into (1):

$$V_T = \frac{Vs}{\sqrt{\rho_w/\rho + (V_s/V_w)^2}}$$

where ρ = density of borehole wall

V_s = shear wave velocity

The velocities of all identified tube waves from each shot record were first measured and then averaged. The velocity obtained is used to represent the tube wave velocity for that particular depth interval. By assuming V_w = 1.46 km/s, ρ_w = 1.00 g/cc, and measured wall rock densities (from density log), the corresponding shear wave velocities were obtained using equation (2). The plots of velocity variations are presented in Figure 52.10.

In general the results exhibited some scattering due to interference from other tube waves. However, with the exception of the interval 94.0-102.0 m they do show relatively low velocities over the depth intervals shallower than 135 m. The same characteristics have also been noted with the TV log, standard logs and tube wave originating depths (see Fig. 52.8 and Appendix 1).

Conclusions and Recommendation

Our experimental work suggests that the identification of tube wave events on borehole seismograms may be used as reliable indicators of fractures open to fluid flow. In addition, the relative amplitudes of tube waves appear to be correlatable with measured hydraulic conductivities and total

Table 52.5

Correlation between tube wave and TV log in CR-9

Tube wave generating depth(m)	Tube wave relative amplitude[1]	TV log Total widths of open fractures per m Depth in m	(widths in mm)
15.91	L	15.0 - 16.0	(11.0)
17.95	M	17.0 - 18.0	(6.0)
21.13	S	21.0 - 22.0	(1.6)
23.39	S	23.0 - 24.0	(1.2)
26.21	M	25.0 - 26.0	(4.0)
44.21	L	44.0 - 45.0	(3.6)
61.65	L	61.0 - 62.0	(1.0)
144.52	VL	144.0 - 145.0	(10.0)
286.82	L	286.0 - 287.0	(15.0)
288.52	L	287.0 - 288.0	(1.5)
289.65	VL	288.0 - 289.0	(6.0)
302.39	L	302.0 - 303.0	(8.0)
305.95	M	305.0 - 306.0	(1.0)
347.95	VL	347.0 - 348.0	(15.0)

[1] Tube wave relative amplitude: visually estimated and subdivided into small (S), medium (M), large (L), very large (VL).

Table 52.6

Correlation between tube wave and TV log in CR-9

Tube wave originating depth(m)	Tube wave relative amplitude[1]	TV log Total widths of large closed fractures per m Depth in m	(widths in mm)
50.78	S	50.0 - 51.0	(2.0)
52.65	S	52.0 - 53.0	(2.0)
83.04	L	83.0 - 84.0	(0.2)
92.21	L	91.0 - 92.0	(1.0)
104.21	L	103.0 - 105.0	(3.2)
118.47	M	117.0 - 119.0	(2.2)
124.10	L	123.0 - 124.0	(2.8)
156.52	S	156.0 - 157.0	(7.5)
176.78	L	176.0 - 177.0	(2.0)
181.08	S	180.0 - 181.0	(1.0)
187.08	S	187.0 - 188.0	(1.0)
192.52	S	192.0 - 193.0	(3.0)
211.82	S	211.0 - 212.0	(1.0)
225.69	S	225.0 - 226.0	(2.0)
240.52	M	239.0 - 240.0	(0.3)
255.69	M	255.0 - 258.0	(3.7)
280.26	M	280.0 - 281.0	(1.2)
312.52	L	312.0 - 313.0	(1.0)
325.65	M	325.0 - 326.0	(3.0)
363.91	L	363.0 - 364.0	(5.0)
372.52	S	372.0 - 373.0	(5.9)
377.95	S	377.0 - 378.0	(2.0)

[1] Tube wave relative amplitudes: visually estimated and subdivided into small (S), medium (M), large (L), very large (VL)

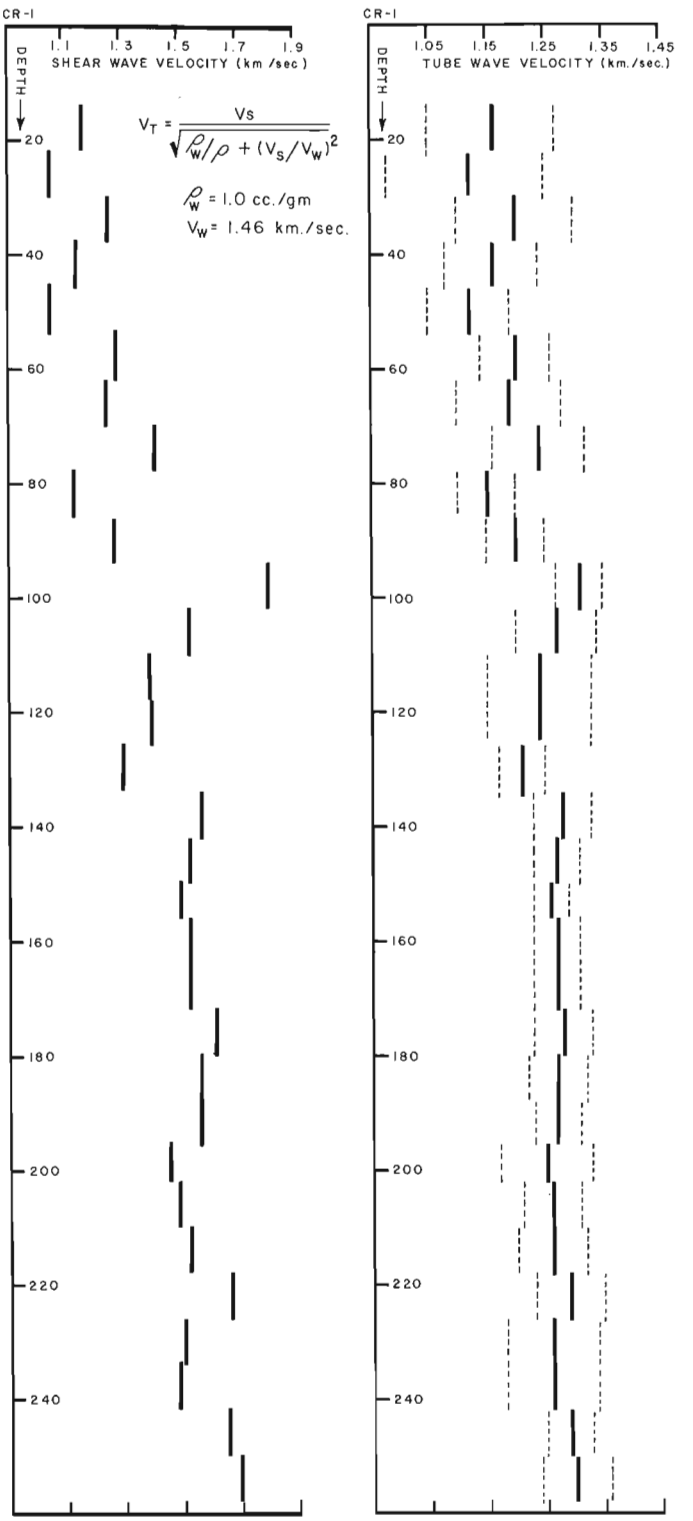

Solid lines: *average tube wave velocities*
Dashed lines: *error bars associate with average tube wave velocities*

Figure 52.10. *Observed tube wave velocities and calculated shear wave velocities in hole CR-1.*

widths of open fractures on the TV log. Studies of the TV log and core log indicate the heavily fractured nature of the borehole wall over the depth interval 395 m-400 m in WN-1 (9 open fractures by TV log and 37 naturally open fractures by core log). However, the results are probably more closely related to porosity rather than permeability. In spite of the large number of open fractures on the borehole wall, permeabilities are actually low. The amplitude of the tube wave is relatively much smaller than that of 416.5 m (Fig. 52.1, 52.7) which has small porosity but high permeability; there is only one partly open fracture of 16.0 mm at 416.22 m by TV log and six naturally open fractures by core log. The differential in fracture permeability is supported by the hydrogeology study. It shows 205-210 μms in aperture of equivalent single open fracture over the interval 415.0-417.97 m and 83-86 μms in aperture over 394.5-397.47 m. The former is hydrologically much more permeable than the latter. Consequently, tube wave results appear to be more directly related to fracture hydrology than TV log and core log. Furthermore, some open fractures which are not observed by core log and TV log are detected by the tube wave analysis and the hydrogeology studies.

Because of the relatively low frequency employed in this seismic study, it is suggested that the tube wave events are effectively sampling a volume of rock within several metres of the borehole. At least a macroscopic bulk property of the rock mass (containing an open fracture) is monitored at the time of incidence of compressional wave onto a fluid-filled fractured zone which intersects the borehole. Hence, the results obtained from this new method can possibly provide the information of fracture permeability with substantial depth penetration into the immediate vicinity of the borehole wall (Huang and Hunter, 1980b).

The tube wave analysis also assures fast data-acquisition in the field. With an active hydrophone array of 12.43 m, a crew of three people can probably cover a 500 m hole within a day. In addition, the preliminary interpretation can be made in the field.

To obtain a better understanding of subsurface fracture permeability it is suggested that borehole data measured by different methods be combined so as to establish the most complete possible mapping of fractures which intersect the borehole.

The testing program is still in its initial phase and several uncertainties remain to be resolved. It is hoped that more quantitative information about fracture permeability in boreholes can be obtained through the detailed studies of the amplitude and the velocity of tube wave events. The following recommendations are made:

1. For some open fractures not recorded by TV log (but indicated by tube wave events), arrangements should be made for hydraulic conductivity testings in holes WN-1, CR-1 and CR-9.
2. More work must be done to obtain correlations between relative amplitudes of tube waves and measured hydraulic conductivities in the borehole. An empirical relationship may be formulated between the sizes of open fractures and relative amplitudes.
3. A detailed study of the velocity variation of the tube waves should be conducted to obtain the relationship between wall rigidity and tube wave velocity.

Acknowledgments

Appreciation is expressed to the management of Atomic Energy of Canada Limited for permission to publish this material. Special thanks are extended to all the employees of the seismic section at the Geological Survey for their assistance in every phase of the work. R.M. Gagne has helped considerably with the drafting. Field assistance was provided by R.A. Burns and R. Good. A. Overton and H.A. MacAulay provided valuable discussions and suggestions concerning field methods and interpretation of our observations. We are sincerely thankful to L.S. Collett for his support and encouragement throughout the course of this study. Thanks also to C. Wright of Earth Physics Branch for fruitful discussions on this study.

Selected References

Biot, M.A.
1952: Propagation of elastic waves in a cylindrical bore containing a fluid; Journal of Applied Physics, v. 23 (9), p. 997-1005.

Davison, C.C.
1979: A progress report on WNRE hydraulic testing program – 1978/79; Atomic Energy of Canada Limited, Technical Record.

Huang, C. and Hunter, J.A.M.
1980a: A progress report on the seismic downhole survey; Atomic Energy of Canada Limited, Technical Record, TR-31.

1980b: A progress report on the identification and correlation of tube wave events on borehole seismic records; Atomic Energy of Canada Limited, Technical Record, TR-32.

Hunter, J.A.M. and Neave, K.G.
1978: A preliminary report on the Downhole Seismic, CR-1; Atomic Energy of Canada Limitd (July, 1978).

Kitsunezaki, C.
1971: Field experimental study of shear waves and the related problems; Contributions, Geophysical Institute, Kyoto University, no. 11, p. 103-177.

Lau, J.
1978a: A report on borehole television survey; Preliminary report; Borehole WN-1; Atomic Energy of Canada Limited (November, 1978).

1978b: A report on borehole television survey, Preliminary report; Borehole CR-1; Atomic Energy of Canada Limited (March, 1979).

1980c: A report on borehole television survey, Preliminary report; Borehole CR-9; Atomic Energy of Canada Limited (March, 1980).

Ording, J.R. and Redding, V.L.
1953: Sound waves observed in mud-filling well after surface dynamite charges; Journal of the Acoustical Society of America, v. 25, p. 719-726.

Paillet, F.
1980: A preliminary draft on acoustic propagation in the vicinity of fractures which intersect a fluid-filled borehole; unpublished report, U.S. Geological Survey, Denver, Colorado.

Riggs, E.D.
1955: Seismic wave types in a borehole; Geophysics, v. 20 (1), p. 53-67.

Sheriff, R.E.
1974: Encyclopedic dictionary of exploration geophysics; Society of Exploration Geophysicists, Tulsa, Oklahoma.

White, J.E.
1965: Seismic waves: radiation, transmission, and attenuation; International Series in the Earth Sciences; McGraw-Hill Book Company, New York, Chapter 4, p. 142-198.

Appendix 1

CR-1 Tube Wave Record Suite

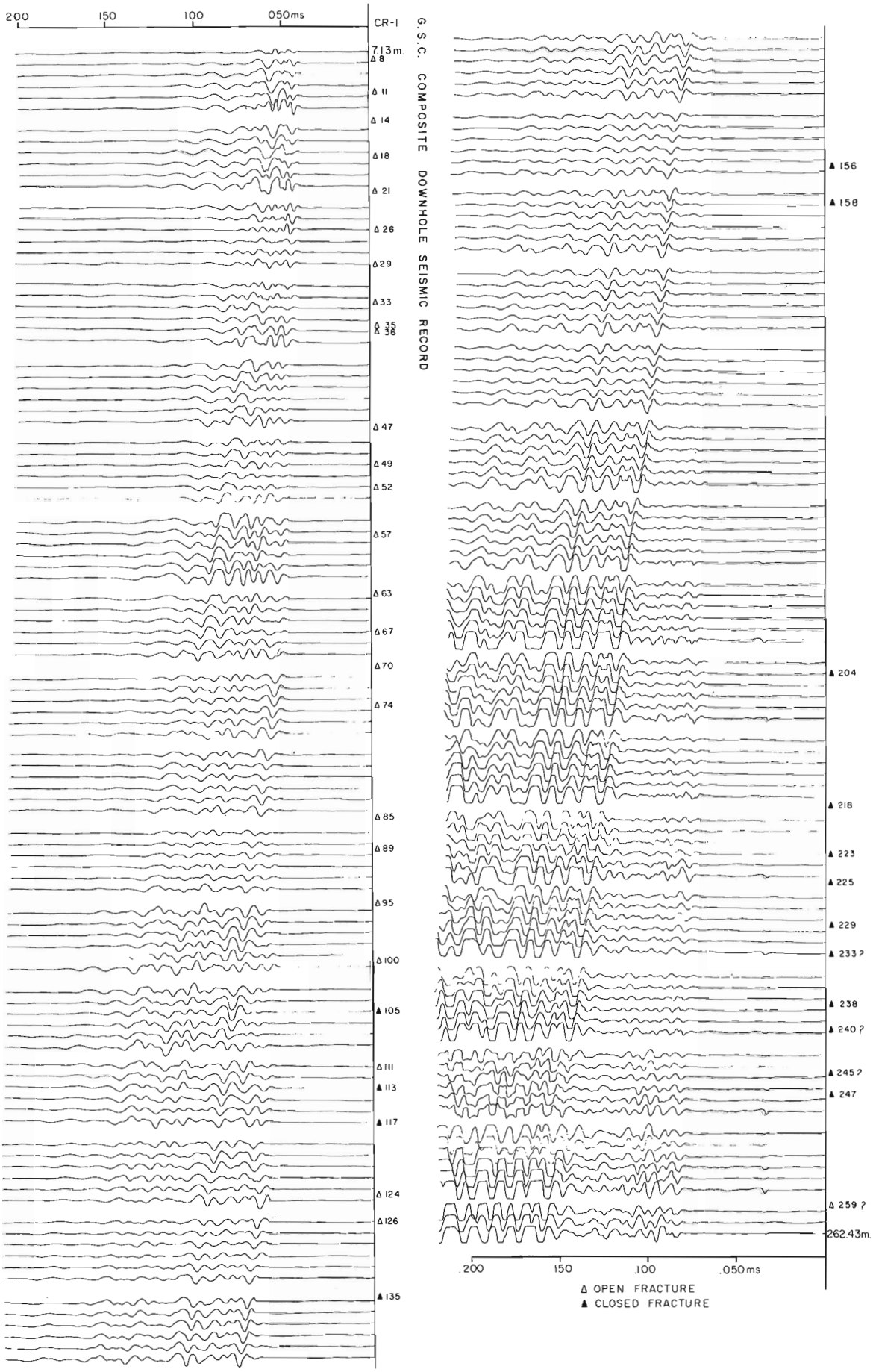

Appendix 2

CR-9 Tube Wave Record Suite

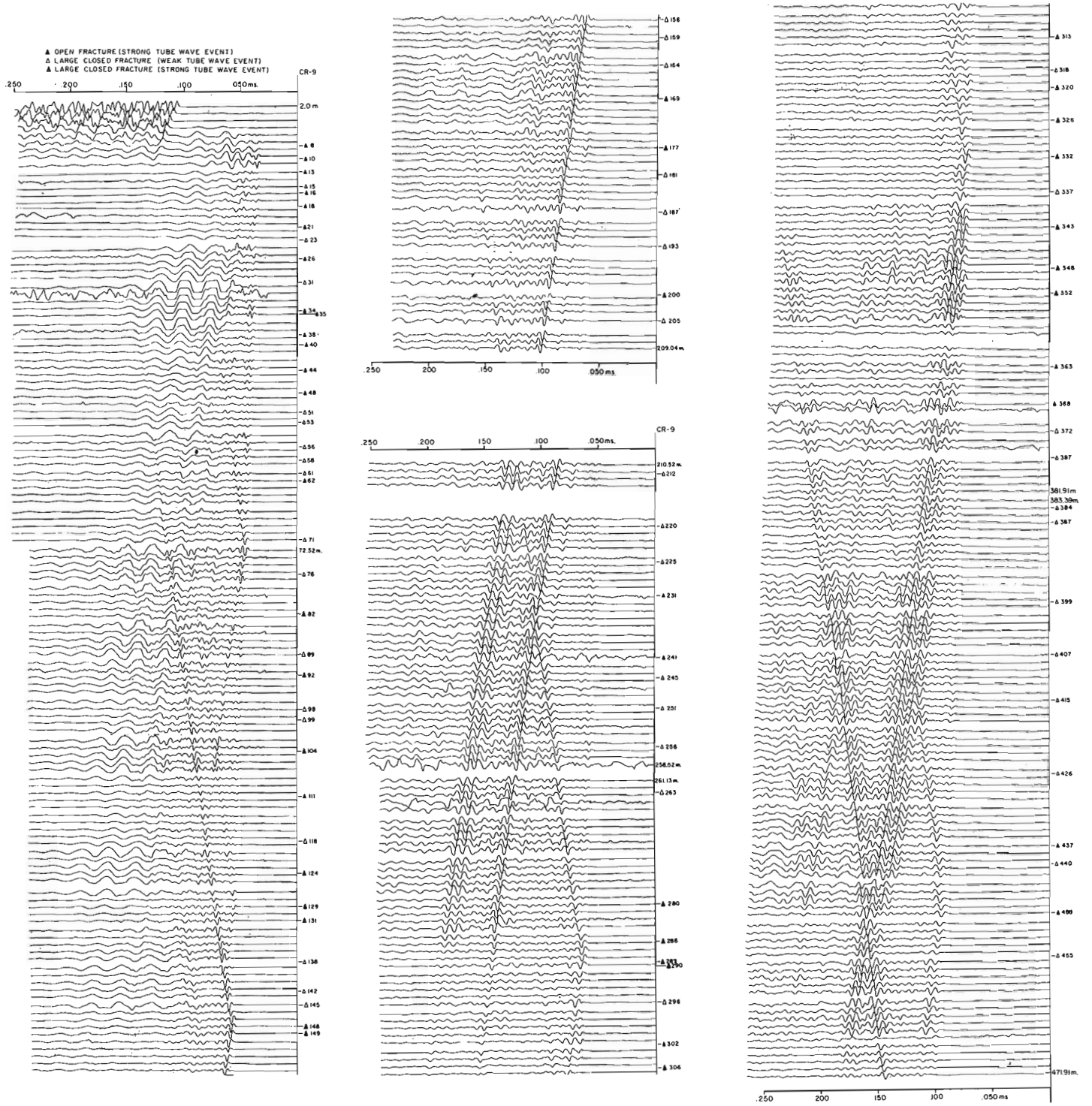

53. TRACE ELEMENTS IN TILL AND ESKER SEDIMENTS IN NORTHWESTERN MANITOBA

Project 800024

L.A. Dredge
Terrain Sciences Division

Dredge, L.A., Trace elements in till and esker sediments in northwestern Manitoba; in Current Research, Part A, Geological Survey of Canada, Paper 81-1A, p. 377-381, 1981.

Abstract

Results from a till and esker sediment sampling program show that background trace element modal values are 10-20 ppm for copper, 20-30 ppm for lead, 30-50 ppm for zinc, 10-20 ppm for cobalt, 20-30 ppm for nickel, and 0.1-0.2 ppm for silver. No anomalously high values were found. Most of the till has been transported 1 to 5 km from source rocks, in a south-southwesterly direction. The highest trace element levels were found in till derived from pelitic biotite gneiss.

Introduction

During the summer of 1975 regional lake sediment (Hornbrook et al., 1976) and airborne radiometric (Resource Geophysics and Geochemistry Division, 1976) surveys were carried out in northwestern Manitoba as part of the Federal-Provincial Uranium Reconnaissance Program (Darnley et al., 1975). In order to provide information to extend the usefulness of the regional reconnaissance surveys, both geochemical and geophysical follow-up investigations were carried out in northwestern Manitoba as described by Coker (1976). This report presents results of overburden sampling in the northeastern part of the Whiskey Jack Lake map area (NTS 64 K/16) where lake sediment sampling had indicated abnormally high silver values.

The objectives of this report are (1) to release the trace element data on the sampled glacial drift; (2) to determine copper, lead, zinc, cobalt, nickel, and silver regional background values in glacial drift; (3) to locate drift anomalous in trace element levels; and (4) to determine the provenance of trace elements present in till and esker sediments by studying glacial dispersal of garnets from known source rocks.

Bedrock and surficial overburden samples were systematically collected from a 133 km^2 area along eight east-west traverses, 1 to 5 km apart, and along one north-south traverse (Fig. 53.1). Every 200 m, 1 kg samples of mineral sediment were collected from bottoms of 60 to 80 cm-deep holes. The samples were from below the B horizon; obviously oxidized sediment was avoided.

Regional Geology

Bedrock Geology

Initial reconnaissance geological mapping of the area was carried out by Currie (1961), and the study area was subsequently remapped by Weber et al. (1975). Bedrock is exposed over about 2 to 5 per cent of the study area, with near-surface bedrock and felsenmeer covering another 2 to 5 per cent. The Precambrian bedrock, Archean and Aphebian, forms part of the Churchill Structural Province. Archean bedrock in the study area consists of plutons of foliated alaskite (Fig. 53.1; Weber et al., 1975). Aphebian rocks lie in the extension of the Wollaston fold belt as defined by Money (1968); these rocks consist of meta-arkose and of lit-par-lit gneisses, composed of various proportions of garnetiferous biotite gneiss, granitic gneiss, and lesser calc-silicate materials.

No mineral occurrences of economic significance have been found, although traces of sulphides have been reported in outcrops along Magas Lake, and malachite (Cu-Zn occurrence) was observed along Dillabough Lake (Weber et al., 1975). In addition, the lake sediment sampling program (Resource Geophysics and Geochemistry Division, 1976) has revealed elevated levels of Fe-Mn-Zn in lakes within the northern belt of biotite gneiss in the study area as well as a silver high in a small lake south of Jackfish Lake (Fig. 53.1); Co-Fe and gamma highs within the alaskite, with a silver anomaly in Hourie Lake; and Pb-Co-Mn and Fe highs in Dillabough Lake.

Surficial Geology

Surficial geological mapping (1:250 000 scale) of the study area was begun in 1976 and finished in 1980. In order of decreasing areal importance the main components are sandy till, bog and fen peat, esker ridge and delta sands, raised beach ridges, bedrock outcrops, and shattered rock (Fig. 53.2).

The till is 1 to 5 m thick with the matrix typically consisting of 65% sand, 30% silt, and 5% clay. The till is composed mainly of quartz, feldspars, and lesser mafic minerals, being derived from a variety of Precambrian igneous and metasedimentary rock sources. The till was deposited by successive ice flows from the north-northeast.

A major esker system trends north-south across the study area. The main ridge is interrupted by nodes which are hillocks of sand spaced 3 to 6 km apart; the nodes represent seasonal stillstands and suggest that the last glacial ice melted back at a rate of 3 to 6 km per year in this area.

Much of northwestern Manitoba has been inundated by glacial lakes before and after the last glaciation. Deposits from these episodes are scarce in the study area, but lacustrine processes have washed the upper part of the till, contributed some fines, and in more exposed places, reworked the till into beaches.

Frost action is most evident in the formation of mudboils and solifluction lobes, in the distortion of primary sedimentary structures, and in the shattering of fissured rocks. Most of the area is underlain by permafrost. Active layer thicknesses are 60 to 80 cm in peat and clay and somewhat greater in coarse grained, better drained mineral soils.

Glacial Dispersal

Trace element contents of the tills can be related to their sources if the direction and distance of glacial transport are known. In order to assess the average distance of transport and extent of lateral mixing in till, the dispersion of red garnets from known source rocks (within pelitic biotite gneiss) was examined. Garnet contents of the fine sand fraction (0.125-0.250 mm) of each till sample were plotted and the values were then contoured (not shown).

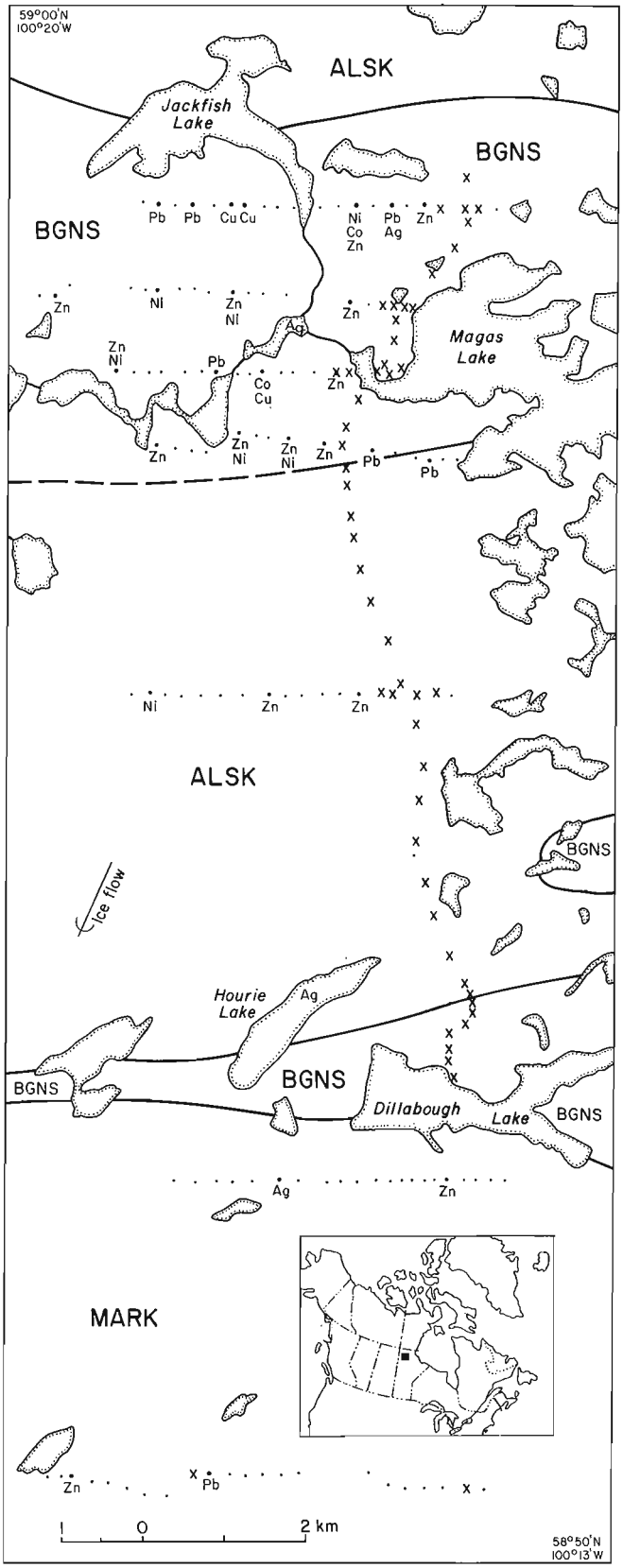

ALSK = foliated alaskite

BGNS = pelitic biotite gneiss, minor calc-silicate

MARK = meta-arkose

(.) samples in till

(x) samples in esker deposits

(•) highest base metal values

Figure 53.1. *Bedrock geology (after Weber et al., 1975) and location of elevated trace metal values (NTS 64 K/16).*

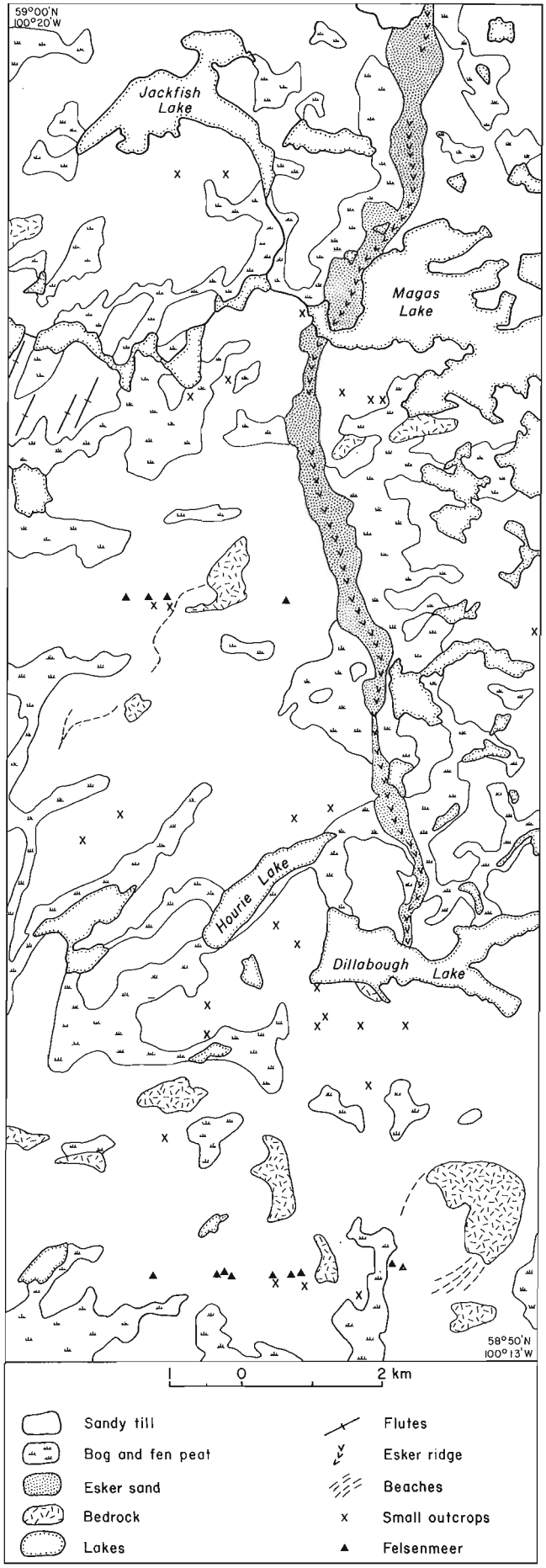

Figure 53.2. *Distribution of surficial materials in the study area.*

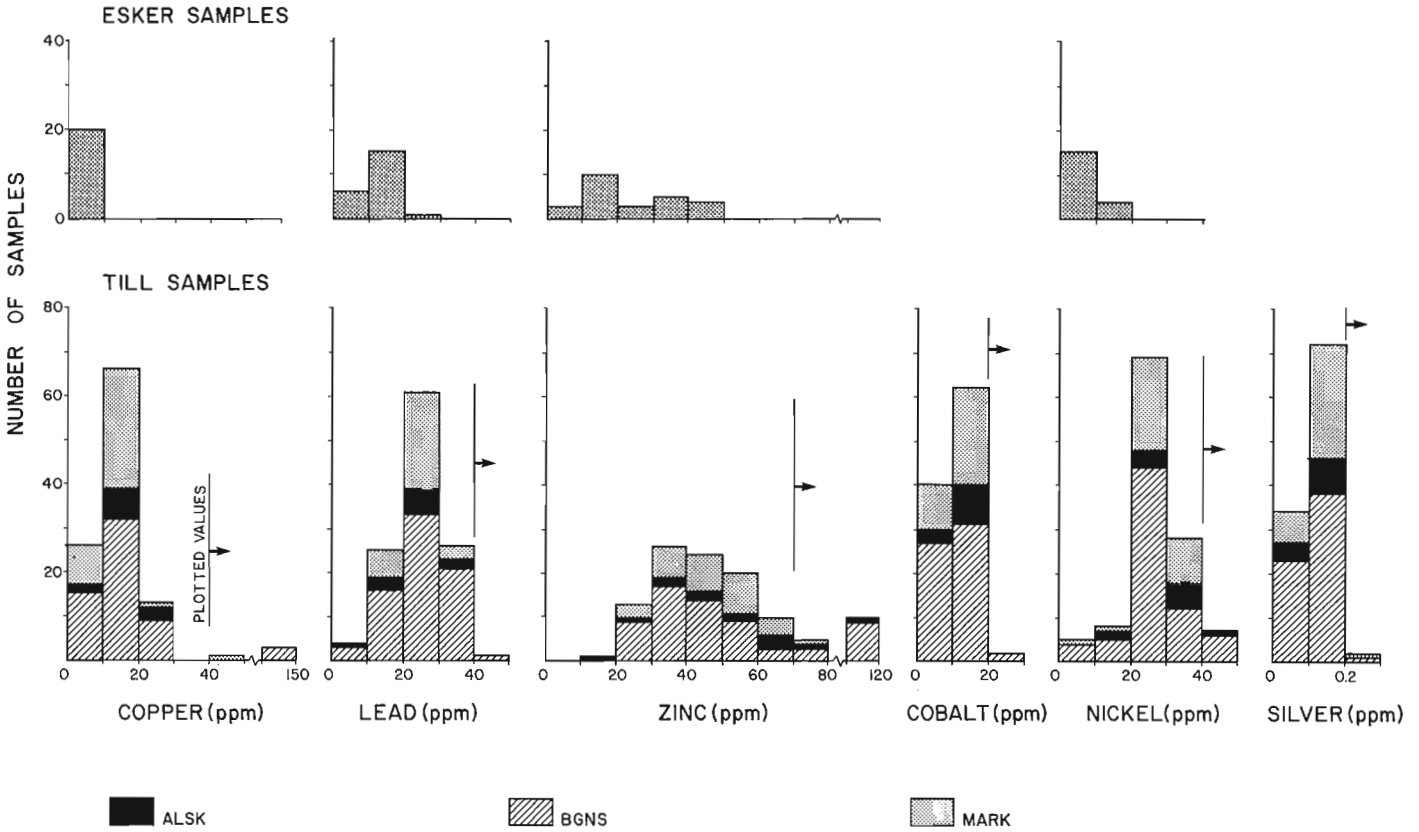

Figure 53.3. *Frequency histograms of selected trace element concentrations in the <2 µm fraction of esker sediments and till. Histograms of till samples represent till over the bedrock indicated. Sites with values exceeding the thresholds indicated are plotted in Figure 53.1.*

The average garnet content of tills in the study area is 20 to 30% of the heavy minerals. Outcrops of biotite gneiss near Jackfish Lake, however, contain up to 68% garnet. The effect of this source is apparent over several traverses, creating a tail of relative highs. The band of attenuation is fairly narrow, having a width of about 400 m (2 sample points) and trending south-southwest, parallel to the direction of glacial flow determined by flutings and regional striae. The concentration of garnet drops rapidly away from the source, with about half the garnets being deposited within 1 km (the nearest adjacent traverse).

Thus, glacial dispersal of sand-sized mineral grains in till within the study area is generally of the order of several hundred metres in the direction of glacial transport, although detection is still apparent up to 5 km from source. Grains are not dispersed laterally more than 0.5 km over this distance. By analogy, the trace element content of the tills would be expected to reflect bedrock sources lying within several kilometres to the north-northeast. Dispersal may be slightly greater than that for garnets because of the finer grain size used for the trace element analysis. Trace element levels in the esker materials represent an average value that is characteristic of multiple sources which may lie several tens of kilometres north.

Geochemistry

Frequency Analysis

Concentrations of copper, lead, zinc, cobalt, nickel, and silver were determined for clay-sized particles (<2 µm diameter) of 131 samples using atomic absorption spectrometry (analyses by Bondar-Clegg and Co. Ltd. Ottawa).

Histograms for each element are shown in Figure 53.3 for the till and esker sand samples. The values obtained are interpreted as background values, reflecting the regional character of the mixture of rocks in the area. Modal values for copper are 10-20 ppm; lead 20-30 ppm; zinc 30-50 ppm; cobalt 10-20 ppm; nickel 20-30 ppm; and silver 0.1-0.2 ppm. Except for silver, these background values are low relative to other areas examined within the Churchill Structural Province but generally are higher than values derived from peat sampling (Coker and DiLabio, 1979) and lake sediment sampling (Resource Geochemistry and Geophysics Division, 1976) in this general area (Table 53.1). Trace element concentrations are lower for the esker samples which represent mixed materials from multiple sources and variable transport distances. Till samples show a greater range of values and derive from local sources.

Areal Distributions

The distributions of elevated trace element values lying at the high end of the histograms have been plotted on Figure 53.1. Most high concentrations occur in the northern part of the study area in tills overlying biotite gneiss. The highest values are from thin tills near outcrops or felsenmeer. There is some consistent clustering of elevated metal levels, particularly the Ni-Zn combination in till associated with biotite gneiss, but scattered occurrences of elevated trace element levels are also found in till associated with this rock and other rock units.

Isopleth maps of element concentrations do not show any trains down-ice from elevated values; from this it is concluded that the transport distance of debris containing these elements is probably less than 1 km.

Table 53.1

Trace element concentrations (ppm) in selected surficial materials in northwestern Manitoba and southern District of Keewatin.

	Northwestern Manitoba (64 K/16)[1]		Northwestern Manitoba (64 K)[2]	Northwestern Manitoba (64 N)[3]	Rankin Inlet, NWT[4]		Baker Lake, NWT[5]
	Till		Lake sediment	Bog peat	Co-Ni-Cu-rich till		Till
	Modal Range	Maximum	Modal Range	Modal Range	Median	Range	Range
Copper	10-20	148	10-20	4-20	278	108-580	78-133
Lead	20-30	41	0-5	3	29	19-50	76-1870
Zinc	30-50	121	50-100	10-100	143	96-186	35-182
Cobalt	10-20	21	0-10	2-4	56	33-112	21-29
Nickel	20-30	48	0-20	1-10	203	94-1840	12-35
Silver	0.1-0.2	0.24	0.05-0.1	-	-	-	-

[1]This report
[2]Hornbrook et al., 1976
[3]Coker and DiLabio, 1979
[4]DiLabio and Shilts, 1977
[5]Shilts and Cunningham, 1977

The major silver anomaly of 17.8 ppm, obtained from a lake sediment sample south of Jackfish Lake, is not reflected in the till. As stated by Coker (W.B. Coker, personal communication, 1980), "This area was chosen for follow-up work because of the north-south string of lakes with elevated levels of Ag (17.8, 3.0, 0.8, and 0.6 ppm) and As in their sediments. Reanalysis of the original 1975 reconnaissance lake sediment samples confirmed these Ag and As values. However, the detailed lake sampling in 1976 produced only one lake sediment sample with a Ag content of 0.2 ppm. All the other samples had Ag contents less than the detection limit (i.e. <0.1 ppm). Therefore we could not confirm the original silver values (perhaps contamination?)." Most silver values in till and esker sediments in this area are 0.1 to 0.2 ppm, with the highest being 0.24 ppm several kilometres north of the lake sediment anomaly. It is unlikely that the till sample marks a significant occurrence of silver; furthermore, the till is probably not a source for the silver extracted from lake sediment.

Very low trace element values are associated with the esker; low values also occur in till but are not related to any one rock type.

Comparison of Till and Regional Lake Sediment Data

Results indicate that trace element values obtained from tills within the study area (NTS 64 K/16) are higher than those obtained from regional lake sediment sampling within NTS 64 K. A direct correspondence between these two data sets is not expected; the two populations reflect bedrock characteristics to different degrees, and analytical procedures differ. It is also possible, however, that the bedrock in the study area has slightly higher trace element levels of Pb, Co, Ni, and Ag than bedrock in the rest of the area.

There is little correspondence between the areal distribution of elevated trace element values determined by lake sediment sampling within the study area and elevated values in the till. Part of this discrepancy may be due to the fact that the till and lake sediment samples were not located close enough to allow comparison; few ground traverses were run across areas where lake samples were taken. In addition, lake sediment is derived from material eroded throughout a drainage basin, whereas most till samples characterize smaller and directionally oriented source areas. The provenance of material obtained by these two methods is therefore not the same.

Summary and Comments

Results

Trace element values are low in this part of northwestern Manitoba and likely represent regional background levels. No anomalies were detected, although some locally elevated values are present and appear to originate primarily in the biotite gneiss around Jackfish Lake.

Till samples show higher trace element values and indicate provenance areas more clearly than esker samples. Elevated trace element values in till samples probably reflect elevated values in bedrock lying several hundred metres to several kilometres north (i.e. up-ice) of the sampling sites. Most probably originate within calc-silicate layers in the pelitic gneiss sequence, because similar layers have been shown to contain anomalous amounts of Cu-Pb-Zn along the Wollaston belt in Saskatchewan (Coombe, 1979).

Sampling Procedures

Glacial dispersal of sand sized particles has been shown to be of the order of 0.5 to 5 km. For this study, east-west traverses were spaced 1 to 4 km apart; as a result, any dispersal trains were difficult to contour and to interpret clearly. A closer grid spacing (e.g. 500 m) in the direction parallel to glacial flow is recommended for a clearer dispersal pattern.

Till samples were taken from a depth of 60 to 80 cm, directly below the B horizon. To obtain regional trace element values, lake sampling or shallow till sampling (such as carried out here) is suitable; for closer inspection of local anomalies, however, deeper till samples are better. Samples taken lower in the soil profile generally have been less diluted and oxidized and are more likely to have been derived from local sources. In addition, much of northwestern Manitoba has been inundated to at least 400 m a.s.l.

by glacial lakes of considerable size. Fines in the upper 50 cm of till may have been introduced during the submergence period and may have a different geochemical nature than those in unmodified till farther down in the soil profile.

Tills in this area are very sandy and contain only small amounts of clay sized particles, most of which are rock flour rather than clay minerals. Labile base metals may not attach to these particles as well as to clay minerals; therefore results are not strictly comparable to those in other areas where the clay content consists of clay minerals. For this area, there may be a higher level of trace element concentrations in the substrate than is indicated by trace element analysis of the <2 μm fraction.

Acknowledgments

This report deals with a small part of a much larger overburden sampling program undertaken by W.B. Coker, Resource Geophysics and Geochemistry Division. All logistical and field support for detailed till sampling was provided by W.B. Coker. This paper was critically read by W.B. Coker and R.N.W. DiLabio.

References

Coker, W.B.
1976: Geochemical follow-up studies, northwestern Manitoba; in Report of Activities, Part C, Geological Survey of Canada, Paper 76-1C, p. 263-267.

Coker, W.B. and DiLabio, R.N.W.
1979: Initial geochemical results and exploration significance of two uraniferous bogs, Kasmere Lake, Manitoba; in Current Research, Part B, Geological Survey of Canada, Paper 79-1B, p. 199-206.

Coombe, W.
1979: Mineral deposits and regional metallogeny, southeastern Shield; in Summary of investigations 1979, Saskatchewan, Geological Survey, M.R. 79-10, p. 120-133.

Currie, K.L.
1961: Geology, Whiskey Jack Lake, Manitoba; Geological Survey of Canada, Map 52-1960, scale 1 inch to 4 miles.

Darnley, A.G., Williams, R.M., Ruzicka, V., Dyck, W., Cameron, E.M., and Richardson, K.A.
1975: The Federal-Provincial Uranium Reconnaissance Programs; in Uranium Exploration '75, p. 49-68; Geological Survey of Canada, Paper 75-26, 71 p.

DiLabio, R.N.W. and Shilts, W.W.
1977: Detailed drift prospecting in the southern district of Keewatin; in Report of Activities, Part A, Geological Survey of Canada, Paper 77-1A, p. 479-483.

Hornbrook, E.H.W., Garrett, R.G., and Lynch, J.J.
1976: Regional lake sediment geochemical reconnaissance data, northwestern Manitoba; NTS 64 K; Geological Survey of Canada, Open File 321.

Money, P.L.
1968: The Wollaston Lake Belt, Saskatchewan, Manitoba, Northwest Territories; in Symposium on basins and geosynclines of the Canadian Shield; Geological Survey of Canada, Paper 70-40, p. 170-197.

Resource Geophysics and Geochemistry Division
1976: Airborne gamma-ray spectrometry data, Whiskey Jack Lake, NTS 64 K; Geological Survey of Canada, Open File 317.

Shilts, W.W. and Cunningham, C.M.
1977: Anomalous uranium concentrations in till north of Baker Lake, District of Keewatin; in Report of Activities, Part B, Geological Survey of Canada, Paper 77-1B, p. 291-292.

Weber, W., Schledewitz, D., Lamb, C., and Thomas, K.
1975: Geology of the Kasmere Lake-Whiskey Jack Lake (north-half) area; Manitoba Mineral Resource Division, Publication 74-2, 163 p.

SCIENTIFIC AND TECHNICAL NOTES
NOTES SCIENTIQUES ET TECHNIQUES

DIRECTION OF MOVEMENT OF GLACIALLY TRANSPORTED BOULDERS NOT NECESSARILY SHOWN BY PRESERVED ICE-MOVEMENT DIRECTION INDICATORS, BAKER LAKE, DISTRICT OF KEEWATIN

Project 800008

Mikkel Schau
Precambrian Geology Division

During bedrock investigations in 56 D (Baker Lake sheet, see Heywood and Schau, this publication, report 36) it became apparent that the directions of dispersal of boulders from easily recognized marker horizons did not coincide with the directions indicated by glacial striae and roche moutonnée. On the sketch map (Fig. 1) positions of such rock units are indicated by letters and derived boulders by the corresponding numeral (Table 1). Also shown are ice-movement directions indicated by glacial striae and roches moutonnées (Wright, 1967; Cunningham and Shilts, 1977; Nadeau and Schau, 1979; Shilts, personal communication). The dispersal of the orthoquartzite is perhaps the most notable. House sized orthoquartzite boulders are found north of their outcrops in the Whitehills region, and southeast of Whitehills, quartzites form a large proportion of the erratics. At a site about 40 km southeast of the orthoquartzite outcrops and in an area underlain by augened granite bedrock, nearly all of the erratic boulders greater than 10 cm in diameter were orthoquartzite.

In the map sheet to the west (66 A), Cunningham and Shilts (1977) observed southward transport of erratics through a region where ice moulded features show a northward direction of ice-movement. The ice divide of the Keewatin ice sheet migrated from northwest to southeast to its final position. The relationship between the dispersal that occurred when the ice divide was at its more westerly positions and dispersal that occurred when it occupied its more easterly positions can readily explain both the dual directions of transport and the lack of correspondence of ice-inscribed features to the main direction(s) of erratic transport (Cunningham and Shilts, 1977, Shilts, personal communication). Whatever the cause, the observation that glacial dispersal is not necessarily indicated by glacial striae or roches moutonnées is of practical importance to people chasing boulder trains.

Table 1

Rock Description	Outcrop Locality	Boulder Locality
Finely layered calc-silicate and marble unit	A	1
Orthoquartzite with small flecks of chrome muscovite	B	2
Red weathering, well layered, carbonated, quartz magnetite iron formation	C	3
Pink arkose	D	4

From: Scientific and Technical Notes in Current Research, Part A; Geol. Surv. Can., Paper 81-1A.

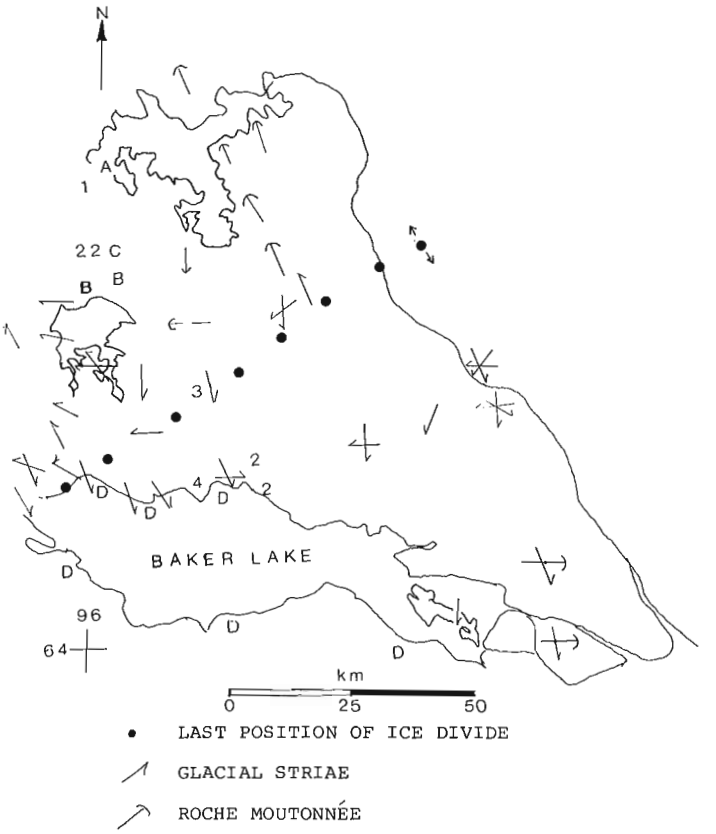

Figure 1. *Ice direction indicators near Baker Lake. Modified from Wright, 1967; Cunningham and Shilts, 1977; Nadeau and Schau, 1979, Shilts, personal communication, and field work.*

Acknowledgments

The author thanks J.G. Fyles and W.W. Shilts for discussing these observations.

References

Cunningham, C.M. and Shilts, W.W.
1977: Surficial Geology of the Baker Lake Area, District of Keewatin; in Report of Activities, Part B, Geological Survey of Canada, Paper 77-1B, p. 311-314.

Nadeau, L. and Schau, Mikkel
1979: Surficial Geology near the Mouth of the Quoich River, District of Keewatin; Scientific and Technical Notes in Current Research, Part A, Geological Survey of Canada, Paper 79-1A, p. 389-390.

Wright, G.M.
1967: Geology of the southeastern barren grounds; Parts of the Districts of Mackenzie and Keewatin; Geological Survey of Canada, Memoir 350.

STRAIN RATIOS MEASURED ACROSS A HUDSONIAN DEFORMATION FRONT AT KAMINAK LAKE, DISTRICT OF KEEWATIN

John Russell Henderson,
Precambrian Geology Division

The distribution, orientation and metamorphism of pre-Hurwitz diabase dykes at Kaminak Lake (Fig. 1) was described by Davidson (1970). Pre-Hurwitz dykes in the Archean craton south of Kaminak Lake strike 010 degrees; in reactivated Archean basement terrane north of Kaminak Lake they strike 030 degrees. Horizontal, upright folds occur in Aphebian Hurwitz Group strata preserved in a narrow synclinorium along the deformation front striking 063 degrees. Fold axes and axial surfaces parallel locally penetrative cataclastic foliation and lineation in underlying Archean basement rocks (Davidson, 1970).

A ratio of principal strains can be determined from the map pattern of the dykes and folds if one assumes that the fold belt parallels the major principal strain axis (λ_1) in the zone of progressive deformation (Fig. 1). For example, Ramsay (1967, p. 130) showed that $(\frac{\lambda_2}{\lambda_1})^{1/2} = \frac{\tan \Theta'}{\tan \Theta}$ where λ_1 and λ_2 are principal quadratic extensions, and, with reference to Figure 2, Θ is the angle between the strike of the Hurwitz fold belt and the undeformed dykes south of Kaminak Lake (53°), and Θ' is the angle between the fold belt and the deformed dykes north of Kaminak Lake (33°). The principal strain ratio thus determined is 0.5. In other words, an imaginary circle of unit radius south of the deformation front (Fig. 1, dash line boundary) would become an ellipse north of the front (Fig. 1, dot line boundary) with a major semi-axis two units along parallel to the Hurwitz fold belt, and a minor semi-axis one-half a unit long normal to the fold belt. This result assumes that horizontal rotation of the dykes is complete at the dot line boundary shown in Figure 1; larger values of $(\frac{\lambda_2}{\lambda_1})^{1/2}$ would be gotten if Θ continued to decrease northward.

If the fold belt parallels the intermediate principal strain axis of the Hudsonian finite strain ellipsoid, simultaneous rotation of the pre-Hurwitz dykes and folding of the Hurwitz beds may be attributed to horizontal shortening and vertical extension of the Archean basement in the more mobile Hudsonian orogen as it was compressed against more rigid Archean basement south of Kaminak Lake.

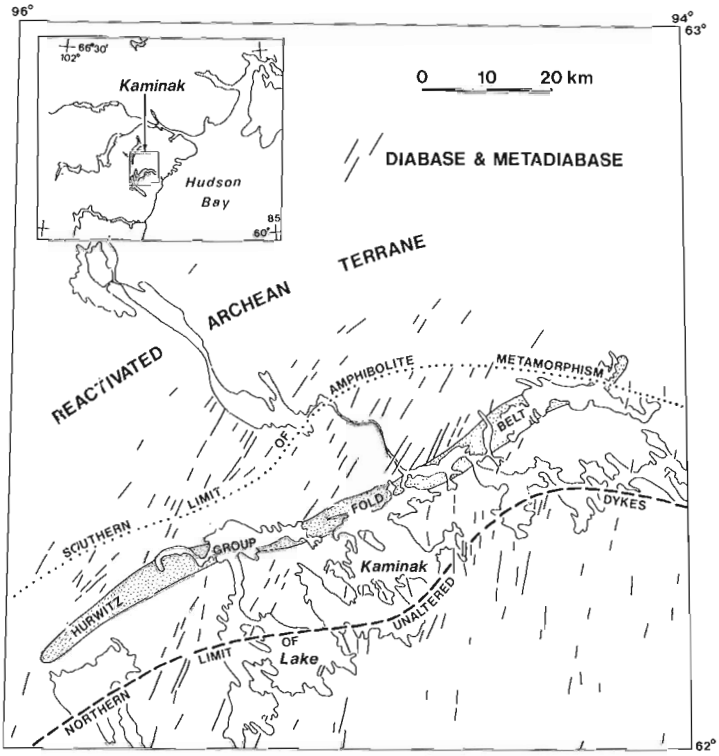

Figure 1. Effect of Hudsonian metamorphism on pre-Hurwitz diabase dykes (from Davidson, 1970).

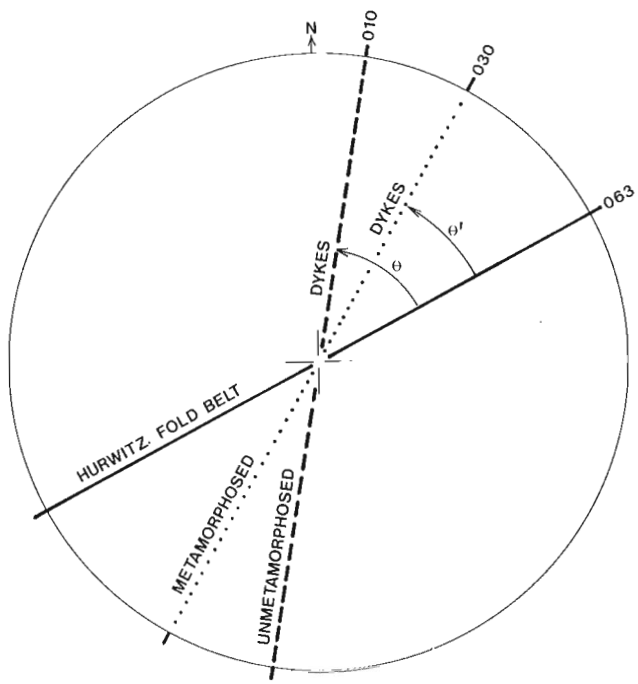

Figure 2. Relationship of diabase dykes and Hurwitz fold belt.

References

Davidson, A.
1970: Precambrian Geology, Kaminak Lake map area, District of Keewatin; Geological Survey of Canada, Paper 69-51 and Map 1285A, 27 p.

Ramsay, J.G.
1967: Folding and Fracturing of Rocks; McGraw-Hill, Inc., New York, 568 p.

From: Scientific and Technical Notes in Current Research, Part A; Geol. Surv. Can., Paper 81-1A.

STABILITY PROBLEMS ASSOCIATED WITH SAND AND GRAVEL PADS, CENTRAL DISTRICT OF KEEWATIN

Project 770035

P.A. Egginton
Terrain Sciences Division

Introduction

Sand and gravel generally are stable materials compared to fine grained sediments. In central District of Keewatin, however, Shilts (1978) identified several natural sand and gravel pads that on the basis of morphology appear to be rafting downslope as largely coherant masses. This note presents data on the displacements of materials associated with one such pad located on the shores of Kaminak Lake, District of Keewatin (Fig. 1).

Acknowledgments

I would like to thank W.W. Shilts for bringing this problem to my attention in 1977 and for suggesting this study.

Nature of Deposits

Sand and gravel have been deposited in central District of Keewatin under a variety of geological environments both during and after the last glaciation. Eskers and kames are common throughout the region but are generally of substantial thickness and pose limited stability problems. On the other hand, sand and gravel deposits resulting from the reworking of glacial deposits by waves during retreat of the postglacial Tyrrell Sea are thinner and vary from a few centimetres to several metres in thickness. They are found at elevations up to 170 m a.s.l. (Lee, 1959; Shilts, 1978).

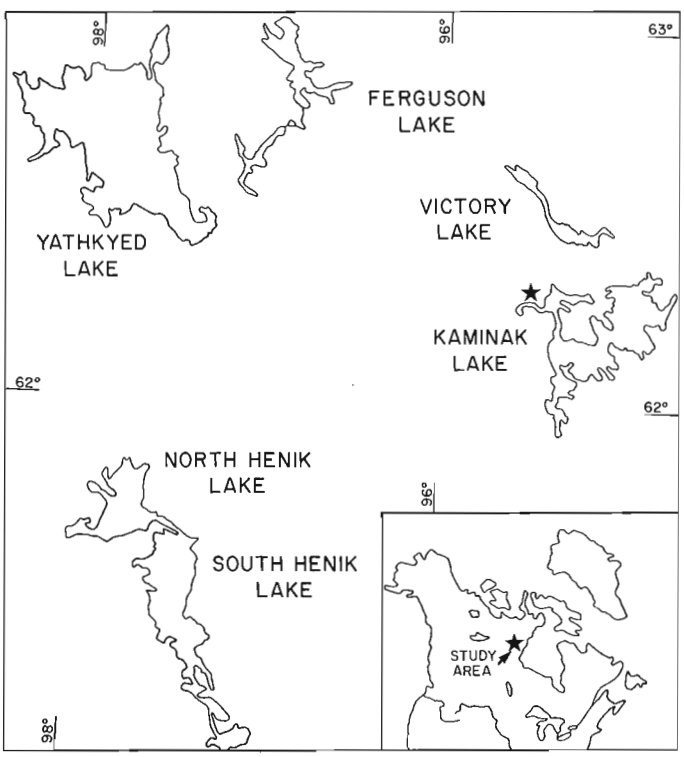

Figure 1. Location map of the study area, Kaminak Lake, District of Keewatin.

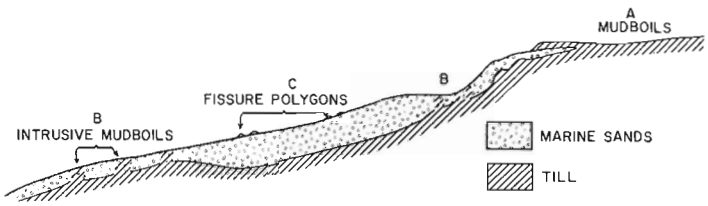

Figure 2. Schematic section through a slope near Kaminak Lake. The stratigraphy was determined from a series of pits dug along the slope. Where the sand deposit is thin and the till mobile, the sand has been incorporated into the till (A). Where the sand is thicker (30-50 cm), till has been intruded into it (B). Only where the deposits are more than 60 cm thick do they remain intact (C). Diagram is not to scale.

Today only parts of these formerly large expanses of sand and gravel remain intact as a continuous surficial deposit covering large areas. This is partly a result of the variability of the depositional environment, which affects both the location and the thickness of the deposit; however, present day periglacial processes are also responsible for the discontinuity of the deposits.

At Kaminak Lake thin (< 30 cm) nearshore deposits typically have been reworked into the underlying till by frost action and solifluction (A of Fig. 2). On some slopes the deposits are of sufficient thickness (30-50 cm) that the sand has not been totally incorporated into the till, rather the till intrudes through the sand producing one variation of the familiar mudboil pattern (B of Fig. 2; Egginton, 1979). Where sand and gravel deposits are more than 60 cm thick they generally persist as undeformed pads, lying on till or other glacial or marine sediments (C of Fig. 2). Thin pads are well vegetated whereas pads 2 m thick are not; the presence or absence of vegetation is controlled by moisture availability through capillarity.

The Kaminak Pad

A sand and gravel pad located on the west arm of Kaminak Lake was studied in some detail (Fig. 3). The pad is composed of coarse beach sand and fine gravel, is less than 2 m thick along its periphery, and overlies till (Shilts, 1978). Pits dug in the pad in late summer intersected free water at depths of 130 cm. On the basis of active layer thicknesses measured in marine deposits of similar texture within 1 km of the site, an active layer of at least 1.7 to 2 m can be expected. The sand is fairly permeable – snowmelt and precipitation percolate rapidly through with little direct runoff.

Over the 1977-1980 study period seepage was always observed downslope of this pad. In late summer 1980, daily seepage rates, from a nearby sand and gravel deposit, were measured at about 0.5 L/minute in spite of an absence of any significant precipitation for at least two weeks prior to the seepage measurements (Fig. 5). The seepage was measured where it collected in a small rill and therefore represents only a small proportion of the total slope seepage from the deposit.

A field-fabricated and uncalibrated lysimeter buried in nearby till gave typical evaporation rates of 3 mm/day. This value is only an estimate but it is likely of the right order of magnitude. On this basis substantial quantities of water can be evaporated from the surface of the till or sand if the water can be drawn to the surface. Given that the till contains a high proportion of silts, it can be expected to have a capillary rise in excess of 3 m; a value of 50 cm or less is probable for the pad (values estimated from tables in Lambe, 1969, p. 246). With rapid evaporation and a capillary

From: Scientific and Technical Notes in Current Research, Part A; Geol. Surv. Can., Paper 81-1A.

Figure 3.

The sand and gravel pad studied at Kaminak Lake. GSC 203502-T

Figure 4

Gravel beaches foundering into underlying and adjacent till near Kaminak Lake. The scar of an old flow phenomenon is visible to the left of centre and a more recent one in the centre of the photograph. (GSC 20445-S, courtesy W.W. Shilts)

rise substantially greater than the active layer thickness (1.5 m), the till dries rapidly throughout the summer. The pad, on the other hand, displays limited capillary rise – values are about 20 per cent of the active layer thickness; it loses little moisture to evaporation. Thus, the majority of water from either snowmelt or rain is available for seepage, and the base of the thaw zone in or under the pad is kept at or near saturation throughout the thaw season.

Mass Movement

Historically, on the basis of morphology, it is apparent that parts of the Kaminak pad along the margin have separated from the main deposit and have been displaced several metres downslope. Shilts (1978) has described a skin flowslide in nearby beach gravels overlying fine grained muds (Fig. 4). In both cases the historical movements appear to have been rapid.

In 1977, 1.5 m-long steel rods were driven into the Kaminak pad along its margin and were contained within the sand and gravel. The relative positions of the rods were determined by taping. Over distances of 30 m the measurements were taken with a precision of ± 3 mm; over shorter distances the precision was greater. Given the nature of material in the pad, it does not seem likely that the rods can move independently of the confining material.

The position of the posts and the relative ground movement, as reflected by the distance change between adjacent posts, is shown in schematic form for various time periods (Fig. 6). Over the study period only relatively minor displacements were recorded. Although there was no rapid displacement, there is some evidence to suggest that parts of the apparently detached segments along the margin of the pad are overriding one another while other parts appear to be experiencing a rotational displacement. For example, the distance between rods no. 3 and no. 4 decreased over the period of observation while the distance between rods no. 2 and no. 3 increased by the same amount; this suggests the movement of one detached part of the pad onto the other. Similarly, in 1980 the distances between rods no. 7 and no. 8 and between rods no. 8 and no. 9 decreased by 9 and 18 mm, respectively (Fig. 6). This latter displacement appears to be associated with a rotational slumping of the outer parts of the pad causing the rods to move closer together.

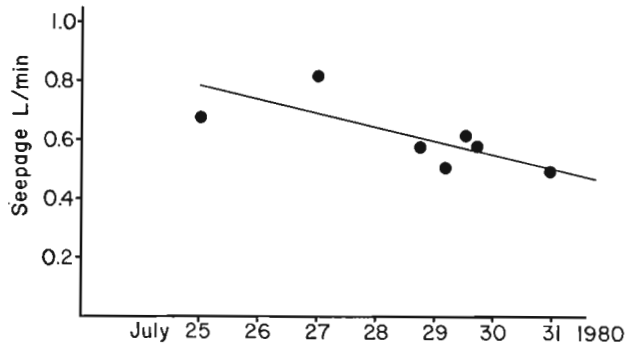

Figure 5. *Seepage from a sand and gravel deposit, Kaminak Lake.*

Discussion

Sands and gravels devoid of fines are inherently stable materials on low angle slopes. It is apparent that the displacements described above are associated with the thaw and subsequent movement of the underlying mud (fine grained marine sediments of till). Maximum annual thaw depths occur in late summer, at which time the thaw table, if the pad is thin enough, descends through the pad into the underlying mud. The presence of seepage indicates that the bottom of the pad typically is saturated throughout the thaw season; the moisture supply may be augmented by late summer rainfall. The ready supply of water and the melting ground ice may cause the muds to liquefy. It is at this time that parts of the relatively rigid pad may move downslope. Liquefaction in subsequent years may be enhanced by the formation of ice lenses in the saturated muds during freeze up.

Egginton (1979) reported typical annual downslope movements of 10 to 40 mm/a in mudboils in the Kaminak region. Thus portions of the Kaminak pad experienced rates of displacement that are similar to those recorded for a nearby till.

Monthly temperature summaries for Ennadai Lake (300 km southwest of the study site) and Baker Lake (200 km north of the study site), the two stations likely to be most representative of the study area, are presented in Figure 7. The historic monthly averages are shown along with the maximum recorded monthly mean. A comparison of these data with monthly averages for 1977, 1978, and 1979 indicate that temperatures in these years did not deviate markedly from the historic averages. Certainly they are substantially less than the recorded monthly maximums. The 1980 data are not available at the time of writing.

Since displacements of the sand and gravel depend upon the active layer penetrating into underlying less stable mud, it seems likely that the greatest and most widespread displacements will occur during unseasonably warm summers when thaw depths are greatest, moisture availability remaining constant. Such extreme conditions were not encountered over the duration of the monitoring period.

Summary

Thin (≤2 m) sand and gravel pads in central District of Keewatin may be displaced downslope by creep or mudflow associated with the liquefaction of the underlying mud. The critical factors are 1) that the underlying material has a high proportion of fines (i.e. is prone to movement), 2) that there is an adequate moisture supply, and 3) that the active layer extends through the pad into the underlying mud. If the pad is thick enough, the underlying mud will remain frozen and stable.

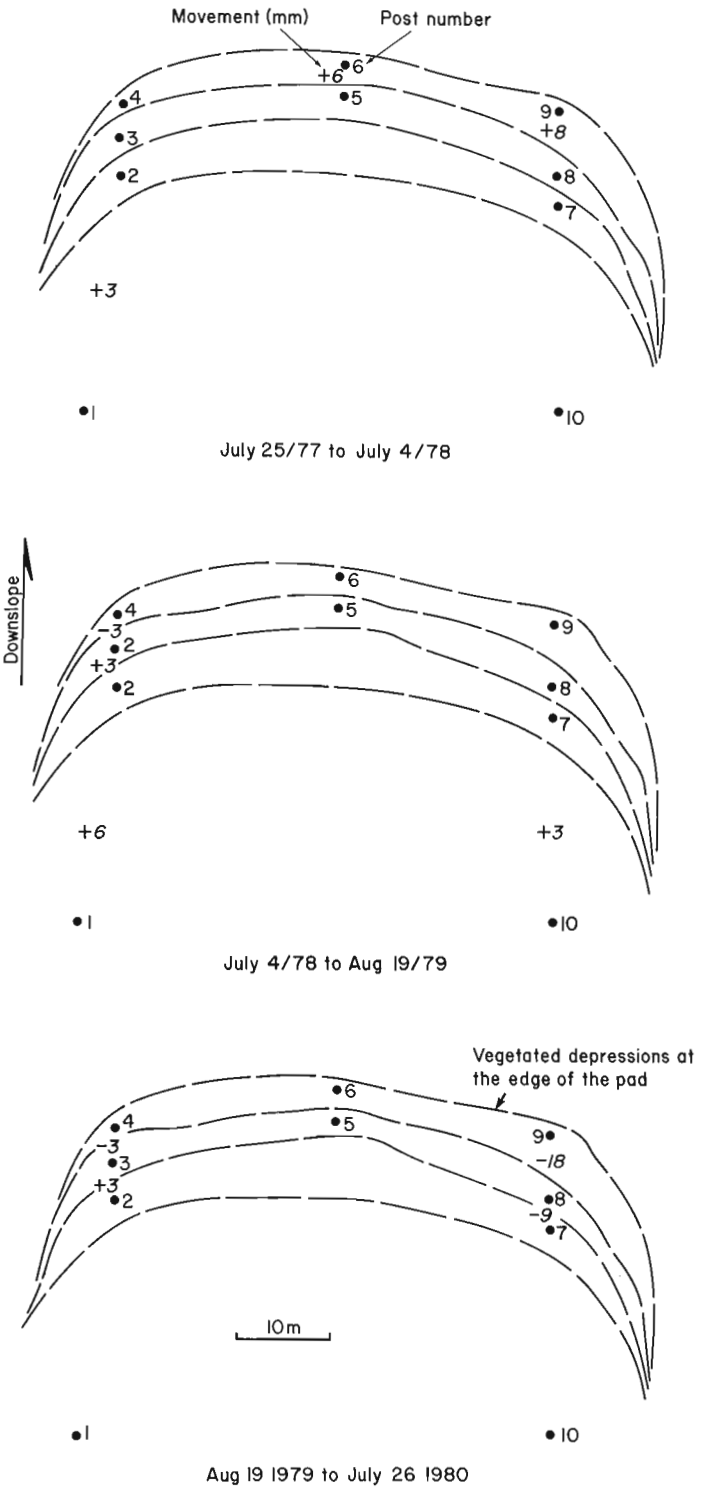

Figure 6. *Relative movements over various time periods of rods located within the margin of a sand and gravel pad at Kaminak Lake. Displacements are shown either as a positive value (indicating the rods moved farther apart) or a negative value (indicating the rods moved closer together).*

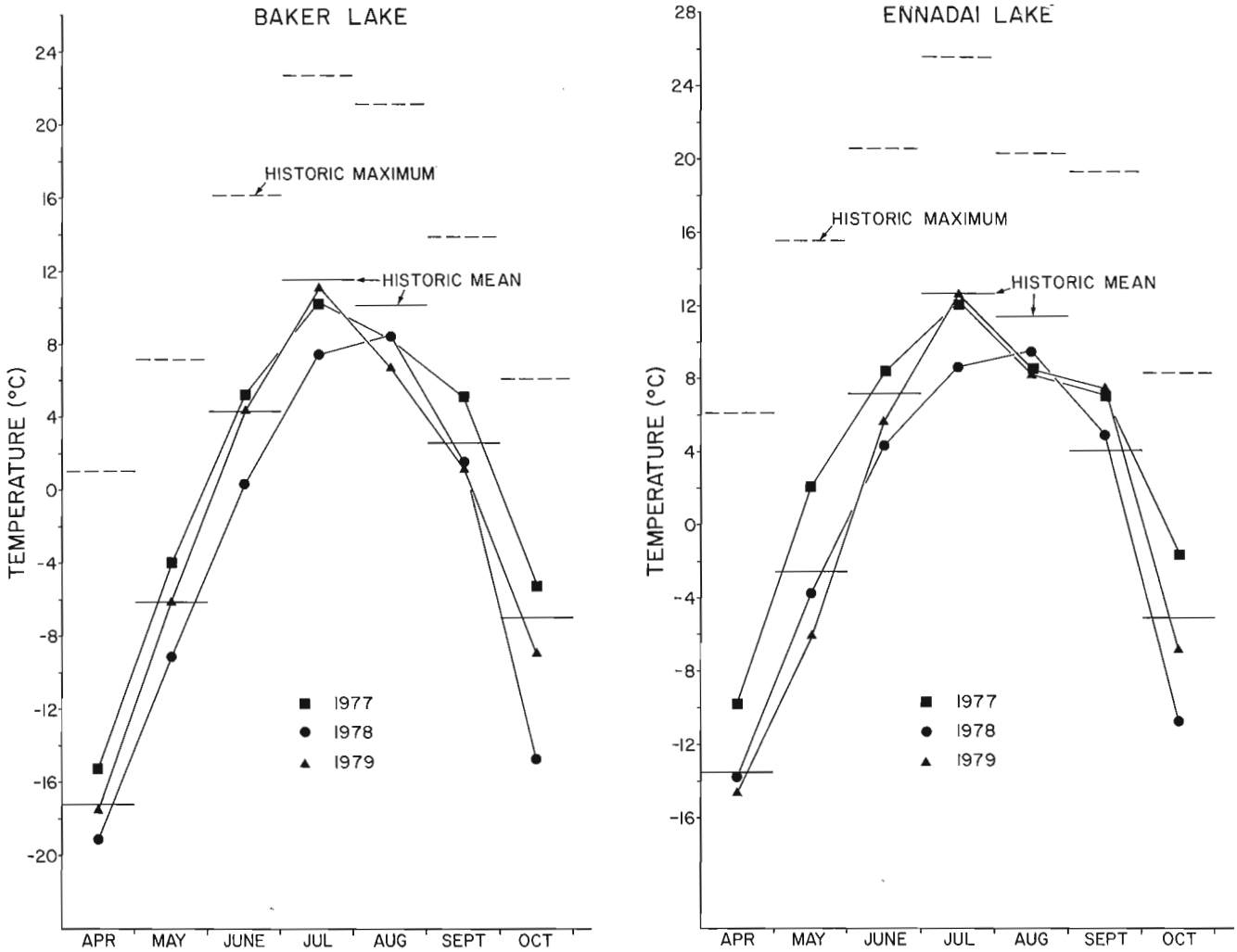

Figure 7. *Temperature summaries compiled for Ennadai Lake and Baker Lake, Northwest Territories. The historic mean monthly temperatures include all available data to 1979 inclusive. The historic maximum monthly mean temperature is also given. The data were compiled from summaries kindly provided by Polar Gas Ltd. and augmented by monthly data from Atmospheric, Environment Service (1975-1980).*

The pad monitored in this study experienced limited movement over the study period form 1977-1980 (maximum recorded value 18 mm/a). On the basis of morphology, however, it appears that this and other pads have been much more mobile in the recent past. It is speculated that yearly displacements greater than those recorded will occur in unseasonably warm years when the thaw depth is greater. Furthermore, in these summers, thicker and normally stable pads will become unstable. For engineering planning purposes in central District of Keewatin, only pads thicker than the maximum expected thaw penetration should be considered stable, if they overlie fine grained marine sediments or till.

References

Atmospheric Environment Service
1975-1980: Monthly record; Atmospheric Environment Service, Environment Canada.

Egginton, P.A.
1979: Mudboil activity, central District of Keewatin; in Current Research, Part B, Geological Survey of Canada, Part 79-1B, p. 349-356.

Lambe, T.W.
1969: Soil mechanics; John Wiley and Sons Inc., New York, p. 246.

Lee, H.A.
1959: Surficial geology of southern District of Keewatin and the Keewatin Ice Divide, Northwest Territories; Geological Survey of Canada, Bulletin 51, 42 p.

Shilts, W.W.
1978: Nature and genesis of mudboils, central Keewatin; Canadian Journal of Earth Sciences, v. 15, no. 7, p. 1053-1068.

NEAR-COASTAL AND INCIPIENT WEATHERING FEATURES IN THE CAPE HERSCHEL – ALEXANDRA FIORD AREA, ELLESMERE ISLAND, DISTRICT OF FRANKLIN

EMR Research Agreement 53-4-79

Stephen H. Watts[1]
Terrain Sciences Division

Introduction

On Ellesmere Island along the south coasts of Alexandra Fiord and Buchanan Bay east of the Royal Canadian Mounted Police (RCMP) post are a number of intensely weathered bedrock features (Fig. 1). Included are examples of grus accumulations, spalled crusts, exfoliated joint blocks, differentially eroded dykes, and minor incipient weathering pits. Field studies were carried out during July 1979 to document the nature and occurrence of these features as part of a regional assessment of the influence of lithology and topographic position on the processes and products of subaerial weathering under arid arctic conditions.

Previous studies in this region have included reconnaissance mapping of the Precambrian-Paleozoic bedrock geology by Christie (1962, 1967) and, more recently, by Frisch et al. (1977). Preliminary evaluation of the glacial history has been undertaken by Blake (1977, 1978).

Acknowledgments

The Polar Continental Shelf Project (G.D. Hobson, Director) generously supported this work by providing both access to the study area by Twin-Otter and to certain sampling localities by Jet-Ranger. Base camp facilities at Alexandra Fiord and at the Cape Herschel Station of the North Water Project were afforded by the Royal Canadian Mounted Police and by the late Dr. F. Müller, Eidgenössische Technische Hochschule, Switzerland, respectively. Generous hospitality and kind co-operation from Dr. W. Blake, Jr. was deeply appreciated in making my first field season in the high Arctic most pleasurable. Financial support in the form of an external research agreement made this study possible.

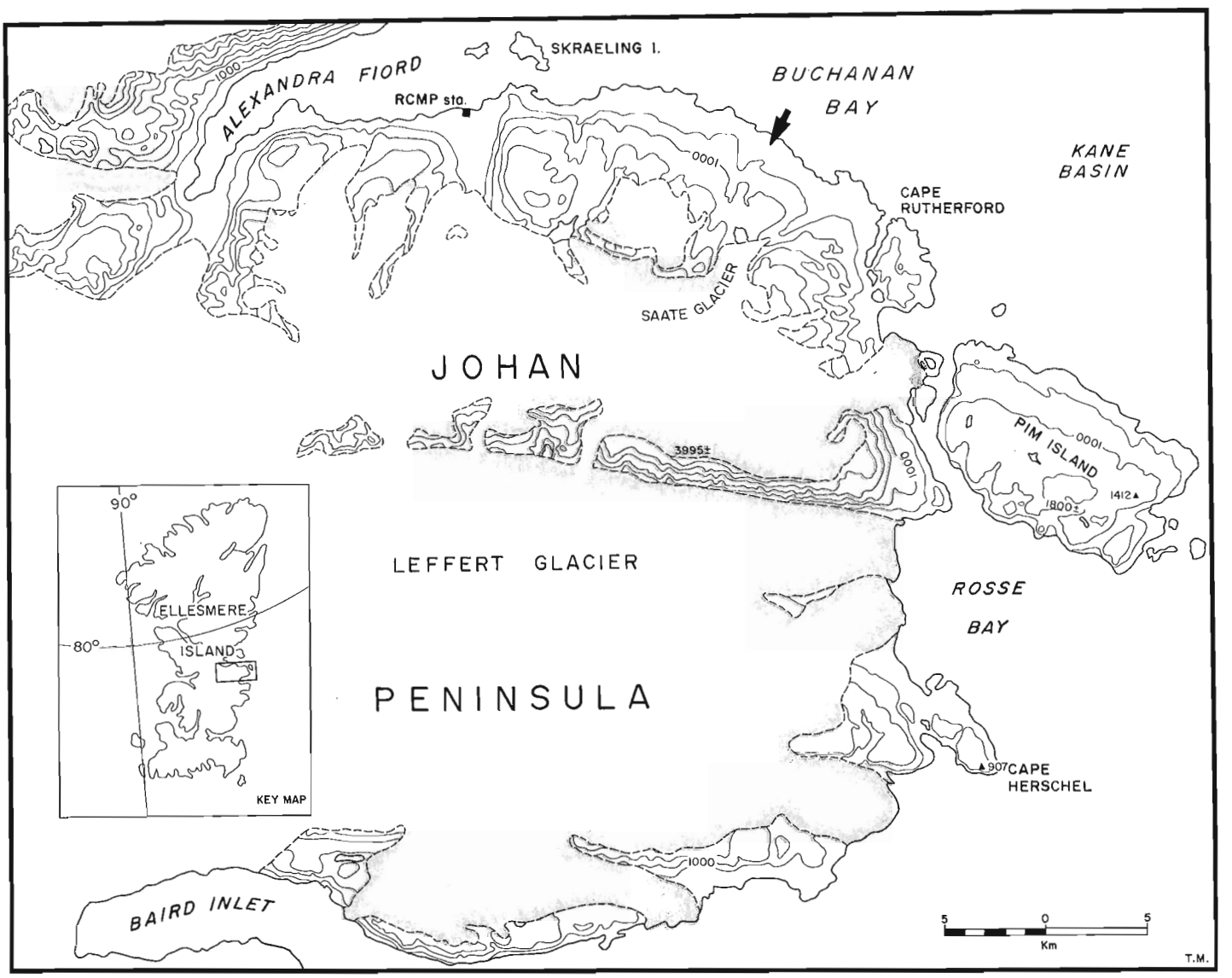

Figure 1. *Field study area. The arrow indicates the position of the ridge whose weathering is illustrated in Figures 2 and 3.*

[1] Geology Department
Sir Sandford Fleming College
P.O. Box 8000
Lindsay, Ontario K9V 5E6

From: Scientific and Technical Notes in Current Research, Part A; Geol. Surv. Can., Paper 81-1A.

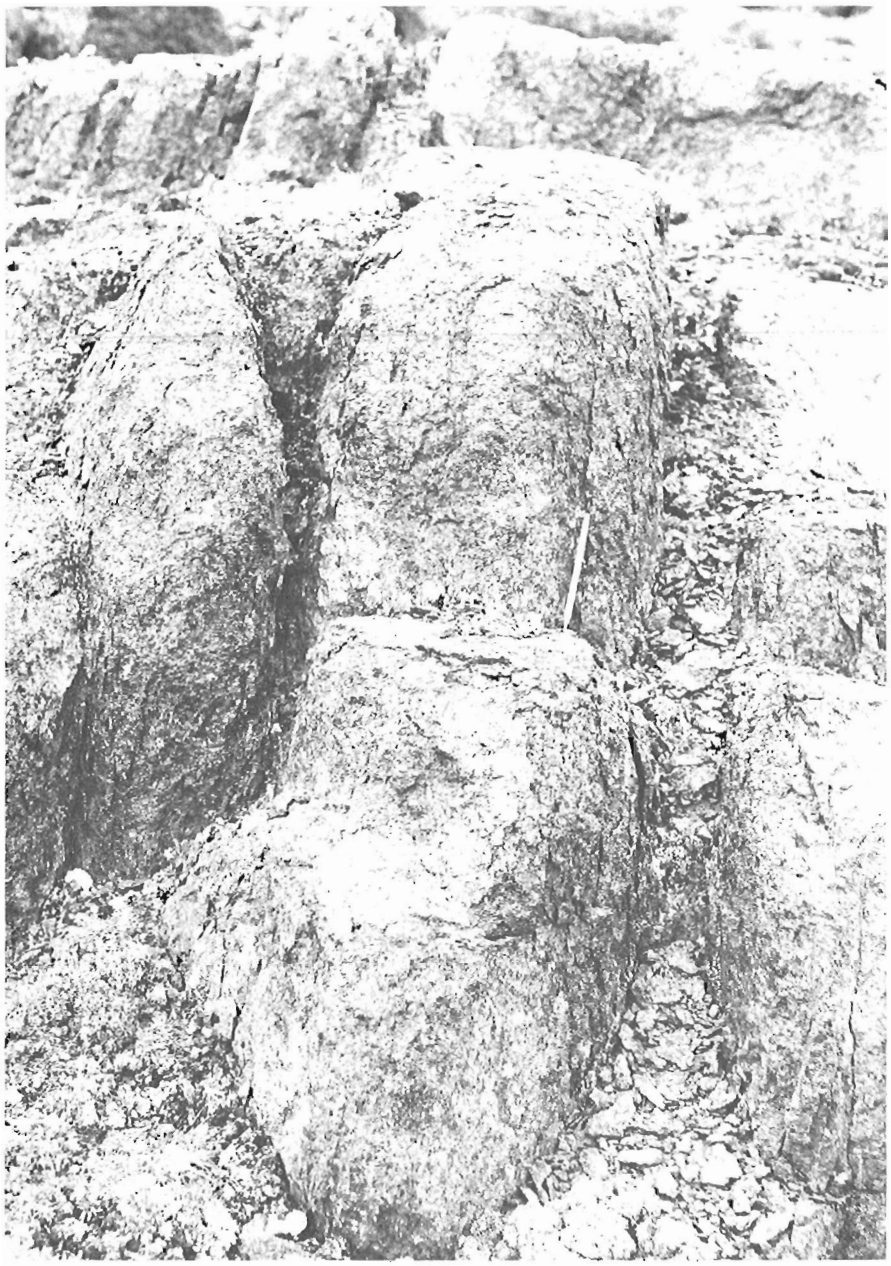

Figure 2

Joint block revealing evidence of disintegration by surface spalling. Although not readily seen in black and white photographs, encrustations of both calcium carbonate and sodium chloride were noted along this ridge (cf. Fig. 1) an on equally intensely weathered outcrops along the south-western coast of Skraeling Island within 20 m of sea level. Salt wedging along joints was also noted at the latter locality. July 17, 1979

Field Observations

The area affords good exposures of quartz feldspar biotite paragneiss merging eastward into more massive, locally gneissic, potassic granite which is particularly well exposed on the plateau on Pim Island and on Cape Herschel (Christie, 1962). Numerous quartz-rich pegmatites are present. More mafic intrusions including granodiorite, diabase, and a rock resembling gabbro in appearance (on Skraeling Island) were noted within the gneiss. Gossan zones containing pyrite, magnetite, and copper sulphides were observed from the air on Skraeling Island and along the north shore of Alexandra Fiord. The study area lies along the northern flank of the Precambrian Shield with lower Paleozoic dolomites, limestones, and sandstones outcropping in steep slopes and vertical cliff faces up to 600 m high across Buchanan Bay to the north. Scattered outliers of Paleozoic strata are preserved at widely varying elevations ranging from within 20 m of high tide level to above 400 m a.s.l. southwest of the RCMP post. An ice cap extends over most of Johan Peninsula to within 2 km of the coast with permanent ice extending to below 750 m a.s.l. Valley glaciers reach to sea level. The broad nature of the valleys suggests that extensive glaciers flowed into Kane Basin via Buchanan Bay.

An interesting example of highly weathered coastal features is an outcrop ridge (Fig. 1-3) approximately 300 m long by 120 m wide by up to 45 m high situated east of a small stream delta draining an ice-dammed lake and part of Saate Glacier (78°52'N, 75°05'W).

During field studies observations also were compiled on the nature of granite exposures on Pim Island and particularly Cape Herschel (Fig. 1). The overridden and deeply sculptured upland surfaces typifying this area have been noted by Blake (1977). Textbook examples of glacial polish, striae, grooves, perched erratics, and roches moutonnées mark the exposures and provide evidence of glacial overriding by southward-flowing late Wisconsin ice (Blake, 1977).

Figure 3. *An exposure about half way up the same outcrop ridge as in Figure 2 (elevation approximately 28 m a.s.l.). Note the difference in degree of physical weathering of adjacent joint blocks. Laboratory data confirm that the unaltered block in the centre of the photograph is a granitic intrusion lacking hornblende but otherwise identical in both composition and texture to the host gneiss. July 17, 1979.*

The condition of the outcrop surfaces in this area immediately following glaciation to a large extent has determined the type of incipient weathering observed in the granite. Many features of glacial erosion on exposures remain intact with virtually no breakdown whatsoever. Preliminary breakdown of the outcrop surface has taken place primarily along joint systems (Fig. 4) and around original breaks in the glacially smoothed surface as, for example, around chattermarks. Localized grus development has resulted from continued flaking on outcrop surfaces. Although glacial polishing appears to hinder direct surface disintegration, flaking has resulted from rock breakdown undercutting surface areas.

That bedrock surface weathering has been limited is attested to by the presence of carbonate crusts up to 0.3 cm thick on both sheltered joint blocks and on exposed faces (Fig. 5; cf. Ford, 1970; Hallet, 1976). These crusts could not have survived intense glacial abrasion and would not likely form on such open, well drained – in places vertical – slopes by evaporation in postglacial time. They are thus believed to be late glacial in origin, formed perhaps during ice stagnation.

Sheeting and exfoliation of bedrock, which would favour further surface weathering, were not widely encountered on the granite outcrop. Plucking has occurred along the distal side of individual outcrop ridges and limited block displacement has resulted. Where standing water occurs, as in upland basins excavated in bedrock or where snowbanks inhibit runoff, in situ frost heaved blocks are evident (cf. Potts, 1970).

Perhaps the most intensely weathered bedrock features in the Cape Herschel – Pim Island area are examples of micropitting covering outcrops in patches up to 10 m across (Fig. 6). A number were noted in the vicinity of Cape Herschel, where they are developed on the up-ice faces of glacially streamlined rock ridges of northerly aspect at various elevations up to 400 m a.s.l. Individual micropits are up to 5 cm across by 2 cm deep but average 2 cm wide by 1.2 cm deep on the basis of 62 examples. Lichens were noted in some micropits. The pits have enlarged through solution and adjacent examples have been joined by continued weathering. Evidence of surface flaking in areas adjacent to the pits was noted. The surfaces on which the pits developed typically slope at 15 to 30 degrees even though the pits commonly have a vertical orientation. Evaluation of aspect, slope, and other environmental conditions suggests that the micropitting has resulted from solution related to snowbank melting in the summer.

Discussion

An initial reaction to the occurrence of the coastal weathering features developed in paragneiss, not only at the site described but also on Skraeling Island and along the north coast of Alexandra Fiord, was that such features were produced over a long period of time and could even be pre-Wisconsin in age, having survived glaciation intact. Their position, however, would apparently preclude this. Any flowage of ice out of the Buchanan Bay area by valley glaciers merging with the main ice mass flowing south out of Kane Basin would have scoured the coastal lowlands along Alexandra Fiord, and particularly Skraeling Island, destroying these features had they predated the last ice advance of the Wisconsin.

Figure 4. *Typical outcrop surface in massive, medium grained granite on the Cape Herschel plateau. Note the smooth unaltered nature of the bedrock with incipient disintegration along joints due to gelifraction. Although not evident in this photograph, minor iron oxides have concentrated as stains along the joints. July 10, 1979. Pen (15 cm) provides scale.*

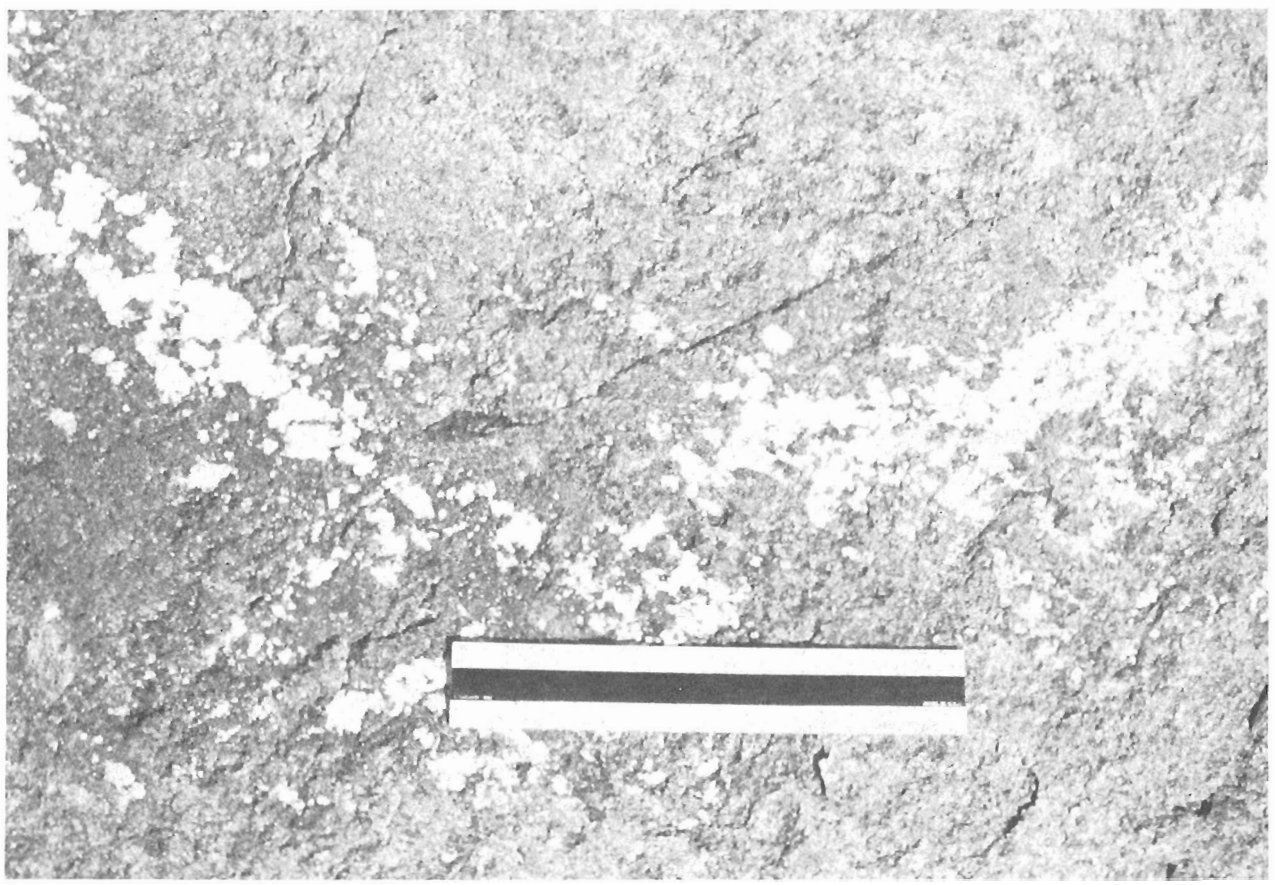

Figure 5. *Carbonate coating on exposed unweathered granite outcrop on west side of upland at 250 m a.s.l. near Cape Herschel station. Photograph was taken on July 10, 1979. Ruler is 15 cm long.*

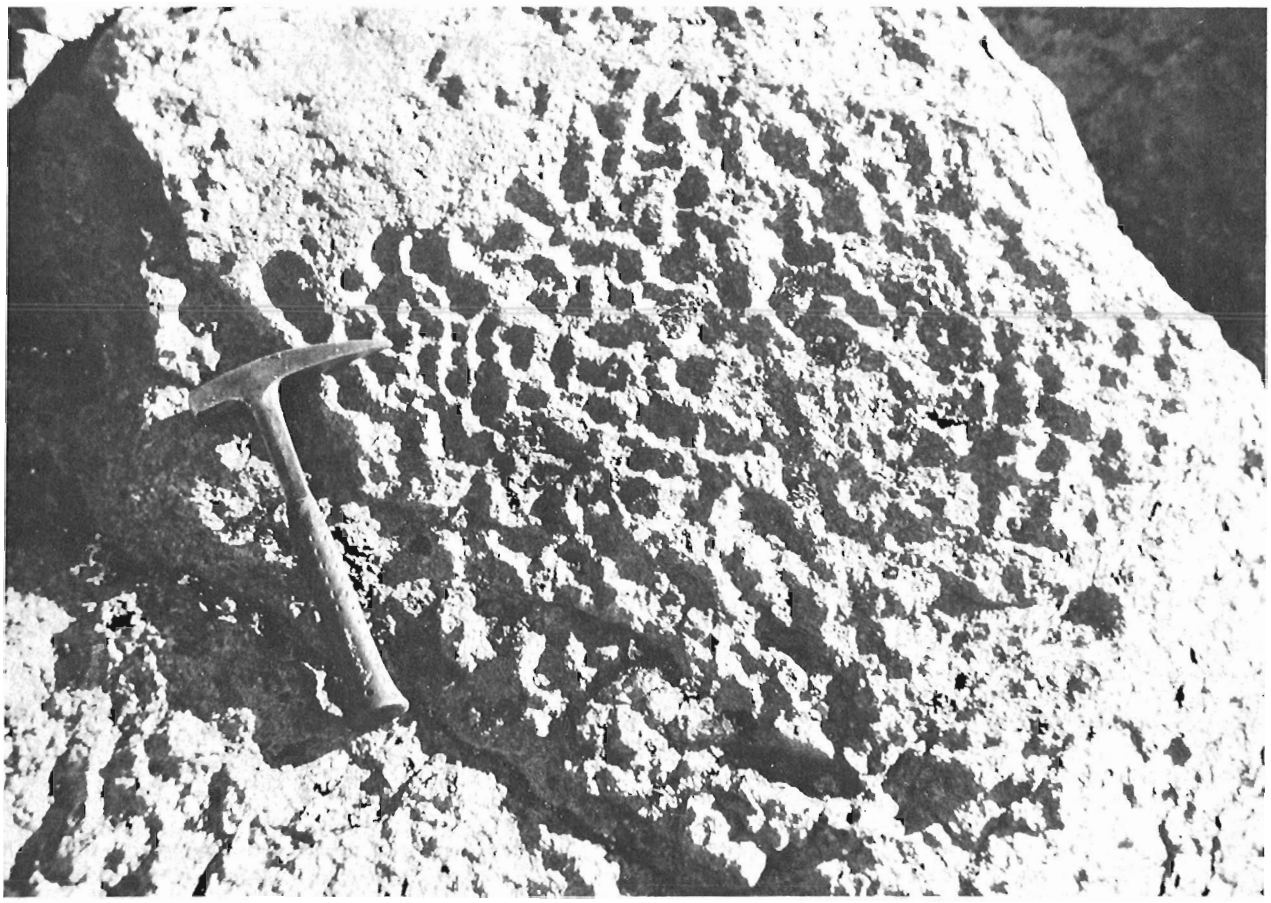

Figure 6. *Close-up view of micropitting developed in a north-facing exposure of granite near the north shore of Cape Herschel peninsula at 55 m a.s.l. This site was beneath the sea 7500 years ago. July 15, 1979.*

Figure 7. *Crusts of sodium sulphate coating till and clay at the edge of a small evaporitic pond located about 10 m a.s.l. on the north shore of Knud Peninsula about 30 km north of the study area. July 26, 1979.*

Marine shells, including single valves and intact pairs of **Mya truncata** (6260 ± 140 years old, GSC-1348), have been collected from sands along a stream immediately east of the RCMP post at about 30 m a.s.l. (Lowdon and Blake, 1973). Shells of the same species collected at 52 m a.s.l. on the north side of Cape Herschel Peninsula are 7210 ± 90 years old (GSC-2525; Blake, 1978). These dates indicate that the bedrock ridge along the coast north of Saate Glacier was beneath the sea in Holocene time (Fig. 1).

In a similar near-coastal position at 10 m a.s.l. efflorescences of sodium salts, including thenardite, were noted in a salt pond several metres across on the north side of the Knud Peninsula 30 km north of the study area (Fig. 7 cf. Nichols, 1969; Tedrow, 1969). It has not been established whether the salts originated from sea spray, from earlier marine incursion, or from Paleozoic evaporite sequences exposed upslope to the south of the site. Davies (1974) has reported similar highly saline lakes in marine silt terraces near sea level in northern Greenland. The mineral mirabilite ($Na_2SO_4.10H_2O$) is the low temperature stable form of sodium sulphate but under drying conditions, as in an arid basin, or in the lab, the mineral readily yields its water, reverting to thenardite (Reeves, 1968). Thenardite also has been identified by X-ray diffraction analysis from material collected in the Lake Hazen area of northern Ellesmere Island (Traill, 1969, p. 560). Elsewhere, in upland areas above both Alexandra Fiord and Cape Herschel, salt encrustations, primarily calcium carbonate and sodium chloride, appear to be mainly concentrated on mafic erratics and may indeed have been derived from leaching of hornblende within the rocks (Bradley et al., 1978). It is thought that intense weathering by salt crystallization at or near – and in some cases initially below – sea level has been largely responsible for the intense weathering of certain lithologies here and elsewhere in postglacial time (cf. Evans, 1970; Goudie, 1974; Birkeland, 1978; Watts, 1979).

Laboratory analyses on water chemistry, bedrock composition, and textural and physical changes accompanying bedrock weathering in the Alexandra Fiord area are currently being completed. An examination of the influence of bedrock lithology and outcrop position, with respect to sea level and to glacial ice, on rates of outcrop weathering under arctic conditions is found in Watts (in press). Incipient weathering features common to coastal granites as reported in this paper no doubt typify exposures of large areas of the Precambrian Shield in Holocene time.

References

Birkeland, P.W.
1978: Soil development as an indication of relative age of Quaternary deposits, Baffin Island, N.W.T., Canada; Arctic and Alpine Research, v. 10, p. 733-747.

Blake, W., Jr.
1977: Glacial sculpture along the east coast of Ellesmere Island, Arctic Archipelago; in Report of Activities, Part C; Geological Survey of Canada, Paper 77-1C, p. 107-115.

1978: Coring of Holocene pond sediments at Cape Herschel, Ellesmere Island, Arctic Archipelago; in Current Research, Part C; Geological Survey of Canada, Paper 78-1C, p. 119-122.

Bradley, W.C., Hutton, J.T., and Twidale, C.R.
1978: Role of salts in development of granitic tafoni, South Australia; Journal of Geology, v. 86, p. 647-654.

Christie, R.L.
1962: Geology, Alexandra Fiord; Geological Survey of Canada, Map 9-1962, scale 1 inch to 4 miles.

1967: Bache Peninsula, Ellesmere Island, Arctic Archipelago; Geological Survey of Canada, Memoir 347, 63 p.

Davies, W.E.
1974: Geological and limnological factors of cold deserts; in Polar Deserts and Modern Man, ed. T.L. Smiley and J.H. Zumberge; University of Arizona Press, Tucson, 173 p.

Evans, I.
1970: Salt crystallization and rock weathering: A review; Revue de geomorphologie dynamique, v. 9, p. 153-177.

Ford, D.C.
1970: Calcite precipitates at the soles of temperate glaciers; Nature, v. 226, no. 5244, p. 441-442.

Frisch, T., Morgan, W.C. and Dunning, G.R.
1977: Reconnaissance geology of the Precambrian Shield on Ellesmere and Coburg islands, Canadian Arctic Archipelago; in Current Research, Part A; Geological Survey of Canada, Paper 77-1A, p. 135-138.

Goudie, A.
1974: Further experimental investigation of rock weathering by crystallization and other mechanical processes; Zeitschrift fur Geomorphologie, Supplementband 21, p. 1-12.

Hallet, B.
1976: Deposits formed by subglacial precipitation of $CaCO_3$; Geological Society of America, Bulletin v. 87, p. 1003-1015.

Lowdon, J.A. and Blake, W., Jr.
1973: Geological Survey of Canada radiocarbon dates XIII; Geological Survey of Canada, Paper 73-7, 61 p.

Nichols, R.F.
1969: Geomorphology of Inglefield Land, North Greenland; Meddelelser om Grønland, v. 188, no. 1, 109 p.

Potts, A.S.
1970: Frost action in rocks: Some experimental data; Transactions of the Institute of British Geographers, Publication 49, p. 109-124.

Reeves, C.C., Jr.
1968: Introduction to Paleolimnology; Elsevier Publishing Company, Amsterdam, 228 p.

Tedrow, J.C.F.
1969: Soil investigations in Inglefield Land, Greenland; Meddelelser om Grønland, v. 188, no. 3, 93 p.

Traill, R.J.
1969: A catalogue of Canadian minerals; Geological Survey of Canada, Paper 69-45, 649 p.

Watts, S.H.
1979: Some observations on rock weathering, Cumberland Peninsula, Baffin Island; Canadian Journal of Earth Sciences, v. 16, p. 977-983.

Bedrock weathering features in a part of eastern High Arctic Canada: Their nature and significance; Annals of Glaciology; Symposium on Processes of Glacial Erosion and Sedimentation (Geilo, Norway), August 1980. (in press)

STRATIGRAPHIC FRAMEWORK OF SOUTHEASTERN SELWYN BASIN, NAHANNI MAP AREA, YUKON TERRITORY AND DISTRICT OF MACKENZIE

Project 790007

S.P. Gordey, D. Wood[1], and R.G. Anderson[2]
Cordilleran Geology Division, Vancouver

Introduction

During the summer of 1980, geologic mapping of Nahanni map area (105 I) at 1:250 000 scale was completed, and limited field work in Sheldon Lake map area (105 J) undertaken in anticipation of future work there. Field work was co-ordinated with other studies by several individuals under a program known as the Nahanni Integrated Multidisciplinary Pilot Project (IMPP). B.S. Norford measured lower Paleozoic and Devonian sections, to provide paleontologic control on certain formations. M.J. Orchard sampled in detail the Devonian Grizzly Bear Formation and its correlatives for conodont study. L. Jackson studied the surficial deposits, their geomorphology and Pleistocene history. W.H. Fritz briefly examined correlatives of the Lower Cambrian Backbone Ranges Formation in Glacier Lake map area. D.H. Wood spent two weeks for a B.Sc. thesis (University of British Columbia) mapping, sampling for K-Ar dating, and examining stratigraphic relations of the South Fork Volcanics, an acid to intermediate volcanic suite in southwestern Sheldon Lake map area. W.D. Goodfellow, I. Jonasson and D. Sangster continued their study of the mineralogy and geochemistry of the Howard's Pass lead-zinc deposit. K.M. Dawson examined several mineral occurrences in Nahanni map area and in conjunction with W.H. Fritz, I. Jonasson and D. Sangster also undertook a study of the types and stratigraphic relations of mineral occurrences in the Sekwi Formation (Lower Cambrian) in Bonnet Plume (106 B), Nadaleen River (106 C), Mount Eduni (106 A) and Sekwi Mountain (105 P) map areas. M.P. Cecile continued his study of the lower Paleozoic platform to basin transition in northeast Niddery Lake map area (105 O).

This report summarizes highlights of the bedrock geology studied during the 1980 field season, and supplements earlier and more complete descriptions of stratigraphy and structure of the Nahanni area by Gordey (1978, 1979, 1980a, b).

Regional Setting

From Early Cambrian through Middle Devonian time in the Nahanni area a shallow water carbonate platform (Mackenzie Platform, Fig. 1) was flanked to the southwest by a deep or restricted basin in which shale, chert, and limestone (Selwyn Basin) were deposited. Another platform to the southwest (Cassiar Platform) accumulated shallow water dolostone and quartz arenite in Siluro-Devonian time, but its earlier history is not well understood. This paleogeographic regime changed dramatically in Late Devonian time with the influx of clastics characterized by shale, quartz-chert sandstone, and chert pebble conglomerate possibly derived from Proterozoic and lower Paleozoic lithologies from within Selwyn Basin. Early Cretaceous deformation produced northwest trending open folds in competent carbonate strata and folds of similar amplitude and wavelength in incompetent basin facies rocks, although the latter are complicated by tight second-order folds and axial-plane slaty cleavage. In mid-Cretaceous time post-tectonic biotite- and biotite-hornblende quartz monzonite plutons intruded to high levels, locally reaching the surface to form the presumably related acid to intermediate South Fork Volcanics.

Selwyn Basin – Cassiar Platform Relations

Figure 2 shows proposed stratigraphic correlations from Cassiar Platform to Selwyn Basin. Cassiar Platform strata comprise tan weathering platy dolomitic siltstone and fine grained sandstone of probable mid- to Late Silurian age overlain by Lower Devonian massive dolostone locally containing two-holed crinoid columnals and corals, in turn overlain by thick massive very clean medium- to coarse-grained quartz arenite (see also Tempelman-Kluit, 1977). The platy siltstone where bioturbated and dolomitic resembles the wispy laminated orange mudstone of the basin facies to which it is partly or wholly equivalent. At section B platy siltstone lithologies are present, although the unit is shalier than typical and locally calcareous. There the base of the platy siltstone is taken as the contact with gun-blue weathering siliceous graptolitic shales of Ordovician and ? Silurian age. The thick Lower Devonian quartzite and dolostone have no known equivalents in the basin presumably reflecting pre-Late Devonian erosion.

Although the early history of Cassiar platform is not revealed in these sections its influence is indicated by control of facies on the southwest side of Selwyn Basin. The proportion of chert in Ordovician – Silurian strata decreases dramatically towards the southwest, indicating if not a shallow water platform, possibly a submarine ridge in this direction. In Early Cambrian time limestone conglomerate, and mature clean massive quartz arenite up to 30 m thick, appear towards the southwest side of the basin. The conglomerate contains a small proportion of oncolitic and/or oolitic limestone clasts. These, as well as finely crystalline grey-limestone clasts of various shapes up to 0.4 m long are

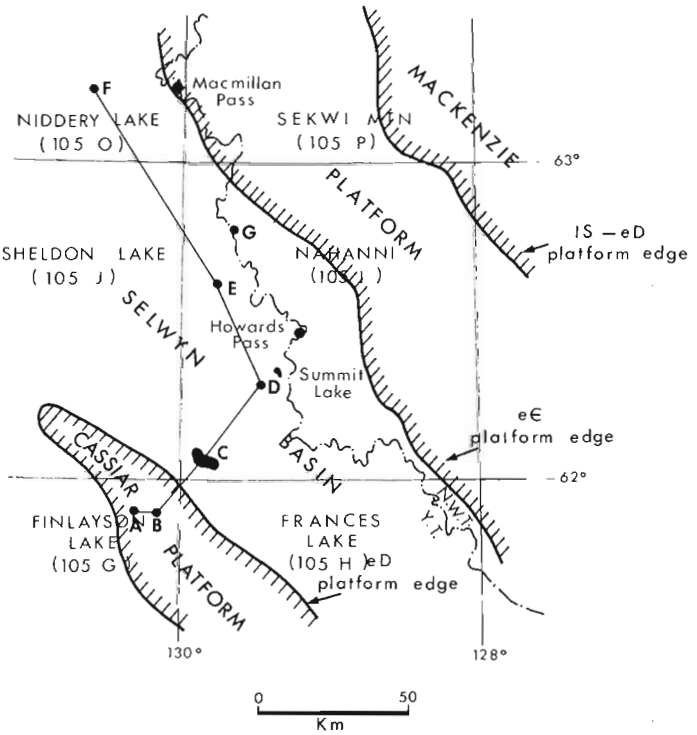

Figure 1. *Location of sections shown in Figure 2. The edge of Cassiar Platform may be in part erosional. The Lower Cambrian platform boundary is taken as the western limit of shallow water facies of the Sekwi Formation. The western limit of shallow water carbonates of the Delorme, Camsel, and Sombre formations here defines the Upper Silurian to Lower Devonian edge of Mackenzie Platform.*

[1]Department of Geology, University of British Columbia, Vancouver, B.C.
[2]Department of Geology, Carleton University, Ottawa, Ontario.

From: Scientific and Technical Notes in Current Research, Part A; Geol. Surv. Can., Paper 81-1A.

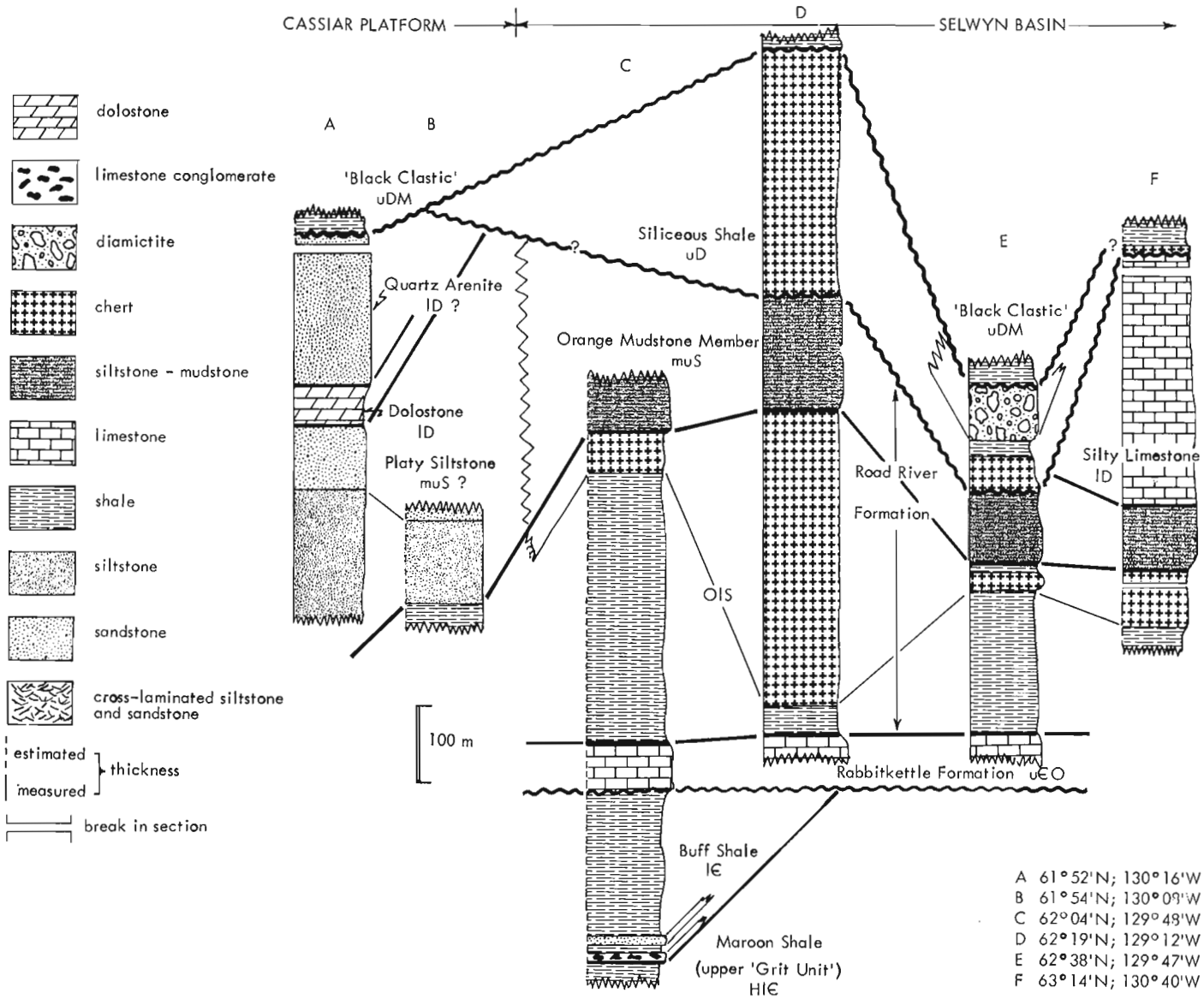

Figure 2. *Proposed correlations from Cassiar Platform to Selwyn Basin. Location of sections shown on Figure 1. Section C is a composite section shown on Figure 1. l = lower, m = middle, u = upper.*

variably oriented in a sandy limestone matrix. The interpretation of these deposits as debris flows, as well as the presence of the clean quartz sand imply a shallow water platform to the south or southwest in Early Cambrian time. Similar conglomerate is found near the margin of Mackenzie Platform (Gordey, 1979).

The orange mudstone unit is a regionally extensive marker found within Selwyn Basin in the Nahanni area and extending at least 140 km north into Niddery Lake area. Monograptids near the base at several localities and one collection within the unit indicate a Middle and Late Silurian age. The younger limit is uncertain as in most places the upper contact is probably unconformable. The platy siltstone unit, its platform ? equivalent is a widespread unit found along Cassiar Platform in both the Yukon and northern British Columbia.

Unconformities

In the Nahanni area three major unconformities interrupt the stratigraphic record. The sub-Cambro-Ordovician (sub-Rabbitkettle) unconformity extends across southeastern Selwyn Basin and is recognized by rapid truncation of underlying units, so that the Rabbitkettle Formation locally rests on the maroon and green shales of the Proterozoic "Grit Unit". The hiatus becomes insignificant in northeastern Nahanni area where little or no strata have been removed by erosion. To the northwest within Selwyn Basin its continuation is uncertain. The Rabbitkettle Formation is well developed in southwesternmost Nahanni area, but correlative strata on nearby Cassiar Platform are not yet recognized.

A regional sub-Upper-Devonian (sub-Siliceous shale) unconformity is postulated to extend across most of, and possibly the entire basin (Fig. 2). It exists as far southwest as Howard's Pass, and on Mackenzie Platform where the siliceous shale unit sits above Lower Silurian and upper Middle Devonian strata (Gordey, 1980b). In the Niddery Lake area (section F) a thin section of siliceous shale overlies thick Lower Devonian silty limestone which in turn overlies a normal thickness of the orange mudstone unit. Southeast along the 'facies trend' (section E), the silty limestone or its shale equivalent is not present and probably removed by erosion. In the centre of the basin (section D) an

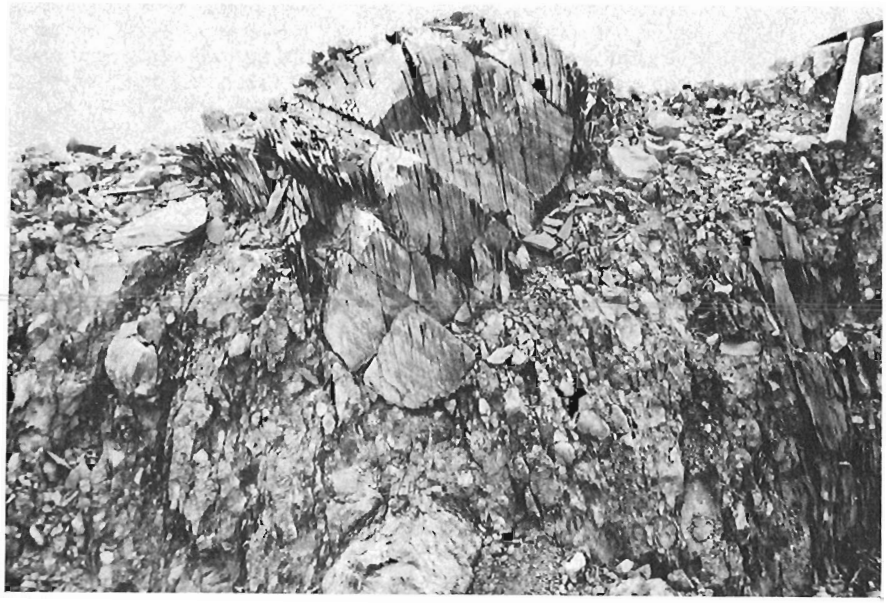

Figure 3

Diamictite in Upper Devonian siliceous shale unit, interpreted as a debris flow deposit. Large clast in centre of photo is shale. Other clast types include chert and coarse grained quartz arenite. The matrix is black shale.

unconformity is favoured on regional evidence although it is not yet proven that all chert of the siliceous shale unit is Late Devonian. The lower part may include Lower or Middle Devonian strata in chert facies. The sub-siliceous shale unconformity and subsequent deposition of the regional blanket of shale and chert terminated the older lower to mid-Paleozoic paleogeographic regime. The local spectacular debris-flow conglomerate within the upper part of the siliceous shale unit (section E, Fig. 2, 3), possibly basin derived, is the earliest indication of rapid differential uplift that occurred within older basin areas and continued into Devono-Mississippian ('black clastic') time.

A regional sub-Devono-Mississippian unconformity (sub-'black clastic') is recognized by highly variable thickness of the underlying siliceous shale unit, and by the sharp upper contact of that unit. Its existence above older Cassiar Platform strata is demonstrated in Section A where brown shale and minor quartz-chert wacke abruptly overlie clean quartz arenite of probable Early Devonian age.

Mississippian and Younger Clastics

In northwestern and northern Nahanni map area, clastic strata of late Paleozoic to Triassic age overlie the Devono-Mississippian 'black clastic' group (Fig. 3). The top of the 'black clastic' is defined at the base of a pure clean quartz arenite unit (A) about 170 m thick. Aside from a thin shale member, the thick bedded to massive sandstone is featureless. The basal contact with brown to black weathering 'black clastic' shale is not well exposed but seems to be gradational over a few metres. Quartzite beds in talus blocks near the base are thin, separated by shale partings and contain laminated quartz siltstone. The top contact with overlying shale (B) is abrupt. Shale above the sandstone resembles that below in weathering dark brown to tan, and being black to blue-grey on fresh surface. It is in turn overlain by orange-weathering, locally ripple-marked, fine- to medium-grained, white quartz arenite. Dark brown to tan weathering grey-green to green shale overlies the quartz arenite, at its base containing scattered spherical barite concretions up to 0.2 m in diameter that diminish in size and quantity upward. The overlying orange-weathering pale green to black chert (C) in lenticular beds to 0.2 m thick contains intervals of pale green shale similar to that found stratigraphically below. Scattered barite nodules up to 0.2 m across are also found in the chert. The base of the chert is marked by a bed of ochre-weathering massive grey limestone (2 m thick) that has yielded Permian conodonts (Orchard, personal communication, 1980). The base of the overlying cross-laminated unit (D) is taken as the top of the uppermost chert bed, which is coincident with the first appearance upwards of dark grey to black siltstone and shale, as opposed to the green shale stratigraphically lower. A thick sequence of monotonous, ripple cross-laminated, variably calcareous, thin-bedded quartzose sandstone and siltstone overlies the thin basal member. The only variation within this thick sequence is in its middle part where the ratio of cross-laminated sandstone to siltstone-shale is low and the interval is recessive weathering. A thin bed of limestone from within this unit has yielded Middle Triassic conodonts (Orchard, personal communication, 1980).

Because of poor paleontologic control the stratigraphic relations of units within the section and their correlation outside the area are not firm. The basal quartz arenite probably corresponds to a similar extensive sandstone unit in western Sekwi Mountain map area, unit 27 of Blusson (1971) where a basal unconformity is recognized. Shale above the quartzite may correspond to shale of Blusson's overlying unit 28. The chert unit, with its thin Permian limestone at the base may be partly equivalent to Blusson's unit 29, of Carboniferous or Permian age, which is characterized by variable amounts of light grey to buff quartzite, dolostone, and interbedded dark shale and minor chert. The thick ripple cross-laminated Triassic sediments, not previously reported from this part of Selwyn Mountains, bear a striking resemblance to Triassic strata elsewhere in the northern Cordillera.

South Fork Volcanics[1]

The South Fork Volcanics between Orchie and Tay lakes in southwestern Sheldon Lake map area can be subdivided into four laterally extensive units. The lower unit of massive porphyritic andesite 130 to 300 m thick is characterized by hornblende phenocrysts which occur with plagioclase and quartz in a dark greenish grey groundmass. The top 10 m of the unit is heavily weathered, possibly reflecting a period of erosion before deposition of the overlying volcaniclastics.

[1] Description by D. Wood

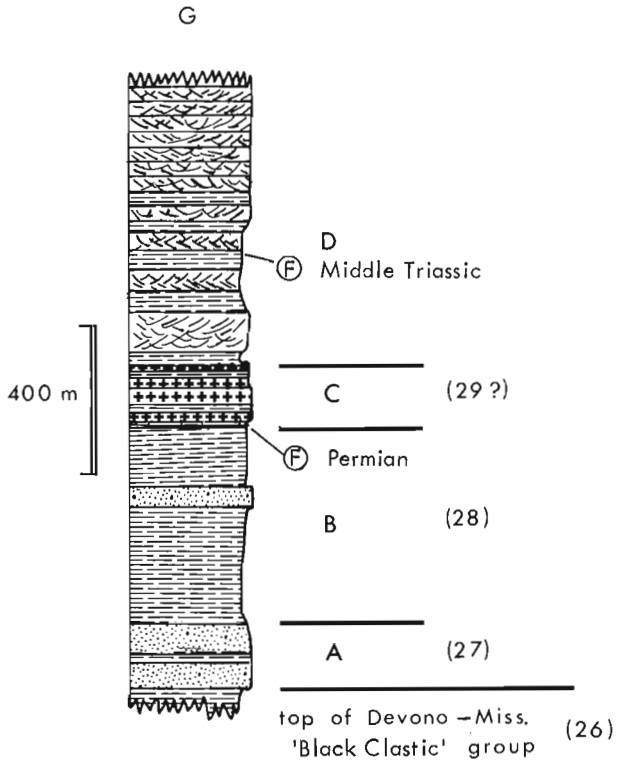

Figure 4. *Post – 'black clastic' stratigraphy, northern Nahanni map area. Units A to D are referred to in text. Also shown is the proposed correlation with units of Blusson (1971) in Sekwi Mountain map area. Section location is 62 48'N; 129 42'W.*

Immature volcaniclastic sandstone, lapilli tuff, and at least one mudflow deposit, in total ranging from 33 m to 45 m thick, directly overlie the andesite. The tuffs contain dark volcanic fragments with wispy outlines in a matrix rich in feldspar and quartz crystals. In the debris flow deposit large angular blocks of andesite and basement derived silty limestone as large as 3 m across are suspended in a carbonaceous mudstone matrix.

The third unit, in sharp contact with the volcaniclastics, is composed of crystal tuff at least 416 m thick. Massive intervals of tuff up to 65 m thick are separated by well bedded, medium bedded units 15 m to 20 m thick. Within these bedded units graded bedding is well developed. The tuffs are composed mostly of quartz and feldspar crystals, and lesser volcanic, chert, and shale fragments.

Porphyritic dacite, presumably overlying the tuff but not observed in stratigraphic contact with it, is at least 250 m thick. The dacite is composed of quartz, feldspar, hornblende, and biotite phenocrysts in a light green to greenish grey groundmass. On the west side of peak 7003 ft., 16 km northeast of Tay Lake similar and possibly correlative dacite is at least 720 m thick.

In the Orchie Lake – Tay Lake area the South Fork Volcanics generally dip from 10 to 30° westerly and overlie with angular unconformity Paleozoic and ? Mesozoic sedimentary rocks folded about west trending axes. At one exposure the basal unit overlies biotite quartz monzonite unconformably. There, a highly weathered zone about 1 m thick in the plutonic rock may reflect a period of pre-volcanic weathering. If the volcanics are a late expression of the mid-Cretaceous plutonic event, it is conceivable that high level plutons could be unroofed before volcanism.

Mineral Occurrences

No new mineral occurrences were found during the present work; however, a small area of previously unmapped Road River shale may be of economic interest. It occurs in the area of section C, on trend with correlative ? strata hosting the Maxi showing of stratiform lead-zinc mineralization thought to be at the same stratigraphic position as the deposits at Howard's Pass (Dawson, 1979). The shale is brown weathering, silty, generally non-calcareous, and except near the top of the unit contains little chert. Superficially it resembles shale of the Devono-Mississippian 'black clastic' but its stratigraphic position and graptolite fauna show it to be of Ordovician and Early Silurian age. Aside from strata of this age (post-Rabbitkettle and pre-orange mudstone) the other unit of economic interest regionally is the siliceous shale which hosts a well known regional barite horizon (Dawson, 1977) and the barite-lead-zinc deposits at Macmillan Pass.

References

Blusson, S.L.
1971: Sekwi Mountain map-area; Yukon Territory and District of Mackenzie; Geological Survey of Canada, Paper 71-22.

Dawson, K.M.
1977: Regional metallogeny of the northern Cordillera; in Report of Activities, Part A, Geological Survey of Canada, Paper 77-1A, p. 1-4.

1979: Regional metallogeny of the northern Cordillera: recent stratiform base metal discoveries in Yukon Territory and District of Mackenzie; in Current Research, Part A, Geological Survey of Canada, Paper 79-1A, p. 375-376.

Gordey, S.P.
1978: Stratigraphy and structure of the Summit Lake area, Yukon and Northwest Territories; in Current Research, Part A, Geological Survey of Canada, Paper 78-1A, p. 43-48.

1979: Stratigraphy of southeastern Selwyn Basin in the Summit Lake area, Yukon Territory and Northwest Territories; in Current Research, Part A, Geological Survey of Canada, Paper 79-1A, p. 13-16.

1980a: Stratigraphic cross-section, Selwyn Basin to Mackenzie Platform, Nahanni map area, Yukon Territory and District of Mackenzie; in Current Research, Part A, Geological Survey of Canada, Paper 80-1A, p. 353-355.

1980b: Geology of Nahanni (105 I) map area, Yukon Territory and District of Mackenzie; Geological Survey of Canada, Open File No. 689.

Tempelman-Kluit, D.J.
1977: Geology of Quiet Lake (105 F) and Finlayson Lake (105 G) map-areas, Yukon Territory; Geological Survey of Canada, Open File No. 486.

PETROLIFEROUS CORE FROM A DIAPIR EAST OF CUMBERLAND SOUND, BAFFIN ISLAND

Project 760015

Brian MacLean and S.P. Srivastava
Atlantic Geoscience Centre, Dartmouth

A 65 cm long drill core composed of dark grey mudstone was recovered by **CSS Hudson** on October 7, 1980 from a ridge structure believed to be of diapiric origin at 64°16.9'N, 61°55.8'W off Cumberland Sound on the Baffin Island continental shelf. The core was recovered by means of the Bedford Institute underwater electric rock core drill.

Preliminary examination at sea indicates that the sample material is poorly lithified and has a mottled, apparently chaotic appearance. The core sample gave off a strong petroliferous odour and bubbles emanated from the core upon recovery.

The sample locality (Fig. 1) lies on a northeasterly trending structure previously delineated and reported by MacLean and Falconer (1979). The locality is 5.5 km north of the seismic profile across the structure shown in Figure 2. The material forming the core of the structure typically is acoustically opaque such as might be caused by the masking effect of gas. The presence of gas bubbling from the core strongly supports this conclusion. In addition to the core material itself, samples of the overlying unconsolidated sediments and of the water column were collected for chemical analysis to provide a further indication of whether gas may be escaping naturally into the sea.

Two seismic refraction profiles run in 1980 across this ridge structure yielded velocities in the range of 2.5 kms^{-1} and 6.1 kms^{-1}. These velocities seem appropriate to represent the sedimentary material in the core of the diapir, and the underlying basement rocks, respectively.

By the end of the 1980 season a series of geophysical profiles spaced at 9.3 km intervals will have been run across the Cumberland Sound offshore area between 64°20'N and 65°00'N. The occurrence of additional ridge structures is indicated.

The presence of petroliferous material and gas in these structures as suggested by our core sample together with the possibilities for entrapment on the flanks indicates that structures of this type may be of resource significance in this area.

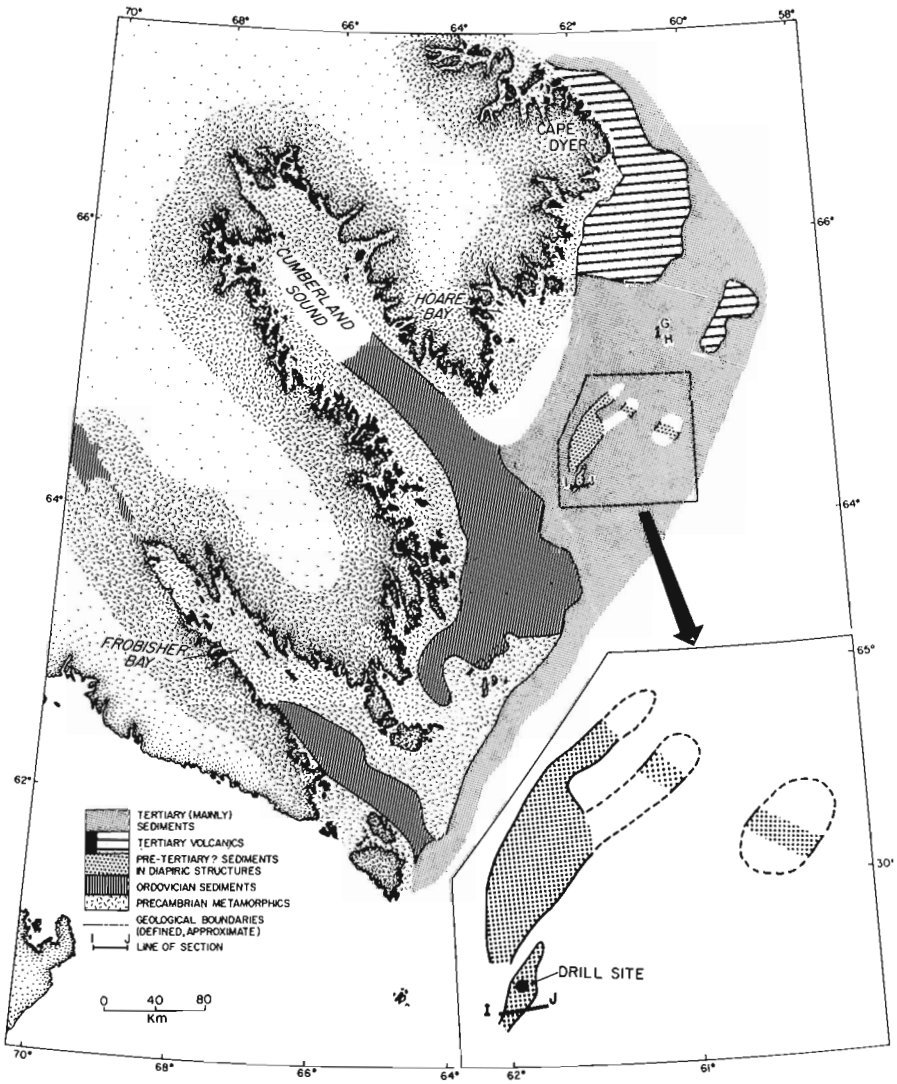

Figure 1. *Regional geological map showing locations of the core site and structure off Cumberland Sound.*

From: Scientific and Technical Notes in Current Research, Part A; Geol. Surv. Can., Paper 81-1A.

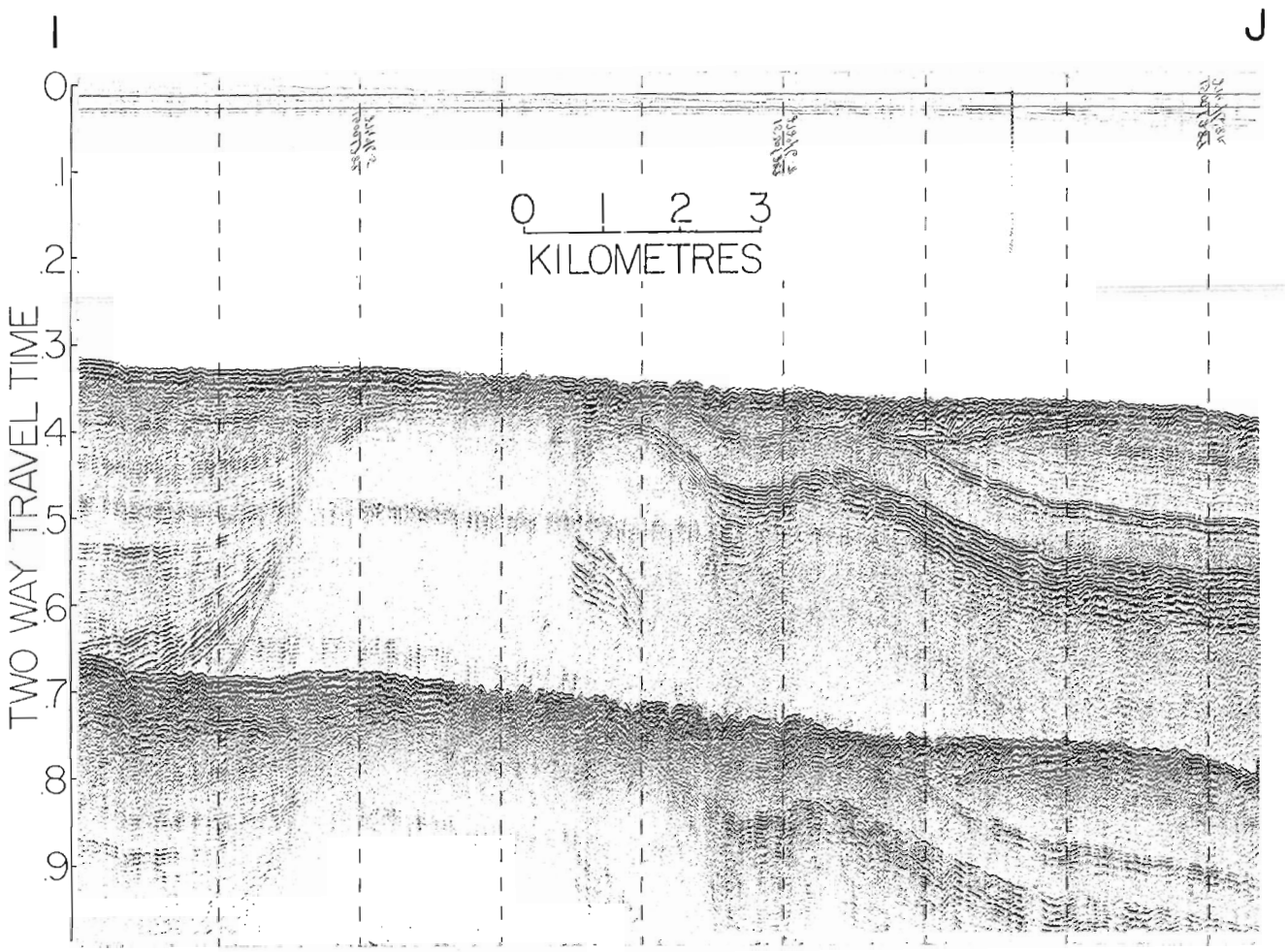

Figure 2. *Profile I-J (see Fig. 1 for location). Seismic reflection record across a diapiric ridge structure east of Cumberland Sound.*

We gratefully acknowledge the co-operation and assistance of Captain F.W. Mauger, Officers, Crew and Scientific Staff aboard **CSS Hudson** without whom this study could not have been undertaken.

Reference

MacLean, B., and Falconer, R.K.H.
1979: Geological/geophysical studies in Baffin Bay and Scott Inlet-Buchan Gulf and Cape Dyer-Cumberland Sound areas of the Baffin Island shelf; in Current Research, Part B, Geological Survey of Canada, Paper 79-1B, p. 231-244.

NATURAL HYDROCARBON SEEPAGE AT SCOTT INLET AND BUCHAN GULF, BAFFIN ISLAND SHELF: 1980 UPDATE

Project 760015

E.M. Levy[1] and B. MacLean
Atlantic Geoscience Centre, Dartmouth

Introduction

Chemical, geological and geophysical investigations carried out in 1977 and 1978 have provided strong evidence that slicks, which are frequently present off the northeast coast of Baffin Island in the vicinity of Scott Inlet and Buchan Gulf are the consequence of natural seepage of petroleum from the seabed (Fig. 1) (Levy, 1979; MacLean, 1978; MacLean and Falconer, 1979). The distributions of petroleum residue concentration anomalies found in the sea surface microlayer, in the water column and surficial bottom sediments, as well as the repeated occurrence of slicks indicated that one of the most active of the seeps is associated with a structural high near the seaward end of the submarine trough that extends across the Baffin Island continental shelf at Scott Inlet. In addition, the data also suggested that other seeps, which may be less persistent, are probably present elsewhere at Scott Trough and also off Buchan Gulf. As all the available chemical and geological data indicated that natural hydrocarbon seepage is occurring at both Scott Trough and Buchan Trough, detailed studies of these areas were carried out in September 1980 **(CSS Hudson,** Cruise 80-028). During this cruise oil droplets were observed erupting at the surface of the sea and forming iridescent patches which quickly spread into slicks. Their number and frequency of arrival was considerably greater than previously observed (Loncarevic and Falconer, 1977). This phenomenon, is the most direct visual indication of seepage yet obtained in this area. In addition, the distribution of slicks is discussed and a brief summary is given of the kinds of chemical, geological and geophysical investigations carried out. More complete results must await the chemical and geological analyses of the samples and interpretation of the geophysical records.

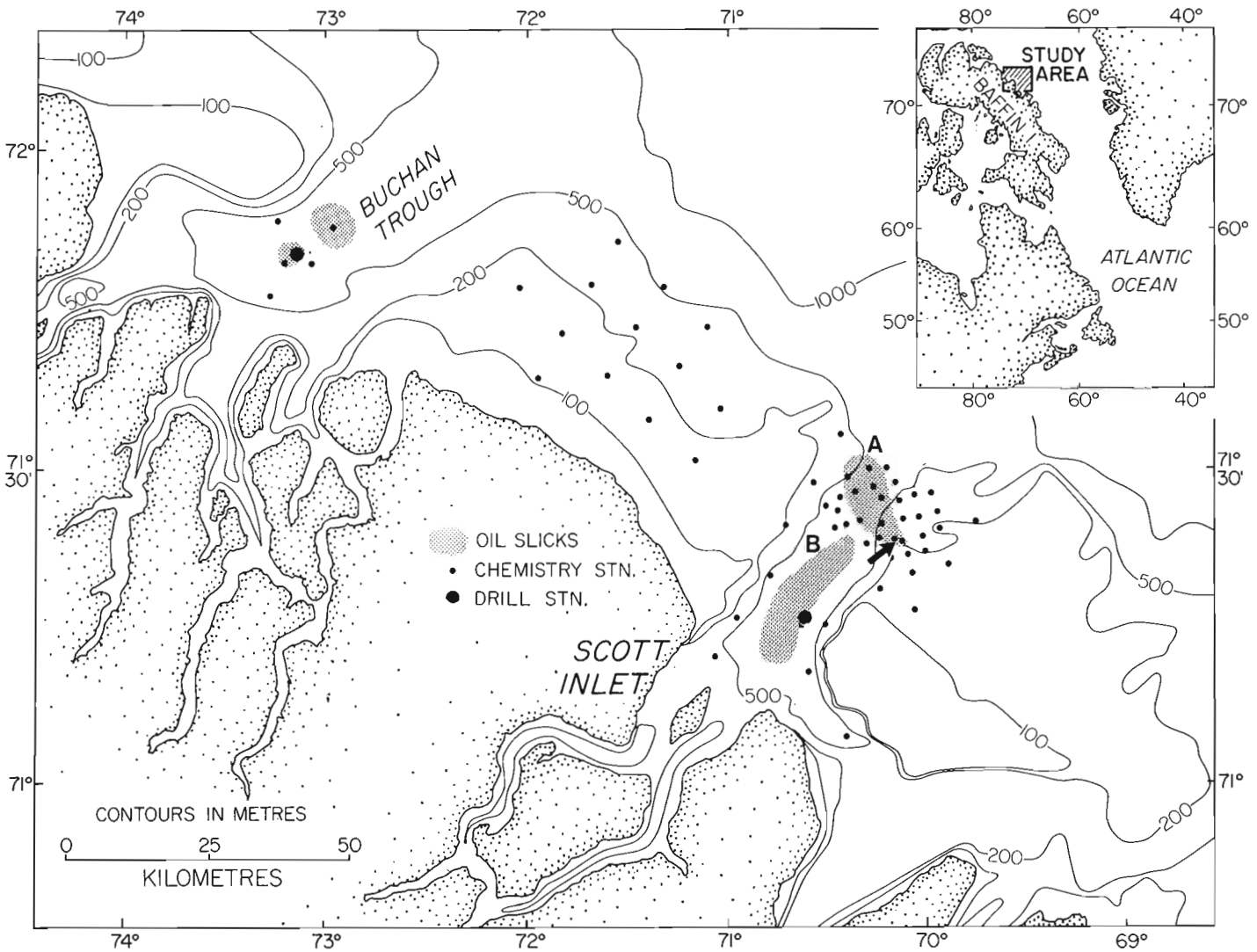

Figure 1. *Scott Inlet – Buchan Gulf area showing chemistry and drill sample locations and areas in which surface slicks were observed. The arrow indicates the outer Scott Trough locality where oil droplets and bubbles were erupting at the sea surface.*

[1]Atlantic Oceanographic Laboratory, Bedford Institute of Oceanography, Dartmouth, N.S.

From: Scientific and Technical Notes in Current Research, Part A; Geol. Surv. Can., Paper 81-1A.

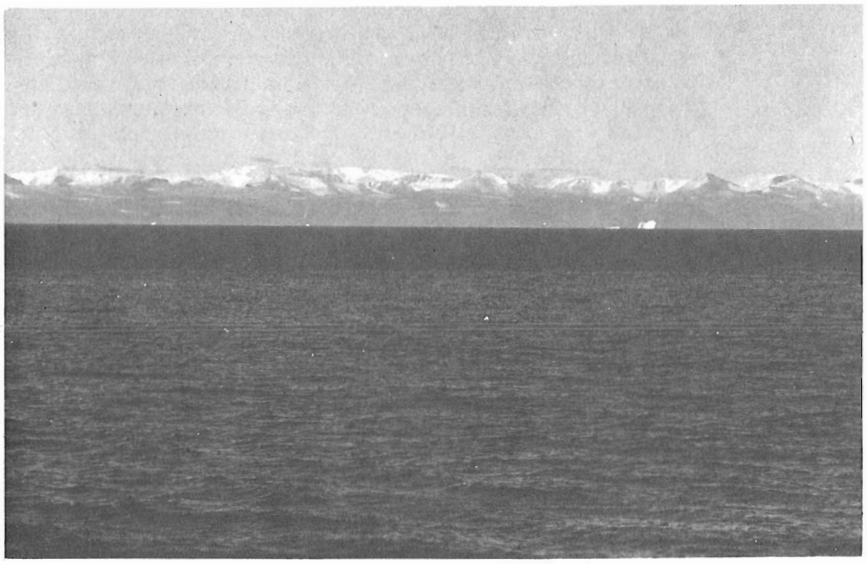

Figure 2

Oil slick at Area A (slick in foreground). GSC 203653

Field Program

During the 1980 cruise, samples of seawater were collected from the sea surface microlayer and at 10 depths throughout the water column at 5 stations at Buchan Trough, 32 at Scott Trough, and 13 over the shelf between the troughs (Fig. 1). Surficial bottom sediment samples were collected at these stations and at an additional 12 stations at Scott Trough. An attempt was also made to collect a sample of the slick-forming material and a piston core was taken at the site where seepage was occurring. Gas chromatographic analyses to determine the concentrations of volatile hydrocarbons (C_1 to C_6) in the water and sediment samples were carried out within a few hours of collection. Water samples were extracted with carbon tetrachloride and sediment samples were frozen for subsequent determination of petroleum residues by fluorescence spectrophotometry and other analyses. In addition, detailed analyses of the hydrocarbon mixtures will be carried out by gas chromatography/mass spectrometry.

Geological and geophysical investigations of the Scott-Buchan offshore area in 1977 and 1978 (MacLean, 1978; MacLean and Falconer, 1979) revealed the presence of Upper Cretaceous (Campanian) and upper Eocene to lower Oligocene strata as well as possibly older sedimentary rocks underlying the seafloor in this region. Upturned strata that flank a structural (basement) high beneath the outer south wall of Scott Trough are believed to be the source of persistent seepage observed in that area. Truncation of strata by erosion provides possible opportunities for escape of formation fluids or gases elsewhere.

Emphasis of the 1980 geological/geophysical program in the Scott-Buchan area was directed toward the collection of additional samples with the Bedford Institute of Oceanography rock core drill in an effort to define more fully the stratigraphic succession. Although the thickness of soft sediment cover over the bedrock in these areas severely limited the number of accessible sites, two bedrock cores were recovered from the floor of Buchan Trough. The cores appear to be lithologically similar to the Campanian strata sampled previously in the floor of Buchan Trough 10 km to the northeast (MacLean and Falconer, 1979; MacLean and Williams, 1980). A short drill core of limestone was recovered from the floor of Scott Trough. Although the age of this material has not yet been determined, it is thought to be part of the Cretaceous or Tertiary sequence.

Additional seismic reflection, magnetic, and gravity profiles were run in several areas to define geological boundaries in greater detail than afforded by previous surveys.

Distribution of Slicks

An attempt was made to determine the distribution of slicks by making visual observations of the sea surface whenever possible throughout the cruise. Although sea conditions were favourable for the formation and observation of slicks none was present during the passage from Thule via north central Baffin Bay to Buchan Gulf. At Buchan Gulf, under very light winds, conditions were ideal for the formation of slicks and excellent light conditions made their observation easy. Thin, scattered slicks were present at the stations at the inner portion of Buchan Trough (Fig. 1). This is the same general area where they were reported in 1978 (Levy, 1979). However, none was present shoreward of the sampling area. Since slicks may be formed by surface active molecules of recent biological origin as well as those derived from petroleum, it is often extremely difficult by visual methods to differentiate between the two. Therefore, the slicks at Buchan Gulf cannot be unequivocally attributed to natural seepage. Samples of water were collected from the surface microlayer and an attempt will be made to provide a definitive identification of the source of the slick-forming material through detailed chemical analyses by gas chromatography/mass spectrometry.

Conditions remained favourable for the formation and observation of surface slicks during most of the sampling program carried out at Scott Trough and the area between Scott Trough and Buchan Trough (Sept. 5-11). Slicks were not present over the shallow area between the two troughs or seaward of region A in Figure 1. Within region A, however, extensive slicks were observed at all stations and at several sites the entire sea surface has a "greasy" appearance (e.g. Fig. 2)*. As there had been several days of light south to southeasterly winds just before surveying this area, the

* It should be appreciated that slicks can only be clearly discerned where there is a distinct boundary between areas where capillary waves are damped by the presence of surface active materials and those where the surface is ruffled by capillary waves. Consequently, in the absence of interference colours and unless this contrast can be seen, it is difficult to decide whether the entire surface visible from the ship is covered with a continuous film or whether no film is present.

source of the slick must have been somewhere to the south or southeast. Slicks were also present on September 7 during a geophysical survey of the central portion of Scott Trough (area B, Fig. 1) where the sea surface again had a greasy appearance. At the rock core drilling station in area B, gas bubbles were observed rising to the sea surface but, because drilling was in progress on the seafloor at the time, it is not certain whether these bubbles were the result of natural gas releases from the seabed or were somehow related to the drilling operation. In either case, however, these bubbles were much larger and definitely not the type resulting from physical turbulence at the sea surface.

Near the southern edge of area A (Fig. 1) on September 11 slicks were sighted from a distance and on closer examination droplets of oil were observed erupting at the sea surface. Attempts were made to obtain some of this material but, because of the erratic random nature of the phenomenon, the thinness of the film and its rapid spreading, and the limited visibility from a dory used to collect the samples, it is doubtful whether sufficient material for detailed chemical analyses was collected. By the time the dory work was completed, the wind began to increase and the slick became much smaller but, at the same time, much better defined. Gas bubbles, some of them of golf ball size were observed erupting at the sea surface while we were collecting a piston core (234 cm) of bottom sediments. Oil was rising to the surface randomly in space and time but at a sufficient rate to maintain a slick over an area of perhaps 2 km by 2 km even with a wind speed of 20 knots. On breaking the surface, the oil droplets spread almost instantaneously into a circular slick about 25 cm in diameter. At first, the layers at the centres of these slicks were of sufficient thickness to display interference colours but immediately spread out to a film of monomolecular thickness within a few seconds. The slicks then drifted downwind and eventually were no longer visible under the wind conditions at the time. The random pattern of eruption suggests that the escape from the seabed occurs over an area, rather than from a single point source, and that the seepage is sporadic.

To have been at the site and to have watched hundreds of such droplets arrive at the sea surface provides more convincing evidence for natural seepage than any photographic or written description – or perhaps even the most sophisticated scientific measurements – can convey.

Acknowledgments

We gratefully thank Captain F.W. Mauger, Officers, Crew and Scientific Staff aboard **CSS Hudson** for their excellent co-operation and assistance in carrying out the field study and R.T. Haworth for review of the manuscript.

References

Levy, E.M.
1979: Further chemical evidence for natural seepage on the Baffin Island shelf; in Current Research, Part B, Geological Survey of Canada, Paper 79-1B, p. 379-383.

Loncarevic, B.D. and Falconer, R.K.H.
1977: An oil slick occurrence off Baffin Island; in Report of Activities, Part A, Geological Survey of Canada, Paper 77-1A, p. 523-524.

MacLean, B.
1978: Marine geological-geophysical investigations in 1977 of the Scott Inlet and Cape Dyer – Frobisher Bay areas of Baffin Island continental shelf; in Current Research, Part B, Geological Survey of Canada, Paper 79-1B, p. 13-20.

MacLean, B., and Falconer, R.K.H.
1979: Geological/geophysical studies in Baffin Bay and Scott Inlet – Buchan Gulf and Cape Dyer – Cumberland Sound areas of the Baffin Island shelf; in Current Research, Geological Survey of Canada, Paper 79-1B, p. 231-244.

MacLean, B. and Williams, G.L.
1980: Upper Cretaceous rocks in Baffin Bay; Geological Association of Canada, Program with Abstracts, v. 5, p. 69.

AUTHOR INDEX

	Page
Anderson, R.G.	395
Annesley, I.R.	275
Ashton, K.E.	269
Bell, R.T.	241
Blake, W., Jr.	191
Campbell, F.H.A.	15
Cameron, B.E.B.	209
Card, K.D.	77
Cecile, M.P.	281
Chandler, F.W.	37
Copeland, M.J.	41
Currie, K.L.	23
Davidson, A.	291
Dewez, V.	327
Dredge, L.A.	377
Dyke, L.D.	157
Eade, K.E.	231
Easton, R.M.	305
Egginton, P.A.	299,385
Ermanovics, I.	69
Fader, G.B.	45
Franklin, J.M.	9
Frisch, T.	31
Frith, R.A.	333
Fritz, W.H.	145
Froese, E.	311
Gabrielse, H.	201
Gall, Q.	311
Geurts, M.A.	327
Gordey, S.P.	395
Gordon, T.M.	315
Guay, F.	327
Henderson, J.B.	175
Henderson, J.R.	384
Heywood, W.W.	259
Hoffman, P.F.	247,251
Hofmann, H.J.	281
Hogarth, D.D.	77
Huang, C.F.	361
Hunter, J.A.	361
King, L.H.	45
Klassen, R.A.	317
Klepacki, D.W.	169
Korstgård, J.A.	69
Lafleur, J.	77
Lamontagne, C.G.	231
Landriault, F.	327
Léveillé, P.	327
Levy, E.M.	401
Lichti-Federovich, S.	57
Littlejohn, A.L.	133
Loveridge, W.D.	33
Mackay, J.R.	63
MacLean, B.	399,401
Meijer-Drees, N.C.	107
Miller, A.R.	231
Monger, J.W.H.	185
Moore, P.R.	95
Morgan, W.C.	291
Morrow, D.W.	107
Nadeau, L.	265
Nance, R.D.	23
Oke, C.	181
Okulitch, A.V.	33
Ollerenshaw, N.C.	341
Orchard, M.J.	357
Parjari, G.E., Jr.	23
Pell, J.	227
Percival, J.A.	77
Pickerill, R.K.	23
Poulsen, K.H.	9
Read, P.B.	169
Rees, C.J.	223
Rimsaite, J.	115
Ruzicka, V.	133
Sangster, D.F.	1
Schau, M.	259,383
Shannon, K.R.	217
Simony, P.S.	181,227
Srivastava, S.P.	399
Stevens, R.D.	37
St-Onge, D.A.	327
St-Onge, M.R.	251
Struik, L.C.	213
Sullivan, R.W.	33
Tella, S.	231
Thompson, P.H.	175
Tipper, H.W.	209
Trettin, H.P.	103
Watkinson, D.H.	349
Watts, S.H.	389
Whittaker, P.J.	349
Wood, D.	395

NOTE TO CONTRIBUTORS

Submissions to the *Discussion* section of *Current Research* are welcome from both the staff of the Geological Survey and from the public. Discussions are limited to 6 double-spaced typewritten pages (about 1500 words) and are subject to review by the Chief Scientific Editor. Discussions are restricted to the scientific content of Geological Survey reports. General discussions concerning branch or government policy will not be accepted. Illustrations will be accepted only if, in the opinion of the editor, they are considered essential. In any case no redrafting will be undertaken and reproducible copy must accompany the original submissions. Discussion is limited to recent reports (not more than 2 years old) and may be in either English or French. Every effort is made to include both *Discussion* and *Reply* in the same issue. *Current Research* is published in January, June and November. Submissions for these issues should be received not later than November 1, April 1, and September 1 respectively. Submissions should be sent to the Chief Scientific Editor, Geological Survey of Canada, 601 Booth Street, Ottawa, Canada, K1A 0E8.

AVIS AUX AUTEURS D'ARTICLES

Nous encourageons tant le personnel de la Commission géologique que le grand public à nous faire parvenir des articles destinés à la section discussion *de la publication* Recherches en cours. *Le texte doit comprendre au plus six pages dactylographiées à double interligne (environ 1500 mots), texte qui peut faire l'objet d'un réexamen par le rédacteur en chef scientifique. Les discussions doivent se limiter au contenu scientifique des rapports de la Commission géologique. Les discussions générales sur la Direction ou les politiques gouvernementales ne seront pas acceptées. Les illustrations ne seront acceptées que dans la mesure où, selon l'opinion du rédacteur, elles seront considérées comme essentielles. Aucune retouche ne sera faite aux textes et dans tous les cas, une copie qui puisse être reproduite doit accompagner les textes originaux. Les discussions en français ou en anglais doivent se limiter aux rapports récents (au plus de 2 ans). On s'efforcera de faire coincider les articles destinés aux rubriques* discussions et réponses *dans le méme numéro. La publication* Recherches en cours *paraît en janvier, en juin et en novembre. Les articles pour ces numéros doivent être reçus au plus tard le 1er novembre, le 1er avril et le 1er septembre respectivement. Les articles doivent être renvoyés au rédacteur en chef scientifique: Commission géologique du Canada, 601, rue Booth, Ottawa, Canada, K1A 0E8.*